Diseases of the Orbit

A Multidisciplinary Approach

2nd Edition

2003

Lippincott Williams & Wilkins

Philadelphia

227 East Washington Square, Philadelphia, PA 19106-3780

0-7817-1512-1

Printed in the United States of America

First edition published in 1988.

9 8 7 6 5 4 3 2 1

Library of Congress Cataloging-in-Publication Data

0-7817-1512-1

Editor

Jack Rootman MD, FRCSC

Professor
Departments of Ophthalmology and Pathology, University of British Columbia and the Vancouver Hospital and Health Sciences Centre, Vancouver, British Columbia, Canada

Secondary Editors

Jonathan Pine

Acquisitions Editor

Carol Field

Developmental Editor

Tim Reynolds

Manufacturing Manager

Cassie Carey

Production Manager

Cathy Hunt

Cover Designer

Robert Elwood

Indexer

Edwards Brothers
Printer

Contributing Authors

Hind Al-Katan MD

Consultant Ophthalmologist & Head
Department of Ophthalmology, Security Forces Hospital; Clinical Assistant Professor, Department of Ophthalmology, King Saud University; Visiting Staff, Department of Pathology, King Khalid Eye Specialist Hospital, Riyadh, Saudi Arabia

Wilma Y. Chang BSc
Department of Ophthalmology, University of British Columbia, Vancouver, British Columbia, Canada

Joseph M. Connors MD, FRCPC

Clinical Professor
Division of Medical Oncology, Department of Medicine, University of British Columbia; Chair, Lymphoma Tumor Group, British Columbia Cancer Agency, Vancouver, British Columbia, Canada

Peter J. Dolman MD, FRCSC

Clinical Associate Professor
Department of Ophthalmology, University of British Columbia and the Vancouver Hospital & Health Sciences Centre, Vancouver, British Columbia, Canada

Randy D. Gascoyne MD, FRCPC

Clinical Professor
Department of Pathology, University of British Columbia; Pathologist, British Columbia Cancer Agency, Vancouver, British Columbia, Canada

Douglas A. Graeb MD, FRCPC

Associate Professor
Division of Neuroradiology, Departments of Radiology, University of British Columbia and the Vancouver Hospital & Health Sciences Centre, Vancouver, British Columbia, Canada

Dean R. Jones MD

Resident
Department of Anesthesiology, Columbia Presbyterian Medical Center, Columbia University, New York, New York, United States

Steven E. Katz MD

Assistant Professor
Department of Ophthalmology, Ohio State University, Columbus, Ohio, United States

Christopher J. Lyons MB, BSc, FRCSC

Associate Professor
Department of Ophthalmology, University of British Columbia; Head, Department of Ophthalmology, British Columbia Children's Hospital, Vancouver, British Columbia, Canada

Thomas R. Marotta MD, FRCPC

Assistant Professor and Interventional Neuroradiologist
Departments of Radiology, St. Michael's Hospital, the University Health Network – Toronto Western Hospital and the University of Toronto, Toronto, Ontario

Robert A. Nugent MD, FRCPC

Associate Professor
Division of Neuroradiology, Department of Radiology, University of British Columbia and the Vancouver Hospital & Health Sciences Centre, Vancouver, British Columbia, Canada

Peerooz Saeed MD
Department of Ophthalmology–Orbital Centre, Academic Medical Center, University of Amsterdam; Consultant Ocular Oncologist, Head and Neck Group, Antonie van Leeuwenhoek Hospital/The Netherlands Institute of Cancer, Amsterdam, The Netherlands

Dinesh Selva MBBS (Hons), FRACS, FRANZCO

Senior Clinical Lecturer
Oculoplastic and Orbital Division, Department of Ophthalmology, Royal Adelaide Hospital, University of Adelaide, Adelaide, Australia

Bruce Stewart BFA
Victoria, British Columbia, Canada

Valerie A. White MD, FRCPC

Associate Professor
Departments of Pathology and Ophthalmology, University of British Columbia and the Vancouver Hospital & Health Sciences Centre, Vancouver, British Columbia, Canada

Preface

The most significant responsibility of the clinical academic endeavor is a commitment to life-long learning, which this book represents. It reflects the need to question, innovate, and analyze what we do as physicians in the context of the intricate bond necessary between teachers, students, and colleagues for the management of disease. *Diseases of the Orbit* is structured in such a way as to provide a graduated approach to knowledge acquisition. First it establishes an essential background knowledge of orbital disease as the basis for the patient encounter, so that the student is able to analyze critical findings and define a management program for the patient. Having acquired such, the section on specific diseases will act as a compendium for individual treatment.

For me, the most striking aspect of this new edition is how much things have changed in my own practice and understanding of these diseases. As we enter the molecular era, new techniques in pathology have allowed us to investigate and understand the pathogenesis of disease better. This has been particularly useful in the fields of inflammation and neoplasia, where we are able to more specifically diagnose and therefore design appropriate therapeutic regimens. This book also reflects a significant change in the way we approach thyroid orbitopathy, based on the management of over 2000 cases and advances in the last decade. The challenge for us remains how to prevent this disorder. Vascular lesions have been a major focus of our clinic, the understanding of which has been vastly improved by advances in interventional neuroradiology and clinicopathologic correlation.

Overall, the content of this text has changed at least 40% to 50% from 1988, which alone justifies the new edition. Equally important, the functional and artistic structure of *Diseases of the Orbit* has changed as a result of our being able to use sophisticated publishing tools. I have attempted as much as possible to integrate case-based visuals with text so that specific examples enhance general knowledge acquisition, providing a basis for algorithmic thinking in patient management. At the same time, this task has highlighted the limitations of our current knowledge and the need to maintain a commitment to learning in order to challenge these limitations.

Acknowledgments

The structure and content of this book reflects the dedicated commitment and creative talents of Wilma Chang, who has maintained my database, helped all our fellows and students, and has become an expert in desktop publishing for this endeavor. This book in its new format simply would not exist if it were not for her efforts, for which I am deeply grateful. My local colleagues in neuroradiology, pathology, oncology, rheumatology, and surgery have been a constant source for learning, inspiration, and cooperative patient care. So far, the Orbit, Ocular Pathology, and Oculoplastics programs at the University of British Columbia have had close to 60 fellows, visitors, and graduate students, all of whom have helped to advance patient care and research at our center. Their presence has contributed in no small way to the constant questioning that was the intellectual basis for a second edition of *Diseases of the Orbit*. They have become members of our extended family worldwide. You will note that a number of them have contributed to this edition by updating and reviewing data in specific areas. In addition, there are contributions to this from many of my colleagues. I, however, have written every word, approved the esthetics, and developed the teaching model for this edition and therefore accept all of its shortcomings. My secretary, Daniela Ciucci, has kept the practice on an even keel and supported cheerfully all the extra efforts necessary in an academic clinical practice.

I wish to thank Carol Field, Cassie Carey, Tim Reynolds, and Jonathan Pine at Lippincott Williams & Wilkins, and particularly want to thank Kathey Alexander, who initiated this project. Of course I wish to thank the University of British Columbia and the Vancouver Hospital & Health Sciences Centre for their constant commitment to my work.

Finally, the core support team is my family, who have always understood and respected the drive for academic and clinical excellence, which has cost them some considerable time and attention.

Contents

Part A

Background Knowledge

Chapter 1

Structure of the Orbit: Anatomic and Imaging Features

Jack Rootman

Robert A. Nugent

The complex of neurosensory, vascular, motor, and secretory structures within the orbit are confined to 30 cm^3, bounded anteriorly by the lids, and surrounded by bone, nasal sinuses, intracranial contents, and deep facial structures. Disease may originate from or affect any of these spaces independently or conjointly and lead to deterioration of visual and/or ocular function. Knowledge of orbital and periorbital anatomy is fundamental to understanding the effect of disease and planning surgical intervention. The important features of orbital anatomy are its relationship to surrounding tissues, its structural integrity, anatomic uniformity, and essential symmetry. Although anatomic variations exist, in clinical and surgical situations we can rely on the fundamental structural uniformity of this organ complex.

Advances in imaging of the orbit provide increasingly exquisite detail with regard to the clinical anatomy. In this chapter, we will try to relate orbital anatomy to the various imaging techniques.

Bony Anatomy

The orbit is pyramidal in shape with an overall volume of 30 cm^3, of which the eye constitutes 7 cm^3 (Fig. 1-1). The base of the pyramid is a quadrangular anterior opening that measures 4 cm horizontally and 3.5 cm vertically. The widest dimension is 1 cm to 1.5 cm from the anterior orbital margin. The apex is formed by the optic canal and the superior orbital fissure.

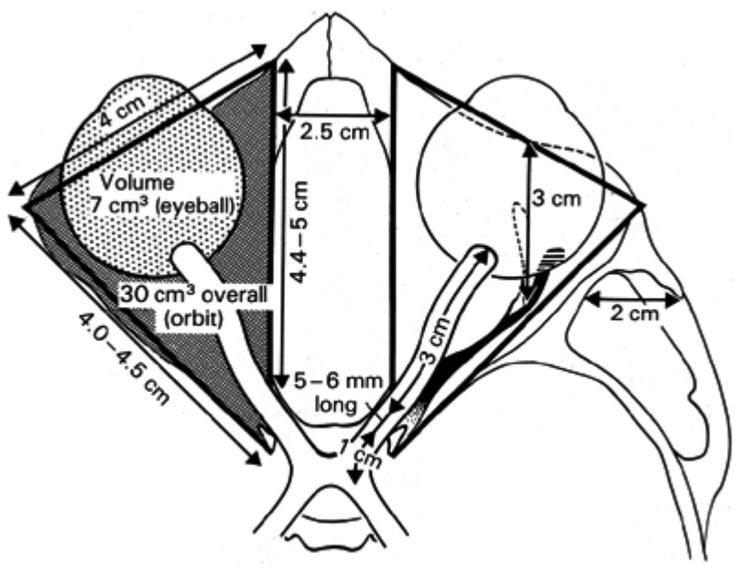

Figure 1-1. Schematic representation of the major orbital dimensions and relationships.

The medial walls of the orbit are 2.5 cm apart, roughly parallel, and 4.4 cm to 5 cm long. The lateral walls are 4.5 cm to 5 cm long at right angles to each other. The distance from the inferior orbital rim anteriorly to the infraorbital groove posteriorly is 2.5 cm to 3 cm. The depth of the temporalis fossa laterally is 2 cm.

Orbital growth is completed between 7 years of age and puberty. It is believed that enucleation in childhood retards bony growth.

The orbital roof (Fig. 1-2) is triangular and composed of the lesser wing of the sphenoid and the frontal bones, which may have within it a posterior extension of the frontal sinus. Apically, the lesser wing contains the optic canal, which is 5 mm to 6 mm in diameter, 10 mm to 12 mm in length (there can be some variability due to the oblique opening), and has an axis of 36 to the sagittal plane. Thus, the optic canals are separated anteriorly by 3 cm and posteriorly by 2.5 cm. The orbital roof is 3 mm thick posteriorly, and is thinnest just behind the superior rim. Anterolaterally is the lacrimal fossa, located just above the frontozygomatic suture line. It is important to recognize that the roof bows upward, just behind the orbital rim, and the floor bows downward (Fig. 1-3).

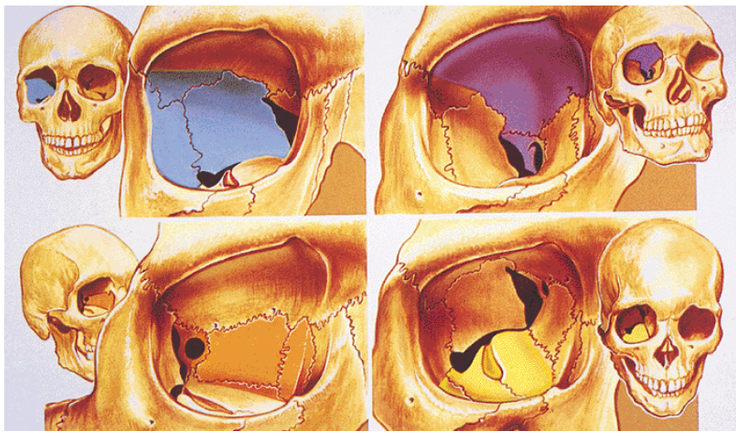

Figure 1-2. Anatomy of the orbital walls. (Reproduced with permission from Rootman J, Stewart B, Goldberg RA. Orbital Surgery: A Conceptual Approach. Philadelphia: Lippincott-Raven, 1995:81.)

The lateral wall (Fig. 1-2) is made up of the greater wing of the sphenoid, frontal, and zygomatic bones, and is at an angle of 45 to the medial wall. It is 4.5 cm to 5.0 cm long, and is the strongest orbital wall. Posteriorly, it is separated from the roof by the superior orbital fissure (which is 2.2 cm long) and from the floor by the inferior orbital fissure (which is 20 mm long). Laterally, it forms a portion of the temporalis fossa and is thinnest at the suture line between the greater wing of the sphenoid and the zygomatic bone (where it can be fractured easily at surgery). Posteriorly, the inferior orbital fissure communicates with the pterygopalatine and infratemporal fossae.

The oblong medial wall is the thinnest (0.2 mm to 0.4 mm) and is made up of the maxillary, lacrimal, ethmoid, and lesser

wing of sphenoid. About 24 mm from the anterior lacrimal crest is the anterior ethmoid foramen, and 12 mm behind this is the posterior ethmoid foramen, which is approximately 6 mm from the optic canal (described by the mnemonic, “24-12-6”). These foramina mark the horizontal level of the cribriform plate at the frontoethmoid suture line. The ethmoid and frequently the sphenoid and maxillary sinuses form part of the medial wall.

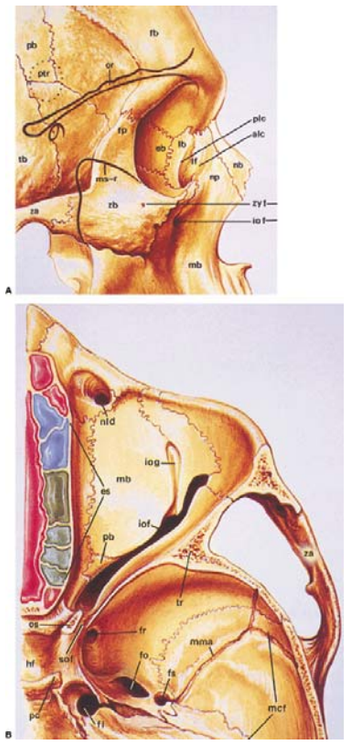

Figure 1-3. (A) Direct lateral view of the bony orbit with a transview of the orbital roof, floor, and optic canal. (B) The orbital floor as seen from above, showing relationships of adjacent cavities and fossae. (Reproduced with permission from Rootman J, Stewart B, Goldberg RA. Orbital Surgery: A Conceptual Approach. Philadelphia: Lippincott-Raven, 1995;80, 82.)

Key (A):

fb	frontal bone
plc	posterior lacrimal crest
alc	anterior lacrimal crest
lb	lacrimal bone
lf	lacrimal fossa
eb	ethmoid bone
nb	nasal bone
np	nasal process of maxilla
zy f	zygomaticofacial foramen
iof	infraorbital foramen
mb	maxillary bone (maxilla)
zb	zygomatic bone (zygoma)
za	zygomatic arch
ms-r	roof of maxillary sinus (transview)
fp	frontal process of zygoma
tb	temporal bone
or	orbital roof (transview)
ptr	pterion
pb	parietal bone

Key (B):

nld	nasolacrimal duct
iog	infraorbital groove (V_2)
iof	inferior orbital fissure
pb	palatine bone
es	ethmoid sinuses
mb	maxillary bone
za	zygomatic arch
tr	trigone of greater wing of sphenoid
mma	groove for middle meningeal artery
mcf	middle cranial fossa
fs	foramen spinosum (for middle meningeal artery)
fo	foramen ovale (V_3)
fr	foramen rotundum (V_2)
fl	foramen lacerum (for internal carotid artery)
sof	superior orbital fissure (tip of greater wing)
os	optic strut
hf	hypophyseal fossa
pc	posterior clinoid process

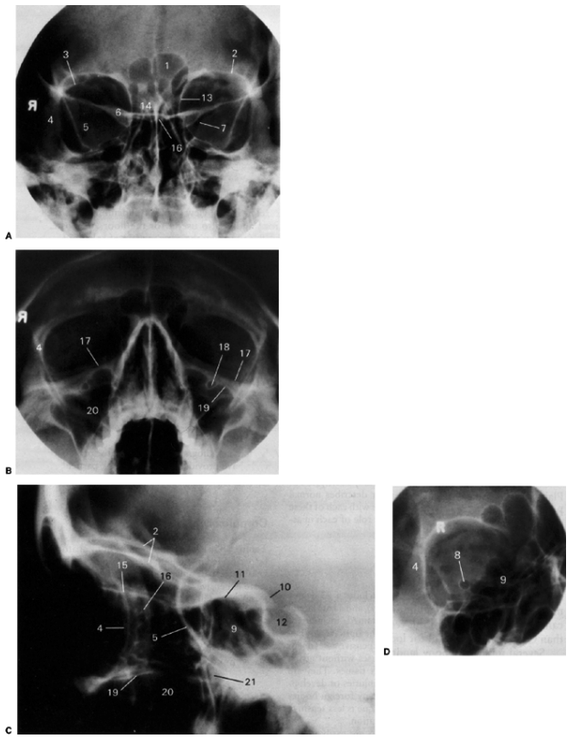

Figure 1-4. Plain film views of the orbits: (A) Caldwell view, (B) Waters' view, (C) lateral view, and (D) optic canal view of the right orbit.

Key:

1 Frontal sinus
2 Orbital roof
3 Superior orbital rim
4 Lateral orbital rim
5 Greater wing of sphenoid
6 Lesser wing of sphenoid
7 Superior orbital fissure
8 Optic canal
9 Sphenoid sinus
10 Anterior clinoid
11 Planum sphenoidale
12 Sella turcica
13 Medial orbital rim
14 Ethmoid sinus
15 Roof of ethmoid sinus
16 Cribriform plate
17 Inferior orbital rim
18 Infraorbital canal
19 Floor of orbit
20 Maxillary sinus
21 Pterygopalatine fossa

The floor (Figs. 1-2 and 1-3) is shorter, triangular, and is made up of the maxillary, zygomatic, and palatine bones. The infraorbital sulcus originates about 2.5 cm to 3 cm from the inferior orbital rim and forms the infraorbital canal halfway along its course, which opens on the maxilla at the infraorbital foramen. The maxillary and often some of the ethmoid sinuses are immediately adjacent to the floor. The floor is 0.5 mm to 1 mm thick. The thinnest point is medial to the infraorbital sulcus and canal, where it can be fractured easily at the time of decompression surgery. Anteromedially is the nasolacrimal fossa (5 mm by 17 mm) and duct formed by the lacrimal and maxillary bones. It contains the lacrimal sac, which drains into the duct. Immediately posterior to the nasolacrimal fossa is the origin of the inferior oblique muscle. The duct is 17 mm to 20 mm long and runs inferolaterally and 15 degrees posteriorly, where it opens under the inferior turbinate at the junction of the anterior one third and posterior two thirds.

Plain Films of the Orbits

Several important bony landmarks are easily identified on plain films. The Caldwell view (Fig. 1-4A) is particularly useful for demonstrating the anterior orbital rim, with the exception of the inferior portion, which is best seen on the Waters' view. In addition, the Caldwell view shows portions of the medial, superior, and posterior walls well, with the superior orbital fissure visualized between the lesser and greater sphenoid wings posteriorly. Frequently, the palpebral fissure will produce a transverse radiolucent line across the orbit that may mimic a fracture line.

The Waters' view (Fig. 1-4B) gives the best demonstration of the orbital floor, lateral rim, and infraorbital canal. It is particularly useful with suspected blowout fractures of the floor.

The lateral view (Fig. 1-4C) demonstrates the orbital roof and is also useful for the floor and posterolateral wall, formed by the greater wing of sphenoid.

The basal view may sometimes give added information about the optic canal. It is particularly useful for assessment of the lateral orbital wall.

The optic canal view is obtained by an oblique apical projection, which allows for views of the optic foramen, optic strut, anterior clinoid process, planum sphenoidale, superior ethmoid air cells, and posterior frontal sinus.

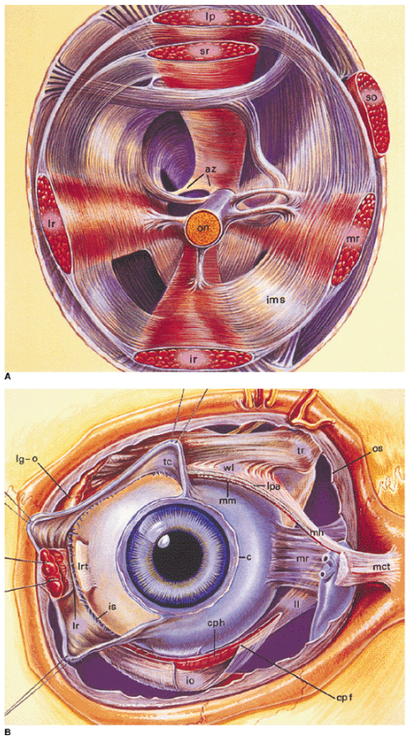

Figure 1-5. (A) Orbital septa and condensations in the posterior orbit. (B) Tenon's capsule and anterior orbital structures and septa. (Reproduced with permission from Rootman J, Stewart B, Goldberg RA. Orbital Surgery: A Conceptual Approach. Philadelphia: Lippincott-Raven, 1995;100-1.)

Key (A):

lp	levator palpebrae muscle
sr	superior rectus muscle
so	superior oblique muscle
mr	medial rectus muscle
ir	inferior rectus muscle
lr	lateral rectus muscle
ims	intramuscular septum
az	annulus of Zinn
on	optic nerve

Key (B):

lg-o	lacrimal gland (orbital lobe)
tc	Tenon's capsule (opened at limbus)
wl	Whitnall's ligament
tr	fascial condensation overlying trochlea
lpa	levator palpebrae aponeurosis (cut edge)
mm	Müller's muscle (cut edge)
mh	medial horn of levator aponeurosis
mr	medial retinaculum
mct	medial canthal tendon (anterior limb, cut)
c	conjunctiva
ll	Lockwood's ligament
cpf	capsulopalpebral fascia (cut edge)
cph	capsulopalpebral head of lower lid retractors
io	inferior oblique muscle blending with Lockwood's ligament
is	intramuscular septal condensation
lrt	lateral rectus tendon (cut)
lr	opening in Tenon's capsule for lateral rectus muscle
os	orbital septum

Periorbita and Septa

The periosteum or periorbita (Fig. 1-5) is generally loosely adherent to the surrounding bones except at the anterior orbital margin, lacrimal crests, and the margins of the fissures and canals. Posteriorly, it is continuous with the dura of the optic nerve and that surrounding the superior orbital fissure, and anteriorly with the periosteum of the orbital margins. Thus, surgery or trauma posteriorly may result in cerebrospinal fluid leaks.

In descriptive terms, the orbit has been divided into the extraperiosteal, extraconal, and intraconal spaces. The latter two are separated by the rectus muscles and intermuscular septa, which are denser in the anterior orbit. Disease processes may be roughly contained within these spaces, thus the concept serves some practical value. However, work by Koornneef has shown that the intraconal and extraconal spaces are highly complex and are divided by radial fibrovascular connective tissue septa, which also bridge between the muscles and the periorbita. Further, these septa connect to and provide support to all of the intraorbital structures, thereby forming complex surgical spaces. They invest the orbital fat that surrounds all the structures as lobules. In general, the septa are more complex and dense anteriorly, where surgical dissection is therefore more difficult. The connective tissue system also supports intraorbital structures and accounts for the anatomic uniformity of the tissue relationships. Roughly, the system is best understood in relationship to the extraocular muscles, as demonstrated schematically in Fig. 1-5 . Disruption of the orbit with alterations in the connective tissue architecture accounts for many of the clinical results of fractures and trauma.

Orbital Contents

Extraocular Muscles

The six striated extraocular muscles, including the four recti and two oblique muscles, control eye movement (Fig. 1-6). The rectus muscles arise from the annulus of Zinn at the apex, where it is continuous with the dural sheath of the optic nerve and periorbita and apical component of the connective tissue system. The annulus has an upper tendon (of Lockwood) and lower tendon (of Zinn). Because of this intimate relationship apical disease frequently affects all of these structures simultaneously. In addition, surgical removal of the optic nerve must be done within the annulus, which is most safely entered superomedially after removing the orbital roof. Anteriorly, the recti insert on the globe 5 mm to 7 mm posterior to the limbus. The superior oblique originates just superior to the annulus, and passes forward through the trochlea (4 mm posterior to the orbital margin just medial to the supraorbital notch) from whence it extends in a slight posterolateral plane to insert on the superior aspect of the globe. The inferior oblique arises from the bone just posterolateral to the nasolacrimal fossa, then extends in a slight posterolateral direction coursing beneath the inferior rectus and inserts on the inferolateral aspect of the eye. The superior oblique is innervated by the trochlear nerve, the lateral rectus by the abducens nerve, and the remaining muscles by the branches of the oculomotor nerve. The levator palpebrae (oculomotor innervation) originates from the annulus and inserts on the upper lid. Müllers' muscle, a sympathetically innervated smooth muscle, is attached anteriorly to the levator muscle and aponeurosis. Disease, such as thyroid orbitopathy, affecting either of these muscles may alter lid position or function. The approximate anterior-posterior length of the recti and the superior oblique muscles is 4 cm. Their nerve supply enters at the junction of the posterior and middle third of the muscle belly. The inferior oblique is 3.5 cm in length, and its motor supply from the inferior division of the oculomotor nerve enters its belly posteriorly after coursing just lateral to the inferior rectus, just behind the equator of the globe.

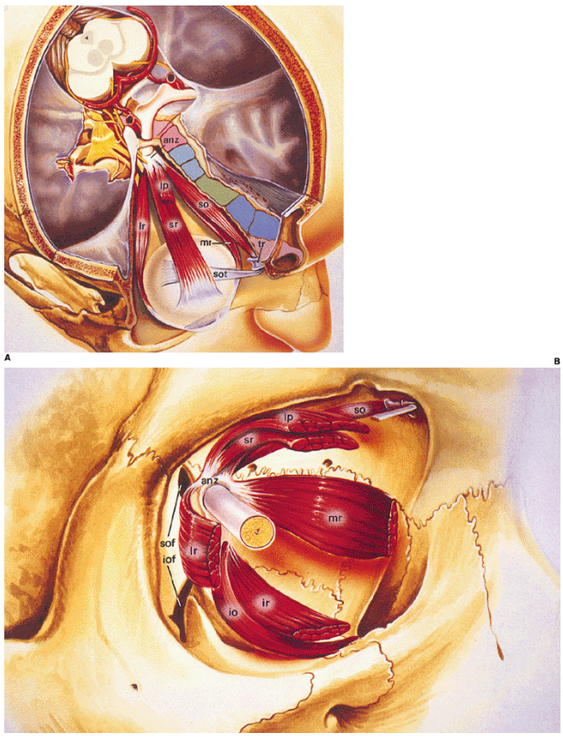

Figure 1-6. (A) Superior panoramic view emphasizing major relationships of the extraocular muscles. (B) Anterolateral view of extraocular muscles. (Reproduced with permission from Rootman J, Stewart B, Goldberg RA. Orbital Surgery: A Conceptual Approach. Philadelphia: Lippincott-Raven, 1995;108-9.)

Key (A):

sot	superior oblique muscle tendon
tr	trochlea
mr	medial rectus muscle
lr	lateral rectus muscle
sr	superior rectus muscle
so	superior oblique muscle
lp	levator palpebrae muscle
anz	annulus of Zinn

Key (B):

so	superior oblique muscle
lp	levator palpebrae muscle
sr	superior rectus muscle
mr	medial rectus muscle
lr	lateral rectus muscle
ir	inferior rectus
io	inferior oblique
sof	superior orbital fissure
iof	inferior orbital fissure
anz	annulus of Zinn

Optic Nerve

The optic nerve (see Fig. 1-1) is a nerve fiber tract, 4.5 cm to 5.0 cm long and about 4 mm in diameter, that extends from the globe to the chiasm. It is divided into four portions: intraocular (1 mm), intraorbital (30 mm), intracanalicular (9 mm to 10 mm), and intracranial (10 mm). Because the distance from the globe to the orbital apex is 20 mm, the intraorbital portion of the nerve tends to form an S-shaped configuration. The subarachnoid space and meningeal linings surround the nerve and extend from the canal forward to the globe. The ophthalmic artery is encased by dura in the optic canal where it lies inferolateral to the nerve. At the orbital end of the canal, it loses the dural coat and crosses medially in the intraconal space. The central retinal artery, a branch of the ophthalmic artery, enters inferomedially about 1 cm behind the globe. The remaining arterial supply of the optic nerve is from collateral branches via the pia-arachnoid. The optic nerve is related intracranially to the frontal lobe, anterior cerebral, anterior communicating, middle cerebral, and internal carotid arteries as well as the cavernous sinus and pituitary gland.

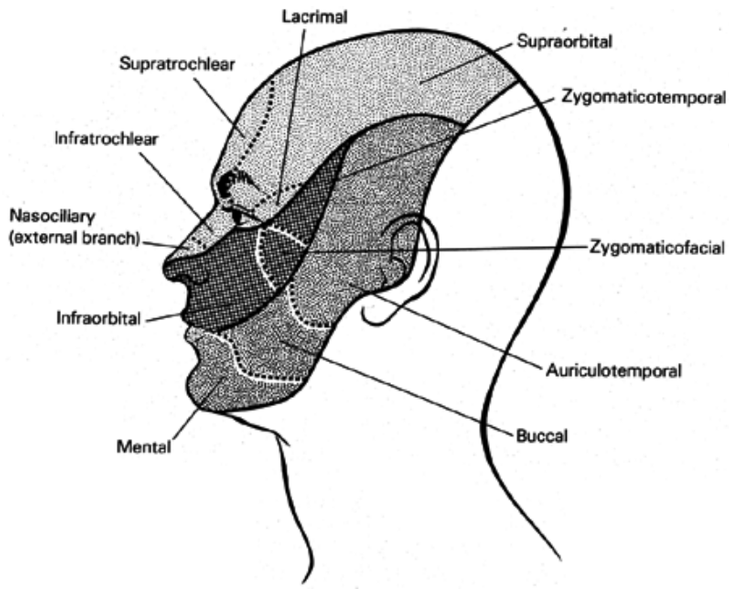

Figure 1-7. Schematic demonstrates the sensory dermatomes of the fifth nerve: V_1 ophthalmic division (fine stippling), V_2 maxillary division (dark stippling), V_3 mandibular division (intermediate stippling).

Peripheral Nerves

The major sensory innervation of the orbit is by means of the ophthalmic division of the trigeminal, with the maxillary (by means of the infraorbital and zygomatic branches) supplying the inferior orbital, cheek, and temporal regions (Fig. 1-7). The frontal and lacrimal branches of the ophthalmic nerve enter the orbit outside the annulus of Zinn and run forward between the periorbita and the levator complex to supply the forehead and lacrimal gland. The nasociliary branch is intraconal, crosses medially over the optic nerve, and terminates as the ethmoidal and infratrochlear nerves. The trochlear nerve extends forward in the same space as the frontal and lacrimal (Fig. 1-8).

The oculomotor nerve enters the muscle cone within the annulus of Zinn as a superior division (supplying the levator and superior rectus) and an inferior division (supplying the medial and inferior rectus and inferior oblique). Just temporal to the optic nerve (1.5 cm to 2 cm from the globe) in the apex is the ciliary ganglion (Fig. 1-9). It is chiefly a

ganglion where the parasympathetic fibers from the inferior division of the oculomotor nerve synapses. In addition, sensory fibers from the nasociliary nerve and sympathetic fibers from the plexus around the internal carotid artery (via the superior orbital fissure) pass through the ganglion. The sensory root subserves the cornea, iris, and ciliary body; the parasympathetic supplies the iris sphincter, ciliary body, and lacrimal gland; and the sympathetic supplies ocular vessels, the iris dilator (by means of ciliary nerves), the lacrimal gland, and sympathetic muscles of the upper and lower lids. The secretary fibers to the lacrimal gland (postganglionic from the sphenopalatine) arrive by the zygomatic and lacrimal nerves.

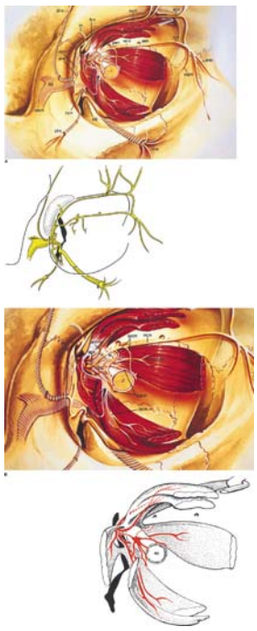

Figure 1-8. Anterolateral view of neural structures with corresponding schematics of the sensory nerves and motor nerves. (Reproduced with permission from Rootman J, Stewart B, Goldberg RA. Orbital Surgery: A Conceptual Approach. Philadelphia: Lippincott-Raven, 1995;115, 120.)

Key (A):

son	supraorbital nerve
stn	supratrochlear nerve
itn	infratrochlear nerve
enn	external nasal nerve
mpn	medial palpebral nerve
ion	infraorbital nerve
zfn	zygomaticofacial nerve
zyn	zygomatic nerve
ztn	zygomaticotemporal nerve
pg	pterygopalatine ganglion (transview)
ana	anastomosis with lacrimal nerve
ln	lacrimal nerve
frn	frontal nerve
gg	Gasserian ganglion
mnn	mandibular nerve (V_3)
opn	ophthalmic nerve (V_1)
ncn	nasociliary nerve
aen	anterior ethmoidal nerve
pen	posterior ethmoidal nerve

Key (B):

ocn-l	oculomotor nerve (III), lower division to inferior oblique muscles
spcn	short posterior ciliary nerves
cg	ciliary ganglion
ocn-lmr	oculomotor nerve (III), lower division to medial rectus muscle
lpcn	long posterior ciliary nerves
ncn	nasociliary nerve
sr	sensory root
spr	sympathetic root from carotid plexus
ocn-u	oculomotor nerve (III), upper division to levator palpebrae and superior rectus muscles

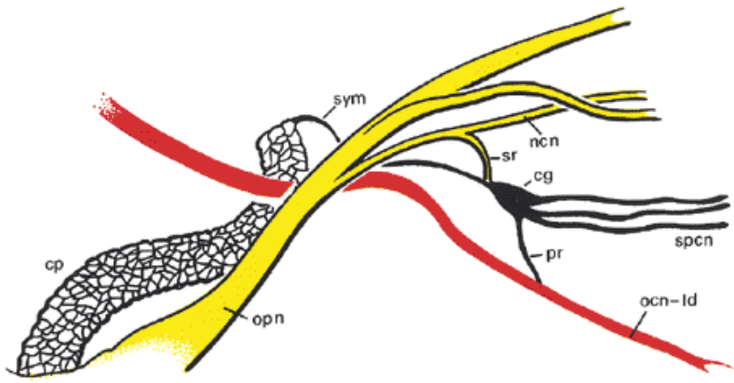

Figure 1-9. Lateral schematic of ciliary ganglion and related nerves. (Reproduced with permission from Rootman J, Stewart B, Goldberg RA. Orbital Surgery: A Conceptual Approach. Philadelphia: Lippincott-Raven, 1995;130.)

Key:

cp	carotid plexus (sympathetic)
sym	sympathetic root
opn	ophthalmic nerve (V_1)
sr	sensory root
ncn	nasociliary nerve
cg	ciliary ganglion
pr	parasympathetic root
spcn	short posterior ciliary nerves
ocn-ld	oculomotor nerve (III), lower division

The seventh nerve is the motor supply for the orbicularis, and by the nervus intermedius gives the parasympathetic supply to the lacrimal gland. The facial nerve enters the parotid gland and divides into temporal facial (upper) and cervical facial (lower) branches. It innervates the orbicularis by the upper division, which forms temporofrontal and zygomatic branches. Numerous anatomic variations exist. Surgically, when operating laterally it is important to avoid this nerve by entering anteriorly over the frontozygomatic process and staying in a plane just superficial to the temporalis fascia.

Vascular Anatomy

Arterial Supply

The major arterial supply of the orbit is from branches of the ophthalmic artery, which generally arises from the internal carotid artery just inferomedial to the optic nerve (Fig. 1-10). Rarely, the ophthalmic artery may arise from the middle meningeal and enter the orbit through the superior orbital fissure. In the optic canal it courses forward and laterally within the dural sheath, and at the orbital apex penetrates laterally through the dura and then crosses in 80% to 85% of subjects to the medial orbit over the nerve. In the remaining 15% to 20% of subjects the artery courses under the nerve. The branches of the ophthalmic artery with some variations in origin are as follows: central retinal, lateral posterior ciliary, lacrimal, medial posterior ciliary, muscular, supraorbital, posterior and anterior ethmoidal, nasofrontal, supratrochlear, and dorsonasal arteries. The ophthalmic artery frequently has anastomotic branches to the external carotid system by means of the middle meningeal and lacrimal arteries, which pass through the superior orbital fissure, and by means of the anterior deep temporal, superficial temporal, and lacrimal arteries (Fig. 1-11). The major distribution and anatomic variations of the ophthalmic artery have been described by Hayreh (Table 1-1).

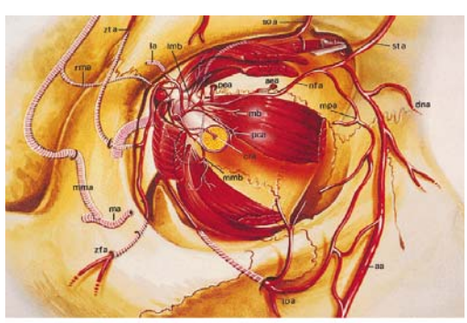

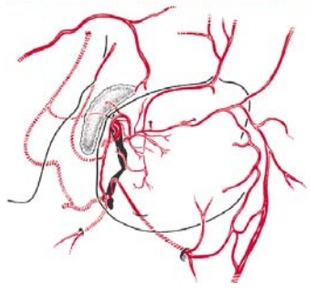

Figure 1-10. Direct anterolateral view of the arteries of the orbit (above), with corresponding schematic (left). (Reproduced with permission from Rootman J, Stewart B, Goldberg RA. Orbital Surgery: A Conceptual Approach. Philadelphia: Lippincott-Raven, 1995;127.)

Key:			
soa	supraorbital artery	pca	posterior ciliary artery
sta	supratrochlear artery	cra	central artery of retina
dna	dorsal nasal artery	mmb	medial muscular artery
aa	angular artery	lmb	lateral muscular artery
ioa	infraorbital artery	la	lacrimal artery
mpa	medial palpebral artery	zta	zygomaticotemporal artery
nfa	nasofrontal artery	rma	recurrent meningeal artery
aea	anterior ethmoidal artery	mma	middle meningeal artery
pea	posterior ethmoidal artery	ma	maxillary artery
mb	muscular artery	zfa	zygomaticofacial artery

Table 1-1. Order of origin of ophthalmic artery branches.

ORDER OF ORIGIN	OPHTHALMIC ARTERY CROSSED	
	Over Optic Nerve	Under Optic Nerve
1	Central retinal and medial posterior ciliary	Lateral posterior ciliary
2	Lateral posterior ciliary	Central retinal
3	Lacrimal	Medial muscular
4	Muscular to superior rectus or levator	Medial posterior ciliary
5	Posterior ethmoid and supraorbital, jointly or separately	Lacrimal
6	Medial posterior ciliary	Muscular to superior rectus and levator
7	Medial muscular	Posterior ethmoid and supraorbital, jointly or separately
8	Muscular to superior oblique and medial rectus, jointly / separately / to either	Muscular to superior oblique and medial rectus, jointly / separately / to either
9	To areolar tissue	Anterior ethmoid
10	Anterior ethmoid	To areolar tissue
11	Medial palpebral or inferior medial palpebral	Medial palpebral or inferior medial palpebral
12	Superior medial palpebral	Superior medial palpebral
Terminal	Dorsal nasal Supratrochlear	Dorsal nasal Supratrochlear

From Hayreh SS. The ophthalmic artery. III: branches. Br J Ophthalmol 1962;46:212-47.

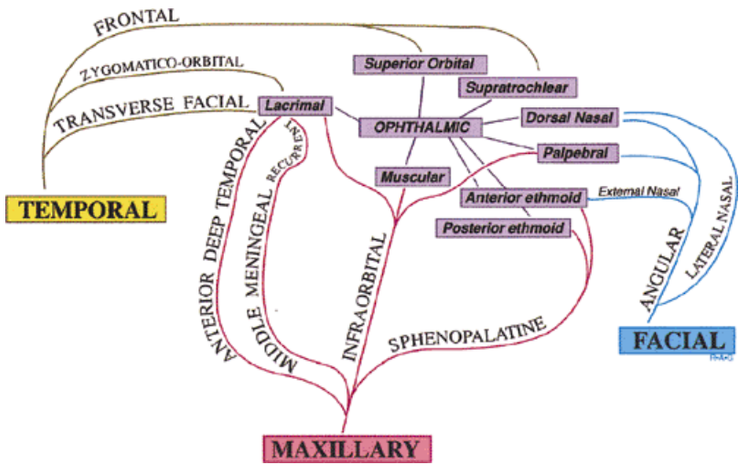

Figure 1-11. Anastomatoses between internal and external carotid artery circulation. (Reproduced with permission from Rootman J, Stewart B, Goldberg RA. Orbital Surgery: A Conceptual Approach. Philadelphia: Lippincott-Raven, 1995;129.)

The posterior ciliary arteries supply the globe by 15 to 20 short (to choroid and optic nerve head) and 2 long (to ciliary muscle, iris, and anterior choroid) branches. There are two main muscular branches, the lateral (supplying the levator, superior rectus, and superior oblique) and the medial (supplying medial and inferior recti and inferior oblique). Anteriorly, the arteries in the recti divide into two anterior ciliary arteries, which supply the anterior globe. The lacrimal artery branches into recurrent meningeal, zygomatic, glandular, and lateral palpebral arteries (which form the arcades of the lid). The zygomatic branches anastomose with the anterior deep temporal (by the zygomaticotemporal) and the transverse facial (by the zygomaticofacial) arteries. The supraorbital artery supplies the eyebrow and forehead and has small branches contributing to the superior rectus, superior oblique, and levator muscles.

The posterior ethmoid artery supplies the posterior ethmoid air cells, and the anterior ethmoid artery supplies the remaining ethmoid cells, frontal sinus, dura in the anterior cranial fossa, and the lateral wall of nose and septum. The marginal arcades of the lid are formed from the medial and lateral palpebral arteries and lie 4 mm from the upper lid margin and 2 mm from the lower. The remaining terminal arteries are the dorsal nasal and supratrochlear branches.

The major external carotid branches supplying the orbit are

the facial (medially), superficial temporal (laterally), and maxillary (deep) arteries. The facial forms the angular branch, which anastomoses with the dorsal nasal artery. The superficial temporal artery forms the transverse facial (which anastomoses with the infraorbital), the zygomatic (anastomoses with lacrimal and palpebral branches of the ophthalmic), and the frontal (anastomoses with the supraorbital and frontal arteries of the ophthalmic). The maxillary artery forms the infraorbital branch (supplying the lacrimal gland, inferior rectus, inferior oblique, lacrimal sac, and lower eyelid) and anastomoses with branches of the facial artery. The collateral circulation is outlined in Fig. 1-11 .

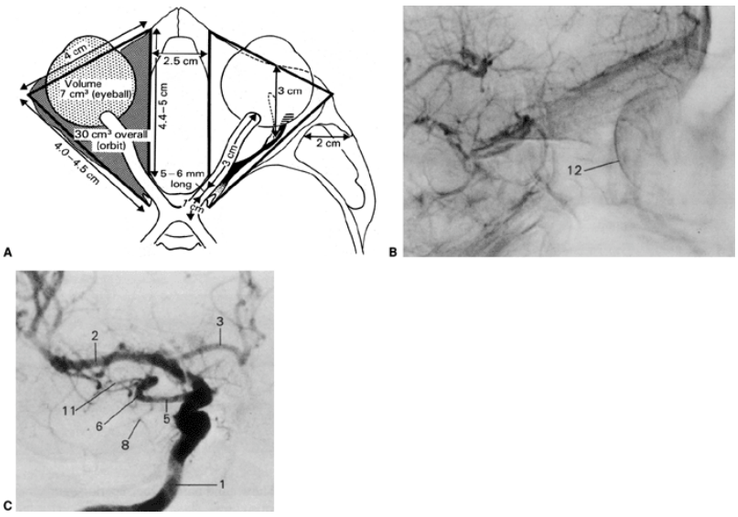

Figure 1-12. Normal orbital angiograms: (A) lateral view obtained during the arterial phase, (B) lateral view obtained during the venous phase, and (C) Caldwell view obtained during the arterial phase.

Key:

1 Internal carotid artery

2 Middle cerebral artery

3 Anterior cerebral artery

4 Ophthalmic artery - intracranial

5 Ophthalmic artery - intraorbital: first portion

6 Ophthalmic artery - intraorbital: second portion

7 Ophthalmic artery - intraorbital: third portion

8 Inferior muscular artery

9 Frontal

10 Angular

11 Lacrimal

12 Choroidal crescent

Orbital Angiography

Angiography remains essential in assessing vascular lesions, particularly arteriovenous malformations and fistulas (Fig. 1-12). Rarely, it may be used in aiding the differential diagnosis of lesions shown on CT or MR imaging, especially meningiomas or vascular tumors. Preoperative assessment of the arterial anatomy may occasionally be desirable.

This technique is invasive, requiring femoral artery puncture and selective catheterization of the internal and external carotid artery. Super-selective catheterization of branches of the external carotid is frequently done as well. The high cost and moderate to high radiation doses are other drawbacks of angiography.

The ophthalmic artery has intracranial, intracanalicular, and intraorbital portions. In more than 80% of patients it originates from the subdural extracavernous portion of the carotid artery prior to entering the optic canal. In approximately 10% of the population it originates from the cavernous portion of the carotid artery and enters the orbit via the superior orbital fissure. Rarely, the ophthalmic artery originates from the middle meningeal artery.

The intracranial portion is relatively short. On a lateral film, it is seen bending superiorly as it passes medial and inferior to the anterior clinoid. In the optic canal, it lies inferior to the optic nerve and is relatively straight as it passes anteroinferiorly. This is well seen on lateral and anterior-posterior films.

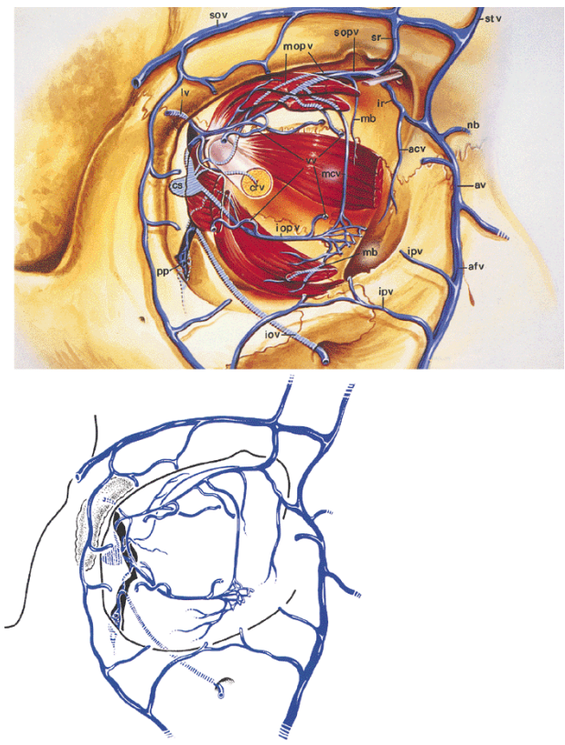

Figure 1-13. Anterolateral view of venous drainage of the orbit (above), with corresponding schematic (left). (Reproduced with permission from Rootman J, Stewart B, Goldberg RA. Orbital Surgery: A Conceptual Approach. Philadelphia: Lippincott-Raven, 1995; 131.)

Key:

sov	supraorbital vein
stv	supratrochlear vein
nb	nasal branch
av	angular vein
afv	anterior facial vein
ipv	inferior palpebral vein
iov	infraorbital vein
sr	superior root of superior ophthalmic vein
sopv	superior ophthalmic vein
mopv	medial ophthalmic vein
ir	inferior root of superior ophthalmic vein
acv	anterior collateral vein
mb	muscular branch
vv	vena vorticosa (superior, lateral, and medial vorticose veins)
mcv	medial collateral vein
iopv	inferior ophthalmic vein
pp	pterygoid plexus
cs	cavernous sinus
crv	central vein of retina
lv	lacrimal vein

The intraorbital portion of the ophthalmic artery consists of three parts. The most posterior portion extends from the optic canal to the point where it starts to bend laterally around the optic nerve. The second portion crosses superior to the optic nerve laterally to medially in more than 80% of patients. In approximately 15% to 20%, the artery passes inferior to the optic nerve. The third part of the orbital portion extends from the superomedial aspect of the optic nerve to pass forward under the superior oblique and above the medial rectus muscles. It passes below the trochlea before dividing into the frontal and angular branches.

The lacrimal artery originates from the second portion of the ophthalmic artery within the orbit, but the proximal portion is not well seen. In the lateral view, this vessel usually projects above the ophthalmic artery and extends anterior to the choroidal crescent, unlike the ciliary arteries. In the anterior-posterior view, it can be seen passing towards the superolateral angle of the orbit.

The supraorbital artery is the most superior vessel on the lateral view, closely related to the orbital roof. In the anterior-posterior view, it courses upward and medially toward the supraorbital foramen. The posterior and anterior ethmoidal arteries are relatively small branches noted in the mid- and posterior orbit. The inferior muscular artery is the most inferior of the branches on the lateral film.

The choroidal crescent is a characteristic vascular blush outlining the posterior two thirds of the globe. It is best seen in the early venous phase and may be indented by intraconal lesions. The superior and inferior vorticose veins can be seen in the venous phase passing posteriorly from the upper and lower margins of the globe. They outline the boundaries of the muscle cone.

Several anastomoses exist between the ophthalmic artery branches and those of the external carotid. In particular, anastomoses are present with the supraorbital, ethmoidal, lacrimal, infraorbital, and zygomaticofacial branches. Therefore, complete vascular assessment of the orbit should also include an external carotid arteriogram (Fig. 1-11).

CT or MR angiography may help delineate vascular lesions without the need for arterial catheterization and the associated risks.

Venous System

The orbital veins (Fig. 1-13) are valveless, the superior ophthalmic draining into the cavernous sinus by the superior orbital fissure, and the inferior into the superior ophthalmic vein and the pterygoid plexus. The venous system has a different course than that of the arteries, and lies within the connective tissue septa of the orbit. In contrast, the arteries pass through the septa. The superior ophthalmic vein is the larger, and is formed by the confluence of the angular, nasofrontal, and supraorbital veins. It has three sections, the first extending posterolaterally to the medial border of the superior rectus in the anterior third of the orbit. The second section of the superior ophthalmic vein enters the muscle cone, passing to the lateral orbit beneath the superior rectus muscle. The third section extends posteromedially along the lateral border of the superior rectus into the superior orbital fissure, where it drains into the cavernous sinus. The more variable inferior ophthalmic vein forms inferolaterally as a plexus and passes posteriorly adjacent to the inferior rectus muscle. It anastomoses with the superior ophthalmic vein, and has a similar branch that connects with the pterygoid plexus through the inferior orbital fissure. The tributaries are muscular, medial collateral, vortex, and lateral collateral.

Anterior venous drainage may be through the facial vein by means of the angular vein medially, and a plexus from the inferior ophthalmic to the facial vein laterally.

Orbital Venography

Orbital venography is rarely used now to assess intraorbital venous abnormalities for the cavernous sinus. In our unit, the majority of venous investigations are by direct intralesional approaches, which will be outlined in the chapter on vascular lesions .

The technique consists of injecting contrast by means of a midline vein in the forehead, while the patient applies finger compression over the area of the angular vein to encourage flow of contrast through the superior ophthalmic vein. Films are obtained in the Caldwell, Waters, and lateral projections (Fig. 1-14). Generally, the superior ophthalmic vein can be identified bilaterally with variable filling of the inferior ophthalmic and connecting channels.

The first segment of the superior ophthalmic vein starts near the trochlea and extends posteriorly in the anterior one third of the orbit, before entering the muscle cone along the medial border of the levator palpebrae superioris. The second part of the superior ophthalmic vein passes posteriorly, superior to the optic nerve and inferior to the superior rectus muscle. The third segment extends between the origins of the lateral and superior rectus muscles, through the superior orbital fissure, and into the anteroinferior part of the cavernous sinus. This vein can be well seen through its entire intraorbital course.

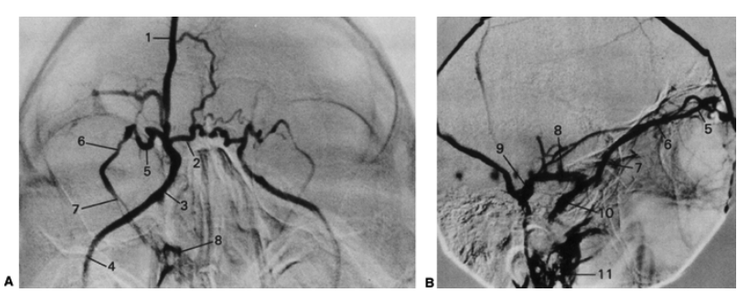

Figure 1-14. Orbital venograms: (A) Waters' view and (B) lateral view.

Key:

1 Frontal vein	5 Superior ophthalmic vein, first segment	9 Superior petrosal sinus
2 Prenasal vein	6 Superior ophthalmic vein, second segment	10 Inferior petrosal sinus
3 Angular vein	7 Superior ophthalmic vein, third segment	11 Deep cervical plexus
4 Facial vein	8 Cavernous sinus	

Cavernous Sinus

The cavernous sinus (Fig. 1-15) lies in the middle cranial fossa adjacent to the sphenoid sinus and pituitary fossa, just below the anterior and posterior clinoid processes and inferomedial to the temporal lobe. It is a dural venous sinus that communicates with the ophthalmic, central retinal, inferior cerebral, superficial middle cerebral, and middle meningeal veins. In addition, it communicates with the inferior and superior petrosal sinuses and the pterygoid plexus. Structurally, the cavernous sinus consists of a complex of venous channels. Within the sinus are the carotid siphon and sympathetic plexus.

The lateral wall contains within its inner loose fibrillar or deep layers the oculomotor, trochlear, abducens, and ophthalmic and maxillary divisions of the fifth nerve. The relationship of these nerves within the sinus changes from posterior to anterior (Fig. 1-15). The oculomotor nerve moves from a superior to an inferior position in relationship to the trochlear nerve, and the abducens shifts down in relationship to the ophthalmic division of the trigeminal nerve. Anterior to the sinus the lacrimal, frontal, and trochlear nerves enter the orbit outside the annulus of Zinn and the oculomotor, abducens, and nasociliary nerves enter the orbit within the annulus (Fig. 1-16). Because of the complex and intimate relationships involved in the cavernous sinus, lesions in this area frequently involve multiple functional abnormalities of the sensory and motor nerves of the orbit.

Contents of Orbital Fissures and Canal

Table 1-2 describes the contents of the orbital fissures and canals, and Fig. 1-16 demonstrates the major neural structures within the orbit and the superior orbital fissure.

Lacrimal System

The lacrimal gland, situated in a shallow fossa in the superolateral orbit, weighs 78 g and measures 20 mm by 12 mm by 5 mm. It is divided into palpebral and orbital (larger) lobes by the lateral horn of the levator aponeurosis (Fig. 1-17). The orbital lobe is superior to the palpebral, and the isthmus between the two extends through a gap in the lateral extension of the levator aponeurosis, which can be best visualized at lacrimal surgery by identifying the levator superiorly and following the fibers of the aponeurosis inferolaterally. The ducts (10 to 12) pass through the palpebral lobe, where they can be seen in the superolateral conjunctival fornix 4 mm to 5 mm from the tarsal border. Thus, resection of the palpebral lobe functionally destroys the gland. The borders of the gland are related anteriorly to the orbital septum, posteriorly to the orbital fat, and medially to the superior rectus, globe, and lateral rectus. The inferior surface rests on the lateral rectus. The lacrimal gland is a serous gland, and the acini have a tubuloracemose arrangement.

The acini consist of columnar cells surrounded by an incomplete layer of myoepithelial cells. Acinar secretions drain into intralobular, then interlobular, and thence into the main ducts. Grossly the lacrimal gland has a nodular surface with a fine connective tissue pseudocapsule. It is pinkish-gray, in contrast to orbital fat, which is yellow-gray. The gland is supported by Whitnall's ligament and the lateral horn of the levator aponeurosis as well as by septal attachments to the superior periorbita. The lacrimal artery penetrates it posteriorly, and the vein from it drains into the superior ophthalmic. Lymphatic drainage is by means of the lid and conjunctiva to the preauricular nodes. The lacrimal nerve and sometimes branches of the zygomatic carry the sensory afferents, the parasympathetic efferents (by the nervus intermedius, facial, greater superficial petrosal, vidian, sphenopalatine ganglion, infraorbital, and lacrimal nerves), and the sympathetic efferents (from the carotid plexus through the sphenopalatine ganglion). This pathway is believed to account for reflex tearing. In addition to the lacrimal gland, there are accessory glands (of Krause and Wolfring) in the lids and conjunctiva. There are 20 to 40 glands of Krause in the upper fornix, and six to eight in the lower fornix. The glands of Wolfring are fewer, consisting of three at the upper border of the superior tarsus and one at the lower border of the inferior tarsus.

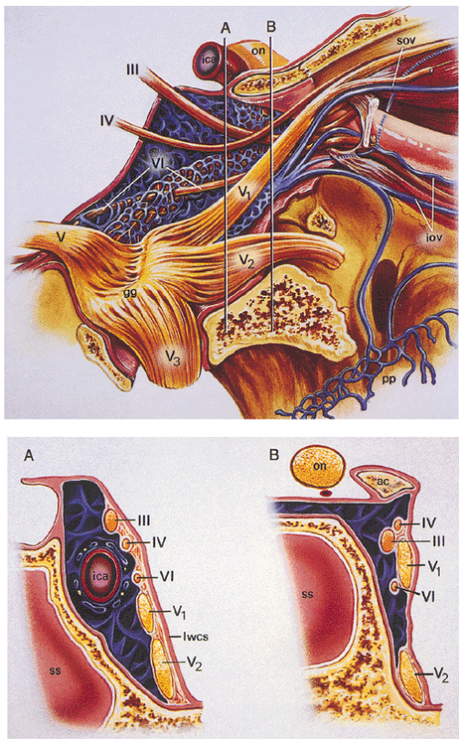

Figure 1-15. Lateral view (top) and cross-sectional views (bottom) of the cavernous sinus and orbital apex. The vertical lines (A and B) correspond to the planes of coronal section in the cavernous sinus. (Reproduced with permission from Rootman J, Stewart B, Goldberg RA. Orbital Surgery: A Conceptual Approach. Philadelphia: Lippincott-Raven, 1995:103.)

Key (top):

ica	internal carotid artery
on	optic nerve
sov	superior ophthalmic vein
iov	inferior ophthalmic veins
pp	pterygoid plexus
gg	Gasserian ganglion
III	oculomotor nerve
IV	trochlear nerve
V_1	trigeminal nerve (ophthalmic division)
V_2	trigeminal nerve (maxillary division)
V_3	trigeminal nerve (mandibular division)
VI	abducent nerve

Key (bottom):

ss	sphenoid sinus (coronal view)
ica	internal carotid artery
on	optic nerve
ac	anterior clinoid process
III	oculomotor nerve
IV	trochlear nerve
V_1	trigeminal nerve (ophthalmic division)
V_2	trigeminal nerve (maxillary division)
lwcs	lateral wall of cavernous sinus (dura)

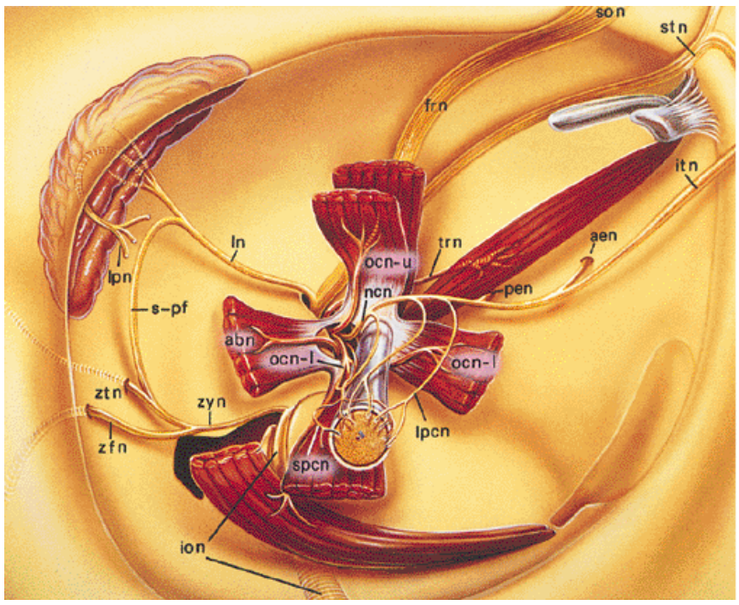

Figure 1-16. Foreshortened view emphasizing the major relationships of the neural structures within the orbit and the superior orbital fissure. (Reproduced with permission from Rootman J, Stewart B, Goldberg RA. Orbital Surgery: A Conceptual Approach. Philadelphia: Lippincott-Raven, 1995;106.)

Key:

frn	frontal nerve (V_1)
son	supraorbital nerve (V_1)
stn	supratrochlear nerve (V_1)
itn	infratrochlear nerve (V_1)
aen	anterior ethmoidal nerve
pen	posterior ethmoidal nerve
trn	trochlear nerve (IV)
ocn-u	oculomotor nerve (III), upper division
ocn-l	oculomotor nerve (III), lower division
ncn	nasociliary nerve (V_1)
abn	abducent nerve (VI)
lpcn	long posterior ciliary nerve
spcn	short posterior ciliary nerve
ion	infraorbital nerve (V_2)
ln	lacrimal nerve (V_1)
zyn	zygomatic nerve (V_2)
s-pf	sensory and parasympathetic fibers to lacrimal gland
lpn	lateral palpebral nerve
ztn	zygomaticotemporal nerve
zfn	zygomaticofacial nerve

Table 1-2. Contents of orbital fissures and canals.

	LOCATION	CONTENTS
Optic canal	Lesser wing of sphenoid	Optic nerve Meninges Ophthalmic artery Sympathetic fibers
Superior orbital fissure	Lesser and greater wing of sphenoid	Nerves Motor: III Superior and inferior divisions IV Trochlear VI Abducens Sensory: V1 Frontal lacrimal, nasociliary Sympathetic fibers Vessels Superior ophthalmic vein Anastomosis of recurrent lacrimal and middle meningeal artery
Inferior orbital fissure	Greater wing of sphenoid, palatine, zygomatic, and maxillary bones	Nerves Sensory: V2 infraorbital and zygomatic Parasympathetic Branches from pterygopalatine ganglion Vessels: Inferior ophthalmic vein and branches to pterygoid plexus
Anterior ethmoid canal	Frontal and ethmoid	Nerve: Anterior ethmoid becomes dorsal nasal Vessel: Anterior ethmoid artery
Posterior ethmoid canal	Frontal and ethmoid	Nerve: Posterior ethmoid Vessel: Posterior ethmoid artery
Nasolacrimal fossa	Lacrimal and maxillary bones	Nasolacrimal sac and duct

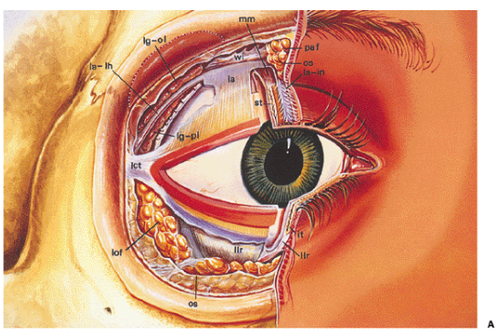

Figure 1-17. (A) Transected and partially dissected upper and lower eyelids. The lateral portion of the orbital septum and the levator have been excised to demonstrate adjacent relationships. (B) Dissection of entire upper and lower lid posterior to orbicularis. (Reproduced with permission from Rootman J, Stewart B, Goldberg RA. Orbital Surgery: A Conceptual Approach. Philadelphia: Lippincott-Raven, 1995;134-5.)

Key (A):

lg-ol	lacrimal gland, orbital lobe
lg-pl	lacrimal gland, palpebral lobe with ductiles piercing conjunctiva (cut)
la-lh	lateral horn of levator aponeurosis
la	levator aponeurosis
wl	Whitnall's ligament
mm	Müller's muscle
paf	preaponeurotic fat
os	orbital septum (cut edge)
la-in	insertion of levator aponeurosis
st	superior tarsus
it	inferior tarsus
llr	lower lid retractors
lof	lateral orbital fat
lct	lateral canthal tendon

Key (B):

wl	Whitnall's ligament
la	levator aponeurosis
sep	orbital septum
soa-n	supraorbital artery and nerves
sta-n	supratrochlear artery and nerves
mfp	medial fat pad
oom-or	origins of orbicularis oculi muscle (orbital portion)
iom	inferior oblique muscle
cfp	central fat pad
ae	arcuate expansion
lfp	lateral fat pad

Tears flow across the eye and are drained into the lacrimal sac through the canaliculi of the upper and lower lid by a pump system initiated by blinking. The tear film consists of a superficial lipid, central aqueous, and deep mucus layer. The upper and lower canaliculi originate at the puncta, and have a 2.0 mm vertical portion and an 8.0 mm horizontal portion, which fuse into a common canaliculus (Fig. 1-18). The common canaliculus enters the lateral wall of the lacrimal sac by means of the valve of Rosenmüller, which prevents reflux. The canaliculi are lined by squamous epithelium, whereas the sac and duct are lined by columnar epithelium, goblet cells, and ciliated cells. The lacrimal sac is 13 mm to 15 mm in vertical length, and has a fundal portion (3 mm to 5 mm) behind and above the medial canthal ligament and a body (10 mm) below it. It fills the lacrimal fossa and is enveloped by the periorbita and the medial canthal ligament, superficial and deep heads of the pretarsal, and deep head of the preseptal muscles. This complex constitutes the lacrimal pump system. The tears drain through the nasolacrimal duct just beneath the inferior turbinate through a fold in the duct (called the valve of Hausner) in the lateral wall of the nose.

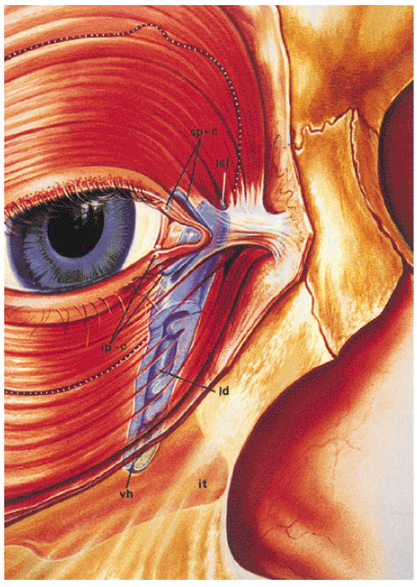

Figure 1-18. Transview to demonstrate the major relationships of the lacrimal outflow system. (Reproduced with permission from Rootman J, Stewart B, Goldberg RA. Orbital Surgery: A Conceptual Approach. Philadelphia: Lippincott-Raven, 1995;141.)

Key:

sp-c	superior punctum and canaliculus
ip-c	inferior punctum and canaliculus
lsf	fundus of lacrimal sac
ld	lacrimal duct with internal valves
vh	valve of Hasner
it	inferior turbinate (transview)

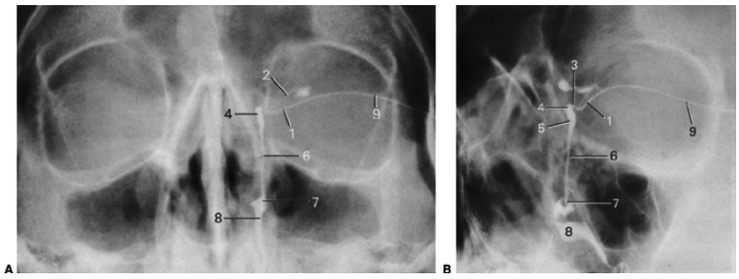

Figure 1-19. Normal dacryocystography: (A) Waters' view and (B) oblique view.

Key:

1 Inferior canaliculus

2 Superior canaliculus

3 Common canaliculus

4 Lacrimal sac

5 Valve of Krause

6 Nasolacrimal duct

7 Valve of Hasner

8 Contrast in nose

9 Cannula

Dacryocystography

Dacryocystography is useful in patients presenting with epiphora, in which there may be a mechanical obstruction, inflammatory disease, tumor, fistula, diverticulum, lacrimal concretion, or postoperative failure (Fig. 1-19). CT scan shows the lacrimal sac and nasolacrimal duct but does not demonstrate the canaliculi or the site of stenosis or occlusion.

When radiographic contrast material, usually a water-soluble agent, is injected via a cannula into the inferior canaliculus, good opacification of the superior, inferior, and common canaliculi will be seen at the medial aspect of the orbit on the anterior-posterior view. The Caldwell view is useful for showing these structures as well as the lacrimal sac and nasolacrimal duct. A narrowing at the inferior margin of the lacrimal sac, relating to the valve of Krause, is normally seen, as is a similar narrowing in the midportion of the nasolacrimal duct at Taillefer's valve. Narrowing at the distal end of the nasolacrimal duct is related to Hasner's valve. Contrast can normally be demonstrated extending into the inferior meatus where the duct empties. This technique has the advantage of being relatively simple and inexpensive, and it provides exquisite anatomical detail of the nasolacrimal system.

Dacryoscintillography is another imaging technique that can be used to demonstrate both anatomic and functional abnormalities of the lacrimal out-flow system.

Lids

The orbit forms a complex interdigitation with the lid and brow region that accounts for the structural barrier of the orbit anteriorly (Figs. 1-20 and 1-21).

The brow is a thick multilaminar structure at the upper orbital margin in men. It is located slightly higher in women.

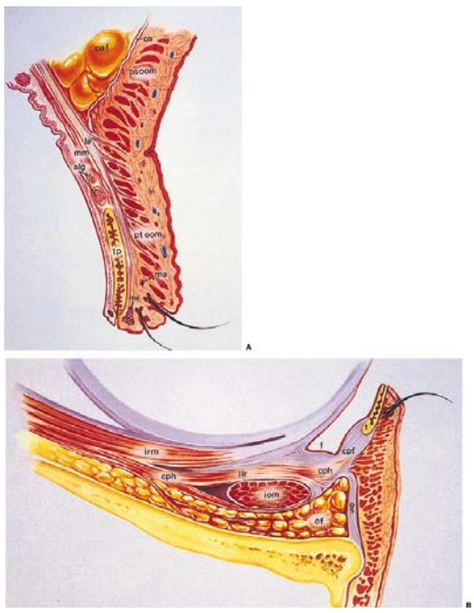

Figure 1-20. (A) Sagittal view of the upper lid. (B) Central sagittal view of the lower lid and adjacent ocular and orbital structures. (Reproduced with permission from Rootman J, Stewart B, Goldberg RA. Orbital Surgery: A Conceptual Approach. Philadelphia: Lippincott-Raven, 1995;136-7.)

Key (A):

os	orbital septum
paf	preaponeurotic fat
la	levator aponeurosis
mm	Müller's muscle
alg	accessory lacrimal glands
tp	superior tarsal plate with Meibomian glands
mr	muscle of Riolan (grey line)
ma	marginal artery
ps oom	preseptal orbicularis oculi muscle
pt oom	pretarsal orbicularis oculi muscle

Key (B):

irm	inferior rectus muscle
cph	capsulopalpebral head of lower lid retractors
llr	lower lid retractors
iom	inferior oblique muscle
f	inferior fornix
cpf	capsulopalpebral fascia
os	orbital septum
of	orbital fat
t	inferior tarsus

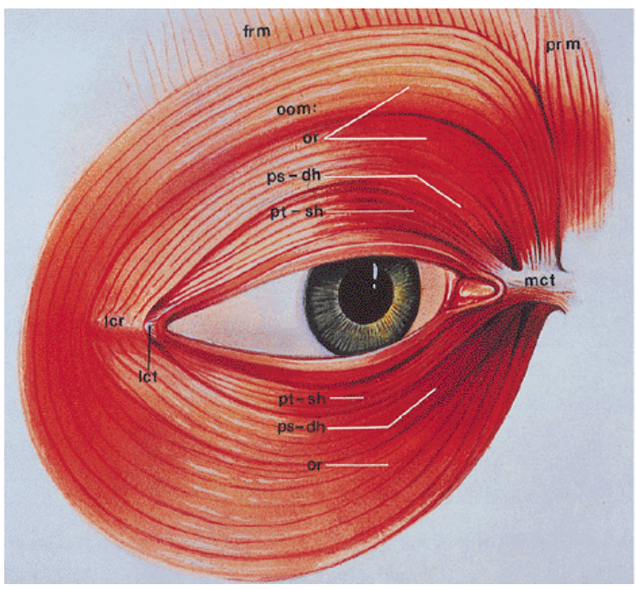

Figure 1-21. Anterior view of the three slips of the orbicularis oculi. (Reproduced with permission from Rootman J, Stewart B, Goldberg RA. Orbital Surgery: A Conceptual Approach. Philadelphia: Lippincott-Raven, 1995;139.)

Key:

frm	frontalis muscle
prm	procerus muscle
oom:or	orbicularis oculi muscle, orbital portion
ps-dh	preseptal portion, deep head
pt-sh	preseptal portion, superficial head
mct	medial canthal tendon
lcr	lateral canthal raphe
lct	lateral canthal tendon

It consists of four layers including a thick skin, muscle, fat, and aponeurotic layer. The muscle layer is made up of the frontalis superiorly, which fuses medially with the vertically oriented procerus muscle and obliquely orientated corrugator superciliaris. The corrugator, procerus, and frontalis are in turn attached to fibers of the orbicularis. Deep to the muscles is a layer of fat, which extends over the brow to lie on the orbital septum. The muscle and adipose tissue are attached to an aponeurotic layer arising from the deep galea insertion, particularly in the medial portion. Laterally, the muscular layers are less firmly attached, which accounts for the development of lateral brow ptosis in this region.

The lids and orbital septum are integral to and form the anterior boundary of the orbit. The anatomy of the upper lid is similar to that of the lower lid, except for differences in the upper and lower lid retractors. Very thin keratinizing epithelium covers the lids and is loosely attached to the underlying orbicularis muscle (Fig. 1-20). This muscle is divided into orbital, preseptal, and pretarsal portions (Figs. 1-18 and 1-21). Laterally, the orbital fibers extend continuously around to the lower lid and attach medially to the orbital margin, frontal bone, and frontal process of maxillary bone.

Medially, the preseptal and pretarsal muscles form a complex relationship to the lacrimal sac and medial canthal ligament by dividing into interdigitating deep and superficial heads. The superficial preseptal head inserts into the medial canthal ligament and the deep head into the fascia of the lacrimal sac. Pretarsal orbicularis divides into an anterior head that attaches to the medial canthal tendon in front of the canaliculus, and a deep head that attaches to the lacrimal fascia and posterior crest. The medial canthal ligament also has a deep head (thin; attached to posterior lacrimal crest), a superficial head (thick; attached to frontal process of maxillary bone), and a fine superior branch. Laterally, the preseptal muscles form an indistinct raphe and the pretarsal muscles form the lateral canthal ligament, which inserts on the lateral orbital tubercle.

Deep to the orbicularis, the orbital septum fuses with the periosteum of the orbital rim peripherally, except medially, where it splits to attach to the anterior and posterior lacrimal crests (see Fig. 1-17). The septum is confluent with the levator aponeurosis in the upper lid and the capsulopalpebral fascia in the lower lid. Preaponeurotic orbital fat is retained by the septum and divided into several pads in the upper and lower lids (see Fig. 1-17).

Both the upper and lower lid retractors attach to anterior orbital condensations, which act as suspensory ligaments. The superior transverse ligament of Whitnall is 15 mm to 20 mm above the tarsus. It attaches medially near the trochlea and laterally through the lacrimal gland to the orbital wall. The aponeurotic portion of the levator begins just below the ligament, as does Müller's muscle. These two lamellae can be separated surgically, Müller's attaching to the upper tarsal border and the aponeurosis to the anterior border of tarsus, orbicularis, and subcuticular tissue. Laterally, the horn of the levator aponeurosis divides the orbital and palpebral lobes of the lacrimal gland and inserts on the lateral orbital tubercle, retinaculum, and tendon. The medial horn attaches posteriorly to the canthal ligament.

In the lower lid the retractors are the capsulopalpebral fascia. This is a fibrous layer that extends from the inferior rectus, surrounds the inferior oblique, and fuses to the suspensory ligament of Lockwood. Thence, it incorporates the inferior tarsal muscle (in the fornix) and inserts as a fascial aponeurosis into the lower lid. Additional attachments are to the septum and Tenon's capsule. The inferior tarsal muscle does not attach to the tarsus, but is incorporated in the fascia 2 mm to 3 mm below it. Lockwood's ligament forms complex attachments to the anterior orbital fascia and the lower lid retractors.

The tarsus is composed of dense regular connective tissue and contains the Meibomian glands (25 in the upper and 20 in the lower). They are sebaceous glands that produce lipid secretions. The follicles of the lids also contain sebaceous glands of Zeis and apocrine glands of Moll. Additionally, the skin of the lids contains eccrine sweat glands. The arterial supply of the pretarsal lid is from the external carotid system by means of the superficial temporal and facial arteries. Venous drainage is through the anterior facial and superior temporal veins. The post-tarsal lid is supplied by the terminal branches of the ophthalmic artery, and is drained by the ophthalmic veins. The lids have lymphatic drainage laterally to the preauricular and intraparotid lymph nodes, and medially to the submental and submandibular nodes. There are no lymphatics in the deep orbit.

Surface Anatomy

The supraorbital notch (present in 75% of persons) or foramen (present in 25%) is palpable at the junction of the medial one third and lateral two thirds of the superior margin (Fig. 1-22). A vertical line from this point intersects the inferior margin 3 mm to 4 mm in front of the origin of the inferior oblique muscle (which is adjacent to the opening of the nasolacrimal duct). Four millimeters directly below is a palpable indentation created by the infraorbital foramen. Medial to the supraorbital notch, the trochlea may be palpated 4 mm posterior to the margin. Below this, the medial canthal ligament can be felt at the level of the upper margin of the lacrimal sac. (Thus, cystic masses felt above it are generally ethmoidal in origin, and below it lacrimal sac in origin.) The frontozygomatic suture can be felt 6 mm above the marginal tubercle of the zygomatic bone and is the surface marking for the inferior border of the lacrimal gland.

The eyelids extend superiorly to the eyebrow and lateral orbital rim and inferiorly to the nasojugal (medial) and malar (lateral) folds. Generally, the upper lid crease is 8 mm to 11 mm above the margin, and is due to the firm attachment of the levator aponeurotic fibers below this point. This fold separates the loosely adherent (upper) preseptal portion from the more firmly attached tarsal portion. The inferior lid crease, which is more evident in the young, is 2 mm to 3 mm below the lower lid margin medially and 5 mm to 6 mm laterally. The lids are divided horizontally by the puncta into an inner (one sixth) lacrimal portion and outer ciliary or bulbar portion. The ciliary portion of the lid margin contains the lashes and adnexa and is separated by the gray line from the tarsal (posterior) portion, which contains the Meibomian orifices. The lateral commissure is at the level of the superior attachment of the helix of the ear.

CT and MR Orbital Anatomy

Computed Tomography

Normal CT Anatomy

Axial and coronal CT views of the orbit are complementary for showing bony and soft tissue anatomy (Fig. 1-23). The axial view is superior for demonstrating the lateral and medial bony margins, the superior orbital fissure, and the optic canal. Coronal views are best for assessing the floor and roof. The lacrimal sac and nasolacrimal duct as well as the inferior orbital fissure and infraorbital canal are equally well seen on axial or coronal images.

The optic nerve has a slightly serpiginous course with minimal inferior and lateral bowing in its midportion. Because of this, thin slices may not show the entire course of the nerve on any one axial slice. The nerve can be well defined through its entire course except within the optic canal. The postcanalicular portion as well as the optic chiasm can be identified. The dural sheath and arachnoid along the optic nerve is particularly well defined with intravenous contrast.

On coronal views immediately posterior to the globe, a small central density within the nerve represents the central retinal artery and vein. The optic canal is best seen when the gantry is tilted to scan on a plane connecting the anterior floor of the orbit with the anterior clinoid.

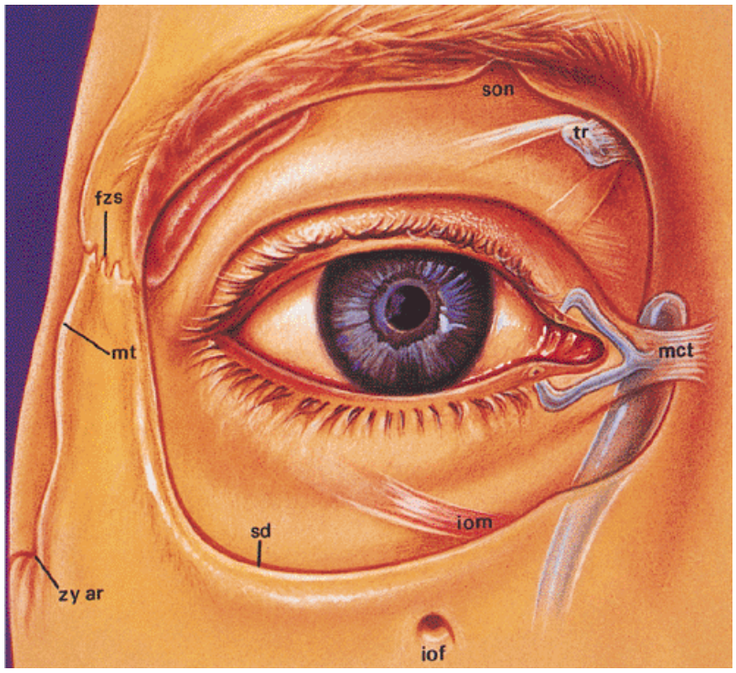

Figure 1-22. Surface anatomy of periorbital region. (Reproduced with permission from Rootman J, Stewart B, Goldberg RA. Orbital Surgery: A Conceptual Approach. Philadelphia: Lippincott-Raven, 1995; 145.)

Key:

son	supraorbital notch
tr	trochlea
fzs	frontozygomatic suture
zy ar	zygomatic arch takeoff
sd	septal demarcation at inferior orbital rim
iof	infraorbital foramen
iom	origin of inferior oblique muscle
mct	medial canthal tendon, anterior limb
mt	marginal tubercle of zygoma

The extraocular muscles generally have a course parallel to the adjacent orbital wall. Consequently, only the medial and lateral rectus muscles may be seen in their entirety on an axial view. The tapering of these muscles in their tendinous portions as well as their origins at the annulus of Zinn are well seen. On a coronal view, they are vertically oriented. The superior and inferior rectus muscles are only partially visualized on any one axial slice and on coronal views are seen cross sectionally to lie in a slightly oblique horizontal plane. This is related to the superior slope of the floor and the inferior slope of the roof from lateral to medial. The levator palpebrae superioris merges with the superior rectus and is only identified separately on anterior coronal images where it diverges and separates from the superior rectus. The superior oblique muscle is best seen on coronal views, lying superior and slightly medial to the medial rectus muscle. The trochlea is well seen on axial views, and is occasionally calcified. The least well-defined muscle is the inferior oblique, with only its insertion well seen on axial views and the muscle belly somewhat poorly defined on anterior coronal views.

The lacrimal gland is readily identified in the lacrimal fossa on both coronal and axial views. The anterior soft tissue densities merging with the globe medially and laterally are the orbital septum, eyelids, and conjunctiva. The lacrimal sac can be identified by noting the position of the anterior and posterior lacrimal crest on axial views. The superior portion of the nasolacrimal duct, where it extends inferiorly from the lacrimal sac, can be readily identified on axial and coronal CT.

Vascular structures in the orbit can be seen without intravenous contrast, but are highlighted with contrast. The ophthalmic artery is seen in the apex of the orbit as it swings laterally before looping over the optic nerve. Several of its branches, including the anterior and posterior ethmoidal and posterior ciliary vessels, can usually be identified.

The superior ophthalmic vein is routinely identified in axial

and coronal views as it courses near the trochlea to pass through the muscle cone inferior to the superior rectus and superior to the optic nerve, to exit the orbit through the superior orbital fissure. The inferior ophthalmic and connecting veins are seen inconsistently.

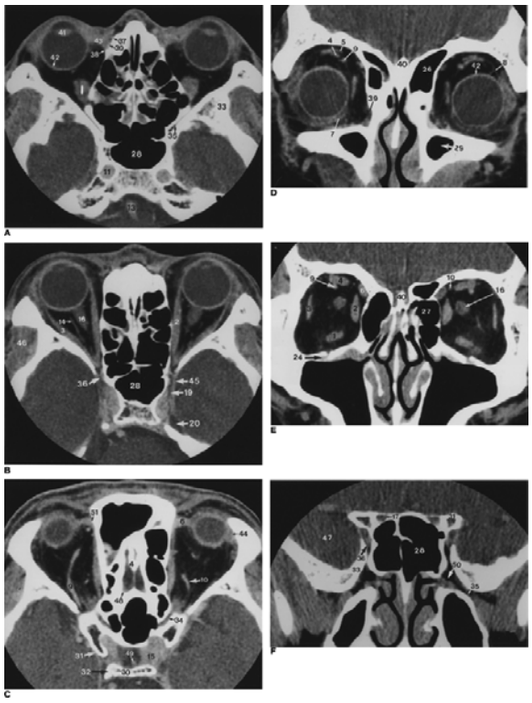

Figure 1-23. Axial CT scans. (A, B, and C) Selected axial scans, performed with intravenous contrast enhancement, demonstrate anatomy progressing from an inferior level to a superior position in the orbit. Coronal CT scans. (D, E, and F) The images progress from anterior to posterior through the orbits.

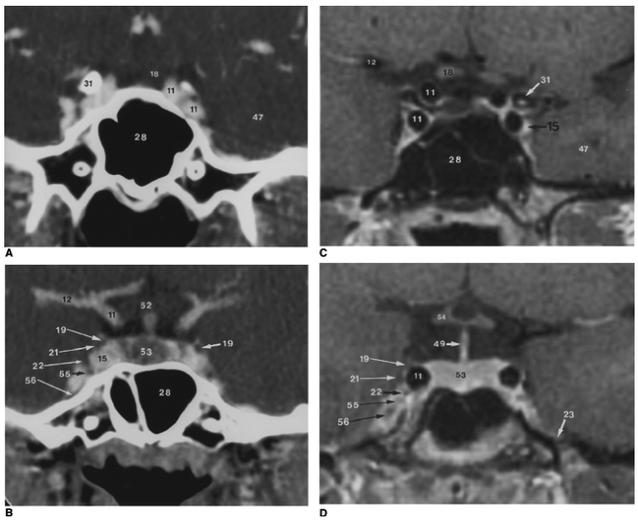

Figure 1-24. Cavernous sinus region. (A and B) Coronal CT images of the cavernous sinus region with contrast enhancement, from anterior to posterior position. (C and D) Corresponding MR images to the CT images.

Key for Figures 1-23 and 1-24:

1 Inferior rectus muscle	20 Gasserian ganglion	39 Lacrimal fossa
2 Medial rectus muscle	21 Cranial nerve (IV)	40 Crista galli
3 Lateral rectus muscle	22 Cranial nerve (VI)	41 Lens
4 Superior rectus muscle	23 Cranial nerve (V_3)	42 Scleral uveal rim
5 Levator palpebrae superioris	24 Infraorbital nerve	43 Orbital septum
6 Superior oblique muscle	25 Frontal nerve	44 Lacrimal gland
7 Inferior oblique muscle	26 Frontal sinus	45 Tentorium
8 Intermuscular septum	27 Ethmoid sinus	46 Temporal fossa
9 Superior ophthalmic vein	28 Sphenoid sinus	47 Temporal lobe
10 Ophthalmic artery	29 Maxillary sinus	48 Olfactory groove
11 Internal carotid artery	30 Dorsum sellae	49 Pituitary stalk
12 Middle cerebral artery	31 Anterior clinoid	50 Pterygopalatine fossa
13 Basilar artery	32 Posterior clinoid	51 Trochlea
14 Posterior ciliary artery	33 Greater wing of sphenoid	52 Optic chiasm
15 Cavernous sinus	34 Optic canal	53 Pituitary gland
16 Optic nerve - intraorbital	35 Inferior orbital fissure	54 Optic tract
17 Optic nerve - intracanalicular	36 Superior orbital fissure	55 V_1
18 Optic nerve - intracranial	37 Anterior lacrimal crest	56 V_2
19 Cranial nerve (III)	38 Posterior lacrimal crest	

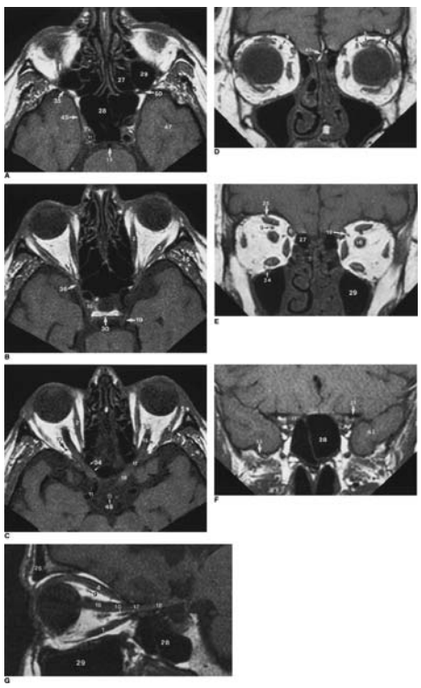

Figure 1-25. Magnetic resonance orbital images: (A, B, and C) axial views; (D, E, and F) coronal views, and (G) saggital view.

Key:

1 Inferior rectus muscle	20 Gasserian ganglion	39 Lacrimal fossa
2 Medial rectus muscle	21 Cranial nerve (IV)	40 Crista galli
3 Lateral rectus muscle	22 Cranial nerve (VI)	41 Lens
4 Superior rectus muscle	23 Cranial nerve (V_3)	42 Scleral uveal rim
5 Levator palpebrae superioris	24 Infraorbital nerve	43 Orbital septum
6 Superior oblique muscle	25 Frontal nerve	44 Lacrimal gland
7 Inferior oblique muscle	26 Frontal sinus	45 Tentorium
8 Intermuscular septum	27 Ethmoid sinus	46 Temporal fossa
9 Superior ophthalmic vein	28 Sphenoid sinus	47 Temporal lobe
10 Ophthalmic artery	29 Maxillary sinus	48 Olfactory groove
11 Internal carotid artery	30 Dorsum sellae	49 Pituitary stalk
12 Middle cerebral artery	31 Anterior clinoid	50 Pterygopalatine fossa
13 Basilar artery	32 Posterior clinoid	51 Trochlea
14 Posterior cerebral artery	33 Greater wing of sphenoid	52 Optic chiasm
15 Cavernous sinus	34 Optic canal	53 Pituitary gland
16 Optic nerve - intraorbital	35 Inferior orbital fissure	54 Optic tract
17 Optic nerve - intracanalicular	36 Superior orbital fissure	55 V_1
18 Optic nerve - intracranial	37 Anterior lacrimal crest	56 V_2
19 Cranial nerve (III)	38 Posterior lacrimal crest	

A line joining the lateral orbital margins in the axial plane will normally intersect the globe near its midportion, with at least one third of the globe posterior to this line. The sclera, choroid, and retina form a well-defined band that enhances with intravenous contrast. The lens is normally high density on CT.

Nerves can occasionally be identified within the orbit, although positions may be variable. In particular, the frontal, supraorbital, and inferior divisions of the third nerve may be seen. However, they may be difficult to differentiate from vascular structures, particularly when the study is done without intravenous contrast.

The cavernous sinus (Fig. 1-24) is particularly well seen with intravenous contrast. The third and fourth nerves, and the first divisions of the fifth nerve and the sixth intracranial nerve appear as round, low-density structures on coronal views through the uniformly enhancing cavernous sinus.

The optic chiasm is more readily identified than the postcanalicular portion of the optic nerves, because the former is surrounded by cerebrospinal fluid in the suprasellar cistern.

Magnetic Resonance Imaging

Soft tissue detail with MRI is very similar to that shown on the CT, with both using orbital fat to highlight other structures (Fig. 1-25). Details of the globe are better defined on

MRI, whereas CT gives better bone detail and is much more sensitive to calcification. MRI is better able to define the intracanalicular portion of the optic nerve as well as the optic chiasm.

Normal MRI Anatomy

MR imaging can take advantage of orbital and periorbital fat to highlight many normal structures. This is best done with thin-sectioned T1-weighted images in which fat will have high intensity (appear bright or white), whereas other structures will be of lower intensity, ranging from very dark to shades of gray on images.

The iris and ciliary muscle can be defined within the globe, with the medial and lateral canthal ligaments and Tenon's capsule appearing relatively dark. The sclera can be clearly separated from retina and choroid, particularly with use of intravenous contrast which will produce further increased intensity of the retina and choroid.

The orbital septum can be well defined as a low intensity band on axial or sagittal images. Similarly, the orbicularis muscle as well as the tarsal plates within the eyelids will appear as thin, dark bands.

Like CT scanning, MR imaging readily defines the extraocular muscles, with somewhat better visualization of the tendinous portions of the muscles. The levator aponeurosis, as a distinct extension of the levator palpebrae superioris, can be defined as it curves downward into the upper lid. Müller's muscle, distinct from the inferior (distal) portion of the levator palpebrae, can be identified as it passes superior to the superior rectus muscle. Both structures are seen well on sagittal and coronal views. The intermuscular septum is well seen between the extraocular muscles in the anterior orbit, becoming much more incomplete in the posterior orbit.

A variety of nerves can be identified as slightly low-intensity, rounded structures passing through the orbital fat on the coronal views. The frontal nerve is well seen and the superior and inferior divisions of the third nerve are often well distinguished, although the position may vary slightly. The infraorbital nerve can be seen as it passes through the infraorbital canal. Other nerves that are frequently seen include the nasociliary, trochlear, zygomaticofacial, and zygomaticotemporal nerves.

The superior as well as inferior ophthalmic veins can be identified as intermediate low intensity structures. Intraorbital arteries tend to be very low intensity due to their flow and include the lacrimal, nasociliary, and supratrochlear branches as well as the ophthalmic artery.

The optic nerve can be readily separated from the subarachnoid space within the optic sheath. Also, this nerve can be well seen passing through the optic canal and posteriorly to the chiasm.

The extraocular muscles readily enhance with contrast, unlike other muscles within the head and neck region. Fat suppressed T1-weighted images are very useful for better definition of enhancing lesions within the orbit, since such lesions would be difficult to separate from normal fat without fat suppression.

Bibliography

General

Doxanas MT, Anderson RL. Clinical Orbital Anatomy. Baltimore: Williams & Wilkins, 1984.

Kikkawa DO, Lemke BN. Orbital and eyelid anatomy. In: Dortzbach RK, ed. Ophthalmic Plastic Surgery: Prevention and Management of Complications. New York: Raven Press, 1993:1-29.

Lange J. Clinical Anatomy of the Nose, Nasal Cavity, and Paranasal Sinuses. New York: Thieme Medical Publishers, 1989.

Lasjunias P, Berenstein A. Surgical Neuro-Angiography. Germany: Springer-Verlag, 1987.

McCord CD, Tannenbaum M, eds. Oculoplastic Surgery, 2nd ed. New York: Raven Press, 1987.

Rootman J, Stewart B, Goldberg RA. Orbital Surgery: A Conceptual Approach. Philadephia: Lippincott-Raven, 1995.

Wigand ME. Endoscopic Surgery of the Paranasal Sinuses and Anterior Skull Base. New York: Thieme Medical Publishers, 1990.

Zide BM, Jelks GW. Surgical Anatomy of the Orbit. New York: Raven Press, 1985.

Bony Anatomy

Goldberg RA, Relan A, Joenig J. Relationship of the eye to the bony orbit, with clinical correlations. Aust N Z J Ophthalmol 1999;27:398-403.

Webster RC, Gaunt JM, Hamdan US, et al. Supraorbital and supratrochlear notches and foramina: anatomical variations and surgical relevance. Laryngoscope 1986;96:311-5.

Optic Canal

Bansberg SF, Harner SG, Forbes G. Relationship of the optic nerve to the paranasal sinuses as shown by computed tomography. Otolaryngol Head Neck Surg 1987;96:331-5.
Goldberg RA, Hannanai K, Toga AW. Microanatomy of the orbital apex: computed tomography and microcryoplaning of soft and hard tissue. Ophthalmology 1992;99:1447-52.
Hayreh SS. The sheath of the optic nerve. Ophthalmologica 1984;189:54-63.
Maniscalco JE, Habal MB. Microanatomy of the optic canal. J Neurosurg 1978;48:402-6.

Periorbita, Septa, and Extraocular Muscles

Anderson RL. Medial canthal tendon branches out. Arch Ophthalmol 1977;95:2051-2.

Apt L. An anatomical reevaluation of rectus muscle insertions. Trans Am Ophthalmol Soc 1980;78:365-75.

Helveston EM, Merriam WW, Ellis FD, et al. The trochlea. A study of the anatomy and physiology. Ophthalmology 1982;89:124-33.

Jones LT. A new concept of the orbital fascia and rectus muscle sheaths and its surgical implications. Trans Am Acad Ophthalmol Otolaryngol 1968;72:755-64.

Koornneef L. Eyelid and orbital fascial attachments and their clinical significance. Eye 1988;2:130-4.

Koornneef L. Orbital septa: anatomy and function. Ophthalmology 1979;86:876-80.

Mustarde JC. The role of Lockwood's suspensory ligament in preventing downward displacement of the eye. Br J Plast Surg 1968;21:73-81.

Sacks JG. The shape of the trochlea. Arch Ophthalmol 1984;102:932-3.

Nerves

Davis RA, Anson BJ, Budinger JM, Kurth L. Surgical anatomy of the facial nerve and parotid gland based upon study of 350 cervicofacial halves. Surg Gynecol Obstet 1956;102:384-412.

Gudmundsson K, Rhoton AL Jr, Rushton JG. Detailed anatomy of the intracranial portion of the trigeminal nerve. J Neurosurg 1971;35:592-600.

Henderson WR. A note on the relationship of the human maxillary nerve to the cavernous sinus and to an emissary sinus passing through the foramen ovale. J Anat 1966;100:905-8.

Ishikawa Y. An anatomical study of the distribution of the temporal branch of the facial nerve. J Craniomaxillofac Surg 1990;18:287-92.

Stuzin JM, Wagstrom L, Kawamoto HK, Wolfe SA. Anatomy of the frontal branch of the facial nerve: the significance of the temporal fat pad. Plast Reconstr Surg 1989;83:265-71.

Vascular

Brismar J. Orbital phlebography. II. Anatomy of the superior ophthalmic vein and its tributaries. Acta Radiol [Diagn] (Stockh) 1974;15:481-96.

Brismar J: Orbital phlebography. III. Topography of intraorbital veins. Acta Radiol [Diagn] (Stockh) 1974;15:577-94.

Hayreh SS. The ophthalmic artery. III: branches. Br J Ophthalmol 1962;46:212-47.

Hayreh SS. Arteries of the orbit in the human being. Br J Surg 1963;50:938-53.

Hayreh SS, Dass R. The ophthalmic artery. I: origin and intracranial and intra-canalicular course. Br J Ophthalmol 1962;46:65-98.

Hayreh SS, Dass R: The ophthalmic artery. II: intra-orbital course. Br J Ophthalmol 1962;46:165-85.

Lang J, Kageyama I. The ophthalmic artery and its branches, measurements and clinical importance. Surg Radiol Anat 1990;12:83-90.

Spektor S, Piontek E, Umansky F. Orbital venous drainage into the anterior cavernous sinus space: microanatomic relationships. Neurosurgery 1997;40:532-40.

Yoshii I, Ikeda A. A new look at the blood supply of the retro-ocular space. Three-dimensional analysis of the arterial pattern of the posterior ciliary artery. Anat Rec 1992;233:321-8.

Orbital Apex and Cavernous Sinus

Ettl A, Zwrtek K, Daxer A, Salomonowitz E. Anatomy of the orbital apex and cavernous sinus on high-resolution magnetic resonance images. Surv Ophthalmol 2000;44:303-23.

Goldberg RA, Hannanai K, Toga AW. Microanatomy of the orbital apex: computed tomography and microcryoplaning of soft and hard tissue. Ophthalmology 1992;99:1447-52.

Govsa F, Kayalioglu G, Erturk M, Ozgur T. The superior orbital fissure and its contents. Surg Radiol Anat 1999;21:181-5.

Harris FS, Rhoton AL. Anatomy of the cavernous sinus. A microsurgical study. J Neurosurg 1976;45:169-80.

Henderson WR. A note on the relationship of the human maxillary nerve to the cavernous sinus and to an emissary sinus passing through the foramen ovale. J Anat 1966;100:905-8.

Housepian EM. Microsurgical anatomy of the orbital apex and principles of transcranial orbital exploration. Clin Neurosurg 1978;25:556-73.

Natori Y, Rhoton AL Jr. Microsurgical anatomy of the superior orbital fissure. Neurosurgery 1995;36:762-75.

Renn WH, Rhoton AL Jr. Microsurgical anatomy of the sellar region. J Neurosurg 1975;43:288-98.

Lacrimal System

Ahl NC, Hill JC. Horner's muscle and the lacrimal system. Arch Ophthalmol 1982;100:488-93.

Anderson RL, Dixon RS. The role of Whitnall's ligament in ptosis surgery. Arch Ophthalmol 1979;97:705-7.

Doane MG. Interactions of eyelids and tears in corneal wetting and the dynamics of the normal human eyeblink. Am J Ophthalmol 1980;89:507-16.

Doane MG. Blinking and the mechanics of the lacrimal drainage system. Ophthalmology 1981;88:844-51.

Gioia VM, Linberg JV, McCormick SA. The anatomy of the lateral canthal tendon. Arch Ophthalmol 1987;105:529-32.

Jones LT. The lacrimal secretary system and its treatment. Am J Ophthalmol 1966;62:47-60.

Jones LT, Wobig JL. Surgery of the Eyelids and Lacrimal System. Birmingham: Aesculapius, 1976:58.

Meyer DR, Linberg JV, Wobig JL, McCormick SA. Anatomy of the orbital septum and associated eyelid connective tissues. Ophthal Plast Reconstr Surg 1991;7:104-13.

Lids

Anderson RL. Medial canthal tendon branches out. Arch Ophthalmol 1977;95:2051-2.

Anderson RL, Beard C. The levator aponeurosis. Attachments and their clinical significance. Arch Ophthalmol 1977;95:1437-41.

Anderson RL, Dixon RS. The role of Whitnall's ligament in ptosis surgery. Arch Ophthalmol 1979;97:705-7.

Collin JRO, Beard C, Wood I. Experimental and clinical data on the insertion of the levator palpebrae superioris muscle. Am J Ophthalmol 1978;85:792-801.

Gentry LR. Anatomy of the orbit. Neuroimaging Clin N Am 1998;8:171-94.

Hawes MJ, Dortzbach RK. The microscopic anatomy of the lower eyelid retractors. Arch Ophthalmol 1982;100:1313-18.

Hayman LA, Maturi RK, Pfleger MJ, Diaz-Marchan P. MR imaging of the eyelids: normal and pathological findings. AJNR 1995;165:639-44.

Hoffman KT, Hosten N, Lemke AJ, et al. Septum orbitale: high-resolution MR in orbital anatomy. AJNR 1998;19:91-4.

Jones LT. The anatomy of the lower eyelid and its relation to the cause and cure of entropion. Am J Ophthalmol 1960;49:29-36.

Jones LT. A new concept of the orbital fascia and rectus muscle sheaths and its surgical implications. Trans Am Acad Ophthalmol Otolaryngol 1968;72:755-64.

Kuwabara T, Cogan DG, Johnson CC. Structure of the muscles of the upper eyelid. Arch Ophthalmol 1975;93:1189-97.

Lemke BN, Stasior OG. The anatomy of eyebrow ptosis. Arch Ophthalmol 1982;100:981-6.

Imaging

Daniels DL, Herfkins R, Gager WE, et al. Magnetic resonance imaging of the optic neves and chiasm. Radiology 1984;152:79-83.

Ettl A, Kramer J, Daxer A, Koornneef L. High resolution magnetic resonance imaging of neurovascular orbital anatomy. Ophthalmology 1997;104:869-77.

Kline LB, Acker JD, Post MJ, Vitak JJ. The cavernous sinus: a computed tomographic study. AJNR 1981;2:2299-305.

Lloyd GAS. Radiology of the Orbit. Philadelphia: WB Saunders, 1975.

Sargent EN, Ebersole C. Dacryocystography: the use of sinografin for visualization of the nasolacrimal passages. Am J Roentgenol Rad Ther Nucl Med 1968;102:4:831-9.

Chapter 2

Anatomic Patterns of Orbital Disease

The effect of any disease is governed not only by the nature of the process (pathophysiology) but also by the anatomic pattern of involvement (location). For instance, a small tumor in the orbital apex may produce an early disturbance of the second, third, fourth, fifth, or sixth nerves, as seen in a cavernous hemangioma that presented primarily with progressive visual loss (Fig. 2-1A). In contrast, a more laterally placed apical meningioma may affect the structures of the superior orbital fissure with or before the optic nerve is involved (Fig. 2-1B). In simple terms, disease can be viewed as having either functional or mass effect. It is the character of these effects that helps to discern disease location. Functional effect interferes with the motor, sensory, or secretory function of orbital structures. Mass effect shifts or displaces orbital structures by occupying space (positive effect), by increasing space (bone expansion, a negative effect), or by cicatrization (negative effect). For instance, an ethmoidal mass causes lateral displacement (positive effect), whereas destruction of the orbital floor leads to enophthalmos and downward displacement (negative effect) (Fig. 2-2). A desmoplastic process such as a metastatic carcinoma may tether and trap structures and lead to traction toward it as well as entrapment (negative effect) (Fig. 2-2).

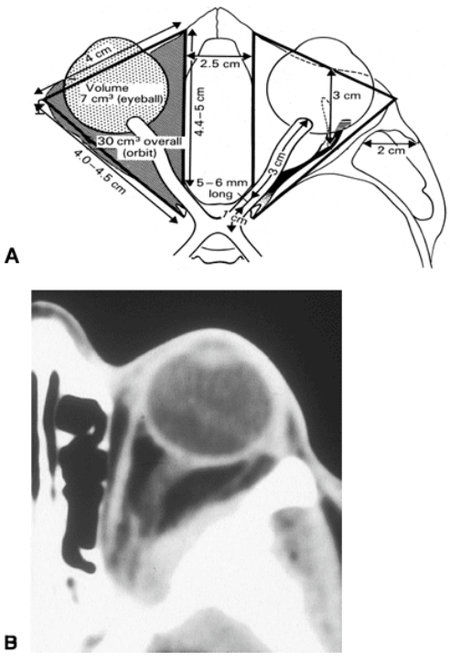

Figure 2-1. Two apical lesions in which slightly different locations affected presentation. (A) This 48-year-old woman presented with decreased vision on the right side in her nonamblyopic eye, which was associated with reduced color vision and a mild central field defect. She had a right afferent pupillary defect of 1.8 log units. MRI revealed a well-defined, apical orbital mass with smooth anterior and posterior margins, which enhanced on contrast. Because of progressive visual loss, the lesion was removed by an extended lateral orbitotomy and proved to be a cavernous hemangioma. (B) This meningioma presented with proptosis, venous congestion, and mild optic neuropathy reflecting compression of structures passing through the superior orbital fissure.

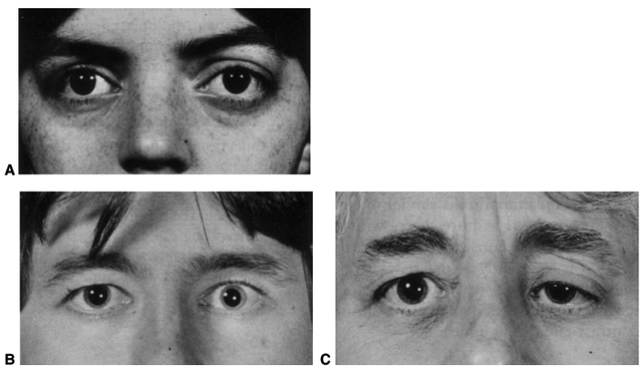

Figure 2-2. Three different mass effects. (A) A positive mass effect led to lateral displacement of the left eye from an ethmoidal fibrous dysplasia. (B) A negative effect of enophthalmos and downward displacement of the left eye was due to a blowout fracture with depression of the orbital floor. (C) A cicatrizing metastatic carcinoma caused a negative effect of left enophthalmos and lid distraction.

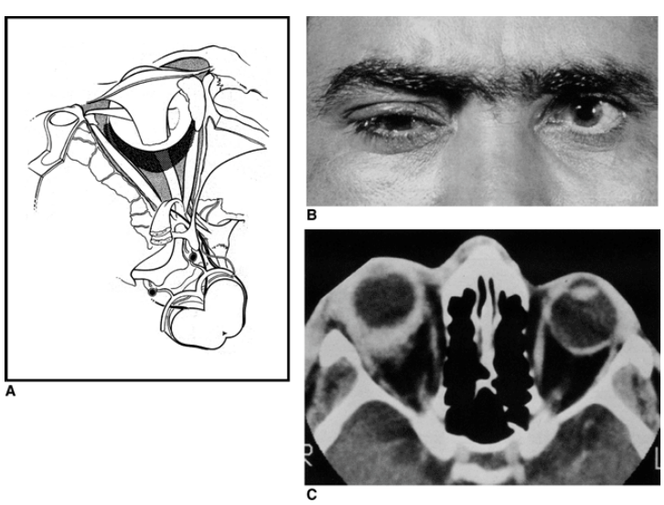

Figure 2-3. (A) Schematic of anterior (periocular) pattern of involvement in a case of acute anterior idiopathic inflammation. (B) Clinically, it was characterized by pain, right ptosis, chemosis, injection, proptosis (3 mm), and minimal exudative retinal detachment with decreased vision (20/60). (C) CT scan with contrast shows an irregular enhancing lesion of the anterior orbit associated with a thickened sclerochoroidal rim. These features may be indistinguishable from scleritis. Biopsy showed nonspecific polymorphous lymphocytic infiltration so the patient was treated with, and responded promptly to, oral corticosteroids.

The patterns of anatomic involvement can be divided into anterior, ocular, lacrimal, lacrimal drainage system, myopathic, intraconal, apical, optic nerve, diffuse, and periorbital. Disease produces signs and symptoms that reflect these locations. Using inflammations as examples, the effect of location on presentation can be demonstrated. For instance, we have classified acute and subacute idiopathic (nonspecific) orbital inflammatory disease using an anatomic model, which includes five locations of anterior, lacrimal, myopathic, apical, and diffuse presentations characterized by clinical features of inflammation that differ on the basis of site and extent of involvement.

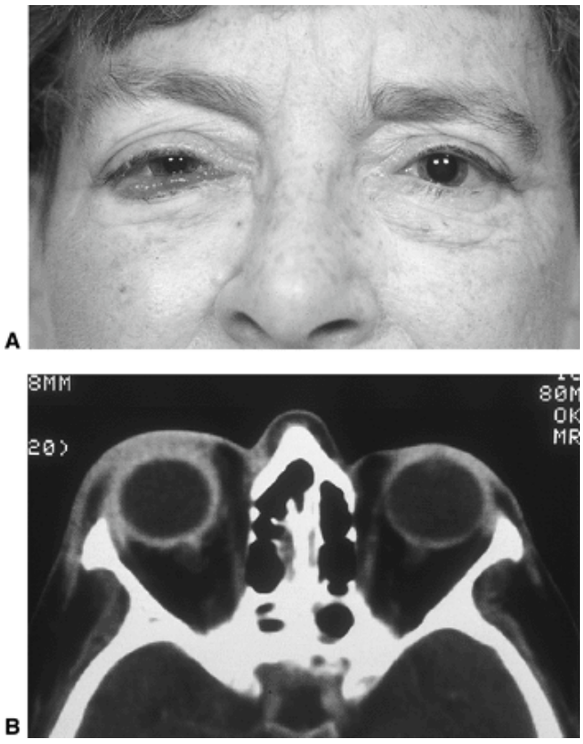

Figure 2-4. (A) This 72-year-old woman presented with sudden onset of swelling, injection, and pain, which was progressive and led to severe chemosis. She had mild proptosis and thickened sclera on slit lamp examination, later confirmed by CT scan. (B) The scan demonstrates relatively diffuse thickening of the globe with infiltration of the anterior orbital fat. Treatment for scleritis with systemic steroids led to rapid resolution.

Anterior

The anterior or periocular idiopathic inflammations may be characterized by pain, chemosis, lid swelling, injection, uveitis, papillitis, optic neuropathy, diplopia, and even exudative inflammatory retinal detachment (Fig. 2-3). All of these features relate to the location and severity of the process occurring anteriorly within the orbit adjacent to and affecting the globe. A typical patient presents with proptosis, chemosis, lid injection, retinal venous dilatation, and possible uveitis. Characteristically, on imaging (CT and MR) a contrast-enhancing anterior orbital infiltration intimately

related to the globe produces scleral and choroidal thickening, obscuring the junction of the globe and optic nerve and extending variably along the sheath. Ultrasonography localizes the anterior inflammatory process and demonstrates a sclerotenonitis.

Ocular

Ocular inflammation obviously can extend to surrounding orbital structures, as demonstrated by a patient presenting with keratitis, chemosis, conjunctival injection, and scleral thickening due to scleritis (Fig. 2-4). In addition, there was clinical evidence of anterior orbital inflammation leading to ptosis and lid swelling. Investigations show thickening of the globe and anterior orbital infiltration on CT scan with evidence of sclerotenonitis on ultrasonography. A conjunctival biopsy confirmed perivasculitis.

Lacrimal

Acute idiopathic lacrimal inflammation typically presents with localized pain, tenderness and injection of the temporal lid and fornix with a palpable lacrimal gland, an S-shaped deformity of the lid, and often pouting of the lacrimal ducts (Fig. 2-5). The anatomic localization on imaging reveals an irregular, poorly-defined infiltrate confined to the superolateral aspect of the orbit. It is adjacent to and obscuring the lateral part of the globe, which is displaced downward and inward.

Lacrimal Drainage System

Inflammation affecting the lacrimal drainage system can lead to tearing, anterior orbital and lid swelling, upward or lateral displacement, and fistulization (Fig. 2-6). The effect depends on the severity and nature of the primary process.

Myopathic

Acute and subacute idiopathic inflammations of muscle are characterized by pain with eye movement, localized injection of the globe over the insertion of the affected muscle, and reduced ocular motility (Fig. 2-7). On CT scan and ultrasonography, the contrast-enhancing irregular infiltrate involves one or more extraocular muscles with relatively diffuse enlargement, extending up to the globe and usually including the tendon.

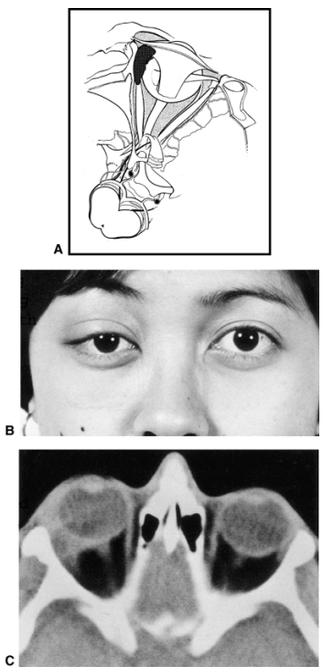

Figure 2-5. (A) Schematic of lacrimal location, which is demonstrated clinically in a 25-year-old woman who presented with an idiopathic inflammatory lesion of the right lacrimal gland. (B) Note superolateral lid swelling, S-shaped deformity of the lid, mild local chemosis, and injection. (C) CT scan shows an irregular lacrimal mass that proved to be inflammatory on biopsy, and responded to oral corticosteroids.

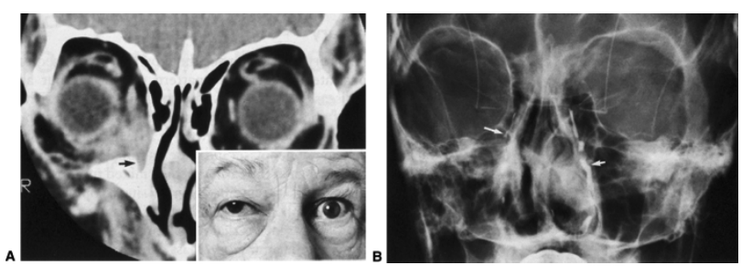

Figure 2-6. (A) Lacrimal drainage system location is demonstrated in a patient who presented with right lower lid swelling, upward globe displacement, limitation of elevation, and tearing. CT scan shows an irregular infiltrative mass (arrow) involving the anterior inferior orbit with entrapment of the inferior oblique muscle and lacrimal drainage system. (B) A dacryocystogram of the same patient shows obstruction on the right (long arrow) in contrast to the open system on the left (short arrow). Biopsy revealed an idiopathic sclerosing inflammatory process. (Reproduced with permission from Rootman J. The clinical evaluation and pathology of tumors of the eye, orbit and lacrimal apparatus. In: Thawley SE, ed. Comprehensive Management of Head and Neck Tumors. Vol 2. Philadelphia: WB Saunders, 1987.)

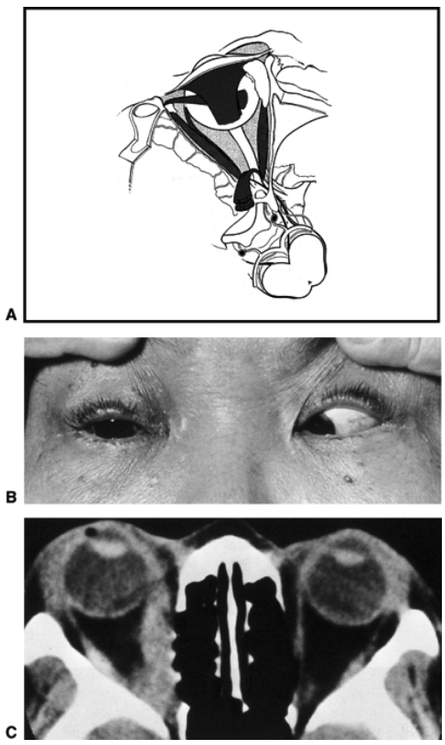

Figure 2-7. (A) Schematic demonstrates myopathic pattern of orbital disease. A 60-year-old woman presented with painful subacute myositis. (B) Note limitation of ocular movement on the right, medial chemosis and injection, swollen lid, and mild ptosis and proptosis. (C) Diffuse swelling and contrast enhancement of the entire medial rectus muscle and tendon confirmed the diagnosis. The patient responded promptly to systemic corticosteroids.

Intraconal

Lesions within the muscle cone produce axial displacement and functional deficit of the eye, optic nerve, muscles, and ciliary ganglion. Figure 2-8 shows bilateral intraconal sclerosing inflammation that led to axial proptosis and limitation of extraocular movements.

Apical

Perineural or apical acute and subacute idiopathic inflammation produces less proptosis, pain, or visible inflammation, but is associated with the early development of optic neuropathy or motor and sensory symptoms (Fig. 2-9). In addition, when an apical process affects the superior orbital fissure, vascular congestion due to superior or inferior ophthalmic vein obstruction may be a clinical feature. Thus, the patient characteristically reports pain, limitation of movement, or visual deficit typical of the so-called orbital apex syndromes. CT scans confirm apical and perineural inflammation consistent with the clinical syndrome.

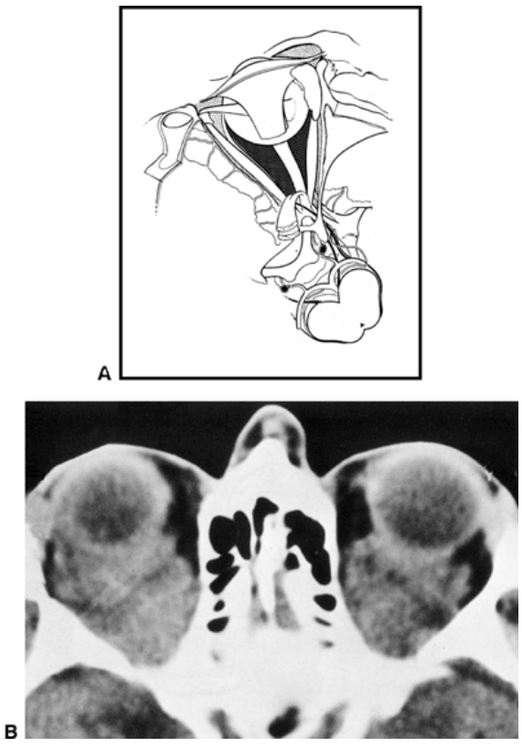

Figure 2-8. (A) Schematic of intraconal location. (B) Clinically, bilateral intraconal infiltrative disease was found, which proved on biopsy to be an idiopathic sclerosing inflammation of the orbit.

Diffuse

Diffuse idiopathic inflammation is similar in clinical presentation to anterior, but is more severe with profound signs

and symptoms (Fig. 2-10). It is frequently associated with optic neuropathy and motor and sensory orbital deficits. The entire orbit is involved by a diffuse, poorly-defined, contrast-enhancing infiltrate.

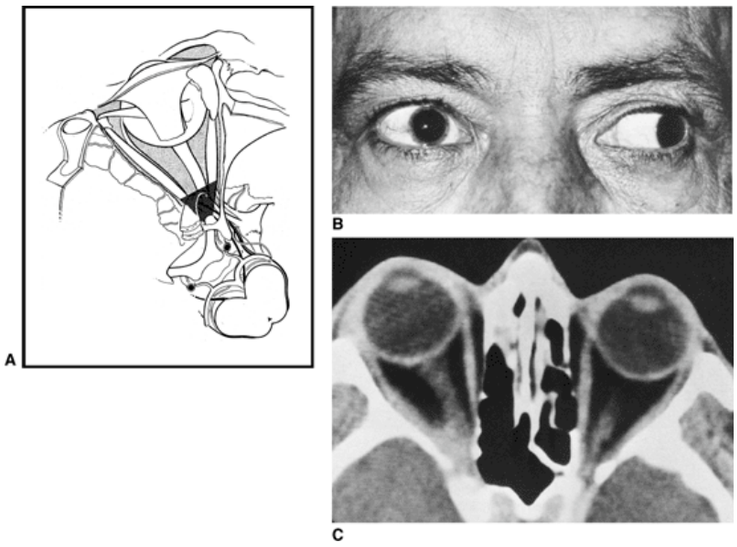

Figure 2-9. (A) Schematic demonstrates the major orbital structures affected by the apical pattern of disease. (B) Clinical features of an acute idiopathic apical inflammatory disease are shown in a middle-aged patient who presented with sudden onset of a painful ophthalmoplegia with limitation of right ocular movements, profound optic neuropathy (hand movements), mild proptosis, and minimal signs of ocular or lid inflammation. (C) CT scan demonstrates an irregular infiltration of the orbital apical structures with mild swelling of the optic nerve. The patient responded rapidly to corticosteroids. Pupils are pharmacologically dilated.

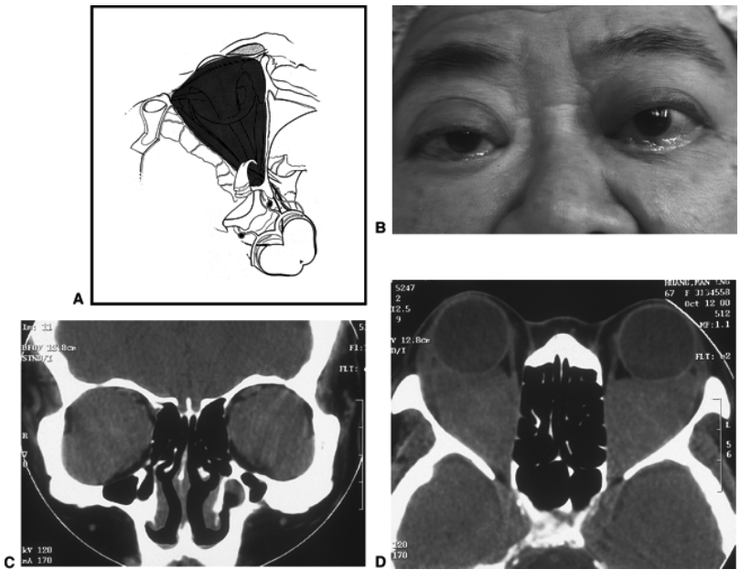

Figure 2-10. (A) Schematic demonstrates the diffuse pattern of orbital disease. (B) This 67-year-old woman presented with a history of progressive proptosis for 1 year associated with decreasing vision. On physical examination, her vision was light perception OD and counting fingers at 4 feet OS with a raised intraocular pressure. She had marked symmetrical restriction of movement, firm orbits, and exophthalmometry measurements of 22 mm right and 21 mm left, with evidence of a slight afferent pupillary defect on the right. The CT scans (C, D) demonstrate a diffuse bilateral infiltration of the orbits, which on biopsy proved to be Erdheim-Chester disease. She had an initial response to pulsed steroids and cyclophosphamide, with vision improving to hand movements OD and 20/40 OS, but deteriorated rapidly and died of a stroke due to hypertension and complications of diabetes mellitus 4 months after her initial visit.

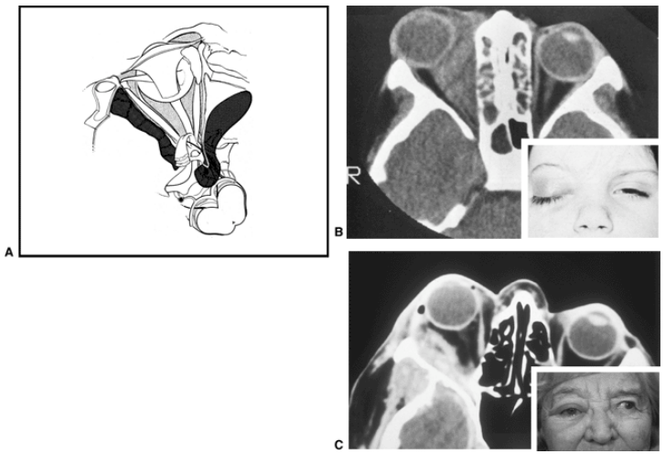

Figure 2-11. (A) Schematic demonstrates periorbital sources of disease, which may arise from the sinuses, bone, or intracranial structures. (B) Ethmoid sinus infection and a subperiosteal abscess caused sudden tense proptosis, lateral displacement, ptosis, and optic neuropathy. (C, inset) This 80-year-old woman presented with a 3 to 4 month history of onset of right proptosis and lid swelling associated with dysesthesia of the right scalp and temple. On physical examination, she had light perception with downward displacement of the globe and marked restriction of movement, as well as infraorbital and supraorbital sensory deficits. (C) CT scan demonstrates a lesion eroding the sphenoid wing and infiltrating the orbit, temporalis fossa, and middle cranial fossa. Biopsy revealed an adenocarcinoma, which was metastatic from a previously occult bowel carcinoma. (Figure 2-11B from Rootman J. The clinical evaluation and pathology of tumors of the eye, orbit and lacrimal apparatus. In: Thawley SE, ed. Comprehensive Management of Head and Neck Tumors, vol 2. Philadelphia: WB Saunders, 1987.)

Periorbital

Diseases originating from the sinuses, face, and intracranial cavity may extend into and affect the orbit by contiguity or as the result of damage to neurosensory or vascular structures shared with the orbit. This is well demonstrated in sinus inflammation where the clinical presentation varies depending on the location of primary sinus disease and the stage of the process. These may include diffuse cellulitis, fistulization, recurrent inflammation, or acute proptosis secondary to subperiosteal abscess formation (Fig. 2-11C). Lesions of the cranial bones may also secondarily affect structures supplying the orbit or may indeed extend into the orbit (Fig. 2-11B).

Optic Nerve

The effect of disease on the optic nerve is governed by whether or not the process is intrinsic to the nerve or from the surrounding sheath. The difference is demonstrated by intrinsic optic neuritis versus optic nerve sheath inflammation (Fig. 2-12). The pathophysiology of the difference is better defined by tumors, where the onset, character, progression, and clinical signs and symptoms may be different for intrinsic tumors (gliomas) versus optic sheath tumors (meningiomas).

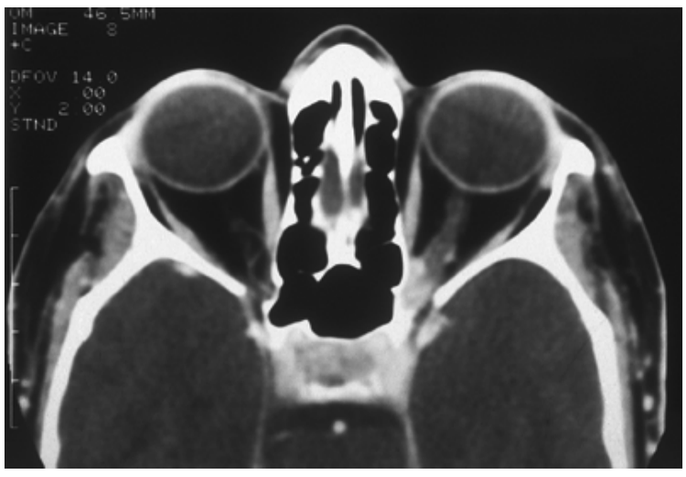

Figure 2-12. This 52-year-old woman developed sudden visual loss and presented with a vision of counting fingers at 2 meters. Her CT scan had multiple areas of dural thickening and enhancement, consistent with dural sarcoid lesions. Systemic evaluation was negative for sarcoid, but the patient responded completely to oral corticosteroids.

Summary

Inflammatory disease has for the most part been used to demonstrate the anatomic pattern of disease, but all other disorders can be viewed in a similar manner. The effects of these processes are governed by the pathophysiologic disturbance they cause in that location. For instance, neoplasia may be lacrimal, periorbital, neural, or apical in the case of benign mixed tumor of the lacrimal gland, carcinoma of the sinus, optic nerve glioma, and sphenoid wing meningioma, respectively. The major difference is that neoplasms are usually dominated by noninflammatory mass effects or infiltration (entrapment). Anterior lesions cause greater direct ocular effects due to the immediate relationship to the globe, whereas diffuse diseases involve motor and sensory structures of the entire orbit and may lead to fixation of the globe and sensory deficits (pain, paresthesia, or loss of visual function). Apical disease tends to affect the optic, motor, and sensory nerves earlier as in a case of minimal apical infiltration by a metastatic carcinoma with profound early motor loss (ptosis and limitation of movement), sensory deficit (paresthesia), and visual loss without much evidence of mass effect (proptosis) (Fig. 2-13). Lacrimal pathology is dominated by functional (tearing or drying) and structural alterations of the gland, lacrimal fossa, and the outer third of the upper lid. A tumor here may cause downward and inward displacement of the globe, sensory defects of the

frontotemporal and frontozygomatic nerves, and an S-shaped deformity of the lid. Myopathic disease such as thyroid ophthalmopathy leads to restriction of ocular movement due to a combination of mass effect, scarring, or neuromuscular dysfunction. Ocular diseases have symptomatic functional changes (e.g., visual loss, floaters, photopsia, pain, photophobia) primarily affecting vision, and are usually readily accessible to clinical examination of the globe. Processes within the tight periorbital space can cause profound and even sudden effects (e.g., an abscess), with the displacement governed by the site of involvement. A mass arising from the ethmoids causes lateral displacement; the roof, downward (Fig. 2-14), and the floor, upward displacement. Disease of the lacrimal drainage system is usually characterized functionally by obstruction leading to tearing with or without recurrent infection. Mass effect here leads to lateral and upward displacement with anterior tumefaction.

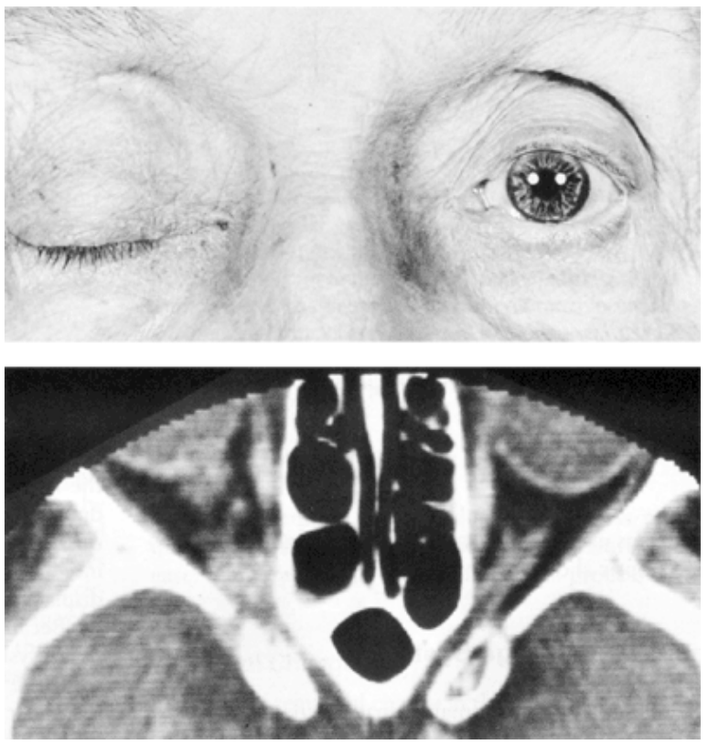

Figure 2-13. (Top) Clinical photograph demonstrates right ptosis, which was associated with compressive optic and motor neuropathy due to an apical metastatic carcinoma (bottom).

Because of the complicated nature of the orbit as an organ system, location of disease can usually be defined from the signs and symptoms produced. Awareness of the effect of site on the signs and symptoms of orbital disease makes clinical analysis more pertinent and accurate.

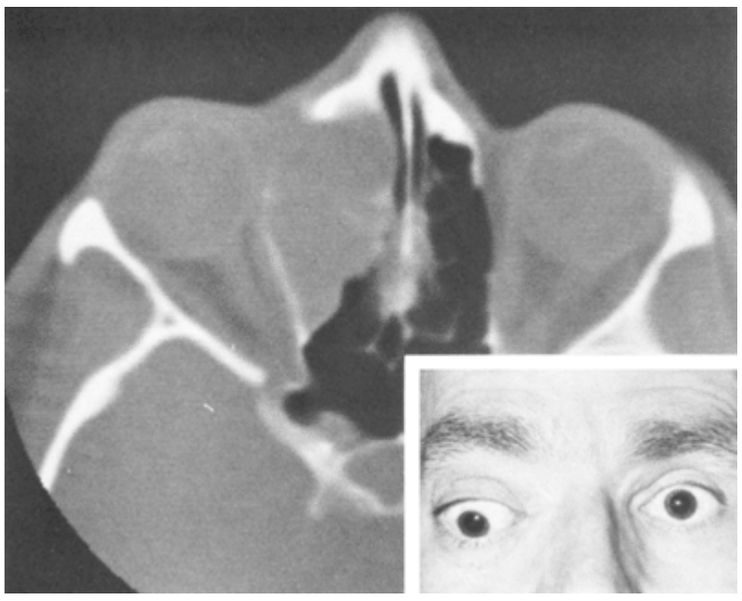

Figure 2-14. A mass (mucocele) arising in the right frontoethmoid complex caused downward and outward displacement of the globe. (Reproduced with permission from Rootman J. The clinical evaluation and pathology of tumors of the eye, orbit and lacrimal apparatus. In: Thawley SE, ed. Comprehensive Management of Head and Neck Tumors. Vol 2. Philadelphia: WB Saunders, 1987.)

Chapter 3

Pathophysiologic Patterns of Orbital Disease

Five processes can occur, either independently or in combination, within and around the orbit: inflammations, neoplasia, structural abnormalities (acquired and congenital), vascular lesions, and degeneration and depositions. The processes are not mutually exclusive and may occur in concert, but for the most part in our experience one process is the dominant underlying pathophysiology of presentation. Based on close to 4,000 patients seen at the Orbit Clinic of the University of British Columbia, their incidence is as follows:

Inflammation (overall)	60.2%
Thyroid orbitopathy	51.7%
Other inflammations	8.6%
Neoplasia	18.1%
Structural abnormality	12.5%
Congenital	4.9%
Acquired	7.7%
Vascular lesions	4.6%
Degeneration and depositions	1.7%

Inflammation

Overall, we found that inflammation accounts for close to 60% of primary orbital disease processes, the majority of which were related to thyroid orbitopathy. The underlying pathophysiologic substrate determines the nature of the clinical presentation and development. This ranges in character from acute inflammatory cells and their chemical intermediates, to insidious infiltrates in the case of some misdirected immune responses or granulomas. Specifically in acute inflammation, polymorphonuclear leucocytes are usually the dominant cells inciting a rapid, frequently destructive process. In contrast, slower, more progressive disorders may have a substrate of lymphocytes, plasma cells, histiocytes, and fibroblasts (idiopathic sclerosing inflammations), or a granulomatous infiltrate (Wegener's granulomatosis). As we learn more about the lymphocyte, it has become evident that these cells can respond with varying onsets ranging from a rapid to slow influx of cells (with and without attracting other cell types or inducing destruction or fibroplasia), with corresponding clinical patterns.

The character and location of the infiltrate affect the clinical presentation, which may be acute (dominated by pain, injection, systemic malaise, and loss of function) to chronic (insidious). The chronic presentation may be characterized by an infiltrative picture dominated by entrapment or may simply produce a mass effect. This scheme reflects the fundamental and established pathophysiologic patterns of inflammatory disease, which may be acute, subacute, or chronic.

Acute Inflammation

Acute inflammation is characterized by rapid development (days) and flagrant features of inflammation (warmth, injection, swelling, malaise, and loss of function). Infective cellulitis is the model. The majority of inflammatory disorders in this category are of sinus origin, especially in children, but they may be ocular, pyemic, or due to secondary infection of a wound. The location of the process determines the effect. For instance, a preseptal infection rarely affects function of orbital tissues initially, but may lead to damage of lid structures (Fig. 3-1). On the other hand, sinusitis with orbital spread may have a profound and sudden effect on optic nerve and orbital function early in the course of the disease (Fig. 3-2).

Pathologically, acute bacterial infections draw polymorphonuclear leucocytes and their pharmacologic intermediates, leading to necrosis and rapid destruction of tissue planes. Thus, the early manifestations are edema, injection, pain, loss of function, and systemic malaise with subsequent abscess formation and fistulization or spread if unchecked. On investigation, the progressive features reflect tissue swelling, infiltration, and destruction with irregular margins, leading to abscess formation, loss of normal planes, separation of structures, and contrast enhancement.

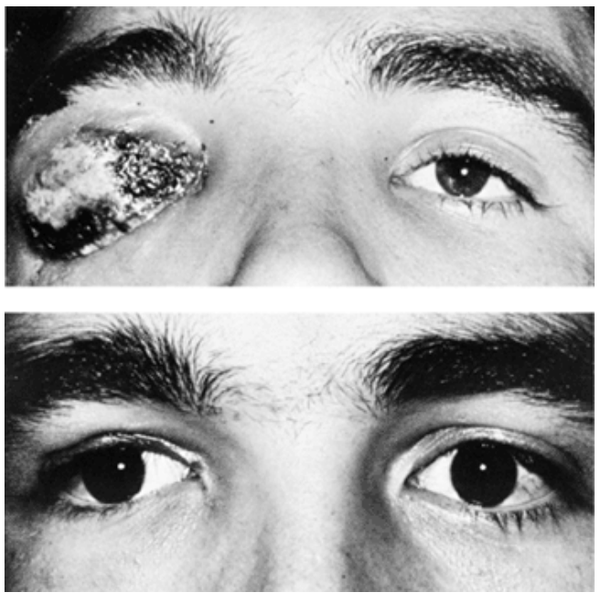

Figure 3-1. An acute necrotizing infective lesion of the preseptal lid is shown before (top) and after treatment (bottom) with systemic antibiotics and local measures. Note minor damage to lid structures only.

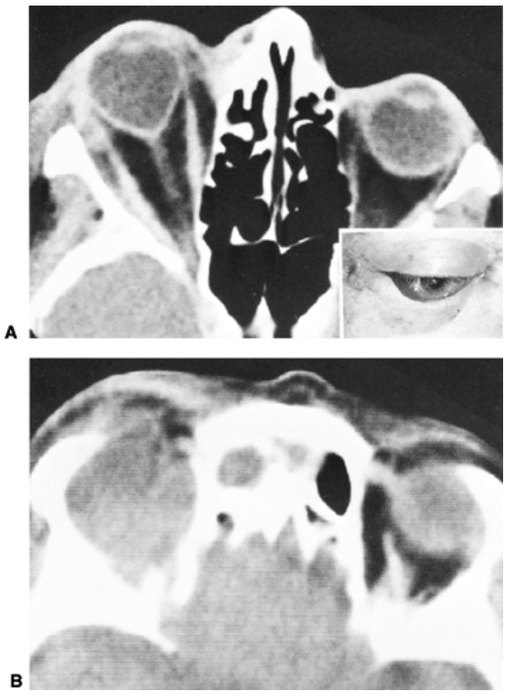

Figure 3-2. Acute sinus infection caused sudden and profound effects on ocular and orbital structures. (A) Note the marked tense proptosis with tenting of the globe and stretching of the optic nerve. (B) Proptosis and orbital tension were due to the sudden extension of purulent material into the superior subperiosteal space from a frontal sinus abscess. (Fig. 3-2A reproduced with permission from Rootman J. The clinical evaluation and pathology of tumors of the eye, orbit and lacrimal apparatus. In: Thawley SE, ed. Comprehensive Management of Head and Neck Tumors. Vol 2. Philadelphia: WB Saunders, 1987.)

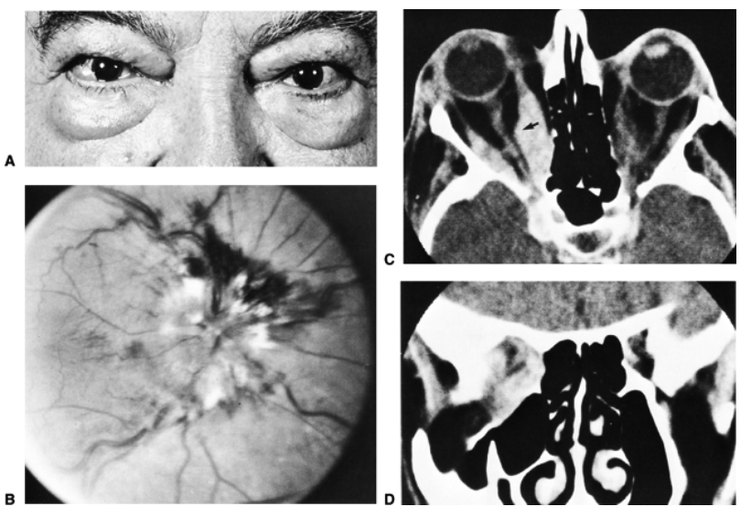

Figure 3-3. Subacute inflammatory disease in a patient with infiltrative thyroid orbitopathy. (A, B) He showed lid swelling, chemosis, symmetrical limitation of movement, and papilledema. (C, D) These features were due to profound apical muscle swelling, leading to compressive optic neuropathy as shown on CT scan. Note posterior angulation of the muscle due to compression of the optic nerve (C, arrow). (Figs. 3-3A, 3-3C, and 3-3D reproduced with permission from Rootman J. The clinical evaluation and pathology of tumors of the eye, orbit and lacrimal apparatus. In: Thawley SE, ed. Comprehensive Management of Head and Neck Tumors, Vol 2. Philadelphia: WB Saunders, 1987.)

The limited and practical differential diagnosis of acute orbital inflammation includes about five disorders: infective cellulitis; acute (nonspecific) idiopathic inflammation; acute ocular inflammation (uveitis, keratitis, scleritis); a sudden event in a pre-existing lesion (e.g., a hemorrhage in a lymphangioma); and more rarely a fulminant neoplasm (such as chloroma, rhabdomyosarcoma, or metastasis). Fulminant neoplasia more commonly present with patterns suggestive of subacute inflammation.

Subacute Inflammation

Subacute inflammation generally has two patterns, which take weeks to develop and tend to be associated with more subtle signs of inflammation. The first is a slow onset of displacement, injection, pain, and loss of function (i.e., mass and functional effects), and the second is a remitting pattern with progressive signs and symptoms.

Many cases of infiltrative thyroid orbitopathy are good examples of a subacute onset of inflammatory disease. The underlying immunopathogenic mechanism consists of lymphocytic, mast cell, and plasmacytic infiltration with increased mucopolysaccharides, connective tissue, and water content, affecting primarily the extraocular muscles and fat. Thus, the clinical pattern consists of swelling of the lids and conjunctiva, proptosis, injection, and diplopia. If the infiltration is significant, problems secondary to proptosis and muscle involvement dominate the pattern. On the other hand, apical disease may affect the optic nerve and extraocular movements regardless of the degree of proptosis (Fig. 3-3).

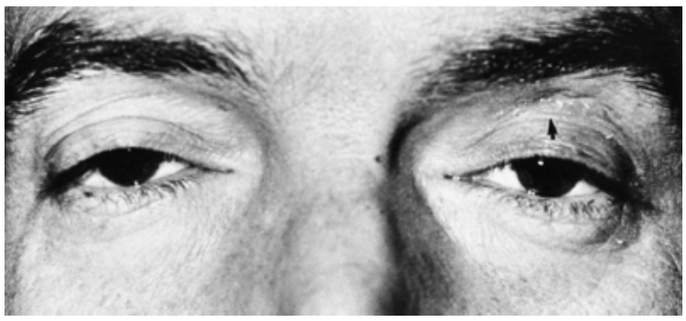

Figure 3-4. The patient demonstrates a fistula (arrow) in the left upper lid, which was due to tracking of pus from the frontal sinus. He suffered from intermittent subacute inflammation as the result of recurrent closing and opening of the fistula.

The second subacute pattern is remitting, which is characterized by abeyance and exacerbations. A good example of this is an orbital inflammation that may occur secondary to sinus disease, especially in the adult. The remitting course is brought about by two factors. The first is the development of natural defense mechanisms such as fistula formation or drainage (Fig. 3-4). The second and more frequent cause is iatrogenic due to incomplete or inappropriate treatment for sinusitis with orbital cellulitis. To summarize, the subacute pattern either is progressive or remitting in character. The basic differential diagnosis includes thyroid orbitopathy, infective cellulitis (especially fungal), idiopathic (nonspecific and specific) orbital inflammations (especially granulomatous or persistent lymphocytic infiltrates), primary ocular inflammation (such as scleritis or uveitis), collagen vascular disease, and rapidly developing (fulminant) malignancies. Occasionally, the vascular dilatation and tissue exudation associated with arteriovenous fistulas may produce a picture that can be confused with inflammation.

Chronic Inflammation

Chronic orbital inflammation is dominated by silent or extremely low-grade signs of inflammation with a progressive pattern of displacement with or without evidence of entrapment and interference with orbital function. Thus, chronic inflammation may produce infiltrative disease (entrapment) or simply act to produce a mass effect. A classic pattern can be seen in the idiopathic sclerosing inflammations and some granulomatous orbital diseases (Fig. 3-5). The inflammation stimulates a desmoplastic response that infiltrates the orbit, leading to fixation of structures. Investigations generally demonstrate loss of tissue planes and an irregular mass. In the case of some destructive lesions, especially those arising from or adjacent to bone, infiltration, destruction, and irregularity of bone may be noted. The differential diagnosis for chronic infiltrative inflammation includes primary and secondary neoplasia, thyroid ophthalmopathy, lymphoproliferative disorders, collagen vascular disease, idiopathic sclerosing inflammations, and rare disorders such as amyloidosis.

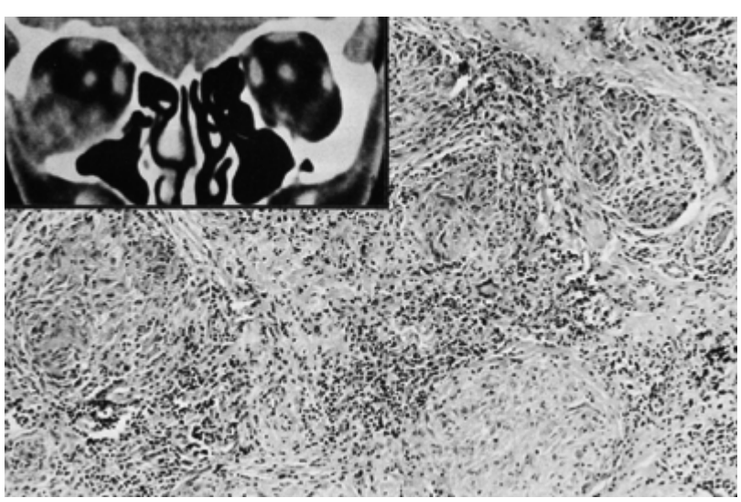

Figure 3-5. Chronic infiltrative granulomatous inflammation of the orbit. Note the irregular infiltration of the inferior and lateral portion of the right orbit. Upgaze and abduction were limited due to entrapment of the inferior and lateral rectus muscles.

On the other hand, chronic inflammatory lesions may simply produce a mass effect without evidence of infiltration or entrapment of orbital structures. The location of the mass will affect the clinical presentation. For example, a case of cholesterol granuloma in the roof of the orbit eroded bone and caused simple downward displacement without features of orbital entrapment (Fig. 3-6). The simple differential diagnosis of chronic inflammatory disease with mass effect includes any primary or secondary mass within the orbit.

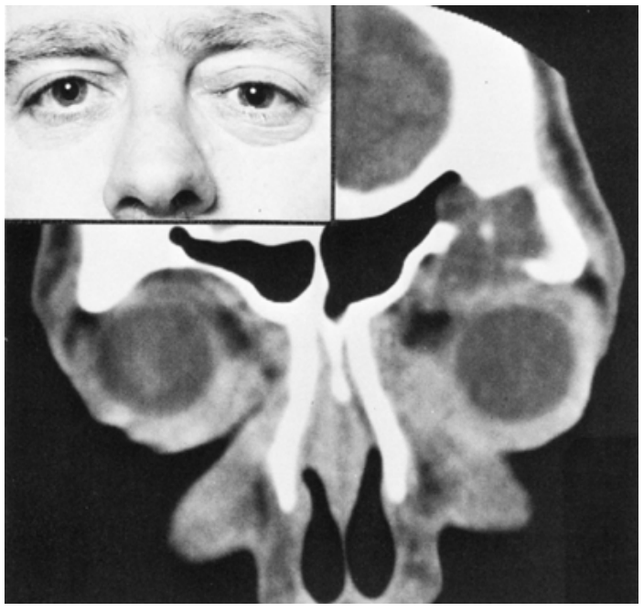

Figure 3-6. This patient demonstrates the mass effect of a cholesterol granuloma that destroyed the superolateral bone of the orbit and displaced the orbital structures downward without infiltrating them. (Reproduced with permission from Rootman J. The clinical evaluation and pathology of tumors of the eye. In: Thawley SE, ed. Comprehensive Management of Head and Neck Tumors. Vol 2. Philadelphia: WB Saunders, 1987.)

Neoplasia

Neoplasia accounts for 18% of the orbital cases we have seen. The specific list of new growths is huge and getting longer all the time. However, from a practical clinical and decision making point of view, they can be defined on the basis of general biologic behavior. That is, they are either benign or malignant and may display infiltrative or noninfiltrative phenomena. Clinically, the benign noninfiltrative masses are usually associated solely with mass effect without destruction or entrapment. In contrast, an infiltrative mass is usually associated with evidence of functional damage or entrapment. On investigation, both types are characterized by mass effect with displacement; however, malignant and infiltrative lesions may have irregular margins, engulf structures, and destroy bone, as opposed to smooth, regular, noninfiltrative masses.

The schwannoma is a good example of a benign, slow-growing, and progressive neoplasm that is associated with displacement of orbital structures. Tumors in this category include an array of soft tissue lesions such as schwannoma and benign fibrous histiocytoma (Fig. 3-7).

Benign tumors are rarely infiltrative in behavior but may be locally invasive. For example, a case of a granular cell tumor that was infiltrating had entrapped the anterior orbital structures, leading to restricted extraocular movements, proptosis, indentation of the posterior pole, and reduced vision (Fig. 3-8). Other benign (nonmetastasizing) neoplasias that may be infiltrative include some fibrous histiocytomas and hemangiopericytomas.

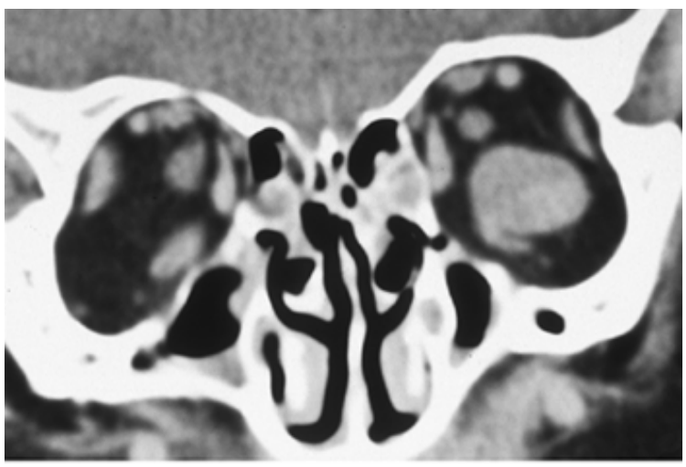

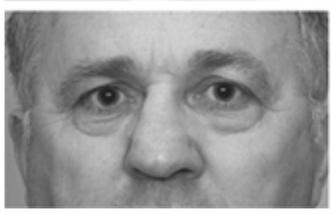

Figure 3-7. This 54-year-old man presented with progressive hyperopic shift and swelling of the left eye. He had 2 mm axial and upward displacement with inferior choroidal folds. On CT scan, there was an intraconal smooth, contoured, noninfiltrative orbital mass, which was of uniform density on ultrasound, and proved to be a schwannoma on removal.

Histologically, malignant lesions can also have these two patterns. This is well demonstrated by two cases of neoplasia of the lacrimal gland that showed infiltrative and noninfiltrative behavior. A 70-year-old man presented with a 10-year history of slowly progressing proptosis and downward displacement of his left eye, with a sudden increase in signs and symptoms over the previous 6 months. He had marked proptosis, edema, ptosis, limitation of movement, and chemosis with a sensory deficit affecting the distribution of the lacrimal division of the fifth nerve. Investigations confirmed an infiltrative mass arising from the lacrimal gland and destroying bone (Fig. 3-9). Histologically, it was a poorly differentiated mucoepidermoid carcinoma.

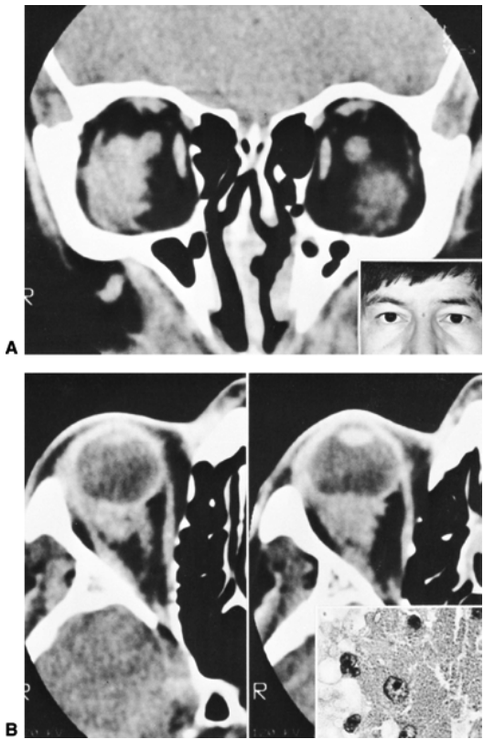

Figure 3-8. (A) This patient has a locally infiltrative benign neoplastic process. (B) A granular cell tumor (inset, H&E, original magnification × 100) infiltrated the anterior portion of the orbit, restricting ocular movements, indenting the posterior pole, and reducing vision.

Malignant lesions usually demonstrate infiltrative and destructive effects leading to displacement (mass effect) and functional deficits (motor, sensory, or visual). On the other hand, histologically malignant lesions can be less aggressive, as shown by another patient with a history of downward displacement of the eye and no evidence of interference with sensory or motor function. She had a lacrimal gland lesion

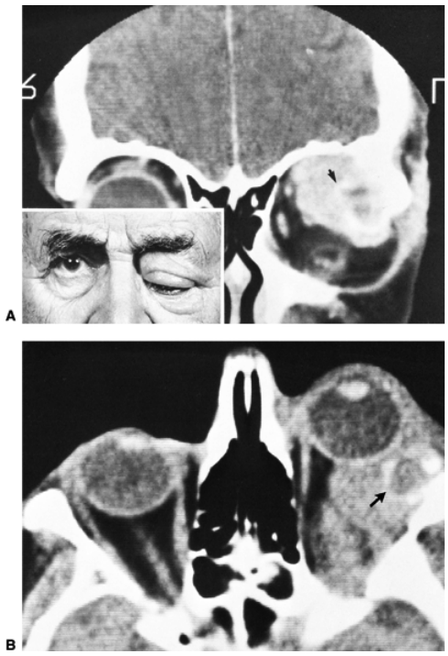

Figure 3-9. The features of an infiltrative malignant epithelial tumor of the lacrimal gland. (A) Clinically, the patient had a longstanding lesion with sudden growth over a 6-month period leading to ptosis, chemosis, and edema with limitation of ocular movements. (B) Note irregular bony invasion and destruction, calcification (arrows), and apical infiltration of the orbit. Histologically, it was a poorly differentiated mucoepidermoid carcinoma.

without bone destruction but with excavation of the lacrimal fossa, which was shown on plain films and CT scans. This was suggestive of a longstanding noninfiltrative mass (Fig. 3-10). At surgery, it was found to be well-encapsulated. It proved to be a lacrimal pleomorphic adenoma with in situ carcinoma.

Structural Abnormalities: Congenital and Acquired

Structural lesions include congenital bony abnormalities such as Crouzon's disease or craniofacial dysostosis, maxillary hypoplasia, and facial asymmetry (Fig. 3-11). Acquired structural abnormalities are really post-traumatic lesions of the orbit, following all types of physical damage. The most common injury is a direct physical blow (Fig. 3-12), but other injuries result from thermal, chemical, and radiation-induced orbital damage. Included in this category are some of the cysts (dermoids, implantations, lacrimal cysts, mucoceles) and ectopias.

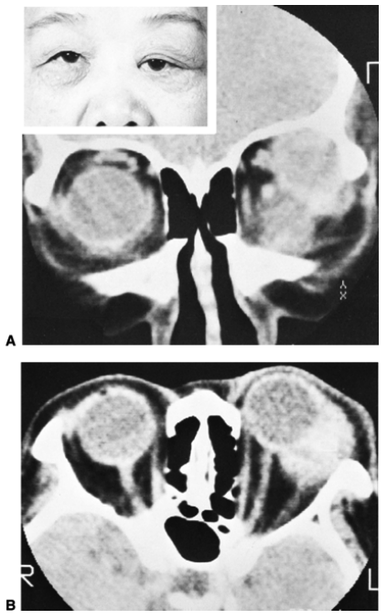

Figure 3-10. (A) This patient had a histologically diagnosed low-grade malignant mucoepidermoid carcinoma of the lacrimal gland with features of longstanding growth. (B) Note bony expansion in contrast to the irregular invasion seen in the malignant mucoepidermoid carcinoma shown in Fig. 3-9. (Reproduced with permission from Rootman J. The clinical evaluation and pathology of tumors of the eye, orbit and lacrimal apparatus. In: Thawley SE, ed. Comprehensive Management of Head and Neck Tumors. Vol 2. Philadelphia: WB Saunders, 1987.)

Vascular Lesions

In our experience, vascular lesions were the fourth most common orbital process. Pathologically, many disorders are included but pathophysiologically, a few fundamental patterns can be seen based on the character of flow or the lack thereof (hemodynamics). The nonobstructive vascular lesions on the arterial side may be either high or low flow (including tumors, malformations, and shunts). Venous malformations are either distensible or nondistensible depending on size and degree of connection to the venous system. Hemodynamically, lymphangiomas are relatively isolated vascular anomalies. There are however many transitional vascular lesions and malformations that consist of a combination of different types of vessels, such as arteriovenous (dural fistula and arteriovenous malformations), venous lymphatic (so-called lymphangiomas), and arteriocapillary (Sturge-Weber and Osler-Rendu or hereditary hemorrhagic telangectasia) lesions. Purely obstructive lesions may be on the arterial or venous side with differing features depending on this relationship.

A classic example of a high-flow tumor on the arterial side is seen in some infantile capillary hemangiomas (Fig. 3-13). These include the strawberry hemangiomas, which may have a spectrum of involvement from local superficial infantile hemangioma to massive facial lesions (complex infantile hemangiomas) with and without multiple external and internal hemangiomatosis. Histologically, they have many vascular channels and typically undergo a cycle of growth followed by spontaneous regression. These high-flow tumors may be intraorbital (deep infantile hemangiomas) and can manifest pulsating exophthalmos due to their rich blood supply.

The cavernous hemangioma is a vascular lesion with low arterial flow. It grows slowly in the orbit of the adult. It is well-defined on ultrasonography, enhances on contrast CT or MR scanning, and shows minimal late pooling on angiography.

With congenital arteriovenous (AV) malformations and acquired arteriovenous fistulas, the communication (shunt)

may also be either large or small, resulting in either high-flow or low-flow lesions. The larger the communication, the more profound the orbital findings. A high-flow acquired shunt demonstrates pulsating exophthalmos, bruit, and marked orbital swelling clinically due to retrograde flow into the venous system, which may be evidenced on CT scan and arteriography. In contrast, a low-flow carotid cavernous fistula may manifest milder elevations of venous pressure leading to dilated episcleral, orbital, and intraocular veins and features of lesser proptosis, raised intraocular pressure, and an absent or minimal bruit. AV malformations in contrast have antigrade flow into and out of the shunt, rather than into the whole of the orbital venous system. Thus they may be characterized by enlarged outflow vessels, pulsation, and intermittent hemorrhage alone.

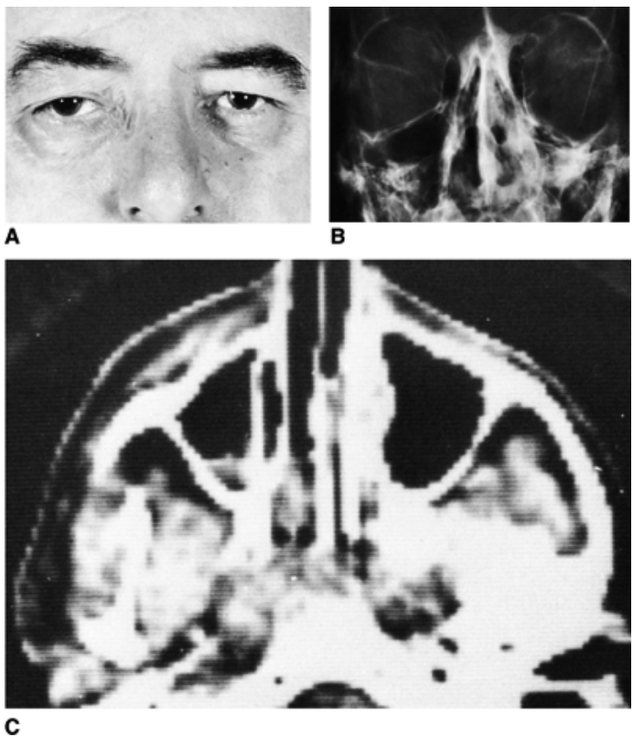

Figure 3-11. (A) A patient with a congenital structural abnormality presented with apparent right proptosis; in fact, he has left enophthalmos. It was due to left maxillary hypoplasia resulting in enlargement of the left orbit, which is shown in radiographs (B) and CT scan (C). (Reproduced with permission from Rootman J. The clinical evaluation and pathology of tumors of the eye, orbit and lacrimal apparatus. In: Thawley SE, ed. Comprehensive Management of Head and Neck Tumors. Vol 2. Philadelphia: WB Saunders, 1987.)

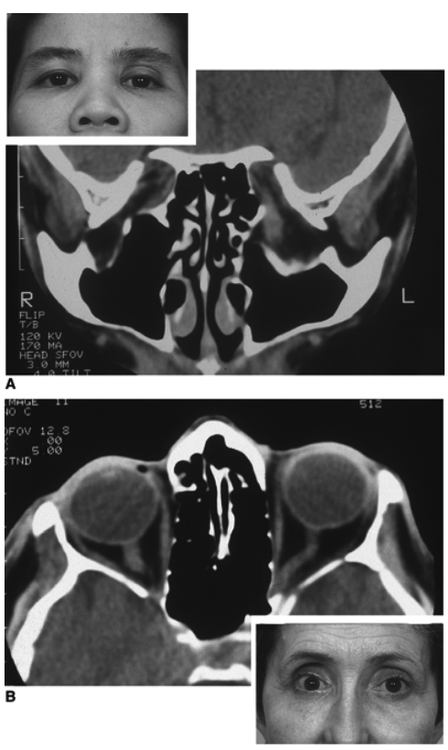

Figure 3-12. Both patients demonstrate post-traumatic enophthalmos with downward displacement of the left (A, inset) and the right (B, inset) eyes and deepening of the superior sulcus secondary to blowout fractures. The CT scans demonstrate blowout of the orbit inferiorly on coronal view (A) and enophthalmos on axial view (B).

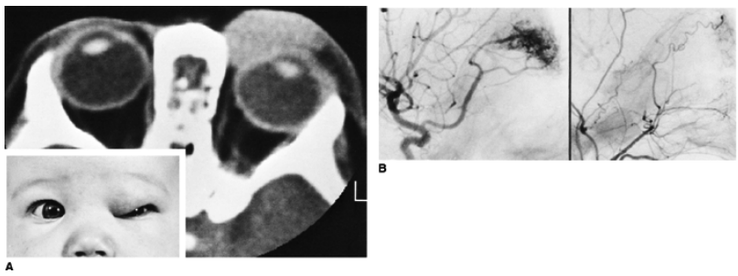

Figure 3-13. This patient demonstrates an infantile capillary hemangioma with high arterial flow. (A) Note the left-sided enhancing mass on CT scan. (B) Rapid arterial filling is shown on both external and internal carotid angiography.

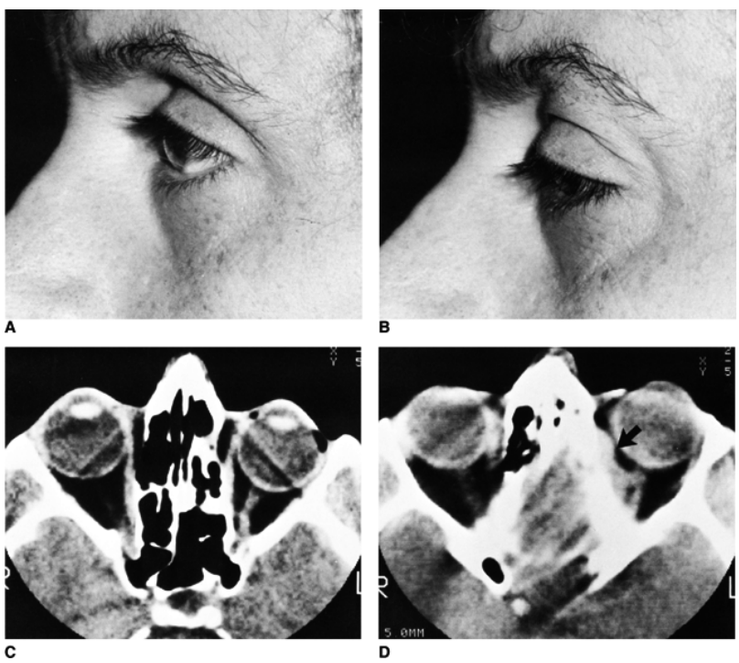

Figure 3-14. This patient has the clinical and CT features of a distensible venous anomaly. (A, C) Note enophthalmos at rest, and (B, D) proptosis on Valsalva maneuver due to filling of the medial varix (arrow). (Figs. 3-14A to C reproduced with permission from Rootman J. The clinical evaluation and pathology of tumors of the eye, orbit and lacrimal apparatus. In: Thawley SE, ed. Comprehensive Management of Head and Neck Tumors. Vol 2. Philadelphia: WB Saunders, 1987.)

On the venous side of the circulation, there are a number of lesions that may have either large venous connections (distensible) or small venous connections (nondistensible). For example, the clinically nondistensible varix has minimal flow, and thus tends to present with spontaneous thrombosis or hemorrhagic episode. However, these may also present as slowly progressive asymptomatic tumors resulting from microscopic thrombosis and hemorrhage. A varix may be, and frequently is, a component of a combined venous lymphatic vascular malformation (so-called lymphangioma). True lymphangiomas are no-flow lesions, as evidenced by persistent pooling following direct injection of contrast dye within them. In contrast, large venous-to-venous shunts (distensible venous vascular malformations) frequently present with enophthalmos and have intermittent proptosis on raising the jugular venous pressure (Fig. 3-14).

Some of the foregoing lesions have either arterial or venous obstructive elements. However, arterial and venous obstruction can be part of other systemic and local processes. An example is a patient who developed postoperative massive swelling of the lid due to a superior ophthalmic vein thrombosis (Fig. 3-15).

Degenerations and Depositions

Degenerations include orbital diseases characterized by atrophy, deposition, and cicatrization. Progressive myopathy and amyloid deposition are examples of degenerative processes and depositions. Another example we encountered is linear scleroderma with facial and orbital atrophy associated with cicatrization of the lid and medial extraocular muscles (Fig. 3-16). On the other hand, orbital fat prolapse through Tenon's capsule may present with the patient having noted a tumor, especially when pressure was applied to the eye. This results from weakening of the orbital connective tissue with age (Fig. 3-17). Progressive myopia is another degenerative process that may present as pseudoproptosis. Finally, localized amyloidosis is an example of a deposition that may occur in the orbit, and leads to functional and structural changes that may reflect an underlying inflammatory or lymphoproliferative pathogenesis.

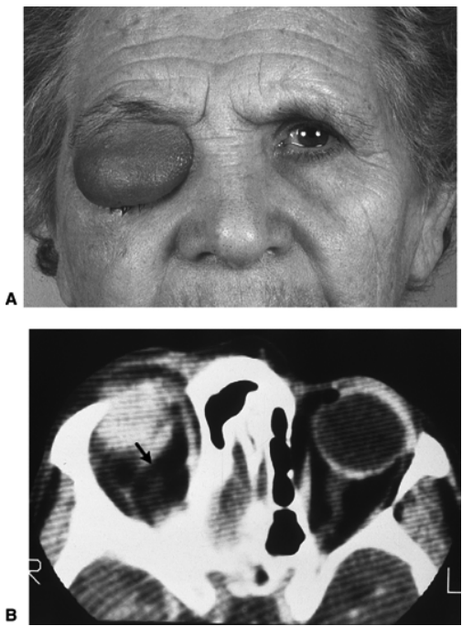

Figure 3-15. (A) This 71-year-old woman presented postcryotherapy for secondary glaucoma with increasing right upper lid pitting edema, which led to peau d'orange, superior chemosis, proptosis (3 mm), and restricted movements. (B) The CT demonstrates the enlarged and obstructing superior ophthalmic vein (arrow). Observation alone led to resolution.

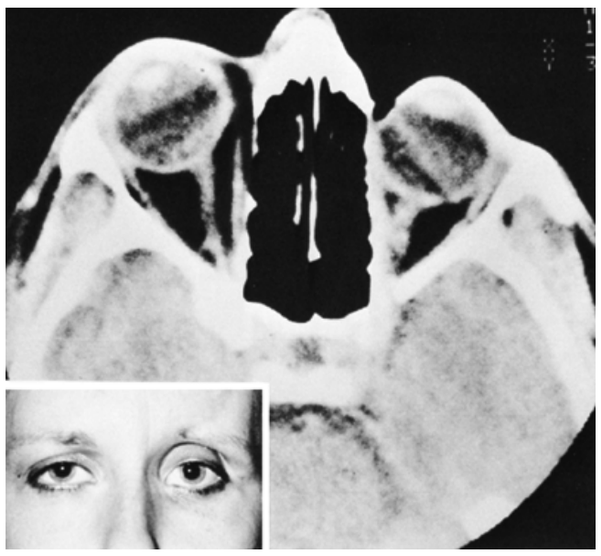

Figure 3-16. This patient has a degenerative disease process. Linear scleroderma was associated with focal frontal dermal and orbital fat atrophy, with scarring of the lid and medial rectus muscle.

The foregoing is meant to serve as a clinically based formulation for thinking about orbital disease. As in all simplifications, it has exceptions. However, for the most part it provides an accurate method of viewing orbital disease in the clinical setting.

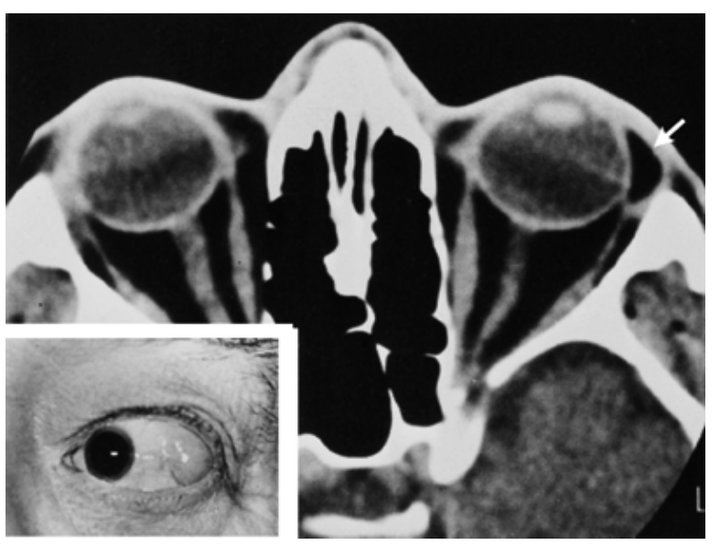

Figure 3-17. A degenerative lesion of the orbit. Note the superior lateral fat prolapse due to a defect in Tenon's capsule (arrow).

Chapter 4

Distribution and Differential Diagnosis of Orbital Disease

Jack Rootman

Wilma Chang

Dean Jones

The aim of this section is to establish a rough context for disease occurrence–in relationship to age, process, diagnosis, and clinical presentation–as a basis for developing differential diagnoses during the patient encounter. The approach should provide a reasoned and focused differential diagnosis appropriate to the individual being examined. Personally, I eschew the philosophy of "listing" diseases, but it is useful to have some broad concept of overall incidence for different age groups and for specific clinical presentations. This chapter will provide an overview of our personal experience as a basis for differential diagnoses for age groups and specific presentations. All of this should be viewed in the context that any series is prejudiced by factors of regional epidemiology, choice of nosology and classification, and special areas of expertise that may lead to referral. Thus, only a broad picture can be obtained from such a review, but it should provide a framework for the analysis of orbital disease. There are a number of excellent series that review orbital disease incidence. The reader is referred to these for comparison with our experience; in particular, the texts by Albert and Jakobiec, Duke-Elder , Henderson , Krohel and coworkers , and Taylor , as well as articles by Kennedy , Iliff and Green , Shields et al. , and Wilson et al.

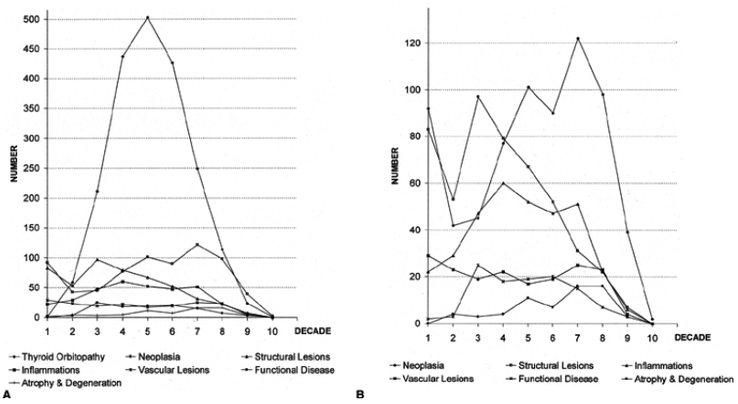

Figure 4-1. Age distribution of all orbital lesions (A) and orbital lesions excluding thyroid orbitopathy (B), University of British Columbia Orbital Clinic, 1976-1999.

Distribution of Orbital Disease

Distribution by Process

Figure 4-1 demonstrates our experience of the broad categories of disease processes encountered at the University of British Columbia Orbital Clinic, and Table 4-1 outlines the specific diagnosis in each category. The major trends noted are the bimodal distribution of neoplasia, the dominance of thyroid orbitopathy in middle life, the gradual decrease in structural disease, and a relatively uniform occurrence of inflammatory, vascular, and degenerative lesions. The changing profiles in each diagnostic category can be seen in Table 4-1 and will be outlined in the next section.

Table 4-1. Age distribution of orbital patients, University of British Columbia Orbital Clinic, 1976-1999

TYPE OF LESION	DECADE 1	2	3	4	5	6	7	8	9	10	TOTAL	%
Thyroid Orbitopathy												
	Thyroid Orbitopathy 52% 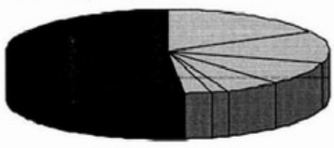											
	1	59	211	437	503	426	249	114	23	1	2024	51.7
Neoplasia												
	Neoplasia 18% 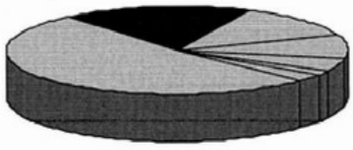											
Neurogenic												
Optic nerve glioma	10	7	4	1	1	1	0	0	0	0	24	0.6
Meningioma												
Optic nerve	0	0	3	6	9	5	5	3	2	0	33	0.8
Sphenoid wing	0	1	2	4	8	11	9	7	0	0	42	1.1
Other	1	0	1	2	2	5	2	0	0	0	13	0.3
Other optic nerve tumors												
Dural melanoma	0	0	0	0	1	0	0	0	0	0	1	0.0
Medulloblastoma	1	0	0	0	0	0	0	0	0	0	1	0.0

TYPE OF LESION	DECADE 1	2	3	4	5	6	7	8	9	10	TOTAL	%
Peripheral nerve sheath tumors												
Neurofibroma	0	0	0	0	1	1	1	0	0	0	3	0.1
Plexiform neurofibroma	2	4	1	2	2	1	0	0	0	0	12	0.3
Schwannoma	1	3	4	6	1	3	2	1	0	0	21	0.5
Schwannoma-malignant	0	0	1	0	1	0	0	0	0	0	2	0.1
Malignant peripheral nerve sheath tumor	2	1	0	0	0	0	0	0	0	0	3	0.1
Neurofibromatosis	7	3	5	4	2	0	2	0	0	0	23	0.6
Rare neurogenic tumors												
Peripheral neuroectodermal tumor (PNET)	2	1	0	0	0	0	0	1	0	0	4	0.1
Granular cell	0	0	0	0	1	0	0	0	0	0	1	0.0
Optic nerve choristoma	0	0	0	1	0	0	0	0	0	0	1	0.0
Other neoplasms of the CNS	0	0	0	0	1	0	0	0	0	0	1	0.0
Lymphoma	0	1	0	0	0	0	0	0	0	0	1	0.0
Astrocytoma	1	0	0	1	1	0	1	0	0	0	4	0.1
Carcinomatous meningitis	0	0	0	1	0	0	0	0	0	0	1	0.0
Dilated optic nerve sheath	0	0	0	0	0	1	0	0	0	0	1	0.0
Total neurogenic	27	21	21	28	31	28	22	12	2	0	192	4.9
Lymphoproliferative												
Lymphocytic												
Reactive lymphoid hyperplasia	0	1	0	0	6	1	0	0	0	0	8	0.2
Atypical lymphoid hyperplasia	0	0	0	0	2	1	0	2	1	0	6	0.2
Lymphoma	0	0	1	1	10	14	24	33	12	1	96	2.5
Conjunctival lymphoma	0	1	1	2	3	2	3	4	1	0	17	0.4
Sclerosing lymphoma	0	0	0	0	0	0	1	1	0	0	2	0.1
Plasma cell tumors												
Reactive	0	0	0	0	0	0	0	1	0	0	1	0.0
Myeloma	0	0	0	0	0	1	3	3	0	0	7	0.2
Plasmacytoma	0	0	0	0	0	1	0	2	0	0	3	0.1
Other												
T-cell lymphoma	0	0	1	0	0	1	0	0	0	0	2	0.1
Hodgkin's	0	0	1	0	0	0	0	0	0	0	1	0.0
Leukemia	0	0	1	0	1	0	2	0	0	0	4	0.1
Chloroma	3	0	0	0	0	0	0	0	0	0	3	0.1
Myelogenous leukemia	0	0	0	1	0	0	0	0	0	0	1	0.0
Histiocytoses												
Langerhans cell histiocytosis	8	0	0	0	0	0	0	0	0	0	8	0.2
Malignant histiocytosis	0	0	0	0	1	0	0	0	0	0	1	0.0
Total lymphoproliferative	11	2	5	4	23	21	33	46	14	1	160	4.1
Vascular Neoplasia												
Capillary hemangioma (infantile)	35	0	0	0	0	0	0	0	0	0	35	0.9
Cavernous hemangioma	0	0	1	17	15	10	3	2	1	0	49	1.3
Hemangiopericytoma	0	0	3	0	0	2	1	1	0	0	7	0.2

TYPE OF LESION	DECADE 1	2	3	4	5	6	7	8	9	10	TOTAL	%
Angiosarcoma	0	0	0	0	0	0	0	1	1	0	2	0.1
Pyogenic granuloma	0	0	0	0	0	0	1	0	0	0	1	0.0
Total vascular neoplasia	35	0	4	17	15	12	5	4	2	0	94	2.4
Secondary Tumors												
Nasopharynx												
Squamous	0	1	0	1	3	1	2	2	0	0	11	0.3
Transitional cell	0	0	0	0	0	0	1	0	0	0	1	0.0
Adenoid cystic	0	0	0	0	0	0	2	1	0	0	3	0.1
Mucoepidermoid	0	1	0	0	1	0	0	0	0	0	2	0.1
Neuroendocrine	0	0	0	0	1	0	0	0	1	0	3	0.1
Melanoma	0	0	0	0	0	0	2	0	0	0	2	0.1
Adenocarcinoma	0	0	0	0	0	1	0	2	0	0	3	0.1
Lymphoma	0	0	0	0	0	0	1	1	0	0	2	0.1
Rhabdomyosarcoma	1	0	0	1	0	0	0	0	0	0	2	0.1
Malignant fibrous histiocytoma	0	0	0	0	0	0	1	0	0	0	1	0.0
Hemangiopericytoma	0	0	0	0	0	0	1	0	0	0	1	0.0
Esthesioneuroblastoma	0	0	1	0	0	0	0	0	0	0	1	0.0
Lid												
Basal cell	0	0	0	0	1	1	3	3	2	0	10	0.3
Squamous	0	0	0	1	0	0	3	1	2	0	7	0.2
Sebaceous	0	0	0	1	0	0	2	1	0	0	4	0.1
Melanoma	0	0	0	0	0	0	0	1	0	0	1	0.0
Pleomorphic adenoma	0	0	0	1	0	0	0	0	0	0	1	0.0
Spindle cell tumor	0	0	0	0	0	1	0	0	0	0	1	0.0
Conjunctiva												
Melanoma	0	0	0	1	0	1	1	1	3	0	7	0.2
Squamous	0	0	0	0	0	0	2	4	2	1	9	0.2
Ocular												
Melanoma	1	0	0	0	0	3	1	1	2	0	8	0.2
Malignant fibrous histiocytoma	1	0	0	0	0	0	0	0	0	0	1	0.0
Lacrimal sac												
Transitional cell	0	0	0	0	0	1	2	0	0	0	3	0.1
Squamous	0	0	0	0	1	0	1	1	0	0	3	0.1
Fibrous histiocytoma	0	0	0	1	0	0	0	0	0	0	1	0.0
Other contiguous site	0	0	0	1	0	0	1	2	0	0	4	0.1
Total secondary tumors	3	2	1	8	7	9	26	21	12	1	92	2.3
Mesenchymal												
Striated muscle												
Rhabdomyosarcoma	5	3	0	0	0	0	0	0	0	0	8	0.2
Fibrous tissue												
Fibrosarcoma	1	0	0	0	0	0	0	0	0	0	1	0.0

TYPE OF LESION	DECADE 1	2	3	4	5	6	7	8	9	10	TOTAL	%
Histiocytic												
Benign fibrous histiocytoma	1	0	0	1	1	1	0	0	0	0	4	0.1
Malignant fibrous histiocytoma	1	0	0	0	0	0	1	0	0	0	2	0.1
Solitary fibrous tumor	0	0	0	0	1	0	0	0	0	0	1	0.0
Reactive bone tumors												
Cholesterol granuloma	0	0	0	1	2	2	0	1	0	0	6	0.2
Giant cell granuloma	0	0	1	0	0	0	0	0	0	0	1	0.0
Aneurysmal bone cyst	1	1	0	0	0	0	0	0	0	0	2	0.1
Brown tumor	0	0	0	0	0	0	1	0	0	0	1	0.0
Benign Fibro-osseous Lesions												
Fibrous dysplasia	1	3	3	2	0	1	1	0	0	0	11	0.3
Osteoma	0	4	2	3	1	0	1	0	0	0	11	0.3
Chondroma	0	0	1	0	0	0	0	0	0	0	1	0.0
Ossifying Fibroma (psammomatoid)	0	0	1	0	0	0	0	0	0	0	1	0.0
Malignant Bone Lesions												
Ewing's sarcoma	2	1	0	0	0	0	0	0	0	0	3	0.1
Chondrosarcoma	0	0	0	0	2	1	0	0	0	0	3	0.1
Osteogenic sarcoma	1	1	0	0	0	0	0	0	0	0	2	0.1
Intraosseous hemangioma	0	0	0	0	0	0	1	0	0	0	1	0.0
Other												
Epithelioid sarcoma	0	1	0	0	0	0	0	0	0	0	1	0.0
Liposarcoma	0	1	1	0	0	0	0	0	0	0	2	0.1
Rhabdoid tumor	1	0	0	0	0	0	0	0	0	0	1	0.0
Leiomyoma	1	0	0	0	0	0	0	0	0	0	1	0.0
Total mesenchymal	15	15	9	7	7	5	5	1	0	0	63	1.6
Metastatic												
Carcinoma												
Breast	0	0	0	2	3	6	7	1	1	0	20	0.5
Prostate	0	0	0	0	0	1	3	2	1	0	7	0.2
Gastrointestinal	0	0	0	0	0	0	1	1	0	0	2	0.1
Lung	0	0	0	0	1	1	2	1	0	0	5	0.1
Thyroid	0	0	0	0	0	0	1	0	0	0	1	0.0
Unknown	0	0	0	0	0	1	1	0	1	0	3	0.1
Pancreas	0	0	0	0	0	1	0	0	0	0	1	0.0
Adenocarcinoma	0	0	0	1	1	0	2	2	3	0	9	0.2
Carcinoid	0	0	0	0	0	0	0	0	1	0	1	0.0
Sarcoma												
Liposarcoma	0	0	0	0	0	0	1	0	0	0	1	0.0
Neuroblastoma	1	0	0	0	0	0	0	0	0	0	1	0.0
Melanoma	0	0	1	1	0	1	4	0	2	0	9	0.2
Fibrosarcoma	0	0	0	0	0	0	0	0	0	0	0	0.0
Total metastatic	1	0	1	4	5	11	22	7	9	0	60	1.5

TYPE OF LESION	DECADE 1	2	3	4	5	6	7	8	9	10	TOTAL	%
Lacrimal												
Benign Epithelial Lesions												
Pleomorphic adenoma	0	0	4	5	5	4	2	2	0	0	22	0.6
Carcinoma in pleomorphic adenoma	0	0	0	1	1	0	0	0	0	0	2	0.1
Myoepithelioma/spindle cell	0	0	0	0	1	0	0	0	0	0	1	0.0
Malignant Epithelial Lesions												
Adenoid cystic	0	2	0	3	5	0	0	2	0	0	12	0.3
Carcinoma ex pleomorphic adenoma	0	0	0	0	1	0	3	1	0	0	5	0.1
Muccepidermoid ex pleomorphic adenoma	0	0	0	0	0	0	2	1	0	0	3	0.1
Adenocarcinoma	0	0	0	0	0	0	0	1	0	0	1	0.0
Polymorphous low-grade adenocarcinoma	0	0	0	0	0	0	1	0	0	0	1	0.0
Ductal adenocarcinoma	0	0	0	0	0	0	1	0	0	0	1	0.0
Total lacrimal	0	2	4	9	13	4	9	7	0	0	48	1.2
Total Neoplasia	**92**	**42**	**45**	**77**	**101**	**90**	**122**	**98**	**39**	**2**	**710**	**18.1**

Structural Lesions

Structural Lesions 13%

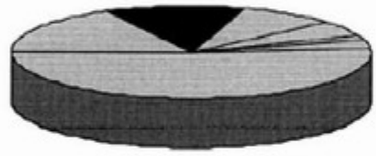

Congenital												
Cystic Lesion												
Dermoids and epidermoids	45	6	9	7	2	2	3	0	1	0	75	1.9
Microphthalmos with cyst	3	0	0	1	0	0	0	0	0	0	4	0.1
Sweat gland cyst	0	0	1	0	1	0	0	0	0	0	2	0.1
Rathke pouch cyst	0	1	0	0	0	0	0	0	0	0	1	0.0
Muscle cyst	0	0	0	0	1	0	0	0	0	0	1	0.0
Other cyst	3	1	1	1	2	0	0	0	0	0	8	0.2
Implantation cyst	1	3	1	1	1	1	0	1	0	0	9	0.2
Arachnoid cyst	0	0	0	0	0	0	0	1	0	0	1	0.0
Respiratory cyst	0	0	1	1	0	0	0	0	0	0	2	0.1
Bone Anomaly												
Asymmetry	4	2	6	10	8	15	4	1	2	0	52	1.3
Shallow orbits	2	0	0	0	0	0	0	0	0	0	2	0.1
Pfeiffer's syndrome	1	0	0	0	0	0	0	0	0	0	1	0.0
Maxillary hypoplasm	0	0	0	0	0	0	1	0	0	0	1	0.0
Other	0	1	0	0	0	1	0	0	0	0	2	0.1
Ectopia												
Dermolipoma	11	3	10	3	1	1	0	0	0	0	29	0.7

TYPE OF LESION	DECADE 1	2	3	4	5	6	7	8	9	10	TOTAL	%
Fat in cavernous sinus	0	0	0	0	0	1	0	0	0	0	1	0.0
Total congenital lesions	70	17	29	24	16	21	8	3	3	0	191	4.9
Acquired												
Cystic Lesion												
Mucocele	0	1	7	9	7	7	5	11	2	0	49	1.3
Implantation cyst (acquired)	0	0	0	0	1	1	0	0	0	0	2	0.1
Lacrimal cyst	1	0	3	6	7	5	1	0	0	0	23	0.6
Polyposis	0	0	0	0	0	2	0	1	0	0	3	0.1
Lacrimal sac mucocele	0	0	0	0	1	0	1	0	0	0	2	0.1
Encephalocele	0	0	0	0	1	0	0	0	0	0	1	0.0
Trauma												
Orbital fracture(s)	8	20	29	17	14	5	6	2	0	0	101	2.6
Soft tissue trauma	1	6	5	2	3	3	2	2	0	0	24	0.6
Foreign body trauma	2	4	4	2	3	2	1	1	0	0	19	0.5
Traumatic hemorrhage	0	1	3	0	0	1	0	0	0	0	5	0.1
Orbital emphysema	0	0	0	0	0	1	0	0	0	0	1	0.0
Post-traumatic neuropathy	1	2	3	4	0	1	1	0	0	0	12	0.3
Post-traumatic enophthalmos	0	0	11	5	8	0	2	0	1	0	27	0.7
Post-traumatic, other	0	0	2	1	2	0	0	0	0	0	5	0.1
Pseudoproptosis	0	0	1	6	2	1	3	1	1	0	15	0.4
Blepharochalasis	0	2	0	1	0	1	1	0	0	0	5	0.1
Lid retraction	0	0	0	2	2	1	0	1	0	0	6	0.2
Total acquired lesions	13	36	68	55	51	31	23	19	4	0	300	7.7
Total structural lesions	**83**	**53**	**97**	**79**	**67**	**52**	**31**	**22**	**7**	**0**	**491**	**12.5**

Inflammatory Lesions

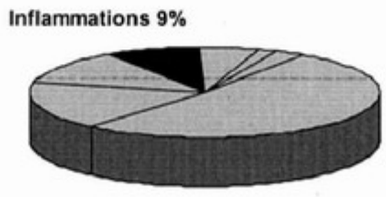

Infectious												
Microbial inflammation												
Sinusitis	7	9	5	4	2	3	4	1	2	0	37	0.9
Other microbial inflammation	2	1	4	5	2	1	3	3	2	0	23	0.6
Conjunctivitis	1	0	0	1	0	1	0	0	0	0	3	0.1
Dacryoadenitis	0	0	1	0	1	2	2	0	0	0	6	0.2
Osteomyelitis	0	0	1	1	0	0	0	1	0	0	3	0.1
Parasitic inflammation	1	0	0	1	1	0	0	0	0	0	3	0.1

TYPE OF LESION	DECADE 1	2	3	4	5	6	7	8	9	10	TOTAL	%
Fungal infection												
Mucormycosis	0	0	0	0	0	1	0	1	0	0	2	0.1
Aspergillosis	0	0	0	0	0	0	1	0	1	0	2	0.1
Other	0	0	0	2	0	0	0	0	0	0	2	0.1
Inflammatory fistula	0	0	0	0	0	1	0	0	0	0	1	0.0
Total infectious	11	10	11	14	6	9	10	6	5	0	82	2.1
Nonspecific Inflammation												
Acute & subacute idiopathic inflammation												
Anterior	1	5	4	4	2	3	3	2	0	0	24	0.6
Diffuse	0	1	0	0	0	0	2	0	0	0	3	0.1
Myositic	3	4	11	13	11	8	5	1	0	0	56	1.4
Apical	0	1	0	0	4	3	2	1	0	0	11	0.3
Lacrimal	0	3	3	6	7	4	3	1	1	0	28	0.7
Superior oblique tendonitis	0	0	0	0	1	1	0	0	0	0	2	0.1
Nonspecific granulomatous inflammation	0	0	2	1	0	1	1	0	0	0	5	0.1
Total nonspecific inflammation	4	14	20	24	25	20	16	5	1	0	129	3.3
Other Orbital Inflammation												
Sarcoidosis	0	1	1	3	1	1	1	1	0	0	9	0.2
Sarcoid reaction	0	0	1	1	1	2	3	2	0	0	10	0.3
Sclerosing nonspecific inflammation	2	1	2	6	3	5	3	1	0	0	23	0.6
Sjogren's Syndrome	0	0	1	2	5	3	1	1	0	0	13	0.3
Vasculitis												
Systemic lupus	0	0	1	0	0	0	0	0	0	0	1	0.0
Wegener's granulomatosis	3	1	3	2	5	1	6	0	0	0	21	0.5
Orbital vasculitis	0	1	0	0	0	0	1	1	0	0	3	0.1
Leukocytoclastic vasculitis	0	0	1	0	0	2	1	1	0	0	5	0.1
Ocular inflammations with orbital signs												
Scleritis	0	1	1	3	4	2	4	3	0	0	18	0.5
Cogan's Syndrome	0	0	0	1	0	0	0	0	0	0	1	0.0
Tolosa-Hunt Syndrome	0	0	2	3	1	1	1	0	0	0	8	0.2
Unknown inflammation	0	0	1	0	0	1	0	0	0	0	2	0.1
Melkersson-Rosenthal syndrome	0	0	0	0	0	0	1	0	0	0	1	0.0
Necrobiotic xanthogranuloma	0	0	0	0	0	0	1	0	0	0	1	0.0
Adult-onset asthma with xanthogranuloma	0	0	0	0	1	0	1	1	0	0	3	0.1
Pseudorheumatoid nodule	1	0	2	0	0	0	0	0	0	0	3	0.1
Angiolymphoid hyperplasia with eosinophillia	1	0	0	1	0	0	1	0	0	0	3	0.1
Total other orbital inflammation	7	5	16	22	21	18	25	11	0	0	125	3.2
Total inflammatory lesions	**22**	**29**	**47**	**60**	**52**	**47**	**51**	**22**	**6**	**0**	**336**	**8.6**

TYPE OF LESION	DECADE 1	2	3	4	5	6	7	8	9	10	TOTAL	%
Vascular Lesions												
	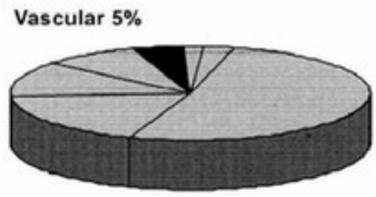											
Arteriovenous Lesion												
Malformation	2	2	0	1	0	0	0	0	0	0	5	0.1
Adult malformation	0	0	1	3	0	0	0	0	0	0	4	0.1
Shunt/Fistula	0	1	1	4	4	10	11	13	3	0	47	1.2
Venous lesion												
Nondistensible varix	3	4	0	3	2	2	1	1	1	0	17	0.4
Distensible Varix	1	2	9	5	5	3	3	3	0	0	31	0.8
Malformation	2	0	0	2	0	1	1	0	0	0	6	0.2
Thrombosis	0	0	0	0	1	0	0	2	0	0	3	0.1
Venous lymphatic malformation												
(lymphangioma)	18	13	6	3	1	0	1	1	0	0	43	1.1
Adult lymphangioma	0	0	0	0	1	2	1	0	0	0	4	0.1
Combined lymphangioma-varix	3	1	0	0	1	0	0	0	0	0	5	0.1
Lymphedema	0	0	1	1	0	0	0	0	0	0	2	0.1
Angioneurotic edema	0	0	1	0	0	0	0	0	0	0	1	0.0
Spontaneous hemorrhage	0	0	0	0	0	1	2	0	0	0	3	0.1
Arterial ischemia	0	0	0	0	0	0	2	2	0	0	4	0.1
Superior ophthalmic vein thrombosis	0	0	0	0	1	0	2	1	0	0	4	0.1
Carotid cavernous aneurysm	0	0	0	0	1	0	1	0	0	0	2	0.1
Total vascular lesions	**29**	**23**	**19**	**22**	**17**	**19**	**25**	**23**	**4**	**0**	**181**	**4.6**
Atrophy and Degeneration												
	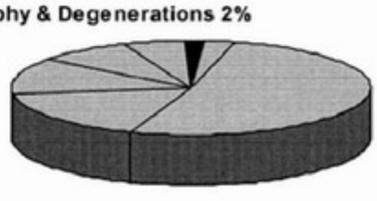											
Post-irradiation	0	1	1	0	2	1	1	2	0	0	8	0.2
Idiopathic (lipodystrophy)	0	0	0	0	0	0	0	1	0	0	1	0.0

TYPE OF LESION	DECADE 1	2	3	4	5	6	7	8	9	10	TOTAL	%
Other												
Myopia	0	0	0	0	0	0	1	0	0	0	1	0.0
Scleroderma	0	0	0	1	1	1	0	0	0	0	3	0.1
Fat Prolapse	0	2	0	0	3	1	11	11	2	0	30	0.8
Progressive external ophthalmoplegia	0	0	1	1	0	0	1	0	0	0	3	0.1
Mitochondrial dystrophy	0	0	0	0	0	1	0	0	0	0	1	0.0
Ptosis	0	2	0	1	2	0	0	1	0	0	6	0.2
Enophthalmos	0	0	1	0	0	1	0	0	0	0	2	0.1
Exophthalmos (due to myopic change)	0	0	0	1	2	0	1	0	0	0	4	0.1
Depositions	0	0	0	0	1	1	1	0	1	0	4	0.1
Orbital nerve palsy	0	0	0	0	0	1	0	1	0	0	2	0.1
Total atrophy and degeneration	**0**	**5**	**3**	**4**	**11**	**7**	**16**	**16**	**3**	**0**	**65**	**1.7**

Functional Disease

Functional Disease 3%

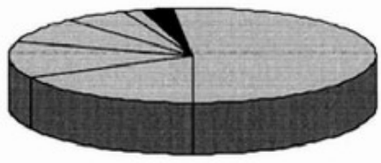

Orbital pain	0	1	9	10	8	9	7	4	2	0	50	1.3
Pseudotumor cerebri	0	1	9	4	4	1	1	0	0	0	20	0.5
Optic nerve sheath swelling												
Ischemic optic neuropathy	0	0	0	1	1	1	1	1	0	0	5	0.1
Papilledema	0	1	3	0	1	1	2	0	0	0	8	0.2
Orbital swelling	0	0	2	2	2	3	1	0	1	0	11	0.3
Chronic chemosis	0	0	0	1	0	0	1	0	0	0	2	0.1
Not yet diagnosed	2	0	2	0	3	5	2	2	0	0	16	0.4
Total functional disease	**2**	**3**	**25**	**18**	**19**	**20**	**15**	**7**	**3**	**0**	**112**	**2.9**

TOTAL	**3919**	**100.0**

Distribution by Diagnosis

The individual diseases will be discussed in detail; however, it is useful to look at their overall occurrence within the broad age groups of childhood and adolescence (age up to 16 years), middle adult life (17 to 64 years), and the elderly (65 years and over).

The incidence of orbital lesions in order of occurrence in childhood and adolescence provide a framework for the differential diagnosis in this age group (Table 4-2). Under the age of two, the two most common lesions were neoplasia and structural disorders, the leading neoplasm being capillary hemangioma and the leading structural lesion being dermoid and epidermoid cysts. Between 2 and 16 years of age, the most common lesions were structural, including orbital trauma, dermoid and epidermoid cysts, and other bony abnormalities. Orbital asymmetry with pseudoproptosis was not infrequent in this age group and should be considered in the differential diagnosis of orbital disease of childhood and adolescence. Neoplasia are the next in order of occurrence and are dominated by neurogenic and mesenchymal tumors. Orbital inflammation was roughly divided 3:2 between infections and acute and subacute idiopathic orbital inflammations, both of which are dominated clinically by obvious inflammatory signs and symptoms. Vascular lesions constituted approximately 14% of all diagnoses and were dominated by combined venous lymphatic malformations (lymphangiomas). Thyroid orbitopathy was the next most common in this age group and was typically mild. We have also noticed a steady decline in neoplasia and structural lesions from age 2 to 17, with a concurrent rise in inflammatory disorders.

In adult life, the order of occurrence of the common lesions was thyroid orbitopathy, neoplasia, structural lesions, and inflammations. Neoplastic disorders in this age group tend to be predominantly primary tumors, particularly neurogenic, lymphoproliferative, vascular, and secondary. About 11% of all neoplasia in this group were secondary in origin. The next category of lesion was structural. These were largely trauma and acquired cystic lesions, such as mucoceles and implantation cysts. In this age group, some congenital bony anomalies also appeared, including orbital asymmetry. Nonspecific and specific orbital inflammations occur with about equal frequency.

Of those patients 65 years of age and older, thyroid orbitopathy remained the most common lesion, followed closely by neoplasia, which were in order of occurrence lymphoproliferative, secondary, and neurogenic. The inflammations seen in this age group were roughly equal in terms of specific disorders and infections. Mucoceles were the most common structural lesions, and acquired arterial venous shunts were the most common vascular disorders.

Table 4-2. Orbital disease by age cohort, University of British Columbia Orbital Clinic, 1976-1999

	NUMBER	% OF COHORT
Age < 2 Years (n=82)		
Neoplasia	**37**	**45.1**
Capillary hemangioma	29	
Structural Lesions	**35**	**42.7**
Congenital cysts	25	
Age 2 to 16 Years (n=280)		
Structural Lesions	**83**	**29.6**
Orbital trauma	31	
Dermoid & epidermoid	31	
Neoplasia	**78**	**27.9**
Neurogenic	38	
Mesenchymal	20	
Inflammation	**43**	**15.4**
Infections	19	
Nonspecific inflammations	14	
Vascular Lesions	**38**	**13.6**
Lymphangioma/combined venous lymphatic lesion	26	
Thyroid Orbitopathy	**27**	**9.6**
Age 17 to 64 Years (n=4126)		
Thyroid Orbitopathy	**1743**	**42.2**
Neoplasia	**377**	**9.1**
Neurogenic	121	
Lymphoproliferative & hematopoietic	68	
Vascular	50	
Secondary	43	
Structural Lesions	**337**	**8.1**
Orbital trauma	152	
Acquired cystic	62	
Congenital bone anomaly	43	
Inflammations	**245**	**5.9**
Nonspecific orbital inflammations	107	
Specific inflammation	95	
Total > 65 Years (n=646)		
Thyroid Orbitopathy	**254**	**39.3**
Neoplasia	**203**	**31.4**
Lymphoproliferative & hematopoietic	83	
Secondary	44	
Neurogenic	27	
Inflammations	**52**	**8.0**
Specific inflammation	22	
Infections	20	

The profile of orbital disease in the various age groups allows for some useful generalizations. For example, non-thyroid orbital inflammatory disease is dominated by infections in childhood; by an equal occurrence of nonspecific and specific inflammations in middle life, and by vasculitic and granulomatous processes in the elderly. Neoplastic disease shows a similar change in pattern. Childhood and adolescence is dominated by primary tumors, while middle life is dominated by the occurrence of primary tumors and lesser numbers of secondary neoplasia. Late adult life is dominated by secondary, metastatic, and generally malignant neoplasia. As would be expected, children and adolescents suffer traumatic and congenital structural lesions, whereas adult and elderly patients develop acquired structural lesions that are primarily mucoceles and posttraumatic disorders. Lymphomas begin to occur in adult life but are the predominant neoplasm of the orbit in the elderly.

Distribution by Location

Some diseases are restricted to or more common in certain orbital areas, and this information can provide a context for differential diagnoses based on location. For instance, in general the most common locations are in the superior and anterior orbit (Tables 4-3 ,4-4 ,4-5). Medial and inferior lesions originate largely from the sinus, whereas lacrimal tumors and inflammations are by definition superolaterally located.

In terms of anterior-posterior location (Table 4-4), lymphoproliferative disease was the commonest anterior disorder, and either vascular malformations or neoplasia dominated the midorbit. The posterior orbit had neurogenic neoplasia as its most common lesion. By quadrant (Table 4-5), lymphoproliferative lesions were the most common superiorly and medially. Neurogenic lesions dominated the central orbit.

Table 4-3. Location of non-thyroid orbital disease, University of British Columbia Orbital Clinic, 1976-1999

	NUMBER	%
Anterior-Posterior Position		
Anterior orbit	693	37
Mid-orbit	486	26
Posterior orbit	302	16
Diffuse	71	4
Quadrant		
Superior	719	38
Lateral	547	29
Medial	401	21
Inferior	296	16
Diffuse	185	10
Central	184	10

Table 4-4. Most common non-thyroid orbital diseases by anterior-posterior location within the orbit, University of British Columbia Orbital Clinic, 1976-1999

	NUMBER	% OF AREA
Anterior orbit (693)		
Lymphoproliferative disease	100	14
Congenital cystic lesion	64	9
Vascular malformation	63	9
Trauma	60	9
Specific inflammation	51	7
Vascular neoplasia	42	6
Secondary neoplasia	41	6
Nonspecific inflammation	40	6
Mid-orbit (486)		
Trauma	63	13
Vascular malformation Lymphangioma (33)	61	13
Vascular neoplasia	47	10
Lymphoproliferative disease	42	9
Neurogenic neoplasia	38	8
Nonspecific inflammation	33	7
Specific inflammation	28	6
Mesenchymal neoplasia	27	6
Posterior orbit (302)		
Neurogenic neoplasia Sphenoid wing meningioma (33) Peripheral nerve sheath (18)	80	25
Vascular malformation Lymphangioma (21) Fistula (13)	57	19
Vascular neoplasia	23	8
Mesenchymal neoplasia	22	7
Specific inflammation	22	7
Diffuse (71)		
Trauma	19	27
Shunt/fistula	8	11
Neurogenic neoplasia	7	10
Asymmetry	6	8

Table 4-5. Most common non-thyroid orbital diseases per orbital quadrant, University of British Columbia Orbital Clinic, 1976-1999

	NUMBER	% OF QUADRANT
Superior (downward displacement) [719]		
Lymphoproliferative disease Lymphoma (72)	96	13
Specific inflammation	67	9
Vascular malformation Lymphangioma (24) Varix (16)	66	9
Congenital cystic lesion Dermoid/epidermoid (55)	64	9
Acquired cystic lesion Mucocele (37)	61	8
Nonspecific inflammation	52	7
Lateral (Inward displacement) [547]		
Lymphoproliferative disease Lymphoma (36)	51	9
Congenital cystic lesion	51	9
Specific inflammation	51	9
Nonspecific inflammation Lacrimal inflammation (29)	50	9
Neurogenic neoplasia Sphenoid wing meningioma (28)	48	9
Medial (outward displacement) [401]		
Lymphoproliferative disease	50	12
Orbital trauma	40	10
Secondary neoplasia	34	8
Acquired cystic lesion Mucocele (33)	34	8
Infection Sinusitis/cellulitis (33)	33	8
Mesenchymal neoplasia	26	6
Inferior (upward displacement) [296]		
Orbital trauma	66	22
Vascular malformation Varix (16) Lymphangioma (10)	33	11
Lymphoproliferative disease	29	10
Vascular neoplasia	23	8
Secondary neoplasia	21	7
Diffuse (axial displacement) [185]		
Orbital trauma	32	17
Asymmetry	21	11
Shunt/fistula	14	8
Central (axial displacement) [184]		
Neurogenic neoplasia Optic nerve meningioma (25) Optic nerve glioma (20)	71	39
Functional disease Optic nerve sheath swelling (13) Pseudotumor cerebri (12)	30	16
Structural lesion Orbital trauma (18)	25	14
Inflammation Specific inflammation (8)	16	9
Vascular neoplasia Cavernous hemangioma (7)	10	5

Distribution by Clinical Presentation

Temporal Onset

Temporal onset has been divided into six categories: congenital, catastrophic (hours to days), acute (days), subacute (days to weeks), chronic-months (1 to 12 months), and chronic-years (over 12 months) (Table 4-6). Catastrophic onset is dominated by infections whereas the majority of acute onset lesions are inflammatory lesions, vascular lesions, and much less frequently, rapidly developing neoplasia. Acute onset diseases are dominated by infection and inflammation, shunts, and more rarely metastatic tumors. Subacute lesions are dominated by neoplasia, inflammations (especially specific), and to a lesser degree lesions of structural origin. Chronic lesions are dominated by the occurrence of neoplasia and specific inflammatory disorders, particularly low-grade and infiltrative inflammations.

Clinical Process

As noted, the major clinical processes that can be identified on examination of a patient are mass effect, inflammation, infiltration, and vascular features of diseases (Table 4-7). The major category of clinical presentation was mass effect; approximately 58% of patients with non-thyroid orbital disease presented with some sort of displacement. The two categories of disease presenting primarily as displacement were neoplasia and structural lesions, and less often either vascular or inflammatory lesions. The most common neoplasia presenting as masses were neurogenic and lymphoproliferative, whereas posttraumatic and congenital lesions dominated the structural diseases with mass effect. In the vascular category, combined venous lymphatic malformations were the most common. Of the inflammations that appeared primarily as masses, these were largely low-grade chronic disorders such as granulomas, sarcoid, and sclerosing inflammations.

Patients who had clinically obvious inflammatory disease were of course primarily those whose final diagnosis included nonspecific inflammations (dominated by myositis), specific inflammations (dominated by granulomatous and sclerosing disorders), and infections largely originating from the sinus. The only other major causes of inflammatory presentations were acquired cystic lesions and posttraumatic inflammation. Of the mucoceles in this category, those associated with inflammation were usually pyomucoceles. Only a small minority of patients with neoplastic and vascular disorders presented with pseudoinflammatory features. The neoplasia that we encountered in this group included occasional lymphomas,

meibomian carcinoma, and secondary neoplasia. Vascular lesions with signs and symptoms suggestive of inflammation were either manifestations of superior ophthalmic vein thrombosis or lymphedema.

ONSET	<2 YEARS	NO.	2 TO 16 YEARS	NO.	17 TO 64 YEARS	NO.	65+ YEARS (n=646)	NO.
Catastrophic	TOTAL	3	TOTAL	31	TOTAL	140	TOTAL	11
	Infection	2	Orbital trauma	28	Orbital trauma	124	Orbital trauma	7
	Trauma	1						
Acute	TOTAL	2	TOTAL	43	TOTAL 169		TOTAL	61
	Lymphoproliferative neoplasia		Inflammations		Orbital inflammations		Infections	11
	Trauma	1	Infections	14	Microbial infections	29	Shunts/fistulas	9
			Sinusitis	11	Specific inflammations	18	Neoplasia	
			Nonspecific inflammations	7	Nonspecific inflammations	34	Lymphoproliferative	7
			Vascular		Vascular lesions	17	Metastatic	5
			Lymphangioma	7	Orbital trauma	11	Secondary	4
					Neoplasia	10		
Subacute	TOTAL	12	TOTAL	22	TOTAL	147	TOTAL	47
	Capillary hemangioma	7	Neoplasia	12	Orbital inflammations		Lymphoproliferative	
			Orbital inflammation	4	Nonspecific inflammations	34	neoplasia	10
			Structural lesions	4	Specific inflammations	21	Orbital inflammations	8
					Neoplasia		Structural lesions	6
					Lymphoproliferative	17		
					Metastatic	11		
					Structural lesions (18)			
					Acquired cystic	7		
					Orbital trauma	7		
Chronic-months	TOTAL	28	TOTAL	67	TOTAL	311	TOTAL	141
	Capillary hemangioma	11	Neoplasia		Neoplasia		Neoplasia	
	Dermoids/epidermoids	10	Neurogenic	11	Lymphoproliferative	27	Lymphoproliferative	53
			Mesenchymal/bone	9	Metastatic	19	Secondary	17
			Vascular lesions	11	Meningioma	16	Structural Lesions	11
			Congenital cysts	10	Cavernous hemangioma	15	Vascular lesions	10
			Orbital inflammations	10	Secondary	15	Orbital inflammations	
					Orbital inflammations		Sarcoid	6
					Nonspecific inflammations	28		
					Specific inflammations	25		
					Vascular lesions	17		
					Structural lesions			
					Acquired	17		
					Congenital	14		
Chronic-years	TOTAL	1	TOTAL	56	TOTAL	392	TOTAL	113
	Vascular neoplasia	1	Neoplasia		Neoplasia		Neoplasia	
			Neurofibromatosis	9	Meningioma	43	Secondary	19
			Optic nerve glioma	6	Other neurogenic neoplasia	33	Neurogenic	14
			Dermoids/epidermoids	11	Vascular neoplasia	23	Lymphoproliferative	13
					Lymphoproliferative	21	Atrophy & degeneration	12
					Secondary	21	Vascular lesions	10
					Mesenchymal	14	Structural lesions	
					Lacrimal	14	Acquired structural lesions	6
					Structural lesions			
					Bone anomalies	25		
					Acquired cysts	16		
					Congenital cysts	14		
					Vascular lesions			
					Varix	20		
					Lymphangioma	11		
					Orbital inflammations	25		
Congenital	TOTAL	35	TOTAL	22	TOTAL	20	TOTAL	0
	Congenital cystic	13	Dermoids/epidermoids	6	Structural lesions	8		
	Vascular neoplasia	10	Vascular lesions	5	Vascular lesions	6		
	Vascular lesion	6	Neoplasia	5	Neoplasia (neurofibromatosis)	3		

Table 4-6. Temporal onset of non-thyroid orbital disease — most common occurence by age cohort, University of British Columbia Orbital Clinic, 1976-1999

MASS EFFECT (n=1103)	Number	%	Total	%
Neoplasia			493	44.7
Neurogenic	125	11.3		
Lymphoproliferative	118	10.7		
Vascular	68	6.2		
Secondary	59	5.3		
Mesenchymal	55	5.0		
Lacrimal	35	3.2		
Metastatic	33	3.0		
Structural			366	33.2
Trauma	132	12.0		
Dermoid/epidermoid	63	5.7		
Dermolipoma	17	1.5		
Acquired				
Mucocele	38	3.4		
Lacrimal cyst	17	1.5		
Asymmetry	42	3.8		
Vascular Lesions			102	9.2
Lymphangioma/combined venous lymphatic	45	4.1		
Varix	21	1.9		
Shunt/fistula	17	1.5		
Inflammations			74	6.7
Specific inflammation	35	3.2		
Infection	19	1.7		
Nonspecific inflammation	18	1.6		

INFLAMMATORY (n=376)	Number	%	Total	%
Inflammation (274)			274	72.9
Nonspecific inflammation (116)				
Myositis	51	13.6		
Lacrimal	24	6.4		
Anterior	20	5.3		
Specific inflammation (91)				
Wegener's granulomatosis	17	4.5		
Scleritis	17	4.5		
Sclerosing	14	3.7		
Sarcoid/sarcoidosis	13	3.5		
Infection (66)				
Sinusitis/cellulitis	49	13.0		
Structural (33)			33	8.8
Acquired cystic	12	3.2		
Trauma	12	3.2		
Mucocele	9	2.4		
Neoplasia (31)			31	8.2
Lymphoproliferative	17	4.5		
Secondary	7	1.9		

INFILTRATIVE DISEASE (n=152)	Number	%	Total	%
Neoplasia			103	67.8
Secondary	42	27.6		
Lymphoproliferative	24	15.8		
Metastatic	18	11.8		
Neurogenic	13	8.6		
Inflammation			27	17.8
Specific inflammation	15	9.9		
Infection	6	3.9		
Nonspecific inflammation	5	3.3		

VASCULAR (n=146)	Number	%	Total	%
Vascular Lesion			127	87.0
Lymphangioma/combined venous lymphatic	38	26.0		
Shunt/fistula	35	24.0		
Varix	29	19.9		
Neoplasia			9	6.3
Vascular	3	2.1		

UNKNOWN (n=40)	Number	%	Total	%
Functional	34	85.0	34	85.0

Table 4-7. Character of non-thyroid orbital disease, University of British Columbia Orbital Clinic, 1976-1999

Patients who presented with clinically infiltrative disease (such as limitation of ocular movement, functional damage, or cicatricial effect) for the most part had secondary or metastatic tumors. We also noted that a significant number of lymphoproliferative disease or neurogenic tumors had features of infiltration. The inflammatory diseases in this group included specific inflammations such as sclerosing inflammatory disease and Wegener's granulomatosis. Patients with nonspecific orbital inflammatory syndromes and infections also did present with infiltrative features. Occasionally, one sees infiltrative features associated with rare disorders, such as amyloid and linear scleroderma.

The patients who presented with an onset indicative of vascular disease included those with arterial, venous, lymphatic, and combined malformations, which were suggested primarily by variable proptosis or obvious surface lesions. The majority of arteriovenous shunts were clinically detectable as vascular disorders. Patients with combined venous lymphatic lesions often had a mass effect but could be suspected on the basis of surface features, suggesting a vascular abnormality. The only other lesions that tend to suggest a vascular cause are some neoplasia, in particular capillary hemangiomas with surface features, and rare dermatotropic vascular tumors.

Symptoms

We analyzed our series in terms of the presenting symptoms both by diagnosis and by location (Table 4-8) (Fig. 4-2). The most common symptoms in order of occurrence of non-thyroid orbital disease was swelling, proptosis, blurring or loss of vision, diplopia, and pain. Overall, there are a number of very interesting generalizations that also provide some framework for thinking about differential diagnoses. For instance, of the neurogenic neoplasia, the major presenting symptoms were obviously visual loss, whereas only meningiomas of the sphenoid wing and peripheral nerve sheath neoplasia were dominated by mass effect. Peripheral nerve sheath neoplasia were also associated with ptosis, evidence of a palpable mass, and pain. In contrast, meningiomas of the sphenoid wing were very frequently associated with periorbital swelling as a result of compression of the apex. In terms of lymphoproliferative neoplasia, the dominating symptoms were swelling, palpable masses, proptosis, and ptosis. A somewhat similar distribution was seen in vascular neoplasia except that a significant number of them had visual loss/blurring. The secondary neoplasia were dominated by features of pain, dysesthesia, or proptosis. Major symptoms associated with bone lesions were proptosis, orbital displacement, or, more rarely, periorbital swelling. In contrast to this, metastatic tumors had a high frequency of diplopia, swelling, ptosis, and visual loss associated with pain. About one third of lacrimal neoplasia were associated with a palpable mass, and half of them with proptosis.

DISORDER	Total with Disorder	Swelling	Proptosis	Diplopia	Pain	Visual Loss/ Blurring	Masses
NEOPLASIA							
Neurogenic neoplasm							
Optic nerve glioma	24		8	3	3	12	
Meningioma - optic nerve	33	2	5	10	7	30	
Meningioma - sphenoid wing	42	18	26	4	8	21	
Peripheral nerve sheath neoplasm	64	10	20	8	13	11	13
Lymphoproliferative neoplasm							
Lymphoma/lymphoid hyperplasia	129	58	30	37	14	20	47
Plasma cell tumors	11	2	8	7	4	4	
Vascular neoplasm	59	15	27	15	9	27	33
Secondary neoplasm							
Nasopharyngeal	30	7	9	10	10	11	2
Lid	24	2		4	2		9
Conjunctival	16		1	2	2		7
Ocular	10	1		1	3	2	3
Mesenchymal neoplasm							
Fibrohistiocytic/Striated muscle	18	5	6	3	2	3	6
Bone lesions	45	10	19	5	11	7	8
Metastatic	60	21	10	29	13	20	7
Lacrimal neoplasm	48	6	17	10	7	4	14
STRUCTURAL LESIONS							
Congenital lesions							
Cystic	103	13	19	17	4	8	60
Bone anomaly	58	8	28	7	15	4	1
Ectopia	30	3	1	8	3	1	21
Acquired lesions							
Cystic	80	26	19	20	18	15	25
Trauma	220	52	19	69	25	56	
INFLAMMATORY LESIONS							
Infection	82	52	19	22	42	18	3
Nonspecific inflammation	129	95	17	43	78	22	3
Specific orbital inflammation							
Sarcoidosis	19	10	1	3	4	6	4
Sclerosing	23	16	7	11	10	4	3
Sjogren's Syndrome	13	10	3	2			2
Vasculitic inflammation	30	17	9	7	12	9	5
Ocular inflammations with orbital signs	19	12	4	3	13	3	
VASCULAR LESION							
Lymphangioma/combined venous lymphatic lesion	52	16	30	8	6	9	11
Arteriovenous lesion	56	27	25	20	16	11	3
Venous lesion	57	16	17	13	19	12	14
TOTAL	1584	530	404	401	373	350	304

DISORDER	Ptosis	Redness	Tearing	Dysesthesia	Enoph-thalmos	Grittiness
NEOPLASIA						
Neurogenic neoplasm						
Optic nerve glioma	1					
Meningioma - optic nerve	1	1	1	2		
Meningioma - sphenoid wing	4	2	3	3	1	1
Peripheral nerve sheath neoplasm	18	1	4		2	
Lymphoproliferative neoplasm						
Lymphoma/lymphoid hyperplasia	22	13	18	2		5
Plasma cell tumors	7			1		
Vascular neoplasm	4	2	2	2		
Secondary neoplasm						
Nasopharyngeal	4	1	6	7		
Lid	1	3				1
Conjunctival		1				
Ocular	2		1			1
Mesenchymal neoplasm						
Fibrohistiocytic/Striated muscle	3					
Bone lesions	4		5	5		
Metastatic	17	4	3	5	2	2
Lacrimal neoplasm	9	2	7	2	1	1
STRUCTURAL LESIONS						
Congenital lesions						
Cystic	8	9	4	2		1
Bone anomaly	4	7	6	2	2	1
Ectopia	1	3	1			
Acquired lesions						
Cystic	9	5	5	1	2	2
Trauma	20	5	4	24	22	1
INFLAMMATORY LESIONS						
Infection	9	19	6	4		1
Nonspecific inflammation	12	31	15			8
Specific orbital inflammation						
Sarcoidosis	4	3	5	1		1
Sclerosing	4	6	3			
Sjogren's Syndrome	2	4	1			1
Vasculitic inflammation	3	9	3			1
Ocular inflammations with orbital signs	3	13	2			1
VASCULAR LESION						
Lymphangioma/combined venous lymphatic lesion	4	5	6	1	1	
Arteriovenous lesion	9	27	1	2		
Venous lesion	4	1	2	3	2	1
TOTAL	193	177	114	69	35	30

Table 4-8. Presenting symptoms of common non-thyroid orbital diseases, University of British Columbia Orbital Clinic, 1976-1999

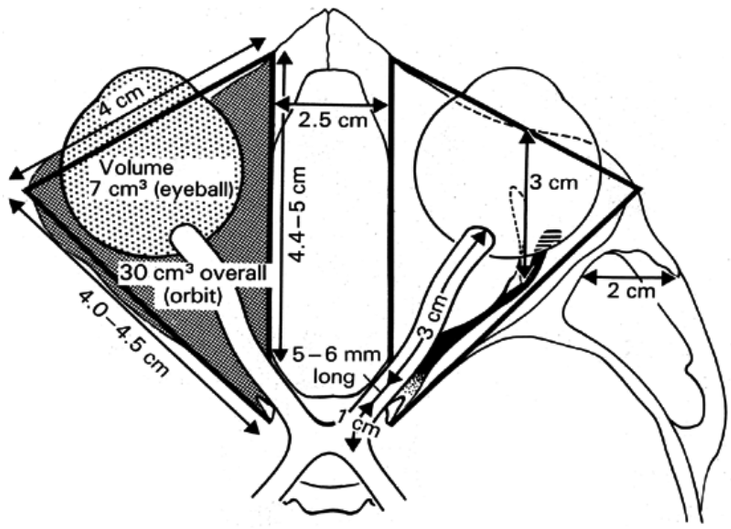

Figure 4-2. Symptomatology by major orbital disease groupings.

In terms of structural lesions, the most common presenting symptoms were awareness of mass and proptosis. Another interesting finding was that bone anomalies were associated with pain in a significant number of cases. The most common symptoms of cystic lesions were palpable swelling, masses, proptosis, and less frequently pain.

Of the inflammatory lesions, infections and nonspecific inflammations were dominated by features of swelling, pain, redness, diplopia, and proptosis, as would be expected. Under the specific orbital inflammatory syndromes, the dominant features were swelling with injection and to a lesser degree, pain. Ocular inflammations in particular were associated with pain. Of the vascular lesions, it is interesting to note that a fair number of arteriovenous and venous lesions were painful, and the remaining clinical symptoms were dominated by diplopia, proptosis, and swelling.

In terms of symptoms versus locations (Fig. 4-3), this is another algorithm that is useful to develop logical differential diagnoses. For instance, anterior lesions are dominated by mass effect. As expected, many of the inflammatory lesions also have an anterior location. Diseases that are located in the pterygopalatine fossa and infratemporal region are dominated by mass effect and psychophysical changes, whereas a midline lesion is characterized by mass effect, inflammation as well as motor signs. The more posterior the lesion, the greater the number of psychophysical and sensory effects are noted in either the orbit or cranial space. The commonest symptoms associated with sinus and nasopharyngeal lesions were inflammatory and mass-related, whereas optic nerve lesions were dominated by psychophysical effects.

The foregoing outline of our experience is not meant to replace a careful clinical analysis of the patient population, but does provide contextual framework for understanding the clinical onset of disease and categorizing patients following clinical examination prior to investigation. Fitting these broad frequency statistics within the context of developing a diagnostic algorithm for an individual patient makes it easier to come up with a specific and useful diagnosis.

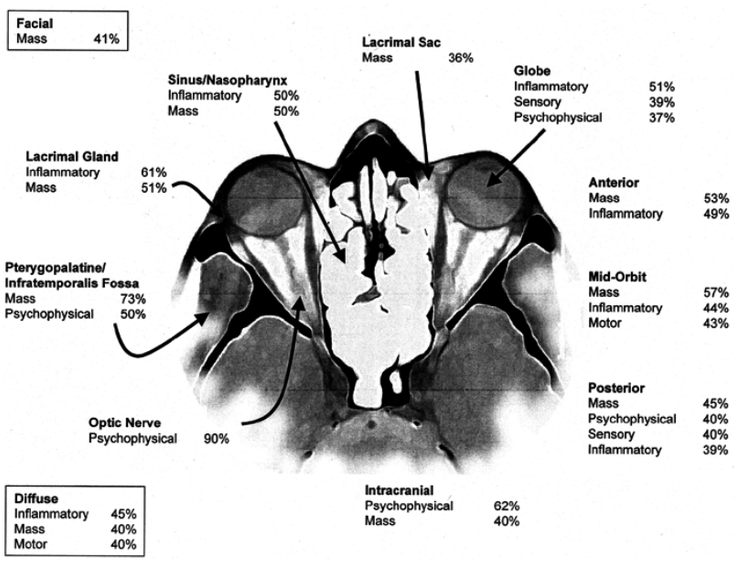

Figure 4-3. Common symptoms encountered in clinical assessment of orbital disease, based on disease location.

Orbital Differential Diagnosis

Bilateral Proptosis

The lesions that can cause bilateral proptosis are listed in Table 4-9 . From a practical point of view, the most common causes include thyroid orbitopathy, acute and subacute idiopathic inflammations, congenital craniofacial disorders, myopia, lymphomas and leukemias, metastatic lesions, and arteriovenous shunts.

Table 4-9. Bilateral proptosis

Inflammation	
	Thyroid orbitopathy
	Acute and subacute idiopathic inflammation
	Vasculitis, including Wegener's granulomatosis
	Idiopathic sclerosing inflammation
	Sarcoidal lesions
	Sjögren's syndrome
Neoplasia	
	Lymphoma and leukemia
	Metastatic carcinoma
	Metastatic neuroblastoma
	Langerhans cell histiocytosis (histiocytosis X)
	Diffuse optic nerve glioma in neurofibromatosis
	Chordoma and chondrosarcoma
	Midline fibrous dysplasia
	Sinus carcinomas
Structural Lesions	
	Congenital craniofacial dysostosis
	Mucocele
	Dacryops
Degenerative	
	Myopia
Vascular Malformation	
	Arteriovenous shunt
	Varices
	Cavernous sinus thrombosis
Bilateral Lacrimal Lesions	
	Lymphoma
	Sarcoid
	Sjögren's syndrome
	Acute and subacute idiopathic inflammation
	Lacrimal cyst

Pseudoproptosis

It is necessary to be aware of a number of disorders that may give the appearance of proptosis, yet not be associated with axial displacement of the globe. These include asymmetries of the bony orbit, globe, and lid fissures.

Table 4-10. Pseudoproptosis

Globe	
	Myopia – asymmetric
	Bupthalmos
	Refractive — anisometropia
Altered Lid Position	
	Ptosis
	Lid retraction
	Surgical recession of muscles
	Third and sixth nerve palsy
Structural Lesions	
	Facial asymmetry
	Contralateral enophthalmos
	Posttraumatic disorders

Enophthalmos

Enophthalmos is an important and subtle, often overlooked, clinical sign. Three mechanisms alone or in combination can lead to enophthalmos: structural abnormality, fat atrophy, and traction (Table 4-11). The structural abnormalities in order of likeliest causes include trauma with expansion of the orbit, orbital asymmetry, destruction of the orbital floor due to maxillary sinusitis or mucocele, and absence of the sphenoid wing in neurofibromatosis. An additional cause is sympathetic paresis, which may be more apparent than real. Causes of orbital atrophy include: posttraumatic, postinflammatory, and postirradiation fat atrophy; distensible orbital varices, and lipodystrophy. The final mechanism for enophthalmos is traction due to cicatrization. The causes include metastatic carcinoma (particularly from breast, stomach, lung, and prostate), postinflammatory cicatrization of muscle, surgical shortening of extraocular muscles, linear scleroderma, and nystagmus retractorius as well as posttraumatic scarring of orbital soft tissue. In our experience, a high percentage of patients with enophthalmos presented with symptoms of apparent exophthalmos, ptosis, or diplopia, which suggests the sign is often missed both by the patient and the physician. Adequate history, photographic review, family study, and orbital imaging should reveal the diagnosis in all cases.

It is of particular note that patients presenting with enophthalmos due to metastases can be missed for significant periods of time. Enophthalmos secondary to maxillary sinusitis is due to erosion of the orbital floor; surgical correction will obviate the enophthalmos, facial pain, and visual symptoms. Cosmetically disfiguring enophthalmos is also treatable whether due to trauma, microphthalmos, or orbital asymmetry, and may be an important contribution to the patient's needs. In the case of asymmetry, a specific diagnosis will allay the patient's concern. Orbital varices that cause significant pain may require surgical intervention. In summary, enophthalmos is a subtle, frequently missed, but important physical sign that can and should be accurately diagnosed. The range of causes underscores the need for careful and thorough diagnosis.

Table 4-11. Enophthalmos

- **Structural Abnormality**
  - Trauma
  - Asymmetry
  - Destruction of the orbital floor
  - Absence of sphenoid wing
  - Sympathetic paresis
  - Distensible varices
- **Atrophy**
  - Post-trauma
  - Postirradiation
  - Lipodystrophy
  - Varix
- **Cicatrization**
  - Post-trauma
  - Postinflammation
  - Metastatic carcinoma
  - Postsurgical shortening
  - Nystagmus retractorius
  - Linear scleroderma

Dynamic Lesions of the Orbit

The dynamic lesions of the orbit include all those entities that either pulsate, vary with positional change, or alter on Valsalva maneuver (Table 4-12). The basic pathophysiologic mechanism consists either of bony absence with communication of intracranial pulsation or a rich communication between the arterial and venous systems. In addition, venous anomalies that have significant communication with the jugular venous system (distensible varices) may cause intermittent proptosis. One unusual dynamic lesion that we saw was a case of absence of the lateral wall of the orbit associated with neurofibromatosis, which led to bobbing of the eye with chewing as a result of transmission of movement from the temporalis fossa induced by mastication. We have seen several patients with ocular bobbing with mastication after extensive removal of the lateral wall of the orbit for decompression.

Table 4-12. Dynamic lesions of the orbit

- **Bone Defect**
  - Congenital absence of the sphenoid wing (neurofibromatosis)
  - Meningoencephalocele
  - Potentially destructive lesions of bone
    - Massive mucocele with intracranial extension
    - Aneurysmal bone cyst
    - Reparative granuloma
    - Xanthomatous lesion of bone
    - Post-traumatic or postsurgical bone dehiscence
    - Dermoid cyst
    - Metastatic lytic tumors of bone (e.g., Wilm's tumor, plasmacytoma, myeloma)
    - Langerhans' cell histiocytosis (histiocytosis X)
- **Arteriovenous Shunts**
  - Capillary hemangioma
  - High-flow congenital and acquired shunts
  - Vascular tumors
    - Thyroid carcinoma
    - Nephroblastoma
    - Prostatic carcinoma
    - Hemangiopericytoma (rare)
- **Venous Anomalies**
  - Distensible varices

Orbital Imaging: Differential Diagnosis

A number of broad categories of orbital lesions form the basis of differential diagnosis based on their appearances with imaging devices. Again, these lists are not meant to substitute for a rational diagnosis within the context of the entire clinical picture, but may help to form a basis for grasping broad groupings.

Isolated Circumscribed Lesions

Isolated circumscribed lesions may be benign or malignant, as described in Table 4-13 . The major isolated noninfiltrative orbital lesions are cavernous hemangiomas, peripheral nerve sheath tumors (including schwannoma and neurofibroma), fibrous histiocytoma, and hemangiopericytoma. Lesions of the lacrimal gland that may be well circumscribed include epithelial neoplasia and sarcoidal inflammation. The other lesions that can appear to be noninfiltrative are essentially very rare aside from lymphomas. Lymphomas may have well-defined margins but they are usually nodular; the overall tumor frequently conforms to the adjacent structures in contrast to the other lesions described, which tend to displace and deform the other structures. Some rhabdomyosarcomas and metastatic tumors may appear as relatively circumscribed lesions on imaging.

Table 4-13. Isolated circumscribed lesions

Benign

- Cavernous hemangioma
- Benign peripheral nerve sheath tumors
- Fibrous histiocytoma
- Hemangiopericytoma
- Benign lacrimal epithelial tumors
- Low-grade orbital and lacrimal inflammation (e.g., sarcoidal)
- Capillary hemangioma (rare)
- Adult isolated lymphangioma
- Amyloidoma

Malignant

- Lymphomas, frequently nodular
- Lacrimal epithelial neoplasia
- Carcinoid
- Rhabdomyosarcoma
- Metastatic tumors
- Optic nerve tumors
- Mesenchymal chondrosarcoma

Table 4-14. Cystic lesions

Epithelial Cysts

- Congenital
  - Dermoid cysts
  - Cystic teratoma
  - Simple epithelial cysts
- Acquired
  - Mucoceles
  - Lacrimal cysts
  - Implantation cysts

Nonepithelial Cysts

- Hematic
  - Spontaneous
  - Associated with a bony lesion
  - Associated with a vascular lesion
- Neurogenic
  - Optic nerve sheath cyst
  - Microphthalmos with cyst
- Infectious
  - Microbial
  - Nonmicrobial/parasitic
- Neoplastic
  - Cystic degeneration in rapidly growing neoplasia (e.g., rhabdomyosarcoma, melanoma, metastases)
  - Cystic or mucinous degeneration in other neoplasia (e.g., benign mixed tumor of the lacrimal gland, schwannoma, isolated neurofibroma, pilocytic astrocytoma)

Cystic Lesions

Cystic lesions are described in the chapter on structural lesions (Chapter 11), wherein they are grouped as epithelial or nonepithelial lesions. Types of cystic lesions and degenerations with cystic change are described in Table 4-14 . The major isolated cystic lesions of the orbit are dermoid and various adnexal cysts. A number of the rapidly growing tumors may undergo cystic degeneration, in particular, rhabdomyosarcomas, melanomas, and metastatic lesions. Some of the benign tumors may undergo mucinous degeneration, including benign mixed tumor, schwannoma, and isolated neurofibroma. Lymphangiomas frequently have multiple low-density cystic areas that may be surrounded by an enhancing rim on contrast CT study. Abscesses, whether they are microbial or parasitic, may also appear as cystic lesions with low-density centers and a contrast-enhancing rim.

Infiltrative Orbital Lesions

The major categories of infiltrative orbital lesions include both benign and malignant neoplastic disease, inflammations, and depositions (Table 4-15). The benign lesions, which may have an infiltrative appearance, are plexiform neurofibromas and capillary hemangiomas. All are easily recognized within the context of age of occurrence and the clinical appearance. The malignant lesions and the chronic orbital inflammations may be difficult to differentiate because the clinical syndrome occurs in a similar age group and is characterized by a desmoplastic or cicatricial (infiltrative) response in the orbit. In particular, metastatic and chronic inflammatory disease fall in this category. The nonspecific inflammatory processes and some fulminant neoplasms, such as leukemias, may present a similar, more rapidly developing clinical picture and may resemble one another on imaging studies. Finally, amyloid deposition may be characterized by infiltration of the orbit with a silent, clinically restrictive disease process.

Table 4-15. Infiltrative orbital lesions

- **Benign Masses**
  - Plexiform neurofibroma
  - Capillary hemangioma
  - Malformations
    - Lymphangioma
    - Arteriovenous malformation
- **Malignant Neoplasia**
  - Metastatic tumors
  - Malignant fibrous histiocytoma
  - Some lymphomas
  - Leukemia
- **Inflammations**
  - Nonspecific orbital inflammations
  - Specific orbital inflammations
- **Depositions**
  - Amyloid

Lesions of Muscle

Lesions of muscle are described in Table 4-16 . In order of occurrence, enlargement of the extraocular muscles can be a result of inflammatory, neoplastic, or vascular disorders. The most common lesions of muscle are inflammatory disorders, which may be clinically and radiologically differentiated. The specific differential diagnosis between thyroid orbitopathy and myositis is discussed in Chapter 12 in the section on acute and subacute idiopathic inflammations of the orbit. Some of the arteriovenous shunts may present a picture that can be confused with inflammatory disease, and on orbital imaging show relatively uniform enlargement of the extraocular muscles. The neoplastic lesions include metastatic carcinoma, particularly from breast, melanoma, and some lymphomas. Metastatic carcinomas are usually associated with a nodular enlargement of the extraocular muscle and reticular infiltration of the adjacent orbit. In contrast, melanomas tend to produce uniform enlargements of the extraocular

Table 4-16. Lesions of muscle

- **Associated with Enlargement**
  - Inflammation
    - Nonspecific orbital inflammations
    - Specific orbital inflammations
  - Vascular
    - Carotid or dural cavernous fistula
    - Arteriovenous malformation
  - Neoplastic
    - Locally invasive orbital tumors (metastatic, secondary, or primary)
    - Discrete metastases to extraocular muscle
    - Paraneoplastic syndromes
  - Infective
    - Secondary involvement in orbital cellulites
    - Primary involvement by viral, bacterial, fungal, or parasitic organisms (e.g., herpes zoster ophthalmicus, Lyme disease, *Cystercercus*, trichinosis
  - Deposition – amyloid
  - Traumatic – blunt/open trauma
  - Iatrogenic
    - After ophthalmic or sinus surgery
    - Lithium-induced myopathy
    - Cloroquine myopathy
  - Congenital
    - Absence of muscles
    - Fibrosis syndromes
    - Enlargement of muscles
    - Neurofibromatosis
  - Miscellaneous (e.g., acromegaly, vitamin E deficiency
- **Associated With Shrinkage**
  - Myopathy
    - Denervation atrophy
    - Myasthenia gravis, mitochondrial cytopathy
    - Linear scleroderma
    - Postinflammation

Modified with permission from Lacey B, Chang W, Rootman J. Nonthyroid causes of extraocular muscle disease. Surv Ophthalmol 1999;44:187-213

muscles, often with central necrosis of the tumor. Lymphomas, when they occur in extraocular muscles, can cause marked enlargement of the muscle and tend to involve preferentially the levator, superior rectus, and medial rectus. Amyloid may also deposit in extraocular muscles as a nodular, irregular enlargement.

Destructive Lesions of Bone

Solid Lesions

A large number of lesions can potentially cause bone destruction with or without a solid soft tissue component. In particular, the inflammatory lesions include chronic sinusitis, osteomyelitis, and Wegener's granulomatosis. Reparative granulomas and aneurysmal bone cysts may also lead to destruction of bone and may have areas of low density within them. Some of the malignancies that have a propensity to involve bone include Langerhans cell histiocytosis, plasmacytoma, and Ewing's sarcoma as well as a number of metastatic tumors, especially neuroblastoma and prostatic carcinoma. Epithelial malignancies of the sinus may and frequently do invade and destroy bone. Some rare lytic meningiomas may also destroy bone.

Table 4-17. Solid lesions of bone

Primary

- Reparative granuloma
- Aneurysmal bone cyst
- Ewing's sarcoma
- Wegener's granulomatosis
- Osteogenic sarcoma
- Fibrosarcoma

Secondary

- Sinusitis – polyposis
- Langerhans cell histiocytosis
- Plasmacytoma
- Bony metastasis
- Epithelial malignancies of the sinus and nasopharynx
- Lytic meningiomas

Cystic Lesions

The category of cystic bone lesions includes dermoid cysts, which often have a low-density area due to the presence of fat; they affect a focal area of bone at the site of the suture line, often with a distinct margin. Mucoceles involve the adjacent sinus and the orbital structures with lysis of the intervening bone. Frequently there is an area of dystrophic calcification within the wall of mucoceles. Reparative granulomas and reactive xanthomatous lesions may also lead to bone destruction, and may have low-density cystic areas. The lesions of bone are discussed in greater detail in Chapter 9 in the section on mesenchymal tumors of the orbit .

Table 4-18. Cystic lesions of bone

- Dermoid cyst
- Mucocele
- Reparative granuloma
- Xanthomatous lesions

Table 4-19. Hyperostotic lesions of bone

- Prostatic carcinoma (metastatic)
- Meningioma
- Osteomyelitis
- Primary bone tumors
  - Fibrous dysplasia
  - Osteoma: ossifying fibroma
  - Osteosarcoma
  - Chondrosarcoma

Hyperostotic Lesions

Prostatic carcinoma has a propensity to cause increased density of bone, especially the sphenoid wing. Some meningiomas and chronic osteomyelitis may also cause hyperostosis. Several of the primary bone tumors are characterized by a high degree of bone and osteoid formation within them, leading to densely calcified, hyperostotic lesions. These include fibrous dysplasia, osteomas, ossifying fibromas, chondrosarcomas, and osteogenic sarcomas.

Optic Nerve Lesions

Optic nerve lesions include neoplastic and nonneoplastic types, as described in Table 4-20 . The differential diagnosis of optic nerve meningioma and glioma is discussed in detail in Chapter 9 in the section on neurogenic tumors . A number of nonneoplastic lesions of the optic nerve may lead to expansion (usually uniform) of the nerve or its sheath. Those lesions associated with sheath expansion include apical compression due to thyroid orbitopathy and raised intracranial pressure, in particular pseudotumor cerebri. Bleeding into the subarachnoid space either due to direct orbital or intracranial trauma also leads to expansion of the optic nerve sheath. Expansion of the nerve itself may be associated with a number of inflammatory conditions including optic neuritis, toxoplasmosis, tuberculosis, and sarcoidosis, all of which lead to a uniform density expansion. In contrast, when the nerve is infarcted either by direct vascular obstruction or due to adjacent inflammatory or vasculitic disease, the central portion of the nerve tends to appear as a low-density or hypointense area.

Table 4-20. Optic nerve lesions

Neoplastic

- Optic nerve glioma
- Optic nerve meningioma
- Plexiform neurofibroma – posterior ciliary nerves
- Angiomeningioma
- Metastases
- Leukemia
- Meningeal spread of tumors

Non-neoplastic

- Sheath expansion
  - Apical orbital crowding in thyroid orbitopathy
  - Pseudotumor cerebri
  - Chronic papilledema
  - Subarachnoid bleeding
  - Patulous optic nerve sheath
- Nerve expansion
  - Optic neuritis
  - Toxoplasmosis
  - Tuberculosis
  - Sarcoidosis
  - Infarction of the optic nerve

Table 4-21. Orbital lesions with calcification and without bone destruction

Dystrophic Calcification

- Phlebolith
- Varix
- Lymphangioma
- Old thrombosis in arteriovenous shunt or malformation
- At a site of old hemorrhage
- Chronic inflammation

Neoplastic

- Malignant and less commonly benign epithelial tumors of the lacrimal gland
- Extraosseous mesenchymal chondrosarcoma
- Meningioma
- Occasional lymphomas – especially plasmacytoid
- Old schwannomas

Osseous and Cartilaginous Soft Tissue Tumors

Cystic Lesions

- Dermoid cyst – conjunctival
- Epithelial cyst – isolated

Calcification in the Globe

Displaced Orbital Bone Following a Fracture

Calcified Trochlea

Orbital Lesions with Calcification

Orbital lesions that show calcification without bone destruction are listed in Table 4-21 .

Typically, lesions that have undergone thrombosis may form phleboliths, including varices, lymphangiomas, and arteriovenous shunts or malformations. Other causes of dystrophic calcification include chronic inflammation. A number of neoplasms are associated with calcification, in particular epithelial tumors of the lacrimal gland. In this category, the malignant epithelial tumors are more commonly calcified than the benign ones. The osseous and cartilaginous soft tissue tumors are frequently calcified. Meningiomas, in particular the psammomatous variant, tend to be calcified. Schwannomas, especially ancient ones, may develop dystrophic calcification usually as a focal site. We have seen two lymphomas with focal dystrophic calcification presumably due to areas of necrosis. The cystic lesions of the orbit, including dermoid cysts, epithelial cysts, and mucoceles, are characterized by a tendency to focal calcification, usually in the wall of the cyst.

The numerous causes of calcification within the globe include phthisis bulbi, osteomas, optic nerve drusen, hyalin plaques, and cartilage within dysgenetic and malformed globes.

The lesions that cause bone destruction (Table 4-22) and may be calcified include the primary fibro-osseous tumors, dermoid cysts, and mucoceles. Both the mucocele and dermoid cyst tend to cause excavation rather than erosion of bone, but we have encountered the rare instance of a ruptured dermoid with granulomatous reaction causing a more irregular infiltration and destruction of bone. The distinguishing feature, however, is the abrupt delimitation to the suture line. The full differential diagnosis of fibro-osseous tumors is discussed in Chapter 9 in the section on mesenchymal tumors .

An Algorithm for Specific Diagnosis

In Chapter 5 (An Approach to Diagnosis), I will emphasize that a confluence of observations and knowledge can lead to appropriate investigation and diagnosis. These factors include a broad understanding based on character of onset, clinical categorization, and location of disease. In real life, the development of a differential diagnosis tends to follow a diminishing algorithm based on clinical examination, pathophysiology, imaging, and ultimately biopsy, which now includes molecular techniques. As an example of this process, I would like to follow the algorithm as it applies in two specific cases, both children. The history for both patients is subacute onset of a temporal orbital mass effect with inflammatory features.

In the first case (Case A, Fig. 4-4), the ophthalmologist could begin by considering the differential diagnosis of a rapidly developing proptosis of a child, based on the clinical presentation (Table 4-23). The major categories of the differential diagnosis should follow broad pathophysiologic concepts and would include the following: sudden recognition of a preexisting lesion; an infection, infestation, or inflammation; a rapid new growth or tumor, and a change in a preexisting lesion. The most common cause of rapidly developing proptosis is sudden recognition of a preexisting lesion, and this would include a myriad of different kinds of tumors that can occur in this age group. Infections, infestations, or inflammations include conditions such as sinusitis, nonspecific inflammatory syndromes, metastatic abscess, parasitic disease, and sclerosing inflammation. The rapid new growths or tumors include capillary hemangioma, rhabdomyosarcoma, metastatic or secondary neoplasms as well as a number of miscellaneous tumors. Finally, a change in a preexisting lesion, such as a lymphangioma, hematic cyst, varix, reparative granuloma, or dermoid cyst, may account for a rapidly developing proptosis in a child.

Table 4-22. Orbital lesions exhibiting intrinsic calcification with bone destruction

- Fibro-osseous tumors
  - Fibrous dysplasia
  - Osteoma
  - Reparative granuloma
  - Solid aneurysmal bone cyst
  - Osteosarcoma
  - Chondrosarcoma
- Dermoid cyst
- Epidermoid cyst
- Mucocele

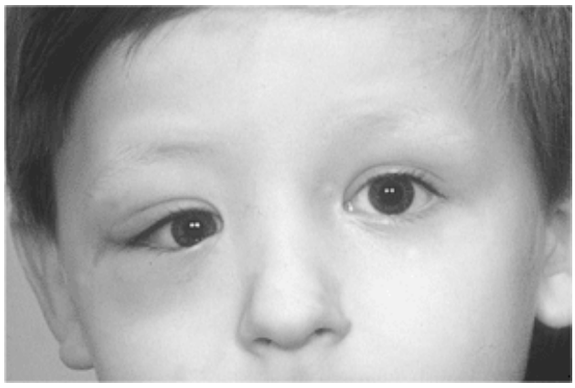

Figure 4-4. Case A. This 4-year-old boy from Bosnia presented with a 3-month history of downward, inward displacement of the right globe, which was associated with a sudden onset of inflammation. Aside from mild injection of the upper lid and globe displacement, his ocular examination was normal.

Table 4-23. Case A – Differential diagnosis of a rapidly developing proptosis in childhood

1. Sudden recognition of a preexisting lesion
   - glioma
   - lacrimal tumor
   - dermoid cyst
   - sphenoid wing meningioma
   - miscellaneous
2. Infection, infestation, inflammation
   - sinusitis
   - nonspecific inflammation
   - metastatic abscess
   - parasitic disease
   - sclerosing inflammation
3. Rapid new growth or tumor
   - capillary hemangioma
   - rhabdomyosarcoma
   - metastatic or secondary neoplasm
   - miscellaneous tumors
4. Change in a preexisting lesion
   - lymphangioma
   - varix
   - hematic cyst
   - reparative granuloma
   - solid aneurysmal bone cyst with bleed
   - bleed in fibrous dysplasia
   - ruptured dermoid cyst

On the other hand, the ophthalmologist may develop a differential diagnosis on the basis of the primary location (Table 4-24). In this instance, locations to consider are lesions of the lacrimal fossa or the lateral orbital bone and rarely, more diffuse soft tissue tumors or inflammations. Lesions of the lacrimal fossa include inflammations, chiefly dacryoadenitis, ruptured dermoid cysts, epithelial tumors, and lymphoproliferative or leukemic disease. The lateral orbital bone may develop meningiomas, reparative granulomas, dermoid cysts, Langerhans cell histiocytosis, lymphomas, or leukemias that could result in this presentation. Finally, nonspecific orbital inflammatory disease or neoplasia may also present in this fashion.

In developing the differential diagnosis, the picture to consider now is the combination of a rapidly developing mass in the lateral orbit of a child (Table 4-25). In terms of sudden recognition of a preexisting lesion, lesions to consider would include lacrimal tumor, dermoid cyst, or sphenoid wing meningioma. Of infections, infestations, and inflammations, likely diagnoses are dacryoadenitis, nonspecific inflammation, parasitic disease, sclerosing inflammation, and a metastatic abscess, which would in fact be rare. A rapid new growth or tumor would include, in order of occurrence, Langerhans cell histiocytosis, reparative granuloma, solid aneurysmal bone cyst, and metastatic tumor such as neuroblastoma, lymphoma, and sarcoma (sarcomas tend to be rare laterally). The final group, change in a preexisting lesion, except for dermoid cysts are mostly rare laterally in this age group.

To focus this clinical differential diagnosis to the likeliest causes in this age group, the most probable cause would be an infection, infestation, or inflammation. For patients in this age group, changes in preexisting lesions rarely involve significant inflammation of subacute onset, and sudden recognition of preexisting lesions are seldom inflamed. Hemorrhages laterally are in fact quite rare. Of rapid new growths or tumors, reparative granulomas and metastatic tumors are also rarely inflamed, whereas Langerhans cell histiocytosis or a leukemic infiltrate can have inflammatory features.

Table 4-24. Case A – Differential diagnosis of a lateral orbital mass in childhood

1. Lesion of the lacrimal fossa
   - inflammation
   - dermoid cyst
   - epithelial tumor
   - lymphoproliferative disease or leukemia
2. Lesion of the lateral orbital bone
   - dermoid cyst
   - meningioma
   - Langerhans cell histiocytosis
   - reparative granuloma
   - solid aneurysmal bone cyst
   - lymphoma or leukemia
   - metastatic neoplasm (neuroblastoma)
3. Soft tissue tumor or inflammation
   - specific and nonspecific inflammation of the orbit, especially lacrimal
   - neoplasm of the lateral orbit

Table 4-25. Case A – Differential diagnosis of a rapidly developing lateral orbital mass in childhood

1. Sudden recognition of a preexisting lesion
   - lacrimal tumor (adenoid cystic)
   - dermoid cyst
   - sphenoid wing meningioma
2. Infection, infestation, inflammation
   - dacryoadenitis
   - nonspecific inflammation
   - metastatic abscess (exceedingly rare)
   - parasitic disease
   - sclerosing inflammation (rare)
   - ruptured dermoid cyst
3. Rapid new growth or tumor
   - Langerhans cell histiocytosis
   - reparative granuloma
   - solid aneurysmal bone cyst
   - metastatic neoplasm (neuroblastoma)
   - lymphoma
   - sarcoma (rare laterally, including rhabdomyosarcoma)
4. Change in a preexisting lesion
   Most are rare laterally

Table 4-26. Case A – Differential diagnosis of an inflamed, isolated, lateral orbital cyst in childhood

1. Sudden recognition of a preexisting lesion
   - not inflamed
2. Infection, infestation, inflammation
   - echinococcus
   - dermoid cyst (ruptured)
3. Rapid new growth or tumor
   - few are lateral, inflamed, or cavitate
4. Change in a preexisting lesion
   - not inflamed

The next level of differentiation uses imaging findings to add specificity. In the case of our first patient, we note a well defined, cystic lesion with excavation of the bone and flattening of the globe, suggesting an inflammatory change in a preexisting lesion (Fig. 4-5). Thus the differential diagnosis now becomes an inflamed lateral, isolated orbital cyst in childhood (Table 4-26). In terms of infections, infestations, or inflammations, such a well defined cyst would most likely be an echinococcus cyst. If a change in a preexisting lesion were to be considered, the cystic options include a dermoid cyst. We have already eliminated recognition of preexisting lesions, as they tend not to be inflamed, and as stated earlier, with new growths or tumors, few are inflamed or cavitate. The focused final diagnosis is either echinococcal or dermoid cyst. Excision of the lesion revealed an echinococcal cyst (Fig. 4-6).

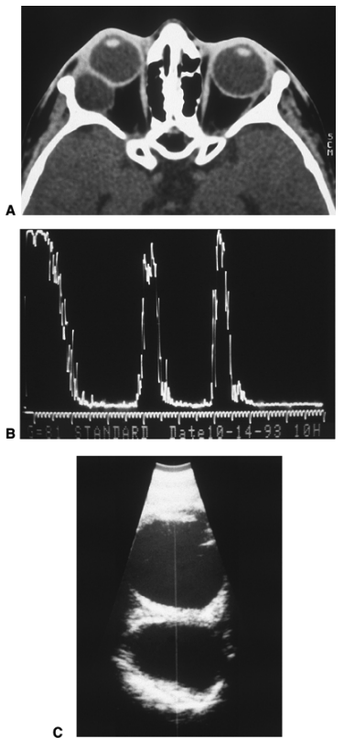

Figure 4-5. Case A. (A) CT scan shows a cystic lesion in the lateral orbit that indents the globe and demonstrates some excavation of the lateral orbit wall, suggesting chronicity. (B) The A- and B-scan ultrasonograms confirmed a cystic lesion.

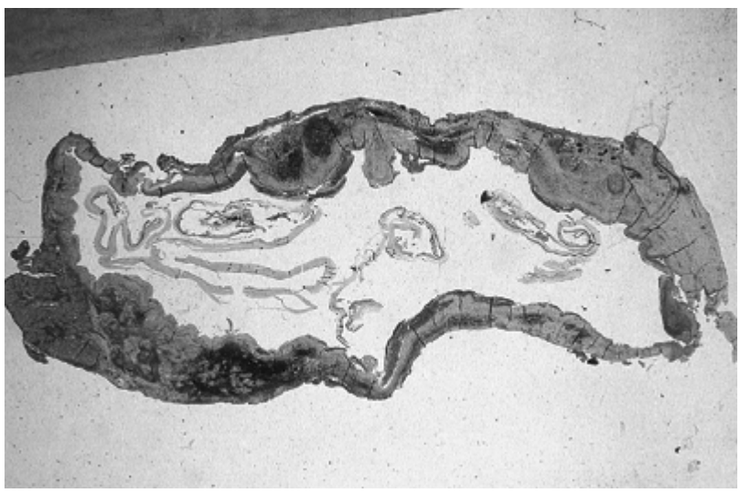

Figure 4-6. Case A. Low-power view of the cyst removed from Case A, which was characteristic for echinococcus (H&E, original magnification × 2).

The second patient (Case B, Fig. 4-7) had on imaging a destructive lesion of bone with a low-density center (Fig. 4-8), which forms the core of the differential diagnosis (Tables 4-27 and 4-28). The differential diagnosis would therefore include a new mass, which in this age group would suggest Langerhans cell histiocytosis and lymphoma. Lymphomas, however, are rarely destructive of bone in this age group. The second likeliest would be a change in a preexisting lesion, such as a dermoid cyst, reparative granuloma (often within a focus of fibrous dysplasia), or a solid aneurysmal bone cyst. Finally, recognition of a preexisting lesion would include dermoid cyst. On biopsy, the patient proved to have Langerhans cell histiocytosis (Fig. 4-9).

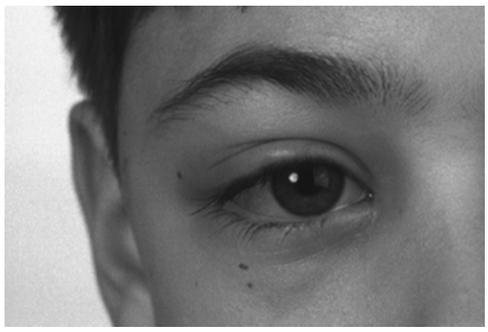

Figure 4-7. Case B. This 10-year-old boy presented with a 3-week history of swelling of his right upper lid. There was downward displacement and axial proptosis with an otherwise normal ocular examination.

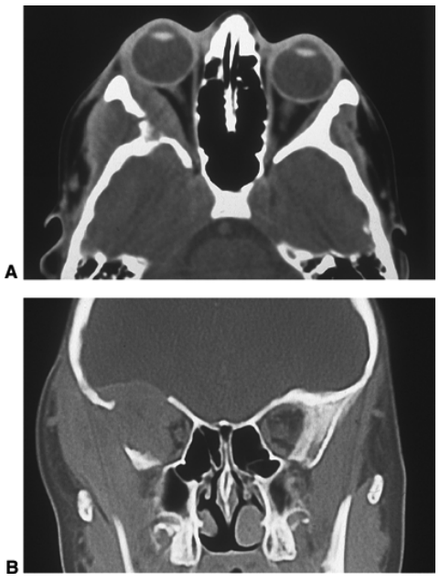

Figure 4-8. Case B. (A) Axial CT scan demonstrates a lytic mass within an enhancing rim. (B) Coronal CT scan on bone setting demonstrates destruction of the bone of the lateral wall and roof of the orbit.

Table 4-27. Differential diagnosis of an inflamed lateral orbital mass in childhood

Infection, infestation, inflammation
- dacryoadenitis
- nonspecific inflammation
- metastatic abscess
- parasitic disease
- sclerosing inflammation
- miscellaneous

Rapid new growth or tumor
- reparative granuloma (rarely inflamed)
- Langerhans cell histiocytosis (rarely inflamed)
- lymphoma or leukemia (rarely inflamed)
- metastatic neoplasm (rarely inflamed)

Change in a preexisting lesion
- dermoid cyst
- hemorrhage

Sudden recognition of a preexisting lesion
- not inflamed

Table 4-28. Differential diagnosis of an inflamed, rapidly developing, lateral orbital mass with a low-density center and bone destruction in childhood

1. Rapid new growth or tumor
   - Langerhans cell histiocytosis
   - lymphoma (bone destruction rare in this age group)
2. Change in a preexisting lesion
   - dermoid cyst
   - reparative granuloma
   - solid aneurysmal bone cyst
3. Recognition of preexisting lesion
   - dermoid cyst ?

The above algorithm is meant to demonstrate the kind of thinking based on careful evaluation and knowledge that allows for meaningful development of a focused differential diagnosis prior to specific management.

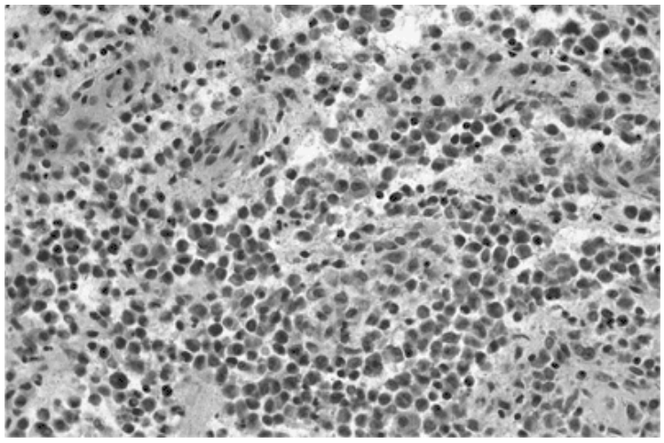

Figure 4-9. Case B. The patient underwent needle biopsy, which confirmed the diagnosis of Langerhans cell histiocytosis (H&E, original magnification × 10). The lesion was curetted.

Bibliography

Adam YG, Farr HW. Primary orbital tumors. Am J Surg 1971;122:726-31.

Cline RA, Rootman J. Enophthalmos: a clinical review. Ophthalmology 1984;91:229-37.

Crawford JS. Disease of the orbit. In: Toronto Hospital for Sick Children, Department of Ophthalmology. The Eye in Childhood. Chicago: Year Book Medical, 1967;331-64.

Dallow RL, Pratt SG, Green JR. Approach to orbital disorders and frequency of disease occurrence. In: Albert DM, Jakobiec FA, eds. Principles and Practice of Ophthalmology. 2nd ed. Philadelphia: WB Saunders, 2000; 3056-67.

Duke-Elder S. System of Ophthalmology. Vol 13, The ocular adnexa. London: Henry Kimpton, 1976.

Dutton JJ, Byrne SF, Proia AD. Diagnostic Atlas of Orbital Diseases. Philadelphia: WB Saunders, 2000.

Eldrup-Jorgensen P. Primary, histologically confirmed orbital tumours in Denmark 1943-1962. Histopathological and prognostic studies. Acta Ophthalmol 1970;48:657-66.

Henderson JW. The tumor survey. In: Henderson JW, ed. Orbital Tumors. 3rd ed. New York: Raven Press, 1994;43-52.

Iliff WJ, Green WR. Orbital tumors in children. In: Jakobiec FA, ed. Ocular and Adnexal Tumors. Birmingham: Aesculapius, 1978;669-84.

Jones IS, Jakobiec FA. Diseases of the Orbit. Hagerstown, MD: Harper & Row, 1979;17-30.

Kennedy RE. An evaluation of 820 orbital cases. Trans Am Ophthalmol Soc 1984;82:134-55.

Krohel GB, Stewart WB, Chavis RM. Orbital Disease: A Practical Approach. New York: Grune & Stratton, 1981.

Moss HM. Expanding lesions of the orbit: a clinical study of 230 consecutive cases. Am J Ophthalmol 1962;54:761-70.

Perez Moreiras JV, Perez Becerra E. Patologia orbitaria: exploracion, diagnostico y cirugia. Tomo 1. Barcelona: Ciba Vision, 2000.

Reese AB. Expanding lesions of the orbit. Bowman lecture. Trans Ophthalmol Soc UK 1971;91:85-104.

Shields JA, Bakewell B, Augsburger JJ, et al. Classification and incidence of space-occupying lesions of the orbit: a survey of 645 biopsies. Arch Ophthalmol 1984;102:1606-11.

Shields JA, Bakewell B, Augsburger JJ, et al. Space-occupying orbital masses in children: a review of 250 consecutive biopsies. Ophthalmology 1986;93:379-84.

Taylor D. Pediatric Ophthalmology. 2nd ed. London: Blackwell Science, 1997.

Templeton AC. Orbital tumours in African children. Br J Ophthalmol 1971;55:254-61.

Wilson MW, Buggage RR, Grossniklaus HE. Orbital lesions in the Southeastern United States. Orbit 1996;15:17-24.

Wilson MW, Grossniklaus HE. Orbital disease in North America. Ophthalmol Clin North Am 1996;9:539-47.

Part B

Patient Encounter

Chapter 5

An Approach to Diagnosis

Evaluation of the patient with orbital disease should seek to glean information regarding pathophysiologic effect and location. History taking and physical examination provide an opportunity to define whether the disease process is characterized by features of inflammation, infiltration, mass effect, or vascular change, and it should define the location of the disorder. These changes are then validated by investigations that evaluate pathophysiologic change, including psychophysical abnormality and motor and sensory effects. Finally, imaging techniques can define the lesion in terms of location, contour or surface features, infiltrative effects, and relationship to and effect on adjacent structures. Imaging can address physiologic issues of vascularity, compressibility, positional change, changes with treatment, and in some instances, function (such as dynamic CT and MR, CTA and MRA, angiography, venography, and PET scanning). This pattern of thinking about and examination of the patient allows for a logical acquisition of information. Development of a differential diagnosis is dependent upon evaluating symptoms and signs, frequency of disease occurrence for age groups, and is contextualized to a specific patient following complete clinical and imaging studies (Fig. 5-1).

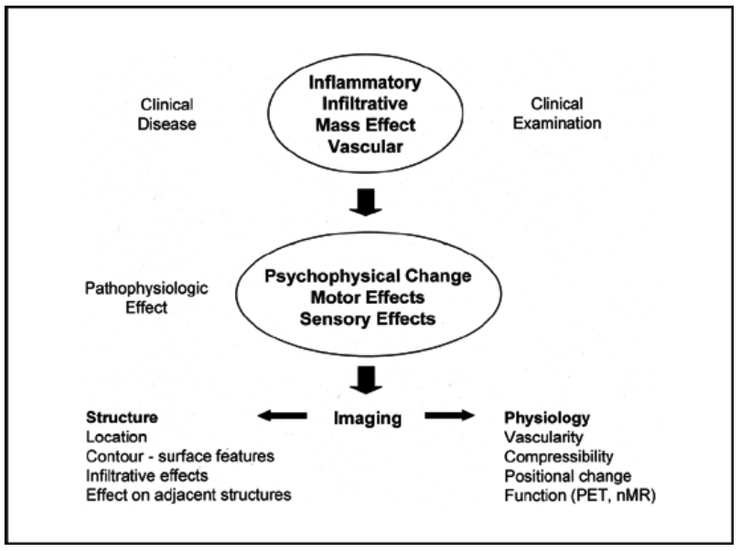

Figure 5-1. An algorithm for clinical and imaging analysis.

Pathophysiologic Approach to Clinical Analysis of Orbital Disease

When confronted with a patient suspected of having orbital disease, the clinician may feel confused. There are, nevertheless, basic patterns that provide a framework for the study of each case. **The clinical analysis sets the stage for other investigations and is our most reliable tool**. I like to analyze a case by trying to locate and characterize the process induced by the disease. Essentially, history taking and physical examination should be directed to answering two questions:

- Where is the disease located?
- How has the disease affected the orbital structures, that is, what dynamic alteration has it caused?

With the answers to these two questions synthesized, the clinician is ready to formulate a plan for investigation.

Principles

Location of Disease

The "where" question is usually the easiest to answer. Clues to location can be obtained by analysis of mechanical displacement of orbital structures. When a process shifts orbital structures, the direction of shift is a clue to the location of the disease. The effect can be viewed as positive if the lesion occupies space and pushes structures away (Fig. 5-2) and negative if it draws structures toward it through cicatrization (Fig. 5-3), excavation (Fig. 5-4), or both. An excavating effect may be due to atrophy of contents or enlargement of the orbit secondary to hypoplasia of adjacent structures, expansion, trauma, or lytic disturbances of bone.

The physical examination should provide information on the degree and direction of displacement of the affected orbital structures. Displacement of the eye should be measured in the following manner:

- Measure horizontal displacement by recording the distance at the level of the canthi from the center of the nose to the medial edge of the limbus with the patient looking in the axial direction (Fig. 5-5A).
- Measure vertical displacement by recording the position of the globe above or below the level of the canthi (Fig. 5-5B).
- Measure proptosis with an exophthalmometer, one eye at a time, with the patient regarding an object (preferably your eye) along their central visual axis (Fig. 5-5C).

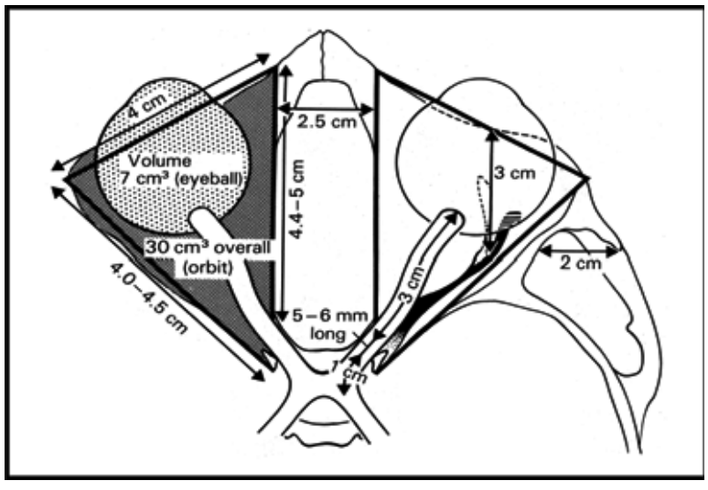

Figure 5-2. Positive effect of orbital disease: the lesion pushes orbital structures (in this case, the globe) away from it. (Reproduced with permission from Rootman J. An approach to diagnosis of orbital disease. Can J Ophthalmol 1983;18:102-7.)

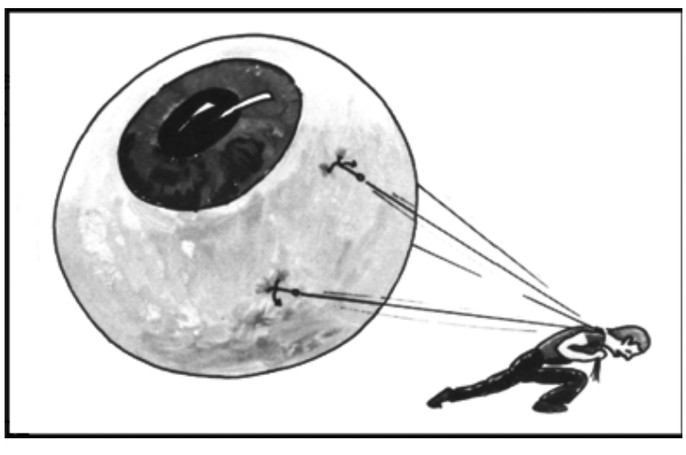

Figure 5-3. Negative effect of orbital disease: the disease process draws structures toward it. (Reproduced with permission from Rootman J. An approach to diagnosis of orbital disease. Can J Ophthalmol 1983;18:102-7.)

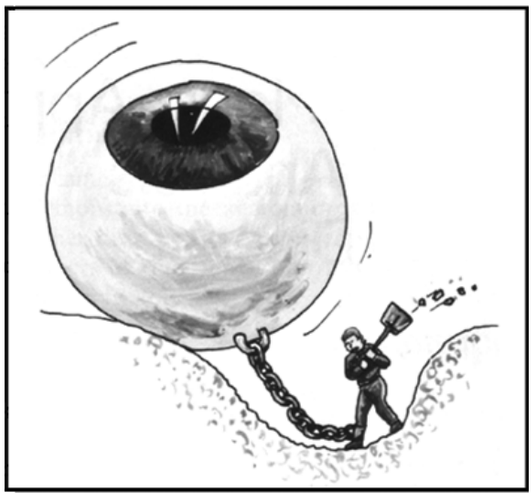

Figure 5-4. Orbital displacement may be due either to cicatrization of orbital contents, or to traumatic or lytic dehiscence of bone with or without surrounding atrophy. (Reproduced with permission from Rootman J. An approach to diagnosis of orbital disease. Can J Ophthalmol 1983;18:102-7.)

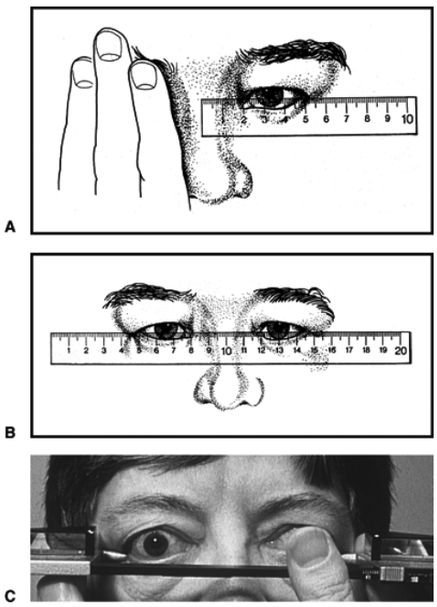

Figure 5-5. (A) Measure horizontal displacement of the eye by recording the distance (in millimeters) at the level of canthi from center of nose to medial edge of limbus. (B) Measure vertical displacement of the eye by recording the position of globe above or below the level of canthi. (C) Measurement of proptosis with an exophthalmometer: with the other eye occluded, patient looks along central visual axis. (In this case, at your left eye with their right eye.)

In addition to mechanical clues to location, functional deficits may help in defining the “where” of disease. For instance, apically located disease may have visual, sensory, and motor deficit disproportionate to what would be expected based on the degree of displacement of structures. A disease that primarily affects motor function may direct attention to the neuromuscular structures of the orbit.

Dynamic Alteration

Dynamic alteration is more difficult to assess and requires the analysis of two basic clinical features of disease: temporal change and the abnormal process.

Temporal Change

Evidence of temporal change, such as diurnal variation and intermittency, should be extracted from the patient's history, with special emphasis on time of onset and rapidity of development. For example, many patients with thyroid ophthalmopathy have more proptosis, lid edema, and diplopia in the morning as a result of accentuation of orbital swelling due to lying prone all night.

Both the time and the rapidity of onset of the change may provide a clue to the nature of the underlying disease. A catastrophic change occurring over several hours suggests either hemorrhage in a preexisting lesion or fulminant inflammation with or without a preexisting lesion. A change that is somewhat less rapid (acute-days or subacute-weeks) but progressive suggests either an inflammatory process or fulminant neoplasia. On the other hand, an insidious change (chronic-months to chronic-years) may be due to low-grade inflammation or neoplasia, either benign or malignant. Finally, an intermittent (or dynamic) change, such as pulsation or alteration with a Valsalva maneuver, suggests either a bony defect in the orbit or a relation between the lesion and the vascular system.

The Abnormal Process

Abnormal changes can be divided into four basic clinically discernible categories, which are not necessarily independent but provide a working framework for characterization of orbital problems. One tends to associate certain clinical signs with each of these processes.

- **Inflammatory effect**. Inflammation is characterized by, and can be inferred from signs and symptoms of, pain, warmth, loss of function, and mass effect. The degree to which one categorizes the process as either acute, subacute, or chronic is related to the severity and rapidity of onset.

- **Mass effect**. A mass effect consists of displacement with or without signs of involvement of sensory or neuromuscular structures. Displacement points to the location of the disease and may help to characterize its nature.
- **Infiltrative change**. Infiltrative diseases are usually associated with evidence of destruction, entrapment, or both. This includes effects on ocular movement or neurosensory function (e.g., diplopia, muscle restriction or fibrosis, optic neuropathy, pain, or paresthesia).
- **Vascular change**. Alteration in the character, size, and structural integrity of vessels may imply an underlying vascular process. The major features implying vascular disease consist of venous dilatation, pulsation, expansion with Valsalva maneuver, tissue exudation, hemorrhage, infarction, and structural alterations of vascular components.

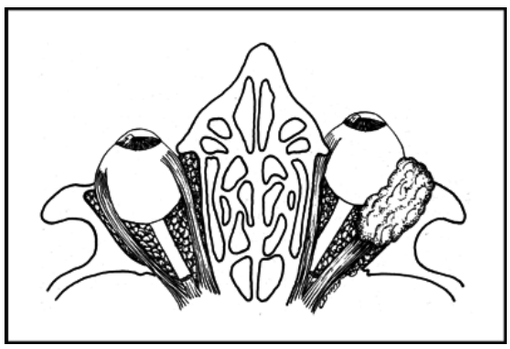

Figure 5-6. Positive mass effect of lacrimal tumor: downward and inward displacement of globe. (Reproduced with permission from Rootman J. An approach to diagnosis of orbital disease. Can J Ophthalmol 1983;18:102-7.)

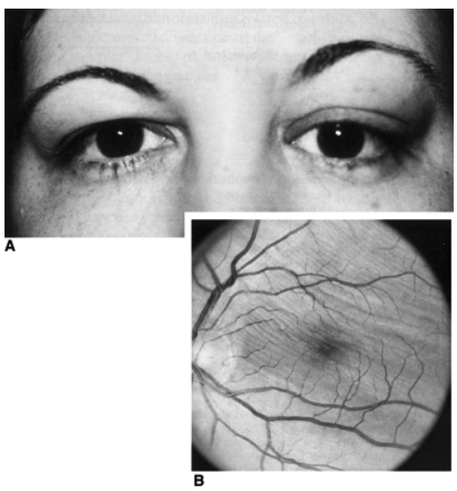

Figure 5-7. (A) Downward and inward displacement of the left globe, with fullness and S-shaped deformity of lid, in a patient with a benign mixed tumor of the lacrimal gland. (B) Superotemporal choroidal folds in the same patient. (Reproduced with permission from Rootman J. An approach to diagnosis of orbital disease. Can J Ophthalmol 1983; 18: 102-7.)

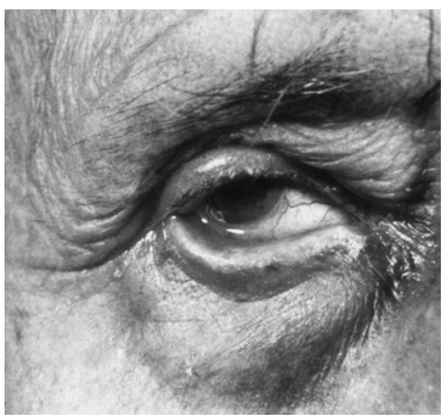

Figure 5-8. Upward and outward displacement of eye and lid in a patient with sclerosing carcinoma in the superolateral orbit. (Reproduced with permission from Rootman J. An approach to diagnosis of orbital disease. Can J Ophthalmol 1983;18:102-7.)

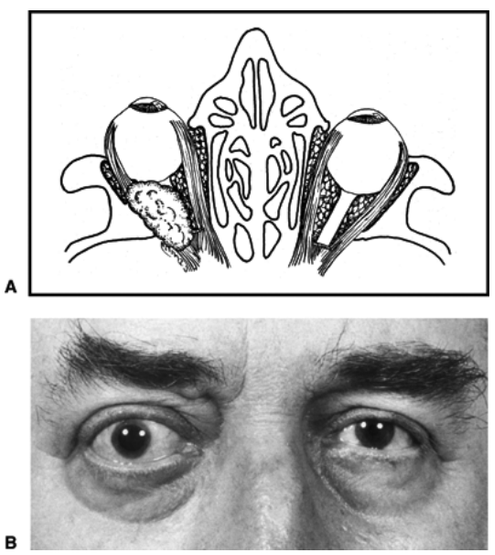

Figure 5-9. (A) Schematic of axial proptosis due to an intraconal mass. (B) Clinical appearance of axial proptosis in a patient with a right-sided intraconal schwannoma. (Reproduced with permission from Rootman J. An approach to diagnosis of orbital disease. Can J Ophthalmol 1983;18:102-7.)

Examples of Pathophysiologic Approach

The foregoing principles can best be appreciated through specific clinical examples that emphasize aspects of this approach.

Location of Disease

Mechanical Features

A mass lesion arising in the area of the lacrimal fossa and producing a positive effect leads to downward and inward displacement with or without indentation of the globe (Fig. 5-6). This picture, associated with superotemporal choroidal folds, was evident in a patient who proved to have a benign mixed tumor of the lacrimal gland (Fig. 5-7). On the other hand, a negative process due to cicatrization in the same area may result in enophthalmos and upward and outward displacement of the globe, as in the patient shown in Figure 5-8 , who had a sclerosing carcinoma.

Within the muscle cone a positive or a negative process produces axial displacement of the globe (Fig. 5-9). For example, an intraconal schwannoma leads to positive displacement and axial proptosis, and an orbital metastasis of sclerosing carcinoma leads to axial enophthalmos (Fig. 5-10). In some instances both a positive and a negative effect may occur under different circumstances. The patient in Figure 5-11 was normally enophthalmic (Fig. 5-11A), but owing to an orbital venous anomaly, showed increasing axial proptosis and fullness of the lid during Valsalva maneuver or when bending over (Fig. 5-11B).

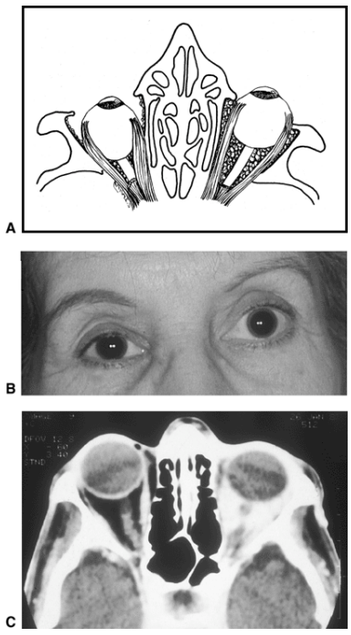

Figure 5-10. (A) Schematic demonstrating axial enophthalmos that may be due to intraconal cicatrization or in some instances, atrophy. (B) Clinical photo of a 67-year-old woman who presented with progressive left enophthalmos and reduced lid and extraocular movements. (C) The CT scan demonstrates the left enophthalmos and orbital infiltration from a cicatrizing metastatic carcinoma of the breast. (Fig. 5-10A reproduced with permission from Rootman J. An approach to diagnosis of orbital disease. Can J Ophthalmol 1983:18:102-7.)

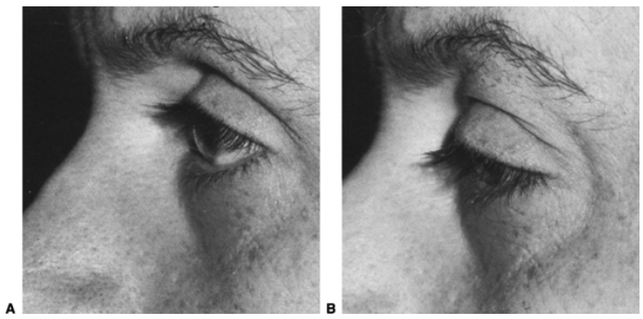

Figure 5-11. (A) Enophthalmos due to fat atrophy and enlargement of the orbit in a patient with distensible orbital venous malformation. (B) Exophthalmos, increased fullness of the lids, and loss of deep upper sulcus in the same patient during Valsalva maneuver. (Reproduced with permission from Rootman J. An approach to diagnosis of orbital disease. Can J Ophthalmol 1983;18:102-7.)

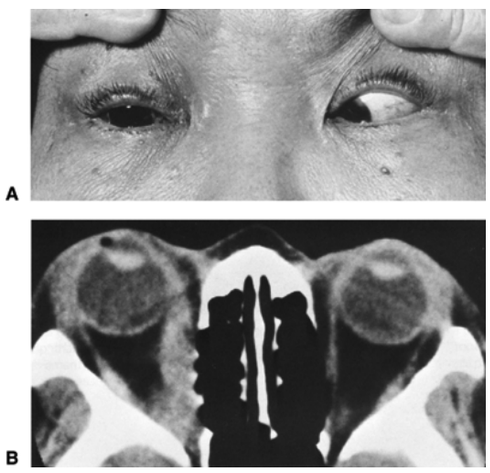

Figure 5-12. (A) Clinical photograph of a patient with myositis demonstrates lid swelling and local injection over the muscle insertion. (B) CT scan demonstrates an enlarged medial rectus muscle and tendon.

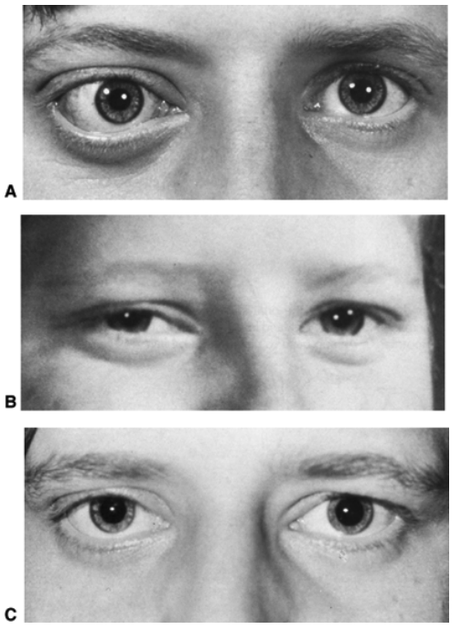

Figure 5-13. (A) Right-sided proptosis and sixth nerve palsy that developed overnight in a 16-year-old boy with an orbital vascular anomaly. (B) Orbital asymmetry in the same boy 5 years earlier. (C) Photograph taken 1 month later demonstrates resorption of blood and minimal residual proptosis. (Figs. 5-13A and B reproduced with permission from Rootman J. An approach to diagnosis of orbital disease. Can J Ophthalmol 1983;18:102-7.)

Functional Features

The patient with myositis shown in Figure 5-12 demonstrates a functional deficit that helps point to location. She had pain on ocular movement, swelling of the lid, and local injection over the affected medial rectus muscle, suggesting a process located in the muscle.

Dynamic Alteration

A catastrophic temporal change suggests either hemorrhage in a preexisting lesion or fulminant inflammation with or without a preexisting lesion. The patient in Figure 5-13 presented with sudden proptosis and sixth nerve palsy after a normal night's sleep (Fig. 5-13A). He proved to have a large orbital hemorrhage within a preexisting vascular lesion. The diagnosis was supported by the orbital asymmetry noted in a photograph taken 5 years earlier (a FAT scan! - family album tour) (Fig. 5-13B), an elicited history of spontaneous proptosis followed by subconjunctival hemorrhage at age 5 years, and the fact that the lesion resolved over the next month while the patient was under observation (Fig. 5-13C). His case demonstrates how eliciting a history of temporal change can aid in precise diagnosis.

Temporal change may be continuous and rapid or insidious, implying different processes. On the other hand, intermittent change, such as pulsation or alteration with Valsalva maneuver, suggests either a bony defect or a relation between the lesion and the vascular system. The child in Figure 5-14 had pulsating exophthalmos due to the rich vascular supply of an infantile orbital hemangioma.

The Abnormal Process

Clinically, inflammation is categorized on the basis of the severity of the signs and the rapidity of their onset. For instance, in acute infective cellulitis there is a sudden development of features of orbital inflammation with marked limitation of movement, proptosis, injection, and pain (Fig. 5-15). In contrast, a more subacute process, such as some cases of idiopathic inflammatory disease or thyroid ophthalmopathy, may have all or most of the features of inflammation, but they will be more subtle (Fig. 5-16).

A mass effect consists of displacement of orbital structures with or without compromise of function. With a well-encapsulated lesion, for instance, there tends to be displacement without much effect, other than mechanical indentation, of the orbital structures.

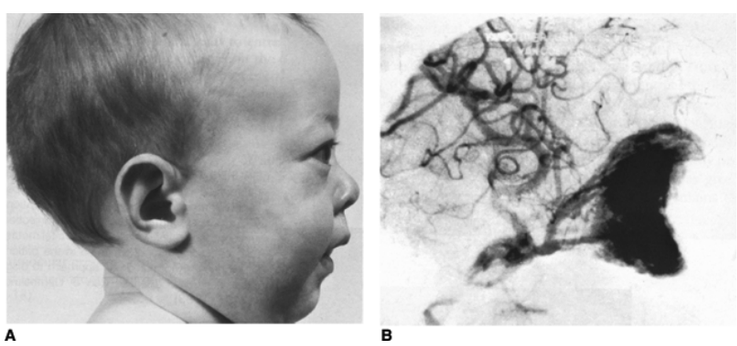

Figure 5-14. (A) Axial proptosis that pulsated. (B) Vascular capillary hemangioma of the orbit, demonstrated by arteriography, in the same infant. (Reproduced with permission from Rootman J. An approach to diagnosis of the orbit. Can J Ophthalmol 1983;18:102-7.)

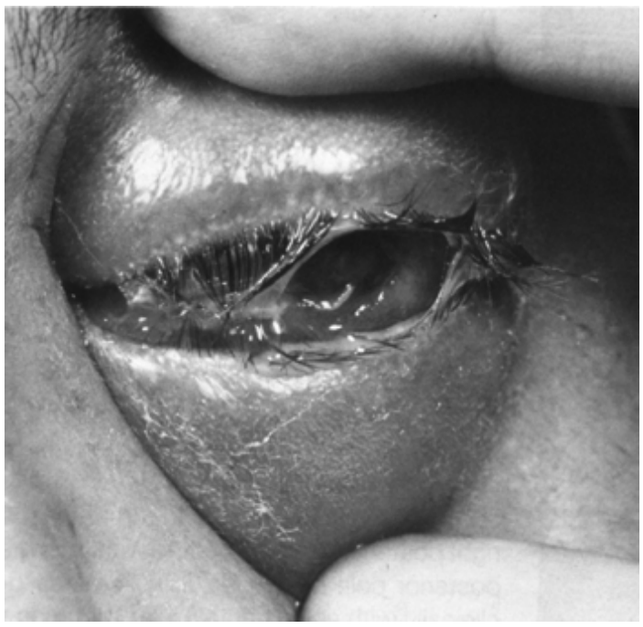

Figure 5-15. Lid edema, injection, and proptosis in a patient with acute orbital cellulitis secondary to pyemic enophthalmitis. The patient also had marked limitation of ocular movements and pain. (Reproduced with permission from Rootman J. An approach to diagnosis of orbital disease. Can J Ophthalmol 1983;18:102-7.)

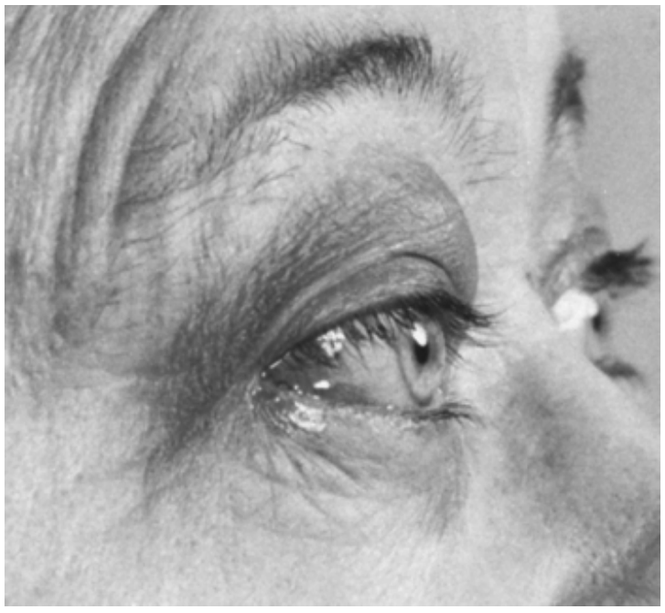

Figure 5-16. Lid edema, injection, and chemosis in a patient with subacute orbital inflammation due to thyroid orbitopathy. The patient also had limited ocular movements, but little pain. (Reproduced with permission from Rootman J. An approach to diagnosis of orbital disease. Can J Ophthalmol 1983;18:102-7.)

The process of infiltration leads to entrapment and damage of orbital structures, as seen in the enophthalmos, ptosis, and limited ocular movements of the patient with an orbital metastasis of sclerosing carcinoma (Fig. 5-10). On the other hand, the patient in Figure 5-17 presented with progressive proptosis, limitation of ocular movement, and papilledema of relatively rapid onset but no clinical evidence of inflammation; these signs pointed to a malignant or a destructive inflammatory process. The patient proved to have an orbital metastasis.

Vascular change is well demonstrated in patients showing episcleral venous dilatation, slightly increased intraocular pressure, retinal venous dilatation, and modest tissue engorgement due to arteriovenous shunts (Fig. 5-18).

Trying to answer the two questions about disease location and resultant dynamic alteration in all cases makes orbital examination more fun, more productive, and more accurate. To make a clinical diagnosis of orbital disease one should bring together information from the history and physical examination that identifies displacement, characterizes temporal development, and defines the disease process. Diseases of the orbit present virtually every combination of location and dynamic alteration. Defining these by clinical means does not necessarily provide absolute proof of the disease, but it does give a reasonable framework for investigation. It remains the most powerful tool for studying the patient.

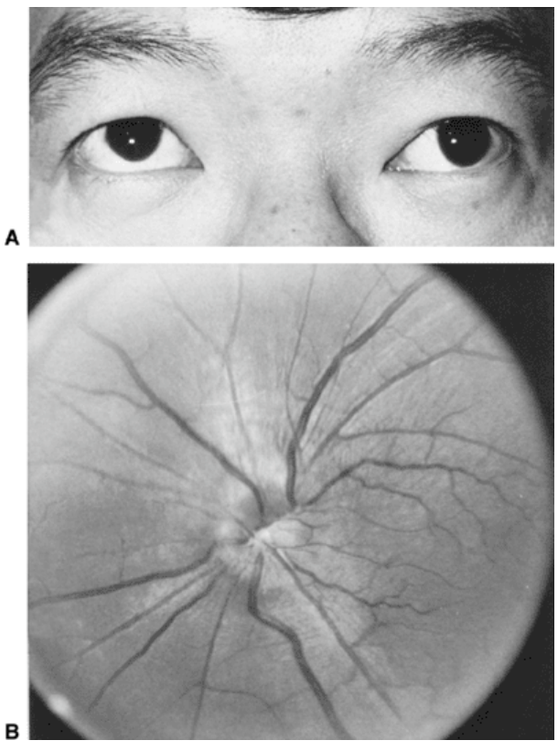

Figure 5-17. (A) Left-sided proptosis and limitation of upgaze (he is looking up) in a patient with rapidly progressive signs of infiltration. (B) Slight papilledema (note superior disc injection and engorged retinal veins) due to orbital metastasis of colonic adenocarcinoma in the same patient. (Reproduced with permission from Rootman J. An approach to diagnosis of orbital disease. Can J Ophthalmol 1983;18:102-7.)

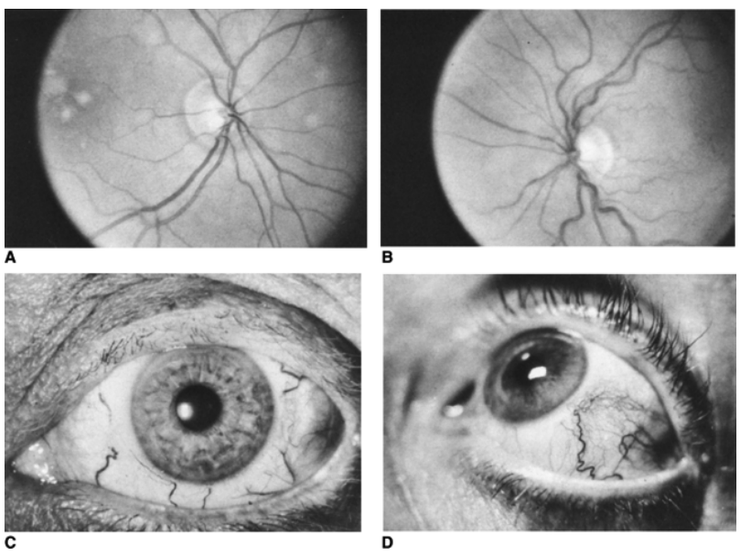

Figure 5-18. Clinical manifestations of low-flow arteriovenous shunts. Vascular dilatation and tortuosity of the left posterior pole is shown (B), compared with a normal right posterior pole (A). This was associated clinically with left epibulbar vascular dilatation (C) and 3 mm of proptosis that occurred in a 72-year-old woman. (D) Epibulbar vascular dilatation and tortuosity in a 74-year-old female who presented with a mild sixth nerve palsy, raised intraocular pressure (34 mmHg), and 2 mm of proptosis due to a low-flow dural arteriovenous shunt.

The Patient Encounter

History Taking (Table 5-1)

For the most part, history taking elucidates the dynamics of disease, particularly in terms of temporal onset and physiologic symptoms. To a lesser degree, it points to location, which is much more evident on physical examination. The temporal dynamics include questions concerning the onset, duration, intermittency, and chronicity of disease. It is frequently useful to ask patients for old photographs (FAT scan - family album tour) or observations of other family members. The symptoms suggesting various physiologic disturbances can be thought of as sensory, motor, psychophysical, structural, and functional.

Sensory

Sensory symptoms include pain, which should be characterized in terms of severity, location, radiation, and associations with ocular movements or exposure to light. Loss of, or modifications in, sensation should be elucidated by seeking symptoms of numbness, tingling, and cold and hot sensations.

Motor

Symptoms suggestive of motor abnormalities include diplopia, which should be characterized in terms of variation with direction of gaze, pain (especially gaze evoked), and any sensations of tightness on movement that may reflect a cicatricial or restrictive component.

Psychophysical

Psychophysical symptoms primarily relate to variations in visual acuity, color vision, and awareness of either positive or negative scotomata. With development of early and often subtle defects of optic nerve function, patients can often be aware of slight graying of their vision or color desaturation, which may be intermittent or gaze-related. It is often necessary to elicit this information specifically.

Structural

Structural changes symptomatically are associated with an awareness of displacement of the globe. Patients may have become aware of proptosis, enophthalmos, or horizontal or vertical displacements. In addition they may be conscious of fullness of the lids, intermittent swelling, or masses, which may or may not be tender.

Vascular

Symptoms reflecting vascular disease include swelling, redness, hyperemia, and epibulbar vascular dilatation.

Other

Other functional abnormalities related to orbital disease include increased lacrimation or dry eyes.

General Inquiry

Orbital disease is often associated with systemic abnormalities. Inquiry concerning the present state of health, current and past drug treatment, allergies, and significant dermatologic abnormalities should be elicited. Past illnesses should also be elicited, particularly endocrine disorder, immunologic disease, cancer, infections, surgery, and major medical disease. Some emphasis should be placed on symptoms of central nervous system disease including headache, sensory, and motor symptoms. Sometimes a family history of disease can aid in uncovering a diagnosis, particularly as relates to immunologic, neoplastic, endocrine, and infectious diseases.

Physical Examination of the Patient

Examination of the orbit should seek to glean information that provides for a pathophysiologic analysis of the patient. Although I disparage a mechanical approach to patients, it is useful to have a conceptual framework for obtaining the necessary information. This information can then be synthesized and an appropriate plan of investigation established.

Physical examination of the orbit can be divided into categories of general, psychophysical, orbital, ocular movement, and ocular assessment.

General assessment of the patient should include observations concerning the facial contours and lateral and vertical symmetry of facial, lid, orbital, and ocular structures. Particular attention should be paid not only to alterations in contour but changes in color (xanthochromia, redness, brawny discoloration) and pigmentation. The orbital and periorbital structures should be palpated as should the preauricular and cervical nodes. The lids and conjunctiva should be assessed for position and alterations in structure. I usually

measure the interpalpebral fissure bilaterally and document both upper and lower lid retraction, margin reflex distance (MRD), lid lag, and degree of scleral show. Measurement of maximum levator function should be included. Injection of both the conjunctiva and lids should be documented and graded (usually I use a three-point system). The degree of preseptal, pretarsal, and conjunctival edema should also be documented (using a subjective or three-point system). Chemosis can be graded as visible (1) to the gray line, (2) to the lid margin, and (3) over the lid margin.

1. **History of Illness**
   - Symptoms
   - Temporal
   - Dynamics
   - Sensory
   - Motor
   - Structural
   - Psychophysical
   - Functional
   - Onset Acuity: acute < 7 days
     subacute 1-4 weeks
     chronic/months > 4 weeks
     chronic/years > 1 year

2. **General Status**
   - Allergies
   - Drugs
   - Past Illnesses
     - Medical & immune diseases
     - Surgical
     - Ocular
   - Social History
     - Tobacco
     - Alcohol
     - Drugs
   - Family History
   - Functional Inquiry

3. **Physical Examination**

a. **Psychophysical** **OD** **OS**
   - Keratometry
   - Visual Acuity
     - without correction
     - with correction
     - manifest
   - Color Vision (Isihara)
   - Visual Field (Confrontation)
   - Amsler Grid
   - Sensory Function - V1, V2, V3
   - Pupils
   - Afferent: __ log units; R / L / none

b. **Eyelids**
   - Facial Contours
   - Edema (0 to 3)
     - Upper preseptal
     - Upper pretarsal
     - Lower preseptal
     - Chemosis
   - Injection (0 to 3)
     - Upper preseptal
     - Conjunctival
   - Lid Margins (mm)
     - Interpalpebral fissure
     - MRD
     - Upper scleral show
     - Lower scleral show
     - Maximum levator function
     - Lagophthlamos
     - Upper lid lag (y / n)
     - Lid fold
   - Auscultation
   - Nodes

Orbital Fat Prolapse
(label figure 0 to +2)

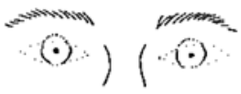

c. **Orbit** **OD** **OS**
   - Displacement (mm)
     - Vertical
     - Horizontal
   - Ballotment – increasing firmness (0 to 3)
   - Exophthalmometry (mm)
     - Hertel
     - Facial
   - Lacrimal Gland Palpation (0 to 2)

d. **Motility**
   - Versions (Hirschberg)

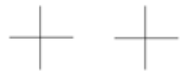

   - Prism Cover Test
     - Manifest tropia
     - (primary position)
   - Forced Ductions
     - Increasing tension (1 to 4)

   - Compliance (tightness of orbit)

e. **Ocular Examination**
   - Biomicroscopy
     - Fornix
     - Cornea – punctate stain (0 to 3)
     - Anterior chamber
     - Iris color/angle
     - Structure - lens
   - Schirmer Test
   - Intraocular Pressure (mmHg)
     - Straight (5° down)
     - Up (max.)
     - Other
   - Vitreous
   - Fundus Examination
     - Disk edema (0 to 3)
     - Optic atrophy (0 to 3)
     - Macula
     - Choroidal folds (draw in)

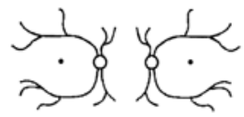

4. **Analysis Profile**
   - Location
   - Dynamics: Temporal
     Physiologic

5. **Investigations**

6. **Diagnosis**

5. **Planned Management**: Conservative
   Medical
   Surgical
   Other

6. **Management**

7. **Outcome**

Table 5-1. New patient profile.

Psychophysical examination includes a study of the best corrected visual acuity, confrontation visual fields, a central visual acuity using an Amsler grid, and color vision assessment. In addition, the sensory functions of the fifth nerve should be assessed both for light touch and pain. Pupillary examination should assess size, symmetry, light, and near reaction as well as check for afferent pupillary defects.

Orbital examination should document the degree of horizontal and vertical displacement of the globe, the ease of ballotment (which can be either measured subjectively in a three-point system or by millimeter measurement). Exophthalmometry should be documented and the width of the exophthalmometer recorded. In general, differences of greater than 2 mm relative protrusion between eyes requires investigation for proptosis or enophthalmos. Normal exophthalmometry measurements will vary according to age, sex, and race. Fledelius and Stubgaard's study of 267 subjects showed that the average protrusion values for those between 10 and 20 years of age were within 1 standard deviation below the values for adults (>19 years). In children aged 5 to 7 years, mean protrusion values were 12.6 mm for females and 13.7 mm for males whilst for 8- to 10-year-olds, the mean values were 14.1 mm for females and 13.7 mm for males. In the adult group (20 years and older), the mean values for females and males were 16.0 mm and 16.5 mm respectively. There is a documented racial difference in protrusion values for adults (Table 5-2); blacks are shown to have greater mean values than Caucasians, with Asians lying somewhere in between the two.

Table 5-2. Normal exophthalmometry measurements (Hertel) in adults

	MALES		FEMALES		
RACE	**Mean (mm)**	**Standard Deviation**	**Mean (mm)**	**Standard Deviation**	**SOURCE**
Black	18.20	2.97	17.46	2.64	Dunsky
Black	18.56*	3.08	17.90*	2.61	Migliori & Gladstone
Asian*	16.73	1.90	16.64	1.81	Quant & Woo
Caucasian-American	16.55*	2.57	**15.46***	2.34	Migliori & Gladstone

* measurements for the right eye used

In instances where one is suspicious for vascular lesions, care should be taken to assess whether or not there is evidence of pulsation, either by carefully looking at the eyes from a lateral point of view or in the mirror of the exophthalmometer. Sometimes, subtle pulsation is only evident on slit lamp examination and, when the lesion originates from an intracranial defect, may have a downward component. In distensible venous anomalies, the normally enophthalmic orbit may be best evaluated hemodynamically by inducing a Valsalva maneuver. This is best achieved by having the patient hold their breath and then bend down in the seated position with their head between their legs, thereby raising the thoracic and abdominal pressure and reducing venous out-flow.

Ocular movements can be documented by recording ductions and versions in the four cardinal positions by degrees. We use the Hirschberg test to measure this with a light reflex at the pupil margin representing 15, in the mid-iris 30, and the limbus 45. Cover and cross cover tests with prism measurements should assess manifest deviations. I also do Maddox rod testing using a Risley prism in the primary position, upgaze, downgaze, right gaze, and left gaze. Any evidence of abnormalities of movements will require a forced duction examination, which can be recorded subjectively as 1 through 3.

Ocular examination should include measurement of the intraocular pressure in the primary position and upgaze. Frequently, in the presence of a duction abnormality there is a pressure rise in the position of gaze opposite to a cicatrized

muscle. Biomicroscopy of the cornea, conjunctiva, and fornices should be carefully done. Finally the fundus, optic nerve head, retinal blood vessels, and choroid should be carefully examined with direct and indirect ophthalmoscopy. In particular, evidence of choroidal folds, disc edema, and optociliary vessels should be ruled out. Indentation of the globe may be noted, and if it is due to a mass the indentation may shift as you observe the fundus with an indirect ophthalmoscope and the patient alters his ocular position.

Following history taking and physical examination, it is useful to develop an analysis profile of the patient in which location and dynamics, both temporal and physiologic, can be summarized. This then should lead to the development of a differential diagnosis and an investigative plan.

Prospective follow-up should include a record of management, outcome, or progression of disease with and without therapy. A chart profile for documentation is provided in Table 5-1 .

Differential Diagnosis - Analysis Profile

The differential diagnosis in a patient should develop a specific analysis profile that is based on the determinant symptoms and symptoms brought about by the history taking and physical examination (Fig. 5-19). This should lead to a supposition concerning the location of the disease and the dynamic alterations brought about by the disease process. For instance, a patient with slow onset disease that is characterized by infiltrative effect and protrusion of the globe would fit into the differential diagnosis of insidious-onset infiltrative disease, and this would be contextualized to the individual depending upon the age and frequency of such diseases at that age. Greater specificity then can be obtained by again placing the patient's clinical findings within the context of specific confirmatory investigations. Prospective follow-up should then include a record of management, outcome, or progression of disease with and without therapy.

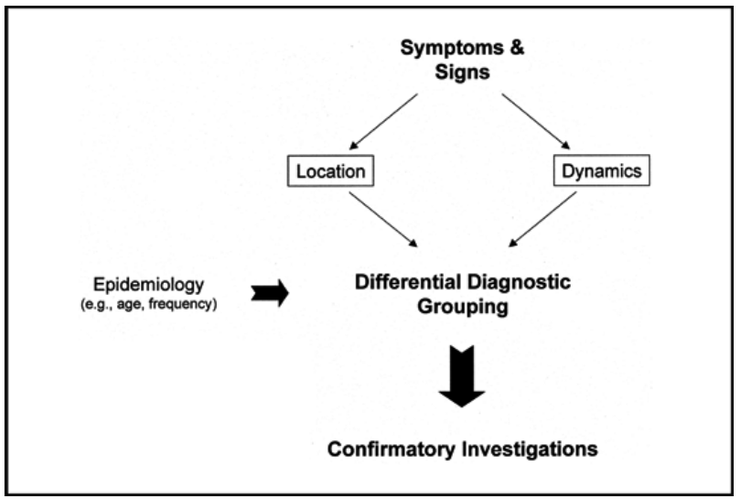

Figure 5-19. Analysis profile for differential diagnosis of orbital disease.

Bibliography

Dunsky IL. Normative data for Hertel exophthalmometry in a normal adult black population. Optom Vis Sci 1992;69:562-4.

Fledelius HC, Stubgaard M. Changes in eye position during growth and adult life as based on exophthalmometry, interpupillary distance, and orbital distance measurements. Acta Ophthalmologica 1986;64:481-6.

Migliori ME, Gladstone GJ. Determination of the normal range of exophthalmometric values for black and white adults. Am J Ophthalmol 1984;98:438-42.

Quant JR, Woo GC. Normal values of eye position and head size in Chinese children from Hong Kong. Optom Vis Sci 1993;70:668-71.

Quant JR, Woo GC. Normal values of eye position in the Chinese population of Hong Kong. Optom Vis Sci 1992;69:152-8.

Rootman J. An approach to diagnosis of orbital disease. Can J Ophthalmol 1983;18:102-7.

Chapter 6

Confirmatory Investigation of Orbital Disease and Effect on Function

Investigative procedures based on a framework of clinical analysis should elucidate a diagnosis by defining the location, dynamics (both temporal and process related), and structure of orbital lesions. The investigations following history and physical examination include ocular and visual function assessment, orbital imaging, systemic survey, and pathologic study. Ocular and psychophysical investigations provide evidence of the functional effect of disease on the visual apparatus. Imaging methods help to pinpoint location and suggest features of inflammatory, mass, infiltrative, vascular, and structural change. Systemic investigation is particularly important in assessment of the patient because endocrine, vascular, infectious, immunologic, and neoplastic disease may have orbital manifestations. Histopathologic analysis, the final arbiter, has become increasingly sophisticated, requiring an awareness of technical change to maximize the value of biopsy material for diagnosis, prognosis, and research. Therapeutic decisions are then made on the basis of the clinical analysis and investigations.

Extraocular and Visual Function Examination in Orbital Disease

To assess the effect of disease on ocular and orbital function, there are an array of methods to study psychophysical function, ocular motility, blood supply, and lacrimal dynamics. Optic nerve function may be delineated by study of color vision, visual fields, and visually evoked responses. Dysfunction of the muscles or neuromuscular apparatus may be detected early, documented, and studied on a temporal basis. Tear production, content, and drainage can be studied with simple or sophisticated techniques.

Psychophysical Study

Although history and physical examination is the cornerstone for diagnosis, psychophysical and electrophysiological investigations frequently contribute to the understanding of the overall clinical picture.

The role of psychophysical (color vision, visual field, and contrast sensitivity testing) and electrophysiological investigations can best be illustrated with cases where these techniques have been helpful. Psychophysics plays a role in several clinical settings: the identification of functional pathology where clinical evidence is scanty or “soft,” confirmation of more obvious clinical findings, and for the follow-up of patients to monitor progression of disease or post-therapeutic change.

Apical Hemangioma, Left Orbit

The patient, a 36-year-old man, had a history of longstanding left proptosis with a recent onset of central visual problems. He had a visual acuity reduced to 20/80 OS (OD 20/20), a slightly swollen optic nerve head, and a small superotemporal focal elevation of the peripapillary retina due to a presumed subretinal hemorrhage. Normal pattern visual evoked potentials (VEP) results were obtained from the right eye with a very prolonged delay and reduction of VEP voltage from the left eye (Fig. 6-1). Color vision assessment showed virtually no pathology on testing with Ishihara and Dvorine plates or the Farnsworth Pane D15, but hue discrimination testing on the FarnsworthMunsell 100 Hue test revealed a marked abnormality of color performance. (The patient's score was 368 for the left eye; the 95th percentile limit for this age group is 120.) Visual field studies show that there was a small central scotoma and expansion of the blind spot (Fig. 6-2A). Imaging revealed a large intraconal enhancing mass crowding the apex of the orbit (Fig. 6-3). Clinically, it appeared to be a hemangioma. It was removed by lateral orbitotomy.

The patient was assessed again 6 months postoperatively. Visual acuity had improved to 20/30. This was confirmed

also by VEP and color vision testing. For the left eye, VEP implicit time had shortened and voltage had increased, though still not to normal values (Fig. 6-1). He had a small persistent visual field defect (Fig. 6-2B) and a focal superotemporal peripapillary scar. The FarnsworthMunsell 100 Hue score had decreased to 200 in the left eye, a significant improvement though still abnormal.

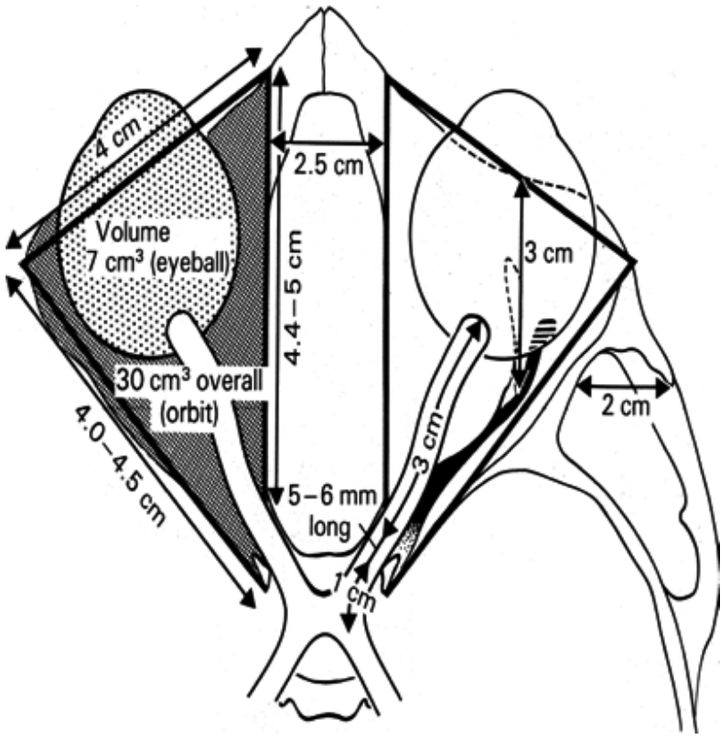

Figure 6-1. Visual evoked potentials (VEP) of normal right eye and abnormal left eye preoperatively and postoperatively in a patient with an apical compressive hemangioma of the orbit. VEP implicit time improved, but not to normal levels.

Comment: The VEP changes in this patient are typical of compressive lesions in the orbit affecting optic nerve function. VEP voltage drops more or less in parallel with the changes in visual acuity, whereas the changes in VEP implicit time indicate better the extent of optic nerve dysfunction. Improvement in visual function was also documented by increased visual acuity and color vision even with a persistent visual field defect.

Thyroid Orbitopathy

Preoperatively, the patient, a women with compressive thyroid orbitopathy (the crowded orbital apex syndrome) and marked soft tissue and oculomotor signs, exhibited visual field defects (greater on the left) and visual acuity of 20/40+ right eye, 20/70 left eye. VEP and color vision assessments were performed also. VEP studies showed normal recordings on the right, but reduced and delayed major peaks from studies of the left (Fig. 6-4). Color vision studies confirmed the left severe optic nerve dysfunction, showing major color confusion errors on Ishihara and Dvorine testing, and predominantly red/green losses on both Farnsworth D15 and FarnsworthMunsell 100 Hue testing. Scores for the right eye were within normal limits on all tests.

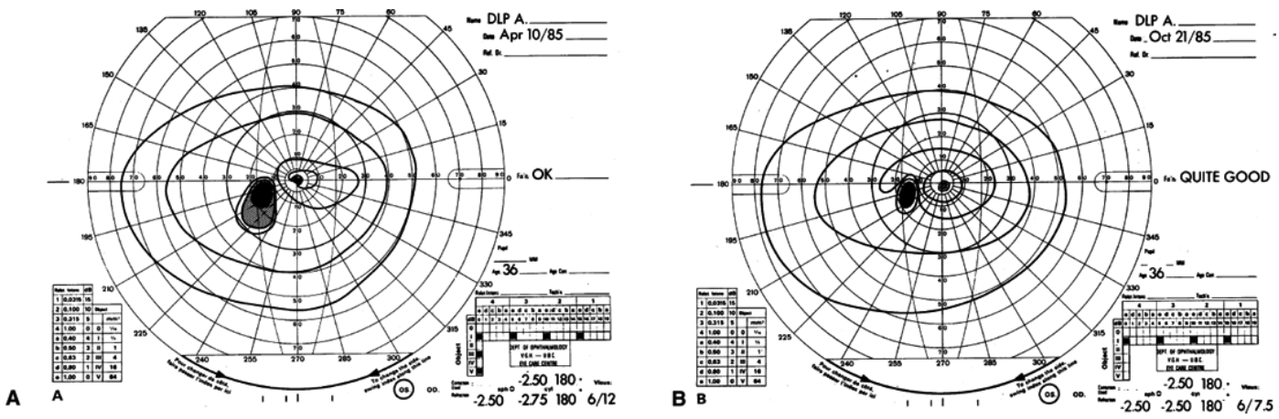

Figure 6-2. (A) Preoperative visual field of the patient demonstrated in Figure 6-1 shows enlargement of the blind spot and a small paracentral relative scotoma. The enlargement of the blind sport corresponded to a focal area of subretinal neovascularization above the disc. Central vision at this point was 20/80. (B) Visual field of the same patient 6 months after removal of an apical cavernous hemangioma. There was an improvement in central visual acuity (20/30), with an increase in the size of the central isopters but a persistence of the scotoma.

Testing was conducted 3 months after orbital decompression. Central visual acuity had worsened somewhat (20/60 right eye, 20/80 left eye), but both VEP and color vision performance had improved significantly (Fig. 6-4). VEP implicit time was nearly normal, although the amplitude of the major positive peak remained in the subnormal range. The acquired red/green defect remained present on color vision assessment, but had decreased in severity.

This case illustrates the fact that VEP and color vision testing can sometimes provide documentation of a visual function change not evident on visual acuity testing alone. The improvement in conduction and decrease in vision pointed to additional retinal pathology rather than persistent compressive optic neuropathy.

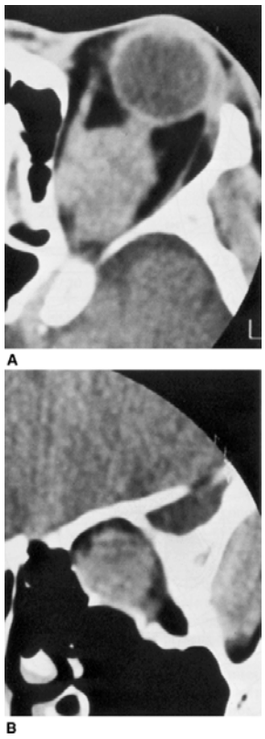

Figure 6-3. Axial and coronal CT scans of the patient in Figs. 6-1 and 6-2 show a well-defined, lobular mass surrounding and obscuring the optic nerve and extending to the orbital apex.

Visual Field Assessment

The function of the optic nerve is frequently impaired by disease of the orbit, optic canal, and intracranial lesions anterior to the chiasm. Although the visual field defects are not pathognomonic of the type of disturbance, whether compressive, infiltrative, or inflammatory, they are more likely to indicate location of disease at these sites. The defect may suggest direction of compression in the case of mass lesions or whether the entire nerve is involved in some infiltrative process. A single examination of the field may not be characteristic, but the type of progression, nature of onset, and possible regression will help in the clinical evaluation of the dynamics of orbital disease.

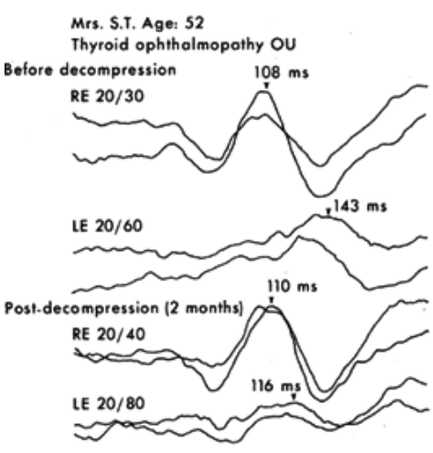

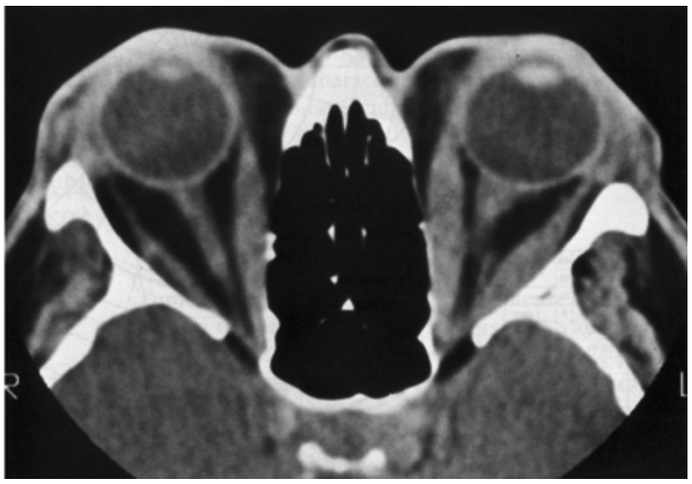

Figure 6-4. (Left) VEP before and after decompression in a patient with compressive thyroid optic neuropathy. Note improvement in the implicit time with slight deterioration of vision, which was due to concurrent retinal pathology. (Right) Axial CT scan of the same patient shows left apical compression. Note distention of the left retrobulbar nerve sheath.

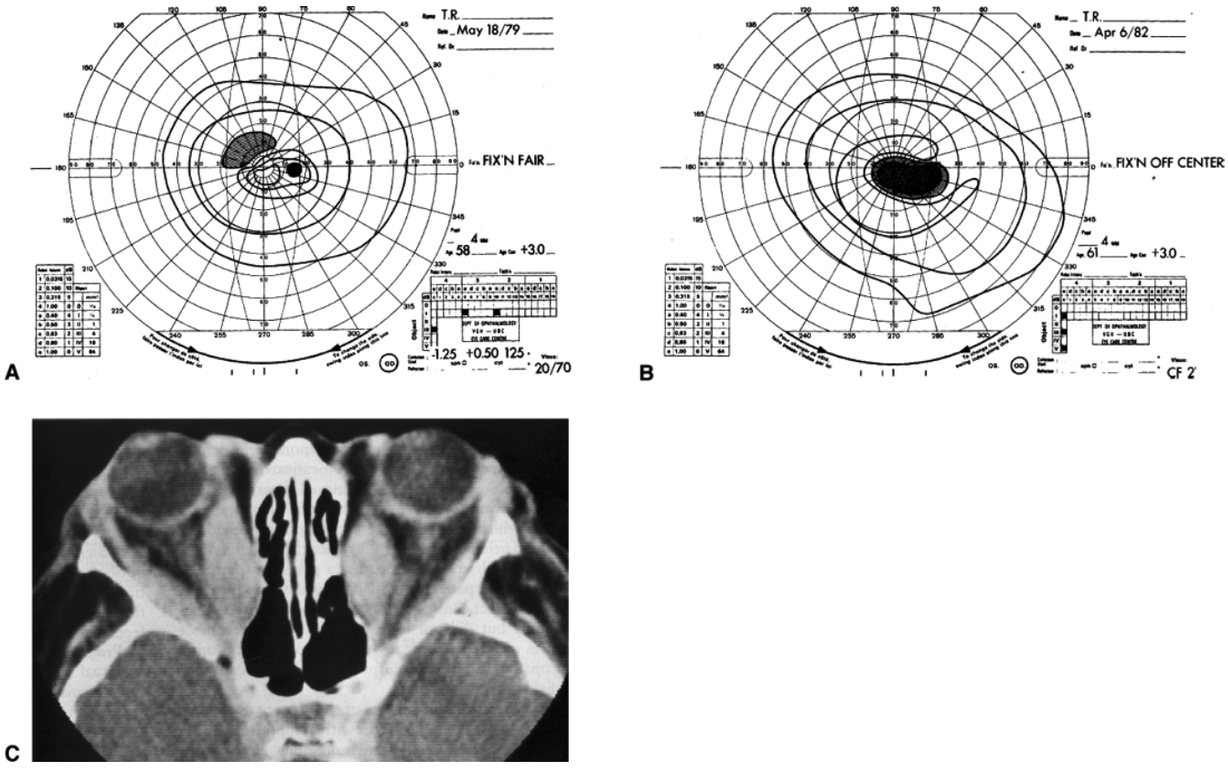

Figure 6-5. Visual fields of a patient with compressive thyroid orbitopathy who showed progression of a central (A) to a centrocecal (B) defect. (C) The patient's axial CT scan shows apical compression and massive medial rectus muscles. Note bilateral bowing of the lamina papyracea (“Coca Cola” sign).

Involvement of the Optic Nerve in the Orbit

Masses in the anterior orbit are less likely to involve the optic nerve than tumors at the apex, where there is less space and the optic nerve is more fixed. Field defects due to apical orbital disease are predominantly centrocecal scotomas, which may be dense when the patient first presents or may start as small paracentral nuclei between the blind spot and fixation, and gradually progress to become centrocecal defects (Fig. 6-5). Such scotomas may break through to the periphery, a feature that we have noted particularly in optic neuropathy of thyroid orbitopathy where the breakthrough is more often inferior than superior (Fig. 6-6). Generalized contraction of the isopters may also occur but is a nonspecific finding and always difficult to interpret. When the patient's visual acuity remains good and there is no disturbance of the clarity of the media (so that no other cause for a contraction of the isopters exists), contraction should raise the suspicion of optic nerve involvement.

The visual field may also show abnormalities of localized sectors. Those most commonly involved are the temporal visual field, from medial compression, and the inferior sectors, presumably from superior pressure or compression of the nerve against superior structures. The visual field defects

of thyroid orbitopathy and compressive tumors at the orbital apex suggest that the temporal and nasal fibers are already well segregated into those that will cross in the chiasm and those that will remain uncrossed on their way to the lateral geniculate body. Therefore, it is not unusual to find evidence of a vertical step in optic nerve compression at the apex. In bilateral orbital disease, particularly thyroid orbitopathy, chiasmal disease may be suspected if both visual fields have a temporal defect with a vertical step. In our series of thyroid orbitopathy with optic neuropathy, there were a number of such cases where chiasmal disease was excluded by CT studies and the orbital pathologic process could not possibly have involved the junction of the optic nerves. Thus, bitemporal field defects may be misleading in terms of the location of the lesion. Additionally, we have had several unusual experiences with patients having thyroid orbitopathy and temporal field defects, which emphasize the necessity for a broad approach to field defects. In one instance the patient had a parasellar dermoid in addition to thyroid orbitopathy; in another, a basilar aneurysm accounted for the field defect. Both patients had thyroid orbitopathy but did not have the usual constellation of features associated with thyroid orbitopathy and optic neuropathy, leading us to suspect another cause for the field defect.

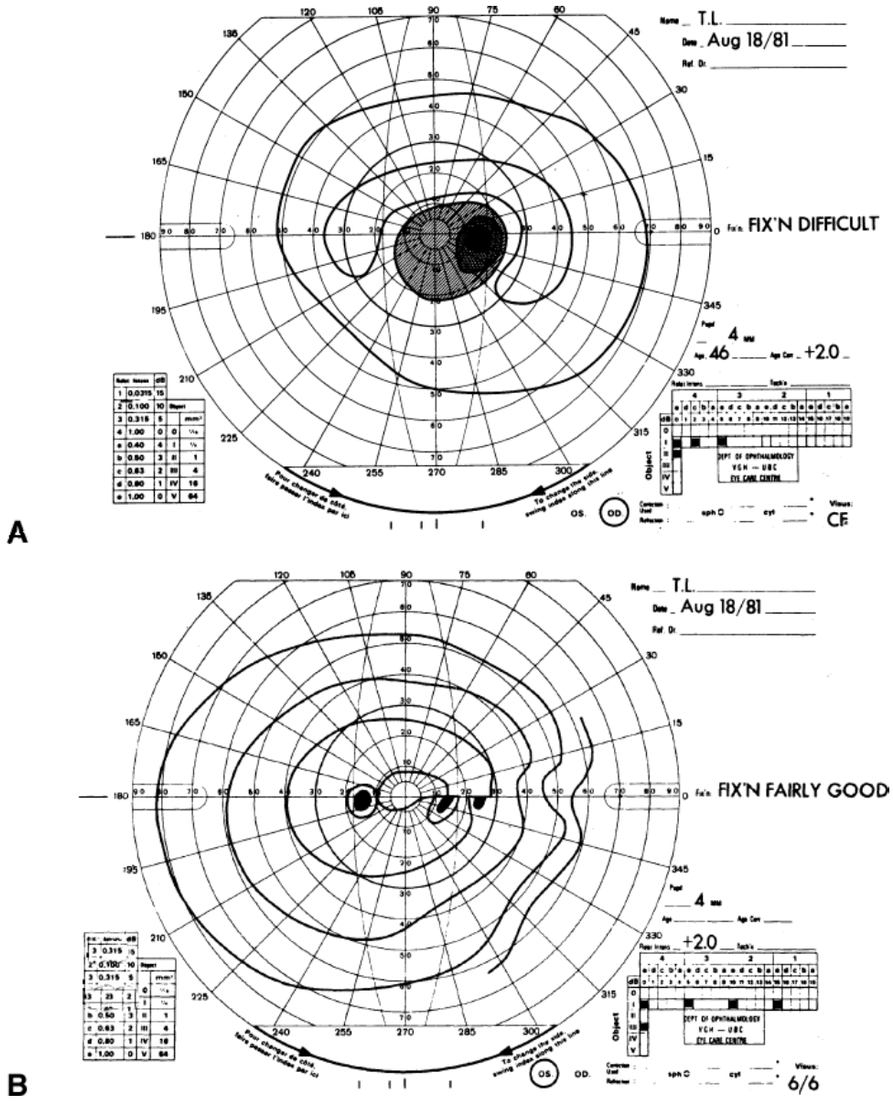

Figure 6-6. Visual fields of a patient with a bilateral longstanding compressive optic neuropathy, which is worse on the right (A) than on the left (B). The right visual field shows a dense centrocecal scotoma whereas the left shows an inferior nerve fiber bundle defect with some nasal peripheral isopter indentation. The early field defect on the left was a frequent type seen in a series of thyroid orbitopathy with optic neuropathy.

Nerve fiber bundle defects of the arcuate or inferior altitudinal types may also occur with compression of the optic nerve. However, they are more unusual.

Intracranial and Cranial Lesions Affecting the Optic Nerve

Intracranial compression will most likely occur from meningiomas of the optic nerve or adjacent structures, aneurysms of the anterior part of the circle of Willis, craniopharyngiomas, and pituitary tumors. Visual field defects in these instances are not unlike those of orbital apex lesions. Centrocecal scotomas, frequently with breakthrough to the superior periphery, are the most common defects. Classic nerve fiber and altitudinal defects are also common. The closer the lesion is to the chiasm, the more likely a defect of the opposite visual field. This produces a junctional scotoma, a temporal defect with a vertical step, which may go on to involve the entire upper temporal quadrant of the opposite field. Visual field study is useful in assessing optic nerve tumor extent and ruling out chiasmal involvement. Although such a combination is suggestive of intracranial optic nerve involvement, we have already noted that in bilateral apical compression due to thyroid orbitopathy, vertical steps and temporal field defects may occur and be misleading.

Disease progression may be monitored with ongoing visual fields, particularly with cranio-orbital meningiomas. The rate of progression of visual field defects due to meningiomas is variable but tends to be slow. Improvement can be noted following surgical decompression of sphenoid wing meningiomas (Fig. 6-7).

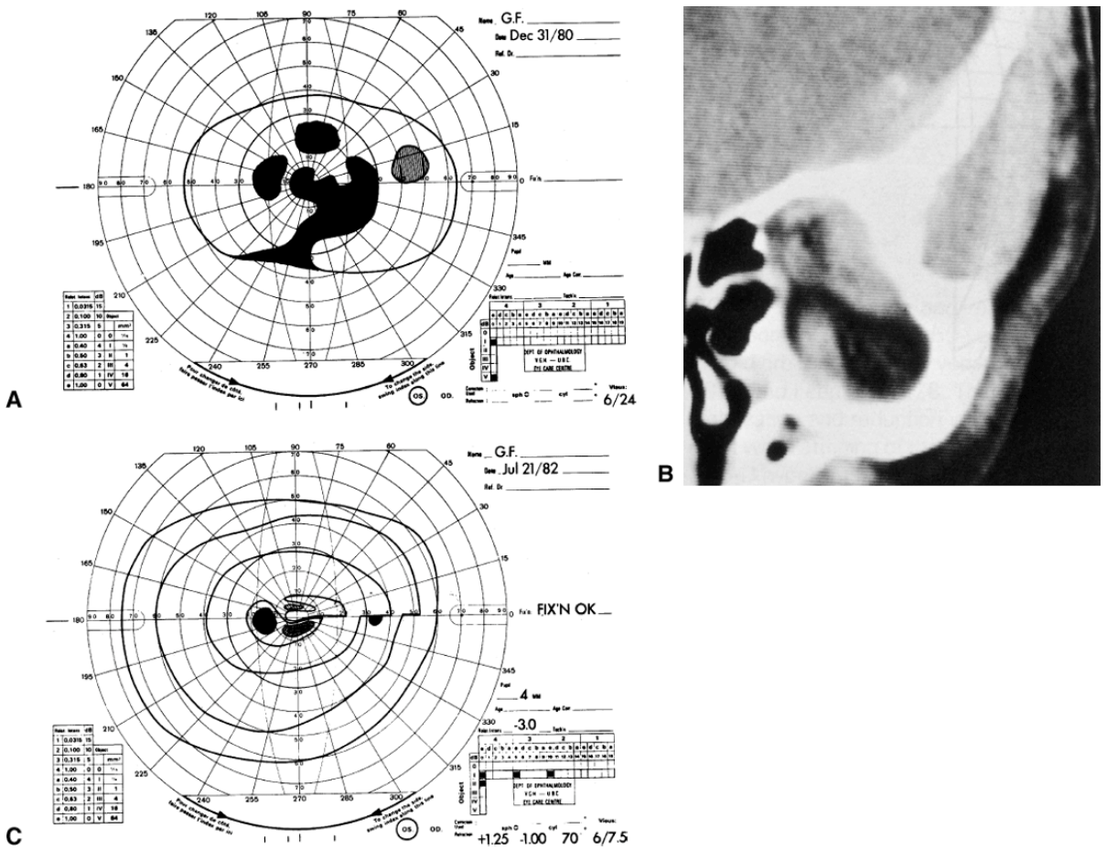

Figure 6-7. (A) Visual field defect in a patient with a sphenoid wing meningioma. The meningioma had encroached on the apical orbit and the optic nerve intracranially. There is a dense central scotoma breaking through inferiorly. Two other dense paracentral scotomas are present. The CT scan (B) shows a meningioma involving the apex of the orbit, temporalis fossa, and anterior cranial fossa. (C) Visual field of the same patient after surgical resection of the meningioma shows improvement of vision from 6/24 to 6/7.5. The central scotoma disappeared with good visual recovery. An upper and lower nerve fiber bundle defect remained.

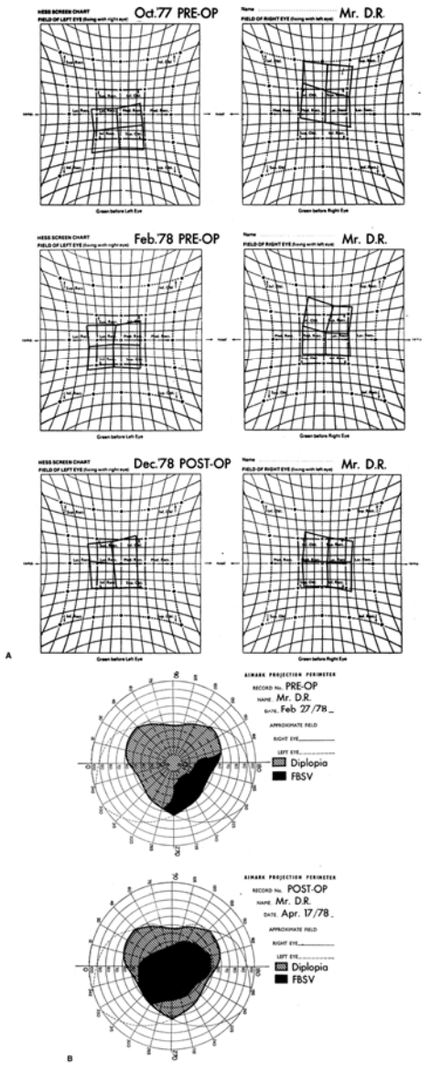

Figure 6-8. (A, top and middle) Preoperative Hess screen tests of a 50-year-old patient with thyroid orbitopathy and myopathy, done in October 1977 and February 1978. There was evidence of stabilization and reduction in the cyclovertical element with flattening of the top and bottom. He had a 25 diopter hypertropia and a 6 diopter exophoria. (A, bottom) Postoperative Hess screen of the same patient following a left inferior rectus adjustable recession. Note marked improvement in vertical element. (B, top) Preoperative binocular field vision of the same patient. (B, bottom) Postoperative binocular field of vision showing restoration of the central field.

Oculomotor Examination

Accurate oculomotor assessment is useful in differentiating between infiltrative and noninfiltrative (cicatricial effect or paresis) restrictions caused by orbital disease. Forced ductions help to distinguish between infiltrative and noninfiltrative myopathies. In addition, prospective evaluation with objective measurements, including Hess screens, allows documentation of primary features and progression of disease. For example, preoperative evaluation of patients with progressive myopathies, particularly when thyroid related, helps to define the need for and timing of intervention (Fig. 6-8A). Documentation of the binocular field of vision is also a useful adjunctive test following treatment (Fig. 6-8B).

Orbital Imaging

Jack Rootman

Robert A. Nugent

Orbital imaging has allowed for increased specificity concerning the position, nature, and progress of lesions. Procedures should be varied and specific, based on the implied clinical location and dynamic character of processes. Imaging can define the location, relationship to adjacent structures, evidence of infiltration, capsular definition, contour, tissue characteristics, dynamic effects (movement and positional change), and relationship to the vascular system allowing greater specificity in diagnosis and management. Imaging can also be useful in procedures such as needle biopsy and both intra- and preoperative localization and

characterization of lesions. In addition, changes in the lesion with time can aid in diagnosis, timing of intervention, and assessment of progression or effect of treatment.

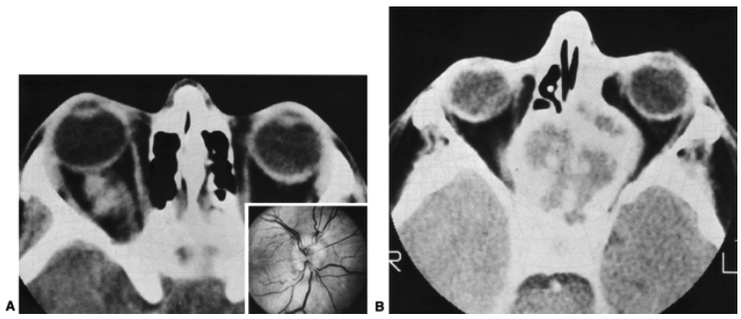

Figure 6-9. These two patients presented with axial proptosis, in one instance due to an intraconal hemangioma with some displacement of the optic nerve (A) and in the other a chondrosarcoma arising from the ethmoid sinus complex (B).

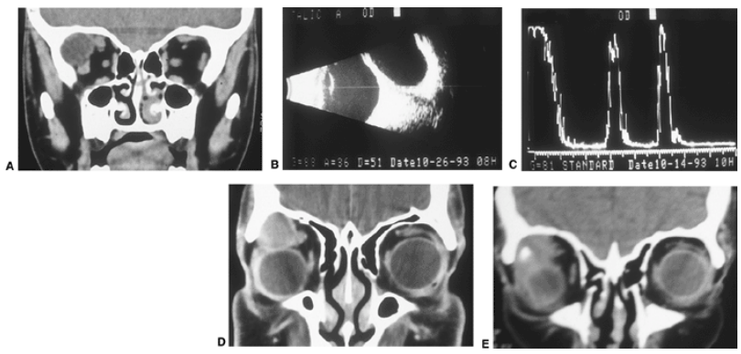

Figure 6-10. (A) Coronal CT scan demonstrates a well-defined cystic lesion in the lacrimal fossa, confirmed on B- and A-scan ultrasonography (B and C). It proved to be a hydatid cyst. (D) This mass presented in a 50-year-old man with a 2-year history of bulging of the right eye. On retrospective photographic review, the lesion had been present at least 5 years. It is a well-marginated, homogeneous, mildly lobulated, enhancing soft tissue density, which displaces the globe inferiorly and anteriorly; the adjacent muscles are also displaced. There was no calcification. Bony remodelling of the lacrimal fossa is noted, suggesting a longstanding lesion. Physical examination revealed 5 mm of proptosis, 10 mm downward displacement, and 4 mm medial displacement with slight limitation of upgaze. The globe appeared indented superolaterally. The tumor was removed en bloc and proved to be a pleomorphic adenoma. (E) This 74-year-old woman presented with a 6-month history of right frontal headache as well as paresthesia of the lateral orbital rim. In addition, she was aware of increasing prominence of the right eye with intermittent vertical diplopia. On physical examination, she had no evidence of dysesthesia but was aware of tenderness in the superolateral orbital rim on the right. A firm nodular mass was palpated. There was a small right hypotropia in extreme upgaze with limitation of movement and there were choroidal folds superotemporally. Coronal CT scan demonstrates an irregular lacrimal mass with focal calcification and a relatively normal-shaped lacrimal fossa. Aspiration needle biopsy revealed an adenoid cystic carcinoma. The patient underwent radical excision of the orbit and adjacent bone. The adjacent bone was involved to the excision borders so the patient underwent radical radiotherapy of 5000 cGy in 25 fractions. She developed local recurrence of disease and ultimately lung metastasis over a 5-year period.

For example, in the differential diagnosis of the patient with axial proptosis, CT scanning localized the disease to the intraconal space in the case of a hemangioma and to the orbital apex and medial wall in a case of chondrosarcoma of the sinus (Fig. 6-9). Imaging can define the difference between cystic, noninfiltrative, and infiltrative masses, as illustrated by cases of hydatid cyst (Figs. 6-10A to C), lacrimal gland adenoma (Fig. 6-10D), and lacrimal carcinoma (Fig. 6-10E). Localization of tumors preoperatively or for ancillary diagnostic procedures, such as aspiration needle biopsy, can be done accurately using CT scan or ultrasound (Fig. 6-11). Finally, disease progress or the effect of treatment can be monitored, as shown in a patient with Ewing's sarcoma of the orbit and nasopharynx before and after treatment with radiotherapy and systemic chemotherapy (Fig. 6-12). MRI is particularly helpful in characterizing, localizing, and studying the extent of lesions of the orbital apex, optic nerve, and central nervous system (Fig. 6-13).

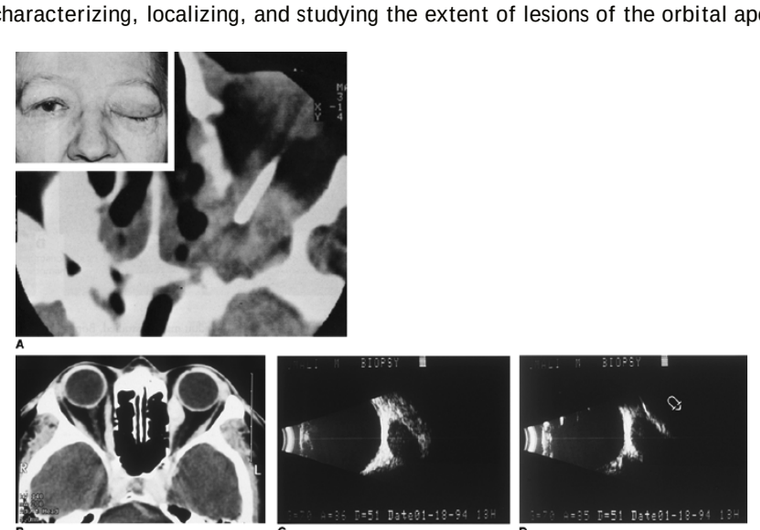

Figure 6-11. (A) This demonstrates the value of orbital imaging for localization during a needle aspiration biopsy of a patient with progressive proptosis, ptosis, third nerve palsy, and an infiltrative mass extending from the apex of the maxillary sinus into the orbit. Ultrasound can be used in the same manner. (B) This axial CT scan demonstrates a 1.5 cm fusiform mass of the left medial rectus and irregular enlargement of the right medial rectus in a 63-year-old man with known metastatic carcinoma of the colon. Ultrasound demonstrates the enlarged medial rectus without (C) and with the aspiration biopsy needle inserted (D, arrow).

Advances in imaging continue to improve soft tissue detail and have superceded traditional techniques, such as plain film radiography. This section discusses available imaging techniques and their essential roles in assessing orbital disease.

Echography

Orbital echography, which is a noninvasive ultrasonographic technique, provides useful information regarding the location, size, shape, tissue characteristics, and vascular features of orbital disease. The technique of standardized echography combines information obtained from Amode, Bmode, and Doppler echography. The reflections of sound waves of an Ascan are emitted from a small probe, and can be displayed on an oscilloscope. These can differentiate the reflectivity, structure, sound attenuation, location, size, borders, mobility, and compressibility of lesions. With the added twodimensional modality of Bscan, location, shape, and size can be graphically demonstrated. Doppler echography provides information concerning vascularity.

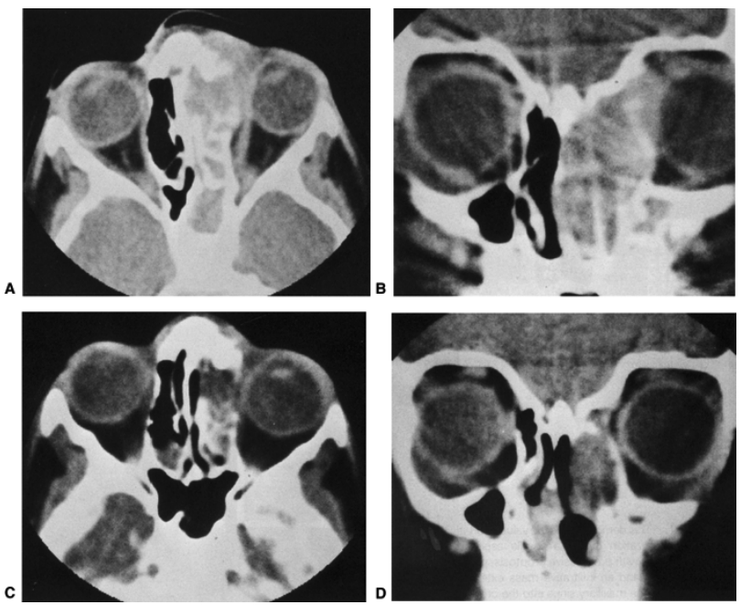

Figure 6-12. Regression of a Ewing's sarcoma can be demonstrated by comparison of axial and coronal scans prior to (A, B) and after (C, D) radiotherapy and chemotherapy.

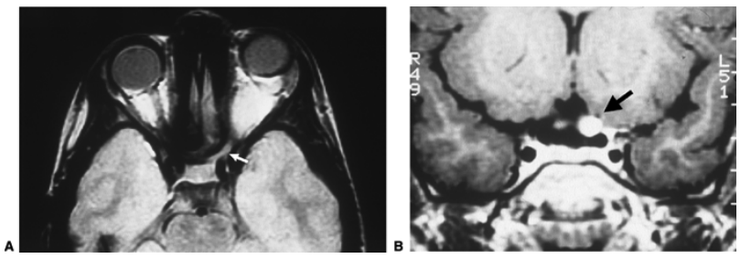

Fig. 6-13. (A) This T2-weighted axial MRI demonstrates an optic nerve glioma extending along the optic canal to the prechiasmal area (arrow). The tumor was excised to within 2 mm of the chiasm but was histologically present at the margin. (B) The coronal view of a T1-weighted MRI of the same patient 2 years later demonstrates growth of the residual tumor.

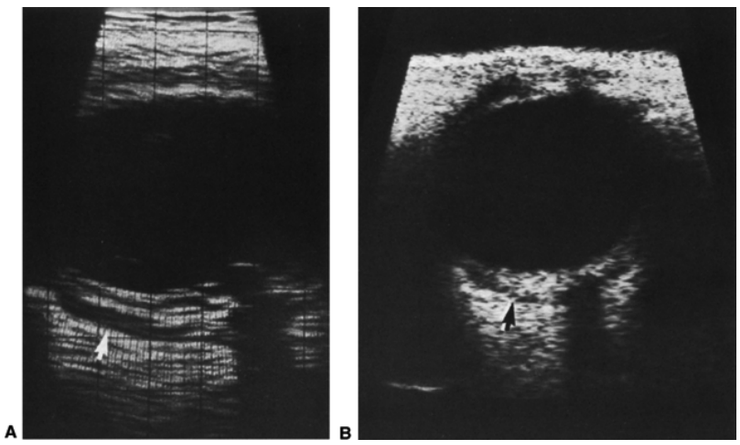

Figure 6-14. These B-mode ultrasound images demonstrate features of posterior scleritis. In both instances, there is evidence of thickening of the scleral envelope posteriorly, and fluid accumulation in Tenon's space (arrow).

Depending on the type of lesion being studied, the overall technique should involve a combination of these methods. We utilize echography primarily as an adjunctive imaging modality. It is particularly useful in assessing lesions that involve the globe and adjacent orbit, such as scleritis (Fig. 6-14). In addition, ultrasonography is good for the study of cystic lesions of the orbit. In the case of tumors, location, tissue density, and margins can be defined and differences between smooth, nodular, and infiltrative lesions documented (Fig. 6-15). Inflammatory lesions, such as myositis or abscesses, may be distinguished with ultrasonography. For anterior lesions particularly, ultrasoundguided needle biopsy is a very useful adjunctive procedure (see Fig. 6-11). Ultrasound can confirm dilatation and collapse of a distended optic nerve sheath using the 30 test (Fig. 6-16).

Computed Tomography

CT provides excellent soft tissue resolution because of the presence of orbital fat, which is low density on CT, and allows identification of orbital structures (Figs. 6-17 and 6-18). CT provides superb detail of bony anatomy and is exquisitely sensitive for calcification as well as high-density foreign bodies, such as metal. It is the imaging technique of choice for primary assessment of orbital disease. This technique does use ionizing radiation; the dose to the lens is approximately 30 mGy (3 rad) for a series of 3 mm axial slices. The cumulative lifetime dose associated with cataract formation is estimated at 200 to 600 rads.

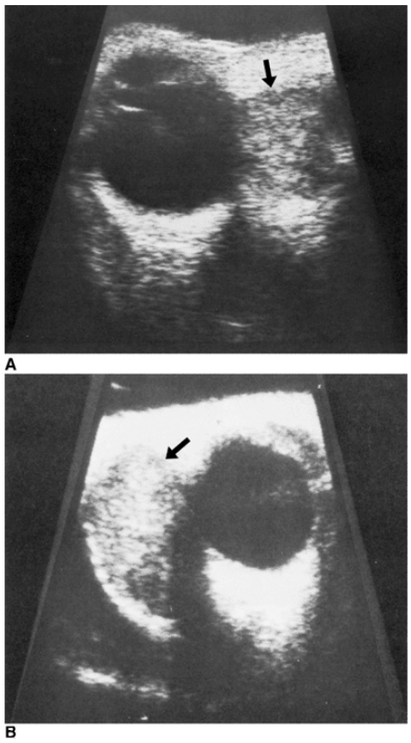

Figure 6-15. Both of these B-mode scans demonstrate large, well-defined masses in the superotemporal orbit (arrows). These are consistent with solid tumors with no cystic or anechoic areas within the lesions. Both were tumors of the lacrimal gland; (A) was a pleomorphic adenoma and (B) an adenoid cystic carcinoma.

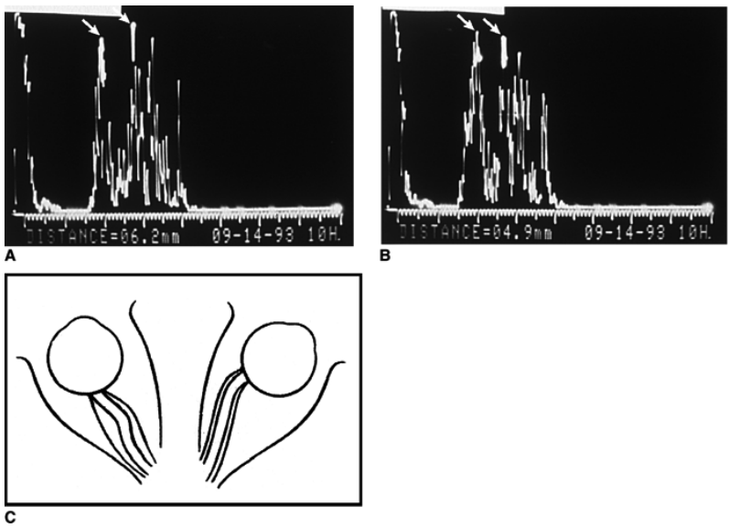

Figure 6-16. The A-scans taken in the axial (A) and abducted (B) positions demonstrate the enlarged optic nerve sheath (A, arrows), which collapses on abduction (B, arrows). This reflects dilatation of the sheath brought about by increased subarachnoid fluid, diagrammatically represented in (C). The patient was a 31-year-old man with benign intracranial hypertension papilledema, and progressive symptomatic visual loss. He underwent a successful optic nerve sheath decompression.

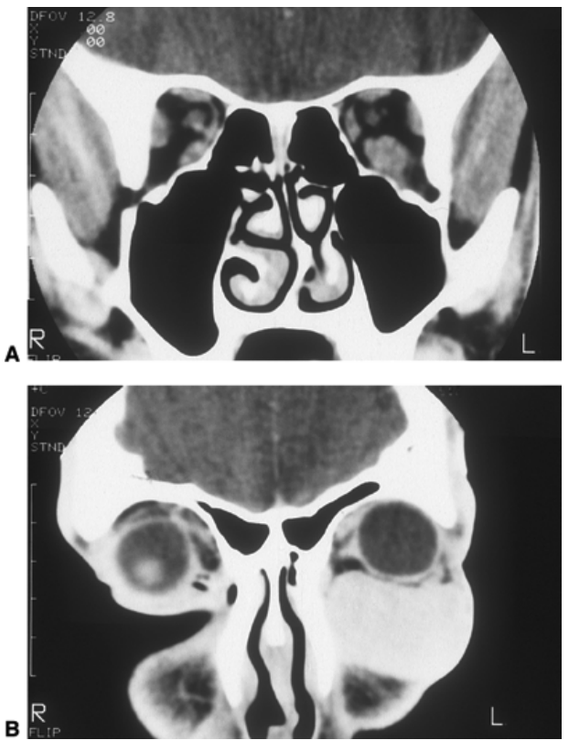

Figure 6-17. These coronal CT scans demonstrate an orbital mass originating in the inferior rectus muscle of the left orbit (A) and extending forward as a large tumor displacing the globe upward (B). This proved to be a liposarcoma in an 18-year-old man.

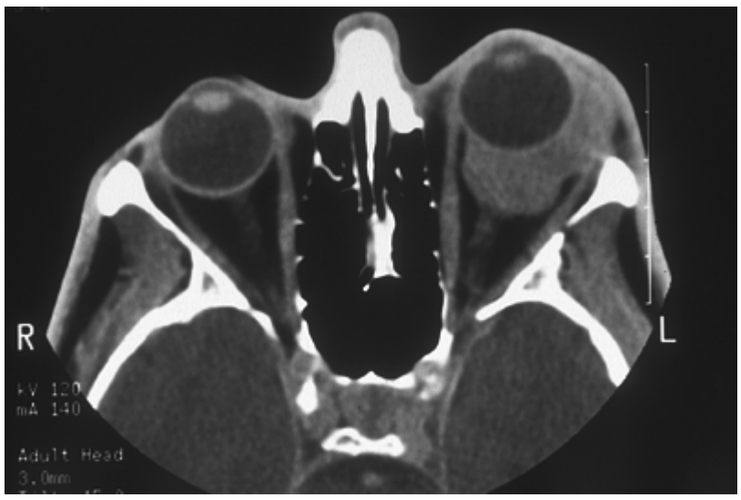

Figure 6-18. This smooth, homogeneous, slightly nodular lesion in the left orbit conforms to the contour of the globe and extends anteriorly beneath Tenon's capsule. This proved to be a maltoma (mucosa-associated lymphoma).

Technique

Routine assessment of the orbits includes contiguous axial and coronal views. These images or “slices” are usually 3 mm in thickness, although this may vary between 1 mm and 5 mm. Thin slices have the advantage of less volume averaging of the adjacent structures and provide finer spatial resolution. However, they have a lower signal to noise and do increase the radiation dose. It may be difficult to obtain high-quality true coronal views in patients with cervical spine disease or in patients who have excessive dental amalgam. In this situation, the recent advent of helical CT is advantageous, as high-quality reformatted images in other planes can be computer generated from the original axial images.

The axial images are normally obtained at an angle parallel to Reid's baseline (inferior orbital rim to the external auditory canal). However, the best view of the optic canal is obtained at an angle of -20 relative to Reid's baseline (this optic canal plane would be parallel to a line from the inferior orbital rim to the superior aspect of the anterior clinoid), since the canal passes inferiorly and obliquely from posterior to anterior.

Role of Intravenous Contrast

The high radiographic density of iodine in the contrast medium provides increased density or “enhancement” because the contrast agent will be more abundant in vascular structures following intravenous infusion. The extraocular muscles demonstrate prominent enhancement, as does the lacrimal gland. The optic nerve has minimal central enhancement with more prominent enhancement of the dural sheath. Arteries and veins within the orbit demonstrate enhancement, as does the scleral uveal rim.

Orbital masses can be readily identified without contrast enhancement because of surrounding low-density fat. However, contrast is essential in identifying extraorbital extension, particularly tumors extending intracranially. Contrast and positional change is also very useful with vascular lesions, such as varices, lymphangiomas (Fig. 6-19), arteriovenous and combined venous lymphatic malformations (Fig. 6-20), and hemangiomas. As well, contrast should always be given with suspected optic nerve lesions such as meningioma and glioma. Enhancement frequently aids in the differential diagnosis, since it may help to define thrombosis and cystic or more solid masses.

The subarachnoid space extends into the optic nerve sheath from the intracranial cerebrospinal fluid compartment. Many patients who have had myelography or cisternography performed with water-soluble agents will show evidence of contrast material within the optic nerve sheath on CT. This technique was occasionally useful in the past but is no longer indicated since MRI can define cerebrospinal fluid around the optic nerve.

Magnetic Resonance Imaging (MRI)

As a result of technological advances, magnetic resonance imaging (MRI) is assuming an increasing role in orbital imaging. MRI signal intensity depends upon several parameters hydrogen proton density as well as T1 and T2 relaxation times, which are specific for different tissues.

MRI has several advantages compared to CT scanning. It does not require ionizing radiation and images may be obtained in a variety of planes without repositioning the patient. It is less susceptible to image degradation from artifact related to dental fillings. Both CT and MRI are severely degraded by braces or other metal, however.

The disadvantages of MRI relative to CT include greater sensitivity to patient motion as well as cost. MRI is contraindicated in patients with cardiac pacemakers, orbital foreign bodies, and most types of intracranial aneurysm clips.

Technique

Like CT, MRI is preferably done with thin slices in the axial and coronal plane. In addition, the sagittal plane can be studied and is frequently useful, particularly for the optic nerve. T1 images (recognized by the dark vitreous and dark cerebrospinal fluid) (Fig. 6-21) provide excellent contrast between the high intensity orbital fat and the muscles and optic nerve. Subtle signal intensity changes, such as within the muscles in Graves' orbitopathy or changes within the optic nerve with optic neuritis, can be best appreciated with proton density or T2 images (recognized by the white vitreous and white cerebrospinal fluid) (Fig. 6-22). High blood flow generates a dark image (flow void) (Fig. 6-23). T2-weighted scans emphasize edema or other fluids, which appear bright. The use of fat suppression techniques may make these intensity changes somewhat more apparent by eliminating the bright signal of adjacent fat (Fig. 6-21). Bone appears dark on MR imaging and is less well delineated than with CT scanning.

The role of intravenous contrast is very similar to the use of contrast with CT scanning. Normal structures with a rich vascular supply, such as the extraocular muscles, or lesions that are vascular, such as meningiomas, will preferentially contain more of the contrast agent, which by shortening the T1 of these tissues will increase their intensity on T1-weighted images. This increased intensity can be better appreciated with fat suppressed images (Fig. 6-21).

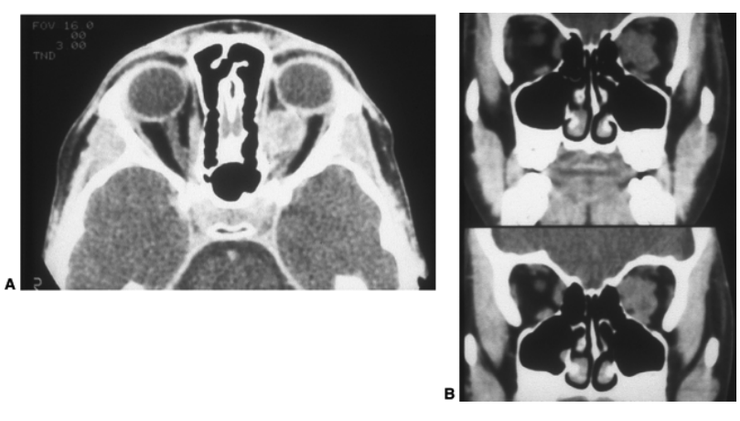

Figure 6-19. These scans demonstrate a medial orbital mass displacing the right optic nerve laterally. This occurred in an 11-year-old boy with a left visual acuity of 20/200 with papilledema. Note that the lesion enhances in an irregular fashion (A; B, upper [without contrast]; B, lower [with contrast]). On excision, it proved to be an isolated venous lymphatic malformation (lymphangioma) with hemorrhage.

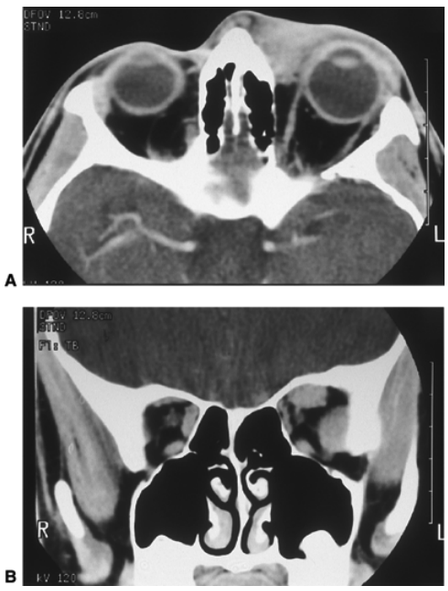

Figure 6-20. (A) The contrast enhanced axial CT scan demonstrates an anterior orbital lesion in an 11-year-old boy. The lesion appeared hemodynamically isolated (negative Valsalva maneuver) on clinical examination but was associated with a deep (apical), distensible venous portion, noted on coronal scan (B), with raised jugular venous pressure. The anterior lesion, which was excised, was histologically consistent with a so-called lymphangioma. The deep lesion was a distensible varix. (Reproduced with permission from Lacey B, Rootman J, Marotta TR. Distensible venous malformations of the orbit. Clinical and hemodynamic features and a new technique of management. Ophthalmology 1999;106:1197-209.)

Surface coil technology has advanced considerably and now allows for exquisite anatomic detail in the orbit with good signal to noise, even when thin slices are obtained. They do have a limitation in that the orbital apex will not be optimally visualized, nor will the area of the cavernous sinus and optic chiasm. These areas require imaging with the head coil.

MRI provides superb detail of the globe, with better anatomic definition than CT as well as better tissue specificity based on signal intensities.

Role of MRI versus CT

Trauma

CT plays a dominant role in these patients, since bony injuries are better defined, as are foreign bodies. Both modalities show hemorrhage and globe rupture. The presence of an intraorbital metallic foreign body is a contraindication to the use of MRI, because the strong magnetic field may damage adjacent structures by moving the foreign body.

Globe injury can be better defined on MRI, as can optic nerve contusion. However, CT scan should be the initial imaging modality.

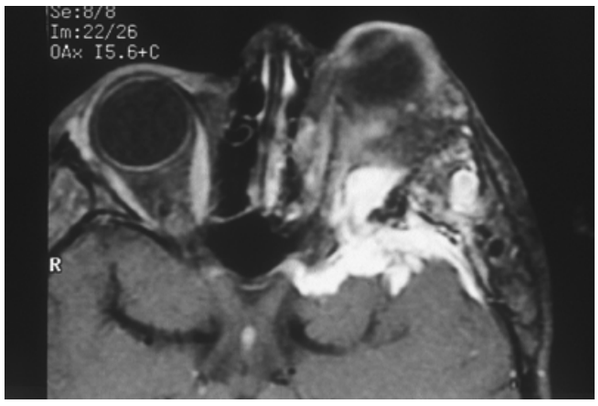

Figure 6-21. The contrast-enhanced, fat suppressed, T1-weighted MR scan demonstrates an extensive venous lesion involving the orbit, temporalis fossa, and brain and dura of the middle cranial fossa. (Reproduced with permission from Lacey B, Rootman J, Marotta TR. Distensible venous malformations of the orbit. Clinical and hemodynamic features and a new technique of management. Ophthalmology 1999;106:1197-209.)

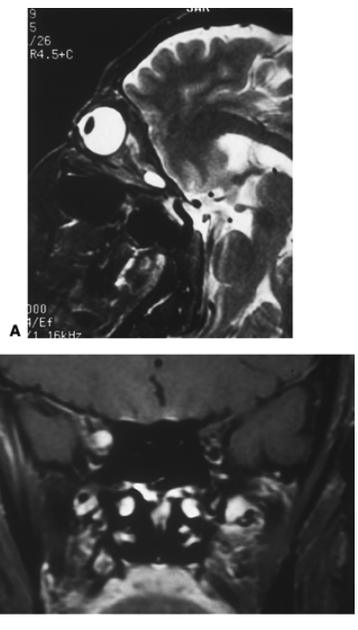

Figure 6-22. T2-weighted sagittal (A) and contrast-enhanced T1-weighted coronal (B) MR scans demonstrate an apical orbital mass, which caused visual loss (decreased visual acuity, color vision, and visual fields) in a 48-year-old woman. The mass was excised via an extended posterolateral orbitotomy and proved to be a cavernous hemangioma.

Orbital Tumors

Intraocular tumors can be more readily identified and characterized with MRI, which is very complimentary with ultrasound. CT is very limited in this regard, although it is excellent for demonstrating calcification within ocular lesions, such as that seen with retinoblastoma.

Retro-ocular mass lesions are readily identified with both modalities. Calcification is again more readily evident on CT scan. MRI sometimes provides more tissue specificity, depending on signal intensities. MRI is also very useful for demonstrating hemorrhage within lesions.

Vascular Lesions

Both MRI and CT are excellent for showing arteriovenous malformations, arteriovenous fistulas, and vascular malformations (Fig. 6-21). Distensible varices sometimes are not apparent unless the patient performs a Valsalva maneuver or is positioned for direct coronal images (see Fig. 6-20). In this situation, MRI could miss the lesion since head position does not have to be changed in the MRI to get different views.

MRI shows high flow vessels as a signal void (Fig. 6-23), whereas CT shows them as enhancement. High flow vessels within the cavernous sinus are better seen on MRI, since enhancement of the cavernous sinus can obscure these vessels on CT whereas the high flow signal void on MRI will be highlighted against the enhancement of the cavernous sinus.

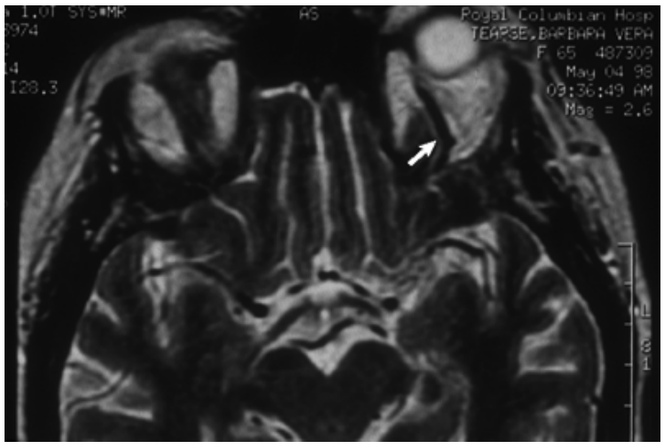

Figure 6-23. The T2-weighted MR scan demonstrates the flow void of an enlarged superior ophthalmic vein (arrow) in a patient with an acquired dural fistula (arrow).

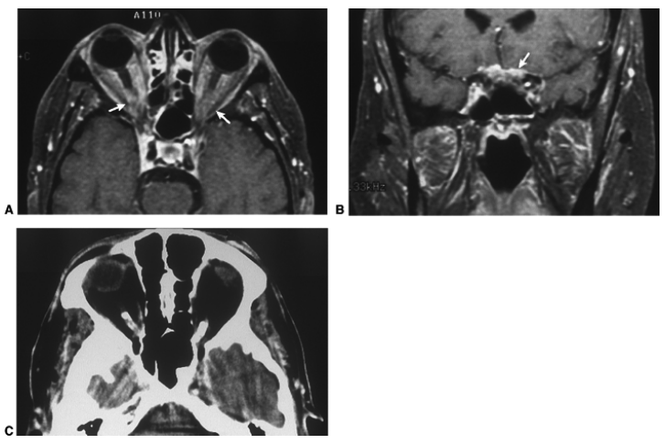

Figure 6-24. (A) This T1-weighted axial MR scan demonstrates infiltration and obliteration of the optic nerve bilaterally in the orbital apex (arrows), which is also demonstrated on coronal T1-weighted contrast enhanced imaging (B). The coronal scan shows bilateral involvement across the optic chiasm and planum sphenoidale (B, arrow). The patient is a 57-year-old man with an 11-year history of progressive visual loss that had been diagnosed as optic neuritis. An axial CT scan (C) taken 2 years prior to referral demonstrates bilateral calcification of the optic nerve, pathognomonic for optic nerve meningioma.

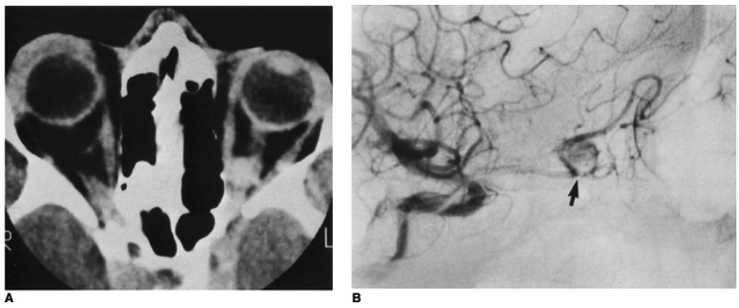

Figure 6-25. (A) CT scan demonstrates a contrast-enhancing apical orbital mass that displaced the optic nerve and led to optic neuropathy. (B) The angiogram demonstrates an early uniform fine mesh of enhancing vessels suggestive of either an angiomeningioma or a vascular tumor.

Optic Nerve Lesions

The optic nerve is well seen on both CT and MRI, although the intracanalicular and intracranial portion is not optimally visualized with CT (Fig. 6-24). Most lesions of the optic nerve are well seen with both modalities, although calcification, as with sheath meningiomas, is much better shown on CT whereas early changes of optic neuritis may only be seen on MRI because of signal intensity changes. The intracranial portion of the optic nerve as well as the optic chiasm is seen with both CT and MRI, although better seen with the latter.

Idiopathic Orbital Inflammation and Graves' Orbitopathy

Both CT and MRI are extremely useful in imaging these conditions. There is some recent evidence that MRI may distinguish idiopathic inflammation from lymphoid tumors.

Both modalities can show changes within extraocular muscles. CT offers a very simple and accurate means of measuring extraocular muscles. MRI may offer early detection as signal intensity changes within the muscles may predate size changes with Graves' orbitopathy. However, CT scan shows low density changes early in the course of Graves' orbitopathy as well.

Vascular Studies and Procedures

Vascular studies in both arterial and venous phases are useful in assessing selected aspects of orbital tumors and vascular lesions. Magnified and subtracted views of the arterial supply can aid in defining the location and the character of the blood supply of tumors preoperatively (Fig. 6-25). Indeed, therapy of highly vascular tumors, malformations (Figs. 6-26 and 6-27), and fistulas can be performed with selected arterial embolization and occlusion. Phlebography is rarely indicated in the study of orbital disease, except for venous malformations where specific localization and definition may be possible (Fig. 6-28). Orbital venograms are routinely done by the angular tributaries, but the venous system may also need to be studied via the retrograde jugular venous supply and direct puncture in selected circumstances (*cf* Vascular Lesions Chapter 13). In some instances, the introduction of digital subtraction methods may circumvent the need for direct and complicated intra-arterial injection studies.

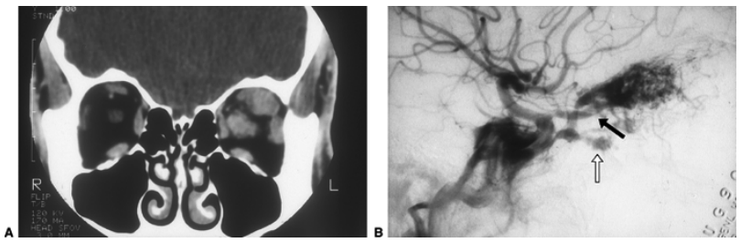

Figure 6-26. (A) This coronal CT scan shows a complex, irregular mass in the orbital apex of a 40-year-old man. He presented with a history of recurrent orbital hemorrhages and pulsating orbital pain induced by Valsalva maneuver or physical stress. (B) Internal carotid angiogram shows filling of a complex arteriovenous malformation. Note the enlarged ophthalmic artery (black arrow) and venous out-flow to the cavernous sinus (outlined arrow).

Methods of Study of the Lacrimal Drainage System

The lacrimal drainage system can be assessed by direct contrast injection, scintillography, and CT or MRI studies. In the case of obstruction, contrast injection of the drainage system can help to outline intraluminal masses or sites of the obstruction secondary to extraluminal pressure. This may be particularly useful in the study of combined nasopharyngeal and orbital lesions or lesions of the lacrimal sac. Biochemical analysis of tear lysozyme and angiotensinconverting factor may help to differentiate between sarcoidosis and Sjögren's disease affecting the lacrimal

gland. (Both angiotensin converting enzyme and tear lysozyme levels increase in sarcoidosis.)

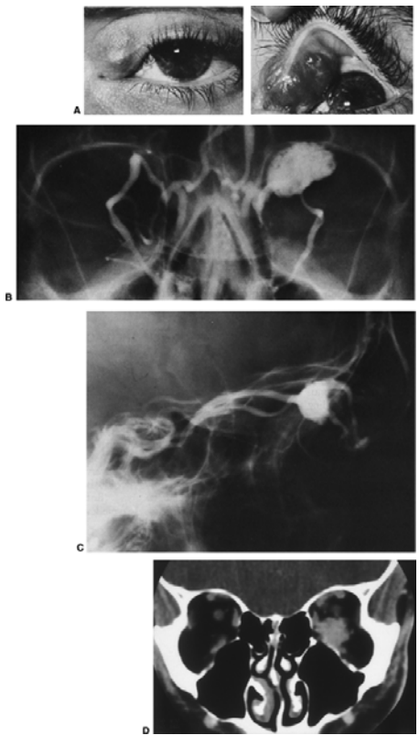

Figure 6-27. The clinical photographs show the anterior component of a varix without (A, left) and with (A, right) distention brought about by a Valsalva maneuver. The venograms (B, C) demonstrate the anterior component of the varix on anterior-posterior and lateral views. (D) A separate deep distensible varix in the inferior orbit was noted on coronal CT scan. This deep varix was not related to the blood flow of the anterior lesion demonstrated above.

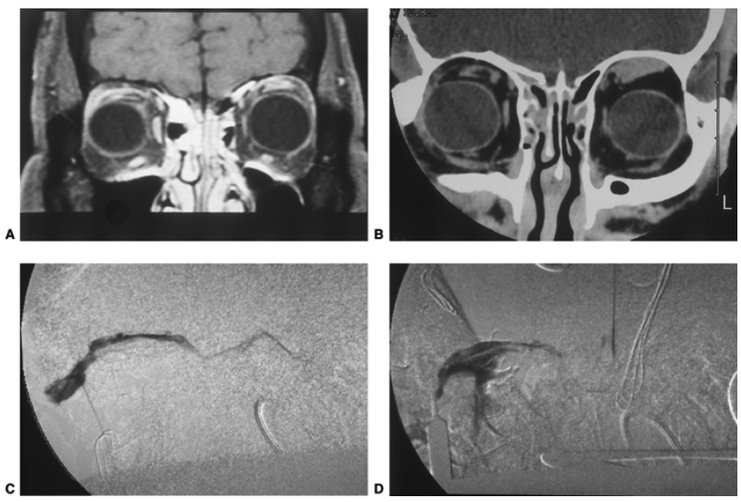

Figure 6-28. Coronal gadolinium-enhanced T1-weighted MR (A) and enhanced CT (B) images revealed the presence of a venous malformation affecting the left superior orbit. The lesion is larger on the CT coronal image because the patient's head was in a dependant hyperextended position to achieve this imaging plane. (Such head positioning is not required to achieve multiplanar images with MRI.) Intraoperatively, a direct intralesional lateral venogram revealed filling of the lesion and its out-flow through a single venous channel at the superior orbital fissure to the cavernous sinus (C). With pressure applied intraoperatively at the superior orbital fissure, control of out-flow is confirmed venographically. (Reproduced with permission from Lacey B, Rootman J, Marotta TR. Distensible venous malformations of the orbit: clinical and hemodynamic features and a new technique of management. Ophthalmology 1999;106:1197-1209.)

Conclusion

Angiography, venography, and dacryocystography are very specific modalities for evaluating orbital disease. Plain films offer only a very basic assessment of bony detail as well as the presence of foreign bodies. CT scan and MRI offer exquisite soft tissue detail and sensitivity to lesions within the orbit and are therefore the mainstay of orbital imaging. CT can be more readily carried out in many situations, although MRI is showing increasing promise for more specificity with orbital disease and particularly ocular disease. These two modalities remain very complimentary.

Pathologic Assessment

Frequently, orbital lesions are not easily accessible and considerable technical expertise is required to obtain material both for biopsy or removal. Once tissue is obtained, it is important to have a clear plan for disposition based on a presumptive diagnosis. The major areas of diagnostic tissue pathology are cytology, histochemistry, immunohistochemistry, electron microscopy, and molecular techniques. The value of these methods (outlined in the chapter on Pathology Chapter 7) can best be demonstrated by a few practical case examples.

Routine cytologic methods and ancillary technology, including histochemistry and electron microscopy, are readily available in most treatment centers. In the orbit, this has

facilitated fine needle aspiration, which is particularly useful in the diagnosis of secondary invasions where this procedure might avoid open biopsy. For instance, aspiration of a progressive infiltrative lesion of the orbit arising from the maxillary antrum (see Fig. 6-11A) yielded a specimen that proved to be a squamous cell carcinoma on histology and electron microscopy (Fig. 6-29).

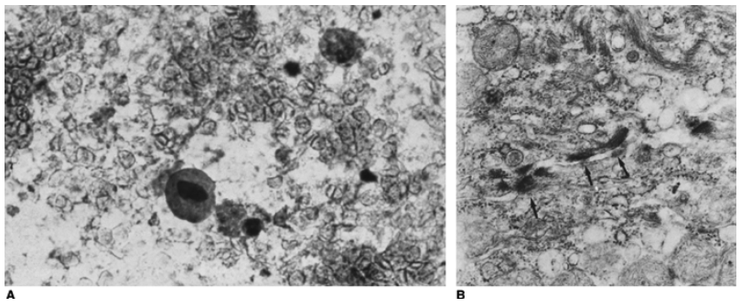

Figure 6-29. (A) Histopathologic photograph of cytology obtained from an aspirate of the tumor shown in Fig. 6-11. Note large squamoid cells (H&E, original magnification × 100). (B) An electron micrograph of the aspirate shows desmosomes (arrows) and subcellular organelles consistent with squamous cell origin. (Rootman J, Quenville N, Owen D. Recent advances in pathology as applied to orbital biopsy. Ophthalmology 1984;91:708-18.)

Routine histochemical methods offer a broad range of standard techniques for identifying myofilaments, amyloid, fibrin, reticulin, neuroglial tissues, and so forth. Further, the introduction of immunohistochemical techniques, particularly the immunoperoxidase method with monoclonal antibodies and polymerase chain reaction (PCR), has allowed for an everincreasing range of specificity in tissue diagnosis. Proper management of the tissues is important to obtain accurate results. Methods for identifying component antigens are routinely available for immunoprotein, muscle, keratin, glial protein, prostatic antigen, endocrine granules, and many others. Immunohistochemical methods can even be applied to aspiration biopsy material.

An example demonstrating the gamut of technology is shown in a case of a nasopharyngeal carcinoma. On routine histology, it appeared to be a poorly differentiated malignancy with a wideranging differential diagnosis (Fig. 6-30A to D). Immunoperoxidase stain ruled out immunoglobulin, myoglobulin, and glial fiber protein. Routine histochemistry stained for argyrophil granules was strongly positive, suggesting a carcinoma with neuroendocrine features (Fig. 6-30E).

Ultrastructural methods are useful in distinguishing tissue types, as demonstrated in the above case, which showed membranebound neuroendocrine granules (Fig. 6-30E). In another case of a child with a poorly differentiated round cell tumor of the nasopharynx, electron microscopy showed pools of glycogen and cell membrane junctions with the absence of other subcellular components. This led to a diagnosis of Ewing's sarcoma (Fig. 6-31), which can now be defined further with molecular techniques. Electron microscopy is valuable in the study of round cell tumors of childhood, where we are attempting to differentiate between rhabdomyosarcoma, lymphoma, neuroblastoma, and rarer tumors such as granulocytic sarcoma, Ewing's sarcoma, and histiocytosis X. In the case of rhabdomyosarcoma, the electron microscope allows identification of the banding typical of myoblastic origin. The pools of glycogen and the presence of cell membrane junctions with the absence of other subcellular components help to identify Ewing's sarcoma. Granulocytic sarcomas contain granules and lysosomes, and in the case of histiocytosis × there are typical Birbeck's granules (X bodies or Langerhans granules). Similarly, electron microscopy of poorly differentiated tumors of the adult can help to distinguish between lymphoma (convoluted nuclei, cytoplasmic indentations, nuclear vacuoles, and nuclear bridges), carcinomas (villi, neuroendocrine granules, intracellular bridges, microgland formation, and so on), and melanomas (melanosomes). It is important following surgical biopsy to get appropriate fixation (glutaraldehyde) and rapid transportation to the lab for maximal electron microscopy results. This applies also to the use of immunohistochemical and molecular techniques, which have

superceded electron microscopy where it is critically important to receive fresh tissue.

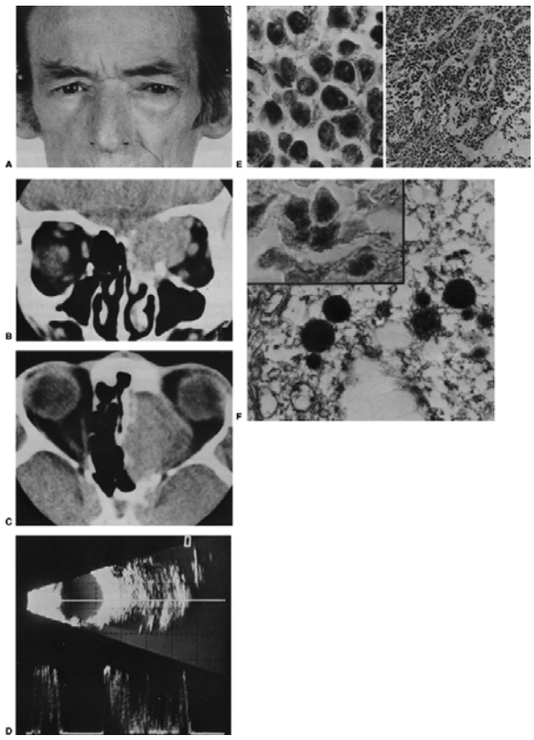

Figure 6-30. (A) This patient presented with lateral and axial displacement of the left globe due to a mass within the sinus and nasopharynx, which is shown on coronal (B) and axial (C) CT scans. Note bone destruction and infiltration. (D) Ultrasound image of the same patient (A and B modes) shows multiple interfaces characteristic of a solid infiltrating orbital mass. (E) Low- and high-power photomicrographs of a biopsy of this lesion. It is a poorly differentiated round cell tumor of the nasopharynx (H&E, original magnifications; left × 10, right × 100). (F, inset) A grimelius stain was positive for argyrophil granules (grimelius, original magnification × 100). (F) The electron micrograph of the same lesion shows membrane-bound neuroendocrine granules, confirming a diagnosis of neuroendocrine carcinoma. (Reproduced with permission from Rootman J, Quenville N, Owen D. Recent advances in pathology as applied to orbital biopsy. Ophthalmology 1984;91:708-18.)

Increasingly, especially in the case of childhood tumors, molecular biologic techniques are being utilized to specify tumor type and have a role in not only determining prognosis but the specific type of treatment that would be best suited for neoplasia.

We do not wish to comprehensively review the myriad of details applied to the technology demonstrated, but rather to emphasize the value of an informed multidisciplinary approach to biopsy. It is not necessary for all of us to be experts in the area of pathology, but to be aware of increasing and changing sophistication and specificity. Practically, the message is that the clinician should have a clear plan for the disposition of the specimen prior to the biopsy. The best way of handling material is to alert the pathologist in advance, discuss the differential diagnosis, and ask for guidance in the handling of the tissue. This will assure maximum diagnostic information.

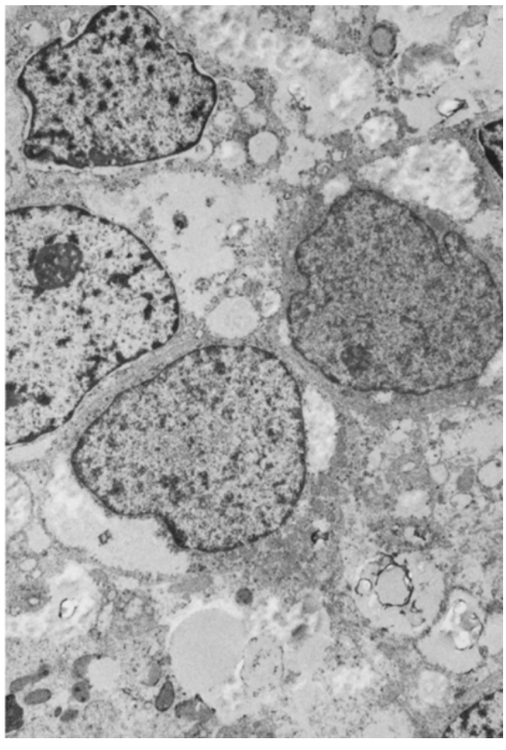

Figure 6-31. Electron micrograph demonstrates pools of glycogen with few subcellular organelles, suggestive of Ewing's sarcoma.

Conclusion

The goal of this section is to provide the basis for a rational approach to investigation of disease processes after clinical evaluation. In particular, it is intended to give the framework for establishing the presence, location, effect, and specific identity of disease. In the final analysis it is the multidisciplinary integration of a broad background of knowledge of anatomy, clinical presentation, pathophysiology, and investigative technology that leads to the rational management of disease in the orbit.

Bibliography

General

DukeElder S. System of Ophthalmology, Vol. 13. London, Henry Kimpton, 1984.

Dutton JJ, Byrne SF, Proia AD. Diagnostic Atlas of Orbital Diseases. Philadelphia: WB Saunders, 2000.

Henderson JW. Orbital Tumors. 2nd ed. Philadelphia: Lippincott-Raven, 1994.

Jakobiec FA (ed). Ocular and Adnexal Tumors. Birmingham: Aesculapius, 1978.

Jones IS, Jakobiec FA. Diseases of the Orbit. New York: Harper& Row, 1979.

Extraocular and Visual Function

Van Lith GHM, Vijfvinkel-Bruinenga S, Graniewski-Wijnands H. Pattern evoked cortical potentials and compressive lesions along the visual pathways. Documenta Ophthalmolgica 1982;52:347-53.

Orbital Imaging

Bailey CC, Kabala J, Laitt R, et al. Cine magnetic resonance imaging of eye movements. Eye 1993;7:691-3.

Breslau J, Dalley RW, Tsurada JS, et al. Phased array surface coil MR of the orbits and optic nerves. AJNR 1995;16:1247-51.

Byrne SF. Standardized echography in the differentiation of orbital lesions. Surv Ophthalmol 1984;29:226-8.

Byrne SF, Glaser JS. Orbital tissue differentiation with standard echography. Ophthalmology 1983;90:1071-90.

Chambers EF, Manelfe C, Cellerier P. Metrizamide CT cisternography and perioptic subarachnoid space imaging. J Comput Assist Tomogr 1981;5:875-80.

Char DH, Sobel D, Kelly WM, et al. Magnetic resonance scanning in orbital tumor diagnosis. Ophthalmology 1985;92:1305-10.

de Potter P, Shields JA, Shields CL. MRI of the Eye and Orbit. Philadelphia: JB Lippincott, 1995.

Deluise VP, Tabbara KF. Quantitation of tear lysozyme levels in dryeye disorders. Arch Ophthalmol 1983;101:634-5.

Dubois PJ, Kennerdell JS, Rosenbaum AE, et al. Computed tomographic localization of fine needle aspiration biopsy of orbital tumors. Radiology 1979;131:149-52.

Ettl AR. High Resolution Magnetic Resonance Imaging Anatomy of the Orbit. Amsterdam: St. Poelten, 1999.

Flaharty PM, Lieb WE, Sergott RC, et al. Color doppler imaging: a new noninvasive technique to diagnose and monitor carotid cavernous sinus fistulas. Arch Ophthalmol 1991;109:522-6.

Herrick RC, Hayman LA, Taber KH, et al. Artifacts and pitfalls in MR imaging of the orbit: a clinical review. Radiographics 1997;17:707-24.

Hurwitz JJ, Welham RAN, Lloyd GAS. The role of intubation macro-dacryocystography in management of problems of the lacrimal system. Can J Ophthalmol 1975;10:361-6.

Levine RA. Orbital ultrasonography. Radiol Clin North Am 1987;25:447-69.

Lloyd GAS. Radiology of the Orbit. Philadelphia: WB Saunders, 1975.

Moström U, Ytterberg C, Bergström K. Eye lens dose in cranial computed tomography with reference to the technical development of CT scanners. Acta Radiol Diagn [Stockh] 1986;27:599-606.

Ossoinig KC. Standardized echography: basic principles, clinical applications, and results. Int Ophthalmol Clin 1979;19:127-210.

Rosenstock T, Hurwitz JJ. Functional obstruction of the lacrimal drainage passages. Can J Ophthalmol 1982;17:249-55.

Sargent EN, Ebersole C. Dacryocystography. The use of sinografin for visualization of the nasolacrimal passages. Am J Roentgenol Radium Ther Nucl Med 1968;102:831-9.

Sharma OP, Vita JB. Determination of angiotensinconverting enzyme activity in tears. A noninvasive test for evaluation of ocular sarcoidosis. Arch Ophthalmol 1983;101:559-61.

Tien RD, Chu PK, Hesselink JR, Szumowski J. Intra- and paraorbital lesions: value of fat-suppression and MR imaging with paramagnetic contrast enhancement. AJNR 1991;12:245-53.

Wilson WB, Dreisbach JN, Lattin DE, Stears JC. Magnetic resonance imaging of nonmetallic orbital foreign bodies. Am J Ophthalmol 1988;105:612-7.

Pathologic Assessment

Amemiya T, Yoshida H. Electron microscope study of the orbital lesion of HandSchüllerChristian disease. J Pediatr Ophthalmol 1977;14:242-7.

Basset F, Escaig J, Le Crom M. A cytoplasmic membranous complex in histiocytosis X. Cancer 1972;29:1380-6.

Churg A, Ringus J. Ultrastructural observations on the histogenesis of alveolar rhabdomyosarcoma. Cancer 1978;41:1355-61.

Crist WM, Edwards RH, Pereira F. Rhabdomyosarcoma diagnosed by electron microscopy in a child with acute lymphocytic leukemia. J Pediatr 1978;93:893-4.

Dresner SC, Kennerdell JS, Dekker A. Fine needle aspiration biopsy of metastatic orbital tumors. Surv Ophthalmol 1983;27:397-8.

Falini B, Taylor CR. New developments in immunoperoxidase techniques and their application. Arch Pathol Lab Med 1983;107:105-17.

Frable WJ. Fineneedle aspiration biopsy: a review. Hum Pathol 1983;14:9-28.

Freeman AI, Johnson WW. A comparative study of childhood rhabdomyosarcoma and virusinduced rhabdomyosarcoma in mice. Cancer Res 1968;28:1490-500.

Friedman B, Gold H. Ultrastructure of Ewing's sarcoma of bone. Cancer 1968;22:307-22.

Friedman B, Hanaoka H. Roundcell sarcomas of bone. A light and electron microscopic study. J Bone Joint Surg Am 1971;53:1118-36.

Ghadially FN. Diagnostic electron microscopy of rumours. London: Butterworth, 1980.

Henderson DW, Raven JL, Pollard JA, Walters MN. Bone marrow metastases in disseminated alveolar rhabdomyosarcoma: case report with ultrastructural study and review. Pathology 1976;8:329-41.

Horvat BL, Caines M, Fisher ER. The ultrastructure of rhabdomyosarcoma. Am J Clin Pathol 1970;53:555-64.

HouJensen K, Priori E, Dmochowski L. Studies on ultrastructure of Ewing's sarcoma of bone. Cancer 1972;29:280-6.

Kadin ME, Bensch KG. On the origin of Ewing's tumor. Cancer 1971;27:257-73.

Kameya T, Shimosato Y, Adacho I, et al. Neuroendocrine carcinoma of the paranasal sinus: a morphological and endocrinological study. Cancer 1980;45:330-9.

Kaminsky DB. Aspiration biopsy for the community hospital. In: Masson Monographs in Diagnostic Cytopathology. New York: Masson, 1981, vol. 2.

Kennerdell JS, Dekker A, Johnson BL, Dubois PJ. Fineneedle aspiration biopsy. Its use in orbital tumors. Arch Ophthalmol 1979;97:1315-7.

Kennerdell JS, Slamovits TL, Dekker A, Johnson BL. Orbital fine-needle aspiration biopsy. Am J Ophthalmol 1985;99:547-51.

Khalil MK, Huang S, Viloria J, Duguid WP. Extramedullary plasmacytoma of the orbit: case report with results of immunocytochemical studies. Can J Ophthalmol 1981;16:39-42.

Kline TS. Handbook of fine needle aspiration biopsy cytology. St. Louis: CV Mosby, 1981.

Knowles DM 2nd, Jakobiec FA. Ocular adnexal lymphoid neoplasms: clinical, histopathologic, electron microscopic, and immunologic characteristics. Hum Pathol 1982;13:148-62.

Kroll AJ, Kuwabara T, Howard GM. Electron microscopy of rhabdomyosarcoma of the orbit. A study of two cases. Invest Ophthalmol 1963;2:523-37.

Kroll AJ. Finestructural classification of orbital rhabdomyosarcoma. Invest Ophthalmol 1967;6:531-43.

Liu D. Complications of fine needle aspiration biopsy of the orbit. Ophthalmology 1985;92:1768-71.

Mahoney JP, Alexander RW. Ewing's sarcoma. A light- and electron-microscopic study of 21 cases. Am J Surg Pathol 1978;2:283-98.

Meis-Kindblom JM, Stenman G, Kindblom L-G. Differential diagnosis of small round cell tumors. Semin Diagn Pathol 1996;13:213-41.

MesaTejada R, Pascal RR, Fenoglio CM. Immunoperoxidase: a sensitive immunohistochemical technique as a “special stain” in the diagnostic pathology laboratory. Hum Pathol 1977;8:313-20.

Mierau GW, Favara BE. Rhabdomyosarcoma in children: ultrastructural study of 31 cases. Cancer 1980;46:2035-40.

Morales AR, Fine G, Horn RC Jr. Rhabdomyosarcoma: an ultrastructural appraisal. Pathol Annu 1972;7:81-106.

Nakayama I, Tsuda N, Muta H, et al. Fine structural comparison of Ewing's sarcoma with neuroblastoma. Acta Pathol Jpn 1975;25:251-68.

Rice RW, Cabot A, Johnston AD. The application of electron microscopy to the diagnostic differentiation of Ewing's sarcoma and reticulum cell sarcoma of bone. Clin Orthop 1973;91:174-85.

Roholl PJ, De Jong ASH, Ramaekers FCS. Application of markers in the diagnosis of soft tissue tumours. Histopathology 1985;9:1019-35.

Rootman J, Quenville N, Owen D. Recent advances in pathology as applied to orbital biopsy: practical considerations. Ophthalmology 1984;91:708-18.

Sarkar K, Tolnai G, McKay DE. Embryonal rhabdomyosarcoma of the prostate. An ultrastructural study. Cancer 1973;31:442-8.

Schyberg E. Fine needle biopsy of orbital tumours. Acta Ophthalmol [Suppl] 1975;125:11.

Shechan DC, Hrapchak BB. Theory and Practice of Histotechnology, 2nd ed. St. Louis: CV Mosby, 1980.

Spoor TC, Kennerdell JS, Dekker A, et al. Orbital fine needle aspiration biopsy with Bscan guidance. Am J Ophthalmol 1980;89:274-7.

Taylor CR. Immunoperoxidase techniques: practical and theoretical aspects. Arch Pathol Lab Med 1978;102:113-21.

Triche TJ. Round cell tumors in childhood: the application of newer techniques to the differential diagnosis. Perspect Pediatr Pathol 1982;7:279-322.

WestmanNaeser S, Naeser P. Tumours of the orbit diagnosed by fine needle biopsy. Acta Ophthalmol 1978;56:969-76.

Winkler CF, Goodman GK, Eiferman RA, Yam LT. Orbital metastasis from prostatic carcinoma: identification by an immunoperoxidase technique. Arch Ophthalmol 1981;99:1406-8.

Zimmerman LE, Font RL, Tso MOM, et al. Application of electron microscopy to histopathologic diagnosis. Trans Am Acad Ophthalmol Otolaryngol 1972;76:101-7.

Part C
Diseases of the Orbit

Chapter 7
The Pathologic Basis of Orbital Disease

Valerie A. White

Jack Rootman

The pathologic processes in the orbit mirror those in the rest of the body and also include some entities that are unique to or have a predilection for this site. This chapter is an attempt to provide a reasonably simple and comprehensible classification of orbital diseases for the ophthalmologist from the point of view of a pathologist. Much of the information is presented in a tabular format to promote a conceptual understanding of the classification of categories of disease and the entities that must be considered in the differential diagnosis. An asterisk beside an entity indicates that it commonly occurs in the orbit relative to the other lesions described.

The handling of specimens by both orbital surgeons and pathologists is of utmost importance in obtaining an accurate diagnosis, particularly when dealing with a suspected neoplasm. The proliferation of new histopathologic techniques is extensive and ophthalmologists cannot be expected to remember what to do in all situations. In addition, cytogenetic and molecular genetic investigation has become an important adjunct to diagnosis in some neoplasms involving the orbit, and these procedures often require special handling of fresh tissue. Therefore, the ophthalmologist should discuss the differential diagnosis and handling of the tissue with the pathologist before biopsy. Guidelines are given in later sections for the disposition of tissue in various disorders.

Although most of the histopathologic descriptions in this chapter are based on light microscopic examination of H&E-stained slides following formalin fixation, paraffin embedding and sectioning, aspiration biopsy, and cytologic examination of H&E- and Giemsa-stained smears have become widely used in the diagnosis of both orbital and intraocular tumors. Table 7-1 gives an overview of techniques which may be used in the diagnosis of orbital disease. The application of cytogenetic and molecular genetic procedures to diagnosis of specific entities is discussed in relevant sections.

Neoplasia

Pathologic analysis of neoplasms addresses two major concerns – whether the tumor is benign or malignant, and the type of tumor. Malignancy and nature of most tumors is generally determined on routine H&E sections by the assessment of mitoses, anaplasia, and invasive margins in the context of clinical history. Typing may require immunohistochemistry, electron microscopy, and/or genetic analysis. Most antigens routinely used in the typing of tumors are preserved by fixation in formalin. We routinely fix a small representative portion of tissue in 2.5% glutaraldehyde for electron microscopy, and the remainder in formalin. Preservation of antigens is greatest when tissues are fixed as soon as possible after removal. In the appropriate situation, and if sufficient tissue is available, a fresh sample is submitted for cytogenetic study and a small portion frozen for future DNA studies. This is particularly important in lesions suspected of being malignant.

Table 7-2 presents definitions of common pathologic terms as related to neoplasia to facilitate an understanding of the classification of orbital neoplasms.

The neoplasms of the orbit will be described under the five major categories of epithelial, mesenchymal, lymphoproliferative and leukemic, melanocytic, and central nervous system (optic nerve), as listed in Table 7-2 . Two additional categories, neoplasms of the orbital bone and lacrimal gland, are described as these unique locations give rise to a differential diagnosis that is more specific. The optic nerve also has a specific differential diagnosis that is not shared by the other sites.

Table 7-1. Pathologic techniques used in diagnosis of orbital disease

TECHNIQUE	DESCRIPTION	USES
Routine light microscopy	Tissues usually fixed in formalin, processed through alcohols into paraffin wax, sectioned at 1-5 um, stained with hematoxylin and eosin (H&E), and examined with a light microscope Other fixatives may be used	Most commonly used pathologic technique First line in diagnosis Allows performance of other techniques, including histochemical and immunohistochemical stains, and extraction of DNA
Fine needle biopsy and cytologic examination	Cells aspirated from a lesion in situ with a thin needle Cells immediately spread on glass slides and stained Cells may be placed in fluid to perform cytospins	Quick method to determine nature of a pathologic process, if adequate numbers of cells can be obtained Diagnosis of recurrences or metastases Cells may be used for flow cytometry or molecular techniques Most useful in non-fibrotic lesions
Immunohistochemistry (IH)	Routinely processed tissues stained with an antibody directed against a specific antigen Site of antigen is visualized by any of a number of processes that produce a colored product	Panels of such antibodies useful in determining nature of undifferentiated neoplasms and detecting presence of different populations of lymphocytes in lymphomas or inflammatory processes
Electron microscopy (EM)	Small pieces of tissue fixed in glutaraldehyde, processed through osmium tetroxide and alcohols into a hard plastic resin Very thin sections of <100 nanometers stained with uranyl acetate and lead citrate and examined with an electron microscope	Gives very high power resolution of a small number of cells Used to determine nature of cell types in neoplasms, although this use has largely been replaced by immunohistochemical staining Often used for research purposes Can be used in association with immunohistochemical staining
Flow cytometry	Suspension of cells stained with fluorescent labeled antibodies and counted singly by a laser	Very useful for determining monoclonal or polyclonal populations of lymphocytes in lymphoproliferative processes For determining DNA content in nuclei from neoplasms
Cytogenetic examination	Suspension of fresh cells grown in culture until metaphases obtained; these are then fixed with methanol and acetic acid and stained with Giemsa to examine the chromosome complement of single cells	Useful in diagnosis of Ewing's sarcoma/peripheral neuroectodermal tumor, myxoid liposarcoma, alveolar rhabdomyosarcoma, and Burkitt's and follicle center cell lymphomas in which specific translocations have been detected
Polymerase chain reaction (PCR) and reverse transcriptase PCR (RT-PCR)	Using DNA extracted from the cells of a tumor, a small specific sequence is amplified until it can be analyzed on an electrophoretic gel or by a DNA probe RT-PCR uses RNA extracted from a tumor to first make a complementary DNA (cDNA), which is then amplified	PCR very useful in determining rearrangement of the immunoglobulin heavy chain gene (IgH RA) or T-cell receptor gene to detect presence of a monoclonal population of lymphocytes in any type of lymphoma RT-PCR used in tumors such as those above to detect the products of specific translocations

In most instances, the histologic diagnosis is obvious; however, when faced with a poorly differentiated or undifferentiated malignancy, the pathologist must first classify the neoplasm as belonging to one of the main categories and then further subclassify it if possible. A battery of certain immunohistochemical stains is helpful in the primary classification of a neoplasm as detailed in Table 7-3 .

Once a neoplasm has been categorized into one of these major classes, further immunohistochemical staining may be required to make a more specific diagnosis. Because immunohistochemistry plays such a large role in the diagnosis of neoplasia, immunohistochemical staining patterns for the various **histologic** categories of neoplasms are grouped in Tables 7-4 ,7-5 ,7-6 .

Table 7-2. Definitions of common pathologic terms related to neoplasia

TERM	DEFINITION
Neoplasia	"New growth": autonomous growth of tissue that exceeds and is uncoordinated with those of the normal tissues of the host and that persists after cessation of the stimulus or stimuli that initiated it
Hyperplasia	Increase in number of cells in an organ or tissue, which may then have an increased volume
Dysplasia	Term which has two meanings, thus important to know context in which it is used: most commonly used in reference to premalignant changes in epithelia which have lost their orderly pattern of maturation and show pleomorphic (variably shaped) cells and mitoses above the basal layer also refers to disorderly growth in the fetal period, which produces an abnormally formed tissue or organ
Benign	Neoplasm that retains some of the properties of the cell from which it is derived Usually has expansile, non-invasive borders and usually does not metastasize or kill patient Benign epithelial tumors are referred to as adenomas prefaced by an adjective indicating site of origin (e.g., sebaceous adenoma) Benign tumors of the mesenchymal tissues are named by adding the suffix A-oma to the cell of origin (e.g., fibroma and osteoma for benign tumors of fibroblasts and osteocytes respectively)
Malignant	Neoplasm that invades surrounding structures and has potential to metastasize and kill patient May be well, moderately, or poorly differentiated depending on resemblance to cell of origin Histologically usually shows some of the following: pleomorphism of cell size and shape, increased nuclear to cytoplasmic ratio, abnormal mitoses, tumor giant cells, disorganization of cellular architecture, necrosis, and/or invasive borders All malignancies can be placed into one of five main categories and then further subdivided according to more specific features: carcinoma-malignant neoplasm of epithelial cells, prefixed by site or cell type of origin (e.g., sebaceous carcinoma) sarcoma-malignant neoplasm of mesenchymal cells, either soft tissue or bone, prefixed by cell of origin (e.g., osteosarcoma) lymphoma-malignant neoplasm of lymphocytes (no benign neoplasm of lymphocytes exists) melanoma-malignant neoplasm of melanocytes (benign counterpart is a nevus) central nervous system neoplasms (optic nerve)
Differentiation	Degree to which a neoplasm resembles its presumed cell of origin
Dedifferentiation	Neoplasm that does not resemble any cell of origin This does not mean that the cells were once differentiated and now are not Means that the stem cells from which the neoplasm is derived have sufficient numbers of mutations that they do not show any evidence of specific differentiation In this circumstance, immunohistochemistry and electron microscopy are most helpful
-blastoma	Suffix usually applied to neoplasms of children that show evidence of immature growth recapitulating the tissues of the fetus (e.g., retinoblastoma)
Teratoma	Tumors usually occurring in brain and/or orbit of children, or the gonads, that show histologic evidence of tissues from all three germ layers: ectoderm, mesoderm, and endoderm
Hamartoma	Benign, disorganized proliferation of tissues normally present in a specific location
Choristoma	Benign, disorganized proliferation of tissues not normally present in that location

Table 7-3. Usual immunohistochemical staining patterns of the major categories of malignant neoplasms

STAIN	SARCOMA	CARCINOMA	MELANOMA	LYMPHOMA
Keratin	-	+	-	-
Vimentin	+	-	+	+
HMB-45	-	-	+	-
Leukocyte common antigen, B- or T-cell antigens	-	-	-	+

+ Usually positive for that stain; - Usually does not stain.

Immunohistochemistry

Each immunohistochemical staining table (Tables 7-4 ,7-5 ,7-6) is based on a general histologic pattern that the pathologist sees on hematoxylin-eosin stain.

Table 7-4. Immunohistochemical staining of spindle-cell neoplasms

NEOPLASM	VIMENTIN	MUSCLE ACTIN	SMOOTH MUSCLE ACTIN	DESMIN	S100	FACTOR VIII-RELATED ANTIGEN	*Ulex europaeus-1* (UEA)	KERATIN	MYOGLOBIN	CD34
Fibrous histiocytoma	+	+/-	+/-	-	-	-	-	-	-	+
Rhabdomyosarcoma	+	+	-	+	-	-	-	-	+/-	-
Leiomyosarcoma	+	+	+	+	-	-	-	-	-	-
Liposarcoma	+	-	-	-	+/-	-	-	-	-	-
Hemangiopericytoma	+	-	-	-	-	-	-	-	-	+
Angiosarcoma	+	-	-	-	-	+/-	+/-	-	-	+
Kaposi's sarcoma	+	-	-	-	-	+/-	+	-	-	+
Schwannoma, neurofibroma	+	-	-	-	+	-	-	-	-	+
Malignant peripheral nerve sheath tumor	+	-	-	-	+/-	-	-	-	-	+/-
Chondrosarcoma	+	-	-	-	+/-	-	-	-	-	-
Spindle-cell carcinoma	+/-	-	-	-	-	-	-	+	-	-

+ Usually stains for that antigen; +/- May or may not stain; - Usually does not stain.

Table 7-5. Immunohistochemical staining of small cell undifferentiated neoplasms

NEOPLASM	LEUKOCYTE COMMON ANTIGEN (LCA)	KERATIN	NEURON-SPECIFIC ENOLASE (NSE)	NEURO-FILAMENT (NF)	DESMIN	O13
Usually Childhood Neoplasms						
Leukemia**	+	-	-	-	-	+/-
Neuroblastoma	-	-	+	+	-	-
Retinoblastoma	-	-	+	+	-	NA
Rhabdomyosarcoma	-	-	-	-	+	-
Ewing's sarcoma	-	-	-	-	-	+
Wilms' tumor	-	+	-	-	$	-
Usually Adult Neoplasms						
Lymphoma	+	-	-	-	-	+/-
Peripheral neuroepithelioma	-	-	+	+	-	+
Olfactory neuroblastoma	-	-	+	+	-	-
Small cell carcinoma	-	+/-	+/-	+/-	-	-

+ Usually stains for that antigen; - Usually does not stain; $ May stain if myoid differentiation is present; +/- May or may not stain.

** Enzyme histochemistry and other immunohistochemical stains required to distinguish histologically between lymphoma and leukemia.

Table 7-6. Immunohistochemical staining of other, usually large cell neoplasms

NEOPLASM	VIMENTIN	KERATIN	EPITHELIAL MEMBRANE ANTIGEN (EMA)	$100	NEURON-SPECIFIC ENOLASE (NSE)	CHROMOGRANIN	SYNAPTOPHYSIN	HMB-45	GLIAL FIBRILLARY ACIDIC PROTEIN (GFAP)	LEUKOCYTE COMMON ANTIGEN (LCA)
Melanoma-uveal, conjunctival, orbital, metastatic	+	-	-	+	+	-	-	+	-	-
Carcinoma-metastatic, locally invasive, lacrimal	LG	+	+	LG	-	-	-	-	LG	-
Large cell lymphoma	+/-	-	-	-	-	-	-	-	-	+
Granular cell tumor	+	-	-	+	-	-	-	-	-	-
Paraganglioma	+	-	-	+/-	+	+	+	-	+/-	-
Carcinoid tumor	-	+	NA	-	+	+	+	-	-	-
Alveolar soft part sarcoma**	+/-	-	-	+/-	+/-	NA	-	-	-	-
Malignant rhabdoid tumor	+	+	+/-	-	-	-	-	-	-	-
Meningioma	+	+/-	+/-	+/-	+/-	NA	NA	-	-	-
Astrocytoma	+	-	-	+/-	+/-	-	-	-	+	-

+ Usually stains for that antigen; - Usually does not stain; +/- May or may not stain; ** Some stain for desmin and muscle actin; LG Lacrimal gland neoplasms may stain for vimentin, S100, and GFAP; NA Data not available.

Mesenchymal Neoplasms of the Orbital Soft Tissue and Bone

Mesenchymal neoplasms of the orbit include both benign and malignant lesions of the soft tissues and bone. The soft tissues include smooth and skeletal muscle, fibrous, adipose, vascular, and peripheral nervous system tissues. The group of all benign and malignant neoplasms of soft tissue is often referred to as “soft tissue tumors,” while malignant tumors of both soft tissue and bone are sarcomas. Another term frequently used synonymously is “spindle cell tumor,” as these neoplasms are often composed of spindle-shaped cells microscopically. The distinction between benign and malignant is usually made on routine light microscopy, although the behavior of some neoplasms does not fall neatly into one category. Also included in spindle cell tumors are those of the peripheral nervous system. Once it has been decided that a neoplasm is in the soft tissue category, it must be subclassified by the type of differentiation it shows and then into a specific entity. Most of the soft tissue neoplasms that have been described elsewhere in the body occur in the orbit. They will be presented under their major categories and specific entities in a tabular format. Also included are some lesions thought to be reactive, as these may form masses and must be considered in the pathologic differential diagnosis of true neoplasms.

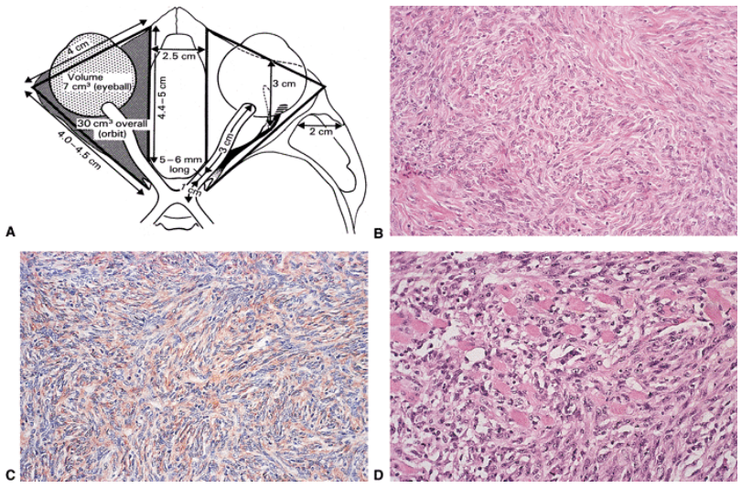

Figure 7-1. (A) Nodular fasciitis. High-power view of cellular periphery with regular-shaped spindle cells and normal mitoses (H&E, original magnification × 25). (B) Benign fibrous histiocytoma. Photomicrograph shows monotonous small spindle cells arranged in a storiform pattern similar to that for solitary fibrous tumor (H&E, original magnification × 25). (C) This tumor stains for CD-34 antigen (indirect immunoperoxidase, anti-CD-34, original magnification × 25). (D) Malignant fibrous histiocytoma. This neoplasm shows pleomorphic nuclei, prominent nucleoli, and numerous mitotic figures as it invades an extraocular muscle (H&E, original magnification × 25).

Mesenchymal Neoplasms of Orbital Soft Tissue

Fibrous and Fibrohistiocytic Neoplasms

Fibroblastic tumors are composed of the basic mesenchymal cell, the fibroblast, which contains vimentin intermediate filaments demonstrable by immunohistochemistry, has rough endoplasmic reticulum (RER), no external lamina, and no desmosomes on electron microscopy. Fibrohistiocytic tumors are more frequent and are distinguished from pure fibroblastic lesions by having a mixture of cell types, including fibroblasts, myofibroblasts, histiocytic-like cells, and undifferentiated mesenchymal cells by light microscopy and electron microscopy. Immunohistochemically, they stain for vimentin and sometimes for actin. The many different entities are distinguished by recognition of histological patterns in the context of clinical findings and imaging.

Table 7-7. Pathologic characteristics of fibroblastic and fibrohistiocytic lesions

TERM AND DEFINITION	GROSS	MICROSCOPIC
Nodular fasciitis (Fig. 7-1A)		
Mass composed of reactive fibroblasts	Firm, white, uncircumscribed	Spindled fibroblasts and myofibroblasts with mitoses, but no atypia Often situated around a central myxoid area
Fibroma and myxoma		
Rare neoplasms composed of fibroblasts with or without a myxoid (mucopolysaccharide containing) background	Firm, white, uncircumscribed, and gelatinous	Spindled fibroblasts in a background of collagen or mucopolysaccharides
***Benign and locally aggressive fibrous histiocytoma** (Figs. 7-1B and C)		
Benign and locally aggressive neoplasms composed mainly of fibroblasts, with occasional histiocyte-like cells	Firm, white to gray, circumscribed	Benign tumors composed of small, thin, or wavy-shaped spindle cells arranged in a storiform or cartwheeling pattern with occasional normal mitoses and no necrosis Locally aggressive fibrous histiocytomas have similar cytology, but have infiltrating borders
***Solitary fibrous tumor**		
Benign tumor composed of fibroblasts	Firm, white to gray, circumscribed	Entity recently described as occurring in many locations in the body, including the orbit Benign fibroblasts arranged in a variety of patterns, including storiform, fascicular, and hemangiopericytoma-like Similar histology to benign fibrous histiocytoma
Giant cell angiofibroma		
Rare, benign tumor composed of fibroblasts, vessels, and giant cells	Occurs in lacrimal gland area	Recently described entity having histology similar to solitary fibrous tumor, but with numerous vascular spaces and giant cells
Fibromatosis		
Group of benign, nonmetastatizing, but locally aggressive fibroblastic proliferations	Firm, white to gray, uncircumscribed	Spindled fibroblasts arranged in fascicles with a background of collagen, small blood vessels, and occasional inflammatory cells Normal mitoses may be present More cellular than a fibroma, but less cellular than a fibrosarcoma
Fibrosarcoma		
Malignant neoplasm of fibroblasts only, with a tendency to occur in children	Firm, white to gray, uncircumscribed	Cellular proliferation of regularly shaped fibroblasts arranged in a herringbone pattern with little intervening collagen Abnormal mitoses and increased cellularity distinguish it from the above neoplasms
Malignant fibrous histiocytoma (Fig. 7-1D)		
Sarcoma composed of malignant fibroblasts with admixtures of myofibroblasts, “histiocytic” cells, and undifferentiated cells	Large, firm, white to gray with areas of necrosis Uncircumscribed, infiltrative	Neoplasm with pleomorphic fibroblastic, myofibroblastic, and undifferentiated cells Abnormal mitoses, necrosis, tumor giant cells often present Infiltrating margins

Skeletal and Smooth Muscle Neoplasms

Soft tissue tumors of muscle are divided into those of skeletal and smooth muscle. Skeletal muscle neoplasms in the orbit are virtually all malignant and require distinction from the many other neoplasia that fall into the large group of “small blue cell” undifferentiated malignancies, which usu ally occur in children and young adults (Table 7-8). All muscle tumors stain immunohistochemically for vimentin, desmin, and muscle specific actin, while smooth muscle tumors also stain for smooth muscle actin.

Table 7-8. Pathologic characteristics of neoplasms of skeletal and smooth muscle

TERM AND DEFINITION	GROSS	MICROSCOPIC	SPECIAL INVESTIGATIONS
Rhabdomyosarcoma			
Malignant soft tissue neoplasm showing differentiation toward skeletal muscle Divided into several histologic subtypes which are prognostic: embryonal is the most frequent subtype in the orbit (Figs. 7-2A and B) spindle cell botryoid alveolar (Fig. 7-2C) undifferentiated and unclassifiable	Soft, fleshy May be circumscribed or infiltrative	Cells with high nuclear to cytoplasmic ratio and little cytoplasm embryonal: hypercellular small round to spindle cells with little cytoplasm; occasional “strap” cells with more cytoplasm showing cross striations spindle cell: low cellularity, small spindle-shaped cells in a fascicular pattern botryoid: occurs beneath epithelial surface with a subepithelial condensation of tumor cells alveolar: cells arranged in alveoli with well preserved cells around edges and necrotic cells centrally, giant cells often present	IH most useful for diagnosis EM used to identify cells containing remnants of sarcomeres with thick myosin and thin actin filaments, and Z-band material Alveolar rhabdomyosarcoma has a specific translocation t(2;13) or t(1;13), the abnormal product of which can be identified by RT-PCR
Leiomyoma			
Benign neoplasm of smooth muscle cells that occurs rarely in the orbit	Firm, white Circumscribed with a whoried cut surface	Spindle-shaped cells arranged in fascicles with a collagenous background	EM shows spindle cells with longitudinal cytoplasmic filaments, dense bodies, pinocytotic vesicles, and external lamina
Leiomyosarcoma			
Malignant neoplasm of smooth muscle cells that occurs rarely in the orbit	Soft, fleshy Uncircumscribed	Spindle-shaped cells with varying degrees of pleomorphism, mitoses Infiltrative margins	Similar, but less well-developed EM findings as a leiomyoma

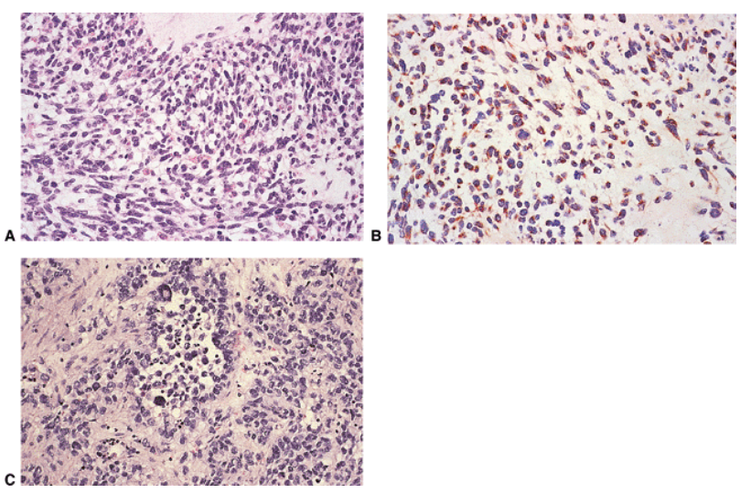

Figure 7-2. Rhabdomyosarcoma. (A) Embryonal rhabdomyosarcoma with small undifferentiated spindle cells and intervening hypocellular areas (H&E, original magnification × 25). (B) Strong staining for desmin, the intermediate filament of muscle cells (indirect immunoperoxidase, desmin, original magnification × 25). (C) An extraorbital alveolar rhabdomyosarcoma showing an “alveolar” space with wellpreserved cells around the periphery and degenerating cells centrally. A tumor giant cell is present in the upper left of the space (H&E, original magnification × 25).

Neurogenic and Neural Crest Neoplasms

Neurogenic and neural crest neoplasia are grouped together because of their proven or presumed origin from components of peripheral nerve, or because they show definite evidence of neural crest or neuroectodermal differentiation.

Peripheral nerve sheath tumors are the most common in this group; the others are rare. Most of these stain for S100 protein immunohistochemically.

Table 7-9. Pathologic characteristics of neoplasms with neurogenic or neuroepithelial differentiation

TERM AND DEFINITION	GROSS	MICROSCOPIC	SPECIAL
Neurofibroma (Figs. 7-3A to C) Benign tumor composed of cells normally found in a peripheral nerve May be associated with von Reckinghausen's neurofibromatosis Three forms	Plexiform: bag of worms appearance, very vascular Isolated: firm, white, circumscribed enlargement of a peripheral nerve Diffuse: irregular increase in density & firmness of tissues	Plexiform: irregular enlargement of many small nerves comprised of cells normally found in peripheral nerve: axons, Schwann cells, endoneurial and perineurial cells Isolated: circumscribed tumor composed of above cell types Diffuse: proliferation of bland spindle shaped cells and ovoid bodies which surround and permeate normal structures without destroying them	All show evidence of axons, Schwann cells and undifferentiated cells by EM
Schwannoma (neurilemmoma) (Fig. 7-3D) Benign tumor composed entirely of Schwann cells	Firm, white, circumscribed, eccentric enlargement of peripheral nerve, frequently supraorbital nerve	Circumscribed tumor composed of spindle cells with long wavy nuclei which may form Verrucay bodies (areas where nuclei line up parallel to each other) Antoni A areas are cellular, Antoni B less cellular like a neurofibroma May show evidence of degeneration in form of cystic areas, collections of foamy macrophages, thick-walled blood vessels and bizarre nuclei	Characteristic pattern of long wrapping cell processes all surrounded by external lamina on EM Long spacing collagen usually present

Figure 7-3. (A) Plexiform neurofibroma. Photomicrograph shows numerous nerves enlarged by spindle cell proliferations, giving a bag of worms appearance responsible for thickening of the eyelid and orbit (H&E, original magnification × 25). (B) Positive staining for protein S100 in the enlarged nerves (indirect immunoperoxidase, S100, original magnification × 10). (C) Areas of diffuse neurofibroma surrounding sebaceous glands in the same patient (H&E, original magnification × 25). (D) Schwannoma (neurilemmoma) showing cellular Antoni A area with Verocay body in the lower half and hypocellular Antoni B area in the upper left (H&E, original magnification × 25). (Fig. 7-3B reproduced with permission from White VA, Rootman J, Orbital pathology. In: Albert DM, Jakobiec FA, eds. Principles and Practice of Ophthalmology. 2nd ed. Philadelphia: WB Saunders, 2000:3816-74.)

Malignant peripheral nerve sheath tumor (malignant schwannoma) Rare sarcoma of peripheral nerve	May show a plexiform growth pattern Important to identify origin from nerve	May have a spindle or epithelioid cell pattern Shows usual features of malignancy	May retain some S100 protein positivity by IH and/or EM characteristics of Schwann cells
Amputation neuroma Reactive proliferation of peripheral nerves and fibrous tissue in response to transection of nerve by previous trauma	Irregular firm white mass with infiltrative margins	Benign, haphazard proliferation of peripheral nerves surrounded by fibrosis secondary to previous trauma	Nerves will be S100 protein positive

Granular cell tumor (Fig. 7-4A) Benign neoplasm thought to be derived from Schwann cells that have developed a facultative histiocytic role	Irregular firm white mass with infiltrative margins	Collections of polygonal cells with abundant eosinophilic granular cytoplasm Positive on PAS and diastase stain, and for S100 protein	EM characteristic with cytoplasm full of single membrane bound lysosomes containing electron dense material

Figure 7-4. Granular cell tumors show abundant granular eosinophilic cytoplasm, which are surrounded by fibrous tissue. (A) The cytoplasm stains strongly PAS positive after diastase treatment (PAS and diastase, original magnification × 25). (B) Extraorbital peripheral neuroepithelioma shows a proliferation of small undifferentiated cells with occasional poorly formed rosettes (indirect immunoperoxidase, neuron-specific enolase, original magnification × 40). (Reproduced with permission from White VA, Rootman J, Orbital pathology. In: Albert DM, Jakobiec FA, eds. Principles and Practice of Ophthalmology. 2nd ed. Philadelphia: WB Saunders, 2000:3816-74.)

Peripheral neuroectodermal tumor (PNET) (Fig. 7-4B) Malignant neoplasm composed of primitive neuroepithelial cells occurring in soft tissues, better differentiated counterpart of Ewing's sarcoma	Soft, fleshy mass with circumscribed or infiltrative borders	Collections of undifferentiated small blue cells which may show some evidence of neural differentiation in the form of rosettes	EM shows occasional cells with processes containing dense core granules and microtubules Has t(11;22), t(21;22) or t(7;22) translocation which can be identified by RT-PCR
Paraganglioma Neural crest tumor of cells derived from the paraganglia	Circumscribed, tan color	Polygonal cells with granular cytoplasm arranged in nests separated by thin-walled blood vessels	Positive on Grimelius stain & for chromogranin by IH EM shows numerous dense core granules and intercellular junctions
Retinal anlage tumor (melanotic neuroectodermal tumor of infancy) Tumor resembling the developing eye thought to arise from displaced neuroepithelium Usually occurs in the maxilla	Pigmented, not circumscribed	Cells arranged in alveolar units lined by pigmented cuboidal cells resembling pigment epithelial cells surrounding a central area containing small neuroblastic cells	
Primary orbital meningioma	Firm, white, circumscribed	Meningioma histologically similar to those occurring in optic nerve, but unattached to nerve or intracranial dura	

Vascular Neoplasms

Vascular lesions consist of malformations, hamartomas, and neoplasms. Capillary and cavernous hemangiomas and lymphangiomas are considered to be hamartomas rather than benign neoplasms. The clinical and radiologic examinations of vascular lesions are much more important than histopathologic examination in establishing a diagnosis, particularly in the malformations, because in some cases little or no tissue will be excised. These lesions are discussed more fully in the chapter on vascular lesions (Chapter 13).

Table 7-10. Pathologic characteristics of vascular neoplasms

TERM AND DEFINITION	GROSS	MICROSCOPIC
Intravascular papillary endothelial hyperplasia Exuberantly organizing thrombus in an artery or vein that produces a mass in anterior orbit/eyelid	Hemorrhagic mass	Organizing thrombus composed of fibrin covered by endothelial cells that produce a papillary pattern May obscure or extend outside of vessel wall making it difficult to recognize its origin
Glomus tumor Tumor arising from the smooth muscle cells of the Sucquet-Hoyer canal, an arteriovenous anastomosis usually present in skin of hands and feet	Well-circumscribed, dark red nodule	Small vascular spaces surrounded by regular, polyhedral glomus cells
Hemangiopericytoma (Fig. 7-5A) Neoplasm derived from pericytes, cells that surround endothelial cells	Circumscribed vascular mass	Sinusoidal or staghorn-shaped vascular spaces lined by endothelial cells and surrounded by small, oval to spindle cells, the pericytes Range from benign to malignant, although all can recur and metastasize, often slowly
Angiosarcoma (Fig. 7-5B) Highly malignant neoplasm of endothelial cells usually involving skin and superficial soft tissue	Hemorrhagic mass	Infiltrating vascular spaces lined by atypical endothelial cells that may become solid in poorly differentiated areas

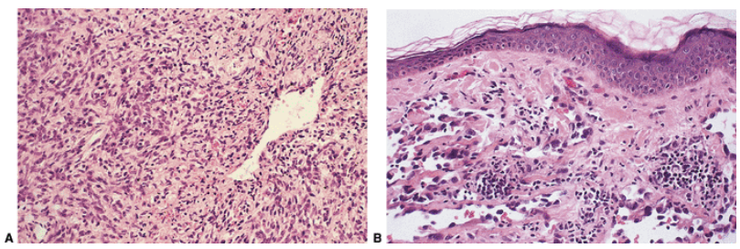

Figure 7-5. (A) Hemangiopericytoma. Large staghorn vessel surrounded by small, regular, spindleshaped pericytes (H&E, original magnification × 25). (B) Angiosarcoma. The dermis is infiltrated by irregular avascular channels lined by malignant endothelial cells with large, dense nuclei (H&E, original magnification × 25). (Fig. 7-5A reproduced with permission from White VA, Rootman J, Orbital pathology. In: Albert DM, Jakobiec FA, eds. Principles and Practice of Ophthalmology. 2nd ed. Philadelphia: WB Saunders, 2000:3816-74.)

Adipose Tissue Neoplasms

Adipose tissue neoplasms are rare in the orbit. Previous surveys of orbital lesions included larger numbers of lipomas, which were probably excised fat nodules.

Table 7-11. Pathologic characteristics of neoplasms of adipose tissue

TERM AND DEFINITION	GROSS	MICROSCOPIC	SPECIAL
Lipoma Rare tumor in orbit composed of benign adipocytes that may have admixed fibrous tissue	Small fatty mass that may have some fibrous areas Encapsulated	Mature adipose tissue admixed with fibroblasts forming a spindle cell lipoma or with small blood vessels forming an angiolipoma	
Liposarcoma (Fig. 7-6) Rare tumor in orbit composed of lipoblasts with admixed fibroblasts and blood vessels Subdivided into four types of which only two have been reported in the orbit: well-differentiated and myxoid	Large fatty mass with fibrous areas Encapsulated or infiltrative	Myxoid: hypocellular, myxoid background containing lipoblasts (round cells with nucleus pushed to one side by a single fat vacuole) and a plexiform vascular pattern Well-differentiated: more mature lipoblasts (may be difficult to distinguish from normal orbital fat) and a fibrous component with pleomorphic fibroblasts	Myxoid type has a specific translocation t(12;16), the abnormal product of which may be identified by RT-PCR

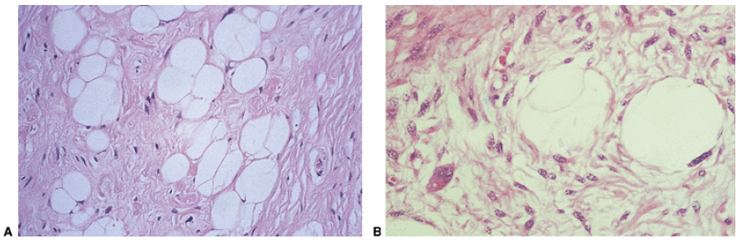

Figure 7-6. (A) Welldifferentiated liposarcoma with sclerosing areas that infiltrate the extraocular muscle. Note the slightly pleomorphic spindleshaped nuclei that are prominent in the sclerosing area. These tumors may become large but can be deceptively bland histologically (H&E, original magnification × 25). (B) Liposarcoma. This myxoid liposarcoma is more poorly differentiated with larger and more irregular cells (H&E, original magnification × 40).

Neoplasms of Uncertain Histogenesis

These rare neoplasms are grouped together because their cells of origin have not been identified with certainty. They consist of immature cells, which frequently show little evidence of specific differentiation or mixed differentiation. Both malignant rhabdoid tumor and epithelioid sarcoma stain for vimentin and epithelial markers.

Table 7-12. Pathologic characteristics of neoplasms of uncertain histogenesis

TERM AND DEFINITION	GROSS	MICROSCOPIC	SPECIAL
Alveolar soft part sarcoma Low grade sarcoma, which may show minimal evidence of skeletal muscle differentiation in some cases	Highly vascular soft tissue neoplasm	Polygonal cells, surrounded by fibrovascular stroma arranged in a pseudoalveolar pattern Occasional cells contain characteristic PAS+D positive crystals	By EM the crystals consist of rectangular membrane bound arrays with a periodicity of 8-10 nm
Malignant rhabdoid tumor Primitive pluripotential sarcoma showing some **histologic** characteristics of a rhabdomyosarcoma	Soft, circumscribed	Monotonous mass of malignant cells having vesicular nucleus that may be indented by a perinuclear, eosinophilic, hyaline cytoplasmic mass Numerous mitoses and necrosis	EM shows that the cytoplasmic mass is composed of a whorled array of intermediate filaments No features of skeletal muscle or other specific differentiation are found
Epithelioid sarcoma (Figs. 7-7A and B) Histologically low grade neoplasm, usually occurring on the extremities, which pursues a relentless course	Nodular pattern with spread along tendons May form fistulous tracts with overlying skin	Nodular formations of large, atypical cells with central necrosis that must be distinguished from a granulomatous process	

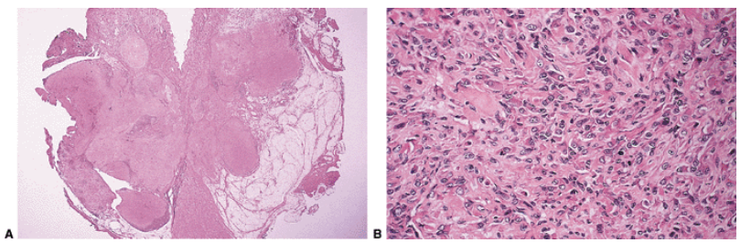

Figure 7-7. Epithelioid sarcoma. (A) Low-power photomicrograph showing nodules of tumor with central areas of necrosis invading the orbital fat (H&E, original magnification × 2.5). (B) Higher power shows the large cells with atypical nuclei and abundant eosinophilic cytoplasm (H&E, original magnification × 25).

Mesenchymal Neoplasms of Orbital Bone

Mesenchymal tumors arising in bone are grouped together because their site of origin dictates a separate differential diagnosis from soft tissue lesions. Understanding bone pathology is difficult and in the head is complicated by the rarity of these tumors and their slightly different histopathologic characteristics from bone tumors elsewhere, probably due to the neural crest origin of the facial bones and their lack of enchondral ossification. These factors result in a blurring of distinctive histopathologic patterns amongst benign lesions, which are more easily distinguishable when

occurring in other bones. We have divided them into fibro-osseous, reactive giant cell, and malignant groups. As with all bone pathology, it is important that the diagnosis be contextualized with the radiologic interpretation. If there is significant disagreement, the diagnosis should be reviewed and consideration given to the possibility that the specimen is not representative or was taken from the periphery of the lesion. The text by Mirra is the most complete reference on bone tumors throughout the body. The articles by ourselves, Fu and Perzin, and Blodi discuss tumors specifically located in the facial bones. It must be emphasized that all bone tumors may involve the adjacent soft tissues of the orbit. We have seen a case of an enchondroma of the orbit, a bony neoplasm that rarely occurs in this location. Various other tumors that occur in the soft tissues of the orbit, including myxoma, lipoma, cavernous hemangioma, hemangioendothelioma, fibrous histiocytoma, and lymphoma, have been infrequently reported in the orbital bones.

Table 7-13. Major mesenchymal tumors of orbital bone

LESION	LOCATION	PATHOLOGY
Fibroosseous Lesions		
Osteoma	Frontal, ethmoidal sinuses	Most osteomas show a peripheral cap of dense lamellar bone with little intervening stroma and a central core of woven bone, lined by osteoblasts and osteoclasts, containing a fibrous stroma
Fibrous dysplasia (Fig. 7-8)	Frontal, ethmoidal, sphenoidal sinuses, maxilla	Irregular trabeculae of woven bone unlined by osteoblasts in a moderately cellular fibrous stroma (one of our cases showed osteo*cartilaginous* foci in a fibrous background)
Ossifying fibroma	All; frontal and ethmoidal most common	Cellular fibrous stroma arranged in whoris; bony trabeculae lined by osteoblasts; psammomatoid variant shows round to oval spicules of bone similar to psammoma bodies
Osteoblastoma	Frontal, ethmoidal	Abundant trabeculae of osteoid and woven bone surrounded by numerous pleomorphic but benign osteoblasts; stroma contains osteoclasts and numerous vessels lined by endothelial cells

Figure 7-8. Fibrous dysplasia. Histopathology shows a fibrous stroma, from which arise small spicules of woven bone unlined by osteoblasts (H&E, original magnification × 25).

Figure 7-9. Cholesterol granuloma (hematic cyst). Orbital tissue shows foamy histiocytes, cholesterol clefts, and hemosiderin deposition (H&E, original magnification × 50). (Reproduced with permission from White VA, Rootman J, Orbital pathology. In: Albert DM, Jakobiec FA, eds. Principles and Practice of Ophthalmology. 2nd ed. Philadelphia: WB Saunders, 2000:3816-74.)

Reactive Giant Cell Lesions		
Giant cell reparative granuloma	Most common in mandible; also in maxilla, temporal, sphenoidal, ethmoidal	Small giant cells grouped around hemorrhagic foci and irregularly spaced in a stroma containing oval and spindle-shaped cells with foci of collagen, hemosiderin, and osteoid
Brown tumor of hyperparathyroidism	Maxilla, ethmoidal, frontal, sphenoidal	Similar histology to giant cell reparative granuloma; can often be diagnosed only by finding abnormal serum calcium and phosphate values
Aneurysmal bone cyst	Sphenoidal, frontal	Blood-filled channels unlined by endothelial cells, surrounded by variably fibrous stroma containing osteoid, giant cells, foci of hemorrhage, and hemosiderin
Cholesterol granuloma (Fig. 7-9)	Most common in frontal; rarely in zygoma, maxilla	Cholesterol clefts surrounded by foreign body giant cells, foci of recent and old hemorrhage, foamy macrophages, lymphocytes, fibrous tissue; may be associated with surrounding abnormal bone
Malignant Neoplasms		
Osteosarcoma (Figs. 7-10A and B)	Maxilla, ethmoidal, frontal; often in patients with germline mutation of retinoblastoma gene	Trabeculae of osteoid arising directly from a malignant fibroblastic stroma showing hypercellularity, anaplasia, mitoses, and invasion of adjacent structures; malignant chondroblastic areas may be present

Figure 7-10. Osteosarcoma. (A) Osteoid surrounded by malignant osteoblasts infiltrates between the normal bone and marrow fat of the orbit (H&E, original magnification × 10). (B) Higher power shows the pleomorphic sarcoma cells infiltrating an extraocular muscle (H&E, original magnification × 25). (Reproduced with permission from White VA, Rootman J, Orbital pathology. In: Albert DM, Jakobiec FA, eds. Principles and Practice of Ophthalmology, 2nd ed. Philadelphia: WB Saunders, 2000:3816-74.)

Chondrosarcoma	Maxilla, ethmoidal	Hyaline cartilaginous tissue showing hypercellularity, nuclear pleomorphism, and binucleate cells within lacunae
Mesenchymal chondrosarcoma	Bones and soft tissues of orbit	Islands of mature hyaline cartilage embedded in a stroma composed of small spindle-shaped cells similar to those in a hemangiopericytoma
Ewing's sarcoma (Figs. 7-11A to D)	Frontal, maxilla, ethmoidal, sphenoidal	Small undifferentiated cells; PAS positive, diastase-sensitive glycogen in cytoplasm; electron microscopy shows cells with few intercellular junctions and organelles; specific translocations involving chromosome 22 as seen in peripheral neuroectodermal tumor (see Table 7-9)

Figure 7-11. Ewing's sarcoma. (A) This tumor shows small undifferentiated (“blue”) cells infiltrating orbital bone. Numerous mitoses are present (H&E, original magnification × 25). (B) The large amount of glycogen frequently seen in this tumor is stained by PAS (PAS, original magnification × 40). (C) The glycogen is removed by pretreating the section with diastase (PAS and diastase, original magnification × 40). (D) This neoplasm stains strongly for O13 (immunoperoxidase, anti-O13, original magnification × 40). (Figs. 7-11B and C reproduced with permission from White VA, Rootman J, Orbital pathology. In: Albert DM, Jakobiec FA, eds. Principles and Practice of Ophthalmology. 2nd ed. Philadelphia: WB Saunders, 2000:3816-74.)

Lymphoproliferative and Leukemic Lesions

Ophthalmic surgeons have an important role in ensuring that the specimen from a patient suspected of having a lymphoproliferative lesion is delivered to the pathologist in a manner that allows the material to be used in the most appropriate way and for the largest number of diagnostic investigations. At our institution, specimens are sent to the laboratory immediately after removal, wrapped in sterile saline-dampened Telfa gauze in a hard plastic container, to avoid crush artifact, rather than a plastic bag. When received, a slide is touched to its surface to pick up cells and an H&E stain is immediately done to confirm a lymphoproliferative process. If lymphocytes are present and sufficient material has been received, the specimen will be divided in the following manner. A piece is fixed in B5 fixative (containing mercuric chloride and formalin) for routine processing, H&E examination, and immunophenotyping on fixed tissue (regular formalin fixation distorts the nuclear features and destroys many of the antigens required for proper classification). A piece of fresh tissue is used for immunophenotyping by flow cytometry and for DNA extraction to detect immunoglobulin gene rearrangement (IgH RA), which is common in all types of B-cell lymphomas, or rearrangement of the *bcl-2* oncogene (the product of the t(14;18) seen in follicular lymphomas). It may also be used to detect T-cell receptor gene rearrangement in the rare T-cell lymphoma of the orbit. These investigations require approximately 0.5 cc of tissue and thus might not be performed on every specimen. The most important factors are that the specimen is not crushed and it is fixed promptly in B5 fixative for histology. If insufficient tissue is received for fresh studies, the amount remaining, after an adequate amount has been placed in B5, may be fixed in formalin since polymerase chain reaction (PCR) for gene rearrangement can be performed from formalin fixed tissue.

B-Cell Lymphomas

Previously, it was thought that differentiation of orbital lymphomas from inflammatory conditions or “pseudotumors” was difficult; however, it is now recognized that most orbital lymphoproliferative lesions are lymphomas and patients should be treated and followed as such. Orbital lymphomas are usually suspected clinically (Fig. 7-12A) and are easy to confirm histologically. The vast majority of these lesions are of B-cell origin, although varying numbers of reactive T-cells will be admixed. Most lesions are composed of “small” B-cells, resembling normal B lymphocytes. Previously difficult to differentiate one from another, the categories of “small cell lymphomas” have been well-delineated in the last several years as outlined in Table 7-14 , which describes the most common categories encountered in the orbit. Immunologic staining by histologic or flow cytometric methods for a variety of lymphocyte differentiation antigens may be required to diagnose these lymphomas accurately. Low grade lymphoma of mucosal associated lymphoid tissue (MALT) is the most frequent category. Two histologic classifications are given in Table 7-14 as both are currently in use, although the REAL (Revised European-American Lymphoma) classification is the most recent, and likely to become incorporated in the future World Health Organization (WHO) classification.

Occasional cases of large cell lymphoma, in which the lymphocyte is about the same size as a histiocyte or endothelial cell, occur in the orbit (Fig. 7-15). In this instance, differentiation from other large cell malignancies, such as a carcinoma or melanoma, may be required, as outlined in Table 7-3 . We reported a single case of signet ring morphology in a mixed small cleaved and large cell lymphoma of the orbit, a cellular pattern seen most frequently in adenocarcinoma, so this diagnosis must be ruled out on the basis of immunopathology and/or electron microscopy. Several cases of orbital large cell lymphoma and Burkitt's lymphoma in patients with AIDS have been reported. Orbital involvement with large cell lymphoma as part of a post-transplant lymphoproliferative disorder has also been reported.

Secondary orbital and adnexal involvement in generalized systemic lymphoma has been reported in up to 5.3% of cases. The histologic types were mainly intermediate grade with large lymphocytes as distinct from primary orbital lymphomas, which are predominantly low grade and composed of small lymphocytes.

Table 7-14. Comparison of REAL (Revised European-American Lymphoma) classification, Working Formulation, histology, and cytology of small cell lymphomas that commonly occur in the orbit

REAL CLASSIFICATION	WORKING FORMULATION	HISTOLOGIC PATTERN	CYTOLOGY	IMMUNOLOGIC PROFILE	MOLECULAR FINDINGS
Extranodal marginal zone B-cell lymphoma (low-grade B-cell lymphoma of MALT type) (Figs. 7-12B to F)	Small lymphocytic	Diffuse, vaguely nodular, germinal centers	Heterogeneous population of lympho-cytes; small, round lymphocytes, cleaved lymphocytes (marginal zone/ monocytoid B-cells), plasma cells	CD5-, CD10-, CD20+, CD23-/+, CD43-/+	IgH RA

Figure 7-12. (A) Clinical photograph of an orbital lymphoma with a subconjunctival involvement, which has the typical salmon flesh appearance. (B) Low-power photomicrograph shows the characteristic dark and pale areas of a MALT lymphoma (H&E, original magnification × 2.5). (C) Higher power shows a germinal center to the left surrounded by small lymphocytes and collections of larger, paler monocytoid B-cells to the right (H&E, original magnification × 40). (D) High-power view of a MALT lymphoma of the lacrimal gland shows lymphoepithelial lesions in which reactive epithelium of ducts is infiltrated by lymphocytes (H&E, original magnification × 25). (E) Another MALT lymphoma shows monoclonality by immunoperoxidase staining for kappa light chains. (F) There is very little staining for lambda light chains. (Not all MALT lymphomas will show monoclonality by immunoperoxidase.) (E and F, immunoperoxidase, anti-light chains, original magnification × 25). (Fig. 7-12A reproduced with permission from White VA, Rootman J, Orbital pathology. In: Albert DM, Jakobiec FA, eds. Principles and Practice of Ophthalmology. 2nd ed. Philadelphia: WB Saunders, 2000:3816-74.)

B-cell chronic lymphocytic leukemia/small lymphocytic lymphoma	Small lymphocytic, consistent with chronic lymphocytic leukemia	Diffuse with pseudofollicles	Small, round lymphocytes	CD5+, CD10-, CD20+, CD23+, CD43+	IgH RA
Lymphoplasmacytoid lymphoma	Small lymphocytic, plasmacytoid	Diffuse	Small, round lympho-cytes, plasmacytoid lymphocytes, plasma cells	CD5-, CD10-, CD23-, CD43-/+	IgH RA
Mantle cell lymphoma (Figs. 7-13A and B)	Diffuse, small cleaved	Diffuse, vaguely nodular, mantle zone, rarely follicular	Small, cleaved lymphocytes; nuclei may be round or oval	CD5+, CD10-/+, CD20+, CD23-, CD43+	IgH RA, t(11;14)

Figure 7-13. Mantle cell lymphoma. (A) Photomicrograph shows lymphocytes with slightly irregular nuclei, compressing residual germinal centers, and admixed with occasional histiocytes (H&E, original magnification × 40). (B) This lymphoma stains for *bcl-1*, the product of the 11;14 translocation, which occurs in mantle cell lymphoma (Immunoperoxidase, anti-*bcl-1*, original magnification × 25).

Follicle center lymphoma, follicular, Grades I–III (Figs. 7-14A to C)	Follicular, predominantly small cleaved cell; follicular, mixed small and large cell	Follicular +/- diffuse areas	Small cleaved lymphocytes with irregular, convoluted nuclei	CD5-, CD10+/, CD20+, CD23-/+, CD43-	t(14;18), IgH RA

Figure 7-14. Follicular lymphoma. (A) Low-power view shows the slightly nodular appearance of this type of lymphoma (H&E, original magnification × 2.5). (B) High-power view shows the cells within the malignant follicle with very irregularly shaped "cleaved" nuclei (H&E, original magnification × 100). (C) This type of lymphoma stains for *bcl-2* protein, the product of the 14;18 translocation seen in follicular lymphomas (immunoperoxidase, anti-*bcl-2*, original magnification × 10). (Fig. 7-14B from White VA, Rootman J, Orbital pathology. In: Albert DM, Jakobiec FA, eds. Principles and Practice of Ophthalmology. 2nd ed. Philadelphia: WB Saunders, 2000:3816-74.)

Follicle center lymphoma	Diffuse, small cleaved cell	Diffuse	Small cleaved lymphocytes	Same as follicle center, follicular	Same as follicle center, follicular

Modified from Tables 2 and 3 with permission from Harris NL, Jaffe ES, Stein H, et al. A revised European-American classification of lymphoid neoplasms: a proposal from the International Lymphoma Study Group. Blood 1994; 84:1361-92.

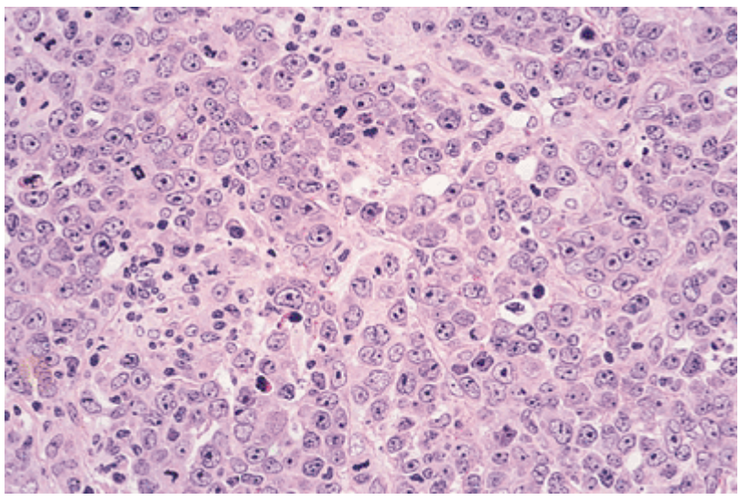

Figure 7-15. Large cell lymphoma. The cells are large with pleomorphic, vesicular nuclei, prominent nucleoli, and numerous mitoses (H&E, original magnification × 40).

Reactive and Atypical Lymphoid Hyperplasia

True reactive lymphoid hyperplasia is infrequent in the orbit and has a variety of definitions. We maintain a strict definition of focal lymphoid collections, often with germinal centres and intact mantle zones, widely separated by orbital fat and fibrous tissue. Lesions with diffuse sheets of lymphocytes do not fall into our definition of reactive hyperplasia.

Occasionally cases will be seen that cannot be easily placed into the reactive or lymphomatous categories. In these instances, it is important that all special modalities, including immunophenotyping and molecular methods, be utilized to aid in diagnosis. If this is done, there should be few lesions that fall into this category. Often this occurs because a biopsy is inadequate in size or was handled inappropriately, and a diagnosis of lymphoma can only be suggested, not made definitively. In these cases, rebiopsy may be required.

T-Cell Lymphoma

Involvement of the orbit in T-cell lymphomas is uncommon and usually occurs at the end-stage of mycosis fungoides when there is widespread disease of the skin and other organs. Case reports describing solitary T-cell lymphoma of the orbit, with eyelid and/or orbital involvement as a presenting sign, have been published. Histologically, malignant T-cells often have a markedly convoluted cerebriform nucleus (Sézary's cells), which may suggest the diagnosis. This is not always the case and confirmation of a T-cell lymphoma depends on the results of immunophenotyping or gene rearrangement studies.

Malignant histiocytosis or histiocytic medullary reticulosis infrequently involves the orbit. The histogenesis of the cells is in some dispute, but studies suggest that in most cases they are of T-cell origin.

Plasmacytomas

Plasmacytomas could have been categorized as B-cell lymphomas because plasma cells are the end-stage of differentiation of B lymphocytes. However, their clinical history and pattern of involvement of the orbit are much different and set them apart. Plasma cell tumors may be seen as soft tissue lesions, either polyclonal reactive or extramedullary monoclonal plasmacytomas, or as a solitary tumor of bone, with or without adjacent soft tissue disease; or orbital bone involvement may be part of the systemic disease, multiple myeloma. If a plasma cell tumor is diagnosed on orbital biopsy, a complete physical examination, skeletal survey for osteolytic bone lesions, bone marrow biopsy, serum protein electrophoresis, and immunoelectrophoresis of serum and urine must be undertaken to rule out systemic disease.

Histopathologically, plasma cells are easy to recognize because of their oval shape, eccentric nucleus with clumped chromatin, perinuclear halo, and amphophilic cytoplasm. Some of these features may be lost in more poorly differentiated neoplasms. Immunoperoxidase staining for cytoplasmic immunoglobulins on Bouin's or B5 fixed tissue may be useful in establishing monoclonality. If a lesion appears immunohistochemically polyclonal, molecular studies for immunoglobulin heavy chain gene rearrangement should be carried out to exclude or confirm monoclonality, as this may impact treatment.

Hodgkin's Lymphoma

Involvement of the orbit in Hodgkin's lymphoma is rare; only a few cases have been reported. It usually occurs in the setting of widespread disease. In one case we encountered, although involvement of the orbit was not diagnosed until 29 months after initial presentation with Hodgkin's disease, orbital asymmetry (documented in old photographs) and radiologic evidence of bony excavation suggested that orbital involvement had been present for a much longer time. Histologic diagnosis of Hodgkin's lymphoma rests on the demonstration of Reed-Sternberg cells, the mirror-image binucleate cells with eosinophilic nucleoli, and vesicular nuclei. Rye's classification of lymphocyte-predominant, mixed cellularity, lymphocyte-depleted, and nodular sclerosing types has been in use for many years. A case of nonspecific orbital granuloma in longstanding Hodgkin's has been described.

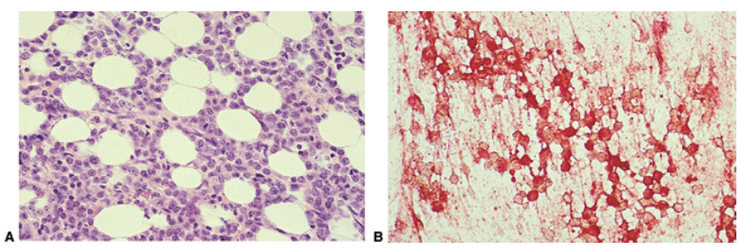

Figure 7-16. Chloroma. (A) Invasion of orbital fat by cells of myeloid leukemia with slightly oval nuclei (H&E, original magnification × 40). (B) Positive chloroacetate esterase stain on a smear of cells from the leukemia in (A) (H&E, original magnification × 40). (Reproduced with permission from White VA, Rootman J, Orbital pathology. In: Albert DM, Jakobiec FA, eds. Principles and Practice of Ophthalmology. 2nd ed. Philadelphia: WB Saunders, 2000:3816-74.)

Leukemia

Ocular involvement is common in leukemia but may not always be clinically evident. In a large autopsy series, ocular involvement was present in 80% of cases, but orbital involvement was present in only 14% of chronic and 7.3% of acute leukemias, most of which were not thought to have been clinically evident. Clinical orbital infiltration may be the presenting sign of an acute leukemia or may occur during its course.

The most characteristic association is the chloroma (or granulocytic sarcoma or *extramedullary myeloid cell tumor* using the most current terminology) with acute myelogenous leukemia but a mass can infrequently occur with acute lymphoblastic leukemia, during the blast crisis of chronic myelogenous leukemia, and with chronic lymphocytic leukemia. We recently saw a patient with orbital involvement associated with prolymphocytic leukemia. If a patient has been identified as having leukemia, the diagnosis will be easy but if an orbital chloroma is the presenting sign, the main problem lies in suspecting the diagnosis. Grossly, the chloroma may show a slight greenish tinge due to the presence of myeloperoxidase.

Histopathologic examination shows a mass of undifferentiated cells, which require distinction from the other “small blue cell tumors” of childhood, the age group in which granulocytic sarcoma is most frequent (Figs. 7-16A and B). To establish the diagnosis of a granulocytic sarcoma, the cytoplasm must be examined for the presence of eosinophilic granules that contain myeloperoxidase, confirmed by the chloroacetate esterase (Leder's) stain or by positive immunohistochemical staining with antilysozyme or antimyeloperoxidase. Ruling out rhabdomyosarcoma, metastatic neuroblastoma, and Ewing's sarcoma is mandatory if there is no evidence of systemic leukemia. Systemic leukemia usually becomes evident at the same time or shortly after a chloroma is diagnosed but in some cases, it has not appeared for up to several months. If the orbital mass occurs in the setting of a lymphoblastic or chronic lymphocytic leukemia, the cells are similar to those described earlier in lymphomas. Examination of bone marrow and peripheral blood is required to aid in making the correct diagnosis.

Benign and Malignant Epithelial Neoplasms of the Orbit

The only epithelial structure in the orbit is the lacrimal gland, so **primary** epithelial neoplasms that involve the orbit arise in the lacrimal gland. All other carcinomas that involve the orbit are either metastatic or involve the orbit by direct extension from adjacent sites.

The lacrimal gland is frequently involved in lymphoproliferative processes, which are similar to those described for B-cell lymphomas and reactive/atypical lymphoid hyperplasia. It is also the site of a number of inflammatory processes, which are listed below. Very uncommonly, it may be involved by soft tissue neoplasms as described in the section on mesenchymal soft tissue neoplasms .

Epithelial Neoplasms of the Lacrimal Gland

The lacrimal gland gives rise to both benign (adenomas) and malignant (carcinomas) epithelial neoplasms, both of which occur commonly in the orbital lobe and less frequently in the palpebral lobe. The neoplasms are the same as those in the salivary glands, although not all the neoplasms that occur in the salivary glands have been described in the lacrimal gland (Table 7-15).

Table 7-15. Pathologic characteristics of epithelial neoplasms of the lacrimal gland

TERM AND DEFINITION	GROSS	MICROSCOPIC
Pleomorphic adenoma (Benign mixed tumor) (Figs. 7-17A and B) Biphasic neoplasm showing a mixture of epithelial and "stromal" areas	Firm white encapsulated, but bosselated, mass May have cystic areas	Two cell patterns are seen in every case Epithelial: small ductules lined by two layers of cells, inner epithelial and outer myoepithelial "Stromal": myxoid areas that appear to be mesenchymal, but that are actually derived from the myoepithelial cells; these areas often contain metaplastic cartilage, and rarely bone or fat

Figure 7-17. Pleomorphic adenoma. (A) Gross photograph of an excised pleomorphic adenoma shows a firm, whitish lesion with a slightly nodular surface at the site of excrescence into the capsule. (B) Microscopic examination shows the typical biphasic pattern with ductules lined by two layers of cells, an inner epithelial layer and outer myoepithelial, merging into the myxoid stroma (H&E, original magnification × 10).

Carcinoma *in* pleomorphic adenoma Areas of carcinoma arising in, but not extending outside, a pleomorphic adenoma	Similar to pleomorphic adenoma	Focal or diffuse areas of cellular and nuclear pleomorphism, mitoses or malignant glands in an obvious background of a pleomorphic adenoma Must **not** have extended outside capsule of pleomorphic adenoma to be classified as such
Oncocytoma Benign epithelial neoplasm composed of oncocytes More common in caruncle and accessory lacrimal glands of eyelids	Firm, circumscribed yellowish-brown mass	Composed totally of oncocytes, large cells with abundant eosinophilic granular cytoplasm packed with mitochondria on electron microscopy Regular nuclei that may have prominent nucleoli
Adenoid cystic carcinoma (Figs. 7-18A and B) Malignant epithelial neoplasm containing both epithelial and myoepithelial cells	Firm, white infiltrative mass	Consists of small, only slightly pleomorphic cells with scant cytoplasm, which form true glands, and gland-like areas where cells are arranged around basement membrane material forming the cribriform pattern Numerous histologic patterns described: cribriform, tubular, basaloid, comedocarcinomatous, and sclerosing Perineural and bone invasion common

Figure 7-18. Adenoid cystic carcinoma. (A) Aspiration biopsy sample shows round and elongated fragments of tissue, consistent with the cribriform and tubular pattern seen in adenoid cystic carcinoma. The cells are minimally atypical (H&E, original magnification × 25). (B) Histopathology reveals cribriform and tubular patterns with perineural invasion at right (H&E, original magnification × 25). (Fig. 7-18A reproduced with permission from White VA, Rootman J, Orbital pathology. In: Albert DM, Jakobiec FA, eds. Principles and Practice of Ophthalmology. 2nd ed. Philadelphia: WB Saunders, 2000:3816-74.)

Carcinoma *ex* pleomorphic adenoma (Malignant mixed tumor) Carcinoma arising in and extending outside of a pleomorphic adenoma, or carcinoma arising in a patient with a previously excised pleomorphic adenoma	Firm, white infiltrative	Carcinoma of adeno-, squamous, mucoepidermoid, or undifferentiated type that arises in a background of a pleomorphic adenoma Must find histologic evidence of a pre-existent pleomorphic adenoma in patients presenting *de novo* with a lacrimal neoplasm
Mucoepidermoid carcinoma Biphasic carcinoma composed of glandular and squamoid areas	Firm, white infiltrative	Two components must be present: single cells or glands with cells containing intracellular mucin and sheets of cells with squamoid or definite squamous differentiation May be well-differentiated in which there is more glandular tissue, which is often cystic, or poorly differentiated in which squamoid areas predominate with only occasional mucous secreting cells
Adenocarcinoma, NOS Carcinoma with no evidence of a pre-existent pleomorphic adenoma	Firm, white infiltrative	Malignant glandular neoplasm May have a pattern similar to ductal carcinoma of breast and other salivary glands and is then called ductal adenocarcinoma (Fig. 7-19) or salivary duct carcinoma

Figure 7-19. Ductal adenocarcinoma of the lacrimal gland with malignant glands containing large cells with pleomorphic nuclei, numerous mitoses, and eosinophilic cytoplasm. This tumor also showed comedonecrosis and vascular invasion (H&E, original magnification × 40). (Reproduced with permission from Katz SE, Rootman J, Dolman PJ, et al. Primary ductal adenocarcinoma of the lacrimal gland. Ophthalmology 1996;103:157-62.)

Rare examples of other benign (monomorphic adenomas and myoepitheliomas) and malignant neoplasms (ductal, acinic cell, and epithelial-myoepithelial carcinomas) have been described in the lacrimal gland.

Epithelial Neoplasms of the Orbital Soft Tissues

As noted, carcinomas, which primarily involve the orbital soft tissues and do not arise in the lacrimal gland, are either metastatic or extend directly from adjacent structures (secondary). The most common primary carcinomas give rise to the largest number of metastases, with breast, lung, gastrointestinal tract, prostate, and kidney as well as cutaneous melanoma being the most frequent in adults. When a metastasis is a diagnostic possibility, the histology of the orbital lesion should be compared with that of the patient's primary, which should be similar. Up to 25% of metastatic tumors may present before a known primary; therefore, this possibility must always be considered in both the clinical and pathologic differential diagnosis. A distinctive feature is the tendency of some tumors to metastasize to specific sites in the orbit, particularly cutaneous melanoma and breast carcinoma to the extraocular muscles, and prostate, renal, and thyroid adenocarcinomas and neuroblastoma to bone (usually the greater wing of sphenoid). Table 7-16 gives brief notes about tumor type, sites of predilection, and pathologic details for the major metastatic orbital tumors, listed in approximate order of frequency. Rare metastases have also been reported from testicular seminomas and ovarian, hepatocellular, and salivary carcinomas. Metastatic tumors in children are listed separately because the metastases in this age group parallel the common pediatric solid tumors.

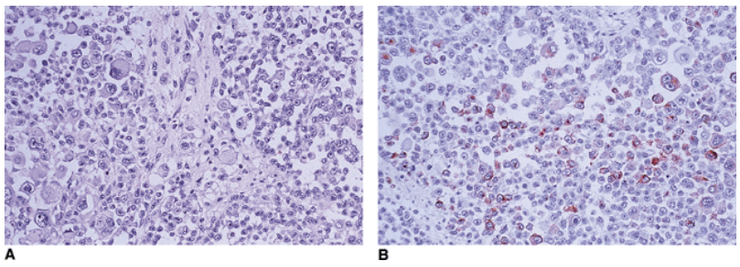

Figure 7-20. Metastatic cutaneous melanoma. (A) Pleomorphic amelanotic melanoma metastatic to the rectus muscle (H&E, original magnification × 25). (B) The tumor cells stain moderately with the antimelanoma antibody HMB45 (indirect immunoperoxidase, original magnification × 25).

Table 7-16. Pathologic characteristics of metastatic orbital tumors

TUMOR	SITES OF METASTASES	HISTOLOGY	HISTOCHEMISTRY	IMMUNOHISTOCHEMISTRY	ELECTRON MICROSCOPY
Metastases in Adults					
Breast carcinoma	Soft tissue, EOM, bone	Glandular, cells in single file, histiocytoid	PAS + diastase, alcian blue	Estrogen, progesterone receptors, B72.3, CEA	Extra- and intracellular lumina; mucin secretory vacuoles
Small cell carcinoma of lung	Soft tissue, bone	Small oval cells in sheets with necrosis; DNA staining of vessels		Keratin, NSE	Dense core granules
Adenocarcinoma of colon, stomach, pancreas, lung	Soft tissue, bone	Glandular, mucinous, signet ring, or papillary patterns	PAS + diastase, mucicarmine	CEA, keratin	Extra- and intracellular lumina; microvilli with filamentous core rootlets
Prostatic adenocarcinoma	Bone, soft tissue	Glandular, single cell infiltration	Alcian blue pH 2.5	Prostatic acid phosphatase; prostate-specific antigen	Extracellular gland formation
Renal adenocarcinoma	Soft tissue, bone	Clear cells in lobules surrounded by vessels; sometimes granular	PAS negative after diastase	Keratin +/- vimentin	Epithelial cells with glycogen and lipid
Cutaneous melanoma (Figs. 7-20A and B)	EOM, soft tissue	Large epithelioid cells; often amelanotic, bizarre cells	Fontana-Masson	S100, HMB-45	Premelanosomes, few junctions, intranuclear cytoplasmic inclusions
Thyroid carcinoma	Soft tissue, bone	Papillary pattern with ground glass nuclei, follicular pattern, or medullary (similar to carcinoid)		Thyroglobulin in follicular; calcitonin in medullary	Papillary shows intranuclear cytoplasmic inclusions; follicular shows epithelial cells with colloid; dense core granules in medullary
Carcinoid	Soft tissue	Regular cells in lobules, trabeculae	Argyrophil +/- argentaffin	Chromogranin, synaptophysin, serotonin	Epithelial cells with irregular dense core granules
Squamous carcinoma	Soft tissue	Polygonal groups and single infiltrating cells with eosinophilic cytoplasm		Keratin	Epithelial cells containing tonofilaments joined by desmosomes
Metastases in Children					
Neuroblastoma	Soft tissue, bone	Small undifferentiated cells with occasional rosette formation		NSE	Cells with cytoplasmic extensions containing dense core granules and microtubules
Ewing's sarcoma	Soft tissue	Small undifferentiated cells	PAS negative after diastase	O13	Cells with poorly formed inter-cellular junctions, few organelles
Wilms' tumor	Soft tissue	Biphasic pattern with tubules and spindle cell stroma			

CEA, carcinoembryonic antigen; EOM, extraocular muscles; NSE, neuron-specific enolase.
Modified with permission from Table 276-4 of White VA, Rootman J. Orbital pathology. In: Albert DM, Jakobiec FA, eds. Principles and Practice of Ophthalmology. 2nd ed. Philadelphia: WB Saunders, 2000:3816-74.

Table 7-17 gives a summary of neoplasms that may involve the orbit by direct extension. In most instances the diagnosis should be obvious clinically or from the patient's past history of an adjacent neoplasm. Not all neoplasms listed in Tables 7-16 and 7-17 are carcinomas but they are included here for the sake of completeness.

Table 7-17. Neoplasms involving the orbit by direct extension

EXTENSION FROM	TUMOR TYPES
Sinuses – maxillary, ethmoidal, frontal	Epithelial-squamous carcinoma, adeno-carcinoma, transitional, adenoid cystic, mucoepidermoid, malignant mixed tumor, carcinoma arising in inverted papilloma Nonepithelial-melanoma, rarely sarcomas
Nose and nasopharynx	Poorly differentiated squamous carcinoma (lymphoepithelioma), esthesioneuroblastoma, angiofibroma, as well as those tumors occurring in the sinuses
Skin of eyelids and surrounding face	Basal cell, squamous and sebaceous carcinomas, cutaneous melanoma, rare sweat gland carcinomas
Conjunctiva	Squamous, spindle cell squamous, mucoepidermoid and oncocytic carcinomas, conjunctival melanoma
Globe	Uveal melanoma, retinoblastoma, medulloepithelioma, carcinoma of pigmented and nonpigmented epithelium of ciliary body
Intracranial cavity and optic nerve	Meningioma, high-grade astrocytoma, chordoma, large pituitary adenoma
Lacrimal sac	Squamous and transitional cell carcinomas, adenocarcinomas arising de novo or in papillomas, adenoid cystic carcinoma, undifferentiated carcinoma; melanoma, rare sarcomas

Modified with permission from Table 276-5 of White VA, Rootman J. Orbital pathology. In: Albert DM, Jakobiec FA, eds. Principles and Practice of Ophthalmology. 2nd ed. Philadelphia: WB Saunders, 2000:3816-74.

Melanocytic Neoplasms involving the Orbit

All melanomas, regardless of origin, have common histologic and immunohistologic features. The cells may range from spindle to polygonal to giant cell in shape, and usually exhibit a moderate to marked degree of nuclear pleomorphism with prominent nucleoli and mitotic figures. The cytoplasm is eosinophilic and varies from having no melanin pigment to being very heavily pigmented so that the gross appearance can range from white to black and any shade in between, often with irregular pigmentation throughout. A Fontana-Masson histochemical stain is useful in identifying melanin. All melanomas will have the immunohistochemical profile indicated in Table 7-3 . With immunohistochemistry, electron microscopy is rarely required but shows melanosomes with varying degrees of melanogenesis.

Melanoma in the orbit usually arises secondarily from direct or metastatic spread of a choroidal, conjunctival, cutaneous, or leptomeningeal melanoma. Primary melanoma of the orbit is a rare condition usually arising in the setting of oculodermal melanocytosis (nevus of Ota), a developmental anomaly more common in Asians and blacks. At least six cases of orbital melanoma have been reported in this syndrome. Pathologic examination has shown a melanoma, similar to a spindle cell choroidal melanoma, which is associated with increased numbers of nonmalignant spindle-shaped melanocytes or a cellular blue nevus in the orbital tissues surrounding the melanoma.

Neoplasms of the Optic Nerve

The optic nerve may be involved by a variety of pathologic processes that occur in the orbital soft tissues, such as inflammation, metastasis, and direct extension from primary intraocular and orbital neoplasms. There are only two major primary optic nerve neoplasms – astrocytomas (also known as gliomas, a more general term referring to both astrocytomas and oligodendrogliomas) and meningiomas. Medulloepitheliomas may occasionally arise in the optic nerve.

Table 7-18. Pathologic characteristics of neoplasms of the optic nerve

TERM AND DEFINITION	GROSS	MICROSCOPIC
Astrocytoma (glioma) (Figs. 7-21A and B) Neoplasm arising from the intrinsic astrocytes within the optic nerve	Fusiform expansion of the nerve confined by dura Cut surface of tumor soft, white, and may be cystic	Expansion of area of nerve within pial septae by slightly hypercellular proliferation of spindle-shaped, pilocytic astrocytes without mitoses Difficult to tell histologically where the tumor ends as cellularity tapers off and glial cells at margin of tumor may be reactive Meninges may be thickened by meningeal proliferation with or without invasion by the glioma May be microcystic spaces containing mucopolysaccharides between tumor cells Eosinophilic collections of glial filaments, known as Rosenthal fibers, may be present in cell processes Occasional gliomas, usually in adults, are malignant, showing marked increase in cellularity, pleomorphic astrocytes, and mitoses

Figure 7-21. Astrocytoma of the optic nerve. (A) Low-power photomicrograph shows widening of the tissue between the pial septae of the nerve (H&E, original magnification × 10). (B) Higher power shows the slightly increased cellularity by minimally atypical cells (H&E, original magnification × 25).

Meningioma (Figs. 7-22A to C) Neoplasm arising from the meninges surrounding the optic nerve	Variable thickening of optic nerve sheath May be invasion of orbital structures	Most optic nerve meningiomas of transitional or meningotheliomatous type Meningotheliomatous types have a sheet-like pattern of growth with indistinct cell borders and oval nuclei with intranuclear cytoplasmic inclusions Transitional types have lobules and whorls of meningothelial cells surrounded by fibroblastic cells, and may contain psammoma bodies Other benign histologic types occur rarely Atypical forms with sheet-like growth and numerous mitoses, and hemangiopericytomatous types, rarely occur

Figure 7-22. Meningioma. (A) Tumor on the left compresses the optic nerve right (H&E, original magnification × 25). (B) Meningotheliomatous histologic type of meningioma with occasional psammoma bodies (H&E, original magnification × 25). (C) Transitional type with numerous small whorls (H&E, original magnification × 40).

Congenital & Structural Lesions

Congenital

It is difficult to classify this group of lesions as many can fall into more than one category. We have presented them from a mechanistic view point.

Malformations

Associated With Orbital Bone and Ocular Malformations

Various congenital structural malformations of the orbital soft tissues and bones occur with histologically normal tissues, and pathologic examination is rarely required. These disorders include orbital asymmetry and craniofacial dysostoses, in which the diagnosis is established clinically and radiologically. Primary globe anomalies, such as anophthalmia, synophthalmia, congenital cystic eye, and microphthalmia also induce disturbances in growth of normal orbital tissue.

Vascular

Malformations of the orbital vessels may occur independently or as part of congenital syndromes such as Sturge-Weber or Wyburn-Mason, or they may be acquired spontaneously or as a result of trauma. Diagnosis rests mainly on hemodynamics, arteriography, venography, and intralesional vascular studies. If tissue is removed, pathologic examination may show a tangled mass of abnormal vessels in which the clear-cut distinction between arteries and veins is lost, with fragmentation of the elastic lamina of arteries and both vessels showing loss of normal muscular layers.

Hamartomas

Vascular

Capillary Hemangiomas

Capillary hemangiomas commonly involve the ocular adnexae, where they may be superficial, deep, or combined. In the early stage, these are cellular lesions composed of proliferating capillaries with little intervening stroma with lumina that may be difficult to visualize (Figs. 7-23A and B). They have an infiltrative growth pattern and may involve all orbital structures. Later on, the capillaries become dilated and filled with red blood cells, and fibrosis and fat are found between the vessels. The vessels at all stages may be outlined with a reticulin stain, and endothelial cells stained immunohistochemically with CD-34, for Factor VIII-related antigen and by lectin binding with *Ulex europaeus*-1.

Lymphangioma

The lymphangioma has been called a “hamartoma” or “choristoma,” depending on whether the component vessels are considered to be true lymphatics or dysplastic blood vessels showing some features of lymphatics. These poorly circumscribed infiltrating lesions occurring in children and young adults may involve the conjunctiva, eyelid, or deep orbit and often can only be partially removed. Histopathologically, they consist of a myriad of irregularly sized and shaped vascular channels with thin walls embedded in a loose fibrous stroma that contains bundles of smooth muscle and collections of lymphocytes. The vascular channels may be filled with red blood cells or may contain serous fluid. Evidence of old hemorrhage is present in the form of hemosiderin and cholesterol clefts, and thrombosis and calcification may be present. Electron microscopy has shown features of both vascular and lymphatic channels. Many of the so-called lymphangiomas are in fact mixed venous lymphatic malformations, which are in discussed in detail later.

Cavernous Hemangioma

Cavernous hemangioma is a well-encapsulated, benign, slowly growing vascular lesion occurring in adults. If proptosis, diplopia, or visual field loss is significant, the lesion

is removed. Grossly, it is a characteristically plum-colored, bosselated, encapsulated mass that has a spongy appearance on the cut surface. Microscopically, it is well encapsulated by fibrous tissue and shows large regularly shaped vascular channels lined by endothelial cells and surrounded by smooth muscle cells. The stroma consists of thick fibrous tissue that may contain bundles of smooth muscle and myxoid foci. The vessels are usually filled with red blood cells. Thrombosis with organization may rarely be present. Tumors may be multiple. Cavernous hemangioma may also occur within the bones of the orbit.

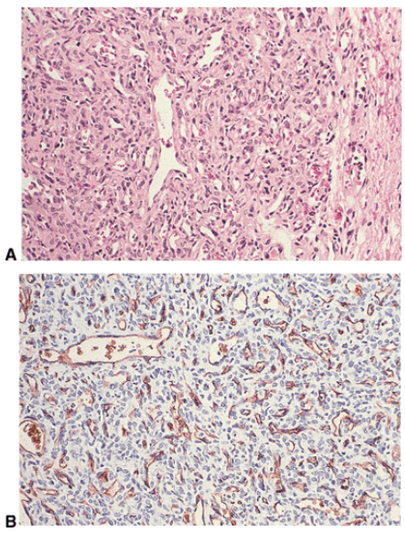

Figure 7-23. Capillary hemangioma. (A) Cellular capillary hemangioma demonstrates small vessels, some of which contain red blood cells, arranged in lobules surrounded by fibrous tissue (H&E, original magnification × 25). (B) Binding of the lectin *Ulex europaeus*1 outlines the numerous small vessels in this lesion (Lectin binding, *Ulex europaeus*1, original magnification × 25). (Reproduced with permission from White VA, Rootman J, Orbital pathology. In: Albert DM, Jakobiec FA, eds. Principles and Practice of Ophthalmology. 2nd ed. Philadelphia: WB Saunders, 2000:3816-74.)

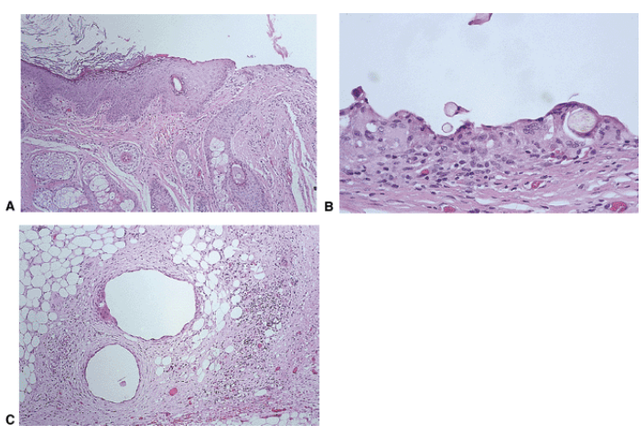

Figure 7-24. Dermoid cyst. (A) Dermoid cyst showing stratified keratinizing squamous epithelium with a hair follicle and sebaceous gland in the wall and hairs and keratin in the lumen (H&E, original magnification × 10). (B) Ruptured dermoid cyst with replacement of epithelium by foreign body giant cells and histiocytes. Note numerous hairs (H&E, original magnification × 25). (C) Orbital lipogranulomatous inflammatory and fibrous reaction to lipid leaked from a ruptured dermoid cyst (H&E, original magnification × 10).

Nonvascular

Cartilaginous Hamartoma

Lesions containing benign cartilage have been reported in the orbit. Some have classified these as tumors rather than hamartomas, but in all instances the histologic appearance has been benign.

Choristomas

Choristomatous Cysts

All congenital epithelial cysts are distinguished by having a lining that recapitulates some of the normal adnexal epithelia. They are all thought to arise from sequestration of normal tissue in abnormal locations during embryonic development and thus are choristomatous cysts.

Dermoid Cysts (Figs. 7-24A to C)

These are the most common congenital epithelial cysts, accounting for 33% of cysts in our series and nearly half of orbital lesions seen in childhood, when they usually present. They typically occur in the superotemporal orbit in relation to the suture lines, often with a bony defect. The lining consists of keratinizing stratified squamous epithelium with various adnexal structures embedded in the wall, including sebaceous glands, hair follicles, and eccrine sweat glands. The cyst contents consist of keratin, sebaceous secretions, and hairs that are usually grossly recognizable. A portion of the wall is often replaced by a giant cell foreign body granulomatous response, indicating previous rupture of the cyst lining. When the oily sebaceous secretions extrude into the surrounding orbital fat, a lipogranulomatous and fibrotic response is initiated and may obscure the original cystic nature of the lesion. Remnants of epithelium and hairs must be looked for to confirm the origin of the inflammation. When no adnexal structures are found in the wall, the lesion is termed an *epidermoid cyst.* Dermoid cysts have recently been described in the lateral rectus muscle. Squamous cell carcinoma has been reported, arising from longstanding, asymptomatic choristomatous cysts in two elderly patients.

Conjunctival Dermoid Cysts

Conjunctival dermoid cysts represent sequestrations of conjunctival and caruncular epithelia, usually occurring in the medial orbit without a bony defect. The cyst lining is composed of a nonkeratinizing stratified squamous or cuboidal epithelium, which may have goblet cells, and the wall contains adnexal structures and occasionally lacrimal gland. The

wall sometimes does not have any adnexal structures, making the lesion a simple conjunctival cyst, analogous to an epidermoid cyst. This type of cyst resembles an acquired conjunctival inclusion cyst and can be differentiated only through a lack of historical or clinical evidence of trauma.

Other Epithelial Cysts

These cysts have a lining that recapitulates the lacrimal duct or apocrine sweat gland epithelium (sudoriferous), or they may show no specific features and be classified as simple. We have encountered two cysts that were lined by pseudostratified ciliated columnar respiratory-type epithelium (endodermal origin) with no connection to the sinuses. A few have been reported, presumably of congenital origin. One enterogenous cyst lined by mucin-secreting epithelial cells resembling gastrointestinal (also endodermal origin) epithelium has been described. Cysts with mixtures of conjunctival and apocrine epithelia, including oncocytic cells, also occur.

Neural

Neural choristomas are composed of glial tissue with occasional neurons or meningeal cells. Encephalocele, meningoencephalocele, and meningocele maintain a connection to the intracranial cavity through a defect in the dura and orbital bone, whereas with ectopic brain no such connection is present. Histopathologically, they consist of disorganized glial and fibrous tissue, often demonstrating occasional neurons and foci of calcification. We have seen a lesion containing cerebellar tissue as well as a cyst with an ependyma-like lining. Microphthalmos with cyst and congenital cystic eye are also in this category as they produce orbital cysts lined by disorganized retinal and glial tissue.

Phakomatous Choristoma

These choristomas occur in the eyelid and anterior orbit and are composed of islands of cataractous lens cortical material surrounded by cuboidal lens epithelium and a PAS-positive capsule. Ellis et al. showed positive immunohistochemical staining with antibodies to alpha, beta, and gamma lens crystallin proteins, and the intermediate filament, vimentin.

Ectopic Lacrimal Gland

The orbital lobe of the lacrimal gland normally extends to the posterior aspect of the globe. More deeply located lobules of ectopic acinar tissue lose their ductal connections, and the buildup of secretions may cause an inflammatory reaction. Rarely, tumors and cysts have arisen in ectopic lacrimal gland.

Teratomas

Teratomas are common in the gonads, mediastinum, and pineal area. More than 50 cases have been reported in the orbit. They may present at any time from the fetal stage to adolescence. Most are benign and localized to the orbit. Some, however, are associated with brain and/or periorbital involvement and may represent extension of a primary teratoma from these sites. Cases with brain and orbital involvement have been diagnosed in utero by ultrasonography. Histologically, the tissues are usually mature and consist of ectoderm represented by keratinizing squamous epithelium and adnexal glandular structures; mesoderm by fibrous tissue, cartilage, fat, muscle, and/or bone; endoderm by gastrointestinal mucosal and glandular tissues, and neuroectoderm by mature brain. When the neural tissue has the appearance of fetal neural tissue, it is said to be immature. This is often seen in primary intracranial teratomas presenting in fetal life with secondary orbital involvement resulting in death.

An allied tumor, usually presenting in the gonads of young children, is the endodermal sinus tumor of which several orbital cases have been reported. This is a tumor derived from embryonic tissue that shows extraembryonic differentiation. Histopathologically, a loose network of stroma is lined by flat to cuboidal epithelium. Papillary structures called Schiller-Duval bodies (vascular cores lined by epithelial cells) are present. Anaplasia, mitoses, hemorrhage, and necrosis are frequent. The cells stain strongly for alpha-fetoprotein. A characteristic feature is numerous PAS-positive, diastase-resistant hyaline globules.

Acquired

Acquired structural lesions are frequently cystic and will therefore come under the differential diagnosis of a cystic mass.

Traumatic

Mucoceles (Figs. 7-25A and B)

Mucoceles usually arise in association with a previous history of chronic sinusitis or fractures involving the sinuses, but occasionally there may be no such history. They are most frequently of frontal or ethmoidal origin but may arise from any sinus. They are thought to occur because of poor

drainage due to an obstructed ostium, which leads to a buildup of secretions. Over time, the mucocele slowly expands, erodes the sinus wall, and extends into the orbit, where it presents as a cystic mass with displacement of the globe. An alternative explanation for those associated with fractures is implantation of sinus mucosa into the orbit at the time of trauma; there it slowly expands as a result of continued secretion. Histologically, these cysts are lined by normal pseudostratified ciliated columnar sinus epithelium with goblet cells. The lining sometimes is atrophic or eroded as a result of pressure. The outer wall of the cyst usually has an extremely dense laminated layer of fibrous connective tissue, often with dystrophic calcification, which is immediately beneath the epithelium, as well as a minimal to marked chronic inflammatory infiltrate of plasma cells and lymphocytes. The contents usually consist of clear to mucoid material containing epithelial debris. They may occasionally be infected, and rarely contain fungal hyphae and numerous eosinophils in allergic persons. Sinus polyposis may cause erosion of the wall with extension of polyps into the orbit. Malignant neoplasms have occasionally been reported in association with mucoceles.

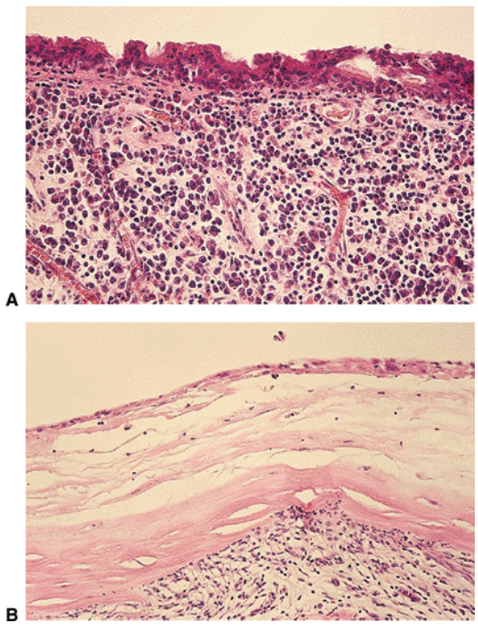

Figure 7-25. Mucocele. (A) Inflamed mucocele with marked chronic inflammation in the wall and slightly degenerated respiratory epithelium (H&E, original magnification × 40). (B) Another area of the same cyst with atrophy of the epithelium and dense laminated connective tissue in the wall (H&E, original magnification × 25). (Reproduced with permission from White VA, Rootman J, Orbital pathology. In: Albert DM, Jakobiec FA, eds. Principles and Practice of Ophthalmology. 2nd ed. Philadelphia: WB Saunders, 2000:3816-74.)

Implantation Cysts

Conjunctival implantation cysts lined by conjunctival epithelium are introduced into the orbit as a result of trauma or surgery, particularly extraocular muscle surgery. They occur in any location and may become large.

Hematic Cysts (see Fig. 7-9)

Blood-filled cysts have been classified into those occurring in the soft tissues of the orbit versus orbital bone. Soft tissue lesions may occur in association with a preexisting lymphangioma or vascular anomaly, or spontaneously with a coagulopathy. One has been described in association with an extramedullary plasmacytoma. Those in bone occur in association with preexisting fibrous dysplasia, aneurysmal bone cyst, or reparative granuloma, or with no evidence of an underlying lesion. The latter lesions have also been referred to as **cholesterol granulomas**. In these heterogeneous cases, the pathology is that of the underlying lesion, with superimposed recent and old hemorrhage consisting of fresh and degenerating red blood cells, cholesterol clefts surrounded by foreign body giant cell reaction, foamy histiocytes, and hemosiderin-laden macrophages.

Nontraumatic

Lacrimal Ductal Cysts (Fig. 7-26)

Lacrimal ductal cysts occur in the superolateral orbit and are easily observed by everting the upper lid, where they are seen in the conjunctival cul-de-sac. They may be bilateral. Histologically, they are lined by two to three layers of epithelium, often containing goblet cells – the inner layer cuboidal to columnar, the outer flattened basal epithelial cells. The wall may contain lacrimal gland acini, inflammation, and fibrosis.

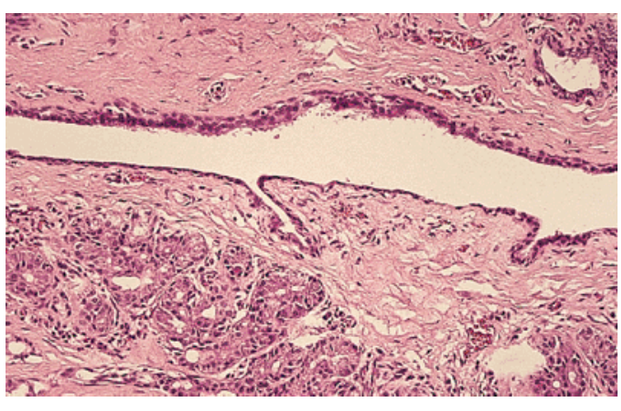

Figure 7-26. Acquired lacrimal ductal cyst lined by two to three layers of cuboidal to columnar epithelium, with lacrimal gland tissue in the wall (H&E, original magnification × 25).

Infectious

We have seen a case of an infectious cyst due to cysticercosis. This was located within the lateral rectus muscle and was surrounded by an intense granulomatous inflammatory reaction containing many eosinophils. Cysticercosis commonly involves the vitreoretinal space and subconjunctival area, but occasional cases have been reported in the orbit and particularly in the extraocular muscles. A more frequent cause of infectious cysts in the orbit is *Echinococcus granulosus*, which is common in the Middle East, East Africa, India, and South America (Fig. 7-27). Other organisms that may cause cysts in the orbit include *Multiceps* species and *Histoplasma duboisii*.

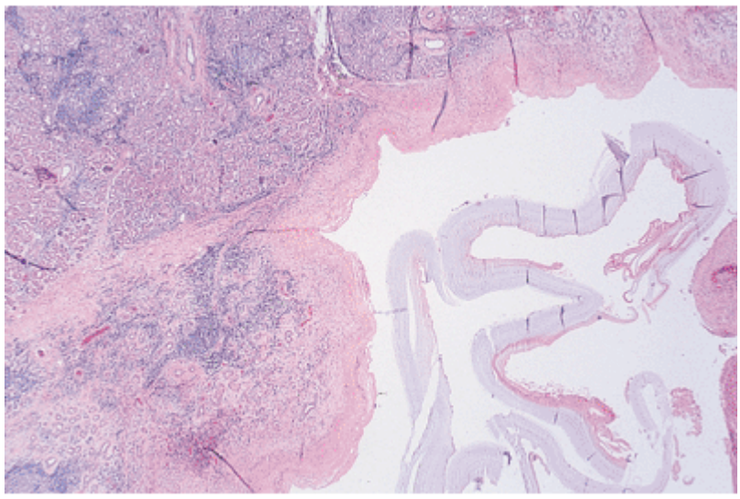

Figure 7-27. Echinococcal cyst. Wall of cyst due to *Echinococcus granulosus* surrounded by heavy granulomatous inflammation containing eosinophils. Note laminated germinal membrane characteristic of this cyst. No organisms remain (H&E, original magnification × 2.5).

Infectious and Inflammatory Disorders

The infectious and inflammatory disorders can be classified in different ways: by time course, site of inflammation, mechanism of production of inflammation, association with systemic disease, or predominant inflammatory cell involved. The latter is the method used by the pathologist when trying to make a diagnosis in a specific case and it is the method of categorization used in this chapter. As with any classification, it must be recognized that the same entity may produce different patterns of inflammation, depending on the time in the course of disease that the biopsy is taken, the immunologic status of the patient, and other unknown factors. This section will only deal with diseases that are biopsied, as many of the acute infectious and acute and subacute nonspecific inflammatory disorders are not usually biopsied unless the course is unusual. In each of these categories, the differential diagnosis may include infectious and noninfectious conditions, so the wise ophthalmologist will consider this and send material for appropriate culture at the time of biopsy.

Acute Inflammation

These disorders are characterized by a predominance of neutrophils or polymorphonuclear leukocytes.

Table 7-19. Pathologic characteristics of acute inflammations of the orbit

TERM AND DEFINITION	PATHOLOGIC APPEARANCE
Acute Infectious	
Acute bacterial infections	Rarely biopsied, as diagnosis usually made clinically Masses of neutrophils, some degranulating, admixed with fewer lymphocytes, macrophages, and plasma cells
Acute Noninfectious	
Vasculitis	These include polyarteritis nodosa, hypersensitivity vasculitis, and rarely Churg-Strauss vasculitis, all characterized by infiltration of vessel walls by neutrophils Fibrinoid necrosis of vessel walls, a deeply eosinophilic discoloration of a vessel wall due to leakage of fibrin into the vessel wall because it has become necrotic, may be present in vasculitis involving larger vessels In hypersensitivity vasculitis involving capillaries and post-capillary venules neutrophils are fragmented, producing neutrophilic dust

Granulomatous Inflammation

This large group of diseases is characterized by granuloma formation, the definition of which is a **collection of epithelioid histiocytes**, often containing giant cells and surrounded by a cuff of lymphocytes and plasma cells. The production of a granuloma is incited by the presence of poorly digestible particles of organisms or foreign bodies, T-cell mediated immunity to the irritant, or both. Because of the requirement for intact cell-mediated immunity, the pattern of response in these diseases may be severely modified in the immunocompromised patient. The importance of recognizing granulomatous inflammation is twofold: first, many chronic infections produce granulomatous inflammation and therefore an infection must always be ruled out by culture and/or special stains, and second, the type of granulomatous pattern in a noninfectious patient may allow recognition of a specific disease entity, which will guide treatment.

Table 7-20. Pathologic characteristics of granulomatous inflammations of the orbit

TERM AND DEFINITION	PATHOLOGIC APPEARANCE
Granulomatous Infections	
Bacterial Granulomatous infection due to *Mycobacterium tuberculosis* or *leprae*	These infections are extremely rare in the orbit The tuberculous granuloma is characterized by *necrotizing granulomatous inflammation*, a caseous necrotic center surrounded by a rim of epithelioid histiocytes and Langhans-type giant cells that are in turn surrounded by lymphocytes and plasma cells The specific diagnosis is made by the finding of a rare acid-fast bacillus on the Zeihl-Neelsen or fluorescent auramine stain
Fungal (Figs. 7-28A to C) Granulomatous infection due usually to *Aspergillus* or *Mucor* species Rare causes include *Pseudoallescheria, Histoplasma, Blastomyces*, and *Sporothrix*	Two histologic patterns In immunologically normal patients there will be necrotizing granulomatous inflammation as described above for mycobacterial infections In immunocompromised patients, there may be minimal to no inflammation and fungal hyphae frequently are angioinvasive, causing necrosis of surrounding tissue Fungal hyphae can often be identified on H&E stains, but will be highlighted on PAS and Grocott stains Hyphae of *Aspergillus* are regularly shaped, septate, and branch at acute angles while those of *Mucor* are irregularly shaped, broader, have a ribbon-like appearance, are nonseptate, and branch at right angles

Figure 7-28. (A) Limited orbital mucormycosis. Biopsy of inflammatory orbital mass shows very occasional nonseptate hyphal fragments surrounded by granulomatous inflammation (H&E, original magnification × 40). (B) Mucormycosis in immunocompromised patient. Invasion of vessels by *Mucor.* Note the broad, ribbonshaped, nonseptate hyphae. The PAS stain highlights the irregularly shaped hyphae but they are equally well seen with the H&E stain (PAS, original magnification × 25). (C) *Pseudoallescheria boydii* (also known as *Scedosporium apiospermum*). Invasion of vessels by *P. boydii* with surrounding necrotic orbital tissue and lack of an inflammatory response. Grocott's stain highlights these organisms, which are morphologically similar to *Aspergillus* and can be distinguished only by culture (Grocott, original magnification × 40). (Fig. 7-28B reproduced with permission from White VA, Rootman J, Orbital pathology. In: Albert DM, Jakobiec FA, eds. Principles and Practice of Ophthalmology. 2nd ed. Philadelphia: WB Saunders, 2000:3816-74.)

Parasitic Granulomatous infection due to a variety of parasitic infestations, most commonly *Echinococcus* species and cysticercosis Rare causes include *Multiceps* species, trichinosis, microfilaria of *Loa loa* and *Oncocerca volvulus*, worms of *Dirofilaria* species, eggs of *Paragonimus* and *Schistosoma hematobium*, *Ascaris* and *Entamoeba* protozoans Rarely ophthalmomyiasis due to infestation by larvae of certain flies causes necrotizing damage to the orbit	Histologically most parasites are surrounded by a granulomatous reaction which has the added feature of numerous eosinophils The particular parasite must be identified morphologically *Echinococcus* produces macroscopically visible cysts which have an outer acellular layer and inner germinal layer from which protrude abortive larvae containing the heads or scolices which are adorned with hooklets; if the lesion is longstanding the cysts may calcify or become necrotic and all that remains may be the hooklets (see Fig. 7-26) Cysticercosis shows the body of a large worm surrounded by a cuticle

Specific Noninfectious Granulomatous Inflammations

Wegener's granulomatosis (Figs. 7-29A and B)
An idiopathic systemic inflammatory vasculitis which may involve kidneys, lungs and upper respiratory tract
Orbital involvement may be the first or only manifestation

Despite the name of this disorder, it is more often characterized by a mixed inflammatory infiltrate which contains moderate numbers of neutrophils, often forming microabscesses or infiltrating small vessel walls producing a vasculitis which is only seen in about half of cases
The inflammatory infiltrate should also contain histiocytes, lymphocytes and plasma cells producing the mixed picture
Eosinophils and giant cells may be present
Granulomas, if present, are vaguely organized and may surround areas of necrosis
Gram, fungal and Zeihl-Neelsen stains should be performed to rule out an infection

Figure 7-29. Wegener's granulomatosis. (A) Vasculitis produced by infiltration of a vessel wall by neutrophils. The surrounding orbital fat shows a heavy mixed acute and chronic inflammatory infiltrate (H&E, original magnification × 40). (B) Poorly formed granuloma surrounding a necrotic area (H&E, original magnification × 25).

Sarcoid and sarcoidal reaction pattern (Fig. 7-30)
A localized or systemic disease characterized by prototypical noninfectious granulomatous inflammation

Nonnecrotizing granulomatous inflammation in which the granulomas are often called “naked” as they are not surrounded by a cuff of lymphocytes; giant cells may be few
When giant cells are present they may contain asteroid bodies, Schaumann bodies and/or crystalline inclusions of calcium oxalate
Lesion may become fibrotic
Called sarcoidosis when systemic disease present and sarcoidal reaction pattern when it is not
May be present in either orbital soft tissue, lacrimal gland or optic nerve

Figure 7-30. Sarcoidal reaction pattern. Biopsy demonstrates well-formed noncaseating granulomas set in a fibrous background (H&E, original magnification × 25).

Figure 7-31. Foreign body granulomatous reaction to a fragment of wood that had become embedded in the orbit after trauma (H&E, original magnification × 25). (Reproduced with permission from White VA, Rootman J, Orbital pathology. In: Albert DM, Jakobiec FA, eds. Principles and Practice of Ophthalmology. 2nd ed. Philadelphia: WB Saunders, 2000:3816-74.)

Foreign body granulomas (Fig. 7-31)
A foreign body giant cell granulomatous response to intrinsic or extrinsic foreign material

Foreign body granulomas differ from the above granulomatous inflammations in that there are usually more giant cells, containing up to 50 nuclei, which are large, irregular, and mold themselves to the shape of the foreign material
Oily materials, such as lipid released from a ruptured dermoid cyst, silicone, and bone wax, produce large irregularly shaped empty spaces (due to lipid dissolved during processing) surrounded by histiocytes and giant cells
Other foreign materials, such as wood and sutures, are intimately surrounded by giant cells

Pseudorheumatoid nodule
Lesion seen in anterior orbit similar to those seen on extremities in patients with rheumatoid diseases

Palisaded granulomatous inflammation around a hyaline, necrobiotic area of collagen that may stain positively for acid mucopolysaccharides or fibrin

Xanthogranulomatous & Histiocytic Inflammations of the Orbit

These lesions are grouped separately from the earlier granulomatous inflammations as they are not characterized by well-formed granulomas, but rather irregular sheets of histiocytes, which do not have an epithelioid appearance. There are no infectious lesions in this group.

Table 7-21. Pathologic characteristics of xanthogranulomatous and histiocytic inflammations of the orbit

TERM AND DEFINITION	PATHOLOGIC APPEARANCE
Xanthogranulomatous inflammations (Non-Langerhans cell histiocytosis) (Figs. 7-32A and B) These are a group of lesions characterized by foamy histiocytes and Touton giant cells The importance of this group is that they may be associated with a systemic disorder such as - adult-onset asthma - necrobiotic xanthogranuloma with paraproteinemia, lymphocyte, or plasma cell disorders - Erdheim-Chester disease with bone, heart, or lung involvement	This group of lesions is characterized by sheets and widespread infiltration of anterior orbital structures, particularly the orbicularis muscle, by foamy histiocytes and Touton giant cells with associated clusters of lymphocytes, often forming follicles with germinal centers, and plasma cells Histologically, it is important to separate this lesion from xanthelasma, which involves the dermis only Scattered, small and poorly defined areas of necrosis may be present in necrobiotic xanthogranuloma with paraproteinemia These lesions are often difficult to separate from each other histologically and patients should have a thorough history, physical exam, and investigation for evidence of occult systemic disease
Langerhans cell histiocytosis (Histiocytosis X) A group of disorders characterized by histiocytes that span the continuum from inflammatory to malignant in their behavior May involve a single site in the orbital bone or eyelid skin, multiple bony sites, or multiple organs	These lesions are composed mainly of Langerhan's cell histiocytes that have bean-shaped nuclei and abundant, slightly eosinophilic cytoplasm These cells stain positively for S100 protein and show Birbeck granules by electron microscopy Eosinophils, lymphocytes, and/or plasma cells may be admixed
Sinus histiocytosis with massive lymphadenopathy Usually involves the cervical lymph nodes of young adults and rarely the orbit	Characterized by masses of large histiocytes with small nuclei surrounded by lymphocytes and plasma cells Divided into lobules by fibrous tissue

Figure 7-32. Necrobiotic xanthogranuloma with paraproteinemia. (A) Facial photograph of a 72yearold woman who presented with progressive ocular irritation and limitation of movement, which was associated with a waxy, yellowish deposition in both upper and lower lids. (B) Biopsy specimen of the anterior orbital mass shows tracts of collagen with focal necrosis, Touton giant cells, and foci of chronic inflammation containing lymphocytes and plasma cells (H&E, original magnification × 25). (Fig. 7-32A reproduced with permission from White VA, Rootman J, Orbital pathology. In: Albert DM, Jakobiec FA, eds. Principles and Practice of Ophthalmology. 2nd ed. Philadelphia: WB Saunders, 2000:3816-74.)

Lymphocytic Inflammations of the Orbit

Lymphocytic inflammations of the orbit are characterized by polymorphous and polyclonal infiltration of the orbital tissues, often with follicle formation and sometimes with destruction of orbital structures.

Table 7-22. Pathologic characteristics of lymphocytic inflammations of the orbit

TERM AND DEFINITION	PATHOLOGIC APPEARANCE
Klmura's disease (Fig. 7-33) Idiopathic inflammatory disorder, involving the cervical lymph nodes, lacrimal gland, and orbit Seen more commonly in Asians May be associated with peripheral eosinophilia	Lymph nodes show reactive lymphoid hyperplasia with the presence of numerous eosinophils Blood vessels are numerous and may show atypical endothelial cells In the orbit and lacrimal gland there is a polymorphous chronic inflammatory infiltrate containing numerous eosinophils
Sjögren's syndrome (Fig. 7-34) Characteristic inflammation of lacrimal and salivary glands often associated with a variety of autoimmune diseases High incidence of lymphoma involving either lymph nodes or glands	Gland shows atrophy of the acini and replacement by a dense infiltrate of lymphocytes with prominent, often large and irregularly shaped germinal centers Later stages may be atrophic and fibrotic Distinction from a mucosal associated lymphoid tissue (MALT) lymphoma may be difficult In the latter, there are well defined epithelial-myoepithelial islands, which are proliferations of residual ducts with infiltration by lymphocytes, and presence of monocytoid lymphocytes Demonstration of a monoclonal population required to diagnose lymphoma

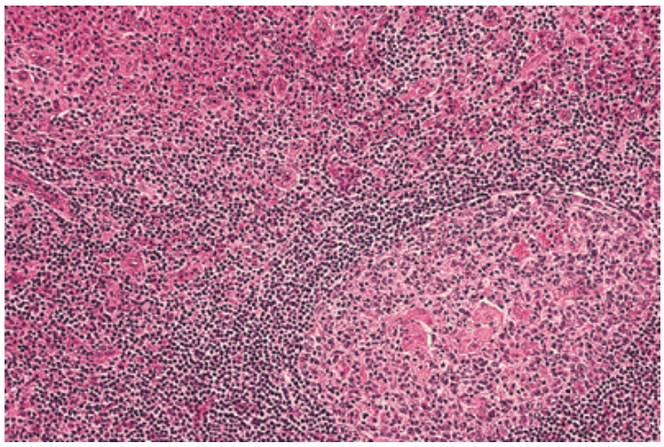

Figure 7-33. Kimura's disease. A reactive germinal center (on the lower right) is surrounded by eosinophils, and a portion of an eosinophilic abscess is seen at upper left (H&E, original magnification × 25). (Reproduced with permission from White VA, Rootman J, Orbital pathology. In: Albert DM, Jakobiec FA, eds. Principles and Practice of Ophthalmology. 2nd ed. Philadelphia: WB Saunders, 2000:3816-74.)

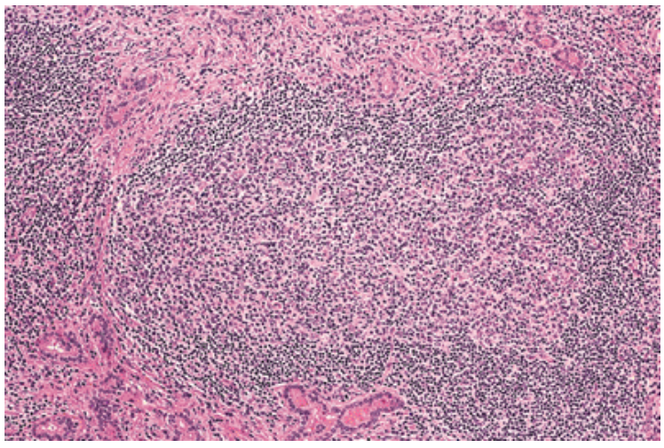

Figure 7-34. Sjögren's syndrome. Large, irregular germinal center in a background of chronic inflammation with loss of the lacrimal acini in a patient with keratoconjunctivitis sicca (H&E, original magnification × 10). (Reproduced with permission from White VA, Rootman J, Orbital pathology. In: Albert DM, Jakobiec FA, eds. Principles and Practice of Ophthalmology. 2nd ed. Philadelphia: WB Saunders, 2000:3816-74.)

Inflammation of the Orbit characterized by Fibrosis

Idiopathic sclerosing inflammation of the orbit is the main entity in this group. It is a diagnosis of exclusion, as other conditions may have a significant fibrotic component. Wegener's granulomatosis may have a fibrotic stage with a less dense inflammatory infiltrate or have large sheets of necrotic tissue mimicking fibrous tissue with a sparse inflammatory infiltrate around the edges of the necrotic tissue. Sarcoidosis and Sjögren's syndrome may have significant fibrosis. Neoplastic lesions, such as sclerosing metastases, particularly from breast carcinoma, and sclerosing lymphoma may also occur. The only way to accurately differentiate these lesions is to always consider them in the differential diagnosis when faced with a lesion of this type, to obtain a full history from the patient, and perform other investigations, such as immunohistochemistry or molecular studies, as required.

Table 7-23. Pathologic features of inflammatory lesions of the orbit characterized by fibrosis

TERM AND DEFINITION	PATHOLOGIC APPEARANCE
Idiopathic sclerosing inflammation of the orbit (Fig. 7-35)	Dense fibrous tissue infiltrates the orbital structures, particularly the fat Inflammation is relatively sparse compared to the above lymphocytic category, and consists of lymphocytes, plasma cells, histiocytes, and occasional lymphoid follicles with germinal centers.
Chronic dacryocystitis (Fig. 7-36) Idiopathic inflammation of the lacrimal gland	Atrophy of the acini with preservation of ducts that are surrounded by fibrosis Sparse chronic inflammatory cell infiltrate May be difficult to differentiate histologically from chronic Sjögren's syndrome, so clinical information and serologic testing may be required

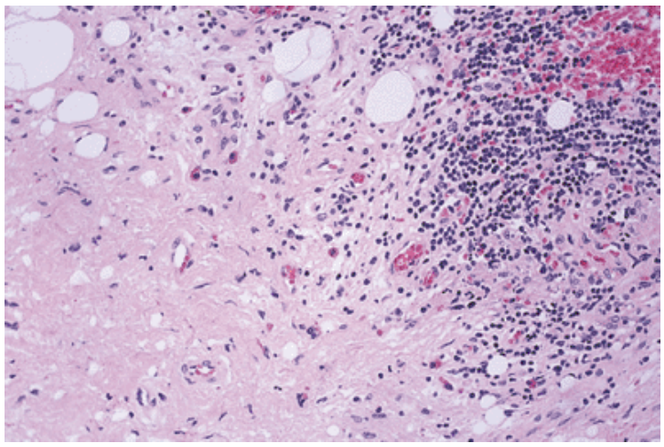

Figure 7-35. Sclerosing inflammation of the orbit shows extensive fibrosis of the fat, a sparse chronic inflammatory infiltrate of lymphocytes and plasma cells, and occasional histiocytes and germinal centers. No neutrophils are present (H&E, original magnification × 25).

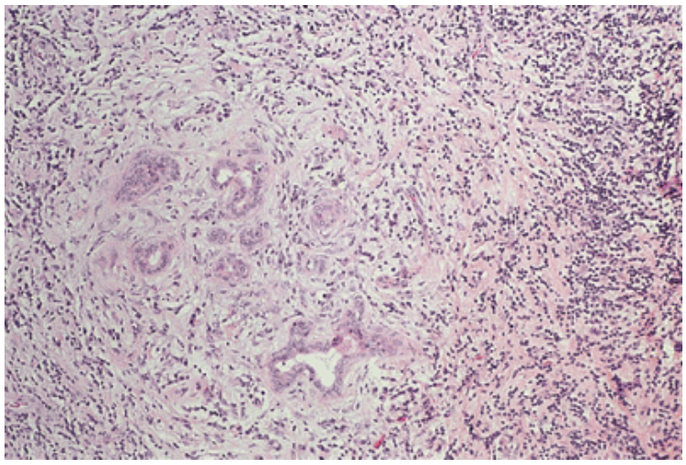

Figure 7-36. Chronic dacryocystitis. Nonspecific inflammation of the lacrimal gland with loss of acini, preservation of ductules, chronic inflammation, and fibrosis (H&E, original magnification × 10). (Reproduced with permission from White VA, Rootman J, Orbital pathology. In: Albert DM, Jakobiec FA, eds. Principles and Practice of Ophthalmology. 2nd ed. Philadelphia: WB Saunders, 2000:3816-74.)

Thyroid Orbitopathy

The histopathologic findings in thyroid orbitopathy are nonspecific by themselves and therefore must be interpreted in the light of clinical, radiological, and thyroid hormone findings. The structures primarily affected are the extraocular muscles, most commonly the medial and inferior recti, which show a sparse to moderate inflammatory infiltrate of lymphoid follicles, macrophages, and occasional plasma cells and mast cells (Fig. 7-37). In the early stages, this is associated with an often dramatic interstitial deposition of acid mucopolysaccharide, as shown by staining with alcian blue at pH 2.5. If biopsy is performed when the disease has been present for a longer time, fibrosis, destruction of muscle fibers, and infiltration by mature fat cells are seen. Inflammation and fibrosis may affect the orbital fat surrounding the muscle, but involvement of the fat primarily is not common.

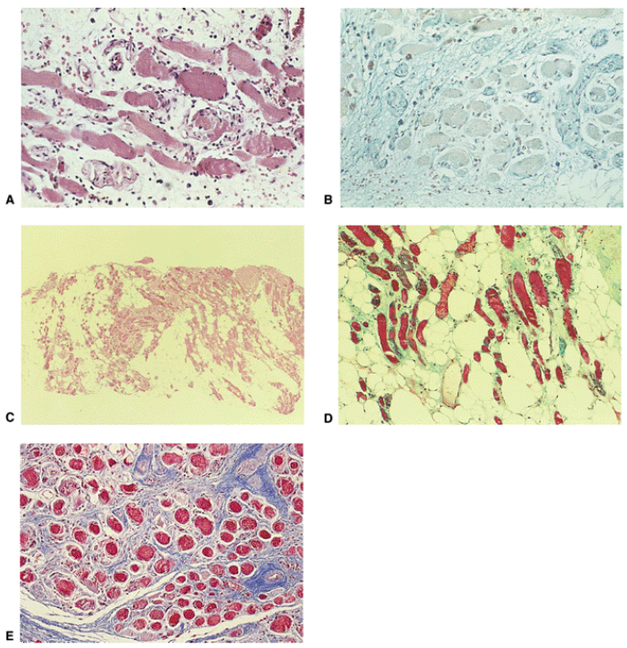

Figure 7-37. Thyroid orbitopathy. (A) This specimen demonstrates a paucicellular inflammatory infiltrate with separation of the extraocular muscle bundles by stromal deposition of glycosaminoglycans (H&E, original magnification × 25). (B) Alcian blue stain demonstrates pools of positive-staining mucopolysaccharides (Alcian blue, original magnification × 25). (C) This low-power view of an extraocular muscle biopsy of a patient with chronic thyroid orbitopathy shows fat replacement (H&E, original magnification × 2.5). (D) Masson's trichrome stain of the specimen in (C) shows a higher power view of the fat replacement (Masson's trichrome, original magnification × 25). (E) Trichrome staining highlights the deposition of fibrous tissue between the muscle fibers (Masson's trichrome, original magnification × 25). (Fig. 7-37E reproduced with permission from White VA, Rootman J, Orbital pathology. In: Albert DM, Jakobiec FA, eds. Principles and Practice of Ophthalmology. 2nd ed. Philadelphia: WB Saunders, 2000:3816-74.)

Amyloid Deposition

Amyloid deposition may be related to systemic or localized disease. When systemic, it may be associated with a plasma cell dyscrasia, a chronic inflammatory condition, or a familial neuropathy. Localized disease may be due to a local lymphoid proliferation, a chronic inflammatory condition, or an organ-limited disease. When amyloid is associated with a plasma cell or lymphoproliferative disease, it has been found to be composed of immunoglobulin light chains. The other groups of amyloid are composed of heterogeneous substances. On H&E staining, amyloid appears as eosinophilic hyaline material, often in round deposits or situated around blood vessels (Figs. 7-38A and B). No matter what the composition of the amyloid, it is orange on Congo red stain and demonstrates red-green dichroism under polarized light. Amyloid may affect many ocular structures and in occasional cases has been found to involve primarily the orbit, including the extraocular muscles and lacrimal gland, usually without systemic disease. We recently reported two cases of localized orbital amyloidosis that showed rearrangement of the immunoglobulin heavy chain gene by molecular analysis indicating the presence of a monoclonal population of plasma cells, which presumably produced the amyloid. One patient had bilateral enlargement of multiple extraocular muscles, but neither patient had evidence of systemic disease. We believe that molecular studies for immunoglobulin heavy chain gene rearrangement should be carried out even if the lesion is polyclonal by immunohistochemistry, as this may dictate appropriate treatment.

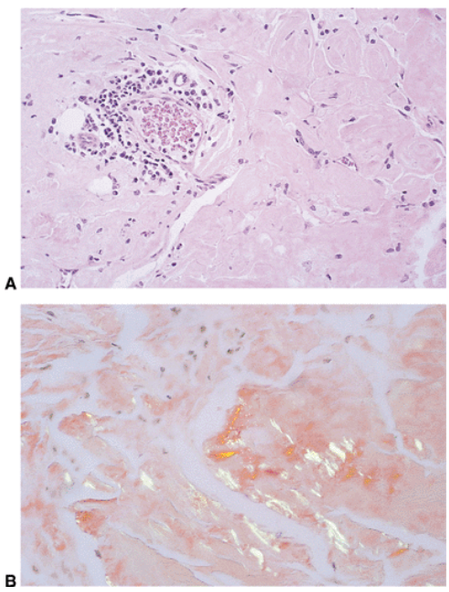

Figure 7-38. Amyloid deposition. (A) Biopsy of anterior orbit shows extensive deposition of amyloid with collections of plasma cells around vessels (H&E, original magnification × 25). (B) Examination of the Congo red stain with polarized light shows applegreen birefringence and redgreen dichroism (Congo red, original magnification × 40).

Bibliography

General

Garner A, White VA, Albert DM. General pathology. In: Albert DM, Jakobiec FA, eds. Principles and Practice of Ophthalmology, vol. 4, 2nd ed. Philadelphia: WB Saunders, 2000: 3575-609.

Glasgow BJ, Foos RY. Ocular Cytopathology. Boston, Butterworth-Heinemann, 1993.

Glasgow BJ, Layfield LJ. Fine-needle aspiration biopsy of orbital and periorbital masses. Diagn Cytopathol 1991;7:132-41.

Prophet EB, Mills B, Arrinton JB, Sobin LH, eds. Laboratory Methods in Histopathology. Washington, DC: American Registry of Pathology, 1992.

White VA, Rootman J. Orbital pathology. In: Albert DM, Jakobiec FA, eds. Principles and Practice of Ophthalmology, vol. 4, 2nd ed. Philadelphia: WB Saunders, 2000: 3816-74.

Zajdela A, Vielh P, Schlienger P, Haye C. Fine-needle cytology of 292 palpable orbital and eyelid tumors. Am J Clin Pathol 1990;93:100-4.

Neoplasia

General

Cotran RS, Kumar V, Collins T. Robbins: Pathologic Basis of Disease, 6th ed. Philadelphia: WB Saunders, 1999.

Immunohistochemistry

Enzinger FM, Weiss SW. Immunohistochemistry of soft tissue lesions. In: Enzinger FM, Weiss SW, eds. Soft Tissue Tumors, 3rd ed. St. Louis: Mosby, 1995:139-63.

Immunohistochemistry in tumor diagnosis. Seminars in Diagnostic Pathology 2000;17:169.

Rosai J. Special techniques in surgical pathology. In: Rosai J, ed. Ackerman's Surgical Pathology, 8th ed. St. Louis: Mosby, 1996:29-62.

Soft Tissue

Dickersin GR. Diagnostic Electron Microscopy: A Text/Atlas. New York: Igaku-Shoin Medical Publishers, 1988.

Enzinger FM, Weiss SW. Soft Tissue Tumors, 3rd ed. St. Louis: Mosby, 1995.

Slominski A, Wortsman J, Carlson A, et al. Molecular pathology of soft tissue and bone tumors: a review. Arch Pathol Lab Med 1999;123:1246-59.

Van Roggen JFG, Bovee JVMG, Morreau J, Hogendoorn PCW. Diagnostic and prognostic implications of the unfolding molecular biology of bone and soft tissue tumours. J Clin Pathol 1999;52:481-9.

Fibrous and Fibrohistiocytic

Allen PW. The fibromatoses: a clinicopathologic classification based on 140 cases. Am J Surg Pathol 1977;1:255-69, 305-21.

Caballero LR, Rodriguez AC, Sopelana AB. Angiomatoid malignant fibrous histiocytoma of the orbit. Am J Ophthalmol 1981;92:13-5.

Cole CH, Magee JF, Gianoulis M, Rogers PCJ. Malignant fibrous histiocytoma in childhood. Cancer 1993;71:4077-83.

Dei Tos AP, Seregard S, Calonje E, et al. Giant cell angiofibroma: a distinctive orbital tumor in adults. Am J Surg Pathol 1995;19:1286-93.

Dorfman DM, To K, Dickersin GR, et al. Solitary fibrous tumor of the orbit. Am J Surg Pathol 1994;18:281-7.

Fisher C. Fibromatosis and fibrosarcoma in infancy and childhood. Eur J Cancer 1996;32A:2094-100.

Fletcher CDM. Benign fibrous histiocytoma of subcutaneous and deep soft tissue: a clinicopathologic analysis of 21 cases. Am J Surg Pathol 1990;14:801-9.

Font RL, Hidayat AA. Fibrous histiocytoma of the orbit: a clincopathologic study of 150 cases. Hum Pathol 1982;13:199-209.

Font RL, Zimmerman LE. Nodular fasciitis of the eye and adnexa: a report of ten cases. Arch Ophthalmol 1966;75:475-81.

Hasegawa T, Hirose T, Seki K, et al. Solitary fibrous tumor of the soft tissue. Am J Clin Pathol 1996;106:325-31.

Hayashi N, Borodic G, Karesh JW, et al. Giant cell angiofibroma of the orbit and eyelid. Ophthalmology 1999;106:1223-9.

Herschorn BJ, Jakobiec FA, Hornblass A, et al. Epibulbar subconjunctival fibroma. Ophthalmology 1983;90:1490-4.

Hidayat AA, Font RL. Juvenile fibromatosis of the periorbital region and eyelid. Arch Ophthalmol 1980;98:280-5.

Hoffman MA, Dickerson GR. Malignant fibrous histiocytoma: an ultrastructural study of eleven cases. Hum Pathol 1983;14:913-22.

Jakobiec FA, Klapper D, Maher E, Krebs W. Infantile subconjunctival and anterior orbital fibrous histiocytoma: ultrastructural and immunohistochemical studies. Ophthalmology 1988;95:516-25.

Jakobiec FA, Tannenbaum M. The ultrastructure of orbital fibrosarcoma. Am J Ophthalmol 1974;77:899-917.

Kaw YT, Cuesta RA. Nodular fasciitis of the orbit diagnosed by fine needle aspiration cytology. Acta Cytol 1993;37: 957-60.

Lieb WE, Goebel HH, Wallenfang T. Myxoma of the orbit: a clinicopathologic report. Graefes Arch Clin Exp Ophthalmol 1990;228:28-32.

Maiuri F, Corriero G, Galicchio B, et al. Myxoma of the skull and orbit. Neurochirurgia 1988;31:136-8.

Montessori GA, North DP. Radiation induced orbital sarcoma in an elderly patient. Can J Ophthalmol 1972;7:381-5.

Scott IU, Tanenbaum M, Rubin D, Lores E. Solitary fibrous tumor of the lacrimal gland fossa. Ophthalmology 1993;103:1613-8.

Smoot CN, Krohel GB, Smith RS. Adult periorbital fibromatosis. Br J Ophthalmol 1989;73:373-5.

Variend S, Bax NMA, Van Gorp J. Are infantile myofibromatosis, congenital fibrosarcoma and congenital haemangiopericytoma histogenetically related? Histopathology 1995;26:57-62.

Waeltermann JM, Huntrakoon M, Beatty EC, Cibis GW. Congenital fibromatosis (myofibromatosis) of the orbit: a rare cause of proptosis at birth. Ann Ophthalmol 1988;20:394-9.

Weiner JM, Hidayat AA. Juvenile fibrosarcoma of the orbit and eyelid: a study of five cases. Arch Ophthalmol 1983;101:253-9.

Westra WH, Gerald WL, Rosai J. Solitary fibrous tumor: consistent CD34 immunoreactivity and occurrence in the orbit. Am J Surg Pathol 1994;18:992-8.

Muscle

Coffin CM. The new International Rhabdomyosarcoma Classification, its progenitors, and considerations beyond morphology. Adv Anat Pathol 1997;4:1-16.

Conlon MR, Rubin PAD, Samy CN, Albert DM. Metastatic orbital leimyosarcoma: a clinicopathological study. Can J Ophthalmol 1994;29:85-9.

Folberg R, Cleasby G, Flanagan JA, et al. Orbital leiomyosarcoma after radiation therapy for bilateral retinoblastoma. Arch Ophthalmol 1983;101:1562-5.

Font RL, Jurco S 3rd, Brechner RJ. Postradiation leiomyosarcoma of the orbit complicating bilateral retinoblastoma. Arch Ophthalmol 1983;101:1557-61.

Hollowood K, Fletcher CDM. Rhabdomyosarcoma in adults. Sem Diagn Pathol 1994;11:47-57.

Jakobiec FA, Mitchell JP, Chauhan PM, Iwamoto T. Mesectodermal leiomyosarcoma of the antrum and orbit. Am J Ophthalmol 1978;85:51-7.

Jakobiec FA, Howard GM, Rosen M, Wolff M. Leiomyoma and leiomyosarcoma of the orbit. Am J Ophthalmol 1975;80:1028-42.

Jolly SS, Brownstein S, Jordan DR. Leiomyoma of the anterior orbit and eyelid. Can J Ophthalmol 1995;30:366-70.

Kodet R, Newton WA Jr, Hamoudi AB, et al. Orbital rhabdomyosarcomas and related tumors in childhood: relationship of morphology to prognosis–an Intergroup Rhabdomyosarcoma Study. Med Pediatr Oncol 1997;29:51-60.

Lyon DB, Dortzbach RK, Gilbert-Barness E. Polyphenotypic small-cell orbitocranial tumor. Arch Ophthalmol 1993;111:1402-8.

Mamalis N, Grey AM, Good JS, et al. Embryonal rhabdomyosarcoma of the orbit in a 35-year-old man. Ophthalmic Surg 1994;25:332-5.

Matsko TH, Schmidt RA, Milam AH, Orcutt JC. Primary malignant ectomesenchymoma of the orbit. Br J Ophthalmol 1992;76:438-41.

Meekins BB, Dutton JJ, Proia AD. Primary orbital leiomyosarcoma: a case report and review of the literature. Arch Ophthalmol 1988;106:82-6.

Meis-Kindblom JM, Stenman G, Kindblom L-G. Differential diagnosis of small round cell tumors. Sem Diagn Pathol 1996;13:213-41.

Parham DM. The molecular biology of childhood rhabdomyosarcoma. Sem Diagn Pathol 1994;11:39-46.

Nakhleh RE, Swanson PE, Dehner LP. Juvenile (embryonal and alveolar) rhabdomyosarcoma of the head and neck in adults: a clinical, pathologic, and immunohistochemical study of 12 cases. Cancer 1991;67:1019-24.

Newton WA Jr, Gehan EA, Webber BL, et al. Classifications of rhabdomyosarcomas and related sarcomas: pathologic aspects and proposal for a new classification–an Intergroup Rhabdomyosarcoma Study. Cancer 1995;76:1073-85.

Newton WA Jr, Soule EH, Hamoudi AB, et al. Histopathology of childhood sarcomas, intergroup rhabdomyosarcoma studies I and II: clinicopathologic correlation. J Clin Oncol 1988;6:67-75.

O'Day MP, Nielsen P, Al-Bozom I, Wilkins IA. Orbital rhabdomyosarcoma metastatic to the placenta. Am J Obstet Gynecol 1994;171:1382-3.

Walton RC, Ellis GS Jr, Haik BG. Rhabdomyosarcoma presumed metastatic to the orbit. Ophthalmology 1996;103:1512-16.

Wiechens B, Werner JA, Luttges J, et al. Primary orbital leiomyoma and leiomyosarcoma. Ophthalmologica 1999;213:159-64.

Neurogenic and Neural Crest

Allaire GS, Laflamme P, Bourgouin P. Granular cell tumour of the orbit. Can J Ophthalmol 1995;30:151-3.

Archer KF, Hurwitz JJ, Balogh JM, Fernandes BJ. Orbital nonchromaffin paraganglioma: a case report and review of the literature. Ophthalmology 1989;96:1659-66.

Bednar MM, Trainer TD, Aitken PA, et al. Orbital paraganglioma: case report and review of the literature. Br J Ophthalmol 1992;76:1983-5.

Dolman PJ, Rootman J, Dolman CL. Infiltrating orbital granular cell tumour: a case report and literature review. Br J Ophthalmol 1987;71:47-53.

Farris SR, Grove AS Jr. Orbital and eyelid manifestations of neurofibromatosis: a clinical study and literature review. Ophthal Plast Reconstr Surg 1996;12:245-59.

Jaeger MJ, Green WR, Miller NR, Harris GJ. Granular cell tumor of the orbit and ocular adnexae. Surv Ophthalmol 1987;31:417-23.

Jakobiec FA, Font FL, Zimmerman LE. Malignant peripheral nerve sheath tumors of the orbit: a clinicopathologic study of eight cases. Trans Am Ophthalmol Soc 1985;83:332-66.

Jakobiec FA, Klepach GL, Crissman JD, Spoor TC. Primary differentiated neuroblastoma of the orbit. Ophthalmology 1987;94:255-66.

Johnson TE, Weatherhead RG, Nasr AM, Siqueira EB. Ectopic (extradural) meningioma of the orbit: a report of two cases. J Pediatr Ophthalmol Strabismus 1993;30:43-7.

Kapadia SB, Frisman DM, Hitchcock CL, et al. Melanotic neuroectodermal tumor of infancy. Am J Surg Pathol 1993;17:566-73.

Kiratli H, Bilgic S, Gedikoglu G, et al. Primitive neuroectodermal tumor of the orbit in an adult. A case report and literature review. Ophthalmology 1999;106:98-102.

Kliewer KE, Wen D-R, Cancilla PA, Cochrane AJ. Paragangliomas: assessment of prognosis by histologic, immunohistochemical and ultrastructural techniques. Hum Pathol 1989;20:29-39.

Lam DSC, Ng JS, To KF, et al. Cystic schwannoma of the orbit. Eye 1997;11:798-800.

Lamping KA, Albert DM, Lack E, et al. Melanotic neuroectodermal tumor of infancy (retinal anlage tumor). Ophthalmology 1985;92:143-9.

Lyons CJ, McNab AA, Garner A, Wright JE. Orbital malignant peripheral nerve sheath tumours. Br J Ophthalmol 1989;73:731-8.

McDonald P, Jakobiec FA, Hornblass A, Iwamoto T. Benign peripheral nerve sheath tumors (neurofibromas) of the lacrimal gland. Ophthalmology 1983;90:1403-13.

Messmer EP, Camara J, Boniuk M, Font RL. Amputation neuroma of the orbit: report of two cases and review of the literature. Ophthalmology 1984;91:1420-3.

Paulus W, Jellinger K, Brenner H. Melanotic paraganglioma of the orbit: a case report. Acta Neuropathol 1989;79:340-6.

Pettinato G, Manivel C, d'Amore ESG, et al. Melanotic neuroectodermal tumor of infancy. Am J Surg Pathol 1991;15:233-45.

Rakes SM, Yeatts RP, Campbell RJ. Ophthalmic manifestations of esthesioneuroblastoma. Ophthalmology 1985;92:1749-53.

Rootman J, Goldberg C, Robertson W: Primary orbital schwannomas. Br J Ophthalmol 1982;66:194-204.

Shields JA, Shields CL, Leib WE, Eagle RC. Multiple orbital neurofibromas unassociated with von Recklinghausen's disease. Arch Ophthalmol 1990;108:80-3.

Singh AD, Husson M, Shields CL, et al. Primary neuroectodermal tumor of the orbit. Arch Ophthalmol 1994;112:217-21.

Woog JJ, Albert DM, Solt LC, et al. Neurofibromatosis of the eyelid and orbit. Int Ophthalmol Clin 1982;22:157-87.

Vascular

Burnstine MA, Frueh BR, Elner VM. Angiosarcoma metastatic to the orbit. Arch Ophthalmol 1996;114:93-6.

Croxatto JO, Font RL. Hemangiopericytoma of the orbit: a clinicopathologic study of 30 cases. Hum Pathol 1982;13:210-8.

Font RL, Wheeler TM, Boniuk M. Intravascular papillary endothelial hyperplasia of the orbit and ocular adnexa. A report of 5 cases. Arch Ophthalmol 1983;101:1731-6.

Henderson JW, Farrow GM. Primary orbital hemangiopericytoma. Arch Ophthalmol 1978;96:666-73.

Hufnagel T, Ma L, Kuo T-T. Orbital angiosarcoma with subconjunctival presentation. Ophthalmology 1987;94:72-7.

Messmer EP, Font RL, McCrary JA 3rd, Murphy D. Epithelioid angiosarcoma of the orbit presenting as Tolosa-Hunt syndrome. Ophthalmology 1983;90:1414-21.

Nappi O, Ritter JH, Pettinato G, Wick MR. Hemangiopericytoma: histopathological pattern or clincopathologic entity. Sem Diagn Pathol 1995;12:221-32.

Neufeld M, Pe'er J, Rosenman E, Lazar M. Intraorbital glomus cell tumor. Am J Ophthalmol 1994;117:539-41.

Nunnery EW, Kahn LB, Reddick RL, Lipper S. Hemangiopericytoma: a light microscopic and ultrastructural study. Cancer 1981;47:906-14.

Sorenson RL, Spencer WH, Stewart WB, et al. Intravascular papillary endothelial hyperplasia of the eyelid. Arch Ophthalmol 1983;101:1728-30.

Weber FL, Babel J. Intravascular papillary endothelial hyperplasia of the orbit. Br J Ophthalmol 1981;65:18-22.

Adipose Tissue

Abdalla MI, Ghaly AF, Hosni F. Liposarcoma with orbital metastases: case report. Br J Ophthalmol 1966;50:426-8.

Bartley GB, Yeatts RP, Garrity JA, et al. Spindle cell lipoma of the orbit. Am J Ophthalmol 1985;100:605-9.

Chang HR, Hajdu SI, Collin C, Brennan MF. The prognostic value of histologic subtypes in primary extremity liposarcoma. Cancer 1989;64:1514-20.

Cockerham KP, Kennerdell JS, Celin SE, Fechter HP. Liposarcoma of the orbit: a management challenge. Opthalmic Plast Reconstr Surg 1998;14:370-4.

Favrot SR, Ridley MB, Older JJ, Szakacs JE. Orbital liposarcoma. Otolaryngol Head Neck Surg 1994;111:111-5.

Feinfeld RE, Hesse RJ, Scharfenberg JC. Orbital angiolipoma. Arch Ophthalmol 1988;106:1093-5.

Jakobiec FA, Rini F, Char D, et al. Primary liposarcoma of the orbit: problems in the diagnosis and management of five cases. Ophthalmology 1989;96:180-91.

Johnson BL, Linn JG Jr. Spindle cell lipoma of the orbit. Arch Ophthalmol 1979;97:133-4.

Koganei Y, Ishikawa S, Abe K, et al. Orbital lipoma. Ann Plast Surg 1988;20:173-82.

Lane CM, Wright JE, Garner A. Primary myxoid liposarcoma of the orbit. Br J Ophthalmol 1988;72:912-7.

Miller MH, Yokoyama C, Wright JE, Garner A. An aggressive lipoblastic tumour in the orbit of a child. Histopathology 1990;17:141-5.

Uncertain Histogenesis

Bunt AH, Bensinger RE. Alveolar soft-part sarcoma of the orbit. Ophthalmology 1981;88:1339-46.

Chase DR, Enzinger FM. Epithelioid sarcoma: diagnosis, prognostic indicators, and treatment. Am J Surg Pathol 1985;9:241-63.

Font RL, Jurco S, 3rd, Zimmerman LE. Alveolar soft-part sarcoma of the orbit. Hum Pathol 1982;13:569-79.

Foschini MP, Eusebi V. Alveolar soft-part sarcoma: a new type of rhabdomyosarcoma? Sem Diagn Pathol 1994;11:58-68.

Lieberman PH, Brennan MF, Kimmel M, et al. Alveolar soft-part sarcoma: a clinicopathologic study of half a century. Cancer 1989;63:1-13.

Niffenegger JH, Jakobiec FA, Shore JW, Albert DM. Adult extrarenal rhabdoid tumor of the lacrimal gland. Ophthalmology 1992;99:567-74.

Parham DM, Weeks DA, Beckwith JB. The clinicopathologic spectrum of putative extrarenal rhabdoid tumors. Am J Surg Pathol 1994;18:1010-29.

Rootman J, Damji KF, Dimmick JE. Malignant rhabdoid tumor of the orbit. Ophthalmology 1989;96:1650-4.

Walford N, Deferrai R, Delemarre JFM, et al. Intraorbital rhabdoid tumour following bilateral retinoblastoma. Histopathology 1992;20:170-3.

Wang NP, Bacchi CE, Jiang JJ, et al. Does alveolar soft-part sarcoma exhibit skeletal muscle differentiation? An immunocytochemical and biochemical study of myogenic regulatory protein expression. Mod Pathol 1996;9:496-506.

White VA, Heathcote JG, Hurtwitz JJ, et al. Epithelioid sarcoma of the orbit. Ophthalmology 1994;101:1680-7.

Wick MR, Ritter JH, Dehner LP. Malignant rhabdoid tumors: a clinicopathologic review and conceptual discussion. Sem Diagn Pathol 1995;12:233-48.

Bone

Abramson DH, Ellsworth RM, Kitchin FD, Tung G. Second nonocular tumors in retinoblastoma survivors: are they radiation-induced? Ophthalmology 1984;91:1351-5.

Abramson DH, Ronner HJ, Ellsworth RM. Second tumors in nonirradiated bilateral retinoblastoma. Am J Ophthalmol 1979;87:624-7.

Blodi FC. Pathology of orbital bones. The XXXII Edward Jackson memorial lecture. Am J Ophthalmol 1976;81:1-26.

Dhir SP, Munjal VP, Jain IS, et al. Osteosarcoma of the orbit. J Pediatr Ophthalmol Strabismus 1980;17:312-4.

Dorfman HD, Czerniak B. Bone Tumors. St. Louis: Mosby, 1998.

Epley KD, Lasky JB, Karesh JW. Osteosarcoma of the orbit associated with Paget disease. Ophthal Plast Reconstr Surg 1998;14:62-6.

Friendly DS, Font RL, Milhorat TH. Hemangioendothelioma of frontal bone. Am J Ophthalmol 1982;93:482-90.

Fu Y-S, Perzin KH. Non-epithelial tumors of the nasal cavity, paranasal sinuses and nasopharynx: a clinicopathologic study. Cancer 1974;34:453-63.

Fu Y-S, Perzin KH. Non-epithelial tumors of the nasal cavity, paranasal sinuses, and nasopharynx: a clinicopathologic study. II. Osseous and fibro-osseous lesions, including osteoma, fibrous dysplasia, ossifying fibroma, osteoblastoma, giant cell tumor, and osteosarcoma. Cancer 1974;33:1289-305.

Hunter JV, Yokoyama C, Moseley IF, Wright JE. Aneurysmal bone cyst of the sphenoid with orbital involvement. Br J Ophthalmol 1990;74:505-8.

Jacobs JL, Merriam JC, Chadburn A, et al. Mesenchymal chondrosarcoma of the orbit: report of three new cases and review of the literature. Cancer 1994;73:399-405.

Johnson TE, Bergin DJ, McCord CD. Aneurysmal bone cyst of the orbit. Ophthalmology 1988;95:86-9.

Khouja N, Ben Amor S, Jemel H, et al. Mesenchymal extraskeletal chondrosarcoma of the orbit. Report of a case and review of the literature. Surg Neurol 1999;52:50-3.

Lam DS, Li CK, Cheng LL, et al. Primary orbital Ewing's sarcoma: report of a case and review of the literature. Eye 1999;13:38-42.

Leone CR, Lawton AW, Leone RT. Benign osteoblastoma of the orbit. Ophthalmology 1988;95:1554-8.

Lowder CY, Berlin AJ, Cox WA, Hahn JF. Benign osteoblastoma of the orbit. Ophthalmology 1986;93:1351-4.

Lyon DB, Tang TT, Kidder TM. Epithelioid hemangioendothelioma of the orbital bones. Ophthalmology 1992;99:1773-8.

Margo CE, Ragsdale BD, Perman KI, et al. Psammomatoid (juvenile) ossifying fibroma of the orbit. Ophthalmology 1985;92:150-9.

Mercado GJV, Gunduz K, Shields CL, et al. Pleomorphic adenoma of the lacrimal gland in a teenager. Arch Ophthalmol 1998;116:962-3.

Miller NR, McCarthy EF, Carter N, et al. Lytic Paget disease as a cause of orbital cholesterol granuloma. Arch Ophthalmol 1999;117:1084-6.

Miller NR, Gray J, Snip R. Giant, mushroom-shaped osteoma of the orbit originating from the maxillary sinus. Am J Ophthalmol 1977;83:587-91.

Moore AT, Buncic JR, Munro IR. Fibrous dysplasia of the orbit in childhood. Ophthalmology 1985;92:12-20.

Moore RT. Fibrous dysplasia of the orbit. Surv Ophthalmol 1969;13:321-44.

Naiman J, Green WR, D'Heurle D, et al. Brown tumor of the orbit associated with primary hyperparathyroidism. Am J Ophthalmol 1980;90:565-71.

Nakagawa K, Takasato Y, Ito Y, Yamada K. Ossifying fibroma involving the paranasal sinuses, orbit, and anterior cranial fossa: case report. Neurosurgery 1995;36:1192-5.

Pasternak S, O'Connell JX, Verchere C, Rootman J. Enchondroma of the orbit. Am J Ophthalmol 1996;122:444-5.

Roarty JD, McLean IW, Zimmerman LE. Incidence of second neoplasms in patients with bilateral retinoblastoma. Ophthalmology 1988;95:1583-7.

Sanerkin NG, Mott MG, Roylance J. An unusual intraosseous lesion with fibroblastic, osteoclastic, osteoblastic, aneurysmal and fibromyxoid elements: “solid” variant of aneurysmal bone cyst. Cancer 1983;51:2278-86.

Sebag J, Chapman P, Truman J, Riemersma RR. Giant cell granuloma of the orbit with intracranial extension. Neurosurgery 1985;16:75-81.

Selva D, White VA, O'Connell JX, Rootman J. Primary bone tumors of the orbit. In: Tasman W, Jaeger EA, eds. Foundations of Clinical Ophthalmology. Philadelphia: Lippincott, Williams and Wilkins, 2000; chap. 44.

Selva D, O'Connell JX, White VA, Rootman J. Pathogenesis of orbital cholesterol granuloma. (in progress).

Sevel D, James HE, Burns R, Jones KL. McCune-Albright syndrome (fibrous dysplasia) associated with an orbital tumor. Ann Ophthalmol 1984;16:283-97.

Shields JA, Peyster RG, Handler SD, et al. Massive juvenile ossifying fibroma of maxillary sinus with orbital involvement. Br J Ophthalmol 1985;69:392-5.

Slem G, Varinli S, Koker F. Brown tumor of the orbit. Ann Ophthalmol 1983;15:811-2.

Small ML, Green WR, Johnson LC. Lipoma of the frontal bone. Arch Ophthalmol 1979;97:129-32.

Swanson PE, Lillemoe TJ, Manivel JC, Wick MR. Mesenchymal chondrosarcoma. Arch Pathol Lab Med 1990;114:943-8.

Voytek TM, Ro JY, Edeiken J, Ayala AG. Fibrous dysplasia and cemento-ossifying fibroma. Am J Surg Pathol 1995;19:775-81.

Whitson WE, Orcutt JC, Walkinshaw MD. Orbital osteoma in Gardner's syndrome. Am J Ophthalmol 1986;101:236-41.

Woodruff G, Thorner P, Skarf B. Primary Ewing's sarcoma of the orbit presenting with visual loss. Br J Ophthalmol 1988;72:786-92.

Yamaguchi K, Hayasaka S, Yamada T, et al. Orbitocranial fibrous dysplasia: a case report. Ophthalmologica 1986;193:225-30.

Lymphoproliferative and Leukemic

Adkins JW, Shields JA, Shields CL, et al. Plasmacytoma of the eye and orbit. Int Ophthalmol 1997;20:339-43.

Bairey O, Kremer I, Rakowksy E, et al. Orbital and adnexal involvement in systemic non-Hodgkin's lymphoma. Cancer 1994;73:2395-9.

Coupland SE, Foss H-D, Assaf C, Auw-Haedrich C, Anastassiou G, Anagnostopoulos I, Hummel M, Karesh JW, Lee WR, Stein H. T-cell and T/Natural killer-cell lymphomas involving ocular and ocular adnexal tissues. Ophthalmology 1999; 106:2109-20.

Coupland SE, Krause L, Delecluse H, et al. Lymphoproliferative lesions of the ocular adnexa. Ophthalmology 1998;105:1430-41.

Davis JL, Parke DW, 2nd, Font RL. Granulocytic sarcoma of the orbit: a clincopathologic study. Ophthalmology 1985;92:1758-62.

De Smet M, Rootman J. Orbital manifestations of plasmacytic lymphoproliferations. Ophthalmology 1987;94:995-1003.

Dolman PJ, Rootman J, Quenville NF. Signet-ring cell lymphoma in the orbit: a case report and review. Can J Ophthalmol 1986;21:242-5.

Fratkin JD, Shammas HF, Miller SD. Disseminated Hodgkin's disease with bilateral orbital involvement. Arch Ophthalmol 1978;96:102-4.

Gonnering RS. Bilateral primary extramedullary orbital plasmacytomas. Ophthalmology 1987;94:267-70.

Gross ND, Wilson DJ, Dailey RA, et al. Nodular sclerosing Hodgkin disease with primary presentation in the orbit. Ophthal Plast Reconstr Surg 1998;14:169-73.

Harris NL, Jaffe ES, Diebold J, et al. World Health Organization classification of neoplastic diseases of the hematopoetic and lymphoid tissues: report of the clinical advisory committee meeting-Airlie House, Virginia, November 1997. J Clin Oncol 1999;17:3835-49.

Harris NL, Jaffe ES, Stein H, et al. A revised European-American classification of lymphoid neoplasms: a proposal from the International Lymphoma Study Group. Blood 1994;84:1361-92.

Henderson JW, Banks PM, Yeatts RP. T-cell lymphoma of the orbit. Mayo Clin Proc 1989;64:940-4.

Jenkins C, Rose GE, Bunce C, et al. Histological features of ocular adnexal lymphoma (REAL classification) and their association with patient morbidity and survival. Br J Ophthalmol 2000;84:907-13.

Kielar RA. Orbital granuloma in Hodgkin's disease. Ann Ophthalmol 1981;13:1197-9.

Kincaid MC, Green WR. Ocular and orbital involvement in leukemia. Surv Ophthalmol 1983;27:211-32.

Kirsch LS, Brownstein S, Codere F. Immunoblastic T-cell lymphoma presenting as an eyelid tumor. Ophthalmology 1990;97:1352-7.

Knowles DM, Jakobiec FA, McNally L, Burke JS. Lymphoid hyperplasia and malignant lymphoma occurring in the ocular adnexa (orbit, conjunctiva, and eyelids). Hum Pathol 1990;21:959-73.

Knowling MA, Harwood AR, Bergsagel DE. Comparison of extramedullary plasmacytomas with solitary and multiple plasma cell tumors of bone. J Clin Oncol 1983;1:255-62.

Lauer SA, Fischer J, Jones J, et al. Orbital T-cell lymphoma in human T-cell leukemia virus-1 infection. Ophthalmology 1988;95:110-5.

Leidenix MJ, Mamalis N, Olson RJ, et al. Primary T-cell immunoblastic lymphoma of the orbit in a pediatric patient. Ophthalmology 1993;100:998-1002.

Lukes RJ, Collins RD. New approaches to the classification of the lymphomata. Br J Cancer 1975;31:1-27.

Lukes RJ, Craver LF, Hall TC, et al. Report of the nomenclature committee. I. Cancer Res 1966;26:1311.

Matzkin DC, Slamovits TL, Rosenbaum PS. Simultaneous intraocular and orbital non-Hodgkin lymphoma in the acquired immune deficiency syndrome. Ophthalmology 1994;101:850-5.

Medeiros LJ, Carr J. Overview of the role of molecular pathology in the diagnosis of malignant lymphomas. Arch Pathol Lab Med. 1999;123:1189-1207.

National Cancer Institute. Summary and description of a working formulation for clinical usage. Cancer 1982;49:2112-35.

Patel S, Rootman J. Nodular sclerosing Hodgkin's disease of the orbit. Ophthalmology 1983;90:1433-6.

Pomeranz HD, McEvoy LT, Lueder GT. Orbital tumor in a child with posttransplantation lymphoproliferative disorder. Arch Ophthalmol 1996;114:1422-3.

Rappaport H. Atlas of Tumor Pathology, Section III, Fascicle 8, Tumors of the Hematopoietic System. Washington, DC: Armed Forces Institute of Pathology, 1966.

Reifler DM, Warzynski MJ, Blount WR, et al. Orbital lymphoma associated with acquired immune deficiency syndrome (AIDS). Surv Ophthalmol 1994;38:371-80.

Roth MJ, Medeiros J, Elenitoba-Johnson K, et al. Extramedullary myeloid cell tumors. Arch Pathol Lab Med 1995;119:790-8.

Rubinfeld RS, Gootenberg JE, Chavis RM, Zimmerman LE. Early onset acute orbital involvement in childhood acute lymphoblastic leukemia. Ophthalmology 1988;95:116-20.

Schwyzer R, Sherman GG, Cohn RJ, et al. Granulocytic sarcoma in children with acute myeloblastic leukemia and t(8;21). Med Pediatr Oncol 1998;31:144-9.

Segal GH, Jorgensen T, Masih AS, Braylan RC. Optimal primer selection for clonality assessment by polymerase chain reaction analysis: I. Low grade B-cell lymphoproliferative disorders of nofollicular center cell type. Hum Pathol 1994;25:1269-75.

Sioutos N, Bagg A, Michaud GY, et al. Polymerase chain reaction versus Southern blot hybridization. Diagn Mol Pathol 1995;4:8-13.

Skinnider LF, Romanchuk KG. Orbital involvement in chronic lymphocytic leukemia. Can J Ophthalmol 1984;19:142-4.

Stenson S, Ramsay DL. Ocular findings in mycosis fungoides. Arch Ophthalmol 1981;99:272-7.

Stockl FA, Dolmetsch AM, Saornil MA, et al. Orbital granulocytic sarcoma. Br J Ophthalmol 1997;81:1084-8.

White VA, Gascoyne RD, McNeil K, et al. Histopathologic findings and frequency of clonality detected by the polymerase chain reaction in ocular adnexal lymphoproliferative lesions. Mod Pathol 1996;9:1052-61.

White WL, Ferry JA, Harris NL, Grove AS Jr. Ocular adnexal lymphoma. Ophthalmology 1995;102:1994-2006.

Wilson MS, Weiss LM, Gatter KC, et al. Malignant histiocytosis: a reassessment of cases previously reported in 1975 based on paraffin section immunophenotyping studies. Cancer 1990;66:530-6.

Benign & Malignant Epithelial Tumors

Lacrimal Gland

Biggs SL, Font RL. Oncocytic lesions of the caruncle and other ocular adnexa. Arch Ophthalmol 1977;95:474-8.

de Rosa G, Zeppa P, Tranfa F, Bonavolonta G. Acinic cell carcinoma arising in a lacrimal gland. Cancer 1986;57:1988-91.

Dolman PJ, Rootman J. In situ malignant mixed tumour of the lacrimal gland: case report and review. Orbit 1987;6:181-7.

Evans HL. Mucoepidermoid carcinoma of salivary glands: a study of 69 cases with special attention to histologic grading. Am J Clin Pathol 1984;81:696-701.

Eviatar JA, Hornblass A. Mucoepidermoid carcinoma of the lacrimal gland: 25 cases with a review and update of the literature. Ophthal Plast Reconstr Surg 1993;9:170-81.

Gamel JW, Font RL. Adenoid cystic carcinoma of the lacrimal gland: the clinical significance of a basaloid histologic pattern. Hum Pathol 1982;13:219-25.

Gormley WB, Sekhar LN, Wright DC, et al. Management and long-term outcome of adenoid cystic carcinoma with intracranial extension: a neurosurgical perspective. Neurosurgery 1996;38:1105-13.

Hartwick RWJ, Shaw PA, Srigley JR, Hurwitz JJ. In situ adenocarcinoma ex pleomorphic adenoma of the lacrimal gland. Can J Ophthalmol 1990;25:213-7.

Harvey PA, Parsons A, Rennie IG. Primary sebaceous carcinoma of lacrimal gland: a previously unreported primary neoplasm. Eye 1994;8:592-5.

Heaps RS, Miller NR, Albert DM, et al. Primary adenocarcinoma of the lacrimal gland. Ophthalmology 1993;100:1856-60.

Henderson JW, Farrow GM. Primary malignant mixed tumors of the lacrimal gland. Report of 10 cases. Ophthalmology 1980;87:466-73.

Iwamoto T, Jakobiec FA. A comparative ultrastructural study of the normal lacrimal gland and its epithelial tumors. Hum Pathol 1982;13:136-62.

Katz SE, Rootman J, Dolman PJ, et al. Primary ductal adenocarcinoma of the lacrimal gland. Ophthalmology 1996;103:157-62.

Lee DA, Campbell RJ, Waller RR, Ilstrup DM. A clinicopathologic study of primary adenoid cystic carcinoma of the lacrimal gland. Ophthalmology 1985;92:128-34.

Luna MA, Batsakis JG, Ordonez NG, et al. Salivary gland adenocarcinomas: a clinicopathologic analysis of three distinctive types. Sem Diagn Pathol 1987;4:117-35.

Ni C, Cheng SC, Dryja TP, Cheng TY. Lacrimal gland tumors: a clinicopathological analysis of 160 cases. Int Ophthalmol Clin 1981;22:99-120.

Ostrowski ML, Font RL, Halpern J, et al. Clear cell epithelial-myoepithelial carcinoma arising in pleomorphic adenoma of the lacrimal gland. Ophthalmology 1994;101:925-30.

Paulino AFG, Huvos AG. Epithelial tumors of the lacrimal glands: a clinicopathologic study. Ann Diagn Pathol 1999;3:199-204.

Perzin KH, Jakobiec FA, Livolsi VA, Desjardins L. Lacrimal gland malignant mixed tumors (carcinomas arising in benign mixed tumors): a clinico-pathologic study. Cancer 1980;45:2593-606.

Rodgers IR, Jakobiec FA, Gingold MP, et al. Anaplastic carcinoma of the lacrimal gland presenting with recurrent subconjunctival hemorrhages and displaying incipient sebaceous differentiation. Ophthal Plast Reconstr Surg 1991;7:229-37.

Rosenbaum PS, Mahadevia PS, Goodman LA, Kress Y. Acinic cell carcinoma of the lacrimal gland. Arch Ophthalmol 1995;113:781-5.

Seifert G, Brocheriou C, Cardesa A, Eveson JW. WHO international histological classification of tumours: tentative histological classification of salivary gland tumours. Pathol Res Pract 1990;186:555-81.

Shields CL, Shields JA, Eagle RC, Rathmell JP. Clinicopathologic review of 142 cases of lacrimal gland lesions. Ophthalmology 1989;96:431-5.

Vangveeravong S, Katz SE, Rootman J, White V. Tumors arising in the palpebral lobe of the lacrimal gland. Ophthalmology 1996;103:1606-12.

Witschel H, Zimmerman LE. Malignant mixed tumor of the lacrimal gland. A clinicopathologic report of two unusual cases. Graefes Arch Clin Exp Ophthalmol 1981;216:327-37.

Wright JE. Factors affecting the survival of patients with lacrimal gland tumours. Can J Ophthalmol 1982;17:3-9.

Wright JE, Rose GE, Garner A. Primary malignant neoplasms of the lacrimal gland. Br J Ophthalmol 1992;76:401-7.

Metastatic and Invasive Neoplasms

Albert DM, Rubenstein RA, Scheie HG. Tumor metastasis to the eye. II. Clinical study in infants and children. Am J Ophthalmol 1967;63:727-32.

Amoaku WMK, Bagegni A, Logan WC, Archer DB. Orbital infiltration by eyelid skin carcinoma. Int Ophthalmol 1990;14:285-94.

Apple DJ. Wilms' tumor metastatic to the orbit. Arch Ophthalmol 1968;80:480-3.

Ballinger WH, Wesley RE. Seminoma metastatic to the orbit. Ophthalmic Surg 1984;15:120-2.

Bonavolonta G, Villari G, de Rosa G, Sammartino A. Ocular complications of juvenile angiofibroma. Ophthalmologica 1980;181:334-9.

Broughton WL, Zimmerman LE. A clinicopathologic study of 56 cases of intraocular medulloepitheliomas. Am J Ophthalmol 1978;85:407-18.

Bullock JD, Yanes B. Ophthalmic manifestations of metastatic breast cancer. Ophthalmology 1980;87:961-73.

Buys R, Abramson DH, Kitchin FD, et al. Simultaneous ocular and orbital involvement from metastatic bronchogenic carcinoma. Ann Ophthalmol 1982;14:1165-71.

Capone A Jr, Slamovits TL. Discrete metastasis of solid tumors to extraocular muscles. Arch Ophthalmol 1990;108:237-43.

Csaky KG, Custer P. Perineural invasion of the orbit by squamous cell carcinoma. Ophthalmic Surg 1990;21:218-20.

Elner VM, Burnstine MA, Goodman ML, Dortzbach RK. Inverted papillomas that invade the orbit. Arch Ophthalmol 1995;113:1178-83.

Ferry AP, Font RL. Carcinoma metastatic to the eye and orbit. I. A clinicopathologic study of 227 cases. Arch Ophthalmol 1974;92:276-86.

Ferry AP, Haddad HM, Goldman JL. Orbital invasion by an intracranial chordoma. Am J Ophthalmol 1981;92:7-12.

Ferry AP, Naghdi MR. Bronchogenic carcinoma metastatic to the orbit. Arch Ophthalmol 1967;77:214-6.

Folberg R, Whitaker DC, Tse DT, Nerad JA. Recurrent and residual sebaceous carcinoma after Mohs' excision of the primary lesion. Am J Ophthalmol 1987;103:817-23.

Font RL, Ferry AP. Carcinoma metastatic to the eye and orbit. III. A clinicopathologic study of 28 cases metastatic to the orbit. Cancer 1976;38:1326-55.

Font RL, Naumann G, Zimmerman LE. Primary malignant melanoma of the skin metastatic to the eye and orbit. Am J Ophthalmol 1967;63:738-54.

Fratkin JD, Purcell JJ, Krachmer JH, Taylor JC. Wilms' tumor metastatic to the orbit. JAMA 1977;238:1841-2.

Freedman MI, Folk JC. Metastatic tumors to the eye and orbit. Arch Ophthalmol 1987;105:1215-9.

Friling R, Marcus M, Monos T, et al. Rhabdomyosarcoma: invading the orbit in an adult. Ophthal Plast Reconstr Surg 1994;10:283-6.

Goldberg RA, Rootman J, Cline RA. Tumors metastatic to the orbit: a changing picture. Surv Ophthalmol 1990;35:1-22.

Gonnering RS, Sonneland PR. Oncocytic carcinoma of the plica semilunaris with orbital extension. Ophthalmic Surg 1987;18:604-7.

Grossniklaus HE, Zimmerman LE, Kachmer ML. Pleomorphic adenocarcinoma of the ciliary body: immunohistochemical and electron microscopic features. Ophthalmology 1990;97:763-8.

Hood CI, Font RL, Zimmerman LE. Metastatic mammary carcinoma in the eyelid with histiocytoid appearance. Cancer 1973;31:793-800.

Hornblass A, Kass LG, Reich R. Thyroid carcinoma metastatic to the orbit. Ophthalmology 1987;94:1004-7.

Howard GM, Jakobiec FA, Trokel SL, et al. Pulsating metastatic tumor of the orbit. Am J Ophthalmol 1978;85:767-71.

Johnson LN, Krohel GB, Yeon EB, Parnes SM. Sinus tumors invading the orbit. Ophthalmology 1984;91:209-17.

Johnson TE, Tabbara KF, Weatherhead RG, et al. Secondary squamous cell carcinoma of the orbit. Arch Ophthalmol 1997;115:75-8.

Kersten RC, Tse DT, Anderson RL, Blodi FC. The role of orbital extenteration in choroidal melanoma with extrascleral extension. Ophthalmology 1985;92:436-43.

Khalil M, Brownstein S, Codere F, Nicolle D. Eccrine sweat gland carcinoma of the eyelid with orbital involvement. Arch Ophthalmol 1980;98:2210-4.

Khalil MK, Duguid WP. Neurotropic malignant melanoma of right temple with orbital metastasis: a clinicopathological case report. Br J Ophthalmol 1987;71:41-6.

Kindermann WR, Shields JA, Eiferman RA, et al. Metastatic renal cell carcinoma to the eye and adnexae. Ophthalmology 1981;88:1347-50.

Malviya VK, Blessed W, Lawrence WD, Deppe G. Retroorbital metastases in ovarian cancer. Gynecol Oncol 1989;35:120-3.

Margo CE, Levy MH. Orbital metastasis from medullary carcinoma of the thyroid. Am J Ophthalmol 1993;115:394-5.

Marquardt MD, Zimmerman LE. Histopathology of meningiomas and gliomas of the optic nerve. Hum Pathol 1982;13:226-35.

McLean IW. Uveal nevi and malignant melanomas. In: Spencer WH, ed. Ophthalmic Pathology, 4th. ed. Philadelphia: WB Saunders, 1996; v. 3; 2121-217.

Mottow-Lippa L, Jakobiec FA, Iwamoto T. Pseudoinflammatory metastatic breast carcinoma of the orbit and lids. Ophthalmology 1981;88:575-80.

Musarella MA, Chan HSL, DeBoer G, Gallie BL. Ocular involvement in neuroblastoma: prognostic implications. Ophthalmology 1984;91:936-40.

Orcutt JC, Char DH. Melanoma metastatic to the orbit. Ophthalmology 1988;95:1033-7.

Polito E, Leccisotti A. Primary and secondary orbital melanomas: a clinical and prognostic study. Ophthal Plast Reconstr Surg 1995;11:169-81.

Rao NA, Font RL. Mucoepidermoid carcinoma of the conjunctiva. Cancer 1976;38:1699-709.

Rao NA, Hidayat AA, McLean IW, Zimmerman LE. Sebaceous carcinomas of the ocular adnexa. Hum Pathol 1982;13:113-22.

Reifler DM. Orbital metastasis with enophthalmos. Henry Ford Hosp Med J 1985;33:171-9.

Reifler DM, Hornblass A. Squamous cell carcinoma of the eyelid. Surv Ophthalmol 1986;30:349-65.

Rootman J, Carruthers JDA, Miller RR. Retinoblastoma. In: Rosenberg HS, Bernstein J, eds. Perspectives in Pediatric Pathology. Basel: Karger, 1987; v. 10; 208-58.

Ruusuvaara P, Setala K, Tarkkanen A. Orbital metastasis from cutaneous malignant melanoma. Acta Ophthalmol 1989;67:325-8.

Satorre J, Rootman J. Paraorbital sinus and nose neoplasms affecting the orbit and eyelids and their treatment. Curr Opin Ophthalmol 1990;1:542-8.

Seretan EL. Metastatic adenocarcinoma from the stomach to the orbit. Arch Ophthalmol 1981;99:1469.

Sher JH, Weinstock SJ. Orbital metastasis of prostatic carcinoma. Can J Ophthalmol 1983;18:248-50.

Shields CL, Shields JA, Yarian DL, Augsburger JJ. Intracranial extension of choroidal melanoma via the optic nerve. Br J Ophthalmol 1987;71:172-6.

Shields JA, Elder D, Arbizo V, et al. Orbital involvement with desmoplastic melanoma. Br J Ophthalmol 1987;71:279-84.

Shields JA, Font RL. Meibomian gland carcinoma presenting as a lacrimal gland tumor. Arch Ophthalmol 1974;92:304-6.

Slamovits TL, Burde RM. Bumpy muscles. Surv Ophthalmol 1988;33:189-99.

Stannard C, Lipper S, Sealy R, Sevel D. Retinoblastoma: correlation of invasion of the optic nerve and choroid with prognosis and metastases. Br J Ophthalmol 1979;63:560-70.

Stefanyszyn MA, Hidayat AA, Pe'er JJ, Flanagan JC. Lacrimal sac tumors. Ophthal Plast Reconstr Surg 1994;10:169-84.

Thomas KM, Cumberworth VL, McEwan J. Orbital and skin metastases in a polymorphous low grade adenocarcinoma of the salivary gland. J Laryngol Otol 1995;109:1222-5.

Tranfa F, Cennamo G, Rosa N, et al. An unusual orbital lesion: hepatoma metastatic to the orbit. Ophthalmologica 1994;208:329-32.

Vanneste JAL. Subacute bilateral malignant exophthalmos due to orbital medulloblastoma metastases. Archives of Neurology 1983;40:441-3.

Weimar VM, Ceilley RI. Basal-cell carcinoma of a medial canthus with invasion of supraorbital and supratrochlear nerves: report of a case treated by Mohs' technique. J Dermatol Surg Oncol 1979;5:279-82.

Weiss R, Grisold W, Jellinger K, et al. Metastasis of solid tumors in extraocular muscles. Acta Neuropathol 1984;65:168-71.

Whyte AM. Bronchogenic carcinoma metastasizing to the orbit. J Maxillofac Surg 1978;6:277-80.

Winkler CF, Goodman GK, Eiferman RA, Yam LT. Orbital metastasis from prostatic carcinoma: identification by an immunoperoxidase technique. Arch Ophthalmol 1981;99:1406-8.

Wollensak G, Witschel H, Bohm N. Signet ring cell carcinoma of the eccrine sweat glands in the eyelid. Ophthalmology 1996;103:1788-93.

Wolter JR, Hendrix RC. Osteoblastic prostate carcinoma metastatic to the orbit. Am J Ophthalmol 1981;91:648-51.

Wright JD, Font RL. Mucinous sweat gland adenocarcinoma of eyelid. Cancer 1979;44:1757-68.

Yeo JH, Jakobiec FA, Iwamoto T, et al. Metastatic carcinoma masquerading as scleritis. Ophthalmology 1983;90:184-94.

Melanocytic

Dutton JJ, Anderson RL, Schelper RL, et al. Orbital malignant melanoma and oculodermal melanocytosis: report of two cases and review of the literature. Ophthalmology 1984;91:497-507.

Ellis DS, Spencer WH, Stephenson CM. Congenital neurocutaneous melanosis with metastatic orbital malignant melanoma. Ophthalmology 1986;93:1639-42.

Gunduz K, Shields JA, Shields CL, Eagle RC Jr. Periorbital cellular blue nevus leading to orbitopalpebral and intracranial melanoma. Ophthalmology 1998;105:2046-50.

Loffler KU, Witschel H. Primary malignant melanoma of the orbit arising in a cellular blue naevus. Br J Ophthalmol 1989;73:388-93.

Tellado M, Specht CS, McLean IW, et al. Primary orbital melanomas. Ophthalmology 1996;103:929-32.

Wilkes TDI, Uthman EO, Thornton CN, Cole RE. Malignant melanoma of the orbit in a black patient with ocular melanocytosis. Arch Ophthalmol 1984;102:904-6.

Optic Nerve

Berry K. Pathologic considerations important in the diagnosis and management of tumors of the nervous system. B C Med J 1995;37:80-5.

Marquardt MD, Zimmerman LE. Histopathology of meningiomas and gliomas of the optic nerve. Hum Pathol 1982;13:226-35.

O'Keefe M, Fulcher T, Kelly P, et al. Medulloepithelioma of the optic nerve head. Arch Ophthalmol 1997;115:1325-7.

Sadun F, Hinton DR, Sadun AA. Rapid growth of an optic nerve ganglioglioma in a patient with neurofibromatosis I. Ophthalmology 1996;103:794-9.

Taphoorn MJ, de Vries-Knoppert WA, Ponssen H, Wolbers JG. Malignant optic glioma in adults. J Neurosurg 1989;70:277-9.

Congenital and Structural Lesions

Bonavolonta G, Tranfa F, de Conciliis C, Strianese D. Dermoid cysts: 16-year survey. Ophthal Plast Reconstr Surg 1995;11:187-92.

Bowen JH, Christensen FH, Klintworth GK, Sydnor CF. A cartilaginous hamartoma of the orbit. Ophthalmology 1981;88:1356-60.

Bullock JD, Fleishman JA, Rosset JS. Lacrimal ductal cysts. Ophthalmology 1986;93:1355-60.

Call NB, Baylis HI. Cerebellar heterotopia in the orbit. Arch Ophthalmol 1980;98:717-9.

de Juan E Jr, Green WR, Iliff NT. Allergic periorbital mucopyocele in children. Am J Ophthalmol 1983;96:299-303.

DiLoreto DA, Rootman J, Neigel JM, Kennedy RA. Infestation of extraocular muscle by *Cystericercus cellulosae*. Br J Ophthalmol 1990;74:751-2.

Ellis FJ, Eagle RC, Shields JA, et al. Phakomatous choristoma (Zimmerman's tumor): immunohistochemical confirmation of lens-specific proteins. Ophthalmology 1993;100:955-60.

Garden JW, McManis JC. Congenital orbital-intracranial teratoma with subsequent malignancy: case report. Br J Ophthalmol 1986;70:111-3.

Goldstein MH, Soparker CNS, Kersten RC, et al. Conjunctival cysts of the orbit. Ophthalmology 1998;105:2056-60.

Green WR, Zimmerman LE. Ectopic lacrimal gland tissue. Arch Ophthalmol 1967;78:318-27.

Gunalp I, Gunduz K. Cystic lesions of the orbit. Int Ophthalmol 1996;20:273-7.

Haik BG, Karcioglu ZA, Gordon RA, Pechous BP. Capillary hemangioma (infantile periocular hemangioma). Surv Ophthalmol 1994;38:399-426.

Harris GJ, Jakobiec FA. Cavernous hemangiomas of the orbit. J Neurosurg 1979;51:219-28.

Harris GJ, Sakol PJ, Bonavolonta G, de Conciliis C. An analysis of thirty cases of orbital lymphangioma. Ophthalmology 1990;97:1583-92.

Hayashi N, Repka MX, Ueno H, et al. Congenital cystic eye: report of two cases and review of the literature. Surv Ophthalmol 1999;44:173-9.

Henderson JW, Farrow GM, Garrity JA. Clinical course of an incompletely removed cavernous hemangioma of the orbit. Ophthalmology 1990;97:625-8.

Holds JB, Anderson RL, Mamalis N, et al. Invasive squamous cell carcinoma arising from aymptomatic choristomatous cysts of the orbit. Ophthalmology 1993;100:1244-52.

Howard GR, Nerad JA, Bonavolonta G, Tranfa F. Orbital dermoid cysts located within the lateral rectus muscle. Ophthalmology 1994;101:767-71.

Iliff WJ, Green WR. Orbital lymphangiomas. Ophthalmology 1979;86:914-29.

Iwamoto T, Jakobiec FA. Ultrastructural comparison of capillary and cavernous hemangiomas of the orbit. Arch Ophthalmol 1979;97:1144-53.

Jakobiec FA, Trokel S, Iwamoto T. Sino-orbital polyposis. Arch Ophthalmol 1979;97:2353-7.

James CRH, Lyness R, Wright JE. Respiratory epithelium lined cysts presenting in the orbit without associated mucocele formation. Br J Ophthalmol 1986;70:387-90.

Katz NNK, Ruymann FB, Margo CE, et al. Endodermal sinus tumor (yolk sac carcinoma) of the orbit. Journal of Pediatric Ophthalmology & Strabismus 1982;19:270-4.

Kaufman SJ. Orbital mucopyoceles: two cases and a review. Surv Ophthalmol 1981;25:253-62.

Kivela T, Tarkkanen A. Orbital germ cell tumors revisited: a clinicopathological approach to classification. Surv Ophthalmol 1994;38:541-54.

Krohel GB, Wright JE. Orbital hemorrhage. Am J Ophthalmol 1979;88:254-8.

Lessner AM, Antle CM, Rootman J, et al. Cystic lesions of the orbit and radiolucent defects of bone. In: Margo CE, Hamed LM, Mames RN, eds. Diagnostic Problems in Clinical Ophthalmology. Philadelphia: W.B. Saunders, 1994; 87-98.

Leventer DB, Merriam JC, Defendini R, et al. Enterogenous cyst of the orbital apex and superior orbital fissure. Ophthalmology 1994;101:1614-21.

Lieb W, Rochels R, Gronemeyer U. Microphthalmos with colobomatous orbital cyst: Clinical, histological, immunohistological, and electronmicroscopic findings. Br J Ophthalmol 1990;74:59-62.

Mamalis N, Garland PE, Argyle JC, Apple DJ. Congenital orbital teratoma: A review and report of two cases. Surv Ophthalmol 1985;30:41-6.

Manschot WA. Coenurus infestation of eye and orbit. Arch Ophthalmol 1976;94:961-4.

Mansour AM, Barber JC, Reinecke RD, Wang FM. Ocular choristomas. Surv Ophthalmol 1989;33:339-58.

Mansour AM, Li HK. Congenital cystic eye. Ophthal Plast Reconstr Surg 1996;12:104-7.

Margo CE, Folberg R, Zimmerman LE, Sesterhenn IA. Endodermal sinus tumor (yolk sac tumor) of the orbit. Ophthalmology 1983;90:1426-32.

Margo CE, Naugle TC, Karcioglu ZA. Ectopic lacrimal gland tissue of the orbit and sclerosing dacryoadenitis. Ophthalmic Surg 1985;16:178-81.

McNab AA, Wright JE. Orbitofrontal cholesterol granuloma. Ophthalmology 1990;97:28-32.

Milne HL, Leone CR, Kincaid MC, Brennan MW. Chronic hematic cyst of the orbit. Ophthalmology 1987;94:271-7.

Mims J, Rodrigues M, Calhoun J. Sudoriferous cyst of the orbit. Can J Ophthalmol 1977;12:155-6.

Morales AG, Croxatto JO, Crovetto L, Ebner R. Hydatid cysts of the orbit. Ophthalmology 1988;95:1027-32.

Newman NJ, Miller NR, Green WR. Ectopic brain in the orbit. Ophthalmology 1986;93:268-72.

Newton C, Dutton JJ, Klintworth GK. A respiratory epithelial choristomatous cyst of the orbit. Ophthalmology 1985;92:1754-7.

Pasquale LR, Romayananda N, Kubacki J, et al. Congenital cystic eye with multiple ocular intracranial anomalies. Arch Ophthalmol 1991;109:985-7.

Pillai AM, Sambasivan R. Congenital cystic eye - a case report with CT scan. Indian J Ophthalmol 1987;35:88-91.

Rappaport K, Liesegang TJ, Menke DH, Czervionke LF. Plasmacytoma manifesting as recurrent cellulitis and hematic cyst of the orbit. Am J Ophthalmol 1996;122:595-7.

Rawlings EF, Olson RJ, Kaufman HE. Polypoid sinusitis mimicking orbital malignancy. Am J Ophthalmol 1979;87:694-7.

Rootman J, Hay E, Graeb D, Miller R. Orbital-adnexal lymphangiomas: a spectrum of hemodynamically isolated vascular hamartomas. Ophthalmology 1986;93:1558-70.

Rose GE, O'Donnell BA. Congenital orbital cysts assoicated with the common sheath of superior rectus and levator palpebrae superioris muscles. Ophthalmology 1995;102:135-8.

Ruchman MC, Flanagan J. Cavernous hemangioma. Ophthalmology 1983;90:1328-36.

Sen DK. Cysticercus cellulose in the lacrimal gland, orbit and eye lid. Acta Ophthalmol 1980;58:144-7.

Shapiro A, Tso MOM, Putterman AM, Goldberg MF. A clinicopathologic study of hematic cysts of the orbit. Am J Ophthalmol 1986;102:237-41.

Sherman RP, Rootman J, Lapointe JS. Orbital dermoids: clinical presentation and management. Br J Ophthalmol 1984;68:642-52.

Shields JA, Kaden IH, Eagle RC Jr, Shields CL. Orbital dermoid cysts: clinicopathologic correlations, classification, and management. Ophthal Plast Reconstr Surg 1997:13:265-76.

Shields JA, Augsburger JJ, Donoso LA. Orbital dermoid cyst of conjunctival origin. Am J Ophthalmol 1986;101:726-9.

Smith S, Rootman J. Lacrimal ductal cysts: presentation and management. Surv Ophthalmol 1986;30:245-50.

Terry A, Patrinely JR, Anderson RL, Smithwick Wt. Orbital meningoencephalocele manifesting as a conjunctival mass. Am J Ophthalmol 1993;115:46-9.

Vinters HV, Murphy J, Wittmann B, Norman MG. Intracranial teratoma: Antenatal diagnosis at 31 weeks' gestation by ultrasound. Acta Neuropathol 1982;58:233-6.

Waring GO, Roth AM, Rodrigues MM. Clinicopathologic correlation of microphthalmos with cyst. Am J Ophthalmol 1976;82:714-21.

Weaver DT, Bartley GB. Malignant neoplasia of the paranasal sinuses associated with mucocele. Ophthalmology 1991;98:342-6.

West JA, Drewe RH, McNab AA. Atypical choristomatous cysts of the orbit. Aust N Z J Ophthalmol 1997;25:117-23.

Wilson RD, Traverse L, Hall JG, et al. Oculocerebrocutaneous syndrome. Am J Ophthalmol 1985;99:142-8.

Infectious and Inflammatory Disorders

Alper MG, Zimmerman LE, La Piana FG. Orbital manifestations of Erdheim-Chester disease. Trans Am Ophthalmol Soc 1983;81:64-85.

Amemiya T, Mori H, Koizumi K. Clinical and histocytopathological study of chronic dacryoadenitis. Graefes Arch Clin Exp Ophthalmol 1983;220:229-32.

Anderson RL, Carroll TF, Harvey JT, Myers MG. *Petriellidium (Allescheria) boydii* orbital and brain abscess treated with intravenous miconazole. Am J Ophthalmol 1984;97:771-5.

Aylward GW, Sullivan TJ, Garner A, et al. Orbital involvement in multifocal fibrosclerosis. Br J Ophthalmol 1995;79:246-9.

Baker RH, Bartley GB. Lacrimal gland ductule stones. Ophthalmology 1990;97:531-4.

Batsakis JG. Antineutrophil cytoplasmic autoantibodies (ANCAs): what's their status? Adv Anat Pathol 1996;3:59-63.

Binford CH, Connor DH. Pathology of Tropical and Extraordinary Diseases. Vol 2. Washington, DC: Armed Forces Institute of Pathology, 1976.

Buggage RR, Spraul CW, Wojno TH, Grossniklaus HE. Kimura disease of the orbit and ocular adnexa. Surv Ophthalmol 1999;44:79-91.

Cernea P, Marculescu A, Constantin F. L'Osteoériostite syphilitique du sommet de l'orbite. Annales Oculiste 1968;201:436-42.

Char DH, Ablin A, Beckstead J. Histiocytic disorders of the orbit. Ann Ophthalmol 1984;16:867-73.

Collison JMT, Miller NR, Green WR. Involvement of orbital tissues by sarcoid. Am J Ophthalmol 1986;102:302-7.

Cornblath WT, Dotan SA, Trobe JD, Headington JT. Varied clinical spectrum of necrobiotic xanthogranuloma. Ophthalmology 1992;99:103-7.

Cornblath WT, Elner V, Rolfe M. Extraocular muscle involvement in sarcoidosis. Ophthalmology 1993;100:501-5.

Damato BE, Allan D, Murray SB, Lee WR. Senile atrophy of the human lacrimal gland: the contribution of chronic inflammatory disease. Br J Ophthalmol 1984;68:674-80.

Devaney KO, Travis WD, Hoffman G, et al. Interpretation of head and neck biopsies in Wegener's granulomatosis. A pathologic study of 126 biopsies in 70 patients. Am J Surg Pathol 1990;14:555-64.

Endicott JN, Kirconnell WS, Beam D. Granuloma inguinale of the orbit with bony involvement. Arch Otolaryngol 1972;96:457-9.

Fartasch M, Vigneswaran N, Diepgen TL, Hornstein OP. Immunohistochemical and ultrastructural study of histiocytosis × and non-X histiocytoses. J Am Acad Dermatol 1990;23:885-92.

Favara BE, McCarthy RC, Mierau GW. Histiocytosis X. Hum Pathol 1983;14:663-76.

Feinberg R, Mark EJ, Goodman M, et al. Correlation of antineutrophil cytoplasmic antibodies with the extrarenal histopathology of Wegener's (pathergic) granulomatosis and related forms of vasculitis. Hum Pathol 1993;24:160-8.

Ferry AP, Abedi S. Diagnosis and management of rhino-orbitocerebral mycormyocosis (phycomycosis). Ophthalmology 1983;90:1096-104.

Fishleder A, Tubbs R, Hesse B, Levine H. Uniform detection of immunoglobulin-gene rearrangement in benign lymphoepithelial lesions. N Engl J Med 1987;316:1118-21.

Floyd BB, Brown B, Isaacs H, Minckler DS. Pseudorheumatoid nodule involving the orbit. Arch Ophthalmol 1982;100:1478-80.

Font RL, Neafie RC, Perry HD. Subcutaneous dirofilariasis of the eyelid and ocular adnexae. Arch Ophthalmol 1980;98:1079-82.

Font RL, Yanoff M, Zimmerman LE. Benign lymphoepithelial lesion of the lacrimal gland and its relationship to Sjogren's syndrome. Am J Clin Pathol 1967;48:365-76.

Foucar E, Rosai J, Dorfman R. Sinus histiocytosis with massive lymphadenopathy (Rosai-Dorfman Disease): review of the entity. Sem Diagn Pathol 1990;7:19-73.

Foucar E, Rosai J, Dorfman RF. The ophthalmologic manifestations of sinus histiocytosis with massive lymphadenopathy. Am J Ophthalmol 1979;87:354-67.

Freyer DR, Kennedy R, Bostrom BC, et al. Juvenile xanthogranuloma: forms of systemic disease and their clinical implications. J Pediatr 1996;129:227-37.

Garrity JA, Kennerdell JS, Johnson BL, Ellis DL. Cyclophosphamide in the treatment of orbital vasculitis. Am J Ophthalmol 1986;102:97-103.

Gephardt GN, Shah LF, Tubbs RR, Ahmad M. Wegener's granulomatosis. Immunomicroscopic and ultrastructural study of four cases. Arch Pathol Lab Med 1990;114:961-5.

Goulart RA, Mark EJ, Rosen S. Tumefactions as an extravascular manifestation of Wegener's granulomatosis. Am J Surg Pathol 1995;19:145-53.

Gutierrez Y. Diagnostic Pathology of Parasitic Infections With Clinical Correlations. Philadelphia: Lea & Febiger, 1990.

Helm CJ, Holland GN. Ocular tuberculosis. Surv Ophthalmol 1993;38:229-56.

Hidayat AA, Cameron JD, Font RL, Zimmerman LE. Angiolymphoid hyperplasia with eosinophilia (Kimura's disease) of the orbit and ocular adnexa. Am J Ophthalmol 1983;96:176-89.

Hornblass A, Herschorn BJ, Stern K, Grimes C. Orbital abscess. Surv Ophthalmol 1984;29:169-78.

Hughes D, Buckley PJ. Idiopathic retroperitoneal fibrosis is a macrophage-rich process. Am J Surg Pathol 1993;17:482-90.

Hui PK, Ng CS, Kung ITM, Gwi E. Lymphadenopathy of Kimura's disease. Am J Surg Pathol 1989;13:177-86.

Jabs DA, Johns CJ. Ocular involvement in chronic sarcoidosis. Am J Ophthalmol 1986;102:297-301.

Jakobiec FA, Gess L, Zimmerman LE. Granulomatous dacryoadenitis caused by *Schistosoma haematobium*. Arch Ophthalmol 1977;95:278-80.

Jakobiec FA, Mills MD, Hidayat AA, et al. Periocular xanthogranulomas associated with severe adult-onset asthma. Trans Am Ophthalmol Soc 1993;91:99-129.

Jakobiec FA, Trokel SL, Aron-Rosa D, et al. Localized eosinophilic granuloma (Langerhans' cell histiocytosis) of the orbital frontal bone. Arch Ophthalmol 1980;98:1814-20.

Kalina PH, Lie JT, Campbell RJ, Garrity JA. Diagnostic value and limitations of orbital biopsy in Wegener's granulomatosis. Ophthalmology 1992;99:120-4.

Kao SCS, Rootman J. Unusual orbital presentations of dural sarcoidosis. Can J Ophthalmol 1996;31:195-200.

Karam F, Chmel H. Rhino-orbital cerebral mucormycosis. Ear Nose Throat 1990;69:187, 91-3.

Karcioglu ZA, Brear R. Conjunctival biopsy in sarcoidosis. Am J Ophthalmol 1985;99:68-73.

Kattah JC, Zimmerman LE, Kolsky MP, et al. Bilateral orbital involvement in fatal giant cell polymyositis. Ophthalmology 1990;97:520-5.

Katz SE, Rootman J. Adverse effects of bone wax in surgery of the orbit. Ophthal Plast Reconstr Surg 1996;12:121-6.

Kennerdell JS, Dresner SC. The nonspecific orbital inflammatory syndromes. Surv Ophthalmol 1984;29:93-103.

Kersten RC, Haglund L, Kulwin DR, et al. Mycoplasma hominis orbital abscess. Arch Ophthalmol 1995;113:1096-7.

Kersten RC, Locastro AJ, Eberhard ML, et al. Periorbital dirofilariasis. Ophthal Plast Reconstr Surg 1994;10:293-6.

Kersten RC, Shoukrey NM, Tabbara KF. Orbital myiasis. Ophthalmology 1986;93:1228-32.

Kestelyn P. Rhinoscleroma with bilateral orbital involvement. Am J Ophthalmol 1986;101:381-2.

Khalil M, Lindley S, Matouk E. Tuberculosis of the orbit. Ophthalmology 1985;92:1624-7.

Klapper SR, Patrinely JR, Kaplan SL, Font RL. Atypical mycobacterial infection of the orbit. Ophthalmology 1995;102:1536-41.

Koyama T, Matsuo N, Watanabe Y, et al. Wegener's granulomatosis with destructive ocular manifestations. Am J Ophthalmol 1984;98:736-40.

Kronish JW, Johnson TE, Gilberg SM, et al. Orbital infections in patients with human immunodeficiency virus infection. Ophthalmology 1996;103:1483-92.

Kuo T, Shih L, Chan H. Kimura's disease. Am J Surg Pathol 1988;12:843-54.

Lawton AW, Karesh JW. Periocular granuloma annulare. Surv Ophthalmol 1986;31:285-90.

Li S, Perlman JI, Edward DP, Weiss R. Unilateral Blastomyces dermatiditis endophthalmitis and orbital cellulitis. Ophthalmology 1998;105:1466-70.

Lowe J, Bradley J. Cerebral and orbital *Aspergillus* infection due to invasive aspergillosis of ethmoid sinus. J Clin Pathol 1986;39:774-8.

Lubin JR, Jallow SE, Wilson WR, et al. Rhinoscleroma with exophthalmos: a case report. Br J Ophthalmol 1981;64:14-7.

MacCumber MW, Hoffman PN, Wand GS, et al. Ophthalmic involvement in aggressive histiocytosis X. Ophthalmology 1990;97:22-7.

Macy JI, Mandelbaum SH, Minckler DS. Orbital cellulitis. Ophthalmology 1980;87:1309-13.

Margo C, Rabinowicz M, Kwon-Chung KJ, Zimmerman LE. Subacute zygomycosis of the orbit. Arch Ophthalmol 1983;101:1580-5.

Mauriello JA, Yepez N, Mostafavi R, et al. Invasive rhinosino-orbital aspergillosis with precipitous visual loss. Can J Ophthalmol 1995;30:124-30.

McCarthy JM, White VA, Harris G, et al. Idiopathic sclerosing inflammation of the orbit: immunohistologic analysis and comparison with retroperitoneal fibrosis. Mod Pathol 1993;6:581-7.

McCurley TL, Collins RD, Ball E, Collins RD. Nodal and extranodal lymphoproliferative disorders in Sjogren's syndrome: a clinical and immunopathologic study. Hum Pathol 1990;21:482-92.

Mehregan DA, Winkelmann RK. Necrobiotic xanthogranuloma. Arch Dermatol 1992;128:94-100.

Mortada A. Orbital pseudo-tumors and parasitic infections. Bull Ophta Soc Egypt 1968;61:393-9.

Nichols CW, Eagle RC, Yanoff M, Menocal NG. Conjunctival biopsy as an aid in the evaluation of the patient with suspected sarcoidosis. Ophthalmology 1980;87:287-91.

O'Keefe M, Haining WM, Young JDH, Guthrie W. Orbital mucormycosis with survival. Br J Ophthalmol 1986;70:634-6.

Olurin O, Lucas AO, Oyediran ABO. Orbital histoplasmosis due to *Histoplasma dubiosii*. Am J Ophthalmol 1969;68:14-8.

Pepose JS, Akata RF, Pflugfelder SC, Voigt W. Mononuclear cell phenotypes and immunoglobulin gene rearrangements in lacrimal gland biopsies from patients with Sjogren's syndrome. Ophthalmology 1990;97:1599-605.

Perry SR, Rootman J, White VA. The clinical and pathologic constellation of Wegener granulomatosis of the orbit. Ophthalmology 1997;104:683-94.

Pillai S, Malone TJ, Abad JC. Orbital tuberculosis. Ophthal Plast Reconstr Surg 1995;11:27-31.

Robin JB, Schanzlin DJ, Meisler DM, et al. Ocular involvement in the respiratory vasculitides. Surv Ophthalmol 1985;30:127-40.

Rootman J. Why “orbital pseudotumor” is no longer a useful concept. Br J Ophthalmol 1998;82:339-40.

Rootman J, McCarthy JM, White VA, et al. Idiopathic sclerosing inflammation of the orbit: a distinct clinicopathologic entity. Ophthalmology 1994;101:570-84.

Rootman J, Nugent R. The classification and management of acute orbital pseudotumours. Ophthalmology 1982;89:1040-8.

Ross MJ, Cohen KL, Peiffer RL Jr, Grimson BS. Episcleral and orbital pseudorheumatoid nodules. Arch Ophthalmol 1983;101:418-21.

Satorre J, Antle CM, O'Sullivan R, et al. Orbital lesions with granulomatous inflammation. Can J Ophthalmol 1991;26:174-95.

Sekhar GC, Lemke BN. Orbital cysticercosis. Ophthalmology 1997;104:1599-1604.

Sen DK. Acute suppurative dacryoadenitis caused by a *Cysticercus cellulosae*. J Pediatr Ophthalmol Strabismus 1982;19:100-2.

Shields JA, Buchanon HW. Solitary orbital involvement with juvenile xanthogranuloma. Arch Ophthalmol 1990;108:1587-9.

Shields JA, Karcioglu ZA, Shields CL, et al. Orbital and eyelid involvement with Erdheim-Chester disease. Arch Ophthalmol 1991;109:850-4.

Streeten BW, Rabuzzi DD, Jones DB. Sporotrichosis of the orbital margin. Am J Ophthalmol 1974;77:750-5.

van Maarsseven ACMT, Mullink H, Alons CL, Stam J. Distribution of T-lymphocyte subsets in different portions of sarcoid granulomas: immunohistologic analysis with monoclonal antibodies. Hum Pathol 1986;17:493-500.

Viale G, Codecasa L, Bulgheroni P, et al. T-cell subsets in sarcoidosis. Hum Pathol 1986;17:476-81.

Vida L, Moel SA. Systemic North American blastomycosis with orbital involvement. Am J Ophthalmol 1974;77:240-2.

Weinreb RN. Diagnosing sarcoidosis by transconjunctival biopsy of the lacrimal gland. Am J Ophthalmol 1984;97:573-6.

Xu K-P, Katagiri S, Takeuchi T, Tsubota K. Biopsy of labial salivary glands and lacrimal glands in the diagnosis of Sjogren's syndrome. J Rheumatol 1996;23:76-82.

Thyroid Orbitopathy

Bahn RS, Heufelder AE. Pathogenesis of Graves' ophthalmopathy. N Engl J Med 1993;329:1468-75.

Trokel SL, Jakobiec FA. Correlation of CT scanning and pathologic features of ophthalmic Graves' disease. Ophthalmology 1981;88:553-64.

Amyloid Deposition

Campos EC, Melato M, Manconi R, Antonutto G. Pathology of ocular tissues in amyloidosis. Ophthalmologica 1980;181:31-40.

Cohen AS, Connors LH. The pathogenesis and biochemistry of amyloidosis. J Pathol 1987;151:1-10.

Gonnering RS, Sonneland PR. Ptosis and dermatochalasis as presenting signs in a case of occult primary systemic amyloidosis (AL). Ophthalmic Surg 1987;18:495-7.

Knowles DM, Jakobiec FA, Rosen M, Howard G. Amyloidosis of the orbit and adnexae. Surv Ophthalmol 1975;19:367-83.

Pasternak S, White VA, Gascoyne RD, et al. Monoclonal origin of localised orbital amyloidosis detected by molecular analysis. Br J Ophthalmol 1996;80:1013-7.

Chapter 8

Thyroid Orbitopathy

Jack Rootman

Peter J. Dolman

Thyroid-related orbitopathy has been recognized by the medical community for 200 years. The ocular changes associated with thyroid disease were first published by Graves in 1835 and by Von Basedow in 1840 but were apparently noted in 1786 by Parry (published posthumously in 1825). The diverse nomenclature, diagnostic groupings, classifications, eponyms, and most importantly the lack of general understanding of its natural history and epidemiology make it difficult in the practical situation to appreciate the nature of this disorder in the individual patient. We have chosen to refer to the orbital and related ocular changes as **thyroid orbitopathy** or **Graves' orbitopathy** because it is an **orbital** rather than an ophthalmic process. The majority of patients have clinical or laboratory evidence of thyroid disease but the orbital process can occur even in the absence of detectable thyroid abnormality. It remains the most common cause of unilateral or bilateral proptosis and is the subject of a vast literature. We will attempt to highlight the clinically relevant features of thyroid orbitopathy based on our experience of over 2000 cases, thereby providing practical guidelines and our current management philosophy. The purpose of this chapter is to contextualize the individual and his or her constellation of symptoms, signs, and imaging features in such a way as to develop a rational management for that patient at the **initial** encounter.

Thyroid orbitopathy is overwhelmingly associated with and usually occurs close to or within 18 months of hyperthyroidism; there is a rough correlation between the nature of hyperthyroidism, its management, and the orbitopathy. Subclinical thyroid abnormalities may be noted in some patients with typical orbitopathy. It is best understood if the dynamics of the pathophysiologic situation are individualized and the physician attempts to deal with the patient on this basis. Management should consist of a coordinated, multidisciplinary, medical-surgical approach based on staging of the disease and knowledge of its effect on the orbital and ocular structures. Broadly speaking, management is directed toward abating or controlling the active phase of the disease, prevention of ocular and psychophysical damage, redressing ocular motor abnormalities, and improving the cosmetic disfigurement.

Pathogenesis, Pathology, and Pathophysiology

Pathogenesis

Thyroid orbitopathy occurs in a genetically preselected population, affecting females four to five times more frequently than males, except in older age groups where the female-male ratio decreases. The propensity for the development and severity of this disorder may be related to genetic and environmental factors. HLA-DR histocompatibility loci (which play a role in T-cell response) have been associated with thyroid orbitopathy but so far no specific gene has been related to the disorder. A specific cause remains unknown

but evidence links the orbitopathy, the immunogenic thyroid disorder, and pretibial myxedema to immune mechanisms of both cellular and humoral mediation.

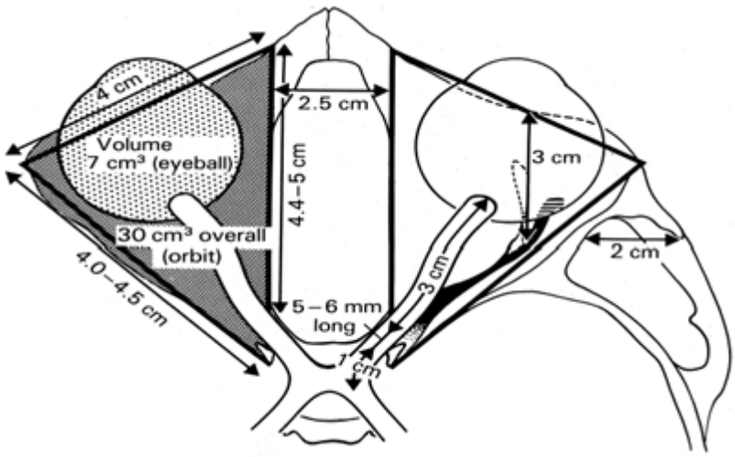

Figure 8-1. Histopathology of the typical features of thyroid orbitopathy. The scattered inflammatory infiltrate has some foci of more intense cellularity consisting of plasma cells, lymphocytes, and occasional mast cells. The muscle fibers appear distended and there is a loose stroma rich in mucopolysaccharides (glycosaminoglycans) (H&E, original magnification × 10).

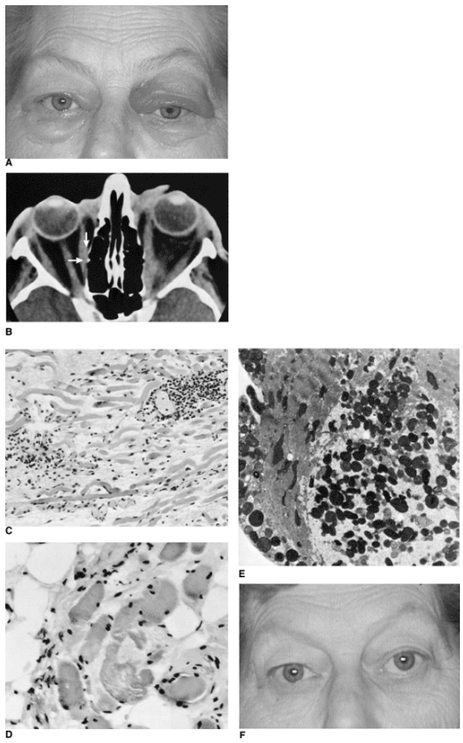

Figure 8-2. (A) This 67-year-old woman was seen 6 months after the onset of a cryptogenic bilateral orbital inflammatory syndrome, which was worse on the left than on the right, and she had not responded to oral steroids prior to referral. It was bilateral and characterized on the left by chemosis (+3), marked lid edema (+3), and injection of the skin and conjunctiva. She had exophthalmometry of 19 mm on the right and 22 mm on the left; 2 mm of downward displacement; marked limitation of elevation (0°), abduction (10°), adduction (15°), and infraduction (50°) of the left globe. She had a 25-diopter left hypotropia due to a restrictive myopathy. Vision was 20/20 on the right and 20/40 on the left, and visually evoked response was delayed on the left with an acquired red/green defect. She had been thoroughly investigated for thyroid disease, and all tests (including TRH stimulation) were negative. (B) Axial CT scan demonstrates bilateral myopathy, enlarged anteriorly displaced lacrimal glands, and some left apical crowding. Note low density areas in the muscles (arrows). On the left side, there is also evidence of infiltration of orbital fat, an unusual (but not unknown) feature of relatively severe, active thyroid orbitopathy. (C) Because of the unusual involvement of orbital fat, a perconjunctival biopsy of orbital muscle was done. It demonstrated infiltration by focal and scattered plasma cells and lymphocytes surrounding blood vessels and adjacent to some muscle fibers. Note the loose mucopolysaccharide-rich stroma with collagen deposition (H&E, original magnification × 10). Degenerative changes (swelling and disruption) of the muscle fibers on light (D) and electron (E) microscopy. The electron micrograph shows massive accumulations of mitochondria (some swollen, others degenerating) within the disrupted muscle fiber (H&E, original magnifications D × 25, E × 11750). The overall picture led to a diagnosis of euthyroid orbitopathy and the patient underwent radiotherapy (2000 cGy) and improved over the next 6 weeks with decreased swelling and increased abduction, but was noted to have increased hypotropia (45 diopter). Within a year she had borderline abnormal TSH stimulation testing but has never developed a clinical thyroid disorder. Over this time, the hypotropia reduced to 30 diopter and upgaze improved to 10° with disappearance of periorbital edema and chemosis. She underwent a left inferior rectus recession on adjustable suture 1 year postradiotherapy and obtained orthophoria in primary position to 10° downgaze. (F) Two years after onset of disease, on questionnaire the patient considered herself 80% recovered.

The orbital connective tissue, lipocytes, and possibly extraocular muscle antigens are thought to be targeted by T-lymphocytes. Thyrotropin receptors (thyroid-stimulating hormone receptor – TSHR) may play a role as an autoantigen in Graves' hyperthyroidism, orbitopathy, and pretibial myxedema. An alternative theory suggests that there is a primary autoantigen in the extraocular muscle. Activated lymphocytes (especially T-cells) infiltrate the orbital tissues (and for that matter, other soft tissues), particularly in the early phase of the disorder, and induce the changes related to the orbitopathy. This infiltration results in cytokine release, which may cause secondary expression of numerous circulating proteins (notably extraocular muscle protein in the 63 to 67 kDa range and the 72 kDa [heat shock] protein). The local response to cytokines, oxygen-free radicals, and fibrogenic growth factors leads to fibroblast stimulation resulting in increased glycosaminoglycan (GAG) synthesis, cell growth, and pre-adipocyte transformation with expression of immunomodulatory molecules. The effect on the orbital tissues, especially fibroblasts in the extraocular muscles and orbital soft tissues, is an increase in orbital hydrophilic GAGs, increase in orbital muscle and fat volumes, inflammatory edema, muscle injury, and scarring. These mechanisms result in the clinical manifestations of increased mass, inflammation, swelling, muscle restriction, and secondary compressive features.

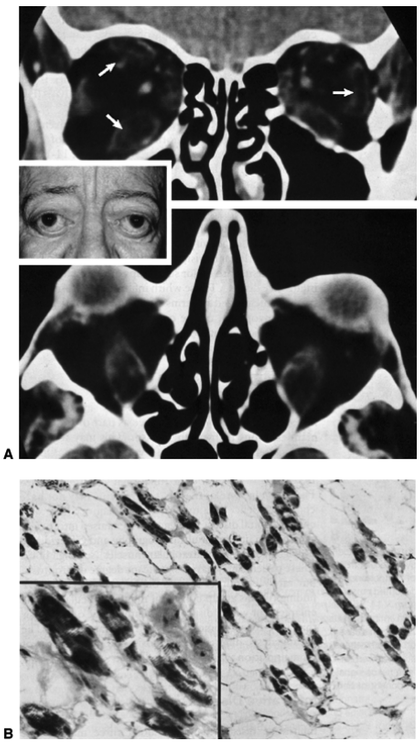

Figure 8-3. (A) This patient demonstrates the features of a longstanding thyroid orbitopathy with severe exophthalmos but no active soft tissue nor motor abnormalities. It had been present for 35 years, and its onset was associated with hyperthyroidism. The axial and coronal CT scans demonstrate enlargement of and multiple low-density foci (arrows) within all of the muscles. He was referred with severe and acute corneal exposure. He underwent decompression, at which time a muscle biopsy was also done. (B) Photomicrograph demonstrates replacement of the degenerated muscle with bundles of fat (PTAH, original magnification × 10, inset × 25).

Pathology

The pathology reflects the immunopathogenic mechanisms suggested. The extraocular muscles are infiltrated by a relatively paucicellular population of lymphocytes (especially T-cells in the early phase), macrophages (particularly early), B-lymphocytes, plasma cells, and mast cells. In addition, there is a deposition of hydrophilic mucopolysaccharides (represented as pools of alcian blue-positive extracellular protein separating the muscle bundles and fibers), which with inflammatory edema reflects target effects on the endomysial and orbital fibroblasts as well as the muscle itself. The pathology varies depending on the intensity and stage of the disease when the tissues are examined. Muscle fibers are separated by the glycosaminoglycan-rich stroma early in the disease (Figs. 8-1 and 8-2). With longer duration, there is an increase in stromal collagen deposition, some muscle degeneration, and ultimately in the quiescent stage replacement of degenerated muscles with fat that corresponds to CT features (Fig. 8-3).

Pathophysiology

The local pathophysiologic change reflects several variable, interacting factors that lead to the clinical spectrum of disease and are of most significance in the more severe presentations. The major primary variables are inflammation during the

active phase; mass effect brought about by enlargement of the extraocular muscles and increased orbital fat, and muscle changes leading to restriction of movement. The secondary factors are orbital compliance and a lack of orbital lymphatics resulting in variable degrees of congestion.

The inflammation induces muscle and soft tissue swelling and contributes to tearing, injection, discomfort, and periorbital edema. Muscle enlargement occurs in the middle and posterior thirds of the orbit. When progressive, it leads to mass effect (proptosis), scarring, and damage, which manifest as the development of increasing motor restriction (including lid retraction), psychovisual effects (optic neuropathy), and exposure. The secondary effects of the disease are governed by the interaction of inflammation, mass effect, and compliance (i.e., tightness of the orbital box including the anterior and intraorbital septal network), leading to venous obstruction and increasing congestion compounded by the absence of deep orbital lymphatics. This venous obstruction results in a disproportionate swelling of the anterior structures by overwhelming the ability of the lymphatics of the lid and conjunctiva to drain fluid. Because of the posterior focus of the disease and the narrowing orbital apex, significant muscle swelling is a major factor in the development of psychophysical deficit, which may be out of proportion to the degree of either inflammation or apparent overall mass effect but usually does correlate with degree of proptosis and especially severity of myopathy. One of the unusual aspects of this orbitopathy is the possibility of differing amounts of single muscle or multiple muscle involvement, reflected in the varying presentations of clinical myopathy in different patients.

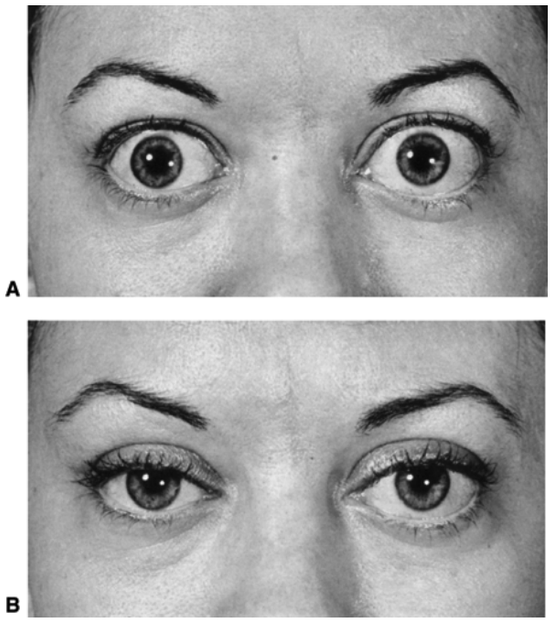

Figure 8-4. (A) This 30-year-old female demonstrates the features of mild, noncicatricial (noninfiltrative) orbitopathy, consisting of mild proptosis and lid retraction occurring concomitant to hyperthyroidism. (B) Photograph taken 1 year later shows her postoperative appearance after a graded upper lid lengthening procedure (müllerectomy).

Classification & Categorization

The classification of thyroid orbitopathy has improved with better understanding of the disease but there is still no universally acceptable or completely satisfactory system. The original NOSPECS classification is of historical interest only and in clinical practice is of little value in categorization or prognostication. This system has been abandoned for assessing subjective (symptomatic) and objective characteristics that determine disease **activity** and **severity** (extent). Readers are referred to papers by Gorman (1991 and 1998), Burch and Wartofsky, Mourits et al., and Bartley et al. for in depth discussions of classification, and to the many papers on quantitative evaluation of the orbit with imaging.

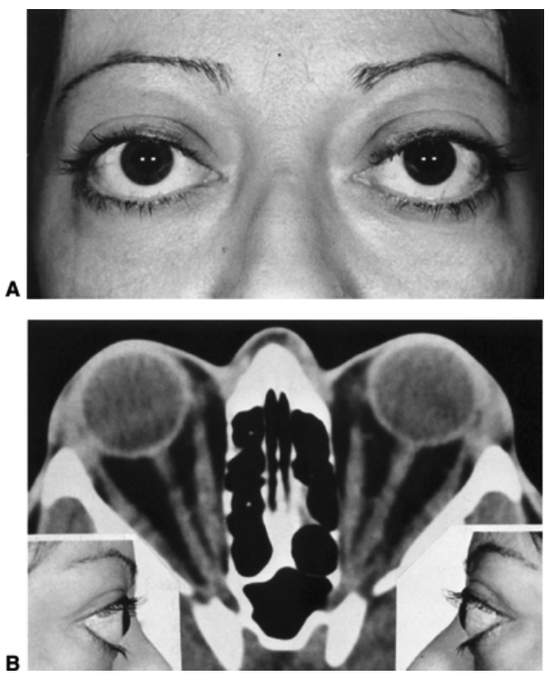

Figure 8-5. (A) This 32-year-old woman demonstrates the features of low-grade (nonactive) thyroid orbitopathy persisting 3 years after the onset and treatment of hyperthyroidism. Her major clinical features are exophthalmos (23 mm right, 24 mm left), normal ocular movements, a 6-mm rise in intraocular pressure on upgaze, and lower lid retraction with an absence of soft tissue swelling. (B) Axial CT scan shows mild bilateral enlargement of the extraocular muscles with an apparent increase in fat volume and anterior displacement of the lacrimal glands.

Although some differences in nomenclature and inferred pathogenesis exist, most authors agree that the **clinically important** differentiation in the management of thyroid orbitopathy is to separate those patients with, or at risk of developing, progressive or severe disease from the majority who have lesser disease. The majority of hyperthyroid patients have subclinical orbital disease as suggested on imaging, but never manifest significant clinical progression. Many authors distinguish these patients into two broad groups of infiltrative versus noninfiltrative disease, or type 1 and type 2 disease, without real evidence for a pathogenetic dichotomy. We prefer to define the disorder in terms of a spectrum of presentation in terms of activity and severity.

Patients with mild disease (particularly adolescent and young adult onset) may simply have lid lag, lid retraction (stare), lagophthalmos, and proptosis alone or in varying combinations as part of the manifestation of active hyperthyroidism (Fig. 8-4). Some of these features may regress in select patients with control of the hyperthyroidism.

Moderate active disease consists of persistent lid retraction, lid lag, proptosis, and some manifestations of soft tissue change with swelling and intermittent myopathy that has an active course but eventually settles, usually within 6 months to a year (Fig. 8-5). This end of the spectrum (so-called noninfiltrative or type 1 disease) rarely leads to serious orbital or ocular problems and stabilizes relatively quickly. The imaging findings in this group consists of mild extraocular muscle enlargement with a disproportionate degree of proptosis that may reflect increase in the fat volume.

With increasing severity, the onset of this disorder is more rapid, occurs more frequently in middle-aged or older patients, and is dominated by inflammatory, cicatricial, and mass effects to varying degrees (so-called infiltrative or type 2 disease).

Many patients have disease that abates spontaneously but clinically significant orbitopathy probably affects 10% to 15% of patients with about 5% to 6% developing severe orbitopathy (Fig. 8-6). The major manifestations of more serious disease are progressive exophthalmos associated with significant soft tissue features, mass change, and myopathy, all of which in general correlate with severity of disease. Compression of the orbital apex leads to the crowded orbital apex syndrome with optic neuropathy.

Clinical Evaluation

General Determinants

Many clinicians find thyroid orbitopathy difficult to manage, largely because of uncertainty regarding the natural history and spectrum of the disorder. In the last 10 to 15 years, we have learned more about the natural history of thyroid orbitopathy, which has in the past been compounded by dissociation of endocrinologists' and the ophthalmic community's interests in this disease. Recent studies have allowed us to reapproach thyroid orbitopathy with more clearly understood paradigms, and to categorize and manage patients more effectively. Our experience at the University of British Columbia Thyroid Orbitopathy Clinic over the last 25 years has led to the development of some critical insights and allowed for appropriate contextualization of affected individuals and better outcomes.

The key issue is to recognize the factors that place a patient at risk for developing progressive disease, in contrast to the majority who will have a relatively mild course. As noted, it is likely that only 10% to 15% of patients with thyroid orbitopathy are going to have the more significant form of the disease. However, it has been suggested that up to 50% (clinically) and perhaps 90% (on imaging) of patients have some form of orbitopathy prior to or following hyperthyroidism, which is mostly milder or subclinical.

In order to manage the individual patient, it is important to understand the key factors that help to predict their probable course. We believe that the earlier patients can be categorized into mild, nonprogressive versus more active and severe disease, the more likely we are able to reduce the severity in the latter group and reassure the former. We have seen an improvement in severe cases by virtue of earlier referral and better endocrine control by the endocrine and general medical community, and earlier intervention by ourselves to reduce the progression of this disorder.

Prognostic Determinants in Decision Making

Historically, clinicians have been advised to wait and watch for progression of disease and intervene only once severe features develop. Our philosophy is to identify those predictive variables of mild versus severe disease to allow earlier management decisions. We attempt to make a decision in a timely manner based on activity and severity thereby treating as early as possible, preferably after the first visit.

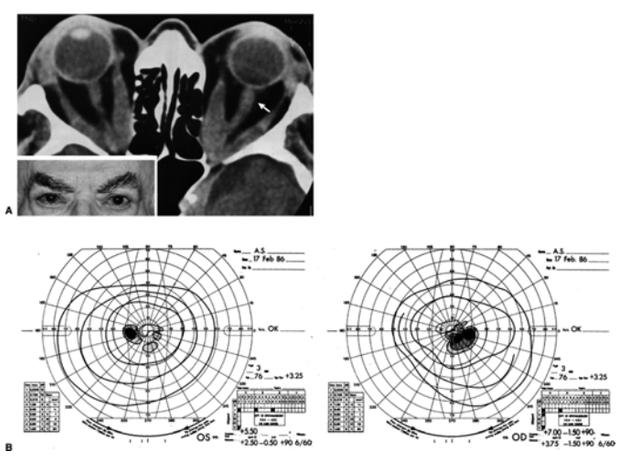

Figure 8-6. This 76-year-old man was referred with severe thyroid orbitopathy that began 4 months after treatment for hyperthyroidism. He had developed progressive proptosis, soft tissue signs (edema +3, injection and chemosis +3), symmetrical and significant limitation of extraocular movements in all positions of gaze, and reduction of vision to counting fingers bilaterally. In spite of treatment with 100 mg prednisone when referred, his vision was 20/400 right and 20/200 left. Exophthalmometry was 21 mm bilaterally, and he had marked symmetrical limitation of ocular movements. Fundus examination revealed choroidal striae. (A) Axial CT scan demonstrates apical compression, proptosis, and anterior displacement of the lacrimal gland with dilatation of the distal optic nerve sheath (arrow). (B) Visual fields show bilateral inferior scotomata that are worse on the right than on the left, and VEPs were abnormal. He underwent bilateral apical decompression with removal of the medial wall and floor. At follow-up 2 months later, his vision was 20/40 bilaterally with persistence of a small paracentral scotoma on the left side.

Age, Sex, and Race

We and others have identified age, sex, and race as important prognostic factors. Young patients generally have milder orbitopathy whilst older patients are prone to more severe disease. We have found that males tend to have worse disease and later onset than females. In our community, we have found that Caucasians tend to have worse disease than Asians, with Asians having less enlargement and fewer numbers of muscles involved and a higher frequency of single muscle involvement.

Acuity of Onset and Severity of Disease

Another important and **often overlooked** factor is the acuity of onset of inflammatory disease. For instance, patients who present with an acute or subacute history of onset that is development and progression over a few weeks of significant features of retrobulbar discomfort, pain on extraocular movement, diplopia, periorbital swelling, limitation of movement, proptosis, visual difficulty, and a widened interpalpebral fissure are more likely to develop severe disease than those who have an insidious onset occurring over more than 4 months and associated with lesser signs and symptoms on referral. From our own review of patients requiring significant intervention for thyroid orbitopathy, those who had acute or subacute onsets of their inflammatory component had four times more likelihood of developing severe disease. Patients with mild or moderate disease were more likely to undergo spontaneous improvement than those with severe disease.

What about the Relationship between Thyroid Function and Orbitopathy?

Graves' orbitopathy can occur in association with hypothyroidism or an euthyroid state but the majority occur in relationship to Graves' hyperthyroidism. About 20% of Graves' orbitopathy occur before hyperthyroidism, 40% at the time of hyperthyroidism, and about 40% after the occurrence of hyperthyroidism. The disorder can be detected in about 90% of patients on imaging and only 50% display some clinical features, but it often improves spontaneously. The natural history within a year of occurrence of orbitopathy is that approximately 22% of patients improve significantly, 42% slightly, 22% remain the same, and about 14% become worse.

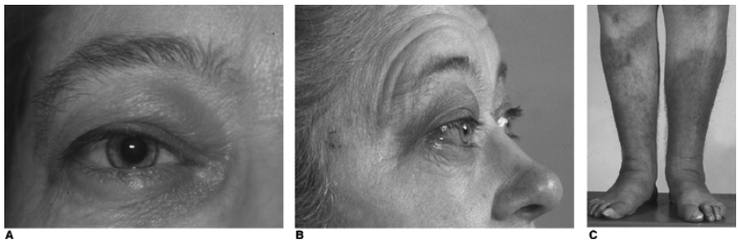

Figure 8-7. (A, B) This 58-year-old woman had a subacute onset (weeks) of tearing, vertical diplopia, and periorbital swelling with proptosis, leading within 3 months (up to presentation) to a decrease in vision, an awareness of color desaturation, and gray-outs on the right side. She had a right afferent pupillary defect with 20/40 vision; 3-mm downward and 2-mm outward displacement, proptosis (26 mm right eye and 16 m left eye), chemosis (+2), lid edema (+2), and both conjunctival and lid injection. She had a 12-diopter left hypertropia with a reduction of elevation of the right eye to 30 and an increase in intraocular pressure by 6 mmHg on upgaze. She was also noted to have right disc edema and pretibial myxedema (C). She responded dramatically to high-dose oral corticosteroids with recovery of vision.

There is a rough correlation between the severity of autoimmune hyperthyroid disease and orbitopathy, and this may be a predictive factor that should be considered at the time of primary treatment of hyperthyroidism. Although some controversy still exists, the general opinion is that the nature of treatment of this disorder is associated with differences in incidence and severity of orbitopathy. In short, the administration of radioactive iodine is associated with a higher incidence of progression and severity of orbitopathy (especially if preexisting) but not so much that one should not consider it as an appropriate treatment in the context of the hyperthyroidism. There is also a general consensus that early and complete control of the hyperthyroidism is important in terms of management of orbitopathy. This is also true if induced hypothyroidism is recognized and controlled early. This does, however, suggest closer monitoring of patients who receive this as a primary treatment.

Treatment with thyroid-suppressive drugs is associated with reduced occurrence and severity of orbitopathy, as is near total thyroidectomy. Another aspect of hyperthyroidism to keep in mind is the timing from hyperthyroidism. In general, the onset of symptoms of orbitopathy within the immediate period of hyperthyroidism (i.e., within 2 to 4 months either before or after) contextualized with other factors such as severity and nature of onset, correlates with the likelihood of progression and the need for intervention.

There is some suggestion that immunosuppression, in this case the use of corticosteroids at the time of treatment of hyperthyroidism, may reduce the severity of orbitopathy and certainly is a factor to consider when confronted with a patient who has active hyperthyroidism and signs of infiltrative orbitopathy. Theoretically, T-cell suppression during early active disease may be a useful consideration for the future.

We have noted that in many cases, spontaneous hypothyroidism is associated with less severe orbitopathy and is therefore a useful prognostic indicator. The association of pretibial myxedema with orbitopathy is also significant. In a broad sense, pretibial myxedema correlates with increased likelihood and severity of orbitopathy and should be part of the primary assessment (Fig. 8-7). This also applies to acropachy and a feature we have noted in more severely affected patients, facial swelling.

Other Prognostic Determinants

Patients who smoke tend to have progressive and more severe orbitopathy and should be advised to discontinue smoking. Although the evidence is not conclusive, there are several studies that suggest severe physical and emotional stress can lead to the development of hyperthyroidism.

Table 8-1. Prognostic determinants for thyroid orbitopathy

CO-FACTORS	BETTER PROGNOSIS	WORSE PROGNOSIS
Age	Younger	Older
Race	Asian	Caucasian
Sex	Female	Male
Onset	Chronic (over 5 months)	Acute and subacute (under 3 months)
Smoking		Yes
Diabetes		Yes
Major life stresses		Yes
Thyroid function		
Clinical Status	Effective early control of hyperthyroidism Spontaneous hypothyroidism Euthyroid Control of induced hypothyroidism at the time of treatment for hyperthyroidism	Hyperthyroid (especially severe) Radioactive iodine treatment at the time of preexisting orbitopathy Residual thyroid tissue post-treatment
Onset of orbitopathy in relation to hyperthyroidism	Distant	Recent
Laboratory		High thyroid-stimulating antibodies (TSAb) Rapid hypothyroidism, thyroid-stimulating hormone (TSH), and TSH receptor antibody elevation post-treatment for hyperthyroidism High pretreatment T3 concentrations
Soft tissue components of Graves' hyperthyroidism	Mild to moderate orbitopathy	Severe orbitopathy Existing orbitopathy when hyperthyroid Pretibial myxedema Acropachy Facial swelling
Steroids at time of hyperthyroidism	Yes	

Consideration should also be given to the coexistence of other autoimmune diseases. From an ophthalmic point of view in particular, there is a significant incidence of co-involvement of the extraocular muscles with myasthenia and thyroid orbitopathy. Diabetes is a negative co-factor in thyroid orbitopathy. It has been our experience that patients with diabetes tend to have more severe and less easily managed orbital disease. In particular, the effect of corticosteroids on their diabetes limits the use of this agent, thus they may need adjuvant immunoregulatory agents. Orbital radiotherapy in this group is contraindicated because of the risk of progression of retinopathy. Other immunoregulatory diseases that may occur in patients with thyroid disease include pernicious anemia and vitiligo.

Radiation of the neck for nonthyroid disorders, such as thyroid carcinoma and Hodgkin's disease, can be associated with a spontaneous development of thyroid orbitopathy. We have experienced six patients with post-Hodgkin's disease in the head and neck region who have developed thyroid orbitopathy, all of whom appeared to have relatively mild orbital involvement.

In summary, the above factors should be considered in the assessment of the individual patient's situation, as they are useful predictive variables for contextualizing their disease. Attention therefore should be paid to age, sex, race, association with smoking, acuity of onset (acute onset patients being four times more likely to have severe disease), and relationship to thyroid disorder. The other factors to consider concern the clinical features, such as symptoms and character of onset of soft tissue signs and motility problems, degree of early physical distortion (proptosis), lid retraction, and rapidity of progression. These factors govern management and prognostication for the individual patient (Table 8-1).

Clinical Features

The clinical aspects of thyroid orbitopathy are best divided into features of soft tissue swelling and infiltration (inflammatory), myopathy, apical compression (visual threat), and abnormalities of ocular and lid position (appearance) as well as function. In general, all of these features tend to occur as a continuum. Assessing an individual patient requires consideration of the constellation of symptomatic and observable disease features in each of these categories in order to determine whether the patient is manifesting significant disease activity and to assess severity.

Soft Tissue Features

As stated previously, the soft tissue features of infiltrative disease consist in general order of occurrence of tearing, lid edema, conjunctival swelling (chemosis), fat prolapse, surface discomfort (which may lead to some visual difficulty), vascular engorgement associated with injection, and lacrimal gland enlargement. As the orbit becomes more congested, the patient becomes aware of a retrobulbar discomfort or aching feeling that they often describe as “something pushing behind the eye.” They may also note pain on eye movement in fields of restriction, suggesting progressive myopathy. In the more severe orbitopathies, these signs appear to develop in an acute or subacute pattern (that is, within approximately weeks up to 3 to 4 months), whereas the more chronic or insidious onset (4 months or more) tends to belie a milder course. The onset and progression of soft tissue features may be intermittent and variable in course and patients should be warned of this. In a retrospective questionnaire to our patients, we found that they are usually aware of a relatively precise onset of soft tissue signs and symptoms and in the more serious cases, are able to pinpoint the time of onset (acuity) and progression of lid swelling and ocular discomfort.

There are a number of practical tips with regard to early clinical diagnosis related to the effect of inflammation and pressure within the orbit. The patient often presents to the general practitioner with intermittent lid swelling that has a diurnal pattern; it is generally worse in the morning after lying prone all night, which may lead to a misdiagnosis of allergic disease. In contrast to allergy, these patients tend to be aware of some retrobulbar discomfort, intermittent asthenopia, tearing, and ocular fatigue (particularly with reading). Further, they do not have evidence of conjunctival follicle formation or seasonal relationships. It is also important to keep in mind that they frequently present with asymmetric disease, one orbit more involved than the other. The inflammation, infiltration, and proptosis affect the conjunctival structures and lead to burning, injection, grittiness, and an excessive outpouring of mucus with intermittent blurring of vision. This coupled with an abnormal lid position and chemosis may cause functional or physical obstruction of the lacrimal drainage system, leading to epiphora with the increase in severity of soft tissue features. Figures 8-8 ,8-9 ,8-10 ,8-11 ,8-12 demonstrate mild, moderate, and severe soft tissue features of thyroid orbitopathy.

We have occasionally encountered some patients who have a disproportionate degree of lid swelling when compared to their epibulbar and myopathic symptoms. They usually evidence a rather pale, edematous, noninjected distention of the lower lids that tends to be sensitive to anti-inflammatory intervention (steroids, radiotherapy), possibly reflecting disproportionate out-flow problems (Fig. 8-13).

It is important to note that the degree of fat prolapse should be evaluated separately from the skin changes associated with active thyroid orbitopathy, since patients can have a disproportionate amount of fat prolapse with very little lid edema or the opposite depending upon factors of age, venous out-flow, and disease activity (Fig. 8-14). Several studies

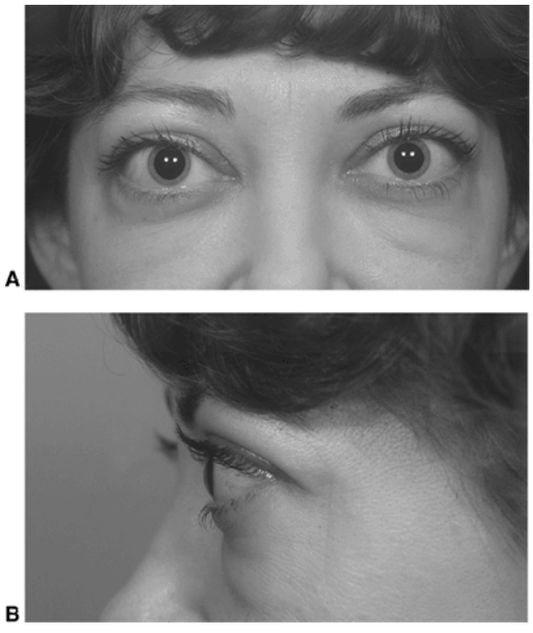

Figure 8-8. Mild thyroid orbitopathy. (A, B) This 37-year-old female was seen 2 years post-radioactive iodine with a 15-month (chronic) onset of variable lid swelling and proptosis. On physical examination, she had minimal pretarsal edema (+1), chemosis (+1), fat prolapse with temporal fullness, exophthalmometry measurements of 23 mm bilaterally (compared to old photographs of 15 mm), slight limitation in abduction bilaterally (to 45°), and widened interpalpebral fissures (13 mm). She was considered to have mild orbitopathy and was observed. Six months later, she was noted to be stable and was offered the options of bilateral müllerectomies with or without decompression and fat resection.

have suggested that there is an increase in some of the anterior orbital fat that accounts for the increasing fullness of the upper lid, particularly temporally.

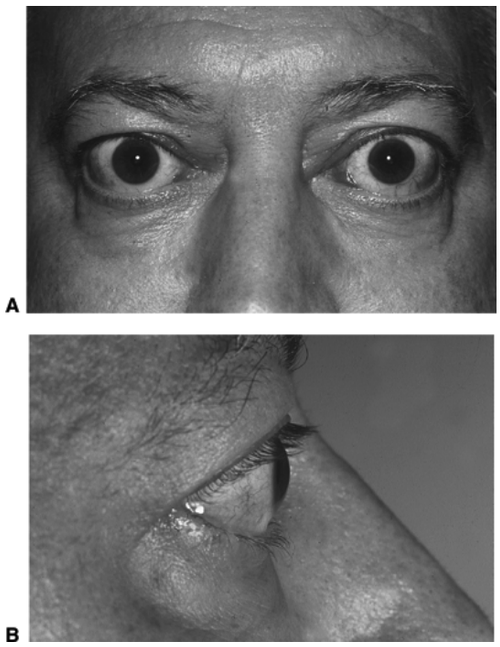

Figure 8-9. Moderate thyroid orbitopathy. (A, B) This 53-year-old man had a 6-month history of progression of thyroid orbitopathy after a subacute onset in spite of oral steroids. On physical examination, he had features of moderate and active orbitopathy with edema (+2), chemosis (+2), conjunctival injection, caruncular swelling, and decreased elevation bilaterally. His intraocular pressures rose from 18 mmHg on the right and 20 mmHg on the left to 28 mmHg and 30 mmHg respectively in upgaze. Exophthalmometry measurements were 25 mm on the right and 26 mm on the left. He underwent orbital radiotherapy followed by decompression after failure of oral steroids for treatment of his disease. His final exophthalmometry measurements were 19 mm bilaterally and he has been stable for 15 years.

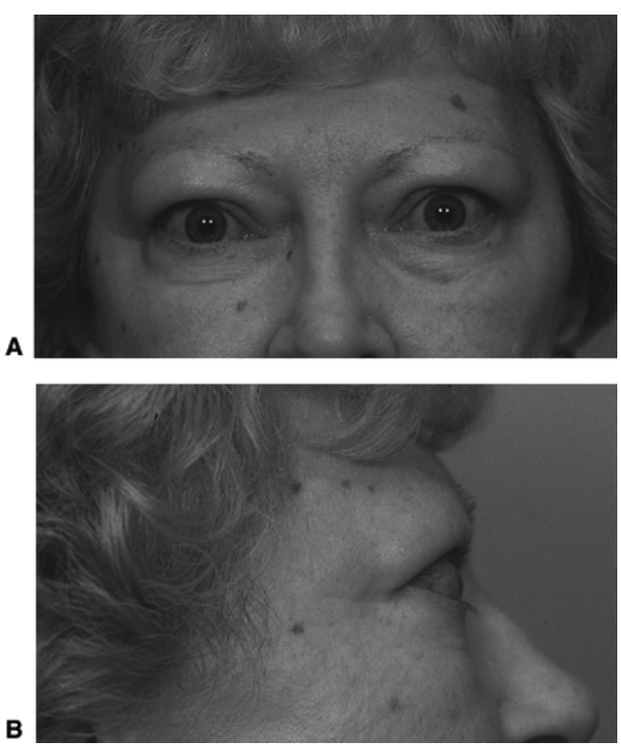

Figure 8-10. Moderate thyroid orbitopathy. (A, B) This 52-year-old female presented with a 2-month history of progressive onset of increasing soft tissue signs and diplopia 1.5 years after radioactive iodine. She had moderate edema (+2) with chemosis (+1), lid retraction, proptosis (18 mm bilaterally), fat prolapse (+2), restriction of upgaze to 10 bilaterally, and a left hypotropia in upgaze. Her intraocular pressures in 5 downgaze were 24 mmHg on the right and 20 mmHg on the left, rising to 42 mmHg and 30 mmHg respectively in upgaze. Her findings of active, moderate orbitopathy were the same 2 months later with a slight increase in diplopia. She underwent a trial of steroids followed by radiotherapy; within 6 months she had markedly reduced edema and an increase of upgaze to 20 with no diplopia with active moderate thyroid orbitopathy. Two years later, she underwent müllerectomy and blepharoplasty and had a full range of ocular movements.

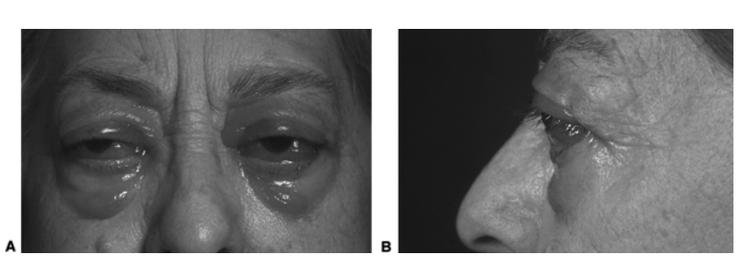

Figure 8-11. Severe thyroid orbitopathy. (A, B) This 60-year-old female had a subacute onset of periorbital swelling and proptosis concurrent with hyperthyroid symptoms. After receiving radioactive iodine, she noted increasing periorbital edema, decreasing vision, gray-outs with color desaturation, and persistent retrobulbar pain. She had reduced vision bilaterally (20/100 right eye, 20/70 left eye), severe edema (chemosis +3, edema +3), severe injection, proptosis (24 mm right, 22 mm left), and reduced extraocular movement in all positions of gaze. Her intraocular pressures were 38 mmHg on the right and 34 mmHg on the left. She underwent high-dose corticosteroid therapy and decompression for this severe active orbitopathy. Within 6 weeks, she had a vision of 20/60 right and 20/30 left with a slight increase in her extraocular movements, improvement of her visual fields and VEP, and reduction of her intraocular pressures to 20 mmHg bilaterally in the 5 downgaze position. She had also developed pretibial myxedema. She was stable 4 months postoperatively.

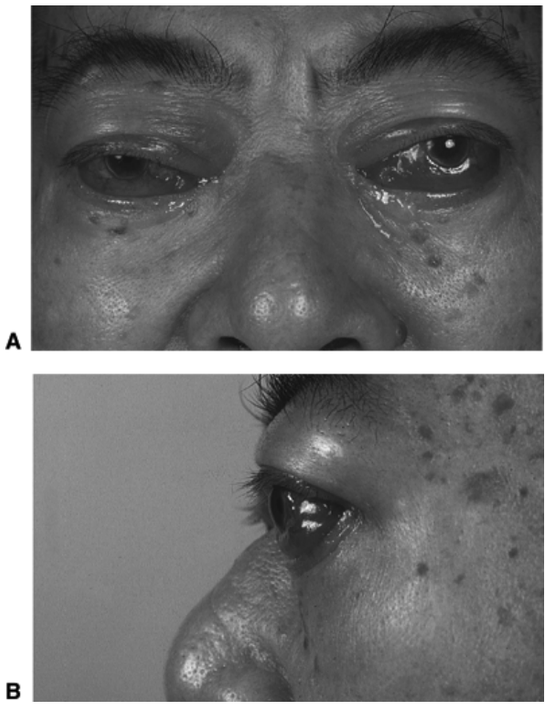

Figure 8-12. Severe thyroid orbitopathy. (A, B) This 75-year-old patient with diabetes had a 1-year history of progressive thyroid orbitopathy occurring 10 years after treatment for hyperthyroidism. He had longstanding macular degeneration on the left and his vision on the right was 20/40. On physical examination, he had severe orbitopathy with an exodeviation, marked restriction of movements in all fields of gaze, edema (+3), chemosis (+3), lid injection, and punctate staining of his cornea. He had the features of a small tight orbit syndrome, which was confirmed on CT scan, with ptosis rather than lid retraction as a result of apical compression and congestion. Because he was diabetic, he underwent urgent bilateral medial and lateral decompression with recovery of vision on the right (see Fig. 8-24). He later underwent lower lid elevations.

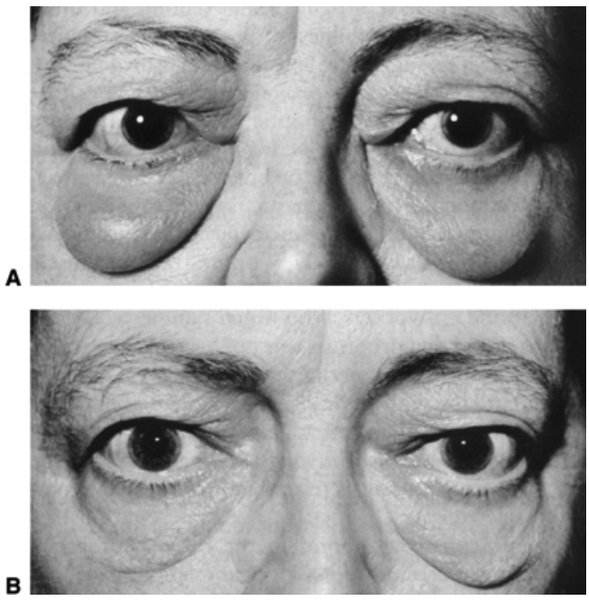

Figure 8-13. (A) This 61-year-old woman with thyroid orbitopathy demonstrates a disproportionate swelling of the anterior soft tissues. It was exquisitely sensitive to steroids, as shown in the lower photograph (B) taken 2 weeks after induction of steroid treatment (30 mg/day tapered to 15 mg/day). In spite of the marked lid swelling, she had 20 mm of proptosis, no chemosis, and mild muscle enlargement on CT scan with normal extraocular movements. Withdrawal of steroids caused recurrence of the lid swelling.

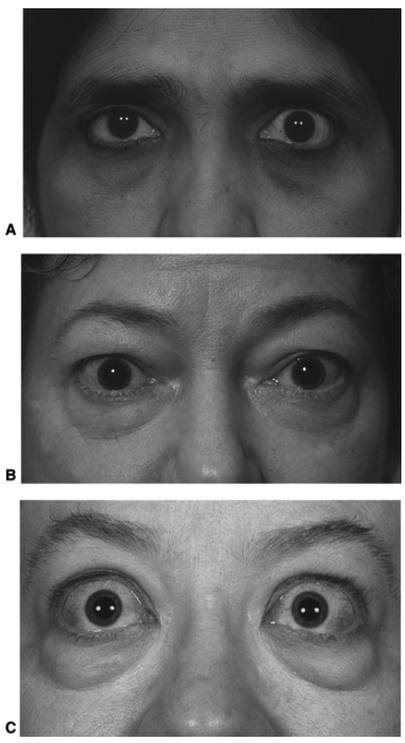

Figure 8-14. These three middle-aged women with thyroid orbitopathy demonstrate mild (A), moderate (B), and severe (C) fat prolapse associated with thyroid orbitopathy.

Table 8-2. Inflammatory index (worse eye).

SOFT TISSUE FEATURE		RATING
Chemosis	0	Absent
	1	Mild (to gray line)
	2	Moderate (to lid margin)
	3	Severe (over lid margin)
Conjunctival injection	0	Absent
	1	Present
Lid injection	0	Absent
	1	Present
Lid edema	0	Absent
	1	Mild
	2	Moderate
	3	Severe
Pain at rest (retrobulbar aching)	0	Absent
	1	Present
Pain on movement	0	Absent
	1	Present

Clinical Evaluation

In evaluating patients for soft tissue inflammatory features, the subjective symptoms that we look for are retrobulbar discomfort at rest and patients' awareness of lid edema. Further, we ask the patients about the speed or acuity of onset of inflammatory features, and whether the disorder has been the same, better, or worse since onset in order to establish the rate of onset and activity. From a physical examination point of view, we look for chemosis (mild, moderate, or severe), conjunctival injection (present or absent), lid injection (present or absent), and lid edema of the upper and lower lids (mild, moderate, or severe). The symptomatic and objective findings combine to establish an inflammatory index, which is assessed for the worse orbit and can result in a maximum of 10 (Table 8-2). Fat prolapse is evaluated as being mild, moderate, and severe. However, it really only reflects volume changes and evaluation can be compounded by the normal relaxation of tissues associated with aging (Fig. 8-14).

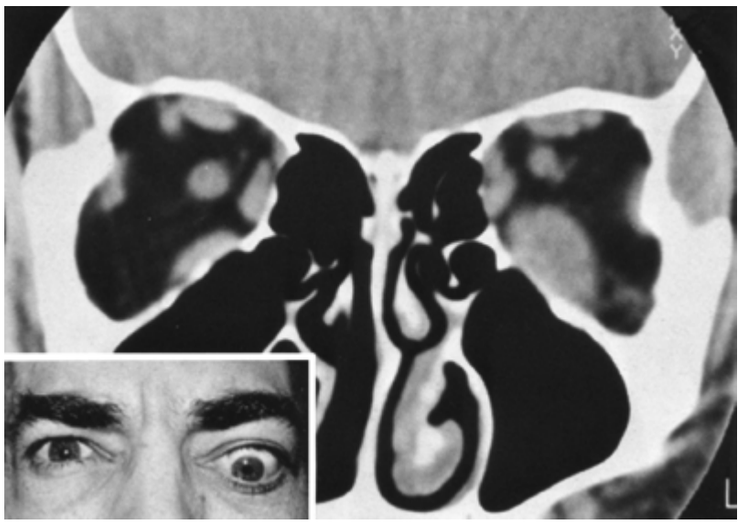

Figure 8-15. Although thyroid orbitopathy is usually characterized by involvement of more than one muscle, this 47-year-old man demonstrates a striking dominance of a left inferior rectus myopathy (30-diopter left hypotropia). Complete investigations, including TRH stimulation test, revealed normal thyroid function. He subsequently developed mild disease affecting the right eye. The coronal CT scan demonstrates the enlarged inferior rectus. After stabilization, the patient underwent left inferior and right superior rectus adjustable recession and achieved orthophoria in the primary position and to 20 upgaze and 50 downgaze. He subsequently underwent bilateral müllerectomies and a left lower lid elevation.

Myopathy

Infiltration, swelling, tightening, and scarring of the muscles generally manifest as diplopia with limitation of ocular movement that is classically intermittent in onset, progressive in more severe cases, occasionally sudden and permanent, and spontaneously reversible in rare instances. Myopathy is frequently associated with the soft tissue inflammatory signs, but it can occur in a few muscle groups, asymmetrically, and with minimal inflammatory signs and symptoms.

One of the early symptoms of myopathy is an awareness of an inability to read for extended periods of time, characterized by fatigability and discomfort. In addition, patients are aware of a tendency to blurring on saccadic movements, which they described as a momentary fogging of vision on horizontal or vertical refixation. (We refer to this as saccadic discord brought about by reduction in peak saccadic velocity, which correlates with increasing muscle size and age.) The early symptoms are also related to the propensity of this disorder to affect the vertical muscles clinically. Thus patients are more vulnerable in positions of gaze requiring use of these muscles and at times of day when orbital edema is maximal (i.e., in the morning and late in the day). They are therefore often aware of diplopia when lying in bed, a position that forces use of the vertical muscles.

With increasing severity of myopathy, the patient first notes a sensation of stretching and later the development of pain on eye movement. In the early stages, diplopia is characteristically present for the first few hours of the day and as the disorder worsens, it becomes more persistent throughout the day. Patients can usually document how long diplopia persists during the day. As the myopathy progresses, the patient becomes aware of increasing pain or a stretching sensation followed by constant diplopia in extremes of gaze, which gradually affects the central positions and ultimately becomes progressive in terms of the increasing separation of images. There are, however, some patients with significant myopathy where the major finding is symmetrical restriction in all fields of gaze with relatively little diplopia in the central positions, since they cannot move off axis. This is reflected in a decreasing range of movements and lesser degrees of deviation because of concomitant involvement of antagonists. **Patients with significant restriction of movement in all positions of gaze are at risk of developing optic neuropathy**.

The frequency of **clinical** occurrence of myopathy in descending order is inferior, medial, superior, and lateral rectus involvement (Figs. 8-15 and 8-16). However, it is important to note that any muscle may be involved in the orbitopathy, including the obliques. In fact in a controlled radiologic study of thyroid orbitopathy, we found that the most frequently involved complex was the superior muscle group. With progression, the degree of deviation increases, particularly in patients who have asymmetrical disease. In addition, the patient obviously moves from a phoric to tropic deviation. The majority of patients have some degree of asymmetry in onset and progression of their myopathy. With increasing involvement of the muscle, the anterior radicals of the muscular vessels become engorged, producing characteristic dilated and visible vessels subconjunctivally over the insertions (see Figs. 8-6 , 8-9 , and 8-10). As the muscles tether, they become rigid on forced duction testing, and the degree to which the intraocular pressure rises on movement of the agonist (especially upgaze related to the tight inferior rectus) correlates positively with severity. A rise of more than 4 mmHg is consistent with the diagnosis of restriction associated with thyroid orbitopathy. The greater the increase of pressure above this level, the more severe the orbitopathy. We noted that a rise of over 9 mmHg correlates with optic neuropathy.

There is an unusual and small subcategory of patients who present with a fulminant inflammatory and myopathic syndrome that mimics acute myositis. We have seen few patients in this category (Fig. 8-17). Their acute myositis is characterized by a very rapid (acute-days) onset of orbital inflammation, congestion, chemosis, injection, and painful limitation of ocular movements. In every respect, the syndrome parallels (and in fact may be) the nonspecific orbital inflammatory myositic syndrome except that it demonstrates associations with an underlying thyroid disorder (i.e., a nonsuppressible thyroid gland). This particular subcategory is exquisitely sensitive to treatment with corticosteroids, and emphasizes the need to rule out thyroid disorders in acute orbital myositis. Only one of our patients who presented primarily with myositis and responded positively to a short course of corticosteroids developed thyroid orbitopathy 10 years later. The differential features of thyroid myopathy and orbital myositis are discussed in the chapter on inflammatory diseases.

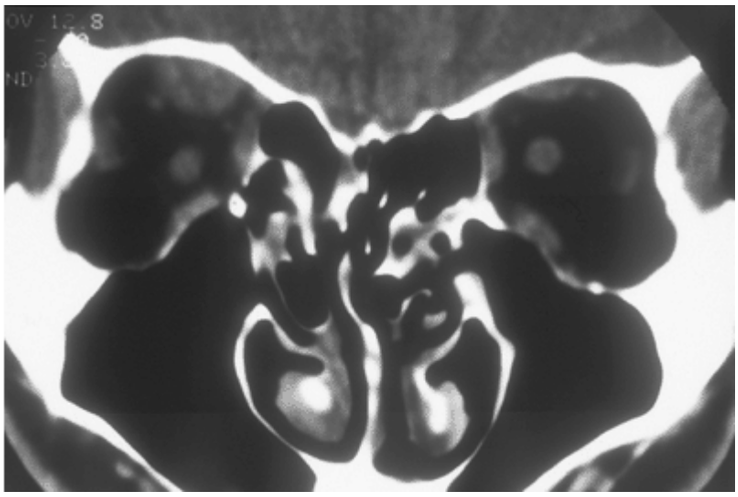

Figure 8-16. This 56-year-old male presented with a 1-month history of epiphora followed by diplopia, which was associated with preseptal edema (+2) and a widened interpalpebral fissure on the right with 1 mm superior scleral show. In addition, there was downward and outward displacement of the globe and restriction of movement on downgaze with a 30-diopter right hypertropia and 6-diopter exotropia. He had a positive forced duction and a nonsuppressible thyroid gland. He was observed for 6 months and noted to be stable so he underwent a right superior rectus recession.

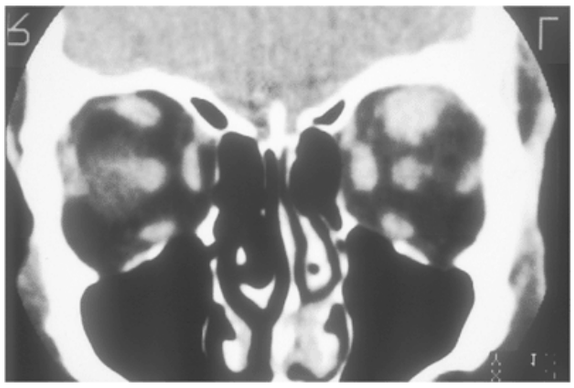

Figure 8-17. This 49-year-old man presented with a 3-week history of painful, tender swelling of the left upper lid, and injection and chemosis associated with ptosis. He had pain on ocular movement and was becoming aware of diplopia on upgaze. Physical examination revealed a left ptosis with 2 mm of downward displacement and 1 mm of proptosis. CT scan demonstrates an enlarged left superior rectus muscle with infiltration of the adjacent orbital fat. From a medical point of view, he had a history of ankylosing spondylitis and on investigation had a normal free thyroxine level, a low TSH level, and a negative response to TRH stimulation. These findings were compatible with euthyroid Graves' disease. The orbital myositis responded dramatically to oral steroids. This patient demonstrates the unusual association of acute myositis with abnormality of thyroid function.

Restrictive strabismus may be the first and only sign of thyroid orbitopathy. We have noted that this presentation is particularly common in the elderly, who may in fact have subclinical thyroid orbitopathy previously. CT scan reveals characteristic muscle enlargement with evidence of fat replacement, suggesting longstanding disease (see Fig. 8-27F).

It should be noted that thyroid orbitopathy has an infrequent association with myasthenia gravis. This should be suspected when the patient demonstrates a variable ptosis, a changing or unusual deviation (particularly exodeviation), a negative or incongruous forced duction test, a positive ice test, or a positive Tensilon test (Fig. 8-18). Another rare association is ocular myotonia, which is characterized by episodic, involuntary, sustained contracture of the extraocular muscles. Finally, some patients describe a phosphene or flashing lights in association with movement, particularly when elevating the eye with tight inferior recti.

Clinical Evaluation

The subjective evaluation of strabismus and motility disorders consists of eliciting visual fatigue, saccadic discord, or with progression, a stretching sensation that develops into pain on extraocular movement and ultimately symptomatic diplopia, which may progress from intermittent to being present only in positions of gaze and before becoming constant. In addition, the patient can define whether the diplopia has been the same, better, or worse on primary and follow-up examinations. The objective findings are evaluated based on ductions and versions, the simplest and most reliable method being measurement of degrees of movement in the horizontal and vertical planes based on a modification of the Hirschberg corneal light reflex method (i.e., at the pupil edge 15 of movement, mid-iris 30 of movement, and limbus 45 of movement). Finally, manifest strabismus is simply measured with prisms in the primary position, upgaze, downgaze, and the horizontal extremes. We then measure the intraocular pressure in the primary position, upgaze, or in the direction opposite to the maximal restriction.

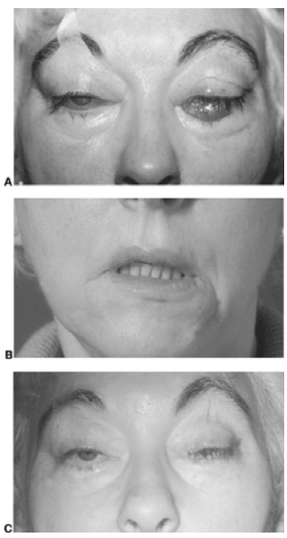

Figure 8-18. (A) This 56-year-old female with known myasthenia gravis developed subacute onset of marked periorbital edema, chemosis, and conjunctival prolapse. On examination, she had almost complete ptosis with severe soft tissue signs and no extraocular movements. She was also noted to have marked dysphonia along with relaxation of the facial muscles (B). On laboratory testing, she had recurrence of hyperthyroidism, which precipitated the dysphonia and orbitopathy. She was treated with high-dose steroids and plasmapheresis for the myasthenia, orbital radiotherapy, and thyroid suppressive drugs. (C) Photograph of the same patient 6 weeks postradiotherapy.

The Crowded Orbital Apex Syndrome – Dysthyroid Optic Neuropathy

As noted earlier with increasing severity of soft tissue swelling, the development of a constant retrobulbar aching or pushing sensation suggests crowding within the confined spaces of the orbit. Ultimately, this crowding of the apex leads to optic neuropathy, which has long been recognized as a serious consequence in severe thyroid orbitopathy. The pathogenesis has been ascribed to many causes, including

toxic optic neuropathy, but more recently has been attributed primarily to apical orbital crowding and increasing orbital pressure. Our review of the clinical and computed tomographic findings of patients with optic neuropathy compared to control thyroid orbitopathy groups confirmed that orbital crowding is the primary mechanism. We identified clinical signs and symptoms that reflect crowding of the orbital apex and lead to a specific psychovisual and motor syndrome (Figs. 8-19 and 8-20). Overall, this syndrome affects approximately 6% of patients with thyroid orbitopathy. We and others have identified a small subgroup with optic neuropathy associated with optic nerve stretching due to increased orbital volume rather than compression of the nerve at the apex (Fig. 8-21).

Clinically the main manifestation of apical compression is optic neuropathy, but there are other features related to crowding, such as proptosis, palpable lacrimal glands, greater increased intraocular pressure in upgaze (generally 9 mm or more), marked ocular motor limitation, and soft tissue components with venous congestion. In short, this group of patients has physical findings that reflect a more severe degree of myopathy, inflammation, and orbital congestion when compared to a control group of patients with thyroid orbitopathy and no optic neuropathy. In addition, the features of the crowded orbital apex (i.e., significant tissue swelling, diplopia, tearing, and discomfort) may obscure the diagnosis of optic neuropathy and dominate the symptoms, leading to a failure of the physician and patient to recognize the optic neuropathy early. Indeed in half of the instances, on referral neither the physician nor the patient was aware of the early signs of optic neuropathy. **This situation implies a need to be particularly vigilant with patients who have the constellation of findings suggesting a predisposition to optic neuropathy**. The progressive symptoms that can be elicited on questioning patients are intermittent gray-outs of vision, decreasing vision, and color desaturation.

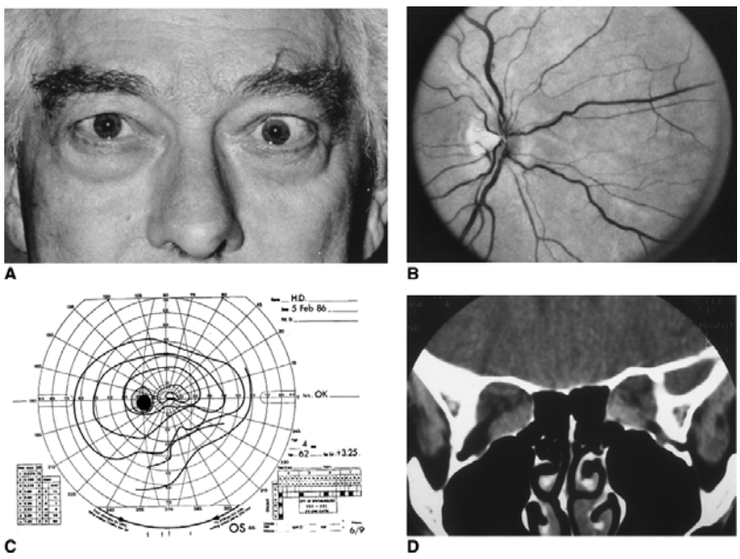

Figure 8-19. (A) This 62-year-old man was referred with diplopia, proptosis, and lid swelling of 1-month's duration, and desaturation of left color vision for 3 months. He had been treated for hyperthyroidism at the onset of his orbitopathy. On physical examination his vision was 20/20 right and 20/25 left. Exophthalmometry was 18.5 mm right and 20.0 mm left, and there was an 8-diopter right hypertropia and 12-diopter esotropia with marked limitation of ductions bilaterally. (B) On fundus examination he had slightly hyperemic discs with minimal blurring of the nasal margin. He had been treated with high-dose steroids and had failed to respond visually. His VEP showed a large delay in implicit times from the left eye, and (C) Goldmann visual fields demonstrated an inferior nasal depression with a small relative paracentral defect. (D) CT scan demonstrated severe apical crowding bilaterally. He underwent bilateral apical decompressions with full recovery of vision and an increase in esotropia to 30 diopters. Subsequently, he had bimedial recession with adjustable sutures and is currently orthophoric.

Patients with optic neuropathy are older at the time of examination and are more likely to be male (Fig. 8-19). Those with diabetes seem to have a greater risk for optic neuropathy, a stormier and more recalcitrant course, and, overall, tend to have more severe optic neuropathy. The chief presenting symptom that differentiates patients with optic neuropathy from others with thyroid orbitopathy is graying of vision or color desaturation. Patients rarely volunteered this information unless specifically questioned. They may have a tight orbital septum, resistance to retropulsion, and often complain of an aching fullness or pressure-like sensation behind the eyes that may be exacerbated on movement.

In our experience, the physical findings that should alert the clinician to a risk of optic neuropathy are more marked proptosis; palpable lacrimal glands; greater increase in intraocular pressure on upgaze; greater restriction of extraocular muscles, particularly in supraduction and abduction,

and greater incidence of vertical tropia. We noted that muscle restriction is often bilateral but asymmetrical, in contrast to Trobe and coworkers, who noted symmetry. Others have suggested that proptosis was not helpful in assessing the risk of optic neuropathy; however, we found that overall patients with optic neuropathy had greater degrees of proptosis. **The most significant correlate is severity of myopathy**, suggesting that the risk of optic neuropathy is related to increase in extraocular muscle volume. There is also a subgroup of patients who do not necessarily have significant proptosis but have a rather narrow orbital apex (particularly Asians) that may lead to earlier compressive features without other significant manifestations.

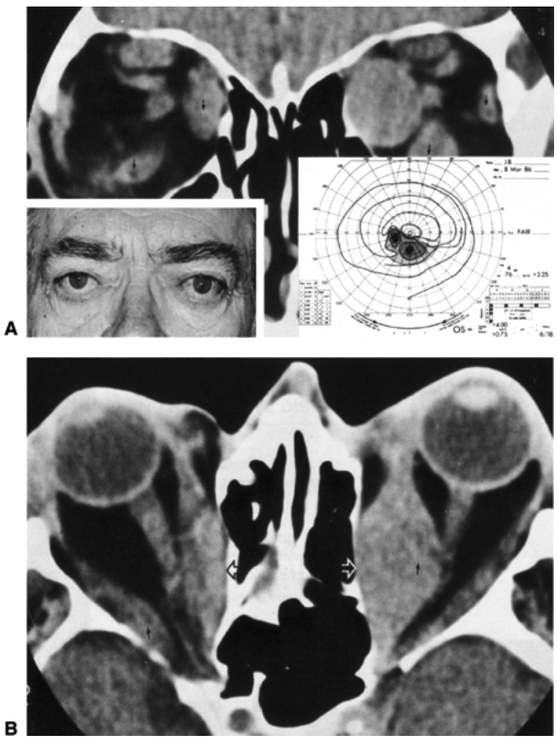

Figure 8-20. (A, left inset) This 76-year-old male developed hyperthyroidism 13 years prior to referral. His initial orbitopathy was noted 5 years after treatment with radioactive iodine. On presentation, he was aware of deteriorating vision (worse on the left than right), increasing proptosis, and fading color vision. On physical examination he had vision of 20/20-1 right and 20/40 unimprovable on the left, palpable lacrimal glands, markedly widened interpalpebral fissures, and 27-mm exophthalmos bilaterally. There was bilateral limitation of elevation and inferior punctate keratopathy. (A, B) CT scans demonstrated apical crowding, worse on the left, with medial bowing (“Coca Cola sign”; large arrows) into the ethmoids, marked proptosis, anterior displacement of lacrimal glands, and low-density areas within muscle (small arrows). (A, right inset) Visual field showed a left inferior arcuate scotoma, and VEP demonstrated bilateral optic neuropathy more severe on the left. In view of the degree of proptosis and the apical orbital crowding, the patient underwent a left three-wall and right two-wall decompression. Postoperatively, his vision improved to 20/25 left, and exophthalmometry was 20 mm bilaterally with recovery of fusion.

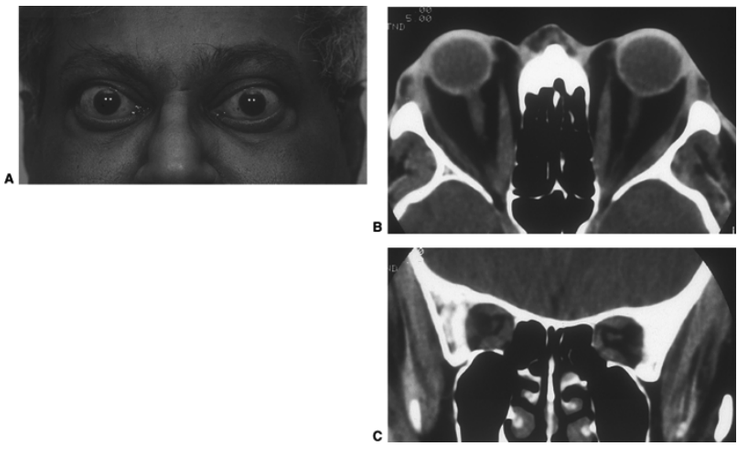

Figure 8-21. (A) This 51-year-old male presented 6 years postradioactive iodine with an 18-month history of progressive proptosis. Over the next 6 months, he developed increasing proptosis and decreasing ocular movements with periorbital swelling. He responded at first to prednisone but ultimately his symptoms recurred on reduction of his steroids (and after receiving radiotherapy) because the pathogenesis, as demonstrated on the CT scans (B, C), was related to axial proptosis and stretching of the optic nerve rather than apical compression. Note low-density areas in the muscles.

Visual acuity was poorer in the optic neuropathy group, but was certainly not as poor as might be expected with some patients still able to read 20/20. Ophthalmoscopy of the optic nerve head is also a less consistent indicator; slightly less than half of the patients we reviewed had normal-appearing discs. Nevertheless, elevation and hyperemia or pallor are significant signs. An afferent pupillary defect is present if the disease is asymmetric; however, its absence may reflect bilateral compression. Visual field abnormalities include increased size of blind spot, paracentral scotoma, nerve fiber bundle defect, central or centrocecal scotoma, and generalized constriction. These defects appear in isolation or in varying combinations. In the majority, nerve fiber bundle defects are inferior (Figs. 8-19 and 8-20). We also noted a vertical step, which may be bilateral. In our experience, color vision is a relatively sensitive indicator of optic nerve dysfunction and is a simple and reliable test that can be routinely applied in the clinical setting. A number of patients with severe apical crowding and venous out-flow problems may have concomitant signs of congestion of the choroid that leads to striae in the posterior pole and progressive hyperopia.

In summary, optic neuropathy is frequently subclinical, may be masked by other symptoms, and may be missed unless specifically elicited. Our observations suggest that the patient to suspect is older, more frequently male, has a later onset of thyroid disease, is a smoker, and is more frequently diabetic. On physical examination, these patients have more proptosis, a higher incidence of significant vertical deviation, and more severe limitation of extraocular movements. Additionally, this greater severity of myopathy was reflected in higher increases in intraocular pressure on upgaze (over 9 mmHg). In effect, the more severe the disease in terms of the myopathy, the greater the index of suspicion for optic neuropathy, which is reflected in tropias, reduced ductions and versions, and increasing tightness on forced duction testing.

Imaging is an important investigation when optic neuropathy is suspected. The findings of apical crowding, increased proptosis, enlarged muscle diameter (particularly apically), increased superior ophthalmic vein diameter, retrobulbar dilatation of the optic nerve sheath, and anterior displacement of the lacrimal gland should alert the clinician to a possible optic neuropathy, and appropriate psychophysical and electrophysiologic testing should be done. Another feature that may indicate apical crowding is evidence of a relatively sudden angulation of the posterior third of the muscle as it abuts on the optic nerve (Fig. 8-22). In particular, coronal scans are most useful in assessing the degree of crowding of the apex and the relief of this following operative decompression. This crowding, along with inflammation, is the physiological basis for the compromised venous out-flow, neuropraxia, reduced axonal transport, and restricted ocular movements that constitute this syndrome. All muscle indices (extraocular muscle diameters; muscle diameter index, i.e., the sum of all mean muscle diameters) were significantly increased in optic neuropathy orbits as opposed to nonneuropathy orbits. Examination of muscle enlargement ratios (i.e., the ratio of maximum muscle diameter of each muscle compared to the same muscle in a group of normal subjects) showed a proportional enlargement of the major muscle groups in neuropathy versus nonneuropathy thyroid orbitopathies, the degree of enlargement being greater in those with optic neuropathy. This suggests that no specific muscle or group of muscles was enlarged out of proportion in neuropathy orbits. The overall constellation of symptoms, signs, psychophysical findings, and imaging outlined should raise the clinical index of suspicion and lead to prompt recognition and management of optic neuropathy.

Clinical Evaluation

Symptomatic evaluation of visual function consists of eliciting the patient's awareness of normal versus abnormal vision and color vision disturbances, and whether or not these have been the same, better, or worse since onset or last examination. Objective findings consist of assessment of central vision with and without glasses and with best corrected vision. We use the Pseudo-isochromatic Plates (American Optical Corporation) to assess color vision in the clinic. (The Ishihara, designed to screen for congenital color vision abnormalities rather than for acquired abnormalities, is less effective in detecting the color vision defects associated with thyroid orbitopathy). We measure the pupils directly and with the swinging eye flashlight test looking for a Marcus-Gunn reflex, which we document with neutral density filters. The fundus examination allows assessment of presence or absence of spontaneous venous pulsation, edema or pallor of the optic nerve head, or the presence of choroidal folds.

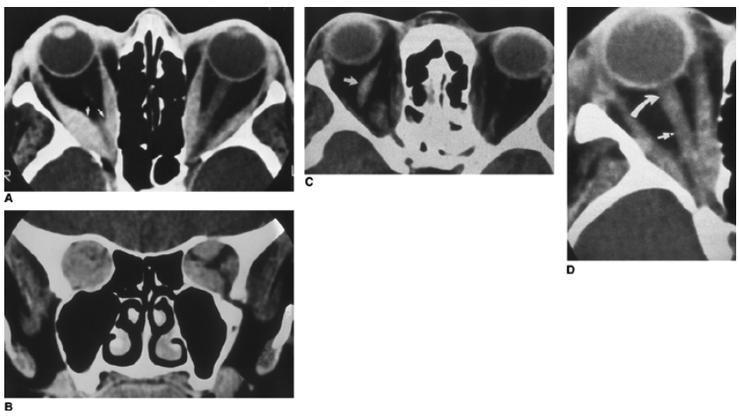

Figure 8-22. Axial (A) and coronal (B) scans demonstrate the features of apical orbital crowding in dysthyroid optic neuropathy. Note the dramatic involvement of the posterior half of the muscle belly and the acute angulation (A, arrows) of the right medial and lateral rectus muscles in the axial scan, as well as obliteration of the perineural fat on the coronal scan. (C) This axial CT scan demonstrates a dilated superior ophthalmic vein in thyroid orbitopathy in a patient who had optic neuropathy. (D) Enlargement of the distal optic nerve sheath and prolapse of the lacrimal gland is demonstrated in this scan of a patient with the crowded orbital apex syndrome. (Figs. 8-22C and D reproduced with permission from Nugent RA, Belkin RI, Neigel JM, et al. Graves orbitopathy: correlation of CT and clinical findings. Radiology 1990;177:675-82.)

It is important to note that there are other causes of visual difficulty that are extremely common with thyroid orbitopathy. These include astigmatism brought about by lid retraction as well as induced hyperopia as a result of flattening of the posterior pole when there are choroidal folds. Commonly, the development of corneal changes may result in significant visual difficulty.

Lid Malposition and Appearance in Thyroid Orbitopathy

Lid malpositions, particularly upper lid retraction, are the most common ocular features of thyroid orbitopathy. However, lower lid retraction, ptosis, and entropion may occur. Lid malpositions contribute to the exposure, tearing, astigmatism, and cosmetic deformity of thyroid orbitopathy. The major pathophysiologic mechanism for lid retraction are fibrosis and contracture of the upper or lower musculoaponeurotic complexes, and possibly sympathetic stimulation or increased sympathetic tone. In addition, proptosis contributes to lid retraction and exposure. The degree of retraction may be variable as a manifestation of sympathetic stimulation, overmedication (thyroid replacement), or natural anxiety level. Upper lid retraction is often worse in acute thyrotoxicosis or when the patient is anxious at the time of examination (a factor that should be taken into account when assessing retraction). It is also important to note that patients with significant inferior rectus tethering, particularly when asymmetrical, may have an accentuation of the degree of upper lid retraction (fixation duress) on attempted upgaze.

Some cases of acute upper lid retraction has been ascribed to sympathetic stimulation or increased sensitivity to circulating catecholamines, a fact that has not been clearly validated. In a clinical, CT, and pathologic study of patients undergoing müllerectomy for lid retraction, we found that features of smooth muscle damage were not evident and the factor best correlating with lid retraction was evidence of involvement of the superior striated muscle complex (Fig. 8-23). Numerous studies have correlated superior muscle complex involvement as the major mechanism for lid retraction.

Upper lid retraction is often the first sign, and may be asymmetrical and intermittent in onset. It is often but not always associated with some evidence of swelling of the lid. There is a tendency for the upper lid to show some lateral arching. On downward pursuit movement, decreased maximum levator function, lid lag, or a staccato-like delayed movement is noted. Mild lid retraction usually implies intersection of

the lid with the upper limbus (margin reflex distance [MRD] 6); moderate suggests 2 mm to 4 mm of scleral show (MRD 6 to 10); and severe suggests more than 4 mm (MRD 10 or more) of scleral show. Generally, as the retraction increases, the maximum levator function decreases.

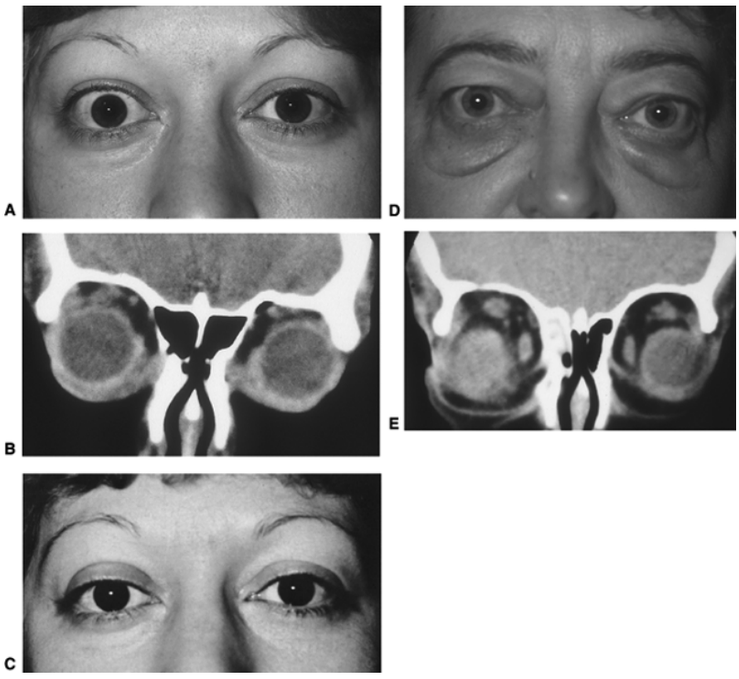

Figure 8-23. (A) This 30-year-old woman presented 4 years after an episode of hyperthyroidism with right lid retraction. (B) The coronal CT scan demonstrates a very slight enlargement of the superior muscle complex. (C) The patient's appearance is shown after a graded right müllerectomy. (D) This 53-year-old woman presented with periorbital edema (+3), proptosis, and lid retraction with normal extraocular movements and no chemosis. (E) Her coronal CT scan demonstrates enlargement of the superior muscle group (SMG), accounting for her lid retraction.

The patient presenting with only lid retraction invokes the differential diagnosis outlined in Table 8-3 . The major causes are neurologic abnormalities, cicatricial processes, and ocular and orbital malposition.

In addition to lid retraction, a small percentage of patients with thyroid orbitopathy develop ptosis. The primary cause is stretching of the capsulopalpebral structures or infrequently, an association with myasthenia gravis. Concurrent myasthenia gravis should be suspected in patients who have variable ptosis, an unusual strabismus (e.g., exodeviation), markedly variable diplopia, or fluctuating lid retraction, and can be validated by appropriate testing. Thus, care should be taken to assess patients for a nonsclerotic component to their myopathy (i.e., negative forced duction or failure of the forced duction to correlate with degree of deviation).

Table 8-3. Differential diagnosis of eyelid retraction in thyroid orbitopathy

- Graves' disease
- Neurologic disease
  - Marcus Gunn phenomena
  - Midbrain disease
  - Hydrocephalus
  - Parinaud's syndrome
  - Trauma to cranial nerve III
  - Aneurysm involving cranial nerve III
- Sympathomimetic drugs
- Cirrhosis
- Congenital
- Postsurgical retraction
  - Ptosis surgery
  - Lid reconstruction
- Post-traumatic lid scarring
- Idiopathic

Longstanding and severe proptosis may lead to ptosis as a result of stretching of the levator structures, wherein there is evidence of thinning of the aponeurosis, absence of an upper lid fold, decreased maximum levator function in upgaze, and general lengthening of the lid. Finally, it should be noted that in our experience, ptosis can occasionally be a feature of severe apical crowding in a particularly tight orbit but is then associated with other manifestations of apical crowding previously described. We have noted in such instances that following decompression, lid retraction usually replaces the ptosis (Fig. 8-24).

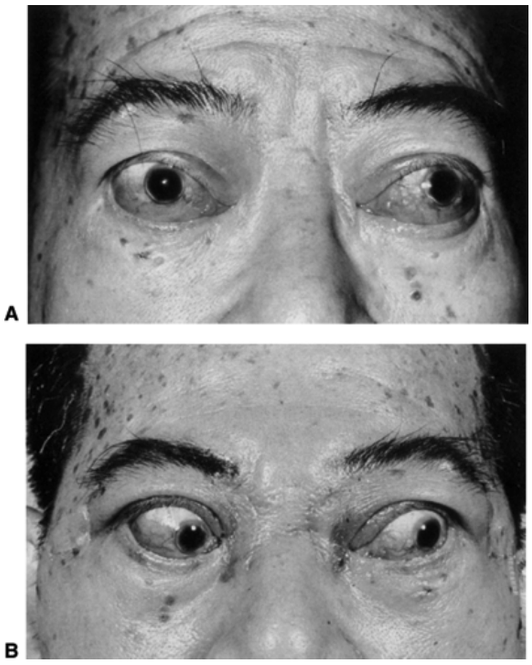

Figure 8-24. This 75-year-old man presented with a severe, active, congestive orbitopathy and optic neuropathy that developed over a 6-month period 8 years after he first noted prominence of his eyes and 5 years after treatment for hyperthyroidism. He had left macular degeneration with hand-movement vision, right visual acuity of 20/100, proptosis of 22 mm left and 21 mm right, severe chemosis, and marked limitation of extraocular movements (A – attempted left gaze). Postoperatively (B – attempted left gaze), note improvement in soft tissue signs, reduction of proptosis, increased lid retraction, and increased extraocular movements. VEP returned to normal postoperatively and vision improved to only 20/70 due to the presence of a cataract. Following cataract extraction, vision on the right side was 20/25. Such dramatic resolution of soft tissue features is often seen due to relief of venous congestion.

Lower lid retraction reflects degree of proptosis and the same pathogenetic mechanisms as with the upper lid, but tends to be more constant in appearance. In combination with proptosis and chemosis, it may significantly increase epiphora, a common feature of thyroid orbitopathy. The poor lid position interferes with the normal flow of tears and the chemosis may act as an obstructive element in the punctal region. Entropion and lateral lid elevation are more commonly seen as a complication of decompressive or lid surgery.

A striking eyelid malposition phenomenon that we have noted in patients with severe proptosis is the tendency for the lower lid to contract in a peculiar manner. These patients demonstrate a retrusion of the lid on horizontal shortening of the lower lid associated with blinking. This contraction of the lid may occasionally be associated with retroplacement of the lower lid behind the equator and an alarming, acute prolapse of the eye that can be reversed by relaxation of the lid and gently applying pressure to the globe.

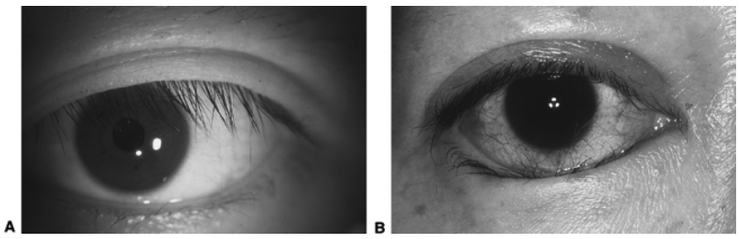

Figure 8-25. (A) This 19-year-old Asian male had a 2-year history of progressive proptosis following hyperthyroidism. His major symptoms were related to corneal irritation brought about by inversion of the upper lashes. (B) This photograph demonstrates eversion of the lashes of the lower eyelid in an Asian patient with thyroid orbitopathy and accentuation of an epiblepharon.

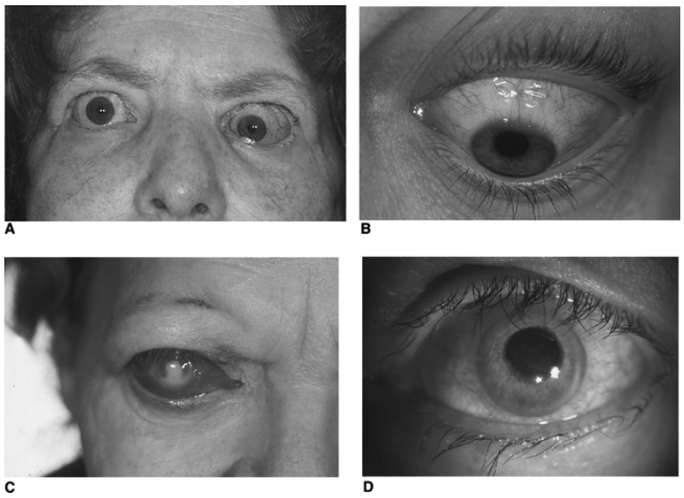

Figure 8-26. The features of corneal exposure in thyroid orbitopathy. (A) This 54-year-old woman was seen 3 years after the concomitant development of hyperthyroidism and orbital disease. She had bilateral corneal exposure due to lid retraction, exophthalmos, marked restriction of upgaze, and an absent Bell's phenomenon. On the left side, she had a hypotropia with trichiasis. (B) The features of superior limbic keratoconjunctivitis are demonstrated. This nonspecific condition has no known cause but when bilateral, it is frequently associated with dysthyroid states. This 41-year-old female developed mild thyroid orbitopathy associated with hyperthyroidism 1 year prior to presentation. (C) This patient presented with a right *Pseudomonas* corneal ulcer secondary to severe exophthalmos, lagophthalmos, and bilateral inferior rectus restrictive myopathy. (D) This 57-year-old woman presented with severe active orbitopathy characterized by proptosis, periorbital edema, corneal exposure due to lagophthalmos, and a lack of a Bell's phenomenon, which led to corneal epithelial damage.

It is of particular note to recognize that Asian patients with thyroid orbitopathy (Fig. 8-25) are prone to the development of corneal problems as a result of the combination of a tight orbital septum, swollen epicanthal folds, and retraction of the posterior lamellae that allow the nonfixed anterior lamellae to roll over the lid margin and create inversion with trauma to the cornea from the lashes (Fig. 8-26).

Another feature that may be seen in patients who have thyroid abnormalities, in particular hypothyroidism, is superior limbic keratitis (Fig. 8-26B), which is characterized by a fine, nodular, superior pannus with slight keratinization of the epithelium. This may occur as a result of lid retraction. It is associated with localized injection and significant symptoms of irritation and foreign body sensation, and there is frequently evidence of adjacent filamentary keratitis. Our preferred management for patients with this feature consists of a topical application with cotton-tipped applicators of silver nitrate 1% to the area of involved conjunctiva and to the upper palpebral conjunctiva. This treatment can be done at decreasing intervals as the disease improves. Failing this, a localized conjunctivectomy is very effective. If the associated lid retraction is severe, it can be dealt with surgically.

Clinical Evaluation

In the clinical evaluation of appearance and exposure, the subjective symptoms that we seek are the presence, absence, variability, or progression of awareness of tearing, foreign body sensation, lid retraction, or proptosis. The patient will also be able to define for you whether these have been the same, better, or worse since onset or since last examination. The objective findings that we look for are the presence or absence of fat prolapse, width of the interpalpebral fissure, and the degree of lid retraction as an expression of the margin reflex distance (MRD) or upper and lower scleral show. Levator function is measured as the difference between the lid position in extreme up and downgazes. As the scarring of the levator increases, there is a decrease of maximum levator function in downgaze compared to a decrease in upgaze when there is aponeurosis weakening. Lagophthalmos is then gauged with a ruler directly on attempted eyelid closure, and exophthalmometry is measured with a Hertel exophthalmometer. Careful biomicroscopy of the cornea, with and without fluorescein, identifies the presence or absence of erosions. We frequently do Schirmer testing and Rose-Bengal staining since a relatively high percentage of women in this age group have dry eyes.

Disease Activity and Severity Determinants

Disease Activity

Interventions are governed by assessment of the two broad categories of disease activity and disease severity. These features have to be individualized to the patient and related to other co-factors that may exist in determining interventions and prognosis. We try to develop disease activity and severity determinants based on the four categories of vision, inflammation, motility, and appearance, which will be discussed later in the chapter. Generally speaking, one can expect spontaneous improvement in patients who have mild or even moderate disease but this is not the case in patients who present with or develop severe disease.

The major indices in the evaluation of thyroid orbitopathy can be divided into those that are largely subjective and relate to evaluating disease activity, and those that are largely objective and relate to severity and extent of disease. As a broad simplification, Table 8-4 defines the major indices in thyroid orbitopathy.

The major clinical determinants of disease activity are acuity of onset of soft tissue features, progression as noted above (i.e., rapid onset, rapid progression in months by history and on close follow-up), and the development of clinical symptoms such as spontaneous retrobulbar pain, discomfort on movement, tearing, features of soft tissue swelling, myopathy, optic neuropathy (gray-outs of vision), and mechanics of the disorder (such as proptosis and lid retraction).

The symptomatic features of the disease should not be overlooked and can be elicited by asking patients about the tempo of onset, disease progression, and change with time as well as the presence or absence of subjective symptoms such as tearing, pain on ocular movement, or persistent deep retrobulbar discomfort (often described as a pressure or pushing sensation). In addition, patients can clearly define their visual difficulties and the degree of swelling that they are experiencing through directed questions concerning:

- the amount of diurnal variation
- their perception of periorbital structures when they are maximally swollen, including the degree of facial swelling
- disturbances of vision (including disturbances brought about by limitation of movement, fatiguability with near tasks, abnormal saccadic movements, diplopia, corneal changes and refractive error, and optic neuropathy) that may be of complex origin but **from the patient's point of view** are defined only as a disturbance.

Table 8-4. Major indices of thyroid orbitopathy

Disease Activity (largely subjective)

Tempo and progression
Acute, subacute, or chronic onset
Slow or rapid development
Subjective symptoms
Spontaneous retrobulbar pain
Pain on extraocular movement
Soft tissue features
Swelling, injection, and chemosis noted by patient
Patient assessment of symptoms and signs
Same, better, or worse

Severity and Extent (largely objective)

Proptosis
Lid and conjunctival swelling
Extraocular muscle function
Optic nerve function
Corneal change
Imaging

We have studied a cohort of recently diagnosed hyperthyroid patients and compared them to newly referred thyroid orbitopathy patients. This study was aimed at the development of a symptomatic screening questionnaire for the early detection of thyroid orbitopathy. The questionnaire explored symptoms in categories relating to exposure, inflammation, proptosis, vision, and strabismus. The results of our study have produced a screening rule, which could identify patients with clinical signs of ophthalmopathy 8 months before they would have been referred through regular channels. The rule, which we have called the “Vancouver Rule,” consists of a positive response in newly diagnosed hyperthyroid patients to one of the following two questions:

- Swelling or feeling of fullness in one or both of your upper eye lids?
- Bags under your eyes?

and any one of the following three questions:

- Redness in your eyes or eyelids?
- Do your eyes seem to be open too wide?
- Is your vision blurry (even with glasses/contacts)?

This simple rule would detect that group of patients requiring early referral and may be a means to institute earlier therapy. The study emphasizes the value of symptom assessment for early detection of activity related to thyroid orbitopathy.

Severity Determinants

After determining disease activity, objective physical examination helps to define how severe the disease is. The key clinical features for determining severity include disturbances of vision (including optic neuropathy), soft tissue involvement (inflammatory and congestive features), degree of motility restriction, proptosis, and restricted venous out-flow that contributes in a mechanical way to the amount of orbital and periorbital edema. In addition, evaluating lid and corneal changes as well as degree of fat prolapse add to the objective determinants. One should also keep in mind the degree to which this disorder interferes with daily life, as a feature of severity determination. CT and MR imaging may also contribute to quantitative evaluation of orbital involvement and in the case of MRI, perhaps response to therapy, but the emphasis in this section is to evaluate the clinical aspects of the disease to determine severity.

The presence or absence of optic neuropathy can be relatively easily determined on the basis of pupillary function, vision, visual fields, color vision, and optic nerve appearance. Soft tissue evaluation should record periorbital edema by classifying the amount of pretarsal and preseptal edema and chemosis into broad categories of 0 to 3. Myopathy can be clinically assessed by viewing the versions or limitation of such using the Hirschberg image in attempted gaze in the cardinal positions. Mechanical issues relate to the degree of proptosis (measured by exophthalmometry), interpalpebral fissure width, lagophthalmos, degree of corneal involvement, and presence or absence of Bell's phenom-enon.

Table 8-5. Normative measures for extraocular muscles (in millimeters)

	CT Rootman et al.	CT Ozgen & Ariyurek	MRI Demer & Kerman	ULTRASOUND Demer & Kerman	ULTRASOUND Byrne et al.
Medial rectus	4.1	4.2	4.50	4.66	3.5
Inferior rectus	4.9	4.8	4.78	3.89	2.6
Superior muscle group	3.8	4.6	5.01	5.19	5.3
Lateral rectus	2.9	3.3	4.76	4.22	3.0
Superior oblique	2.4				
Sum of all muscles (muscle diameter index)	18.2	16.9	19.07	17.97	14.4
Superior ophthalmic vein: Axial	1.8				
Coronal	2.7				
Optic nerve sheath:					
Retrobulbar	5.5				
Waist	4.2				

Imaging as a Means of Determining Disease Activity and Severity

For the most part, we believe good clinical criteria can define the severity of the disease quite well and correlate significantly with CT or MRI findings. However, there are a number of things to keep in mind with regard to imaging. One can, by comparing the degree of muscle enlargement, nature of muscle infiltration, features of apical compression, and degree of fat involvement, define severity criterion that may require intervention. In particular, are there features that suggest the disease is active or either visually or mechanically threatening?

In quantitative evaluation of the extraocular muscles, it is important to have normative data to establish variations from the norm. Generally, increasing extraocular muscle size or volume correlates with increasing severity of disease. In many of the studies done, there are some variations between CT, MRI, and ultrasound observations. Table 8-5 provides data from several studies done on muscle size and muscle diameter index.

As to activity, we have noted for many years that an acute case of significant orbitopathy is associated with very fine low density infiltration of the muscles (see Figs. 8-2B , 8-5 , 8-6 , 8-16 , 8-19 , 8-20 , 8-22 , and 8-27E), in contrast to chronic cases where the muscle tends to be replaced by fat (see Figs. 8-3 and 8-27F). We have already noted that with rapid onset infiltrative orbitopathy, there is sometimes evidence of infiltration of the adjacent fat (see Fig. 8-2) but for most cases the fat remains well delineated from the muscle margin.

Some authors have noted that MR imaging is particularly useful for assessing the degree of fat effacement at the apex as well as measuring optic nerve thickness in apical disease. In addition, it has been suggested that the T2 relaxation times of extraocular muscles were longer in patients with Graves' orbitopathy. The probability of response to treatment increased with higher mean T2 relaxation times of the extraocular muscles prior to therapy. It has been suggested that this would be a useful rough index of activity, which decreases with treatment. Prummel et al. have recently suggested, however, that quantitative orbital MRI is less accurate in predicting outcome of radiotherapy and more useful in detecting the fibrotic end stage than the active stage of Graves' ophthalmopathy.

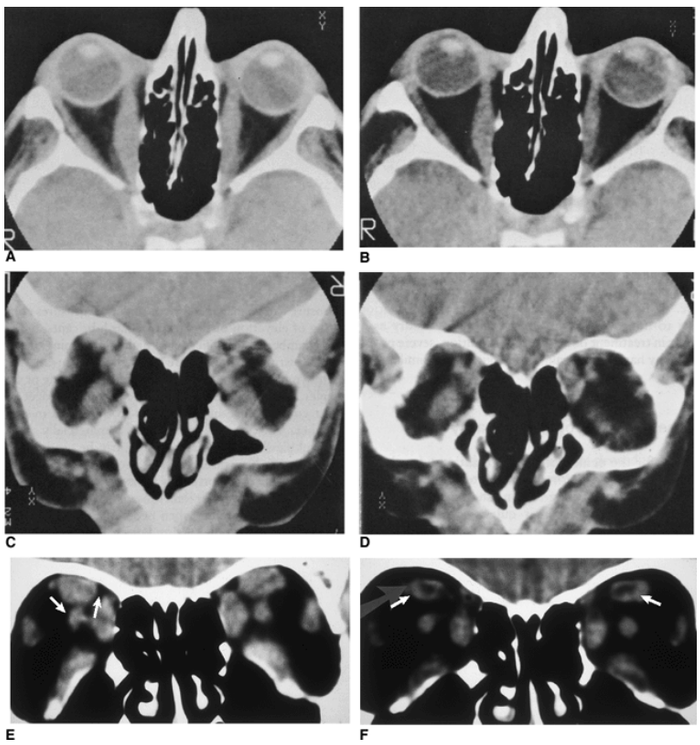

Figure 8-27. Improvement in extraocular muscle size is demonstrated on axial CT scans taken before (A) and 1 month after (B) orbital radiotherapy for a euthyroid orbitopathy. This was associated with significant soft tissue signs, exophthalmometry of 18 mm right and 17 mm left, and a 10-diopter esotropia. Clinically, the patient showed dramatic resolution of chemosis with improvement of lid edema and ocular comfort. The esotropia remained stable. He subsequently underwent a right medial rectus recession with adjustable suture. Reduction in muscle mass is shown on coronal CT scans taken before (C) and 4 months after (D) orbital radiotherapy for marked soft tissue signs and symptoms that developed 3 months after treatment for hyperthyroidism in this 70-year-old man. (E) CT appearance of thyroid orbitopathy that was associated with significant inflammatory features prior to treatment with radiotherapy. Note small low density areas (small arrows) in the muscles. (F) The same orbit 5 years postradiotherapy. Note large areas of fatty deposition within the muscles (arrows) and mild shrinkage of the muscles. (Fig. 8-27F reproduced with permission from Kao SCS, Kendler DL, Nugent RA, et al. Radiotherapy in the management of thyroid orbitopathy: computed tomographic and clinical outcomes. Arch Ophthalmol 1993;111:819-23.)

The best correlations with severity of disease are seen in the group of patients who have dysthyroid optic neuropathy, the major features of which are associated with significant apical crowding on direct coronal scanning with evidence of loss of the perineural fat at the apex, enlargement of the retrobulbar optic nerve sheath, dilatation of the superior ophthalmic vein, degree of proptosis, enlargement, and prolapse of the lacrimal gland (see Figs. 8-6 , 8-19 , 8-20 , and 8-22). Rarely, optic neuropathy may correlate with stretching of the optic nerve (see Fig. 8-21).

Management

Interventional Criteria

In order to develop a decision-making paradigm, one has to understand the background described and be able to separate patients into prognostic categories on the basis of the symptoms, signs, and imaging features outlined. Interventional criterion should be based upon factors that determine disease activity and severity in each category of manifestation (i.e., inflammatory, visual, motor, and appearance), which define appropriate management. In general, assessment of activity defines when to intervene, and severity determines the means of intervention.

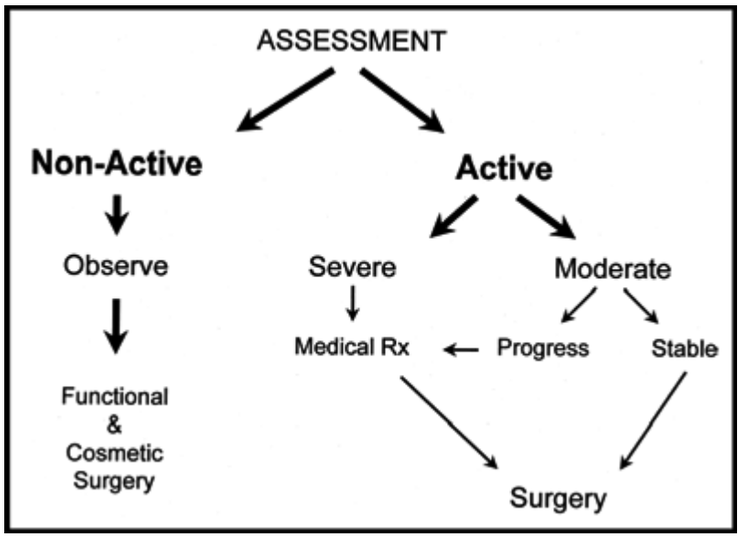

Figure 8-28. Paradigm for assessment and management of thyroid orbitopathy.

The question arises as to when does one intervene with any modality that might affect or modify the disease activity. In reviewing the above, patients with minimal inflammatory or infiltrative disease can generally be observed or treated conservatively. On the other hand, patients with rapid onset and progressive, inflammatory, mass, and infiltrative components require disease modification. Features such as significant progressive soft tissue swelling (particularly of rapid and symptomatic onset) with and without myopathy are criteria for disease modification. Generally, we propose that a decision whether to intervene should be made on the **primary** visit in patients with significant disease or after closely watching those with moderate soft tissue features (i.e., review within 2 months).

There are some instances, however, where patients present suddenly, such as abrupt recognition of what has in fact been an insidious but mild disease or some elderly patients with sudden onset of diplopia in the absence of inflammatory or infiltrative features. The latter represent a break down in control of movement on the background of old thyroid orbitopathy, which can be readily defined by the lack of correlation between the degree of restriction and the lack of symptoms and signs of acute soft tissue features. In addition, this group will typically have evidence of longstanding disease on imaging, such as low-density fatty infiltration of the muscles.

Patients with a progressive mechanical threat, such as corneal exposure and for that matter optic neuropathy, may require aggressive disease modification followed by surgery. In some very severe sight-threatening situations, primary surgery can be carried out at the same time as anti-inflammatory therapy. Finally, patients who have run the course of their disease, be it moderate or severe, have some degree of disfigurement that requires surgical redress. The overall paradigm is shown in Fig. 8-28 . Once the patient's situation is assessed from a historical and clinical point of view as mild, moderate, or severe disease, those patients with mild involvement are reassured and observed, and functional and cosmetic surgery carried out after stability has been established for a significant period of time (usually 1 year).

Patients with more active disease, on the other hand, can be divided into those who have severe versus moderate disease. Severe disease denotes a relatively rapid onset of

inflammatory and infiltrative features that lead to early mechanical and significant soft tissue involvement. Those with severe disease should be treated with medical interventions, such as corticosteroids or radiotherapy with or without immunoregulatory agents, to dampen the activity of the disease and then observed off of therapy for a period of time for nonprogression. Once nonprogression is established, appropriate surgery can then be performed (usually within 6 months to 1 year). Patients who present with moderate disease should be observed fairly closely, probably every 2 to 3 months depending on their symptoms. **They should be warned about features of progression** (i.e., inflammatory, visual, motor, and appearance) **and told to return sooner if concerned**. If they remain stable, then surgical redress of mechanical problems can be performed at a later date. Should the disease progress, patients may need medical intervention to modify the severity of the disease until stabilized. Severe apical crowding and clinical features of congestion and optic neuropathy may precipitate earlier medical intervention and surgery. Generally, medical intervention can antecede the surgery.

Medical Treatment

Treatment of Thyroid Disease and Prevention of Thyroid Orbitopathy

In general, we support the concept of treating hyperthyroidism using thyroid suppressive drugs to first restore euthyroidism. After this is achieved, either radioactive iodine or surgery may be required as thyroid suppressive drugs have a relatively high incidence of recurrence and our goal is to obtain permanent control since the persistence of hyperthyroidism is bad for orbitopathy. It remains to be evaluated whether orbitopathy can be modified in terms of incidence or progression by the use of immunoregulatory or anti-inflammatory agents at the time of treatment of the hyperthyroidism but some theoretical basis exists for this hypothesis, particularly if thyroid orbitopathy occurs concomitantly with treatment of hyperthyroidism.

Controversy still exists regarding the treatment of hyperthyroidism and its relationship to orbitopathy but several points have been made. As stated earlier, thyroid suppression and thyroidectomy are associated with a smaller incidence of developing progression of mild and moderate orbitopathy than is the case with radioactive iodine. However, many authors feel that radioactive iodine is of significant benefit and associated with better long-term control of hyperthyroidism. In addition, many feel that prevention of hypothyroidism following treatment is extremely important in reducing the incidence and severity of orbitopathy. Furthermore, the use of corticosteroids at the time of treatment with I^{131} significantly reduces severity and progression of mild and moderate orbitopathy. The use of corticosteroids is recommended in those patients who have active orbitopathy at the time of I^{131} administration and negative prognostic determinants, particularly smoking, high TSH, and high thyroid-stimulating antibodies. It has been suggested that treating with steroids should continue until the thyroid-stimulating antibodies (when present) decrease postradioactive iodine.

For the patient who presents primarily with features of thyroid orbitopathy and no clinical thyroid abnormality, the laboratory investigations recommended by our endocrinologists include sensitive TSH, free T4 or total T4 (if TSH is low or altered), T3 (if TSH is low), and normal T4 testing. Additionally, there are a few ancillary tests that may be of use, including thyroid antibody titre and TSH receptor antibody test.

Treatment of Thyroid Orbitopathy

As to active medical treatment of the orbitopathy, this consists of conservative measures when mild, or the use of either corticosteroids and/or radiotherapy for active, progressive disease. The simple conservative measures include elevating the head of the patient's bed to reduce periorbital edema, cool compresses (gel pads are ideal), and the use of moisture chambers to protect the cornea (which can be simply made using clear plastic food wrap). We do not recommend taping since with significant lid retraction the lid almost always opens underneath the tape and causes abrasion. For minor amounts of diplopia, we recommend the use of Fresnel prisms while the patient is stabilizing. The other important conservative measure that we have adopted is to advise patients to stop smoking because of its known association with severity. In addition, we recommend that patients wear dark glasses and avoid direct exposure to sun, which tends to accentuate the amount of swelling. Although diuretics are frequently prescribed by clinicians, we believe they have little or no effect on periorbital disease.

It has been recently suggested that mild and moderate Graves' ophthalmopathy may respond to oral antioxidant agents but no case-controlled study has yet been done.

We use adjuvant immunosuppressive drugs or cyclosporine in patients who may not have responded to other measures or are diabetic. The immunosuppressives we use as adjuvants are given in doses that are generally agreed upon as being adequate for inflammatory-based conditions. For azathioprine, the recommended dosage is 12 mg/kg up to 14 mg/kg; the usual dosage is 50 mg twice a day for 1 week. If the patient is found to be stable after a hematologic

profile, the dosage can be increased to 50 mg three times a day. Generally, the white cell count should be monitored once a month. Methotrexate is usually given in doses of 525 mg once per week with regular monthly monitoring of the white cell count. Cyclophosphamide can be administered intravenously in pulsed doses of 5001000 mg every 4 to 8 weeks, or daily orally at 12 mg/kg (generally in the 100200 mg range). Cyclosporine is administered 50 mg twice a day with an upper range of 200 mg twice a day. The usual dosage is 100 mg twice a day.

Some authors have suggested that early combinations of corticosteroids and immunosuppressive drugs may reduce disease severity. There is still not enough evidence to suggest any single modality is of profound value in established disease but we believe that severity can be lessened by medical interventions.

The role of corticosteroids in the treatment of this disorder is well established. Glucocorticocoids appear to affect not only the inflammatory component of this disorder but retrobulbar fibroblastic proliferation and function. Our current preference is to use pulsed steroids in doses of 1 g intravenous methylprednisolone delivered under supervision 3 times in 1 week, following which the patient is monitored for improvement or nonimprovement of their signs and symptoms usually within 1 month to 6 weeks. The pulse corticosteroids given in this dose have the added benefit of lymphocytolysis rather than suppression of inflammation alone that is associated with lower doses of oral corticosteroids. This protocol can be repeated at varying time intervals. We have repeated pulses as much as six times but most patients require three or less pulses, generally given 6 weeks apart. Many of the patients show reduction of the inflammatory features of the disorder with only about one third responding in terms of improved extraocular movements.

We have become less prone to use oral corticosteroids because of the many known side effects and the tendency for recrudescence of disease after dosage reduction or discontinuance. The efficacy of steroids should be balanced against the many systemic side effects. In our experience, titrating the doses downward usually takes a long time, and to control soft tissue symptoms patients may be receiving intermittent steroids for anywhere between 3 months and 1 year. We have been impressed with the frequency with which patients receiving continuous oral corticosteroids suffer side effects, even with small doses. The severity varies from full-blown Cushing's syndrome to minimal side effects. These patients, who are already suffering significant physical changes, now have the added problems of weight gain, acne, hirsutism, facial rubor, and weakness. We have also been impressed by the frequency at which patients complain of the effect of corticosteroids on their personality, producing depression in some, and hyperactivity and sleeplessness in others. Aside from these side effects, one should be aware of the potential for osteoporosis, secondary infections, and glucose intolerance. Because of these many side effects, we have developed a philosophy of avoiding the long-term use of oral steroids, using them in relatively low doses (starting at 30 mg to 40 mg daily decreasing over a 6- to 9-week period) as an adjunctive measure, for short periods of time. Alternatively, we prefer pulses to oral doses to reduce the side effects. If oral corticosteroids are preferred in the treatment of optic neuropathy, the recommended doses start at 100 mg to 120 mg prednisone per day but as noted our preference is to use pulsed steroids in this circumstance.

Orbital irradiation using modern techniques appears to be efficacious and **careful limited irradiation** produces rapid palliative relief of congestion and enhances comfort and vision. Clinically, one can expect 60% to 70% of patients to have a good response (Fig. 8-27). The response is generally obtained in the abatement of soft tissue signs and symptoms and improvement of movement. Soft tissue changes respond in 4 to 6 weeks. Proptosis and ophthalmoplegia respond little to any form of conservative medical therapy. In our treatment center, the technique has been modified to use supervoltage irradiation (2000 cGy in 10 fractions over 12 days using a 4-MeV linear accelerator) delivered only to the posterior two thirds of the orbit and avoiding the globe itself. We found that the extraocular muscle and orbital CT changes tend to parallel the response after radiotherapy. Only 14% of our patients had recurrence of symptoms following radiotherapy. An added benefit is that this appears to be a single-course treatment modality.

There are a number of questions about the use of radiotherapy in Graves' orbitopathy; “Why does it work?” is not the least of them. Local immunosuppression is an attractive theory and was the initial impetus for using this modality. If an abnormal systemic immune response is the basis of the disease process, it is surprising that symptomatic local recurrences are not more common. Possibly, orbital radiotherapy interferes with a target other than just the inflammatory cells, such as the muscle membrane or fibroblastic component, to prevent the development of progressive infiltrative changes. We believe that orbital radiotherapy is indicated for rapidly progressive severe orbitopathy, for troublesome moderate to severe soft tissue signs and symptoms and progressive myopathy, for patients in whom steroids are contraindicated, or for those not controlled by or who develop side effects on modest doses of steroids. The effect of radiotherapy as a primary modality in very early disease is not known, and potentially may lead to permanent arrest of disease progression and prevent disabling and disfiguring problems. Generally speaking, we have tended to avoid the use of radiotherapy in young patients

because the disease tends to be much milder and the long-term effects of radiotherapy are not known. An additional important contraindication to radiotherapy is known diabetes or vascular disease as radiotherapy may significantly accelerate the course of vascular retinopathy.

Although many papers, including our own, supporting the use of radiotherapy have been published, the major limitation has been lack of effective patient controls. There is a general consensus in the community that radiotherapy is of benefit but a need for case-controlled studies remains. A recent study by Mourits et al. suggests that a major effect of radiotherapy in moderate disease is on improvement of extraocular muscle function rather than soft tissue signs. Gorman et al. have also challenged the value of radiotherapy in treatment of moderate disease. For patients with optic neuropathy, before considering radiotherapy we will pulse them with corticosteroids and then proceed to radiotherapy or in some instances, decompression depending on the configuration of the orbit and the response to pulsed steroids (Fig. 8-29). We have noted that approximately 20% of patients receiving radiotherapy experience an exacerbation of their soft tissue signs following the second or third treatment, which we usually manage by administering oral corticosteroids in doses of 20 mg to 30 mg per day decreased over a 2- to 3-week period.

Other treatments (that have not been fully validated) include the use of octreotide (somatostatin analogues, which are expensive) or plasmapheresis. Immunoglobulins have also been used in the treatment of thyroid orbitopathy but carry with them significant expense as well as concern about the risks of using plasma-derived products. A more recent suggestion is that the future may see the use of cytokine antagonists to block the disease induction. In practical terms, we feel that the most reliable medical treatment modalities widely available to us at this point in time are corticosteroids with or without immunosuppression and radiotherapy. In our experience, earlier referral and more rigorous therapy of hyperthyroidism has significantly decreased the incidence and severity of this disease.

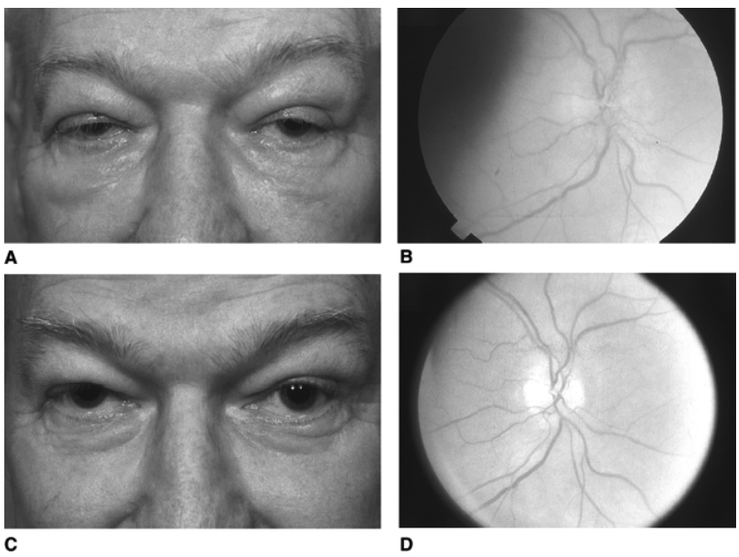

Figure 8-29. (A) This 66-year-old man presented 1-year after receiving radioactive iodine for hyperthyroidism with a subacute onset and 5-month progression of lid swelling, double vision, and retrobulbar discomfort. On examination he had moderate periorbital edema (+2), chemosis (+2), ptosis, lid injection, and bilateral severe restriction of movement in all directions of gaze (less than one third of normal). In addition, he had bilateral papilledema (B right eye shown), visual field defect, and reduced color vision. He was treated with high-dose pulsed methylprednisolone therapy (1 g IV × 3) followed by radiotherapy and within 20 days, his vision returned to normal and there was an improvement of soft tissue signs. (C, D right eye shown) These photographs taken 2 months postradiotherapy demonstrate the absence of periorbital edema and regression of the papilledema.

Generally in terms of monitoring the effect of treatment, one can rely on observations related to subjective and objective features of improvement. Imaging such as ultrasound, MRI, and CT scan may validate the improvement. Overall, it is expected that the majority of patients with mild and moderate disease improve but only approximately 60% of those with severe disease will improve.

In conclusion, from a medical point of view we favor managing thyroid orbitopathy by early restoration of euthyroidism with antithyroid drugs followed by definitive treatment with radioactive iodine or thyroidectomy. Medical management of mild (and some moderate) disease should be focussed on protection and moderate doses of corticosteroids administered when necessary. For severe and some moderate orbitopathies, we advocate the use of high-dose pulsed steroids followed by radiotherapy and possible surgical intervention.

Raised Intraocular Pressure in Thyroid Orbitopathy

It has been our experience that patients are frequently misdiagnosed and treated for raised intraocular pressure, largely because of failure to measure intraocular pressure in 5 downgaze, thereby avoiding the inferior rectus tethering that contributes to the raised intraocular pressure. Several studies suggest that glaucoma is in fact no more frequent in thyroid orbitopathy. We have also noted that in patients who undergo decompression, the intraocular pressure drops due to the reduction in passive venous congestion.

Surgical Management

From the above, you will recognize that our essential management philosophy is to categorize patients into prognostic groups based on disease activity and severity, intervene medically till stabilized, and then treat surgically. There are very few instances in our experience where surgery need be urgent, and it is much easier and fraught with fewer complications to operate on patients whose disease has become quiescent to some degree. We find that in the majority, aggressive medical intervention even for apical compression with significant visual threat leads to improvement of symptoms relatively quickly (i.e., within weeks) and allows a more contemplative approach to surgery.

The surgical indications and approaches for thyroid orbitopathy have been discussed and illustrated in detail in “Orbital Surgery: A Conceptual Approach” by Rootman et al. Herein we will discuss primarily the general approaches.

There are really only two instances in which relatively emergent surgery is necessary, and decompression should be combined with aggressive anti-inflammatory medical therapy to minimize the effect of surgical trauma. The situations necessitating urgent decompression are 1) corneal exposure with damage as a result of marked proptosis and lid retraction and 2) uncontrolled apical compression with evidence of significant visual threat. We have shifted our opinion with regard to optic neuropathy management. Overall, we do not believe that decompression is urgent if one can first medically control visual symptoms either with high-dose pulse corticosteroids or radiotherapy, particularly in orbits where there is mainly apical compression without a great deal of proptosis. Patients who have severe proptosis with apical crowding or corneal threat need to have an adequate decompression, which addresses both the degree of proptosis and apical compression. Patients who do not have significant proptosis with apical compression (small tight orbit) are first treated with an aggressive medical regimen to see if we can reverse or halt the phenomenon, obviating surgery and its attendant risks and complications (Fig. 8-29). As long as nerve functions are improving, one can delay decompression until the inflammatory and infiltrative effects are stabilized. We have had some cases where eyelid lengthening surgery as well as muscle surgery (inferior rectus to restore Bell's phenomenon) became necessary as an emergent procedure in order to achieve adequate corneal coverage.

The major consideration for surgical management of optic neuropathy is adequate relief of orbital pressure, especially in the apex, and there are a number of ways in which this can be achieved through removal of various combinations of orbital walls or fat (Fig. 8-30) (Table 8-6). The apex can be relieved best medially but relief can be also achieved by a lateral approach (by removing the greater wing of sphenoid), inferior apical decompression, and more rarely superior decompression using medial (caruncular), combined lateral, swinging eyelid, and coronal approaches. The appearance following treatment can be tailored to the desired outcome.

The order of elective surgery has to be governed by the effects of various procedures on orbital structures and in principle should first involve decision making about decompression, since this may affect lid position and ocular deviation (Fig. 8-31). The second procedure to consider is muscle surgery, since strabismus surgery may affect lid position. Finally, lid surgery is carried out to address malpositions, which may have been altered by the antecedent surgeries. It should be noted that the order has to be individualized, depending upon the approach chosen by the surgeon. We now often combine internal blepharoplasty and fat dissection and in some cases, lower lid elevation. On occasion, a decompression, upper lid procedure, and muscle surgery is done to protect the cornea and repair Bell's phenomenon in cases of very severe corneal threat.

The factors that affect surgical decision making include epidemiologic considerations such as age, sex, and race as well as individual patient features related to current and past surgical and medical problems, smoking, past physical appearance, and patient expectations. The individual physical features that have to be considered are specific facial contour, the status of the sinuses, thickness of the bones particularly the sphenoid wing, narrowness of the apex, size of the globe, refractive error, contour and status of the lids, and the status of the cornea and tear film. There are also numerous disease-related factors that should be considered in surgical management. These include the degree and nature of muscle involvement, degree of proptosis, and orbital compliance. A final consideration includes psychosocial factors related to the disfigurement.

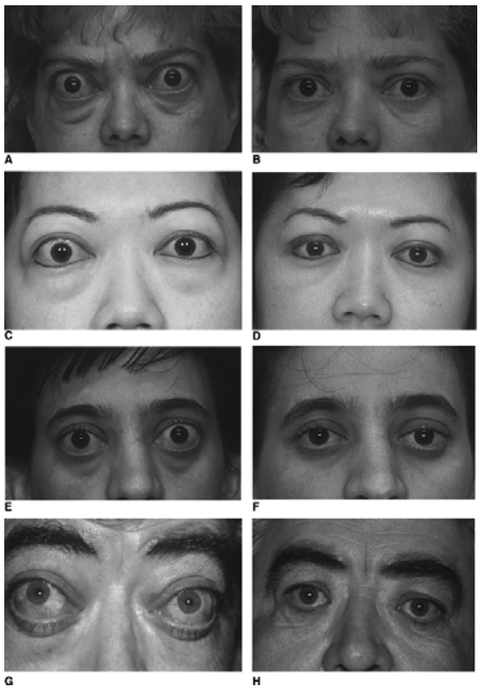

Figure 8-30. These photographs demonstrate the preoperative (left photos) and postoperative (right photos) appearances of patients who have undergone decompression as part of their therapy for thyroid orbitopathy. (A, B) Clinical photographs of a 34-year-old woman who presented with a longstanding history of stable nonactive orbitopathy characterized by severe exophthalmos (27 mm right, 26 mm left) with fat prolapse, lid retraction, and minimal soft tissue signs. She underwent bilateral three-wall orbital decompression and müllerectomies, achieving a final result of exophthalmometry 20 mm right and 19 mm left, and interpalpebral fissures of 11 mm right and 12 mm left with no deviation. (C, D) This 43-year-old Asian woman had active orbitopathy characterized by chemosis (+2) and lid edema (+1). Exophthalmometry measurements were 24 mm bilaterally with some restriction of upgaze, more on the right than the left. This was associated with corneal exposure as a result of lid retraction. Her CT scan demonstrated mild apical crowding with extraocular muscle enlargement. She underwent orbital radiotherapy and within a month showed improvement in periorbital swelling, which had stabilized by 5 months postpresentation. She underwent bilateral two-wall decompressions and subsequent müllerectomies with upper lid blepharoplasties. Her resulting interpalpebral fissure measurements were 9 mm bilaterally and exophthalmometry was 18 mm right and 19 mm left. (E, F) This 24-year-old woman presented with proptosis and lid retraction as part of a stable, nonactive orbitopathy with exophthalmometry measurements of 25 mm right and 26 mm left. She underwent three-wall decompression and müllerectomy, which resulted in interpalpebral fissures of 8 mm right and 9 mm left and exophthalmometry of 19 mm bilaterally. (G, H) Active severe orbitopathy in a 45-year-old man. He had chemosis (+3), edema (+3), severe exophthalmos (29 mm right, 30.5 mm left), and bilateral restriction of up- and downgazes. He underwent treatment with oral prednisone followed by radiotherapy. Six months postradiotherapy, he also underwent bilateral three-wall orbital decompression followed by müllerectomy. His final exophthalmometry measurements were 20 mm bilaterally and his interpalpebral fissures were 11 mm right and 9 mm left with a full range of ocular movements.

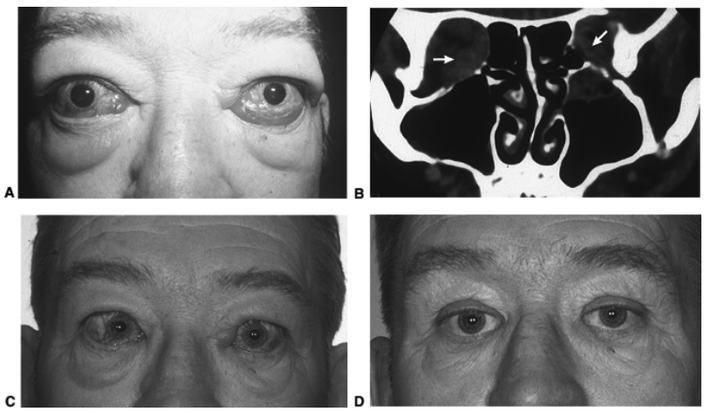

Figure 8-31. (A) This 60-year-old man presented 8 months postradioactive iodine with a 2-month history of subacute onset of periorbital edema, pain, and a recent decrease in vision. On presentation, his vision was reduced; he had an abnormal VEP and paracentral visual field defects on both sides with edema (+3), chemosis (+3), and significant exophthalmos measuring 26 mm on the right and 27 mm on the left. In addition, he had severe restriction of ocular movements in all positions of gaze and his intraocular pressures went from 22 mmHg on the right and 25 mmHg on the left to 32 mmHg and 37 mmHg respectively on upgaze. (B) His CT scan demonstrated a severe apical crowding. Note low density foci in the muscles (arrows). He was admitted to the hospital and treated with oral corticosteroids followed by decompression. One month postdecompression, his vision had returned to normal and exophthalmometry measurements were 21 mm right and 20 mm left; however, within 3 months he had a 30 diopter esotropia with marked injection. (C) By 6 months, his esotropia had increased to 45 diopters with a 6-diopter right hypotropia and marked restriction of upgaze. He underwent strabismus surgery consisting of four bimedial recessions on adjustable sutures and a bilateral inferior rectus recession with a right adjustable suture to correct an absent Bell's phenomenon. This was combined with müllerectomy. (D) Fifteen months after presentation, his exophthalmometry was 16 mm right and 17 mm left and he had normal vision and fundus with no evidence of soft tissue signs.

Table 8-6. Technical options in decompression

Floor and medial wall

Anterior

- Medial skin
- Medial upper eyelid
- Caruncular

Sinus approach

- Ogura
- Transnasal endoscopic

Lateral wall ± floor ± roof ± augmentation or bony advancement

Swinging eyelid approach

Lateral upper eyelid approach

Burke-Kronlein + medial approach

Burke-Kronlein + Ogura or transnasal endoscopic

Coronal approach

Soft tissue

Orbital fat excision

Blepharoplasty

- External
- Internal

We now tend, in situations where we are using a swinging eyelid approach, to do lower lid-lengthening procedures and internal blepharoplasties at the same time as the decompressive surgery. This may require a later minor cosmetic touch-up in some cases. Usually, we wait until after vertical muscle surgery to consider upper lid-lengthening procedures because inferior and superior rectus tethering can affect the degree of lid retraction. In addition, we have noted that a number of patients with fairly compressed orbits show an increase rather than a decrease in lid retraction after decompression; therefore, upper lid procedures should be generally avoided until such time as decompression has been performed. Using the above philosophy, we have experienced minimal postoperative diplopia and have had reasonable cosmetic results.

Decompression

Surgical approaches to decompression may to some degree be determined by the skill set of the surgeon but it is our belief that surgery for thyroid orbitopathy should be part of a comprehensive armamentarium that includes the ability to use tailored interventional techniques. These would include the ability to provide decompression through the medial wall, floor, lateral and posterolateral walls, and roof with or without augmentation or bony advancement (Table 8-6). In addition, an ability to deal with soft tissues by fat resection and blepharoplasty is important. Our current technical preferences are to minimize skin incisions by using swinging eyelid approaches, caruncular incisions, and skin-based lid incisions. We have avoided primary sinus approaches because of the higher incidence of myopathic complications; we prefer anterior direct approaches. In principle, we aim to provide a balanced decompression to avoid implosion into single cavities (i.e., medial plus lateral, inferomedial plus lateral). The key to management of optic neuropathy is adequate apical decompression via medial and/or lateral approaches with or without fat resection. Using the above philosophy, we have minimized as much as possible new postoperative strabismus and have had reasonable cosmetic results (Figs. 8-30 and 8-31).

Myopathy

Jack Rootman

Christopher J. Lyons

Patients with myopathy and strabismus should not normally undergo muscle surgery unless stable in terms of the thyroid disease, off medical treatment of orbitopathy, and inactive for at least 6 months. There are however some circumstances in which earlier treatment of the myopathy becomes necessary or useful, particularly in instances of inferior rectus tethering with an absence of the Bell's phenomenon (and resultant corneal exposure, especially if lagophthalmos is present). Stable orthoptic measurements should be documented for at least 6 months prior to surgery. Careful attention should be paid to incomitance in the cardinal positions of gaze and measurement of deviation in the reading position. A useful but not totally accurate method for assessing stability of the deviation is persistent flattening of the base of the Hess screen, which usually infers a stable end to the cicatricial process (Fig. 8-32). Regular measurement of deviations in all positions of gaze is the most practical method for follow-up of myopathy to assess stabilization.

The majority of patients with strabismus in our experience have combined vertical and horizontal deviations with a smaller percentage demonstrating pure vertical or pure horizontal deviation. About equal numbers have an increase or decrease in the esodeviation in downgaze (V- and A-patterns). In addition as stated earlier, the degree of deviation, nature of muscle involvement, clinical indices of proptosis, and degree of forced duction abnormality correlate well with CT findings. The degree of limitation of duction correlates very well with forced duction testing.

One should avoid progressive or traditional bifocals in patients with vertical rectus involvement, since the restricted vertical excursion may make the add segment inaccessible or place it within the diplopic field. Instead, separate single vision glasses should be used at near and distance. Prisms are of limited use due to the incomitant nature of the deviation in most patients. When used, Fresnel prisms may be preferable as they are cheaper and easily replaced when the deviation changes. Botulinum toxin has a short-lived effect but can be considered, particularly in early disease where the deviation may largely be caused by the combination of inflammatory muscle spasm and scarring.

The goal in surgical management of the myopathy is restoration of as large an area of fused single binocular vision as possible. Particular emphasis should be placed on obtaining fusion in the primary position and downgaze for reading and negotiating stairs. Preoperative counseling is important regarding the aims of surgery, which is 1) to enlarge the field of binocular vision and 2) to bring it in to the most useful zone, that is around the primary position and in downgaze (reading). Patients should be warned that they will still experience double vision postoperatively but not in the principal gaze directions. The likelihood of multiple surgeries being necessary to solve the problem should also be discussed, since this is higher in thyroid orbitopathy than in nonrestrictive strabismus. Preoperative field of binocular single vision measurements are helpful to describe the aim of surgery to the patient. Adjustable surgery is preferable, although it is recognized to be less predictable in thyroid

orbitopathy than in normal muscle surgery. Resection should be avoided because of the inherent scarring and contracture produced by the myopathy and the risk of recrudescence of disease. Using adjustable sutures, an attempt should be made to do all of the surgery as a single procedure. Preoperative and intraoperative forced duction testing must be used and the surgeon should be prepared to change the operative plan depending upon the results of the forced duction.

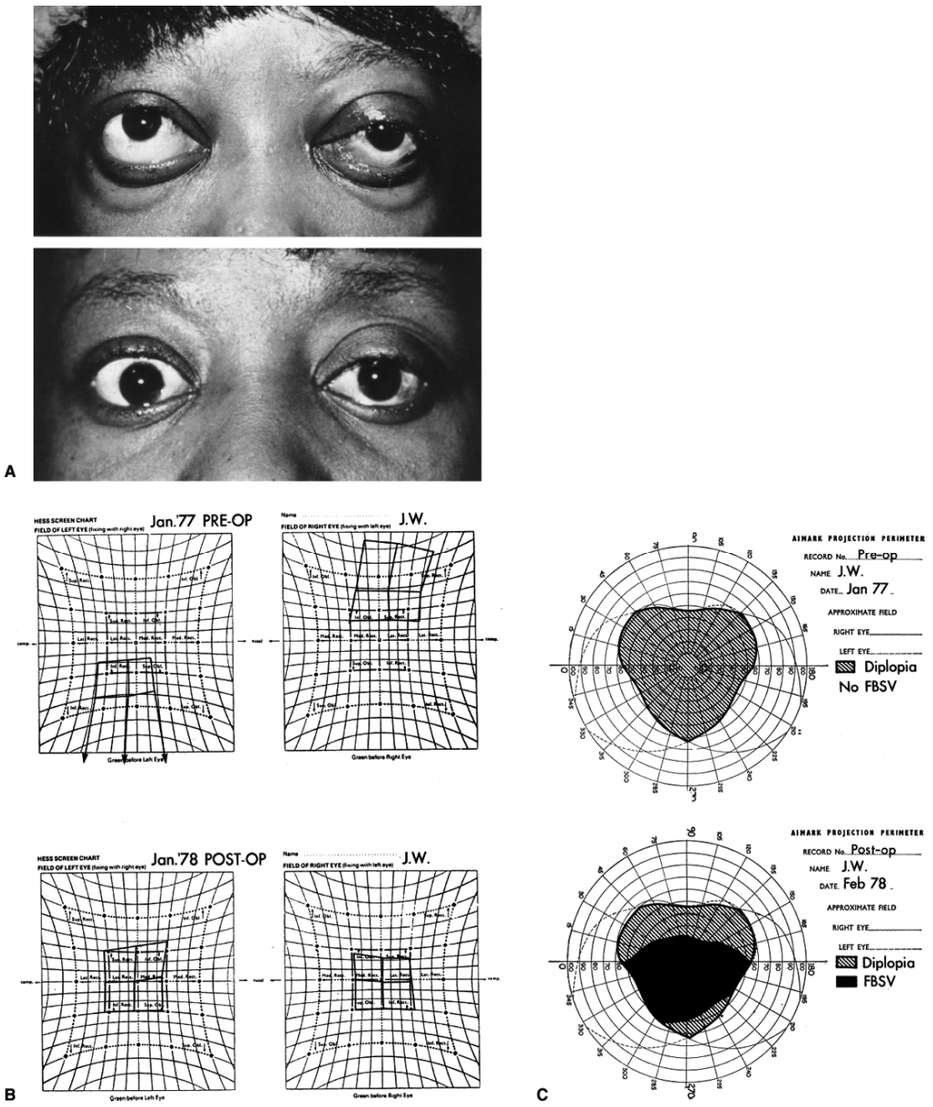

Figure 8-32. (A) This patient demonstrates the various stages of management of severe thyroid orbital disease. (A, top) She presented with severe congestive orbitopathy, corneal exposure, optic neuropathy with a vision of 20/200 right and 20/30 left, exophthalmometry of 25 mm right and 20 mm left, and a marked vertical deviation. She was treated with a short course of corticosteroids and underwent bilateral transantral orbital decompression (procedure preferred in dark-skinned individuals to avoid keloid formation) with recovery of vision. She subsequently underwent left inferior rectus recession and right superior rectus recession on adjustable suture for restriction of the inferior and superior recti. Postoperatively, she was orthophoric in primary position and downgaze, and had 18 mm of proptosis on the right and 16 mm on the left. (B) The pre- and postoperative Hess screens show flattening of the base postoperatively and recovery of binocularity following surgery. (C) The pre- and postoperative field of binocular single vision (FBSV).

Inferior rectus involvement may cause hypotropia but also esotropia. Before recessing a medial rectus in patients with inferior rectus involvement and esotropia, repeat the forced duction test after the inferior rectus insertion has been divided. If abduction remains limited on forced duction testing, medial rectus recession is indicated; if not, the medial rectus may be spared. A large unilateral inferior rectus recession leads to hypertropia in downgaze and ipsilateral lower lid retraction. The latter may be reduced by careful dissection of the lower lid retractors from the inferior surface of the inferior rectus. Late consecutive hypertropia is a common sequel of inferior rectus recession. This is usually caused by some unsuspected fixation duress from the contralateral eye in which the inferior rectus is also involved, leading to increased superior rectus tone and driving the ipsilateral superior rectus by Hering's law. Ipsilateral superior rectus involvement is another cause of consecutive hypertropia. Both these can be determined by careful forced duction testing at the start of surgery. In a patient with consecutive hypertropia, readvancement of the inferior rectus alone is futile. It should be combined with surgery on the yoke muscle or antagonist, depending on duction and forced duction test results. Large bilateral inferior rectus recessions may be necessary to treat restrictions, resulting in downgaze limitation, particularly in abduction. The superior obliques are then the only functional depressors, resulting in symptomatic intorsion and exotropia in downgaze. The A-pattern associated with superior oblique overaction may be treated by posterior tenotomy of the superior obliques. The A-pattern may also be reduced to some extent by nasal transposition of the inferior recti by a half or one tendon width at the time of recession.

The following outlines the surgical technique that we prefer. The adjustable suture method is carefully explained to the patient to ensure postoperative cooperation. The anesthetist is instructed to use minimal narcotic, sedative, or anesthetic agents. Forced duction testing is done at the start of the procedure and the results recorded. The plan of surgery is adjusted according to the forced duction findings. We prefer a conjunctival incision 2 mm to 4 mm posterior to the limbus, isolation of the muscle on a muscle hook, and deep dissection of all the check ligaments and fibrous bands attached to the periphery and belly of the muscles. Dissection often goes far enough posteriorly to expose the plane of the vortex veins adjacent to the grossly enlarged muscles, where direct trauma should be avoided. Meticulous attention in freeing all adhesions and connections between the lower lid retractors and the inferior rectus muscle is necessary. We use a double-armed absorbable suture threaded through the muscle at the insertion, locking it on either side. The muscle is disinserted with scissors if there is moderate tethering but a scalpel is used to cut through the tendon on to a preplaced muscle hook if more severely tethered. Forced duction testing is then repeated to identify any persistent tethering and the remaining bands are recessed. The suture is secured to the insertion site and allowed to retract, using a double throw followed by a half bow allowing the muscles to hang back the desired amount (Fig. 8-33).

Repeat forced duction is performed after conjunctival closure to rule out conjunctival tethering. If after suturing the conjunctiva forced duction demonstrates more tethering than before closure, we recess the conjunctiva as needed. About 4 hours later, using topical anesthesia a final adjustment is made. Using the above principles and adjustable sutures, we are able to obtain fusion in the primary and downgaze positions in a single surgical procedure in 75% of our cases, and fusion in primary gaze alone in 85% of cases.

Generally, we have found with multiple muscle involvement one can correct about 2.5 to 3 diopters of deviation per millimeter of recession, whereas with single muscle involvement 3 diopters and even up to 5 diopters can be achieved with 1 mm of recession. Usually, more effect is obtained the more the recessed muscle is restricted. From our study, we noted that when adjustable inferior rectus recession surgery alone was performed, an average correction of 3.4 diopters per millimeter of surgery could be expected. If both medial recti were recessed, 2.5 diopters of deviation are corrected per millimeter of surgery. When operating on combined deviations, horizontal changes of 3.3 diopters per millimeter and vertical changes of 2.7 diopters per millimeter of

surgery were obtained. Recession of the inferior rectus alters its adducting influence and promotes exodeviation, thus accounting for this greater horizontal measurement. This can be corrected by medial transposition of the inferior rectus insertion. Generally speaking, the maximum recessions done are 8 mm on the inferior rectus, 8 mm on the medial rectus, and 5 mm on the superior rectus. There is some possibility that recessing the medial and inferior recti more than 6 mm may lead to a duction deficit, which has to be considered in the context of the overall deviation, so that consideration should be given to operating on the contralateral eye. Over-recessions may lead to problems, particularly in downgaze, and should be avoided. These figures can be used as preoperative guidelines to help predict the amount of surgery necessary.

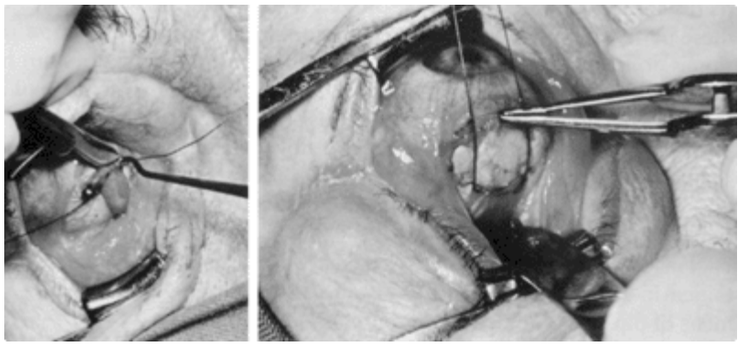

Figure 8-33. Photographs demonstrate the disinsertion of a muscle at the time of strabismus surgery (left), and placement of an adjustable suture (right) for thyroid myopathy.

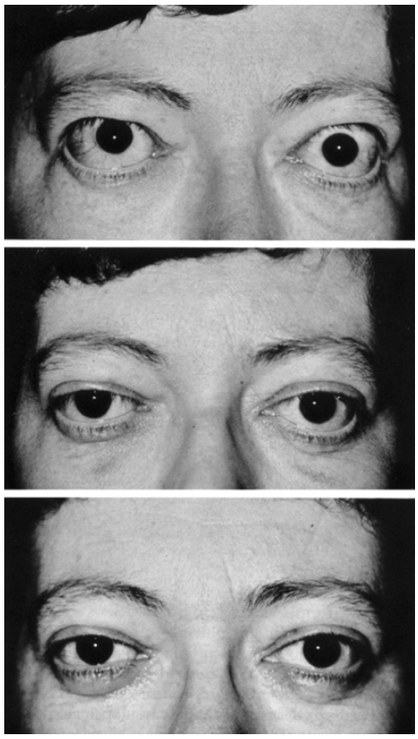

Figure 8-34. (Top) This 36-year-old woman presented 1 year after treatment of her hyperthyroidism with radioactive iodine. She had a 16-diopter left hypotropia and a 10-diopter esotropia. Exophthalmometry measurements were 23 mm right and 24 mm left, with marked upper lid retraction. She underwent an adjustable left inferior rectus recession and right medial rectus recession, followed by a müllerectomy (center) and bilateral lower lid elevation (bottom).

The major complication of strabismus surgery in our experience has been lower lid retraction despite meticulous dissection of the lower lid retractors. If this is cosmetically noticeable and disturbing, corrective procedures can be done at a later stage under local or general anesthetic (Fig. 8-34). Some authors have advocated release of the lower lid retractors at the time of inferior rectus surgery but because this is an unpredictable complication, we advocate waiting and then correcting.

In patients with lesser degrees of restriction, we have done adjustable surgery with local anesthetic by injecting small amounts of lidocaine into the tendon after topical anesthesia has been instilled, and adjusting on the table. However, we generally find that if one has to do several muscles or if they are particularly tight, it is easier to proceed with general anesthesia followed by adjustment postanesthetic.

There are two special aspects of strabismus surgery for thyroid oculomyopathy that should be reemphasized. The first is awareness of the importance of the forced duction test. There are a small percentage of patients (roughly 8% of those operated upon in our series) that have superior rectus involvement accounting for a hyperdeviation rather than the usual contralateral inferior rectus tethering. It is important to recognize these patients so that appropriate superior rectus recession is done in these circumstances. In general, it is important to assess restriction of movement of the agonist muscle in order to avoid postoperative overcorrections. The other caveat in strabismus surgery is that one should aim for single binocular vision in the primary position and 20 to 30 degrees of downgaze. Patients who do not achieve single binocular vision in downgaze may be particularly upset, because this makes it difficult to read and to negotiate stairs.

A rare complication of muscle surgery believed to be more common in thyroid orbitopathy is anterior segment ischemia, which we have not encountered. For this reason, operations on more than two muscles per eye in a single setting should generally be avoided. One can also use techniques of vessel preservation to avoid this complication.

In summary, we suggest that strabismus surgery in thyroid myopathy should aim for cure in the primary position and downgaze, be done on a patient who does not have active thyroid disease, and involve release of a restricted muscle by recession rather than resection. Furthermore, the amount of recession and the choice of muscle should be planned on the basis of degree of involvement (clinical deviation and ductions), symmetry, forced duction testing (prior to and repeated during surgery), and amount of scarring noted intraoperatively. The use of adjustable sutures is strongly advocated.

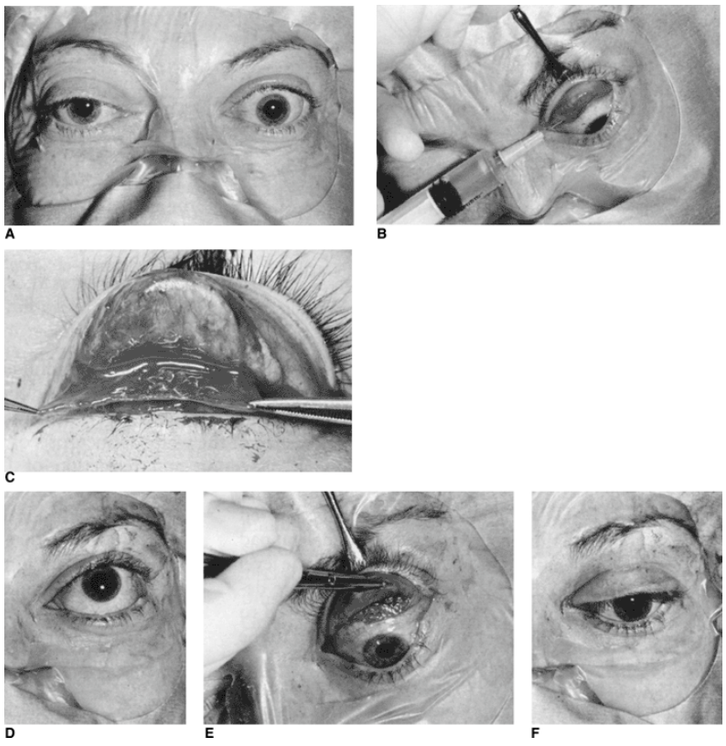

Figure 8-35. These photographs demonstrate a graded müllerectomy for left upper lid retraction (A). The lid is everted over a pediatric Desmarres retractor and a local anesthetic with epinephrine is injected subconjunctivally (B). A buttonhole incision is then made in the conjunctiva at the tarsal margin, and the conjunctiva is elevated, detached, and dissected free of the underlying Müller's muscle. Müller's muscle is buttonholed and detached from the tarsal plate then dissected free of the underlying levator aponeurosis (C). The patient's lid position is assessed (D). Note persistent lateral arching. The lid is then everted over the Desmarres retractor, and the lateral half to two thirds of the levator aponeurosis is incised and allowed to retract (E) to achieve a normal lateral curvature (F).

Lid Retraction

Lid retraction may be treated medically by adrenergic blocking agents; however, the results are inconsistent and often locally irritating. Haddad has reported better and more consistent results. Some patients require the addition of weak topical steroids to deal with the injection associated with guanethidine. Guanethidine (5%) is not routinely available in many centers.

Surgical management of lid retraction may be most gratifying. The procedure we prefer for upper lid retraction is graded Müllers' and aponeurosis weakening under local anesthetic to permit intraoperative evaluation of lid condition and function (Fig. 8-35). This is achieved by local subconjunctival injection along the upper tarsal border and fornix after everting the lid over a pediatric Desmarres retractor. The conjunctiva and Müllers' muscle is disinserted from the border of the tarsus using a cutting cautery. Müllers' muscle is then dissected from the underlying levator aponeurosis and the incision carried laterally along the very edge of the upper tarsal border. One should be careful not to dissect the conjunctiva in the superolateral fornix in order to avoid the lacrimal ducts. Müllers' muscle can be allowed to either retract or may be excised. The levator aponeurosis is then identified as a smooth white surface. The patient is allowed to sit up and their lid level evaluated to determine if an appropriate degree of ptosis is achieved. Because residual retraction is almost universally present laterally, lysis of the outer one half to one third of the levator aponeurosis is routinely performed. This can be safely achieved by everting the tarsus and incising the levator aponeurosis at the very tarsal margin, avoiding the lacrimal ducts. If retraction is severe and persistent, a graded recession of the levator aponeurosis is then performed. If a patient has more than 4 mm or 5 mm of scleral show and less than 10 mm of maximum levator function on downgaze, we tend to prefer an anterior lid crease approach with disinsertion of the levator and Müllers' muscle and placement of a scleral graft. It should be noted that the posterior approach can also be utilized for graft placement and in the majority of cases is adequate for lid lengthening. Additional techniques including marginal myotomies of the levator may be also be utilized to add lid length.

As a general guideline for the surgical management of lid retraction, if the upper lid is at the limbus or is retracted up to 3 mm, a müllerectomy with lateral tenotomy as described is usually adequate. In addition, marginal myotomy from an anterior route may correct relatively small degrees of lid retraction. Lid retraction of 3 mm to 5 mm requires a recession of either the levator muscle or the aponeurosis along with the müllerectomy. Lid retraction of 5 mm or greater may require a müllerectomy, levator recession, and a scleral graft.

Lower Lid Elevation

Lower lid retraction contributes to the appearance of proptosis and degree of exposure, and may be a complication of operations on the inferior rectus muscle. In essence, all of the procedures on the lower lid achieve their results by disinsertion of the capsulopalpebral fascia from the lower tarsus with placement of a spacer using sclera, cartilage, fascia, or hard palate.

The method we prefer can be done under local or general anesthesia. A suture is placed in the lid, which is everted over a Desmarres retractor. A conjunctival capsulopalpebral fascia incision is made at the lower tarsal border using a cutting cautery and the conjunctival fascial plane is dissected to the fornix. The conjunctiva and retractors are allowed to retract further by making lateral and medial radial incisions. A scleral graft of a width two to three times the amount of retraction is then prepared and sutured to the capsulopalpebral fascia. The other margin of the graft is then attached at the lower edge of the tarsus. The conjunctiva is left recessed to epithelialize over the graft. In greater degrees of retraction or in the case of a recurrence, we prefer the use of an ear cartilage graft. An alternative is to use alloplastic implants in the lid in order to elevate it.

Blepharoplasty

Blepharoplasty is another procedure that should attend to the nature of the abnormality produced by the disease. One should assiduously avoid blepharoplasty on patients who have severe, active, preseptal edema; that is, one should await resolution or manage the medical aspects of the disease prior to surgery. By and large, these patients do not have the kind of fat prolapse or, for that matter, the kind of skin that you see in senile patients, and they require more radical excision of anterior orbital and infrabrow fat and less excision of their often thickened skin. Thus, blepharoplasty should include blunt dissection behind the orbital septum with more radical removal of anterior orbital fat. Avoid excessive skin resection because complications of lagophthalmos can result. This is best accomplished by doing it under local anesthesia and maintaining a conservative attitude toward vertical skin resection. Rather, the contour of the lid should be altered by the fat resection and lateral tension rather than by vertical shortening. As stated earlier when we use a swinging eyelid approach, we routinely do an internal blepharoplasty.

DISEASE ONSET - Orbit		**Thyroid**
Symptoms:		
Date of Onset:		
Rate of Onset:	Acute (days) / Subacute (weeks) / Chronic (months) A / S / C	A / S / C
Progress:	Same / Better / Worse s / b / w	s / b / w
Tests:		
Treatment:		

SUBJECTIVE	OBJECTIVE	OD	OS	GRADE/ SEVERITY	MANAGEMENT	RESPONSE TO THERAPY
VISION						
Vision: Normal / abnormal	Central Vision sc/cc	20 /__	20 /__	W: ___ + ___ X ___ ___ + ___ X ___	Normal	Nil	
	cM	20 /__	20 /__	W: ___ + ___ X ___ ___ + ___ X ___	Refractive error	Correction	
Color Vision: Normal / abnormal	Color Vision Errors (AO)				Corneal changes	Lubricants, moisture chamber, müllerectomy, release of inferior rectus, decompression if severe proptosis	
	Pupils (afferent defect)	y / n	y / n				
	Spont. Venous Pulsation	y / n	y / n				
	Optic Nerve: edema	y / n	y / n				
	Pallor	y / n	y / n		Optic neuropathy	Oral steroids IV Steroids/radiotherapy Surgical decompression	If not effective, try next level of therapy
	Choroidal Folds	y / n	y / n				
Progress from Onset: Same/ better/ worse							
INFLAMMATORY						
Orbital Pain At rest: y / n With gaze: y / n	Chemosis (0-3)	**Inflammatory Index (worse eye)**		Absent	Observe and consider surgery as required	
	Conjunctival Injection (0-1)		Chemosis (0-3):			
	Lid Injection (0-1)		Conjunctival injection (0-1):	Mild	Nonsteroidal drugs Cool compresses Elevate head of bed	Follow in 4 months, if worsens, treat as moderate disease
	Lid Edema: Upper (0-3)		Lid injection (0-1):			
Lid Edema: y / n	Lower (0-3)		Lid edema (0-3):			
			Pain at rest (0-1):			
			Pain on movement (0-1):	Moderate	Trial of oral steroids (corticosteroids 50 mg x 3 days) or pulsed steroids with 4-6 week follow-up	If responsive, consider radiotherapy
			TOTAL (10):			
				Severe	Oral steroids Pulse steroids Radiotherapy Immunosuppressives	Generally requires aggressive treatment; if poorly responsive, try next level of therapy; consider possibility of orbital congestion or tight orbit requiring surgical decompression
Progress: Same/ better/ worse						
STRABISMUS / MOTILITY						
Diplopia: None Intermittent With gaze Constant	Ductions (degrees)	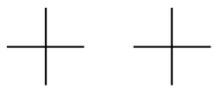		Absent	No treatment	
				Intermittent	Follow closely for worsening severity (monitor versions and amount of strabismus)	If strabismus becomes progressively more severe, consider oral/IV steroids or radiotherapy
				Present with gaze	Treat if versions or symptoms worsen	
		Strabismus: y / n Prism measurement:		Manifest strabismus	Fresnel prisms or patch one eye until inflammation is quiescent; once strabismus is stable for over 4-6 months, plan surgical realignment or permanent prism glasses; if orbital decompression planned, this is performed prior to strabismus repair	
Progress: Same/ better/ worse		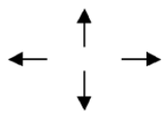				
APPEARANCE / EXPOSURE						
Lid Retraction: y / n	Fat Prolapse	y / n	y / n	Proptosis	If orbital inflammation present, treat medically first. Once inflammation resolved, may plan surgery – orbital decompression	Repeat as necessary
	Interpalpebral Fissure	__ mm	__ mm			
	Lid Retraction:					
	Upper MRD-4	__ mm	__ mm			
	Upper scleral show	__ mm	__ mm			
	Lower scleral show	__ mm	__ mm			
	Levator Function	__ mm	__ mm			
	Lagophthalmos	__ mm	__ mm	Lid retraction	Upper lid: mullerectomy, levator recession Lower lid: elevate with scleral or cartilage graft	
	Exophthalmometry	__ mm	__ mm			
Proptosis: y / n Tearing: y / n Foreign Body Sensation: y / n				Fat prolapse	Blepharoplasties and/or fat resection	
Biomicroscopy	Corneal Erosions	y / n	y / n	Corneal erosions	Lubricants, moisture chamber, müllerectomy, release of inferior rectus, decompression	
	IOP Straight	mmHg	mmHg			
	Up	mmHg	mmHg			
	Down (if primary position)	mmHg	mmHg			
	Other					
Progress: Same/ better/ worse						

Table 8-7. Evaluation and management of thyroid orbitopathy

Summary Paradigm for Assessment and Management of Thyroid Orbitopathy

Our experience at the University of British Columbia Thyroid Orbitopathy Clinic over the last 25 years has emphasized the broad spectrum of this disorder, its profound effects on patients and the benefit of individualizing care, and prognostication, which helps to allay very early the fears of patients regarding the long-term outcome as it relates to this disease. Overall, the majority of patients with milder disease can achieve relatively normal status within 9 months and those with more severe disease can expect to obtain relatively stable end states including surgical treatment within 24 months. In order to provide a final conceptual framework for management, we have produced a summary table of the assessment and management of patients with thyroid orbitopathy (Table 8-7). This is based on the practical division of symptoms and signs and is related to activity and severity determinants in each area of vision, inflammatory findings, strabismus, and appearance.

Bibliography

General

Char DH. Thyroid Eye Disease, 3rd ed. Boston: Butterworth-Heinemann, 1997.

Gorman CA, Waller RR, Dyer JA. The Eye and Orbit in Thyroid Disease. New York: Raven Press, 1984.

Tucker SM, Tucker NA, Linberg JV. Thyroid eye disease. In: Tasman W, Jaeger EA, eds. Clinical Ophthalmology, vol 2. Philadelphia: Lippincott-Raven, 1994; chap 36.

Pathogenesis

Bahn RS, Dutton CM, Natt N, et al. Thyrotropin receptor expression in Graves' orbital adipose/connective tissues: potential autoantigen in Graves' ophthalmopathy. J Clin Endocrinol Metab 1998;83:998-1002.

Bahn RS, Heufelder AE. Pathogenesis of Graves' ophthalmopathy. New Engl J Med 1993;329:1468-75.

Burch HB, Wartofsky L. Graves' ophthalmopathy: current concepts regarding pathogenesis and management. Endocrine Rev 1993;14:747-93.

Chang TC, Huang KM, Chang TJ, Lin SL. Correlation of orbital computed tomography and antibodies in patients with hyperthyroid Graves' disease. Clin Endocrinol 1990;32:551-8.

Crisp M, Starkey KJ, Lane C, et al. Adipogenesis in thyroid eye disease. Invest Ophthalmol Vis Sci 2000;41:3249-55.

Frueh BR, Musch DC, Grill R, et al. Orbital compliance in Graves' eye disease. Ophthalmology 1985;92:657-65.

Gunji K, Kubota S, Swanson J, et al. Role of the eye muscles in thyroid eye disease: identification of the principal autoantigens. Thyroid 1998;8:553-6.

Heufelder AE, Joba W. Cellular immunity and orbital antigens in thyroid-associated orbitopathy. Exp Clin Endocrinol Diabetes 1999;107(suppl 5):S152-7.

Heufelder AE. Retro-orbital autoimmunity. Baillière's Clin Endocrinol Metab 1997;11:499-520.

Hosal BM, Swanson JK, Thompson CR, et al. Significance of serum antibodies reactive with flavoprotein subunit of succinate dehydrogenase in thyroid associated orbitopathy. Br J Ophthalmol 1999;83:605-8.

Hufnagel TJ, Hickey WF, Cobbs WH, et al. Immunohistochemical and ultrastructural studies on the exenterated orbital tissues of a patient with Graves' disease. Ophthalmology 1984;91:1411-9.

Jacobson DH, Gorman CA. Endocrine ophthalmopathy: current ideas concerning etiology, pathogenesis, and treatment. Endocrine Rev 1984;5:200-20.

Kazim M, Goldberg RA, Smith TJ. Insights into the pathogenesis of thyroid-associated orbitopathy: evolving rationale for therapy. Arch Ophthalmol 2002;120:380-6.

Kennerdell JS, Rosenbaum AE, El-Hoshy MH. Apical optic nerve compression of dysthyroid optic neuropathy on computed tomography. Arch Ophthalmol 1981;99:807-9.

Kubota S, Gunji K, Stolarski JS, et al. Reevaluation of the prevalences of serum autoantibodies reactive with “64-kd eye muscle proteins” in patients with thyroid-associated ophthalmopathy. Thyroid 1998;8:175-9.

Ludgate M, Crisp M, Lane C, et al. The thyrotropin receptor in thyroid eye disease. Thyroid 1998;8:411-3.

McKenzie JM. Thyroid-stimulating antibody (TSAb) in Graves' disease. Thyroid Today 1980;3:1.

Pappa A, Lawson JMM, Calder V, et al. T cells and fibroblasts in affected extraocular muscles in early and late thyroid associated ophthalmopathy. Br J Ophthalmol 2000;84:517-22.

Rootman J, Patel S, Berry K, Nugent R. Pathological and clinical study of Müller's muscle in Graves' ophthalmopathy. Can J Ophthalmol 1987;22:32-6.

Sergott RC, Glaser JS. Graves' ophthalmopathy: a clinical and immunologic review. Surv Ophthalmol 1981;26:1-21.

Shokeir MO, Pudek MR, Katz S, Rootman J, Kendler DL. The relationship of thyrotropin receptor antibody levels to the severity of thyroid orbitopathy. Clin Biochemistry 1996;29:187-9.

Trokel SL, Jakobiec FA. Correlation of CT scanning and pathologic features of ophthalmic Graves' disease. Ophthalmology 1981;88:553-64.

Walfish PG, Wall JR, Volpe R. Autoimmunity and the Thyroid. Orlando: Academic Press, 1985.

Wang C, Crapo LM. The epidemiology of thyroid disease and implications for screening. Endocrinol Metab Clin N Am 1997;26:189-218.

Weetman AP. Recent progress in thyroid autoimmunity: an overview for the clinician. Thyroid Today 1996;14:1.

Weetman AP. Thyroid-associated eye disease: pathophysiology. Lancet 1991;338:25-8.

Yamada M, Li AW, Wall JR. Thyroid-associated ophthalmopathy: clinical features, pathogenesis, and management. Critical Rev Clin Lab Sci 2000;37:523-49.

Classification & Natural History

Arneja J, Dolman PJ, Kendler DL, Rootman J. Predictive variables of disease severity in thyroid-related orbitopathy. In progress.

Bartley GB, Gatourechi V, Kadrmas EF, et al. Long-term follow-up of Graves ophthalmopathy in an incidence cohort. Ophthalmology 1996;103:958-62.

Gorman CA. The measurement of change in Graves' ophthalmopathy. Thyroid 1998;8:539-43.

Gorman CA. Clever is not enough: NOSPECS is form in search of function. Thyroid 1991;1:353-5.

Hales IB, Rundle FF. Ocular changes in Graves' disease: a long-term follow-up study. Quarter J Med 1960;29:13-26.

Jacobson DL, Gange SJ, Rose NR, Graham NMH. Epidemiology and estimated population burden of selected autoimmune diseases in the United States. Clin Immunol Immunopathol 1997;84:223-43.

Linder M, Rootman J, Dolman P, et al. Development of a symptom-based screening rule for early detection of thyroid orbitopathy. In progress.

Mourits MPh, Koornneef L, Wiersinga WM, et al. Clinical critieria for the assessment of disease activity in Graves' ophthalmopathy: a novel approach. Br J Ophthalmol 1989;73:639-44.

Perros P, Kendall-Taylor P. Natural history of thyroid eye disease. Thyroid 1998;8:423-5.

Perros P, Kendall-Taylor P. Natural history of thyroid associated ophthalmopathy. Clin Endocrinol 1995;42:45-50.

Rasmussen AK, Nygaard B, Feldt-Rasmussen U. (131)I and thyroid-associated ophthalmopathy. Eur J Endocrinol 2000;143:155-60.

Rundle FF. Management of exophthalmos and related ocular changes in Graves' diseaes. Metabolism 1957;6:36-48.

Rundle FF, Wilson CW. Development and course of exophthalmos and ophthalmoplegia in Graves' disease with special reference to the effect of thyroidectomy. Clin Sc 1944;5:177-94.

Rundle FF, Wilson CW. Bulging of the eyelids with exophthalmos. Clin Sc 1944;5:31-45.

Rundle FF, Wilson CW. Ophthalmoplegia in Graves' disease. Clin Sc 1944;5:17-29.

Streeten DHP, Anderson GH Jr, Reed GF, Woo P. Prevalence, natural history and surgical exophthalmos. Clin Endocrinol 1987;27:125-33.

Terwee CB, Gerding MN, Dekker FW, et al. Development of a disease specific quality of life questionnaire for patients with Graves' ophthalmopathy: the GO-QOL. Br J Ophthalmol 1998;82:773-9.

Wang C, Crapo LM. The epidemiology of thyroid disease and implications for screening. Endocrinol Metab Clin N Am 1997;26:189-218.

Weetman AP, McGregor AM, Hall R. Ocular manifestations of Graves' disease: a review. J R Soc Med 1984;77:936-42.

Werner SC. The eye changes of Graves' disease: overview. Mayo Clin Proc 1972;47:969-74.

Clinical Evaluation

Anonymous. Classification of eye changes in Graves' disease. Thyroid 1992;2:235-6.

Bartley GB. Evolution of classification systems for Graves' ophthalmopathy. Ophthal Plast Reconstr Surg 1995;11:229-37.

Bartley GB, Fatourechi V, Kadrmas EF, et al. Long-term follow-up of Graves ophthalmopathy in an incidence cohort. Ophthalmology 1996;103:958-62.

Bartley GB, Gorman CA. Diagnostic criteria for Graves' ophthalmopathy. Am J Ophthalmol 1995;119:792-5.

Brix TH, Hansen PS, Kyvik KO, Hegedüs L. Cigarette smoking and risk of clinically overt thyroid diseaes: a population-based twin case-control study. Arch Int Med 2000;160:661-6.

Byrne SF, Gendrom EK, Glaser JS, et al. Diameter of normal extraocular recti muscles with echography. Am J Ophthalmol 1991;112:706-13.

Chung SM, Lee AG, Holds JB, et al. Ocular neuromyotonia in Graves dysthyroid orbitopathy. Arch Ophthalmol 1997;115:365-70.

Danks JJ, Harrad RA. Flashing lights in thyroid eye disease: a new symptom described and (possibly) explained. Br J Ophthamol 1998;82:1309-11.

Demer JL, Kerman BM. Comparison of standardized echography with magnetic resonance imaging to measure extraocular muscle size. Am J Ophthalmol 1994;118:351-61.

Feldon SE, Levin L, Liu SK. Graves' ophthalmopathy: correlation of saccadic eye movements with age, presence of optic neuropathy, and extraocular muscle volume. Arch Ophthalmol 1990;108:1568-71.

Feldon SE, Muramatsu S, Weiner JM. Clinical classification of Graves' ophthalmopathy: identification of risk factors for optic neuropathy. Arch Ophthalmol 1984;102:1469-72.

Feldon SE, Unsöld R. Graves' ophthalmopathy evaluated by infrared eye-movement recordings. Arch Ophthalmol 1982;100:324-8.

Fells P, McCarry B. Diplopia in thyroid eye disease. Trans Ophthalmol Soc U. K. 1986;105:413-23.

Fernandez-Soto L, Gonzalez-Jimenez A, Excobar-Jimenez F. Smoking and autoimmune thyroid disease [letter]. Ann Intern Med 1997;126:1005.

Gamblin GT, Harper DG, Galentine P, et al. Prevalence of increased intraocular pressure in Graves' diseaseevidence of frequent subclinical ophthalmopathy. N Engl J Med 1983;308:420-4.

Gerding MN, van der Meer JWC, Broenink M, et al. Association of thyrotrophin receptor antibodies with the clinical features of Graves' ophthalmopathy. Clin Endocrinol 2000;52:267-71.

Given-Wilson R, Pope RM, Michell MJ, et al. The use of real-time orbital ultrasound in Graves' ophthalmopathy: a comparison with computed tomography. Br J Radiol 1989;62:705-9.

Guimarães FC. Cruz AAV. Palpebral fissure height and downgaze in patients with Graves' upper eyelid retraction and congenital blepharoptosis. Ophthalmology 1995;102:1218-22.

Hamed LM, Lessner AM. Fixation duress in the pathogenesis of upper eyelid retraction in thyroid orbitopathy: a prospective study. Ophthalmology 1994;101:1608-13.

Hosten N, Sander B, Cordes M, et al. Graves ophthalmopathy: MR imaging of the orbits. Radiology 1989;172:759-62.

Jim K, Rootman J, Nugent RA, Dolman PJ. Clinical and radiologic differences in the extraocular muscles of Asian and Caucasian populations affected by thyroid orbitopathy. In progress.

Kalmann R, Mourits MPh. Diabetes mellitus: a risk factor in patients with Graves' orbitopathy. Br J Ophthalmol 1999;83:463-5.

Kalmann R, Mourits MPh. Prevalence and management of elevated intraocular pressure in patients with Graves' orbitopathy. Br J Ophthalmol 1998;82:754-7.

Kazuo K, Fujikado T, Ohmi G, et al. Value of thyroid stimulating antibody in the diagnosis of thyroid associated ophthalmopathy of euthryoid patients. Br J Ophthalmol 1997;81:1080-3.

Kendall-Taylor P, Perros P. Clinical presentation of thyroid associated orbitopathy. Thyroid 1998;8:427-8.

Kendler DL, Lippa J, Rootman J. The initial clinical characteristics of Graves' orbitopathy vary with age and sex. Arch Ophthalmol 1993;111:197-201.

Khalil HA, de Keizer RJW, Kijlstra A. Analysis of tear proteins in Graves' ophthalmopathy by high performance liquid chromatography. Am J Ophthalmol 1988;106:186-90.

Lyons CJ, Rootman J. Inflammatory disorders. In: Taylor D, ed. Pediatric Ophthalmology, 2nd ed. London: Blackwell Science, 1997:393-9.

Marcocci C, Bruno-Bossio G, Manetti L, et al. The course of Graves' ophthalmopathy is not influenced by near total thyroidectomy: a case-control study. Clin Endocrinol 1999;51:503-8.

Marino M, Barbesino G, Pinchera A, et al. Increased frequency of euthyroid ophthalmopathy in patients with Graves' disease associated with myasthenia gravis. Thyroid 2000;10:799-802.

Metz H. Saccadic velocity measurements in strabismus. Trans Am Ophthalmol Soc 1983;81:630-92.

Metz H. Saccadic velocity studies in patients with endocrine ocular disease. Am J Ophthalmol 1977;84:695-9.

Mourits MPh, Prummel MF, Wiersinga WM, Koornneef L. Clinical activity score as a guide in the management of patients with Graves' ophthalmopathy. Clin Endocrinol 1997;47:9-14.

Mourits MPh, Prummel MF, Wiersinga WM, Koornneef L. Measuring eye movements in Graves' ophthalmopathy. Ophthalmology 1994;101:1341-6.

Nianiaris N, Hurwitz JJ, Chen JC, Wortzman G. Correlation between computed tomography and magnetic resonance imaging in Graves' orbitopathy. Can J Ophthalmol 1994;29:9-12.

Nugent RA, Belkin RI, Neigel JM, et al. Graves orbitopathy: correlation of CT and clinical findings. Radiology 1990; 177:675-82.

Ohnishi T, Noguchi S, Murakami N, et al. Levator palpebrae superioris muscle: MR evaluation of enlargement as a cause of upper eyelid retraction in Graves disease. Radiology 1993;188:115-8.

Ozgen A, Ariyurek M. Normative measurements of orbital structures using CT. AJR 1998;170:1093-6.

Panzo GJ, Tomsak RL. A retrospective review of 26 cases of dysthyroid optic neuropathy. Am J Ophthalmol 1983;96:190-4.

Patrinely JR, Osborn AG, Anderson RL, Whiting AS. Computed tomographic features of nonthyroid extraocular muscle enlargement. Ophthalmology 1989;96:1038-47.

Prummel MF, Gerding MN, Zonneveld FW, Wiersinga WM. The usefulness of quantitative orbital magnetic resonance imaging in Graves' ophthalmopathy. Clin Endocrinol 2001;54:205-9.

Sergott RC. Oculocutaneous manifestations of thyroid disease. In: Callen JP, Eiferman RA, eds. Ocutaneous Diseases. Boston: Little, Brown & Co, 1985:117.

Spierer A, Eisenstein Z. The role of increased intraocular pressure on upgaze in the assessement of Graves ophthalmopathy. Ophthalmology 1991;98:1491-4.

Streeten DHP, Anderson GH Jr, Reed GF, Woo P. Prevalence, natural history and surgical exophthalmos. Clin Endocrinol 1987;27:125-33.

Tellez M, Cooper J, Edmonds C. Graves' ophthalmopathy in relation to cigarette smoking and ethnic origin. Clin Endocrinol 1992;36:291-4.

Terwee CB, Gerding MN, Dekker FW, et al. Development of a disease specific quality of life questionnaire for patients with Graves' ophthalmopathy: the GO-QOL. Br J Ophthalmol 1998;82:773-9.

Uretsky SH, Kennerdell JS, Gutai JP. Graves' ophthalmopathy in childhood and adolescence. Arch Ophthalmol 1980;98:1963-4.

Wouters RJ, van den Bosch WA, Lemij HG. Saccadic eye movements in Graves' disease. Invest Ophthalmol Vis Sci 1998;39:1544-50.

Management

Bartley GB, Fatourechi V, Kadrmas EF, et al. The treatment of Graves' ophthalmopathy in an incidence cohort. Am J Ophthalmol 1996;121:200-6.

Bartalena L, Pinchera A, Marcocci C. Management of Graves' ophthalmopathy: reality and perspectives. Endocrine Rev 2000;21:168-99.

Medical

Bartalena L, Marcocci C, Bogazzi F, et al. Relation between therapy for hyperthyroidism and the course of Graves' ophthalmopathy. N Engl J Med 1998;338:73-8.

Bartalena L, Marcocci C, Pinchera A. Management of Graves' ophthalmopathy: reality and perspectives. Endocr Rev 2000;21:168-99.

Bartalena L, Marcocci C, Pinchera A. Treating severe Graves' ophthalmopathy. Baillieres Clin Endocrinol Metab 1997;11:521-36.

Bartalena L, Marcocci C, Pinchera A. Cytokine antagonists: new ideas for the management of Graves' ophthalmopathy. J Clin Endocrinol Metab 1995;81:446-8.

Bartalena L, Marcocci C, Bogazzi F, et al. Use of corticosteroids to prevent progression of Graves' ophthalmopathy after radioiodine therapy for hyperthyroidism. N Engl J Med 1986;321:1349-52.

Bartalena L, Marcocci C, Chiovato L, et al. Orbital cobalt irradiation combined with systemic corticosteroids for Graves' ophthalmopathy: comparison with systemic corticosteroids alone. J Clin Endocrinol Metab 1983;56:1139-44.

Beckendorf V, Maalouf T, George JL, et al. Place of radiotherapy in the treatment of Graves' orbitopathy. Int J Radiat Oncol Biol Phys 1999;43:805-15.

Bouzas EA, Karadimas P, Mastorakos G, Koutras DA. Antioxidant agents in the treatment of Graves' ophthalmopathy. Am J Ophthalmol 2000;129:618-22.

Degroot LJ. Radioiodine and the immune system. Thyroid 1997;7:259-64.

Degroot LJ, Gorman CA, Pinchera A, et al. Therapeutic controversies: radiation and Graves' ophthalmopathy. J Clin Endocrinol Metab 1995;339-49.

Donaldson SS, Bagshaw MA, Kriss JP. Supervoltage orbital radiotherapy for Graves' ophthalmopathy. J Clin Endocrinol Metab 1973;37:276-85.

El Sheikh M, McGregor AM. Graves' ophthalmopathy: medical management. Curr Ther Endocrinol Metab 1997;6:90-4.

Erickson BA, Harris GJ, Lewandowski MF, et al. Echographic monitoring of response of extraocular muscles to irradiation in Graves' ophthalmopathy. Int J Radiat Oncol Biol Phys 1995;31:651-60.

Feldon SE. Radiation therapy for Graves' ophthalmopathy: trick or treat? Ophthalmology 2001;108:1521-2.

Glinoer D, Schrooyen M. Plasma exchange therapy for severe Graves' ophthalmopathy. Horm Res 1987;26:184-9.

Glinoer D, Etienne-Decerf J, Schrooyen M, et al. Beneficial effects of intensive plasma exchange followed by immunosuppressive therapy in severe Graves' ophthalmopathy. Acta Endocrinolog 1986;111:30-8.

Gorman CA, Garrity JA, Fatourechi V, et al. A prospective, randomized, double-blind, placebo-controlled study of orbital radiotherapy for Graves' ophthalmopathy. Ophthalmology 2001;108:1523-34.

Guy JR, Fagien S, Donovan JP, Rubin ML. Methylprednisolone pulse therapy in severe dysthyroid optic neuropathy. Ophthalmology 1989;96:1048-53.

Haddad HM. Mueller's muscle: to relax or to incise. Metab Pediatr Syst Ophthalmol 1995;18:15-8.

Hurbli T, Char DH, Harris J, et al. Radiation therapy for thyroid eye diseases. Am J Ophthalmol 1985;99:633-7.

Just M, Kahaly G, Higer HP, et al. Graves ophthalmopathy: role of MR imaging in radiation therapy. Radiology 1991;179:187-90.

Kao SCS, Kendler DL, Nugent RA, et al. Radiotherapy in the management of thyroid orbitopathy: computed tomographic and clinical outcomes. Arch Ophthalmol 1993;111:819-23.

Karadimas P, Bouzas EA, Topouzis F, et al. Hypothyroidism and glaucoma. A study of 100 hypothyroid patients. Am J Ophthalmol 2001;131:126-8.

Kazim M, Trokel S, Moore S. Treatment of acute Graves' orbitopathy. Ophthalmology 1991;98:1443-8.

Keltner JL. Is Graves' ophthalmopathy a preventable disease? Arch Ophthalmol 1998;116:1106-7.

Kinyoun JL, Kalina RE, Brower SA. et al. Radiation retinopathy after orbital irradiation for Graves' ophthalmopathy. Arch Ophthalmol 1984;102:1473-6.

Lazarus JH. Relation between thyroid eye disease and type of treatment of Graves' hyperthyroidism. Thyroid 1998;8:437.

Leone CR Jr. The management of ophthalmic Graves' disease. Ophthlamology 1984;91:770-9.

Lloyd WC III, Leone CR Jr. Supervoltage orbital radiotherapy in 36 cases of Graves' disease. Am J Ophthalmol 1992;113:374-80.

Marcocci C, Bartalena L, Bogazzi F, et al. Progress in thyroid-associated ophthalmopathy. Orbit 1996;15:197-203.

Marcocci C, Bartalena L, Tanda ML, et al. Graves' ophthalmopathy and 131I therapy. Quart J Nucl Med 1999;43:307-12.

Marcocci C, Bruno-Bossio G, Manetti L, et al. The course of Graves' ophthalmopathy is not influenced by near total thyroidectomy: a case-control study. Clin Endocrinol 1999;51:503-8.

Mourtis MP, van Kempen-Harteveld ML, Garcia MBG, et al. Radiotherapy for Graves' orbitopathy: randomised placebo-controlled study. Lancet 2000;355:1505-9.

Mourits MPh, Prummel MF, Wiersinga WM, Koornneef L. Clinical activity score as a guide in the management of patients with Graves' ophthalmopathy. Clin Endocrinol 1997;47:9-14.

Nakahara H, Noguchi S, Murakami N, et al. Graves ophthalmopathy: MR evaluation of 10-Gy versus 24-Gy irradiation combined with systemic corticosteroids. Radiology 1995;196:857-62.

Ohnishi T, Noguchi S, Murakami N, et al. Extraocular muscles in Graves' ophthalmopathy: usefulness of T2 relaxation time measurements. Radiology 1994;190:857-62.

Olivotto IA, Ludgate CM, Allen LH, Rootman J. Supervoltage radiotherapy for Graves' ophthalmopathy: CCABC technique and results. Int J Radiat Oncol Biol Phys 1985;11:2085-90.

Pfluger T, Wendt T, Toroutoglou N, et al. Retrobulbarbestrahlung bei endokriner Ophthalmopathie: Vergleich zwischen 10 und 16 Gy Herddosis. Strahlenther Onkol 1990;166:673-7.

Rush S, Winterkorn JM, Zak R. Objective evaluation of improvement in optic neuropathy ofllowing radiation therapy for thyroid eye disease. Int J Radiat Oncol Biol Phys 2000;47:191-4.

Smitt MC, Donaldson SS. Radiation therapy for benign disease of the orbit. Semin Radiat Oncol 1999;9:179-89.

Tallstedt L, Lundell G. Radioiodine treatment, ablation, and ophthalmopathy: a balanced perspective. Thyroid 1997;7:241-5.

Tallstedt L, Lundell G, Torring O, et al. Occurrence of ophthalmopathy after treatment for Graves' hyperthyroidism. N Engl J Med 1992;326:1733-8.

Tsujino K, Hirota S, Hagiwara M, et al. Clinical outcomes of orbital irradiation combined with or without systemic high-dose or pulsed corticosteroids for Graves' ophthalmopathy. Int J Radiation Oncology Biol Phys 2000;48:857-64.

Van Ruyven RLJ, Van den Bosch WA, Mulder PGH, et al. The effect of retrobulbar irradiation on exophthalmos, ductions and soft tissue signs in Graves' ophthalmopathy: a retrospective analysis of 90 cases. Eye 2000;14:761-4.

Weetman AP, Wiersinga WM. Current management of thyroid-associated ophthalmopathy in Europe. Results of an international survey. Clin Endocrinol 1998;49:21-8.

Wiersinga WM. Preventing Graves' ophthalmopathy. N Engl J Med 1998;338:121-2.

Wiersinga WM, Prummel MF. An evidence-based approach to the treatment of Graaves' ophthalmopathy. Endocrinol Metab Clin North Am 2000;29:297-319.

Wiersinga WM, Smit T, Schuster-Uittenhoeve ALJ, et al. Therapeutic outcome of prednisone medication and of orbital irradiation in patients with Graves' ophthalmopathy. Ophthalmologica 1988;197:75-84.

Surgical

Bayliss HI, Call NB, Shibata CS. The transantral orbital decompression (Ogura technique) as performed by the ophthalmologist: a series of 24 patients. Ophthalmology 1980;87:1005-12.

Carter KD, Frueh BR, Hessburg TP, Musch DC. Long-term efficacy of orbital decompression for compressive optic neuropathy of Graves' eye disease. Ophthalmology 1991;98:1435-42.

Dev S, Damji KF, DeBacker CM, et al. Decrease in intraocular pressure after orbital decompression for thyroid orbitopathy. Can J Ophthalmol 1998;33:314-9.

Dixon R. The surgical management of thyroid-related upper eyelid retraction. Ophthalmology 1982;89:52-7.

Fatourechi V, Garrity JA, Bartley GB, et al. Graves' ophthalmopathy: results of transantral orbital decompression performed primarily for cosmetic indications. Ophthalmology 1994;101:938-42.

Garrity JA, Fatourechi V, Bergstralh EJ, et al. Results of transantral orbital decompression in 428 patients with severe Graves' ophthalmopathy. Am J Ophthalmol 1993;116:533-47.

Garrity JA, Saggau DD, Gorman CA, et al. Torsional diplopia after transantral orbital decompression and extraocular muscle surgery associated with Graves' orbitopathy. Am J Ophthalmol 1992;113:363-73.

Goldberg RA. The evolving paradigm of orbital decompression surgery. Arch Ophthalmol 1998;116:95-6.

Goldberg RA, Perry JD, Hortaleza V, Tong JT. Strabismus after balanced medial plus lateral wall versus lateral wall only orbital decompression for dysthyroid orbitopathy. Ophthal Plast Reconstr Surg 2000;16:271-7.

Grove AS Jr. Upper eyelid retraction and Graves' disease. Ophthalmology 1981;88:499-506.

Grove AS Jr. Eyelid retraction treated by levator marginal myotomy. Ophthalmology 1980;87:1013-8.

Harvey JT, Anderson RL. The aponeurotic approach to eyelid retraction. Ophthalmology 1981;88:513-24.

Hedin A. Eyelid surgery in dysthyroid ophthalmopathy. Eye 1988;2:201-6.

Hudson HL, Feldon SE. Late overcorrection of hypotropia in Graves ophthalmopathy: predictive factors. Ophthalmology 1992;99:356-60.

Hurwitz JJ, Freeman JL, Eplett CJ, et al. Ethmoidectomy decompression for the treatment of Graves' optic neuropathy. Can J Ophthalmol 1992;27:283-7.

Hurwitz JJ, Birt D. An individualized approach to orbital decompression in Graves' orbitopathy. Arch Ophthalmol 1985;103:660-1.

Kazim M, Trokel SL, Acaroglu G. Elliot A. Reversal of dysthyroid optic neuropathy following orbital fat decompression. Br J Ophthalmol 2000;84:600-5.

Kazim M, Trokel S, Moore S. Treatment of acute Graves' orbitopathy. Ophthalmology 1991;98:1443-8.

Kennerdell JS, Maroon JC. An orbital decompression for severe dysthyroid exophthalmos. Ophthalmology 1982;89:467-72.

Leatherbarrow B, Lendrum J, Mahaffey PJ, et al. Three wall orbital decompression for Graves' ophthalmopathy via a coronal approach. Eye 1991;5:456-65.

Leone CR Jr, Piest KL, Newman RJ. Medial and lateral wall decompression for thyroid ophthalmopathy. Am J Ophthalmol 1989;108:160-6.

Leone CR Jr. The management of ophthalmic Graves' disease. Ophthalmology 1984;91:770-9.

Linberg JV, Anderson RL. Transorbital decompression: indications and results. Arch Ophthalmol 1981;99:113-9.

Lueder GT, Scott WE, Kutschke PJ, Keech RV. Long-term results of adjustable suture surgery for strabismus secondary to thyroid ophthalmopathy. Ophthalmology 1992;99:993-7.

Lyons CJ, Rootman J. Orbital decompression for disfiguring exophthalmos in thyroid orbitopathy. Ophthalmology 1994;101:223-30.

McCord CD Jr. Current trends in orbital decompression. Ophthalmology 1985;92:21-33.

McCord CD Jr. Orbital decompression for Graves' disease: exposure through lateral canthal and inferior fornix incision. Ophthalmology 1981;88:533-41.

Mourits MPh, Sasim IV. A single technique to correct various degrees of upper lid retraction in patients with Graves' orbitopathy. Br J Ophthalmol 1999;83:81-4.

Mourits MPh, Koornneef L, Wiersinga WM, et al. Orbital decompression for Graves' ophthalmopathy by inferomedial, by inferomedial plus lateral, and by coronal approach. Ophthalmology 1990;97:636-41.

Mourits MPh, Koornneef L, van Mourik-Noordenbos AM, et al. Extraocular muscle surgery for Graves' ophthalmopathy: does prior treatment influence surgical outcome. Br J Ophthalmol 1990;74:481-3.

Paridaens DA, Verhoeff K, Bouwens D, van den Bosch WA. Transconjunctival orbital decompression in Graves' ophthalmopathy: lateral wall approach ab interno. Br J Ophthalmol 2000;84:775-81.

Prendiville P, Chopra M, Gauderman WJ, Feldon SE. The role of restricted motility in determining outcomes for vertical strabismus surgery in Graves' ophthalmopathy. Ophthalmology 2000;107:545-9.

Remulla HD, Gliklich RE, Metson R, Rubin PAD. Delayed orbital infection after endoscopic orbital decompression for dysthyroid orbitopathy. Ophthalmology 2000;107:947-50.

Seiff SR, Shorr N. Nasolacrimal drainage system obstruction after orbital decompression. Am J Ophthalmol 1988;106:204-9.

Shorr N, Neuhaus RW, Baylis HI. Ocular motility problems after orbital decompression for dysthyroid ophthalmopathy. Ophthalmology 1982;89:323-8.

Small RG, Meiring NL. A combined orbital and antral approach to surgical decompression of the orbit. Ophthalmology 1981;88:542-7.

Thaller VT, Kaden K, Lane CM, Collin JRO. Thyroid lid surgery. Eye 1987;1:609-14.

Trokel S, Kazim M, Moore S. Orbital fat removal. Decompression for Graves' orbitopathy. Ophthalmology 1993;100:674-82.

Wilson WB, Manke WF. Orbital decompression in Graves' disease: the predictability of reduction of proptosis. Arch Ophthalmol 1991;109:343-5.

Chapter 9

Neoplasia

Neurogenic Tumors

Neurogenic tumors are a group of lesions originating from the neuroectoderm and from nonmesenchymal support cells that are, in turn, derived from the neural crest. The four cell lines included in this category are schwannian, melanocytic, ganglion, and leptomeningeal. The important clinical features of derivative tumors will be emphasized.

Optic Nerve Glioma

Pilocytic (Juvenile) Astrocytoma

Gliomas of the anterior visual pathway can be a clinical challenge, with multiple factors determining presentation, management, and outcome. The key issues to consider are histogenesis, location, extent, association with neurofibromatosis, and biologic activity. Optic nerve gliomas are low grade pilocytic (juvenile) astrocytomas that parallel the biology and behavior of similar tumors seen elsewhere in the central nervous system. The majority are isolated lesions, but a significant proportion arise within the context of neurofibromatosis (an average of one third of patients in optic nerve glioma series) where the biologic behavior and systemic features are different. Diffuse optic nerve gliomas are pathognomonic for neurofibromatosis type 1 (NF1).

In 1969, Hoyt and Baghdassarian suggested that optic nerve gliomas of childhood had a good prognosis for survival and behaved more like hamartomas than neoplasia, based on an apparent tendency for early growth followed by long-term quiescence. Imes and Hoyt reviewed the same population of patients 17 years later. They concluded that the behavior of this tumor was neoplastic and that the prognosis was less favorable, as 57% (16/28) of their patients died. However, they noted that only five of the patients died directly from the chiasmal glioma and that the deaths occurred largely during the first decade of follow-up. They also noted that of the 16 patients with neurofibromatosis, 9 (56%) died, a comparable figure to patients without neurofibromatosis.

Further, two third of NF1 patients who died did so from nonchiasmal gliomas and sarcomas. The 12 patients who survived have had stable vision and a good quality of life. Recent reviews counter these findings and suggest that about 8% to 15% of patients with NF1 have optic pathway gliomas, and that approximately 30% of patients presenting with optic nerve gliomas have NF1. In addition, patients with NF1 have better 5– and 10–year survival rates than non-NF1 patients, and only 12% compared to 63% (in non-NF1) have evidence of progression. The visual prognosis for patients with NF1 is better and the tumor behaves in a more indolent manner. Overall, therefore, NF1 is a favorable prognostic marker for visual pathway gliomas.

Neurofibromatosis was originally considered a single condition but genetically is in fact a group of distinct neurocristopathies with differing clinical manifestations. Although both NF1 and neurofibromatosis type 2 (NF2) are the most common and have ophthalmic manifestations, it is NF1 that is of greatest importance from an orbital point of view (Table 9-1). NF1 has multiple manifestations including Lisch nodules, café au lait spots, neurofibromas, optic nerve and central nervous system tumors, and occasionally tumors of the spinal cord, sympathetic nerves, and adrenals. Aside from central nervous system meningiomas and acoustic neuromas, NF2 has the major ocular manifestation of presenile lens opacities and is about 10 times rarer than NF1. About one third of patients with optic nerve pathway gliomas that present with visual symptoms have NF1. The major differences as applied to NF1 and non-NF1 optic nerve gliomas are outlined in Table 9-2 .

Although gliomas isolated to the optic nerve have been reported as female preponderant, my review of the literature suggests equal numbers of males and females. About 71% are seen in the first decade of life and 90% in the first two decades. Defining the location and extent of these tumors is difficult but about one quarter are limited to the optic nerve alone and three quarters involve the chiasm, with 40%

having extrachiasmal involvement. The important factors to establish in optic nerve gliomas (for that matter, in any instance of visual deterioration due to an optic nerve tumor) are a correct and specific diagnosis; the extent of the lesion; functional deficits caused by the tumor; and the predictable biologic behavior. They are slow-growing pilocytic astrocytomas. The general principle of management is essentially conservative. When limited to the orbit or the prechiasmal optic nerve and either large or rapidly progressive, excision is recommended. Visual acuity tends to fall into two groups with about 25% of non-NF1 cases having vision between 20/20 and 20/40, and 60% having 20/300 or less. When there is significant chiasmal or parachiasmal involvement with stability, gliomas can be observed, but if they progress, chemotherapy, radiotherapy, and/or shunting procedures may be necessary. There is, however, no definitive evidence that radiotherapy or chemotherapy alter the long-term prognosis.

Table 9-1. Diagnostic criteria for neurofibromatosis types 1 and 2

NEUROFIBROMATOSIS TYPE 1 (NF1)	NEUROFIBROMATOSIS TYPE 2 (NF2)
The diagnostic criteria are met if two or more of the following are found	NF2 may be diagnosed when one of the following is present
Six or more café au lait macules over 5 mm in greatest diameter in prepubertal patients and over 15 mm in greatest diameter in postpubertal patients Two or more neurofibromas of any type **or** plexiform neurofibroma Freckling in the axillary or inguinal regions Optic glioma Two or more Lisch nodules (iris hamartomas) A distinctive osseous lesion such as sphenoid dysplasia or thinning of long bone cortex, with or without pseudoarthrosis A first-degree relative (parent, sibling, or offspring) with NF1 by the above criteria	Bilateral eighth nerve masses seen by appropriate imaging techniques (e.g., CT scan or MRI). Preferably MRI with gadolinium* A parent, sibling, or child with NF2 and either unilateral eighth nerve mass or any two of the following - neurofibroma - meningioma - glioma - schwannoma - juvenile posterior subcapsular lens opacity

Table modified with permission from Lyons CJ. The neurofibromatoses. In: Taylor D, ed. Pediatric Ophthalmology. 2nd ed. London: Blackwell Science, 1997;309-21; and National Institutes of Health. National Institutes of Health consensus development conference statement: neurofibromatosis. Neurofibromatosis 1988;1:172-8.
* From Mulvihill JJ, Parry DM, Sherman JL, et al. NIH Conference. Neurofibromatosis 1 (Recklinghausen disease) and neurofibromatosis 2 (bilateral acoustic neurofibromatosis). An update. Ann Int Med 1990;113:39-52.

Table 9-2. Characteristics of optic nerve glioma with and without neurofibromatosis type 1

	NON-NEUROFIBROMATOSIS TYPE 1	NEUROFIBROMATOSIS TYPE 1
Presentation	Visual loss; strabismus; proptosis	Asymptomatic; routine examination finding; visual loss
Progression	63%	12%
Visual Outcome	Poor	Good
Growth Rate	Faster – 2.4/yr; occasionally rapid	Stable-slow progression – 8.4/yr; fluctuating vision
Tumor Distribution (Location)	Discrete; unilateral; may be chiasmatic	Multifocal; diffuse; bilateral; may be chiasmatic
Survival	5-year survival = 83% 10-year survival = 63%	5-year survival = 93% 10-year survival = 81%
Radiographic Findings	Fusiform optic nerve enlargement; loss of perineural space; may kink distally	Fusiform optic nerve enlargement; high signal intensity of perineural arachnoid gliomatosis on T2-weighted MRI; kinking of intraorbital nerve
Histology	Obliteration of perineural space by expanding optic nerve; intrinsic lesion	Arachnoid gliomatosis; perineural gliomatous and mucinous accumulation; paraxial
Associated Features	None	Café au lait spots; Lisch nodules; other tumors
Chiasmal & Hypothalamic Lesions	More frequently relapse; precocious puberty frequent	Indolent; precocious puberty infrequent
Hydrocephalus	79% (radiologically)	Exceedingly rare
Follow-up	Regular imaging	Not routine unless symptomatic

Modified with permission from Lyons CJ, Rootman J. Neurogenic tumours. In: Taylor D, ed. Pediatric Ophthalmology. 2nd ed. London: Blackwell Science, 1997:322-33.

Histopathology

Optic nerve gliomas are well-differentiated pilocytic astrocytomas with two growth patterns. The majority arise intrinsically, expanding the individual fascicles and the overall dimension of the nerve. The second pattern is extension of glioma into the arachnoid space, as seen in NF1 (perineural gliomatosis) (Fig. 9-1). Not infrequently, there is hyperplasia of the surrounding arachnoidal cells, which may lead to an incorrect diagnosis of meningioma from small biopsy specimens (Figs. 9-1F and 9-2B). Gliomas characteristically do not invade the dura. They are composed of fibrillary astrocytes, which may develop many brightly eosinophilic nodes (called Rosenthal fibers) in their processes. Optic nerve gliomas rarely have malignant degenerative features or mitoses; however, cystic and mucinous changes are frequently noted (Fig. 9-2B). These may correlate clinically with apparent growth (Fig. 9-3) and may also help to distinguish them from meningiomas, which are not mucin-producing. Histologically, there may be considerable sparing of the axonal component of the nerve (Fig. 9-2B). Vascular proliferation and atypia are common and do not indicate malignancy. However, mitotic figures and necrosis are frequently associated with malignant degeneration. Thus, factors that may cause clinical expansion or growth of gliomas include deposition of mucin, astrocytic proliferation, and less frequently necrosis, hemorrhage, and arachnoidal hyperplasia.

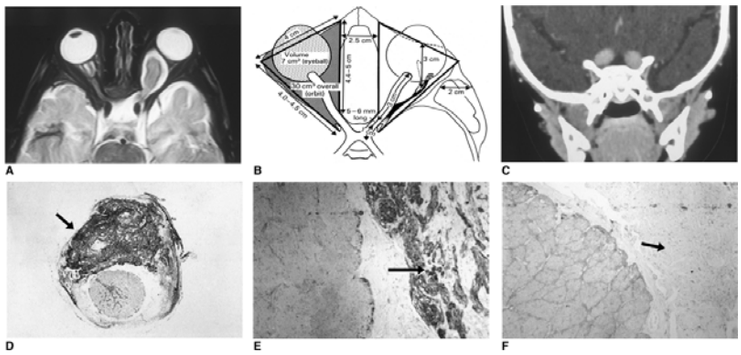

Figure 9-1. Case 6 (see Table 9-3). MR and CT imaging of a 1-year-old girl who presented with left proptosis and exodeviation at birth due to a diffuse glioma. Note that on T2-weighted MRI (A), the subarachnoid space shows high signal intensity and contrast enhancement (B; T1 imaging with fat suppression) due to the perineural arachnoidal gliomatosis associated with a diffuse optic nerve glioma in neurofibromatosis type 1. Coronal CT scan (C) demonstrates enlargement of the optic canal and bilateral involvement. The left orbital component was removed because of progressive proptosis and blindness. The glioma had evidence of perineural gliomatosis and arachnoidal hyperplasia. (D) Cross-section of this patient's optic nerve (marked “ON”) stained for glial fibrillary acidic protein (GFAP) demonstrates arachnoidal gliomatosis (arrow), which is also shown in (E) at a higher power (arrow) (GFAP, original magnifications; D × 5, E × 10). (F) Similar stain in another area demonstrates negativity where there was arachnoidal hyperplasia (arrow) in addition to the gliomatosis (GFAP, original magnification × 10).

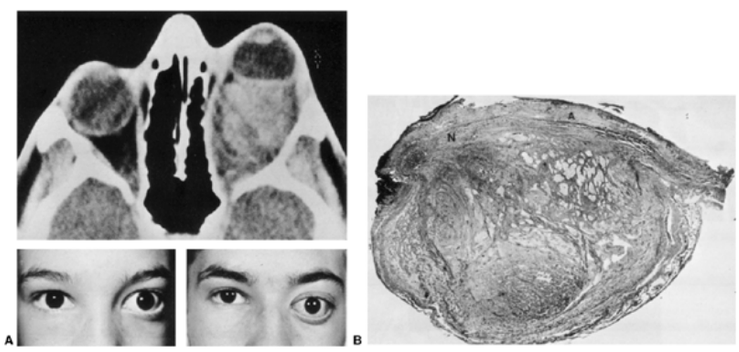

Figure 9-2. Case 18 (see Table 9-3). Clinical features of a developing optic nerve glioma. This boy presented at age 11 years (A, left inset) with a history of proptosis first noted at age 6 years, and documented progressive anisometropic hyperopia. There was no clinical evidence of neurofibromatosis. At this stage, his vision was 20/70 with a +3.50 sphere; in addition, he had 7 mm of proptosis, an afferent pupillary defect, and a raised gliotic disc. Over the next 5 years he showed documented fluctuations of vision between 20/40 and 20/80 with progressive proptosis and increasing hyperopia. At age 16 years (A, right inset), he had 11 mm of proptosis, 7 diopters of hyperopia, increased optic nerve atrophy, and an unsightly globe. (A) Axial CT scan done at that time shows a massive inhomogeneous lesion that has led to flattening of the posterior aspect of the globe and expansion of the orbit. The tumor and optic nerve were removed. (B) The massive glioma had multiple cystic areas and hyperplasia of the arachnoid *A* with considerable preservation of the axonal elements *N* (luxol fast blue hematoxylin, original magnification × 4).

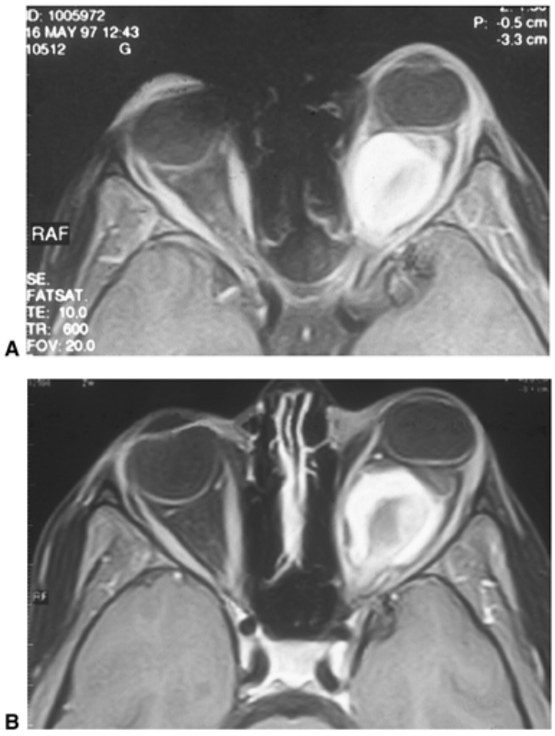

Figure 9-3. Case 20 (see Table 9-3). This optic nerve glioma was seen in 12-year-old girl (with no evidence of neurofibromatosis) who presented in March 1997 with a 2-year history of bulging of the left eye. On examination, she had 20/20 vision on the right and 20/30 left with a 0.6 neutral density filter left relative afferent pupillary defect. This was associated with a decrease in vision, papilledema, gliosis, and pallor over the next 6 months when she was noted to have progression of her proptosis. The T1-weighted, contrast-enhanced, fat-suppressed MR images (A, B) performed 7 months apart demonstrate cystic expansion of the lesion with increased proptosis and flattening of the globe. Histologically, expansion was due to cystic degeneration.

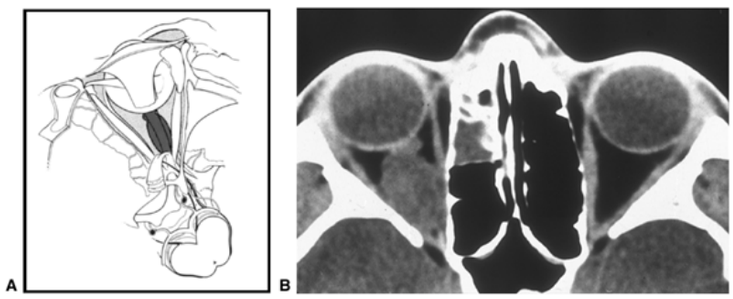

Figure 9-4. Schematic diagram (A) and CT scan (B) of a typical configuration of an intraorbital optic nerve glioma showing smooth fusiform expansion of the nerve with characteristic kinking at the distal end.

As noted, a small or peripheral biopsy specimen may only include an area of arachnoidal hyperplasia, which can be difficult to distinguish from a meningioma. Occasionally, gliomas within the subarachnoid space may be confused with a peripheral nerve sheath spindle cell tumor. They may be distinguished by histochemical stains for glial fibrillary acidic protein (GFAP) (Fig. 9-1) and phosphotungstic acid-hematoxylin (PTAH) to identify glial filaments. Electron microscopically, astrocytomas usually have a very loose, lacy appearance and only rarely demonstrate basement membranes. Rosenthal fibers are electron-dense condensations of glial filaments that are unique to astrocytes and help to distinguish them from peripheral nerve sheath tumors.

The clinical character and management of optic nerve gliomas can be best understood by dividing them into orbital, orbitocranial, chiasmal, and diffuse types.

Orbital Pilocytic Astrocytoma of the Optic Nerve

Clinical Features

Approximately 25% of optic nerve gliomas are orbital (Fig. 9-4) where they present with proptosis (frequently nonaxial and temporal), visual loss (85%), optic atrophy (60%), strabismus, limitation of elevation (50%), and unilateral papilledema (approximately 50%). They are seen in patients between the ages of 4 and 12 (average 8.8) years. The degree of visual loss tends to be profound at initial diagnosis, but may be minimal (Figs. 9-2 and 9-5). Proptosis is usually insidious in onset but may occur rapidly as a result of increased mucosubstance, necrosis, or hemorrhage (Fig. 9-3).

Examination reveals decreased vision, afferent pupillary abnormalities, visual field changes (including irregular defects, increased blind spot, altitudinal scotoma, and peripheral contraction), and strabismus in some younger patients.

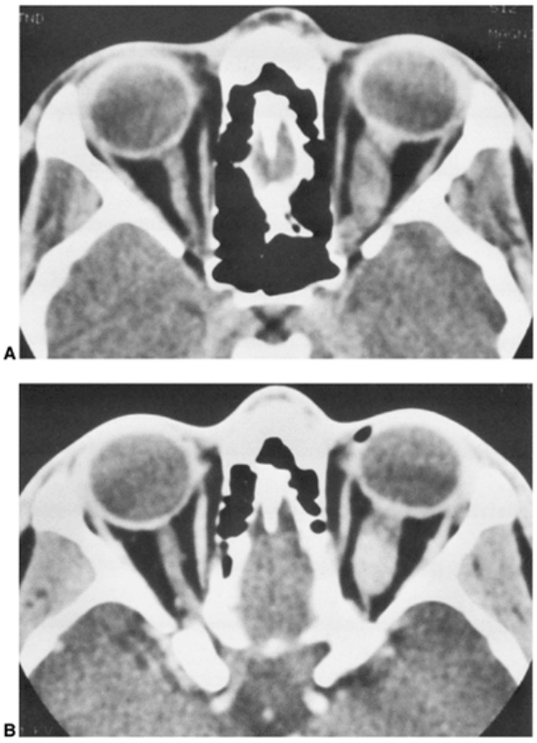

Figure 9-5. Case 17 (see Table 9-3). This 22-year-old woman had noted left visual problems for 4 years. On primary examination, she had 20/15-1 on the right and 20/20-1 on the left with a left relative afferent pupillary defect, 2 mm of proptosis, and a mild diffuse optic nerve atrophy. Her visual fields demonstrated a paracentral scotoma, and she had an abnormal VEP. (A, B) Axial CT scans show a fusiform dilatation of the optic nerve head with slight kinking of the anterior portion of the nerve due to a glioma. Clinically there was no evidence of neurofibromatosis, and she has been followed for 14 years without deterioration of vision or significant change in her tumor.

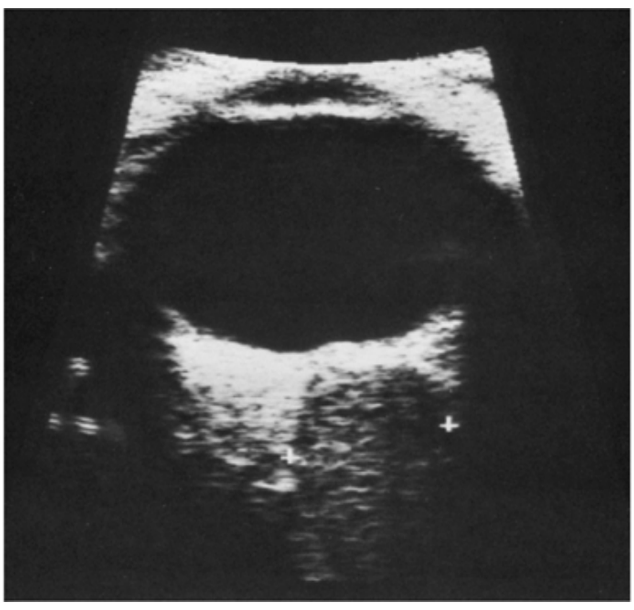

Figure 9-6. Case 9 (see Table 9-3). B-scan ultrasound demonstrates enlargement of the optic nerve by a solid glioma.

Disk swelling, or more commonly pallor, may be noted but optociliary shunts are quite rare. Patients with the stigmata of NF1 are more commonly seen with orbitocranial or diffuse optic nerve glioma and they can present with relatively good visual acuity, which may fluctuate at follow-up with spontaneous improvement. Isolated (non-NF1) gliomas are the majority of optic nerve gliomas restricted to the orbit alone, and are more frequently characterized by progressive visual loss, visual field defects, optic atrophy, proptosis, papilledema, and, rarely, the development of optociliary shunts.

Imaging

In patients with positive clinical features, the imaging of optic nerve gliomas is so characteristic that biopsy is rarely needed and may indeed be meddlesome, leading to visual loss. On CT scan, gliomas present as enlarged fusiform optic nerves with smooth, well-defined, intact dural margins (Figs. 9-4 and 9-5). Involvement of the entire orbital optic nerve is common. Anterior kinks adjacent to the globe reflecting pliability of the nerve, and low density cystic areas reflecting focal areas of degeneration within the tumor are both characteristic of optic nerve gliomas (Figs. 9-3 ,9-4 ,9-5). Calcification that is visible on CT scan is exceedingly rare. The density of these lesions is similar to normal optic nerve and shows uniform intense enhancement after contrast infusion. A central linear lucency within the optic nerve sheath, as seen in meningiomas after contrast infusion, is not noted in orbital optic nerve gliomas on CT scanning. Angiographically, they do not demonstrate a tumor blush, in contrast to optic nerve meningiomas. Ultrasonographic examination demonstrates either relatively homogeneous enlargement of the optic nerve or cystic changes (Fig. 9-6).

Magnetic resonance imaging is the modality of choice for evaluation and follow-up in optic nerve gliomas. It allows for accurate assessment of prechiasmal and chiasmal involvement (Figs. 9-1 , 9-3 , and 9-7 ,9-8 ,9-9). Gliomas are isointense or slightly hypointense on T1-weighted scans and hyperintense on T2. Optic nerve gliomas in NF1 are characterized by arachnoidal gliomatosis with mucinous accumulation in the perineural space (Fig. 9-1), in contrast to non-NF1 patients where the subarachnoid space is usually obliterated and the nerve intrinsically expanded (Figs. 9-7 and 9-8A). T2-weighted images of NF1 gliomas show an area of high signal intensity (corresponding to the mucinous elements) surrounding a central core of lower intensity (the intraneural tumor), which can be mistaken for subarachnoid fluid. Intrinsic mucin accumulation and anterior subarachnoid expansion may account for some cystic changes (Fig. 9-3).

Management

Isolated (non-NF1) intraorbital gliomas have a good prognosis for life (12% mortality rate) but a poor one for vision. Their slow progression and tendency to a declining growth pattern with time implies that the clinician's responsibilities are to establish that they are isolated and to observe the patient unless there is disfiguring proptosis (Fig. 9-2) or significant progression, particularly posteriorly. Practically speaking, patients with a unilateral optic nerve glioma, good vision, and no evidence of chiasmal involvement should be followed regularly with clinical, functional, and imaging (MRI) studies.

Visual deterioration unassociated with fluctuations or NF1 may be an indication for treatment with chemotherapy or radiotherapy. Disfiguring proptosis or significant progression warrant an adequate resection of the tumor, which may be achieved through a lateral orbital approach; however, I believe a frontotemporal panoramic orbitotomy is the method of choice, since the onus on the surgeon at the time of extirpation is to achieve a complete removal. The reason for this preferred route is based on intervention only for tumors that are of significant size, extend to the apex, or show some evidence of rapid progression. The tumor should be excised within the dura of the optic nerve distally at the globe, and the proximal extent should be identified grossly, resected, and defined histologically as clear. Several reports, including those of pilocytic astrocytomas of the central nervous system, have suggested that even incompletely excised gliomas may not progress.

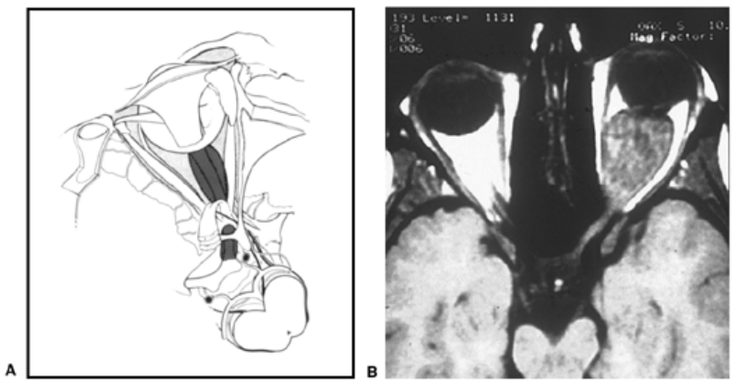

Figure 9-7. Case 12 (see Table 9-3). (A) Schematic diagram of an orbitocranial glioma extending to the chiasmal region. (B) The T1-weighted MR image demonstrates an orbital glioma that does not involve the proximal optic nerve. This was seen in a patient without evidence of neurofibromatosis. The lesion had been present since childhood but over a 2-year period, her vision deteriorated and the proptosis progressed to become unsightly. She underwent an excision to the prechiasmal region in 1990 via a panoramic orbitotomy, and has been disease free for 7 years follow-up.

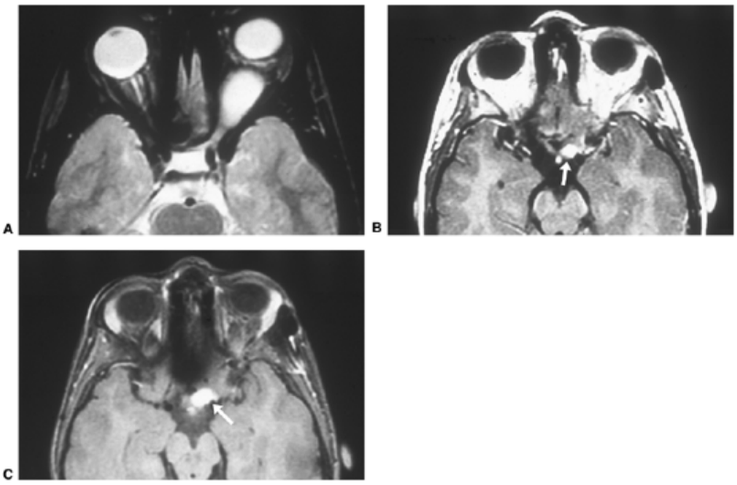

Figure 9-8. Case 15 (see Table 9-3). This girl presented at age 8 with a 4-year history of progressive visual loss. She had light perception vision on the left and on T2-weighted MR scan (A), appeared to have a tumor extending up to the optic canal. She underwent a craniotomy and at the time of excision was noted to have a slightly enlarged optic nerve that involved the prechiasmal and left chiasmal region. (B) A T1-weighted contrasted MRI done 7 months later demonstrates residual tumor (arrow) in the prechiasmal and chiasmal regions. This residuum grew over the next 6 months, as demonstrated on T1-weighted MR imaging with contrast enhancement and fat suppression (C, arrow). She underwent chemotherapy and was stable for 5 years but has recently demonstrated growth.

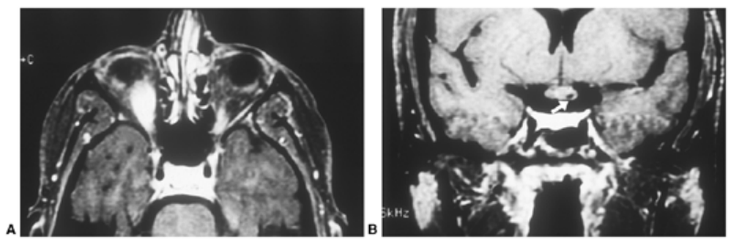

Figure 9-9. Case 16 (see Table 9-3). This 25-year-old woman was diagnosed at the age of 4 years with a left optic nerve glioma and underwent at that time an optic canal decompression. On examination, her vision was 20/200 with decreased color vision, a left relative afferent pupillary defect with temporal pallor, and 4 mm of proptosis. She had no stigmata of neurofibromatosis type 1, and visual field examination revealed a central scotoma. (A, B) The MR images demonstrate an orbitocranial lesion involving the chiasm (arrow). She has remained stable with an additional 4 years of follow-up.

Orbitocranial Gliomas

The second group of optic nerve gliomas are those with both orbital and intracranial involvement. They fall into three subgroups: anterior to the chiasm; with chiasmal involvement; and with adjacent parachiasmal involvement. The first subgroup consists of tumors that extend from the orbit up to, but not involving, the chiasm. These patients generally require more prompt surgical action, because once tumors involve the chiasm, excision is impossible. The patient may have evidence of tumor involving the nerve but not the chiasm on the basis of absence of contralateral visual field defect and careful imaging of the optic canal and chiasmal region (Figs. 9-8 and 9-10). MRI is the modality of choice but may not be completely accurate as to extent (Fig. 9-8B). When they extend into the optic canal, there is a smooth enlargement of the bony structures (Figs. 9-1 and 9-10). This subgroup of optic nerve astrocytomas can be managed by en bloc surgical excision of the involved nerve up to the chiasm with confirmation of clear margins.

Chiasmal Gliomas

Clinical Features

It appears that two thirds to three quarters of optic nerve gliomas involve the chiasm in one way or another. They may either be restricted to the chiasm or involve the parachiasmal structures including the optic nerve, third ventricle, and adjacent brain (Fig. 9-11). They are seen in a slightly older age group than isolated optic nerve glioma. Generally, they present with bilateral visual loss but may be discovered on investigation for hydrocephalus, endocrine dysfunction, or on routine neuroimaging studies. Visual loss is usually slow but may occur suddenly as a result of hemorrhage within the tumor. Strabismus and dissociated nystagmus mimicking spasmus nutans may be other presenting features. These tumors may even extend into the optic tracts. Hypothalamic involvement produces various endocrine abnormalities, including precocious puberty, growth retardation, diabetes insipidus, and obesity. Tumors isolated to the optic nerve and chiasm have a 10-year mortality rate of approximately 17%. However, if there is chiasmal and hypothalamic, or third ventricle involvement on presentation, the mortality rate becomes 50%.

Imaging

Chiasmal gliomas may be associated with suprasellar masses including cystic lesions, extension into the hypothalamus, hydrocephalus, and involvement of the higher visual pathways. These gliomas are best demonstrated on MR imaging. Noncontiguous intracranial tumors may be seen in about 4% of patients with NF1.

Management

The majority of chiasmal gliomas are indolent but those that McDonnell and Miller describe as posterior have a more serious prognosis. Surgical intervention is only useful for significant exophytic components such as suprasellar masses or tumors compressing the chiasm or optic nerves. Direct surgery on the chiasm risks hypothalamic syndromes, sudden death, and bilateral visual loss. The management options continue to be chemotherapy and radiotherapy but considerable controversy exists concerning indications and the value of these treatments. In general, most authors suggest chemotherapy as a primary choice unless the tumors are of

large size or involve the hypothalamus, third ventricle, or optic tract. Chemotherapy may also be very useful to avoid the adverse effects (mental and growth retardation, psychiatric problems, and induction of second tumors) of radiotherapy by delaying it until the child has matured. Although chemotherapy may delay radiation, the majority of children eventually relapse. In the absence of controlled prospective trials, a careful review of the literature in balance does not confirm a benefit from radiotherapy. However, the introduction of fractionated stereotactic radiotherapy may prove to be a better treatment modality for optic nerve glioma.

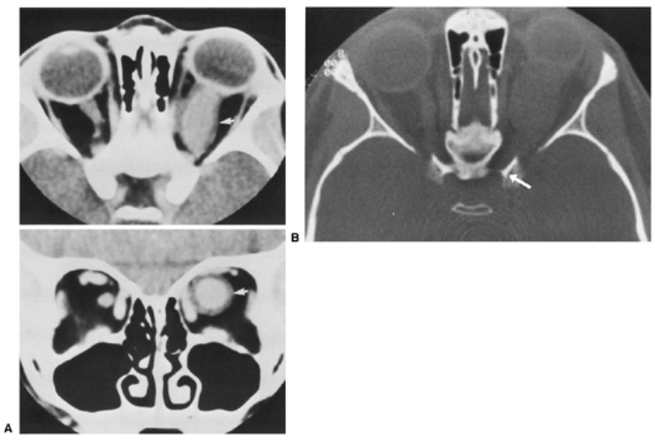

Figure 9-10. Case 14 (see Table 9-3). (A) Axial and coronal contrast-enhanced CT scan of a 5-year-old child shows a fusiform optic nerve lesion causing flattening of the posterior margin of the globe. There was no evidence of neurofibromatosis type 1 except for a single café au lait spot. Note the low-density expansion of the left optic nerve sheath that corresponded histologically to arachnoidal meningeal hyperplasia (arrow). Clinically, the patient had slight proptosis and mere light perception. (B) Axial CT scan of the same patient with bone settings demonstrates widening of the left optic canal (arrow) due to involvement of the intracanalicular portion of the nerve. The patient underwent resection to the prechiasmal region and has had no recurrence for 9 years.

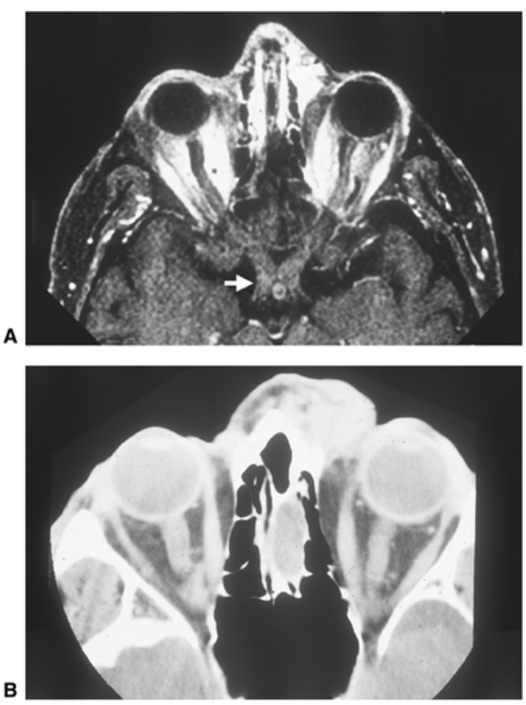

Figure 9-11. Case 23 (see Table 9-3). The T1-weighted MRI (A) and CT scan (B) demonstrate bilateral optic nerve and chiasmal (arrow) glioma. This was seen in a 41-year-old man with a history of neurofibromatosis type 1 and a vision of 20/400 right and 20/200 left. He has been stable for 10 years of follow-up. Note plexiform neurofibroma of the anterior orbital and periorbital region.

Patients with features of NF1, largely those with orbitocranial or diffuse gliomas, are more likely to have tumors that behave in an indolent fashion with good preservation of vision, although fluctuations of vision are well known to occur (Fig. 9-12). This group in particular should be managed conservatively.

Diffuse and Bilateral Pilocytic Astrocytoma

Diffuse and multifocal optic nerve gliomas with perineural gliomatosis are pathognomonic for NF1 (Figs. 9-1 , 9-12 , and 9-13). These tumors have a good visual prognosis, even without intervention, so that these patients are best observed (Fig. 9-12). It is worth emphasizing that patients with neurofibromatosis are prone to sarcomas and malignant gliomas in other sites and bear close follow-up. Bilateral optic nerve gliomas may be seen in the absence of systemic evidence of NF1 (Cases 7 and 8 – Table 9-3).

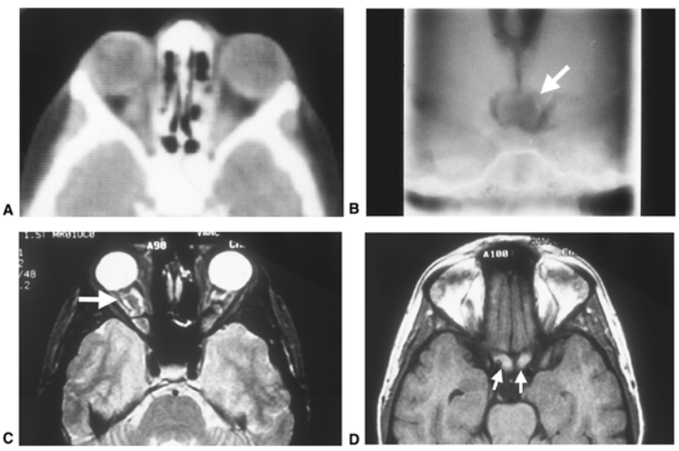

Figure 9-12. Case 2 (see Table 9-3). This child with neurofibromatosis type 1 presented at 4 years of age with prominence of her left eye and vision of 20/40 right and 20/200 left, which was associated with mild optic atrophy. CT scan performed at that time (A) demonstrates a diffuse optic nerve glioma involving both orbital portions, and the pneumoencephalogram (B) demonstrates the chiasmal involvement (arrow). This patient has been observed over 13 years with variable and fluctuating vision in the 20/40 range on the right and 20/50 on the left. At last visit (age 17 years), her vision was 20/20 bilaterally. MR images (C, D) taken at that time shows typical perineural arachnoidal gliomatosis on the T2-weighted image (C, arrows) with chiasmal intracranial involvement (B, C, D, arrows).

Our experience with 24 cases (8 diffuse, 8 orbitocranial, 4 orbital, 3 chiasmal, 1 malignant) reflects the clinical spectrum of optic nerve glioma (Table 9-3). Of those with diffuse or bilateral glioma (6 females, 2 males), six had systemic features of NF1, two of which were bilaterally blind, four had reduced vision, and two had normal vision. Fluctuations in vision were observed in this group of patients, one in particular (Case 2 – Table 9-3) had vision that varied between 20/20 and 20/200 and stabilized at 20/20 bilaterally in adulthood with 13 years of follow-up (Fig. 9-12). Seven cases presented in early childhood and one was picked up because her child had NF1 (Case 4 – Table 9-3). Three of the diffuse optic nerve gliomas included involvement of the optic radiations, and two of the patients had developmental delay. One patient with bilateral optic nerve glioma had a large suprasellar mass (Fig. 9-14) extending from the chiasm with involvement of the optic radiations.

The second group (5 females, 3 males) had lesions extending to the chiasm. None of these patients had NF1 but two had three or less café au lait spots without other stigmata. Five underwent resection for growth or progressive visual loss (one also received radiotherapy). All are alive and well. One of the patients (Case 15 – Table 9-3) had tumor at the resection margin 2 mm from the chiasm and has had growth of the residual within a year, leading to chemotherapy and stability for 5 years (Fig. 9-8). She now demonstrates further growth and will be considered for stereotactic radiosurgery if definitive growth occurs. One patient (Case 10 – Table 9-3) has been observed without progression for 2 years.

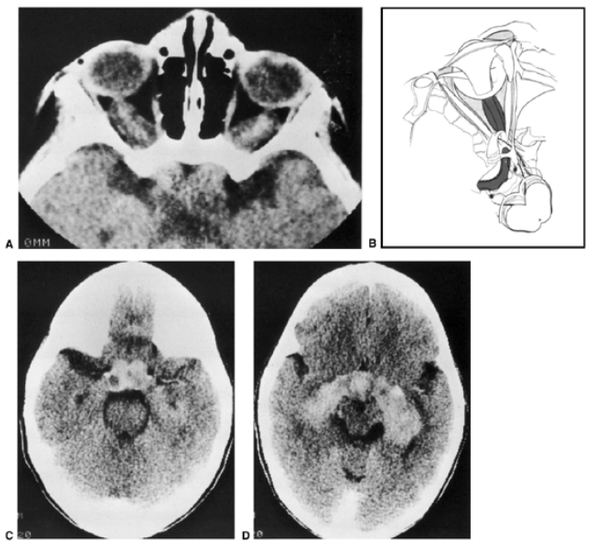

Figure 9-13. Case 3 (see Table 9-3). Axial CT scans show a diffuse glioma involving both optic nerves (A), the chiasm (C), and optic tracts (D), which is schematically represented in (B). The patient was a 5-year-old boy with neurofibromatosis type 1; he had bilateral blindness and optic pallor.

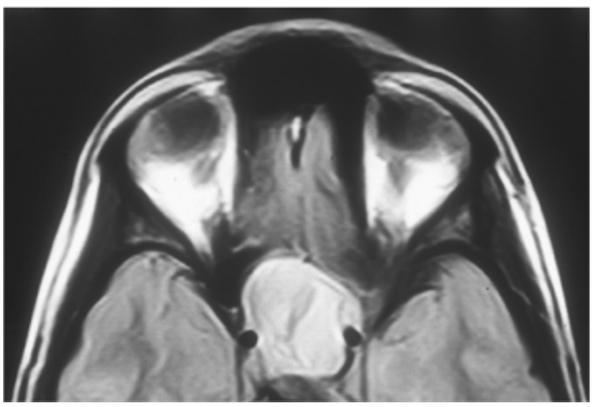

Figure 9-14. Case 8. This T2-weighted MRI demonstrates significant intracranial involvement of a suprasellar mass in a 3-year-old child, who had a bilateral glioma and developmental delay. She did not have stigmata for neurofibromatosis type 1 and she had bilateral optic atrophy. She was treated with chemotherapy and has been stable for 11 years.

Of our four orbital cases, two have been observed only (5 and 14 years) without progression. The remaining two cases underwent surgical excision for growth, both largely due to cystic change. Neither have recurred.

We had three isolated chiasmal and parachiasmal optic nerve gliomas. One (Case 22 – Table 9-3), with precocious puberty and NF1, underwent radiotherapy for progressive visual loss with good response; however, the patient subsequently died of a second glioma. The remaining two have been observed for 22 and 10 years and are stable.

The single case of malignant optic nerve glioma died within 6 months of diagnosis.

The major lesion to differentiate from optic nerve gliomas remains optic nerve meningioma. The numerous epidemiologic, clinical, orbital imaging, and histopathologic differences between these two lesions are summarized in Table 9-4 .

Table 9-3. Optic nerve gliomas seen at the University of British Columbia Orbital Clinic, 1976-99

CASE	ONSET (age)	AGE SEEN (years)	SEX	NERUO-FIBRO-MATOSIS	PRESENTATION	IMAGING	MANAGEMENT	FOLLOW-UP
DIFFUSE (n = 8)								
With Perineural Gliomatosis								
1 (DC)	2 years	2	F	+	Right pupil noted to be larger than left; 4 months of progressive right proptosis (OD 14 mm, OS 8 mm)	Diffuse optic nerve and chiasm	Under observation	Stable for 14 years
2 (JC)	4 years	4	F	+	Left eye prominent for several months; vision 20/40 OD, 20/200 OS; mild optic atrophy	Diffuse optic nerve and chiasm	Observed; variable vision, fluctuates to levels of 20/40 OD 20/50 OS	Follow-up for 13 years; vision now 20/20 OU
3 (JH)	1 year	4	M	+	Bilateral blindness progressive since age 1 year; nystagmus; optic atrophy	Optic nerves, chiasm, and radiations	Observed	Follow-up for 1 year
4 (CP)	2 years	12	F	+	Left proptosis; visual loss; bilateral optic atrophy	Bilateral optic nerve sella, brain stem, anterior cranial fossa	Multiple debulking	Minimal growth; follow-up for 13 years
5 (GS)	Aniso-metropic, amblyopic age 6 years	36	F	+	Family history of stigmata; examined because of child with NF1; pale left optic nerve head; vision slow 20/20	Left optic nerve and chiasm	Observed	Stable for 6 years
6 (AW)	Birth	1.1	F	+	Bilaterally raised gliotic disk; left proptosis	Diffuse, involves radiations	Debulking of left orbital component 1998	Stable for 5 years, strabismus surgery at 5 years
Bilateral without Perineural Gliomatosis								
7 (BL)	2 years	2	M	-	Developmental delay	Bilateral optic nerves and chiasm	Observed	No follow-up since seen in 1987
8 (TT)	Infancy	2	F	-	Poor fixation OD with optic atrophy OD and temporal pallor OS; developmental delay	Diffuse and radiations with suprasellar mass	Chemotherapy when vision deteriorated and tumor growth noted (age 3)	Stable for 11 years; bilaterally blind

ORBITOCRANIAL (n = 8)								
9 (HD)	13 years	14	F	-	8 months progressive right visual loss (counting fingers 40 cm); elevated optic nerve head	Right optic nerve anterior to chiasm	Resection	No recurrence at 16 years
10 (JD)	8 years	16	M	3 café au lait spots	7-year history of progressive visual loss right eye; now no light perception	Right optic nerve	Observation	No progression at 2 years; no follow-up since
11 (NE)	Mid-teens	63	M	-	Progressive visual loss to blindness over 48 years	Left optic nerve to chiasm, expansion between 1995 and 1998	Diagnostic excision of intracranial component	Developed neovascular glaucoma at 4 years
12 (KK)	14 years	14	F	-	Photographic evidence of proptosis since childhood; progressive proptosis with decrease in vision and growth over 2 years	Involved to optic canal but not beyond on MRI and CT	Excision (1990) to just anterior of the chiasm; free at margins	No recurrence for 7 years
13 (KL)	25 years	30	F	-	Decreased right vision for 5 years; diagnosis astrocytoma grade II; treated with radiotherapy 5600 rad, resected (elsewhere)	Right optic nerve to chiasm	Observation	Enucleation following radiation keratopathy and painful eye
14 (AQ)	Infancy	6	F	1 café au lait spot	Strabismus left eye since age 9 months; proptosis age 4 years; light perception only left eye	Left optic nerve to chiasm	Resected; gross complete, microsocpic residual	No recurrence for 9 years
15 (NR)	4	8	F	-	Left light perception only with progressive loss	Progressive growth and involvement to chiasm	Excision to chiasm; histologically involved at margins	Enlargement of nodule within a year with contralateral visual field change; chemotherapy then stable for 6 years with slight growth
16 (JS)	4	25	F	-	History of poor fixation at 11 months of age; 20/20 OD 20/200 OS; loss of color vision; 2 mm proptosis; slight downward and medial displacement of left globe; moderate temporal optic disk pallor	Left optic nerve and left portion of chiasm	Bony decompression (age 4 years); observed since	No progression for 4 years
ORBITAL (n = 4)								
17 (RF)	18 years	22	F	-	4 years decreased vision OS; 2 mm proptosis; optic atrophy	Left orbit	Observed	No growth for 14 years
18 (TH)	8 years	11	M	-	Changing refraction for 1 year; increased hyperopia; vision 20/25; 7 mm proptosis; disc pallor	Left orbit	Observed 4 years; vision 20/80; marked proptosis - 11 mm; optociliary shunt; resected	No recurrence for 5 years

19 (DK)	unknown	13	M	-	Vision right eye reduced 20/25	Right optic nerve enlarged	Observed since 1981	No change at 5 years
20 (BS)	2 years	12	F	-	Left proptosis; 20/30 OS with 0.9 RAPD; progressive visual loss to count fingers over the next 6 months with papilledema, gliosis, and pallor	Intraconal increase in size	Resected 1998; margins involved with astrocytic hyperplasia	No recurrence for 3 years
CHIASMAL AND PARACHIASMAL (n = 3)								
21 (DA)	Childhood	7	M	-	Visual loss left eye	Left optic nerve to chiasm	Biopsied and irradiated prior to referral	22 years no light perception left eye with optic atrophy and right nasal field defect
22 (KC)	2 years	9	M	+	Decreased vision bilaterally; 20/400 OD, 20/200 OS; bilateral optic atrophy OD greater than OS; precocious puberty	Chiasmal	Observed for 2 years; decreased vision to 20/400 OD, 20/60 OD; led to radiotherapy 5000 rad	Vision improved to 20/100 OD, 20/40 OS at 2 years; second cerebral glioma at 3 years; bilateral nasal field defect at 5 years; died at age 15
23 (GH)	Childhood	41	M	+	20/400 OD, 20/200 OS; Decreased color vision; Lisch nodules; fundus melanocytic hyperplasia; seizures since childhood	Chiasm, bilateral optic nerves, posterior thalamus, right middle cerebral peduncle, plexiform neurofibroma of lid	Observed	Stable for 10 years
MALIGNANT (n = 1)								
24 (WM)	54 years	54	M	-	Blurred vision OS, vision 20/20 OD, count fingers OS; bilateral temporal field defect	Chiasm, hypothalamus	Biopsy - glioblastoma, radiotherapy	Dead in 6 months

Malignant Optic Nerve Glioma (Glioblastoma) of Adulthood

In 1973, Hoyt and coworkers described a malignant optic nerve glioma of adulthood. It appeared to constitute a distinct syndrome occurring in middle-aged males, causing rapid deterioration of vision mimicking optic neuritis with relentless progression to blindness and fatality. The early symptoms consisted of monocular visual blurring, retrobulbar pain, features of increased venous congestion, edema, and infarction of the nerve at the disc. The tumor progresses to cause blindness, hemiparesis, and hypothalamic abnormalities. Pathologically, it is an aggressive glioblastoma that invades the surrounding tissues, leading to a rapid downhill course and death. Most patients were not diagnosed before craniotomy or autopsy.

More recently, the syndrome has been broadened to include the middle-aged of both sexes (roughly in equal proportion) with binocular visual symptoms in 50%. In spite of visual and retrobulbar symptoms, 25% of cases show normal ophthalmologic and neuroradiologic findings. Roughly 50% have or develop disc edema and may go on to hemorrhagic glaucoma and orbital involvement (proptosis and ophthalmoplegia) as a result of growth and extension. The ocular symptoms occur early and as the tumor rapidly extends into the nervous system, neurologic symptoms develop. CT scanning will demonstrate enlargement of the optic nerve or chiasm in 75% of patients. Diagnosis is by open biopsy. Spoor et al. have described one case in which the biopsy was made by fine needle aspiration. The fulminant and relentless course of this disease is unaffected by any therapeutic modality. Histologically, the majority of cases have been glioblastoma multiforme with a few described as histologically more well-differentiated astrocytomas.

Table 9-4. Major features of optic nerve glioma and optic nerve meningioma

	OPTIC NERVE GLIOMA	OPTIC NERVE MENINGIOMA
Epidemiology		
	Age Median 5 years (may be first symptomatic after age 20 years 71% in first decade; 90% by second decade Associations: approximately 30% have NF1 Bilateral involvement frequently associated with NF1 Sex: slight female dominance	Age: mean 41 years (4% under 20) Associations: rare association with NF2 Bilateral involvement is not associated with NF1 Sex: significant female dominance
Clinical Features: Visual		
	Disproportionate visual loss (85% have some visual loss and 60% have 20/30 or less) with minimal proptosis Optociliary shunt rare Optic atrophy in 60% Papilledema in 50%, especially in orbital glioma Patients with NF1 have a better visual prognosis	Disproportionate visual loss to degree of proptosis Optociliary shunt a characteristic feature in 25% Optic atrophy in 55% Papilledema in 42%
CT Features		
	Intact dura, smooth margins Most are fusiform May have central remnant of optic nerve (especially with NF1) Kinking and cystic degeneration Very rare and sparse calcification Rare bone change Cystic change not infrequent	If tumor extends through dura or has irregular margins, then orbital invasion likely (15%) Diffuse with polar bulbous enlargement Railroad tracking a characteristic feature (20% to 25%) Straight or splinted Calcification when present and dense is a typical feature (20% to 25%) Hyperostosis of adjacent bone may occur Cystic change is very rare
MRI Features		
	Tubular, fusiform, or lobulated Smooth margins Anterior kinking T1: low intensity; T2: variable Perineural arachnoidal gliomatosis: increased T2 intensity and gadolinium enhancement Intracranial involvement: high T2 intensity	Variable (hyper-, hypo-, and isointense) T2-weighted changes Most are isointense to gray matter (T1) Increased enhancement with gadolinium, frequently perineural
Histologic Features		
	Astrocytic filaments (PTAH and GFAP) Rosenthal fibers Arachnoidal hyperplasia frequent	Intranuclear pseudoinclusions Clusters and whorls All are meningothelial or transitional PAS-positive glycoprotein in cytoplasm
Electron Microscopy Features		
	Elongated and spindle-shaped Abundant cytoplasmic glial filaments Focal degeneration Rosenthal; electron-dense condensations of glial filaments	Intertwining cell processes with many desmosomes Little extracellular space or matrix Cytoplasm numerous filaments Few organelles
Immunohistochemical		
	GFAP (glial fibrillary acidic protein) positive EMA (epithelial membrane antigen) negative	GFAP negative EMA positive (80%)

Meningiomas

Meningiomas may affect the orbit when they arise intracranially, from the optic nerve, or rarely de novo in the orbital soft tissues. They are usually slow-growing and declare clinically by compression and/or encasement of normal structures. Visual loss is frequent; those from the optic nerve sheath usually cause unilateral deterioration whereas those arising intracranially often ultimately affect vision bilaterally. The more confined the space and the closer to the optic nerve, the earlier their effect on vision. As such, even small tumors of the optic canal can cause early visual disturbances while more remote lesions cause structural displacement and disfigurement first, with functional deficits later. To date, we have seen 88 meningiomas, 33 of which were optic nerve sheath in origin and the remaining arose elsewhere involving either the sphenoid wing (42) or other sites (13). Sphenoid wing meningiomas account for 20% of intracranial meningiomas, and 90% of orbital meningiomas arise intracranially. Only one of our cases appeared to be a primary tumor of the soft tissues of the orbit. Most intracranial meningiomas that affect orbital or visual structures arise from the dura of the sphenoid bone (ridge, planum, parasellar region, or optic canal). Predisposing factors are female sex (progesterone receptors), previous ionizing radiation, and neurofibromatosis type 2 (deletion of chromosome 22).

Histogenesis and Growth

The meningothelial cap cells of the arachnoid villi (pacchionian granulations) are the stem cells of meningiomas. They arise from and incorporate the middle meningeal layer adjacent to the pia-arachnoid. Growth is slow and usually in cohesive clusters with or without evidence of encapsulation. When invading soft tissues, there is frequently reactive desmoplasia. Infiltration of bone can cause hyperostosis, making them difficult to distinguish from primary bone tumors. Meningiomas tend to displace structures, extend along paths of least resistance through foramina and adventitial spaces, encase structures in dense connective tissue, or cause compression due to hyperostosis and expansion of bone.

There are a number of histologic patterns but the fundamental cell is usually round or polygonal, or may be more spindle-shaped. Varying admixtures of blood vessels, fibroblasts, and psammoma bodies account for the differing patterns. Although they usually arise as a cohesive mass that develops in continuity, concurrent multiple sites of occurrence and seeding have been described.

Overall, two third of meningiomas are meningotheliomatous (syncytial) (41%), consisting of sheets of polygonal cells, or transitional (mixed-psammomatous) (25%) where they are composed of eddies or whorls of spindle cells that frequently surround a central psammoma body. Dense, randomly woven bundles of spindle-shaped meningothelial cells and fibroblasts constitute the fibrous pattern (approximately 19%). Meningiomas may be quite vascular (Fig. 9-15) and are rarely cystic.

The two aggressive patterns are angioblastic (capillary hemangioblastoma) and sarcomatous. Angioblastic meningiomas are exceedingly rare, constituting 3% of meningeal tumors. It is thought that the majority of these lesions are hemangiopericytic with very few that are hemangioblastic. Angioblastic meningiomas have a tendency to recur, and up to one third are reported to metastasize eventually. The spread of angioblastic meningiomas is not predictable histologically. Sarcomatous (anaplastic) intracranial meningiomas occur in a younger age group (second decade), are more pleomorphic and invasive, and may metastasize outside the central nervous system. Histologically, they are divided into benign (94%), atypical (5%), and anaplastic (1%).

Intracranial Meningiomas

Clinical Features and Topography

Meningiomas constitute 20% of adult and 2% of childhood intracranial tumors. The major sites affecting orbital and visual structures are the sphenoid ridge, suprasellar area (tuberculum sellae, parasellar), and olfactory groove. Overall, 18% to 20% of all intracranial meningiomas occur in the sphenoid wing, 8% suprasellar region, and 8% along the olfactory groove. Tumors of the middle portion of the sphenoid ridge arise from the posterior margins of the lesser wing (Fig. 9-16). The deep inner or clinoidal portion and the middle third of the sphenoid ridge make up the medial portion and by contiguity affect neural and vascular structures passing through the optic canal and superior orbital fissure early in their course. Similarly, parasellar meningiomas affect adjacent vessels and structures of the cavernous sinus early, leading to motor, sensory (25%), or visual deficits (50%) (Fig. 9-16). In contrast, tumors of the olfactory groove and lateral third of the greater wing of sphenoid (Fig. 9-16) tend to be large and globular before causing symptoms of raised intracranial pressure or displacement. En plaque meningiomas have a propensity to occur along the greater wing of the sphenoid and are frequently desmoplastic, infiltrative, and hyperostotic.

The orbital and visual manifestations reflect location with the more medial tumors causing cranial nerve palsies, visual deficits, and venous obstructive signs and symptoms (edema and chemosis). More remote tumors exert their effect by raised intracranial pressure or mass effect. Those of the greater wing of the sphenoid may manifest enlargement

of the temporalis fossa with late intracranial symptoms, while those of the olfactory groove present with both intracranial and visual symptoms. Physical distortion of the orbit is the result of expanded bone and/or tumor invading soft tissues. Expansion of the temporalis fossa may be easily noted in patients wearing glasses wherein the gap between the temporalis and the temple of the glasses is narrow compared to the other side. Retrospective review of photographs can often be useful in assessing this feature or orbital displacement (Figs. 9-15 and 9-17). By the time tumors of the olfactory groove present with visual loss, they are often bilateral.

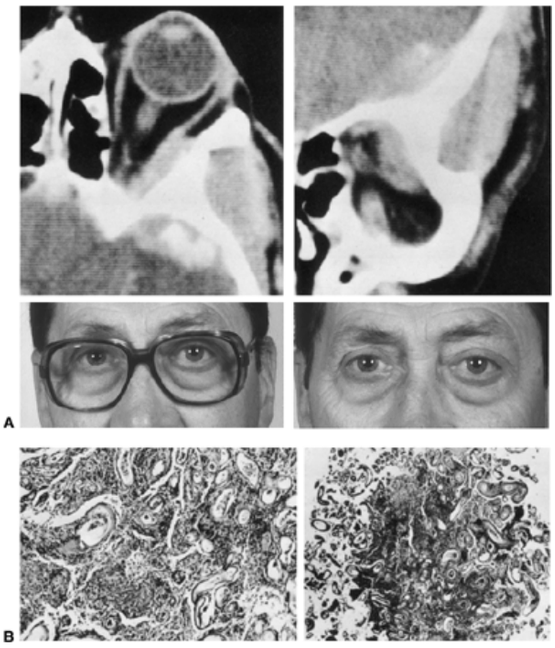

Figure 9-15. (A) This meningioma of the outer two third of the sphenoid wing is causing hyperostosis with an associated soft tissue mass involving the adjacent lateral orbit and middle cranial and temporalis fossae (axial and coronal contrast-enhanced CT scans). Note fullness of the left temporalis fossa in the clinical photograph of this 67-year-old man, who had become aware of a decrease in his vision. Clinically, there was medial displacement (2 mm), proptosis (7 mm), and decreased visual field. He underwent resection of the tumor and bone, with recovery of field and vision. (B) Histopathology of the lesion shown in (A). Note rich vascular pattern with islands of meningothelial cells (H&E, original magnifications; left × 10, right × 2.5).

Figure 9-16. Schematic diagram demonstrates the sites of nonoptic nerve meningiomas that may affect vision and the orbit: (1) inner, (2) middle, and (3) outer thirds of the sphenoid; (4) olfactory groove, (5) parasellar, and (6) intraorbital.

Intracranial meningiomas occur three times more frequently in women than in men and are usually seen in the fifth decade. In contrast, Wright noted that optic nerve and orbital meningiomas are female predominant but may have a bimodal peak in the second and fifth decades. Our combined series of 88 cases did not demonstrate a bimodal peak. Those in the young are said to be more aggressive. Multifocal simultaneous meningiomas may occur, and there is an increased frequency of intracranial and orbital meningiomas in neurofibromatosis type 2 (12% of patients).

In a summary of data from prospective studies, Wilson noted that visual loss in intracranial meningiomas is slowly progressive in 90%, acute in 8% to 12%, and may be slow but intermittent in about 12%. Fifty percent have initial unilateral loss with bilateral visual loss occurring in the remainder, except for olfactory groove meningiomas, which have a higher incidence of bilateral loss. Deterioration of color vision is an earlier and more sensitive index of compression of the optic nerve.

Investigations

The most useful imaging modalities for meningiomas are CT and MR imaging. Bony change, hyperostosis, and lysis are particularly well shown on CT scan (Fig. 9-18), and the soft tissue component of the tumor is readily visible with MRI, especially with gadolinium enhancement. The lesion is well defined, homogeneous, and characteristically of increased density with uniform enhancement post-contrast infusion. In addition, the tumor may show encasement of adjacent structures (Fig. 9-19). Smaller intracranial meningiomas can be identified with CT but are particularly visible on MR imaging (Fig. 9-20). Contrast angiography is most useful for adjunctive embolization preoperatively and has been replaced as a routine imaging technique by MRI and CT. Fine calcification may be evident in highly psammomatous lesions. Three-dimensional reconstruction can demonstrate relationships to other structures including blood vessels.

Management

The development of multidisciplinary and microsurgical approaches has substantially improved management. Providing the tumor is well defined, excision is extremely effective. However, invasion of bone and adjacent soft tissues or encasement of vital structures may obviate complete excision. Major debulking can be effective in improving cosmesis and alleviating compressive symptoms with reversal or postponement of visual loss. In the management of sphenoid wing meningiomas, combined neurosurgical-orbital panoramic orbitotomies have in our hands allowed for aggressive excision or debulking of these tumors with orbital reconstruction and minimal morbidity. The introduction of postoperative radiotherapy has improved the results for patients with residual or recurrent tumors, with overall time to and rates of recurrence reduced by adjuvant treatment. Our current approach is to aggressively debulk, and where possible, completely remove the tumors. Radiotherapy is utilized for cavernous sinus or known residual disease. We have removed 19 sphenoid wing meningiomas, ten of which underwent gross total removal, six aggressive subtotal removal, and three partial removal. All of them underwent orbital reconstruction with a reduction in proptosis in all 19, residual proptosis of less than 2 mm in two, and enophthalmos in two. Surgical limits were determined by cavernous sinus involvement in one, subarachnoid seeding in one, extensive bony disease in three, infratemporal fossa disease in one, and age-associated disease in one. Seven of our patients underwent adjunctive radiotherapy, five for incomplete removal, one for CT scan residual, and one following cavernous sinus dissection. Major indications for surgery were proptosis and temporal fullness with orbital congestion and impaired vision. All of the patients with impaired vision achieved improvement. The principal complications in surgery consisted of two instances of diplopia in extreme gaze, five of temporalis fossa excavation, two with dysesthesia, two with ptosis, and one with frontalis palsy. To date, we have had no recurrences requiring secondary removal. Our overall philosophy is that sphenoid wing and skull base orbitocranial meningiomas respond well to aggressive but limited surgery, which has low morbidity, no mortality, and is able to preserve or improve vision. They also achieve good cosmetic results and are best operated on early with radiotherapy utilized as an adjunct.

It is necessary, however, to plan for follow-up on these patients with at least a 10- to 20-year perspective since recurrence rates are significant. Antiprogesterone therapy may have had some success and other types of hormonal therapies are being explored. Image-guided techniques may also play a role in future therapy of these lesions, both surgically and in stereotactic radiosurgical techniques.

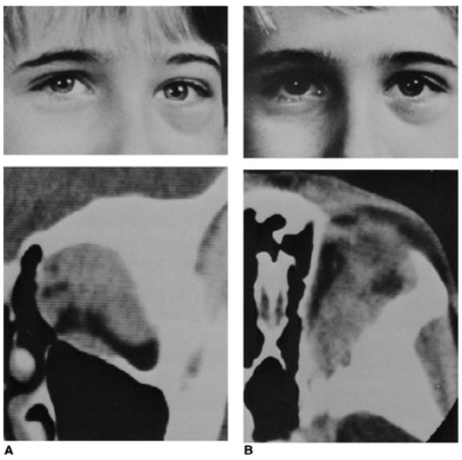

Figure 9-17. (A, top) Clinical photography of an 11-year-old boy who presented with a left proptosis (8 mm) with downward (3 mm) and inward (2 mm) displacement. A photograph taken 2 years earlier (B, top) demonstrates prior “swollen lids.” Axial (A, bottom) and coronal (B, bottom) CT scans of the meningioma demonstrate hyperostosis of the orbital roof and lateral wall. Clinical features consisted of temporal and supraorbital pain with proptosis for a 5-year period. The patient had slight decreased vision (20/25) with minimal temporal pallor. The patient also demonstrated lid swelling and chemosis due to venous obstruction, a common feature of apically located meningiomas. She had lid retraction, making the differential diagnosis one of thyroid orbitopathy.

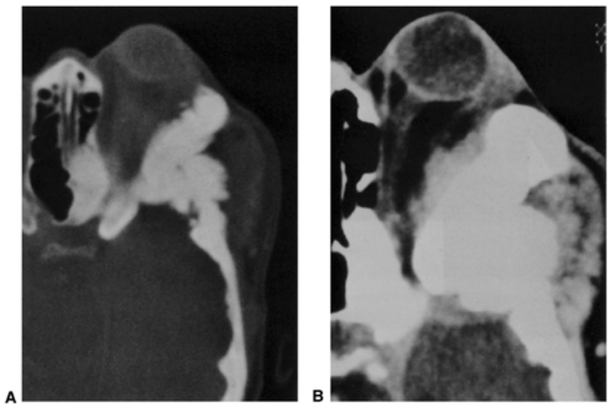

Figure 9-18. Axial CT scans with bone (A) and soft tissue (B) settings demonstrate the bony and soft tissue components of an extensive meningioma affecting the orbit and adjacent structures. Note the marked proptosis.

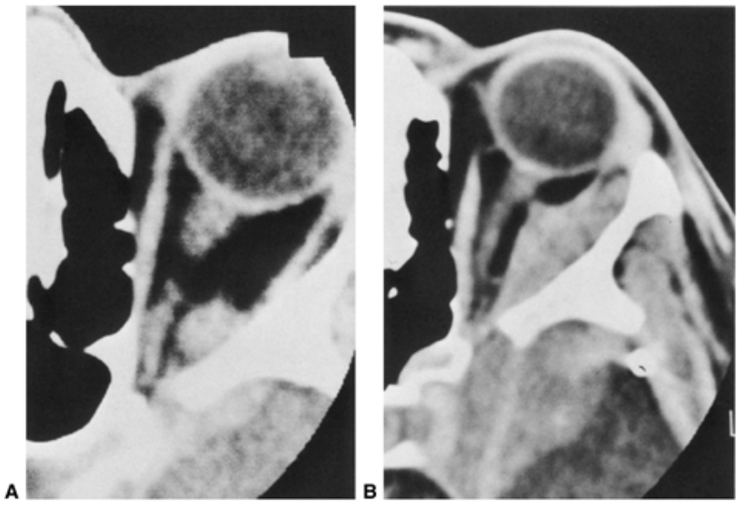

Figure 9-19. Axial CT features of two different meningiomas of the sphenoid wing show variation in patterns of growth and biologic character. (A) This lesion was seen in a 57-year-old woman who presented with visual deterioration for 1 year, lid swelling, and proptosis for 7 years. She had 2 mm of downward and inward displacement, 6 mm of proptosis, a minimal afferent pupillary defect, and decreased color vision. Note small en plaque meningioma of both sides of the inner sphenoid wing. In contrast, the patient in (B) was a 21-year-old woman with a 2-month history of progressive proptosis (6 mm), slight decreased color vision, and reduction of extraocular movements in left abduction. A large meningioma involves the orbit, middle fossa, cavernous sinus, and temporal fossa.

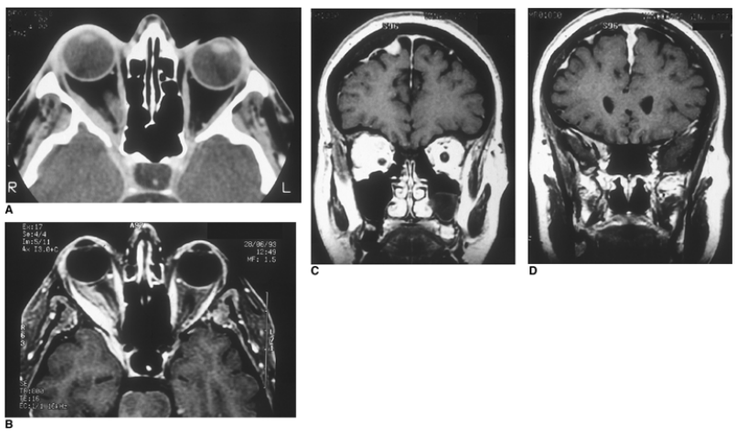

Figure 9-20. This 53-year-old woman presented with a 1-year history of pressure behind the right eye, which was associated with lid swelling. Her ocular examination was essentially normal, including visual acuity, color vision, pupillary examination, and visual fields. Her eye movements were also normal and exophthalmometry was 17 mm on the right and 13 mm on the left. A CT scan (A) demonstrated a thickening of the lateral rectus muscle with a slight increase in the size of the cavernous sinus and some infiltration of the orbital apex. (B) The T1-weighted, gadolinium-enhanced, fat-suppressed MRI demonstrated infiltration of the muscle, adjacent fat, and the cavernous sinus, and MR scans of the head (C, D) revealed additional meningiomas involving the convexity and the falx, as well as extension of the meningioma along the wing of the sphenoid. The patient had received low-dose radiotherapy to her scalp as a child, which is associated with a potential for multiple meningiomas later in life.

Clinical features of regrowth of medial tumors that involve the cavernous sinus are neuropraxias of the cranial nerves III, IV, and VI, whereas regrowth in the infratemporal fossa are associated with facial hypesthesia, trismus, and referred otalgia. Posterior regrowth along the petrous bone may result in internal auditory involvement with tinnitus, hearing loss, unsteadiness, and occasional facial twitching.

Optic Canal Meningiomas

Canal meningiomas typically present with early visual loss due to compression of the optic nerve. Even with the use of thin section axial and coronal CT scans, it may be very difficult to identify small tumors of the canal. Subtle, round expansion of the orbital end of the optic canal should be sought. MR imaging, particularly with gadolinium enhancement, is very useful in the study of the intracanalicular as well as the proximal and distal optic nerve. These tumors may spread posteriorly and extend over the planum to affect the opposite optic nerve, even 10 to 20 years after initial diagnosis. Because of their intimate relationship to the vascular supply in the optic canal, excision without damage to the nerve is highly unlikely. Radiation, with or without canal decompression particularly using stereotactic methods, may be useful for slowing or arresting progress. With evidence of spread toward the chiasm or the opposite optic nerve, total excision is desirable. It has been suggested that bilateral optic nerve meningiomas may represent multicentric origin, but in our combined series of 88 optic nerve meningiomas, involvement of the planum sphenoidale was detectable in 2 of 4 of our cases and a third case was noted at the time of intracranial surgery for basilar aneurysm (Fig. 9-21). Bilaterality is also a feature of basofrontal (planum sphenoidale) or more rarely sphenoid meningiomas, especially if they are of the en plaque variety.

Optic Nerve Meningiomas

Jack Rootman

Peerooz Saeed

Histogenesis

Optic nerve meningiomas are almost always transitional or meningotheliomatous in pattern. They are characterized by slow growth as cohesive tumors with a propensity to invade via emmissaria through the dura, thereby extending into adjacent tissues. We have shown that a subgroup of optic nerve meningiomas with low growth potential is densely psammomatous and calcified. Three basic gross patterns occur within the optic nerve sheath: extradural, subdural (intrasheath), or combined. Nerve sheath meningiomas have a propensity to breach the dural sheath and grow as nodular cohesive extradural masses, which may invade fat and muscle in the adjacent orbit.

Clinical Manifestations

The majority occur between the third and sixth decades (mean onset 40 years in our series) with up to 80% affecting females. Approximately 4% to 7% occur in childhood where they behave in a more aggressive fashion, and in some instances, may be associated with neurofibromatosis type 2.

The essential clinical feature is a slowly developing compressive optic neuropathy with several types of onset and progression. They can present with decreased vision, transient visual obscurations similar to those occurring in papilledema, or duction-induced visual change in extremes of gaze (particularly noted in apical lesions). In our series, 80% presented with decreased visual acuity and 15% with transient visual obscurations while 97% had optic disc change (55% atrophy, 42% swelling, 25% optociliary shunts) (Table 9-5). The early symptoms consist of minimal visual impairment, mild dyschromatopsia, enlargement of the blind spot, and contraction of the visual field. On examination the optic nerve head may be mildly edematous in spite of apparently normal visual acuities. The patient's subjective complaint of visual difficulty may be substantiated by psychophysical testing, such as contrast sensitivity and color vision studies. The onset symptoms and signs may be difficult to differentiate from other entities with similar clinical presentations, such as diabetic papillopathy, thyroid optic neuropathy, congenital pseudopapilledema, perineuritis, asymmetric or unilateral papilledema, benign intracranial hypertension, apical tumors, papillophlebitis, disc drusen, and some inflammatory lesions of the optic nerve.

Table 9-5. Clinical symptoms and signs of optic nerve sheath meningiomas. Combined data from the University of British Columbia (Vancouver, Canada) and the Academic Medical Center (Amsterdam, The Netherlands) (n = 88)

CLINICAL PRESENTATION	% OF SERIES
Symptoms	
Decreased vision	80
Transient visual obscurations	15
Pain	7
Diplopia	4
Signs	
Disc atrophy	55
Disc swelling	42
Optociliary shunts	25
Proptosis	30
Extraocular muscle restriction or deviation	39

From Saeed P, Rootman J, Nugent RA, et al. Optic nerve sheath meningiomas. Submitted, Ophthalmology, 2002.

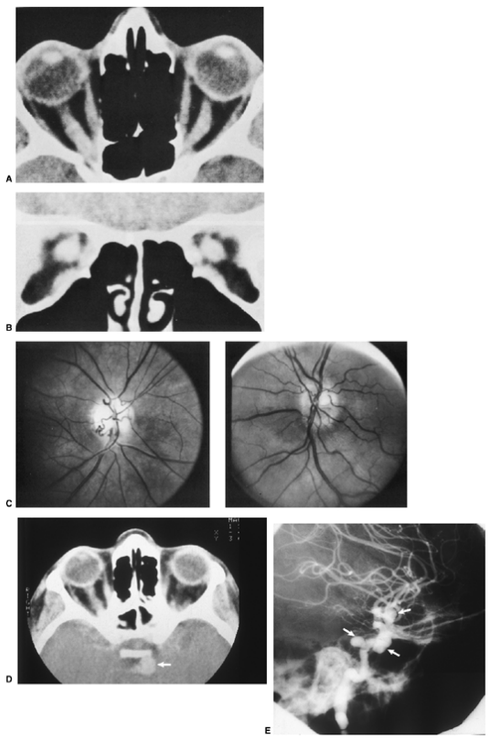

Figure 9-21. Axial (A) and coronal (B) CT scans show diffuse bilateral optic nerve meningioma in a 33-year-old woman who presented with an 8-year history of intermittent reduction of vision. She had no light perception on the right, and a right afferent pupillary defect and 20/30 vision on the left. She had concurrent basilar aneurysms. The meningioma was proven on biopsy, and continuity was noted over the planum sphenoidale at the time of aneurysm surgery following an intracranial hemorrhage. (C) Photographs of the fundi of the patient shown in (A) demonstrate chalky white pallor and optociliary shunts (on the right) with superior temporal pallor. The CT scan (D) demonstrates an aneurysm arising from the basilar artery (arrow), and the internal carotid angiogram (E) reveals multiple aneurysms arising from the left carotid siphon (arrows).

With growth, greater impairment of vision and psychophysical function occur. Proptosis may increase, but is usually mild (between 2 mm and 6 mm) and was seen in only 30% of our patients. There is progressive constriction of the visual fields, leading to residual visual islands. Increasing disc edema is associated with dilatation of papillary and peripapillary vessels, progressive gliosis, and the appearance of refractile bodies. Vascular compromise may be associated with the development of optociliary shunt vessels (Fig. 9-21) and choroidal folds. Ultimately, the nerve becomes increasingly gliotic, the refractile bodies disappear, and atrophy supervenes. Progression is usually slow, providing a safe temporal framework for evaluation and follow-up of these patients. We found that 71% of our patients who presented with vision of 20/50 or better retained a good level of acuity for 5 years or more in follow-up. It should be noted that in combined series, well over 90% of patients have visual loss (45% have 20/40 and 25% have counting fingers or worse), 66% atrophy, 65% proptosis, 50% disk edema, and 32% have optociliary shunts.

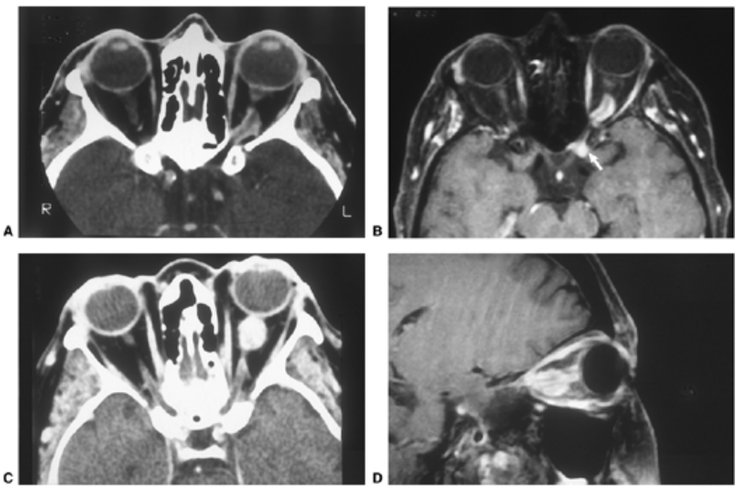

Figure 9-22. Tubular patterns. (A, B) The CT and MR images demonstrate a biopsy proven tubular-diffuse meningothelial meningioma, which was seen in a 54-year-old woman who presented with transient amaurosis, left afferent pupillary defect, and 20/15 vision. The tumor did not show evidence of intracranial involvement on CT scan (A) but was noted to have an intracranial extension on the T1-weighted, gadolinium-enhanced, fat-suppressed MRI (B, arrow). A tubular optic nerve sheath meningioma with evidence of anterior globular expansion, shown on this contrast enhanced CT scan (C), was seen in a 51-year-old woman with 20/30 vision and 2 mm of proptosis. (D) Sagittal view MRI (T2-weighted with gadolinium enhancement and fat suppression) demonstrates a tubular optic nerve sheath meningioma with apical expansion due to exophytic growth. Note irregular margins in the fat, suggesting invasion. The patient is a 40-year-old woman with a vision of 20/30 and 1 mm of proptosis. (Reproduced with permission from Saeed P, Rootman J, Nugent RA, et al. Optic nerve sheath meningiomas. Submitted, Ophthalmology, 2002.)

Imaging

MRI and high-resolution CT scan are the mainstay of investigation for definition of size, location, and extension. Careful axial CT cuts in the plane of the optic nerve along with coronal and sagittal scans will define extent, and subtle expansion of the optic canal may be seen. MR imaging, particularly T1-weighted with gadolinium enhancement and fat suppression, allows recognition and better definition of meningiomas within the orbit, optic canal, and intracranially. The CT scan is most useful for assessing overall configuration, calcification, and bone changes, whereas MR imaging is superior for evidence of soft tissue involvement in the orbit as well as intracranial extension.

Optic nerve meningiomas demonstrate four general patterns: tubular (either diffuse, or with anterior or posterior expansion (Fig. 9-22)), globular (Figs. 9-23A and B), fusiform (Figs. 9-23C and D), and focal (Fig. 9-23E). We found that 80% had smooth borders while 20% had irregular margins. The irregular margins correlated with fat invasion in the

orbit (Fig. 9-23A). Central lucent areas or tram-tracking occur in approximately one quarter of cases and identify the residual optic nerve. Dense uniform enhancement of the meningioma occurs and, in contrast to optic nerve gliomas, buckling or kinking of the optic nerve is not seen. A pathognomonic subgroup of optic nerve meningiomas are calcified (31%) (Fig. 9-24), and we have shown that diffuse calcification is associated with indolent tumor behavior with very slow growth at one sixth the rate of other optic nerve meningiomas. Gadolinium-enhanced MRIs of optic nerve meningiomas appear as regions of high signal intensity, that are sharply defined from the normal optic nerve. This method is very effective for defining the location, extent, and contour of the lesion, and is particularly useful in identifying proximal intracranial involvement (Fig. 9-22B). Fat suppressed MR imaging is particularly useful in identifying intraorbital extension (Fig. 9-25). A significant feature on imaging is evidence of a finely nodular surface reflecting the typical extradural growth pattern. This particular appearance is in contrast to gliomas, which retain a smooth, well-defined margin. Ultrasonography may help to define nodular margins, the presence of calcification (Fig. 9-26), and the absence of cystic change (a feature more characteristic of glioma). The clinical syndromes of optic nerve glioma and meningioma infrequently overlap because of the large difference in age. However, on imaging there is an overlapping pattern noted in both optic nerve glioma and meningioma consisting of a fusiform diffuse expansion of the nerve (Fig. 9-27), which may be better defined with MR imaging.

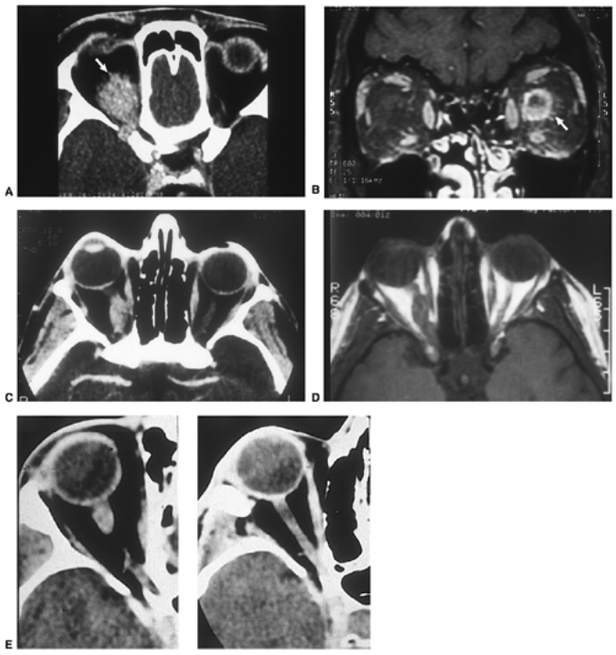

Figure 9-23. (A) This CT scan demonstrates the irregular margins (arrow) of an exophytic, invasive optic nerve sheath meningioma in a 37-year-old woman. She had 6 mm of proptosis and 20/25 vision in the right eye. (B) T1-weighted, gadolinium-enhanced, coronal MRI shows a tubular meningioma with irregular extension into the adjacent orbital fat (arrow). The patient, a 45-year-old woman, had a stable visual acuity of 20/25 for 4 years. (C) This optic nerve sheath meningioma was seen in a 35-year-old woman with a 2-month history of blurred vision on the right side. On physical examination, her vision was 20/30 with evidence of an inferior arcuate scotoma and decreased color vision. Over a 1-year period, her vision deteriorated to light perception only. A CT scan was performed (C) and showed a fusiform optic nerve sheath meningioma, which enhanced and appeared attached to the medial rectus muscle. This feature was also noted on T1-weighted MR imaging (D). She underwent an en bloc excision and the tumor was dissected from the medial rectus muscle. Histology demonstrated a mixed meningothelial and transitional meningioma with invasion both intra- and extradurally. (E) These CT scans were taken before (left) and after (right) excision of a localized, anterior, superior optic nerve sheath meningioma. The scan on the right demonstrates focal absence of the dural sheath postoperatively. This was done on a 35-year-old man who presented with a 5-month history of progressive visual loss and visual field defects. His vision recovered from 20/80 to 20/30, and he has remained stable for 13 years. (Figs. 9-23A to D reproduced with permission from Saeed P, Rootman J, Nugent RA, et al. Optic nerve sheath meningiomas. Submitted, Ophthalmology 2002. Fig. 9-23E reproduced with permission from Rootman J, Stewart B, Goldberg RA. Orbital surgery: A Conceptual Approach. Philadelphia: Lippincott-Raven, 1995;318.)

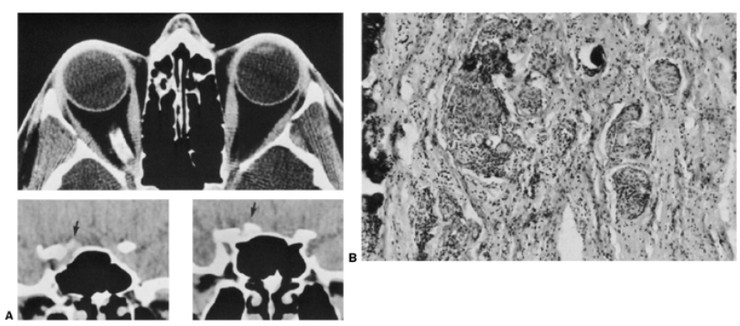

Figure 9-24. (A) Axial CT scan of a calcified meningioma of the optic nerve that occurred in a 41-year-old woman with progressive reduction in vision. Note slight central lucency in the nerve. The coronal scans (A, insets) demonstrate an intracranial component (arrow). The lesion was successfully resected by combined panoramic orbitotomy. (B) Histopathology of the meningioma revealed invasion by the psammomatous meningioma into the optic nerve and dural sheath (H&E, original magnification × 10).

Polar expansion of optic nerve meningiomas in the posterior orbit is associated with a higher incidence of intracranial involvement (Fig. 9-23). Childhood onset is associated with more aggressive or rapid tumor growth as well as more frequent occurrence and greater size of an intracranial component.

Approximately 6% of optic nerve sheath meningiomas are bilateral. Dutton has suggested that a high proportion of tumors occurring in the optic canal are bilateral (about 40%). Bilaterality is associated with poor visual outcome, and in our study, other intracranial pathology was noted (multiple meningiomas or intracranial aneurysms). Half of our bilateral patients demonstrated involvement of the planum sphenoidale in continuity with the lesions of both optic canals (Fig. 9-28). In unilateral cases, other intracranial meningiomas occur in 5% of cases.

Meningioma and glioma are not the only lesions to enlarge the optic nerve. Expansion may be seen in the perineuritis of multiple sclerosis, wherein the optic nerve sheath may enhance. Perineural hemorrhage may be seen as a high-density sleeve on noncontrast CT (MRI and ultrasound features)

scan surrounding the optic nerve. Tubular enlargement of the optic nerve may be noted with leukemic infiltration or lymphoma, papilledema, optic neuritis, idiopathic orbital inflammatory disease (apical type), dural sarcoid (see Fig. 12-52), dural sclerosing inflammation, localized amyloidosis, metastatic tumors, meningiomatosis, and patulous subarachnoid space. The differential diagnostic features of optic nerve meningiomas and gliomas have been described (see Table 9-4).

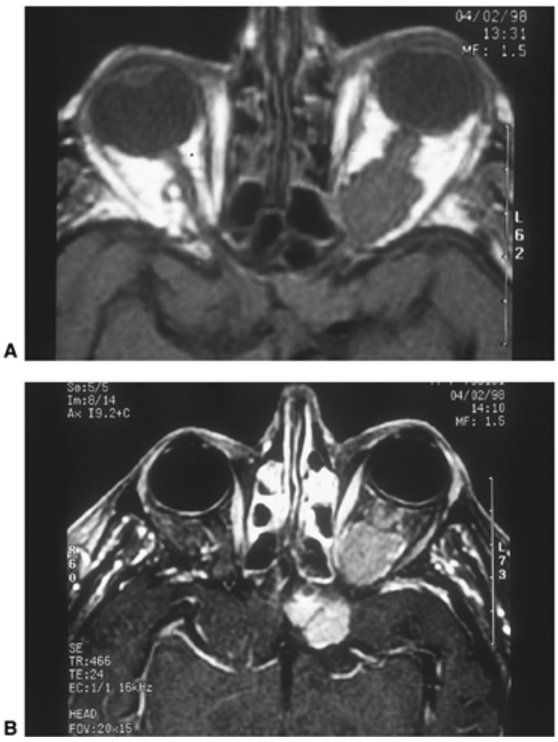

Figure 9-25. (A, B) Axial, T1-weighted MR scans demonstrate a posterior, globular, exophytic meningioma. Note how distinctive the intracranial component appears with contrast enhancement (B). This was seen in a 76-year-old woman with no perception of light on the right side and 3 mm of proptosis.

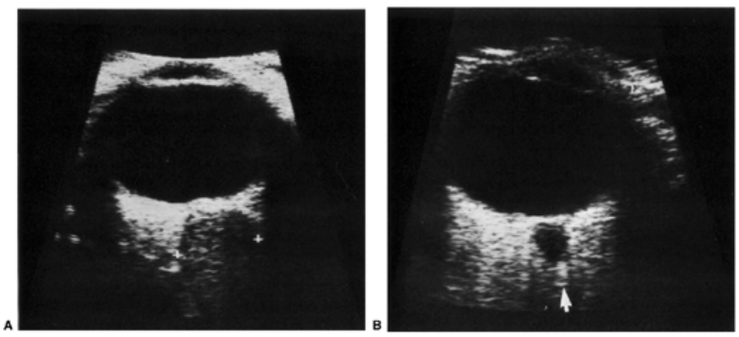

Figure 9-26. (B) B-scan ultrasonography demonstrates enlargement of the optic nerve due to a solid glioma. (B) In contrast, B-scan ultrasonography also shows a lesion of the optic nerve with increased irregular high reflectivity due to the presence of calcium. This lesion was an optic nerve meningioma.

Management

The major therapeutic determinants of optic nerve meningiomas are progression, size, location, evidence of soft tissue infiltration, patient's age, and intracranial involvement. Younger patients are more likely to have larger or rapidly developing tumors, thus requiring careful investigation, earlier intervention and treatment, and vigilant follow-up. Patients who present with visions better than 20/50 are likely to retain their vision for a longer period (generally 5 years) and therefore warrant careful follow-up alone. As to imaging characteristics, a posterior location has a worse visual prognosis than anterior tumors and is associated with a higher incidence of

intracranial involvement. Significant calcification correlates with slower growth. Irregular margins imply orbital involvement, which must be addressed if a surgical decision is made and may require more radical excision. Finally, the presence of intracranial involvement and its extent may determine the need for excision or radiotherapy.

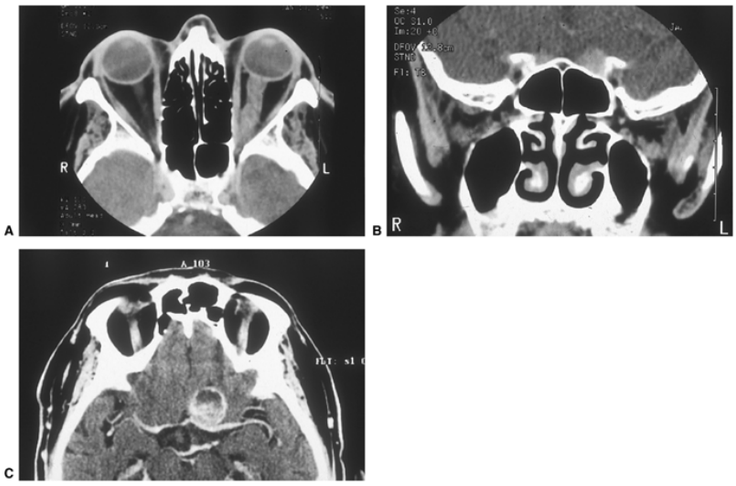

Figure 9-27. (A) Axial CT scan demonstrates a fusiform thickening of the optic nerves, which was seen in a 69-year-old man with a history of decreasing vision since age 17. He had become aware of complete loss of vision only 9 to 10 weeks before presentation. (B) The coronal CT scan demonstrates a intracranial component. The patient was followed over the next 3 years and on repeat scan (C), showed an increase in size of the intracranial component with development of a cystic area. He underwent excision of the intracranial tumor mass, which proved to be a well differentiated pilocytic astrocytoma.

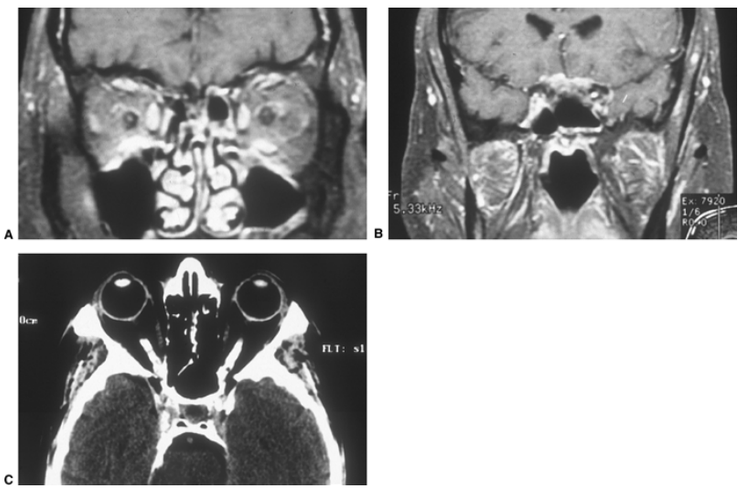

Figure 9-28. This 57-year-old man presented with an 11-year history of progressive visual loss that had been diagnosed as optic neuritis. (A) T1-weighted, axial MR scan demonstrates infiltration of the optic nerve sheath bilaterally. There is also bilateral involvement across the optic chiasm and planum sphenoidale (B, arrow). (C) An axial CT scan shows bilateral calcification of the optic nerve, which is pathognomonic for optic nerve meningioma. (Reproduced with permission from Saeed P, Rootman J, Nugent RA, et al. Optic nerve sheath meningiomas. Submitted, Ophthalmology 2002.)

The only optic nerve meningiomas that can be excised locally appear to be those that are anteriorly located with focal involvement of the dural sheath (see Fig. 9-23E). More extensive lesions that have been excised, particularly those that are circumferential (which most are), have either recurred or led to a complete loss of vision.

Overall, when the visual acuity is stable and 20/50 or better, observation with clinical workup, patient self-evaluation and reporting, visual fields (every 6 months), and neuroimaging annually is indicated. When the patient is younger than 30 years of age or has posteriorly-located, canalicular, or intracranial extension, semiannual clinical evaluation, visual fields, and annual MR imaging are indicated. In patients with progressive visual deterioration, visual field restriction, and/or visual acuity of less than 20/50, radiotherapy is indicated and useful for retaining and improving vision. This generally implies 5500 cGy over a 6-week period. Stereotactic radiotherapy may be considered for small, posteriorly-located lesions.

Excisional surgery may be indicated in prechiasmal lesions, particularly with a large intracranial component or when the planum sphenoidale is involved. These lesions when possible should be excised en bloc. In older patients, it may be sufficient to just remove the intracranial portion of the tumor and treat the remaining portion with radiotherapy. Recurrent tumors that have significantly infiltrated the orbit and failed to respond to radiotherapy may require exenteration as part of an en bloc resection. Patients with a blind eye and significant proptosis (which were few in our series) are also candidates for surgery, involving a total excision of the meningioma and optic nerve sheath. If the tumor has invaded the orbit in this subgroup, exenteration should be included in the en bloc resection. Rapid, progressive, visual deterioration occurring over less than year or with atypical imaging findings, should prompt biopsy.

Other Optic Nerve Tumors

The majority of remaining optic nerve tumors that are clinically relevant are either metastatic or spread from the central nervous system. There are also a large number of nonneoplastic causes of optic nerve enlargement including inflammatory, structural, and choristomatous lesions.

Medulloepitheliomas (Neuroepitheliomas)

Medulloepithelioma of the optic nerve is a clinical curiosity usually seen in children. It affects the nerve head and extends into the substance of the optic nerve. The tumors arise from the medullary epithelium of the optic vesicle and are more common in the ciliary body region. Several cases of benign and malignant medulloepitheliomas of the optic nerve have been described. The important differential diagnosis is optic nerve glioma.

Secondary and Metastatic Tumors

Tumors arising from the globe and surrounding tissues may invade and extend down the optic nerve. The clinical context is usually obvious in the case of retinoblastoma and melanoma, unless the lesion arises within a phthisical eye. Retinoblastoma has a greater propensity to involve the optic nerve, a feature readily detectable with CT, MR, or ultrasound imaging.

A significant cause of optic nerve tumors is metastatic and primary central nervous system neoplasia. In particular, leukemia can affect the central nervous system, and hence the optic nerve and eye, usually in the late and aggressive stages because of the relative pharmacologic isolation of these sites. Leukemia frequently affects the optic nerve head but may independently deposit in the arachnoid sheath as part of a widespread meningeal process. Generalized meningiomatosis from carcinomas, meningiomas, lymphomas, and other rare brain tumors may also infiltrate the optic nerve or its sheath. In the case of carcinomatous meningiomatosis, the patient presents with papilledema, a known history of carcinoma, and negative CT or MR imaging findings because of widespread superficial involvement of the meninges without significant mass effect. The diagnosis can be secured by cytologic examination of cerebrospinal fluid. We have encountered five cases of meningiomatosis with optic nerve involvement: two were due to metastatic carcinomas (both breast), one with a metastatic melanoma of skin, and two with leukemia. The diagnosis was made on cerebrospinal fluid tap in the presence of normal imaging. Direct metastases to the substance of the optic nerve may also cause primary nerve enlargement. We have encountered three such cases, one from breast, one in adenocarcinoma of the bowel, and one from an unknown source.

Primary neoplasia in the central nervous system may also extend into the optic nerve. We have had five cases, three from B-cell lymphomas arising in the central nervous system, one from a medulloblastoma, and one from a dural melanoma (see Fig. 9-96). Several of these were diagnosed

by direct aspiration needle biopsy under CT scan-control of the affected nerve sheath. The primary large B-cell lymphoma of the brain has a specific propensity for ocular involvement, usually as a cryptogenic chronic uveitis and vitritis, but may spread from an intracranial site to involve the optic nerve sheath. We have encountered a single case of cavernous angioma of the optic canal presenting as a tumor of the proximal end of the canal, which led to unilateral optic nerve dysfunction. Optic neuropathy may also occur as a rare paraneoplastic syndrome.

Hemangiopericytoma

Hemangiopericytoma has been discussed as part of the vascular tumors. It should, however, be noted that a significant number of the hemangiopericytomas of the orbit are in fact tumors of the optic nerve. Overall, they have a tendency to local regrowth and progression, which may go on to intracranial involvement in spite of treatment by excision and radiotherapy.

Nonneoplastic Enlargement of the Optic Nerve

There are a number of inflammatory processes affecting the orbit or the optic nerve that may lead to swelling of the nerve, including dural sarcoid, apical nonspecific inflammatory disease, post-infectious infiltration of the optic nerve sheath, primary dural sclerosing inflammation, dural Wegener's granulomatosis, and optic neuritis (see Chapter 12 – Inflammatory Diseases).

Arachnoidal cysts of the optic nerve may simulate a neoplasm and can be effectively treated by a surgical window in the optic nerve sheath. However, it is important to rule out the possibility of an undetected small tumor of the optic canal, which may obstruct the cerebrospinal fluid and distend the subarachnoid space. Nevertheless, true arachnoid cysts have been repeatedly described. The subarachnoid space may become patulous in any instance of raised intracranial pressure, particularly pseudotumor cerebri. In such instances, a dural window may relieve chronic papilledema. It is of note, however, that patulous optic nerves may be seen as a normal variant.

The nonneoplastic causes of optic nerve enlargement that we have encountered include pseudotumor cerebri (13), patulous optic nerve (3), sarcoid (3), sclerosing inflammation (3), chronic papilledema (3), ischemic optic neuropathy (3), Wegener's granulomatosis (2), nonspecific inflammation (2), post-cellulitis (2), and arachnoid cyst (1).

Peripheral Nerve Sheath Tumors

Tumors of nerve sheath origin include a number of entities but in the clinical setting only two, neurofibromas and schwannomas (neurilemmomas), are frequent in the orbit. These tumors share schwannian origin but have differing associations, histopathology, and prognosis. In brief, schwannomas are composed of Schwann cells and are localized, slow-growing, benign tumors of the adult. On the other hand, neurofibromas are made up of a mixture of schwannian, perineural, and fibroblastoid cells, and often contain residual axons. They are plexiform, fusiform, or diffuse and may be less well circumscribed. When not isolated, they often are associated with neurofibromatosis (implying an underlying tendency to widespread involvement, progression, mesodermal defects, and rare malignant transformation). Most series suggest an overall 2:1 occurrence of neurofibroma versus schwannoma. Overall, peripheral nerve tumors constitute 4% of all orbital neoplasia – 2% occurring as plexiform neurofibromas, 1% as isolated neurofibromas, and 1% as schwannomas. In our clinic, we have seen 21 patients with schwannomas, 2 with malignant schwannomas, 31 neurofibromatoses (including 12 with plexiform neurofibromas), and 3 patients with isolated neurofibromas.

Neurofibromas

Neurofibromas occur in three different settings: as isolated (generally dermal) tumors; as diffuse infiltrations; and as plexiform lesions. All three types can be seen as part of the protean manifestations of neurofibromatosis. Isolated, solitary neurofibromas (versus multiple) are in 90% of instances unassociated with neurofibromatosis. It should be noted, however, that neurofibromatosis has 100% penetrance but very low and variable expressivity. Thus a patient with a single neurofibroma may carry the gene but not show the disease. Diffuse neurofibromas are part of the syndrome in about 10% of occurrences. In contrast, many believe that clinically apparent (versus small, histologically diagnosed) plexiform lesions are virtually pathognomonic of von Recklinghausen's disease. The fundamental pathologic abnormality in each consists of a proliferation of schwannian and endoneurial elements with separation of the component axons of the nerve of origin.

The Neurofibromatoses

The neurofibromatoses are a group of up to seven genetically distinct neurocristopathies. Practically speaking, they have common cutaneous manifestations (neurofibromas,

café au lait patches, and plexiform neurofibromas) and may have central nervous system tumors. The most frequent neurocristopathies associated with orbital features are neurofibromatosis types 1 and 2.

Neurofibromatosis Type 1 (NF1)

NF1 (formerly known as peripheral neurofibromatosis) is the most common gene disorder affecting the central nervous system (1 in 3,000 people). It is autosomal dominant with variable expressivity and has a high spontaneous mutation rate. It is on the long arm of chromosome 17. The malignant lesion in NF1 may involve deletion of both copies of the tumor suppressor gene.

The major ocular manifestations are Lisch nodules and the orbital features of plexiform neurofibromas, dysplasia of the sphenoid wing, and optic nerve glioma (Table 9-6) (Fig. 9-29). The Lisch nodules appear progressively with age such that 33% of 2.5-year-olds, 50% of 5-year-olds, 75% of 15-year-olds, and all of the adults have them. Prominent corneal nerves (25% of cases), perilimbal neurofibromas, congenital megaloglobus (Fig. 9-30), glaucoma, and pigmentary hamartomas of the uveal tract (35%) may be seen. Rare retinal features include astrocytic hamartomas, combined retinal and pigment epithelial hamartomas, and retinal hemangiomas.

Café au lait spots appear by age 1, enlarge at puberty, and are most common in the trunk and axilla but are absent from the scalp and eyebrows.

The central nervous system tumors include optic nerve (12%) and other gliomas, vascular anomalies, and arachnoid cysts.

Table 9-6. Diagnostic criteria for neurofibromatosis type 1

The diagnostic criteria are met if two or more of the following are found:

1. Six or more café au lait macules over 5 mm in greatest diameter in prepubertal individuals and over 15 mm in greatest diameter in postpubertal individuals.
2. Two or more neurofibromas of any type or one plexiform neurofibroma.
3. Freckling in the axillary or inguinal regions
4. Optic glioma
5. Two or more Lisch nodules (iris hamartomas)
6. A distinctive osseous lesion such as sphenoid dysplasia or thinning of long bone cortex, with or without pseudoarthrosis.
7. A first degree relative (parent, sibling, or offspring) with neurofibromatosis type 1 by the above criteria.

Reproduced with permission from Lyons CJ. The neurofibromatoses. In, Taylor D, ed. Pediatric Ophthalmology, 2nd ed. London: Blackwell Science, 1997;366-81.

Other systems that may be involved include the spinal cord, sympathetic nerves, and adrenals (pheochromocytoma). In addition, multiple neurofibromas of the gastrointestinal tract and various osseous abnormalities may occur.

Neurofibromatosis Type 2 (NF2)

This type, previously called central neurofibromatosis, is characterized by the development of acoustic neuromas and less frequently, meningiomas, spinal nerve root schwannomas, and presenile lens opacities. It is autosomal dominant but ten times more rare than NF1. The gene for NF2 is situated on chromosome 22.

Patients with NF2 have few café au lait spots (less than six), and the cutaneous lesions are usually schwannomas (Table 9-7). The most important hallmark is the presence of bilateral vestibular schwannomas. More rarely, the trigeminal nerve may be involved. Astrocytomas are rare in the central nervous system but relatively common in the spinal cord. NF2 patients typically develop tumors of the neural coverings or linings, such as meningiomas, schwannomas, and ependymomas. The major ocular findings, which may antecede central nervous system involvement, include the development of presenile central posterior subcapsular lens opacities in 55% to 87% of patients. Lisch nodules are rare but it is of note that several patients with NF2 have presented with third nerve palsies. Lesions of the posterior segment include combined retinal and pigment epithelial hamartomas, epiretinal membranes, astrocytic hamartomas, and optic disk gliomas. Optic nerve sheath meningiomas may also be bilateral. Since many of the manifestations occur early in life, it is important for ophthalmologists to be aware of this disorder.

Table 9-7. Diagnostic criteria for neurofibromatosis type 2

NF2 may be diagnosed when one of the following is present:

Bilateral eighth nerve masses seen by appropriate imaging techniques (e.g., CT scan or MRI), preferably MRI with gadolinium

A parent, sibling or child with neurofibromatosis type 2 and either unilateral eighth nerve mass or any two of the following:

- Neurofibroma
- Meningioma
- Glioma
- Schwannoma
- Juvenile posterior subcapsular lens opacity

Reproduced with permission from National Institutes of Health. National Institutes of Health consensus development conference statement: neurofibromatosis. Neurofibromatosis 1988;1:172-8.

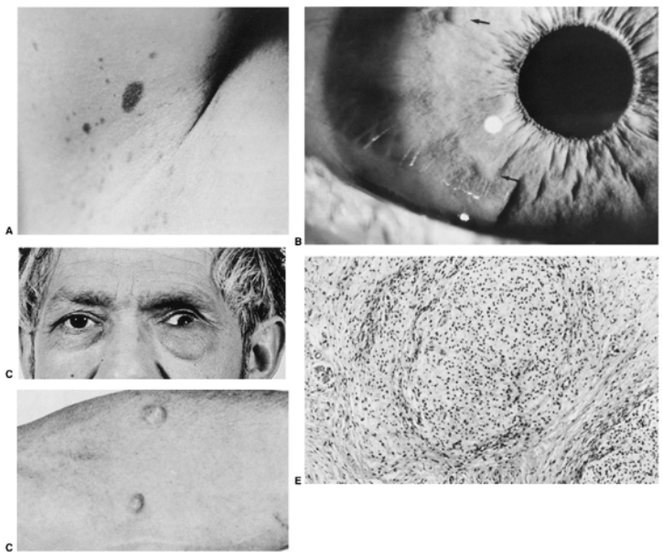

Figure 9-29. (A) Typical site and appearance of café-au-lait spots in the axilla of a 9-year-old child with neurofibromatosis. (B) The iris shown in this photograph demonstrates the characteristic round, dome-shaped, Lisch nodules that are found in a large proportion of patients with neurofibromatosis. (C) This 50-year-old man has a plexiform neurofibroma of the lower lid, which was associated with multiple neurofibromas throughout the body (D). In addition, he had diffuse neurofibromatosis of the uveal tract and iris, which led to glaucoma and phthisis of the left globe. (E) Histopathology of the patient's plexiform neurofibroma demonstrated loosely arranged, swollen nerve bundles surrounded by fibroblasts and collagen (H&E, original magnification × 10).

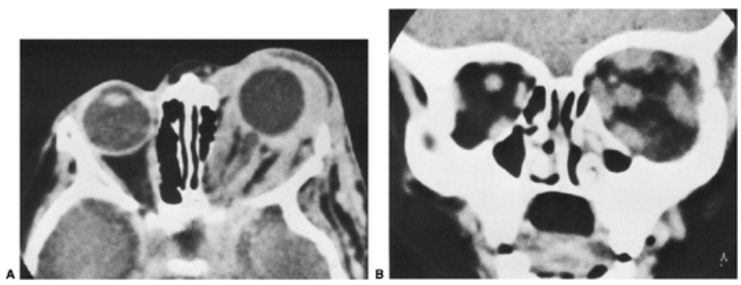

Figure 9-30. Axial (A) and coronal (B) CT scans of a 1-year-old child who presented at birth with an enlarged left eyeball and glaucoma due to uveal neurofibromatosis. On clinical examination, he had left proptosis, a thickened doughy lid with megaloglobus, thickened iris, and pale choroid. The axial CT scan demonstrates extensive orbital plexiform neurofibroma with the full constellation of findings. The left orbit is enlarged. The left ethmoid and maxillary sinuses are small. The upper eyelid and periorbital soft tissues, both medially and laterally, are thickened as are the four rectus muscles. There is increased density of the intraconal fat with several linear densities, and a thickened irregular optic nerve sheath complex due to posterior ciliary involvement. The left globe is buphthalmic and proptotic. The contrast-enhanced axial scan shows marked thickening and enhancement of the uveal-scleral layer. The optic nerve is a central low-density area surrounded by the irregular enhancing plexiform neurofibroma. The cavernous sinus and the superior orbital fissure are enlarged on the left side.

Plexiform Neurofibromas

Plexiform neurofibromas are the most common and complex peripheral nerve tumors of the orbit. Because of the association with neurofibromatosis, they are of early onset (first decade) and have variable manifestations. Pathologically, they consist of diffuse intertwining bundles of Schwann cells, axons, and endoneural fibroblasts surrounded by a cellular perineural sheath. They are not encapsulated, grow along the nerves of origin in a centripetal manner, and insinuate throughout the orbital tissues. Virtually any of the cranial, sympathetic, and parasympathetic nerves may be involved with a propensity to affect sensory nerves in the orbit. With special stains, the axons are demonstrable throughout the fascicles of these grossly distorted nerves. The overlying skin may be thickened (elephantiasis neuromatosa; Figs. 9-31 and 9-32). The tortuous, rope-like, tangled nerves produce a characteristic palpable “bag of worms.” Plexiform neurofibromas are vascular and so diffusely intertwined with the normal tissues that complete removal is associated with hemorrhage and is extremely difficult, if not impossible. Combined with a tendency to continued growth, management can be a surgical frustration. However, it can be aided by the use of the CO_2 laser at surgery. Malignant transformation of plexiform neurofibromas of the orbit is exceedingly rare.

Clinical and Imaging Features

The clinical and investigative findings of plexiform neurofibromatosis consist of soft tissue, bony, and ocular abnormalities. The soft tissues of the lid, periorbita, and face are thickened, hypertrophied, or even pendulous producing varying degrees of proptosis or facial disfigurement or both. Thirty-one percent of plexiform neurofibromas occur in the lid and periorbital region. CT scanning demonstrates the changes as contrast-enhancing, irregular soft tissue infiltration involving these structures (Figs. 9-31 ,9-32 ,9-33 ,9-34). The extraocular muscles may be enlarged due to nerve involvement (Fig. 9-30). In addition, the retrobulbar fat may show increased density and when the nerves in the cavernous sinus are involved, it is enlarged (Fig. 9-30). Plexiform neurofibromas appear on MRI as irregular, poorly defined, diffusely insinuating masses that may extend through the superior orbital fissure. They are heterogeneous and hypointense on T1-weighted images, and have a high-signal intensity on T2-weighted images with respect to orbital fat. They show variable enhancement (Fig. 9-35) with gadolinium and are best appreciated with fat suppression.

Bony changes may be primary mesodermal defects or compensatory with expansion due to mass effect. They consist of enlargement of the orbit, widening of the superior and inferior orbital fissures (Figs. 9-31 and 9-34), hypoplasia of

the ethmoid and maxillary sinuses (Figs. 9-31 , 9-33 , and 9-34), abnormalities of the sphenoid (defects in the greater wing, elevation of the lesser wing) (Figs. 9-30 , 9-31 , 9-33 , and 9-34), and enlargement and distortion of the middle cranial fossa (Fig. 9-33).

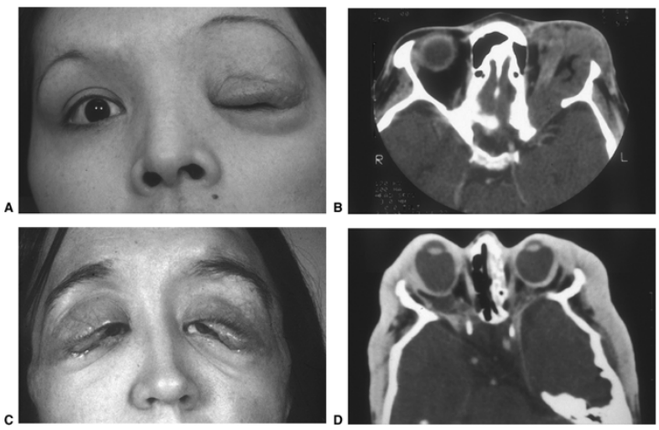

Figure 9-31. (A) This 27-year-old woman with neurofibromatosis type 1 and a positive family history had a progressively thickened, ptotic left lid since birth, which had been debulked at age 9. She had a visual acuity of 20/70 and decreased corneal sensation. The lid had a ropy feel and the globe was proptotic (15 mm OD, 20 mm OS). There was a 16 diopter hypertropia and a 20 diopter left exotropia with latent nystagmus. (B) CT scan demonstrated an irregular soft tissue mass in the enlarged orbit, extending out on to the lid. There is also dysplasia of the sphenoid wing and an adjacent arachnoidal cyst (arrow). (C) This 33-year-old woman with neurofibromatosis type 1 had a right congenital glaucoma. (D) There is a plexiform lesion of the lids, face, and globes and dysplasia of the sphenoid wings. She had light perception only on the right and 20/30 vision on the left. Her mother and three of her siblings had neurofibromatosis type 1.

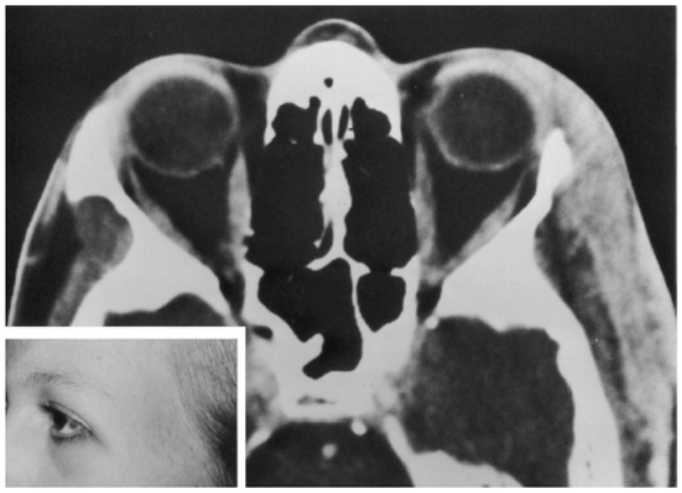

Figure 9-32. This 19-year-old woman presented with a left periorbital lesion that had been increasing over a 3-year period. It had a cordlike consistency with thickening of the overlying skin (elephantiasis neuromatosa) and was associated with an isolated neurofibroma of the left iris (Lisch nodule). The axial CT scan demonstrates thickening of the lateral portion of the lid and the skin in the subcuticular tissue overlying the temporalis fossa.

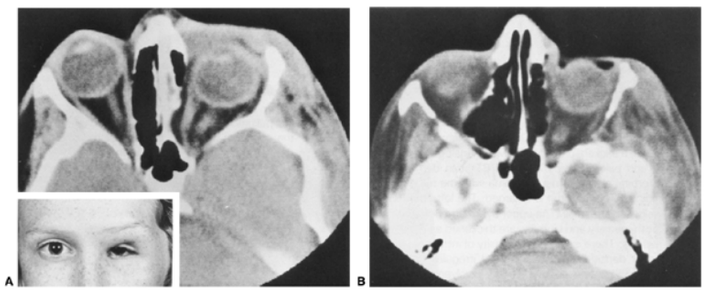

Figure 9-33. (A, inset) A 15-year-old boy presented with a progressive enophthalmic appearance noted since age 2 years. It was associated with thickening of the skin of the upper lid and over the temporalis fossa. In addition, he had a light pigmentary patch in the temporal region of his forehead. On physical examination, he had 11 mm of enophthalmos with spongy thickening of the superior lid, infraorbital region, and zygomatic arch. (A) The enhanced axial CT scan shows marked thickening of the upper eyelid and periorbital soft tissues on the left. The globe is enophthalmic because of enlargement of the orbit, reduction in the size of the ethmoid sinus, and decrease in the volume of intraconal fat. The intraconal fat also shows increased density compared to the normal side. (B) The patient also had absence of a portion of the sphenoid wing and lateral orbital wall, which was associated with an unusual feature of ocular bobbing on mastication due to the intimacy of the periorbita and temporalis muscle.

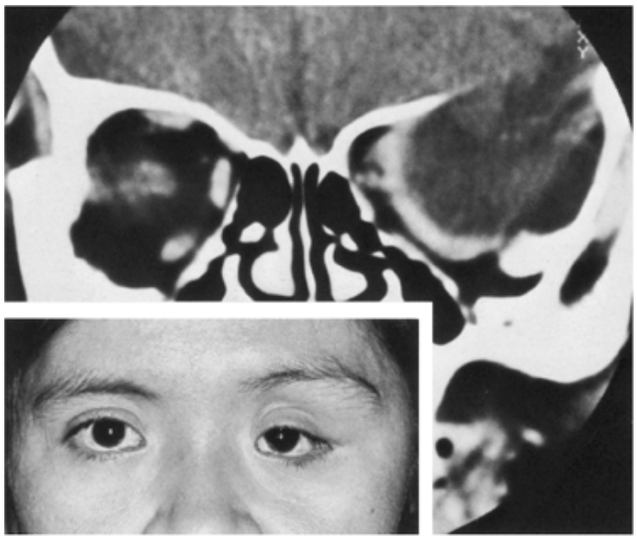

Figure 9-34. (Inset) A 28-year-old woman presented with a throbbing, rhythmic pulsation of the left eye associated with drooping of the lid; the condition had been present for many years. On physical examination, she had 4 mm of downward globe displacement, a deepened superior sulcus, and 3 mm of enophthalmos. A rhythmic pulsation of the left orbit was noted, and she had multiple café au lait spots as well as Lisch nodules of the iris. Axial CT scan demonstrates absence of the greater sphenoid wing with herniation of the contents of the temporal fossa.

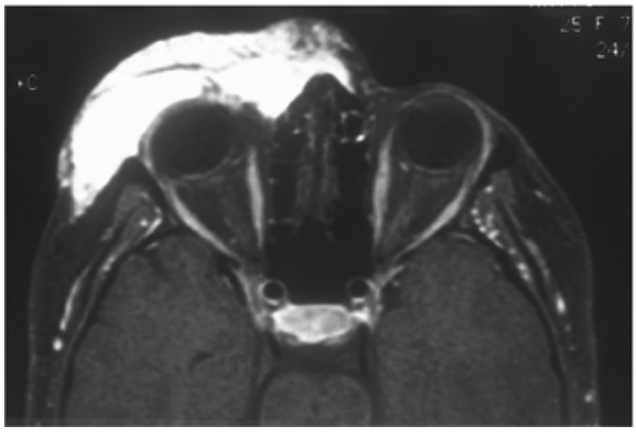

Figure 9-35. This T1-weighted, gadolinium-enhanced, fat-suppressed MRI shows bright enhancement of a thick neurofibroma of the lid, temporalis region, and nose in a patient with neurofibromatosis type 1.

In our experience, the most severe ocular involvement correlated with childhood glaucoma, diffuse uveal neurofibroma (enlarged and thickened globes), and marked orbital anomalies, including irregular nodular thickening of the optic nerve sheath outline with central lucency reflecting plexiform neurofibromas of the perineural and ocular emmissaria, which can be mistaken for an optic nerve glioma (Fig. 9-30). Involvement of single or multiple nerve bundles may produce dramatic enlargement (Fig. 9-36).

Management

The management of plexiform neurofibromas is difficult, treacherous, and frustrating, and usually produces cosmetically inadequate and temporary results. This has led some authors to suggest that in the case of significant involvement, only exenteration will produce an effective result. The usual surgical management is cosmetic, consisting of repeated debulking or orbital bony surgery or both by combined cranial-facial teams; it produces less than gratifying results in most instances. Radiotherapy is both inappropriate and ineffective for plexiform neurofibromas. Absence of the sphenoid wing with enophthalmos can be rectified by a combined orbitocranial reconstruction.

Solitary (Isolated) Neurofibromas

An exact incidence of localized neurofibromas in the orbit is hard to obtain because statistics may be marred by the inclusion of cases that may be the early manifestation of neurofibromatosis. This lesion (when compared to occurrence elsewhere in the body) is infrequent in the orbit. Henderson reported that 8 of 35 neurofibromas were solitary, and Kuo et al. reported a 0.6% occurrence in a large series of orbital tumors. We have encountered 3 cases of solitary neurofibromas and 21 schwannomas. Rose and Wright have reported an equal occurrence of isolated neurofibromas and schwannomas in their series.

Clinical, Histologic, and Imaging Features

These lesions tend to be seen in middle-aged persons, and manifest as solitary masses frequently in the upper quadrants (Fig. 9-37A). Clinically they are solid, isolated, circumscribed, slow-growing masses leading to displacement and/or localized expansion of the orbit. When in the lacrimal fossa, they may be virtually indistinguishable preoperatively from a benign mixed tumor. Because they

mainly affect sensory nerves, anesthesia, paresthesia, and hypesthesia have been common.

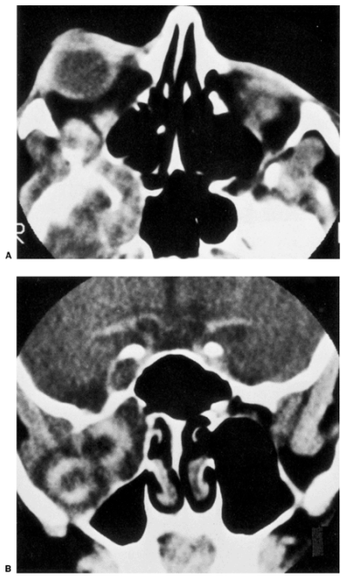

Figure 9-36. Axial (A) and coronal (B) contrast-enhanced CT scans demonstrate a neurofibroma that appears to involve primarily the second division of the fifth nerve with a small first division component. Note expansion of the cavernous sinus, infraorbital fissure, pterygopalatine fossa, and apical orbit. Two areas of ring enhancement surround the lesion. The patient was 34-years-old and was known to have neurofibromatosis.

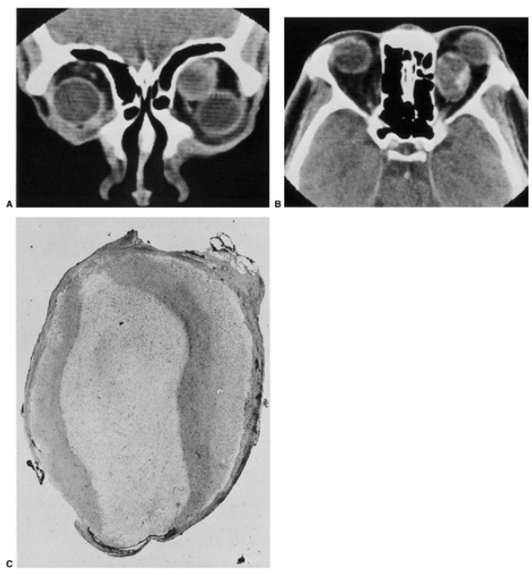

Figure 9-37. Coronal (A) and axial (B) CT scans demonstrate a well-defined, isolated, superior medial orbital mass. The downward displacement of the globe, and capsular and focal density reflect a largely myxomatous component (particularly centrally) shown in (C) under low power.

Grossly, at surgery they are noted to arise from a major nerve and appear as well-defined, firm, circumscribed, rubbery, gray masses with little vascularity. Histologically, they may not be well encapsulated (rather, they show condensation of adjacent tissues) and contain loosely arranged, interlacing bundles of spindle cells (two to three cells thick) and collagen fibrils within a mucoid matrix (Figs. 9-37B and C).

Small, frequently varicose axons may be demonstrated throughout the tumor with special stains. The common histologic variants include a cellular type with dense Schwann cell populations and myxoid neurofibromas having a striking mucoid component (Fig. 9-37B). In addition there are several of interest only to the pathologist, including pacchionian, epithelioid, pigmented, and granular neurofibromas. Malignant transformation is exceedingly rare, but is believed to be more common than in the case of schwannomas.

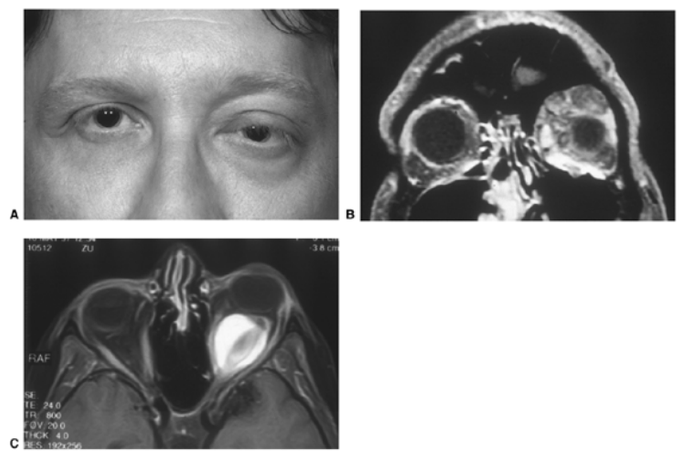

Figure 9-38. (A) This 36-year-old man without stigmata of neurofibromatosis type 1 presented with longstanding proptosis (6 mm) and downward displacement (4 mm) of the left globe. The MRIs demonstrate two lobulated masses in the orbit anteriorly above the globe that converged into one mass posteriorly (B, C). Note the enlarged orbit and high intensity of the peripheral portion of the neurofibroma on T2-weighted MRI (C).

On CT and MR scanning, solitary neurofibromas appear as well-circumscribed, usually homogeneous masses, and on ultrasonography they display low reflectivity. They may in fact be elongated and lobulated. Although multiple tumors may be evident at the time of surgery, these are rarely detected preoperatively. A unique CT and MRI feature that we have noted in two of our cases is a central lucency surrounded by a more dense component due to the central nerve component and surrounded by the proliferating cells (Figs. 9-37 and 9-38).

Management

Management of solitary neurofibromas does not imply the same problems noted in the hereditary forms, and they can be removed even partially with impunity. At surgery they appear as isolated tumors but require careful dissection of the capsule, which can be adherent in areas. Recurrences may represent undetected multiple lesions. Resection implies the frequent necessity to transect the nerve of origin, leading to postoperative neurosensory loss. Thus, before resecting it, care should be taken to identify it as a sensory rather than motor nerve.

Diffuse Neurofibromas

Diffuse neurofibroma is a rare dermal form characterized by infiltration and envelopment of normal structures. It is histologically ill-defined and made up of cells with ovoid nuclei mainly growing diffusely, but in some areas showing an arrangement reminiscent of Wagner-Meissner corpuscles. A variable amount of collagen is present. About 10% of diffuse neurofibromas occur in the context of neurofibromatosis. The majority of these lesions do not imply a high risk of malignant change. Their rare occurrence in the orbit is characterized by a diffuse infiltration of fat, muscles, and soft tissues. Resection implies the same frustrations as plexiform neurofibromas.

Amputation Neuromas

In spite of frequent nerve transection in the orbit, amputation neuromas rarely occur. We have encountered a single case of amputation neuroma. They are a regenerative overgrowth of transected peripheral nerves and may be associated with pain that is curable by excision. It is believed that mechanical factors such as movement, pressure, and scar

tissue contribute to and increase irritation, and this may explain the relative infrequency of these lesions in the orbit. Grossly, they are circumscribed and continuous with the transected nerve. Histologically, they consist of a disorganized proliferation of nerve fascicles with a background of collagen.

Schwannoma (Neurilemmoma)

Schwannomas are well-defined, encapsulated, slowly progressive tumors that develop as eccentric growths from peripheral nerves. They are usually solitary, occur between the ages of 20 and 50 years, and have a predilection for the head and neck region. In general series, they may be noted in association with von Recklinghausen's disease (18% of schwannomas and 1.5% of patients with neurofibromatosis). In the orbit they represent 1% to 2% of tumors; in our series they constituted 1.2% of non-thyroid orbital lesions and about 3.2% of neoplasia. They are occasionally multiple, and malignant transformation is rare.

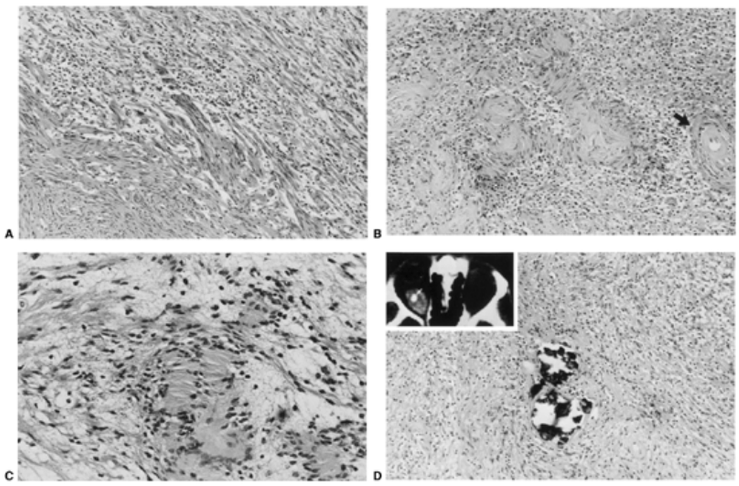

Figure 9-39. (A) Histopathology of an intraconal schwannoma demonstrates an admixture of compactly arranged interlacing fascicles (Antoni A pattern, lower left) and more loosely arranged cells separated by a clear matrix (Antoni B pattern) with a background of lymphocytoid cells. (B) Histopathology of another area of the same tumor shows a hyalinized vessel (arrow) with an organoid cellular pattern centrally (Verocay body). Background pattern is essentially Antoni B with lymphocytoid and lipid-laden foam cells. (C) A higher-power view of a Verocay body. (D) Light microscopy of the intraconal schwannoma shown in axial CT scan (D, inset). Note the smooth, well-defined, oval intraconal mass with central calcification (H&E, original magnifications; A × 10, B × 10, C × 25, D × 10). (Reproduced with permission from Rootman J, Goldberg C, Robertson W. Primary orbital schwannomas. Br J Ophthalmol 1981;66:194-204.)

The proliferating Schwann cells within the perineural capsule displace and may compress the nerve of origin. The characteristic pathology is an admixture of tight cellular Schwann cells (Antoni A area) and a loosely arranged component (Antoni B area) within the capsule (Fig. 9-39). Axons are not noted within the substance of the tumor but rather are seen as eccentric nerve bundles in the capsule. They contain less acid mucopolysaccharide than neurofibromas, have many reticulin fibers, and are S-100 protein positive. On electron microscopy, in contrast to neurofibromas, schwannomas are made up almost exclusively of Schwann cells and their processes. In the Antoni A areas, stacks of processes are surrounded by a well-marked basal lamina (500 nm) while in the Antoni B areas, the processes are less

densely arranged. Long spacing collagen is often seen in schwannomas. The cytoplasm contains few mitochondria, microfibrils, occasional lysosomes, and rarely cilia, and the nucleus is usually flat.

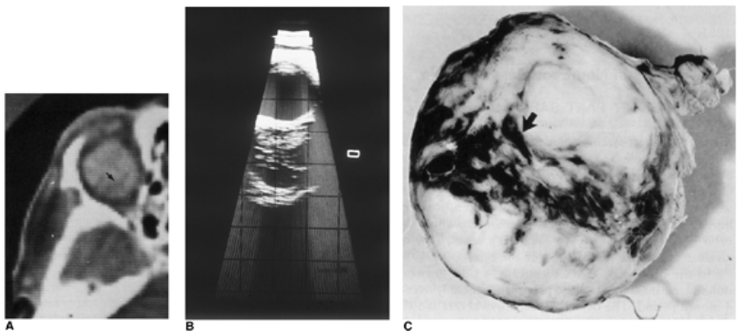

Figure 9-40. (A) Axial CT scan with contrast injection demonstrates a well-defined, mildly enhancing intraconal schwannoma (arrow). (B) B-scan ultrasonography shows the retrobulbar mass with flattening of the globe. (C) Gross photograph of the excised schwannoma shows focal necrosis and hemorrhage in the center of the lesion (arrow), which reflected the low-density nonenhancing areas noted on axial CT scan. (Figs. 9-40A and C reproduced with permission from Rootman J, Goldberg C, Robertson W. Primary orbital schwannomas. Br J Ophthalmol 1981;66:194-204.)

Aside from these typical areas, there is a range of findings that reflect varying organization and maturational features. This includes characteristic organoid cellular patterns (Verocay bodies; Fig. 9-39C), palisading lymphocytoid cells, and hyalinized vessels (Fig. 9-39B) (with PAS-positive basement membrane). Because they are slow growing and late in presentation, features of degeneration may dominate the larger masses. These include cyst formation, hemorrhage (Fig. 9-40), calcification (Fig. 9-39D), collagen deposition, and hyalinization with infiltration of siderophages and lipid-laden Schwann cells. In addition, ancient lesions may display distressing nuclear atypia with large hyperchromatic, frequently multilobed nuclei without mitoses; yet they usually behave as benign lesions. Ten percent of schwannomas occur in neurofibromatosis and 50% of malignant schwannomas occur within this group. The clinical development, investigational features, and management of schwannomas reflect the underlying pathology.

Clinical and Imaging Features

No single feature is pathognomonic but a multiplicity of clinical, imaging, and surgical features point to the diagnosis of schwannoma. It is a tumor that occurs largely in adults (in the third to the seventh decade with a range from childhood to the seventh decade), has an insidious onset, is slow-growing, and is noninvasive with findings governed by the position and size of the lesion (mass effect) (Fig. 9-41). In our experience, when intraconal, the major findings were proptosis, lid swelling, posterior indentation of the globe, and diplopia in extremes of gaze. With apically located tumors, the major findings included central scotoma with papilledema and possible fluctuation of vision on lateral movement. Extraconal schwannomas may occur virtually anywhere in and about the orbit including the sinuses, the gasserian ganglion, cavernous sinus, and the lacrimal gland or sac fossa. We have seen tumors in the ethmoid (one of which presented with sinusitis; Fig. 9-42), lid, and in the roof of the orbit (Fig. 9-41). The majority are localized, characterized by mass effect, but the apical tumors may extend through the superior orbital fissure to involve the cavernous or gasserian ganglion, producing an orbital apex syndrome in some instances (Figs. 9-43 and 9-44). Most series suggest that sensory nerves are more commonly involved in the orbit but numerous cases involving the motor nerves have been described.

On imaging, features of longstanding pressure effect with expansion may be noted when the tumor is next to bone (Fig. 9-45), and rarely focal intratumoral calcification may be seen (Fig. 9-39). Two major types of lesion noted are rounded, well-defined tumor masses or, in the instances of

those involving the cavernous sinus or gasserian ganglion, elongated masses extending through the superior orbital fissure. CT scanning demonstrates well-defined, smooth, rounded contours (both anterior and posterior) with variation in density based on cyst formation, degeneration, and lipid deposition in some tumors (Figs. 9-40 and 9-45). Schwannomas may also be nodular in configuration. Those extending into the cavernous sinus may appear more lucent than the surrounding tissues because of fat content (Fig. 9-45). On MR imaging, the lesions appear ovoid to fusiform and are either homogeneous or heterogenous, isointense to hyperintense in relation to extraocular muscles, and hypointense with respect to orbital fat on T1-weighted images. They may have variable signal intensity on T2-weighted images with the myxoid portion appearing to have greater signal intensity (Fig. 9-44). Overall, these lesions are not distinctive enough to differentiate from cavernous hemangioma, neurofibroma, fibrous histiocytoma, and hemangiopericytoma with assurance. On contrast injection, mild enhancement may be noted; and arteriography is generally negative, showing displacement (except in one of our cases where a blush was observed). Ultrasonography will confirm discrete, generally solid tumor masses with occasional cysts in some.

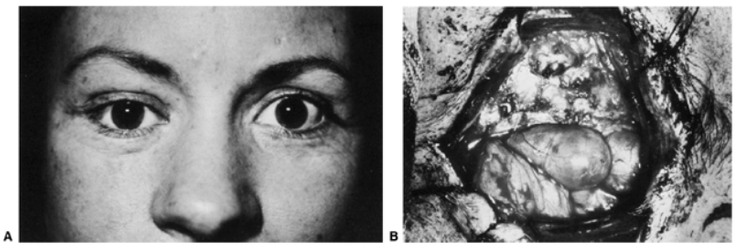

Figure 9-41. (A) This 32-year-old woman had 4 mm downward displacement of the right globe and slight facial asymmetry. (B) Intraoperative photograph of the superior orbital schwannoma that was removed from this patient. There is a multilobular solid tumor mass with slightly varicose surface vessels. (Reproduced with permission from Rootman J, Goldberg C, Robertson W. Primary orbital schwannomas. Br J Ophthalmol 1981;66:194-204.)

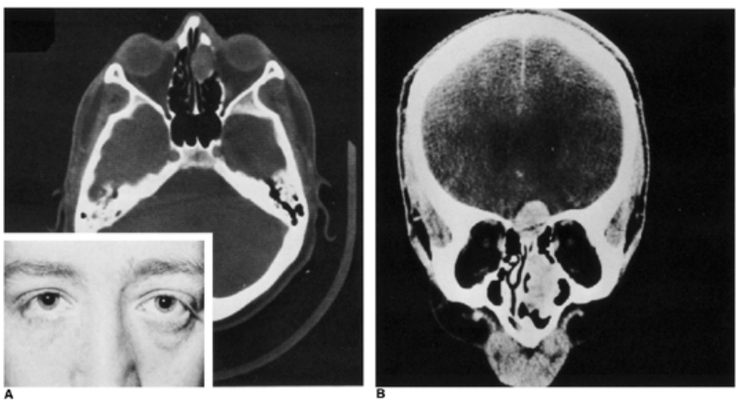

Figure 9-42. (A) This 23-year-old man had mild periorbital swelling, proptosis, and displacement of the left eye as a result of the presence of a mass in the anterior ethmoid portion of the sinus shown on CT scan. Surgically, it was associated with an accumulation of mucopurulent material and an underlying tumor mass, which proved to be a schwannoma with slight cellular atypia. (B) Coronal CT scan of the same patient taken 3 years later shows extension and growth of a residual tumor into the anterior cranial fossa and nasopharynx. He underwent a combined craniotomy-ENT resection, and is alive and well 4 years later. (Reproduced with permission from Rootman J, Goldberg C, Robertson W. Primary orbital schwannomas. Br J Ophthalmol 1981;66:194-204.)

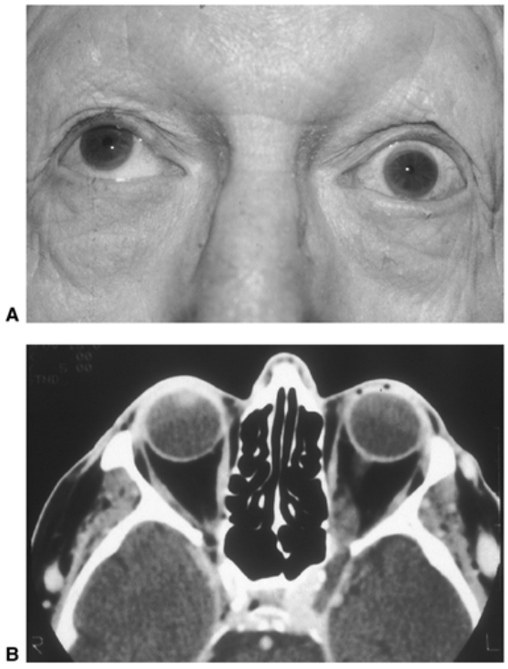

Figure 9-43. (A) This 70-year-old man presented with a 15-year history of progressive but intermittent diplopia, which was particularly notable when looking up and to the right. He had been observed to have a small left pupil and was also aware of a slight left ptosis. On physical examination, he had normal vision with 1 mm of left ptosis, exophthalmometry measurements of 12 mm on the right and 16 mm on the left, normal sensation, and pupillary measurements of 2 mm on the right and 1 mm on left. On extraocular motor examination, he had a right hypertropia in left gaze. His overall features demonstrated a partial third nerve palsy and a possible sympathetic lesion. (B) On CT scan, an apical, smooth-contoured, soft tissue mass was identified extending posteriorly through the superior orbital fissure into the region of the cavernous sinus. Multiple scans suggested that this appeared posteriorly to lie in continuity with the third nerve as it coursed through the superior aspect of the cavernous sinus. Because of the longstanding nature of the lesion and its CT appearance, a diagnosis of schwannoma was made. The patient has been observed without progression.

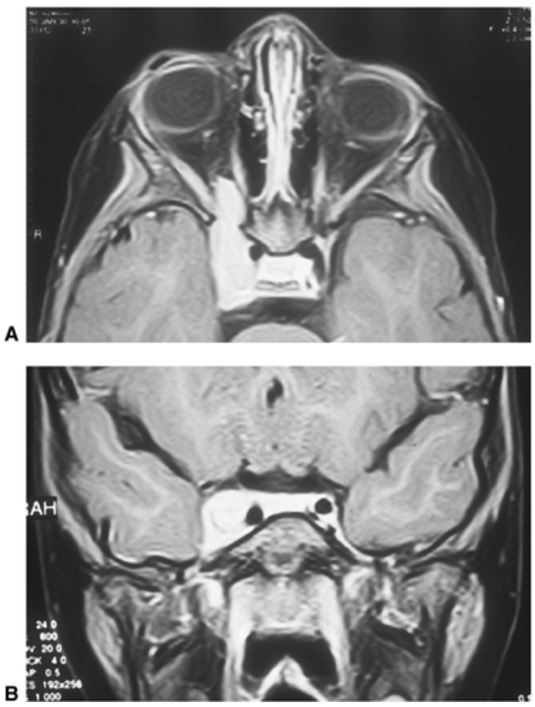

Figure 9-44. This 19-month-old boy presented with a history of an abnormality of the right pupil, noted since age 2 months, followed by a slowly progressive third nerve palsy. He had peripheral stigmata of neurofibromatosis. (A, B) The T2-weighted, post-contrast MR scans demonstrated a uniformly enhancing soft tissue mass extending from the right orbital apex to just posterior to the posterior clinoid, filling the cavernous sinus and Meckel's cave and extending through the superior orbital fissure. The right internal carotid artery is medially displaced. A differential diagnosis of schwannoma versus meningioma was made with a preference for schwannoma. The patient has been followed for 3 years without progression of the lesion, suggesting that the lesion is a schwannoma.

Management

Large or symptomatic tumors can be managed definitively by surgery, the approach being governed by location. At

surgery, they are characteristically yellow-tan, solid, and encapsulated, and often have varicose, violaceous tumor vessels on the surface (Fig. 9-41B). When there is a high fat content, the tumor may be bright yellow, and when degenerated, cystic. Because they arise as outpouchings, they may be stripped off the nerve of origin by microsurgical technique. Removal may be total or subtotal, in piecemeal fashion, or by evacuation of the tumor within its capsule. When critically located, evacuation of these tumors may be wise and can be aided by using ultrasonic fragmentation suction devices, such as CUSA (Cavitron Ultrasonic Aspiration) or laser. Overall, recurrence is extremely rare even when the tumor is only partially removed.

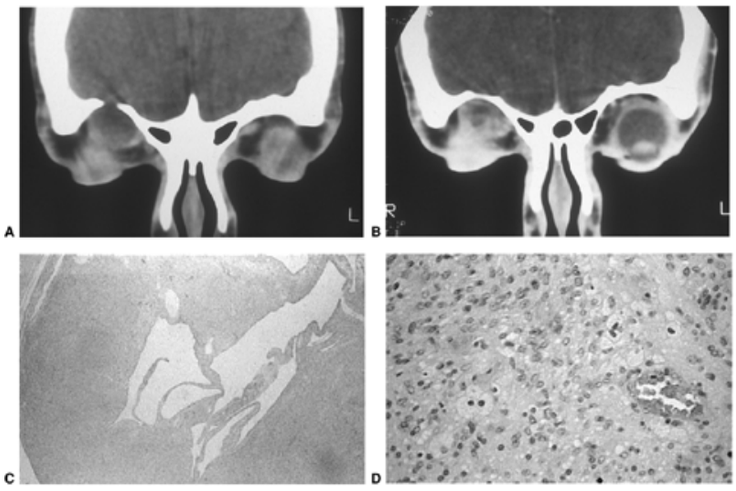

Figure 9-45. This 21-year-old woman had a 2-year history of progressive right ptosis. On physical examination, the only findings were 3 mm of ptosis, 2 mm of downward displacement of the right globe, and 1 mm of proptosis on the right. There was a palpable mass under the superior orbital rim. On CT scan (A, B) there was a smooth, superior orbital mass, which was heterogeneous and had eroded the orbital roof. The lesion was removed by anterior orbitotomy, and histologically was a well-encapsulated spindle cell tumor with large cystic spaces centrally (C) (H&E, original magnification × 2.5). This spindle cell tumor had numerous areas containing foamy as well as hemosiderin-laden macrophages, and there was a fragment of peripheral nerve in a portion of the capsule (D) (H&E, original magnification × 25). The histologic diagnosis was a cystically degenerated schwannoma with marked lipidization.

In summary, schwannomas are rare periorbital and orbital tumors with variable anatomic and pathologic features. They are slow growing, solitary, noninfiltrative, and almost universally benign. A constellation of investigative features points to this diagnosis and surgical intervention, when indicated, is successful.

Malignant Peripheral Nerve Sheath Tumors

The principal malignancy among nerve sheath tumors is malignant schwannoma, but not all tumors in this group arise exclusively from Schwann cells, and they may have diverse histologic manifestations reflecting a pluripotential neural crest origin. Thus, some may arise principally from neural fibroblasts or perineural cells. In the past, these tumors have been described as neurofibrosarcoma, neurogenic sarcoma, and malignant schwannoma. The term “malignant peripheral nerve sheath tumor” is a broader umbrella for lesions in this category, since they are a diverse group of tumors with features of neurodifferentiation that are part of the differential diagnosis of spindle cell neoplasia.

These tumors represent 10% of all soft tissue sarcomas throughout the body with approximately half occurring within the context of neurofibromatosis. Three percent to 13% of patients with neurofibromatosis will develop a malignant peripheral nerve sheath tumor with a latent period

of 10 to 20 years. They largely occur between the second and fifth decades. In the context of neurofibromatosis, they are noted earlier, and males dominate females. Most arise from major nerves and are associated with mass effect and variable sensory and motor symptoms. They usually arise from deeper nerves, and few are seen in the head and neck. There is a high incidence of local recurrence, metastases, and a poor prognosis, in part based on their large size at diagnosis. They generally have a much poorer prognosis when associated with von Recklinghausen's disease.

In the orbit, malignant peripheral nerve sheath tumors are exceedingly rare; Schatz has documented 14, Henderson 3, and Jakobiec and colleagues 8 cases. The age occurrence in this site is wide (2 to 75 years). About one quarter of the patients described have had lesions arising within the context of longstanding neurofibromatosis. Several cases of metastatic malignant peripheral nerve sheath tumors to the orbit have been described.

Biologically, these are usually locally aggressive tumors. Thus, the onset when de novo or due to transformation in the context of neurofibromatosis is usually over several months. More indolent and slowly recurrent tumors have been described. A higher incidence of superior nasal lesions has been noted and affectation of the frontal or supraorbital nerve may be associated with pain, paresthesia, and tenderness in its distribution. Patients with known neurofibromatosis may have a more indolent course or sudden explosive onset of mass and infiltrative effect. Because of frequent incomplete excision or simple biopsy as the initial procedure, rapid recurrence within 3 to 6 months is common. In addition, a propensity for extension along the nerve sheath and systemic or regional spread make these a prognostically poor neoplasm.

Microscopically, the majority of these tumors resemble fibrosarcomas. However, the cells are arranged in a more irregular pattern with wavy, often buckled or comma-shaped nuclei (Fig. 9-46B). In addition, myxoid areas may be noted,

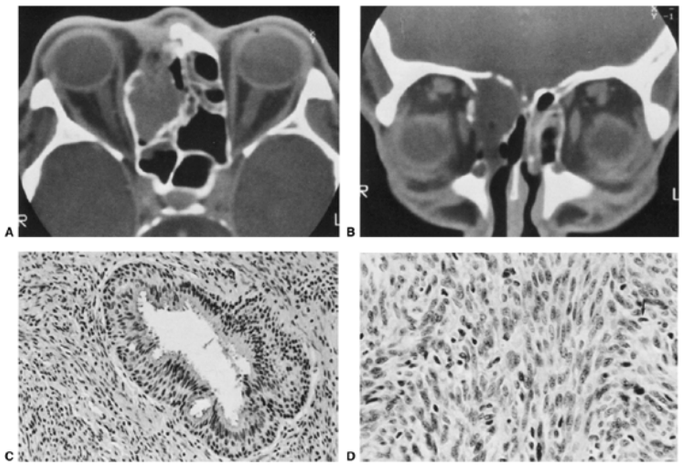

Figure 9-46. Axial (A) and coronal (B) CT scans of a 45-year-old patient who presented with a complaint of tearing present over the previous 2 years. Investigations revealed an ethmoid mass that was believed to be a nasopharyngeal carcinoma. However, biopsy revealed a spindle cell tumor diagnosed as a low grade malignant schwannoma. The lesion had destroyed the cribriform plate and medial orbital wall. The patient underwent a combined craniofacial excision of the mass, and is alive and well 1 year later. (C, D) Histologically, the mass was a low grade malignant schwannoma infiltrating beneath the sinus mucosa. The pattern is one of a spindle cell neoplasm with plump, ovoid, slightly irregular nuclei and occasional comma shapes (arrow) arranged in fascicles (H&E, original magnifications; C × 10, D × 40).

particularly in the context of neurofibromatosis. More common features of Schwann cell character may be seen, including palisading. Heterotopic elements such as bone, skeletal muscle, glandular tissue, and cartilage may be noted. Many of these tumors contain an epithelioid cell component in addition to the spindle-cell proliferation (biphasic). Rhabdomyosarcomatous differentiation and glandular formation have been noted elsewhere but not in the orbital cases. Electron-microscopy and immunohistochemistry (S-100 protein) may help to differentiate these tumors from other spindle-cell and epithelioid neoplasias.

Management of malignant peripheral nerve tumors implies radical and complete excision, which in the orbital context infers exenteration. Because of a propensity to spread along the nerves, combined craniotomy with frozen section may be required. Although recommended, radiotherapy and chemotherapy are not of proven value. Overall, the prognosis for survival is poor, but some tumors may display low-grade behavior with multiple recurrences before succumbing to the malignancy. The introduction of more radical craniofacial techniques may improve the prognosis.

We have encountered five cases of malignant peripheral nerve sheath tumor, all of which appeared to have arisen from the sinuses and secondarily involved the orbit. Two were malignant schwannomas and three would be classified as malignant peripheral nerve sheath tumors. Both of the schwannomas were low-grade recurrences (Figs. 9-42 and 9-46) and managed by combined craniofacial orbital resection. The patients were without recurrence for 1 and 3 years before being lost to follow-up. The remaining three occurred in childhood or adolescence, two arising from the maxillary sinus (Fig. 9-47). All patients underwent radical resection; two are alive and well without recurrence with 7 and 10 years of follow-up. The other patient received adjunctive chemotherapy but has had marginal recurrence adjacent to the orbit and metastasis to the lung (Fig. 9-48).

Rare Tumors of Neuroectodermal Origin

Alveolar Soft Part Sarcoma

Alveolar soft part sarcoma constitutes 0.5% to 1% of all soft tissue sarcomas. It most frequently occurs on the extremities, particularly the lower and on the right side. Overall, it tends to occur in adolescents and young adults with a 3:1 female preponderance. In children, it is believed to affect the head and neck more often, where the orbit is a preferential site. In Enzinger and Weiss' series, 11% of alveolar soft part sarcomas were in the orbit.

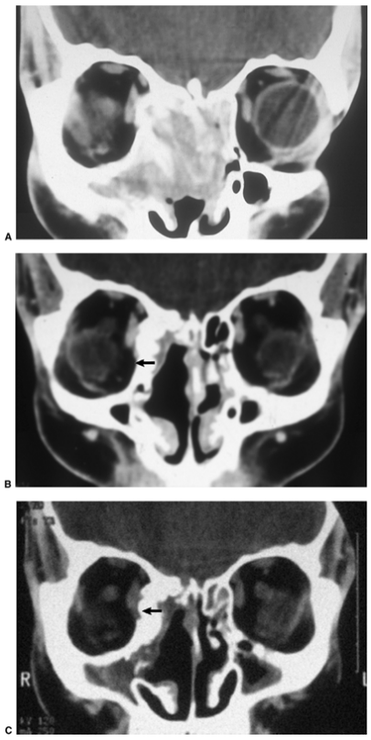

Figure 9-47. This 19-year-old woman presented with a 5-year history of sinus congestion, aching of the right eye, and anosmia. (A) CT scan demonstrated a midline mass with bony hyperostosis. Biopsy proved the mass to be a peripheral nerve sheath tumor, and she underwent excision of the mass. (B) CT scan performed 15 months after presentation demonstrates the persistent thickening of the medial wall of the orbit with a small mass adjacent to the medial rectus muscle (arrow), which was also noted one year later having slightly increased (C). This small mass was biopsied and proved to be a recurrence of tumor so she underwent excision of the medial wall and periorbita. She has been free of tumor for 6 years.

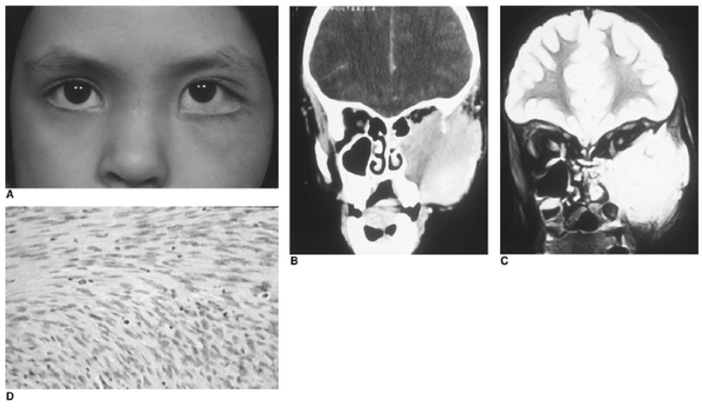

Figure 9-48. (A) This 5-year-old girl presented with progressive swelling of the left lower lid and face, with upward displacement of the globe and proptosis. There was a nodular, soft tissue mass in the lower lid with distortion of the maxilla, mandible, and roof of mouth. (B) CT scan demonstrated a massive lesion arising from the maxillary sinus and extending to involve the bones and soft tissues of the inferior, lateral, and posterolateral orbit. (C) T2-weighted MRI demonstrated a hyperintense lesion, which on biopsy proved to be a spindle cell tumor (D) (H&E, original magnification × 10). The patient underwent radical craniofacial resection, and pathologic examination with special stains led to a diagnosis of malignant peripheral nerve sheath tumor. She has received adjunctive chemotherapy but has had local bony recurrence and metastasis to the lung.

In the orbit, it is characteristically a slow-growing noninvasive mass that leads to proptosis, generally over a 4-month period. The overall 5-year survival rate is 59% and the 20-year rate is 47%. In contrast, when it occurs in the orbit the survival rate is 77%. It is a locally aggressive tumor with a protracted course when it recurs locally. In contrast to rhabdomyosarcoma, it occurs in a slightly older age group and is associated more frequently with decreased vision and proptosis.

Grossly, it is a relatively circumscribed, tan-to-red, vascularized tumor. The characteristic histologic pattern is one of an organoid arrangement of plump, rounded to polygonal cells. The reticulin pattern emphasizes the organoid or nestlike arrangement and the presence of dilated vascular channels. The cells have a rich eosinophilic, occasionally vacuolated cytoplasm with vesicular nuclei. The cytoplasm in 80% of these tumors contains a characteristic PAS-positive, diastase-resistant crystalline material. The electron-microscopic picture identifies within the abundant cytoplasm numerous mitochondria, a prominent smooth endoplasmic reticulum and Golgi apparatus, and rod-shaped crystalloid bodies with occasional electron-dense secretory granules. The crystals and dense granules are characteristically membrane-bound and have a lattice pattern with 100-nm periodicity. These diastase resistant crystals characteristically occur in the paranuclear region.

Several theories of histogenesis have emerged. There have been numerous suggestions that this tumor may be of neural origin, and more recently it has been noted that they may originate from a modified mural cell that stains positively for renin. Thus, an alternative name of malignant angioreninoma has been suggested. A myogenic origin also has been suggested.

Wide local excision is the recommended form of treatment. Radiotherapy and chemotherapy are felt to be only modestly effective and are used for recurrences or incomplete excision. Exenteration is advised in lesions that cannot be completely excised or for local recurrence. Survival following successful excision of the primary tumor and its metastatic lesions has been reported.

Granular Cell Tumor

The majority of cases of granular cell tumor occur in the tongue and subcutaneous tissues. These tumors rarely occur in the orbit where they may have a propensity to involve

muscle. In addition, cases in or near the eye have been noted arising in uvea, conjunctiva, caruncle, lacrimal sac, eyebrows, and eyelids.

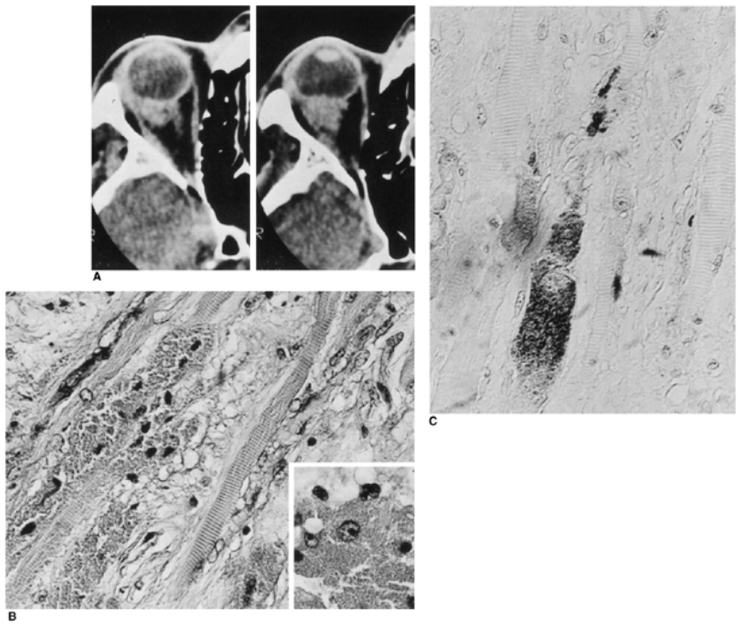

Figure 9-49. (A) Axial CT scans show an irregular right retrobulbar mass displacing the optic nerve medially and indenting the globe: (A, left) superior and (A, right) inferior cuts. The mass was seen in a 44-year-old man who presented with horizontal diplopia and restricted extraocular movements of 10 months' duration. Vision was 20/60, and the globe was elevated 2 mm and proptosed 3 mm. He had posterior choroidal folds. (B) Tumor from the orbit shows plump granular cells invading striated muscle. (B, inset) There were also individual cells with prominent nucleoli and cytoplasmic granules (H&E, original magnifications; B × 10, inset × 40). (C) Granular tumor cell positive for S100 lies among nonstaining striated muscle cells (H&E, original magnification × 25). (Reproduced with permission from Dolman PJ, Rootman J, Dolman CL. Infiltrating orbital granular cell tumour: a case report and literature review. Br J Ophthalmol 1986;71:47-53.)

The tumor may occur at any age, most commonly between 40 and 70 years. There is a female predominance. The typical presentation is a solitary, nontender, firm nodule less than 6 cm in diameter that has been present for less than 1 year. It may be well circumscribed or may infiltrate into surrounding tissues (Fig. 9-49). Throughout the body, 10% to 15% are multicentric and 1% to 3% are malignant. In the orbit, they may occur as discrete or infiltrating, indolently growing tumors of soft tissue or extraocular muscle.

The tumor consists of nests and ribbons of large, round, and polygonal cells. The cells have paracentral, vesicular nuclei with prominent nucleoli and abundant cytoplasm replete with striking coarse eosinophilic granules. The cells lie close to peripheral nerve bundles and normal striated muscle (Figs. 9-49B and C). They are well differentiated and no mitotic activity is noted.

The cytoplasmic granules are PAS-positive and diastase resistant. They may also stain with Sudan black B, India red, Masson trichome, and oil red O. The cytoplasm may be S-100 positive. The characteristic ultrastructural features demonstrate clusters of cells with short interdigitating processes and rare primitive intercellular junctions. The nuclei

are irregularly oval or round with dispersed chromatin and medium-sized nucleoli. Within the cytoplasm are numerous pleomorphic lysosomal-like round bodies lined by single and occasionally double limiting membranes and filled with granular dense material, numerous small vesicles, and concentric laminated bodies. A second, usually more sparse population of spindled mesenchymal cells is frequently noted. They often contain oblong, filamentous, angulate bodies surrounded by a unit membrane. The histogenesis of granular cell tumor remains controversial, but a neural origin is favored.

The treatment of granular cell tumor is wide surgical excision because the clinical behavior is usually benign. For those lesions that are infiltrative, excision with frozen section control is recommended. The reported local recurrence rate is less than 7%. Primary malignant granular cell tumor of the orbit has not been reported; however, it has been described metastatic to the orbit.

Chemodectoma (Paraganglioma)

Chemodectomas are said to arise from the chemoreceptor system, particularly the carotid and jugulotympanic bodies. They are also called nonchromaffin paragangliomas and arise from a widely dispersed collection of chemoreceptor cells of neural crest origin. They occur most commonly in the carotid body; 10% to 20% may have multiple site occurrence, and metastases are seen in 5%. Overall, there is no sex dominance and they occur between 3 and 70 years of age. In addition, they may be sporadic, familial, or multiple. They have a tendency to recur following resection and may metastasize.

In the orbit they are exceedingly rare; 10 of these were collected from 1951 to 1980 throughout China. The previously reported malignant cases are believed to be alveolar soft part sarcomas. Clinically, they usually have been associated with slowly developing (years) proptosis, visual loss, diplopia, and occasionally a throbbing orbital pain. They can, however, have a short history, presenting over months. Some tumors reported were attached to extraocular muscles. These tumors may be locally infiltrative but are usually well defined at the time of surgery. A case of extraorbital extension intracranially has also been described.

Pathologically, these firm or rubbery, reddish-to-tan lesions appear circumscribed and vascular. The component cells are arranged in an organoid or nestlike (Zellballen) pattern and the individual tumor cells are polygonal or ovoid with abundant pale or eosinophilic granular or slightly vacuolated cytoplasm. These nests are surrounded by reticulin. The cell nuclei have finely clumped chromatin (Fig. 9-50). The

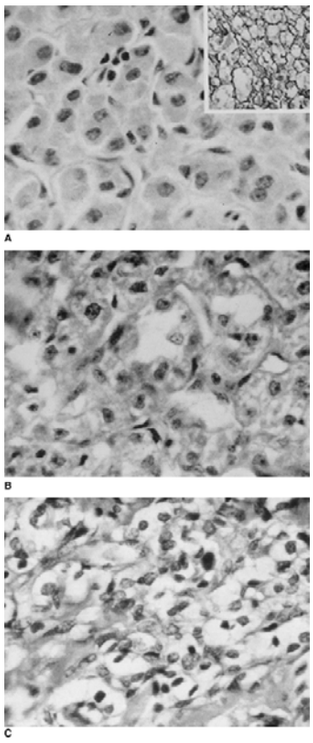

Figure 9-50. (A) Histopathology of an orbital paraganglioma shows nests of plump, regular eosinophilic cells surrounded by reticulin (A, inset) (H&E, original magnifications; A × 40, inset × 10). (B) Orbital paraganglioma demonstrates a more organoid arrangement (H&E, original magnification × 40). (C) Orbital paraganglioma demonstrates nests of vacuolated cells, some of which resemble lipoblasts (H&E, original magnification × 40). (Photos courtesy of Dr. Zhang.)

cytoplasmic granules may be argentaffin- or argyrophil-positive, reflecting small amounts of catecholamines that may be more reliably identified using a formaldehyde-induced fluorescence.

These tumors have a relatively high frequency of recurrence in the orbit as opposed to other sites of the body, so the recommended treatment is excision with frozen section control. In addition, paragangliomas are radiosensitive.

Primary Orbital Carcinoid

Carcinoids characteristically occur as slow-growing neoplasia of the gut, arising from the Kulchitsky's cells. They belong to a larger group of tumors arising from amine precursor uptake and decarboxylation (APUD) cells, which may arise in the pituitary, hypothalamus, adrenal medulla, thyroid, pancreas, and lung. These cells and the tumors derived from them are distinguished by their ability to synthesize bioactive amines or polypeptide hormones. Of tumors arising from this system, 81% are in the upper and lower gastrointestinal tract, 14% occur in the lungs and bronchi, and 5% occur in all other sites. About 5% to 10% of patients with gastrointestinal carcinoid develop the carcinoid syndrome due to a significant hepatic metastatic load producing serotonin and other secretory products. Degradation to 5-hydroxyindoleacetic (5HIAA), which can be detected in the urine, is a marker for this syndrome. Although slow-growing, they are potentially malignant.

Zimmerman and colleagues describe a single case of apparent primary orbital carcinoid with an 11.5-year history of progressive proptosis, leading to exenteration. The orbit contained a tumor made of two cell types arranged in basaloid, tubular, trabecular, and rosette patterns. The tumor cells had either a clear cytoplasm with faint eosinophilic granules and a light basophilic central nucleus with stippled chromatin, or an eosinophilic cytoplasm and densely basophilic nucleus. It had an intense argentaffic reaction (Grimelius) and a light argyrophilic reaction. The patient had no primary lesion detected and was alive and well without recurrence 3 years after exenteration.

It should be noted however that a primary carcinoid of the gut may be exceedingly small and not declare itself, even in the presence of metastasis. We have seen a single case of an orbital carcinoid that presented as a lesion of the inferior rectus of an 83-year-old woman. The lesion was diagnosed by fine needle aspiration biopsy as a carcinoid. The patient refused further treatment and investigation, and ultimately presented 3 years later with a bowel obstruction due to a primary carcinoid, which led to her demise. Several authors have noted that a long delay between recognition of a metastasis and a primary carcinoid is not uncommon.

Neuroepithelial Tumors

The neuroepithelial tumors are a family of neoplasia thought to have arisen from the primitive neuroectoderm. They bear close histologic resemblance and differences are based on sites of origin: the neuroblastoma and ganglioneuroma arise from the sympathetic system, the neuroepithelioma arises from the peripheral nerve, and the olfactory neuroepithelioma arises from the olfactory placode.

Neuroepithelioma

Neuroepithelioma is an exceedingly rare tumor that occurs at any age (most are over 20 years) and is thought to arise from peripheral nerves. Histologically, it is composed of sheets or lobules of rounded cells with indistinct cytoplasm. Some of these groups of cells may form neurotubular units. In addition, they form Homer-Wright or true rosettes as well as perivascular pseudorosettes. They may have a specific chromosomal translocation (11;22). Clinically, they behave in an aggressive fashion and may not respond to either surgery or radiotherapy.

Esthesioneuroblastoma (Olfactory Neuroblastoma)

Esthesioneuroblastoma (olfactory neuroblastoma) is a tumor that arises from the olfactory epithelium in the upper nasal cavity and may extend into the orbit secondarily. Histologically, it is similar to neuroblastoma except for site and age of occurrence. In contrast to neuroblastoma, the frequency of this tumor characteristically has a bimodal peak in the second and fifth decades.

They are made up of sheets of small cells and may or may not have rosettes. They are frequently mistaken for other small cell tumors. Ultrastructurally, they have dense core (neurosecretory granules) and neuritic processes. Olfactory rosettes differing from the Homer-Wright type may be seen in those that demonstrate olfactory differentiation. These are lined by pseudostratified columnar cells with central mucin in the lumina. Neuroblastomas have been divided into two groups: those without olfactory differentiation and those with olfactory differentiation. The latter group may include ganglioneuroblastomatous differentiation (olfactory neurocytoma). Those with olfactory neuroblastomatous differentiation occur in patients of mean age 50 years, and the

less differentiated neuroblastomatous type occurs in patients with a mean age of 20 years. The tumor is rarely seen in patients under the age of 10. The histologic diagnosis may be difficult, requiring both immunohistochemical techniques and electron microscopy.

Rakes and coworkers have emphasized the common occurrence of ophthalmic manifestation in these tumors, noting that 53% of their cases had ocular or orbital manifestations at presentation and an additional 21% developed them later. Indeed, many of the different tumors of the sinus have ocular manifestations at the time of presentation and a small percentage of these patients may be first seen by an ophthalmologist. The common ocular complaints are periorbital pain, lacrimation, and visual disturbance, which usually reflect a tumor in a more advanced stage than those presenting with primary nasal or nonocular symptoms. Additional ocular features include periorbital edema, ptosis, injection, proptosis, epiphora, or cranial nerve palsies.

These tumors have been staged according to site and extent: those in the nasal cavity are group A; those involving the paranasal sinuses are group B; and tumors extending beyond the sinuses into the cranium or orbit are group C. Elkon and coworkers have noted 5-year survival rates of 75% (group A), 68% (group B), and 28% (group C). There has been an increase in survival with the advent of aggressive craniofacial surgery and adjunctive radiotherapy and chemotherapy. Preoperative radiotherapy and chemotherapy may be part of the treatment regimen, along with postoperative chemotherapy for extensive tumors.

Primary Neuroblastoma and Ganglioneuroma

Primary neuroblastoma and ganglioneuroma are thought to arise from the neuroblasts of the sympathetic nervous system. Neuroblastoma is the second most common orbital malignancy of childhood and is overwhelmingly metastatic in origin; it is discussed in the section on metastatic tumors . Primary differentiated neuroblastoma has been described in the orbit on two occasions, both in adults and both had progressive disease requiring radiation and exenteration.

Systemically, ganglioneuromas are three times more common than neuroblastomas but occur at an older age (average 10 years) and in the posterior mediastinum and retroperitoneum, in contrast to the younger age occurrence and adrenal site of neuroblastoma. They are by definition well-circumscribed, benign tumors that contain a histologically uniform population of cells. Scattered nests of mature ganglion cells are seen within a matrix of Schwann cells. Histologically confirmed primary occurrence of this lesion in the orbit has not been described, but a single case of secondary extension from the sinus has been noted.

Primary Orbital Melanoma

Primary melanoma of the orbit is a rare tumor and must be distinguished from the more common occurrence of metastases and secondary melanomas arising from the globe, lid, and conjunctiva. Late recurrence of uveal melanoma has been reported even 42 years after enucleation. Nevertheless, primary melanomas within the orbit do occur. They originate from melanocytes of the leptomeninges, ciliary nerves, and emmissaria or from ectopic rests. They may arise de novo or commonly in association with ocular and oculodermal melanocytosis, or rarely in association with a cellular blue nevus. The oculodermal melanocytosis may be of a limited variety, and features of dermal pigmentation in the first and second divisions of the fifth nerve should be carefully sought. According to Hidano and associates, up to the 65% of patients with the nevus of Ota will have evidence of pigmentation of the ocular tissues.

The clinical onset of primary orbital melanoma is usually described as a rapidly growing tumefaction, which may or may not be infiltrative. CT scans in cases described demonstrate a well-defined enhancing mass with variable low-density or cystic areas in some.

At surgery, they are usually pigmented and may even be black and necrotic, making gross distinction from a hematoma difficult. These tumors may be rarely circumscribed at the time of surgery and are more frequently infiltrative. Histologically, primary melanomas usually consist of a mixture of spindle and epithelioid cells with a high mitotic index. Some melanomas may be mostly spindle cell or epithelioid in character and amelanotic. If associated with a nevus of Ota, scattered melanocytes in the remaining orbital tissues or rests of a cellular blue nevus may be identified. It has been suggested that poor prognostic indicators are mixed cell type with high mitotic count, greater patient age, and the presence of congenital melanosis.

These tumors have a poor prognosis because of their propensity to escape the local confines by perineural routes and adjacent foramina or the bloodstream. Treatment is by complete excision, usually requiring exenteration, and in some circumstances, superexenteration. A few cases of low-grade tumors have been locally resected. Adjuvant radiotherapy and chemotherapy is considered for diffuse, recurrent, metastatic, or incompletely excised lesions.

Retinal Anlage Tumor (Pigmented Retinal Choristoma)

Retinal anlage tumor is a curiosity that characteristically occurs in the head and neck (usually in the upper or lower jaw) of an infant in the first year of life. Its interest to the ophthalmologist lies in its characteristic morphology, which reflects features of the retinal pigment epithelium and neuroblastic cells. In addition, this tumor occasionally involves the orbit by contiguity. Diverse names have been given, including pigmented neuroectodermal tumor of infancy, melanotic progonoma, congenital melanocarcinoma, melanotic adamantinoma, and pigmented epulis of infancy, reflecting differing theories of histogenesis. There has been some argument about the tumor's origin, either from a neuroectoderm or neural crest, but recent evidence suggests neural crest origin. Zimmerman has emphasized the characteristic morphologic features of the pigment within the tumor cells as being of retinal pigment epithelial type, and has proposed the name pigmented retinal choristoma.

The typical histopathologic feature is the presence of alveolar spaces lined by pigmented cuboidal cells. In addition, nests of nonpigmented, small, round cells may be seen within the alveoli or the surrounding fibrous stroma. Neurofibrillary material may be seen in association with these cells, which resemble benign neuroblasts.

The tumor usually presents as a mass involving the upper or lower jaw. Characteristically, the mass is radiolucent and may be locally destructive. Other sites include the skin, ovary, uterus, brain, and epididymis. In the head and neck, they may be locally recurrent in about 10% to 15% of cases. Multifocal lesions have been described and about 4% have been malignant with metastases.

Treatment is complete excision of the involved bone and soft tissue.

Ectomesenchymal Tumors

Because the mesenchyme of the head and neck is largely of neural crest origin (ectomesenchyme, mesectoderm), some tumors derived from these tissues may recapitulate a mixture of fibroblastic, muscle cell, and schwannian elements. Thus, schwannian tumors may have evidence of striated muscle components. More complex admixtures of pigmented, fibroblastic, and myoblastic tissues in these unusual tumors may be noted. These tumors have largely been described in the head and neck region and in the globe, but both primary and secondary ectomesenchymal tumors have occurred in the orbit.

Mesenchymal Tumors

The lesions in this section can be grouped under a broad umbrella of mesenchymal and fibro-osseous tumors by suggesting that a primitive mesenchymal stem cell is capable of developing into a variety of cell types. These cell lines may undergo developmental arrest at varying stages of maturation and produce benign or malignant proliferations with differences in biologic behavior. The orbital tissues of mesenchymal origin include striated and smooth muscle, fibrous tissue, fat, cartilage, and bone. Embryologically, orbital mesenchyme is from the neural crest (ectomesenchyme or mesoectoderm); however, lesions in this location do not differ in biologic behavior from the same elsewhere in the body. Because of their common progenitor, most of these tumor lines may share a continuum of histologic features. In addition, many have a variable pattern and may be composed of cells and single cell lines expressing different functional states, for example, a collagenizing fibroblast, a myofibroblast, or a fibroblastic histiocyte. Myofibroblasts have features of both fibroblasts and smooth muscle cells. Similarly, osteoblasts and chondroblasts share features noted in both cartilaginous and bone-producing tumors.

We have seen 63 mesenchymal lesions of the orbit, comprising 1.6% of all orbital cases and 8.9% of neoplasia. Amongst children, they constitute about 5% of orbital disease. The undifferentiated embryonal mesenchymal tumors and tumors of muscle are classified together on the basis of similar histology, clinical behavior, or features of myopathic differentiation. They include embryonal sarcoma, rhabdomyosarcoma, and rare smooth muscle tumors. Despite the wealth of cellular anlage, adipose and fibrous tissue tumors of the orbit are rare. In contrast, fibrous histiocytomas and solitary fibrous tumors appear to have an orbital predilection. The largest group of mesenchymal lesions derives from bone and includes dysplasias, reactive lesions, and neoplasia.

Striated Muscle Tumors

Rhabdomyosarcoma

Rhabdomyosarcoma invokes the differential diagnosis in childhood of acute and subacute proptosis clinically, and small, round, and spindle cell tumors of the orbit pathologically. It has a distinctive age and site predilection and pathologic appearance. Modern advances in therapy have markedly improved the prognosis, particularly in the orbital cases.

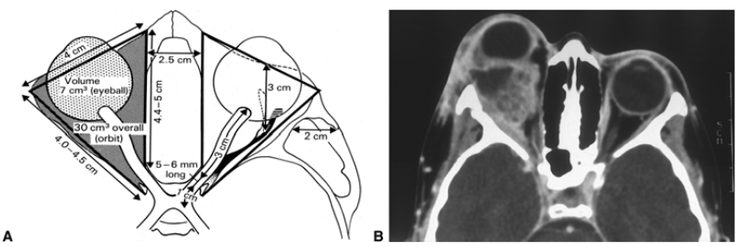

Figure 9-51. (A) This CT scan demonstrates a large infiltrating orbital mass seen in a 9-year-old girl with a history of rapid-onset right proptosis and pain on extraocular movement, which occurred over a 2-week period. On physical examination, she had vision of 20/50 on the right and 20/20 on the left with right afferent pupillary defect, 7 mm downward and 2 mm outward displacement of the globe, and 11 mm of exophthalmos. In addition, she had indentation of the globe and a swollen disc. She underwent a biopsy and debulking of 60% of the tumor, which histologically proved to be an alveolar rhabdomyosarcoma but had no evidence of alveolar rhabdomyosarcoma fusion on molecular studies. Over the next week while awaiting oncology conferencing, the tumor regrew significantly, as shown on contrast CT scan (B). She underwent chemotherapy and radiotherapy and had regression of the tumor with good ocular function 6 months following treatment.

Rhabdomyosarcoma is the most common childhood soft tissue sarcoma, and approximately 10% occur in the orbit. It is the most common primary malignant tumor in childhood. In our series, it constituted 1% of orbital neoplasia and from pooled series, 2% of orbital diseases of children and 6% of childhood orbital tumors. In all sites, about 70% occur in the first decade but it has been reported from birth to the seventh decade. There is a bimodal peak paralleling histology, with embryonal and alveolar types occurring in childhood and adolescence, respectively, and the rare anaplastic (pleomorphic) variety in older people. In the orbit, some series suggest a male predominance and others indicate an equal sex distribution. The average age of presentation of orbital rhabdomyosarcoma is 7 to 8 years, and the majority are embryonal.

The histogenesis is thought to reflect the embryogenesis of muscle with the tissue of origin being pluripotential mesenchyme. This theory is supported by a tendency for the tumor to occur in the orbital soft tissue and not in the extraocular muscles. The embryonal type corresponds to developing muscle at the 7 to 10 week fetal stage, and the alveolar type to the hollow tube stage. The anaplastic (pleomorphic) type is thought to have arisen de novo as a result of dedifferentiation of adult muscle.

Most rhabdomyosarcomas arise spontaneously although familial occurrences (often with a positive history of malignancy – Li-Fraumeni syndrome related to a mutation of the tumor suppressor p53 gene), associations with congenital malformations, and occurrences as second tumors in hereditary retinoblastomas have been cited.

Presentation

Orbital rhabdomyosarcomas present with rapidly developing exophthalmos (over weeks), reflecting the fulminant growth pattern of this tumor (Fig. 9-51). Two thirds are superonasal and thus present with downward and outward displacement of the globe, which is frequently associated with injection and swelling of the lids. About one third to one half have ptosis and a palpable mass. Pain, decreased vision, or epiphora are uncommon presenting signs. About half of the tumors are retrobulbar and a small percentage of rhabdomyosarcomas with orbital presentation arise from the paranasal sinuses, nasal cavity, pterygopalatine fossa, and parapharyngeal space. These may secondarily invade the orbit, thus presenting occasionally with features of nasal obstruction and epistaxis (Fig. 9-52). The clinical differential diagnosis include some acute and subacute orbital inflammations, capillary hemangiomas, aggressive fibromatoses, and numerous undifferentiated or poorly differentiated tumors of epithelial, mesenchymal, neural, or lymphoreticular origin in childhood (*c.f.* chapter 7 – Pathology).

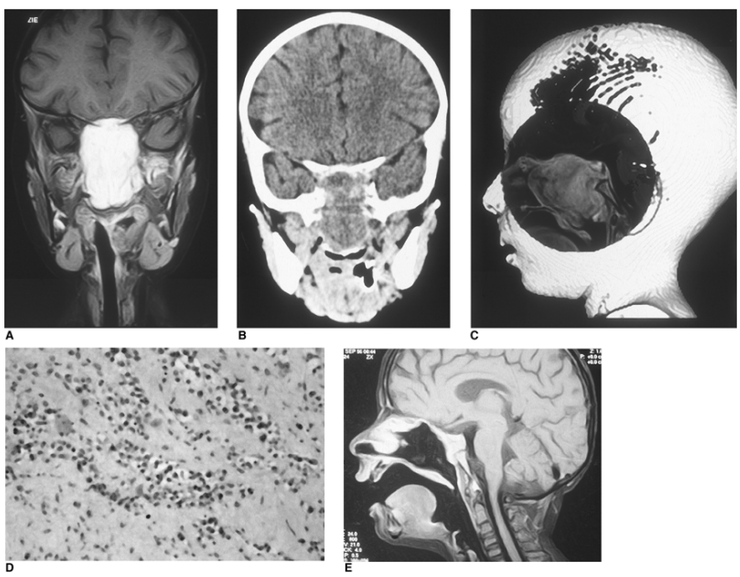

Figure 9-52. This 5-year-old boy presented with nasal obstruction and headache that had been present for approximately 3 weeks. He had a 3-day history of decreased vision bilaterally and progressive ptosis. On physical examination, he had bilateral third nerve palsies, equivocal light perception with bilateral optic atrophy, dilated pupils, and minimal response to light. On MR (A) and CT (B) imaging, he demonstrated a massive tumor of the midline sinus and nasal structures with erosion into the skull base. The three-dimensional reconstruction (C) demonstrates the extent of the tumor in the midline. (D) Biopsy revealed an alveolar rhabdomyosarcoma (H&E, original magnification × 10). He therefore underwent debulking of this tumor (to relieve optic nerve pressure; E, postoperative scan), radiotherapy, and chemotherapy. He has been followed for 5 years without recurrence of disease and is able to read N6 at near on the right and has light perception with perhaps projection on the left.

Imaging

On CT scan, the tumors appear as homogeneous, well defined, soft tissue masses without bone destruction (Fig. 9-51). They are isodense in relation to normal muscle and when larger, may be less well defined with invasion of surrounding structures. Areas of focal hemorrhage or necrosis may appear heterogeneous on CT scan (Figs. 9-51 and 9-53). They demonstrate moderate to marked contrast enhancement.

On MR imaging, they appear isointense or slightly hypointense compared to brain on T1-weighted images, and hyperintense on T2-imaging (Figs. 9-54). Areas of chronic hemorrhage may show focal areas of increased signal on T1- and T2-weighted images. The tumors appear hyperintense after contrast injection, particularly on fat suppression.

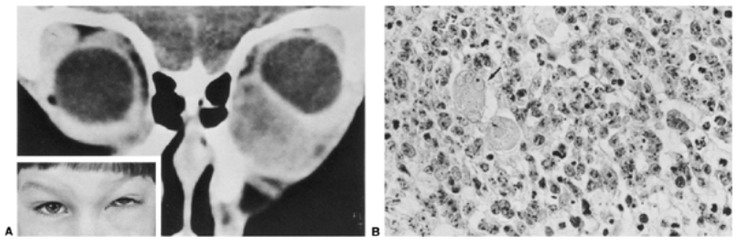

Figure 9-53. (A) A 7-year-old boy with an embryonal rhabdomyosarcoma presented with a mass involving the left lower lid and orbit that developed over a 5-week period. On palpation, it was firm, slightly nodular with a tan-pink subconjunctival component. The coronal CT scan demonstrates a solid tumor with areas of low density, which indented and displaced the globe upward. At orbitotomy, a circumscribed, slightly nodular, pale tan mass was excised. Histologically, there were areas of loose (myxoid) and compact cellularity and distinct perivascular mantles of tumor. The myxoid areas correspond to the low-density foci noted on CT scan. (B) The cell population consisted of pleomorphic round and oval cells with hyperchromatic nuclei and dense nucleoli. In addition, there were large rhabdomyoblasts with eosinophilic fibrillar cytoplasm (arrow) (H&E, original magnification × 40). The patient was treated with combined chemotherapy (modified VAC) and radiotherapy (4140 rad), and is alive and well 10 years later.

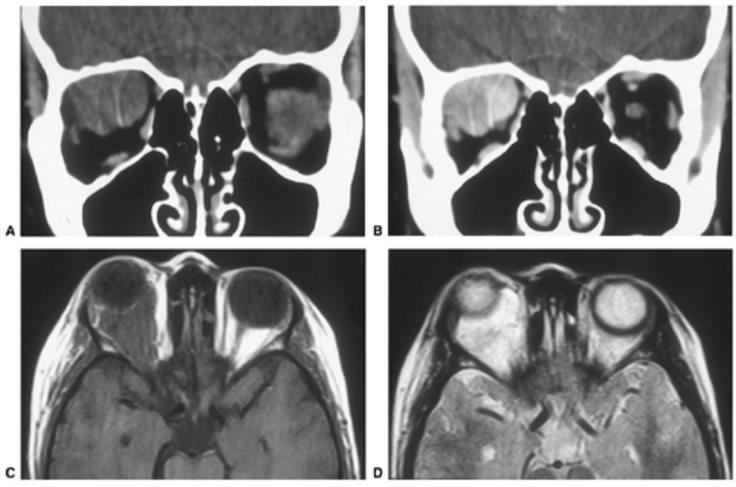

Figure 9-54. This patient with an embryonal rhabdomyosarcoma presented at 9 years of age. Over a 1.5-week period, he had developed diplopia and swelling of the right upper lid with proptosis. He had 6 mm of downward and 3 mm of outward displacement; almost 9 mm of axial proptosis; limitation of upgaze, adduction, and abduction, and 25 diopter right hypotropia in primary position. On CT scan (A), he had a large, inhomogeneous retrobulbar mass, which showed enhancement in some areas (B). (C) T1-weighted MRI demonstrates the mass enveloping the globe and displacing the orbital fat. (D) On T2 MRI, it appeared hyperintense in an irregular fashion. He underwent partial resection, chemotherapy, and radiation therapy and is now 1.5 years posttreatment with 20/20 vision on the right and 20/25 on the left, a full range of ocular movements, and exophthalmometry of 11 mm right and 12 mm left.

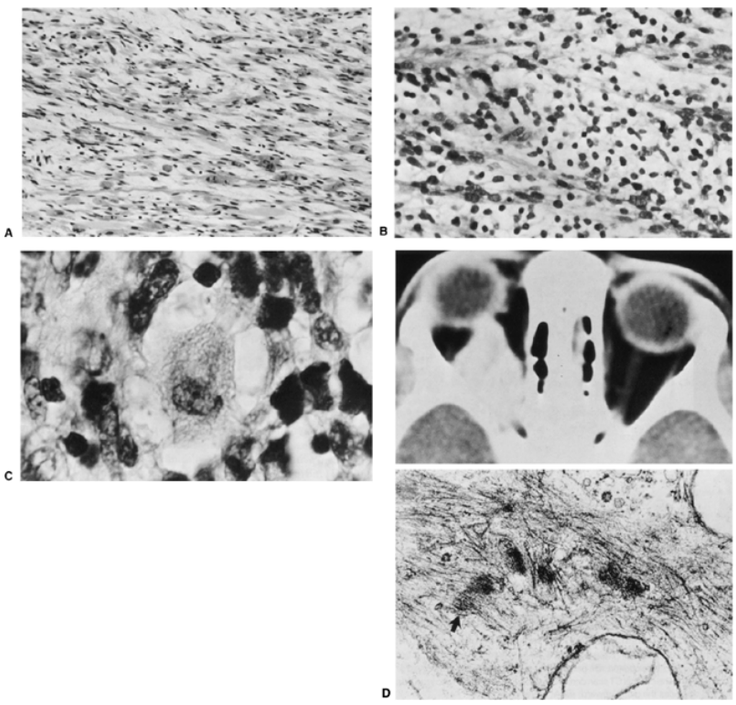

Figure 9-55. (A, B) Photomicrographs of areas of embryonal rhabdomyosarcoma with varying features show elongated, strap-like rhabdomyoblasts, some rounded plump cells, and an admixture of loosely arranged cells (H&E, original magnifications; A × 10, B × 25). (C) Rhabdomyoblasts with a central tumor cell demonstrating vacuolated cytoplasm secondary to lysis of glycogen (“spider web” cell) (H&E, original magnification × 100). (D, top) Contrast-enhanced axial CT scan demonstrates a slightly nodular intraconal mass extending toward the orbital apex. This occurred in a 4-year-old boy who developed rapid prominence of the eye over a 1-week period. (D, bottom) Electron microscopic features from biopsy of the mass above. Note the myofilamentary structure with Z-band densities (arrow). These features suggest early sarcomeric organization substantiating a diagnosis of rhabdomyosarcoma.

Pathology

Rhabdomyosarcomas fall into three broad categories depending on the overall morphologic pattern (embryonal, alveolar, undifferentiated, and anaplastic). Central to the diagnosis is some form of microscopic, immunohistochemical, or electron microscopic demonstration of rhabdomyoblasts. Rhabdomyoblasts may be identified by the presence of cross striations but these are frequently absent and the cells are more often characterized by an abundant eosinophilic cytoplasm containing fibrillary material or cells of spindle, irregular, tadpole, racquet, or angulated shape (Figs. 9-53 and 9-55). They may have a markedly vacuolated cytoplasm suggesting the appearance of a spider web (Fig. 9-55C).

Histochemistry with Masson trichrome, phosphotungstic acid-hematoxylin (PTAH), and periodic acid Schiff (PAS) with and without diastase confirm empiric features of acidophilia and glycogen deposition. Immunoperoxidase techniques, particularly for desmin, muscle-specific actin,

and myoglobulin, help identify the myoblastic nature of the tumor. Ultrastructurally, the degree of differentiation of the tumor varies greatly, with the least differentiated cells demonstrating thin (actin) myofilaments (60 to 80 nm) and the more differentiated thicker (myosin) filaments (120 to 150 nm) (Fig. 9-55D). More obvious characteristics of muscle may be noted with A and I banding and Z lines (Fig. 9-55D). The cytoplasm may also contain a prominent Golgi apparatus, polyribosomes associated with myofilaments, glycogen, lipid, lysosomes, and incomplete basal lamina with pinocytotic vesicles.

The histopathologic classification of orbital rhabdomyosarcoma favored by the Intergroup Rhabdomyosarcoma Study divides these tumors into embryonal, alveolar, undifferentiated, and anaplastic sarcoma. In the orbit, about 80% of rhabdomyosarcomas are embryonal, the majority of which have a classic pattern, followed in order by spindle cell, botryoid, and anaplastic types. Each of these categories is subdivided on the basis of the degree of differentiation from poorly differentiated to moderately to highly differentiated categories. About three quarters of the embryonal rhabdomyosarcomas are minimally differentiated. The alveolar and undifferentiated sarcomas have a poorer prognosis and tend to occur at a younger age (under 1 year) than embryonal rhabdomyosarcomas. Alveolar rhabdomyosarcomas that are primary in the orbit are rare and tend to occur inferiorly. The overall survival rate for alveolar was 74% whereas the embryonal group had an overall survival rate of 94% with the undifferentiated subgroup having a 97% survival rate. Recent studies suggest that genetic analysis may aid in prognostic categorization of rhabdomyosarcomas. In addition, fine needle aspiration biopsy may be successful in diagnosing this tumor, although categorization is more difficult without open biopsy.

Differential Diagnosis

The clinical differential diagnosis includes progressive rapidly developing masses and inflammatory conditions of childhood, such as neuroblastoma, chloroma, lymphangioma, infantile hemangioma, cellulitis, and nonspecific inflammatory diseases. The histopathologic differential diagnosis of childhood round cell tumors includes neuroblastoma, neuroepithelioma, Ewing's sarcoma, angiosarcoma, synovial sarcoma, malignant melanoma, granulocytic sarcoma, rhabdoid tumor, alveolar soft part sarcoma, and malignant lymphoma. Focal myoblastic differentiation can occur as part of other types of tumors, such as the neuroectodermal neoplasia. Some inflammatory conditions may resemble it, including nodular fasciitis and destructive inflammations affecting muscle.

Management

The introduction of the combination of surgery, adjuvant chemotherapy, and radiotherapy in the late 1960s has improved the overall prognosis for survival from roughly 30% to over 90%.

Management involves pathologic confirmation and histopathologic typing as well as tumor staging. The current staging system of the Intergroup Rhabdomyosarcoma Study finds that the overwhelming majority of orbital rhabdomyosarcomas are localized with some residual disease. Staging is done by review of imaging, clinical examination, and the surgeon's opinion (Table 9-8). In addition, the patient should be worked up for metastases with chest X-ray, full blood count, renal and liver function test, bone marrow aspiration for cytology, and bone scan. The cerebral spinal fluid should be cytologically examined if there is any suggestion of meningeal spread. Metastases from orbital sites are to lung and bone with very rare lymphatic extension.

Table 9-8. The Surgical-Pathologic Grouping System used in Intergroup Rhabdomyosarcoma Study Group trials

GROUP NUMBER	CRITERIA
I	Localized disease, completely resected
	Confined to the organ or muscle of origin
	Infiltration outside organ or muscle of origin; regional lymph nodes not involved
II	Compromised or regional resection of three types, including:
	Grossly resected tumors with microscopic residual
	Regional disease, completely resected, in which lymph nodes may be involved and/or extension of tumor into an adjacent organ may be present
	Regional disease with involved lymph nodes, macroscopically resected but with evidence of microscopic residual
III	Incomplete resection or biopsy with macroscopic residual disease
IV	Distant metastases present at onset

Reproduced with permission from Lawrence W Jr, Anderson JR, Gehan EA, Maurer H. Pretreatment TNM staging of childhood rhabdomyosarcoma: a report of the Intergroup Rhabdomyosarcoma Study Group. Children's Cancer Study Group. Pediatric Oncology Group. Cancer 1997;80:1165-70.

Patients in whom a localized tumor has been completely resected are usually treated with chemotherapy alone to avoid the complications of radiotherapy. Patients that are in Groups II, III, and IV usually receive radiation, generally in the range of 4500 to 5000 cGy over 4 to 5 weeks. When there is evidence of intracranial spread, whole cranial irradiation and intrathecal chemotherapy may be added. Gross evidence of residual tumor or distant metastases imply repetitive pulses of chemotherapy.

The overwhelming majority of recurrences occurs within 3 years of the original presentation and can be treated by chemotherapy with local, or more often radical, excision of tumor. Overall survival is excellent for Groups I, II, and III patients because of the favorable site.

Complications of Treatment

Ninety percent of patients posttreatment with radiotherapy develop cataract. Other ocular sequelae include keratoconjunctivitis, dry eyes, radiation retinopathy, and facial asymmetry associated with bony hypoplasia. Lacrimal duct stenosis and dental defects also occur. Incidental irradiation of the pituitary is associated with growth retardation. Secondary neoplasms are rare, the major ones being osteogenic sarcoma and lymphoblastic leukemia. These tend to occur in patients treated with alkylating agents and radiotherapy or in those with a family history suggestive of the Li-Fraumeni syndrome.

Rhabdoid Tumor

Malignant rhabdoid tumor is a highly aggressive tumor of the infant kidney that resembles rhabdomyosarcoma by light microscopy but lacks rhabdomyoblastic findings on electron microscopy. Morphologically similar tumors have been described in multiple extrarenal sites, including the orbit (in 6 instances) where its behavior has also been aggressive. In the orbit, it presents as a rapidly growing, relatively poorly defined tumor in both adults and children.

Histopathologically, these tumors have a characteristic pattern consisting of dense infiltrations of large, oval, or polygonal cells with large vesicular nuclei, prominent nucleoli, abundant eosinophilic cytoplasm, and filamentous cytoplasmic inclusions. Cytoplasmic inclusions consist of parallel intermediate filaments of 6 to 9 nm in diameter. These inclusions have been reported in numerous other tumors, including rhabdomyosarcoma (rhabdomyosarcoma with rhabdoid features), melanoma, malignant peripheral nerve sheath tumor, colonic adenocarcinoma, endometrial sarcoma, and numerous benign conditions. Immunohistochemistry is characteristically positive for vimentin, cytokeratin, and epithelial membrane antigen, and negative for muscle markers, histiocytic markers, HMB-45, and S-100 protein. Because the phenotype resembles the renal tumor, these neoplasms have been called extrarenal rhabdoid tumors. Some authors, however, believe that a more appropriate designation would be “malignant undifferentiated neoplasms with rhabdoid features.”

Overall in extrarenal sites, these tumors have a dismal prognosis with a 15% survival. Of the orbital cases, half of those described have survived with treatment consisting of multimodality chemotherapy and radiotherapy. We described the first case seen in the orbit (Fig. 9-56).

Rhabdomyoma

Rhabdomyoma (adult type) of the orbit has been reported with assurance on two occasions. This is a benign tumor that consists of well-differentiated striated muscle cells in a collagenous stroma. The cells are large, round to polygonal with an abundant granular, acidophilic cytoplasm and lack nuclear atypia. When well defined, these tumors can be excised or partially resected and observed.

Endodermal Sinus Tumor

Like orbital teratomas, endodermal sinus tumors are of germ cell origin and thought to arise from the yolk sac. These malignant tumors usually occur in gonadal sites but have been described rarely in the orbit where they present as a fulminant neoplasm in early childhood (mean age 13 months), similar to the clinical presentation of rhabdomyosarcoma. Although it has a frequently fatal outcome elsewhere, the orbital lesions may have a better prognosis because of early recognition. Histologically, it is a tumor made up of cords of cells, which form a pseudopapillary pattern with a fine, intervening stroma. The epithelial cells are anaplastic and there may be focal, myxomatous, or necrotic areas. In contrast to rhabdomyosarcoma, the cells are positive for alpha fetoprotein. Treatment is surgery combined with triple-drug chemotherapy. This tumor is not of myoblastic origin but is included here because it is part of the differential diagnosis for rhabdomyosarcoma.

Smooth Muscle Tumors

Orbital smooth muscle tumors may arise from vessels, the smooth muscle overlying the inferior orbital fissure, and the capsulopalpebral muscles of Müller. Both the benign and malignant variants are exceedingly rare.

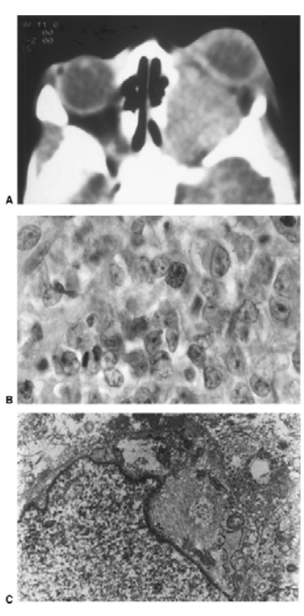

Figure 9-56. A 6-week-old infant presented with a 4.5-week history of progressive left proptosis. (A) Contrast-enhanced CT scan demonstrates a large, dense, intraconal soft tissue mass in the left orbit. The mass does not show any significant contrast enhancement. The orbit was expanded and there was evidence of pressure erosion. The patient also had widening of the superior orbital fissure, with tumor extension in both the superior and inferior orbital fissures. (B) Biopsy of the mass showed round-to-oval cells with vesicular, eccentric nuclei and conspicuous nucleoli (H&E, original magnification × 40). (C) Electron microscopy demonstrates a filamentous cytoplasmic inclusion composed of parallel intermediate filaments indenting the nucleus (original magnification × 19000). (Figs. 9-56A and B reproduced with permission from Rootman J, Damji KF, Dimmick JE. Malignant rhabdoid tumor of the orbit. Ophthalmology 1989;96:1650-4.)

Leiomyoma

Orbital leiomyoma is a curiosity. They are well encapsulated, slowly progressive, isolated orbital tumors that occur in the third and fourth decades. On MR and CT imaging, they are well defined lesions. The more vascular types may have high velocity flow on Doppler ultrasound. Histologically, these solid tumors consist of bundles of palisading cells. The cytoplasm characteristically stains intensely with trichrome and contains filaments; considerable basement membrane is noted on PAS staining, and they are positive for desmin and muscle-specific actin. There may be a prominent vascular component. They can be excised in toto but are frequently very adherent, requiring microdissection. Recurrence, which may be very slow, reflects incomplete excision, and they are not radiosensitive. Because leiomyomas may demonstrate collagen deposition and are spindle cell tumors, confusion with nerve sheath tumors and fibrous histiocytomas is common.

Leiomyosarcoma

Leiomyosarcomas are rare orbital tumors of varying degrees of malignancy, characterized by local invasion and potential for metastasis. They either occur de novo in older individuals (sixth decade) or as radiation-induced sarcomas in younger patients. Clinically, they are relatively rapidly developing and usually infiltrative masses. The histologic diagnosis rests on the demonstration of smooth muscle origin (i.e., cytoplasmic filaments on trichrome stain or electron-microscopy, positive actin and desmin) but this may be difficult. The tumors are characteristically vascular and densely cellular, and demonstrate foci of necrosis, mitoses, or nuclear pleomorphism. Because of their usual infiltrative nature, the treatment of choice is exenteration; however, several cases have been managed successfully by local excision. Both radiotherapy and chemotherapy have been used for recurrent lesions.

A highly aggressive mesoectodermal leiomyosarcoma with neurogenic features has been reported arising from the antrum and invading the orbit.

Adipose Tumors

Although fat constitutes the largest component of the orbit, unequivocal lipomas and liposarcomas are exceedingly rare in this site.

Lipoma

The frequency of lipomas varies from 0% to 9% of orbital tumors, and generally is closer to 0% where strict histopathologic criteria govern reporting. Many reported cases may have been simple fat prolapse.

A lipoma by definition should exist as an independent mass within the orbit, and growth would displace rather than insinuate into other soft tissues. A few cases of orbital spindle cell lipoma have been documented, and proptosis has been reported with disseminated benign lipomas of lipomatosis. Clinically, lipomas develop slowly without infiltration, and at surgery appear circumscribed and slightly more yellow than normal orbital fat. Because of their circumscription, lipomas can be treated by simple excision. They may be hyperintense on T1-weighted MRI studies.

Liposarcoma

Liposarcoma is the most common soft tissue sarcoma of adult life (16% to 18%); however, it is distinctly rare in the orbit. Only 1% of liposarcomas occur in the face; the overwhelming majority are retroperitoneal or involve the thigh. It is believed to develop from undifferentiated mesenchyme and not primarily from fat. There are four histologic types: well-differentiated, myxoid, round cell, and pleomorphic liposarcoma. Overall, prognosis is largely related to size and site of the initial lesion and to pathologic type and grade. The pleomorphic and round cell variants are more locally aggressive and likely to metastasize.

In the orbit, liposarcomas have usually presented as slowly developing mass lesions and were often difficult to diagnose from a clinical and pathological viewpoint. Central to the pathologic diagnosis is the demonstration of lipoblasts, which may vary in appearance from bloated, vacuolated cells to signet ring or round cells with lesser amounts of fat. In the orbit, most cases have been lower-grade, either well-differentiated or myxoid liposarcomas. A preoperative diagnosis is unlikely and is compounded by the possibility that these lesions may be quite circumscribed in appearance and cause little orbital dysfunction. On CT scanning, they appear cystic due to the fat content, which may be confirmed as hyperintense on T1-weighted MR imaging.

Management is governed by the location and possible circumscription of the tumor. Most are infiltrative and should be treated by radical excision, which usually implies exenteration. Some circumscribed and low-grade tumors have been successfully excised. Elsewhere, liposarcomas have been regarded as radiosensitive and in selected cases, adjunctive radiotherapy has been advocated. Metastatic liposarcoma can occur and we have seen one case. We have encountered two primary liposarcomas. The first was a very slow-growing, myxoid liposarcoma that progressed over an 8-year period and was originally mistaken for a neurofibroma (Fig. 9-57). The CT scan showed low-density (fat) infiltrations of the lateral rectus muscle with extension of the lesion into the adjacent fat. The patient underwent exenteration without recurrence of disease over 5 years of follow-up. The second case of liposarcoma was seen in an adolescent with a rapidly developing, malignant, myxoid lesion. The patient underwent exenteration and has been disease free for 9 years of follow-up (Fig. 9-58).

Fibrous Tissue Tumors

Although fibrous tissue tumors constitute an important aspect of the soft tissue lesion systemically, a limited number of them affect the orbit.

Fibroma

Fibroma is the least common and most differentiated fibrous tissue tumor of the orbit. In fact, the diagnosis in a modern setting is of questionable validity and this lesion may be of historical significance only. It has been characterized as a clinically slow, noninfiltrative mass most commonly seen in men and in the medial orbit. Histologically, it is a paucicellular lesion with dense interwoven collagen bundles and few vessels with no evidence of inflammation. There may be areas that are more loosely arranged and some slightly more cellular foci. The major histologic differential diagnosis is keloid or severe fibrosis following orbital inflammatory disorders, or sclerosing inflammation of the orbit. They are relatively well circumscribed and dense. Treatment is by excision, and they recur if removal is incomplete.

Nodular Fasciitis

Nodular fasciitis is one of the most common fibrous tumors in the body, usually involving the upper limb and trunk and presenting as a rapidly developing (weeks to months), tender, solitary mass in young adults. Head and neck lesions are rare and generally occur in children. In the orbital region, it usually affects the adnexa or conjunctiva. Orbital occurrence is rare and usually anterior, where it grows over months and may be tender.

Grossly, they are nodular or well-circumscribed lesions. Histologically, there is a richly cellular, loosely arranged, reactive process. The basic cell population is a plump myofibroblast with a stellate appearance (resembling fibroblasts

in tissue culture). Nodular fasciitis may be more cellular and less differentiated, and the diagnosis is based more on the architecture of the lesion, which often has central necrosis and peripheral “reactive” features. Myxoid areas and mitoses are noted, and account for the frequent confusion with fibrosarcoma. However, nodular fasciitis is less cellular, and has better differentiated cells and normal mitotic figures. More ancient lesions may have foci of collagen deposition. Treatment is by complete excision with an overall recurrence rate of 1% to 2%.

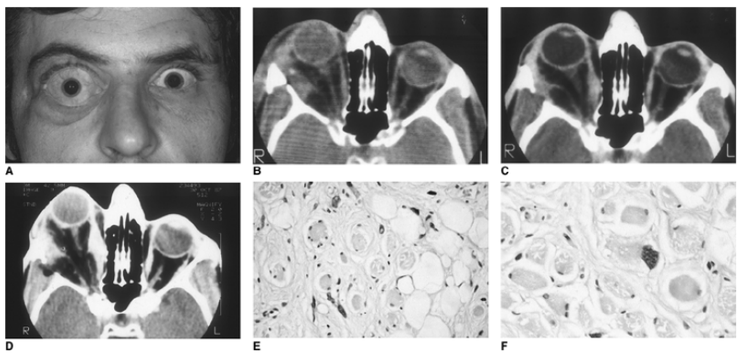

Figure 9-57. (A) This 34-year-old man (shown here in 1987) had a 7-year history of slowly progressive proptosis. In 1982, his CT scan (B) demonstrated a thickened lateral rectus muscle with radiolucencies, and an orbitotomy at that time revealed a 40 × 20 × 8 mm lobulated, rubbery, yellowish mass that infiltrated adjacent tissues. He was diagnosed as a lipoma versus neurofibroma with lipomatous degeneration. A repeat scan 1 year later (C), by which time he had 12 mm of proptosis, demonstrated an increased area of low density in the lateral rectus muscle. At this point, the patient still had 20/20 vision and only slight restriction of movement. He was followed until late 1986 when he had 15 mm of proptosis. A CT scan (D) done at that time demonstrated extension of the low-density area through the orbitotomy defect and involvement of the medial rectus muscle. A review of the original biopsy slides led to the diagnosis of liposarcoma and an exenteration was performed. He is alive and well with 5 years follow-up. (E, F) Histopathologically, his tumor was a myxoid liposarcoma with large lipoblasts infiltrating the deeper orbit and muscle (H&E, original magnifications; E × 25, F × 40). (Figs. 9-57B and C reproduced with permission from Jakobiec FA, Rini F, Char D, Orcutt J, Rootman J, Baylis H, Flanagan J. Primary liposarcoma of the orbit: problems in the diagnosis and management of five cases. Ophthalmology 1989;96:180-91.)

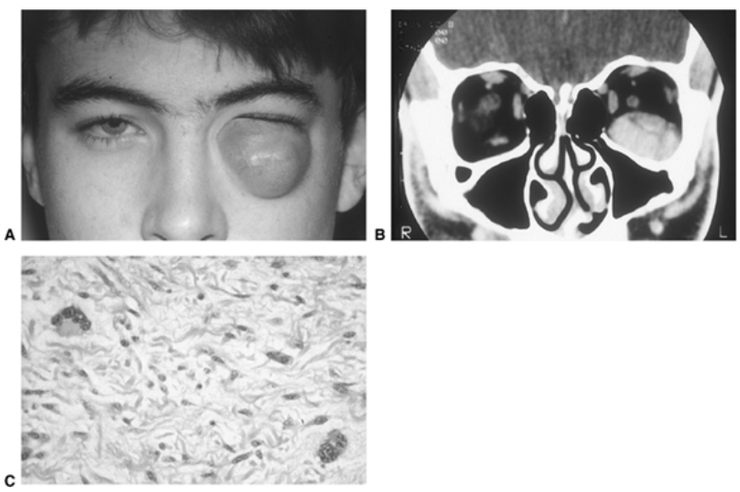

Figure 9-58. (A) This 18-year-old boy presented with a 3-month history of progressive proptosis and upward displacement of the left eye, and the development of a large, rubbery mass in the lower lid. (B) On CT scan, the mass was relatively well defined and extended to the deep orbit, obliterating the inferior structures. Biopsy led to a diagnosis of malignant sarcoma, and an exenteration with frozen control was performed. (C) The mass was seen to originate from the inferior rectus and diagnosed as a dedifferentiated liposarcoma (H&E, original magnification × 40). The patient is alive and well with no recurrence at 9 years follow-up.

Fibromatosis

Fibromatoses are a complicated group of fibrous soft tissue lesions that primarily affect the musculoaponeurotic tissues; they are distinctly rare in the head. Their biologic behavior places them clinically and histopathologically between benign fibrous lesions and fibrosarcoma. Many subtypes have been defined based on sites of occurrence and histopathology. Overall, because they are locally infiltrative and often rapidly growing, distinction from fibrosarcoma may be difficult; however, they are generally less cellular and have focal maturation and collagenization, none or few mitotic figures, and benign-appearing fibroblasts.

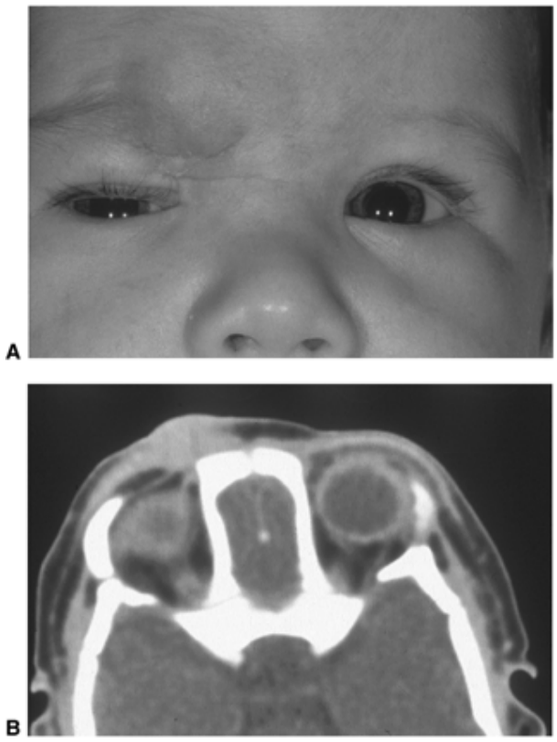

Figure 9-59. (A, B), This 3-month-old boy was born with an infiltration that caused thickening and deformity of the right upper lid and glabellar region. On biopsy, it proved to be a childhood fibromatosis. (Photos courtesy of Jeffrey A. Nerad, MD.)

The most common type affecting the orbit are the extra-abdominal variants of deep (musculoaponeurotic) fibromatoses. They may develop rapidly and involve the orbit by contiguity or as a primary site. Histologically, they are poorly circumscribed and made up of slender, spindle-shaped, uniform cells with abundant collagen.

Fibromatosis occurs twice as often in men and is more frequent in childhood. There are some differences based on age, with certain types characteristically occurring in childhood and infancy, including the infantile form of deep fibromatosis (desmoid type) and infantile myofibromatosis (congenital generalized fibromatosis). The infantile fibromatosis behaves in a fashion similar to the deep fibromatosis of the adult, but may be more rapid in development (Fig. 9-59). In the orbit, they tend to occur inferiorly and may invade from sinuses secondarily. Clinically, they may have overlying inflammatory features. Histopathologically, they are made up of well-differentiated fibroblasts with a varying spectrum of maturity from primitive to more mature-appearing fibroblasts. The infantile myofibromatosis is most often multiple, with a tendency to local aggressiveness and recurrence. These usually have a benign course and tend to regress unless they involve vital viscera. Half the cases are solitary, whereas the remainder have multiple or generalized lesions. The histologic spectrum ranges from dense collagenous to more cellular lesions. Microscopically, the lesions resemble smooth muscle tissue whilst electron-microscopically, they consist of an admixture of fibroblasts and myofibroblasts containing intracytoplasmic myofilaments.

Treatment of the fibromatoses is wide surgical excision because of a high rate of recurrence. Adjunctive radiotherapy has been recommended but carries a risk of sarcomatous degeneration. In addition, radiotherapy may be of limited use and its main value may be to cause cessation of growth. Steroids may be helpful in slowing the growth of these lesions. In instances where the pathology is more aggressive, these are best thought of as low-grade fibrosarcomas. Spontaneous regression and maturation of fibromatoses may occur.

Fibrosarcoma

Fibrosarcoma has been over-diagnosed in the past, resulting in an exaggerated incidence. The introduction of new concepts and terminology such as malignant fibrous histiocytoma, fibromatoses, and numerous other spindle cell tumors has made it an uncommon lesion. Occurrence in the head and neck is distinctly rare other than in the nasal cavity.

The orbit may be involved primarily or by contiguity. When they occur in the orbit, fibrosarcomas tend to have a relatively short history measured in months. Although some may be circumscribed, they usually are infiltrative and insinuate themselves posteriorly, engulfing adjacent structures, and causing functional deficits. They may occur anywhere in the orbit and when primary in that site, they are more common in the elderly.

Microscopically, these neoplasms are made up of interwoven, fasciculated, densely packed, parallel, spindle cells. The degree of differentiation varies and correlates with both local aggressiveness and a tendency to metastases. Secondary histopathologic features may occur, such as osseous and cartilaginous metaplasia as well as mucoid deposition. These secondary features were more commonly reported in the older literature, and when present should invoke the possibility of a malignant fibrous histiocytoma rather then fibrosarcoma. Although the smaller tumors are grossly circumscribed, they often have satellite lesions accounting for recurrence after apparent total excision.

Fibrosarcomas are locally aggressive lesions. They are commonly incompletely removed and tend to be clinically more aggressive following recurrence. The greater the degree of differentiation, the slower the clinical development. In any site, a 50% recurrence rate is not uncommon and can be greatly reduced by radical excision. Both patients and surgeons are less inclined to radical therapy when this lesion occurs in the orbit, making recurrence, extension, and metastases common. Exenteration or wide local excision with margins is the recommended therapy.

Postirradiation fibrosarcomas may arise in the soft tissues or bone of the orbit, particularly as second tumors in patients with the genomic mutation of retinoblastoma (Fig. 9-60). In this circumstance, fibrosarcoma is second only to osteogenic sarcoma in incidence. These second tumors usually occur in patients who have been irradiated, but they may also appear de novo in this group. Postirradiation fibrosarcomas tend to be histologically more bizarre and aggressive.

Solitary Fibrous Tumor

Since the early 1990s, solitary fibrous tumors have been recognized in the orbit. It was first noted in the pleura and has a fibroblastic phenotype (vimentin positive), but it is CD34 positive in contrast to fibrous histiocytoma, which is its main histopathologic differential diagnosis. In the orbit, they have been described in all age groups where they characteristically present as well-circumscribed but not encapsulated lesions, thus they have a tendency to recur if not completely excised. Histologically, they consist of haphazard bundles of spindle cells with scant cytoplasm admixed with dense hypocellular collagenous areas. They have a characteristic imaging feature on MR of heterogeneity and low T2 signal intensity (Fig. 9-61).

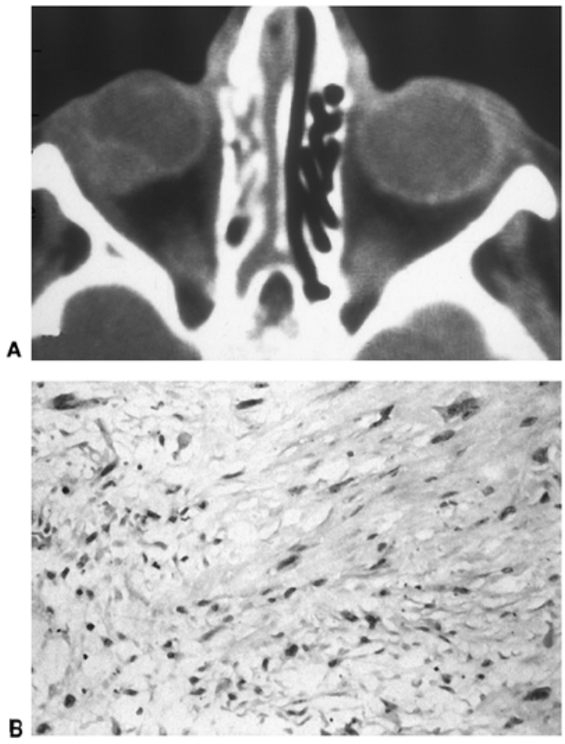

Figure 9-60. (A) This posterior scleral lesion occurred in the right eye of a child born with bilateral retinoblastoma, which had been treated with external beam radiotherapy. The scleral lesion occurred 4 years after treatment and was diagnosed as a malignant fibrosarcoma (B) (H&E, original magnification × 10). He underwent exenteration of the right orbit and is alive well 13 years later.

Epithelioid Sarcoma

Epithelioid sarcoma with both epithelial and mesenchymal features is a rare, aggressive malignancy that commonly affects the tendon sheath. We have described one of the first cases in the orbit where they behave in an infiltrative and aggressive fashion. Histopathologically, they are made up of epithelial-appearing cells with areas of collagen deposition and necrosis, and with very irregular infiltrating margins (Fig. 9-62). In one instance noted in the literature, the patient had multiple recurrences and died of hepatic metastases.

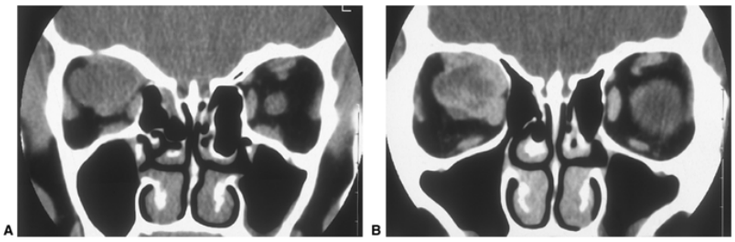

Figure 9-61. This 3 cm × 2 cm relatively well defined orbital mass occurred in a 42-year-old man with slowly developing proptosis. It was heterogeneous (A) with areas of low attenuation and some slight peripheral enhancement (B). It proved histologically to be a solitary fibrous tumor.

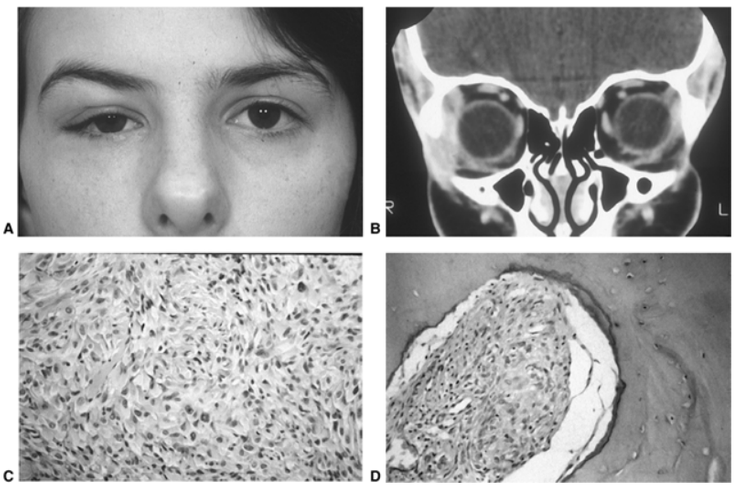

Figure 9-62. This 17-year-old woman presented with a 9-month history of a growth in the right lateral orbit, which extended over the rim. (A) On physical examination, there was a very firm, immobile, bilobed mass that extended from the rim and adjacent orbit inferolaterally to the superolateral orbit, producing an S-shaped deformity of the lid. Exophthalmometry measurements were 15 mm bilaterally, and her ocular movements were normal. (B) The CT scan demonstrated a homogeneous mass infiltrating the lateral orbit. (C, D) The lesion was biopsied and consisted of a homogeneous population of plump spindle to polygonally-shaped cells within the nodular lesion (H&E, original magnifications; C × 25, D × 10). There were areas of frank necrosis surrounded by tumor cells, which had pleomorphic vesicular nuclei and occasional small nucleoli. The cytoplasms of some cells was densely eosinophilic. The tumor was markedly positive for vimentin and focally positive for keratin epithelial membrane antigen and neuron-specific enolase. It was negative for desmin, HMB-45, *Ulex europaeus*, leukocyte common antigen, chromogranin, neurofilament, or myoglobulin. The case was reviewed by Dr. Sharon Weiss, who confirmed the diagnosis of epithelioid sarcoma. The patient underwent an exenteration including the lateral and superolateral orbital wall, which demonstrated invasion of the tumor into the bone. The patient is alive and well 8 years following exenteration. (Fig. 9-62B reproduced with permission from White VA, Heathcote JG, Hurwitz JJ, et al. Epithelioid sarcoma of the orbit. Ophthalmology 1994;101:1680-7.)

Congenital and Infantile Fibrosarcoma

Congenital and infantile fibrosarcoma is a rare, rapidly growing sarcoma with a low incidence of metastasis (0% to 8%). Histologically, the tumor is composed of uniform spindle cells arranged in interwoven bundles and the more differentiated lesions show a characteristic herringbone pattern. Electron-microscopy has shown that the cells are embryonic fibroblasts that contain electron-dense material (Fig. 9-63). Overall, these tumors have a considerably better prognosis than the adult counterpart, and treatment is by radical local excision. We have had a single case of a metastasis of a congenital fibrosarcoma to the globe with extension posteriorly into the orbit. The patient was exenterated following an enucleation, and has had no recurrence for 5 years.

Myxoma

The diagnosis of myxoma in the orbit and elsewhere in the body is complicated by the large number of soft tissue tumors that can have a myxoid appearance. Malignant myxoid lesions must be ruled out, including malignant fibrous histiocytoma, liposarcoma, myxosarcoma, and rarely rhabdomyosarcoma, chondrosarcoma, peripheral nerve sheath tumor, and hemangiopericytoma. Careful analysis of the entire specimen is necessary to substantiate this diagnosis. True orbital myxomas are exceedingly rare, and the few that have been described have been characterized by a clinical picture of indolence and noninfiltrative features despite the lack of a true capsule. This probably reflects on the soft consistency of the tumor. They more commonly occur subconjunctivally. Histologically, it is made up of a population of stellate or spindle cells dispersed in a rich mucinous matrix of hyaluronic acid derived from altered fibroblasts. At the time of surgery, these lesions are apparently indistinctly separated from adjacent tissues, which accounts for a significant risk of recurrence.

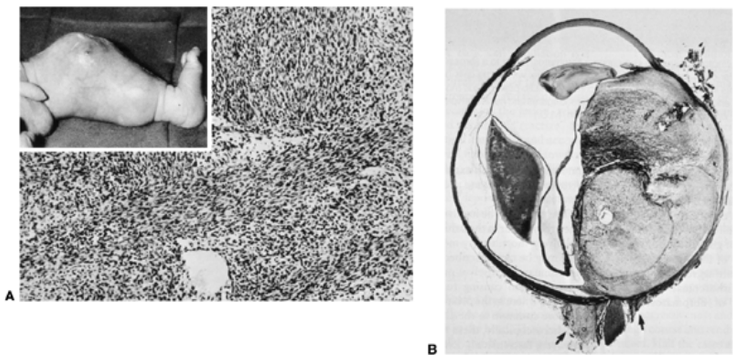

Figure 9-63. (A) Low-power photomicrograph of a primary congenital fibrosarcoma of the leg (A, inset) that occurred at birth. Note the dense zones of interwoven bundles of spindle cells (H&E, original magnification × 10). (B) Gross specimen of globe enucleated 2 years after the primary tumor. There was a uveal metastasis with a temporal serous detachment and orbital extension of the tumor around the optic nerve (arrows) (H&E, original magnification × 2).

Giant Cell Angiofibroma

Giant cell angiofibroma is a rare occurrence in the orbit. It usually arises anteriorly or in the eyelid, particularly in the superolateral orbit where it appears as a palpable mass. Rarely, it leads to proptosis or diplopia. Histopathologically, giant cell angiofibromas consist of a spindle cell tumor with a network of vessels and a background of giant cells within the stroma and the blood vessel linings. The differential diagnosis includes solitary fibrous tumor, hemangiopericytoma, and giant cell fibroblastoma of soft tissue. These tumors are best treated by surgical excision and may recur locally.

Dermatofibroma Protuberans

Although a common lesion, particularly occurring subcutaneously throughout the body, dermatofibrosarcoma protuberans has been rarely described in the orbit. It has a propensity to invade adjacent tissues and recur. We have experienced a single case of this lesion arising subcutaneously in the superomedial eyelid. The lesion was found to extend into the orbit in the trochlear region, and was removed using Mohs' surgery followed by radiotherapy. It has not recurred over 7 years' of follow-up.

Histiocytic Tumors

Fibrous Histiocytoma

Fibrous histiocytomas are mesenchymal tumors that involve fascia, muscle, and soft tissues of the body. They were first well described in the 1960s, and the orbit was identified as site of predilection by Zimmerman in 1967. In fact, fibrous histiocytoma is the most common adult mesenchymal tumor of the orbit.

It is seen in middle adult life, with equal occurrence in males and females. The most common location is the upper nasal quadrant. Most are slow-growing, relatively firm masses but more aggressive growth may be noted. The major presenting clinical signs are proptosis, mass effect with decreased vision, and less frequently diplopia, pain, lid swelling, tearing, ptosis, and restriction of extraocular movements.

This neoplasm is usually characterized by infiltrative features with a tendency to local recurrence and very rare metastases. The specific biology parallels the underlying histopathology such that the slower growing, less bulky tumors reflect a benign variant and the faster growing, locally aggressive large tumors a malignant variant. Between the two is an intermediate group that is characterized primarily by locally aggressive behavior. Thus, duration of symptoms, size, frequency and rapidity of local recurrence, and tendency to metastatic or widespread local aggressive behavior parallels the underlying histopathologic characteristics.

These tumors are made up of fibrous-appearing histiocytic cells that tend to form a characteristic cartwheel or storiform pattern. The benign type is the most common; histologically, it is well circumscribed or has a fine capsule and is made up of benign-looking histiocytic cells with occasional well-differentiated multinucleated histiocytes (Fig. 9-64). Necrosis and mitoses are not major features. A more cellular subtype has been noted within the benign group. The locally aggressive or intermediate fibrous histiocytoma is characterized by increased cellularity without significant pleomorphism and an infiltrating margin. Mitotic figures are generally few and typical in appearance. Both the benign and the intermediate group may have areas with myxoid patterns (Fig. 9-65), and about one third of the tumors show marked vascularity. The least frequent variant is the malignant fibrous histiocytoma, which has the hallmarks of malignancy including necrosis, mitotic activity with abnormal mitoses, tumor giant cells, and pleomorphism (Figs. 9-66 and 9-67). The cellular pattern may be either storiform, pleomorphic, or myxoid. Some of the cells may be vacuolated and contain fat, and the myxoid areas contain acid mucopolysaccharide sensitive to hyaluronidase.

Management of fibrous histiocytoma is essentially surgical and should be aimed at complete resection of local disease to prevent recurrence, since there is some potential (particularly in the intermediate group) to undergo malignant transformation on recurrence. Usually this can be accomplished by removal of the tumor alone. However, widespread tumor infiltration may require more radical exenteration of tissues. The majority of tumors will fall into the benign and intermediate groups, and recurrences from the intermediate

group tend to occur over relatively long periods of time. The management of recurrences should be governed by the biological behavior (i.e., the more rapidly occurring should be treated more aggressively). Radiotherapy is of no benefit and chemotherapy has not been assessed.

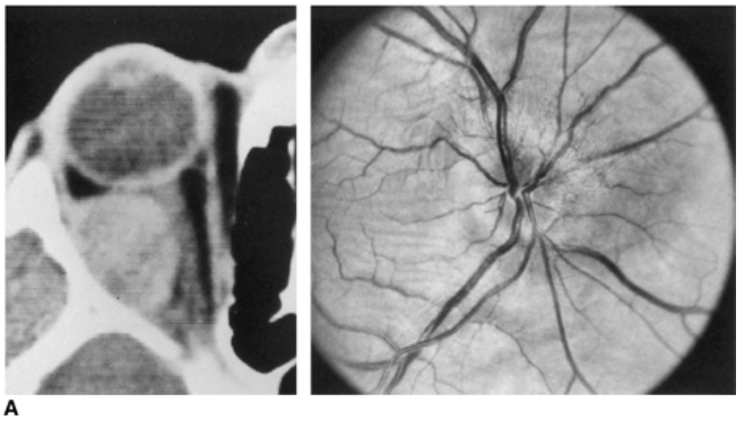

Figure 9-64. CT scan (A, left) and retinal photograph (A, right) of a 38-year-old man who had a history of decreasing vision on the right side for 6 months. He had noted increasing prominence of the eye for 6 weeks. The vision was reduced to 20/70 and there was 5 mm of proptosis. The fundus demonstrates nasal choroidal folds and elevation of the superior margin of the disk. The axial CT scan shows a well-circumscribed homogeneous lateral orbital mass that displaces the optic nerve medially. The patient is well with no recurrence 6 years after removal of the tumor. Diagnosis was confirmed with electron microscopy and on review by Dr. Ramon Font.

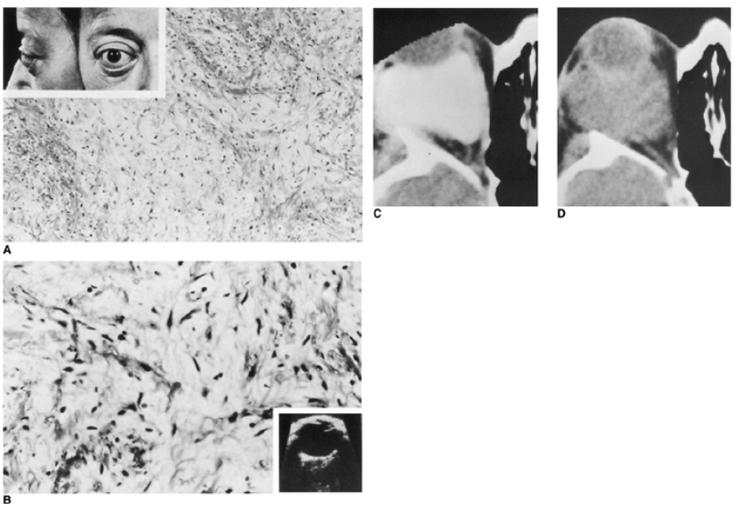

Figure 9-65. (A, B) This 38-year-old woman presented 9 years following removal of a intermediate fibrous histiocytoma that had a myxoid stroma with stellate fibrous histiocytic cells (H&E, original magnifications; A × 10, B × 25). The axial, noncontrasted (C) and contrasted (D) CT scans demonstrated an uniformly enhancing, sharply demarcated retrobulbar mass molding to the shape of the globe, sparing the apex, and herniating through the previous lateral orbitotomy defect. Ultrasonography (B, inset) revealed a somewhat irregular mass directly behind the globe with marked sound wave attenuation. This mass was excised without recurrence over 1 year.

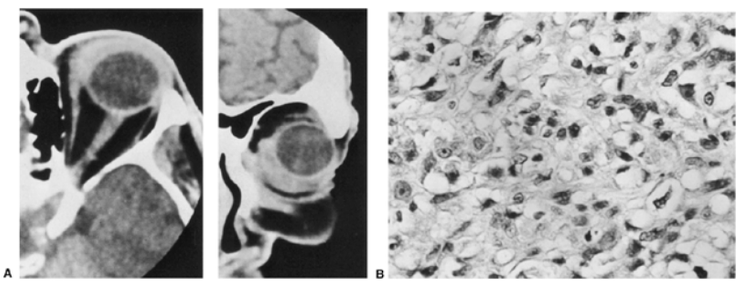

Figure 9-66. (A) Axial and coronal CT scans of a left orbit demonstrate a well-defined soft tissue mass on the anterior, inferior, and medial portions of the globe extending into the medial and inferior rectus muscles. The patient was a 64-year-old farmer who had been aware of increasing left ocular irritation and a “growth” on his sclera. He had been treated 5 years earlier with chemotherapy and prophylactic central nervous system irradiation for a diffuse, poorly differentiated lymphocytic lymphoma involving the cervical nodes, pleura, and lung. (B) Biopsy revealed a malignant spindle-cell soft tissue tumor. Note the sworling arrangement of anaplastic cells in a collagen matrix. The cytoplasm of the fibrous histiocytes is slightly foamy (H&E, original magnification × 40). The histopathologic features are consistent with the diagnosis of malignant fibrous histiocytoma.

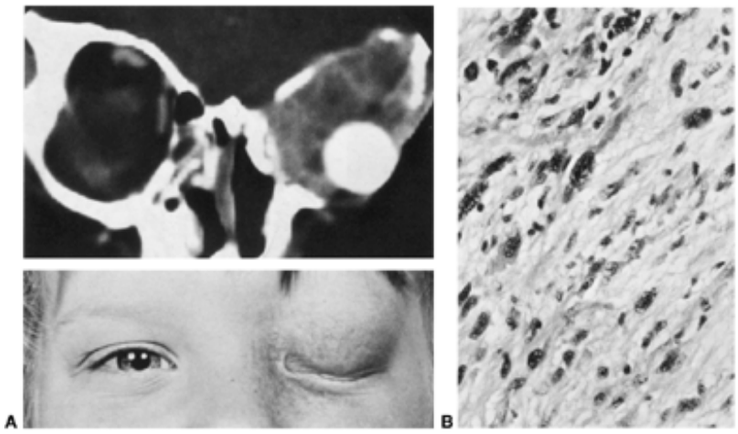

Figure 9-67. (A, bottom) A 6-year-old boy presented with progressive displacement of the implant in his anophthalmic left orbit. He had been treated 3 years earlier for a retinoblastoma with extrascleral extension by enucleation and postoperative radiotherapy. (A, top) Coronal CT scan demonstrates a large infiltrating soft tissue mass in the posterior, superior, and medial portion of the orbit with displacement of the prosthesis. Permeative destruction of the orbital roof and medial and lateral orbital walls was present. (B) Histopathology revealed a highly anaplastic spindle cell tumor with some multinucleate cells and considerable pleomorphism. The cytoplasm of the histiocytic cells is slightly foamy. The final diagnosis was a malignant fibrous histiocytoma (H&E, original magnification × 40).

The malignant fibrous histiocytoma in the orbit usually arises de novo. However, there is a group of malignant fibrous histiocytomas that tend to occur following orbital radiotherapy, particularly in children with the genomic mutation of retinoblastoma. We have seen three cases of malignant fibrous histiocytoma, all following radiotherapy in the orbital region. One was in a child with retinoblastoma (Fig. 9-67), and another was in an adult who had been previously treated for lymphoma of the head and neck by radiotherapy and chemotherapy (Fig. 9-66). Our third case was a patient with sino-orbital malignant fibrous histiocytoma 13 years following radiotherapy (Fig. 9-68). In addition to the usual sites of orbital occurrence, fibrous histiocytoma has been described in the lacrimal sac.

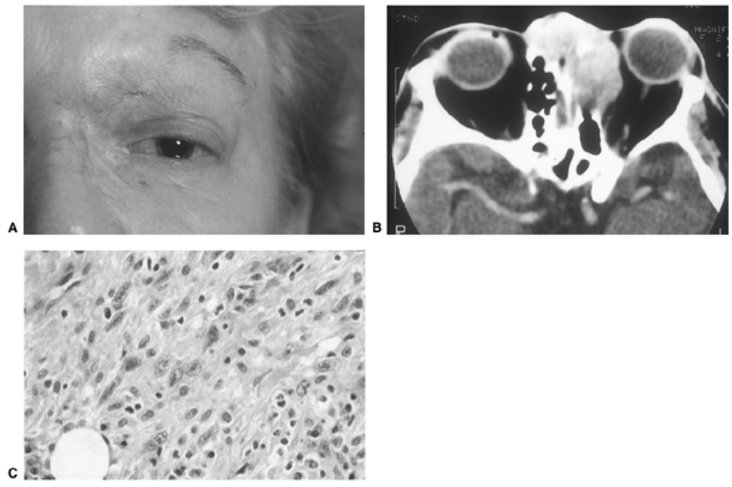

Figure 9-68. (A) This 63-year-old woman developed a shiny, firm area in the superomedial lid and forehead with loss of adjacent brow and downward, inward displacement of the globe. She had had a squamous cell carcinoma of her nose, which had been excised but recurred in the inner canthal region, where it was treated following surgery with radiotherapy 15 years earlier. (B) On CT scan, she demonstrates an invasive lesion destroying the adjacent sinus and base of nose. This proved on biopsy (C) to be a malignant fibrous histiocytoma with large spindle and multinucleate cells. She declined further therapy and died of her lesion 1 year later (H&E, original magnification × 40).

Primary Bone Tumors of the Orbit

Jack Rootman

Dinesh Selva

General Considerations

Primary bone tumors comprise 0.6 to 2% of all tumors of the orbit. Their rarity in conjunction with often similar histology in related lesions has led to poor characterization of this group as a whole. Furthermore, the microscopic and radiologic appearances occasionally differ from that seen in alternate sites. Close cooperation between clinician, radiologist, and histopathologist is a mandatory prelude to accurate diagnosis based on a constellation of all of these features.

Our experience over a 24-year period has yielded 62 cases of primary tumors of the orbital bones (Table 9-9). Fibrous dysplasia and osteoma are the conditions most likely to be encountered in an orbital practice.

The bony lesions can be defined along pathophysiologic lines as dysplastic, reactive, and neoplastic. This simplification allows characterization of each clinically and pathologically. The dysplasias and related fibro-osseous tumefactions include fibrous dysplasia, osteoma, ossifying fibroma, and osteoblastoma, all of which are associated with slowly developing noninfiltrative mass effect with or without facial disfigurement or orbital dystopia. The reactive lesions, on the other hand, include a group of entities with similar behavior and some shared histologic features reflecting their tendency to sudden hemorrhagic episodes. Although several are difficult to define histopathologically, they bear sufficient similarity to blur distinctions between them. They affect adjacent bone and soft tissue structures primarily by displacement. Their major difference from dysplastic lesions is their tendency toward erosion of adjacent bone, loose vascularity, hemorrhage, and local recurrence in some instances. The reactive lesions in our series included reparative granuloma, aneurysmal bone cyst, Brown tumor of hyperparathyroidism, and xanthomatous tumors. In spite of their tendency to involve adjacent bone, all of these displace rather than infiltrate soft tissues; this feature provides a major distinction from the more aggressive malignant lesions.

The neoplasms include many primary tumors, which fall into two broad clinical groups. Both categories produce unrelenting, progressive mass effect; the major difference is the presence or absence of infiltrative features, which reflects biologically more aggressive tumor growth. Neoplasms such as chondrosarcoma and chordoma may be extremely slow growing and noninfiltrative. On the other hand, the more aggressive tumors in orbital bone, such as Ewing's sarcoma, malignant fibrous histiocytoma, osteogenic sarcoma, lymphoma, plasmacytoma, and Langerhans cell histiocytosis, characteristically infiltrate surrounding soft tissue structures, producing restrictive and compressive effects.

Table 9-9. Clinicopathologic classification of primary orbital bone disorders, University of British Columbia Orbital Clinic, 1976-1998

DISORDER	NUMBER OF LESIONS	TOTAL
Benign Fibro-osseous & Cartilaginous Lesions		24
Osteoma	11	
Fibrous dysplasia	11	
Ossifying fibroma	1	
Chondroma	1	
Osteoblastoma	0	
Reactive Bone Lesions		10
Cholesterol granuloma	6	
Aneurysmal bone cyst	2	
Giant cell granuloma	1	
‘Brown tumor’ of hyperparathyroidism	1	
Neoplasms		24
Hematopoietic and histiocytic lesions		
Langerhans' cell histiocytosis	8	
Myeloma	7	
Osteosarcoma	3	
Ewing's sarcoma	3	
Chondrosarcoma	3	
Mesenchymal chondrosarcoma	0	
Giant cell tumor	0	
Vascular		1
Intraosseous hemangioma	1	
Miscellaneous	3	3

From a pathologic point of view, we were struck by the similarities between many of the primary bone tumors rather than their clear-cut differences, particularly between the groups we have classified as dysplasias and reactive tumefactions. Fibrous dysplasia, for example, is defined histologically as foci of osteoid and immature woven bone formation within a fibrous mesodermal matrix. Yet variations in the classical pattern are common, including some osteoblastic rimming, psammomatoid features, foci reflecting recurrent hemorrhage, fibroproliferation, and reparative phenomena. Similarly, reparative granuloma and solid aneurysmal bone cyst are

dominated by reactive fibroplasia with an admixture of giant cells and features of recurrent hemorrhage; however, these lesions are often associated with dysplastic bone formation and, in some respect, reflect features described in fibrous dysplasia. Osteomas also appear to have a spectrum of pathologic findings that relate to fibrous dysplasia. Classically, they are described as solid tumors with compact or cancellous bone formation. However, within osteomas, areas of osteoid, dysgenetic bone, mesodermal fibroplasia, giant cells, and even psammomatoid change may be noted. In many respects, the distinction between dysplasias, osteomas, and reactive lesions may be difficult, and numerous authors have suggested these may be part of a spectrum of dysplastic bone formation. Certainly, the reactive and dysplastic lesions as defined in our series have a fundamental biologic difference from neoplasia; that is, their tendency to remain isolated to bone and not infiltrate soft tissue structures.

Clinical Patterns

There are three clinical patterns of presentation of primary orbital bone tumors.

Slow Progressive Noninfiltrative Mass Effect

The prototypical presentation in this group is that of a benign fibro-osseous lesion, such as an osteoma. Proptosis, globe displacement, and deformity are the most common manifestations with the temporal course being measured in years. Any functional deficits such as decreased vision or diplopia are due purely to mechanical or compressive effects.

Subacute Mass Effect ± Sudden Soft Tissue Displacement

The reactive lesions of bone, such as aneurysmal bone cyst, giant cell granuloma, and cholesterol granuloma, often fall within this category. The evolution of the mass effect in these cases is usually weeks to months, but can extend to years. In addition, they may be subject to intralesional hemorrhage, leading to sudden proptosis or displacement.

Relentless Progression of Mass Effect ± Infiltrative Features

Neoplasia, such as osteosarcoma, Ewing's sarcoma, myeloma and chondrosarcoma, frequently present in this manner. The acuity of onset, with the exception of chondrosarcoma, is somewhat quicker than in than in the first category and signs of infiltration, such as significant pain, decreased vision, or restriction of ocular movement, may be present.

Clinicopathological Classification of Major Orbital Bone Tumors

The clinical patterns detailed above correlate reasonably well with the clinicopathologic classification outlined in Table 9-9 and detailed below.

Benign Fibro-osseous and Cartilaginous Lesions

Osteoma

A true osteoma is a tumorlike mass of bony tissue that is histologically similar to normal bone. Its pathogenesis remains unclear, though traumatic, infective or hamartomatous theories have been proposed. Others have suggested that they arise exclusively at the junction of bones of cartilaginous and membranous origin. None of these theories satisfactorily account for the facts.

The most common sites of origin are the paranasal sinuses, skull, and facial bone. The fact that osteomas were found in 0.42% (15 out of 3510) of plain sinus radiographs reflects their prevalence. Within the sinuses, 50% occur in the frontal sinus with the ethmoid, maxillary, and sphenoid involved in descending order of frequency. Most orbital osteomas are secondary invaders from adjacent sinuses, though on occasion may arise primarily within the orbit. In contrast to the sinus distribution, however, we and others have noted that orbital osteomas appear to have a roughly equal origin from the ethmoid (Fig. 9-69), frontoethmoid, or frontal regions. This perhaps reflects the relatively thin barrier to expansion of the medial orbital wall.

The age range of cases runs the gamut from 10 to 82 years with the highest prevalence in the fourth and fifth decades. Males and females are represented equally.

Clinical Features

The majority of sinus osteomas are solitary and asymptomatic. However, when large enough to encroach on the orbits, a gradual evolution of proptosis and/or globe displacement over many years can occur. There may be an associated headache due to expansion of overlying cortex and periosteum, and a bony mass is often palpable in the superior or superomedial orbit. Obstruction of the sinus ostia may lead

to chronic sinusitis or mucocele, particularly as we have noted in frontal or frontoethmoid lesions (Fig. 9-70). Features reported more rarely include an acquired Brown syndrome, gaze-evoked amaurosis or pain, subluxation of the eye and erosion leading to orbital emphysema, or cerebral spinal fluid rhinorrhea. The sphenoid sinus, though a rare site, has significance as even a small lesion may lead to an orbital apex syndrome.

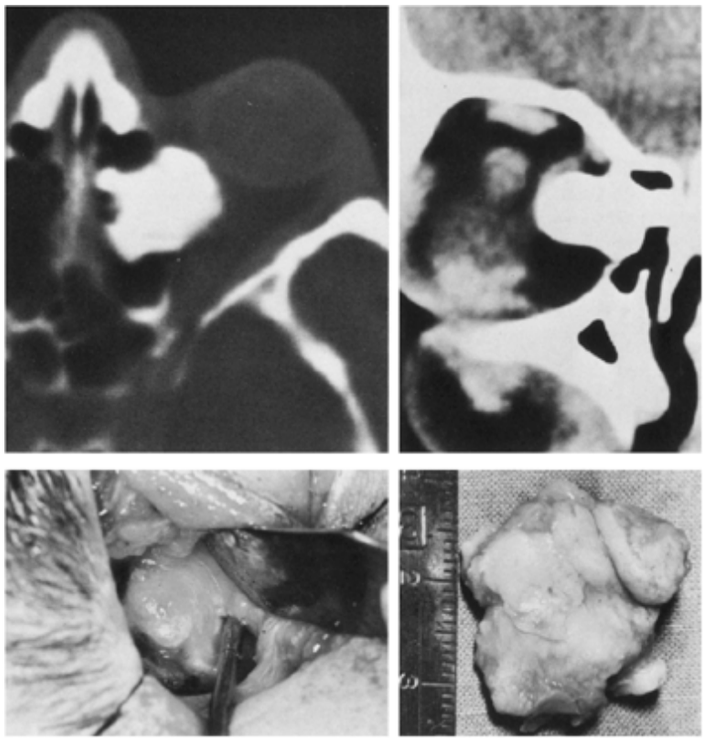

Figure 9-69. Axial (top left) and coronal (top right) CT scans show a compact (ivory) osteoma involving the left ethmoid sinus (axial scan reversed) and extending into the orbit with displacement of the medial rectus muscle. This 23-year-old man had suffered two episodes of subluxation of the globe in a 12-month period. Ocular function was within normal limits aside from proptosis and lateral displacement. He underwent an anterior orbitotomy with excision of a well-defined bosselated osteoma (bottom left and right), and has had normal follow-up examinations over a 2-year period.

An uncommon but important systemic association is Gardner's syndrome. This autosomal dominant syndrome of osteomas, soft tissue tumors, and peripheral congenital retinal pigment epithelial hypertrophy also includes the development of colonic polyposis with subsequent malignant transformation. One should note in this context that multiple osteomas are frequent. Our patient with Gardner's had only a single tumor in the sinuses but an additional one was noted on a skull CT scan. Furthermore, as bony lesions may predate the colonic pathology, patients with osteoma warrant a dilated fundoscopy and referral to a gastroenterologist.

Imaging

The plain X-ray and CT appearances consist of an osteoblastic round or ovoid, sharply circumscribed mass, usually arising in the sinus and invading the orbit. Tumors growing within a sinus conform to its internal contour and often have a bosselated surface. Osteomas may be sessile or pedunculated and generally have a diameter between 1 to 5 cm. Bone settings on CT imaging often show a very dense periphery with a more cancellous internal structure (Fig. 9-71). However, the relative proportions of the two densities may vary with the size of the lesion.

Histopathology

It is important to distinguish osteomas from reactive osteomatous responses to infection, trauma, and chronic inflammation. The clinical and radiological appearances are often invaluable in this regard.

Macroscopically, true osteomas have smooth or bosselated contours with glistening white or pinkish coloration. A covering of mucoperiosteum or periorbita may be seen, depending on the site of origin.

They have been classified histologically into three groups depending on the predominant tissue present: compact (cortical, ivory), cancellous (trabecular, spongy), and fibrous. Fu and Perzin have postulated that the histological type is partly dependent on the age of the lesion, with the compact group representing the most mature and the fibrous the least.

The fibrous subtype may, in fact, be part of a continuum incorporating ossifying fibroma and fibrous dysplasia.

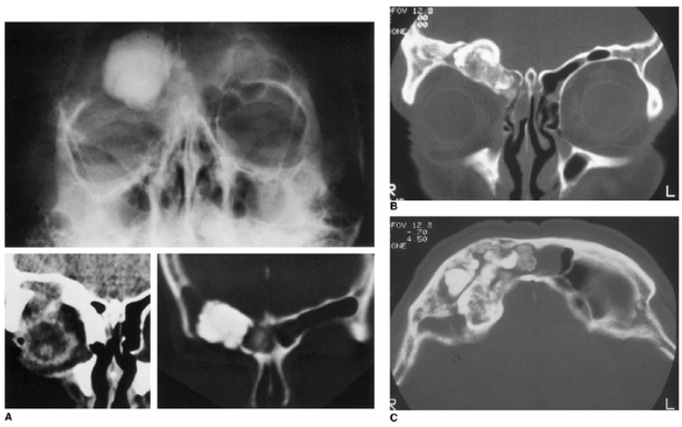

Figure 9-70. Plain film appearance (A, top) of a large ivory osteoma involving the medial portion of the right frontal sinus and ethmoids. This 68-year-old man presented with a 5-month history of right ptosis and paresthesia of the frontal region. In retrospect, he had always noted a drooping right upper lid. On physical examination he had slight restriction of upgaze and 5 mm downward displacement of the globe. Coronal CT scan (A, bottom right) shows a dense bony lesion in the medial portion of the right frontal sinus with a mucocele expanding the lateral portion of the sinus and extending into the orbit through a bony defect (A, bottom left). The osteoma had a bosselated appearance. The mucocele and osteoma were excised by a right frontoethmoidectomy route. Six years later, he developed periorbital and supraorbital nocturnal pressure and pain, and CT scans on bone settings (B, C) demonstrated extensive recurrence of osteoma. This required craniofacial resection and reconstruction.

The compact areas resemble normal cortical bone with dense bony areas and haversian systems. However, there are subtle differences in the arrangement of the haversian canals, which is often evident to the experienced bone pathologist. The cancellous areas consist of anastomosing trabeculae with an intervening fibrovascular stroma. There may also be fatty and hematopoietic elements present in the stroma as well as evidence of osteoblastic activity along the trabeculae. The fibrous region is made up primarily of loose fibrovascular tissue with a few irregular bony trabeculae and osteoid elements.

In our series of nine surgically treated cases, we noted that while the three types of tissue were present in varying admixtures, in all cases there was a remarkably consistent pattern of arrangement. The most peripheral zone was comprised of compact bone; however, moving toward the center or base of the lesion, there was an intermediate zone of increased osteoblastic activity, osteoid, and vascularity. The innermost region consisted of a loose fibrous stroma with a greater number of blood vessels, few trabeculae, and many plump osteoblasts (Figs. 9-71B and C). This configuration has been described previously by Albert et al. and is illustrative of the growth of these lesions.

The outermost zone presumably represents more mature bone and the activity seen centrally suggests that this is where growth is initiated. This implies that extirpation of the central region is probably required to prevent recurrence. It may also explain why leaving residual peripheral areas does not usually lead to regrowth. Finally, the histological subtyping into compact, cancellous, and fibrous lesions probably has little practical significance as there appears to be no correlation with the clinical course.

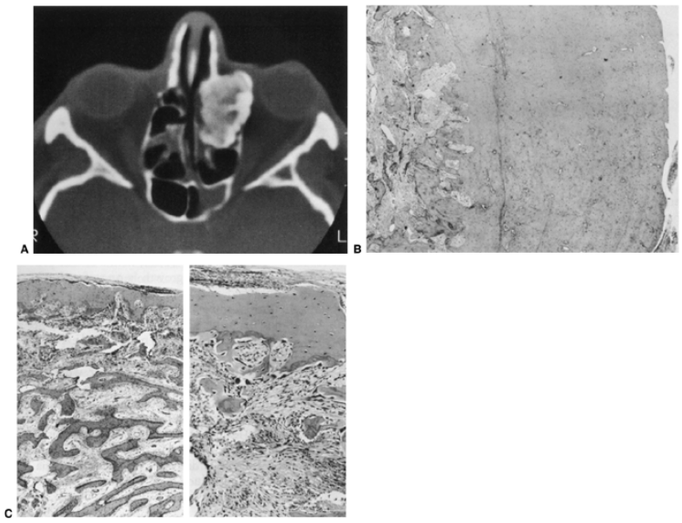

Figure 9-71. The CT appearance of a mass in the anterior ethmoid complex in a 32-year-old man who presented with a 3-month history of painful left proptosis. In retrospect, the proptosis had been noted for 10 years. Vision was 20/70 OS, and remaining ocular functions were normal. The mass shown on bone settings had a dense cortex with a more lucent central component. The patient underwent ethmoidectomy for removal of the tumor affecting the anterior ethmoids and frontoethmoid canal. The mass was removed piecemeal by coring the central portion out and collapsing the walls. (B) The histopathology of the dense portion of this osteoma shows thick bone with a haversian system and a more fibrous trabecular core (H&E, original magnification × 2.5). (C) A portion of the mass with a more trabecular appearance and a vascular stromal component is shown (C, left). Note osteoblasts lining the bony trabeculae (H&E, original magnifications; left × 2.5, right × 10).

Management

Generally, asymptomatic osteomas can be treated conservatively. The only possible exception to this is in the sphenoid sinus, as it is technically easier to remove a small lesion in this location before it has encroached on the orbital apex and optic canal.

If symptomatic and located in the anterior orbit, osteomas can be removed via an anterior orbitotomy. For anterior ethmoid tumors presenting in the superomedial orbit, a modified Lynch incision is often used. Excision can sometimes be aided by coring the lesion and collapsing the cortex for removal. For more posteriorly located tumors involving the roof or cribriform plate, a combined orbitocranial approach via a bicoronal incision is favored. Recurrence is rare, even following a partial resection. We have had only one recurrence (Fig. 9-70).

Fibrous Dysplasia

Fibrous dysplasia is a benign disorder characterized by proliferation of fibrous tissue and osteoid, which replaces and distorts medullary bone. The etiology is unknown though past theories include a maturation arrest at the woven bone stage, or alternatively, hamartomatous proliferation. More recently, the discovery of a postzygotic mutation in the G protein in McCune-Albright syndrome suggests that the bone dysplasia in these patients is a manifestation of a somatic mosaic state.

There are three forms described: monostotic fibrous dysplasia, polyostotic fibrous dysplasia, and McCune-Albright syndrome. Monostotic fibrous dysplasia accounts for 75% to 80% of cases, of which 20% affect the craniofacial bones. In the skull, the frontal bone is most frequently involved, followed by the sphenoid and ethmoid. The majority of those

with orbital involvement have monostotic fibrous dysplasia, though the disease has generally involved contiguous bones at presentation. Polyostotic fibrous dysplasia makes up 20% of all cases and half of these have head and neck involvement. McCune-Albright syndrome occurs largely in females and incorporates the triad of polyostotic fibrous dysplasia, sexual precocity, and cutaneous pigmentation. This pigmentation appears as brown macules, usually six or less in number, with irregular “coast of Maine” borders.

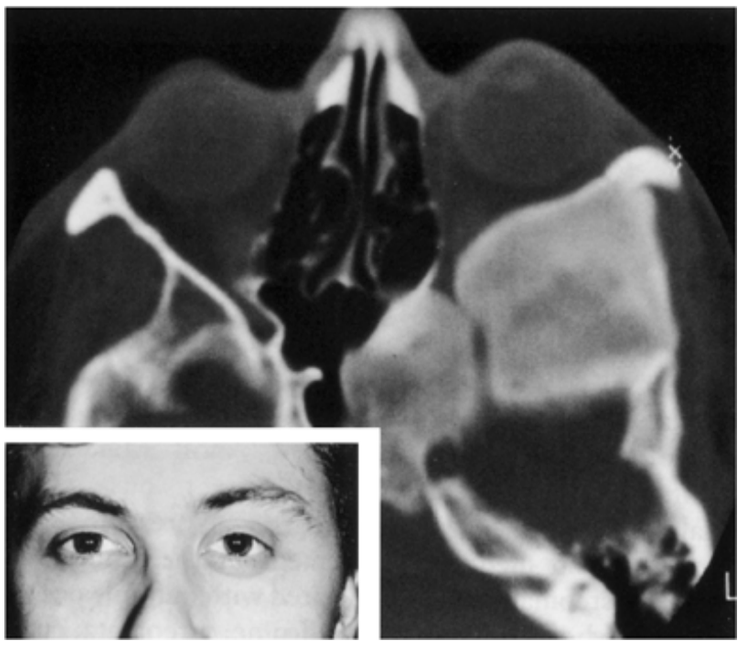

Figure 9-72. A 24-year-old man (inset) presented with an 8-month history of vague aches in the left temporal region. On physical examination, he had completely normal ocular functions with fullness of the left temporalis fossa and proptosis. Retrospective photographic documentation revealed proptosis of 4 years' duration. Axial CT scan on bone settings demonstrates the sclerotic type of fibrous dysplasia involving primarily the sphenoid bone and sinus. No progression was seen after 15 years' of follow-up.

Fibrous dysplasia is generally recognized before the age of 30, though mild or asymptomatic cases may escape detection into late adult life. The gender distribution is roughly equal in monostotic fibrous dysplasia while a female predilection prevails in polyostotic fibrous dysplasia.

Clinical Features

The major clinical signs and symptoms reflect displacement, distortion, and compression of orbital structures, which vary according to site and extent of disease. Facial asymmetry, proptosis, and globe displacement evolving over many years are the most common manifestations (Fig. 9-72). Nasolacrimal duct blockage, diplopia, nasal obstruction, malocclusion, raised intracranial pressure, and cranial nerve palsies also occur. Acute or subacute compressive optic neuropathy can arise due to intralesional hemorrhage, sphenoidal mucocele, or secondary aneurysmal bone cyst (Figs. 9-73 and 9-74). A more chronic visual loss, though less commonly reported, may occur due to compression in the optic canal or at the chiasm (Fig. 9-75). On occasion, a superimposed ischemic neuropathy in the context of chronic compression leads to an acute on chronic deterioration in vision.

This clinical spectrum is reflected in our own experience of ten cases. Changes in facial contour (7/10), proptosis (7/10), globe dystopia (6/10), and decreased vision (3/10) were the major signs. Interestingly, seven patients also had pain either localized to the orbit or described as a diffuse ipsilateral headache.

Overall, the natural history is one of slow growth. Though this was previously thought to cease in adult life, there is evidence that fibrous dysplasia may progress well past the fourth decade.

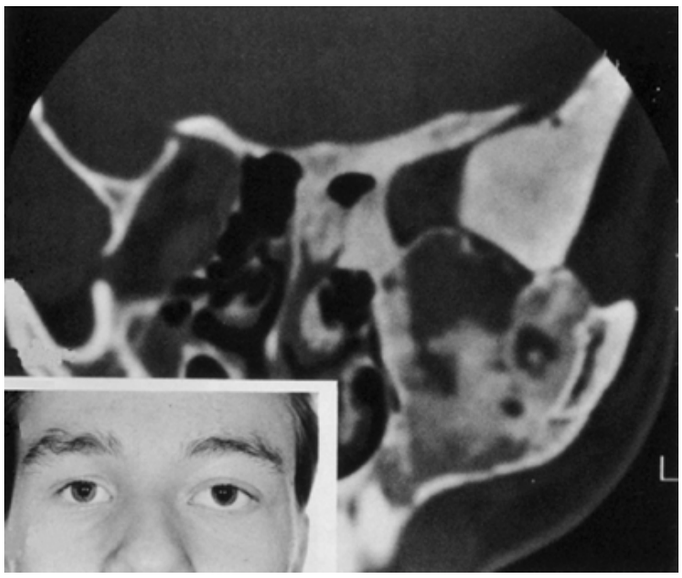

Figure 9-73. This 20-year-old man (inset) presented with a 4-month history of proptosis and 8 months of reduced vision on the left side. On physical examination, his vision was 20/60, and he had left papilledema with a full range of ocular movements, elevation of the left globe, and proptosis. Psychophysical and electrophysiologic functions revealed a field reduction and a delayed VEP. Retrospective study of photographs showed the changes had been present for at least 5 years. The coronal CT scan photographed on bone settings demonstrates both basic patterns of fibrous dysplasia with areas of lucency and sclerosis (pagetoid lesion) involving the maxilla and lesser wing of sphenoid and the ground-glass sclerotic pattern affecting the greater wing of sphenoid. These changes have resulted in compression of the orbital apex. His vision returned to 20/20, and the papilledema had disappeared without recurrence when he was seen at follow-up 18 months later. Systemic investigation revealed fibrous dysplasia involving the rib cage and femur, but normal endocrine function.

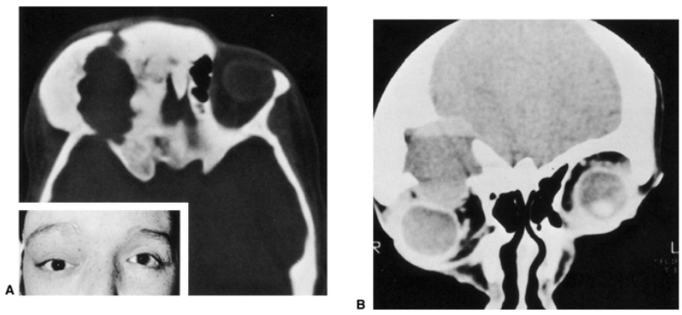

Figure 9-74. (A, inset) This 24-year-old woman with cavitary fibrous dysplasia presented with a 1-month history of right proptosis, visual blurring, and pain following a whiplash injury. Crouzon's disease had been diagnosed 12 years prior to presentation, and she stated that the right side had been abnormal since birth. Vision was 20/60 on the right, with downward and outward displacement of the globe and limitation of upgaze. VEP was delayed because of the optic nerve compression. Axial (A) and coronal (B) CT scans show fibrous dysplasia involving an extensive portion of the frontal and ethmoid bones. In the center of the dysplasia is a large cyst that shows a fluid interface in the coronal scan and indentation of the globe by the portion extending into the orbit. The coronal view was obtained with a “hanging head” position, so the denser dependent blood appears superior on the image. The axial image is photographed to maximize bone detail. The clinical diagnosis was fibrous dysplasia with “aneurysmal bone cyst.” The patient underwent surgical drainage of xanthochromic fluid and debris in the cyst, with removal of the lining and immediately adjacent bone. Her vision returned to 20/20, and there was no recurrence at 6-month follow-up examination.

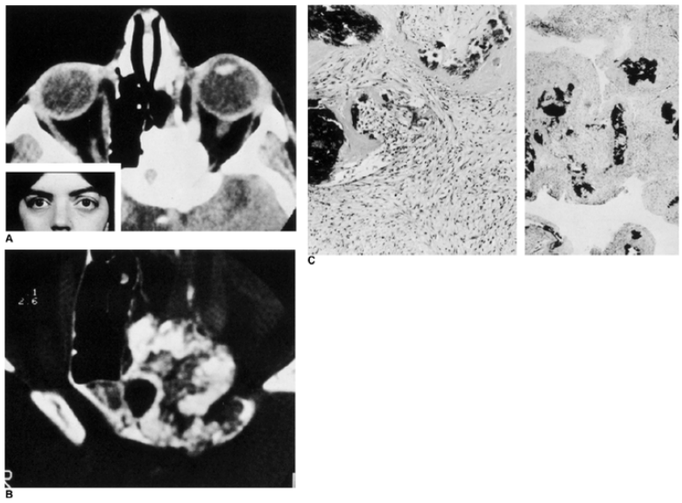

Figure 9-75. (A, inset) Clinical photograph shows a 19-year-old woman who presented with outward displacement of the left globe in 1977. She had a history of a 2-week onset, and ocular function was normal. X-rays and CT scans done at that time showed involvement of the ethmoid sinus by an irregular, diffuse, inhomogeneous bony lesion. She underwent external ethmoidectomy and debulking, and was found to have fibrous dysplasia and a chronic sinusitis, which was drained. Over the next 6 years, her disease progressed, and she had debulking procedures on two separate occasions. Axial CT scans on standard (A) and bone (B) settings show the nodular, inhomogeneous (pagetoid) appearance in 1983. At that time, she presented with a 2-month history of reduced visual acuity that occurred in the latter months of pregnancy, 9 years after the initial diagnosis. Her vision was 20/200, and she had slight temporal pallor on the left side. She underwent combined craniotomy-orbitotomy and radical removal of the dysplastic bone affecting the ethmoid sinus, sphenoid sinus, and optic canal. (C) Histopathology of the lesion shows immature, woven, partially calcified bone within a fibrous matrix with absence of osteoblasts (H&E, original magnifications; left × 10, right × 2.5). Her vision improved to 20/60 and she has remained stable for 16 years.

Rarely, malignant transformation to osteosarcoma, fibrosarcoma, chondrosarcoma, and giant cell sarcoma can occur and is often signaled by a more rapid progression, increased pain, and infiltrative features. The incidence of this complication is estimated at 0.4% to 0.5%, rising to approximately 15% with prior radiotherapy.

Imaging

Within the craniofacial bones, fibrous dysplasia tends to expand the bone with thinning of the overlying cortex. The margins are poorly defined and the dysplasia transgresses suture lines with the proportion of mineralized to fibrous tissue determining the degree of radiolucency. Where the fibrous element is predominant, there may be cyst-like areas, while a preponderance of mineralized tissue results in a homogeneous, sclerotic, “ground-glass” picture. The majority of cases demonstrate a relatively equal mixture resulting in a pagetoid appearance. Fries et al. reviewed 39 patients with fibrous dysplasia of the craniofacial bones and found a pagetoid pattern to be the most common (56%) followed by sclerotic (23%) and cyst-like (21%) appearances.

The primary differential diagnosis is hyperostotic meningioma, which is discussed earlier in the section on meningioma . Meningioma is distinguished by its occurrence in an older age group and by the presence of an associated enhancing soft tissue component, best seen on MRI (Fig. 9-76). Furthermore, meningioma often causes a more homogeneous thickening of bone, which in contrast to fibrous dysplasia does not leave a discernible cortical rim. MRI shows meningioma to have a signal isointense to gray matter on both T1- and T2-weighted images. Fibrous dysplasia, on the other hand, tends to have a lower intensity on T1 and a heterogeneous signal on T2. MRI may also have a role in fibrous dysplasia in the evaluation of mucoceles and recent hemorrhage.

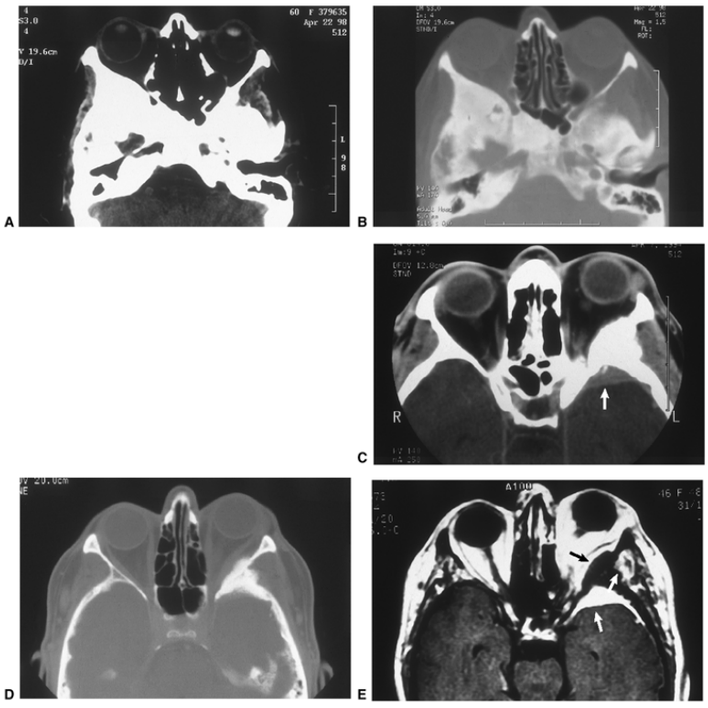

Figure 9-76. (A) Axial CT scan of a woman who presented with subtle proptosis on the right side. (B) CT scan on bone setting confirms a diagnosis of fibrous dysplasia of bone, which is characterized by the presence of a smooth cortex and a ground-glass appearance of the thickened bone. (C) Axial CT scan of a patient with a sphenoid wing meningioma that led to a similar deformity to that of the patient shown in (A) and (B). The contrast-enhanced CT scan demonstrates a nodular thickening of the orbital wall and the associated focal enhancement in the middle cranial fossa (arrow). (D) Bone setting CT scan demonstrates a loss of the smooth cortex with irregularity of the bony margins, and the T1-weighted, contrast-enhanced MR scan (E) shows the enhancing soft tissue component of the meningioma in the temporalis fossa, middle cranial fossa, and orbit lateral to the lateral rectus muscle (arrows).

On occasion, Paget's disease and less commonly cystic bone lesions, such as localized Langerhans cell histiocytosis (eosinophilic granuloma), also enter into the differential diagnosis. Paget's disease arises beyond the age of 40, is usually bilateral, and radiologically may show areas of cotton wool-type density that are not usually seen in fibrous dysplasia.

Histopathology

Macroscopically, fibrous dysplasia consists of gritty, white-to-pink tissue often with blood or serous-filled, cystic areas.

Histologically, there is a fibrous background containing trabeculae of woven bone. The stroma has variable amounts of collagen, fibroblasts, and vascularity. There may also be myxomatous areas and secondary aneurysmal bone cysts. The curvilinear bone trabeculae take on a variety of configurations, including C- or Y-shapes (so-called “Chinese characters”). These trabeculae sometimes have irregular margins due to the attachment of collagen fibers arising in the stroma. While cartilaginous nodules as well as small foci of lamellar bone are occasionally seen, the vast majority of lesions contain immature woven bone. At its periphery, fibrous dysplasia permeates normal bone and there may be areas of reactive bone with more prominent lamellar bone formation and osteoblastic rimming. Sequential biopsies of fibrous dysplasia from childhood to adult life have shown that the histological picture does not change with time.

Within the skull, the major histological differential is ossifying fibroma. The latter, however, is a more circumscribed lesion that displays prominent production of lamellar bone with osteoblastic rimming.

Management

Traditionally, there has been a conservative approach to surgery for fibrous dysplasia with intervention reserved for gross deformity, functional deficits, pain, or sarcomatous transformation. The procedures included resection if the lesion was well localized, curettage with bone grafting, or contouring. The last two decades have seen a shift to more aggressive and earlier intervention. A multidisciplinary craniofacial approach has been advocated, wherein as much affected bone as possible is removed and the resulting defects reconstructed in a single operation. The indications for intervention include those previously mentioned with the added rationale of attempting to prevent complications such as optic nerve compression. However, long-term follow-up data comparing outcomes with the natural history of the disease is lacking. Furthermore there have been two reports of blindness complicating prophylactic optic nerve decompression. Thus the question of the need for prophylactic treatment is controversial and is not recommended unless a functional deficit develops. A large review of fibrous dysplasia of the facial bones suggests that visual complications are indeed rare, supporting a conservative approach.

Ossifying Fibroma (Fibro-osseous Dysplasia)

There is some controversy as to whether ossifying fibroma exists as a distinct clinicopathological entity, with some authors believing it to be a variant of fibrous dysplasia. Nevertheless, there appear to be enough disparate features to characterize it as a benign fibro-osseous neoplasm.

Ossifying fibroma occurs most frequently in the mandible in the first two decades of life, with a proclivity for females. Only rarely does it arise in the orbit, with the frontal bone most commonly involved followed by the ethmoid and the maxillary bones. There are 37 orbital cases reported in the literature with an age range of 4 months to 52 years and an approximately equal male-female ratio.

Clinical Features

As a result of its slow growth, ossifying fibroma generally manifests as a gradual, painless globe displacement with a temporal course measured in years. The mass effect may also lead to proptosis, diplopia, and, if situated more posteriorly, compression of apical structures.

Imaging

Ossifying fibroma commences as a monostotic lesion that expands the bone of origin in a well-circumscribed manner. However, with growth it may spread to involve adjacent bones and may even extend across the midline to involve both orbits. The characteristic CT appearance is of a round or ovoid mass with a well-defined, thin sclerotic margin (Fig. 9-77). Centrally, there is often a patchy pattern of osteoblastic and osteolytic areas.

Histopathology

Macroscopically, the lesional tissue is white to red and has a largely soft fibrous texture with variable grittiness, dependent on the amount of osteoid.

Microscopically, it consists of a cellular vascular stroma containing trabeculae of lamellar bone. These bony trabeculae often have a thin surrounding of osteoid and in contrast to fibrous dysplasia, display prominent osteoblastic rimming. There may also be osteoblasts as well as a few foci of giant cells within the stroma. If larger specimens are available, they may demonstrate a "zonation phenomenon" seen as an increasing maturity of bone as one moves towards the periphery.

In the psammomatoid variant described by Margo et al., at least half of the tumor contains sphericular ossicles. This histological pattern has been correlated with a more aggressive local behavior and a tendency to recur following incomplete excision.

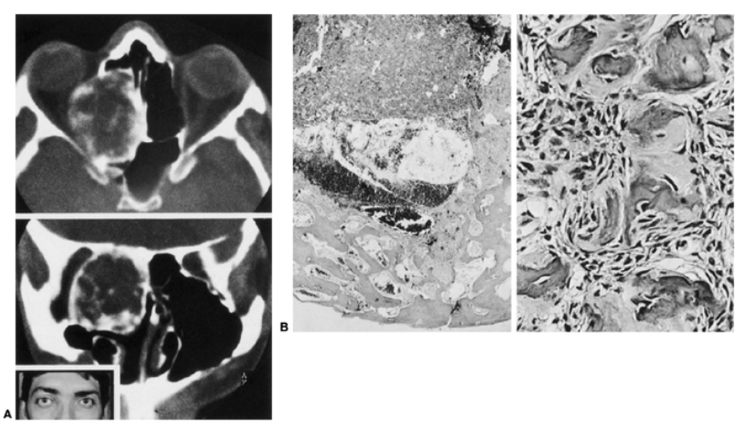

Figure 9-77. (A) This 25-year-old man presented with a 15-year history of lateral displacement of the right globe. He had previously undergone ethmoidal and sphenoidal surgery for removal of an ossifying fibroma. He had a 1-year history of increasing headache on the right side. On physical examination, there was lateral displacement and proptosis of the right globe with some restriction of abduction. Psychophysical findings were normal. The mass was debulked by an ethmoidectomy (lateral rhinotomy route) with improvement of physical appearance. He had remained stable for 1 year, with some residual tumor noted on CT scan. Axial and coronal scans on bone settings emphasize the expansion of the right ethmoid sinus, the corticated shell, and the mixed inner pattern of the tumor. (B, left) A portion of the mass shows a central, dense, hypercellular vascular core and an outer cortex of lamellar bone. (B, right) A high-power photograph shows a fibrous stroma with bony ossicles, suggesting a diagnosis of psammomatoid ossifying fibroma (H&E, original magnifications; left × 2.5, right × 25).

Management

The natural history of ossifying fibroma is one of inexorable progression and thus surgical intervention is generally required. As the propensity for recurrence after incomplete excision is well recognized, the surgical objective should be complete removal. This is particularly applicable in the case of the psammomatoid variant.

For anterior, relatively small lesions, this may be achieved via a percutaneous or bicoronal approach. However, most tumors tend to be sizable (5 cm diameter) at presentation. Thus for these lesions as well as those located more posteriorly, combined orbital, neurosurgical, and rhinological approaches are usually necessary.

Osteoblastoma

Osteoblastoma is a rare benign tumor composed of osteoblasts that produce osteoid and bone. It usually arises in the vertebrae and long bones, and its occurrence in the craniofacial region is extremely rare. These tumors are most frequently seen in the second and third decades and have a male-female ratio of 2:1.

There have been seven cases with orbital involvement reported in the last 30 years. In four of these the tumors appear to arise from the orbital roof, with the remainder originating in the ethmoid sinuses. The natural history is of slow growth, though a minority display a more aggressive behavior (“aggressive” osteoblastoma).

Clinical Features

The presentation in all cases was of a slowly progressive mass effect with proptosis and either downward or outward displacement of the globe. Pain or discomfort was a feature in several cases.

Imaging

In the long bones, osteoblastoma produce cortical expansion and have a lytic center. They can also simulate a large osteoid osteoma with a lucent halo and central ossification.

The different morphology of the orbital bones means that the tumor appears as an osteolytic lesion with a sclerotic margin and may have ossification of the matrix.

Histopathology

The gross appearance is of a relatively gritty or friable tissue, reddish-brown in color.

There is a broad spectrum of histological appearances. The typical picture is of a network of osteoid trabeculae with osteoblastic rimming. These osteoblasts generally have abundant cytoplasm and regular nuclei. However, in some tumors, large epithelioid osteoblasts or a pseudosarcomatous appearance can be observed and leads to confusion with osteosarcoma. In contradistinction to osteosarcomas, however, even atypical osteoblastomas show a tendency toward peripheral maturation and do not permeate surrounding bone. Some authors have suggested that this atypical appearance may correlate with a more aggressive clinical course and have used the term “aggressive osteoblastoma” to define a separate clinicopathologic entity. It is a rare variant with only one case being reported in the skull.

The histology of osteoblastoma is similar to osteoid osteoma, with the latter being distinguished by a size smaller than 1.5 cm as well as a somewhat less cellular and vascular stroma. Nevertheless, they may represent a spectrum of disease, a fact somewhat supported by the recent finding of a common clonal chromosomal abnormality in both tumors. Osteoid osteoma, however, has not been reported in the orbit.

Management

Excision is generally curative; however, there is one report of recurrence of an orbital tumor following a piecemeal removal. There have also been descriptions of a benign osteoblastoma of the skull that developed into an osteosarcoma following an incomplete excision, as well as a case of aggressive osteoblastoma of the temporal bone. In view of this, osteoblastomas should be completely removed under direct vision, where possible, to accurately determine the margins. This usually entails an orbitocranial approach for tumors of the roof and a combined orbitorhinological approach for those arising in the sinuses.

Chondroma

These benign cartilaginous tumors usually occur as asymptomatic lesions in the sinuses and nasal cavity, and only rarely occur in the orbit where they present as slow-growing, painless, firm lumps often near the orbital rim or the trochlea. They have on occasion also been described within the soft tissues of the orbit. Radiologically, they are seen as well-circumscribed, dense masses that histologically consist of lobulated mature hyaline cartilage. Mature chondrocytes are seen within the cartilage along with a variable fibrous or myxoid stroma. Surgical excision is always curative.

A variety of other benign cartilaginous tumors, including osteochondromas, enchondromas (Fig. 9-78), and fibrochondromas, have also rarely been described in the orbit

though the histological documentation is not always convincing.

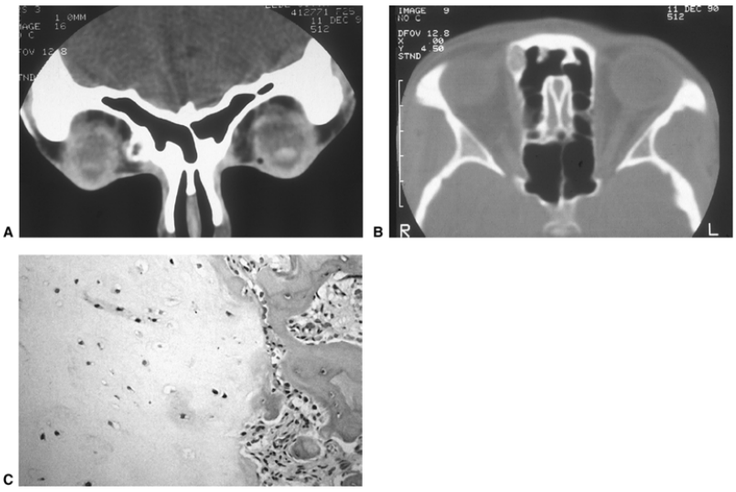

Figure 9-78. This 25-year-old woman presented with an asymptomatic, painless, hard nodule in the superomedial orbit, just anterior to the trochlea. (A, B) CT scans disclosed a nodular, irregular, calcified lesion within the bone. The mass was excised en bloc and was found to be composed of hyalin cartilage (C) surrounded by lamellar bone trabeculae, diagnostic of an enchondroma (H&E, original magnification × 10). (Fig. 9-78B reproduced with permission from Pasternak S, O'Connell JX, Verchere C, Rootman J. Enchondroma of the orbit. Am J Ophthalmol 1996;122:444-5.)

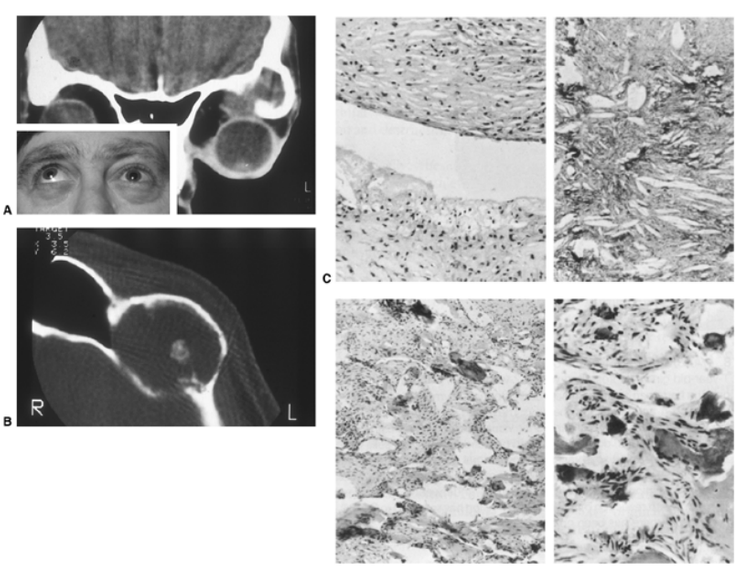

Figure 9-79. (A, inset) This 35-year-old man presented with a 4-week history of diplopia on upgaze and an 8-week history of left ptosis. He had 5 mm downward displacement, 5 mm proptosis, a delayed VEP with a vision of 20/20, and acute choroidal striae. Coronal (A) and axial CT scans revealed a soft tissue mass invading the superolateral orbit, eroding bone, and expanding the diploic spaces of the left frontal bone. (B) A posterior portion (CT bone setting) of the tumor extended through the roof into the anterior cranial fossa. The central portion appeared more radiolucent. The hemorrhagic mass was excised by a combined craniotomy-orbitotomy. (C) The bulk of the tumor consisted of a fibrous lining with many lipid-laden histiocytes in the wall (C, left). In addition, there were large areas of cholesterol granuloma (H&E, original magnifications; left × 10; right × 2.5). (D) At the margin of the lesion, there were some spicules of osteoid within a fibrovascular stroma, which suggested reactive bone or a possible origin of the lesion from dysplastic bone of aneurysmal bone cyst (H&E, original magnifications; left × 10, right × 25).

Reactive Lesions

Cholesterol Granuloma

A cholesterol granuloma is a foreign body response to the presence of crystallized cholesterol. The common sites are the middle ear and pneumatized portions of the temporal bone. In the orbit, it occurs almost exclusively in the diploë of the frontal bone overlying the lacrimal fossa, though it has also been reported in the zygoma.

Theories of pathogenesis include a purely traumatic intradiploic hematoma or a hemorrhage occurring within a preexisting bony anomaly. A breakdown of blood products then leads to cholesterol deposition and a granulomatous response. An analysis of 75 reported cases of orbital cholesterol granulomas, which is also called xanthomatous lesion of bone, revealed a marked preponderance of males in the fourth and fifth decades of life.

Clinical Features

A superolateral mass effect occurring over weeks to years is the typical mode of presentation. This leads to inferior globe displacement, proptosis, and diplopia in upgaze (Fig. 9-79). There may be some associated headache or pain and one third of patients recall a prior trauma.

Imaging

The granuloma arises in the diploë of the frontal bone, causing expansion and eventually erosion of the inner and outer tables. CT reveals it to be osteolytic with a density equivalent to brain, and occasional intralesional bone fragments. Mature lesions display high T1 and T2 signal intensities on MRI. The most commonly evoked differentials in this setting are dermoid cysts and lacrimal gland carcinomas.

Histopathology

These cysts usually contain yellow-brown viscous material with friable tissue and porous bone at the periphery.

Histologically, the principle feature is the dominance of cholesterol clefts surrounded by granulomatous inflammation with conspicuous foreign body giant cells. A variable fibrous stroma is present and usually contains extensive blood-derived debris in the form of extra- and intracellular hemosiderin as well as more recent hemorrhage.

There should be no evidence of epithelial elements, ruling out a diagnosis of epidermoid or dermoid cyst. The prominence of the xanthomatous components also serves to differentiate this condition from giant cell granuloma and aneurysmal bone cyst.

We have seen six cases of cholesterol granuloma, two of which had histological evidence of dysplastic-looking bone at their peripheries. This lends some support to the theory of a preexisting dysplastic bony abnormality.

Management

A percutaneous approach and curettage is almost always curative with only one well documented case of recurrence that occurred when peripheral bone containing lesional tissue was not removed. If there is an extensive intracranial component, a combined orbitocranial operation may be required. None of cases have recurred after curettage.

Aneurysmal Bone Cyst

This benign cystic lesion occurs most frequently in the metaphyses of long bones and in the spine. The pathogenesis is not known, although 30% to 50% occur secondary to other bone diseases including fibrous dysplasia, giant cell granuloma, giant cell tumor, osteoblastoma, osteosarcoma, and intraosseous hemangioma. There is also evidence that some aneurysmal bone cysts may arise as a reactive change to a preexisting arteriovenous malformation. Aneurysmal bone cyst occurs rarely in the skull and of those with orbital involvement, the frontal bone appears to be the most common location. An analysis of 24 recorded orbital cases, including two from our own series, revealed an age range of 11 months to 42 years. The majority presented in the second decade and there was a female preponderance of 5:3.

Clinical Features

The usual signs and symptoms include proptosis, displacement of the eye, and diplopia. Masses in the midline can cause optic nerve compression. As most aneurysmal bone cysts arise in the orbital roof, intracranial extension can rarely give rise to raised intracranial pressure. While typically subacute or chronic in evolution, sudden progression may occur due to intralesional hemorrhage.

Imaging

Aneurysmal bone cysts occurring in long bones have a characteristic uni- or multilocular expansile appearance. However, the radiology in orbital bones is not specific and consists of destruction or expansion (Fig. 9-80). If expansile, the mass may have a thin cortical margin though this is often absent as a result of erosion through to periorbita or dura. The central area is inhomogeneous, shows patchy enhancement, and can have multiple fluid levels, particularly in the more mature lesions. MRI may demonstrate recent hemorrhage in cases with acute onset.

Histopathology

The gross specimen almost always consists of curettings of reddish-brown tissue with a texture that varies from friable to fibrous or gritty. More solid lesions may yield softer, pink to gray-white tissue. If larger samples are available, one may see honeycombed areas of serosanguinous or blood-filled cavitation.

The cardinal microscopic features are cavernous blood-filled spaces that lack endothelial lining, pericytes, or smooth muscle. These spaces are bounded by a fibrous stroma that contains giant cells, hemosiderin-laden macrophages, lymphocytes, and trabeculae of osteoid and bone. The osteoid may lack osteoblastic rimming and seem to arise from the stroma in a metaplastic fashion. Degenerating chondromyxoid areas may surround the osteoid and can display partial calcification (Figs. 9-80B to D).

In 1983, Sanerkin and coworkers described a solid variant of aneurysmal bone cyst in which the aneurysmal sinusoids were either seen only in small foci or were absent. In our experience, we have seen two cases that fit this histological description. It is evident that this picture, apart from the chondromyxoid and sinusoidal foci may bear a very close resemblance to giant cell granuloma.

Finally, in any case of aneurysmal bone cyst, one should conduct a meticulous search for a primary pathology such as fibrous dysplasia.

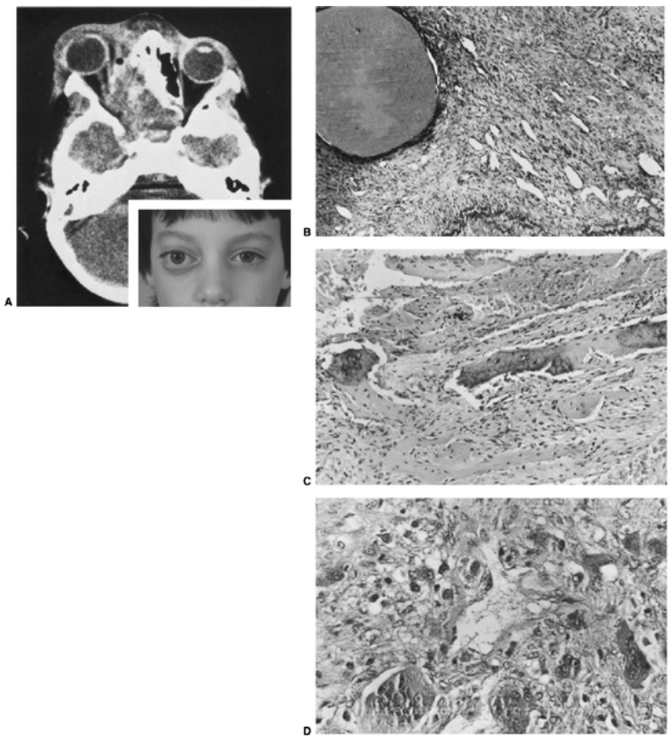

Figure 9-80. Aneurysmal bone cyst. (A) Axial CT scan of an 8-year-old boy who presented with reduced right visual acuity associated with swelling, proptosis, and mild ptosis of 1 month's duration. He had 5 mm downward and 3 mm outward displacement of the globe with paresthesia involving the right cheek. A mixed-density mass lesion expanding and destroying bone was noted. It involved the ethmoid, maxillary, and sphenoid complex. He underwent a combined procedure with excision and curettage of the mass following frozen-section biopsy. (B) The bulk of the mass consisted of a stellate reactive fibroblastic tissue with large vascular spaces, and spicules of bone and osteoid consistent with a diagnosis of solid aneurysmal bone cyst (H&E, original magnification × 10). (C) A higher-power view of both spicules in a fibrous stroma (H&E, original magnification × 10). (D) Reactive fibrous stroma with osteoclastic giant cells (H&E, original magnification × 25). The patient has been observed for 4 years without recurrence.

Management

Curettage is typically curative, and in the absence of an underlying bony abnormality, orbital recurrence is rare and usually occurs within the first 6 months. In such cases, a repeat curettage is generally successful. Resolution has also been reported following incomplete excisions. Radiotherapy has been used for recurrent aggressive lesions, but entails a small yet definite risk of postirradiation sarcoma.

Giant Cell Granuloma

Giant cell granuloma is a benign granulomatous proliferation of unknown etiology. It is also called giant cell reparative granuloma, reflecting a theory of a reparative process in response to trauma and hemorrhage.

Giant cell granuloma occurs most commonly in the mandible, maxilla, and phalanges. Cases with orbital involvement have been reported rarely, arising in the maxilla, frontal, ethmoid, and sphenoid bones with equal frequency. There are nine cases reported in the literature and with the inclusion of our own case, these range in age from 5 to 54 years (average 18.6 years) and have a male-female ratio of 3:2. This corresponds with the epidemiology of giant cell granuloma elsewhere in the skeleton, which generally presents in the first two decades of life with an equal male-female ratio.

Clinical Features

Proptosis and ocular displacement are the most common presentations, though headache and pain may be prominent (Fig. 9-81). Diplopia and decreased vision also occur depending

on the site of the mass. The time course is variable, ranging from months to years, and may be complicated by a rapid progression of symptoms due to hemorrhage.

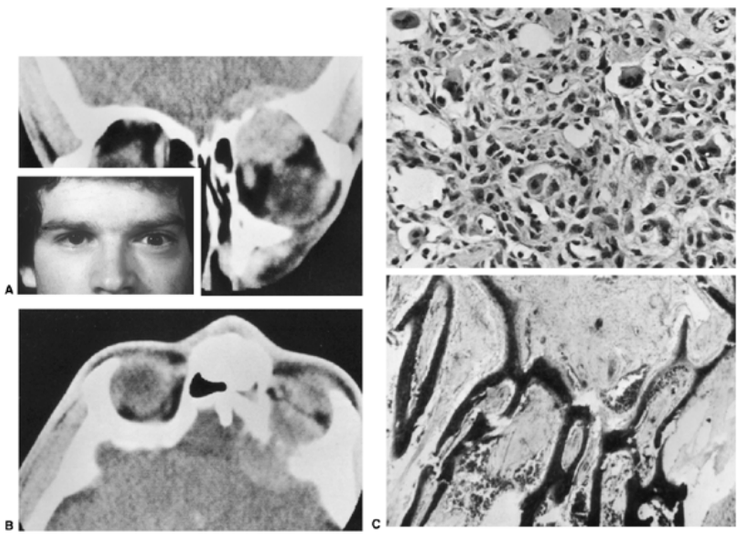

Figure 9-81. Coronal (A) and axial (B) CT scans demonstrate a superior left orbital mass eroding the roof and extending into the anterior cranial fossa. This 24-year-old man (A, inset) presented with sudden onset over a 24-hour period of painless proptosis, downward displacement of the left globe, and diplopia. The lesion had irregular borders with adjacent destruction of bone, and was originally thought to be a malignancy with intralesional hemorrhage. Only blood was obtained on needle aspiration biopsy, and the patient underwent excision of the lesion by a combined craniotomy-orbitotomy. A hemorrhagic mass was removed from the roof of the orbit and some abnormal adjacent bone was noted at the time of surgery. Biopsy specimen revealed two elements. The bulk of the lesion consisted of a spindle-cell stroma containing scattered osteoblastic giant cells, deposits of hemosiderin, and small vascular spaces (C, top). At the margin of the lesion, spicules of osteoid and new bone formation were noted (C, bottom) (H&E, original magnifications; top × 2.5, bottom × 25). The diagnosis was reparative granuloma. The patient has been observed for 5 years without recurrence.

Imaging

Giant cell granuloma typically manifests as a destructive lesion with erosion of adjacent bone. It may have indistinct or sclerotic margins and show moderate enhancement of an often inhomogeneous central matrix.

Histopathology

Macroscopically, the granuloma consists of soft, friable, tan to brown tissue, typically in the form of curettings.

A fibrous stroma with giant cells clustered around foci of hemorrhage is the dominant histology. This stroma contains ovoid and spindle-shaped fibroblasts with a variable amount of fibrosis and evidence of old and new hemorrhage. Reactive bone formation is common (75%) and consists of trabeculae of woven and lamellar bone, which may or may not demonstrate osteoblastic rimming. Areas of secondary aneurysmal bone cyst formation may also be seen.

When the preceding histologic pattern is seen, investigations to exclude Brown tumor of hyperparathyroidism are necessary. Once the latter diagnosis is ruled out, the histological differential includes giant cell tumor and the solid areas in an aneurysmal bone cyst. It is important to differentiate giant cell tumor from giant cell granuloma, as the former is more aggressive and can undergo malignant transformation. Hirsch and Katz have outlined the histologic criteria for this differentiation. The major differences are that in giant cell tumor, the stroma is made up of largely plump, round, oval cells and displays less fibrosis than the often spindle cell stroma of giant cell granuloma. Furthermore, the giant cells in giant cell tumor tend to be larger with more nuclei (>20) and are more diffusely distributed rather than being centered around hemorrhagic foci as in giant cell granuloma. In addition, reactive bone formation is not a conspicuous feature of giant cell tumor. Nevertheless, the distinction between the two entities is not always sharply delineated.

Management

Giant cell granuloma generally responds well to curettage (as did our patient) with or without bone grafting. There is a variable recurrence rate reported for lesions elsewhere in the body but most appear to be cured with a second curettage. This generalization appears to hold true for most orbital cases. However, there is a case reported by Sood et al. where the tumor behaved in a locally aggressive fashion requiring three operations and ultimately radiotherapy.

“Brown tumor” of Hyperparathyroidism

“Brown tumor” represents a benign reactive proliferation with a virtually identical histological appearance to giant cell granuloma. Its association with primary or secondary hyperparathyroidism, however, differentiates the former.

Brown tumors arise as a consequence of the increased osteoclastic activity associated with hyperparathyroidism. This leads to focal areas of bone resorption and hemorrhage. Histologically-proven orbital Brown tumors have been described in 14 cases in the literature. They appeared in an older age group (range 10-70 years; average 33 years) with a more marked female preponderance (5:2) when compared to giant cell granuloma. Eight cases were associated with primary hyperparathyroidism and six with hyperparathyroidism secondary to renal dysfunction. The maxilla, followed by the frontal bone, were the most favored sites.

Brown tumors tend to have a temporal onset usually measured in months, and like giant cell granulomas, are prone to intralesional hemorrhage. Patients with Brown tumors will also demonstrate abnormalities in serum calcium, phosphate, alkaline phosphatase, and parathormone levels, and require skeletal surveys.

The radiological and histological appearances are essentially the same as those for giant cell granuloma (Fig. 9-82). With regard to management, however, treatment of the hyperparathyroidism often results in spontaneous resorption and healing of the bony lesion. Hence, a careful clinical evaluation for manifestations of hypercalcemia or renal dysfunction may obviate the need for surgery.

Neoplasms

Osteosarcoma

Osteosarcoma (osteogenic sarcoma) is the most common primary neoplasm of bone. Long bones are the most frequent site, with orbital involvement being rare and usually from a maxillary focus. In most cases, the tumor arises de novo; however, some are secondary to Paget's disease, fibrous dysplasia, radiation therapy, giant cell tumor, or osteoblastoma. Osteosarcomas are also seen as a second tumor in patients with familial retinoblastoma even in the absence of radiotherapy. Furthermore, a proportion of de novo osteosarcomas have been found to share the deletion of chromosome 13, which renders the retinoblastoma anti-oncogene inactive.

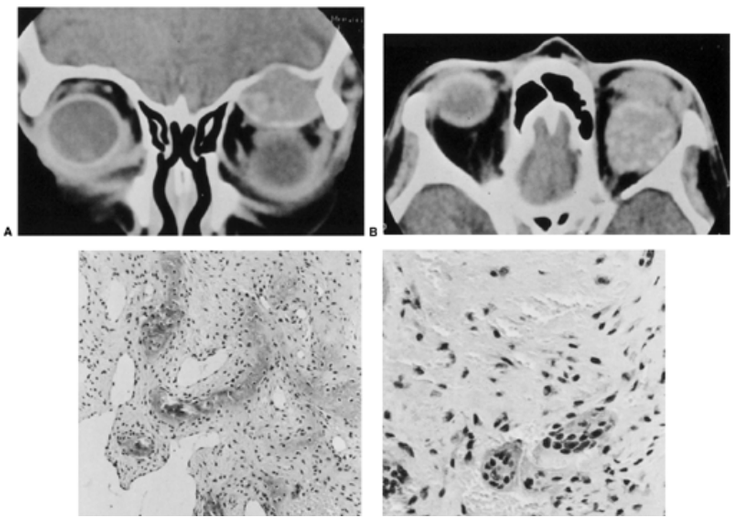

Figure 9-82. Coronal (A) and axial (B) CT scans demonstrate a mass in the roof of the left orbit with erosion of the bone. The patient was a 69-year-old woman who had a 1-month history of painful swelling of the left upper lid. The tumor consisted of a uniformly enhancing soft tissue mass with a calcific rim and central punctate foci of calcification. The mass was extirpated. (C, D) Histologically, it consisted of a fibrous stroma with large vascular channels, many osteoclastic giant cells, and foci of bone formation (H&E, original magnifications; C × 10, D × 25). The findings led to a suspicion of Brown tumor of hyperparathyroidism, which was confirmed on systemic evaluation. The parathyroid adenoma was removed. There has been no recurrence after a 1-year follow-up.

De novo tumors are most prevalent in the second decade with a slight male predilection; however, osteosarcomas involving the orbit afflict an older population, being most frequent in the fourth and fifth decades (range 10-54 years). The common precursor lesions for secondary tumors in the orbit appear to be radiation therapy, Paget's disease, and fibrous dysplasia.

Clinical Features

The course is typically more rapid than the benign tumors discussed previously, averaging approximately 4 to 6 months. In addition to any mass effect, there may be significant pain and infiltration leading to diplopia and decreased vision.

Imaging

A mixed lytic and sclerotic mass with indistinct margins is the usual CT appearance (Figs. 9-83 and 9-84). Soft tissue infiltration of the orbit may also be evident, and the mass may contain foci of mineralization producing “fluffy” densities. MRI can be of value in delineating the extent of any soft tissue component.

Histopathology

Gross specimens contain infiltrative tumor, which may be white, tan, or hemorrhagic in parts, with a soft to firm or gritty texture depending on the stromal components.

The stroma contains sarcomatous cells and must show at least some foci of osteoid production. The anaplastic cells have a variety of histologic subtypes, including osteo-, chondro-, and fibroblastic. In most high-grade lesions, the cells are markedly malignant though they become less so when incorporated into the osteoid (so-called “normalization” of malignant osteoid). The osteoid itself may assume a characteristic delicate filigreed or lacelike pattern.

Management

The regime for osteosarcoma involves preoperative chemotherapy, resection, and then continuation of the chemotherapy with modifications based on the pathology of the resected specimen. Radiotherapy has an adjunctive postoperative role for residual tumor.

These therapies have improved the five-year survival rate from 20% up to 70% for resectable lesions. However, the prognosis in the skull is poorer due to delayed diagnosis and inability to obtain complete resection once the tumor has gained access to the skull base or intracranial space. We have had two patients with osteogenic sarcoma, one occurring in the maxillary antrum and orbit as a second tumor 19 years following retinoblastoma. The tumor was resected en bloc and the patient died 3 years later of leukemia (Fig. 9-83). The other patient had a spontaneously occurring tumor secondary to longstanding fibrous dysplasia (Fig. 9-84).

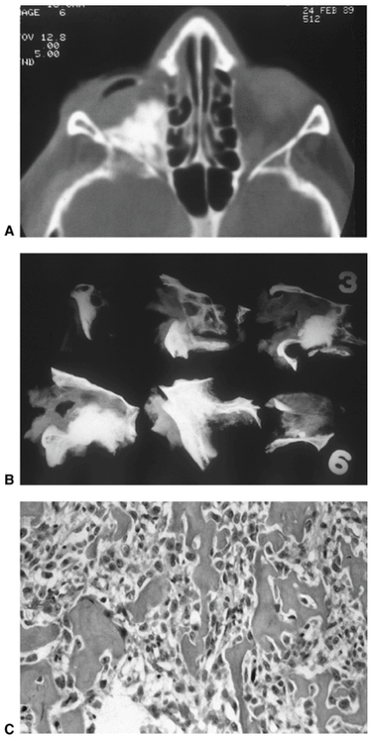

Figure 9-83. (A) This dense, calcified tumor mass occurred in the orbit of an anophthalmic patient, who was treated previously for bilateral retinoblastoma. At age 19, he presented with an extrusion of his prosthesis. Biopsy led to a diagnosis of osteogenic sarcoma, and he underwent an en bloc orbitectomy. (B) The post-orbitectomy X-rays show the completely excised mass. (C) Histology demonstrates a well differentiated osteosarcoma (H&E, original magnification × 25). He lived for 2 years subsequent to the orbitectomy before succumbing to leukemia.

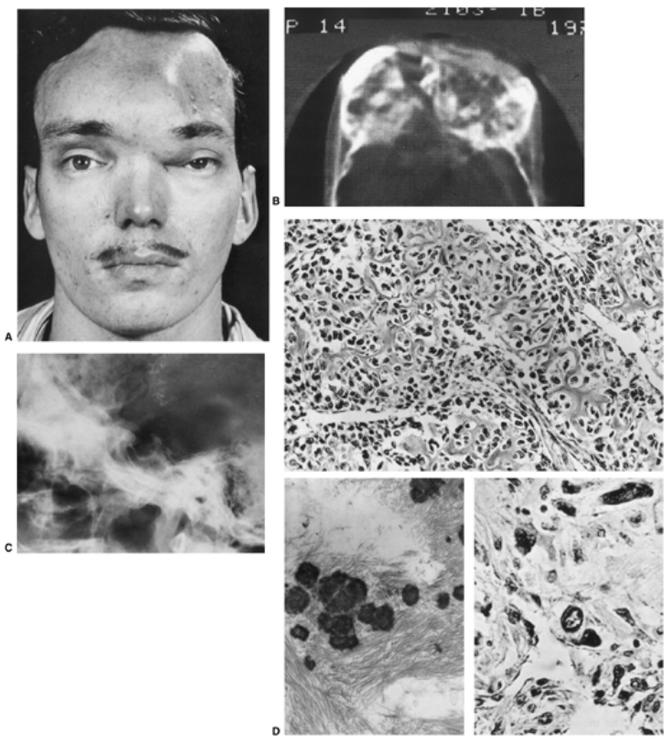

Figure 9-84. This 41-year-old man presented with severe orbital pain and reduced visual acuity to no light perception. It occurred over a 3-week period and was associated with paresthesia. (A) The clinical photograph demonstrates his appearance 15 years earlier with a cosmetic deformity due to fibrous dysplasia. (B) A massive lytic lesion involving the lateral wall, frontal bone, temporal fossa, sphenoid ridge, and orbital soft tissues with intracranial extension was noted on CT scan. (C) Lateral view of skull X-ray shows pagetoid fibrous dysplasia of the orbital roof, demineralization of the sella, and a destructive lesion of the sphenoid bone. (D) Histologic analysis showed a poorly differentiated osteogenic sarcoma with foci of osteoid. The electron micrograph demonstrates osteoid formation in the tumor (H&E, original magnifications; top × 10, bottom × 40, electron micrograph × 1520). A diagnosis of osteosarcoma was made, and the patient was treated palliatively. Within 1 month, the left orbit became involved and he died 6 months after onset.

Chondrosarcoma

This malignant tumor is characterized by chondroid production and occurs most frequently in the lower extremities and pelvis. Orbital involvement is generally secondary to tumors arising in the sinuses and nasal cavity. Craniofacial chondrosarcomas have a male-female ratio of 2:1 and are prevalent in the fifth and sixth decades with a wide age range. Biologically, they are nonmetastasizing, extremely slow-growing, locally aggressive tumors that can cause proptosis and lateral displacement of the globe.

Clinical Features

Due to their frequent sinus origin, chondrosarcomas usually manifest symptoms of nasal and sinus obstruction. Orbital mass effects often occur medially or inferiorly and consist of proptosis, ocular displacement, and epiphora secondary to nasolacrimal duct obstruction. There may be a variable degree of pain or headache as well as infiltrative features. Posterior growth leads to compromise of the optic nerve and apical structures. The course is usually prolonged and symptom duration averages 2 to 3 years.

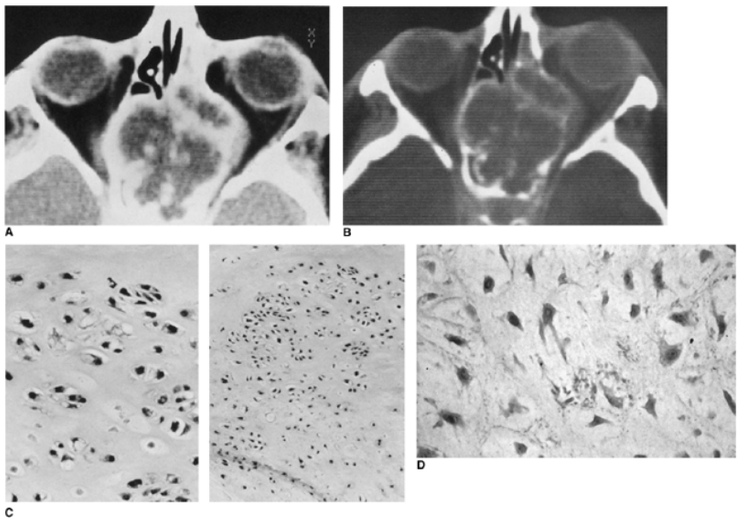

Figure 9-85. Axial CT scans demonstrate an expansile, lytic lesion involving the ethmoid and sphenoid sinus with left proptosis and lateral displacement (A, standard and B, bone settings). This 44-year-old woman had a 5-month history of proptosis. Transnasal biopsy revealed a low-grade chondrosarcoma, and she underwent a multidisciplinary debulking of the tumor followed by radiotherapy. There has been no recurrence after a 19-year follow-up. (C, D) Pathology of the low-grade chondrosarcoma. Note chondrocytes within lacunae (H&E, original magnifications: C, left × 25; C, right × 10; D × 40).

Imaging

Chondrosarcomas appear as well-defined osteolytic lesions with stippled or mottled densities indicative of mineralization (Fig. 9-85). Higher-grade tumors tend to have irregular margins with nonuniform calcification in the form of amorphous cloud-like densities.

The noncalcified regions show T1 signal intensities that are lower than or equal to gray matter on MRI. T2 signals are isointense to the cortex and the masses usually display moderate enhancement.

Histopathology

Grossly, the tissue is white to blue-gray with a discernible lobular pattern. Histologically, there are irregular lobules

of hypercellular cartilage with lacunae containing plump bi- or multinucleated chondrocytes, separated by fibrous stroma or reactive bony trabeculae. The stroma may be myxoid in areas and shows a wide variability in the amount of cellularity, atypia, and chondroid matrix, which has led to a grading system. The Grades 1 through 3 appear to have some correlation with prognosis. This is manifest in tumors involving the orbit, which are mostly Grades 1 or 2 and exhibit slow growth with a low incidence of metastasis.

The major histological differential diagnosis for conventional chondrosarcomas in the orbit are chondromas and chondroblastic osteosarcomas.

Management

Ablative surgery is the goal for resectable chondrosarcomas. However, for craniofacial tumors, this is often not possible and due to their indolent growth, a protracted course with multiple recurrences is frequent. Though not particularly radio- or chemosensitive tumors, both these modalities have been used in an adjunctive role for incompletely excised lesions. We have treated two cases of extensive Grade 2 chondrosarcoma with radical debulking. One case received postoperative radiotherapy and has been free of recurrence for 19 years (Fig. 9-85). The other case occurred in a 46-year-old man, who developed a large midline mass. This was resected but recurred 3 years later (Fig. 9-86). He underwent repeat resection of the apical lesion and has been free of disease for 3 years. A third case was too extensive for complete local resection but underwent debulking with ultimate recurrence.

Mesenchymal Chondrosarcoma

Mesenchymal chondrosarcoma is a variant of chondrosarcoma, which commonly arises in the jaw. Within the orbit, it favors the soft tissues though bony involvement can occur. It is seen in a younger age group and in the orbit has a female predilection.

In contrast to conventional chondrosarcoma, this tumor progresses more rapidly and presents with proptosis and infiltrative effects of less than a year's duration. Radiologically it appears on CT as a nonspecific, irregular, mottled, soft tissue mass while the MRI characteristics are similar to the noncalcified areas of the conventional type. Histologically the mesenchymal variant consists of lobules of cartilage arising in a highly cellular stroma of malignant, small round cells. The chondroid production serves to differentiate it from other small round cell tumors such as Ewing's sarcoma.

Due to its origin in the soft tissues, mesenchymal chondrosarcoma is typically treated with exenteration. Despite the small number of reported orbital cases, it appears that resection is adequate therapy in certain patients. More recent reports suggest that mesenchymal chondrosarcoma may also be successfully managed by local resection with adjuvant chemo- and radiotherapy thus obviating the need for exenteration. In comparison to the usual chondrosarcoma, it has a more rapid course and a propensity for early spread, particularly to the lungs.

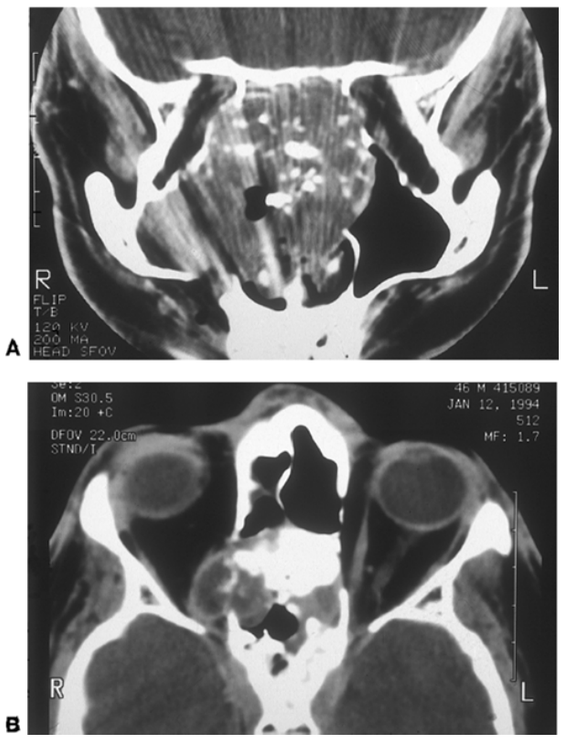

Figure 9-86. This 46-year-old man with a history of a midline chondrosarcoma (A) underwent resection. He presented three years later with a right optic neuropathy due to apical recurrence (B), which was further resected. Note the mottled areas of mineralization within the matrix of the chondrosarcoma. He is alive and well 3 years after his second resection.

Ewing's Sarcoma

Ewing's sarcoma is a small round cell tumor that usually arises in bone. The characteristic chromosomal translocations (t(11;22)(q24:q12)) and proto-oncogenes expressed in this neoplasm suggest that it is an undifferentiated neuroectodermal tumor (PNET).

The majority of cases arise in the first two decades with a predilection for males (1.5:1). The tumor is uncommon among blacks. Incidence in the head and neck is approximately

4% and favors the mandible and maxilla. Most orbital cases represent metastases or direct extension with only a handful of primary orbital lesions reported. Hence, an orbital presentation should institute a rigorous search for a primary.

Clinical Features

Nonaxial proptosis of relatively short duration is the usual presentation. We have encountered two cases of primary orbital Ewing's sarcoma involving bone, aged 6 and 10 years respectively. Both were males and presented with a four-week history of ocular displacement. One tumor arose from the maxilla (Fig. 9-87) and the other from the nasopharynx. We have also seen one patient with metastatic Ewing's sarcoma to posterolateral orbital bone with soft tissue expansion into the orbit. In addition, we have seen one case of an extraosseous Ewing's sarcoma of the orbit in a 72-year-old man (Fig. 9-88).

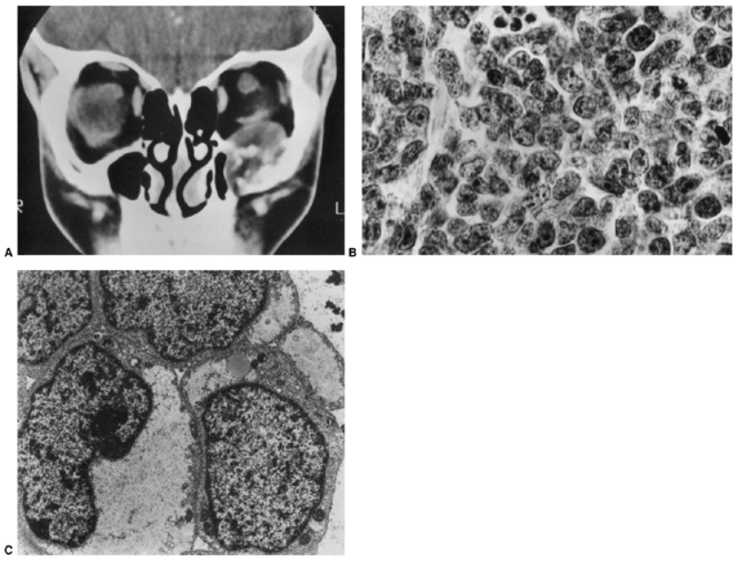

Figure 9-87. (A) Coronal CT scan demonstrates a destructive lesion of the left maxillary sinus and floor of the orbit, and a well-circumscribed soft tissue component invading the orbit. It was seen in a 12-year-old boy who had a 6-week history of a puffy left lower lid. His vision was reduced to 20/60, and he had 6 mm of elevation, 2 mm of proptosis, and a palpable mass in the left lower lid. He underwent incisional biopsy, with frozen section diagnosis of a poorly differentiated round-cell tumor. (B) Histopathology of his biopsy demonstrates a densely packed cellular tumor with PAS-positive, diastase-resistant cytoplasmic vacuoles (H&E, original magnification × 100). (C) Electron microscopy demonstrates the primitive cells with no junctions, large nuclei, scant organelles, and pools of glycogen typical of Ewing's sarcoma. The patient was treated with chemotherapy and radiotherapy, and is alive and well with no local or systemic recurrence with 16 years' follow-up. (Fig. 9-87C courtesy of J. Dimmick, MD.)

Imaging

The CT appearance is of an expansile or permeating mass that shows mottled bone destruction (Fig. 9-87). There may be an associated soft tissue component.

Histopathology

The tumor consists of firm, white tissue made up microscopically of sheets and clusters of uniform, small round cells. Cytoplasmic glycogen as demonstrated by PAS positivity, is present in 90% of cases. Ultrastructurally, there is evidence of glycogen and a sparsity of organelles.

The criteria for distinguishing Ewing's from neuroectodermal tumor of bone have not been well elucidated as yet. In broad terms, however, Ewing's should not demonstrate signs of neuroectodermal differentiation on light or electron microscopy. Although they probably reflect different points in a spectrum of differentiation, the distinction continues to

be made in part due to the poorer prognosis of the neuroectodermal tumors of bone.

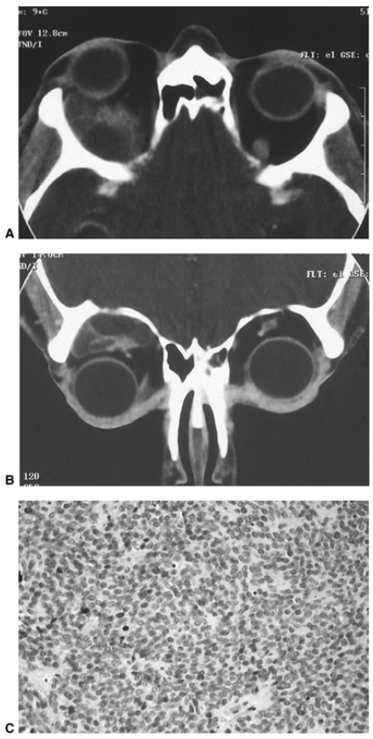

Figure 9-88. Axial (A) and coronal (B) CT scans demonstrate an extraosseous superior orbital mass that occurred in a 72-year-old man, who had noted downward displacement of his globe post-cataract surgery. On physical examination, he had 8 mm of right exophthalmos, 1 mm of downward and inward globe displacement, and limitation of upgaze. He underwent excision of a dark, vascular appearing mass in the orbital apex. (C) This proved to be a densely packed, cellular neoplasm with vesicular nuclei. It proved on molecular studies to be cytogenetically positive for Ewing's sarcoma. He has undergone orbital radiotherapy and chemotherapy, and is alive and well without recurrence 2 years later.

The other differentials to be considered are metastatic neuroblastoma and chloroma in patients under 5 years of age and lymphoma in older patients. Mesenchymal chondrosarcomas and the small cell variant of osteosarcoma are distinguished primarily by the appropriate matrix production.

Management

Induction multi-agent chemotherapy followed by radical local surgery or radiotherapy has resulted in improved 5-year survival rates of up to 74%. Unfortunately, 17% to 20% of survivors subsequently develop a second primary, most commonly osteosarcoma. Due to factors such as improved local control and postirradiation malignancies, surgery is currently favored over radiotherapy for resectable lesions.

Hematopoietic and Histiocytic Lesions Affecting Bone

Myeloma

Multiple myeloma and more rarely solitary plasmacytoma may involve orbital bone. These tumors affect those over the age of 50 and present with a subacute onset of pain and proptosis. In the case of multiple myeloma, there are usually systemic manifestations such as bone pain, fever, and fatigue, as well as urinary and serum protein abnormalities. Radiologically, an osteolytic area with a contiguous soft tissue mass is the rule. Histologically, the tumors are composed of broad sheets of malignant plasma cells varying in appearance from mature to blast-like.

Langerhans Cell Histiocytosis

Langerhans cell histiocytosis (LCH) consists of a variety of syndromes due to proliferation of Langerhans cells, and is discussed in Chapter 10 . Localized bone involvement (eosinophilic granuloma) is prevalent in males between the ages of 3 to 10 years. These children characteristically develop proptosis due to focal lytic superolateral lesions associated with soft tissue expansion. We have seen 6 cases of localized LCH and each demonstrated a characteristic CT appearance of a central radiolucent area with an enhancing rim. Histologically, there is a granulomatous and histiocytic infiltrate with Langerhans cells and prominent eosinophils. Localized periorbital disease is responsive to curettage, intralesional steroid injections, or low-dose radiotherapy. The prognosis is poorer in younger patients with visceral involvement.

Giant Cell Tumor

Giant cell tumor is usually found in the long bones in the third to fifth decades with a slight female predominance. It rarely occurs in the sphenoid, temporal, or ethmoid bones with a primary orbital site having been reported on one occasion. Most cases with orbital involvement originate in the sphenoid and present with headaches, diplopia, decreased vision, and multiple cranial nerve palsies. The sphenoidal lesions are radiologically apparent as either lytic or soft tissue masses eroding the sella.

This friable tumor is composed of uniformly distributed osteoclast-like giant cells. Occasionally, a giant cell tumor may display clinical and histologic evidence of malignancy and metastasize to the lungs.

There is a 30% to 50% recurrence rate following curettage, and thus the goal is complete excision if possible. Radiotherapy has been reserved for inaccessible lesions due to the risk of inducing malignancy.

Vascular Tumors

Aside from one report of a hemangioendothelioma of orbital bone, the only other vascular bony tumor described in the orbit has been the cavernous hemangioma of bone. The hemangioendothelioma presented as an aggressive and lytic infiltrative lesion that recurred following resection.

Intraosseous Hemangioma

These benign vascular tumors of bone, like their counterparts in the orbital soft tissues, are probably hamartomatous in origin. While common in the calvarium and spine, they are rare in the orbit. Any of the orbital bones may be involved, though the frontal bone is the most frequent site. Including one case of our own, there are 20 cases in the literature. These indicate an average age within the fifth decade and a slight female preponderance.

Clinical Features

A slowly developing orbital mass, often associated with pain or tenderness, is typical. There may be a palpable mass in the anterior orbit.

Imaging

Intraosseous hemangiomas present as well-defined, radiolucent masses that expand the inner and outer tables of the bone, often in an asymmetrical fashion. Approximately half will show the classical picture of a sunburst, striated, or honeycombed internal pattern (*c.f.* Vascular Lesions – chapter 13). On selective angiography, they appear as a tangle of vessels.

Histopathology

The specimen consists of soft, violaceous masses with intervening trabeculae of reactive bone. Microscopically, the majority are hemangiomas with large, thin-walled, endothelially lined, blood-filled vascular spaces.

Management

Surgical treatment consists of excision with a rim of normal bone. Preoperative angiography should be performed and strong consideration given to embolization prior to resection, as these tumors can bleed in a profuse and persistent manner.

Miscellaneous

There have been two reports of intramedullary lipoma of the frontal bone, which led to chronic painless expansion simulating fibrous dysplasia. There have also been cases of intraosseous myxoma presenting in a similar fashion. Both malignant fibrous histiocytoma and fibrosarcoma can rarely arise in orbital bone, often as postirradiation neoplasms.

Differential Diagnosis

At the University of British Columbia Orbital Clinic, primary tumors made up 23% of all lesions involving bone. The remainder were comprised of a large variety of pathological processes that involved bone as a secondary phenomenon. These are outlined in Table 9-10 .

We have excluded traumatic and infectious etiologies as they usually pose no diagnostic dilemma with primary bone tumors. Similarly, congenital anomalies such as craniosynostosis, infantile cortical hyperostosis, progressive diaphyseal dysplasia (Engelmann's disease), and osteopetrosis are not typically part of the differential diagnosis.

Inflammatory lesions are distinguished by the presence of clinical inflammatory signs, lack of an epicenter in bone, and have significant soft tissue component. Primary orbital bone tumors, on the other hand, have a focus in bone and, aside from some malignant cases, generally do not have an associated soft tissue mass. These radiological features also serve to distinguish them from sinus epithelial malignancies that secondarily invade the orbit.

Metastases with a bony epicenter may more commonly create confusion with primary orbital bone tumors. Clinically, they tend to present with a more rapid course dominated by

pain, mass effect, and infiltration. Radiologically, they are classified as osteolytic, mixed, or osteoblastic. The majority are osteolytic or mixed. However, metastases from prostate and carcinoid usually result in osteoblastic lesions (Fig. 9-89). Breast, lung, gastrointestinal, and renal metastases may also uncommonly be osteoblastic. Hyperostotic meningiomas have been discussed previously.

Table 9-10. Orbital lesions demonstrating bone involvement (excluding primary bone tumors), University of British Columbia Orbital Clinic, 1976-1999

DISORDER	NUMBER OF LESIONS	TOTAL
Neoplastic		
Lymphoproliferative and hematopoietic		7
Lymphoma	3	
Plasmacytoma – myeloma	2	
Leukemia - prolymphocytic	1	
Chloroma	1	
Metastatic		14
Carcinoma		
Breast	5	
Prostate	3	
Unknown	3	
GI	1	
Thyroid	1	
Neuroblastoma	1	
Secondary		
Intracranial		50
Sphenoid wing meningioma	42	
Other	8	
From sinus		31
Epithelial	23	
Malignant schwannoma	2	
Rhabdomyosarcoma	2	
Lymphoma	2	
Melanoma	1	
Neurofibroma	1	
From lacrimal gland (with bone invasion)		8
Carcinoma ex pleomorphic adenoma	3	
Adenoid cystic carcinoma	2	
Carcinoma in pleomorphic adenoma	1	
Ductal adenocarcinoma	1	
Spindle cell myoepithelioma	1	
From face		1
Squamous cell	1	
Structural lesions of bone		78
Mucoceles	40	
Dermoid cysts	37	
Respiratory cyst	1	
Inflammatory lesions with bone destruction		16
Sinusitis	10	
Wegener's granulomatosis	6	

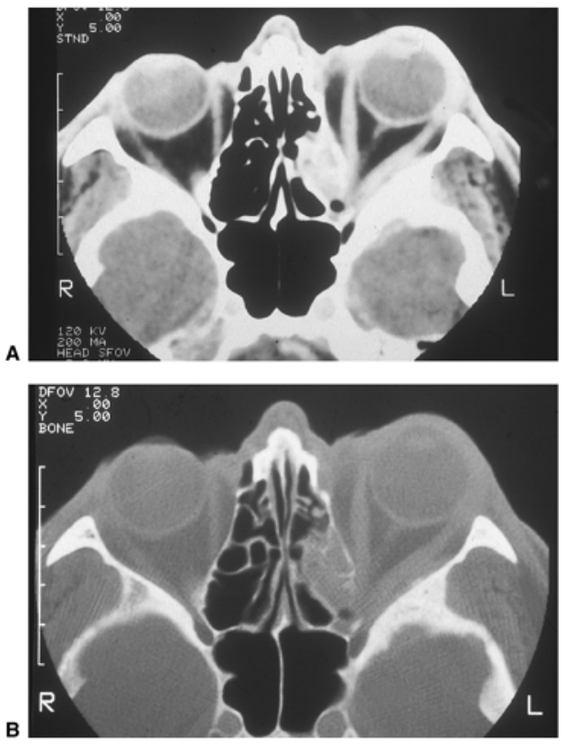

Figure 9-89. (A, B) These axial CT scans demonstrate an osteoblastic metastatic prostate carcinoma, which occurred in a 61-year-old man who developed swelling of his left lid. This was associated with a rapidly decreasing vision over a 2-week period. He had vision of counting fingers at 2 feet on the left, a marked left afferent pupillary defect with ptosis, and a firm, proptotic left orbit. He underwent a needle biopsy under CT scan control, which confirmed a metastatic prostate carcinoma.

Structural lesions such as dermoid or epidermoid cysts may give rise to confusion with cystic bone tumors. MRI can be helpful in excluding the nonlipid-containing lesions but may not be able to differentiate cholesterol granulomas

Orbital bone may also be secondarily invaded by chordoma, a rare slow-growing intraosseous tumor arising from notochordal remnants. When located in the dorsum sella or clivus, it may grow anteriorly to involve the orbital apex. Radiologically, it appears as a heterogeneous destructive lesion with an extraorbital focus. Histologically, it is characterized by the presence of large vacuolated (physaliphorous) cells (see Secondary Tumors of the Orbit , Fig. 9-95).

Primary intraosseous lymphomas have not been reported as orbital lesions, but our experience includes two cases of paraorbital involvement. Both patients had disseminated recurrent lymphoma and developed an intraosseous tumor in the region of the sphenoid sinus with subsequent orbital invasion. In addition, we have also seen intraosseous plasmacytomas, myelomas, chloromas, and one prolymphocytic leukemia. In all such instances, there is often a significant soft tissue component along with evidence of bony lysis.

Conclusion

Primary orbital bone tumors are rare, with osteoma and fibrous dysplasia being the entities most likely to be encountered by the clinician. The presentation is usually a gradual mass effect, with infiltration and acute hemorrhage being features of malignant and reactive lesions respectively. Radiologically, the appearances may be nonspecific, and histology often demonstrates some overlap between related lesions. An accurate diagnosis is therefore dependent on a careful assessment of clinical and radiological information in conjunction with the histology.

Secondary Tumors of the Orbit

Jack Rootman

Steven E. Katz

Secondary tumors include all lesions that extend into the orbit from the adjacent structures of the nasopharynx, sinuses, bone, intracranial cavity, eyelids, conjunctiva, lacrimal sac, and globe. They account for approximately one quarter of all neoplasia in our series (Table 9-11). The main emphasis of this section will be on orbital extension of lesions of epithelial origin and selected tumors arising from the adnexa, eye, and intracranial cavity.

Neoplasia of the Sinus and Nasopharynx

Malignant neoplasms of the sinus account for 0.2% to 0.8% of all systemic malignancies, 3% of malignancies involving the upper aerodigestive tract, and 6% of head and neck cancers. Men outnumber women 2 to 1 and the peak age range is between 40 and 60 years. The incidence of nasopharyngeal carcinoma is 0.5 to 2.0 per 100,000 per year, and etiologic factors may include the Epstein-Barr virus, nitrosamines, cigarette smoking, and various occupational exposures.

The orbit is at risk because it shares three thin, bony walls with the nasal cavity and the sinuses: the roof, medial wall, and floor. Neoplasias can extend into the orbit by bony destruction, through suture lines and natural dehiscences of

walls (i.e., lacrimal fossa, inferior orbital fissure, infraorbital groove, and pterygopalatine fossa), and via the emissarial blood vessels and nerves that perforate the orbital walls.

Table 9-11. Incidence and type of secondary tumors of the orbit, University of British Columbia Orbital Clinic, 1976-1999

TUMOR TYPE	NUMBER	TOTAL
Nasopharynx and Sinus (epithelial and soft tissue)		43
Epithelial	29	
Lymphoma	3	
Rhabdomyosarcoma	3	
Malignant schwannoma	2	
Melanoma	2	
Malignant fibrous histiocytoma	1	
Esthesioneuroblastoma	1	
Hemangiopericytoma	1	
Neurofibroma	1	
Bone		48
Osteoma	11	
Fibrous dysplasia	11	
Histiocytosis X	8	
Myeloma	7	
Ewing's sarcoma	3	
Chondrosarcoma	3	
Osteogenic sarcoma	2	
Chondroma	1	
Fibrosarcoma	1	
Ossifying fibroma (psammomatoid)	1	
Intracranial		44
Sphenoid wing meningiomas	42	
Dural melanoma	1	
Medulloblastoma	1	
Eyelid		26
Basal cell	10	
Squamous cell	7	
Meibomian (sebaceous)	4	
Angiosarcoma	2	
Melanoma	1	
Spindle cell sarcoma	1	
Pleomorphic adenoma	1	
Conjunctiva		16
Squamous carcinoma	9	
Melanoma	7	
Ocular		10
Melanoma	8	
Malignant fibrous histiocytoma	1	
Retinoblastoma	1	
Lacrimal Sac		7
Transitional carcinoma	3	
Squamous carcinoma	3	
Fibrous histiocytoma	1	

Table 9-12. Site and histology of epithelial malignancies of orbit and sinus/nasopharynx. Combined data from the University of British Columbia Orbital Clinic and the Johnson et al. series*

	MAXILLARY	ETHMOID	SPHENOID	NASOPHARYNX AND NOSE	DIFFUSE	TOTAL HISTOLOGIC TYPE
Squamous	5 (25)	2		4	2	38
Transitional		2 (3)		1 (1)		7
Adenocarcinoma	1 (3)	1 (1)		1		7
Adenoid cystic	3 (3)					6
Mucoepidermoid	(1)	1			1	3
Neuroendocrine		1	1		1	3
Basal cell				1		1
Total Sites	**41**	**11**	**1**	**8**	**3**	**65**

* Data from Johnson et al. study in parentheses
Johnson et al. data from Johnson LN, Krohel GB, Yeon EB, Parnes SM. Sinus tumors invading the orbit. Ophthalmology 1984;91:209-17

The incidence of ophthalmoneurologic manifestations in primary nasopharyngeal tumors varies from 36% to 59%. Neoplasia of the sinus and nasopharynx account for 5% of orbital neoplasia in our series and 22% of all secondary tumors.

Epithelial Malignancies of the Sinus and Nasopharynx

Epithelial malignancies of the sinuses frequently spread to the orbit. Conley noted that 75% have extension beyond the sinus, 45% of which have orbital invasion. About 80% of sinus and nasopharyngeal tumors with orbital invasion are epithelial. The specific site of origin and histologic types seen by us and by Johnson et al. are summarized in Table 9-12 . Two thirds originated from the maxillary sinus, and 60% were squamous cell. Epithelial malignancies of the sinus and nasopharynx are classified according to the extent of local invasion and regional nodal spread, and by definition, orbital involvement reflects an advanced stage.

Batsakis divided epithelial malignancies into two groups: (1) those arising from metaplastic epithelium, including squamous cell carcinoma and "transitional" tumors; and (2) those arising from the mucoserous epithelium, including adenocarcinoma and salivary gland neoplasia (e.g., adenoid cystic carcinoma, mucoepidermoid carcinoma, and rare malignant salivary neoplasia). Squamous cell carcinoma is by far the most frequent malignancy of the nose and paranasal sinuses, accounting for up to 80% of cancers in these locations.

Clinical Presentation

The clinical hallmark of these secondary epithelial tumors is **nonaxial globe displacement** associated with infiltration of orbital and paraorbital structures, leading to pain, paresthesia, decreased vision, and reduced extraocular movements. It is the features of chronic, progressive, and relentless pain, paresthesia, and nonaxial displacement that help to distinguish secondary epithelial malignancies from practically every other tumefaction of the orbit. In our experience, metastatic disease was painful in about 25% of cases, and proptosis was usually axial. In contrast, the secondary malignancies were associated with pain and paresthesia in 60% of cases and nonaxial displacement in 48% (Table 9-13). Only 12% of patients in our series had proptosis without nonaxial displacement. The major nasal symptoms experienced were obstruction or epistaxis. The frequency and severity of ocular and orbital symptoms attest to the relatively silent origin and late stage of presentation.

The dominant orbital signs reflect the site of origin and since most arise in the maxillary sinus, upward globe displacement, fullness of the lower lid, infraorbital pain or paresthesia, and distortion of the maxilla are characteristic (Fig. 9-90). In contrast, lesions arising from the ethmoid complex cause outward and downward displacement of the globe. In all of these instances, inflammatory signs may be suggested by injection, chemosis, and edema; however, tenderness and significant rubor are unusual.

Table 9-13. Signs and symptoms of sinus and nasopharyngeal carcinomas. (Total number of patients participating in the study = 25.)

SYMPTOMS AND SIGNS	NUMBER
Ocular and Orbital	
Facial pain and paresthesia	15
Gobe displacement Axial proptosis only (3) Nonaxial component (12)	15
Extra-ocular muscle restriction Subjective diplopia (8)	12
Decreased vision	10
Lid and conjunctival edema	10
Tearing	9
Lid mass	3
Retrobulbar pain	1
Ocular invasion and glaucoma	1
Papilledema	1
Total patients with some eye or orbit symptoms/signs	20
Nasal, Oral, and Neck	
Nasal obstruction	7
Nodes in neck	5
Epistaxis	4
Chronic sinusitis	2
Gum ulcer	1
Vocal cord paralysis	1
Total patients with some nasal, oral, or neck symptoms/signs	17
Other	
Headache	2

Reproduced with permission from Katz SE, Rootman J, Goldberg RA. Secondary and metastatic tumors of the orbit. In: Tasman W. Jaeger EA, eds. Duane's Clinical Ophthalmology. Philadephia: Lippincott-Raven, 1996; chap. 46.

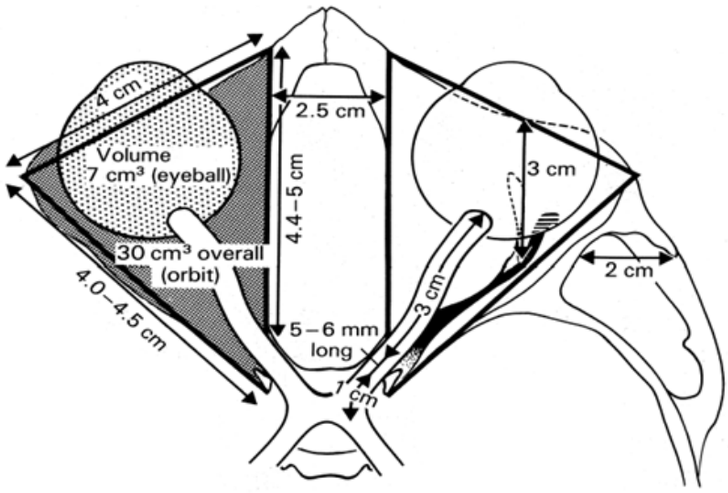

Figure 9-90. A 59-year-old woman presented with a 6-month history of left infraorbital pain and dysesthesia. She was found to have maxillary and antral squamous cell carcinoma and was treated with radiotherapy. Ten months after radiotherapy, she developed severe left ocular and orbital pain associated with tearing and blurred vision. On examination, vision was 20/40 with a fixed mitotic pupil. A firm mass in the floor of the anterior orbit displaced the globe superiorly 5 mm and anteriorly 2 mm. Inferior chemosis, moderate restriction of upgaze, and an intraocular pressure of 30 mmHg (increasing to 40 mmHg on upgaze) were noted. Despite maxillectomy, orbital exenteration, and orbital radiotherapy, the patient had local recurrence and diffuse metastatic disease, and she died 10 months after orbital presentation. (Reproduced with permission from Katz SE, Rootman J, Goldberg RA. Secondary and metatstatic tumors of the orbit. In: Tasman W, Jaeger EA, eds. Duane's Clinical Ophthalmology. 2nd ed. Philadelphia: Lippincott-Raven, 1996; vol. 2; chap. 46.)

Imaging

Radiologic findings consist of either focal or widespread destruction of the sinuses, with invasion of the adjacent structures by a solid tumor mass (Fig. 9-91). The mass is usually large; however, sometimes it may be relatively small when it extends to adjacent structures (Figs. 9-92 and 9-93), particularly in the case of adenoid cystic carcinoma. The sinus and orbit may be the only structures involved, but there is frequently extension to the base of the skull.

Management

Overall, the prognosis has been dismal, with a 5-year survival of approximately 35%. Patients with T3 and T4 staging have had survival rates of 31% and 10%, respectively. Mortality is largely related to the inability to eradicate local disease. Flores and colleagues, reporting on the experience at the British Columbia Cancer Agency, emphasized that during the last decade encouraging results have been obtained with a combination of radiotherapy and surgery in the treatment of epithelial malignancies of the sinuses. Their overall crude 5-year survival for all patients was 46%; a combined treatment consisting of irradiation and surgery in selected patients generated a 5-year survival rate of 74%, as compared with 42% in patients receiving irradiation alone. The important factors in management consist of accurate surgical pathologic staging, a combination of a full course of curative irradiation (60 Gy in 25 treatments over 5 weeks or 50 to 55 Gy in 15 treatments in 3 weeks), and radical surgical resection as the treatment of choice for most paranasal sinus malignancies. In addition, patients with regional nodal disease but without distant metastases are potentially curable and should be treated aggressively. This individualized treatment based on a realistic knowledge of the exact extent of the disease has produced encouraging results in the management of these malignancies.

In recent years, there has been a shift toward preservation of the ocular structures with reconstruction of surrounding

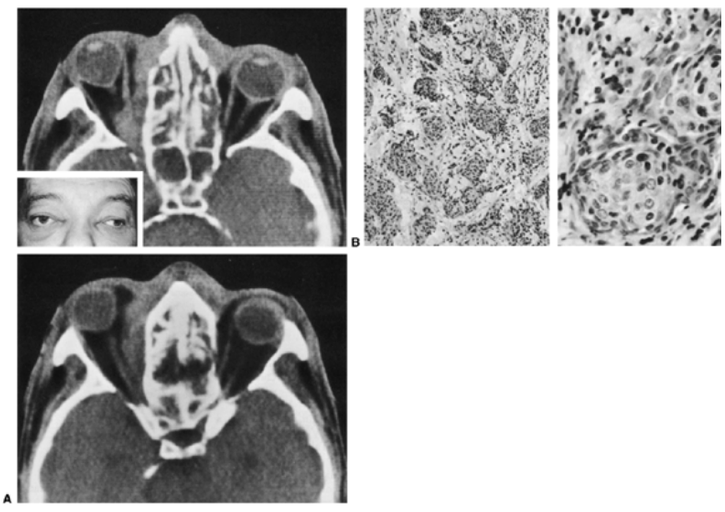

Figure 9-91. (A, inset) This 47-year-old man presented with a progressive right ophthalmoplegia, restriction of medial rectus function, and swelling of the medial canthi and upper lids. In addition, he was aware of some retrobulbar pain and progressive loss of vision on the right. On examination he had vision of 20/200 OD with an afferent pupillary defect, limitation of abduction, and slight proptosis with notable thickening of the base of his nose and medial canthal region. Axial CT scans (A) demonstrate opacification of the ethmoids with multiple subtle focal areas of bone destruction and infiltration of the right orbit and medial canthi bilaterally by a soft tissue mass. (B) Percutaneous biopsy revealed a diffuse, gritty, subcutaneous lesion consisting of cords of neoplastic cells surrounded by a desmoplastic and inflammatory reaction. It was a poorly differentiated neoplasm that had the tinctorial and electron microscopic features of a mucoepidermoid carcinoma (H&E, original magnification; left × 10, right × 25). He underwent radiotherapy and systemic chemotherapy with regression of local disease, but died 1 year later of cerebral extension.

tissues in all instances where possible. This is particularly true where there is evidence of only minimal invasion of the orbit or extraperiosteal involvement.

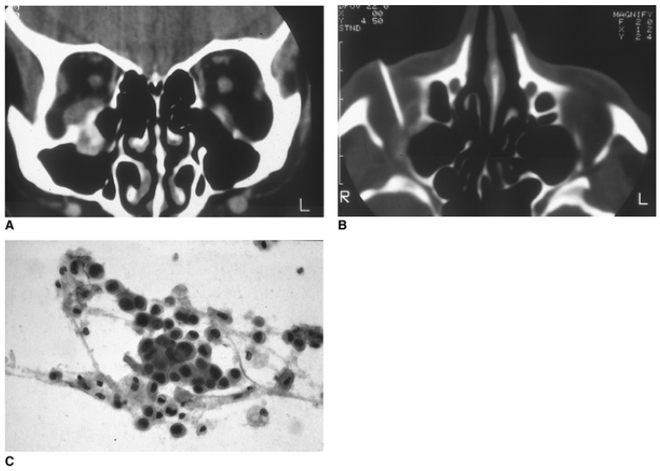

Fig. 9-92. A 73-year-old man presented with a 2-year history of infraorbital numbness and burning sensation, which had progressed to include the supraorbital region, forehead, and lower face during the past 6 months. He had been treated with radiotherapy for prostate carcinoma 7 months before presentation. Examination was significant for proptosis of 2 mm and dysesthesia, including corneal numbness, in all three divisions of cranial nerve V. (A) CT scan revealed a soft tissue mass in the inferior orbit contiguous with the inferior rectus muscle. The lesion extended through the infraorbital canal to involve the pterygopalatine fossa and was associated with soft tissue hanging into the upper portion of the maxillary sinus. (B) An axial CT scan-guided aspiration biopsy was performed and revealed squamous cell carcinoma. Groups of cohesive malignant squamous epithelial cells (C) were noted to have pleomorphic nuclei and abundant eosinophilic to orange cytoplasm, with no features of mucinous differentiation (H&E, original magnification × 100). (Figs. 9-92A and C reproduced with permission from White VA, Rootman J. Orbital pathology. In: Albert DM, Jakobiec FA, eds. Principles and Practice of Ophthalmology. 2nd ed. Philadelphia: WB Saunders, 2000:3816-74.)

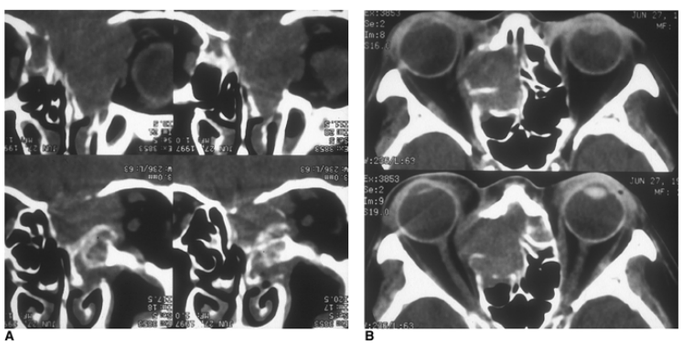

Figure 9-93. (A) These CT scans demonstrate local invasion of the orbit from a recurrent adenocarcinoma of the frontal ethmoid sinus. This occurred in a 75-year-old man who was seen 2 years after craniofacial resection and had a history of multiple intranasal recurrences. He underwent a multidisciplinary cranial, orbital, and ENT microsurgical resection and reconstruction of the periorbita and orbit. The patient is alive and well without recurrence 3 years later.

Tumors Arising from Metaplastic Epithelium

Squamous Cell Carcinomas

Squamous cell carcinomas do not declare themselves clinically until they have breached their sinus of origin in more than 90% of instances. Up to 80% arise within the maxillary sinus, with the ethmoids being the next most common site. The signs and symptoms of maxillary tumors are oral (pain in the teeth, trismus, a full alveolus, and palatal erosion), nasal (obstruction, epistaxis, and chronic sinusitis), ocular (tearing, diplopia, displacement, pain, and proptosis), and facial (paresthesia, swollen cheek, pain, and facial asymmetry). Tumors arising from the posterior portion of the maxillary sinus have a worse prognosis because of proximity to the orbit, cribriform plate, and pterygoid region. In fact, 10% to 22% of squamous cell carcinomas have regional lymph node metastases on initial presentation. Progression and death are usually related to complications of local invasion but approximately 18% develop distant metastases. Histopathologically, the majority of cases consist of moderately well-differentiated keratinizing squamous carcinoma but they may be anaplastic.

Transitional Carcinomas

Transitional carcinomas originate from the schneiderian epithelium of the nasal cavity and paranasal sinuses. The majority of lesions of this histopathologic type are benign papillomas characterized by multiple and multifocal occurrence and local recurrence. Histologically, they may be either papillary (exophytic) or inverted. They occasionally may have ciliated or cylindrical cells. Though recurrent, the large majority of schneiderian papillomas remain benign but a small percentage undergo malignant transformation (7% to 9%), particularly those of the lateral nasal wall or the inverted type. Thus, transitional carcinomas invading the orbit characteristically arise from the ethmoid sinuses or nasopharynx. Treatment is radical surgery, radiotherapy, or both.

Tumors Arising from the Mucoserous Epithelium

Adenoid Cystic Carcinomas

Adenoid cystic carcinomas arise in minor salivary glands and most commonly involve the maxillary antrum and lower nasal cavity. Biologically, these are locally aggressive tumors with extensive limits of involvement (evident in 75% of cases at presentation); they may present as localized masses but are characterized by a course of indolence, recurrence (sometimes over very long periods of time), and ultimately death, usually from spread to contiguous structures. Their hallmark is perineural spread, which accounts for the facial pain noted by many patients, usually in the maxillary division of cranial nerve V. The tumor spreads into the pterygopalatine fossa via the infraorbital nerve and from there to the orbital apex and cranial fossa. The most likely cause of death is relentless and often prolonged local invasion of tumor into the skull base. In addition, 14% of these tumors spread to regional lymph nodes, whereas 40%

have hematogenous metastases. Overall, these are seen in a slightly younger age group than are other sinus and nasopharyngeal tumors, and they are associated with less local reaction in the orbit and more indolent mass effect. In Henderson's series of secondary epithelial neoplasms of the orbit, 22 (85%) of 26 patients with adenoid cystic carcinoma of the sinuses had died (mean secondary survival 7.5 years). The general trend in management is toward less aggressive surgery and to radiotherapy to control local manifestations.

Adenocarcinomas

Adenocarcinomas usually occur more frequently in the sinuses and nasopharynx, typically in the ethmoids, and are seen in unusually high numbers in woodworkers. Their local behavior is similar to that of adenoid cystic carcinoma but development is more rapid. Aggressive surgical treatment is recommended because they are not significantly radiosensitive.

Melanomas

Melanomas rarely occur in the nasopharynx and account for approximately 3.5% of all sinonasal tract neoplasias. They tend to occur in the anterior part of the nasal cavity, presenting as bulbous masses with nasal obstruction and epistaxis. The 5-year survival is 17% to 38% (Fig. 9-94).

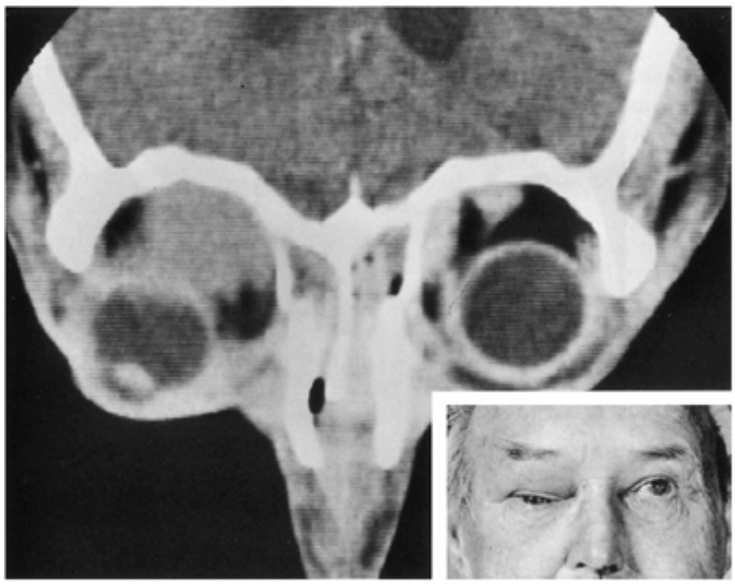

Figure 9-94. This 66-year-old man presented with the sudden development of a superior orbital mass on the right side and a known history of melanoma of the nasopharynx. He had previously been treated on the left side with radiotherapy and had lost vision. Coronal CT scan demonstrates midline involvement and extension of the lesion into the right superomedial orbit and residual tumor in the left superolateral orbit. He was treated urgently with radiotherapy and had local regression of disease, but died 6 months later of disseminated melanoma.

Esthesioneuroblastomas

Esthesioneuroblastomas are rare tumors of neural crest origin that arise from the sensory olfactory epithelium and can invade the cribriform plate, ethmoid sinuses, and orbit. These tumors have a predilection for the young with a peak incidence in the second to third decades, but they do occur with advanced age as well. Histologically, they are made up of sheets of small cells with or without rosettes. They are frequently mistaken for other small cell tumors. Ultrastructurally, they have dense core (neurosecretory) granules and neuritic processes. Olfactory rosettes differing from the Homer-Wright type may be seen in those that demonstrate olfactory differentiation; these are lined by pseudostratified columnar cells with central mucin in the lumina. Neuroblastomas have been divided into two groups based on the presence or absence of olfactory differentiation. The latter group may include ganglioneuroblastomatous differentiation (olfactory neurocytoma). Olfactory neuroblastomatous differentiation occurs in patients with a mean age of 50 years, and the less differentiated neuroblastomatous type occurs in patients with a mean age of 20 years.

In a review of olfactory neuroblastomas by Rakes et al., ophthalmic signs or symptoms occurred in 28 (73%) of 38 cases. The most commonly reported ocular symptoms were periorbital pain, epiphora, decreased vision, and diplopia. Patients presenting primarily with ocular complaints generally have a more advanced tumor stage than those presenting primarily with nasal or nonocular symptoms. The most commonly detected ocular signs included eyelid edema,

proptosis, globe injection, ptosis and cranial nerve palsies, while the most common nonocular signs and symptoms were nasal obstruction, bloody nasal discharge, and headache. Henderson reported surgically proven orbital extension in 6 (23%) of 26 new cases of esthesioneuroblastoma registered at the Mayo Clinic between 1976 and 1987.

These tumors have been staged according to site of confinement: Group A (nasal cavity), Group B (paranasal sinuses), and Group C (extension beyond the sinuses into the cranium or orbit). Elkon et al. have noted 5-year survival rates of 75% (Group A), 68% (Group B), and 28% (Group C). In a review of 26 cases, Levine and coworkers noted a dramatic increase in survival with the advent of aggressive craniofacial surgery and adjunctive radiotherapy and chemotherapy. They recommended combined preoperative radiotherapy and craniofacial resection for Group A and B disease, and the addition of pre- and postoperative antineoplastic agents (vincristine and cyclophosphamide) for Group C disease.

Odontogenic Tumors

Odontogenic tumors (ameloblastoma, ameloblastic fibrosarcoma, and calcifying epithelial odontogenic tumor) and cysts may rarely involve the orbit. Ameloblastomas are locally invasive, benign (2% are malignant) epithelial tumors that arise from the mandible in 80% of cases. Among the remaining 20% that originate from the maxilla, local growth and extension may lead to orbital involvement. Treatment is by local resection, after which about one third of tumors may recur. Radiotherapy is palliative, not curative.

Neuroendocrine Carcinomas

Neuroendocrine carcinomas are rare epithelial malignancies arising in the nose or paranasal sinuses.

Summary

Epithelial malignancies arising from the nose, nasopharynx, and sinuses are characterized by an infiltrative, nonaxial mass effect with significant neurosensory and motor deficit. They are occult neoplasms, and orbital involvement represents a late presentation with a grim prognosis.

Extension of Intracranial Tumors

Meningiomas, which account for 18% of all adult intracranial tumors, are the most common to involve the orbit, and invasion by any other intracranial tumor is exceedingly rare. Most meningiomas that affect the orbital or visual structures arise from the dura of the sphenoid bone (i.e., ridge, planum, parasellar region, or optic canal).

Amongst other primary tumors of the central nervous system, few affect the orbit. Intracranial glioblastoma multiforme is highly malignant and may enter the orbit by gross destruction of orbital bone, extension through the optic canal and superior orbital fissure, or growth through a previous craniotomy site into the scalp and forehead and then over the superior orbital rim into the anterior orbit.

Pituitary tumors and craniopharyngiomas have been rarely described as invading the orbit, but when they do it usually reflects malignancy and skull base invasion.

Tumors of Bone

Tumors of bone may affect the orbit and are described elsewhere in this chapter. One in particular, the chordoma, when it occurs in the skull base, is often relentless, slow-growing, locally malignant, and midline; thus they grow into the nasopharynx or orbits (Fig. 9-95).

Meningeal Spread of Central Nervous System Tumors

Other meningeal tumors that have involved the optic nerve and sometimes the orbit are leukemic infiltrations and generalized carcinomatous meningiomatosis. Leukemia can affect the central nervous system and thus the optic nerve and eye, usually in the late stages. The optic nerve head is frequently affected, but leukemia may independently deposit in the arachnoid of the sheath as part of a widespread meningeal process. With carcinomatous meningiomatosis, the patient typically presents with papilledema, a known history of carcinoma, and negative CT scan findings because of widespread superficial involvement of the meninges without significant mass effect. Little et al. found no history of malignancy in 14 (48%) of 29 cases of meningeal carcinomatosis. The diagnosis may be more apparent on a gadolinium enhanced MRI and can be confirmed by cytologic examination of the cerebrospinal fluid. We have encountered three cases of meningiomatosis due to metastatic tumors: two in patients with breast carcinoma and one in a patient with malignant melanoma of the skin. In all instances, the diagnosis was made on the basis of the cytologic results of a cerebrospinal fluid tap in the presence of a normal CT scan.

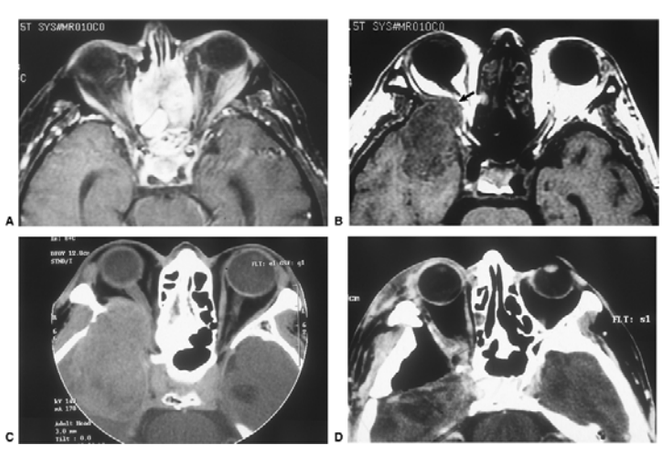

Fig. 9-95. This 67-year-old man presented in 1999 with a history of having had an extensive, midline, solid chordoma, which is shown on T1-weighted, fat-suppressed MRI as a hyperintense midline mass (A). This had been resected in 1994. In June 1996, he developed headaches, cranial nerve VI, X, XI, and XII involvement due to a recurrent clivus chordoma, which was then resected and irradiated. He presented in February 1999 with recurrent right lateral orbital and middle cranial involvement (B). The mass impinged on the temporal lobe, as shown on T1-weighted MRI (B, arrow). (C) CT scan demonstrates bone destruction and a large temporal mass. He underwent a combined orbitocranial resection, as demonstrated in the postoperative CT scan (D). He is alive and well without recurrence to date.

We have seen two cases of primary neoplasia of the central nervous system extending into the optic nerve. One was a medulloblastoma that spread bilaterally along the optic nerves, and the other was a dural melanoma of the spinal cord that subsequently presented as a large mass extending into the orbit around the peripheral and optic nerve structures. Both were diagnosed by aspiration needle biopsy of the affected nerve sheath (Fig. 9-96).

Large cell lymphomas of the central nervous system are prone to ocular involvement, often presenting as papillitis or uveitis with vitritis. There are, however, instances where lymphomas of the central nervous system may spread throughout brain via the cerebrospinal fluid in the subarachnoid space and even invade the dura. Finally, some of the lymphomas, particularly myeloma and plasmacytoid tumors, may involve the bones of the orbit.

Orbital Extension of Eyelid Tumors

Eyelid tumors accounted for 26 (13%) of 194 secondary orbital invasion in our series. Any primary tumor of the skin and ocular adnexa may invade the orbit for the following reasons: (1) late presentation; (2) multiple recurrence following incomplete excision (as is the case with basal cell carcinoma); (3) more rapid and aggressive growth (as in some squamous cell carcinomas); (4) insidious onset that masquerades as some other condition (as in the case of sebaceous carcinoma), and (5) perineural spread as in some squamous cell carcinomas and melanomas. There is a large variety of unusual and rare adnexal tumors that may affect the skin of the lid and rarely invade the orbit, but basal cell, squamous cell, and sebaceous carcinomas represent the most important and common epithelial malignancies of the lid that extend in this fashion.

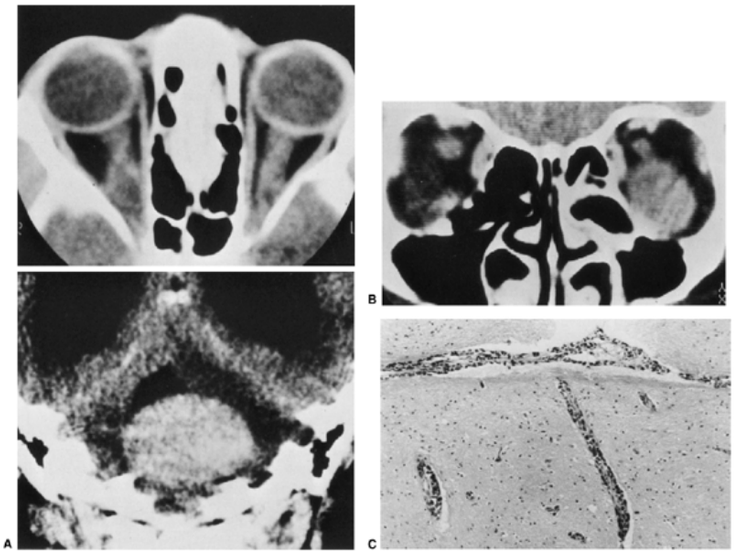

Figure 9-96. (A, top) Axial CT scan demonstrates bilateral enlargement of the optic nerves. This occurred in a 5-year-old girl who had been treated (radiotherapy and resection) 6 months earlier for a medulloblastoma, shown in the coronal CT scan (A, bottom). She presented with hand movements vision and an afferent pupillary defect on the right and 20/30 vision on the left. In addition, there was right optic atrophy with some slight pallor of the left disk. Aspiration needle biopsy of the right optic nerve revealed the presence of medulloblastoma. Coronal (B) CT scan demonstrates a large, well-defined left inferior orbital mass. The patient was a 45-year-old woman who presented with proptosis that had developed over a 2-month period. Several months earlier, she had undergone surgery for a dural melanoma of the spinal cord. Aspiration needle biopsy of the orbital tumor revealed cells consistent with the melanoma removed from the dura. The patient died within 1 week of diagnosis. (C) Autopsy showed diffuse involvement of the meninges with extension into the subarachnoid sheath of the optic nerve and around peripheral nerves of the orbit (H&E, original magnification × 25).

Basal Cell Carcinoma of the Lid

Basal cell carcinoma accounts for more than 80% of malignant eyelid tumors. In most series, however, its frequency in terms of orbital invasion equals squamous cell carcinoma, reflecting the more aggressive nature of squamous cell carcinoma. The indolent and painless course of basal cell carcinoma (median duration about 3 years at presentation) may contribute to late presentation with orbital invasion, usually as a part of advanced disease, recurrence, or a morpheic (sclerosing) variant.

These carcinomas generally occur in the fifth to eighth decades with a male predominance, although approximately 3% of lesions occur in persons less than 35 years of age. Overall, 52% are seen in the lower lid, 27% in the inner canthus, 15% in the upper lid, and 6% in the outer canthus. Orbital extension is more common with inner canthal lesions because of the anatomic intimacy of bone and lacrimal system, as well as the propensity for surgeons to under treat lesions in this locale to avoid damaging the lacrimal apparatus. With modern controlled techniques of management, orbital extension from this site is no more frequent than from any other site.

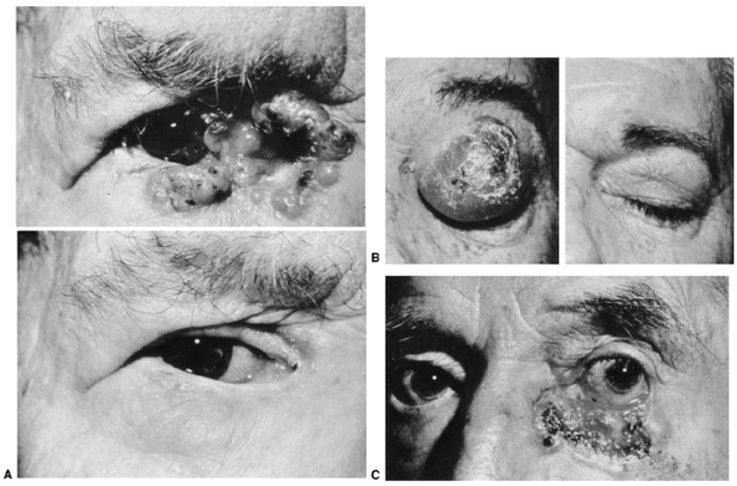

Figure 9-97. Advanced basal cell carcinoma of the lid in three different patients. (A) This 71-year-old man presented in 1971 with an extensive ulcerated medial canthal lesion (A, top). Note the large, nodular, pearly, raised edges. For the previous 3 years, he had noted a “boil” that constantly broke down and gradually increased in size. It was treated with 5000 rad over 22 days (A, bottom). The disease recurred 2 years after presentation, which was managed with local surgery. When last seen in 1977, he had no evidence of recurrent disease. (B) This 62-year-old man presented to the British Columbia Cancer Agency in 1965 with a large cystic basal cell carcinoma (B, left) He underwent radiotherapy with 4000 rad over 10 days with remission (B, right). He had no evidence of recurrence over the next 9 years, when he died of an unrelated esophageal stricture. (B, right) Photograph of the patient taken 1 year after radiotherapy. (C) This 76-year-old chronic alcoholic presented with an ulcerated lesion of the left lower lid. It had been present for 20 years and ulcerated for 2 years. He received 4500 rad over 23 days. He had no recurrence of local disease over the next 11 years, when he died of chronic obstructive pulmonary disease.

The majority of basal cell carcinomas have a typical clinical picture, starting as pearly, raised nodules that develop central ulceration and characteristically extend radially. These can ultimately ulcerate and erode through adjacent tissues, producing grotesque local disfigurement, yet they generally do not metastasize (Fig. 9-97).

There are a large number of histologic variants, including solid (majority), adenoid, keratotic, mixed, and sclerosing (morpheiform). The sclerosing variety has a notorious reputation for extension, largely because it has clinically and pathologically indistinct margins. Clinically, the only clue to extension may be a tendency for the overlying skin to appear pale, very thin, and slightly telangiectatic with loss of adnexa (i.e., cilia). Histopathologically, these lesions consist of minute cords of cells in a dense, fibrous stroma.

Invasion of the orbit usually occurs after incomplete and often multiple excisions. It is heralded by infiltrative features affecting the anterior structures, including extraocular movement restriction, cicatrization and induration of the lid structures, and fixation to adjacent bone. Henderson has noted that the soft tissues of the lid are frequently involved in a circumferential manner before deep orbital invasion occurs.

The management of basal cell carcinoma with orbital invasion demands a firm resolve to use radical therapy that incorporates the entire lesion. Wide excision should be controlled by pathologic confirmation of free borders and may require exenteration, bony removal, and even extirpation of dura. Reconstruction may require a craniofacial surgical team. Leshin and Yeatts reported a success rate of greater

than 95% with excision of basal cell carcinoma using Mohs' microscopic surgical technique in a large series. Anscher and Montano had equal success with modern radiotherapy techniques, particularly in treating smaller lesions. Avoiding surgery that could be cosmetically disfiguring may be advantageous for persons unwilling or medically unfit for surgery.

Chemotherapy with cisplatin alone or in combination with doxorubicin has been used primarily to decrease tumor size before local excision and in conjunction with radiotherapy for patients who refuse or must delay exenteration.

Squamous Cell Carcinoma of the Lid and Adnexa

Squamous cell carcinoma accounts for 7% to 9% of all malignant eyelid lesions. The major predisposing factor is sun exposure in fair-skinned persons, but exposure to carcinogenic agents (e.g., arsenic, irradiation, psoralen-ultraviolet A [PUVA]) as well as genetic factors (e.g., xeroderma pigmentosum) may have a role.

The clinical signs of squamous cell carcinoma develop faster (mean 1 year) than those of basal cell carcinoma, and consist of focal hyperkeratotic lesions that slowly extend and ulcerate. They are more common at the lid margin and in the lower lid by a ratio of 1.4:1. Rarely, papillary forms may be seen. Orbital extension of squamous cell carcinoma is usually associated with long-term neglect by the patient or by a history of chronic and repeated recurrence of lesions following treatment. Once the orbit is invaded, the tumor tends to spread along fascia and fatty planes relatively rapidly compared with basal cell carcinoma. Perineural invasion, even with small or cryptic primaries, may occur and is associated with pain or ophthalmoplegia (Fig. 9-98). Also in contrast to basal cell carcinoma, squamous cell carcinoma is capable of metastasis, usually to the regional preauricular or submandibular lymph nodes. The incidence of regional spread varies from 1% to 21%, but is generally closer to the lower figure. The overall mortality rate is about 15%. Management of squamous cell carcinoma of the lid is usually surgical, with care being taken to obtain adequate controlled margins with the use of frozen sections or Mohs' technique. Fitzpatrick et al. reported a control rate of 93% with radiotherapy; however, squamous cell carcinoma is thought to be less sensitive to radiotherapy than basal cell carcinoma, so higher doses are usually recommended. For deep orbital invasion, radical therapy (either exenteration or radical radiotherapy) is indicated.

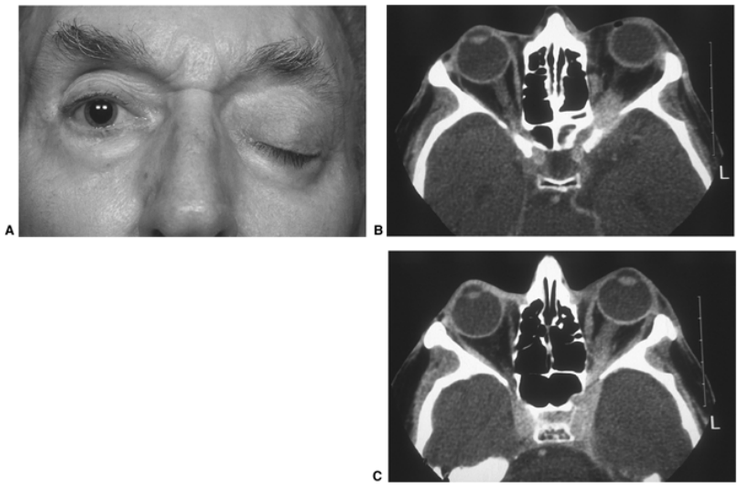

Figure 9-98. (A) This 83-year-old man presented with complete left ptosis. He had undergone two excisions, 3 years previously, of a left supraorbital squamous cell carcinoma. He developed progressive pain and tingling in the forehead, vertical diplopia, and finally general malaise lasting 18 months, ultimately requiring hospitalization. He was treated with corticosteroids for presumed Tolosa-Hunt syndrome and was discharged after showing minimal improvement. Over a 2-month period, he developed decreased vision, ptosis, and bulging of the eye. On presentation, his vision was 20/80 with a relative afferent pupillary defect. There was hypesthesia in the distribution of cranial nerve V1 and hyperesthesia in V2. He had a palpable fixed cord in the forehead in the distribution of the supraorbital nerve, complete ptosis, ophthalmoplegia, and 7 mm of proptosis. CT scan showed local infiltration along the supraorbital nerve with extension of a soft tissue mass along the orbital roof to the orbital apex (B), through a widened superior orbital fissure, and into the cavernous sinus (C). Orbital biopsy revealed cords of squamous cells and evidence of infiltration of a small branch nerve sheath. A single fraction of 10 Gy was given as palliative treatment for pain control. (Reproduced with permission from Katz SE, Rootman J, Goldberg RA. Secondary and metatstatic tumors of the orbit. In: Tasman W, Jaeger EA, eds. Duane's Clinical Ophthalmology. 2nd ed. Philadelphia: Lippincott-Raven, 1996; vol. 2; chap. 46.)

Sebaceous Carcinoma of the Ocular Adnexa

Sebaceous carcinoma represents 1% to 5% of all eyelid malignancies, where it occurs more commonly than elsewhere in the body. Of epithelial malignancies invading the orbit, about one third are sebaceous carcinomas. It is more prevalent in Asian populations. The upper lid is the usual site in approximately two thirds of the cases; about 20% involve the lower lids or are diffuse, and a small percentage involve the caruncle. It is a neoplasm of the elderly (peak occurrence in the seventh decade) and has a slight female predominance.

Sebaceous carcinoma is notoriously difficult to diagnose correctly in the early stages. It may masquerade as a chronic chalazion, blepharoconjunctivitis, basal cell carcinoma, keratoconjunctivitis, or very rarely as a primary orbital tumor. Another reason for confusion has been pathologic misdiagnosis, most commonly being mistaken for basal cell or squamous carcinoma. Increasing awareness of the characteristic presentation, along with earlier and more accurate clinical and pathologic diagnosis, has decreased the mortality associated with this tumor. The blepharoconjunctivitis associated with this lesion is the result of intraepithelial (pagetoid) spread. The usual clinical appearance is a thickening of the conjunctiva associated with frank injection in areas of invasion (Fig. 9-99). A careful biomicroscopic examination reveals yellowish, plaque-like foci within the affected epithelium.

The incidence of orbital extension varies from 6% to 35% in large series and is associated with a 70% mortality rate. These tumors have a propensity to spread to the lymphatic system and subsequently to the lung, liver, brain, or skull. Seventy percent of those that extend into the orbit have preauricular, cervical, or submaxillary adenopathy, compared with an overall incidence of approximately 19% for all sebaceous gland carcinomas of the lid and adnexa.

The pathologic diagnosis is based on evidence of sebaceous origin. They are usually lobular or consist of cords of cells with a varying degree of sebaceous differentiation and infiltration. The degree of differentiation tends to progress from the periphery toward the center of lobules, mimicking the normal pattern of sebaceous glands. Cells that are differentiated have a foamy or vacuolated, slightly basophilic cytoplasm. In contrast, the less differentiated tumors have cells that are more deeply basophilic and anaplastic, and have more mitotic figures. The peripheral location of the basophilic, less vacuolated cells produces a pattern similar to basal cell carcinoma, but the cells are more anaplastic. Sebaceous carcinomas have a propensity toward pagetoid spread, invading the basal layers of skin and mucous membranes in a radial fashion. These tumors characteristically contain fat; thus, frozen sections and fat stains are useful in diagnosis and at the time of controlled resection.

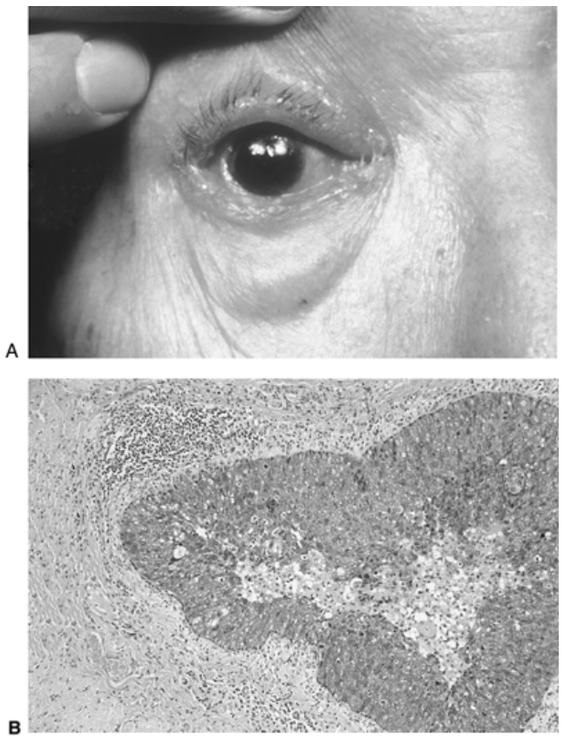

Figure 9-99. (A) This 79-year-old man presented with a chronic history (several years) of a lid lesion treated variably as inflammatory. He had almost total symblepharon and thickened, brawny, immobile upper and lower lids, which was associated with a few pale yellowish infiltrations of the lid margins. (B) Biopsy of his lesion demonstrates a cord of infiltrating sebaceous carcinoma with typical features of central or apical necrosis of the sebaceous cells (H&E, original magnification × 10). (Fig. 9-99B reproduced with permission from Katz SE, Rootman J, Goldberg RA. Secondary and metastatic tumors of the orbit. In: Tasman W, Jaeger EA, eds. Duane's Clinical Ophthalmology. 2nd ed. Philadelphia: Lippincott-Raven, 1996; chap. 46.)

The overall 5-year mortality rate for sebaceous carcinoma of the lids is approximately 15%. The clinical and pathologic features associated with a bad prognosis are vascular or lymphatic invasion, upper and lower lid involvement, orbital invasion, poor differentiation, pagetoid invasion, tumors larger than 10 mm, multicentric origin, infiltrative pattern, and duration of symptoms more than 6 months.

Sebaceous carcinoma of the lid is best managed surgically. Doxanas and Green emphasized the improvement in mortality afforded by early recognition and wide excision with frozen-section control. Although microscopically controlled excision may be attempted in orbital invasion, this circumstance usually necessitates exenteration. The frequent association with lymphatic spread suggests a need to assess spread, obtain histologic proof of involvement, and carry out radical resection of parotid, submaxillary, and cervical nodes. Several reports on radiotherapy indicate that when given in adequate doses (generally more than 45 Gy), this tumor can be treated in patients who refuse to undergo excision or who have contraindications to surgery. In addition, it is a useful palliative treatment.

Malignant Melanoma of the Skin

Malignant melanoma from the skin of the lid is exceedingly rare, constituting 1% of all malignant eyelid lesions, less than 1% of secondary orbital tumors, and less than 0.2% of cutaneous melanomas involve the eyelids. We encountered only one melanoma arising from the skin of the lid that led to orbital invasion and required exenteration. Comparatively, conjunctival melanoma is a more common precursor of orbital invasion, perhaps because of later recognition and contiguity.

Clark and associates are primarily responsible for the classification and framework of our understanding of the biologic behavior of cutaneous melanomas. Most melanomas arise de novo but some are thought to develop from preexistent moles. There are three recognizable precursor lesions. The most important in terms of the lid is *lentigo maligna* (Hutchinson's melanotic freckle), followed by *dysplastic nevus* (B-K mole) syndrome and *giant nevocytic nevi.* Giant nevocytic nevi are childhood lesions that rarely occur in the scalp and are readily recognized. The dysplastic nevus may occur either as an autosomal dominant or sporadic trait that is first noted in childhood and progresses throughout life. These patients are at high risk for cutaneous melanomas. The major features that differentiate these nevi from others are their multiple early occurrence, large size (generally over 5 mm to 10 mm), and flat, irregular surface and margins with haphazard pigmentation.

Melanomas are thought to undergo two phases of growth, a radial intraepidermal extension followed by vertical growth into the deeper layers of the skin. Nodular melanomas are the exception to this biphasic pattern, since they have no clinically discernible radial growth phase. Cutaneous melanomas have been divided into four different types based on patterns of clinical development and histopathology: superficial spreading melanoma (70%), nodular melanoma (de novo, 16%), acral lentiginous melanoma and others (9%), and lentigo maligna (5%).

Superficial spreading melanoma can occur anywhere but is more common in the areas exposed to intermittent and sudden bursts of sun, such as the lower legs of women and the chest and back of men. These appear as raised nodules, 2 to 3 cm in diameter, with bizarre coloration varying from black or brown to rose. Characteristically they have an irregular border. *Nodular melanoma* is a relatively rapidly developing focal tumor without clinically perceptible antecedent radial growth. It may be brown to black or amelanotic and can involve exposed areas of skin or mucous membrane. It invades more deeply than the other types of skin melanoma. *Acral lentiginous melanoma* occurs primarily in the distal extremities or mucosal surfaces, particularly vaginal mucosa. *Lentigo maligna* usually arises in middle-aged and elderly persons with sun-damaged facial skin. Clinically, they are usually large, irregular, pale brown patches with a fine, peppered distribution of increased pigmentation. The lesions usually have a long history of radial extension, which may wax and wane. It is believed that 25% to 30% undergo malignant transformation, which is heralded by the development of nodular, elevated black or brown areas.

The prognosis correlates with the depth of penetration and clinical stage. The revised staging system for malignant melanoma is based on the measured depth of invasion (in millimeters), Clark level, and the presence of nodal or distant metastases (Table 9-14). Stage IA primary cutaneous melanomas treated with wide excision are associated with a 95% 10-year survival, whereas distant metastases are common in stage IIB (50% survival) and stage III (60% to 85% survival). Other factors indicative of poor prognosis include tumor type (nodular worse than superficial spreading), amelanosis, and lack of inflammation.

With increasing awareness of epidemiologic factors (e.g., ultraviolet light, fair skin, hair color) and the nature of melanoma types and premelanotic lesions, the emphasis is shifting to prevention and early identification. Because melanomas have a propensity to regional nodal and widespread systemic metastases, treatment is wide local excision with or without nodal resection or systemic chemotherapy. The role of node dissection is controversial, and chemotherapy remains palliative.

Table 9-14. Staging system for malignant melanoma of the eyelid (American Joint Committee on Cancer)

STAGE	CRITERIA	TNM
IA	Localized melanoma < or equal to 0.75 mm and invades the papillary dermis (Clark's Level II)	T1N0M0
IB	Localized melanoma 0.76-1.5 mm and/or invades to the papillary-reticular dermal interface (Clark's Level III)	T2N0M0
II	Localized melanoma 1.5-4 mm and/or invades the reticular dermis (Clark's Level IV)	T3N0M0
IIIA	Localized melanoma >4 mm and/or invades the subcutaneous tissue and/or satellite(s) within 2 cm of the primary tumor (Clark's Level V)	T4N0M0
IIIB	Metastasis < or equal to 3 cm in any regional lymph node(s)	Any T, N1M0
IIIC	Metastasis >3 cm in any regional lymph node(s) and/or in-transit metastasis*	Any T, N2M0
IV	Distant metastasis	Any T, any N, M1

* In-transit metastasis involves skin or subcutaneous tissue more than 2 cm from the primary tumor not beyond the regional lymph nodes.

Reproduced with permission from Katz SE, Rootman J, Goldberg RA. Secondary and metastatic tumors of the orbit. In: Tasman W, Jaeger EA, eds. Duane's Clinical Ophthalmology. Philadelphia: Lippincott-Raven, 1996; chap. 46.

Other Adnexal Tumors

Merkel cell carcinoma is an uncommon eyelid neoplasm. Overall, 50% of these tumors occur in the head and neck region and 10% in the eyelid or periocular region. It generally appears near the lid margin as a bulging reddish lesion with overlying telangiectatic vessels in the elderly (sixth to seventh decades). The tumor may mimic lymphoma or undifferentiated carcinoma, and the diagnosis can be confirmed by the characteristic immunocytochemical and electron microscopic features. Merkel cell carcinoma is associated with local recurrence and satellite lesions in one third of cases, regional nodal metastases in two thirds, and distant metastases and death in about one half. Orbital invasion is generally associated with tumor recurrence and may lead to intracranial spread. Because chemotherapy and radiation for distant metastases is only palliative, early aggressive surgical excision with wide margins and postoperative radiotherapy are recommended.

The adnexa may also give rise to rare apocrine and eccrine carcinomas that may invade the orbit. This includes the *mucinous sweat gland adenocarcinoma,* which tends to occur in the elderly and rarely invades the orbit and adjacent structures (there are only five reported cases). An unusual and exceedingly rare eccrine adenocarcinoma with a tendency for orbital invasion is the *infiltrating signet-ring carcinoma.* Because of its histiocytoid appearance, metastases from other sites (especially breast) should be ruled out. Finally, *apocrine gland carcinomas* arise from the gland of Moll. At least one case of orbital invasion by this locally aggressive tumor has been reported.

Secondary Tumors Arising from the Conjunctiva

Conjunctival neoplasms accounted for 16 (8%) of 194 secondary orbital neoplasms in our series, consisting of 9 melanomas and 7 squamous cell carcinomas. These two tumors constitute the vast majority of conjunctival neoplasms that invade the orbit.

Squamous Cell Carcinoma of the Conjunctiva

Conjunctival squamous cell carcinoma usually occurs at the limbus, arising in a preexisting carcinoma in situ, solar keratosis, or epithelial dysplasia. It is indolent and seen primarily in men in the sixth and seventh decades. It is believed to arise secondary to longstanding actinic exposure or chronic irritation; thus in the tropics it is more often seen in young adults.

The initial clinical appearance is a whitish, rough, dry, irregular leukoplakic lesion or a telangiectatic, gelatinous,

epibulbar mass. In rare instances, these tumors may be papillary, exophytic, or fixed to the underlying sclera. When confined to the conjunctiva, it can masquerade as conjunctivitis (Fig. 9-100). The usual course is superficial invasion and slow growth because the majority are well-differentiated tumors. It may be locally aggressive and invade intraocularly in less than 10% of cases (this more commonly occurs in mucoepidermoid carcinomas of the conjunctiva), and in about an equal percentage of cases, orbital invasion or nodal metastases occur. Orbital invasion may be heralded by the development of a mass lesion with fixation of the globe. In addition, because these lesions develop insidiously, patients may present with draining fistulas (Fig. 9-101) or apparent orbital cellulitis (Fig. 9-102). Orbital invasion may follow multiple attempts at excision. In underdeveloped countries, higher rates of orbital invasion and metastases have been noted because of late presentation. Even with orbital invasion, death from metastases is exceedingly rare.

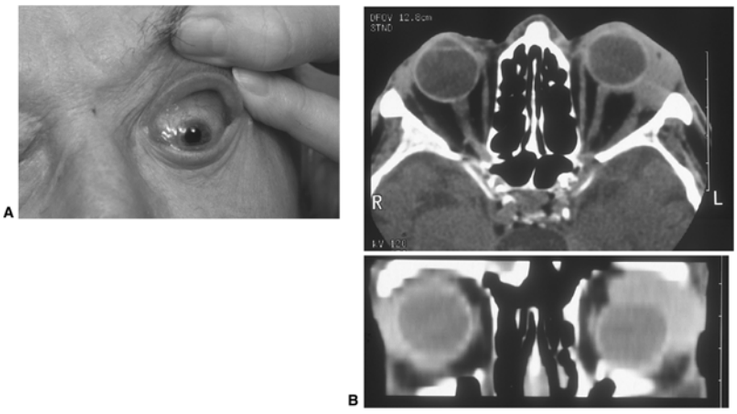

Figure 9-100. (A) This 91-year-old man presented with a 1-year history of left retrobulbar pressure. In addition, he was aware of left supraorbital pain, proptosis, and diplopia. On physical examination, there was 4 mm of proptosis, 4 mm of inward displacement, and marked restriction of movement in all fields of gaze on the left. There was a firm, palpable superotemporal mass (B). This was associated with a subconjunctival salmon patch and conjunctival injection, which was thought to be conjuncivitis. Biopsy revealed a squamous carcinoma that arose from the conjunctiva. He underwent exenteration and was alive and well 2 years following surgery.

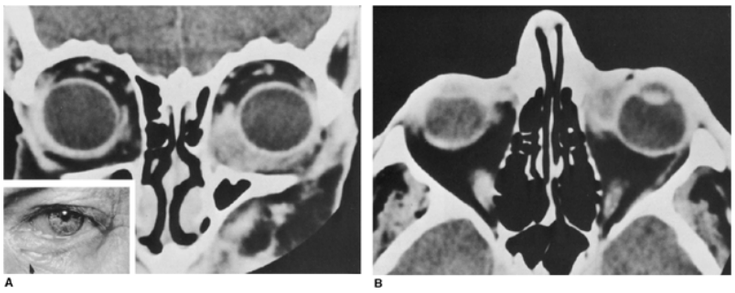

Figure 9-101. (A, inset) This 61-year-old man presented with a chronic fistula (arrow) of the left lower lid and medial canthal region. It was associated with limitation of abduction and a palpable mass in the inferomedial orbit. The coronal (A) and axial (B) CT scans demonstrate an inferomedial infiltrating orbital mass. On biopsy, it proved to be a poorly differentiated squamous cell carcinoma arising from mucous epithelium of either the conjunctiva or lacrimal sac. The patient refused exenteration, and underwent radical radiotherapy with regression of the lesion.

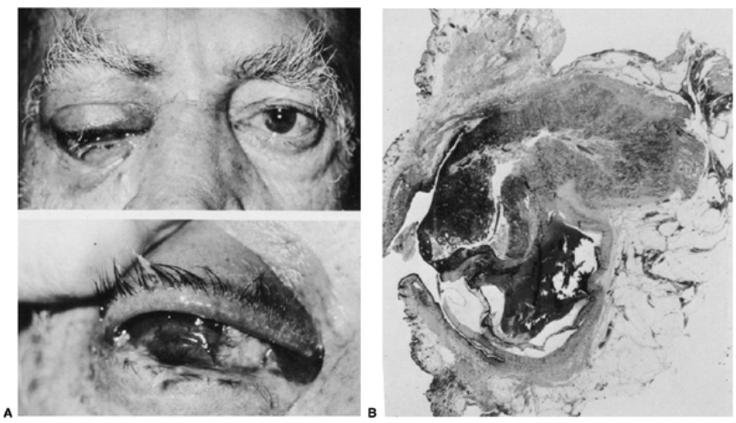

Figure 9-102. (A) This 64-year-old chronic alcoholic presented with a 4- to 5-day history of a painful right eye and proptosis. He claimed to have had no vision in his right eye for years and had recurrent infections in the same eye, which usually responded to minimal conservative treatment. On this occasion, in spite of local antibiotic treatment, there had been no response. On examination, there was 6 mm lateral, 8 mm inferior, and 9 mm axial displacement of the right eye with fullness of the upper lid and erythema of the overlying skin. There was restricted extraocular movements, a purulent discharge, and a boggy, indurated, red, superior conjunctiva. Biopsy of the conjunctiva revealed a well-differentiated squamous cell carcinoma. The patient underwent exenteration after CT scan demonstrated orbital involvement, and he had no evidence of local lymph node or systemic disease. The photomicrograph (B) demonstrates a well-differentiated squamous cell carcinoma infiltrating deeply into the orbit, and invading and perforating the globe (H&E, original magnification × 2). The patient has been observed without recurrence for 6 years. (Reproduced with permission from Rootman J, Roth AM, Crawford JB, et al. Extensive squamous cell carcinoma of the conjunctiva presenting as orbital cellulitis: the hermit syndrome. Can J Ophthalmol 1987;22:40-88.)

The majority are well-differentiated squamous cell carcinomas. The two more aggressive variants, spindle cell carcinoma and mucoepidermoid carcinoma, have a greater tendency to invade the orbit. A pigmented variant of ocular surface squamous cell carcinoma has been described.

Local lesions of the conjunctiva can be treated adequately with histologically controlled conjunctival resection, with or without superficial sclerectomy. In addition, local cryotherapy is useful adjunctively in the management of these lesions. Recurrence rates after excision average 30%, but may be as low as 5% if free surgical margins are obtained. Local excision combined with brachytherapy has also been proposed in selected cases. Topical mitomycin C has also been used in the treatment of squamous cell carcinoma of the conjunctiva, as has topical 5-fluorouracil. Massive conjunctivectomy may be necessary for more rapidly developing and diffuse lesions, whereas orbital extension requires exenteration. Evidence of regional nodal involvement

should be managed with radical node dissection. Radical radiotherapy may be considered for the elderly or for extensive lesions.

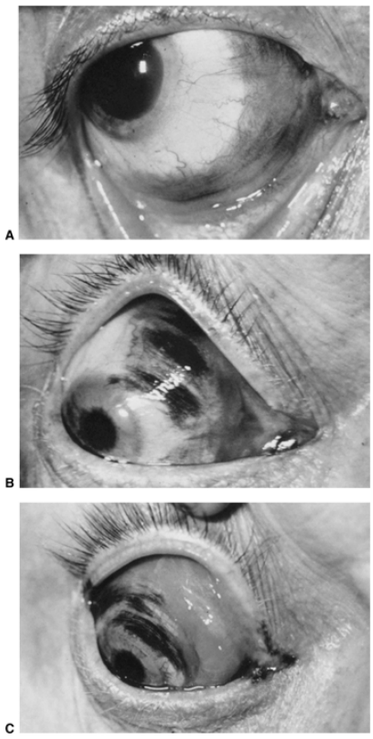

Figure 9-103. This 59-year-old man was referred after having noted a red right eye over a 2-month period. (A) He had been observed for 4 years prior to presentation with a progressive pigmented lesion. (B) demonstrates the lesion 2 years prior to presentation. (C) Upon referral, he was noted to have a large nodular melanoma involving the entire superior fornix. Biopsy revealed a stage IIB diffuse nodular melanoma arising from primary acquired melanosis. He underwent exenteration, and at follow-up 6 years later was alive and well.

Malignant Melanoma of the Conjunctiva

Primary malignant melanoma of the conjunctiva is much less common than intraocular or skin melanomas. In Henderson's series, orbital extension from intraocular melanomas outnumbered extension from conjunctival melanomas by a ratio of 23:4.

Conjunctival melanomas may arise in primary acquired melanosis, from preexistent nevi, or as de novo lesions, and it may be difficult to ascertain the precursor lesion. Many series suggest that approximately 50% arise in primary acquired melanosis, 25% from nevi, and 25% as de novo lesions, although Folberg et al. suggests that primary acquired melanosis is present in 75% of cases.

Primary acquired melanosis is typically a lesion of middle-aged whites and is extremely rare in the younger population. The natural history begins with the development of superficial epithelial involvement with a characteristic peppered distribution of variegated pigment. These lesions can evolve over many years, extending in a radial fashion over larger areas of conjunctiva and skin. In addition, they may wax and wane over time. Ultimately, nodular melanomas may arise within primary acquired melanosis, invade deeper tissues, and metastasize (Fig. 9-103). Biopsy of primary acquired melanosis may help to predict the ones that are prone to progression. Folberg et al. found that primary acquired melanosis with cytologically atypical melanocytes progresses to melanoma in 46% of cases, whereas primary acquired melanosis without atypia does not progress to melanoma.

Malignant melanomas arising from nevi usually appear as a change in known pigmented lesions of the conjunctiva, but it may be impossible to establish a clear clinical history of a preexisting history of nevus. At the time of excision of a melanoma, however, nevoid rests are seen histologically in about one third of cases and are noted in about one quarter of melanomas in primary acquired melanosis. Development of a melanoma from a nevus may be heralded by increasing nodularity, variegated pigmentation, bleeding, or inflammation (Fig. 9-104).

Melanomas arising de novo in conjunctiva parallel the so-called nodular melanoma of skin in that a clinically and histologically recognizable radial growth phase is not noted. Epibulbar melanomas arising de novo can be ulcerative, amelanotic, papillary, or fungating. It is important to be

aware of the possibility of satellite lesions in the conjunctiva and local lymphatic spread, which should be sought carefully on a prospective basis (Fig. 9-105).

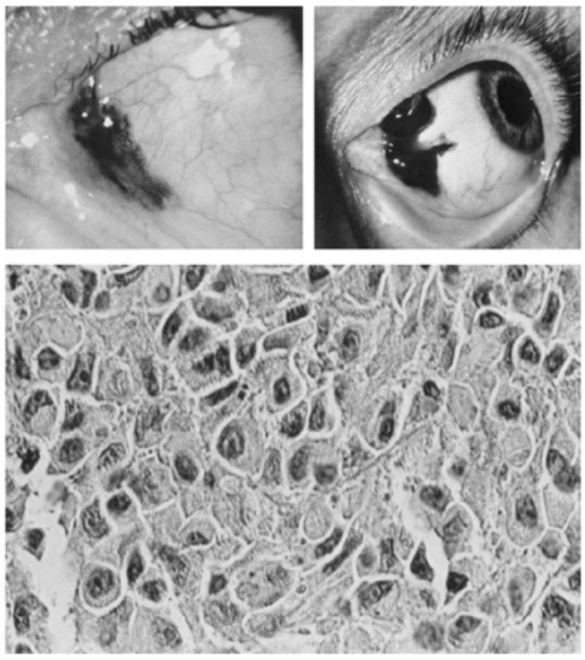

Figure 9-104. This 61-year-old man was referred with the lesion shown (top, right). He had been aware for many years of a pigmented lesion in the medial canthal region. (Top, left) The lesion is shown 6 years earlier. At the time of referral, the lesion had been bleeding intermittently. It was a nodular malignant melanoma, and he underwent resection, cryotherapy, and reconstruction of the medial canthal region. However, he developed a local recurrence 1 year later that required exenteration. He is alive and well with 4 years' follow-up. (Bottom) Histologically, the anaplastic lesion appeared to have arisen from a nevus, which is not shown (H&E, original magnification × 40).

In a recent clinicopathologic study of 256 cases of conjunctival melanoma, Paridaens et al. found 5- and 10-year survival rates of 83% and 69%, respectively. The following prognostic factors associated with a higher mortality are listed in increasing order of risk:

Twofold risk:	Tumors in unfavorable locations (e.g., palpebral conjunctiva, fornices, plica, caruncle, lid margins)
Threefold risk:	Mixed cell types compared with pure spindle cell types
Fourfold risk:	Histologic evidence of lymphatic invasion; initial thickness greater than 4 mm for tumors in unfavorable locations only (Fig. 9-105)
Fivefold risk:	Multifocal tumors in patients with lesions in favorable (epibulbar) locations only.

Our understanding of premalignant and malignant melanocytic lesions of the conjunctiva has advanced considerably in recent years, which, along with biopsy and treatment of potentially aggressive lesions, should lead to decreased morbidity and mortality. The primary treatment for conjunctival malignant melanoma is wide surgical excision combined with cryotherapy. Even extensive conjunctival disease is amenable to removal of the nodular component and repeated local treatment with cryotherapy. Lederman et al. reviewed a series of 184 melanomas of conjunctiva treated with radiotherapy and found that lesion site, macroscopic appearance, and type of lesion bear significantly on the type of treatment and likelihood of response. Limbal tumors arising from nevi respond well, nodular de novo melanomas respond poorly, and widespread malignant acquired melanosis responds less well than localized lesions. For superficial lesions and marginal residuum, we have also used Strontium-90 plaque treatment in doses of 5500 rads over a 1-week period. More recently, mitomycin C has been introduced as a method of treating primary acquired melanosis and early melanoma.

Significant orbital invasion requires exenteration which is subtotal if there is no evidence of radial extension of the lesion to the skin of the anterior lid. Exenteration may not affect survival and is primarily for local control. Nodal involvement indicates widespread metastatic disease, but occasional cases have been cured by node resection.

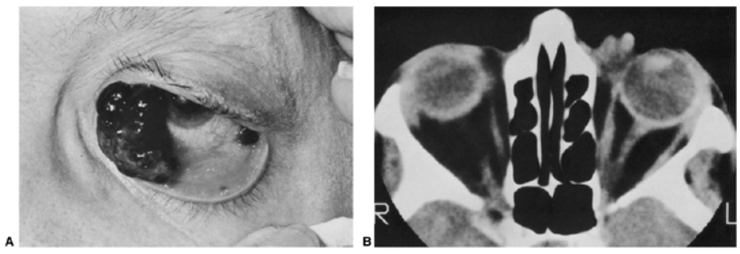

Figure 9-105. (A) This 81-year-old woman had been aware of a pigmented lesion in the left caruncular region for 18 months. It was gradually increasing in size and had bled on several occasions. In addition, she was aware of a lump present for 6 weeks on the left side of her neck. On physical examination, she had vision of 20/200 on the left (compared to 20/40 on the right) and lateral displacement of the left globe with some limitation of abduction. This massive pigmented lesion was associated with thickening and induration of the tarsal conjunctiva and a nodular satellite lesion in the temporal aspect of the inferior fornix due to local lymphatic spread. (B) The axial CT scan demonstrates the irregularly shaped homogeneous density in the anterior orbit. The patient refused exenteration and was managed by local resection and cryotherapy with removal of involved nodes. Two of the 31 neck nodes were positive for metastatic disease. Subsequently, she presented with a nodular recurrence in the left jaw, and died 1 year after treatment without evidence of local recurrence.

Orbital Extension of Ocular Malignancies

Orbital extension of intraocular malignancies accounted for 10 (5%) of 194 secondary orbital neoplasms in our series, consisting of five malignant melanomas, one congenital melanoma, and one retinoblastoma. The incidence of extraocular extension of intraocular tumors has decreased with the advent of screening programs and improved methods of evaluation and treatment.

Extrascleral and Orbital Extension of Uveal Melanoma

Uveal melanoma has a number of distinct biologic characteristics that has made it the center of some controversy in recent years. The core of the controversy concerns the role of extirpation (whether by local resection, enucleation, or in the case of extrascleral extension, exenteration) in the management of this tumor. Zimmerman et al. summarized the major controversies regarding pathogenesis of spread, which includes trauma of enucleation, decreased host resistance incurred by removal, and increased virulence concomitant with the appearance of clinical symptoms. These issues have led to more “conservative” management in selected circumstances (including observation, local radiotherapy, and local resection), greater attention to atraumatic enucleation techniques, and prospective multicenter studies aimed at ultimately resolving these important issues.

The cumulative mortality rate associated with uveal melanoma after enucleation is 30% at 5 years, 40% at 10 years, and 1% per year thereafter. The major negative factors affecting survival are larger intraocular tumor size, the presence of mixed or epithelioid cell type, evidence of extrascleral extension, and mitotic activity. Melanomas gain access to the orbit by paraemissarial extension and less often by intraemissarial growth. The incidence of orbital recurrence is approximately 3% in patients enucleated for melanoma and increases to 18% when there is histologic evidence of extrascleral extension at the time of enucleation. Factors that increase orbital recurrence rates include larger tumor size; epithelioid, mixed, or necrotic cell types; and nonencapsulated or surgically transected epibulbar tumors. Transection of the tumor is associated with a 50% orbital recurrence.

Extrascleral extension occurs in 10% to 15% of patients with uveal melanomas and may present clinically as a visible anterior or posterior nodule, as proptosis in patients with known intraocular tumor (Fig. 9-106), with phthisis and unsuspected tumor, or as a mass in orbital recurrence. Orbital recurrence associated with hepatic metastasis has been described as late as 42 years after primary enucleation. Orbital extension may only become evident at the time of surgery (Fig. 9-107); however, the use of ultrasonography and CT scan may lead to increasing preoperative detection of extrascleral nodules (Fig. 9-108).

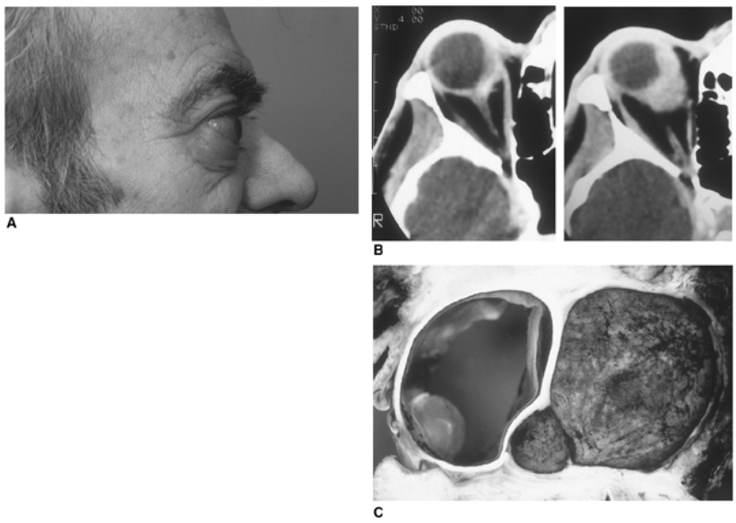

Figure 9-106. (A) This man presented in 1983 at age 59 with an 18 × 16 × 8 mm uveal melanoma, for which he refused therapy. The CT at that time (B, left) demonstrated extrascleral extension. Enucleation was recommended but the patient refused any form of therapy. By 1989 (B, right), he had marked proptosis with restricted ocular movements, an intraocular of 42 mmHg, and neovascularization of the iris with cataract. He underwent subtotal exenteration for local control. (C) Histologically, the tumor was predominantly spindle cell type and was fully resected. In 1999, he developed hepatic and peritoneal metastases. (Reproduced with permission from Katz SE, Rootman J, Goldberg RA. Secondary and metastatic tumors of the orbit. In: Tasman W, Jaeger EA, eds. Duane's Clinical Ophthalmology. 2nd ed. Philadelphia: Lippincott-Raven, 1996; chap. 46.)

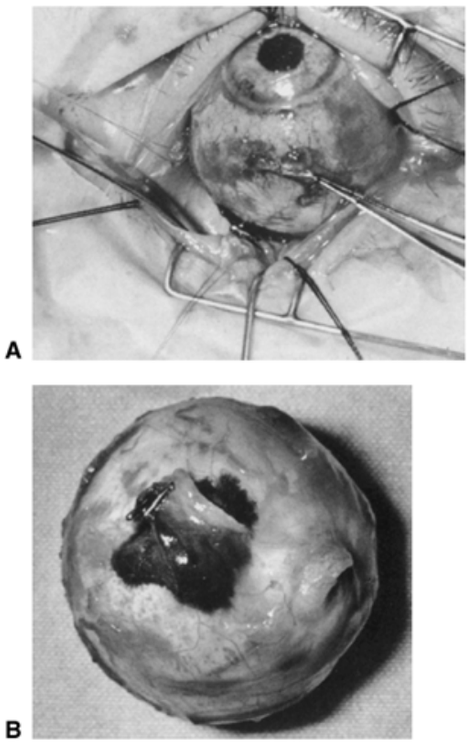

Figure 9-107. An epibulbar extension of melanoma noted at enucleation. (A) The globe and adjacent Tenon's capsule were resected. (B) The tumor after enucleation and removal of Tenon's capsule. The patient developed metastases 8 months following surgery.

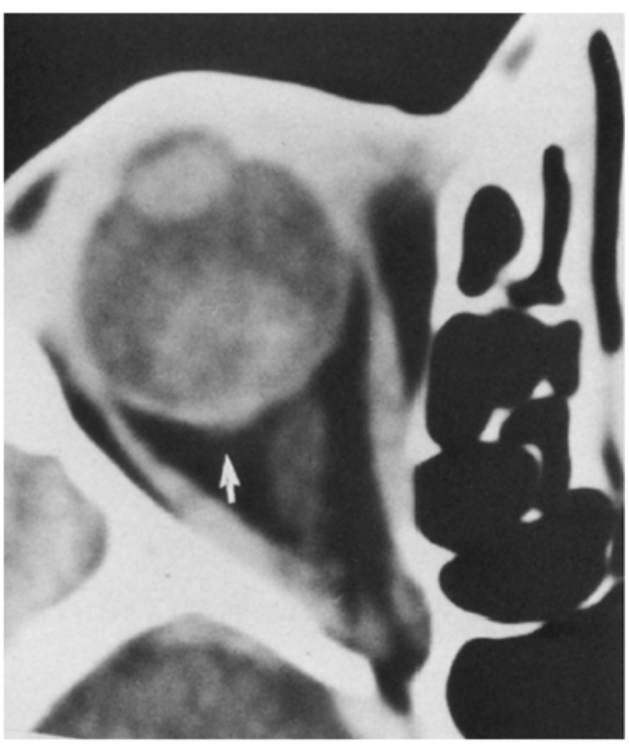

Figure 9-108. Axial CT scan demonstrates a large right intraocular melanoma with posterior extension (arrow). It was seen in a 73-year-old woman who underwent primary subtotal exenteration. The patient died 2 years later of metastatic disease.

The controversy over the management of orbital recurrence parallels that of intraocular melanoma. By the time extrascleral and orbital extension is evident, other biologic factors are already in play that dominate the grave mortality rate, which is 73% to 81% in these circumstances. The role of exenteration has not yet been defined in a prospective controlled study but there is strong retrospective evidence suggesting that exenteration does not afford protection from metastases, except perhaps in cases of frank transaction or nonencapsulation at enucleation. Shields et al. have summarized their current management (Table 9-15) based on the type of extrascleral extension (flat, nodular, vortex vein, or recurrence after enucleation) and the timing of detection (clinical examination, at surgery, or pathologically after enucleation). Essentially, the trend is toward resection only of adjacent tissues when the lesion is nodular, whereas exenteration (which can usually be subtotal) is reserved for instances where there is evidence of tumor transection at the time of enucleation. In these circumstances, exenteration may be only a palliative measure. The role of preoperative and postoperative radiotherapy has not been clearly determined but is unlikely beneficial. Orbital recurrence for similar reasons requires exenteration, although low-grade spindle cell tumors may be curable in such circumstances. The biologic factors outlined appear to dominate the poor prognosis in orbital melanoma.

Table 9-15. Management options of extrascleral extension of posterior uveal melanomas*

TYPE OF EXTRASCLERAL EXTENSION	DETECTED CLINICALLY	DETECTED AT SURGERY	DETECTED PATHOLOGICALLY AND AFTER ENUCLEATION
Flat	Plaque radiotherapy Modified enucleation with tenonectomy	Plaque radiotherapy Modified enucleation with tenonectomy	If encapsulated, observation If nonencapsulated, tenonectomy with removal of ball implant followed by orbital radiotherapy (optional)
Nodular (small)	Plaque radiotherapy Preoperative orbital radiation followed by modified enucleation with tenonectomy	Plaque radiotherapy Modified enucleation with tenonectomy and post-operative orbital radiotherapy	If encapsulated, radiotherapy If nonencapsulated, tenonectomy with removal of ball implant followed by orbital radiotherapy
Nodular (large)	Preoperative orbital radiation followed by modified exenteration	Modified exenteration followed by orbital radiotherapy	Exenteration
Vortex vein		Vortex vein resection followed by modified enucleation or plaque radiotherapy	Tenonectomy Orbital radiotherapy
Recurrence after enucleation	Preoperative orbital radiation followed by exenteration		

* Dependent on size of tumor, patient age, and other factors
Reproduced with permission from Shields JA. Intraocular Tumors: A Text and Atlas. Philadelphia: WB Saunders, 1992:175.

Orbital Extension of Retinoblastoma

Retinoblastoma, the most common intraocular tumor of childhood, accounts for 1% of childhood cancer deaths in the United States and 5% of blindness in children. The incidence is 1 in 15,000 to 1 in 20,000 live births. With modern diagnostic and therapeutic advances, the mortality rate from metastatic or recurrent retinoblastoma has been as low 5%. In underdeveloped countries, patients characteristically present with extensive local and widespread disease; thus, mortality rates range between 90% and 100%. The most common clinical presentation is leukocoria or strabismus; however, ocular inflammation, hyphema, and glaucoma also occur.

A major biologic characteristic of retinoblastoma, like all other malignancies, is the ability to invade and spread. Most retinoblastomas remain for a long time within the confines of the globe, except perhaps for blood-borne metastases, but the barriers to egress are ultimately penetrated. Depending on the site of the primary lesion, retinoblastoma may spread by means of the choroid to the adjacent orbital structures, by the optic nerve (particularly when the origin is peripapillary) to the central nervous system, and by the vascular system to distant metastatic sites.

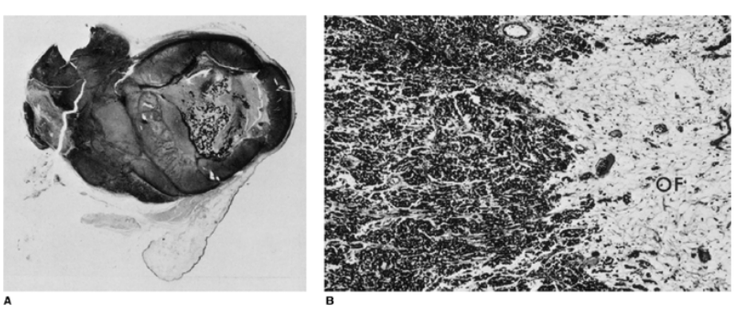

Figure 9-109. (A) A retinoblastoma that had occupied the entire globe and eroded through it into the adjacent orbit (H&E, original magnification × 2). (B) Orbital fat (OF) infiltrated by retinoblastoma (H&E, original magnification × 10).

Bruch's membrane initially resists invasion, but is eventually eroded, leading to choroidal growth. Once the tumor cells reach this choroidal network of fine vascular channels, growth appears to accelerate, as evidenced by three clinical features: rapid growth over a period of days or weeks, high elevation on a narrow pedunculated stalk, and a yellow color at the summit, suggesting the lamina vitrea has been pushed forward ahead of the tumor. Once in the choroid, the tumor spreads diffusely and rapidly in a lateral fashion. Choroidal invasion is more frequent in retinoblastoma than was previously thought and does not necessarily carry a grim prognosis. Metastases relate more closely to a critical mass of the tumor within the sponge-like network of choroidal vessels than to the presence of cells within the choroid.

As soon as there is extensive involvement of the choroid, egress from the confines of the globe follows. Routes of retinoblastoma spread from the globe to the surrounding tissues are via emissarial or globe erosion (Fig. 9-109). An enucleated globe has three features that may suggest the possibility of orbital recurrence: spread in continuity to episcleral nodules, periemissarial retinoblastoma not extending to the surface, and significant invasion of the choroid. The loose periemissarial connective tissue provides a natural plane for tumor growth; therefore, massive posterior choroidal involvement has a greater opportunity for access to the many posterior emissaries.

Lateral growth from the adventitial coats of the intrascleral emissaries may also lead to lamellar separation of the sclera and ultimately destruction of the ocular coats. Once outside the globe, the orbit provides a rich, loose tissue plane and growth accelerates further, leading to a large orbital mass.

Retinoblastoma may gain direct egress by means of the optic nerve to the central nervous system. Access to the subarachnoid space occurs by growth along the optic nerve to the site of penetration of the central retinal artery and vein or by extension to the pia arachnoid, allowing direct egress into the subarachnoid space. The degree of optic nerve extension has been correlated with prognosis and mortality as follows: superficial invasion of the optic nerve head, or grade 1 (10%); involvement up to and including the lamina cribrosa, or grade 2 (29%); involvement posterior to the lamina cribrosa, or grade 3 (42%), and involvement to the line of surgical transaction, or grade 4 (78%).

A more unusual mode of egress into the central nervous system is via the posterior ciliary circulation. Tumors that involve the peripapillary choroid can also reach the subarachnoid space along the radicals of the posterior ciliary vessels that supply the optic nerve head and the pia-arachnoid of the distal optic nerve. Another unusual route of spread into the optic nerve is through the orbit into the subarachnoid space. Once in the cerebrospinal fluid, the tumor circulates and sets up malignant rests.

Awareness of the significance of optic nerve invasion led to the development of adequate techniques of enucleation and improvement in survival in the last century. Although invasion up to but not beyond the lamina cribrosa has relatively little prognostic significance, invasion to the line of transection carries a poor prognosis and suggests the need for cytopathologic examination of the cerebrospinal fluid and

possibly additional therapy. Tumor extending beyond the lamina cribrosa, but not to the line of transection, may also carry a poor prognosis if it extends to the pia arachnoid and indicates a need for cytologic study of the cerebrospinal fluid. A multivariate analysis by Kopelman et al. suggested that invasion of the tumor to the optic nerve or orbit were most highly predictive of death from retinoblastoma.

Retinoblastoma has metastatic potential in addition to local invasion. Tumor-related death occurs solely from central nervous system involvement in 29% to 75% (average 46%) and from distant metastases in 25% to 71% (average 54%). The combined potentials of orbital, intracranial, and systemic spread determine the form of therapy after primary enucleation. Spread from the orbit may reach regional lymph nodes, and autopsy studies have revealed both regional and widespread involvement in 33% to 47% of cases. The sites of hematogenous spread are bone (especially the long bones and skull) and viscera (most often the liver, but also the pancreas, kidney, spleen, testes, ovaries, and uterus).

Management after enucleation for retinoblastoma is based on the presence or likelihood of extraocular spread as determined by pathologic examination of the globe. Therapy consists of adjuvant combined chemotherapy with local orbital and central nervous system irradiation if central nervous system spread is confirmed. The pathologic criteria that suggest orbital or systemic spread and indicate treatment of the orbit as well as systemic chemotherapy are extrabulbar retinoblastoma, orbital recurrence, and massive (particularly posterior) choroidal extension with periemissarial invasion.

There are three pathologic criteria that suggest a need to investigate and treat the central nervous system: tumor cells in the cerebrospinal fluid, extension in the optic nerve to the line of transection, and extension beyond the lamina cribrosa with retinoblastoma adjacent to the pia arachnoid.

Although orbital extension of the tumor has been associated previously with a mortality of 67% to 100%, modern chemotherapeutic and radiotherapeutic techniques are now producing better results. Orbital recurrences of retinoblastoma are managed by an aggressive chemotherapeutic and radiotherapeutic regimen directed toward systemic and central nervous system spread.

Orbital Extension of Neuroepithelial Tumors of the Ciliary Body

The neuroepithelial tumors of the ciliary body can be divided into congenital and acquired tumors, either of which may be benign or malignant.

Medulloepitheliomas

Medulloepitheliomas are embryonal tumors that arise from the neuroepithelium in the ciliary body region in children (mean age 5 years at diagnosis). More rarely, they occur adjacent to and extend into the optic nerve.

Histologically, they are composed of cords of nonpigmented and pigmented cells resembling the optic vesicle or optic cup. They often have areas of undifferentiated cells that resemble retinoblastoma with Homer-Wright and Flexner-Wintersteiner rosettes. The tumor cells can elaborate vitreous-like material. Heteroplastic elements, such as cartilage, brain tissue, and striated muscle, may be noted in the so-called teratoid medulloepitheliomas.

Medulloepitheliomas may be divided pathologically into benign and malignant variants. In a series of 56 cases, Broughton and Zimmerman noted 66% had histologic evidence of malignancy, although they emphasized the characteristic slow growth and locally invasive nature of the tumor. The single most important life-threatening prognostic factor was evidence of extraocular spread. Typically, the presentation is with poor vision, pain, leukocoria, and ciliary body mass in childhood. Of the 56 patients, 8 presented with proptosis or orbital mass. Four patients died of medulloepithelioma, all with orbital extension; nodal metastases developed in one patient, and the remaining three died because of local extension of the tumor intracranially. Of the remaining cases of extraocular extension, the major factor in survival appeared to be complete local excision. Tumors occurring in the optic nerve region are more treacherous because they tend to be identified later and have easier access to the orbital and intracranial structures.

Treatment is with wide local excision. Preoperative imaging may allow for clearer identification of extension and facilitates appropriate planning.

Acquired Neuroepithelial Tumors of the Ciliary Body

The majority of acquired neuroepithelial tumors are benign hyperplasias or adenomas. Malignant variants are rare and most arise in previously traumatized, chronically inflamed eyes. Tumor-related mortality is generally due to contiguous invasion, but widespread metastatic disease may occur. Treatment is wide local excision.

Extension from the Lacrimal Sac

Tumors of the lacrimal sac constitute a small number, but a wide variety of lesions may invade the orbit. They are best viewed within the context of mass lesions of the medial and inferomedial orbit, the large majority of which are secondary to sinus disease and have been discussed earlier. Neoplasia of the lacrimal sac must be differentiated from all other tumefactions in this location, including acute and chronic inflammations. Inflammatory lesions, including granulomas and nonspecific inflammation, account for approximately 25% of lacrimal sac tumors in some series. The remaining tumors are true neoplasms, of which 55% are malignant.

From combined series, primary epithelial neoplasms accounted for 73% of all lacrimal sac tumors (73% of these were malignant) and mesenchymal tumors accounted for 14% (62% of these were malignant). Lymphomas (8%), malignant melanomas (4%), and neural tumors (1%) were also noted.

The general clinical progression is of epiphora followed by simulated dacryocystitis, nonreducible swelling, and eventual tumor extension outside the sac. The benign lesions have a tendency toward slower growth, obstructive symptoms, and recurrent dacryocystitis that may mimic inflammation of the lacrimal sac. The malignancies may initially present similarly; however, the infiltrative nature of tumors in a higher risk category will eventually dominate the clinical picture. Features suggestive of malignancy include a mass extending above the medial canthal ligament, telangiectasis or ulceration of the overlying skin, serosanguineous discharge or bloody reflux after irrigation, local invasion of the adjacent bone and orbit with occasional pain, restricted extraocular movements, nonaxial proptosis, and an overall relentless progressive course. Dacryocystography may be helpful in the diagnosis of suspected lacrimal sac tumors. Findings suggestive of neoplasia include a distended lacrimal sac with a mottled density or filling defect, and delayed emptying.

Epithelial Tumors

Ryan and Font divided the epithelial malignancies into papillomas and de novo tumors. The papillomas display three growth patterns: exophytic, inverted, and mixed types. Additionally, they can be subdivided histologically into squamous, transitional, and mixed cell papillomas. The *exophytic papillomas* tend toward multiple occurrences that affect the whole of the epithelium of the nasolacrimal system, particularly when they are of the transitional cell type (Fig. 9-110). The *inverted papillomas* are more prone to developing focally invasive carcinoma, usually of a low-grade variety. *Mixed papillomas* have mixed clinical and histopathologic features of exophytic and inverted types. In the Armed Forces Institute of Pathology series, papillomas occurred in persons aged 9 to 88 years (mean 44 years). Stefanyszyn et al. also reported that 6 (14%) of 44 papillomas developed into carcinoma or had foci of carcinoma.

De novo carcinomas have been divided into papillary and nonpapillary types on the basis of their gross pattern of involvement. Carcinomas occur in persons ranging in age from 16 to 89 years (mean and median both 59 years). De novo carcinomas may include squamous cell, transitional cell, adenoid cystic, mucoepidermoid, and poorly differentiated carcinomas as well as adenocarcinomas; however, the majority are squamous cell carcinomas. Other less commonly reported epithelial lesions of the lacrimal sac include benign mixed tumors and oncocytomas, which tend to be noninvasive.

Management should be based on histopathologic type and degree of extension. The papillomas, particularly when focal invasion is demonstrated, should be treated with total excision of the lacrimal system, followed by careful observation for any evidence of recurrence in the nose (Fig. 9-110). More aggressive carcinomas should be treated with wide local excision, including the bone of the nasolacrimal system, the adjacent orbit, and the sinus wall. Postoperative radiotherapy is advocated for more aggressive lesions, and significant orbital involvement is an indication for exenteration. In our experience, both transitional cell carcinoma and squamous cell carcinoma of the lacrimal sac with orbital invasion have also been responsive to radical local radiotherapy alone (Fig. 9-111).

Nonepithelial Tumors

Nonepithelial tumors include mesenchymal lesions (fibrous histiocytoma [Fig 9-112], hemangiopericytoma, and lipoma), lymphomas, malignant melanomas, granulocytic sarcomas, and neural tumors (neurilemmoma and neurofibroma). Locally aggressive lesions such as fibrous histiocytomas should be widely excised and carefully followed, whereas malignant lesions should be treated with wide local excision, with or without radiotherapy. Lymphomas should be treated with radiotherapy and/or chemotherapy, depending on the systemic status of the patient. Malignant melanomas of the lacrimal sac share the grim prognosis of other malignant melanomas of mucosal surfaces because of the lack of early detection.

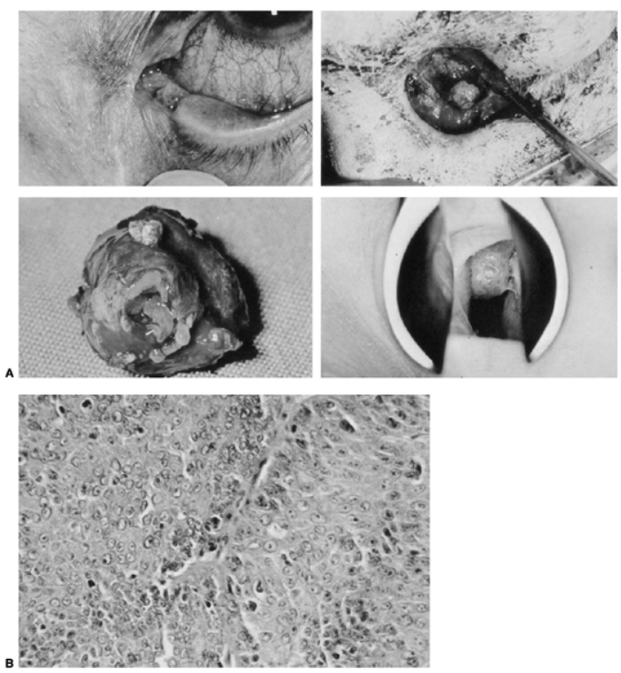

Figure 9-110. (A) The patient, a 69-year-old woman, presented in 1976 with a longstanding history of recurrent papillary lesions in the medial canthal region for which she had undergone multiple local resections. She had a palpable anterior inferior medial orbital mass. The medial canthal region and adjacent lacrimal sac were resected en bloc (A, bottom left) and the nasolacrimal duct was also noted to be involved (A, top right). A lateral rhinotomy with removal of the nasolacrimal canal was undertaken. On routine follow-up 5 years later, a papillary lesion of the nose was noted and an inferior turbinectomy was done. She is alive and well without recurrence 5 years after nasal surgery. (B) Histologically, the orbital lesion proved to be a low-grade papillary transitional cell carcinoma with some inverted areas (H&E, original magnification × 25).

Summary

Secondary tumors of the orbit are a diverse group whose clinical behavior reflects both the site of origin and the underlying tumor biology. Sinus and nasopharyngeal tumors commonly extend into the orbit and generally present with nonaxial displacement of the globe in association with pain and infiltrative features. Sphenoid wing meningiomas, the most common secondary orbital tumors arising intracranially, are slow-growing, compressive lesions. Their hallmark is proptosis (axial, downward, and medial globe displacement) with or without optic or cranial neuropathies, depending on whether the optic canal, superior orbital fissure, or cavernous sinus are involved.

Basal cell carcinoma is by far the most common epithelial eyelid malignancy; however, the frequency of orbital invasion is roughly equivalent to that for the more invasive squamous cell carcinoma and the often delayed diagnosis in sebaceous cell carcinoma. The majority of conjunctival squamous cell carcinomas and malignant melanomas arise from precursor lesions, and early invasion may be clinically silent. The incidence of orbital extension of ocular tumors has declined, in large part due to screening programs, earlier

diagnosis, and treatment options for both retinoblastoma and choroidal melanoma. Lacrimal sac tumors are uncommon and may go unrecognized until dacryocystorhinostomy is performed for nasolacrimal duct obstruction.

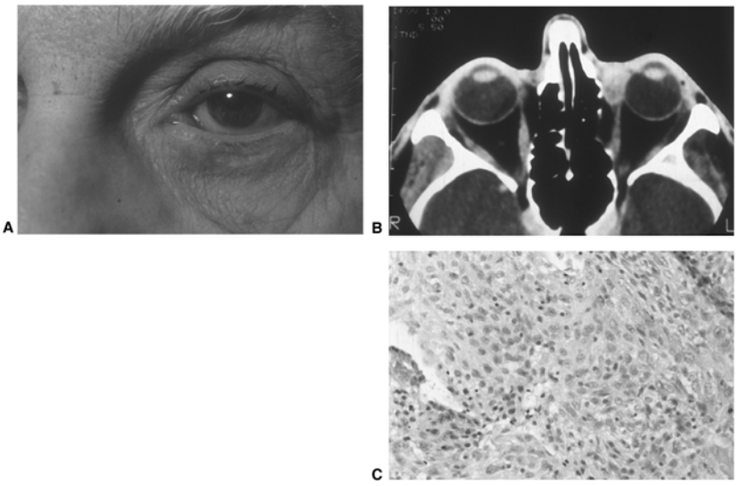

Figure 9-111. A 63-year-old man presented with a 6-month history of left inferomedial canthal swelling, epiphora, and recurrent ectropion (history of ectropion repair 4 years prior). (A) On examination, he had a visible mass below the level of the medial canthal ligament associated with medial ectropion, local conjunctival injection, and minimal decreased abduction. (B) Axial CT scan demonstrates a mass lesion in the region of the lacrimal sac, with no evidence of bony erosion or infiltration into the nose or paranasal sinuses. (C) Biopsy revealed a low-grade transitional carcinoma of the lacrimal sac (H&E, original magnification × 25). The patient underwent radiotherapy with 52.5 Gy in 15 fractions over 3 weeks with regression of the tumor and no evidence of recurrence in 7 years of follow-up. He remains with good visual function and persistent epiphora due to punctal stenosis, atrophy of the lacrimal drainage system, scarring, and contracture of medial lower lid with persistent ectropion. He has refused to undergo conjunctival dacryocystorhinostomy or excision of scar tissue with skin graft. (Figs. 9-111A and B reproduced with permission from Katz SE, Rootman J, Goldberg RA. Secondary and metastatic tumors of the orbit. In: Tasman W, Jaeger EA, eds. Duane's Clinical Ophthalmology. 2nd ed. Philadelphia: Lippincott-Raven, 1996; chap. 46.)

Recognition of the individual clinical features of these tumors is based on anatomic location and tumor biology. Defining the extent of the lesion and structures involved may require directed imaging studies. Ultimately tissue diagnosis, extent of the lesion, and individual patient characteristics will guide specific therapy in each case. Surgical excision, radiotherapy, or other local modalities in combination may be indicated. The goal of treatment is generally complete eradication of the tumor; however, when this cannot be achieved, preservation of visual function, cosmesis, and comfort direct the interventions.

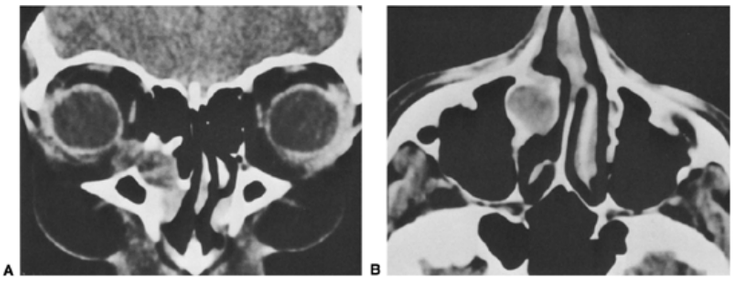

Figure 9-112. Coronal (A) and axial (B) CT scans demonstrate a mass lesion of the right lacrimal sac, nasolacrimal system, and nose in a 38-year-old woman who presented with a 2-year history of epiphora. She was noted to have a mass at the time of dacryocystorhinostomy. Biopsy of the mass revealed a spindle cell tumor consistent with fibrous histiocytoma. We performed a medial orbitotomy and lateral rhinotomy to remove the entire lacrimal sac along with the involved medial nasal and sinus walls. The patient had a local recurrence 8 months later, underwent further resection, and has been disease-free for 15 years.

Orbital Metastases

The diversity of clinical presentations of orbital metastases relates to the biology of the primary and may be associated with misdiagnosis or delay of diagnosis. The ophthalmologist may play a significant role by establishing the tissue of origin through investigation, including biopsy, which may guide specific therapy. Although the prognosis for metastatic cancer remains grim, combined therapy can be palliative and may induce remission and even a cure in some patients. We have published an extensive review of the University of British Columbia Orbital Clinic experience and have updated it for this section.

Prevalence, Incidence, and Location

The increasing frequency of orbital metastases reflects the change in natural history and prolonged longevity of cancer patients. Large clinical and radiographic series suggest that 1.5% to 3.3% of all orbital cases are metastatic. In Henderson's series of orbital neoplasia, 8% were metastatic, and in ours 7% were metastasic. On the whole, orbital metastases are less frequent than ocular metastases.

Combined series from the literature yields a relative prevalence of the various primary tumor types. Breast, lung, and prostate cancer, and melanoma constitute the largest groups (Fig. 9-113). Approximately 11% are of unknown type. These combined clinical and pathologic series do not necessarily illustrate the true distribution of primary tumors metastatic to the orbit but serve to reflect the typical clinical situation.

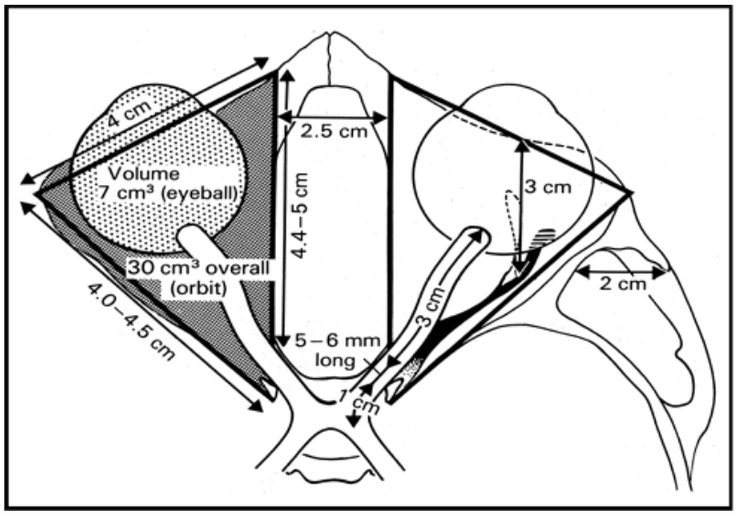

Figure 9-113. Prevalence of various primary types, in combined series. “Other” includes the following: neuroblastoma (1.6%); testicle (1.2%); adrenal, pancreas, and thyroid (0.8% each); bile duct, carcinoid, fibrosarcoma, choroidal melanoma, ovary, parotid, and uterus (0.4% each). (Reproduced with permission from Goldberg RA, Rootman J, Cline RA. Tumors metastatic to the orbit: a changing picture. Surv Ophthalmol 1990;35:1-24.)

There does not appear to be a significant predilection for either orbit but about 7% of cases are bilateral. Additionally, in our own series 39% were in the lateral orbit, 32% superior, 20% medial, and 12% inferior. Metastases to bone and fat are two times more frequent than to muscle. There are, however, differences depending upon the primary tumor type. For instance, prostate carcinoma has a strong tendency to metastasize to bone (Fig. 9-114). In contrast, breast carcinoma tends to localize in orbital fat and muscle, and melanoma has the strongest predilection for metastasis to muscle (Figs. 9-115 and 9-116).

Temporal Characteristics

In the majority of patients, the primary tumor is known, but at least one quarter of patients present with an orbital mass. It is worthwhile to note that patients often neglect to disclose a history of known cancer because of denial, embarrassment, forgetfulness, or lack of association. Certain carcinomas are more likely to have an antecedent history, such as melanoma and breast carcinoma, whereas renal and lung carcinoma are the least likely to have a known primary. The fact that systemic metastatic cancer may manifest first as an orbital process in more than one quarter of cases emphasizes the role of the ophthalmologist, who will be the first physician to evaluate these patients.

The average survival is approximately 9 months from the time of orbital presentation and generally, the primary cancer occurred 31 months before ophthalmic presentation. Certain tumors have a long temporal course such as breast cancer, which has an average delay of 3 years, and thyroid

cancer, with an average delay of 5 years. Melanoma is intermediate and has an average of almost 2 years between diagnosis of the primary and orbital presentation but may have unusually long latencies. More fulminant tumors, such as those from the lung and gastrointestinal tract, are often diagnosed shortly before or even sometimes after orbital presentation and have a rapid course thereafter (average survival 6 months after ophthalmic presentation). Because of their early metastases, these tumors are considered silent primaries.

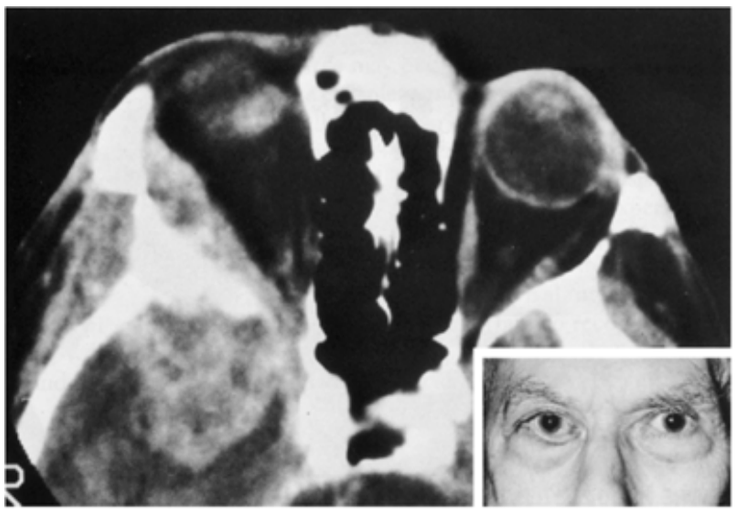

Figure 9-114. This 80-year-old man was referred 6 months after excision of an “adenocarcinoma” of the right parotid. He had developed a prominent right eye with periorbital pain and infraorbital numbness. On physical examination, he had a right tarsorrhaphy, reduced vision on the right side to 20/200, 3 mm of inward and downward displacement and 9 mm of right proptosis. In addition, he had a right afferent pupillary defect and on fundus examination had five choroidal metastases on the right and two on the left. The contrast-enhanced axial CT scan demonstrates a right-sided mass involving the lateral orbital wall, associated with hyperostosis and soft tissue components in the temporalis fossa and in the middle cranial fossa. Note choroidal metastasis on the right side. The bone appears irregular and partially destroyed, and the soft tissue density in the orbit obscured the lateral rectus muscle. On retrospective investigation, the patient was noted to have had a carcinoma of the prostate diagnosed on cystoscopy 4 months prior to this referral. Review of the original tissue specimen led to a diagnosis of metastatic prostatic carcinoma to the right parotid with extension into the infratemporal fossa, right orbit, and right middle cranial fossa as well as bilateral uveal metastases.

Concurrent metastases occur in approximately half of the cases, including to the choroid. There are exceptions, however, such as metastatic carcinoid and renal cell carcinoma, where there may be a single, very slow-growing, solitary orbital metastasis that may be managed with surgical extirpation or excision.

Clinical Presentation

Compared with other types of orbital neoplasia, metastases have a relatively rapid onset of symptoms. The average duration of symptoms until presentation was 3.6 months: metastases from lung and pancreatic cancer and melanoma tended toward a more precipitous onset and earlier presentation, whereas metastases from breast and thyroid cancer were characterized by a longer average duration of symptoms before presentation.

Proptosis and motility disturbances are the most common presenting symptoms and signs (Table 9-16). Motility disturbance out of proportion to the degree of proptosis can occur and is somewhat characteristic of an orbital metastasis.

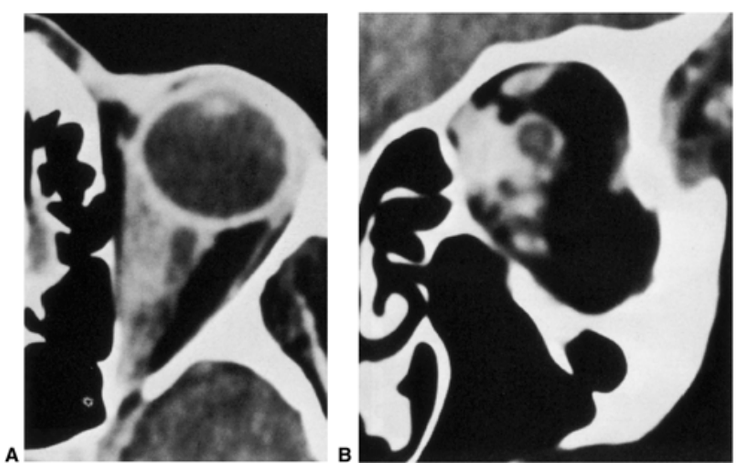

Figure 9-115. Axial (A) and coronal (B) CT scans show an infiltrative mass involving the medial rectus, adjacent orbital fat, and optic nerve. The patient was a 64-year-old woman with carcinoma of the breast, which had been diagnosed 14 years earlier. She had suffered from bone pain for 4 years and, 1 year prior to presentation, had bony metastases diagnosed. She presented with a 3-month history of a firm lump in the inner canthus of the left eye. Physical examination revealed a superomedial mass with 3 mm of enophthalmos and reduction in upgaze and abduction due to an orbital metastasis.

Pain was noted in 23% of cases and may be present early in the course, in contrast to other tumors in which pain is typically a late symptom. The single exception to this are tumors that invade by contiguity, where pain or paresthesia is the most frequent early symptom. Palpable mass, blepharoptosis, and decreased vision were also common signs and symptoms. Pulsation of the orbit may occur when destruction of orbital bone allows transmission of brain pulsation. Vascular metastases, particularly of thyroid and renal origin, can pulsate due to high internal blood flow.

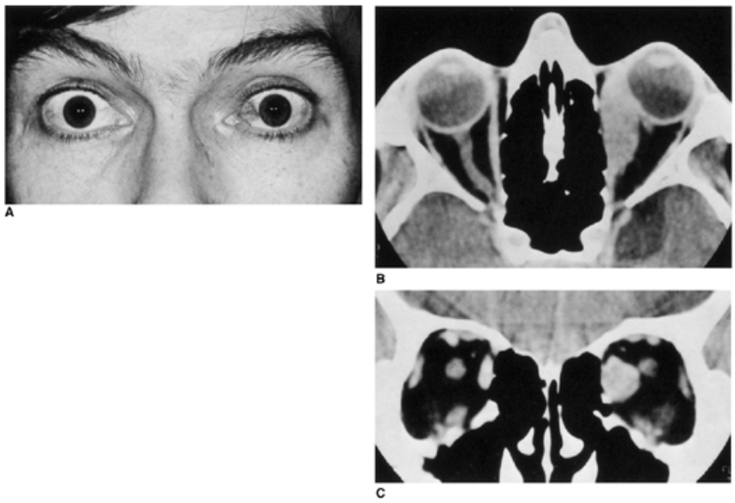

Figure 9-116. (A) This 30-year-old man with a known diagnosis of metastatic melanoma of skin presented with left retrobulbar pain, which was accentuated by eye movement and associated with increasing injection of the medial portion of the globe. Axial (B) and coronal (C) CT scans reveal a homogeneous, enhancing mass due to the metastatic melanoma. The mass involved the medial rectus muscle without infiltration of the adjacent fatty tissues.

Table 9-16. Presenting symptoms and signs of orbital metastatic tumors

	NUMBER (%)
Reported symptoms	
Diplopia	81 (38)
Proptosis	76 (35)
Pain	50 (23)
Decreased vision	44 (20)
Blepharoptosis	35 (16)
Mass	28 (13)
Observed signs	
Proptosis	138 (64)
Motility disturbance	125 (58)
Palpable mass	58 (27)
Decreased vision	48 (22)
Blepharoptosis	45 (21)
Displacement	39 (18)
Chemosis	32 (15)
Enophthalmos	22 (10)
Disc edema	17 (8)
Retinal folds or striae	9 (4)
Paresthesia	7 (3)
Pulsation	3 (1.5)

Modified with permission from Katz SE, Rootman J. Secondary and metastatic tumors of the orbit. In: Tasman W, Jaeger EA, eds. Foundations of Clinical Ophthalmology. 2nd ed. Philadelphia: JB Lippincott, 1996; vol 2; chap 46.

Enophthalmos is a frequently overlooked sign present in 10% of reported cases, of which metastatic breast cancer accounts for approximately 80%. The mechanism is contraction of fibroblasts in the diffuse scirrhous tumor leading to posterior traction on the globe. Destruction of the bony walls of the orbit, resulting in a “biologic orbital decompression,” may rarely play a role.

Although the tabulation of signs and symptoms is helpful, it does not by itself provide a clinical framework for evaluating and categorizing the diverse group of patients with orbital metastases. Clinical presentations of orbital metastatic disease can be generalized into five basic types: mass, infiltrative, functional, inflammatory, and silent (Table 9-17).

Table 9-17. Clinical presentations of orbital metastatic disease

Mass	Primary mass effect, either palpable (anterior) or causing axial or nonaxial displacement of the globe
Infiltrative	Diffuse or localized infiltration of orbital tissues characterized by diplopia, enophthalmos, limitation of eye movements or frozen globe, and a firm orbit (increased resistance to retro-displacement)
Functional	Decrease in cranial nerve function (II,III,IV,V,VI) out of proportion to mass or infiltration
Inflammatory	Acute or subacute onset of inflammatory signs and symptoms including pain (which may be worse on eye movement), chemosis, injection, erythema, and lid swelling
Silent	No orbital signs or symptoms; discovered serendipitously on CT scan performed for some other reason, or during enucleation or other unrelated orbital surgery

Reproduced with permission from Katz SE, Rootman J. Secondary and metastatic tumors of the orbit. In: Tasman W, Jaeger EA, eds. Foundations of Clinical Ophthalmology. 2nd ed. Philadelphia: JB Lippincott, 1996; vol 2; chap 46.

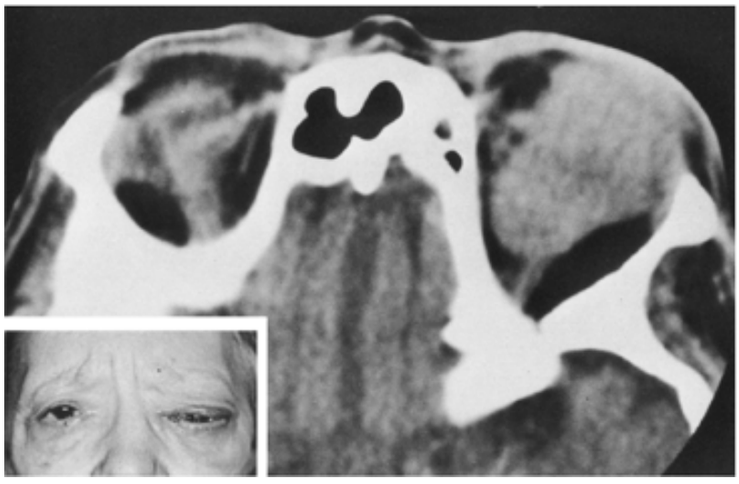

Figure 9-117. Clinical presentation – mass. This 75-year-old woman (inset) was referred from a long-term care facility because of recently noted swelling of her left eye. This had been present for an unknown period of time. Physical examination revealed a left ptosis of 4 mm with reduced levator function, downward displacement of the globe, and 2 mm of proptosis. The upper lid appeared somewhat injected and swollen, and she had chemosis with restriction of upgaze. On palpation there was an indurated mass in the left upper lid and the orbit felt firm. The axial CT scan demonstrates a homogeneous mass in the superior orbit with well-defined, relatively smooth borders. A biopsy was done through a superior fornix incision, and histologically the tumor consisted of a poorly differentiated small cell malignancy that had a trabecular pattern and was associated with considerable tumor cell necrosis. Cytologically, both on section and imprint, the tumor was consistent with a poorly differentiated small cell carcinoma. Electron microscopy confirmed the epithelial nature of the tumor, and many cells contained uniform dense core granules. The findings were consistent with a small cell carcinoma, in particular metastatic oat cell carcinoma. Chest x-ray showed a mass in the right hilum with probably parenchymal nodule in the right lobe.

Syndromes of Presentation

The syndromes of presentation are rarely pure but the overall pattern is clear in the majority of cases (Table 9-17). The syndrome of mass at presentation is the most common (66%), with globe displacement as the predominant sign; pain, inflammation, and secondary motility disturbances are often present as well (Fig. 9-117). The second most frequent presentation is infiltrative (24%), characterized by restricted motility and enophthalmos. This is notable in cases of metastatic breast carcinoma, particularly the scirrhous-type (Figs. 9-115 and 9-118). This infiltrative pattern can

also be seen in gastrointestinal, prostate, lung, and other primary tumors. The least common presentations are inflammatory (5%) (Fig. 9-119) and functional (5%). Functional presentations usually reflect a tumor in a small tight place, such as the optic canal or orbital apex (Fig. 9-120). Finally, orbital metastases may be discovered secondary to imaging done for other reasons.

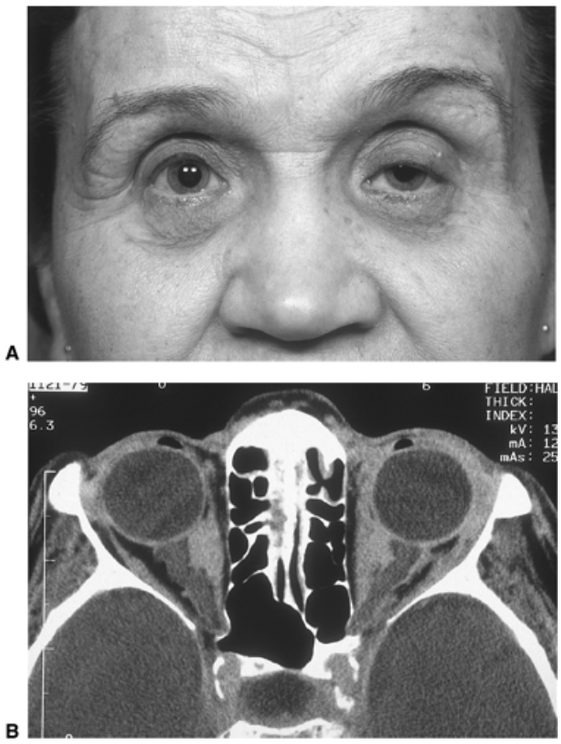

Figure 9-118. Clinical presentation – infiltrative. (A) This 71-year-old woman presented with a 2-year history of drooping of the left upper lid associated with mild swelling, which had occurred just prior to diagnosis of breast carcinoma. The carcinoma was extensive and was treated with radiotherapy and chemotherapy with disappearance of the lid retraction and swelling. Since that time, she had noted marked deepening of her eyes, particularly on the left side. She was unaware of diplopia and on physical examination, had normal vision, left ptosis, and bilateral deep superior sulci. The inferior sulcus on the left side is also deep. On palpation, a dense orbital mass was felt just behind the orbital rim and there was bilateral restriction of ocular movement, worse on the left than the right. (B) The CT scan demonstrates bilateral orbital infiltration, particularly affecting the medial recti. She underwent bilateral orbital radiotherapy.

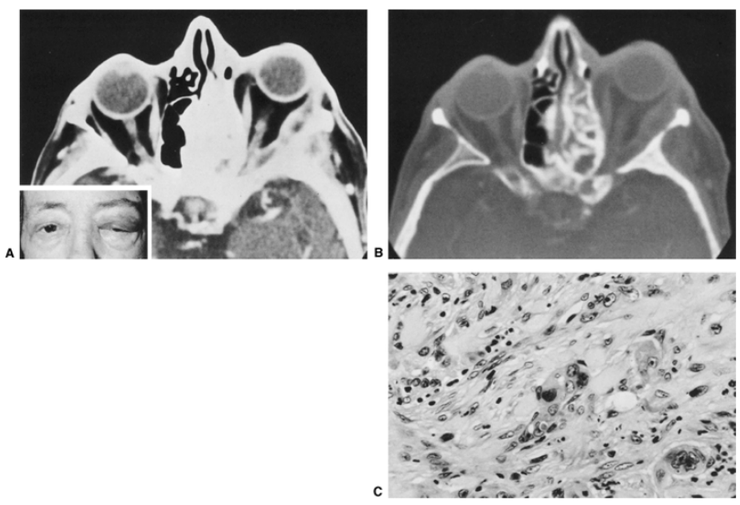

Figure 9-119. Clinical presentation – inflammatory. (A, inset) This 85-year-old woman presented with swelling of the left eye for approximately 4 months. It was associated with mild intermittent supraorbital ache and some diplopia. On physical examination, she had a left afferent pupillary defect with a vision of 20/40. The lid was edematous and injected suggesting inflammation, and she had superior chemosis with a narrow interpalpebral fissure. There was 5 mm of proptosis and marked limitation of movement, especially in abduction and elevation. The left temporalis fossa appeared slightly fuller than the right. The axial CT scans on soft tissue (A) and bone windows (B) settings demonstrate left proptosis with sclerotic changes in the greater sphenoid wing and ethmoid sinus. This is associated with a soft tissue mass in the lateral, posterior, and apical portion of the orbit. The mass is predominantly low-density but had some rim enhancement medially. In addition to bony sclerosis, there is soft tissue opacification of the ethmoid and sphenoid sinuses. The patient had no systemic complaints on admission to hospital but soon developed some abdominal distress with distention. (C) She underwent a small percutaneous biopsy of the orbit. Histopathology revealed dense, focally inflamed fibrotic tissue extensively infiltrated by a poorly differentiated mucin-secreting adenocarcinoma, consistent with a metastatic colonic carcinoma. Systemic investigation revealed a rectal tumor, which on biopsy proved be an adenocarcinoma (H&E, original magnification × 40).

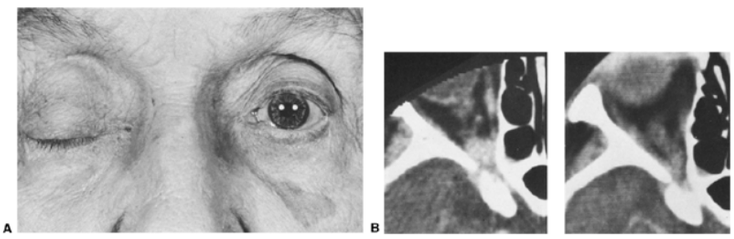

Figure 9-120. Clinical presentation – functional. (A) This 81-year-old woman suddenly developed ptosis on the right side, and complete ophthalmoplegia over several weeks. It was associated with a decrease of vision to hand movements, a fixed pupil, 3 mm of proptosis, and reduced sensation of the first and second divisions of the fifth nerve. (B) CT scans show a well-demarcated, enhancing apical orbital mass that extends into the optic canal and minimally through the superior orbital fissure. A complete systemic survey with a potential diagnosis of metastatic disease disclosed no primary tumor. She died within 2 months of widespread carcinomatosis; the primary remained unidentified.

An interesting syndrome of presentation may be seen with seminoma, which can rarely present as a bilateral nonspecific inflammatory or Graves' disease-like orbitopathy. The etiology is unknown; nevertheless, it does not appear to be related to direct orbital metastasis, as demonstrated by autopsy in one case, and has shown regression in response to corticosteroids or excision of the primary tumor. An endocrine mechanism has been proposed, and although two of the three reported cases were associated with an elevated serum human chorionic gonadotropin level, no direct link has been established. Direct metastasis of seminoma must be carefully excluded. In addition, a giant cell orbital myositis may rarely be seen associated with a known systemic cancer. Table 9-18 summarizes the general clinical and special features of orbital metastases.

Diagnostic Pitfalls

Misdiagnosis and delay in diagnosis are common in metastatic orbital cancer because of protean clinical manifestations, lack of clinical suspicion, and difficulty in obtaining a complete history with regard to previous cancer. The most common misdiagnoses occur in patients presenting with inflammatory syndromes, including cellulitis, myositis, endophthalmitis, and idiopathic orbital inflammatory syndrome. The clinician does not automatically consider an orbital metastasis in a patient who presents with a “hot” orbit and, indeed, this differential diagnosis properly resides fairly low down on the list. A history of previous cancer should alert the clinician to the possibility of metastasis; however, in some patients the inflamed orbit will be the first sign of cancer with a negative past history. From a clinical point of view, features that suggest metastasis are a firm orbit associated with brawny induration and a progressive (usually weeks), unrelenting course dominated by these features along with infiltrative phenomena (Fig. 9-119).

The infiltrative syndrome of presentation has been misdiagnosed as dysthyroid ophthalmopathy or idiopathic orbital fibrosis. Patients with a functional syndrome of presentation have been misdiagnosed as myasthenia gravis and sixth or third nerve palsies. The remaining misdiagnoses reflect the lengthy differential diagnoses of orbital masses, including lacrimal gland tumor, mucocele, meningioma, and chocolate cyst. Although history, examination, and special diagnostic studies will often narrow the likely possibilities, biopsy is required in the majority of cases for definitive diagnosis.

Diagnosis

History and Clinical Examination

Careful and directed history taking combined with routine ophthalmologic and orbital examination is the cornerstone of evaluating patients with orbital metastasis. A general physical examination is indispensable in patients with known or suspected metastatic disease. Breast and prostate primaries in adults, for example, and abdominal neuroblastoma in children often can be readily detected on physical examination. The diagnosis of orbital metastasis can be supported by recognition of the primary lesion during the initial visit to the ophthalmologist.

Laboratory Tests

Both nonspecific and specific laboratory tests help in the work-up of patients suspected of harboring an orbital metastasis. A nonspecific test that can be useful in the differential diagnosis of suspected metastases is the carcinoembryonic antigen (CEA). This may be elevated in patients with metastatic disease, and the degree of elevation may relate to total tumor load. Bullock and Yanes found that an elevated CEA level was specific for metastasis in their series of 42 patients with proptosis; however, the test was not very sensitive, as only 5 of 13 patients with metastatic orbital tumors had CEA levels that were significantly elevated (> 5 ng/mL). Therefore a negative test may not rule out metastatic disease.

Specific tests can be useful in tumors that secrete a measurable substance into the blood stream. Of the tumors that frequently metastasize to the orbit, prostate cancer (producing prostatic acid phosphatase) and seminoma (producing human chorionic gonadotropin) elaborate specific proteins that can be measured for diagnosis, staging, treatment, and follow-up. Carcinoid tumors may elaborate 5-hydroxyindolacetic acid into the urine, particularly in the presence of hepatic metastases and in association with the carcinoid syndrome (i.e., flushing, diarrhea, lacrimation, conjunctival injection, and other vasomotor instabilities), which usually reflects a significant tumor load.

A general evaluation by an oncologist for other metastases is important for diagnosing and staging.

Table 9-18. Summary of orbital metastasis

General Clinical Features	Temporal features	Generally occur within 6 months of primary Relentless development over 3 to 4 months Rarely acute
	General physiologic features	Infiltrative effects Motor – ptosis, decreased extraocular movements Sensory – pain Structural – mass effect or enophthalmos
	Age occurrence	Children and infants Undifferentiated sarcomas Neuroblastoma Ewing's sarcoma Wilms' tumor Medulloblastoma Adults – Postembryonal carcinoma
	Sex	Male predominance- Neuroblastoma (in children) Lung GI Hypernephroma Testicle Prostate Female predominance- Breast Adrenal Thyroid
Special Features of Histologic Types in the Orbit	Orbital propensity	Neuroblastoma Breast Ewing's sarcoma
	Cicatrizing subgroup (± enophthalmos)	Breast GI Prostate Lung
	Bone metastases	Breast – osteolytic > osteoblastic Prostate – osteoblastic > osteolytic Thyroid – osteolytic Ewing's sarcoma
	Vascular with pulsation	Thyroid Hypernephroma
	Bilateral	Breast Stomach Neuroblastoma (40%)
	Particularly painful	Mucin-secreting adenocarcinoma
	Muscle metastases	Skin melanoma – smooth contour on CT Breast – irregular and focal enlargement Oat cell
	Hemorrhage and necrosis (ecchymosis)	Neuroblastoma
	Orbital metastases as a presenting sign	Neuroblastoma (8%) Prostate Stomach Lung Kidney Gall bladder Pancreatic Testicular Undifferentiated
	Nonmetastatic proptosis	Seminoma

Imaging

CT is the practical standard for the diagnosis of orbital disease, and metastatic tumors are no exception. It not only allows for localization but can also provide important clues regarding tissue characteristics. The CT findings in metastatic orbital tumors are variable, but they can be simplified into four basic categories (Table 9-19).

The most common CT presentation is a mass (58%), followed by bone (25%), muscle (9%), and diffuse involvement (8%). Breast carcinoma favors a mass presentation and muscle involvement, prostate carcinoma strongly tends toward bone involvement (Fig. 9-114), and melanoma (Fig. 9-116) has the highest affinity for muscle.

Tumors that metastasize to bone can produce either hyperostotic or lytic change with corresponding changes on CT. Prostate carcinoma particularly tends to produce a hyperostotic response with increased density and thickness of bone, and thyroid metastases commonly cause a lytic response.

MRI provides similar information, including direct sagittal images. Superior soft tissue differentiation of MRI over CT may augment our diagnostic capabilities. For example, signal intensity on T2-weighted images is helpful in distinguishing idiopathic orbital inflammatory tumor (low intensity) from lymphoma or metastasis (high intensity). CT scan is better for evaluating bone involvement.

Needle Biopsy

One of the best applications of needle biopsy is in the setting of suspected metastatic tumors, which when successful, can save the patient from undergoing an open biopsy. In our experience, fine needle aspiration biopsy for orbital metastatic disease in adults is 90% successful in obtaining a diagnosis. If an adequate specimen can be obtained, hormone receptor and surface antigen studies for tissue source identification can be performed directly on the tissue fragment recovered from the needle (e.g., in cases of metastatic prostate carcinoma). In sclerosing lesions, such as scirrhous breast and gut metastases, needle biopsy tends to produce "dry taps" with little or no tissue retrieval.

Pathologic Techniques

The overwhelming majority of metastases are poorly differentiated or "round cell" tumors; thus, diagnosis often requires special histochemical, immunohistochemical, and electron microscopic techniques. Furthermore, in the case of hormonally responsive tumors, steroid receptor studies on the biopsy tissue are important from a therapeutic standpoint. If metastasis is being considered in the differential diagnosis, the surgeon should discuss the case with the pathologist in advance and provide an adequate amount of nontraumatized fresh tissue so that the appropriate receptor or immunohistochemical studies can be performed. The range of typical histologic features, variants, and specific distinguishing features of common orbital metastases has been outlined in the pathology chapter (*c.f.* Chapter 7). The field of immunohistochemistry is rapidly evolving, developing a broader range of specific monoclonal antibodies that identify tissue of origin. Careful, delicate handling and appropriate transmission of an adequate biopsy are critical responsibilities of the ophthalmic surgeon.

Table 9-19. CT and MRI findings in metastatic orbital tumors

Mass	Intraorbital discrete solid mass, typically well-defined and mildly contrast-enhancing; may involve or be associated with orbital structures such as bone, muscle and lacrimal gland; indents rather than invades the globe; calcification very unusual, as is cystic appearance denoting central necrosis (Fig. 9-117)
Diffuse	Diffuse mildly enhancing involvement of orbital tissues with blurring of borders and obscuration of normal orbital structures; enophthalmos may be apparent
Bone	Primarily bone involvement; may be hyperostotic (osteoblastic) or hypostotic (osteolytic); moth-eaten appearance of bone may be present in either type; large areas of bone destruction may be present; all lesions should be assessed using appropriate bone settings on CT (Figs. 9-114 and 9-119); MR imaging may recognize marrow replacement by metastasis
Muscle	Enlargement of one or more extraocular muscles; may appear smooth or have nodular reticulated borders infiltrating adjacent tissues (Figs. 9-115,9-116,9-117,9-118)

Reproduced with permission from Katz SE, Rootman J. Secondary and metastatic tumors of the orbit. In: Tasman W, Jaeger EA, eds. Foundations of Clinical Ophthalmology. 2nd ed. Philadelphia: JB Lippincott, 1996; vol 2; chap 46.

Treatment

Although it is generally true that patients with orbital metastases have a short expected life span, there are many cancers for which excellent treatment exists, and the list of treatable tumors continues to expand. Even in the case of tumors for which no direct treatment is available, troubling

symptoms such as decreased vision or pain can often be relieved with orbital radiotherapy or chemotherapy. To a person with a limited number of weeks or months of life remaining, the ability to maintain visual function and comfort is profoundly important. The principal modalities for treating patients with metastatic cancer are radiation, hormonal therapy, chemotherapy, and surgery. The diverse clinical behaviors and treatments of the common metastatic tumors to the orbit are summarized in Table 9-20 .

Table 9-20. Summary of the characteristics and treatment of common primary types of orbital metastases

TUMOR TYPE	CLINICAL CHARACTERISTICS	DIAGNOSIS	TREATMENT
Breast	Enophthalmos, infiltrative pattern of presentation; long latency; may metastasize many years after primary cancer discovered	CT: Bone and muscle involved, possibly with diffuse infiltration; needle biopsy typically unsuccessful; hormone receptors (estrogen, progesterone) on fresh biopsy tissue	Hormonal therapy; radiotherapy
Lung	Short latency, often “silent” primary (chest x-ray may be normal); rapid progression of symptoms; patient often systemically ill, survival poor		Radiotherapy; chemotherapy (oat cell)
Prostate	Older patient; may have pain; long survival possible	CT: Bony involvement, often hyperostotic; needle biopsy useful; can often use special immunohistologic stains on needle biopsy specimen	Hormonal therapy; orchiectomy; radiotherapy
Melanoma	Long latency; may metastasize many years after primary skin cancer discovered; short survival after metastatic disease	CT: Often involves muscle	Radiotherapy; chemotherapy
Gastrointestinal	Short latency, may be “silent” primary; may have infiltrative syndrome of presentation		Radiotherapy
Thyroid	Primary thyroid tumor may have been read as “benign”; long latency, long survival; may have pulsation	CT: Bone involvement, may be osteolytic	Radiotherapy; radioactive iodine
Carcinoid	Long latency, long survival; may have carcinoid syndrome; potentially isolated metastasis	CT: Typically well-defined mass; urinary 5-hydroxyindolacectic acid may be elevated, especially with liver involvement	Radiotherapy; surgical excision if isolated
Renal	Varied; may be fulminant or latent; may have pulsation		Radiotherapy
Seminoma	Young males; nonmetastatic proptosis		Radiotherapy (very radiosensitive)
Pancreas	Fulminant onset, short survival		Radiotherapy

Reproduced with permission from Goldberg RA, Rootman J, Cline RA. Tumors metastatic to the orbit: a changing picture. Surv Ophthalmol 1990;35:1-24.

Radiotherapy

Radiotherapy is extremely useful in treatment. Typically, a total of 30 to 40 Gy is given in divided doses in a period of 1 to 2 weeks. Dramatic improvement in orbital signs and symptoms, including recovery of vision when impairment is secondary to orbital mass effect, is not uncommon. In published series (which include patients with lymphoma and leukemia), the success rate is reported to be 70% to 90%. Success has been reported even in metastatic carcinoid tumors, which are traditionally considered to be fairly radioresistant. Radiotherapy for orbital metastasis is generally associated with few complications, particularly if care is taken with dosing, field placement, and shielding of the globe. However, Mortada noted a 50% occurrence of cataract in 13 patients undergoing radiotherapy for orbital metastasis. As patients treated for orbital metastatic cancer continue to survive longer, we may observe more ocular radiation complications. Still, to ameliorate symptoms of otherwise untreatable orbital tumors, radiation therapy remains the mainstay of treatment.

Hormonal Therapy

Certain cancers originating in organs that participate in hormonal axes have hormone receptors and if these cancers remain fairly well differentiated, they may show a modulation of growth in response to therapeutic hormonal manipulation. The presence of hormone receptors on the surface of these tumors can be detected and measured in the laboratory with adequate specimens of fresh tissue.

Excellent results have been obtained with hormonal therapy of prostate and breast carcinoma metastatic to the orbit. Particularly in the case of prostate carcinoma, virtual reversal of orbital symptoms and occasional long-term survival have been reported (Fig. 9-121). Diethylstilbestrol, with or without orchiectomy, has been the mainstay of hormonal therapy for prostate cancer since the 1950s. Specific luteinizing hormone-releasing hormone agonists have recently been introduced, which may avoid the feminizing side effects of diethylstilbestrol or orchiectomy. However, the luteinizing hormone-releasing hormone agonists do not seem to offer improved palliation or survival over diethylstilbestrol, and are associated with an initial testosterone surge and tumor growth period of several weeks' duration. This contraindicates their use in compressive spinal cord lesions and presumably in compressive orbital apex lesions as well.

Metastatic breast carcinoma is temporarily responsive to hormonal manipulation in the majority of cases. The importance of screening for estrogen receptors on tissue biopsy is illustrated by McGuire, who found that 55% to 60% of metastatic breast tumors with positive estrogen receptors are responsive to endocrine therapy. The presence of progesterone receptors adds even greater predictive value.

Chemotherapy

With the advent of more aggressive and specific chemotherapeutic protocols, chemotherapy for metastatic disease has become increasingly important and often plays an adjunctive role in palliative therapy. Of the common metastases to the orbit, small cell carcinoma of the lung and neuroblastoma are particularly chemosensitive.

Surgery

In general, patients with metastatic orbital tumors are not candidates for therapeutic surgical intervention. Their disease is systemic, and radical surgery cannot offer a cure. Furthermore, radiotherapy and in some cases hormonal therapy offer alternatives that often provide significant palliation.

Regardless, there are cases in which surgery is indicated. Metastatic carcinoid tumors sometimes grow so slowly that for practical purposes they are isolated tumors. In these cases, excision of the metastatic tumor (along with the primary if it can be found and safely excised) can provide long-term relief of symptoms and perhaps improved survival. Renal cell carcinoma may also present with solitary metastases; although the prognosis is still poor, surgical excision may be indicated for apparently isolated orbital metastases.

Some metastatic tumors produce intolerable symptoms, such as pain or gross proptosis. If radiotherapy, chemotherapy, or other medical approaches are unsuccessful at relieving symptoms, surgical debulking may be indicated for palliation despite the poor prognosis for survival.

Metastatic Orbital Tumors in Children

Metastatic tumors in the pediatric population deserve special mention because they are very different from those seen in adults. In contrast to adults, they are typically sarcomas rather than carcinomas, and orbital involvement is much more common than uveal involvement. Neuroblastoma and Ewing's sarcoma account for the vast majority of pediatric orbital metastases; however, Wilms' tumor, testicular embryonal sarcoma, ovarian sarcoma, and renal embryonal sarcoma have been reported.

Neuroblastoma

Neuroblastoma is the most common solid tumor of childhood, accounting for 10% to 15% of all pediatric cancer. It is second only to rhabdomyosarcoma as the most frequent orbital malignancy of childhood, and it constitutes greater than 90% of pediatric orbital malignancies. Neuroblastomas arise from embryonic neural crest tissue of the postganglionic sympathetic nervous system. The most common primary is the abdomen; however, they may originate in thoracic, cervical, or pelvic sites. The tumor may present any time in the first two decades, although the vast majority present before 3 years of age.

The orbital presentation is characterized by sudden onset and rapid progression of proptosis, which may be unilateral or bilateral, and is often accompanied by periorbital edema, ecchymosis, and ptosis. This presentation evokes a differential diagnosis, including orbital cellulitis, other rapidly developing orbital tumors (e.g., rhabdomyosarcoma, Ewing's sarcoma, medulloblastoma, Wilms' tumor), and hemorrhage into a preexisting lymphangioma. The most common orbital sites are the superolateral orbit and zygoma with

secondary extension (Fig. 9-122). A combination of bone and soft tissue involvement is common, and there may be evidence of bone destruction and other foci of cranial metastases on radiologic evaluation. Other ophthalmic manifestations may include Horner's syndrome due to mediastinal or cervical sympathetic chain involvement, opsoclonus and myoclonus, tonic pupils as a paraneoplastic effect, and metastasis to the iris or choroid. Histology and distinguishing features of neuroblastoma were described earlier in Table 7-16 (*c.f.* Pathology chapter).

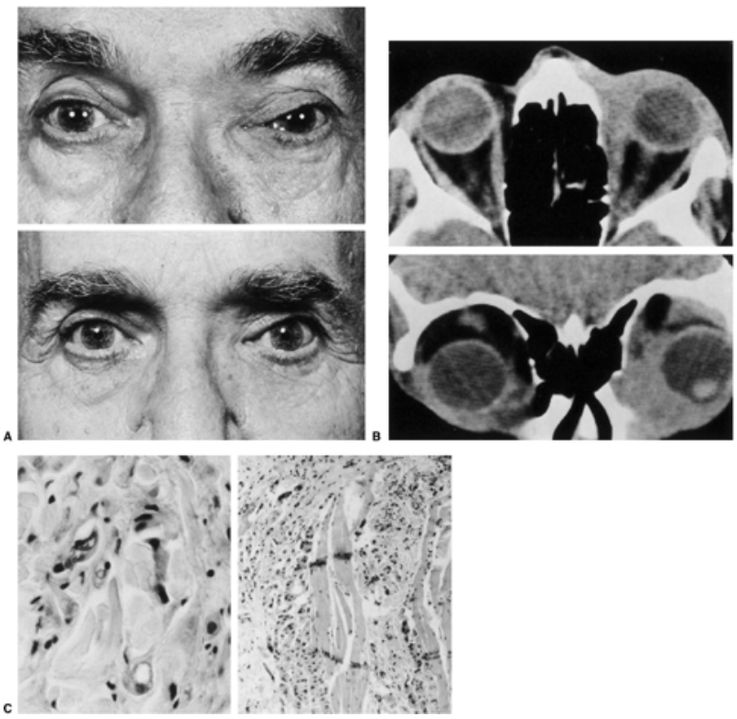

Figure 9-121. (A, top) This 65-year-old man presented with a history of chronic progressive epiphora on the left. He had become aware of a ptosis and thickening of the lid for about 1 year. On physical examination, he demonstrated 4 mm of lateral displacement of the globe with 3 mm of proptosis, and a solid infiltration of the medial orbit and upper and lower lids. It was associated with a limitation in upgaze. (B, top) Axial CT scan demonstrates a diffuse medially-located infiltrating mass involving the anterior and medial portion of the left orbit and lid, whereas the coronal scan (B, bottom) shows that the involvement surrounds the left globe. (C) Biopsy revealed an infiltrating adenocarcinoma characterized by small cords and an irregular pseudoglandular arrangement associated with a marked desmoplastic response. The tumor cells demonstrated mucin secretion within the glandlike structures as well as some intracytoplasmic mucin. Systemic investigation revealed an enlarged prostate, and biopsy confirmed a poorly differentiated, diffusely infiltrating adenocarcinoma. The patient was treated with diethylstilbestrol (Stilbestrol), and had a dramatic response. (A, bottom) One year after initiation of therapy, the patient demonstrates almost total resolution of local infiltrative disease. He is alive and well 14 years following diagnosis.

The prognosis in metastatic neuroblastoma remains poor and varies with age (more favorable in patients less than 1 year), site of primary (thoracic lesions better than abdominal), and extent of disease. Musarella et al. found that 3-year survival rates correlated with type of ocular involvement: orbital metastases (11%), Horner's syndrome (79%), and opsoclonus-myoclonus (100%). Orbital lesions are treated with radiotherapy and chemotherapy in combination with surgery for systemic disease. Aggressive combination chemotherapy with a variety of agents (e.g., cisplatin, adriamycin, cyclophosphamide, vincristine, carmustine, melphalan), with or without total body irradiation and autologous bone marrow rescue, are required for disseminated disease. Elevated urinary vanillylmandelic acid levels due to catecholamine secretion by the tumor are found in 90% of patients and can be helpful in diagnosing disease and monitoring treatment.

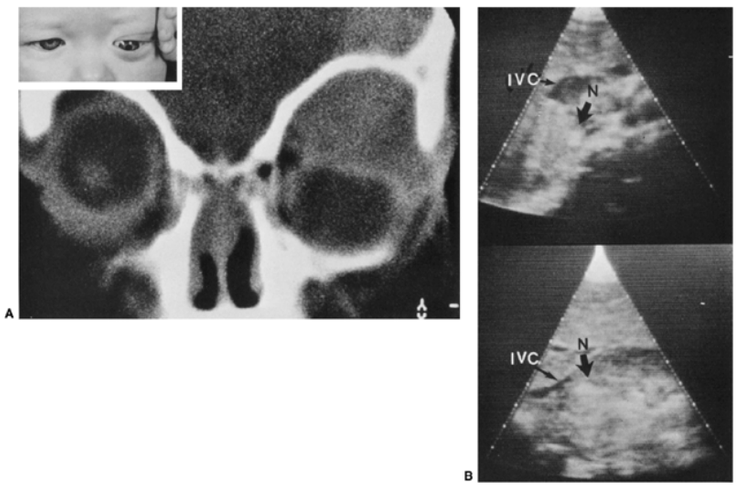

Figure 9-122. (A, inset) This 1-year-old child presented with a 2-week history of redness and crusting of the left eye associated with gradual protrusion and downward displacement. A contrast-enhanced coronal CT scan (A) demonstrated a large, irregularly enhancing orbital mass, which flattened the globe and extended through the orbital roof (area of bone destruction not shown) into the anterior cranial fossa. In the section shown, the orbital roof is slightly bowed superiorly and the anterior cranial fossa mass is seen. (B) Ultrasonography demonstrated a 3-cm to 4-cm mass (N) in the region of the right adrenal gland (B, top – transverse scan; B, bottom – coronal scan). A tumor was also noted in the region of the vena cava (IVC). The bone marrow biopsy revealed heavy infiltration with neuroblastoma, and bone scan demonstrated a metastatic lesion in the left femur. The patient was treated with systemic chemotherapy and orbital radiotherapy, but died of stage IV neuroblastoma within 1 year.

Ewing's Sarcoma

Ewing's sarcoma is a highly malignant, small, round cell tumor of primitive mesenchymal cells in the bone marrow. The majority arise in the lower extremity or pelvis, but they occasionally arise from soft tissue as an extraskeletal variant. We have seen both metastatic and primary soft tissue Ewing's sarcomas of the orbit (Fig. 9-123). Four percent of primary tumors occur in the head and neck, with the maxilla and mandible affected more commonly than the orbital roof. The tumor most commonly presents in the second decade and is rare in Asians and black Americans. Orbital presentation is generally a rapidly progressing proptosis with or without orbital hemorrhage. On a typical CT scan, the involved bone has a “moth-eaten” appearance associated with a soft tissue component of the tumor. The histologic and distinguishing features of Ewing's sarcoma, which is now

considered to be a primitive neuroectodermal tumor (PNET), are presented in Table 7-16 . Treatment generally involves a combination of radiotherapy and chemotherapy. Local disease control may consist of resection of the primary tumor after a course of induction chemotherapy. Clear margins may obviate the need for radiotherapy, although these tumors are quite radiosensitive. With modern chemotherapeutic regimens in combination with surgery or radiation, the 5-year survival rate has improved to 80%. There is a risk of both late recurrence and development of a second primary (typically osteogenic sarcoma); therefore, these patients should have long-term follow-up.

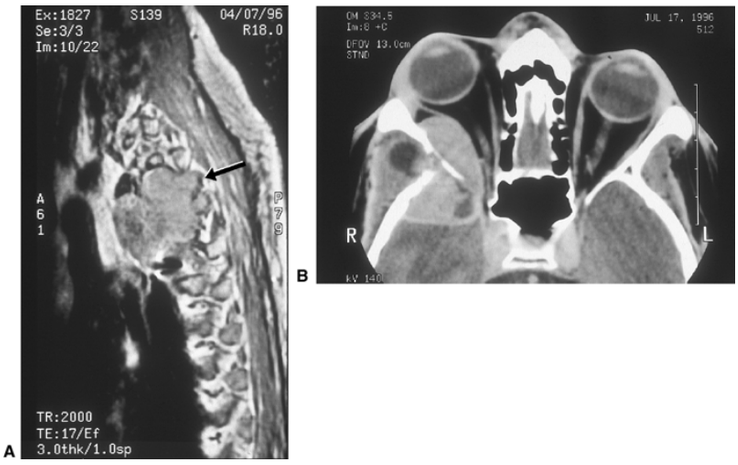

Figure 9-123. (A) This MRI demonstrates a local recurrent Ewing's sarcoma (arrow) of the spinal cord, which was associated with an orbital metastasis. The orbital metastasis appeared with a 4- to 5-week swelling of the right upper lid, more recently associated with fullness of the temporalis fossa. The patient had decreased sensation in V_1 with 3 mm of proptosis and limitation of adduction. (B) He demonstrates a large tumor mass eroding the sphenoid wing and associated with low density areas of necrosis. Aspiration needle biopsy demonstrated metastatic Ewing's sarcoma.

Oncologic Considerations

Metastatic Cancer of Unknown Origin

An important group of orbital metastases are those seen in patients with unknown primaries, which comprised 11% of the patients in a combined series (see Fig. 9-113). In large studies of patients with metastatic cancer of unknown origin, more than half remained undiagnosed despite extensive investigations. Even autopsy was unsuccessful at diagnosing the primary cancer in approximately 10% to 30% of cases. Tumors that are typically “silent,” metastasizing early in their course, constitute the majority of these unknown primaries, including lung, stomach, colon, pancreas, thyroid, and ovarian cancers. Diagnostic efforts in this difficult group of patients are best directed toward ruling out as efficiently as possible those cancers for which there is reasonably effective treatment or palliation.

Breast, prostate, and endometrial cancers have the potential for successful palliation with hormonal therapy. Germ cell tumors, lymphomas, and leukemias can sometimes be virtually cured with combination therapy. Ovarian and small cell lung cancers have curative potential, and thyroid and pancreatic tumors can be successfully palliated. A thoughtfully directed oncologic work-up can investigate these possibilities while minimizing the need for time-consuming, painful, and potentially invasive tests in these patients, for whom the limited time remaining is of great importance.

Summary

Orbital metastases are a heterogeneous group of neoplasms whose clinical behavior reflects, to a large extent, the biology of the underlying primary cancer. They can be divided into five basic syndromes of presentation: mass, infiltrative, functional, inflammatory, and silent.

The clinical presentations of metastatic tumors are diverse, but some general trends help differentiate them from other orbital tumors. A history of cancer may be obtainable (sometimes requiring considerable diligence), but in many cases the orbital symptoms are the first manifestation of systemic cancer. The onset of symptoms is typically rapid, unrelenting, and progressive over a few weeks or months. Motility disturbance is common, sometimes out of proportion to the degree of proptosis, and when present, pain often occurs early in the clinical course. Patients with breast and other scirrhous carcinomas can present with a diagnostically challenging infiltrative syndrome characterized by enophthalmos

and limitation of eye movements; these signs are easily overlooked or misinterpreted.

Investigative goals include identification of the orbital tumor as a metastasis and, when possible and without undue hardship to the patient, diagnosis of the underlying primary cancer. The ophthalmologist can play a role not only in the former, utilizing advanced imaging and needle or open biopsies where necessary, but in the latter by facilitating special histologic studies on orbital tissue. A multidisciplinary approach involving the ophthalmologist, family doctor, pathologist, and oncologist is essential for proper diagnosis and management of this challenging group of patients.

Treatment from an ophthalmologic standpoint includes preservation of vision and relief of pain. Radiotherapy and hormonal therapy can often achieve these goals, sometimes dramatically. Radical surgery is contraindicated except in extreme cases requiring palliative debulking or in cases of unusual tumors, such as carcinoid and renal carcinoma, which may have isolated metastases that can be afforded long-term cure via surgery. It is important to avoid having a hopeless or helpless attitude. With modern treatments, patients with metastatic cancer are surviving longer, and virtual cures are occasionally possible. Even in patients with limited survival, preservation of vision has a dramatic impact on the quality of life.

Tumors of the Lacrimal Gland

Jack Rootman

Valerie A. White

Hind Al-Katan

The main focus of this section will be a discussion of primary epithelial tumors. It is, however, important to consolidate knowledge of these within the context of all space-occupying lesions of the lacrimal fossa. The main categories of tumefaction here include infiltrations (primarily lymphoproliferative or inflammatory), primary epithelial tumors, and structural lesions. Appropriate management of lacrimal masses demands accurate clinical assessment and investigation in order to define the correct medical or surgical intervention.

It has been emphasized that inflammatory and infiltrative lesions are dominated by disorders frequently associated with systemic disease, which include such conditions as infections and infestations, lymphoma, sarcoid, sclerosing inflammation, Wegener's granulomatosis, and nonspecific dacryoadenitis. In the case of clinically active inflammation, the majority are nonspecific dacryoadenitis but sarcoid and Wegener's granulomatosis may present with acute or subacute inflammatory signs. Once infective lesions are ruled out, biopsy is frequently necessary because of systemic associations, as we have previously emphasized.

Noninflammatory masses infiltrating the lacrimal gland and adjacent tissue include lymphoproliferative disease, sarcoid, Sjögren's, sclerosing inflammation, Wegener's granulomatosis, and rarely amyloid. This implies the necessity to biopsy infiltrations that clinically behave as masses and frequently involve the adjacent tissues on imaging.

In contrast, neoplasia of the lacrimal gland, especially those that are epithelial, are characterized by a mass effect. Thus it becomes important to differentiate those that can potentially behave in an aggressive fashion (malignancies – chiefly adenoid cystic carcinoma) versus those that behave in a more benign fashion (primarily pleomorphic adenoma). It is commonly held that malignancies require incisional biopsy to determine the right treatment modality and that benign lesions of the lacrimal gland require complete extirpation. The key issue is to develop a management plan that allows one to arrive at the correct diagnosis and minimize the risk of local recurrence of a pleomorphic adenoma. In the modern context, the overwhelming majority of lesions can be appropriately managed based on careful clinical evaluation and accurate imaging. There remain, however, instances where one cannot be a hundred percent certain that they are handling a malignant versus benign epithelial neoplasm. In these situations, one should approach the tumor surgically as if it is a pleomorphic adenoma. We believe there is little harm done by either a preoperative fine needle biopsy or an intraoperative incisional biopsy and frozen section to differentiate between a malignant and benign lesion, followed by definitive therapy based on the frozen section.

Incidence and Pathophysiology

The major tumefactions we encountered were neoplastic, inflammatory, and structural (Table 9-21), all of which caused a clinical mass effect. The major clinical differences were between those with and without inflammatory features. Inflammatory lesions characteristically present as acute and subacute inflammations with an abrupt onset (days to weeks), accompanied by pain, localized tenderness, injection, S-shaped deformity of the lid, pouting of the lacrimal ducts, localized chemosis, and mild to moderate tumefaction. In contrast, chronic inflammatory processes are dominated by mass effect alone with subtle features of inflammation, and cannot readily be distinguished on clinical grounds from intrinsic and extrinsic neoplasms of the lacrimal fossa. Lymphoproliferative disorders are characterized by a noninflammatory mass effect, developing usually in less than 1 year and associated with little functional change. In contrast,

epithelial neoplasia are dominated by the presence of firm masses that indent, excavate, or erode adjacent structures. The more invasive or aggressive an epithelial lesion, the more it is characterized by infiltrative features that are associated clinically with pain and restriction of movement, and on imaging with infiltration of soft tissue and bone.

Table 9-21. Space-occupying lesions of the lacrimal fossa, University of British Columbia Orbital Clinic, 1976-1999

TUMOR TYPE	NUMBER OF LESIONS	TOTAL
INTRINSIC		
Neoplastic		**73**
Epithelial – benign (25)		
Pleomorphic adenoma	22	
Carcinoma in pleomorphic adenoma	2	
Rare benign tumors	1	
Epithelial – malignant (23)		
Adenoid cystic carcinoma	12	
Carcinoma ex pleomorphic adenoma	5	
Mucoepidermoid carcinoma	3	
Adenocarcinoma	1	
Polymorphous low-grade adenocarcinoma	1	
Ductal adenocarcinoma	1	
Lymphoproliferative	24	
Nonepithelial		
Spindle cell sarcoma	1	
Inflammatory		**75**
Infections		
Bacterial	6	
Viral (zoster)	1	
Noninfective		
Idiopathic	30	
Specific		
Sjögren's syndrome	10	
Sarcoidosis	12	
Wegener's granulomatosis	16	
Structural		**20**
Lacrimal cysts	20	
EXTRINSIC		
Neoplastic and Reactive		**5**
Myeloma	2	
Hodgkin's disease	1	
Eosinophilic granuloma	1	
Brown tumor (hyperparathyroidism)	1	
Inflammatory		**10**
Granulomatous	3	
Reactive xanthomatous lesion of bone	2	
Nonspecific sclerosing inflammation	5	
Structural		**10**
Dermoid	5	
Mucocele	4	
Implantation cyst	1	

Table 9-22. Armed Forces Institute of Pathology 1996 classification of salivary gland tumors

- **Benign Epithelial Neoplasms**
  - Mixed tumor (pleomorphic adenoma)
  - Myoepithelioma
  - Warthin's tumor
  - Basal cell adenoma
  - Canalicular adenoma
  - Oncocytoma
  - Cystadenoma
  - Ductal papillomas
    - Sialadenoma papilleferum
    - Inverted ductal papilloma
    - Intraductal papilloma
  - Lymphadenomas and sebaceous adenomas
  - Sialoblastoma
- **Malignant Epithelial Neoplasms**
  - Mucoepidermoid carcinoma
  - Adenocarcinoma
  - Acinic cell adenocarcinoma
  - Adenoid cystic carcinoma
  - Polymorphous low-grade adenocarcinoma
  - Malignant mixed tumors
    - Carcinoma ex mixed tumor
    - Carcinosarcoma
    - Metastasizing mixed tumor
  - Squamous cell carcinoma
  - Basal cell adenocarcinoma
  - Epithelial-myoepithelial carcinoma
  - Clear cell adenocarcinoma
  - Cystadenocarcinoma
  - Undifferentiated carcinomas
    - Small cell undifferentiated carcinoma
    - Large cell undifferentiated carcinoma
    - Lymphoepithelial carcinoma
  - Oncocytic carcinoma
  - Salivary duct carcinoma
  - Sebaceous adenocarcinoma and lymphadenocarcinoma
  - Myoepithelial carcinoma
  - Adenosquamous carcinoma
  - Mucinous adenocarcinoma
- **Mesenchymal Neoplasms**
  - Benign
  - Sarcoma
- **Malignant Lymphomas**
- **Metastatic Tumors**
- **Non-neoplastic Tumor-like Conditions**

Reproduced with permission from Ellis GL, Auclair PL. Atlas of Tumor Pathology, 3rd Series, Fasc. 17. Washington, DC, Armed Forces Institute of Pathology, 1996.

All of these lesions may occur both as intrinsic tumefactions of the lacrimal gland or extrinsic lesions in the lacrimal fossa (Table 9-21). The reader is referred to the appropriate sections in this book for further discussion of specific lesions.

Epithelial Tumors of the Lacrimal Gland

Classification

In the last four decades, epithelial tumors of the lacrimal gland have undergone reclassification, allowing for a more clear-cut definition of the biology and the expected clinical behavior of these tumors. Increasingly, the list of these rare tumors approaches the diversity and specificity of those of the salivary gland tumors (Table 9-22). We have therefore chosen to classify the epithelial tumors of the lacrimal gland, based on the salivary gland experience, into benign and malignant epithelial neoplasia (Table 9-23). In our series, approximately half of the epithelial tumors were benign (largely pleomorphic adenoma) and the remaining half had malignant features. Review of lacrimal series in the literature shows that the experience varies depending upon the timing of the review and the particular institution, but generally speaking the above applies (Table 9-24).

Benign Epithelial Neoplasia

Pleomorphic Adenoma

Forty-six percent of our cases and approximately half of epithelial tumors of the lacrimal gland published in the literature are pleomorphic adenomas. Typically they occur at a younger age (generally in the second to fifth decades) than malignant lacrimal tumors. They may, however, be seen in any age group and are generally distributed equally between males and females.

Clinical Presentation

The characteristic presentation is of a slowly progressive (more than a year), painless proptosis, downward globe displacement, and swelling of the upper lid, unassociated with inflammatory symptoms or signs. Larger tumors may be associated with blurring of vision and choroidal folds due to ocular indentation, and may have mass-induced diplopia. The range of symptoms in our experience has been proptosis (48%), progressive upper lid swelling or lateral ptosis (42%), redness or tearing (29%), diplopia (19%), visual problems (14%), pain (10%), and dysesthesia (5%). Symptom duration is commonly 3 years or more.

Table 9-23. Proposed classification of epithelial neoplasms of the lacrimal gland based on classification of salivary gland neoplasms, personal experience, and literature review

A. Benign epithelial neoplasms
   i. Pleomorphic adenoma
   ii. Carcinoma in pleomorphic adenoma
   iii. Oncocytoma
   iv. Warthin's tumor
   v. Myoepithelioma.
B. Malignant epithelial neoplasms
   i. Adenoid cystic carcinoma
   ii. Carcinoma ex pleomorphic adenoma
   iii. Mucoepidermoid carcinoma
   iv. Adenocarcinoma and ductal carcinoma
   v. Low-grade carcinoma
   vi. Other rare neoplasms
      - Acinic cell
      - Epithelial-myoepithelial carcinoma
      - Sebaceous adenocarcinoma

The common signs consist of palpable superotemporal mass (90%), downward and inward globe displacement (76%), proptosis (67%), S-shaped contour of the lid (14%), reduced visual acuity (14%), and restricted upgaze (10%). Fundus examination demonstrated globe indentation in half of our patients and choroidal folds in 10%. Sensory disturbance was noted in a fifth of the patients. Palpebral lobe tumors typically present as a nontender, upper, outer eyelid mass.

Imaging

The quintessential feature of pleomorphic adenomas is best seen on CT scan, which demonstrates pressure indentation and expansion of the lacrimal fossa in most cases (Fig. 9-124). This is usually a diffuse enlargement but may be bosselated with nodular indentation (Figs. 9-125 ,9-126 ,9-127). The globe may be indented (Figs. 9-125 and 9-126). About 30% of cases have no bony enlargement. The tumor is usually well circumscribed and may have a slightly nodular configuration. On standardized A-mode echography, there may be a definable pseudocapsule. In our series, half of the

tumors were nodular, three quarters were nonhomogeneous, and three quarters had excavation (smooth contour – pressure effect) of the adjacent bone. Calcification can be present and we noted it in a third of our cases.

Table 9-24. Incidence of benign and malignant epithelial tumors in reported series of lacrimal gland lesions

	Reese 1956	Ashton 1975	Font & Gemel 1978	Stewart et al 1979	Wright et al 1982	Kennedy 1984	Shields et al 1989	Ni & Kuo 1992	Henderson 1994	Rootman 1999
Benign										
Pleomorphic	25	30	136	14	30	12	17	140	25	22
Other	2	–	–	–	–	4	8	–	–	3
Total (%)	27(50)	30(56)	136(51)	14(45)	30(56)	16(76)	25(78)	140(51)	25(38)	25(52)
Malignant										
Adenoid cystic carcinoma	?	13	70	7	11	3	2	68	22	12
Carcinoma ex pleomorphic adenoma	?	2	43	2	3	–	3	25	10	5
Other	?	9	25	8	10	2	2	39	9	6
Total (%)	27(50)	24(44)	129(49)	17(55)	24(44)	5(24)	7(22)	132(49)	41(62)	23(48)
Total-All	54	54	265	31	54	21	32	272	66	48

Reese data from Reese AB. The treatment of expanding lesions of the orbit with particular regard to those arising in the lacrimal gland. Am J Ophthalmol 1956;41:3-11. Ashton data from Ashton N. Epithelial tumors of the lacrimal gland. Mod Probl Ophthalmol 1975;14:306-23. Font & Gamel data from Font RL, Gamel JW. Epithelial tumors of the lacrimal gland: an analysis of 265 cases. In: Jakobiec FA, ed. Ocular and Adnexal Tumors. Birmingham, Alabama: Aesculapius, 1978. Stewart et al. data from Stewart WB, Krohel GB, Wright JE. Lacrimal gland and fossa lesions: an approach to diagnosis and management. Ophthalmology 1979;86:886-95. Wright et al. data from Wright JE. Factors affecting the survival of patients with lacrimal gland tumours. Can J Ophthalmol 1982; 17:3-9. Kennedy data from Kennedy RE. An evaluation of 820 orbital cases. Trans Am Ophthalmol Soc 1984;82:134-57. Rootman data from Rootman J. Diseases of the Orbit: A Multidisciplinary Approach. Philadelphia: JB Lippincott, 1988. Shields et al. data from Shields CL, Shields JA, Eagle RC, Rathmell JP. Clinicopathologic review of 142 cases of lacrimal gland lesions. Ophthalmology 1989;96:431-5. Ni & Kuo data from Ni C, Kuo P-K. Histopathological classification of 272 primary epithelial tumors of the lacrimal gland. Chin Med J 1992;105:481-5. Henderson data from Henderson JW. Orbital Tumors. 3rd ed. New York: Raven Press, 1994.

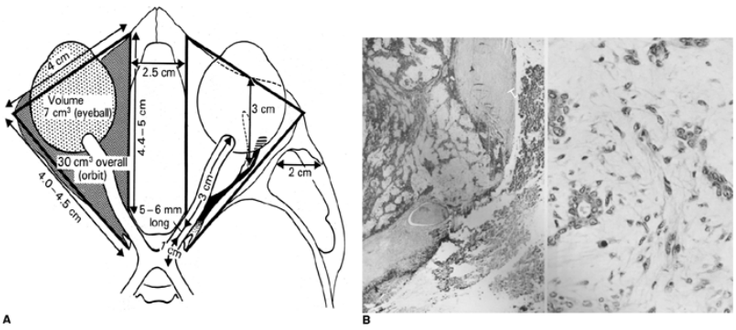

Figure 9-124. (A, right) This 50-year-old woman presented with a longstanding history of progressive right proptosis, which was evident on retrospective photographs taken 5 years earlier (A, left). On coronal CT scan (bottom), she shows a multilobular well-defined mass with smooth excavation of the adjacent orbital roof and a focal absence of the lateral orbital wall. (B) Histopathology of this benign mixed tumor was obtained from a complete excision of the mass and adjacent lacrimal gland. Note the two typical morphologic components of a loosely arranged stroma containing stellate cells and islands or tubules surrounded by ductal epithelium. The low-power photomicrograph (B, left) demonstrates an excrescence extending through the pseudocapsule (white arrow) (H&E, original magnifications; left × 2.5, right × 25). The patient is alive and well 19 years later.

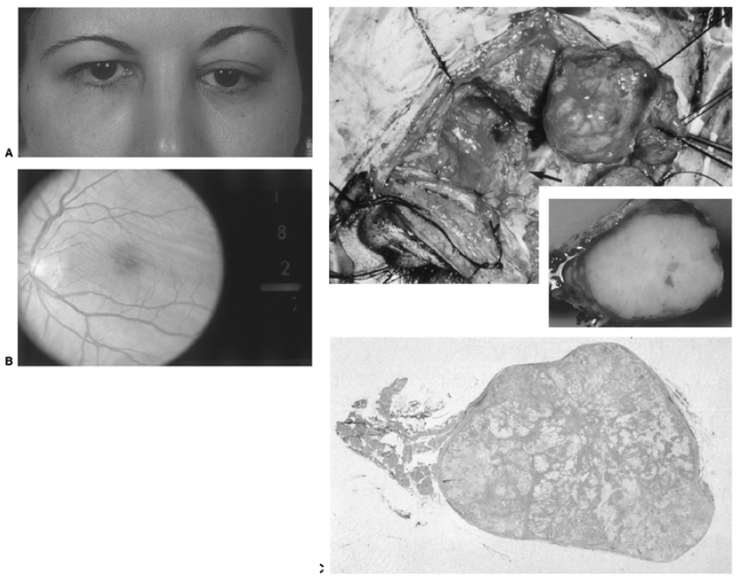

Figure 9-125. (A) This 38-year-old woman presented with a history of a slowly developing mass (1.5 years) in the left orbit and downward globe displacement with some distortion of vision. On physical examination, she demonstrated indentation of the globe with choroidal folds in the superotemporal quadrant (B). She underwent complete extirpation of this mass with the periorbital and surrounding tissue via lateral orbitotomy. (C) This composite demonstrates the surgical, gross, and low-power microscopic features of a benign mixed tumor of the lacrimal gland. Note the bosselated surface with corresponding excavation of bone (arrows) and the “mixed” nature of the tumor (H&E, original magnification × 2).

Ultrasound may reflect the histologic pattern with a highly reflective pseudocapsule, cystic spaces, and a well demarcated mass. On A-scan, there may be moderate to high internal reflectivity with multiple septae and moderate sound attenuation (Fig. 9-126E).

On MR imaging, a diffuse, nodular, well demarcated mass with fossa formation is common. It has a smooth contour and on T2-weighted images, may be heterogeneous and isointense to brain. Pleomorphic adenomas show moderate to marked enhancement with contrast both on CT and MR imaging.

Pathology

These tumors are typically firm, grayish-white, bosselated, and solitary masses grossly. Histologically, they are made up of an epithelial component derived from the ducts, which may be double layered or occur in sheets, solid masses, or narrow cords. Frequently, these foci may undergo squamous metaplasia (Fig. 9-127D). The myoepithelial component consists of an outer spindle layer that merges with the surrounding tissue. They may also undergo metaplasia into myxoid (Fig. 9-127C) or pseudocartilaginous areas, and may occasionally appear as solid sheets. The diverse patterns of the two components account for the name, pleomorphic adenoma. On average, the epithelial component accounts for two-thirds of the tumor. An important feature is the presence of microscopic nodular extensions (Fig. 9-124B) into the pseudocapsule, which is seen in approximately 60% of our cases. (This may account for the tendency in the past for the tumor to recur when appropriate margins are not taken.) Cytogenetics

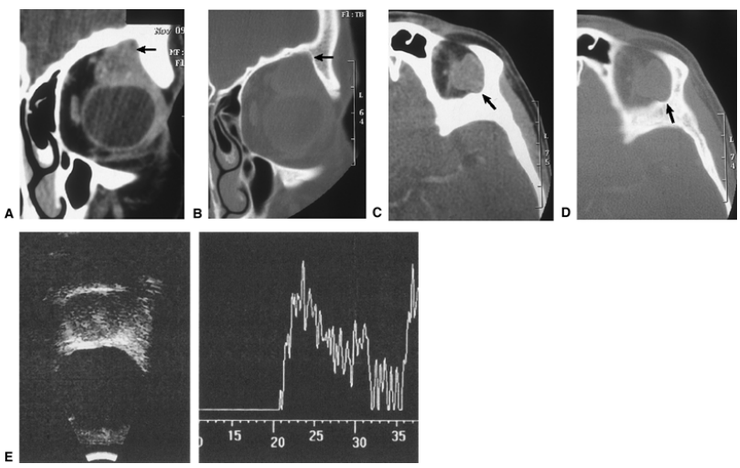

Figure 9-126. These coronal (A, B) and axial (C, D) CT scans demonstrate a firm, slightly nodular lacrimal mass indenting the globe and excavating the adjacent lacrimal fossa (arrows). The patient, a 40-year-old woman, had a 3-year history of progressive droopiness of the left upper lid without pain, swelling, or numbness. There was 4 mm each of downward and inward displacement, 3 mm of proptosis, limitation of elevation, and superior indentation of the fundus. (E, left) B-scan ultrasound demonstrated superior globe indentation by a large, well-defined, homogeneous oval mass. On A-scan (E, right) it was 15.9 × 12.8 × 13.3 mm with medium to low, slightly irregular interval reflectivity. Pathologically, it was composed largely of fibromyxoid material with few foci of pleomorphic adenoma. The tumor was excised en bloc and proved to be a pleomorphic adenoma. It has not recurred over 2 years.

of pleomorphic adenomas showing structural rearrangements involving the 3p, 8q, or 12q chromosomes have been documented by ourselves and others.

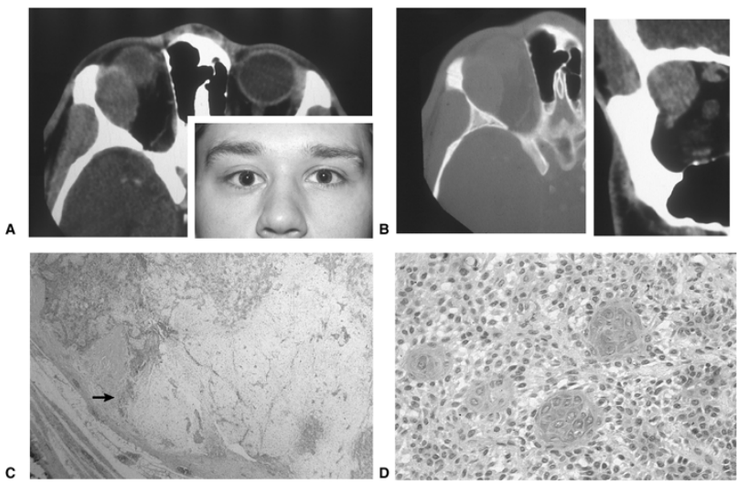

Figure 9-127. These CT scans (A, B) demonstrate coronal and axial images of a mass that occurred in a 23-year-old man with a 1-year history of protrusion of the right globe. He had 4 mm each of inward and downward displacement, and 4 mm of proptosis with restriction of upgaze and indentation of the globe. The mass was excised completely and found to be a pleomorphic adenoma of the lacrimal gland. (C) Low-power histology demonstrates myxoid and more solid portions of the tumor. Note extension into the capsule (arrow) (H&E, original magnification × 4). (D) On high power, squamous metaplasia forming eddies is noted (H&E, original magnification × 40). He has been disease free for 6 years.

Management and Prognosis

In a modern setting with a high accuracy of preoperative diagnosis and complete excision, tumor recurrence should be minimal. The two major factors to prevent recurrence are careful surgical excision without capsular rupture and a preoperative diagnosis without incisional biopsy. It should be noted, however, that incisional biopsy may still be performed in 10% to 15% of cases and if it does, careful removal of the tumor, periorbita and adjacent tissue, and the tract is associated with a virtually zero recurrence rate.

Effective management implies complete extirpation via a modified lateral orbitotomy. The important aspects are wide surgical exposure, excision of the periorbita, careful manipulation of the tumor to avoid rupture, removal of a margin or adjacent tissue, and where possible, preservation of the uninvolved palpebral lobe (reducing the incidence of postoperative filamentary keratopathy). Over the last 25 years, we have had no recurrences of 22 pleomorphic adenomas.

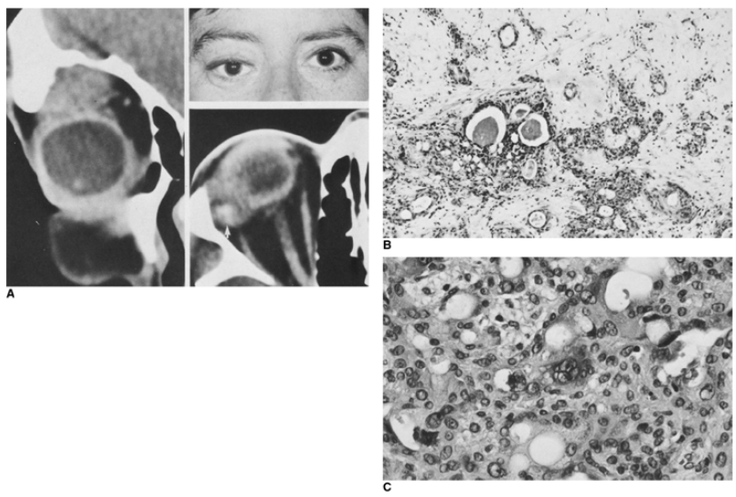

Figure 9-128. (A) This 35-year-old woman presented with a 5-year history of downward displacement of the right eye, increased tearing, and double vision in extreme right gaze. On physical examination, she had a firm, nodular mass protruding just behind the junction of the outer one third and inner two thirds of the superior orbital rim. The globe was displaced 1 mm inward and 6 mm downward, and was 3 mm proptosed. CT scan showed a soft tissue mass with focal calcification (arrow) and excavation of the adjacent bone. The patient underwent an excisional biopsy of the tumor, lacrimal gland, and adjacent soft tissues with gross total removal within the capsule. (B) Histopathologically, the lesion had the typical features of a benign mixed tumor the of lacrimal gland, but in focal areas (C) there was evidence of malignant transformation with large anaplastic cells. The final diagnosis was benign mixed tumor of the lacrimal gland with in situ malignant transformation (H&E, original magnifications; B × 10, C × 40).

Carcinoma in Pleomorphic Adenoma (Circumscribed)

It has been well established that in both salivary and lacrimal pleomorphic adenomas, the longer they are present the more likely malignant transformation may occur, with less than 3% transformation in 10 years and between 10% and 20% transformation over 20 years. It is therefore not surprising that a range of malignant transformations exists and are grouped under the term, “malignant mixed tumors.” It is important, however, to differentiate between a circumscribed, or noninvasive, carcinoma within a pleomorphic adenoma (previously called “carcinoma in situ”) versus a noncircumscribed, or invasive, carcinoma originating from pleomorphic adenoma. Those cases that represent circumscribed carcinoma are mainly benign pleomorphic adenomas with focal areas of malignant transformation. From a clinical point of view, they have the typical symptoms, signs, and radiologic presentation of pleomorphic adenoma but microscopically have circumscribed areas with histologic evidence of malignancy, such as mitoses, malignant gland formation, or cytologic atypia without extension into adjacent tissue (Fig. 9-128). The anaplastic component is usually

adenocarcinoma but rarely can be adenoid cystic, squamous, or sarcomatoid. The clinical appearance may be heralded by the sudden expansion of a heretofore indolent lacrimal mass.

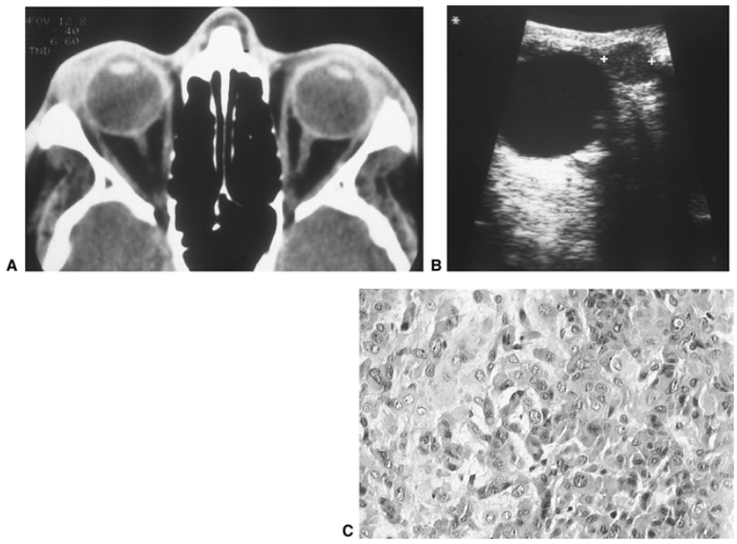

Figure 9-129. The axial CT scan (A) and B-scan ultrasound (B) demonstrate a well-defined, palpebral lobe mass that occurred in a 46-year-old man with a history of having noted the mass for 1.5 years. It was nonsymptomatic aside from its physical presence and was freely mobile. The mass was completely excised and histologically was found to be a pleomorphic adenoma with dominant cellular features of oncocytic change (D) (H&E, original magnification × 40). Note well-defined cells with granular cytoplasm. He has been alive and well without recurrence for 9 years. (Fig. 9-129B reproduced with permission from Vangveeravong S, Katz SE, Rootman J, White V. Tumors arising in the palpebral lobe of the lacrimal gland. Ophthalmology 1996;103:1606-12.)

Management

Since recognition of circumscribed carcinoma is a postoperative histologic diagnosis (arising from an operative procedure for a benign mixed tumor), the treatment is virtually identical to that for benign mixed tumors.

Rare Benign Tumors of the Lacrimal Gland

Oncocytoma

Although we have not encountered a pure oncocytoma, we have had a palpebral lobe tumor dominated by oncocytic metaplasia (Fig. 9-129). We note that this features is not infrequent in salivary gland tumors, including acinic cell carcinoma, pleomorphic adenoma, and mucoepidermoid carcinoma. The criteria for diagnosis include large polygonal cells with abundant, finely granular eosinophilic cytoplasm, and small dark cells with deeply eosinophilic compressed cytoplasm and hyperchromatic nuclei. These cells form solid trabeculae or microacini with empty lumena and little intervening stroma.

In the orbit, oncocytomas have more frequently been described in the lacrimal sac, conjunctiva, accessory lacrimal glands in the caruncle (where it is most common), and rarely in the lacrimal gland itself. Clinically, they are slow growing, reddish, discreet epibulbar masses. In the lacrimal gland, they behave as benign tumors, requiring excision.

Warthin's Tumor

Although this is the second most common benign parotid gland tumor, it accounts for approximately 4% of epithelial tumors in this site. It has been rarely noted in the lacrimal gland. Bonavolonta and colleagues described a case associated with mass effect in the lacrimal fossa arising from a cystic tumor, which was dealt with by complete excision.

Warthin's tumor is thought to have arisen from the ducts within preexisting lymphoid tumor. Microscopically, there is a double layer of epithelial cells and dense intervening lymphoid stroma, sometimes with germinal centers. The deeper epithelial layer is cuboidal or polygonal and the surface layer is columnar with fine, granular eosinophilic cytoplasm resembling oncocytic cells.

Myoepithelioma

Myoepithelioma is a benign tumor of the lacrimal and salivary glands. It is believed to be at one end of the spectrum of epithelial tumors of the glands, with pleomorphic adenoma

at the center and monomorphic adenoma (composed of benign epithelial cells only) at the other end. Although composed primarily of myoepithelial cells, about 10% can be ductal. The tumors can be spindle cell, plasmacytoid, or combined cells. Few cases exist in the lacrimal literature and all behaved clinically and radiologically like pleomorphic adenomas.

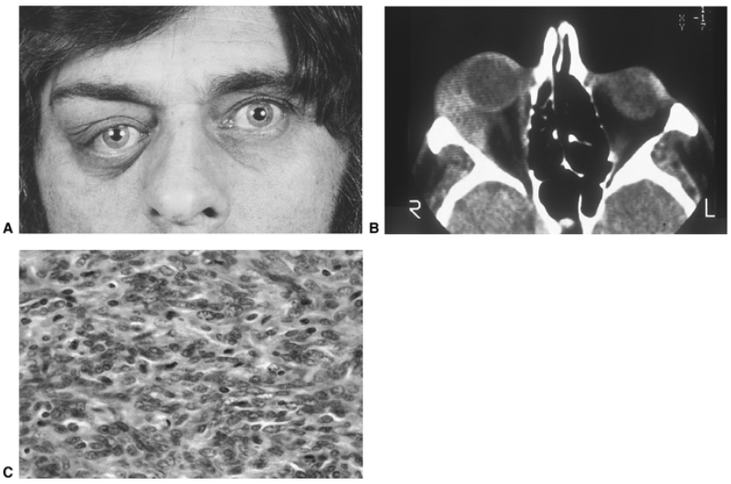

Figure 9-130. (A) This 41-year-old man presented with a 5-year history of a progressive, painless, superotemporal orbital mass on the right (B), which led to 8 mm downward and 4 mm outward displacement and no evidence of paresthesia or pain. The tumor was excised en bloc and consisted of a spindle cell infiltration of myoepithelioid cells associated with preexisting dilated lacrimal ducts (C) (H&E, original magnification × 25). He is alive and well without recurrence 16 years after excision.

We have encountered one case of a spindle cell myoepithelioma in a 40-year-old man with a 5-year history of slowly growing, painless, superolateral orbital mass (Fig. 9-130). This proved to be a well-defined tumor of the lacrimal fossa with slight enlargement of the bone. It was completely excised and has not recurred with 16 years follow-up.

Malignant Epithelial Neoplasia

Adenoid Cystic Carcinoma

Adenoid cystic carcinoma of the lacrimal gland shares with its salivary counterpart a grim reputation based on cardinal biologic features of indolence, persistence, recurrence, metastasis, and death. It is the most common malignant epithelial tumor of the lacrimal gland and it occurs in either sex with perhaps a slight female dominance. The peak incidence is in the fourth decade with a tendency to a bimodal occurrence in the second and fourth decades. It may occur slightly earlier than other malignant epithelial tumors of the lacrimal gland but a broad range of ages implies that it can be seen from adolescence to old age.

Clinical Presentation

The most important clinical features relate to tempo of onset and presence of pain. Generally, these tumors have an onset of less than 10 months, and pain has been reported in variable numbers ranging from 30% (our series) to 79%. The character of the pain is important insofar as it is persistent and, of particular note, associated with paresthesia. Persistent pain with paresthesia is rare (but not unheard of) in other lesions of the lacrimal fossa. Other clinical features include a frontotemporal mass, proptosis (80%), globe displacement, ptosis, and decreased vision, all of which are less specific.

Imaging

An important imaging feature is evidence of lytic (irregular) change in the adjacent bone. These tumors are frequently globular and often lead to expansion of the lacrimal fossa. Other features that may be suggestive but are not absolutely consistent, and may be infrequent, are irregular margins and extension toward the apex of the orbit in an almond shape (Figs. 9-131 and 9-132). In our experience, the presence or absence of calcification is of little use in differentiating these lesions from other tumors of the lacrimal fossa. On CT scan, the intrinsic lesion is usually well defined, solid, and homogeneous.

MR imaging may be more useful for defining evidence of perineural invasion, cavernous sinus involvement, or marrow replacement. T1-weighted, contrast-enhanced MRI usually shows diffuse enhancement, and T2-weighted images demonstrate the tumor as isointense to brain and extraocular muscles (Figs. 9-133A to C , and 9-134).

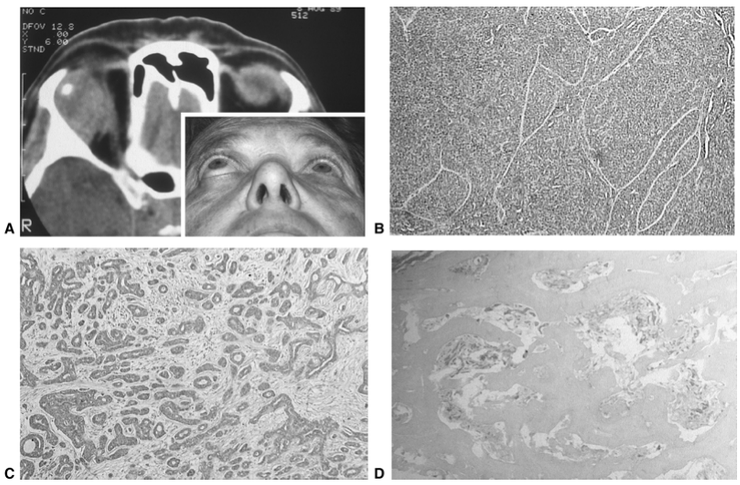

Figure 9-131. (A, inset) This 74-year-old woman presented with a 12-month history of pain, proptosis, and diplopia. She had 5 mm of exophthalmos, 4 mm downward and 2 mm inward globe displacement, and decreased sensation involving V1. (A) The CT scan demonstrated an almond-shaped lacrimal mass that appeared to erode the adjacent bone. An aspiration needle biopsy revealed a probable adenoid cystic carcinoma, which was confirmed by an excisional biopsy. She underwent a superexenteration of the orbit and adjacent bony structures with a myocutaneous graft. (B, C) The tumor was made up of a solid (basaloid) pattern mixed with a tubular pattern, and the bone was invaded by tumor (D; H&E, original magnifications; B × 10, C × 20, D × 20). She underwent radical radiotherapy and died with metastasis 8 years following surgery.

Pathology

Grossly, adenoid cystic carcinomas are usually grayish-white, firm, and may appear deceptively circumscribed, pseudoencapsulated, or nodular. During surgery, the dissection is usually more difficult compared with pleomorphic adenoma, and fine irregularity of the bone with focal bleeding is also more common.

Histopathologically, the tumor cells are small, hyperchromatic, basophilic, and of both ductal and myoepithelial type. Five histologic patterns have been described in the lacrimal gland: cribriform (glandular, Swiss cheese) (Fig. 9-135), solid (basaloid) (Figs. 9-131 and 9-132), tubular (ductal) (Fig. 9-134), sclerosing, and comedocarcinomatous (Fig. 9-132). In salivary gland tumors, cribriform, tubular, and solid types have been described. It is however important to realize that all or several of these patterns may be present in one tumor (Figs. 9-131 , 9-132 , and 9-134). The epithelial structures are usually sharply demarcated from surrounding connective tissue, and perineural (or intraneural) or perivascular spread is very characteristic (Fig. 9-134). These tumors often infiltrate to the margins of resection and often into bone (Figs. 9-131D and 9-132).

In practical terms, the most common morphologic pattern is cribriform, which is seen in the majority of cases. A dominant basaloid pattern is the least common but is felt to be associated with more aggressive behavior. Wright et al. found that disease-free survival was significantly reduced for patients with adenoid cystic carcinoma where half or more of the biopsy specimen showed basaloid differentiation.

Management and Prognosis

The prognosis for adenoid cystic carcinoma remains dismal, and the clinical course is one of painful local and

regional recurrence followed by distant metastasis, usually to the lung. The course is frequently prolonged and distressing (most dying within 5 years of recurrence). Because of this tumor's ability to recur even at a very late date (24 years in one of our cases), the incidence of disease-free patients decreases over time approaching zero by 20 years. Often the die is cast at the time of presentation, the tumor having clearly escaped the bounds of surgical extirpation. Biologically, complete excision would be ideal because conventional radiotherapy has not been shown to be efficacious except as an adjuvant following gross total removal. Immediacy of the cranial nerves allows a high proportion of tumors to extend beyond the bounds of excision into the Gasserian ganglion and cavernous sinus. Current regimens really should aim for local control.

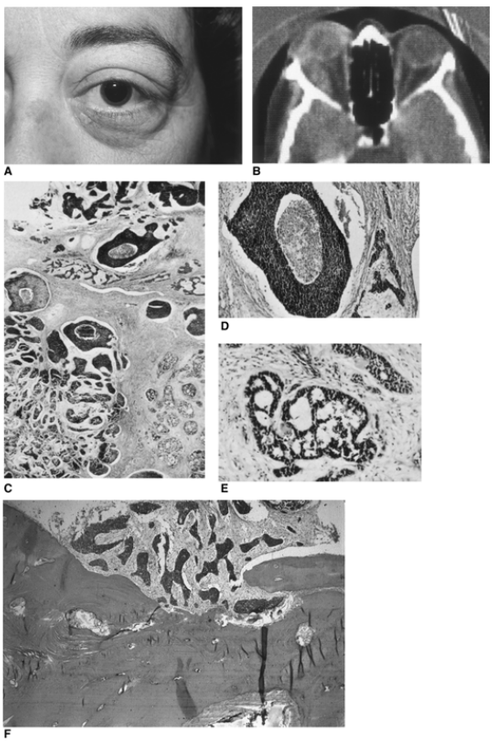

Figure 9-132. Basaloid, comedocarcinomatous, and cribriform patterns. (A, B) This 39-year-old woman presented with a 1-year history of lid swelling associated with proptosis but unassociated with pain or diplopia. She had downward, inward displacement of the globe with proptosis and a sensory deficit in V1. Incisional biopsy revealed a solid carcinoma of the lacrimal gland. She underwent a superexenteration of the orbit and adjacent tissues, and the tumor was found to have a mixture of a basaloid and comedocarcinomatous pattern. (C, D) The histology showed an aggressive, widely infiltrating mass of cords (H&E, original magnifications; C × 2.5, D × 10). Note the solid tumor cells with central foci of necrosis (comedocarcinomatous), and there was a focal area of a more typical adenoid cystic pattern (E) (H&E, original magnification × 10). (F) The tumor invaded the adjacent bone, in cords of solid basaloid cells (H&E, original magnification × 2.5). She died of pulmonary metastasis 2 years following surgery.

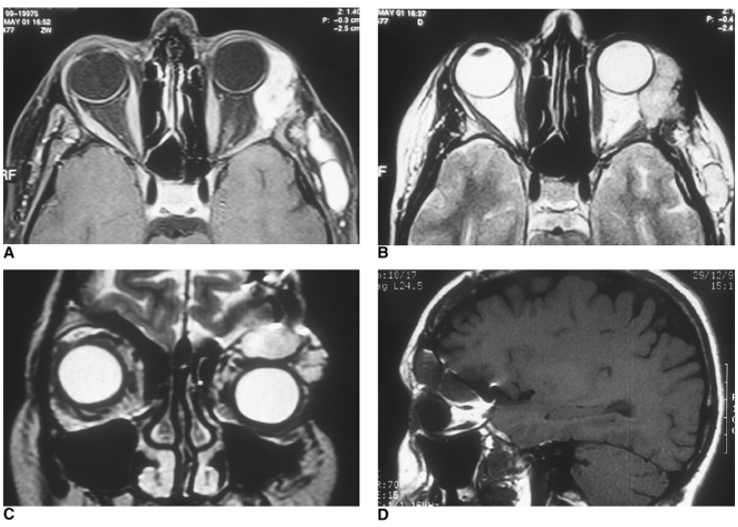

Figure 9-133. This adenoid cystic carcinoma was seen in a 41-year-old woman who had had a previous local excision at age 17 and repeat removals at ages 27 and 36 with a partial removal of the bone. Again, she underwent another local removal 2 years later with a rapid recurrence within a year, leading to downward, inward displacement of the globe and evidence of a superotemporal mass invading the residual bone, sinus, and temporalis fossa. (A) T1-weighted MRI with gadolinium enhancement and fat suppression demonstrates a hyperintense homogeneous lesion of the lacrimal fossa invading the residual bone and associated with second lesions in the temporalis fossa. (B) T2-weighted imaging shows the same mass, which is isointense to brain. (C) The T2-weighted coronal MRI shows tumor invasion of the orbital roof and part of the frontal sinus, which is also demonstrated on T1-weighted sagittal view (D). The patient refused radical therapy and underwent local excision only, developing recurrent disease within 2 years with involvement of the ipsilateral and opposite cervical lymph nodes.

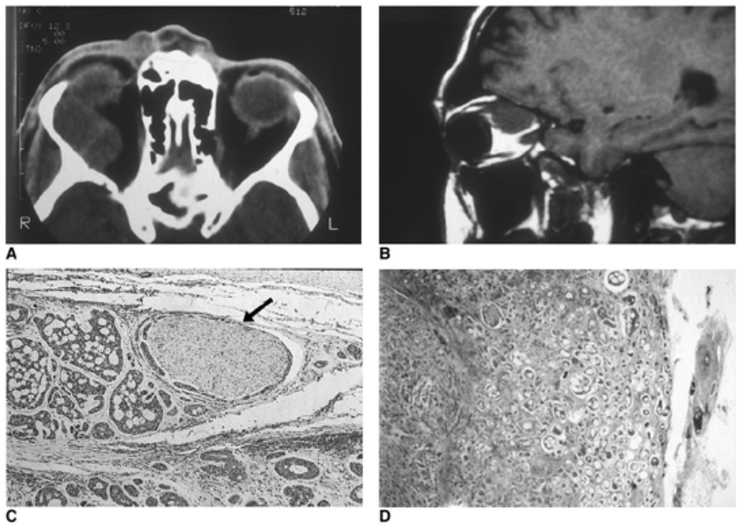

Figure 9-134. This 36-year-old man presented with blurring of vision on the right side, which had been present for a month, without any symptoms of pain or awareness of mass or distortion. There was no evidence of hypesthesia but there was 2 mm of downward displacement of the right globe with 5 mm of exophthalmos and slight limitation of abduction. On CT (A) and MR imaging (B), a mass was noted extending into the posterolateral orbit. Bone settings on CT scan showed slight irregularity of the lateral orbital wall. He underwent an incisional biopsy, which demonstrated an adenoid cystic carcinoma. (C, D) The carcinoma had both a tubular and cribriform pattern but was dominantly tubular, consisting of bilayered epithelial ductal structures or strands surrounded by desmoplastic stroma. It was noted to have invaded perineurally (arrow) (H&E, original magnifications; C × 10, D × 10). He underwent exenteration with removal of the adjacent bone followed by orbital radiotherapy. He has been followed for 9 years without recurrence or metastasis.

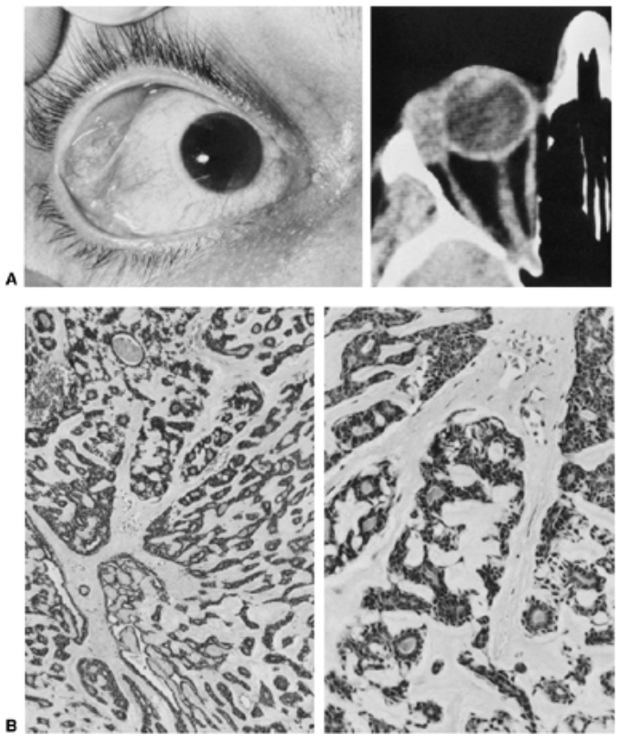

Figure 9-135. (A) Clinical photograph and axial CT scan of a patient who presented with a focal palpable tumor mass in the lacrimal fossa with slight flattening of the globe. There were no features of orbital infiltration or sensory loss. The lesion was removed totally by lateral orbitotomy. (B) Histopathologically, the mass proved to be an adenoid cystic carcinoma with a typical cribriform pattern or glandular pattern, consisting of epithelial nests or islands permeated by cylindrical spaces, which are pseudocysts containing proteoglycans and basement membrane-like material (so-called Swiss cheese appearance) (H&E, original magnifications; left × 2.5, right × 10). Myoepithelial cells surround the pseudocysts, and infrequent true glands with inconspicuous lumena-containing secretory material are surrounded by cuboidal ductal cells. Note the cords of epithelial cells are surrounded by dense connective tissue. In view of the diagnosis, a wide local excision of the adjacent bone and soft tissues (excluding the extraocular muscles and eye) was done. There has been no recurrence to date with 16 years' follow-up.

For tumors that are reasonably well defined, local excision along with the adjacent bone followed either by brachytherapy or radical external beam therapy affords the best potential for a disease-free interval or even local cure. Tumors that have extended into the bone or the soft tissues of the orbit may require radical en bloc orbitectomy by a multidisciplinary team. The excision should include the orbital roof, lateral wall, lids, and anterior portion of the temporalis muscle where the zygomaticofrontal and zygomaticotemporal nerves extend. Reconstruction can involve a myocutaneous flap to allow for postoperative radical radiotherapy. The role of local regional or systemic chemotherapy remains unclear in what is essentially an indolent tumor.

Young patients may have a better prognosis, possibly due to less aggressive histologic features. Two of our cases, who presented as early adolescents, have survived for 12 and 17 years, respectively.

We have had 12 adenoid cystic carcinomas. Four patients underwent en bloc excision (orbitectomy), three of which were followed by radiotherapy. One died at 2 years and a second at 8 years, with metastasis in both and local recurrence additionally in one. The remaining two are alive without recurrence at 1 and 12 years follow-up respectively. Four patients underwent local excision with adjacent bone

and lacrimal nerve. In this group, two recurred at 24 and 2 years while two are alive without recurrence, both after 17 years of follow-up. One of our patients underwent exenteration followed by radiotherapy and is alive without recurrence at 9 years. One patient refused therapy and died with metastasis at 3 years.

Carcinoma ex Pleomorphic Adenoma (Noncircumscribed)

As noted earlier, malignant transformation of pleomorphic adenomas is a time dependent phenomenon; thus on the average, these patients are 10 to 20 years older than patients with pleomorphic adenoma. A pleomorphic adenoma that gives rise to noncircumscribed carcinoma is an invasive tumor originating from a pleomorphic adenoma, in contrast to carcinoma in pleomorphic adenoma, which demonstrates noninvasive intralesional carcinomatous foci. This malignancy occurs in salivary gland tumors with varying rates of 2% to 23%. In the lacrimal gland, the malignant transformation rates vary from 4% to 24%. Font and Gamel suggest that such transformations of recurrent pleomorphic adenomas occur in 10% after 20 years and 20% after 30 years.

Clinical Presentation

There are four clinical circumstances in which noncircumscribed carcinoma ex pleomorphic adenoma present. The first is a sudden growth of a longstanding lacrimal mass, reflecting malignant transformation. The second is an indolent lacrimal mass. The third parallels those seen in other lacrimal epithelial malignancies arising de novo and includes rapid growth, pain, and bony infiltration. The fourth circumstance is a sudden recurrence of a previously excised mixed tumor of the lacrimal gland.

Imaging

CT scanning may demonstrate features of both benign mixed tumor (i.e., central lucent areas or inhomogeneity, nodularity, bosselation, and expansion of the lacrimal fossa) and invasive carcinoma (uniformly dense irregular margin corresponding to a rim of invasive carcinoma) (Fig. 9-136). True bone erosion is present in a small percentage of patients. Calcification may raise the index of suspicion but is an unreliable feature in lacrimal gland tumors.

Pathology

The proportion and type of noncircumscribed carcinoma arising from pleomorphic adenoma can vary from tumor to tumor. The majority will show both components but an essentially monomorphic carcinoma may have only small foci of the pleomorphic adenoma. Many different types of carcinoma ex pleomorphic adenoma have been described. The most common is the undifferentiated adenocarcinoma but mucoepidermoid, squamous, mixed, adenoid cystic, and sarcomatoid types have been described. In our series we had five invasive carcinoma ex pleomorphic adenomas, three of which were mucoepidermoid (previously classified as primary mucoepidermoid but on careful review of the blocks, pleomorphic components were identified), one polymorphous low-grade adenocarcinoma, and one adenocarcinoma.

Management and Prognosis

Overall it has been suggested that the prognosis for invasive carcinoma ex pleomorphic adenoma arising from recurrent disease is worse than the de novo lesions. The influence of therapy on outcome is difficult to assess because of the few numbers, but overall in the case of primary occurrences, a one-stage surgical procedure with radiotherapy is the most effective means of local and systemic control. Specific treatment would depend on the tumor size, degree of infiltration of the orbit and adjacent tissues, and systemic evaluation, particularly of the lung. Significant orbital infiltration along with bony involvement implies the need for orbitectomy. Henderson has noted that patients with an original benign mixed tumor live longer (mean 19.2 years) than those with a de novo variety of malignant mixed tumor (mean 7.7 years).

Mucoepidermoid Carcinoma

Mucoepidermoid carcinoma is a malignant epithelial tumor composed of mucinous and squamous cells that are derived from modified luminal epithelial and myoepithelial cells. Although common in the salivary gland, they are rare in the lacrimal gland (representing approximately 2% of epithelial tumors).

Clinical Presentation and Imaging Features

Eviatar and Hornblass reviewed 25 cases of mucoepidermoid carcinoma, noting that the average onset age was in the fifth decade and that the tumor usually presented as a slowly growing mass in the lacrimal fossa. Other features may include pain or epiphora. This tumor may also present as a rapidly growing mass (Fig. 9-137).

Imaging demonstrates a lacrimal mass with possible posterior extension, frequently with cystic components (Fig. 9-138). Invasion of the bone can occur rarely.

Pathology

These tumors are graded according to the degree of differentiation and relative numbers of mucin producing cells. Generally, higher-grade tumors are dominated by epidermoid or squamous cell features, and lower-grade tumors have more mucin producing cells. Mucoepidermoid carcinomas are classified as grade 1, 2, and 3 based on degrees of cellularity, hyperchromatism, and frequency of mitotic figures.

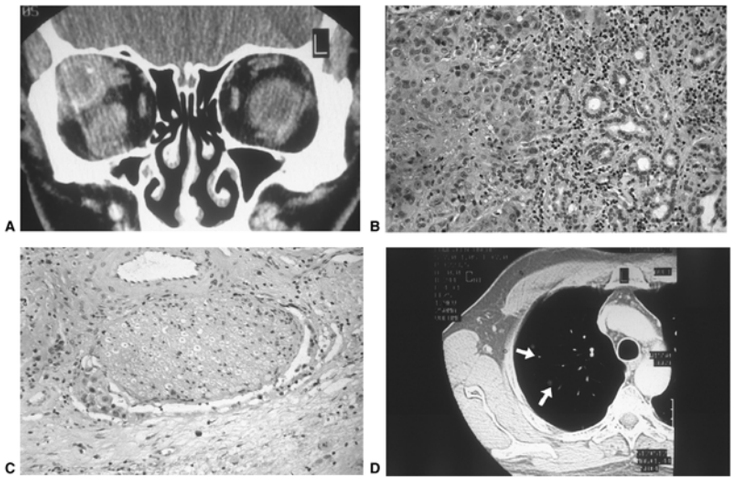

Figure 9-136. Carcinoma ex pleomorphic adenoma. This 64-year-old man presented with a mass noted in the superolateral right orbit for 2 years. (A) His CT scan demonstrates a superolateral mass with irregular margins and some molding of the bone. An excisional biopsy revealed an irregular mass that proved to be an adenocarcinoma ex pleomorphic adenoma. (B) This tumor invaded the lacrimal gland and had some perineural invasion (C, arrow) (H&E, original magnifications; B × 25, C × 25). Systemic investigation revealed multiple pulmonary nodules of metastatic tumor. (D) This CT scan demonstrates multiple pulmonary metastases (arrows), which were proven to be adenocarcinoma on biopsy.

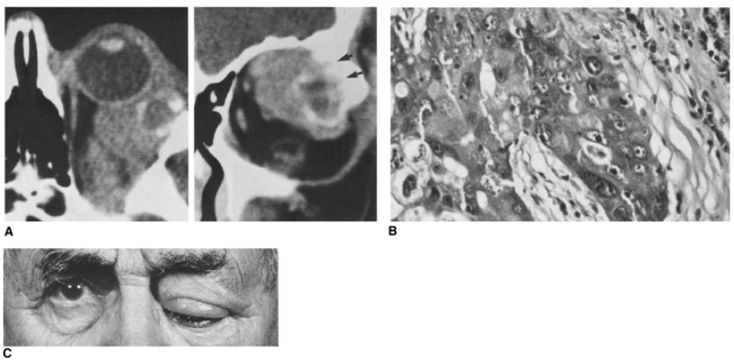

Figure 9-137. Axial (A, left) and coronal (A, right) CT scans and histopathologic features (B) of a rapidly developing infiltrative tumor the of lacrimal gland (H&E, original magnification × 25). It proved to be a poorly differentiated, high-grade mucoepidermoid carcinoma, probably arising from a pleomorphic adenoma. This 77-year-old man (C) presented with 13 mm of proptosis, marked limitation of ocular movements, counting fingers vision, marked swelling, and firm tumefaction of the superolateral orbital soft tissue. Irregular erosion of adjacent bone (A, arrows) due to invasion by the tumor and calcification within favor a malignancy. This patient died of metastatic disease 4 years after debulking and radiotherapy.

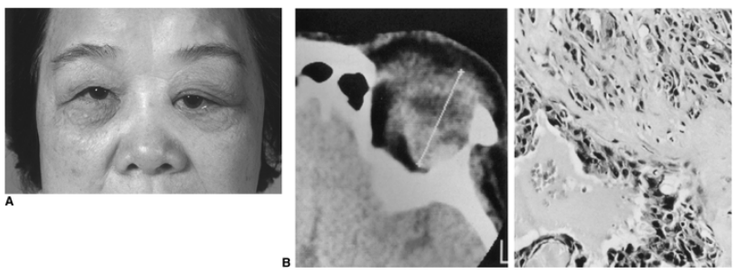

Figure 9-138. (A) This 67-year-old woman presented with a recently noted left superolateral orbital mass, which was a well-defined, slow-growing lacrimal mass that on axial CT scan (B, left) demonstrates excavation of the adjacent orbital wall and inhomogeneous pattern. This tumor was completely excised along with the adjacent lacrimal gland. (B, right) It had a dense capsule containing cords of both mucin-producing and epidermoid cells. Note pools of mucin (H&E, original magnification × 10). It was histologically classified as a low-grade mucoepidermoid carcinoma with a single focus of pleomorphic adenoma. The patient was alive and well without recurrence 20 years following presentation.

Management and Prognosis

The single most important prognostic factor appears to be grade of tumor. Low-grade tumors (grades 1 and 2) generally have a favorable prognosis with a relatively high survival rate (Fig. 9-138) whilst high-grade tumors (grade 3) have a poor survival rate (Fig. 9-137). The recommended treatment for low-grade tumors is complete excision with or without adjuvant radiotherapy. Higher-grade tumors require exenteration or orbitectomy with radiotherapy, after careful metastatic workup.

All three of our cases arose from preexisting pleomorphic adenomas, one in the palpebral lobe of the lacrimal gland and the remaining two in the orbital lobe. The patients with low-grade and palpebral lobe (intermediate grade) tumors are alive and well at 5 and 20 years. The patient with the high-grade tumor died of metastatic disease 4 years after debulking and irradiation.

Adenocarcinomas

In the salivary gland and increasingly in the lacrimal gland, a wide range of adenocarcinomas has been described based on the dominant cell type. At least 10 types have been noted in the salivary gland and six in the lacrimal gland (Tables 9-22 and 9-23).

Adenocarcinoma

By definition, an adenocarcinoma is a neoplasm that shows glandular or ductal differentiation and infiltrative growth with striking cytologic atypia, which does not allow for subtyping. The largest lacrimal series reported is by Heaps and colleagues and includes 13 patients from multiple centers. The tumors usually presented as rapidly growing, aggressive masses, and patients presented with proptosis, pain, visual loss, ptosis, and tearing. Half of the patients died, one quarter were alive with recurrence, and the remainder were alive and disease-free. The authors concluded that a shorter duration of symptoms appeared to correlate with a decreased chance of metastasis and an increased long-term survival. Recommended treatment is exenteration followed by radiotherapy. These tumors may present with simultaneous metastasis and progress very rapidly.

Polymorphous Low-Grade Adenocarcinoma

This is a malignant epithelial tumor that is common in the minor salivary glands, where it is usually circumscribed but not encapsulated. It responds well to wide surgical excision with a 17% recurrence rate and a nodal metastasis rate of approximately 10%.

The importance of this lesion is that it demonstrates a wide range of growth patterns, including solid, trabecular, ductular, and tubular formations. In addition, cribriform, cystic, and papillary-cystic features may be present. They can infiltrate into surrounding tissue including perineurally. The tumor cells, however, are well differentiated with few mitoses. Because of these varying patterns, it is important to recognize this tumor, since it may resemble adenoid cystic carcinoma.

We have seen a single case of polymorphous low-grade adenocarcinoma arising from a small focus of pleomorphic

adenoma. It was a longstanding mass that caused focal thinning and excavation of the lateral orbital wall. The patient underwent local excision with adjacent bone and has been disease free for 10 years.

Ductal Adenocarcinoma

We have described one case of ductal adenocarcinoma (Fig. 9-139) and are now aware of several cases in other centers. Our patient presented with a 6-month history of ptosis and proptosis secondary to a painless mass in the lacrimal fossa. Imaging revealed an irregular nodular mass that extended posteriorly with no bone destruction. On pathology, the tumor had glandular structures in a cribriform pattern with apocrine features. In addition, comedonecrosis and vascular and perineural invasion were present. He underwent an en bloc orbitectomy and radiotherapy and has been disease free for 5 years. The histology was equivalent to that of salivary duct carcinoma.

Sebaceous Adenocarcinoma

Sebaceous adenocarcinoma rarely arises de novo in the salivary glands where it behaves as an intermediate-grade tumor. It recurs in approximately one third of cases. Few cases have been described in the lacrimal gland, the majority of which have developed from a preexisting benign mixed tumor or an anaplastic carcinoma.

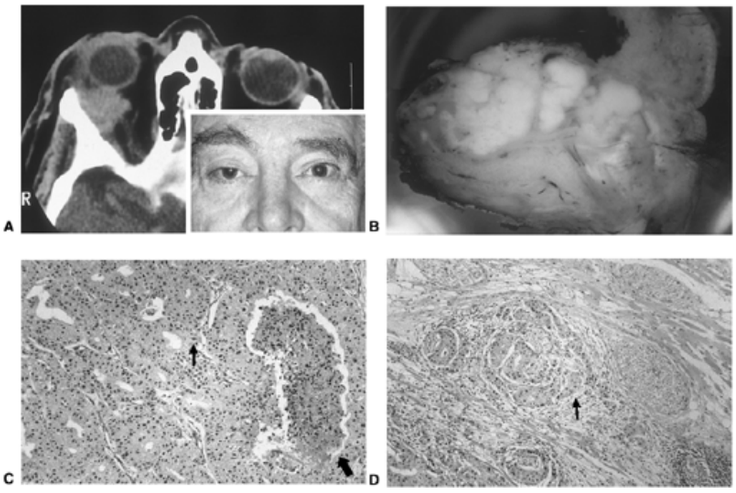

Figure 9-139. (A, inset) This 68-year-old man presented with right ptosis associated with proptosis and downward displacement of the globe. A nodular mass was demonstrated on axial CT scan (A), which had irregular borders and extended posteriorly. (B) Gross photograph of the exenterated orbit demonstrates a nodular pale mass, which proved on histology (C, D) to consist of glandular structures in a cribriform pattern (small arrows) with apocrine features. Comedonecrosis was also demonstrated (C, large arrow). He is alive and well 4 years after exenteration and radiotherapy. (Fig. 9-139A reproduced with permission from Katz SE, Rootman J, Dolman PJ, et al. Primary ductal adenocarcinoma of the lacrimal gland. Ophthalmology 1996;103:157-62.)

Acinic Cell Adenocarcinoma

Acinic cell adenocarcinoma is a malignant epithelial neoplasm of acinar cells and is the third most common epithelial malignancy of the salivary gland. Its primary histopathologic feature is the presence of neoplastic acinar cells with PAS-positive granules. A broad spectrum of histopathologic and cytologic features is present in these tumors, and vacuolated cells are not infrequent.

It has been described in two instances in the lacrimal gland. One was a primary tumor that appeared as a partially cystic mass in the lacrimal fossa, which was histologically characteristic with a low mitotic index and encapsulated. Treatment was local excision alone. The second case was that of an 18-year-old woman who had a recurrence after a lateral orbitotomy and external beam irradiation. She was treated by exenteration and had no recurrence in 4.5 years.

Basal Cell Adenocarcinoma

Basal cell adenocarcinoma has the cytologic features of basal cell adenoma but is infiltrative and, in the salivary gland, has a very low potential for metastasis. It is noted to be encapsulated and homogeneous. Histologically, it is made up of basaloid epithelial cells in a solid or trabecular pattern with a collagenous fibrous stroma. In the lacrimal gland, a single case has been reported by Khalil and Arthurs, which had on an earlier occasion been diagnosed as a solid adenoid cystic carcinoma. The patient was a 36-year-old woman with a 3-year history of a lacrimal mass and a 1-year history of mild pain. On CT scan, there was a homogeneous tumor without erosion of bone. The tumor was removed along with the bony rim after frozen section diagnosis. It was found to be incompletely excised on the basis of microscopic extension beyond the pseudocapsule. A radical exenteration was then carried out and the patient has had no recurrence in 10-years' follow-up (Fig. 9-140).

Epithelial – Myoepithelial Carcinoma

Epithelial-myoepithelial carcinoma is a biphasic tumor of myoepithelial and ductal cells. Usually the myoepithelial component dominates these tumors in the salivary gland and the behavior is one of a relatively low-grade, locally invasive malignancy. A single case has been reported in the lacrimal gland arising from a pleomorphic adenoma.

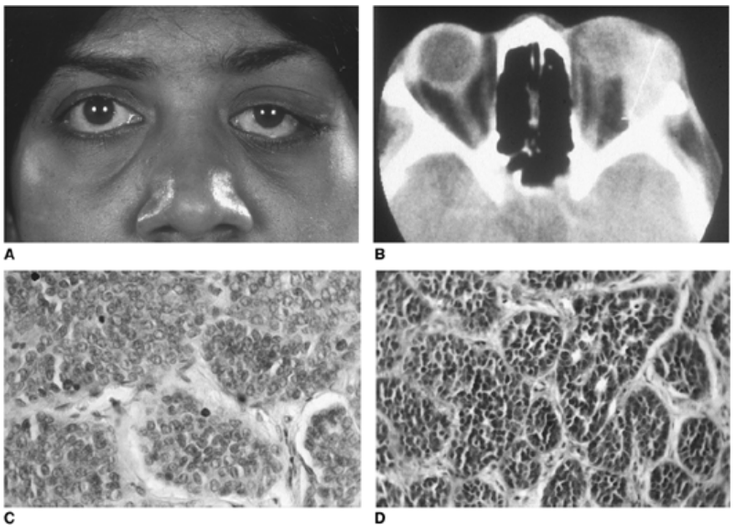

Figure 9-140. (A) This 36-year-old woman presented with a mass in the superotemporal region of her left orbit, which the patient described as slowly progressive over a 3-year period. It was associated with an 8-year history of transient discomfort and for the past 12 months, a constant mild pain during the day. She also had proptosis and downward displacement of the globe. (B) CT scan demonstrates a large homogeneous mass with smooth borders in the lacrimal gland region with no bony erosion. The mass was removed via a lateral orbitotomy. Histopathologically, it was enveloped by a pseudocapsule and was also found to be incompletely excised. The patient's left orbit was then exenterated. (C) and (D) demonstrate cords of basaloid epithelial cells, previously misdiagnosed as a solid adenoid cystic carcinoma. (Figs. 9-140A and B reproduced with permission from Khalil M, Arthurs B. Basal cell adenocarcinoma of the lacrimal gland. Ophthalmology 2000;107:164-8. Figs. 9-140C and D courtesy of Dr. Mourad Khalil.)

Benign versus Malignant Epithelial Tumors

In order to deal with both inflammatory and noninflammatory tumefactions of the lacrimal gland, we have provided an algorithm that includes assessment of the tempo, clinical presentation, imaging, and management of these lesions (Fig. 9-141). In essence, the major clinical characteristics that differentiate the risk of malignant versus benign lesions are based on clinical features of duration of symptoms, persistence of pain, and evidence of sensory loss. The radiologic symptoms that help to differentiate between these two groups of entities are the shape of the mass, evidence of molding, tumor calcification, invasion of bone, and duration of symptoms in relation to the tumor size. Rose and Wright have summarized this in their management plan for masses in the orbital lobe of lacrimal gland (Table 9-25).

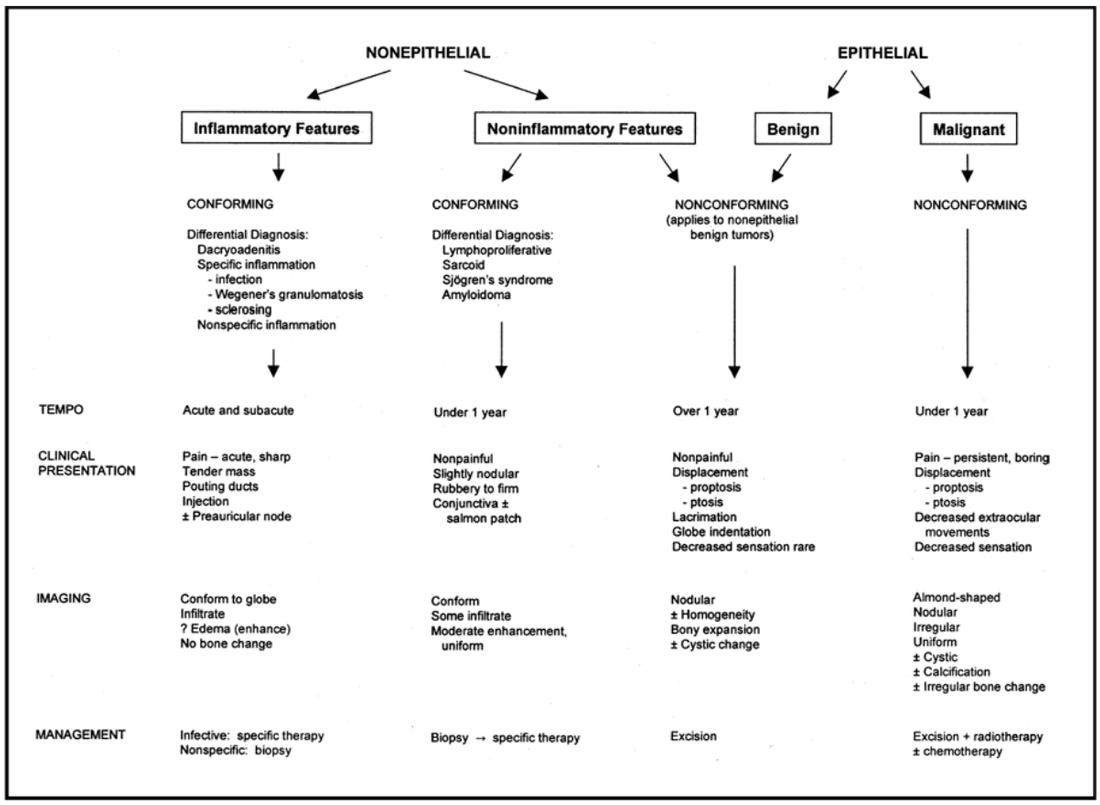

Figure 9-141. Algorithm for diagnosis and management of lacrimal tumor masses.

Table 9-25. Management plan for masses within the orbital lobe of the lacrimal gland

	SCORE	
CHARACTERISTIC	**-1**	**+1**
Clinical		
Duration of acute symptoms	< 10 months	> 10 months
Persistent pain	Present	Absent
Sensory loss	Present	Absent
Radiological*		
Well-defined round or oval mass	Absent	Present
Molding of mass to globe or along the lateral orbital wall	Present	Absent
Tumor calcification	Present	Absent
Bone Invasion	Present	Absent
Duration of symptoms in relation to tumor size	Large tumors; short symptoms	Small tumor; long symptoms

* Features on high-resolution CT studies

Total score: -8 to +2, probably carcinoma (for incisional biopsy); -6 to +2, probably malignant mixed tumor (for incisional or excisional biopsy); +3 to +8, probably pleomorphic adenoma (for excision without prior biopsy)

Reporoduced with permission from Rose GE, Wright JE. Pleomorphic adenoma of the lacrimal gland. Br J Ophthalmol 1992;76:395-400.

Bibliography

Neurogenic Neoplasia

Optic Nerve Gliomas

Albers GW, Hoyt WF, Forno LS, Shratter LA. Treatment response in malignant optic glioma of adulthood. Neurology 1988;38:1071-4.

Alvord EC Jr, Lofton S. Gliomas of the optic nerve or chiasm. Outcome by patients' age, tumor site, and treatment. J Neurosurg 1988;68:85-98.

Anderson DR, Spencer WH. Ultrastructural and histochemical observations of optic nerve gliomas. Arch Ophthalmol 1970;83:324-35.

Brauner R, Malandry F, Rappaport R, et al. Growth and endocrine disorders in optic glioma. Eur J Pediatr 1990;149:825-8.

Brodovsky S, ten Hove MW, Pinkerton RMH, et al. An enhancing optic nerve lesion: malignant glioma of adulthood. Can J Ophthalmol 1997;32:409-13.

Brodsky MC. The "pseudo-CSF" signal of orbital optic glioma on magnetic resonance imaging: a signature of neurofibromatosis. Surv Ophthalmol 1993;38:213-8.

Bruggers CS, Friedman HS, Phillips PC, et al. Leptomeningeal dissemination of optic pathway gliomas in three children. Am J Ophthalmol 1991;111:719-23.

Bynke H, Kagstrom E, Tjernstrom K. Aspects of the treatment of gliomas of the anterior visual pathway. Acta Ophthalmol (Copenh) 1977;55:269-80.

Charles NC, Nelson L, Brookner AR, et al. Pilocytic astrocytoma of the optic nerve with hemorrhage and extreme cystic degeneration. Am J Ophthalmol 1981;92:691-5.

Charrow J, Listernick R, Greenwald MJ, et al. Carboplatin-induced regression of an optic pathway tumor in a child with neurofibromatosis. Med Pediatr Oncol 1993;21:680-4.

Cnossen MH, Stam EN, Cooiman LC, et al. Endocrinologic disorders and optic pathway gliomas in children with neurofibromatosis type 1. Pediatrics 1997;100:667-70.

Danoff BF, Kramer S, Thompson N. The radiotherapeutic management of optic nerve gliomas in children. Int J Radiat Oncol Biol Phys 1980;6:45-50.

de Keizer RJW, de Wolff-Rouendaal D, Bots GTAM, et al. Optic glioma with intraocular tumor and seeding in a child with neurofibromatosis. Am J Ophthalmol 1989;108:717-25.

Debus J, Kocagoncu JO, Hoss A, et al. Fractionated stereotactic radiotherapy (FSRT) for optic glioma. Int J Radiat Oncol Biol Phys 1999;44:243-8.

Delfini R, Missori P, Tarantino R, et al. Primary benign tumors of the orbital cavity: comparative data in a series of patients with optic nerve gliomas, sheath meningioma, or neurinoma. Surg Neurol 1996;45:147-54.

Deliganis AV, Geyer JR, Berger MS. Prognostic significance of type 1 neurofibromatosis (von Recklinghausen disease) in childhood optic glioma. Neurosurgery 1996;38:1114-8.

Dosoretz DE, Blitzer PH, Wang CC, Linggood RM. Management of glioma of the optic nerve and/or chiasm. Cancer 1980;45:1467-71.

Dutton JJ. Gliomas of the anterior visual pathway. Surv Ophthalmol 1994;38:427-52.

Dutton JJ. Optic nerve gliomas and meningiomas. Neurol Clin 1991;9:163-77.

Flickinger JC, Torres C, Deutsch M. Management of low-grade gliomas of the optic nerve and chiasm. Cancer 1988;61:635-42.

Glaser JS, Hoyt WF, Corbett J. Visual morbidity with chiasmal glioma. Long term studies of visual fields in untreated and irradiated cases. Arch Ophthalmol 1971;85:3-12.

Haik BG, Saint Louis L, Bierly J, et al. Magnetic resonance imaging in the evaluation of optic nerve gliomas. Ophthalmology 1987;94:709-17.

Harper CG, Stewart-Wynne EG. Malignant optic gliomas in adults. Arch Neurol 1978;35:731-5.

Harter DJ, Caderao JB, Leavens ME, Young SE. Radiotherapy in the management of primary gliomas involving the intracranial optic nerves and chiasm. Int J Radiat Oncol Biol Phys 1978;4:681-6.

Hochstrasser H, Boltshauser E, Valavanis A. Brain tumors in children with von Recklinghausen neurofibromatosis. Neurofibromatosis 1988;1:233-9.

Holman RE, Grimson BS, Drayer BP, et al. Magnetic resonance imaging of optic gliomas. Am J Ophthalmol 1985;100:596-601.

Horwich A, Bloom HJG. Optic gliomas: radiation therapy and prognosis. Int J Radiat Oncol Biol Phys 1985;11:1067-79.

Hoyt WF, Baghdassarian SA. Optic glioma of childhood. Natural history and rationale for conservative management. Br J Ophthalmol 1969;53:793-8.

Hoyt WF, Meshel LG, Lessell S, et al. Malignant optic glioma of adulthood. Brain 1973;96:121-32.

Imes RK, Hoyt WF. Childhood chiasmal gliomas: update on the fate of patients in the 1969 San Francisco Study. Br J Ophthalmol 1986;70:179-82.

Jakobiec FA, Depot MJ, Kennerdell JS, et al. Combined clinical and computed tomographic diagnosis of orbital glioma and meningioma. Ophthalmology 1984;91:137-55.

Janss AJ, Grundy R, Cnaan A, et al. Optic pathway and hypothalamic/chiasmatic gliomas in children younger than age 5 years with a 6-year follow-up. Cancer 1995;75:1051-9.

Jenkin D, Angyalfi S, Becker L, et al. Optic glioma in children: surveillance, resection, or irradiation? Int J Radiat Oncol Biol Phys 1993;25:215-25.

Kestle JR, Hoffman HJ, Mock AR. Moyamoya phenomenon after radiation for optic glioma. J Neurosurg 1993;79:32-5.

Levin LA, Jakobiec FA. Optic nerve tumors of childhood: a decision-analytical approach to their diagnosis. Int Ophthalmol Clin 1992;32:223-40.

Lewis RA, Gerson LP, Axelson KA, et al. von Recklinghausen neurofibromatosis. II. Incidence of optic gliomata. Ophthalmology 1984;91:929-35.

Lim YJ, Leem W. Two cases of Gamma Knife radiosurgery for low-grade optic chiasm glioma. Stereot Funct Neurosurg 1998;66(suppl 1):174-83.

Listernick R, Charrow J, Greenwald M, Mets M. Natural history of optic pathway tumors in children with neurofibromatosis type 1: a longitudinal study. J Pediatr 1994;125:63-6.

Listernick R, Darling C, Greenwald M, et al. Optic pathway tumors in children: the effecto of neurofibromatosis type 1 on clinical manifestations and natural history. J Pediatr 1995;127:718-22.

Liu GT, Lessell S. Spontaneous visual improvement in chiasmal gliomas. Am J Ophthalmol 1992;114:193-201.

Lovblad KO, Remonda L, Ozdoba C, et al. Dural ectasia of the optic nerve sheath in neurofibromatosis type 1: CT and MR features. J Comput Assist Tomogr 1994;18:728-30.

Lowes M, Bojsen-Moller M, Vorre P, Hedegaard O. An evaluation of gliomas of the anterior visual pathways: a 10-year survey. Acta Ncurochir (Wien) 1978;43:201-6.

Lyons CJ. The neurofibromatoses. In: Taylor D, ed. Pediatric Ophthalmology, 2nd ed. London: Blackwell Science, 1997;322-33.

Marquardt MD, Zimmerman LE. Histopathology of meningiomas and gliomas of the optic nerve. Hum Pathol 1982;13:226-35.

Massry GG, Morgan CF, Chung SM. Evidence of optic pathway gliomas after previously negative neuroimaging. Ophthalmology 1997;104:930-5.

McDonnell P, Miller NR. Chiasmatic and hypothalamic extension of optic nerve glioma. Arch Ophthalmol 1983;101:1412-5.
Medlock MD, Madsen JR, Barnes PD, et al. Optic chiasm astrocytomas of childhood. 1. Long-term follow-up. Pediatr Neurosurg 1997;27:121-8.
Moghrabi A, Friedman HS, Burger PC, et al. Carboplatin treatment of progressive optic pathway gliomas to delay radiotherapy. J Neurosurg 1993;79:223-7.
North K, Cochineas C, Tang E, Fagan E. Optic gliomas in neurofibromatosis type 1: role of visual evoked potentials. Pediatr Neurol 1994;10:117-23.
Packer RJ, Bilaniuk LT, Cohen BH, et al. Intracranial visual pathway gliomas in children with neurofibromatosis. Neurofibromatosis 1988;1:212-22.
Parker JC Jr, Smith JL, Reyes P, Vuksanovic MM. Chiasmal optic glioma after radiation therapy. Neuro-ophthalmologic/pathologic correlation. J Clin Neuroophthalmol 1981;1:31-43.
Redfern RM, Scholtz CL. Long-term survival with optic nerve glioma. Surg Neurol 1980;14:371-5.
Richards RD, Lynn JR. The surgical management of gliomas of the optic nerve. Am J Ophthalmol 1966;62:60-5.
Richardson AE. Optic pathway turnors. Trans Ophthalmol Soc U K 1976;96:424-6.
Robertson AG, Brewin TB. Optic nerve glioma. Clin Radiol 1980;31:471-4.
Rothfus WE, Curtin HD, Slamovits TL, Kennerdell JS. Optic nerve/ sheath enlargement. A different approach based on high-resolution CT morphology. Radiology 1984;150:409-15.
Rush JA, Younge BR, Campbell RJ, MacCarty CS. Optic glioma: long-term follow-up of 85 histopathologically verified cases. Ophthalmology 1982;89:1213-9.
Sadun F, Hinton DR, Sadun AA. Rapid growth of an optic nerve ganglioglioma in a patient with neurofibromatosis 1. Ophthalmology 1996;103:794-9.
Seiff SR, Brodsky MC, MacDonald G, et al. Orbital optic glioma in neurofibromatosis: magnetic resonance diagnosis of perineural arachnoidal gliomatosis. Arch Ophthalmol 1987;105:1689-92.
ShuperA, Horev G, Kornreich L, et al. Visual pathway glioma: an erratic tumour with therapeutic dilemmas. Arch Dis Child 1997;76:259-63.
Spencer WH. Diagnostic modalities and natural behavior of optic nerve gliomas. Ophthalmology 1979;86:8815.
Spoor TC, Kennerdell JS, Martinez AJ, Zorub D. Malignant gliomas of the optic nerve pathways. Am J Ophthalmol 1980;89:284-92.
Spoor TC, Kennerdell JS, Zorub D, Martinez AJ. Progressive visual loss due to glioblastoma: normal neuroroentgenoradiographic studies. Arch Neurol 1981;38:196-7.
Stein BM. Surgical lesions of the intracranial optic nerves and optic chiasm. Ophthalmology 1979;86:308-12.
Stern J, Jakobiec FA, Housepian EM. The architecture of optic nerve gliomas with and without neurofibromatosis. Arch Ophthalmol 1980;98:505-11.
Swenson SA, Forbes GS, Younge BR, et al. Radiologic evaluation of tumors of the optic nerve. AJNR 1982;3:319-26.
Taphoorn MJ, de Vries-Knoppert WA, Ponssen H, Wolbers JG. Malignant optic glioma in adults. Case report. J Neurosurg 1989;70:277-9.
Taveras JM, Mount LA, Wood EH. The value of radiation therapy in the management of glioma of the optic nerves and chiasm. Radiology 1956;66:518-28.
Tenny RT, Laws ER Jr, Younge BR, Rush JA. The neurosurgical management of optic glioma: Results in 104 patients. J Neurosurg 1982;57:452-8.
Wong JY, Uhl V, Wara WM, Sheline GE. Optic gliomas. A reanalysis of the University of California, San Francisco experience. Cancer 1987;60:1847-55.
Wright JE, McNab AA, McDonald WI. Optic nerve gliomas and the management of optic nerve tumours in the young. Br J Ophthalmol 1989;73:967-74.
Wulc AE, Bergin DJ, Barnes D, et al. Orbital optic nerve glioma in adults. Arch Ophthalmol 1989;107:1013-6.
Zimmerman LE. Arachnoid hyperplasia in optic nerve glioma. Br J Ophthalmol 1980;64:638-40.
Zimmerman LE, Arkfeld DL, Schenken JB, et al. A rare choristoma of the optic nerve and chiasm. Arch Ophthalmol 1983;101:766-70.

Meningiomas

Burger PC, Scheithauer BW. Tumors of the Central Nervous System, 3rd Ser, Fasc 10. Washington, DC: Armed Forces Institute of Pathology, 1994
Cushing H, Eisenhardt L. Meningioma. Their Classification, Regional Behavior, Life History and Surgical End Results. Springfield, IL: Charles C Thomas, 1962.
Henderson JW. Orbital Tumors, 3rd ed. Philadelphia, Raven Press, 1994:377-90.

Intracranial, Intracanalicular, and Orbital Meningiomas

Als E. Intraorbital meningiomas encasing the optic nerve. A report of two cases. Acta Ophthalmol (Copenh) 1969;17:900-3.
Andrews BT, Wilson CB. Suprasellar meningiomas: the effect of tumor location on postoperative visual outcome. J Neurosurg 1988;69:523-8.
Barnett GH, Steiner CP, Weisenberger J. Intracranial meningioma resection using frameless stereotaxy. J Image Guid Surg 1995;1:46-52.
Black PM. Meningiomas. Neurosurgery 1993;32:643-57.
Cophignon J, Lucena J, Clay C, Marchac D. Limits to radical treatment of spheno-orbital meningiomas. Acta Neurochir [Suppll (Wien) 1979;28:375-80.
Craig WM, Gogela LJ. Intraorbital meningiomas. A clinicopathologic study. Am J Ophthalmol 1949;32:1663-80.
Crouse SK, Berg BO. Intracranial meningiomas in childhood and adolescense. Neurology 1972;22:135-41.
Deen HG Jr, Scheithauer BW, Ebersold MJ. Clinical and pathological study of meningiomas of the first two decades of life. J Neurosurg 1982;56:317-22.
DeMonte F. Surgical treatment of anterior basal meningiomas. J Neurooncol 1996;29:239-48.
Ehlers N, Malmros R. The suprasellar meningioma. A review of the literature and presentation of a series of 31 cases. Acta Ophthalmol Suppl 1973;121:1-74.
Gregorius FK, Hepler RS, Stern WE. Loss and recovery of vision with suprasellar meningiomas. J Neurosurg 1975;42:69-75
Hart WM Jr, Burde RM, Klingele TG, Perlmutter JC. Bilateral optic nerve sheath meningiomas. Arch Ophthalmol 1980;98:149-51.
Holden J, Dolman CL, Churg A. Immunohistochemistry of meningiomas including the angioblastic type. J Neuropathol Exp Neurol 1987;46:50-6.
Horten BC, Urich H, Rubenstein LJ, Montague SR. The angioblastic meningioma: a reappraisal of a nosological problem. Light-, electron-microscopic, tissue, and organ culture observations. J Neurol Sci 1977;31:387-410.
Karp LA, Zimmerrnan LE, Borit A, et al. Primary intraorbital meningiomas. Arch Ophthalmol 1974;91:24-8.
Kennerdell JS, Maroon JC. Intracanalicular meningioma with chronic optic disc edema. Ann Ophthalmol 1975;7:507-12.
Leonetti JP, Reichman OH, Smith PG, Grubb RL, Kaiser P. Meningiomas of the lateral skull base: neurotologic manifestations and patterns of recurrence. Otolaryngol Head Neck Surg 1990;103:972-80.
Little HL, Chambers JW, Walsh FB. Unilateral intracranial optic nerve involvement: neurosurgical significance. Arch Ophthalmol 1965;73:331-71.

MacMichael IM, Cullen JF. Primary intraorbital meningiomas. Br J Ophthalmol 1969; 53:169-73.
Maroon JC, Kennerdell JS, Vidovich DV, Abla A, Sternau L. Recurrent spheno-orbital meningioma. J Neurosurg 1994;80:202-8.
Mathiesen T, Lindquist C, Kihlstrom L, Karlsson B. Recurrence of cranial base meningiomas. Neurosurgery 1996;39:2-9.
McDermott MW, Durity FA, Rootman J, Woodhurst WB. Combined frontotemporal-orbitozygomatic approach for tumors of the sphenoid wing and orbit. Neurosurgery 1990;26:107-16.
Mehra KS, Khanna SS, Dube B. Primary meningioma of the intraorbital optic nerve. Ann Ophthalmol 1979;11:758-60.
Mirra SS, Miles ML. Unusual pericytic proliferation in a meningotheliomatous meningioma: an ultrastructural study. Am J Surg Pathol 1982;6:573-80.
Moore CE. Sphenoidal ridge meningioma with optic nerve metastases. Br J Ophthalmol 1968;52:636-9.
Peele KA, Kennerdell JS, Maroon JC, et al. The role of posteoperative irradiation in the management of sphenoid wing meningiomas. A preliminary report. Ophthalmology 1996;103:1761-7.
Popoff NA, Malinin TI, Rosomoff HL. Fine structure of intracranial hemangiopericytoma and angiomatous meningioma. Cancer 1974;34:1187-97.
Rootman J, Durity FA. Orbital surgery. In: Sekhar LN, Janecka IF, eds. Surgery of Cranial Base Tumors: A Color Atlas. New York: Raven Press, 1992; 769-86.
Samii M, Tatagiba M, Monteiro ML. Meningiomas involving the parasellar region. Acta Neurochir Suppl (Wien) 1996; 65:63-5.
Susac JO, Smith JL, Walsh FB. The impossible meningioma. Arch Neurol 1977;34:36-8.
Terstegge K, Schorner W, Henkes H, et al. Hyperostosis in meningiomas: MR findings in patients with recurrent meningioma of the sphenoid wings. AJNR 1994;15:555-60.
Trobe JD, Glaser JS, Post JD, Page LK. Bilateral optic canal meningiomas: a case report. Neurosurgery 1978;3:68-74.
Walsh FB. Meningioma, primary within the orbit and optic canal. In: Smith JL, ed. Neuro-ophthalmology Symposium of the University of Miami and the Bascom Palmer Eye Institute. Vol 5. St. Louis: CV Mosby, 1970; 240-66.
Wilson WB. Meningiomas of the anterior visual system. Surv Ophthalmol 1981;26:109-27.
Wilson WB, Gordon M, Lehman RAW. Meningiomas confined to the optic canal and foramina. Surg Neurol 1979;12:218.
Wolter JR, Benz SC. Ectopic meningioma of the superior orbital rim. Arch Ophthalmol 1976;94:1920-2.
Yao YT. Clinicopathologic analysis of 615 cases of meningioma with special reference to recurrence. J Formos Med Assoc 1994;93:145-52.

Optic Nerve Meningiomas

Alper MG. Management of primary optic nerve meningiomas. Current status - therapy in controversy. J Clin Neuroophthalmol 1981;1:101-17.
Boniuk M, Messmer EP, Font RL. Hemangiopericytoma of the optic nerve. A clinicopathologic report including electron microscopic observations. Ophthalmology 1985;92:1780-7.
Boschetti NV, Smith JL, Osher RH, et al. Fluorescein angiography of optociliary shunt vessels. J Clin Neuroophthalmol 1981;1:9-30.
Cibis GW, Whittaker CK, Wood WE. Intraocular extension of optic nerve meningioma in a case of neurofibromatosis. Arch Ophthalmol 1985;103:404-6.
Clark WC, Theofilos CS, Fleming JC. Primary optic nerve sheath meningiomas. Report of nine cases. J Neurosurg 1989;70:37-40.
Dutton JJ. Optic nerve sheath meningiomas. Surv Ophthalmol 1992;37:167-83.
Dutton JJ. Optic nerve gliomas and meningiomas. Neurol Clin 1991;9:163-77.
Eggers H, Jakobiec FA, Jones IS. Tumors of the optic nerve. Doc Ophthalmol 1976;41:43-128.
Ellenberger C. Perioptic meningiomas. Syndrome of long-standing visual loss, pale disk edema, optociliary veins. Arch Neurol 1976;33:671-4.
Eng TY, Albright NW, Kuwahara G, Akazawa CN, Dea D, Chu GL, Hoyt WF, Wara WM, Larson DA. Precision radiation therapy for optic nerve sheath meningiomas. Int J Radiat Oncol Biol Phys 1992;22:1093-8.
Frisen L, Hoyt WF, Tengroth BM. Optociliary veins, disc pallor and visual loss. A triad of signs indicating spheno-orbital meningioma. Acta Ophthalmol (Copenh) 1973;51:241-9.
Hart WM Jr. Burder RM, Klingele TG, Perlmutter JC. Bilateral optic nerve sheath meningiomas. Arch Ophthalmol 1980;98:149-51.
Hendrix LE, Kneeland JB, Haughton VM, et al. MR imaging of optic nerve lesions: value of gadopentetate dimeglumine and fat-suppression technique. AJR 1990;155:849-54.
Jakobiec FA, Depot MJ, Kennerdell JS, et al. Combined clinical and computed tomographic diagnosis of orbital glioma and meningioma. Ophthalmology 1984;91:137-55.
Kennerdell JS, Maroon JC, Malton M, Warren FA. The management of optic nerve sheath meningiomas. Am J Ophthalmol 1988;106:450-7.
Klink DF, Miller NR, Williams J. Preservation of residual vision 2 years after stereotactic radiosurgery for a presumed optic nerve sheath meningioma. J Neuroophthalmol 1998;18:117-20.
Kuroda R, Nakatani J, Yorimae A, Nakao Y, Ohtori T. Clinial experience of intraorbital optic nerve sheath meningioma - report of eight cases. Neurol Med Chir (Tokyo) 1990;30:468-75.
Lawton AW, Leone CR Jr, Hunter DM. Optic nerve pseudomeningioma secondary to localized amyloidosis. Ophthal Plast Reconstr Surg 1989;5:52-5.
Lindblom B, Truwit CL, Hoyt WF. Optic nerve sheath meningioma: definition of intraorbital, intracanicular, and intracranial components with magnetic resonance imaging. Ophthalmology 1992;99:560-6.
Mark LE, Kennerdell JS, Maroon JC, et al. Microsurgical removal of a primary intraorbital meningioma. Am J Ophthalmol 1978;86:704-9.
Marquardt MD, Zimmerman LE. Histopathology of meningiomas and gliomas of the optic nerve. Hum Pathol 1982;13:226-35.
McNab AA, Wright JE. Cysts of the optic nerve: three cases associated with meningioma. Eye 1989;3:355-9.
Rothfus WE, Curtain HD, Slamovit TL, et al. Optic nerve/sheath enlargement: a different approach based on high-resolution CT morphology. Radiology 1984;150;409-15.
Sarkies NJ. Optic nerve sheath meningioma: diagnostic features and therapeutic alternatives. Eye 1987;1:597-602.
Schatz H, Green WR, Talamo JH, Hoyt WF, Johnson RN, McDonald HR. Clinicopathologic correlation of retinal to choroidal venous collaterals of the optic nerve head. Ophthalmology 1991;98:1287-93.
Saeed P, Rootman J, Nugent RA, et al. Optic nerve sheath meningiomas. Submitted, Ophthalmology, 2001.
Sibony PA, Krauss HR, Kennerdell JS, et al. Optic nerve sheath meningiomas. Clinical manifestations. Ophthalmology 1984;91:1313-26.
Smith JL, Vuksanovic MM, Yates BM, Bienfang DC. Radiation therapy for primary optic nerve meningiomas. J Clin Neuroophthalmol 1981;1:85-99.
Spencer WH. Primary neoplasms of the optic nerve and its sheaths: clinical features and current concepts of pathoogenetic mechanisms. Trans Am Ophthalmol Soc 1972;70:490-528.
Wright JE. Primary optic nerve meningiomas: clinical presentation and management. Trans Am Acad Ophthalmol Otolaryngol 1977;83:617-25.
Wright JE, Call NB, Liaricos S. Primary optic nerve meningioma. Br J Ophthalmol 1980;64:553-8.
Wright JE, McNab AA, McDonald WI. Primary optic nerve sheath meningioma. Br J Ophthalmol 1989;73:960-6.

Yuceer N, Erdogan A, Ziya H. Primary optic nerve sheath meningiomas: report of seven cases (clinical, neuroradiological, pathological and surgical considerations in seven cases). J Neurosurg Sci 1994;38:155-9.
Zimmerman CF, Schatz NJ, Glaser JS. Magnetic resonance imaging of optic nerve meningiomas. Enhancement with gadolinium-DTPA. Ophthalmology 1990;97:585-91.

Other Optic Nerve Tumors

Bedotto J, Spier CM, Paquin ML, Grogan TM, Ahmann FR, Greenberg BR. Mantle zone lymphoma with central nervous system involvement. Cancer 1986;58:2125-9.
Brown GC, Shields JA. Tumors of the optic nerve head. Surv Ophthalmol 1985;29:239-64.
Christmas NJ, Mead MD, Richardson EP, Albert DM. Secondary optic nerve tumors. Surv Ophthalmol 1991;36:196-206.
Malik S, Furlan AJ, Sweeney PJ, Kosmorsky GS, Wong M. Optic neuropathy: a rare paraneoplastic syndrome. J Clin Neuroophthalmol 1992;12:137-41.
Noda S, Hayasaka S, Setogawa T. Intraocular lymphoma invades the optic nerve and orbit. Ann Ophthalmol 1993;25:30-4.
Sato K, Kubota T, Kitai R. Cavernous angioma of the optic canal: role of CT and MRI. J Comput Assist Tomogr 1994;18:990-1.

Peripheral Nerve Sheath Tumors

Neurofibromas

The Neurofibromatoses

Bardelli AM, Hadjistilianou T. Buphthalmos and progressive elephantiasis in neurofibromatosis. A report of three cases. Ophthal Pediatr Genet 1989;10:279-86.
Bouzas EA, Parry DM, Eldridge R, Kaiser-Kupfer MI. Familial occurrence of combined pigment epithelial and retinal hamartomas associated with neurofibromatosis 2. Retina 1992;12:103-7.
Bouzas EA, Freidlin V, Parry DM, et al. Lens opacities in neurofibromatosis 2: further significant correlations. Br J Ophthalmol 1993a:77:354-7.
Brodsky MC. The “pseudo-CSF” signal of orbital optic glioma on magnetic resonance imaging: a signature of neurofibromatosis. Surv Ophthalmol 1993;38:213-8.
Dervin JE, Beaconsfield M, Wright JE, Moseley IF. CT findings in orbital tumours of nerve sheath origin. Clin Radiol 1989;40:475-9.
Dossetor FR, Landau K, Hoyt WF. Optic disk glioma in neurofibromatosis type 2. Am J Ophthalmol 1989;108:602-3.
Evans DG, Huson SM, Donnai D, et al. A genetic study of type 2 neurofibromatosis in the United Kingdom. II. Guidelines for genetic counselling. J Med Genet 1992;29:847-52.
Font RL, Ferry AP. The phakomatoses. Intl Ophthalmol Clin 1972;12:1-50.
Good WV, Brodsky MC, Edwards MS, Hoyt WF. Bilateral retinal hamartomas in neurofibromatosis type 2. Br J Ophthalmol 1991;75:190.
Jackson IT, Carbonnel A, Potparic Z, Shaw K. Orbitotemporal neurofibromatosis: classification and treatment. Plast Reconstr Surg 1993;92:1-11.
Jamjoom AB, Malabarey T, Jamjoom ZA, et al. Cerebro-vasculopathy and malignancy: catastrophic complications of radiotherapy for optic nerve glioma in a von Recklinghausen neurofibromatosis patient. Neurosurg Rev 1996;19:47-51.
Kaiser-Kupfer MI, Freidlin V, Datiles MB, et al. The association of posterior capsular lens opacities with bilateral acoustic neuromas in patients with neurofibromatosis type 2. Arch Ophthalmol 1989;107:541-4.
Kaye L, Rothner A, Beauchamp G, et al. Ocular findings associated with neurofibromatosis type 2. Ophthalmology 1992;99:1424-9.
Krohel GB, Rosenberg PN, Wright JE, Smith RS. Localized orbital neurofibromas. Am J Ophthalmol 1985;100:458-64.
Landau K, Dossetor FM, Hoyt WF, Muci-Mendoza R. Retinal hamartoma in neurofibromatosis 2. Arch Ophthalmol 1990;108:328-9.
Landau K, Yasargil GM. Ocular fundus in neurofibromatosis type 2. Br J Ophthalmol 1993;77:646-9.
Listernick R, Charrow J, Greenwald MJ, Esterly NB. Optic gliomas in children with neurofibromatosis type 1. J Pediatr 1989;114:788-92.
Lyons CJ. The neurofibromatoses. In: Taylor D, ed. Pediatric Ophthalmology, 2nd ed. London: Blackwell Science, 1997:309-21.
Mautner VF, Tatagiba M, Guthoff R, et al. Neurofibromatosis 2 in the pediatric age group. Neurosurgery 1993;33:92-6.
McDonald P, Jakobiec FA, Hornblass A, Iwamoto T. Benign peripheral nerve sheath tumors (neurofibromas) of the lacrimal gland. Ophthalmology 1983;90:1403-13.
Meyer D, Wobig JL. Bilateral localized orbital neurofibromas. Ophthalmology 1992;99:1313-7.
Mulvihill JJ, Parry DM, Sherman JL, et al. NIH Conference. Neurofibromatosis 1 (Recklinghausen disease) and neurofibromatosis 2 (bilateral acoustic neurofibromatosis). An update. Ann Int Med 1990;113:39-52.
National Institutes of Health. National Institutes of Health consensus development conference statement: neurofibromatosis. Neurofibromatosis 1988;1:172-8.
Ragge NK. Clinical and genetic patterns of neurofibromatosis 1 and 2. Br J Ophthalmol 1993;77:662-72.
Riccardi VM. Neurofibromatosis: Phenotype, Natural History, and Pathogenesis, 2nd Ed. Baltimore: Johns Hopkins University Press, 1992.
Rose GE, Wright JE. Isolated peripheral nerve sheath tumours of the orbit. Eye 1991;5:668-73.
Rouleau GA, Merel P, Lutchman M, et al. Alteration in a new gene encoding a putative membrane-organizing protein causes neurofibromatosis type 2. Nature 1993;363:515-21.
Schachat AP, Shields JA, Fine SL, et al. Combined hamartomas of the retina and retinal pigment epithelium. Ophthalmology 1984;91:1609-15.
Shields JA, Shields CL, Lieb WE, Eagle RC Jr. Multiple orbital neurofibromas unassociated with von Recklinghausen's disease. Arch Ophthalmol 1990;108:80-3.
Sivalingam A, Augsburger J, Perilongo G, et al. Combined hamartoma of the retina and retinal pigment epithelium in a patient with neurofibromatosis type 2. Journal of Pediatroc Ophthalmology and Strabismus 1991;28:320-2.
Snyder BJ, Hanieh A, Trott JA, David DJ. Transcranial correction of orbital neurofibromatosis. Plast Reconstruct Surg 1998;102:633-42.
Stallard HB. A case of intra-ocular neuroma (von Recklinghausen's disease) of the left optic nerve head. Br J Ophthalmol 1938;21:11.
Tonsgard JH, Oesterle CS. The ophthalmologic presentation of NF-2 in childhood. Journal of Pediatric Ophthalmology and Strabismus 1993;30:327-30.
Trofatter JA, MacCollin MM, Rutter JL, et al. A novel moesin-, ezrin-, radixin-like gene is a candidate for the neurofibromatosis 2 tumor suppressor. Cell 1993;72:791-800.
von Recklinghausen FD. Ueber die multiplen Fibrome der Haut und ihre Beziehung zu den multiplen Neuromen. Festschrift zur Feier des fünfundzwanzigjährigen Bestchens des pathologischen Instituts zu Berlin; Herrn Rudolf Virchow dargebracht. Berlin: Hirschwald, 1882.
Warwar RE, Bullock JD, Shields JA, Eagle RC Jr. Coexistence of 3 tumors of neural crest origin: neurofibroma, meningioma, and uveal malignant melanoma. Arch Ophthalmol 1998;116:1241-3.

Plexiform Neurofibromas

Tada M, Sawamura Y, Ishii N, et al. Massive plexiform neurofibroma in the orbit in a child with von Recklinghausen's disease. Childs Nerv Sys 1998;14:210-2.

Solitary (Isolated) Neurofibromas

Erlandson RA, Woodruff JM. Peripheral nerve sheath tumors: an electron microscopic study of 43 cases. Cancer 1982;49:273-87.
Francois J. Ocular aspects of the phakomatoses. In: Vinken PJ, Bruyn GW, eds. Handbook of Clinical Neurology. New York: American Elsevier, 1972; 624.
Gogi R, Nath K, Kahn AA, Hameens PN. Peripheral nerve tumours of the orbit. Indian J Ophthalmol 1976;24:1-5.
Krohel GB, Rosenberg PN, Wright JE, Smith RS. Localized orbital neurofibromas. Am J Ophthalmol 1985;100:458-64.
Kuo PK, Ni C, Seddon JM, et al. Orbital tumors among Chinese in the Shanghai area. Int Ophthalmol Clin 1982;22:87-98.
McDonald P, Jakobiec FA, Hornblass A, Iwamoto T. Benign peripheral nerve sheath tumors (neurofibromas) of the lacrimal gland. Ophthalmology 1983;90:1403-13.
Rose GE, Wright JE. Isolated peripheral nerve sheath tumours of the orbit. Eye 1991;5:668-73.

Amputation Neuromas

Blodi FC. Amputation neuroma in the orbit. Am J Ophthalmol 1949;32:929-32.
Glatt HJ, Googe PB, Powers T, Apple DJ. Anophthalmic socket pain. Am J Ophthalmol 1993;116:357-62.
Messmer EP, Camara J, Boniuk M, Font RL. Amputation neuroma of the orbit. Report of two cases and review of the literature. Ophthalmology 1984;91:1420-3.
Okubo K, Asai T, Sera Y, Okada S. A case of amputation neuroma presenting proptosis. Ophthalmologica 1987;194:5-8.

Schwannoma

Allman M, Frayer WC, Hedges TR Jr. Orbital neurilemmoma. Ann Ophthalmol 1977;9:1409-13.
Anegawa S, Hayashi T, Torigoe R, et al. [Orbital neurinoma presenting orbital apex syndrome]. No Shinkei Geka - Neurological Surgery 1997;25:473-7.
Barat JL, Marchal JC, Bracard S, et al. Neurinomes des nerfs oculomoteurs. A propros de deux observations. Neuro-chirurgie 1992;38:183-7.
Byrne BM, van Heuven WAJ, Lawton AW. Echographic characteristics of benign orbital schwannomas (neurilemomas). Am J Ophthalmol 1988;106:194-8.
Capps DH, Brodsky MC, Rice CD, et al. Orbital intramuscular schwannoma. Am J Ophthalmol 1990;110:535-9.
Chisholm IA, Polyzoidis K. Recurrence of benign orbital neurilemmoma (schwannoma) after 22 years. Can J Ophthalmol 1982;17:271-3.
Cockerham KP, Cockerham GC, Stutzman R, et al. The clinical spectrum of schwannomas presenting with visual dysfunction: a clinicopathologic study of three cases. Surv Ophthalmol 1999;44:226-34.
Dahl I. Ancient neurilemmoma (schwannoma). Acta Pathol Microbiol Scand [A] 1977;85:812-8.
Del Priore LV, Miller NR. Trigeminal schwannoma as a cause of chronic, isolated sixth nerve palsy. Am J Ophthalmol 1989;108:126-9.
Dervin JE, Beaconsfield M, Wright JE, Moseley IF. CT findings in orbital tumours of nerve sheath origin. Clin Radiol 1989;40:475-9.
Faucett DC, Dutton JJ, Bullard DE. Gasserian ganglion schwannoma with orbital extension. Ophthal Plast Reconstr Surg 1989;5:235-8.
Izumi AK, Rosato FE, Wood MG. Von Recklinghausen's disease associated with multiple neurilemomas. Arch Dermatol 1971;104:172-6.
Jakobiec FA, Font RL, Iwamoto T. Diagnostic ultrastructural pathology of ophthalmic tumors. In: Jakobiec FA, ed. Ocular and Adnexal Tumors. Birmingham: Aesculapius, 1978; 359-453.
Lam DS, Ng JS, To KF, et al. Cystic schwannoma of the orbit. Eye 1997;11:798-800.
Messmer EP, Font RL. Applications of immunohistochemistry to ophthalmic pathology. Ophthalmology 1984;91:701-7.
Razzuk MA, Urschel HC Jr, Martin JA, et al. Electron microscopical observations on mediastinal neurilemmoma, neurofibroma, and ganglioneuroma. Ann Thorac Surg 1973;15:73-83.
Rootman J, Goldberg C, Robertson W. Primary orbital schwannomas. Br J Ophthalmol 1982;66:194-204.
Rose GE, Wright JE. Isolated peripheral nerve sheath tumours of the orbit. Eye 1991;5:668-73.
Rottino A, Kelly AJ. Specific nerve sheath tumor of orbit. Arch Ophthalmol 1941;26:478-88.
Schatz H. Benign orbital neurilemoma. Sarcomatous transformation in von Recklinghausen's disease. Arch Ophthalmol 1971;86:268-73.
Schmitt E, Spoerri O. Schwannomas of the orbit. Acta Neurochir (Wien) 1980;53:79-85.
Shen WC, Yang DY, Ho WL, et al. Neurilemmoma of the oculomotor nerve presenting as an orbital mass: MR findings. AJNR 1993;14:1253-4.
Shields JA, Kapustiak J, Arbizo V, et al. Orbital neurilemoma with extension through the superior orbital fissure. Arch Ophthalmol 1986;104:871-3.
Stefansson K, Wolimann R, Jerkovic M. S-100 protein in soft tissue tumors derived from Schwann cells and melanocytes. Am J Pathol 1982;106:261-8.
Stout AP. The peripheral manifestations of specific nerve sheath tumor (neurilemoma). Am J Cancer 1935;24:751-96.
Sun CN, White HJ. An electron-microscopic study of a schwannoma with special reference to banded structures and peculiar membranous multiple-chambered spheroids. J Pathol 1974;114:13-6.
Weiss SW, Langloss JM, Enzinger FM. Value of S-100 protein in the diagnosis of soft tissue tumors with particular reference to benign and malignant Schwann cell tumors. Lab Invest 1983;49:299-308.

Malignant Peripheral Nerve Sheath Tumors

D'Agostino AN, Soule EH, Miller RH. Primary malignant neoplasm of nerves (malignant neurilemmomas) in patients without manifestations of multiple neurofibromatosis (von Recklinghausen's disease). Cancer 1963;16:1003-14.
D'Agostino AN, Soule EH, Miller RH. Sarcomas of the peripheral nerves and somatic soft tissues associated with multiple neurofibromatosis (von Recklinghausen's disease). Cancer 1963;16:1015-27.
Erzurum SA, Melen O, Lissner G, et al. Orbital malignant peripheral nerve sheath tumors. Treatment with surgical resection and radiation therapy. J Clin Neuroophthalmol 1993;13:1-7.
Grinberg MA, Levy NS. Malignant neurilemoma of the supraorbital nerve. Am J Ophthalmol 1974;78:489-92.
Guccion JG, Enzinger FM. Malignant Schwannoma associated with von Recklinghausen's neurofibromatosis. Virchows Arch A Pathol Anat Histol 1979;383:43-57.
Jakobiec FA, Font RL, Zimmerman LE. Malignant peripheral nerve sheath tumors of the orbit: a clinicopathologic study of eight cases. Trans Am Ophthalmol Soc 1985;83:332-66.
Lyons CJ, McNab AA, Garner A, et al. Orbital malignant peripheral nerve sheath tumours. Br J Ophthalmol 1989;73:731-8.
Mortada A. Solitary orbital malignant neurilemmoma. Br J Ophthalmol 1968;52:188-90.
Sangueza OP, Requena L. Neoplasms with neural differentiation: a review. Part II: malignant neoplasms. Am J Dermatopathol 1998;20:98-102.
Schatz H. Benign orbital neurilemoma. Sarcomatous transformation in von Recklinghausen's disease. Arch Ophthalmol 1971;86:268-73.

Weiss SW, Langloss JM, Enzinger FM. Value of S-100 protein in the diagnosis of soft tissue tumors with particular reference to benign and malignant Schwann cell tumors. Lab Invest 1983;49:299-308.

Rare Tumors of Neuroectodermal Origin

Alveolar Soft Part Sarcoma

Abrahams IW, Fenton RH, Vidone R. Alveolar soft-part sarcoma of the orbit. Arch Ophthalmol 1968;79:185-8.
Altamirano-Dimas M, Albores-Saavedra J. Alveolar soft part sarcoma of the orbit. Arch Ophthalmol 1966;75:496-9.
Auerbach HE, Brooks JJ. Alveolar soft part sarcoma. A clincopathologic and immunohistochemical study. Cancer 1987;60:66-73.
Bunt AH, Bensinger RE. Alveolar soft-part sarcoma of the orbit. Ophthalmology 1981;88:1339-46.
Christopherson WM, Foote FW Jr, Stewart FW. Alveolar soft part sarcomas: structurally characteristic tumors of uncertain histogenesis. Cancer 1952;5:100-11.
DeSchryver-Kecskemeti K, Kraus FT, Engleman W, Lacy PE. Alveolar soft part sarcoma-a malignant angioreninoma: histochemical, immunocytochemical, and electron-microscopic study of four cases. Am J Surg Pathol 1982;6:5-18.
Enzinger FM, Weiss SW. Malignant soft tissue tumors of uncertain type. In: Enzinger FM, Weiss SW, eds. Soft Tissue Tumors. 3rd ed. St Louis: CV Mosby, 1995; 1067-93.
Fisher ER, Reidbord H. Electron microscopic evidence suggesting the myogenous derivation of the so-called alveolar soft part sarcoma. Cancer 1971;27:150-9.
Font RL, Jurco S IIIrd, Zimmerman LE. Alveolar soft part sarcoma of the orbit: a clinicopathologic analysis of 17 cases and a review of the literature. Hum Pathol 1982;13:569-79.
Grant GD, Shields JA, Flanagan JC, Horowitz P. The ultrasonographic and radiologic features of a histopathologically proven case of alveolar soft-part sarcoma of the orbit. Am J Ophthalmol 1979;87:773-7.
Jordan DR, MacDonald H, Noel L, et al. Alveolar soft-part sarcoma of the orbit. Ophthalmic Surg 1995;26:269-70.
Lieberman PH, Foote FW Jr, Stewart FW, Berg JN. Alveolar soft-part sarcoma. JAMA 1966;198:1047-51.
Nirankari MS, Greer CH, Chaddah MR. Malignant non-chromaffin paraganglioma in the orbit. Br J Ophthalmol 1963;47:357-63.
Mukai M, Torikata C, Iri H, et al. Histogenesis of alveolar soft part sarcoma. An immunohistochemical and biochemical study. Am J Surg Pathol 1986;10:212-8.
Shipkey FH, Lieberman PH, Foote FW Jr, et al. Ultrastructure of alveolar soft part sarcoma. Cancer 1964;17:821-30.
Simmons WB, Haggerty HS, Ngan B, Anonsen CK. Alveolar soft part sarcoma of the head and neck. A disease of children and young adults. Int J Pediatr Otorhinolaryngol 1989;17:139-53.
Unni KK, Soule ED. Alveolar soft part sarcoma. An electron microscopic study. Mayo Clin Proc 1975; 50:591-8.
Varghese S, Nair B, Joseph TA. Orbital malignant non-chromaffin paraganglioma. Br J Ophthalmol 1968;52:713-5.
Welsh RA, Bray DM 3rd, Shipkey FH, Meyer AT. Histogenesis of alveolar soft part sarcoma. Cancer 1972;29:191-204.

Granular Cell Tumor

Allaire GS, Laflamme P, Bourgouin P. Granular cell tumour of the orbit. Can J Ophthalmol 1995;30:151-3.
Armin A, Connelly EM, Rawden G. An immunoperoxidase investigation of S-100 protein in granular cell myoblastomas: evidence for Schwann cell derivation. Am J Clin Pathol 1983;79:37-44.
Callejo SA, Kronish JW, Decker SJ, et al. Malignant granular cell tumor metastatic to the orbit. Ophthalmology 2000;107:550-4.
Chaves E, Oliveira AM, Arnaud AC. Retrobulbar granular cell myoblastoma. Br J Ophthalmol 1972;56:854-6.
Dolman PJ, Rootman J, Dolman CL. Infiltrating orbital granular cell tumour: a case report and literature review. Br J Ophthalmol 1986;71:47-53.
Drummond JW, Hall DL, Steen WH Jr, Maxey SA. Granular cell tumor (myoblastoma) of the orbit. Arch Ophthalmol 97:1979;1492-4.
Dunnington JH. Granular cell myoblastoma of the orbit. Arch Ophthalmol 1948;40:14-22.
Fisher ER, Wechsler H. Granular cell myoblastoma-a misnomer: electron microscopic and histochemical evidence concerning its Schwann cell derivation and nature (granular cell schwannoma). Cancer 1962;15:936-54.
Goldstein BG, Font RL, Alper MG. Granular cell tumor of the orbit: a case report including electron microscopic observations. Ann Ophthalmol 1982;14:231-2, 236-8.
Gonzalez-Almaraz G, de Buen S, Tsutsumi V. Granular cell tumor (myoblastoma) of the orbit. Am J Ophthalmol 1975;79:606-12.
Hashimoto M, Ohtsuka K, Suzuki T, Nakagawa T. Orbital granular cell tumor developing in theinferior oblique muscle. Am J Ophthalmol 1997;124:404-6.
Ingram DL, Mossier J, Snowhite J, et al. Granular cell tumors of the breast: steroid receptor analysis and localization of carcinoembryonic antigen, myoglobin and S100 protein. Arch Pathol Lab Med 1984;108:897-901.
Jaeger MJ, Green WR, Miller NR, Harris GJ. Granular cell tumor of the orbit and ocular adnexae. Surv Ophthalmol 1987;31:417-23.
Karcioglu ZA, Hemphill GL, Wool BM. Granular cell tumor of the orbit: case report and review of the literature. Ophthalmic Surg 1983;14:125-9.
Lack EE, Worsham GF, Callihan MD, et al. Granular cell tumor: a clinicopathologic study of 110 patients. J Surg Oncol 1980;13:301-16.
Miettinen M, Lehtonen E, Lehtola H, et al. Histogenesis of granular cell tumor - an immunohistochemical and ultrastructural study. J Pathol 1984;142:221-9.
Morgan G. Granular cell myoblastoma of the orbit. Report of a case. Arch Ophthalmol 1976;94:2135-42.
Morgan LR, Fryer MP. Granular cell myoblastoma of the eye. Case report. Plast Reconstr Surg 1969;43:315-7.
Moriarty P, Garner A, Wright JE. Case report of granular cell myoblastoma arising within the medial rectus muscle. Br J Ophthalmol 1983;67:17-22.
Obayashi K, Yamada Y, Kozaki M. [Granular cell myoblastoma in the orbit.] Nippon Ganka Kiyo 1969;20:566-74.
Rode J, Dhillon AP, Papadaki L. Immunohistochemical staining of granular cell tumor for neurone specific enolase: evidence in support of a neural origin. Diagn Histopathol 1982;5:205-11.
Sakamaki Y. Case of intraorbital myoblastoma. J Clin Ophthalmol [Tokyo] 1963;17:883-4.
Shimoyama I, Hinokuma K, Endo M, et al. [Granular cell myoblastoma in the orbit.] Neurol Med Chir (Tokyo) 1984;24:355-8.
Singleton EM, Nettleship B. Granular cell tumor of the orbit: a case report. Ann Ophthalmol 1983;15:881-3.
Stefansson K, Wollmann RL. S-100 protein in granular cell tumors (granular cell myoblastomas). Cancer 1982;49:1834-8.
Timm G, Timmel H. Zum Myoblastenmyom am Auge. Klin Monatsbl Augenheilkd 1966;148, 665-71.

Chemodectoma (Paraganglioma)

Ahmed A, Dodge OG, Kirk RS. Chemodectoma of the orbit. J Clin Pathol 1969;22:584-8.
Archer KF, Hurwitz JJ, Balogh JM, Fernandes BJ. Orbital nonchromaffin paraganglioma: a case report and review of the literature. Ophthalmology 1989;96:1659-66.
Deutsch AR, Duckworth JK. Nonchromaffin paraganglioma of the orbit. Am J Ophthalmol 1969;68:659-63.
Fisher ER, Hazard JB. Nonchromaffin paraganglioma of the orbit. Cancer 1952;5:521-4.

Glenner GG, Grimley PM. Tumors of the extra-adrenal paraganglion system (including chemoreceptors). An Atlas of Tumor Pathology, 2nd series, Fascicle 9. Washington, DC: Armed Forces Institute of Pathology, 1974.
Kadoya M, Amemiya T. [A case of orbital paraganglioma.] Nippon Ganka Gakkai Zasshi 1979;83:977-85.
Venkataramana NK, Kolluri VR, Kumar DV, et al. Paraganglioma of the orbit with extension to the middle cranial fossa: case report. Neurosurgery 1989;24:762-4.

Primary Orbital Carcinoid

Braffman BH, Bilaniuk LT, Eagle RC Jr, et al. MR imaging of a carcinoid tumor metstatic to the orbit. J Comput Asst Tomogr 1987;11:891-4.
El-Toukhy E, Levine MR, Abdul-Karim FW, Larson DW. Carcinoid tumors of the orbit: a dilemma of diagnosis and treatment. Ophthal Plast Reconst Surg 1996;12:279-83.
Godwin JD 2nd. Carcinoid tumors. An analysis of 2837 cases. Cancer 1975;36:560-9.
Riddle PJ, Font RL, Zimmerman LE. Carcinoid tumors of the eye and orbit: a clinicopathologic study of 15 cases with histochemical and electron microscopic observations. Hum Pathol 1982;13:459-69.
Shields CL, Shields JA, Eagle RC Jr, et al. Orbital metastasis from a carcinoid tumor: computed tomography, magnetic resonance imaging, and electron microscopic findings. Arch Ophthalmol 1987;105:968-71.
White VA. Carcinoid tumor metastatic to the orbit diagnosed by fine needle aspiration biopsy. Canadian Ophthalmic Pathology Society Meeting, Ottawa, Ontario, June 21, 1996.
Zimmerman LE, Stangl R, Riddle PJ. Primary carcinoid tumor of the orbit. A clinicopathologic study with histochemical and electron microscopic observations. Arch Ophthalmol 1983;101:1395-8.

Neuroepithelial Tumors

Neuroepithelioma

Arora R, Sarkar C, Betharia SM. Primary orbital primitive neuroectodermal tumor with immunohistochemical and electron microscopic confirmation. Orbit 1993;12:7-
Bolen JW, Thorning D. Peripheral neuroepithelioma: a light and electron microscopic study. Cancer 1980;46:2456-62.
Griffin CA, McKean C, Israel MA, et al. Comparison of constitutional and tumor-associated 11;22 translocations. Nonidentical breakpoints on chromosomes 11 and 22. Proc Natl Acad Sci USA 1986;83:6122-6.
Howard GM. Neuroepithelioma of the orbit. Am J Ophthalmol 1965;59:934-7.
Seemayer TA, Thelmo WL, Bolande R, Wiglesworth FW. Peripheral neuroectodermal tumors. Perspect Pediatr Pathol 1975;2:151-72.
Shuangshoti S, Menakanit W, Changwaivit W, Suwanwela N. Primary intraorbital extraocular primitaive neuroectodermal (neuroepithelial) tumour. Br J Ophthalmol 1986;70:543-8.
Singh AD, Husson M, Shields CL, et al. Primitie neuroectodermal tumor of the orbit. Arch Ophthalmol 1994;112:217-21.
Wilson WB, Roloff J, Wilson HL. Primary peripheral neuroepithelioma of the orbit with intracranial extension. Cancer 1988;62;2595-601.

Esthesioneuroblastoma

Bobele GB, Sexauer C, Barnes PA, et al. Esthesioneuroblastoma presenting as an orbital mass in a young child. Med Pediatr Oncol 1994;22:269-73.
Chaudhry AP, Haar JG, Koul A, Nickerson PA. Olfactory neuroblastoma (esthesioneuroblastoma): a light and ultrastructural study of two cases. Cancer 1979;44:564-79.
Elkon D, Hightower SI, Lim ML, et al. Esthesioneuroblastoma. Cancer 1979;44:1087-94.
Homzie MJ, Elkon D. Olfactory esthesioneuroblastoma - variables predictive of tumor control and recurrence. Cancer 1980;46:2509-13.
Hurtado-Sarrio M, Artacho-Tejederas JR, Riblon-Bornao F, et al. Esthesioneuroblastoma presenting with epiphora in a young child. Arch Ophthalmol 1997;115:1330-1.
Kadish S, Goodman M, Wang CC. Olfactory neuroblastoma. A clinical analysis of 17 cases. Cancer 1976;37:1571-6.
Knobber D, Lobeck H, Schnoy N. Asthesioneuroblastom: Diagnosesidnerung durch Immunhistologie und Elektronenmidroskopie. Laryngorhinootologie 1993;72:391-7.
Levine PA, McLean WC, Cantrell RW. Esthesioneuroblastoma: the University of Virginia experience 1960-1985. Laryngoscope 961986;:742-6.
Oberman HA, Rice DH. Olfactory neuroblastoma: a clincopathologic study. Cancer 1976;38:2494-502.
Rakes SM, Yeatts RP, Campbell RJ. Ophthalmic manifestations of esthesioneuroblastoma. Ophthalmology 1985;92:174953.
Valles San Leandro L, Arcas Martinez-Salas I, Villegas Perez MP, et al. Esthesioneuroblastoma: an atypical form of manifestaion. Eur J Ophthalmol 1994;4:118-22.

Primary Neuroblastoma and Ganglioneuroma

Bullock JD, Goldberg SH, Rakes SM, et al. Primary orbital neuroblastoma. Arch Ophthalmol 1989;107:1031-3.
Jakobiec FA, Klepach GL, Crissman JD, Spoor TC. Primary differentiated neuroblastoma of theorbit. Ophthalmology 1987;94:255-66.
Stout AP. Ganglioneuroma of sympathetic nervous system. Surg Gynecol Obstet 1947;84:101-10.
Toppozada HH. Ganglioneuroma of the left maxilla and orbit. J Laryngol 1958;72:733-42.

Primary Orbital Melanoma

Allen JC, Jaeschle WH. Recurrence of malignant melanoma in the orbit after 28 years. Arch Ophthalmol 1966;76:79-81.
Coppeto JR, Jaffe R, Gillies CG. Primary orbital melanoma. Arch Ophthalmol 1978;96:2255-8.
Drews RC. Primary malignant melanoma of the orbit in a Negro. Arch Ophthalmol 1975;93:335-8.
Dutton JJ, Anderson RL, Schelper RL, et al. Orbital malignant melanoma and oculodermal melanocytosis: report of two cases and review of the literature. Ophthalmology 1984;91:497-507.
Gündüz K, Shields JA, Shields CL, Eagle RC Jr. Periorbital cellular blue nevus leading to orbitopalpebral and intracranial melanoma. Ophthalmology 1998;105:2046-50.
Hagler WS, Brown CC. Malignant melanoma of the orbit arising in a nevus of Ota. Trans Am Acad Ophthalmol Otolaryngol 1966;70:817-22.
Haim T, Meyer E, Kerner H, Zonis S. Oculodermal melanocytosis (nevus of Ota) and orbital malignant melanoma. Ann Ophthalmol 1982;14:1132-6.
Hidano A, Kajima H, Ikeda S, et al. Natural history of nevus of Ota. Arch Dermatol 1967;95:18795.
Jakobiec FA, Ellsworth R, Tannenbaum M. Primary orbital melanoma. Am J Ophthalmol 1974;78:24-39.
Jay B. Malignant melanoma of the orbit in a case of oculodermal melanosis. (Naevus of Ota). Br J Ophthalmol 1965;49:359-63.
Loffler KU, Witschel H. Primary malignant melanoma of the orbit arising in a cellular blue naevus. Br J Ophthlmol 1989;73:388-93.
Reese AB. Tumors of the Eye. 3rd ed. Philadelphia: Harper & Row, 1976; 210.
Rottino A, Kelly AS. Primary orbital melanoma: case report with review of literature. Arch Ophthalmol 1942;27:934-49.

Shields JA, Augsberger JJ, Donoso LA, et al. Hepatic metastasis and orbital recurrence of uveal melanoma after 42 years. Am J Ophthalmol 1985;100:666-8.
Shields JA, Shields CL, Eagle RC Jr, et al. Necrotic orbital melanoma arising de novo. Br J Ophthalmol 1993;77:187-9.
Tellado M, Specht CS, McLean IW, et al. Primary orbital melanomas. Ophthalmology 1996;103:929-32.
Wilkes TDI, Uthman EO, Thornton CN, Cole RE. Malignant melanoma of the orbit in a black patient with ocular melanocytosis. Arch Ophthalmol 1984;102:904-6.
Wolter JR, Arbor A, Blackhurst RT. Primary orbital melanoma. Eye Ear Nose Throat Mon 1966;45:64.

Retinal Anlage Tumor (Pigmented Retinal Choristoma)

Blanc WA, Rosenblatt P, Wolff JA. Melanotic progonoma ("retinal anlage" tumor) of the shoulder in an infant: a case report. Cancer 1958;11:959-63.
Borello ED, Gorlin RJ. Melanotic neuroectodermal tumor of infanc - a neoplasm of neural crest origin. Cancer 1966;19:196-206.
Cutler LS, Chaudhry AP, Topazian R. Melanotic neuroectodermal tumor of infancy: an ultrastructural study, literature review, and reevaluation. Cancer 1981;48:257-70.
Dehner LP, Sibley RK, Sauk JJ Jr, et al. Malignant melanotic neuroectodermal tumor of infancy: a clinical, pathologic, ultrastructural and tissue culture study. Cancer 1979;43:1389-410.
Hall WC, O'Day DM, Glick AD. Melanotic neuroectodermal tumor of infancy. An ophthalmic appearance. Arch Ophthalmol 1979;97:922-5.
Khoddami M, Squire J, Zielenska M, Thorner P. Melanotic neuroectodermal tumor of infancy: a molecular genetic study. Pediatr Developmental Pathol 1998;1:295-9.
Koudstaal J, Oldhoff, J Panders AK, et al. Melanotic neuroectodermal tumor in infancy. Cancer 1968;22:151-61.
Lamping KA, Albert DM, Lack E, et al. Melanotic neuroectodermal tumor of infancy (retinal anlage tumor). Ophthalmology 1985;92:143-8.
Lurie HI. Congenital melanocarcinoma, melanotic adamantinoma, retinal anlage tumor, progonoma, and pigmented epulis of infancy. Summary and review of the literature and report of the first case in an adult. Cancer 1961;14:1090-108.
Lurie HI, Isaacson C. A melanotic progonoma in the scapula. Cancer 1961;14:1088-9.
Misugi K, Okajima H, Newton WA, et al. Mediastinal origin of a melanotic progonoma or retinal anlage tumor: ultrastructural evidence for neural crest origin. Cancer 1965;18:477-84.
Navas Palacios JJ. Malignant melanotic neuroectodermal tumor: light and electron microscopic study. Cancer 1980;46:529-36.
Nitta T, Endo T, Tsunoda A, et al. Melanotic neuroectodermal tumor of infancy: a molecular approach to diagnosis. Case report. J Neurosurg 1995;83:145-8.
Ricketts RR, Majmudarr B. Epididymal melanotic neuroectodermal tumor of infancy. Hum Pathol 1985;16:416-20.
Stowens D, Lin TH. Melanotic progonoma of the brain. Hum Pathol 1974;5;105-13.
Templeton AC. Orbital tumours in African children. Br J Ophthalmol 1971;55:254-13.
Zimmerman LE. Discussion. Melanotic neuroectodermal tumor of infancy (retinal anlage tumor). Ophthalmology 1985;92:149-50.

Ectomesenchymal Tumors

Enzinger FM, Weiss SW. Soft Tissue Tumors. 3rd ed. St Louis: CV Mosby, 1995; 568-70.
Jakobiec FA, Font RL, Tso MOM, Zimmerman LE. Mesectodermal leiomyoma of the ciliary body: a tumor of presumed neural crest origin. Cancer 1977;39:2102-13.
Jakobiec FA, Iwamoto T. Ocular adnexa: introduction to lids, conjunctiva, and orbit. In: Jakobiec FA, ed. Ocular Anatomy, Embryology, and Teratology. Philadelphia, Harper & Row, 1982; 677-731.
Jakobiec FA, Mitchell JP, Chauhan PM, Iwamoto T. Mesectodermal leiomyosarcoma of the antrum and orbit. Am J Ophthalmol 1978;85:51-7.
Karcioglu Z, Someren A, Mathes SJ. Ectomesenchymoma. A malignant tumor of migratory neural crest (ectomesenchyme) remnants showing ganglionic, schwannian, melanocytic, and rhabdomyoblastic differentiation. Cancer 1977;39:2486-96.

Mesenchymal Tumors

General

Batsakis JG. Tumors of the Head and Neck: Clinical and Pathological Considerations. 2nd ed. Baltimore: Williams & Wilkins, 1979.
Enzinger FM, Weiss SW. Soft Tissue Tumors. 3rd ed. St Louis: CV Mosby, 1995.
Forrest AW. Intraorbital tumors. Arch Ophthalmol 1949;41:198-232.
Jakobiec FA, Bilyk JR, Font RL. Mesenchymal Tumors. In: Spencer WH, ed. Ophthalmic Pathology: An Atlas and Textbook. 4th ed. Philadelphia: WB Saunders, 1996; 2569-629.
Jakobiec FA, Jones IS. Mesenchymal and fibro-osseous tumors. In: Jones IS, Jakobiec F, eds. Diseases of the Orbit. Philadelphia: Harper & Row, 1979; 461-502.
Jakobiec FA, Tannenbaum M. Embryological perspectives on the fine structure of orbital tumors. Int Ophthalmol Clin 1975;15:85-110.
Ni C, Albert DM. Tumors of the Eyelid and Orbit: A Chinese American Collaborative Study, Vol 22. Boston: Little, Brown, 1982.
Spranger JW, Langer LO, Wiedemann H-R. Bone Dysplasias: An Atlas of Constitutional Disorders of Skeletal Development. Philadelphia: WB Saunders, 1974.

Striated Muscle Tumors

Rhabdomyosarcoma

Abramson DH, Ellsworth RM, Tretter P, et al. The treatment of orbital rhabdomyosarcoma with irradiation and chemotherapy. Ophthalmology 1979;86:1330-5.
Abramson DH, Notis CM. Visual acuity after radiation for orbital rhabdomyosarcoma. Am J Ophthalmol 1994;118:808-9.
Alvarez Silvan AM, Garcia Canton JA, Pineda Cuevas G, Alfuro Gutierrez J. Successful treatment of orbital rhabdomyosarcoma in two infants using chemotherapy alone. Med Pediatr Oncol 1996;26:286-9.
Arora R, Betharia SM. Fine needle aspiration biopsy of pediatric orbital tumors. An immunohistochemical study. Acta Cytologica 1994;38:511-6.
Ashton N, Morgan G. Embryonal sarcoma and embryonal rhabdomyosarcoma of the orbit. J Clin Pathol 1965;18:699-714.
Atahan S, Aksu O, Ekinci C. Cytologic diagnosis and subtyping of rhabdomyosarcoma. Cytopathology 1998;9:389-97.
Bale PM, Parson RE, Stevens MM. Diagnosis and behavior of juvenile rhabdomyosarcoma. Hum Pathol 1983;14:596-611.
Baron EM, Kersten RC, Kulwin DR. Rhabdomyosarcoma manifesting as acquired nasolacrimal duct obstruction. Am J Ophthalmol 1993;114:239-42.
Calhoun FP Jr, Reese AB. Rhabdomyosarcoma of the orbit. Arch Ophthalmol 1942;27:558-78.
Cassady JR, Sagerman RH, Tretter P, Ellsworth RM. Radiation therapy for rhabdomyosarcoma. Radiology 1968;91:116-20.

Cavazzana AO, Schmidt D, Ninfo V, et al. Spindle cell rhabdomyosarcoma. A prognostically favorable variant of rhabdomyosarcoma. Am J Surg Pathol 1992;16:229-35.
Chess J, Ni C, Yin RQ, et al. Rhabdomyosarcoma. Int Ophthalmol Clin 1982;22:163-82.
Dagher R, Helman L. Rhabdomyosarcoma: an overview. Oncologist 1999;4:34-44.
Frayer WC, Enterline HT. Embryonal rhabdomyosarcoma of the orbit in children and young adults. Arch Ophthalmol 1959;62:203-10.
Goddard AG, Harris SJ, Plowman PN, et al. Growth hormone deficiency following radiotherapy for orbital and parameningeal sarcomas. Pediatr Hematol Oncol 1999;16: 23-33.
Grosfeld JL, Weber TR, Weetman RM, Baehner RL. Rhabdomyosarcoma in childhood: analysis of survival in 98 cases. J Pediatr Surg 1983;18:141-6.
Haik BG, Jereb B, Smith ME, et al. Radiation and chemotherapy of parameningeal rhabdomyosarcoma involving the orbit. Ophthalmology 1986;93:1001-9.
Hasegawa T, Matsuno Y, Niki T, et al. Second primary rhabdomyosarcomas in patients with bilateral retinoblastoma: a clinicopathologic and immunohistochemical study. Am J Surg Pathol 1998;22:1351-60.
Jones IS, Reese AB, Kraut J. Orbital rhabdomyosarcoma. An analysis of 62 cases. Am J Ophthalmol 1966;61:721-36.
Kahn HJ, Yeger H, Kassim O, et al. Immunohistochemical and electron microscopic assessment of childhood rhabdomyosarcoma. Increased frequency of diagnosis over routine histologic methods. Cancer 1983;51:1897-903.
Kingston JE, McElwain TJ, Malpas JS. Childhood rhabdomyosarcoma: experience of the Children's Solid Tumor Group. Br J Cancer 1983;48:195-207.
Knowles DM, Jakobiec FA, Potter GD, Jones IS. Ophthalmic striated muscle neoplasms. Surv Ophthalmol 1976;21:219-61.
Knowles DM IInd, Jakobiec FA, Potter GD, Jones IS. The diagnosis and treatment of rhabdomyosarcoma of the orbit. In: Jakobiec FA, ed. Ocular and Adnexal Tumors. Birmingham: Aesculapius, 1978; chap 49.
Kodet R, Newton WA Jr. Hamoudi AB, et al. Orbital rhabdomyosarcomas and related tumors in childhood: relationship of morphology to prognosis – an Intergroup Rhabdomyosarcoma study. Med Pediatr Oncol 1997;29:51-60.
Kodet R, Newton WA Jr. Hamoudi AB, et al. Childhood rhabdomyosarcoma with anaplastic (pleomorphic) features. A report of the Intergroup Rhabdomyosarcoma Study. Am J Surg Pathol 1993;17:443-53.
Kroll AJ. Fine-structural classification of orbital rhabdomyosarcoma. Invest Ophthalmol 1967;6:531-43.
Lawrence W Jr, Anderson JR, Gehan EA, Maurer H. Pretreatment TNM staging of childhood rhabdomyosarcoma: a report of the Intergroup Rhabdomyosarcoma Study Group. Children's Cancer Study Group. Pediatric Oncology Group. Cancer 1997;80:1165-70.
Leuschner I, Harms D. Pathologie der Rhabdomyosarkome des Kindes-und Adoleszentenalters. Ein Bericht des Kindertumorregisters bei der Gesellschaft fur Padiatrische Onkologie und Hematologie. Pathologe 1999;20:87-97.
Mafee MF, Pai E, Philip B. Rhabdomyosarcoma of the orbit. Evaluation with MR imaging and CT. Radiol Clin North Am 1998;36:1215-27.
Mannor GE, Rose GE, Plowman PN, et al. Multidisciplinary management of refractory orbital rhabdomyosarcoma. Ophthalmology 1997;104:1198-201.
Messmer EP, Font RL. Applications of immunohistochemistry to ophthalmic pathology. Ophthalmology 1984;91:701-7.
Morales AR, Fine G, Horn RC Jr. Rhabdomyosarcoma: an ultrastructural appraisal. Pathol Annu 1972;7:81-106.
Notis CM, Abramson DH, Sagerman RH, Ellsworth RM. Orbital rhabdoymosarcoma: treatment or overtreatment. Ophthalmic Genet 1995;16:159-62.
Palmer NF, Foulkes M. Histopathology and prognosis in the second Intergroup Rhabdomyosarcoma Study (IRS-II). ASCO Abstracts, C897, p 229, 1983.
Palmer NF, Sachs N, Foulkes M. Histopathology and prognosis in rhabdomyosarcoma (IRS-I). ASCO Abstracts, C660, p 170, 1982.
Pappo AS, Shapiro DN. Rhabdomyosarcoma: biology and treatment. In: Walterhouse DO, Cohn SL, eds. Diagnostic and Therapeutic Advances in Pediatric Oncology. Boston: Kluwer Academic, 1997; 309-39.
Polack FM, Kanai A, Hood CI. Light and electron microscopic studies of orbital rhabdomyosarcoma. Am J Ophthalmol 1971;71:75-83.
Porterfield JF, Zimmerman LE. Rhabdomyosarcoma of the orbit: a clinicopathologic study of 55 cases. Virchow Arch Path Anat 1962;335:329-44.
Qualman SJ, Coffin CM, Newton WA, et al. Intergroup Rhabdomyosarcoma Study: update for pathologists. Pediatr Dev Pathol 1998;1:550-61.
Rodary C, Gehan EA, Flamant F, et al. Prognostic factors in 951 nonmetastatic rhabomyosarcoma in children: a report from the International Rhabdomyosarcoma Workshop. Med Pediatr Oncol 1991;19:89-95.
Rousseau P, Flamant F, Quintana E, et al. Primary chemotherapy in rhabdomyosarcomas and other malignant mesenchymal tumors of the orbit: results of the International Society of Pediatric Oncology MMT 84 Study. J Clin Oncol 1994;12:516-21.
Sagerman RH, Cassady JR, Tretter P. Radiation therapy for rhabdomyosarcoma of the orbit. Trans Am Acad Ophthalmol Otolaryngol 1968;72:849-54.
Sohaib SA, Moseley I, Wright JE. Orbital rhabdomyosarcoma – the radiological characteristics. Clin Radiol 1998;53:357-62.
Stobbe GD, Dargeon HW. Embryonal rhabdomyosarcoma of the head and neck in children and adolescents. Cancer 1950;3:826-36.
Stout AP. Tumors of the soft tissues. In: Atlas of Tumor Pathology, Sect 2, Fasc 5. Washington DC: Armed Forces Institute of Pathology, 1953; 89.
Sun XL, Zheng BH, Li B, et al. Orbital rhabdomyosarcoma. Immunohistochemical studies of seven cases. Chin Med J 1990;103:485-8.
Sutow WW, Lindberg RD, Gehan EA, et al. Three-year relapse-free survival rates in childhood rhabdomyosarcoma of the head and neck: report from the Intergroup Rhabdomyosarcoma Study: Cancer 1982;49:2217-21.
Tefft M, Lindberg RD, Gehan EA. Radiation therapy combined with systemic chemotherapy of rhabdomyosarcoma in children. Local control in patients enrolled in the Intergroup Rhabdomyosarcoma Study. Natl Cancer Inst Monogr 1981;56:75-81.
Tsokos M, Howard R, Costa J. Immunohistochemical study of alveolar and embryonal rhabdomyosarcoma. Lab Invest 1983;48:148-55.
Weichselbaum RR, Cassady JR, Albert DM, Gonder JR. Multimodality management of orbital rhabdomyosarcoma. Int Ophthalmol Clin 1980;20:247-59.
Wharam M, Beltangady M, Hays D, et al. Localized orbital rhabdomyosarcoma: an interim report of the Intergroup Rhabdomyosarcoma Study Committee. Ophthalmology 1987;94:251-4.

Rhabdoid Tumor

Gunduz K, Shields JA, Eagle RC Jr, et al. Malignant rhabdoid tumor of the orbit. Arch Ophthalmol 1998;116:243-6
Kodet R, Newton WA Jr, Sachs N, et al. Rhabdoid tumors of soft itssues: a clinicopathologic study of 26 cases enrolled on the Intergroup Rhabdomyosarcoma Study. Hum Pathol 1991;22:674-84
Rootman JR, Damji KF, Dimmick JE. Malignant rhabdoid tumor of the orbit. Ophthalmology 1989;96:1650-4.

Rhabdomyoma

Hatsukawa Y, Furukawa A, Kawamura H, et al. Rhabdomyoma of the orbit in a child. Am J Ophthalmol 1997;123:142-4

Knowles DM Iind, Jakobiec FA. Rhabdomyoma of the orbit. Am J Ophthalmol 1975;80:1011-8

Endodermal Sinus Tumors

Katz NNK, Ruymann FB, Margo CE, et al. Endodermal sinus tumor (yolk-sac carcinoma) of the orbit. J Pediatr Ophthalmol Strabismus 1982;19:270-4.
Kivela T, Tarkkanen A. Orbital germ cell tumors revisited: a clinicopathological approach to classification. Surv Ophthalmol 1994;38:541-54.
Margo CE, Folberg R, Zimmerman LE, et al. Endodermal sinus tumor (yolk sac tumor) of the orbit. Ophthalmology 1983;90:1426-32.

Smooth Muscle Tumors

Badoza D, Weil D, Zarate J. Orbital leiomyoma: a case report. Ophthal Plast Reconstr Surg 1999;15:460-2.
Folberg R, Cleasby G, Flanagan JA, et al. Orbital leiomyosarcoma after radiation therapy for bilateral retinoblastoma. Arch Ophthalmol 1983;101:1562-5.
Font RL, Jurco S 3rd, Brechner RJ. Postradiation leiomyosarcoma of the orbit complicating bilateral retinoblastoma. Arch Ophthalmol 1983;101:1557-61.
Jakobiec FA, Howard GM, Rosen M, Wolff M. Leiomyoma and leiomyosarcoma of the orbit. Am J Ophthalmol 1975;80:1028-42.
Jakobiec FA, Mitchell JP, Chauhan PM, Iwamoto T. Mesectodermal leiomyosarcoma of the antrum and orbit. Am J Ophthalmol 1978;85:51-7.
Klippenstein KA, Wesley RE, Glick AD. Orbital leiomyosarcoma after retinoblastoma. Ophthalmic Surg Lasers 1999;30:579-83.
Sanborn GE, Valenzuela RE, Green WR. Leiomyoma of the orbit. Am J Ophthalmol 1979;87:371-5.
Wiechens B, Werner JA, Luttges J, et al. Primary orbital leiomyoma and leiomyosarcoma. Ophthalmologica 1999;213:159-64.
Wojno T, Tenzel RR, Nadji M. Orbital leiomyosarcoma. Arch Ophthalmol 1983;101:1566-8.

Adipose Tumors

Lipoma

Bartley GB, Yeatts RP, Garrity JA, et al. Spindle cell lipoma of the orbit. Am J Ophthalmol 1985;100:605-9.
Brown HH, Kersten RC, Kulwin DR. Lipomatous hamartoma of the orbit. Arch Ophthalmol 1991;109:240-3.
Feinfield RE, Hesse RJ, Scharfenberg JC. Orbital angiolipoma. Arch Ophthalmol 1988;106:1093-5.
Johnson BL, Linn JG Jr. Spindle cell lipoma of the orbit. Arch Ophthalmol 1979;97:133-
Koganei Y, Ishikawa S, Abe K, et al. Orbital lipoma. Ann Plast Surg 1988;20:173-82.
Morris DA, Henkind P. Fatty infiltration of orbits and heart. Am J Ophthalmol 1970;69:987-93.
Reese AB. Expanding lesions of the orbit (Bowman lecture). Trans Ophthalmol Soc UK 1971;91:85-104.
Silva D. Orbital tumors. Am J Ophthalmol 1968;65:318-39.

Liposarcoma

Abdalla MI, Ghaly AF, Hosni F. Liposarcoma with orbital metastases. Case report. Br J Ophthalmol 1966;50:426-8.
Cockerham KP, Kennerdell JS, Celin SE, Fechter HP. Liposarcoma of the orbit: a management challenge. Ophthal Plast Reconstr Surg 1998;14:370-4.
Enterline HT, Culberson JD, Rochlin DB, et al. Liposarcoma. A clinical and pathological study of 53 cases. Cancer 1960;13:932-50.
Enzinger FM, Weiss SW. Soft Tissue Tumors. 3rd ed. St Louis: CV Mosby, 1995.
Fezza J, Sinard J. Metastatic liposarcoma of the orbit. Am J Ophthalmol 1997;123:271-2.
Jakobiec FA, Rini F, Char D, et al. Primary liposarcoma of the orbit: problems in diagnosis and management of five cases. Ophthalmology 1989;96:180-91.
Lane CM, Wright JE, Garner A. Primary myxoid liposarcoma of the orbit. Br J Ophthalmol 1988;72:912-7.
Miller MH, Yokoyama C, Wright JE, Garner A. An aggressive lipoblastic tumour of the orbit in a child. Histopathology 1990;17:141-5.
Mortada A. Rare primary orbital sarcomas. Am J Ophthalmol 1969;68:919-25.
McNab AA, Moseley I. Primary orbital liposarcoma: clinical and computed tomographic features. Br J Ophthalmol 1990;74:437-9.
Naeser P, Mostrom U. Liposarcoma of the orbit: a clinicopathological case report. Br J Ophthalmol 1982;66:190-3.

Fibrous Tissue Tumors

Fibroma

Case TD, LaPiana FG. Benign fibrous tumor of the orbit. Ann Ophthalmol 1975;7:813-5.
Fowler JG, Terplan KL. Fibroma of the orbit. Arch Ophthalmol 1942;28:263-71.
Mortada A. Fibroma of the orbit. Br J Ophthalmol 1971;55:350-2.

Nodular Fasciitis

Font RL, Zimmerman LE. Nodular fasciitis of the eye and adnexa. A report of ten cases. Arch Ophthalmol 1966;75:475-81.
Levitt JM, deVeer JA, Oguzhan MC. Orbital nodular fasciitis. Arch Ophthalmol 1969;81:235-7.
Meacham CT. Pseudosarcomatous fasciitis. Am J Ophthalmol 1974; 77:747-9.
Perry RH, Ramani PS, McAllister V, et al. Nodular fasciitis causing unilateral proptosis. Br J Ophthalmol 1975;59:404-8.
Sakamoto T, Ishibashi T, Ohnishi Y, Inomata H. Immunohistological and electron microscopical study of nodular fasciitis of the orbit. Br J Ophthalmol 1991;75:636-8.
Shields JA, Shields CL, Christian C, Eagle RC Jr. Orbital nodular fasciitis simulating a dermoid cyst in an 8-month-old child. Ophthal Plast Reconstr Surg 2001;17:144-8.
Tolls RE, Mohr S, Spencer WH. Benign nodular fasciitis originating in Tenon's capsule. Arch Ophthalmol 1966;75:482-3.

Fibromatoses, Fibrosarcoma, and Myxoma

Abramson DH, Ellsworth RM, Zimmerman LE. Nonocular cancer in retinoblastoma survivors. Trans Am Acad Ophthalmol Otolaryngol 1976;81:454-7.
Abramson DH, Ronner HJ, Ellsworth RM. Second tumors in nonirradiated bilateral retinoblastoma. Am J Ophthalmol 1979;87:624-7.
Balsaver AM, Butler JJ, Martin RG. Congenital fibrosarcoma. Cancer 1967;20:1607-16.
Chung EB, Enzinger FM. Infantile fibrosarcoma. Cancer 1976;38:729-39.

Eifrig DE, Foos RY. Fibrosarcoma of the orbit. Am J Ophthalmol 1969;67:244-8.
Enzinger FM, Weiss SW. Soft Tissue Tumors. 3rd ed. St Louis: CV Mosby, 1995.
Gonzales-Crussi F. Ultrastructure of congenital fibrosarcoma. Cancer 1970;26:1289-99.
Hidayat AA, Font RL. Juvenile fibrosarcomatosis of the periorbital region and eyelid. A clinicopathologic study of six cases. Arch Ophthalmol 1980;98:280-5.
Jakobiec FA, Tannenbaum M. The ultrastructure of orbital fibrosarcoma. Am J Ophthalmol 1974;77:899-917.
Mortada A. Rare primary orbital sarcomas. Am J Ophthalmol 1969;68:919-25.
Nasr AM, Blodi FC, Lindahl S, Jinkins J. Congenital generalized multicentric myofibromatosis with orbital involvement. Am J Ophthalmol 1986;102:779-87.
Paton KE, Rootman J. Unusual second tumors in retinoblastoma. In: Frezzotti R, Balestrazzi E, Falco L, Esente S, eds. Proceedings of the International Symposium on Intraocular and Epibulbar Tumors, Florence, Italy, March 3-5, 1994. Bologna, Italy: Monduzzi Editore, 1994; 41-4.
Rootman J, Carvounis EP, Dolman CL, Dimmick JE. Congenital fibrosarcoma metastatic to the choroid. Am J Ophthalmol 1979;87:632-8.
Sagerman RH, Cassady JR, Tretter P, Ellsworth RM. Radiation induced neoplasia following external beam therapy for children with retinoblastoma. Am J Roentgenol Radium Ther Nucl Med 1969;105:529-35.
Schutz JS, Rabkin MD, Schutz S. Fibromatous tumor (desmoid type) of the orbit. Arch Ophthalmol 1979;97:703-4.
Weiner JM, Hidayat AA. Juvenile fibrosarcoma of the orbit and eyelid. A study of five cases. Arch Ophthalmol 1983;101:253-9.
Yanoff M, Scheie HG. Fibrosarcoma of the orbit. Report of two patients. Cancer 1966;19:1711-6.

Solitary Fibrous Tumor

Alexandrakis G, Johnson TE. Recurrent orbital solitary fibrous tumor in a 14-year-old girl. Am J Ophthalmol 2000;130:373-6.
DeBAcker CM, Bodker F, Putterman AM, Beckmann E. Solitary fibrous tumor of the orbit. Am J Ophthalmol 1996;121:447-9.
Dorfman DM, To K, Dickersin GR, et al. Solitary fibrous tumor of the orbit. Am J Surg Pathol 1994;18:81-7.
Fukanaga M, Ushigome S, Nomura K, Ishikawa E. Solitary fibrous tumor of the nasal cavity and orbit. Pathol Int 1995;45:952-7.
Gigantelli JW, Kincaid MC, Soparkar CNS, et al. Orbital solitary fibrous tumor: radiographic and histopathologic correlations. Ophthal Plast Reconstr Surg 2001;17:207-14.
Heathcote JG. Pathology update: solitary fibrous tumour of the orbit. Can J Ophthalmol 1997;32:432-5.
Kim HY, Lee SY, Kang SJ, Kim HJ. Solitary fibrous tumor of the orbit; a poorly-recognized orbital lesion. Acta Ophthalmol Scand 1999;77:704-8.
Lanuza A, Lazaro R, Salvador M, et al. Solitary fibrous tumor of the orbit. Report of a new case. Int Ophthalmol 1998;22:265-8.
McElvanney AM, Noble JL, O'Donovan DG, et al. Solitary fibrous tumour: an atypical presentation within the orbit. Eye 1996;10:396-9.
Morgan MB, Smoller BR. Solitary fibrous tumors are immunophenotypically distinct from mesothelioma(s). J Cutaneous Pathol 2000;27:451-4.
Ramdial PK, Nadvi S. An unusual cause of proptosis: orbital solitary fibrous tumor: case report. Neurosurgery 1996;38:1040-3.
Sciot R, Goffin J, Fossion E, et al. Solitary fibrous tumor of the orbit. Histopathology 1996;28:188-91.
Scott IU, Tanenbaum M, Rubin D, Lores E. Solitary fibrous tumor of the lacrimal gland fossa. Ophthalmology 1996;103:1613-8.
Westra WH, Gerald WL, Rosai J. Solitary fibrous tumor. Consistent CD34 immunoreactivity and occurrence in the orbit. Am J Surg Pathol 1994;18:992-8.
Woo KI, Suh YL, Kim YD. Solitary fibrous tumor of the lacrmal sac. Ophthal Plast Reconstr Surg 1999;15:450-3.

Epithelioid Sarcoma

White VA, Heathcote JG, Hurwitz JJ, et al. Epithelioid sarcoma of the orbit. Ophthalmology 1994;101:1680-7.

Myxoma

Gifford SR. Multiple myxoma of the orbit. Arch Ophthalmol 1931;5:445-8.
Jakobiec FA, Jones IS. Mesenchymal and fibro-osseous tumors. In: Jones IS, Jakobiec F, eds. Diseases of the Orbit. Philadelphia: Harper & Row, 1979; 461-502.
Kreuger EG, Polifrone JC, Baum G. Retrobulbar orbital myxoma and its detection by ultrasonography. Case report. J Neurosurg 1967;26:87-91.

Giant Cell Angiofibroma

Dei Tos AP, Seregard S, Calonje E, et al. Giant cell angiofibrom. A distinctive orbital tumor in adults. Am J Surg pathol 1995;19:1286-93.
Ganesan R, Hammond CJ, van der Walt JD. Giant cell angiofibroma of the orbit. Histopathology 1997;30:93-6.

Histiocytic Tumors

Fibrous Histiocytoma

Biedner B, Rothkoff L. Orbital fibrous histiocytoma in an infant. Am J Ophthalmol 1978;85:548-50.
Caballero LRC, Rodriguez AC, Sopelana AB. Angiomatoid malignant fibrous histiocytoma of the orbit. Am J Ophthalmol 1981;92:13-5.
Enzinger FM. Angiomatoid malignant fibrous histiocytoma: a distinct fibrohistiocytic tumor of children and young adults simulating a vascular neoplasm. Cancer 1979;44:2147-57.
Font RL, Hidayat AA. Fibrous histiocytoma of the orbit. A clinicopathologic study of 150 cases. Hum Pathol 1982;13:199-209.
Hoffman MA, Dickersin GR. Malignant fibrous histiocytoma: an ultrastructural study of eleven cases. Hum Pathol 1983;14:913-22.
Jakobiec FA, Howard GM, Jones IS, Tannenbaum M. Fibrous histiocytomas of the orbit. Am J Ophthalmol 1974;77:333-45.
Kauffman SL, Stout AP. Histiocytic tumors (fibrous xanthoma and histiocytoma) in children. Cancer 1961;14:469-82.
O'Brien JE, Stout AD. Malignant fibrous xanthomas. Cancer 1964;17:1445-55.
Ozzello L, Stout AP, Murray MR. Cultural characteristics of malignant histiocytomas and fibrous xanthomas. Cancer 1963;16:331-44.
Rodrigues MM, Furgiuele FP, Weinreb S. Malignant fibrous histiocytoma of the orbit. Arch Ophthalmol 1977;95:2025-8.
Singh B, Shaha A, Har-El G. Malignant fibrous histiocytoma of the head and neck. J Cranio Maxillo Fac Surg 1993;21:262-5.
Soule EH, Enriquez P. Atypical fibrous histiocytoma, malignant fibrous histiocytoma, malignant histiocytoma, and epithelioid sarcoma. A comparative study of 65 tumors. Cancer 1972;30:128-43.
Stewart WB, Newman NM, Cavender JC, Spencer WH. Fibrous histiocytoma metastatic to the orbit. Arch Ophthalmol 1978;96:871-3.
Tewfik HH, Tewfik FA, Latourette HB. Postirradiation malignant fibrous histiocytoma. J Surg Oncol 1981;16:199-202.

Turner RR, Wood GS, Beckstead JH, et al. Histiocytic malignancies. Morphologic, immunologic and enzymatic heterogeneity. Am J Surg Pathol 1984;8:485-500.
Weiss SW, Enzinger FM. Malignant fibrous histiocytoma: an analysis of 200 cases. Cancer 1978;41:2250-66.

Primary Bone Tumors of the Orbit

General

Barnes L. Surgical Pathology of the Head and Neck. Vol 2. New York: Marcel Dekker, 1985.
Blodi FC. Pathology of orbital bones. The XXXII Edward Jackson Memorial Lecture. Am J Ophthalmol 1976;81:1-26.
Dahlin DC, Unni KK. Bone Tumors: General Aspects and Data on 8,542 Cases. 4th ed. Springfield: Thomas, 1986.
Fu YS, Perzin KH. Non-epithelial tumors of the nasal cavity, paranasal sinuses, and nasopharynx: a clinicopathologic study. II: Osseous and fibro-osseous lesions, including osteoma, fibrous dysplasia, ossifying fibroma, osteoblastoma, giant cell tumor and osteosarcoma. Cancer 1974;33:1289-305.

Benign Fibro-osseous and Cartilaginous Tumors

Osteomas

Albert DA, Ni C, Sebag J, Renna T. Rare orbital tumors. Int Ophthalmol Clin 1982;22:183-205.
Biedner B, Monos T, Frilling F, et al. Acquired Brown's syndrome caused by frontal sinus osteoma. J Ped Ophthalmol Strabismus 1988;25:226-9.
Cecire A, Harrison HC, Ng P. Ethmoid osteoma, orbital cellulitis and orbital emphysema. Aust NZ J Ophthalmol 1988;16:11-4.
Ciappetta P, Delfini R, Iannetti G, et al. Surgical strategies in the treatment of symptomatic osteomas of the orbital walls. Neurosurgery 1992;31:628-35.
Dal Cin P, Sciot R, Samson I, et al. Osteoid osteoma and osteoblastoma with clonal chromosome changes. Br J Cancer 1998;78:344-8.
Fu YS, Perzin KH. Nonepithelial tumors of the nasal cavity, paranasal sinuses and nasopharynx: a clinicopathologic study. II. Osseous and fibro-osseous lesions, including osteoma, fibrous dysplasia, ossifying fibroma, osteoblastoma, giant cell tumor, and osteosarcoma. Cancer 1974;33:1289-305.
Gardner EJ. Genetic and clinical study of intestinal polyposis, predisposing factor for carcinoma of colon and rectum. Am J Hum Genet 1951;3:167-70.
Gardner EJ, Richards RC. Multiple cutaneous and subcutaneous lesions occurring simultaneously with hereditary polyposis and osteomatosis. Am J Hum Genet 1953;5:139-47.
Grove AS, Jr. Osteoma of the orbit. Ophthalmic Surg 1978;9:23-39.
Henderson JW. Fibro-osseous, osseous, and cartilaginous tumors of orbital bone. In: Henderson JW, ed. Orbital Tumors, 3rd ed. Philadelphia: Raven Press, 1994; 153-99.
McNab AA. Orbital osteoma in Gardner's syndrome. Aust NZ J Ophthalmol 1998;26:169-70.
Miller NR, Gray J, Snip R. Giant, mushroom-shaped osteoma of the orbit originating from the maxillary sinus. Am J Ophthalmol 1977;83:587-91.
Mirra JM. Bone Tumors: Clinical, Radiologic and Pathologic Correlations. Philadelphia: Lea & Febiger, 1989; 174-82.
Mortada A. Orbital osteomata within the domain of opthalmic surgery. Can J Ophthalmol 1969;4:258-65.
Perez Moreiras JV, Prada Sanchez MC. Patologia Orbitaria. Tomo 1. Barcelona: Ciba Vision, 2000.
Whitson WE, Orcult JC, Walkinshaw MD. Orbital osteoma in Gardner's syndrome. Am J Ophthalmol 1986;101:236-41.
Wilkes SR, Trautmann JC, DeSanto LW, Campbell RJ. Osteoma: an unusual case of amaurosis fugax. Mayo Clin Proc 1979;54:258-60.

Fibrous Dysplasia

Albright F, Butler AM, Hampton AO, Smith P. Syndrome characterized by osteitis fibrosa disseminata, areas of pigmentation and endocrine dysfunction with precocious puberty in females. N Engl J Med 1937;216:727-46.
Benedict PH, Szabo G, Fitzpatrick TB, Sinesi SJ. Melanotic macules in Albright's syndrome and neurofibromatosis. JAMA 1968;205:618-26.
Bianco P, Kuznetsov SA, Riminucci M, et al. Reproduction of human fibrous dysplasia of bone in immunocompromised mice by transplanted mosaics of normal and Gsalpha-mutated skeletal progenitor cells. J Clin Invest 1998;101:1737-44.
Bibby K, McFadzean R. Fibrous dysplasia of the orbit. Br J Ophthalmol 1994;78:266-70.
Edelstein C, Goldberg RA, Rubino G. Unilateral blindness after ipsilateral prophylactic transcranial optic canal decompression for fibrous dysplasia. Am J Ophthalmol 1998;126:469-71.
Fries JW. The roentgen features of fibrous dysplasia of the skull and facial bones. Am J Roentgenol Radium Ther Nucl Med 1957;77:71-88.
Hansen-Kuarhoi M, Poole MD. Preoperative difficulties in differentiating intraosseous meningiomas and fibrous dysplasia around the orbital apex. J Cranio Maxillo Fac Surg 1994;22:226-30.
Jackson IT, Hide TA, Gomuwka PK, et al. Treatment of cranio-orbital fibrous dysplasia. J Maxillofac Surg 1982;10:138-41.
Katz BJ, Nerad JA. Opthalmic manifestations of fibrous dysplasia: a disease of children and adults. Ophthalmology 1998;105:2207-15.
Liakos GM, Walker CB, Carruth JAS. Ocular complications in craniofacial fibrous dysplasia. Br J Ophthalmol 1979;63:611-6.
Melen O, Weinberg PE, Kim KS, al e. Fibrous dysplasia of bone with acute visual loss. Ann Ophthalmol 1980;12:734-9.
Moore AT, Buncic JR, Munro IR. Fibrous dysplasia of the orbit in childhood. Ophthalmology 1985;92:12-20.
Osguthorpe JD, Gudeman SK. Orbital complications of fibrous dysplasia. Otolaryngol Head Neck Surg 1987;97:403-5.
Papay FA, Morales L, Jr, Flaharty P, et al. Optic nerve decompression in cranial base fibrous dysplasia. J Craniofac Surg 1995;6:5-14.
Posnick JC. Fibrous dysplasia of the craniomaxillofacial region: current clinical perspectives. Br J Oral Maxillofac Surg 1998;36:264-73.
Reed RJ. Fibrous dysplasia of bone. A review of 25 cases. Arch Pathol 1963;75:480-95.
Seiff SR. Optic nerve decompression in fibrous dysplasia: indications, efficacy and safety [letter]. Plast Reconstr Surg 1997;100:1611-2.
Yabut SM, Kenan S, Sissons HA. Malignant transformation of fibrous dysplasia. A case report and review of the literature. Clin Orthop 1988;228:281-9.

Ossifying Fibroma (Fibro-osseous Dysplasia)

Dahlin DC, Unni KK. Bone Tumors: General Aspects and Data on 8,542 Cases, 4th ed. Springfield, IL: Charles C. Thomas, 1986; 84-7.
Khalil MK, Leib ML. Cemento-ossifying fibroma of the orbit. Can J Ophthalmol 1979;14:195-200.
Lehrer HZ. Ossifying fibroma of the orbital roof. Arch Neurol 1969;20:536-41.
Margo CE, Ragsdale BD, Perman KI, et al. Psammomatoid (juvenile) ossifying fibroma of the orbit. Ophthalmology 1985;92:150-9.
Margo CE, Weiss A, Habal MB. Psammomatoid ossifying fibroma. Arch Ophthalmol 1986;104:1347-51.
Marks MW, Newman MH. Transcoronal removal of an atypical orbitoethmoid osteoma. Plast Reconstr Surg 1983;72:874-7.
Nakagawa K, Takasato Y, Ito Y, Yamada K. Ossifying fibroma involving the orbit, paranasal sinuses and anterior cranial fossa. Neurosurgery 1995;36:1192-5.

Scott M, Prale AR, Croissant PD. Intracranial midline anterior fossa ossifying fibroma invading orbits, paranasal sinuses and right maxillary antrum. Case report. J Neurosurg 1971;34:827-31.
Shields JA, Nelson LB, Brown JF, Dolinskas C. Clinical, computed tomographic and histopathologic characteristics of juvenile ossifying fibroma with orbital involvement. Am J Ophthalmol 1983;96:650-3.
Shields JA, Peyster RG, Handler SD, et al. Massive juvenile ossifying fibroma of maxillary sinus with orbital involvement. Br J Ophthalmol 1985;69:392-5.
Thomas GK, Kasper KA. Ossifying fibroma of frontal bone. Arch Otolaryngol 1966;83:43-6.

Osteoblastoma

Abdalla MI, Hosni F. Osteoclastoma of the orbit: case report. Br J Ophthalmol 1966;50:95-8.
Adler M, Hnatuk L, Mock D, Freeman JL. Aggressive osteoblastoma of the temporal bone: a case report. J Otolaryngol 1990;19:307-10.
Bertoni F, Unni KK, Mcleod RA, Dahlin DC. Osteosarcoma resembling osteoblastoma. Cancer 1985;55:416-26.
Bettelli G, Tigani D, Picci P. Recurring osteoblastoma initially presenting as a typical osteoid osteoma. Report of two cases. Skeletal Radiol 1991;20:1-4.
Clutter DJ, Leopold DA, Gould LV. Benign osteoblastoma. Arch Otolaryngol 1984;110:334-6.
Dal Cin P, Sciot R, Samson I, et al. Osteoid osteoma and osteoblastoma with clonal chromosome changes. Br J Cancer 1998;78:344-8.
Figarella-Branger D, Perez-Castillo M, Garbe L, et al. Malignant transformation of an osteoblastoma of the skull. J Neurosurg 1991;75:138-42.
Freedman SR. Benign osteoblastoma of the ethmoid bone. Am J Clin Pathol 1975;63:391-6.
Leone CR, Jr, Lawton AW, Leone RT. Benign osteoblastoma of the orbit. Ophthalmology 1988;95:1554-8.
Lowder CY, Berlin AJ, Cox WA, Hahn JR. Benign osteoblastoma of the orbit. Ophthalmology 1986;93:1351-4.
Morton KS, Quenville NF, Beauchamp CP. Aggressive osteoblastoma. A case previously reported as a recurrent osteoid osteoma. J Bone Joint Surg 1989;71:428-31.
Ruggieri P, McLeod RA, Unni KK, Sim FH. Mayo Clinic Tumor Rounds: osteoblastoma. Orthopedics 1996;19:621-4.
Shepherd WFI, Maguire CJF, Bailey IC. Benign osteoblastoma of the orbit [abstract]. Irish J Med Sci 1977;146:150.

Chondroma

Blodi FC. Pathology of orbital bones. The XXXII Edward Jackson Memorial lecture. Am J Ophthalmol 1976;81:1-26.
Bowen JH, Christensen FH, Klintworth GK, Sydnor CF. A clinicopathologic study of a cartilaginous hamartoma of the orbit: a rare cause of proptosis. Ophthalmology 1981;88:1356-60.
Fu YS, Perzin KH. Non-epithelial tumors of the nasal cavity, paranasal sinuses and nasopharynx: a clinicopathologic study. III. Cartilaginous tumors (chondroma, chondrosarcoma). Cancer 1974;34:453-63.
Jepson CM, Wetzig PC. Pure chondroma of the trochlea: a case report. Surv Ophthalmol 1966;11:656-9.
Pasternak S, O'Connell JX, Verchere C, Rootman J. Enchondroma of the orbit. Am J Ophthalmol 1996;122:444-5.

Reactive Bone Lesions

Cholesterol Granuloma

Dickey JB, Mullenix CD, O'Grady RB. Atypical magnetic resonance findings in an orbitofrontal cholesterol granuloma. Ophthalmic Plast Reconstr Surg 1992;8:215-20.
Eijpe AA, Koornneef L, Verbeeten B, Jr, et al. Cholesterol granuloma of the frontal bone: CT diagnosis. J Comp Assist Tomogr 1990;14:914-7.
Eisenberg MB, Haddad G, Al-Mefty O. Petrous apex cholesterol granulomas: evolution and management. J Neurosurg 1997;86:822-9.
Fukuta K, Jackson IT. Epidermoid cyst and cholesterol granuloma of the orbit. Br J Plast Surg 1990;43:521-7.
Heaton RB, Ross JJ, Jochum JM, Henry MR. Cytologic diagnosis of cholesterol granuloma: a case report. Acta Cytolgica 1993;37:713-6.
Hill CA, Moseley IF. Imaging of orbitofrontal cholesterol granuloma. Clin Radiol 1992;46:237-42.
Loeffler KU, Kommerell G. Cholesterol granuloma of the orbit: pathogenesis and surgical management. International Ophthalmology 1997;21:93-8.
McNab AA, Wright JE. Orbitofrontal cholesterol granuloma. Ophthalmology 1990;97:28-32.

Aneurysmal Bone Cyst

Bealer LA, Cibis GW, Barker BF, et al. Aneurysmal bone cyst: report of a case mimicking orbital tumor. J Ped Ophthalmol Strabismus 1993;30:199-200.
Citardi MJ, Janjua T, Abrahams JJ, Sasaki C. Orbitoethmoid aneurysmal bone cyst. Otolaryngol Head Neck Surg 1996;114:466-70.
Fite JD, Schwartz JF, Calhoun FP. Aneurysmal bone cyst of the orbit. A clinicopathologic case report. Trans Am Acad Ophthalmo Otolaryngol 1968;72:614-8.
Hunter JV, Yokoyama C, Moseley IF, Wright JE. Aneurysmal bone cyst of the sphenoid with orbital involvement. Br J Ophthalmol 1990;74:505-8.
Johnson TE, Bergin DJ, McCord CD. Aneurysmal bone cyst of the orbit. Ophthalmology 1988;95:86-8.
Klepach GH, Ho REM, Kelly JK. Aneurysmal bone cyst of the orbit. A case report. J Clin Neuro Ophthalmol 1984;4:49-52.
Lucarelli MJ, Bilyk JR, Shore JW, et al. Aneurysmal bone cyst of the orbit associated with fibrous dysplasia. Plast Reconstr Surg 1995;96:440-5.
Martinez V, Sissons HA. Aneurysmal bone cyst. A review of 123 cases including primary lesions and those secondary to other bone pathology. Cancer 1988;61:2296-304.
O'Gorman AM, Kirkham TH. Aneurysmal bone cyst of the orbit with unusual angiographic factors. Am J Roentgenol 1976;126:896-9.
Patel BC, Sabir DI, Flaharty PM, Anderson RL. Aneurysmal bone cyst of the orbit and ethmoid sinus [letter]. Arch Ophthalmol 1993;111:586-7.
Powell JO, Glaser J. Aneurysmal bone cyst of the orbit. Arch Ophthalmol 1975;93:340-2.
Ronner HJ, Jones IS. Aneurysmal bone cyst of the orbit: a review. Ann Ophthalmol 1983;15:626-9.
Sanerkin NG, Mott MG, Roylance J. An unusual intraosseous lesion with fibroblastic, osteoclastic, osteoblastic and fibromyxoid elements. Cancer 1983;51:2278-86.
Yee RD, Cogan DG, Thorp TR, Schut L. Optic nerve compression due to aneurysmal bone cyst. Arch Ophthalmol 1977;95:2176-9.

Giant Cell Granuloma

Friedberg SA, Eiserstein R, Wallner LJ. Giant cell lesions involving the nasal accessory sinuses. Laryngoscope 1969;79:763-6.
Hoopes PC, Anderson RL, Blodi FC. Giant cell (reparative) granuloma of the orbit. Ophthalmology 1981;88:1361-6.
Jaffe HL. Giant cell reparative granuloma, traumatic bone cyst and fibrous dysplasia of the jawbones. Oral Surg 1953;6:159-75.
Rhea JT, Weber AL. Giant cell granuloma of the sinuses. Radiology 1983;147:135-7.
Scully RE, Mark EJ, McNeely BU. Case records of the Massachusetts General Hospital. Weekly clinicopathologic exercises. Case 10-1984. N Engl J Med 1984;310:642-8.

Sood GC, Malik SRK, Gupin DK, Kakar PK. Reparative granuloma of the orbit causing unilateral proptosis. Am J Ophthalmol 1967;63:524-7.
Spraul CW, Wojno TH, Grossniklaus HE, Lang GK. Reparative giant cell granuloma with orbital involvement. Klin Monatsbl Augenheilkunde 1997;211:133-4.

"Brown Tumor" of Hyperparathyroidism

Bedard CH, DNichols RP. Osteitis fibrosa (brown tumor) of the maxilla. Laryngoscope 1974;84:2093-100.
Block MB. Brown tumor of the orbit [letter to the editor]. JAMA 1978;239:1037.
Ferry AP. Brown tumors (fibro-osseous bone replacement and overgrowth) of the orbit in hyperparathyroidism. Metab Pediatr Syst Ophthalmol 1979;3:67-75.
Friedman WH, Pervez N, Schwartz AE. Brown tumor of the maxilla in secondary hyperparathyroidism. Arch Otolaryngol Head Neck Surg 1974;100:151-9.
Gay I, Viskoper JR, Chowers I. Maxillary tumor as a presenting sign of secondary hyperparathyroidism due to renal insufficiency. J Larnyngol Otol 1971;83:737-42.
Holzer NJ, Croft CB, Walsh JB, et al. Brown tumor of the orbit. JAMA 1977;238:1758-9.
Naiman J, Green WR, d'Heurk D, et al. Brown tumor of the orbit associated with primary hyperparathyroidism. Americal Journal of Ophthalmology 1980;90:565-71.
Parrish CM, O'Day DM. Brown tumor of the orbit. Arch Ophthalmol 1986;104:1199-202.
Slem G, Varinli S, Koker F. Brown tumor of the orbit. Ann Ophthalmol 1983;15:811-2.

Neoplasms

Osteogenic Sarcoma

Abramson DH, Ronner HJ, Ellsworth RM. Second tumors in non-irradiated bilateral retinoblastoma. Am J Ophthalmol 1979;87:624-7.
Benedict WF, Fung YK, Murphree AL. The gene responsible for the development of retinoblastoma and osteosarcoma. Cancer 1988;62:1691-4.
Bone RC, Biller HF, Harris BL. Osteogenic sarcoma of the frontal sinus. Ann Otolaryngol 1973;82:162-5.
Dhir SP, Munjal VP, Jain IS, et al. Osteosarcoma of the orbit. J Pediatr Ophthalmol 1980;17:312-4.
Draper GJ, Sanders BM, Kingston JE. Second primary neoplasms in patients with retinoblastoma. Br J Cancer 1986;53:661-71.
Dryja TP, Rapaport JM, Epstein J, et al. Chromosome 13 homozygosity in osteosarcoma without retinoblastoma. Am J Hum Genet 1986;38:59-66.
el Quessar A, Boumedin H, Chakir N, et al. Primary osteosarcoma of the skull. J Neuroradiol 1997;24:70-4.
Glasser DB, Lane JM, Huvos AG, et al. Survival, prognosis and therapeutic response in osteogenic sarcoma. The Memorial Hospital experience. Cancer 1992;69:698-708.
Mark RJ, Sercarz JA, Tran L, et al. Osteogenic sarcoma of the head and neck. The UCLA experience. Arch Otolaryngol 1991;117:761-6.
Trevisani MG, Fry CL, Hesse RJ, Willis GW. A rare case of orbital osteogenic sarcoma [letter]. Arch Ophthalmol 1996;114:494-5.

Chondrosarcoma & Mesenchymal Chondrosarcoma

Evans HL, Ayala AG, Romsdahl MM. Prognostic factors in chondrosarcoma of bone: a clinicopathologic analysis with emphasis in histologic grading. Cancer 1977;40:818-31.
Finn DG, Goepfert H, Batsakis JG. Chondrosarcoma of the head and neck. Laryngoscope 1984;94:1539-44.
Jacobs JL, Merriam JC, Chadburn A, et al. Mesenchymal chondrosarcoma of the orbit. Report of three new cases and review of the literature. Cancer 1994;73:399-405.
Lauer SA, Friedland S, Goodrich JT, Dorfman H. Mesenchymal chondrosarcoma with secondary orbital invasion. Ophthalmic Plast Reconstr Surg 1995;11:1802-6.
Miyamoto H, Yoshii M, Murakami A, et al. [A case of primary orbital chondrosarcoma]. Nippon Ganka Gakkai Zasshi - Acta Societatis Ophthalmologicae Japonicae 1997;101:192-6.
Potts MJ, Rose GE, Hilroy C, Wright JE. Dedifferentiated chondrosarcoma arising in the orbit. Br J Ophthalmol 1992;76:49-51.
Pritchard DJ, Lunke RJ, Taylor WF, et al. Chondrosarcoma: a clinicopathlogic and statistical analysis. Cancer 1980;45:149-57.
Rosenthal DI, Schiller AL, Mankin HJ. Chondrosarcoma: correlation of radiological and histological grade. Radiology 1984;150:21-6.
Ruark DS, Schlehaider UK, Shah JP. Chondrosarcomas of the head and neck. World J Surg 1992;16:1010-6.
Stapleton SR, Wilkins PR, Archer DJ, Uttley D. Chondrosarcoma of the skull base: a series of eight cases. Neurosurgery 1993;32:348-55.

Ewing's Sarcoma

Alvarez-Berdecia A, Schut L, Bruce DA. Localized primary intracranial Ewing's sarcoma of the orbital roof. Case report. J Neurosurg 1979;50:811-3.
Howard DJ, Lund VJ. Primary Ewing's sarcoma of the ethmoid bone. J Larnyngol Otol 1985;99:1019-23.
Jurgens H, Exner U, Gadner H, et al. Multidisciplinary treatment of primary Ewing's sarcoma of bone. A 6-year experience of a European Cooperative Trial. Cancer 1988;61:23-32.
McKeon C, Thiele CJ, Ross RA, et al. Indistinguishable patterns of protooncogene expression in two distinct but closely related tumors: Ewing's sarcoma and neuroepithelioma. Cancer Res 1988;48:4307-11.
Nesbit ME, Jr., Gehan EA, Burgert EO, Jr., et al. Multimodal therapy for the management of primary, nonmetastatic Ewing's sarcoma of bone. A long-term follow-up of the First Intergroup Study. J Clin Oncol 1990;8:1664-74.
O'Connor MI, Pritchard DJ. Ewing's sarcoma. Prognostic factors, disease control and the re-emerging role of surgical treatment. Clin Orthop 1991;262:78-87.
Steiner GC. Neuroectodermal tumor versus Ewing's sarcoma-immunohistochemical and electron microscopic observations. Curr Top Pathol 1989;80:1-29.
Turc-Carel C, Aurias A, Mugneret F, et al. Chromosomes in Ewing's sarcoma. I. An evaluation of 85 cases of remarkable consistency of t(11:22) (q24:q12). Cancer Genet Cytogent 1988;32:229-38.
Wilkins RM, Pritchard DJ, Burgert EO, Jr., Unni KK. Ewing's sarcoma of bone. Experience with 140 patients. Cancer 1986;58:2551-5.
Woodruff G, Thorner P, Skarf B. Primary Ewing's sarcoma of the orbit presenting with visual loss. Br J Ophthalmol 1988;72:786-92.

Hematopoietic and Histiocytic Lesions Affecting Bone

Baghdassarian SA, Shammas HF. Eosinophilic granuloma of orbit. Ann Ophthalmol 1977;9:1247-51.
Frassica DA, Frassica FJ, Schray MF, et al. Solitary plasmacytoma of bone: Mayo clinic experience. Int J Radiation Oncology Biol Phys 1989;16:43-8.
Jordan DR, McDonald H, Noel L, Nizalik E. Eosinophilic granuloma. Arch Ophthalmol 1994;111:134-5.
McFadzean RM. Orbital plasma cell myeloma. Br J Ophthalmol 1975;59:164-5.
Mewis-Levin L, Garcia CA, Olson JD. Plasma cell myeloma of the orbit. Ann Ophthalmol 1981;17:477-81.
Navert C, Zornoza J, Ayala A, Harle TS. Eosinophilic granuloma of bone: diagnosis and management. Skeletal Radiol 1983;10:227-35.

Risdall RJ, Dehner LP, Duray P, et al. Histiocytosis × (Langerhans' cell histiocytosis): prognostic role of histopathology. Arch Pathol Lab Med 1983;107:59-63.
Rodman HI, Font RL. Orbital involvement in multiple myeloma: review of the literature and report of three cases. Arch Ophthalmol 1972;87:30-5.

Giant Cell Tumor

Friendly DS, Font RL, Milhorat T. Hemangioendothelioma of frontal bone. Am J Ophthalmol 1982;43:482-90.
Suster S, Porges R, Tobias J, Nanes M. Giant cell neoplasm of the sphenoid sinus. Mt Sinai J Med 1989;56:118-22.
Tandon DA, Deka RC, Chaudhary C, Misra NK. Giant cell tumor of the temporosphenoidal region. J Larnyngol Otol 1988;102:449-51.

Vascular Tumors

Brackup AH, Haller MD, Danber MM. Hemangioma of the bony orbit. Am J Ophthalmol 1980;90:258-61.
Gross HJ, Roth AM. Intraosseous hemangioma of the orbital roof. Am J Ophthalmol 1978;86:565-9.
Hornblass A, Zaidman GW. Intraosseous orbital cavernous hemangioma. Ophthalmology 1981;88:1351-5.
Relf SJ, Bartley GB, Unni KK. Primary orbital intraosseous hemangioma. Ophthalmology 1991;98:541-7.
Wold LE, Swee RG, Sim FH. Vascular lesions of bone. Pathol Annu 1985;20:101-37.
Zucker JJ, Levine MR, Chu A. Primary intraosseous hemangioma of the orbit. Ophthalmic Plast Reconstr Surg 1989;5:247-55.

Differential Diagnosis

Small ML, Green WR, Johnsen LC. Lipoma of the frontal bone. Arch Ophthalmol 1979;97:129-32.
Maiuri F, Corriero G, Galicchio B, et al. Myxoma of the skull and orbit. Neurochirurgia 1988;31:136-8.
Candy EJ, Miller NR, Carson DS. Myxoma of bone involving the orbit. Arch Ophthalmol 1991;109:919-20.
Capanna R, Bertoni F, Bacchini P, et al. Malignant fibrous histiocytoma of bone. The experience at the Rizzoli Institute: report of 90 cases. Cancer 1984;54:177-87.
Font RL, Hidayat AA. Fibrous histiocytoma of the orbit: a clincopathologic study of 150 cases. Human Pathology 1982;13:199-209.
Tewfik HH, Tewfik FA, Latourette HB. Postirradiation malignant fibrous histiocytoma. J Surg Oncol 1981;16:199-202.
Weatherby RP, Dahlin DC, Ivins JC. Postradiation sarcoma of bone. Review of 78 Mayo Clinic cases. Mayo Clin Proc 1981;56:294-306.
Ferry AP, Haddad HM, Goldman JL. Orbital invasion by an intracranial chordoma. Am J Ophthalmol 1981;92:7-12.

Secondary Tumors

Affeldt JC, Minckler DS, Azen SP, Yeh L. Prognosis in uveal melanoma with extrascleral extension. Arch Ophthalmol 1980;98:1975-9.
American Joint Committee on Cancer. AJCC Cancer Staging Manual, 5th ed. Philadelphia: Lippincott-Raven, 1997.
Andrews TM, Gluckman JL, Weiss MA. Primary mucinous adenocarcinoma of the eyelid. Head Neck 1992;14:303-7.
Anscher M, Montano G. Management of periocular basal cell carcinoma: Mohs' micrographic surgery versus radiotherapy. II. Radiotherapy. Surv Ophthalmol 1993;38:203-210.
Aoyama I, Makita Y, Nabeshima S, et al. Extradural nasal and orbital extension of glioblastoma multiforme without previous surgical intervention. Surg Neurol 1980;14:343-7.
Aurora AL, Blodi FC. Reappraisal of basal cell carcinoma of the eyelids. Am J Ophthalmol 1970;70:329-36.
Barth A, Morton DL. The role of adjuvant therapy in melanoma management. Cancer 1995;75(suppl):726-34.
Bastiaensen LA, Leyten AC, Tjan TG, Misere JF. Chondroid chordoma of the base of the skull: orbital and other neuro-ophthalmological symptoms. Doc Ophthalmol 1983;55:5-15.
Batsakis JG. Pathology of tumors of the nasal cavity and paranasal sinuses. In: Thawley SE, Panje WR, eds. Comprehensive Management of Head and Neck Tumors. Vol 1. Philadelphia: WB Saunders, 1987; 327.
Batsakis JG, Regezi JA, Solomon AR, Rice DH. The pathology of head and neck tumors: mucosal melanomas, part 13. Head Neck Surg 1982;4:404-18.
Batsakis JG, Rice DH, Solomon AR. The pathology of head and neck tumors: squamous and mucous-gland carcinomas of the nasal cavity, paranasal sinuses, and larynx, part 6. Head Neck Surg 1980;2:497-508.
Berezin M, Gutman I, Tadmor R, et al. Malignant prolactinoma. Acta Endocrinol 1992;127:476-80.
Boniuk M, Zimmerman L. Sebaceous carcinoma of the eyelid, eyebrow, caruncle, and orbit. Trans Am Acad Ophthalmol Otolaryngol 1968;72:619-42.
Bridger MWM, Beale FA, Bryce DP. Carcinoma of the paranasal sinuses-a review of 158 cases. J Otolaryngol 1978;7:379-88.
Broughton WL, Zimmerman LE. A clinicopathologic study of 56 cases of intraocular medulloepitheliomas. Am J Ophthalmol 1978;85:407-18.
Buuns DR, Tse DT, Folberg R. Microscopically controlled excision of conjunctival squamous cell carcinoma. Am J Ophthalmol 1994;117:97-102.
Christensen WN, Smith RRL. Schneiderian papillomas: a clinicopathologic study of 67 cases. Hum Pathol 1986;17:393-400.
Christmas NJ, Mead MD, Richardson EP, Albert DM. Secondary optic nerve tumors. Surv Ophthalmol 1991;36:196-206.
Clark WH, Jr, Ainsworth AM, Bernardino EA, et al. The developmental biology of primary human malignant melanomas. Semin Oncol 1975;2:83-103.
Clark WH, Jr, From L, Bernardino EA, Mihm MC. The histogenesis and biologic behavior of primary human malignant melanomas of the skin. Cancer Res 1969;29:705-27.
Clark WH, Jr, Mastrangelo MJ, Ainsworth AM, et al. Current concepts of the biology of human cutaneous malignant melanoma. Adv Cancer Res 1977;24:267-338.
Clark WH, Jr, Reimer RR, Greene M, et al. Origin of familial malignant melanomas from heritable melanocytic lesions: “The B-K mole syndrome.” Arch Dermatol 1978;114:732-8.
Clouston PD, Sharpe DM, Corbett AJ, et al. Perineural spread of cutaneous head and neck cancer: its orbital and central neurologic complications. Arch Neurol 1990;47:73-7.
Cohen BH, Green WR, Iliff NT, et al. Spindle cell carcinoma of the conjunctiva. Arch Ophthalmol 1980;98:1809-13.
Conley J. Concepts in Head and Neck Surgery. New York: Grune & Stratton, 1970:5.
Cross KR, Cooper TJ. Intracranial neoplasms with extracranial metastases. Report of two cases. J Neuropathol Exp Neurol 1952;11:200-8.
Csaky KG, Custer P. Perineural invasion of the orbit by squamous cell carcinoma. Ophthalmic Surg 1990;21:218-20.
Demaerel P, Mosely IF, Scaravilli F. Recurrent craniopharyngioma invading the orbit, cavernous sinus and skull base: a case report. Neuroradiology 1993;35:261-3.
De Potter P, Shields CL, Shields JA, Menduke H. Clinical predictive factors for development of recurrence and metastasis in conjunctival melanoma: a review of 68 cases. Br J Ophthalmol 1993;77:624-30.
Devesa SS. The incidence of retinoblastoma. Am J Ophthalmol 1975;80:263-5.

Doxanas MT, Green WR. Sebaceous gland carcinoma. Review of 40 cases. Arch Ophthalmol 1984;102:245-9.
Duke-Elder S. Diseases of the lacrimal passages. In: Duke-Elder S, ed. Textbook of Ophthalmology. St. Louis: CV Mosby, 1952; v. 5, 5279-368.
Dunphy EB. The story of retinoblastoma. The XX Edward Jackson Memorial Lecture. Am J Ophthalmol 1964;58:539-52.
Dutton JJ. Management of periocular basal cell carcinoma: Mohs' micrographic surgery versus radiotherapy. III. Editorial. Surv Ophthalmol 1993;38:210-2.
Elder DE, Goldman LI, Goldman SC, et al. Dysplastic nevus syndrome: a phenotypic association of sporadic cutaneous melanoma. Cancer 1980;46:1787-94.
Elkon D, Hightower SI, Lim ML, et al. Esthesioneuroblastoma. Cancer 1979;44:1087-94.
Elwood JM, Gallagher RP, Hill GB, et al. Pigmentation and skin reaction to sun as risk factors for cutaneous melanoma: Western Canada Melanoma Study. Br Med J 1984;288:99-102.
Fandi A, Altun M, Azli N, et al. Nasopharyngeal cancer: epidemiology, staging, and treatment. Semin Oncol 1994;21:382-97.
Ferry AP, Haddad HM, Goldman JL. Orbital invasion by an intracranial chordoma. Am J Ophthalmol 1981;92:7-12.
Fitzgerald GWN, Frenkiel S, Black MJ, et al. Ameloblastoma of the jaws: a 12 year review of the McGill experience. J Otolaryngol 1982;11:23-8.
Fitzpatrick PJ, Thompson GA, Easterbrook WM, et al. Basal and squamous cell carcinoma of the eyelids and their treatment by radiotherapy. Int J Radiat Oncol Biol Phys 1984;10:449-54.
Flanagan JC, Stokes DP. Lacrimal sac tumors. Ophthalmology 1978;85:1282-7.
Flores AD, Anderson DW, Doyle PJ, et al. Paranasal sinus malignancy - a retrospective analysis of treatment methods. J Otolaryngol 1984;13:141-6.
Folberg R, McLean IW, Zimmerman LE. Malignant melanoma of the conjunctiva. Hum Pathol 1985;16:136-43.
Folberg R, McLean IW, Zimmerman LE. Primary acquired melanosis of the conjunctiva. Hum Pathol 1985;16:129-35.
Font RA. Eyelids and lacrimal drainage system. In: Spencer WH, ed. Ophthalmic Pathology. 4th ed. Philadelphia: WB Saunders, 1996; 2218-437.
Frucht-Pery J, Rozenman Y. Mitomycin C therapy for corneal intraepithelial neoplasia. Am J Ophthalmol 1994;117:164-8.
Frucht-Pery J, Sugar J, Baum J, et al. Mitomycin C treatment for conjunctival-corneal intraepithelial neoplasia. Ophthalmology 1997;104:2085-93.
Ginsberg J. Present status of meibomian gland carcinoma. Arch Ophthalmol 1965;73:271-7.
Gluckman JL. Nasal cavity and paranasal sinuses. In: Gluckman JL, Gullane PJ, Johnson JT, eds. Practical Approach to Head and Neck Tumors. New York: Raven Press, 1994; 115.
Godtfredsen E. On the frequency of secondary carcinomas in the choroid. Acta Ophthalmol 1944;22:394-
Godtfredsen E, Lederman M. Diagnostic and prognostic roles of ophthalmoneurologic signs and symptoms in malignant nasopharyngeal tumors. Am J Ophthalmol 1965;59:1063-9.
Harris MN, Shapiro RL, Roses DF. Malignant melanoma. Primary surgical management (excision and node dissection) based on pathology and staging. Cancer 1995;75(suppl):715-25.
Henderson JW. Orbital Tumors, 3rd ed. New York: Raven Press, 1994.
Hendley RL, Rieser JC, Cavanaugh HD, et al. Primary radiation therapy for meibomian gland carcinoma. Am J Ophthalmol 1979;87:206-9.
Holds JB, Haines JH, Mamalis N, et al. Mucinous adenocarcinoma of the orbit arising from a stable, benign-appearing eyelid nodule. Ophthalmic Surg 1990;21:163-6.
Homer F. Carcinom der dura mater. Klin Monatsbl Augenheilkd 1864;2:186.
Hornblass A, Jakobiec FA, Bosniak S, Flanagan J. The diagnosis and management of epithelial tumors of the lacrimal sac. Ophthalmology 1980;87:476-90.
Hoyt WF, Piovenetti E, Malamud N, Wilson CB. Cranio-orbital involvement in glioblastoma multiforme. Neurochirurgia 1972;15:1-8.
Ide CH, Ridings GR, Yamashita T, Buesseler JA. Radiotherapy for a recurrent adenocarcinoma of the meibomian gland. Arch Ophthalmol 1968;79:540-4.
Iliff WJ, Marback R, Green WR. Invasive squamous cell carcinoma of the conjunctiva. Arch Ophthalmol 1975;93:119-22.
Jackson RT, Fitz-Hugh GS, Constable WC. Malignant neoplasms of the nasal cavities and paranasal sinuses: (a retrospective study). Laryngoscope 1977;87:726-36.
Jakobiec FA, Folberg R, Iwamoto T. Clinicopathologic characteristics of premalignant and malignant melanocytic lesions of the conjunctiva. Ophthalmology 1989;96:147-66.
Jakobiec FA, Rim FJ, Fraunfelder FT, Brownstein S. Cryotherapy for conjunctival primary acquired melanosis and malignant melanoma. Experience with 62 cases. Ophthalmology 1988;95:1058-70.
Jauregui HO, Klintworth GK. Pigmented squamous cell carcinoma of the cornea and conjunctiva. A light microscopic, histochemical, and ultrastructural study. Cancer 1976;38:778-88.
Johnson LN, Krohel GB, Yeon EB, Parnes SM. Sinus tumors invading the orbit. Ophthalmology 1984;91:209-17.
Jones IS. Tumors of the lacrimal sac. Am J Ophthalmol 1956;42:561-6.
Kass LG, Hornblass A. Sebaceous carcinoma of the ocular adnexa. Surv Ophthalmol 1989;33:477-90.
Kersten RC, Tse DT, Anderson RL, Blodi FC. The role of orbital exenteration in choroidal melanoma with extrascleral extension. Ophthalmology 1985;92:436-43.
Khalil M, Brownstein S, Codere F, Nicolle D. Eccrine sweat gland carcinoma of the eyelid with orbital involvement. Arch Ophthalmol 1980;98:2210-4.
Kincaid MC, Green WR. Ocular and orbital involvement in leukemia. Surv Ophthalmol 1983;27:211-32.
Kivela T, Tarkkanen A. The Merkel cell and associated neoplasms in the eyelids and periocular region. Surv Ophthalmol 1990;35:171-87.
Kodilinye HC. Retinoblastoma in Nigeria: problems of treatment. Am J Ophthalmol 1967;63:469-81.
Kopelman JE, McLean IW, Rosenberg SH. Multivariate analysis of risk factors fo metastasis in retinoblastoma treated by enucleation. Ophthalmology 1987;94:371-7.
Kremer I, Sandbank J, Weinberger D, et al. Pigmented epithelial tumours of the conjunctiva. Br J Ophthalmol 1992;76:294-6.
Kwitko ML, Boniuk M, Zimmerman LE. Eyelid tumors with reference to lesions confused with squamous cell carcinoma. I. Incidence and errors in diagnosis. Arch Ophthalmol 1963;69:693-7.
Lawton AW, Karesh JW. Intracranial glioblastoma invading the orbit. Arch Ophthalmol 1986;104:806.
Lederman M, Wybar K, Busby E. Malignant epibulbar melanoma: natural history and treatment by radiotherapy. Br J Ophthalmol 1984;68:605-17.
Lee GA, Hirst LW. Ocular surface squamous neoplasia. Surv Ophthalmol 1995;39:429-50.
Leshin B, Yeatts P. Management of periocular basal cell carcinoma: Mohs' micrographic surgery versus radiotherapy. I. Mohs' micrographic surgery. Surv Ophthalmol 1993;38:193-203.
Leshin B, Yeatts P, Anscher M, et al. Management of periocular basal cell carcinoma: Mohs' micrographic surgery versus radiotherapy. Surv Ophthalmol 1993;38:193-212.
Levine PA, McLean WC, Cantrell RW. Esthesioneuroblastoma: the University of Virginia experience 1960-1985. Laryngoscope 1986;96:742-6.
Little JR, Dale AJD, Okazaki H. Meningeal carcinomatosis: clinical manifestations. Arch Neurol 1974;30:138-43.
Lloyd WC IIIrd, Leone CR Jr. Malignant melanoma of the lacrimal sac. Arch Ophthalmol 1984;102:104-7.
Lumenta CB, Schirmer M. The incidence of brain tumors: a retrospective study. Clin Neuropharmacol 1984;7:332-7.

Luxenberg MN, Guthrie TH, Jr. Chemotherapy of basal cell and squamous cell carcinoma of the eyelids and periorbital tissues. Ophthalmology 1986;93:504-10.
Macklin MT. A study of retinoblastoma in Ohio. Am J Hum Genet 1960;12:1-43.
Magramm I, Abramson DH, Ellsworth RM. Optic nerve involvement in retinoblastoma. Ophthalmology 1989;96:217-22.
Malik MOA, El Sheikh HE. Tumors of the eye and adnexa in the Sudan. Cancer 1979;44:293-303.
McDermott MW, Durity FA, Rootman J, Woodhurst WB. Combined frontotemporal-orbitozygomatic approach for tumors of the sphenoid wing and orbit. Neurosurgery 1990;26:107-16.
McDonald HR, Char DH. Adenoid cystic carcinoma presenting as an orbital apex syndrome. Ann Ophthalmol 1985;17:757-9.
McDonnell JM, Carpenter JD, Jacobs P, et al. Conjunctival melanocytic lesions in children. Ophthalmology 1989;96:986-93.
McLean IW, Foster WD, Zimmerman LE. Prognostic factors in small malignant melanomas of choroid and ciliary body. Arch Ophthalmol 1977;95:48-58.
Merriam GR. Retinoblastoma: analysis of seventeen autopsies. Arch Ophthalmol 1950;44:71-108.
Midena E, Degli Angeli C, Valenti M, et al. Treatment of conjunctival squamous cell carcinoma with topical 5-fluorouracil. Br J Ophthalmol 2000;84:268-72.
Mihm MC Jr, Clark WH Jr, Reed RJ. The clinical diagnosis of malignant melanoma. Semin Oncol 1975;2:105-18.
Milder B, Smith ME. Carcinoma of lacrimal sac. Am J Ophthalmol 1968;65:782-4.
Morley M, Finger PT, Perlin M, et al. Cis-platinum chemotherapy for ocular basal cell carcinoma. Br J Ophthalmol 1991;75:407-10.
Nerad JA, Whitaker DC. Periocular basal cell carcinoma in adults 35 years of age and younger. Am J Ophthalmol 1988;106:723-9.
Neudorfer M, Merimsky O, Lazar M, Geyer O. Cisplatin and doxorubicin for invasive basal cell carcinoma of the eyelids. Ann Ophthalmol 1993;25:11-3.
Ni C, Dryja TP, Albert DM. Sweat gland tumors in the eyelids: a clinicopathological analysis of 55 cases. Int Ophthalmol Clin 1982;22:1-22.
Ni C, D'Amico DJ, Fan CQ, Kuo PK. Tumors of the lacrimal sac: a clinicopathological analysis of 82 cases. Int Ophthalmol Clin 1982;22:121-40.
Ni C, Searl SS, Kuo PK, et al. Sebaceous cell carcinomas of the ocular adnexa. Int Ophthalmol Clin 1982;22:23-61.
Paridaens ADA, Minassian DC, McCartney ACE, Hungerford JL. Prognostic factors in primary malignant melanoma of the conjunctiva: a clinicopathologic study of 256 cases. Br J Ophthalmol 1994;78:252-9.
Patipa M, Hull DS. Chronic unilateral conjunctivitis: consider malignancy. Am Fam Physician 1980;22:69-70.
Paul EV, Parnell BL, Fraker M. Prognosis of malignant melanomas of the choroid and ciliary body. Int Ophthalmol Clin 1962;2:387-402.
Peele KA, Kennerdell JS, Maroon JC, et al. Malton M. Goodglick T. Rosen C. The role of postoperative irradiation in the management of sphenoid wing meningiomas. A preliminary report. Ophthalmology 1996;103:1761-6.
Pe'er JJ, Stefanyszyn M, Hidayat AA. Nonepithelial tumors of the lacrimal sac. Am J Ophthalmol 1994;118:650-8.
Peksayar G, Soyturk MK, Demiryont M. Long-term results of cryotherapy on malignant epithelial tumors of the conjunctiva. Am J Ophthalmol 1989;107:337-40.
Phillips PP, Gustafson RO, Facer GW. The clinical behavior of inverting papilloma of the nose and paranasal sinuses: report of 112 cases and review of the literature. Laryngoscope 1990;100:463-9.
Radnot M, Gall J. Tumoren des Tranensackes. Ophthalmologica 1966;151:2-22.
Rakes SM, Yeatts RP, Campbell RJ. Ophthalmic manifestations of esthesioneuroblastoma. Ophthalmology 1985;92:1749-53.
Rao NA, Font RL. Mucoepidermoid carcinoma of the conjunctiva: a clinicopathologic study of five cases. Cancer 1976;38:1699-709.
Rao NA, Hidayat AA, McLean J W, Zimmerman LE. Sebaceous carcinomas of the ocular adnexa: a clinicopathologic study of 104 cases with five year follow-up data. Hum Pathol 1982;13:113-22.
Redler LD, Ellsworth RM. Prognostic importance of choroidal invasion in retinoblastoma. Arch Ophthalmol 1973;90:294-6.
Reese AB. Invasion of the optic nerve by retinoblastoma. Arch Ophthalmol 1948;40:553-7.
Reese AB. Precancerous melanoma and diffuse malignant melanoma of the conjunctiva. Arch Ophthalmol 1938;19:354-65.
Reifler DM, Hornblass A. Squamous cell carcinoma of the eyelid. Surv Ophthalmol 1986;30:349-65.
Rootman J. Diseases of the Orbit: A Multidisciplinary Approach. Philadelphia: JB Lippincott, 1988.
Rootman J, Durity F. Orbital surgery. In: Sekhar LN, Janecka IP, eds. Surgery of Cranial Base Tumors. New York: Raven Press, 1993; 769-85.
Rootman J, Ellsworth RM, Hofbauer J, Kitchen D. Orbital extension of retinoblastoma: a clinicopathological study. Can J Ophthalmol 1978;13:72-80.
Rootman J, Hofbauer J, Ellsworth M, Kitchen D. Invasion of the optic nerve by retinoblastoma: a clinicopathologic study. Can J Ophthalmol 1976;11:106-4.
Rootman J, Roth AM, Crawford JB, et al. Extensive squamous cell carcinoma of the conjunctiva presenting as orbital cellulitis: the hermit syndrome. Can J Ophthalmol 1987;22:40-88.
Ryan SJ, Font RL. Primary epithelial neoplasms of the lacrimal sac. Am J Ophthalmol 1973;76:73-.9.
Sammartino A, Bonavolonta G, Pettinato G, Loffredo A. Exophthalmos caused by an invasive pituitary adenoma in a child. Ophthalmologica 1979;179:83-9.
Schenck NL, Ogura JH, Pratt LL. Cancer of the lacrimal sac. Presenatation of 5 cases and review of the literature. Ann Otol Rhinol Laryngol 1973;82:153-61.
Seregard S, Kock E. Conjunctival malignant melanoma in Sweden 1969-91. Acta Ophthalmol 1992;70:289-96.
Shammas HF, Blodi FC. Orbital extension of choroidal and ciliary body melanomas. Arch Ophthalmol 1977;95:2002-5.
Shields JA, Augsburger JJ, Corwin S, et al. The management of uveal melanomas with extrascleral extension. Orbit 1986;5:31-7.
Shields JA, Augsburger JJ, Donoso LA, et al. Hepatic metastasis and orbital recurrence of uveal melanoma after 42 years. Am J Ophthalmol 1985;100:666-8.
Shields JA, Shields CL. Management and posterior uveal melanoma. In: Shields JA, ed. Intraocular Tumors: A Text and Atlas. Philadelphia: WB Saunders, 1992; 171-205.
Shields JA, Shields CL. Management and prognosis of retinoblastoma. In: Shields JA, ed. Intraocular Tumors: A Text and Atlas. Philadelphia: WB Saunders, 1992; 390.
Skolnik EM, Massari FS, Tenta LT. Olfactory neuroepithelioma. Review of the world literature and presentation of two cases. Arch Otolaryngol 1966;84:644-53.
Small IA, Waldron CA. Ameloblastomas of the jaws. Oral Surg 1955;8:281-97.
Smith JB, Bishop VLM, Francis IC, et al. Ophthalmic manifestations of perineural spread of facial skin malignancy. Aust N Z J Ophthalmol 1990;18:197-205.
Smith JL, Wheliss JA. Ocular manifestations of nasopharyngeal tumors. Trans Am Acad Ophthalmol Otolaryngol 1966;66:659-64.
Spiro RH, Hajdu SI, Lewis JS, Strong EW. Mucous gland tumors of the larynx and laryngopharynx. Ann Otol Rhinol Laryngol 1976;85:498-503.
Stannard C, Lipper S, Scaly R, Sevel D. Retinoblastoma: correlation of invasion of the optic nerve and choroid with prognosis and metastases. Br J Ophthalmol 1979;63:560-70.
Starr HJ, Zimmerman LE. Extrascleral extension and orbital recurrence of malignant melanomas of the choroid and ciliary body. Int Ophthalmol Clin 1962;2:369-85.
Stefanyszyn MA, Hidayat AA, Pe'er JJ, Flanagan JC. Lacrimal sac tumors. Ophthal Plast Reconstr Surg 1994;10:169-84.

Tabbara KF, Kersten R, Daouk N, Blodi FC. Metastatic squamous cell carcinoma of the conjunctiva. Ophthalmology 1988;95:318-21.
Tahery DP, Goldberg R, Moy RL. Malignant melanoma of the eyelid. A report of eight cases and review of the literature. J Am Acad Dermatol 1992;27:17-21.
Taktikos A. Investigation of retinoblastoma with special reference to histology and prognosis. Br J Ophthalmol 1966;50:225-34.
Tenzel RR, Stewart WB, Boynton JR, Zbar M. Sebaceous adenocarcinoma of the eyelid. Definition of surgical margins. Arch Ophthalmol 1977;95:2203-4.
Trobe JD, Hood CI, Parsons JT, Quisling RG. Intracranial spread of squamous carcinoma along the trigeminal nerve. Arch Ophthalmol 1982;100:608-11.
Ullman S, Augsburger JJ, Brady LW. Fractionated epibulbar I-125 plaque radiotherapy for recurrent mucoepidermoid carcinoma of the bulbar conjunctiva. Am J Ophthalmol 1995;119:102-3.
Vaziri M, Buffam FV, Martinka M, et al. Clinicopathologic features and behavior of cutaneous eyelid melanoma. Accepted, Ophthalmology, 2000.
Weiss JS, Bressler SB, Jacobs EF Jr, et al. Maxillary ameloblastoma with orbital invasion. A clinicopathologic study. Ophthalmology 1985;92:710-3.
Yeatts RP, Ford JG, Stanton CA, Reed JW. Topical 5-fluorouracil in treating epithelial neoplasia of the conjunctiva and cornea. Ophthalmology 1995;102:1338-44.
Zehetmayer M, Menapace R, Kulnig W. Combined local excision and brachytherapy with ruthenium-106 in the treatment of epibulbar malignancies. Ophthalmologica 1993;207:133-9.
Zimmerman LE. Verhoeff's "terato-neuroma." A critical reappraisal in light of new observations and current concepts of embryonic tumors. The Fourth Frederick H. Verhoeff Lecture. Am J Ophthalmol 1971;72:1039-57.
Zimmerman LE. Squamous cell carcinoma and related lesions of the bulbar conjunctiva. In: Boniuk M, ed. Ocular and Adnexal Tumors: New and Controversial Aspects. St. Louis: CV Mosby, 1964; 49-75.
Zimmerman LE, McLean IW, Foster WD. Does enucleation of the eye containing a malignant melanoma prevent or accelerate the dissemination of tumour cells? Br J Ophthalmol 1978;62:420-5.
Zimmerman LE, McLean IW, Foster WD. Statistical analysis of follow-up data concerning uveal melanomas, and the influence of enucleation. Ophthalmology 1980;87:557-64.

Orbital Metastases

Albert DM, Rubenstein RA, Scheie HG. Tumor metastasis to the eye: I. Incidence in 213 adult patients with generalized malignancy. Am J Ophthalmol 1967;63:723-6.
Albert DM, Rubenstein RA, Scheie HG. Tumor metastasis to the eye: II. Clinical study in infants and children. Am J Ophthalmol 1967;63:727-32.
Alvarez-Berdecia A, Schut L, Bruce DA. Localized primary intracranial Ewing's sarcoma of the orbital roof. Case report. J Neurosurg 1979;50:811-3.
Apple DJ. Wilms' turner metastatic to the orbit. Arch Ophthalmol 1968;80:480-3.
Arnott EJ, Greaves DP. Metastases in the orbit. Br J Ophthalmol 1965;49:43-5.
Ashton N, Morgan G. Discrete carcinomatous metastases in the extraocular muscles. Br J Ophthalmol 1974;58:112-7.
Ballinger WH, Jr, Wesley RE. Seminoma metastatic to the orbit. Ophthalmic Surg 1984;15:120-1.
Bardenstein DS, Char DH, Jones C, et al. Metastatic ciliary body carcinoid tumor. Arch Ophthalmol 1990; 108:1590-4.
Bedford PD, Daniel PM. Discrete carcinomatous metastases in the extrinsic ocular muscles: a case of carcinoma of the breast with exophthalmic ophthalmoplegia. Am J Ophthalmol 1960;49:723-6.
Bersani TA, Costello JJ, Mango CA, Streeten BW. Benign approach to a malignant orbital tumor: metastatic renal cell carcinoma. Ophthal Plast Reconstr Surg 1994;10:42-4.
Bloch RS, Gartner S. The incidence of ocular metastatic carcinoma. Arch Ophthalmol 1971;85:673-5.
Boldt HC, Nerad JA. Orbital metastases from prostate carcinoma. Arch Ophthalmol 1988;106:1403-8.
Braffman BH, Bilaniuk LT, Eagle RC, Jr, et al. MR imaging of a carcinoid tumor metastatic to the orbit. J Comput Assist Tomogr 1987;11:891-4.
Brini M. Discussion. Appeimans M, Michiels J, Jansen E. Metastases orbitaires bilaterales d'un cancer du sein; detection par le phosphore radioactif. Bull Mem Soc Fr Ophtalmol 1954;67:415-427.
Bullock JD, Yanes B. Metastatic tumors of the orbit. Ann Ophthalmol 1980;12:1392-4.
Bullock JD, Yanes B. Ophthalmic manifestations of metastatic breast cancer. Ophthalmology 1980;87:961-73.
Carbajal UM. Metastases in retinoblastoma. Am J Ophthalmol 1959;48:47-69.
Carriere VM, Karcioglu DA, Apple DJ, Insler MS. A case of prostate carcinoma with bilateral orbital metastases and the review of the literature. Ophthalmology 1982;89:402-6.
Cibis GW, Freeman AI, Pang V, et al. Bilateral choroidal neonatal neuroblastoma. Am J Ophthalmol 1990;109:445-9.
Cline RA, Rootman J. Enophthalmos: a clinical review. Ophthalmology 1984;91:229-37.
Conlon MR, Rubin PAD, Samy CN, Albert DM. Metastatic orbital leiomyosarcoma: a clinicopathologic study. Can J Ophthalmol 1994;29:85-9.
Cuttone JM, Litvin J, McDonald JE. Carcinoma metastatic to an extraocular muscle. Ann Ophthalmol 1981;13:213-6.
De Lorimier AA, Bragg KU, Linden G. Neuroblastoma in childhood. Am J Dis Child 1969;118:441-50.
Denby P, Harvey L, English MG. Solitary metastasis from an occult renal cell carcinoma presenting as a primary lacrimal gland tumour. Orbit 1986;5:21-4.
Divine RD, Anderson RL. Metastatic small cell carcinoma masquerading as orbital myositis. Ophthalmic Surg 1982;13:483-7.
Divine RD, Anderson RL, Ossoinig KC. Metastatic carcinoid unresponsive to radiation therapy presenting as a lacrimal fossa mass. Ophthalmology 1982;89:516-20.
Fan JT, Buettner H, Bartley GB, Bolling JP. Clinical features and treatment of seven patients with carcinoid tumor metastatic to the eye and orbit. Am J Ophthalmol 1995;119:211-8.
Feinmesser M, Hurwitz JJ, Heathcoate JG. Pleural malignant mesothelioma metastatic to the orbit. Can J Ophthalmol 1994;29:193-7.
Fekrat S, Miller NR, Loury M. Alveolar rhabdomyosarcoma that metastasized to the orbit. Arch Ophthalmol 1993;111:1662-4.
Ferry AP, Font RL. Carcinoma metastatic to the eye and orbit: I. A clinicopathologic study of 227 cases. Arch Ophthalmol 1974;92:276-86.
Ferry AP. The biological behavior and pathological features of carcinoma metastatic to the eye and orbit. Trans Am Ophthalmol Soc 1973;71:373-425.
Fidler IJ, Hart IR. Principles of cancer biology: cancer metastasis. In: Devita VT, Hellman SA, eds. Cancer: Principles and Practice of Oncology. Philadelphia: JB Lippincott, 1985; 113-24.
Font RL, Ferry AP. Carcinoma metastatic to the eye and orbit: III. A clinicopathologic study of 28 cases metastatic to the orbit. Cancer 1976;38:1326-35.
Fratkin JD, Purcell JJ, Krachnier JH, Taylor JC. Wilms' turner metastatic to the orbit. JAMA 1977;238:1841-2.
Freedman MI, Folk JC. Metastatic tumors to the eye and orbit. Patient survival and clinical characteristics. Arch Ophthalmol 1987;105:1215-9.
Gibbs J, Appleton RE, Martin J, Findlay G. Congenital Horner syndrome associated with non-cervical neuroblastoma. Dev Med Child Neurol 1992;34:642-4.
Glassburn JR, Klionsky M, Brady LW. Radiation therapy for metastatic disease involving the orbit. Am J Clin Oncol 1984;7:145-8.

Goldberg RA, Rootman J. Clinical characteristics of metastatic orbital tumors. Ophthalmology 1990;97:620-4.
Goldberg RA, Rootman J, Cline RA. Tumors metastatic to the orbit: a changing picture. Surv Ophthalmol 1990;35:1-24.
Green AA, Hayes FA, Hustu HO. Sequential cyclophosphamide and doxorubicin for induction of complete remission in children with disseminated neuroblastoma. Cancer 1981;48:2310-7.
Green AA, Hustu HO, Palmer R, Pinkel D. Total-body sequential segmental irradiation and combination chemotherapy for children with disseminated neuroblastoma. Cancer 1976;38:2250-7.
Harris AL, Montgomery A. Orbital carcinoid tumor. Am J Ophthalmol 1980;90:875-7.
Harris AL, Montgomery A, Reyes RR, et al. Carcinoid tumor presenting as an orbital metastasis. Clin Oncol 1981;7:365-72.
Hartmann O, Benhamou E, Beaujean F, et al. Repeated high dose chemotherapy followed by purged autologous bone marrow transplantation as consolidation therapy in metastatic neuroblastoma. J Clin Oncol 1987;5:1205-11.
Hartmann O, Pinkerton CR, Philip T, et al. Very high-dose cisplatinum and etoposide in children with untreated advanced neuroblastoma. J Clin Oncol 1988;6:44-50.
Hayes FA, Thompson EI, Parvey L, et al. Metastatic Ewing's sarcoma: remission, induction and survival. J Clin Oncol 1987;5:1199-204.
Healy JF. Computed tomographic evaluation of metastases to the orbit. Ann Ophthalmol 1983;15:1026-9.
Heckemann R, Schmitt G. Ergebnisse der Strahlentherapie metastatischer orbitatumoren. Strahlentherapie 1978;154:179-81.
Henderson JW, Campbell RJ, Farrow GM, Garrity JA (collaborators). Metastatic carcinomas. In: Henderson JW, ed. Orbital Tumors, 3rd ed. New York: Raven Press, 1994; 361-75.
Hesselink JR, David KR, Weber AL, et al. Radiological evaluation of orbital metastases, with emphasis on computed tomography. Radiology 1980;137:363-6.
Holmes FF, Fouts TL. Metastatic cancer of unknown primary site. Cancer 1970;26:816-20.
Hornblass A, Kass LG, Reich R. Thyroid carcinoma metastatic to the orbit. Ophthalmology 1987;94:1004-7.
Houghton JD. Solitary metastasis of renal cell carcinoma. Am J Ophthalmol 1956;41:548-9.
Howard GM, Jakobiec FA, Trokel SL, et al. Pulsating metastatic turner of the orbit. Am J Ophthalmol 1978;85:767-71.
Huh SH, Nisce LZ, Simpson LD, Chu FC. Proceedings: value of radiation therapy in the treatment of orbital metastasis. Am J Roentgenol Radium Ther Nucl Med 1974;120:589-94.
Hutchison DS, Smith TR. Ocular and orbital metastatic carcinoma. Ann Ophthalmol 1979;11:869-73.
Jaffe N, Paed D, Traggis D, et al. Improved outlook for Ewing's sarcoma with combination chemotherapy (vincristine, actinomycin D and cyclophosphamide) and radiation therapy. Cancer 1976;38:1925-30.
Jakobiec FA, Bilyk JR, Font RL. Secondary tumors, mucoceles, and metastatic tumors. In: Spencer WH, ed. Ophthalmic Pathology. 4th ed. Philadelphia: WB Saunders, 1996; 2770-810.
Jakobiec FA, Rootman J, Jones IS. Secondary and metastatic tumors of the orbit. In: Jones IS, Jakobiec FA, ed. Diseases of the Orbit. Hagerstown: Harper & Row, 1979; 503-69.
Jampol LM, Cottle E, Fischer DS, Albert DM. Metastasis of Ewing's sarcoma to the choroid. Arch Ophthalmol 1973;89:207-9.
Jensen OA. Metastatic tumours of the eye and orbit. A histopathologic analysis of a Danish series. Acta Pathol Microbiol Scand Suppl 1970;212(suppl):201.
Kattah JC, Chrousos GC, Roberts J, et al. Metastatic prostate cancer to the optic canal. Ophthalmology 1993;100:1711-5.
Kennedy RE. An evaluation of 820 orbital cases. Trans Am Ophthalmol Soc 1984;82:134-57.
Kennerdell JS, Dekker A, Johnson BL, Dubois PJ. Fine needle aspiration. Its use in orbital tumors. Arch Ophthalmol 1979;97:1315-7.
Kieran MW, Longeneeker BM. Organ specific metastasis with specific reference to avian systems. Cancer Metastasis Rev 1983;2:165-82.
Knapp A. Metastatic thyroid tumor in the orbit. Arch Ophthalmol 1923;52:68.
Kopelman JE, McLean IW, Rosenberg SH. Multivariate analysis of risk factors for metastasis in retinoblastoma treated by enucleation. Ophthalmology 1987;94:371-7.
Kopelman JE, Shorr N. A case of prostatic carcinoma metastatic to the orbit diagnosed by fine needle aspiration and immunoperoxidase staining for prostatic specific antigen. Ophthalmic Surg 1987;18:599-603.
Leyson JF. Mediastinal seminoma associated with exophthalmos and gynecomastia. Urology 1974;3:366-9.
Loo KT, Tsui WMS, Chung KH, et al. Hepatocellular carcinoma metastasizing to the brain and orbit: report of three cases. Pathology 1994;26:119-22.
Mackay B, Ordonez NG. The role of the pathologist in the evaluation of poorly differentiated tumors. Semin Oncol 1982;9:396-415.
Mann AS. Bilateral exophthalmos and seminoma. J Clin Endocrinol Metab 1967;27:1500-2.
McCurrach F, Hurley I, Taylor H. Chronic corneal ulceration. An unusual presentation of metastatic breast carcinoma. Aust NZ J Ophthalmol 1993;21:191-2.
McGuire WL. Current status of estrogen receptors in human breast carcinoma. Cancer 1975;36:638-44.
Middleton RG. Surgery for metastatic renal cell carcinoma. J Urol 1967;97:973-7.
Mortada A. Roentgenography in orbital metastases with exophthalmos. Am J Ophthalmol 1968;65:48-53.
Mottow-Lippa L, Jakobiec FA, Iwamoto T. Pseudoinflammatory metastatic breast carcinoma of the orbit and lids. Ophthalmology 1981;88:575-80.
Mouridsen H, Palshof T, Patterson J, Battersby L. Tamoxifen in advanced breast cancer. Cancer Treat Rev 1978;5:131-41.
Musarella MA, Chan HS, De Boer G, Gallie BL. Ocular involvement in neuroblastoma: prognostic implications. Ophthalmology 1984;91:936-40.
Neumann KH, Nystrom JS. Metastatic cancer of unknown origin: nonsquamous cell type. Semin Oncol 1982;9:427-34.
Penn RF, Godwin RC. Diffuse peritoneal mesothelioma with metastasis to the orbital area as a presenting symptom. Am J Ophthalmol 1957;43:213-9.
Petrelli RL, Labay GR, Schwarz GS. Adenoid cystic carcinoma with orbital and cranial metastases: case report. Ann Ophthalmol 1978;10:611-5.
Peyster RG, Shapiro MD, Haik BG. Orbital metastasis: role of magnetic resonance imaging and computed tomography. Radiol Clin North Am 1987;25:647-62.
Philip T, Bernard JL, Zucker JM, et al. High-dose chemotherapy with bone marrow transplantation as consolidation treatment in neuroblastoma: an unselected group of stage IV patients over 1 year of age. J Clin Oncol 1987;5:266-71.
Reese AB. Expanding lesions of the orbit (Bowman Lecture). Trans Ophthalmol Soc UK 1971;91:85-104.
Reifler DM. Orbital metastases with enophthalmos: a review of the literature. Henry Ford Hosp Med J 1985;33:171-
Reifler DM, Kini SR, Liu D, Littleton RH. Orbital metastasis from prostatic carcinoma. Identification by immunocytology. Arch Ophthalmol 1984;102:292-5.
Riddle PJ, Font RL, Zimmerman LE. Carcinoid tumors of the eye and orbit: a clinicopathologic study of 15 cases, with histochemical and electron microscopic observations. Hum Pathol 1982;13:459-69.
Robert NJ, Garnick MB, Frei E 3rd. Cancers of unknown origin: current approaches and future perspectives. Semin Oncol 1982;9:526-31.
Roden DT, Savino PJ, Zimmerman RA. Magnetic resonance imaging in orbital diagnosis. Radiol Clin North Am 1988;26:535-45.
Rootman J. Diseases of the Orbit: A Multidisciplinary Approach. Philadelphia: JB Lippincott, 1988.
Rosenkranz L, Schroeder C. Recurrent malignant melanoma following a 46-year disease-free interval. NY State J Med 1985;85:95.

Rush JA, Older JJ, Richman AV. Testicular seminoma metastatic to the orbit. Am J Ophthalmol 1981;91:258-60.
Rush JA, Waller RR, Campbell RJ. Orbital carcinoid tumor metastatic from the colon. Am J Ophthalmol 1980;89:636-40.
Schaerer JP, Whitney RL. Prostatic metastases simulating intracranial meningioma. J Neurosurg 1953;10:546-
Schwab L, Doshi H, Shields JA, et al. Hepatocellular carcinoma metastatic to the orbit in an African patient. Ophthalmic Surg 1994;25:105-6.
Sedlacek SM, Horwitz KB. The role of progestins and progesterone receptors in the treatment of breast cancer. Steroids 1984;44:467-84.
Selva D, Dolman PJ, Rootman J. Orbital granulomatous giant cell myositis: case report and review. Clin Exp Ophthalmol 2000;28:65-8.
Sekimoto M, Hayasaka S, Setogawa T, Kishi K. Presumed iris metastasis from abdominal neuroblastoma. Ophthalmologica 1991;203:8-11.
Seretan EL. Metastatic adenocarcinoma from the stomach to the orbit. Arch Ophthalmol 1981;99:1469.
Sher JH, Weinstock SJ. Orbital metastasis of prostatic carcinoma. Can J Ophthalmol 1983;18:248-50.
Shields CL, Shields JA, Peggs M. Tumors metastatic to the orbit. Ophthal Plast Reconstr Surg 1988;4:73-80.
Shields CL, Shields JA, Eagle RC Jr, et al. Orbital metastases from a carcinoid tumor: computed tomography, magnetic resonance imaging, and electron microscopic findings. Arch Ophthalmol 1987;105:968-71.
Shields JA, Bakewell B, Augsburger JJ, Flanagan JC. Classification and incidence of space-occupying lesions of the orbit. A survey of 645 biopsies. Arch Ophthalmol 1984;102:1606-11.
Shumway EA. Metastatic carcinoma of the orbit, with the report of a case. Trans Am Ophthalmol Soc 1909;12:191.
Silva D. Orbital tumors. Am J Ophthalmol 1968;65:318-39.
Slamovits TL, Burde RM. Bumpy muscles. Surv Ophthalmol 1988;33:189-99.
Spaeth EB. Ocular tumors. A study of incidence of the various types and their mortality rates. Arch Ophthalmol 1951;46:421-3.
Tabbara KF, Kersten R, Daouk N, Blodi FC. Metastatic squamous cell carcinoma of the conjunctiva. Ophthalmology 1988;95:318-21.
Taylor JB, Soloman BH, Levine RE, Ehrlich RM. Exophthalmos in seminoma. Regression with steroids and orchiectomy. JAMA 1978;240:860-2.
Tolia BM, Whitmore WF. Solitary metastasis from renal cell carcinoma. J Urol 1975;114:836-8.
Wakisaka S, Tashiro M, Nakano S, et al. Intracranial and orbital metastasis of hepatocellular carcinoma: report of two cases. Neurosurgery 1990;26:863-6.
West CE, Repka MX. Tonic pupils associated with neuroblastoma. J Pediatr Ophthalmol Strabismus 1992;29:382-3.
White VA, Rootman J. Orbital pathology. In: Albert DM, Jakobiec FA, eds. Principles and Practice of Ophthalmology, 2nd ed. Philadelphia: WB Saunders, 2000; 3816-74.
Whyte AM. Bronchogenic carcinoma metastasizing to the orbit. A case report. J Maxillofac Surg 1978;6:277-80.
Woodruff G, Buncic JR, Morin JD. Horner's syndrome in children. J Pediatr Ophthalmol Strabismus 1988;25:40-4.
Zizmor J, Fasano CV, Smith B, Rabbett W. Roentgenographic diagnosis of unilateral exophthalmos. JAMA 1966;197:343-6.

Tumors of the Lacrimal Gland

General

Ashton N. Epithelial tumors of the lacrimal gland. Modern Problems in Ophthalmology 1975;14:306-23.
Duke-Elder S, MacFaul PA. The ocular adnexa. Part II. Lacrimal, orbital and para-orbital diseases. In: Duke-Elder S, ed. System of Ophthalmology. London: Henry Kimpton, 1974; v. 13; 596-1163.
Ellis GL, Auclair PL. Tumors of the salivary gland. Washington, DC: Armed Forces Institute of Pathology, 1996.
Font RL, Gamel JW. Epithelial tumors of the lacrimal gland: an analysis of 265 cases. In: Jakobiec FA, ed. Ocular and Adnexal Tumors. Birmingham, Alabama: Aesculapius, 1978; 787-805.
Foote FW, Jr, Frazell EL. Tumors of the major salivary glands. Cancer 1953;6:1065-133.
Forrest AW. Lacrimal gland tumors. In: Tasman W, Jaeger EA, eds. Duane's Clinical Ophthalmology. Philadelphia: JB Lippincott, 1991; v. 2; 1-16.
Forrest AW. Epithelial lacrimal gland tumors: pathology as a guide to prognosis. Trans Am Acad Ophthalmol 1954;58:848-65.
Godtfredsen E. Pathology of mucous and salivary gland tumors in the lacrimal gland and the relation to extra orbital mucous and salivary gland tumors. Br J Ophthalmol 1948;32:171-9.
Grossniklaus HE, Abbuhl MF, McLean IW. Immunohistologic properties of benign and malignant mixed tumor of the lacrimal gland. Am J Ophthalmol 1990;110:540-9.
Henderson JW. Orbital Tumors. 3rd ed. New York: Raven Press, 1994.
Jakobiec FA, Bilyk JR, Font RL. Lacrimal gland tumors. In: Spencer WH, ed. Ophthalmic Pathology: An Atlas and Textbook. 4th ed. Philadelphia: WB Saunders, 1996; 2485-525.
Jakobiec FA, Yeo JH, Trokel SL, et al. Combined clinical and computed tomographic diagnosis of primary lacrimal fossa lesions. Am J Ophthalmol 1982;94:785-807.
Kennedy RE. An evaluation of 820 orbital cases. Trans Am Ophthalmol Soc 1984;82:134-57.
Lloyd G. Lacrimal gland tumors: the role of CT and conventional radiology. Br J Radiol 1981;54:1034-8.
Mafee MF, Edward DP, Koeller KK, Dorodi S. Lacrimal gland tumors and simulating lesions: clinicopathologic and MR imaging features. Radiol Clin North Am 1999;37:219-39.
Mafee MF, Haik BG. Lacrimal gland and fossa lesions: role of computed tomography. Radiol Clin North Am 1987;25:767-79.
McLean IW, Burnier MN, Zimmerman LE, Jakobiec FA. Tumors of the eye and ocular adnexa. Atlas of Tumor Pathology, 3rd Series, Fasc. 12. Washington, DC: Armed Forces Institute of Pathology, 1994.
Ni C, Cheng SC, Dryja TP, Cheng TY. Lacrimal gland tumors: a clinicopathological analysis of 160 cases. Int Ophthalmol Clin 1981;22:99-120.
Ni C, Kuo P-K. Histopathological classification of 272 primary epithelial tumors of the lacrimal gland. Chin Med J 1992;105:481-5.
Reese AB. The treatment of expanding lesions of the orbit with particular regard to those arising in the lacrimal gland. Am J Ophthalmol 1956;41:3-11.
Riedel KG, Markl A, Hasenfratz G, et al. Epithelial tumors of the lacrimal gland: clinico-pathologic correlation and managment. Neurosurg Rev 1990;13:289-98.
Rootman J. Diseases of the Orbit: A Multidisciplinary Approach. Philadelphia: JB Lippincott, 1988.
Rootman J, Stewart B, Goldberg R. Orbital Surgery: A Conceptual Approach. Philadelphia: Lippincott-Raven Press, 1995.
Sanders TE. Mixed tumor of the lacrimal gland. Arch Ophthalmol 1939;21:239-60.
Sandros J, Stenman G, Mark J. Cytogenetic and molecular observations in human and experimental salivary gland tumors. Cancer Genet Cytogenet 1990;44:153-67.
Seifert G, Brocheriou C, Cardesa A, Eveson JW. WHO international histological classification of tumours: tentative histological classification of salivary gland tumours. Pathol Res Pract 1990;186:555-81.
Shields CL, Shields JA. Lacrimal gland tumors. Int Ophthalmol Clin 1993;33:181-8.
Shields CL, Shields JA. Review of lacrimal gland lesions. Trans Pa Acad Ophthalmol Otolaryngol 1990;42:925-30.
Shields CL, Shields JA, Eagle RC, Rathmell JP. Clinicopathologic review of 142 cases of lacrimal gland lesions. Ophthalmology 1989;96:431-5.

Stewart WB, Krohel GB, Wright JE. Lacrimal gland and fossa lesions: an approach to diagnosis and management. Ophthalmology 1979;86:886-95.
Wenig BM, Hitchcock CL, Ellis GL, Gnepp DR. Metastasizing mixed tumor of salivary glands. Am J Surg Pathol 1992;16:845-58.
Wright JE. Factors affecting the survival of patients with lacrimal gland tumours. Can J Ophthalmol 1982;17:3-9.
Wright JE, Stewart WB, Krohel GB. Clinical presentation and management of lacrimal gland tumors. Br J Ophthalmol 1979;63:600-6.
Zimmerman LE, Sanders TE, Ackerman LV. Epithelial tumors of the lacrimal gland: prognostic and therapeutic significance of histologic types. Int Ophthalmol Clin 1962;2:337-67.

Epithelial Lacrimal Neoplasia

Pleomorphic Adenoma

Auran J, Jakobiec FA, Krebs W. Benign mixed tumor of the palpebral lobe of the lacrimal gland: clinical diagnosis and appropriate surgical management. Ophthalmology 1988;95:90-9.
Bullerdiek J, Bartnitzke S, Weinberg M, et al. Rearrangements of chromosome region 12q13-q15 in pleomorphic adenomas of the human salivary gland (PSA). Cytogenet Cell Genet 1987;45:187-90.
Bullerdiek J, Hutter K-J, Brandt G, et al. Cytogenetic investigations on a cell line derived from a carcinoma arising in a salivary gland pleomorphic adenoma. Cancer Genet Cytogenet 1990;44:253-62.
Bullerdiek J, Takla G, Bartnitzke S, et al. Relationship of cytogenetic subtypes of salivary gland pleomorphic adenomas with patient age and histologic type. Cancer 1989;64:876-80.
Erlandson RA, Cardon-Cardo C, Higgins PJ. Histogenesis of benign pleomorphic adenoma (mixed tumor) of the major salivary glands. An ultrastructural and immunohistochemical study. Am J Surg Pathol 1984;8:803-20.
Higashi K, Jin Y, Heim S, et al. Chromosome abnormalities in a carcinoma in pleomorphic adenoma of the lacrimal gland. Cancer Genet Cytogenet 1991;55:125-8.
Hrynchak M, White V, Berean K, Horsman D. Cytogenetic findings in seven lacrimal gland neoplasms. Cancer Genet Cytogenet 1994;75:133-8.
Mark J, Dahlenfors R. Cytogenetical observations in 100 human benign pleomorphic adenomas: specificity of the chromosomal aberrations and their relationship to sites of localized oncogenes. Anticancer Res 1986;6:299-308.
Mercado GJV, Gunduz K, Shields CL, et al. Pleomorphic adenoma of the lacrimal gland in a teenager. Arch Ophthalmol 1998;116:962-3.
Nishimura T, Furukawa M, Kawahara E, Miwa A. Differential diagnosis of pleomorphic adenoma by immnuhistochemical means. J Laryngol Otol 1991;105:1057-60.
Parks SL, Glover AT. Benign mixed tumors arising in the palpebral lobe of the lacrimal gland. Ophthalmology 1990;97:526-30.
Riley FC, Henderson JW. Report of a case of malignant transformation in benign mixed tumor of the lacrimal gland. Am J Ophthalmol 1970;70:767-70.
Rose GE, Wright JE. Pleomorphic adenoma of the lacrimal gland. Br J Ophthalmol 1992;76:395-400.
Spencer WH. Ophthalmic Pathology: An Atlas and Textbook. Philadelphia: WB Saunders, 1986; 2496-524.
Stead RH, Qizilbash AH, Kontozoglou T, et al. An immunohistochemical study of pleomorphic adenomas of the salivary gland: glial fibrillary acidic protein-like immunoreactivity identifies a major myoepithelial component. Hum Pathol 1988;19:32-40.
Stenman G, Sahlin P, Mark J, Landys D. Structural alterations of the c-mos locus in benign pleomorphic adenomas with chromosome abnormalities of 8q12. Oncogene 1991;6:1105-8.
Vangveeravong S, Katz SE, Rootman J, White V. Tumors arising in the palpebral lobe of the lacrimal gland. Ophthalmology 1996;103:1606-12.
Wharton JACL, O'Donnell BA. Unusual presentations of pleomorphic adenoma and adenoid cystic carcinoma of the lacrimal gland. Aust N Z J Ophthalmol 1999;27:145-8.

Carcinoma in Pleomorphic Adenoma

Dolman PJ, Rootman J. In situ malignant mixed tumour of the lacrimal gland: case report and review. Orbit 1987;6:181-7.
Hartwick RWJ, Shaw PA, Srigley JR, Hurwitz JJ. In situ adenocarcinoma ex pleomorphic adenoma of the lacrimal gland. Can J Ophthalmol 1990;25:213-7.
Hrynchak M, White V, Berean K, Horsman D. Cytogenetic findings in seven lacrimal gland neoplasms. Cancer Genet Cytogenet 1994;75:133-8.
LiVolsi VA, Perzin KH. Malignant mixed tumors arising in salivary glands. I. Carcinomas arising in benign mixed tumors: a clinicopathologic study. Cancer 1977;39:2209-30.
Perzin KH, Jakobiec FA, Livolsi VA, Desjardins L. Lacrimal gland malignant mixed tumors (carcinomas arising in benign mixed tumors): a clinico-pathologic study. Cancer 1980;45:2593-606.
Ryan RE, Jr, DeSanto LW, Weiland LH, et al. Cellular mixed tumors of the salivary glands. Arch Otolaryngol 1978;104:451-3.
Wright JE, Rose GE, Garner A. Primary malignant neoplasms of the lacrimal gland. Br J Ophthalmol 1992;76:401-7.

Oncocytoma

Ferreiro JA, Stylopoulos N. Oncocytic differentiation in salivary gland tumours. J Laryngol Otol 1995;109:569-71.
Pecorella I, Garner A. Ostensible oncocytoma of accessory lacrimal glands. Histopathology 1997;30:264-70.

Warthin's Tumor

Bonavolonta G, Tranfa F, Staibano S, et al. Warthin tumor of the lacrimal gland. Am J Ophthalmol 1997;124:857-8.

Myoepithelioma

Alos L, Cardesa A, Bombi JA, et al. Myoepithelial tumors of salivary glands: a clinicopathologic, immunohistochemical, ultrastructural, and flow-cytometric study. Sem Diagn Pathol 1996;13:138-47.
Dardick I. Myoepithelioma: definitions and diagnostic criteria. Ultrastruct Pathol 1995;19:335-45.
Dardick I, Kahn HJ, Van Nostrand AWP, Baumal R. Salivary gland monomorphic adenoma: ultrastructural, immunoperoxidase, and histogenetic aspects. Am J Pathol 1984;115:334-48.
Dardick I, Thomas MJ, van Nostrand AWP. Myoepithelioma - new concepts of histology and classification: a light and electron microscopic study. Ultrastruct Pathol 1989;13:187-224.
Font RL, Garner A. Myoepithelioma of the lacrimal gland: report of a case with spindle cell morphology. Br J Ophthalmol 1992;76:634-6.
Grossniklaus HE, Wojno TH, Wilson MW, Someren AO. Myoepithelioma of the lacrimal gland. Arch Ophthalmol 1997;115:1588-90.
Heathcote JG, Hurwitz JJ, Dardick I. A spindle cell myoepithelioma of the lacrimal gland. Arch Ophthalmol 1990;108:1135-9.
Michal M, Skalova A, Simpson RHW, et al. Clear cell malignant myoepithelioma of the salivary glands. Histopathology 1996;28:309-15.
Nagao T, Sugano I, Ishida Y, et al. Salivary gland malignant myoepithelioma: a clinicopathologic and immunohistochemical study of ten cases. Cancer 1998;83:1292-9.

Ostrowski ML, Font RL, Halpern J, et al. Clear cell epithelial-myoepithelial carcinoma arising in pleomorphic adenoma of the lacrimal gland. Ophthalmology 1994;101:925-30.
Seifert G, Brocheriou C, Cardesa A, Eveson JW. WHO international histological classification of tumours: tentative histological classification of salivary gland tumours. Pathol Res Pract 1990;186:555-81.
Simpson RH, Jones H, Beasley P. Benign myoepithelioma of the salivary glands: a true entity? Histopathology 1995;27:1-9.
Singh R, Cawson RA. Malignant myoepithelial carcinoma (myoepithelioma) arising in a pleomorphic adenoma of the parotid gland: an immunohistochemical study and review of the literature. Oral Surg Oral Med Oral Pathol 1988;66:65-70.
Takai Y, Dardick I, Mackay A, et al. Diagnostic criteria for neoplastic myoepithelial cells in pleomorphic adenomas and myoepitheliomas. Immunocytochemical detection of muscle-specifc actin, cytokeratin 14, vimentin, and glial fibrillary acidic protein. Oral Surg Oral Med Oral Path Oral Radiol Endod 1995;79:330-41.

Malignant Epithelial Lacrimal Neoplasia

Adenoid Cystic Carcinoma

Dagher G, Anderson RL, Ossoinig KC, Baker JD. Adenoid cystic carcinoma of the lacrimal gland in a child. Arch Ophthalmol 1980;98:1098-100.
Eibling DE, Johnson JT, McCoy JP, Jr, et al. Flow cytometric evaluation of adenoid cystic carcinoma: correlation with histologic subtype and survival. Am J Surg 1991;162:367-72.
Ellis GL, Auclair PL. Tumors of the salivary gland. Washington, DC: Armed Forces Institute of Pathology, 1996.
Font RL, Gamel JW. Adenoid cystic carcinoma of the lacrimal gland: a clinicopathologic study of 78 cases. In: Nicholson D, ed. Ocular Pathology Update. New York: Masson USA, 1980; 277-83.
Franchi A, Gallo O, Bocciolini C, et al. Reduced E-cadherin expression correlates with unfavorable prognosis in adenoid cystic carcinoma of salivary glands of the oral cavity. Am J Clin Pathol 1999;111:43-50.
Gamel JW, Font RL. Adenoid cystic carcinoma of the lacrimal gland: the clinical significance of a basaloid histologic pattern. Hum Pathol 1982;13:219-25.
Griffin BR, Laramore GE, Russel KJ, et al. Fast neutron radiotherapy for advanced malignant salivary gland tumors. Radiother Oncol 1988;12:105-11.
Hendrix LE, Massaro BM, Daniels DL, et al. Surface coil MR evaluation of a lacrimal gland carcinoma. J Comp Assist Tomogr 1988;12:866-8.
Horiuchi J, Shibuya H, Suzuki S, et al. The role of radiotherapy in the management of adenoid cystic carcinoma of the head and neck. Int J Radiat Oncol Biol Phys 1987;13:1135-41.
Hrynchak M, White V, Berean K, Horsman D. Cytogenetic findings in seven lacrimal gland neoplasms. Cancer Genet Cytogenet 1994;75:133-8.
Huang MX, Ma DQ, Sun KH, et al. Factors influencing survival rate in adenoid cystic carcinoma of the salivary glands. Int J Oral Maxillofac 1997;26:435-9.
Jin Y, Mertens F, Limon J, et al. Characteristic karyotypic features in lacrimal and salivary gland carcinomas. Br J Cancer 1994;70:42-7.
Lee DA, Campbell RJ, Waller RR, Ilstrup DM. A clinicopathologic study of primary adenoid cystic carcinoma of the lacrimal gland. Ophthalmology 1985;92:128-34.
Malberger E, Gdal-On M. Adenoid cystic carcinoma of the orbit diagnosed by means of aspirative cytology. Ophthalmologica 1985;190:125-7.
Matsuba HM, Spector GJ, Thawley SE, et al. Adenoid cystic salivary gland carcinoma: a histopathologic review of treatment failure patterns. Cancer 1986;57:519-24.
Nordkvist A, Mark J, Gustafsson H, et al. Non-random chromosome rearrangements in adenoid cystic carcinoma of the salivary glands. Genes Chromosomes Cancer 1994;10:115-21.
Perzin KH, Gulane P, Clairmont AC. Adenoid cystic carcinomas arising in the salivary glands. Cancer 1978;42:265-82.
Santucci M, Bondi R. Histologic-prognostic correlations in adenoid cystic carcinoma of major and minor salivary glands of the oral cavity. Tumori 1986;72:293-300.
Shields JA, Shields CL, Eagle RC, Jr, et al. Adenoid cystic carcinoma of the lacrimal gland simulting a dermoid cyst in a 9-year-old boy. Arch Ophthalmol 1998;116:1673-6.
Spencer WH. Ophthalmic Pathology: An Atlas and Textbook. Philadelphia: WB Saunders, 1986; 2496-524.
Spiro RH, Huvos AG, Strong EW. Adenoid cystic carcinoma: factors influencing survival. Am J Surg 1979;138:579-83.
Stenman G, Sandros J, Dahlenfors R, et al. 6q- and loss of the y chromosome–two common deviations in malignant human salivary gland tumors. Cancer Genet Cytogenet 1986;22:283-93.
Sur RK, Donde B, Levin V, et al. Adenoid cystic carcinoma of the salivary glands: a review of 10 years. Laryngoscope 1997;107:1276-80.
Tellado M, Specht CS, McLean IW, et al. Primary orbital melanomas. Ophthalmology 1996;103:929-32.
Tellado MV, McClean IW, Specht CS, Varga J. Adenoid cystic carcinomas of the lacrimal gland in childhood and adolescence. Ophthalmology 1997;104:1622-5.
Vrielinck LJ, Van Damme B, van den Bogaert W, et al. The significance of perineural spread in adenoid cystic carcinoma of the major and minor salivary glands. Int J Oral Maxillofac 1988;17:190-3.
Wright JE, Rose GE, Garner A. Primary malignant neoplasms of the lacrimal gland. Br J Ophthalmol 1992;76:401-7.

Carcinoma ex Pleomorphic Adenoma

Auclair PL, Ellis GL. Atypical features in salivary gland mixed tumors: their relationship to malignant transformation. Mod Pathol 1996;9:652-7.
Brandwein M, Huvos AG, Dardick I, et al. Noninvasive and minimally invasive carcinoma ex mixed tumor: a clinicopathologic and ploidy study of 12 patients with major salivary tumors of low (or no?) malignant potential. Oral Surg Oral Med Oral Pathol Oral Radiol Endod 1996;81:655-64.
Bullerdiek J, Bartnitzke S, Weinberg M, et al. Rearrangements of chromosome region 12q13-q15 in pleomorphic adenomas of the human salivary gland (PSA). Cytogenet Cell Genet 1987;45:187-90.
Font RL, Patipa M, Rosenbaum PS, et al. Correlation of computed tomographic and histopathlogic features in malignant transformation of benign mixed tumor of lacrimal gland. Surv Ophthalmol 1990;34:449-52.
Font RL, Smith SL, Bryan RG. Malignant epithelial tumors of the lacrimal gland: a clinicopathologic study of 21 cases. Arch Ophthalmol 1998;116:613-6.
Gerughty RM, Scofield HH, Brown FM, Hennigar GR. Malignant mixed tumors of salivary gland origin. Cancer 1969;24:471-86.
Henderson JW, Farrow GM. Primary malignant mixed tumors of the lacrimal gland. Report of 10 cases. Ophthalmology 1980;87:466-73.
Jakobiec FA. Discussion. Primary malignant mixed tumors of the lacrimal gland. Report of 10 cases. Ophthalmology 1980;87:473-5.
Lauer SA, Levin RJ, Bradley MK, et al. An immortalized cell culture from a malignant mixed tumor of the lacrimal gland. Ophthal Plast Reconstr Surg 1997;13:168-73.
LiVolsi VA, Perzin KH. Malignant mixed tumors arising in salivary glands. I. Carcinomas arising in benign mixed tumors: a clinicopathologic study. Cancer 1977;39:2209-30.
Ludwig ME, LiVolsi VA, McMahon RT. Malignant mixed tumor of the lacrimal gland. Am J Surg Pathol 1979;3:457-62.
Riley FC, Henderson JW. Report of a case of malignant transformation in benign mixed tumor of the lacrimal gland. Am J Ophthalmol 1970;70:767-70.

Shields JA, Shields CL. Malignant transformation of presumed pleomorphic adenoma of lacrimal gland after 60 years. Arch Ophthalmol 1987;105:1403-5.
Tortoledo ME, Luna MA, Batsakis JG. Carcinomas ex pleomorphic adenoma and malignant mixed tumors: histomorphologic indexes. Arch Otolaryngol 1984;110:172-6.
Waller RR, Riley FC, Henderson JW. Malignant mixed tumor of the lacrimal gland. Arch Ophthalmol 1973;90:297-9.
Wright JE, Rose GE, Garner A. Primary malignant neoplasms of the lacrimal gland. Br J Ophthalmol 1992;76:401-7.

Mucoepidermoid Carcinoma

Evans HL. Mucoepidermoid carcinoma of salivary glands: a study of 69 cases with special attention to histologic grading. Am J Clin Pathol 1984;81:696-701.
Eveson JW, Cawson RA. Salivary gland tumours. A review of 2410 cases with particular reference to histological types, site, age and sex distribution. J Pathol 1985;146:51-8.
Eviatar JA, Hornblass A. Mucoepidermoid carcinoma of the lacrimal gland: 25 cases with a review and update of the literature. Ophthal Plast Reconstr Surg 1993;9:170-81.
Gamel JW, Font RL. Adenoid cystic carcinoma of the lacrimal gland: the clinical significance of a basaloid histologic pattern. Hum Pathol 1982;13:219-25.
Kalmovich B, Kuten A, Robinson E. [Malignant salivary gland tumors]. Harefuah 1995;129:308-12, 67-8.
Levin LA, Popham J, To K, et al. Mucoepidermoid carcinoma of the lacrimal gland: report of a case with oncocytic features arising in a patient with chronic dacryops. Ophthalmology 1991;98:1551-5.
Spitz MR, Batsakis JG. Major salivary gland carcinoma: descriptive epidemiology and survival of 498 patients. Arch Otolaryngol 1984;110:45-9.
Spiro RH. Salivary neoplasms: overview of a 35-year experience with 2,807 patients. Head Neck Surg 1986;8:177-84.
Wagoner MD, Chuo N, Gonder JR, et al. Mucoepidermoid carcinoma of the lacrimal gland. Ann Ophthalmol 1982;14:383-5.

Adenocarcinoma

Aberle AM, Abrams AM, Bowe R, et al. Lobular (polymorphous low-grade) carcinoma of minor salivary glands: a clinicopathologic study of twenty cases. Oral Surg Oral Med Oral Pathol 1985;60:387-95.
Anderson C, Krutchkoff D, Pedersen C, et al. Polymorphous low grade adenocarcinoma of minor salivary gland: a clinicopathologic and comparative immunohistochemical study. Mod Pathol 1990;3:76-82.
Batsakis JG, Pinkston GR, Luna MA, et al. Adenocarcinomas of the oral cavity: a clinicopathologic study of terminal duct carcinomas. J Laryngol Otol 1983;97:825-35.
de Rosa G, Zeppa P, Tranfa F, Bonavolonta G. Acinic cell carcinoma arising in a lacrimal gland. Cancer 1986;57:1988-91.
Ellis GL, Corio RL. Acinic cell adenocarcinoma: a clinicopathologic analysis of 294 cases. Cancer 1983;52:542-9.
Evans HL, Batsakis JG. Polymorphous low-grade adenocarcinoma of minor salivary glands: a study of 14 cases of a distinctive neoplasm. Cancer 1984;53:935-42.
Faraci RP, Chretien PB. Adenocarcinoma of the lacrimal gland with simultaneous pulmonary metastases. Archives of Surgery 1974;109:107-10.
Gnepp DR, Chen JC, Warren C. Polymorphous low-grade adenocarcinoma of minor salivary gland: an immunohistochemical and clinicopathologic study. Am J Surg Pathol 1988;12:461-8.
Harvey PA, Parsons A, Rennie IG. Primary sebaceous carcinoma of lacrimal gland: a previously unreported primary neoplasm. Eye 1994;8:592-5.
Heaps RS, Miller NR, Albert DM, et al. Primary adenocarcinoma of the lacrimal gland. Ophthalmology 1993;100:1856-60.
Jordan DR, Addison DJ, Watson AG, McLeish WA. Adenocarcinoma of the lacrimal gland with metastasis to the preauricular lymph nodes and parotid gland. Can J Ophthalmol 1988;23:136-40.
Katz SE, Rootman J, Dolman PJ, et al. Primary ductal adenocarcinoma of the lacrimal gland. Ophthalmology 1996;103:157-62.
Khalil M, Arthurs B. Basal cell adenocarinoma of the lacrimal gland. Ophthalmology 2000;107;164-8.
Konrad EA, Thiel H-J. Adenocarcinoma of the lacrimal gland with sebaceous differentiation. Graefes Arch Clin Exp Ophthalmol 1983;221:81-5.
Luna MA, Batsakis JG, Ordonez NG, et al. Salivary gland adenocarcinomas: a clinicopathologic analysis of three distinctive types. Sem Diagn Pathol 1987;4:117-35.
Perzin KH, LiVolsi VA. Acinic cell carcinomas arising in salivary glands. Cancer 1979;44:1434-57.
Rodgers IR, Jakobiec FA, Gingold MP, et al. Anaplastic carcinoma of the lacrimal gland presenting with recurrent subconjunctival hemorrhages and displaying incipient sebaceous differentiation. Ophthal Plast Reconstr Surg 1991;7:229-37.
Rosenbaum PS, Mahadevia PS, Goodman LA, Kress Y. Acinic cell carcinoma of the lacrimal gland. Arch Ophthalmol 1995;113:781-5.
Simpson RHW, Clarke TJ, Sarsfield PTL, et al. Polymorphous low-grade adenocarcinoma of the salivary glands: a clinicopathological comparison with adenoid cystic carcinoma. Histopathology 1991;19:121-9.
Spiro RH, Huvos AG, Strong EW. Acinic cell carcinoma of salivary origin. Cancer 1978;41:924-35.
Witschel H, Zimmerman LE. Malignant mixed tumor of the lacrimal gland. A clinicopathologic report of two unusual cases. Graefes Arch Clin Exp Ophthalmol 1981;216:327-37.

Epithelial-Myoepithelial Carcinoma

Herrera GA. Light microscopic, ultrastructural immunocytochemical spectrum of malignant lacrimal and salivary gland tumors. Pathology 1990;58:312-22.
Luna MA, Batsakis JG, Ordonez NG, et al. Salivary gland adenocarcinomas: a clinicopathologic analysis of three distinctive types. Sem Diagn Pathol 1987;4:117-35.
Ostrowski ML, Font RL, Halpern J, et al. Clear cell epithelial-myoepithelial carcinoma arising in pleomorphic adenoma of the lacrimal gland. Ophthalmology 1994;101:925-30.
Seifert G, Brocheriou C, Cardesa A, Eveson JW. WHO international histological classification of tumours: tentative histological classification of salivary gland tumours. Pathol Res Pract 1990;186:555-81.

Chapter 10
Lymphoproliferative, Leukemic, and Histiocytic Lesions of the Orbit

Jack Rootman

Valerie A. White

Joseph M. Connors

Randy D. Gascoyne

Over the last 20 years, our understanding of orbital lymphoproliferative lesions has undergone profound change. The primary impetus has been the advent of increasingly sophisticated and specific immunodiagnostic and molecular techniques in tissue pathology. This has led to the recognition that lymphomas are neoplasia derived from the immune system and has resulted in new classifications of the lymphoid tumors.

For front line clinicians encountering patients with lymphoproliferative disorders, the latest technological advances and classifications may seem somewhat intimidating. Yet, in the practical situation, diseases in this category tend to develop along relatively well-defined lines that allow for ease of categorization and management. The most important clinical issue is to recognize that lymphoproliferative disorders are distinct from inflammctory lesions, in particular the so-called “inflammatory pseudotumor,” and should be managed accordingly. The inflammatory disorders are either specific or nonspecific as previously outlined. Their pathologic infiltrate parallels and reflects the clinical course of the inflammations; generally, they are responsive to anti-inflammatories when they are of a nonspecific character, or to specific treatment directed at their causative agent (microbial, toxic, foreign body, or other). Histopathologically, they are distinguished on the basis of predominant features that are clearly inflammatory, such as polymorphic infiltrates and fibrosis, or by other features of inflammations, such as granulomatous reactions. It is particularly important to separate these from the lymphoproliferative disorders, which behave in a much different fashion.

In contrast to inflammatory disease, lymphoproliferative disorders represent a group with a basic unifying histopathologic substrate of a densely cellular infiltrate that is comprised mostly of small lymphocytes. The lymphoproliferative disorders include reactive and lymphomatous lesions of the non-Hodgkin's variety. With newer technologies, the overwhelming majority of these lesions can now be divided into clonal or nonclonal lesions. Of those appearing in the orbit, a large number seem to be low- to intermediate-grade when lymphomas, and behave in a relatively localized, indolent fashion when they are lymphoid hyperplasias.

In this section, the lesions discussed include the lymphocytic tumors (the majority being small B-cell tumors), plasma cell tumors, and a variety of other lymphoproliferative and leukemic lesions (Table 10-1).

Clinical Spectrum & Presentation

In spite of the diversity of these lesions, it has been our experience that four clinical syndromes can be recognized. These syndromes and the common disease processes included in each category are summarized in Table 10-2 and illustrated in Fig. 10-1 . The most common presentation of lymphoproliferative and leukemic lesions (type 1) is insidious development of painless orbital masses (frequently anterior), which lead to little if any functional interference. On imaging, they tend to be cohesive and mold to adjacent structures. This group of patients is collectively the largest in this category of diseases and is mainly made up of individuals with low-grade, slowly-developing lymphoproliferations. The major differential diagnosis relates to the insidious development of asymptomatic orbital masses, which includes many well-differentiated and encapsulated tumors as well as numerous noninfiltrative disorders such as localized granulomatous inflammations, isolated circumscribed tumors, ectopias, and cysts.

Patients who present with fulminant orbital infiltration (type 2) have a more rapid onset of orbital mass and infiltrative effect. This includes for the most part those with lymphoproliferative

or leukemic disorders, either in a late accelerated phase or of a more aggressive variety such as high-grade lymphomas or the acute leukemias, and rare histiocytic malignancies. In addition, these patients are prone to secondary infectious disorders due to immunoregulatory dysfunction as a result of their underlying disease or treatment. Thus, the differential diagnosis incorporates presumed inflammations of the orbit in an immunocompromised host. The most frequent pathogens in this setting are bacterial, but the possibility of fungal infections must be considered. The distinction between progression and infection can be quite difficult, particularly when the patient is immunocompromised because of B- or T-cell dysfunction.

Table 10-1. Modified Non-Hodgkin's lymphoma classifications with occurrence in orbit

REVISED EUROPEAN-AMERICAN LYMPHOMA (REAL) CLASSIFICATION	WORKING FORMULATION	KIEL CLASSIFICATION	WORLD HEALTH ORGANIZATION CLASSIFICATION
Clinically Indolent (Low-risk)			
Chronic lymphocytic leukemia (CLL) or small lymphocytic lymphoma	Small lymphocytic lymphoma (SLL) consistent with CLL	B-cell CLL/lymphoplasmacytoid immunocytoma	Chronic lymphocytic leukemia (CLL) or small lymphocytic lymphoma
Lymphoplasmacytic lymphoma	SLL with plasmacytoid differentiation	Lymphoplasmacytic immunocytoma	Lymphoplasmacytic lymphoma
Follicular lymphoma, grades I-II	Follicular small cleaved and follicular mixed	Centroblastic/centrocytic, follicular	Follicular lymphoma, grades I-II
Marginal-zone lymphoma, extranodal, nodal, and splenic	SLL	Monocytoid lymphoma including marginal-zone	Splenic marginal-zone lymphoma (MZL), nodal MZL, extranodal MZL of MALT (mucosal-associated lymphoid tissue) type
Plasmacytoma/myeloma	Plasmacytoma	Plasmacytic lymphoma	Plasmacytoma/myeloma
Mycosis fungoides/Sézary syndrome	Mycosis fungoides	Mycosis fungoides/Sézary syndrome	Mycosis fungoides/Sézary syndrome
Clinically Aggressive (Intermediate-risk)			
Follicular lymphoma, grade III	Follicular large cell lymphoma	Centroblastic, follicular	Follicular lymphoma, grade III
Diffuse large B-cell (DLBC) lymphoma	Diffuse mixed, diffuse large cell lymphoma	Centroblastic/centrocytic, diffuse	DLBC lymphoma*
DLBC lymphoma	Immunoblastic lymphoma	Immunoblastic lymphoma	Immunoblastic variant of DLBC
Mantle cell lymphoma	Diffuse small cleaved lymphoma	Centrocytic lymphoma	Mantle cell lymphoma
B-cell prolymphocytic leukemia	SLL	B-cell prolymphocytic leukemia	B-cell prolymphocytic leukemia
Peripheral T-cell lymphomas (PTCL) and anaplastic large cell lymphoma (ALCL)	Diffuse mixed, Diffuse large cell, immunoblastic	PTCL and ALCL	Peripheral T-cell lymphomas (PTCL) and analplastic large cell lymphoma (ALCL)
Clinically Very Aggressive (High-risk)			
Lymphoblastic lymphoma	Lymphoblastic lymphoma	Lymphoblastic lymphoma	Lymphoblastic lymphoma
Burkitt's lymphoma	Small noncleaved lymphoma - Burkitt's	Burkitt's lymphoma	Burkitt's lymphoma
Adult T-cell leukemia/lymphoma	Diffuse mixed, diffuse large cell lymphoma	Pleomorphic medium & large - HTLV-1	Adult T-cell leukemia/lymphoma

* Diffuse large B-cell lymphoma In the World Health Organization classification includes three histologic subtypes (mediastinal large B-cell lymphoma, primary effusion lymphoma, and intravascular large B-cell lymphoma) and the recognition of six morphologic variants including centroblastic, immunoblastic, T-cell/histiocyte-rich, lymphomatoid granulomatosis type, anaplastic large B-cell, and plasmablastic.

Table 10-2. Common or typical clinical spectrum of lymphoproliferative and leukemic lesions of the orbit

CLINICAL SYNDROME	DISEASES	DIFFERENTIAL DIAGNOSES
Type 1 Lesions Orbital mass	B-cell lymphomas, small cell Atypical lymphoproliferations Reactive lymphoproliferations Reactive lymphoproliferations Soft tissue plasmacytomas	Solid orbital tumors Cysts Chronic inflammation Ectopias
Type 2 Lesions Fulminant orbital infiltration	Leukemia (especially acute lymphoblastic or accelerated phases of hematopoietic malignancies) Hodgkin's lymphoma Malignant histiocytosis Occasionally myeloma	Orbital cellulitis Fungal infections NSOIS (nonspecific orbital inflammatory syndromes) Secondary infection (immunocompromised host)
Type 3 Lesions Secondary orbital infiltration From bone From skin	B-cell lymphoma, large cell Plasma cell tumors Langerhans' cell histiocytosis Burkitt's lymphoma Myeloid leukemia T-cell lymphomas	Lytic tumors of bone Granulomas of bone
Type 4 Lesions Neuro-ophthalmic	Late disseminated leukemia Late disseminated lymphoma Histiocytic malignancies Late myeloma Late Burkitt's lymphoma	Intracranial malignancies Low-grade intracranial infections and inflammations

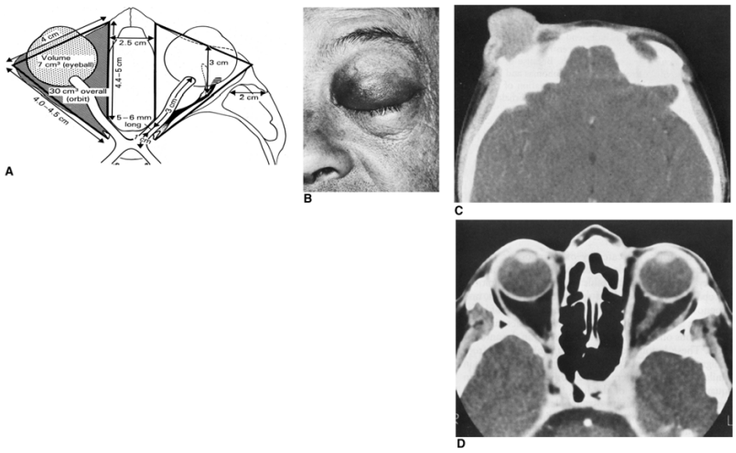

Figure 10-1. (A) Type 1 lymphoproliferative disease orbital mass. This midorbit CT scan shows bilateral orbital masses due to low-grade lymphoma of the lacrimal glands. The lesions are well defined, extraconal in location, and relatively symmetrical. They mold to the lateral margins of the globe and to the bony orbit. Punctate calcification, a rare finding, is present in the posterior portion of the right lesion. This was a B-cell lymphoma. (B) Type 2 lymphoproliferative disease fulminant infiltration. Clinical photograph of a patient who developed a rapidly infiltrating lesion of the left orbit during a relapse of a poorly differentiated lymphocytic lymphoma. This demonstrates typical clinical presentation of type 2 syndrome fulminant orbital infiltration due to lymphoma. It was responsive to reinstitution of systemic chemotherapy. (C) Type 3 lymphoproliferative disease secondary orbital infiltration. CT scan through the superior orbit demonstrates lid invasion from Langerhans' cell histiocytosis arising in the underlying bone. (D) Type 4 lymphoproliferative disease neuro-ophthalmic. Midorbit CT scan demonstrates left cavernous sinus expansion; the latter involvement represents a neuro-ophthalmic complication of a lymphoproliferative lesion. Clinically, the patient presented with cranial nerve palsies.

Another category of patients (type 3) develop orbital manifestations of disease secondary to involvement of adjacent structures. The temporal onset and character of progression reflects the diversity of the underlying lesions. For the most part, these represent disease that has a propensity to involve bone, such as diffuse large B-cell lymphoma, multiple myeloma, or Burkitt's lymphoma, but may also arise from the adjacent paranasal sinuses or skin (e.g., T-cell lymphomas and some types of leukemias). When lesions involve bone and invade the orbit secondarily, the onset may appear to be relatively rapid with evidence on imaging of periorbital or orbital masses associated with bone destruction. Although the most widely recognized in this category are diffuse large B-cell lymphoma and multiple myeloma, other lesions to consider in the differential diagnosis include metastatic carcinoma (particularly thyroid, kidney, prostate, lung, and breast), large arteriovenous malformation or fistula, aneurysmal bone cyst, or lytic meningioma.

The remaining clinical syndrome (type 4) is seen in patients who present with neuro-ophthalmic complications of either lymphoproliferative or leukemic disorders. This category includes some lymphomas and leukemias that have invaded the central nervous system or the ocular structures, or both. Because of the increasing survival of patients with lymphomas and leukemias and the relative pharmacologic isolation of the central nervous system, ocular and neuro-ophthalmic complications are not infrequent.

The above clinical classification includes a wide variety of lymphoproliferative and hematopoietic lesions, all of which may produce signs and symptoms characteristic of any of the four syndromes outlined. The remainder of this chapter will address each of the disorders by dividing them along histopathologic lines into lymphocytic lesions, plasma cell tumors, and miscellaneous lymphoproliferative and leukemic lesions of the orbit.

Biopsying Techniques

The anterior, well-defined location of the majority of these lesions usually allows easy access for biopsy by direct means. If the orbital lesion is the primary presentation of a lymphoproliferative disorder, there is an obligation to establish an accurate histopathologic diagnosis. Biopsy can be done by an open incisional technique or by fine needle aspiration of the orbital mass. We still prefer direct incisional biopsy. One cubic centimeter of tissue is adequate to establish the architecture and provide tissue for immunophenotyping and molecular studies. Characteristically, the tissue is friable and should be handled with care to minimize potential artefact. Although these lesions are readily amenable to needle biopsy, it is less specific as there is no architecture, it may be difficult to subclassify the lesion, and there might be insufficient tissue for ancillary investigations. For the above reasons, incisional biopsy is still our preferred technique; however, needle biopsy can be readily achieved with a 2325 gauge needle core sampling. To do this, three passes are made in slightly different directions with the needle. The needle is then withdrawn and submitted with the syringe in a puncture-proof container to the cytology technician, who should ideally be on-site. This technique is often employed when the patient has previously diagnosed or concurrent lymphoma, and pathological confirmation of orbital involvement is required.

Lymphocytic Tumors

Clinically, the orbital manifestations of lymphocytic tumors are strikingly similar and characterized by an insidious onset of painless mass effect in the sixth or seventh decade of life, typically in the anterior orbit. The lesion does not usually affect vision or optic nerve function, but in a few instances may cause significant globe displacement or diplopia. There is usually mild to moderate proptosis and if there is visible conjunctival involvement, the tumors mold to the globe and appear as a pink, fleshy subconjunctival mass. A slight majority of them are superotemporal and most are predominantly extraconal within the orbit, which is reflected in a nonaxial (often inferior) displacement. The tissue may have a firm or rubbery consistency with nodular borders and is often mobile when palpated. The edge may also conform to fill potential tissue spaces, creating a smooth, narrow, and slightly rounded palpable margin (pancake-like). About a third of patients have some involvement of the opposite orbit. Typically, there are no overlying skin changes such as induration, brawniness, yellowing, or lichenification (a feature more common with dermatotropic T-cell lymphomas and some leukemic infiltrates) nor is there any evidence of adjacent sinus involvement. Twenty-two percent of our patients with orbital lymphocytic lymphomas had contiguous conjunctival involvement. An additional 22% had purely subconjunctival involvement.

In many respects, the lymphoproliferative disorders of the orbit parallel the same kind of lesions in other extranodal sites. In addition, the pathogenesis may bear some identifiable relationship because these extranodal sites are characterized by similar histopathology, disease course, and prognosis, and appear to be mucosal- or epithelial-related or occur in sites of chronic antigenic stimulation. Related examples would include those of the stomach and the lung, where chronic inflammation and associated immune phenomena may give rise to polyclonal or monoclonal lymphoproliferative disorders that recapitulate the mucosal immune system. It should be clear that all of these sites are known to be affected by related disorders that may have an organ-specific autoimmune basis and are the site of diseases that may undergo systematization, whether they are polyclonal or monoclonal in nature.

The occurrence of various lymphoproliferative lesions of the orbit in our practice is shown in Table 10-3 . It is worthwhile to mention that historically there is an increasing frequency of lymphoma, which in our cancer center parallels the increased frequency of lymphoma in general.

With the evolution of the newer diagnostic technologies, increasingly fewer cases fit into the so-called atypical lymphoid hyperplasias in our experience. The majority can now be classified as lymphomas with few reactive lymphoid hyperplasias.

Reactive Lymphoid Hyperplasia

It is our view that a strict definition of reactive lymphoid hyperplasia consists of histologically identifiable focal lymphoid collections, including secondary lymphoid follicles with germinal centers and intact mantle zones that are widely separated by orbital fat and fibrous tissue. Lesions that consist of diffuse sheets of cells do not fall into our definition of reactive hyperplasia and consequently in our recent review, we have identified few reactive hyperplasias. In other words, the reactive lymphoid hyperplasias have the hallmarks of nonclonal infiltrates, including such findings as lymphoid follicles, polyclonality, polymorphous infiltration, vascular hyalinization, hemosiderin deposition, and endothelial proliferation. Polyclonality is defined both by immunophenotypic analysis and molecular methods.

Clinically, these patients usually have an indolent course and the lesions appear as firm to rubbery, slightly nodular anterior orbital infiltrations with lesser involvement of the deeper structures. They are usually painless and do not lead to any functional deficit. On imaging, they tend to mimic the appearance of other lymphoproliferative disorders of the orbit with perhaps slightly more infiltrative margins and less smooth nodularity, as compared with the lymphomas.

Reactive lymphoid hyperplasia may not necessarily be isolated to the orbit, and we and others have noted that there has been incidences of multisystem polyclonal disease (Fig. 10-2). This phenomenon is not unusual because histologically similar lesions occurring in other tissues, such as the salivary gland, gastrointestinal, and respiratory tracts, have been noted to develop multisystem disease that is truly polyclonal. Whether or not they can undergo malignant transformation is a moot point since some of the previously diagnosed “reactive lymphoid hyperplasias” were probably mucosa-associated, follicular, or mantle cell lymphomas, a feature that we have noted in a recent review and reclassification of our patients.

Table 10-3. Frequency of lymphoproliferative disease, University of British Columbia Orbital Clinic, 1976-99

LYMPHOPROLIFERATIVE DISORDER	NUMBER
Lymphocytic	
Reactive lymphoid hyperplasia	6
Indeterminate lymphoid hyperplasia	6
Lymphoma	79
Isolated conjunctival lymphoma	16
Sclerosing lymphoma	2
Plasma cell tumors	
Reactive	1
Myeloma	7
Plasmacytoma	3
Other	
T-cell lymphoma	1
Hodgkin's Disease	1
Leukemia	4
Chloroma	2
Myelogenous leukemia	1
Histiocytoses	
Histiocytosis × - localized	5
Histiocytosis × - multifocal	2
Histiocytosis × - diffuse	1
Malignant histiocytosis	1
TOTAL	138

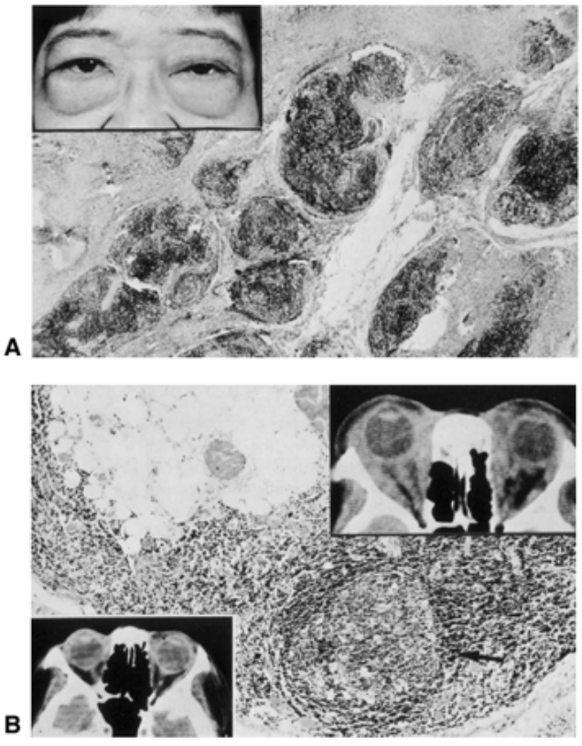

Figure 10-2. (A, inset) Clinical photograph of a 46-year-old woman with bilateral nodularity and thickening of her lids, which had been slowly developing for 16 years. She also had a history of a lesion of the right buttock and glandular enlargement of the iliac and lower paravertebral lymph nodes, diagnosed 17 years earlier as Hodgkin's lymphoma. Retrospective review at this presentation led to a diagnosis of lymphoplasmacytosis within a hyperplastic lymph node. (A) Histology of the orbital lesion shows a low-power view of reactive lymphoid hyperplasia with large collections of lymphocytes invading orbital tissue (H&E, original magnification × 2.5). (B) Higher power view of a reactive lymphoid follicle (arrow) (H&E, original magnification × 10). (B, upper inset) Axial CT demonstrates diffuse bilateral extraconal and intraconal orbital infiltration. (B, lower inset) CT scan after steroid treatment shows marked reduction of the bilateral orbital lesions. This case is an example of a reactive multisystem polyclonal disease. Over the next several years, the patient had multiple recurrences and eventually remained in remission after a course of steroids and azathioprine. (Reproduced with permission from Rootman J, Patel S, Jewell L. Polyclonal orbital and systemic infiltrates. Ophthalmology 1984;91:1112-7.)

Regarding treatment, the reactive lesions appear to be steroid-sensitive and respond to medium to moderate doses of prednisone (Fig. 10-3). Failure to respond or widespread involvement can be treated with good results either by the addition of a cytotoxic agent or local, relatively low-dose radiotherapy (2000 cGy). Two of our cases were resistent to radiotherapy and required immunosuppression.

Indeterminate Lymphoproliferative Lesions

Only six (4%) of our patients remain in the category of having indeterminate lymphoid lesions. By definition, these are lesions with worrisome morphology that fall short of lymphoma and lack either immunophenotypic or molecular genetic evidence of clonality. From a practical point of view, they probably have similar prognostic implications when compared to the low-grade B-cell lymphomas of the orbit, and they can be part of a widespread lymphoreticular process similar to such lesions of the salivary gland or gastrointestinal and respiratory tracts. Thus, indeterminate lymphoproliferative lesions differ very little in presentation and clinical course from low-grade lymphomas of the orbit. In addition, these lymphoproliferations are not uncommonly associated with certain systemic disorders characterized by disturbed immunoregulation. They can be resistant to corticosteroids and may require treatment with immunosuppressive drugs or radiotherapy.

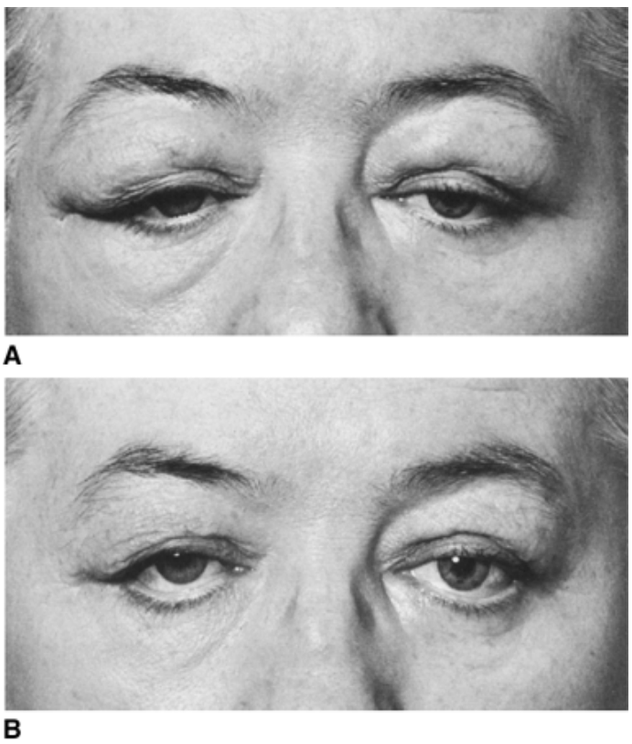

Figure 10-3. (A) Clinical photograph demonstrates bilateral diffuse swelling and nodular tumefaction of the lids. The patient had an 8-year history of progressive lid involvement but retained normal tear secretion. Biopsy showed a reactive lymphoproliferative disease. (B) The same patient after 1 week of corticosteroid therapy demonstrates dramatic resolution. (Reproduced with permission from Rootman J, Patel S, Jewell L. Polyclonal orbital and systemic infiltrates. Ophthalmology 1984;91:1112-7.)

Lymphomas

Pathology and Classification

The understanding of non-Hodgkin's lymphoma continues to undergo evolutionary change due to the explosion in knowledge and new technology available to study the immune system.

A historical perspective is useful for understanding the current classification in widest use, the Working Formulation for Clinical Usage. Before the 1960s, lymphomas were divided into lymphosarcoma and reticulum cell sarcoma. In 1966, Rappaport presented the first reasonable and prognostically useful histopathologic classification of non-Hodgkin's lymphomas. He categorized the lymphomas into well-differentiated and poorly-differentiated lymphocytic, histiocytic, and undifferentiated categories and further subdivided them based on architecture into nodular and diffuse. This classification is still partially in use. In 1975, Lukes and Collins published their classification based on new technologies that allowed differentiation of lymphomas into B- and T-cell subsets and further subdivision by the stages of lymphoid differentiation in the normal lymph node.

About the same time, the Kiel classification (Lennert) became popular in Europe. In 1982, the Working Formulation for Clinical Usage was introduced in North America as a formulary for understanding the myriad of classification schemes currently in use at that time. It was a clinically driven characterization of the non-Hodgkin's lymphomas and although never intended as a classification scheme, it became widely used around the world. The Working Formulation failed to recognize that lymphomas were of distinct lineages (B-cell, T-cell, and natural killer) and grouped unique entities as defined by morphology, immunophenotype, molecular genetic, and cytogenetic criteria as a spectrum of clinical behavior. In fact, within specific disease entities (as defined by morphology, immunophenotype, molecular genetic, and cytogenetic criteria), a spectrum of clinical behavior can be seen that is characteristic of these diseases.

More recently, the International Lymphoma Study Group (ILSG) proposed the Revised European-American Lymphoma (REAL) classification in an attempt to incorporate new knowledge of the immune system and genetic abnormalities associated with non-Hodgkin's lymphoma, and to describe several previously unrecognized types of lymphoma. This proposal has been clinically evaluated and shown to be readily applied and to identify clinically distinctive types of non-Hodgkin's lymphoma. The World Health Organization (WHO) classification has been published recently. The WHO classification incorporates many of the principles and nomenclature of the REAL proposal. The WHO classification, REAL proposal, Kiel classification, and Working Formulation for clinical usage as applied to most orbital lymphomas are compared in Tables 10-1 and 10-4 .

In terms of prognostication, much of our understanding has come from studies by Jakobiec, Knowles, and coworkers. They have drawn a number of conclusions based on their work:

- The site of the lymphoproliferative process is paramount, in that 67% of patients with eyelid lesions, 35% of patients with orbital lesions, and only 20% of patients with conjunctival lesions developed systemic lymphoma during a follow-up of approximately 4 years.
- The histologic classification was important in distinguishing those in the small cell lymphoproliferative categories (hyperplasia, small lymphocytic lymphoma, small cleaved cell lymphoma) from those in all other categories (mixed and large cell) to determine prognosis, where 27% versus 46% of patients developed systemic lymphoma, respectively.
- Approximately one third had systemic lymphoma regardless of whether the lesion was immunophenotypically monoclonal or polyclonal.

In our recent study of 48 patients with orbital lymphoproliferative lesions having a mean follow-up of 8 years, we found that 55% (25) of patients had or developed systemic lymphoma, 11 of which died of disease and 6 were alive with disease. This is a higher percentage of patients presenting with or developing systemic disease than in other reports, probably because of the longer follow-up. All except six lesions could be classified as an indolent type of small cell lymphoma. We used polymerase chaine reaction (PCR) with consensus primers to detect immunoglobulin heavy chain gene rearrangements in paraffin-embedded or fresh frozen tissue in 31 cases. Seventy-four percent of lesions classified histologically as lymphoma were clonal. There was no significant difference between the number of patients in the clonal and nonclonal groups who developed systemic disease. Lack of clonality in a histologically diagnosed lymphoma was due to failure of amplification of that particular patient's immunoglobulin heavy chain gene rearrangement, rather than lack of a clonal population of lymphocytes. Thus, the PCR is more useful for confirming the diagnosis of lymphoma in equivocal cases than predicting which patients will develop systemic disease.

Table 10-4. Comparison of the World Health Organization (WHO) classification, Working Formulation, and histology of small cell lymphomas commonly occurring in the orbit

WHO CLASSIFICATION	WORKING FORMULATION	PATTERN	CYTOLOGY
B-cell chronic lymphocytic leukemia/small lymphocytic lymphoma	Small lymphocytic, consistent with chronic lymphocytic leukemia	Diffuse with pseudofollicles	Small, round lymphocytes
Lymphoplasmacytic lymphoma	Small lymphocytic, plasmacytoid	Diffuse or interfollicular	Small, round lymphocytes, plasmacytoid lymphocytes, plasma cells (± inclusions)
Mantle cell lymphoma	Diffuse, small cleaved	Diffuse, vaguely nodular, mantle-zone	Small, irregular lymphocytes; lack of large cells with nucleoli, epithelioid histiocytes
Follicle center lymphoma, follicular, Grades I-II	Follicular, predominantly small cleaved cell; follicular, mixed small and large cell	Follicular ± diffuse areas	Small cleaved lymphocytes with some large noncleaved cells
Diffuse follicle center lymphoma	Diffuse, small cleaved cell	Diffuse, often vaguely nodular	Small cleaved lymphocytes
Extranodal marginal-zone B-cell lymphoma of MALT type	Small lymphocytic	Diffuse, vaguely nodular, germinal centers	Heterogeneous; small, round lymphocytes, irregular lymphocytes (marginal zone/monocytoid B-cells), plasma cells

Modified from Tables 3 and 4 of Harris NL, Jaffe ES, Stein H, et al. A revised European-American classification of lymphoid neoplasms: a proposal from the International Lymphoma Study Group. Blood 1994;84:1361-92, and from Harris NL, Jaffe ES, Diebold J, et al. World Health Organization classification of neoplastic diseases of the hematopoietic and lymphoid tissues: report of the Clinical Advisory Committee Meeting-Airlie House, Virginia, November 1997. J Clin Oncol 1999;17:3835-49.

In recent publications (including ours) of orbital lymphomas using the REAL classification, the dominant orbital and adnexal lesions are marginal zone B-cell lymphomas of MALT (mucosa-associated lymphoid tissue) type, implying indolence. These studies have also confirmed the prognostic value of the REAL classification of non-Hodgkin's lymphoma.

More than half of these patients have systemic lymphoma at the time of orbital diagnosis or will develop the systemic disease, which is usually indolent. Thus, it is essential that all patients with a histopathologically verified lymphoproliferative lesion of the ocular adnexae be investigated, including a complete systemic evaluation by a hemato-oncologist at the time of diagnosis and at regular follow-up intervals.

Small B-cell Lymphomas

The majority of orbital lymphoproliferations are of B-cell origin, although varying numbers of reactive T-cells will be admixed. Most are composed of “small” B-cells closely resembling normal lymphocytes, which has led to the historical difficulties in distinguishing reactive lesions from those that were true lymphomas. These categories of “small B-cell lymphomas” have been well-delineated in the last several years (Tables 10-1 and 10-4). Small lymphocytic lymphomas (SLL) have a monotonous population of almost normal-appearing lymphocytes, some of which may have plasmacytoid features. A characteristic histologic finding, growth centers, is present in virtually every case and uniquely identifies both SLL and the related chronic lymphocytic leukemia (CLL). Multinucleated cells called polykaryocytes, deposits of hemosiderin, and prominent vessels may be present. Lymphomas of mucosa-associated lymphoid tissue, or MALT lymphomas, are a recently well-delineated entity usually involving mucosal or epithelial surfaces throughout the body. Histologically they demonstrate a characteristic triad including small atypical lymphocytes, reactive lymphoid follicles, and lymphoepithelial lesions. In the orbit as in other sites, MALT lymphoma has a **low** proclivity for systemic involvement. This type of lymphoma is common in the orbit and conjunctiva. In the conjunctiva, however, they much more rarely develop systemic involvement. Mantle cell lymphomas, which are more aggressive (intermediate risk), may have a vaguely nodular or diffuse pattern and are composed of small lymphocytes with slightly enlarged, irregularly shaped nuclei, scattered epithelial histiocytes, and mitotic figures. Lymphoplasmacytoid lymphoma (low risk) is an uncommon small B-cell lymphoma with a prominent plasma cell component and frequent Russell and Dutcher bodies; it is often associated with a monoclonal serum protein. Follicle center or small cleaved cell lymphomas (low risk), which are usually follicular or vaguely diffuse, have a monotonous population of small cleaved lymphocytes. The above are the most common categories of lymphoma in the orbit.

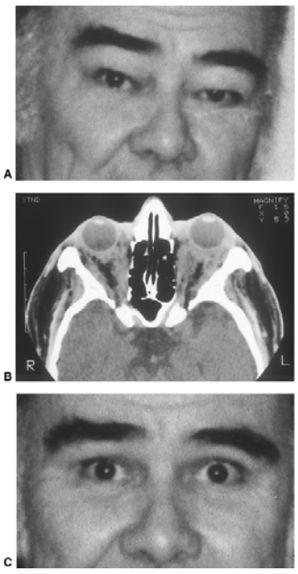

Figure 10-4. (A) This 62-year-old man presented with subacute onset over a 1-month period of lid swelling, tearing, and mild lid retraction. He had a known lymphocytosis due to chronic lymphocytic leukemia. (B) On CT scan there was a ragged infiltration of the orbit bilaterally, an unusual presentation for a lymphoma. (C) The patient responded dramatically to systemic chemotherapy and was free of orbital disease 2 years later.

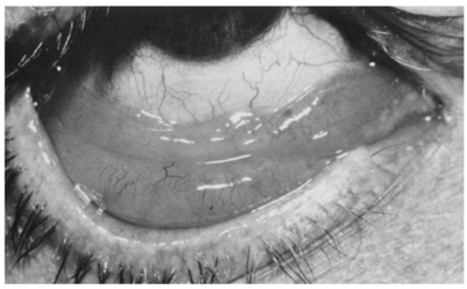

Figure 10-5. Diffuse lymphocytic lymphoma. The large, confluent, salmon-colored fleshy plaque in the inferior fornix is typical of a subconjunctival extension of lymphoma.

Occasional cases of high risk or large cell lymphomas, in which the neoplastic lymphocytes are the same size or larger than reactive histiocytes in the same section respectively, have been described in the orbit. We have encountered several large cell lymphomas, one in a patient with AIDS. Cases of Burkitt's lymphoma in this setting have been described. We reported a single case of follicular lymphoma with signet ring morphology in a mixed small cleaved and large cell lymphoma of the orbit, a cellular pattern seen most frequently in adenocarcinomas, so this diagnosis must be ruled out on the basis of immunopathology and electron microscopy.

Clinical Features

The small B-cell lymphomas are usually characterized by an onset in the sixth and seventh decade of life of a slow mass effect (type 1 lesion). There are, however, occasional instances where they present and progress in a more rapid fashion (Fig. 10-4). Most occur primarily in the anterior orbit and may be associated with pink, fleshy subconjunctival tumefaction (22%) that tends to mold to the shape of the globe (Fig. 10-5). When there is no visible subconjunctival component, these lesions tend to be palpably nodular with relatively well-defined margins and have a slightly friable texture at the time of surgery, resembling pink fish flesh. They may have a rich, fine vascularity and can usually be encompassed surgically, but may also be nodular with infiltrative edges.

On CT scan they are usually well defined and tend to mold to or encompass adjacent ocular and orbital structures without producing functional deficits (Fig. 10-6). They tend to be homogeneous and extraconal, and are predominantly located in one quadrant but may extend intraconally and into adjacent quadrants in a confluent manner. They may rarely occur primarily as a diffuse intraconal lesion or in a perineural location (Fig. 10-7). Lacrimal gland involvement is common and may be the only site of tumefaction (Fig. 10-6). On imaging, they are well defined, often have a lobulated or nodular edge (Fig. 10-8), and are homogeneous in texture. Most involve the orbital soft tissues alone but rarely can be seen as a primary presentation in extraocular muscle (Figs. 10-9 and 10-10). They are isodense to extraocular muscle. Globe displacement, usually in an inferomedial direction, and mild proptosis may be noted.

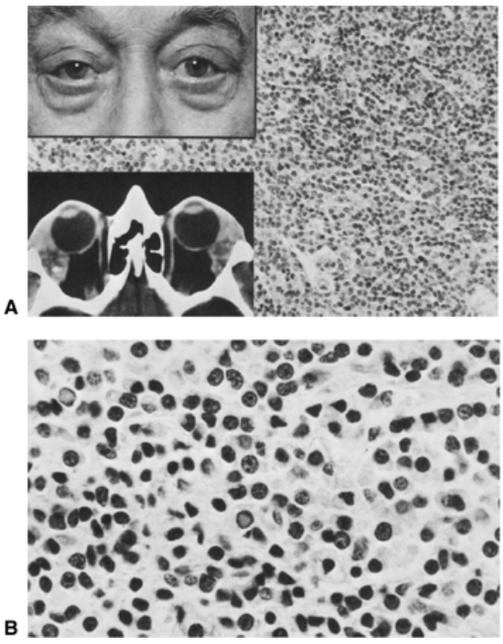

Figure 10-6. This 78-year-old male presented with a 2-month history of epiphora and superolateral orbital soreness with normal tear secretion. (A, top inset) Clinical photograph demonstrates bilateral lacrimal masses. (A, bottom inset) Axial CT scan at mid-orbit level shows bilateral symmetrical inhomogeneous extraconal lesions that mold to the lateral margins of the globe and adjacent bone structures. Coarse punctate calcification is noted in the posterior portion of the right lacrimal lesion. (A, B) Pathology showed a diffuse plasmacytoid small cell lymphocytic lymphoma (low-grade) (H&E, original magnifications; A × 25, B × 40).

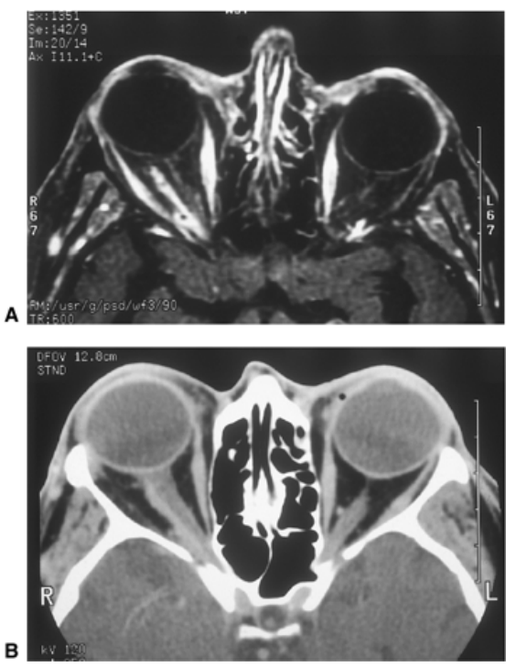

Figure 10-7. This 71-year-old woman presented with onset of right ocular pain over a 2-month period associated with decreased vision, photopsia, and mild increased ocular prominence. Vision was 20/50 on the right with an afferent pupillary defect, scotoma, and 1 mm of proptosis. On T2-weighted, gadolinium-enhanced, fat suppressed MR (A) and CT (B) scans, there was evidence of a perineural infiltrate with a differential diagnosis of lymphoma, dural sarcoid, chronic inflammation, or perhaps a neurogenic tumor. Biopsy and investigation demonstrated a MALT lymphoma without systemic involvement, which responded to radiotherapy. The patient had a return of central vision and was free of disease 3 years later.

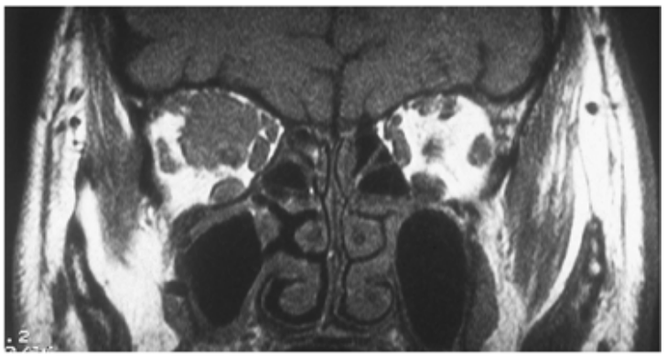

Figure 10-8. This 62-year-old man presented with a chronic progressive proptosis over a 1.5-year period. On physical examination, his vision was 20/25 on the right with 4 mm of proptosis and a slight right afferent pupillary defect. On T1-weighted, contrast enhanced MR scan, there was a large, superior, perineural mass with a differential diagnosis of lymphoma versus exophytic meningioma or neurogenic tumor. Biopsy showed a MALT lymphoma. Systemic investigations were negative so the patient was treated with 2500 cGy to the orbit and underwent complete resolution. However, he was diabetic and developed a radiation-induced retinopathy 2 years later.

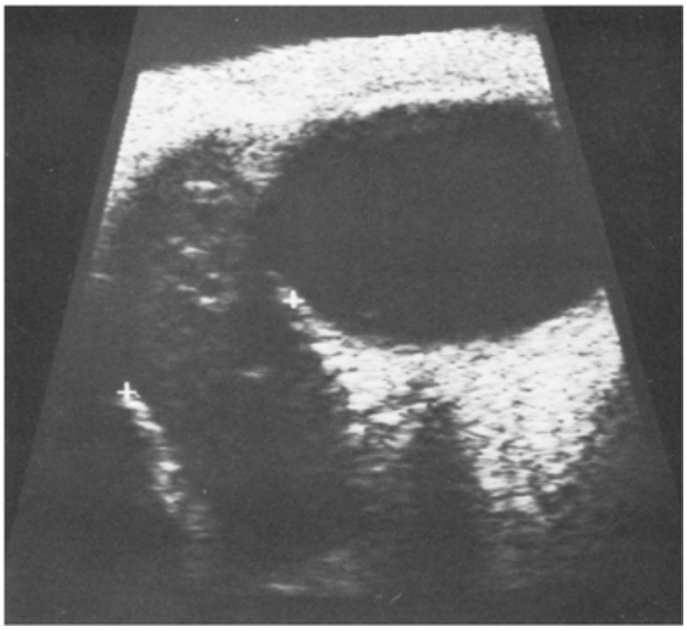

Figure 10-9. B-mode ultrasonogram of a patient with a low-grade orbital lymphoma involving the medial rectus muscle.

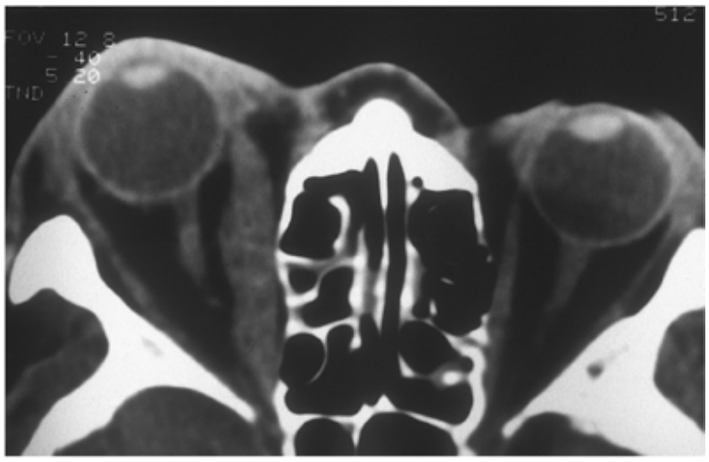

Figure 10-10. This 69-year-old Asian male had a 20-year history of mild progressive proptosis with recent onset of minimal diplopia. On physical examination, he had normal vision, color vision, and pupils. He had fullness of the right orbit with a slightly rubbery feel to the lower lid and increased vascularity over the medial rectus with chemosis. On exophthalmometry, he measured 25 mm on the right and 21 mm on the left, with full eye movements. In addition, he had a mass in the upper cervical chain and parotid region, which he said had been present for at least 10 years. CT demonstrates a nodular, irregular medial rectus. Biopsy showed a small lymphocytic lymphoma with systemic involvement. This indolent lymphoma was treated with oral chlorambucil with a slow but minimal response over the next year. Radiotherapy was then offered but the patient refused. His disease remained minimally changed over the next 2 years, then he developed a bronchiogenic carcinoma with metastasis.

Calcification within the lesion occurs in only 4% and may be diagnostically helpful in subclassifying the tumors into having a plasmacytoid component or in redirecting the investigation toward another etiology. Very few (5%) of the lesions have a multifocal presentation in the orbit but about one quarter are bilateral. Bilateral disease is more common in the rare aggressive variants. The margins of the lesions are either smooth, nodular, or irregular. Approximately half of the patients show globe displacement in a nonaxial direction. Rare but well-recognized patterns of involvement include the solitary lacrimal mass, a posterior intraconal lesion (Fig. 10-8), perineural involvement, spread into the pterygopalatine fossa, and primary extraocular muscle involvement, which may simulate thyroid orbitopathy (Fig. 10-10).

On ultrasound, lymphoproliferative lesions characteristically are acoustically homogeneous and of low reflectivity. They are poorly compressible and have variable outlines. Ultrasound-guided needle biopsy may be useful in diagnosis.

The imaging features on MRI are nonspecific and the masses are isodense to hyperintense when compared to extraocular muscles and **hypodense** when compared with orbital fat on T1-weighted images. On T2-weighted images, the tumor will tend to appear hyperintense compared with both fat and muscle. Gadolinium causes enhancement of the signal on T1 images, which is more easily appreciated with fat suppression (Fig. 10-7). Currently, MRI cannot reliably distinguish between subtypes of lymphoproliferative lesions, although varying pulse sequences may help to characterize these tissues in the future. In summary, fat-suppressed and gadolinium-enhanced T1-weighted MR scans are the most helpful techniques in delineating the extent of tumor. At present, however, MRI offers little advantage over computed tomography.

In our experience, about 25% of our patients presented with antecedent or concurrent systemic lymphoma and over a 10-year period, half of the patients went on to systemic manifestations. The high-grade lesions have a greater incidence of systemic involvement. As noted earlier, underlying systemic disorders, including Sjögren's syndrome, collagen vascular disease, and both hematologic and nonhematologic malignancies, are not uncommon in patients with lymphoid lesions of the ocular adnexa. Overall, the monoclonal B-cell extranodal lymphocytic lymphomas follow a relatively indolent clinical course associated with long-term survival, even with minimal therapeutic intervention for the lower-grade lesions. The exception is mantle cell lymphoma, which tends to behave aggressively and usually requires therapeutic intervention.

Treatment of these patients rests upon obtaining an adequate orbital biopsy for histologic assessment, a proper staging workup, and a strategy based upon the extent of involvement. The overall management of patients is best provided by a multidisciplinary team with special interest in lymphomas. Those lesions that are localized to the orbit can be treated with local radiotherapy (Fig. 10-11) or observed until more widespread disease develops requiring chemotherapeutic intervention (Fig. 10-12). There is evidence to suggest that observation alone for low-grade lymphomas does not alter the prognosis or affect institution of later treatment. Other patients are treated on the basis of age, overall systemic tumor load, and histological tumor grade. Generally, the less well-differentiated tumors are treated promptly with systemic chemotherapy or low-dose (3000 to 3500 cGy) radiotherapy, or both. Overall, prognosis is excellent for these patients and any decision to give specific treatment should be weighed against the associated morbidity.

The recent introduction of monoclonal antibodies against specific lymphocytes may change significantly the treatment of lymphoma.

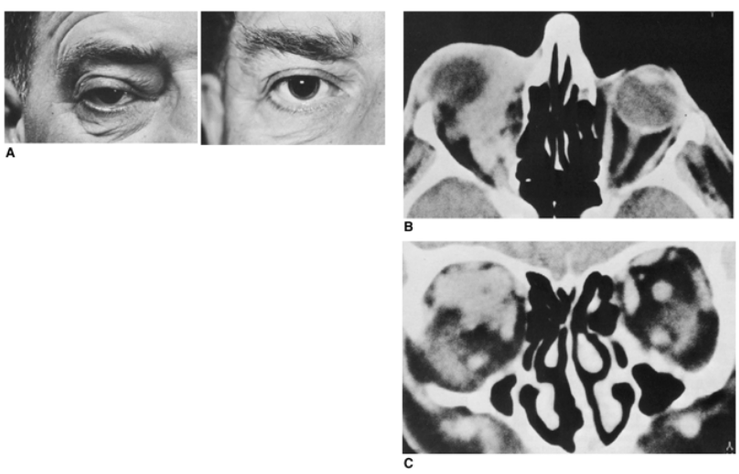

Figure 10-11. (A, left) This 54-year-old man had a 4-year history of a slowly progressive lesion in the superomedial right orbit. The lesion was antecedent to axillary and subcuticular masses, which were treated with local radiotherapy 9 and 7 years earlier, respectively. (A, right) His orbital lesion was also treated with radiotherapy (1500 rad in 5 fractions over 7 days with a 4 mV linear accelerator). (B, C) Axial and coronal CT scans demonstrate a superior, predominantly intraconal, nodular mass that molds to and obscures local structures and is displacing the globe anteriorly and inferiorly. Histologically, the lesion was a small cell lymphocytic lymphoma (low-grade). Fourteen years after presenting with his orbital lesion, he developed a mass in his chest wall that was diagnosed as a plasmacytoma and treated with radiotherapy. He developed a lymphoma at the angle of his left jaw 7 years later, which was treated with oral chlorambucil because of the size. Investigations at that time (1999) showed no systemic bone marrow or lymph node involvement.

Conclusion

Patients with lymphoproliferative disease of the orbit typically present in later life with insidious onset mass effect. Even when histologically nonmalignant (polyclonal), they should be regarded as potential multisystem disorders that may undergo transition to frank malignancy or behave in an aggressive fashion. Furthermore, lesions of this type are not uncommonly associated with underlying systemic disorders related to disturbed immunoregulation. Thus, management requires careful primary and prospective follow-up for local spread and systemic involvement. Those lesions that are truly localized (whether polyclonal or well-differentiated monoclonal) can usually be observed if no functional deficit occurs. If the lesions are bulky and clearly reactive histologically, they may respond to corticosteroid treatment. When atypical or low-grade localized lymphoma is bulky or associated with functional deficit, these lesions can be treated with local modalities, such as low-dose irradiation or rarely resection. Patients who have orbital involvement as part of their systemic disease or higher-grade tumors should be managed promptly by an oncologist with systemic therapy and local treatment as necessary.

Other Lymphomas

Diffuse Large B-cell Lymphomas

Amongst the systemic lymphoid neoplasms, diffuse large B-cell (DLBC) lymphoma is one of the most common (30%) of non-Hodgkin's lymphomas diagnosed in North America. Although uncommon in the orbit, DLBC lymphomas represent the second most frequent orbital non-Hodgkin's lymphoma after the diffuse and follicular small B-cell lymphomas. These aggressive, intermediate, or high-risk orbital lymphomas may represent systemic spread or occasionally the primary presentation of a *de novo* non-Hodgkin's lymphoma. Orbital involvement from DLBC lymphoma arising in the paranasal sinuses is common. This type of lymphoma consists of diffuse sheets of large neoplastic lymphoid cells and biologically represents a heterogeneous spectrum of disorders, including those cases related to the germinal center and others representing transformation of underlying low-grade B-cell lymphoma of MALT type. Their distinction from T-cell lymphomas and other malignant disorders with morphological overlap is usually easily made using routine paraffin section immunostaining techniques.

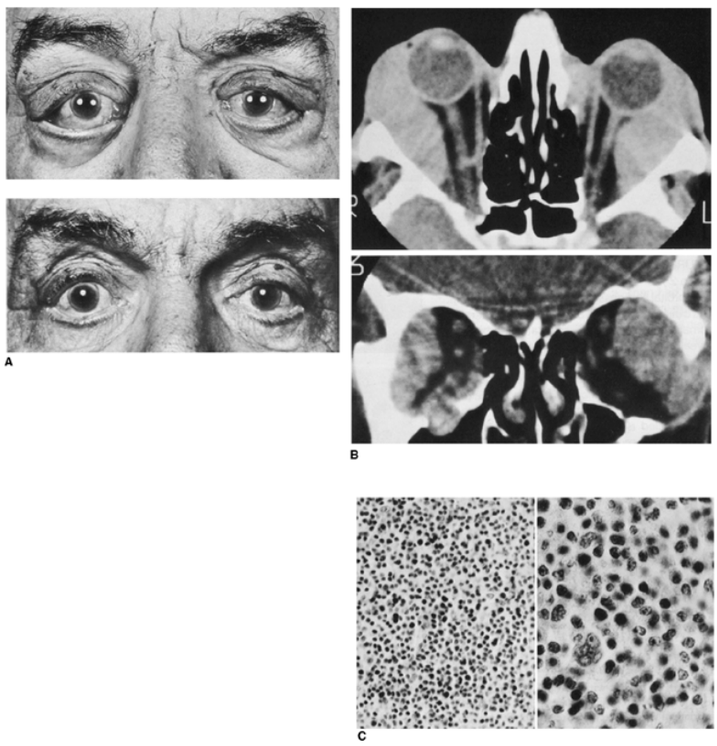

Figure 10-12. (A, top) This 78-year-old man presented with a 3-month history of uncomfortable gritty eyes with increasing proptosis and diplopia due to a small cell (well-differentiated) widespread lymphocytic lymphoma. He had bilateral masses in the lacrimal fossa with S-shaped deformities of the lid and downward, inward displacement of the globes. In addition, salmon-colored infiltrates of the conjunctiva were noted, along with dry eyes. (A, bottom) After several months of systemic chemotherapy, the patient improved dramatically. Axial (B, top) and coronal (B, bottom) CT scans of the same patient demonstrate bilateral, homogeneous, predominantly extraconal smooth masses in the temporal portion of the orbits. Slight nodularity of the margins is noted and the tumors mold to the shape of the globe. The coronal view shows expansion of the right inferior orbital fissure with soft tissue extension into the superior portion of the maxillary sinus. (C) Sections of the orbital biopsy from this patient show extensive replacement of the tissue by a small cell lymphoma with a diffuse pattern (low-grade). On touch preparation, the cells had the morphology of small, mature but slightly atypical lymphocytes, some with slight plasmacytoid features and a few with nuclear clefting. Occasional mitotic features were present. The immunoperoxidase stains were not specific but showed changes suggestive of an IgG monoclonal pattern (H&E, original magnifications: C, left × 25; C, right × 40). The patient died of systemic lymphoma 4 years after presentation.

Burkitt's Lymphoma

Burkitt's lymphoma is a high-grade (high risk) undifferentiated lymphocytic neoplasm endemic to Central Africa that also occurs sporadically worldwide. This disease is of great interest because evidence exists of a chromosomal translocation of the c-myc gene and for cofactors involving the Epstein-Barr virus and states of chronic immune stimulation like malaria or HIV infection.

Clinically, this lymphoma rapidly disseminates but usually presents as a solitary fulminant growth at a median age of 7 years in males predominantly (2:1). African Burkitt's lymphoma presents as a facial tumor in 60%, abdominal mass in 25%, and with paraplegia in 15% of cases. In younger patients (3 to 5 years of age), the maxilla and jaw are more frequent sites of presentation. Although the orbit is ultimately involved in most facial lesions, usually by contiguity, only 13% to 16% present with exophthalmos. Dissemination may occur to the central nervous system (meningeal) and bone marrow. In contrast, the non-African cases are seen in the first three decades (median age 11 years), and are more frequently abdominal with only one third of cases involving the jaw. Burkitt's lymphoma may present as an extranodal tumor of the central nervous system leading to cranial neuropathies or papilledema.

These lymphomas are an outgrowth of B-cells from germinal centers (small noncleaved follicular center cell). The dominant cells are intermediate-sized lymphocytes with round or oval nuclei, multiple small nucleoli, basophilic cytoplasm, and a high mitotic rate. These cells commonly contain fat-filled cytoplasmic vacuoles. The sheets of lymphocytes are interspersed by phagocytic histiocytes, which give the characteristic “starry sky” pattern to the tumor.

Originally, the outlook for this fulminant neoplasm was uniformly poor but the introduction of chemotherapy and adjuvant radiotherapy has greatly improved the prognosis, with dramatic regressions and cures. The major chemotherapeutic agents used are cyclophosphamide, methotrexate, and vincristine. Younger age and localized disease at onset are associated with a better prognosis.

T-cell Lymphomas

The broad spectrum of T-cell neoplasms can be divided into three main categories: the precursor T-cell lymphomas, peripheral T-cell lymphomas, and a special category of disease collectively referred to as cutaneous T-cell lymphoma. The precursor category contains a single lymphoma subtype, lymphoblastic lymphoma, which is closely related to T-cell acute lymphoblastic leukemia (ALL) except that it tends to favor tissue involvement as opposed to primary presentation in the blood and bone marrow. This subtype has a predilection for the anterior mediastinum, central nervous system, and the peripheral blood but may involve the orbital soft tissues during the course of the disease. The diagnosis relies on recognition of a characteristic histology with a leukemic growth pattern, lymphoid cells with intermediate nuclear size, fine chromatin, indistinct nucleoli, and frequent mitotic figures. A battery of immunostains amenable to routine paraffin sections can help to establish the diagnosis.

The peripheral T-cell lymphoma category encompasses a variety of clinicopathologic entities, including such disorders as angioimmunoblastic lymphadenopathy with dysproteinemia (AILD)-type and anaplastic large cell lymphoma. Although more common in Asia, these lymphomas account for approximately 10% to 15% of lymphomas in North America. Extranodal presentations of peripheral T-cell lymphomas are frequent but because they are uncommon non-Hodgkin's lymphomas, orbital involvement is rarely encountered. When they occur in the orbit, most T-cell lymphomas are secondary manifestations of systemic disease of poor prognosis. Most subtypes have unique histologic and phenotypic features but are also associated with characteristic clinical syndromes that facilitate diagnosis. T-cell lineage can usually be established using routine paraffin section immunostaining techniques, but in difficult cases both molecular genetic studies and cytogenetics may be required to establish clonality. The so-called angiocentric lymphomas, now referred to as nasal T/NK (T-cell/natural killer cell) lymphomas have in the past been classified as lethal midline granulomas and polymorphic reticulosis (Figs. 10-13 and 10-14). This subgroup of lymphomas has a propensity to involve the midline structures of the face, and may involve the orbit by contiguity as with one case we have seen. Coupland et al. have described two cases of T/NK lymphoma, both of which were fulminant and associated with systemic involvement – one involving the eye and orbit and the other the orbit alone.

The category of cutaneous T-cell lymphomas (CTCL) typically includes two related entities, mycosis fungoides and Sézary syndrome. Although many lymphomas, particularly those of T-cell type, involve the skin, the CTCLs characteristically are epidermotropic. These diseases for the most part represent overlapping disorders, with Sézary syndrome having a characteristic clinical presentation of diffuse erythematous skin involvement, lymphadenopathy, typical cells in the peripheral blood, and organomegaly. Mycosis fungoides involves the skin and has three progressive stages: erythematous, infiltrative plaque, and tumor (Fig. 10-14). Circulating cells can be found in the peripheral blood in some cases but unlike Sézary syndrome, this is not a major site of disease. Biopsy of the plaque stage is usually diagnostic

with evidence of lymphoid cells with hyperconvoluted nuclei within the upper dermis and involving the epidermis, including characteristic microabscess formation (Pautrier microabscesses). The final stage is the development of ulcerating tumors, which may involve the eyelid, conjunctiva, and orbit. Rarely, this disorder may present primarily in the tumor stage involving the lid and invading the orbit. Histopathologic diagnosis rests with identification of the characteristic morphology together with immunologic techniques to confirm a T-cell lineage. In difficult cases, molecular genetic studies usin PCR may be necessary to establish clonality.

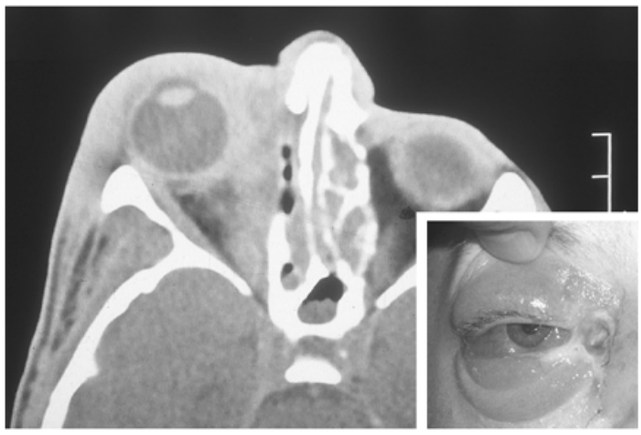

Figure 10-13. (Inset) This 43-year-old woman presented with a unique history of 10 years of waxing and waning bouts of sinusitis and progressive orbital inflammation with multiple sinus surgeries. This was suspected either to be fungal or bacterial in origin and was treated with antibiotics and antifungal drugs to no avail. One year prior to presentation, she underwent an uneventful dacryocystorhinostomy. Six months after surgery, she developed a fistula that infiltrated the medial orbit and adjacent sinus, which was obliterated using a myocutaneous flap. However, the fistula recurred. An extensive orbital biopsy was performed and a diagnosis of T-cell/natural killer cell lymphoma was made. The patient received chemotherapy and radiotherapy, but has developed submantle and pulmonary nodules. (Photos courtesy of Stephen M. Baker, MD.)

Clinical Features

For the most part the orbital and ocular manifestations are a reflection of systemic disease or result from extension of local skin lesions, and usually present late in the course of the disease. The cutaneous T-cell lymphomas are subdivided according to major site of skin involvement into epidermotropic and nonepidermotropic stages. These lymphomas are more common in men and usually occur after the fourth decade of life (Fig. 10-15).

Ocular and orbital involvement usually reflect extracutaneous spread and include deep lid, conjunctival, and caruncular lesions. Keratitis, uveitis, and optic nerve lesions have also been described. T/NK lymphomas are responsible for characteristic midfacial lesions, which may lead to secondary orbital involvement (Figs. 10-13 and 10-14). Further, involvement of the central nervous system can occur with nasal T/NK lymphomas, which may lead to cranial nerve palsies. This disease is characteristically seen in late adult life but has been described even in children. Rarely, the orbit may develop secondary lesions from extraorbital sites.

Management

Treatment of T-cell lymphoma is usually based on the extent of involvement. When primarily dermal, radiotherapy,

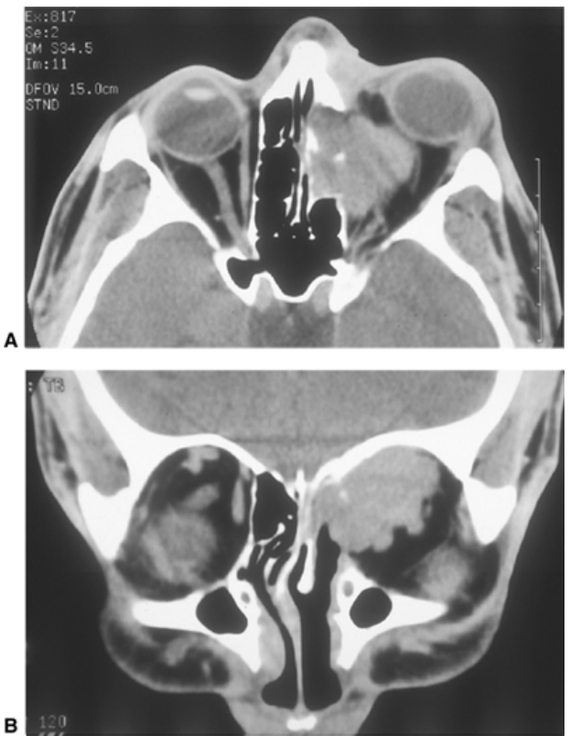

Figure 10-14. This 27-year-old sibling of a patient with retinoblastoma presented with a 6-week history of progressive swelling of the left lid and orbit with erythema and mild edema. He had been treated with antibiotics for 2 weeks to no avail, after which steroids were introduced for a putative nonspecific orbital inflammatory syndrome. The steroids led to resolution for 1 week only. A CT scan performed at that point showed a sino-orbital infiltrate so he underwent an external and internal ethmoidectomy followed by antibiotics. However, the disorder progressed and he was referred to the Orbital Clinic after having a negative sinus biopsy. On referral, he had right proptosis and 8 mm of lateral, 3 mm downward, and 7 mm axial displacement with reduced extraocular movements. Axial (A) and coronal (B) CT scans demonstrated a focal sinus infiltrate with an adjacent orbital involvement. He underwent direct orbital biopsy for a lesion which proved to be a T-cell lymphoma. Systemic assessment demonstrated a stage 1AE diffuse large cell lymphoma of the T-cell phenotype. He was treated with four cycles of ACOP (Adriamycin, cyclophosphamide, vincristine, and prednisone) followed by high-dose ECV therapy (etoposide and cyclophosphamide) with intrathecal methotrexate prophylaxis. He was alive and well 42 months later without recurrence of disease.

photochemotherapy, and topical antineoplastics can be used. In disseminated disease, systemic chemotherapy provides the best disease control, offering occasional cure. The mainstay of treatment for nasal T/NK lymphoma is irradiation because this type is uniquely resistant to chemotherapy.

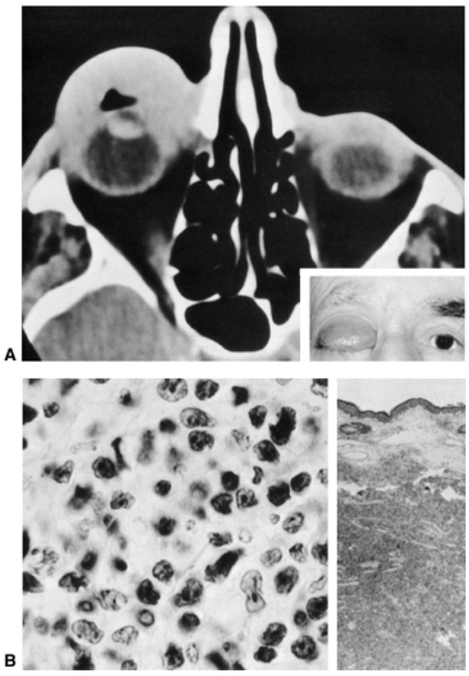

Figure 10-15. (A, inset) This 59-year-old man presented with a 6-week history of increased thickening of the right lid. On physical examination, it was associated with loss of brow hair and cilia. There were some typical salmon patches beneath the conjunctiva on the affected right side. He also had numerous raised, rather injected areas of skin throughout the head and neck region (note left brow). (A) Axial CT scan demonstrates diffuse involvement of the lid and the anterior orbit. (B) Biopsy shows infiltration of the subcuticular tissues by sheets of atypical lymphoid cells. The cells have large nuclei with a distinct nucleolus and a crenated or convoluted nuclear envelope. Immunoperoxidase staining was positive for a T-cell lymphoma, and multiple patches of mycosis fungoides involving the head and neck region were noted. He was treated but died of disease 1 year later.

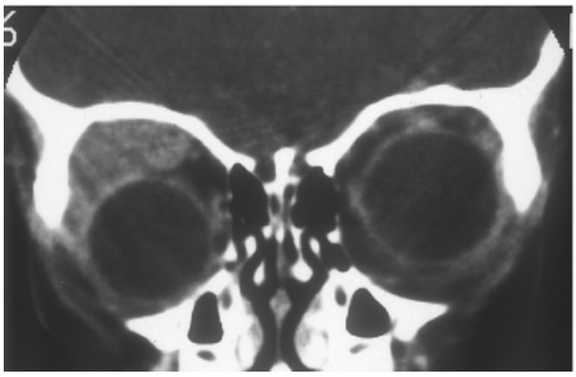

Figure 10-16. This CT scan demonstrates a lacrimal mass in a 5-year-old boy with a 3-week history of proptosis and downward displacement of the right globe. The lesion molded to the shape of the globe. Biopsy showed a chloroma, and systemic evaluation revealed myeloblastic marrow involvement.

Leukemic and Other Lesions

Granulocytic Sarcoma

Granulocytic sarcoma (chloroma or extramedullary myeloid cell tumor) represents a localized, usually extramedullary, form of acute myeloblastic leukemia or of chronic granulocytic leukemia entering blast crisis. It occurs in 8% of patients with myeloid leukemia. When seen in the context of acute myelomonocytic leukemia, orbital involvement heralds a more aggressive systemic disease. In children there is a characteristic predilection for the orbit and surrounding bone. It occurs usually as a rapidly expanding tumor. The mean age of onset is 7 years with a male (3:2) and non-Caucasian predominance. In these cases, the orbit is usually the site of initial presentation but the disease ultimately progresses to full-blown acute myeloblastic leukemia 2 months to 3 years later.

The sites of orbital involvement may include the soft tissues, lacrimal gland (Fig. 10-16), or bones. In 10% of cases bilateral disease is present (Fig. 10-17). Because the clinical presentation is fulminant, confusion with local inflammations and other malignant diseases may occur and warrants rapid consideration of biopsy. Biopsy reveals a poorly differentiated high-grade malignancy that must be distinguished from other childhood round blue cell tumors (neuroblastoma, Ewing's sarcoma, and rhabdomyosarcoma).

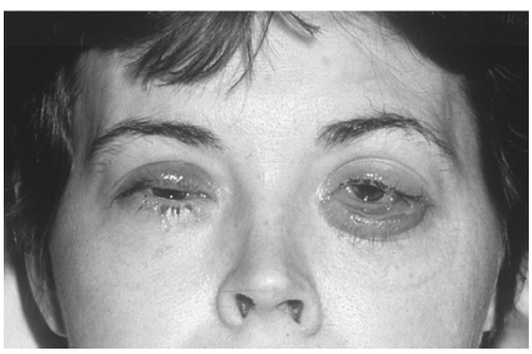

Figure 10-17. This 37-year-old woman presented with a maculopapular rash in the upper body including the eyelids, which developed into nodular cutaneous lesions due to acute myelogenous leukemia. She underwent systemic therapy and bone marrow transplant but died 38 days post-transplant.

In contradistinction to granulocytic sarcoma, true orbital lymphoma is exceedingly rare in childhood.

Histologically, the myeloid origin of the blast cell population can be confirmed by the presence of cytoplasmic granules or Auer rods, or both. The cytology is best assessed with Giemsa-stained imprints and smears. Characteristically, the presence of myeloperoxidase in the tissue imparts a green color to the tumor, accounting for the original designation of this tumor as a chloroma. Cells of myeloid origin can be identified in formalin-fixed tissue by the Leder stain for chloroacetate esterase (a neutrophil enzyme). Paraffin section immunostains for myeloperoxidase, neuraminidase, and CD43 are also helpful for resolving the differential diagnosis. Newer cytogenetic and PCR technologies allow for more specific classification of leukemias. There is a strong association between orbital granulocytic sarcoma T(8;21) and AML-m2 in children. The orbital tumor may develop before, during, or after the occurrence of systemic leukemia.

The prognosis for patients with this aggressive tumor is universally poor. Treatment consists of local irradiation and intensive chemotherapy, which if instituted early, may prolong disease-free survival.

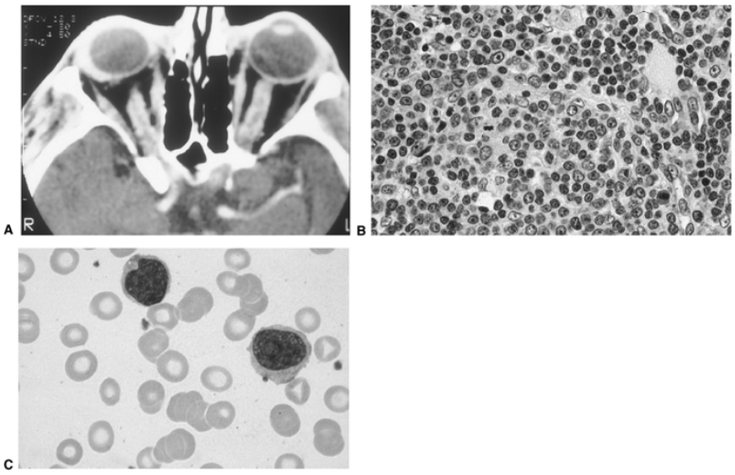

Figure 10-18. (A) CT scan demonstrates a diffuse perineural orbital infiltrate in a 65-year-old man with an ocular history of decreased vision and papilledema. Systemically, he had cervical, axillary, and inguinal lymphadenopathy; splenomegaly; high white cell count, and a IgM monoclonal peak due to an apparent chronic lymphocytic leukemia. A course of oral chlorambucil and prednisone led to only partial improvement of his symptoms with a gradual deterioration of vision and increased splenomegaly. He had progressive reduction of vision, mild proptosis, a dense afferent pupillary defect, and a thickened right lower lid with marked nodularity. Biopsy from the right lower lid (B) demonstrated a lymphoma (H&E, original magnification × 25). Analysis of his peripheral blood (C) revealed that he had prolymphocytes (greater than 55%) of B-cell lineage, which was morphologically suggestive of B-cell prolymphocytic leukemia (Giemsa, original magnification × 100). In spite of aggressive chemotherapy and radiotherapy, the patient died.

Leukemia

There are a host of leukemic disorders, both acute and chronic, which fall mainly in the lymphoid and myeloid groups. The eye and adnexa are not infrequently involved, usually as a complication of late-stage disease. Generally, soft tissue involvement of the orbit is more frequent in acute (especially lymphoblastic) rather than in chronic leukemias. In childhood malignancies of the orbit, acute leukemia and granulocytic sarcoma are a frequent cause of unilateral proptosis (11 %), second only to rhabdomyosarcoma in frequency. Bilaterality is seen in 2% of patients with orbital leukemia. Involvement may be due to soft tissue infiltration or hematoma and is characteristically sudden in onset. Soft tissue hemorrhage is more common in the myeloid group. Involvement of optic nerve (prelaminar and retrolaminar), meninges, uvea, and vitreous may also lead to ocular manifestations. In all of these circumstances orbital disease usually heralds a rapid demise, but local irradiation and both intrathecal and systemic chemotherapy may significantly prolong survival, thus emphasizing the importance of prompt recognition and management (Figs. 10-17 and 10-18).

Plasma Cell Tumors

In many respects, the plasma cell tumors parallel the lymphoproliferative lesions just described. In fact, the diffuse lymphomas of B-cell origin contain within their spectrum variants that have B-cell surface markers and intracytoplasmic immunoglobulins, and display secretory activity. These so-called plasmacytoid lymphomas may secrete IgM paraprotein in sufficient quantities to cause a monoclonal peak in the serum. This is classically seen in Waldenström macroglobulinemia. Plasma cell neoplasms are far less frequent in and around the orbit than B-cell lymphomas and mainly comprise the myeloma end of the spectrum. Patients may present with solitary, well-defined soft tissue lesions (plasmacytoma and reactive plasma cell granulomas), fulminant orbital infiltrations (as part of the manifestations of multiple myeloma or supervening infection in an immunosuppressed host), or, most commonly, with an orbital tumor arising from within adjacent bone either as a solitary plasmacytoma or as part of generalized osseous involvement in multiple myeloma. Finally, certain ocular and neuro-ophthalmic complications are characteristic of multiple myeloma and lymphoplasmacytic lymphoma. Ocular lesions in these two diseases can reflect a hyperviscosity state induced by high levels of the circulating monoclonal paraprotein. Such hyperviscosity is much more commonly seen with the IgM secreting lymphoplasmacytic lymphoma than with myeloma, which more characteristically secretes IgG or IgA. Typical findings include retinal venous engorgement, hemorrhages, microaneurysms, vein thrombosis, sludging, and peripheral pars plana ciliary body cysts. Furthermore, neuro-ophthalmic complications may be a manifestation of direct central nervous system involvement or secondary to erosion of the bones of the skull in multiple myeloma.

The role of an ophthalmologist encountering plasma cell lesions parallels that for all lymphoproliferative disorders. Patients with a primary orbital or periorbital presentation require a full clinical workup and biopsy to establish a histopathologic diagnosis. Further definition requires categorization into benign or reactive lesions, solitary plasma cell tumors, or plasma cell tumors associated with frank multiple myeloma. In some patients, orbital and ocular phenomena develop as a complication of an underlying systemic illness related to disturbed immunoregulation and reduced host defenses.

Plasma cell neoplasias characteristically occur in the bone marrow as multiple focal lesions associated with a variable degree of marrow failure. In a minority of patients, the neoplastic process is truly localized (solitary plasmacytoma of bone or soft tissue). Soft tissue and extramedullary plasmacytomas without bony involvement also occur, of which three quarters are seen in the upper respiratory tract and oropharynx. In general, 90% of plasma cell disorders turn out to be multiple myeloma and 10% solitary plasmacytoma of bone, or extramedullary plasmacytoma. Solitary osseous plasmacytomas appear to be an early form of multiple myeloma in the majority of patients, whereas extramedullary plasmacytomas tend to remain localized or spread to regional lymph nodes.

Histopathology

The plasma cell is characteristically oval to pear-shaped with an eccentric nucleus containing chromatin with a “clock-face” distribution and a paranuclear halo or clear zone representing the Golgi apparatus (“Hof”). These cells can be binucleate and may contain intracytoplasmic (Russell) or intranuclear (Dutcher) inclusions of immunoglobulin crystals (Fig. 10-19). Immunophenotypic stains demonstrate these proteins to be immunoglobulins that are monoclonal in the malignant disorders and polyclonal in the reactive lesions. The cells are typically PAS-positive and diastase-resistant with a pyroninophilic cytoplasm. The electron microscopic features show numerous mitochondria, a characteristically stacked rough endoplasmic reticulum, and a prominent Golgi apparatus. In addition, membrane-bound crystals may be present. The cytologic spectrum varies from

this well-defined mature cell to larger, immature plasma cells with increased mitotic activity and bearing only slight resemblance to the mature cell. Some lesions may show the full spectrum of differentiation. Plasma cell tumors may be associated with amyloid deposition, and we have described two such cases of monoclonal localized orbital amyloidosis, one presenting as a focal nodular infiltrate and the other as diffuse involvement of the fat and muscles. Fine needle aspiration biopsy is a very useful ancillary diagnostic measure in the management of plasma cell tumors.

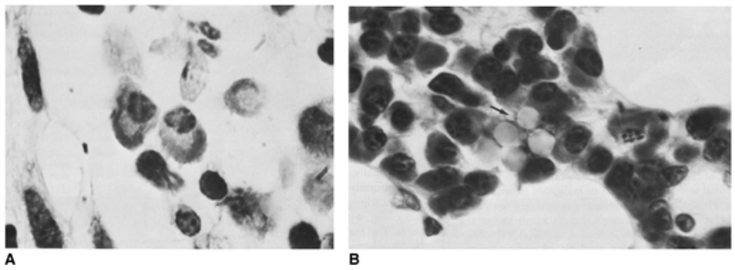

Figure 10-19. (A) Photomicrograph shows normal plasma cells with coarse “cartwheel” nuclear chromatin and paranuclear halo (H&E, original magnification × 100). (B) Dense infiltrate of plasma cells that contain Russell's bodies (arrow) (Masson Trichrome, original magnification × 40).

Spectrum of Orbital Plasma Cell Tumors

Orbital involvement by plasmacytic lymphoproliferative disorders is rare. The spectrum of clinical involvement ranges from reactive disorders to widespread multiple myeloma. The pathologic features of these tumors can be misleading and the use of ancillary diagnostic methods, such as electron microscopy and immunochemistry and PCR, may be necessary to define these lesions accurately. They may present as localized masses (type 1), fulminant orbital infiltrations (type 2), secondary orbital infiltrations particularly from bone (type 3), or neuro-ophthalmic complications of the disease (type 4). Each of these four categories can be further subdivided and discussed along two broad lines, soli tary lesions or tumors associated with widespread involvement.

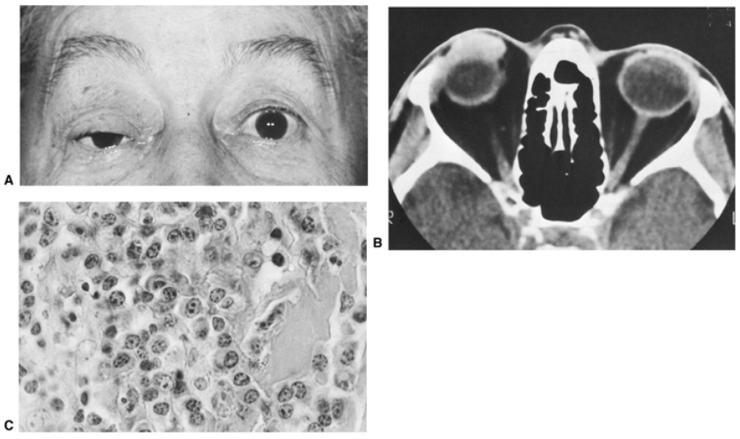

Figure 10-20. (A) This 71-year-old woman demonstrates ptosis (3 mm), downward displacement, and proptosis (3 mm) of the right globe due to a palpable superior orbital mass present for 4 months. (B) Unenhanced axial CT scan of the patient demonstrates an anterior superior homogeneous mass lesion with distinct borders that molds to the contours of the globe. (C) A magnified view of the histopathology from the same patient demonstrates the polymorphous cellular infiltrate and shows numerous plasma cells, lymphocytes, and a few macrophages, some of which contain tingible bodies (H&E, original magnification × 40). Immunocytochemistry was polyclonal. The patient was free of disease 15 years after presentation.

Solitary Plasma Cell Tumors

Clinically, solitary plasma cell tumors include slow-growing, circumscribed soft tissue tumors of the orbit and solitary plasmacytomas of bone. The histopathologic groups are similar to those seen in lymphoproliferative diseases insofar as they may be polyclonal reactive lesions or monoclonal plasma cell tumors.

Polyclonal Plasma Cell Tumor

The polyclonal lesions consist of a heterogeneous population of plasma cells and lymphocytes associated with reactive changes. These lesions may display a follicular organization with varying morphologic features (including tingible body macrophages) in a more or less abundant reactive connective tissue stroma. A proliferation of capillaries and swollen endothelial cells is also seen. The spectrum of reactive plasma cell proliferations is diverse, including plasma cell granuloma and orbital manifestations of the plasma cell variant of Castlemans disease. The distinction from a malignant plasma cell disorder is usually easily made using

kappa and lambda paraffin section immunostains for light-chain clonality. A mixture of kappa and lambda expressing plasma cells will confirm a polyclonal infiltrate. Rarely, PCR techniques are required to assess clonality. The reactive lesions may contain dense, eosinophilic, PAS-positive deposits of immunoglobulins that may include amyloid (which may also be seen as part of monoclonal disorders).

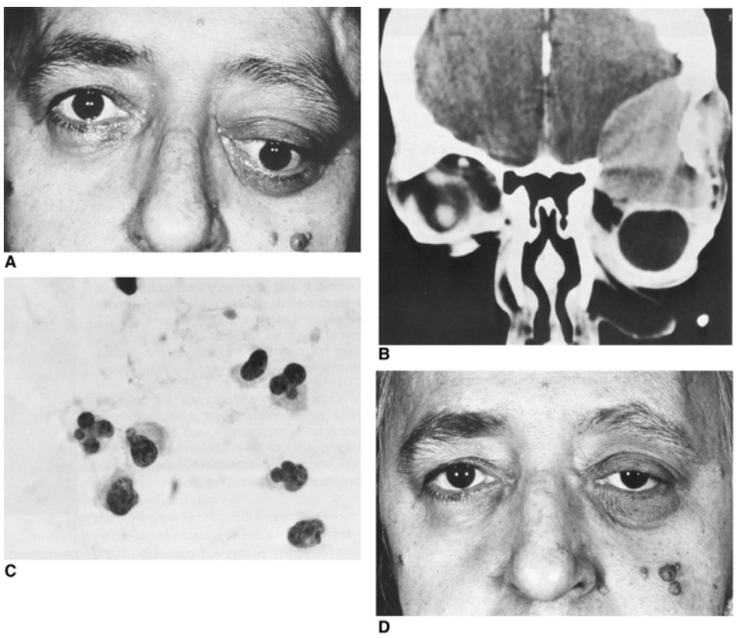

Figure 10-21. (A) This 56-year-old female with a left temporal and brow mass had inferior (9 mm), medial (2 mm), and axial (12 mm) displacement of her eye. The mass, which developed over a 6- to 8-week period, demonstrated pulsation. Sharp, bony defects were palpated at the margins. (B) Enhanced coronal CT (soft tissue technique) demonstrated a large, soft tissue mass in the left superior orbit, invading the anterior cranial and temporalis fossa and displacing the globe inferiorly. Note destruction of the orbital roof and orbital process of the frontal bone. (C) Aspiration biopsy from this patient shows immature plasma cells with binucleate and multinucleated forms; several of the nuclei are irregular in shape (H&E, original magnification × 100). Cytoplasmic immunoperoxidase was strongly positive for IgG and monoclonal lambda light chain. Because systemic investigation showed no other lesions, the final diagnosis was plasmacytoma. (D) Four months after radiotherapy (3600 rad over a 3-week period), the patient showed marked reduction in the size of the mass. The bony defect healed, and she had only minimal proptosis. Two years after treatment, she developed recurrence in her dorsal spine, right humerous, and left femur, for which she received single-dose palliative radiotherapy to each site. The patient died 1 year later.

These lesions are more common in the conjunctiva but have been described in orbital soft tissues. We have encountered one such case, presenting as a well-defined, molding, anterior superior orbital mass (Fig. 10-20). Therapy consists of excising as much of the tumor as possible. Regression of any residual mass will usually occur. An inaccessible or extremely large tumor will respond to low-dose radiotherapy. Corticosteroids have been used but with only moderate responses.

Solitary Plasmacytoma

Solitary extramedullary plasmacytomas are rare monoclonal infiltrates of soft tissue or bone, representing about 3% of all plasma cell neoplasms. The male to female ratio is about 3:1. Lesions develop most frequently in the sixth and seventh decades and have been very rarely described in childhood. Most occur in the oronasopharynx or upper respiratory tract. Extramedullary solitary soft tissue plasmacytomas are associated with prolonged survival (mean 8.3 years), which has led Wiltshaw to consider this as a condition distinct from multiple myeloma. Prolonged survival does not usually occur with solitary plasmacytomas of bone, which are essentially localized forms of myeloma.

Isolated orbital involvement is exceedingly uncommon. Patients characteristically present with proptosis and ptosis. Other symptoms reflect a mass effect and include tearing and blurred vision, followed by diplopia and conjunctival congestion. Pain is rare even though local bony erosion is present at the time of diagnosis in about half of the cases (Fig. 10-21). Orbital involvement may also develop secondary to a paranasal sinus tumor. Rarely, bilateral plasmacytomas occur.

Histologically, the lesions consist of a monomorphous cellular infiltrate of plasma cells. Some variable and binucleate

forms are common; the nuclei may show some irregularity with lobulation, and some may be immature with finer chromatin and increased nuclear/cytoplasmic ratios. There is usually a sparse, delicate, fibrous stroma with thin-walled vessels. The degree of differentiation has some bearing on prognosis with less differentiated tumors being more likely to disseminate, particularly to bone. Immunohistochemistry demonstrates monoclonality with rare tumors having a biclonal light chain.

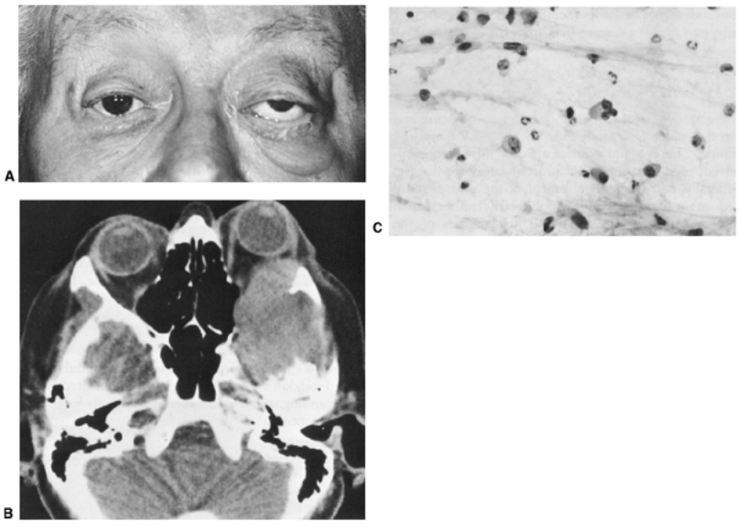

Figure 10-22. (A) This 60-year-old female had a 1-year history of multiple myeloma, a 3-month history of progressive left-sided superotemporal and zygomatic numbness, left ptosis, downward displacement (5 mm), proptosis (8 mm), and edema of her lids. She had also noted diplopia. (B) An enhanced CT scan of this patient shows a large left posterior orbit and middle fossa homogeneous soft tissue mass that has caused partial destruction of the lateral orbital wall, temporal bone, and sphenoid bone. The globe is displaced anteriorly. (C) The aspiration smears demonstrated numerous larger plasma cells. Some relatively mature-appearing plasma cells were present, whereas others had the appearance of plasmablasts. Binucleate and even multinucleate plasma cells were present (H&E, original magnification × 40).

On histologic grounds alone, solitary plasmacytoma cannot be distinguished from multiple myeloma. The distinction is based on the absence of other findings on careful clinical evaluation, including skeletal survey and bone marrow biopsy. Paraproteinemia can be seen in association with solitary plasmacytomas and is, in part, a function of tumor size. Persistence of or increase in paraprotein levels after treatment indicates residual or recurrent disease and warrants reassessment and further therapy. These tumors may be locally invasive, leading to considerable bone destruction and pathologic fractures, and rarely are associated with osteosclerosis. The tumor usually spreads to the regional lymph nodes or occasionally to nonmarrow-containing bones. Progression to multiple myeloma is not as common as previously believed. As stated earlier, bone involvement is really a localized form of myeloma.

Therapy consists of local irradiation at doses of 4000 to 5000 rad. Surgery and chemotherapy are reserved for persistent, recurrent, or unresponsive disease.

Orbital Involvement in Multiple Myeloma

Multiple myeloma rarely involves the orbital tissues. When it occurs, however, in most it is the initial presentation of the disease. Rodman and Font described 30 patients presenting mostly with proptosis, although at the time of diagnosis all had some systemic manifestations including bone pain, fatigue, recurrent infection, pathologic fractures, anemia, hyperglobulinemia, Bence Jones proteinuria, and abnormal immunoelectrophoresis (Fig. 10-22). In the latter stages of known myelomatosis, conjunctival involvement may be seen either as a discrete mass or, on occasion, as diffuse thickening or conjunctivitis. Systemic myeloma may present with bilateral orbital muscle swelling and proptosis secondary to paraproteinemia, which responds to plasmapheresis, and is not due to direct cellular infiltration of the extraocular muscles.

In addition, systemic myeloma can be associated with the development of necrobiotic xanthogranuloma.

Histologically, there may be a wide variation in the degree of differentiation. These tumors have been confused with idiopathic lymphoproliferative disorders, undifferentiated sarcoma, large-cell lymphoma, and amelanotic melanoma. In most cases, myeloma can be differentiated from these lesions by routine paraffin section immunostaining. Documented monoclonal light-chain staining confirms the diagnosis; only rarely are additional ancillary tests such as PCR required.

Clinically, patients with orbital involvement related to multiple myeloma present at an older age than those with solitary extramedullary plasmacytoma, usually in the seventh or eighth decade, with 60% being male. The median survival is around 30 months and death is generally due to infection or renal insufficiency. Particular care should be taken at the time of surgery as these patients may develop acute renal failure as a result of anesthesia or exposure to intravenous contrast material. Therapy consists of systemic chemotherapy and radiation for control of locally invasive lesions.

In disseminated multiple myeloma, soft tissue involvement often heralds the terminal disease stage. Because of the fulminant nature of this infiltration, it may be difficult to distinguish clinically between neoplastic infiltration and a supervening opportunistic infection. Myeloma may present with the clinical features of orbital cellulitis, either secondary to paranasal sinus involvement or orbital hemorrhage with cellulitis, in which case biopsy will show that the orbital infiltrate consists of malignant plasma cells (Fig. 10-23). It is also worth noting that myeloma may lead to immunocompromised states and secondarily cause bacterial or fungal orbital cellulitis.

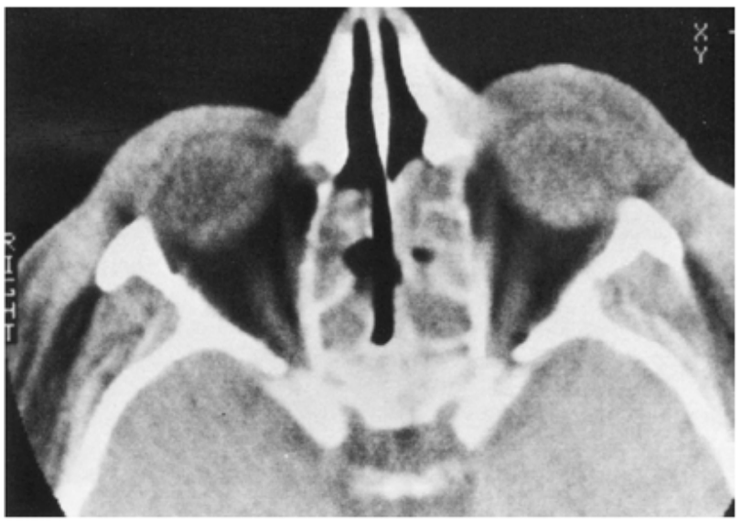

Figure 10-23. An enhanced CT scan in this 57-year-old male, with known myeloma for 2 years and a 6-week history of periorbital pain, swelling, stuffiness of his sinuses and nasopharynx, pyrexia, and fatigue, demonstrates diffuse soft tissue swelling of the left upper lid. Note the opacification of the adjacent ethmoid and sphenoid sinuses due to myeloma infiltrate.

Finally, multiple myeloma is associated with certain ocular and central nervous system manifestations. Patients may show venous engorgement, focal ischemia with cotton-wool spots, retinal hemorrhages, microaneurysms, and cysts of the pars plana and ciliary epithelium. Retinal vascular changes are seen in about two thirds of patients with myeloma, and cysts are seen in approximately one third. The cysts may be sufficiently large to cause anterior displacement of the lens. Central nervous system involvement (thrombosis, intracranial bleeding, meningeal involvement, skullbase erosion) can cause raised intracranial pressure with papilledema, or may lead to cranial nerve palsies involving the ocular and orbital nerve supply (type 4 presentation).

In summary, the spectrum of plasma cell tumors parallels that of the lymphoproliferative groups with disseminated myeloma having a much poorer prognosis. Clinically, these patients present with a variety of manifestations, including localized, well-defined orbital infiltration with tumefaction; periorbital bony involvement; fulminant orbital infiltrations, and central nervous system complications.

Hodgkin's Lymphoma

Clinical Features

In contrast to non-Hodgkin's lymphoma, orbital manifestations of Hodgkin's lymphoma are rare but when they occur, most take place during the terminal phases of the disease. Extranodal Hodgkin's lymphoma, including primary presentation in the orbit, is extremely rare and should raise concerns about the accuracy of diagnosis. The usual clinical syndrome is an orbital mass developing relatively quickly in a patient with known Hodgkin's lymphoma. We have reported a single case of nodular sclerosing Hodgkin's lymphoma of the orbit associated with a longstanding, noninvasive mass effect and local bone excavation (Fig. 10-24).

Pathology

Histologically, Hodgkin's lymphoma is a spectrum of five subtypes with characteristic features (Table 10-5). The key

diagnostic feature is the presence of large neoplastic mononuclear or multinucleate giant cells, known as Reed-Sternberg cells or variants, in a prominent background of reactive cells including small lymphocytes, plasma cells, eosinophils, histiocytes, neutrophils, and fibroblasts. The pathognomonic Reed-Sternberg cells are usually large and binucleate with prominent nucleoli, vesicular nuclear chromatin, and moderate amounts of amphophilic cytoplasm. For many years the cell of origin remained an enigma but recent work has shown that most cases are abnormal B lymphocytes, likely derived from the germinal center. In general, we divide Hodgkin's lymphoma into two broad categories including nodular lymphocyte predominance, which is phenotypically a B-cell disorder, and "classical Hodgkin's lymphoma," which includes nodular sclerosis, mixed cellularity, lymphocyte depletion, and a new entity, lymphocyte-rich, classical Hodgkin's lymphoma. The latter subtypes are B-cell tumors at the molecular level but characteristically fail to express functional immunoglobulin. Rather, the Reed-Sternberg cells in this group of classical Hodgkin's lymphoma typically express CD15 and CD30 markers, thus allowing easy distinction from lymphocyte predominance subtype. In general, the histologic subtypes of Hodgkin's lymphoma represent a continuum from a small number of Reed-Sternberg cells and variants with a predominant reactive background, to cases with relatively few reactive cells and numerous neoplastic Reed-Sternberg cells.

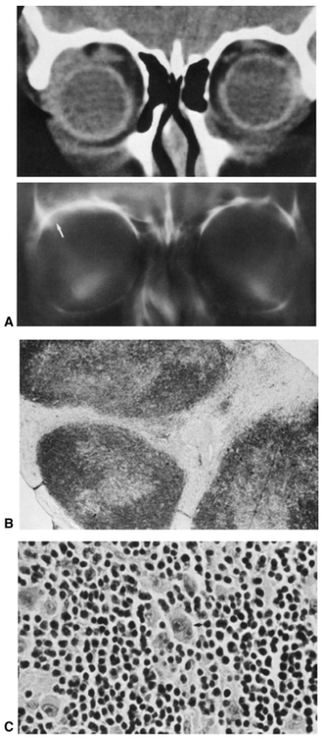

Figure 10-24. (A, top) This 27-year-old woman had a 29-month history of orbital asymmetry, recent onset of swelling of the right upper lid, and known systemic diagnosis of Hodgkin's lymphoma. Coronal CT scan shows a soft tissue mass in the right lacrimal fossa. Note the localized smooth excavation of bone. (A, bottom) Anterior-posterior polytomogram reveals localized expansion of bone adjacent to the right lacrimal fossa without evidence of bony destruction (arrow). This suggested a long-standing lesion with pressure effect but no bony invasion. (B) Photomicrograph of tissue obtained at biopsy of this patient illustrates a lymphoproliferative lesion with dense septae (H&E, original magnification × 25). (C) A polymorphic population of lymphocytes, plasma cells, eosinophils, and diagnostic Reed-Sternberg cells (arrow) are present. The final diagnosis was nodular sclerosing Hodgkin's lymphoma of the orbit (H&E, original magnification × 40). (Reproduced with permission from Rootman J, Patel S, Jewell L. Polyclonal orbital and systemic infiltrates. Ophthalmology 1984;91:1112-7)

Table 10-5. World Health Organization classification of Hodgkin's lymphoma (Hodgkin's disease)

- Nodular lymphocyte-predominant Hodgkin's lymphoma
- Classical Hodgkin's lymphoma
  - Nodular sclerosis Hodgkin's lymphoma
  - Lymphocyte-rich classical Hodgkin's lymphoma
  - Mixed cellularity Hodgkin's lymphoma
  - Lymphocyte depletion Hodgkin's lymphoma

Patients with Hodgkin's lymphoma are divided clinically into four subtypes, according to the Rye classification (Table 10-6). Prognosis is in part based on the amount of immune reaction to the tumor: the fewer the number of lymphocytes, the more aggressive the disease. Prognosis is also

closely related to the staging of the tumor by anatomic involvement (Table 10-6). The variable cellularity of this lesion makes it not infrequently a diagnostic conundrum for the pathologist, who must differentiate it from inflammatory and numerous neoplastic lesions.

Table 10-6. Rye classification of staging for Hodgkin's lymphoma

Staging* - Criteria for Evaluation
Disease limited to one anatomic region (stage I_1) or to two contiguous anatomic regions on the same side of the diaphragm (stage I_2)
Disease in more than two anatomic regions or in two noncontiguous regions on the same side of the diaphragm
Disease on both sides of the diaphragm but not exceeding beyond the involvement of lymph nodes, spleen, or Waldeyer's ring
Involvement of the bone marrow, lung parenchyma, pleura, liver, bone, skin, kidneys, gastrointestinal tract, or any tissue or organ in addition to lymph nodes, spleen, or Waldeyer's ring

* All stages will be subclassified as A or B to indicate absence or presence, respectively, of systemic symptoms (fever, night sweats, weight loss >10% of baseline).

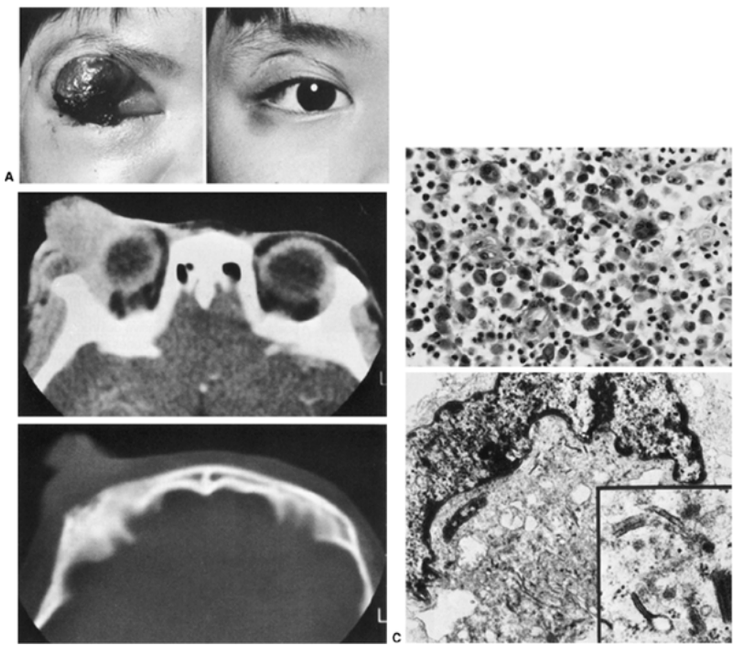

Figure 10-25. This 7-year-old girl presented with a 3-month history of a right upper lid lesion characterized by a waxing and waning course with swelling of the lid. (A, left) On presentation, she had a mass lesion that had eroded through the upper lid and appeared to be infiltrating the lower lid. (A, right) The same patient a few months after radiotherapy (1200 rad in 4 fractions over 4 days with a 4 mV linear accelerator). (B, top) Axial CT scan shows the mass extending through the upper lid, surrounding the lateral margin of the globe, and displacing the globe posteriorly. (B, bottom) Axial CT scan (bone setting) shows that the mass has caused erosion of the underlying bone. (C) The pathologic picture shows plump cells with abundant cytoplasm and vesicular nuclei with well-demarcated large nucleoli and an inflammatory background (H&E, original magnification × 40). (D) Electron micrograph shows C-shaped or indented nucleus and abundant × bodies, Birbeck or Langerhans' granules (D, inset), diagnostic for histiocytosis × (original magnification × 17100; inset × 63000). The patient was disease-free 18 years after presentation.

Management

Overall, the management of Hodgkin's lymphoma represents one of the therapeutic triumphs of modern oncology. Prognosis for low-stage tumors and prospects for cure are remarkably good. However, orbital involvement usually augurs poorly since it frequently reflects disseminated and aggressive disease. Treatment consists of irradiation and chemotherapy.

Histiocytoses

Langerhans' Cell Histiocytosis

Three disorders (Hand-Schuller-Christian disease, Letterer-Siwe disease, and eosinophilic granuloma) have traditionally been categorized as “histiocytosis X” because of their unknown etiology and the similarity of the observed histiocytes. “Langerhans' cell histiocytosis” (LCH) has now replaced the term “histiocytosis X” to reflect the origin of this disease from a somatic mutation in the Langerhans' cell or its precursor. Because these lesions did not behave as true neoplasia, it had been suggested that the pathogenesis may be related to abnormal immune regulation with proliferation of Langerhans' cells and abnormalities of T-suppressor cells. However, recent studies using sophisticated molecular techniques have confirmed that LCH is a clonal disorder.

These disorders are rare (0.6 cases per 1 million children younger than 15 years versus 42.1 cases per 1 million for acute leukemia), occurring most commonly in children. Ophthalmologic manifestations are seen in about 10% of cases. The disease has worldwide incidence and male predominance (2:1). Approximately one third of patients present with disseminated disease, which has a 50% mortality rate. The remaining two thirds have either unifocal or multifocal bone involvement, which can follow either an indolent or a progressive clinical course.

Histogenesis and Pathology

The LCH syndromes are thought to result from abnormal accumulations of specialized histiocytes of the dendritic cell family, specifically the Langerhans' cell, of the epidermis. These cells are part of a larger family of specialized histiocytes known as antigen-presenting cells. The cell can be identified by the presence of characteristic “racquet-shaped” cytoplasmic granules (Birbeck granules) on electron microscopy or by multiple immunohistochemical stains (Fig. 10-25). On routine microscopy, these relatively large mononuclear cells (12 mm) have a moderate amount of granular (occasionally vacuolated) eosinophilic cytoplasm and an indented nucleus with a characteristic linear groove.

The wide clinical disease spectrum is reflected in variations in the pathology and in the site and progression of the process. In addition, LCH has been subdivided into localized and disseminated forms, either of which may be acute or chronic in presentation. There is a characteristic granulomatous-histiocytic infiltrate, often associated with accumulations of granulocytes (especially eosinophils) and lymphocytes. Typically, one sees histologic variation and progression through necrosis, xanthomatous change, and ultimately, fibrosis in the late stage. Multinucleated giant cells may be present. Lesions often involve bone (especially the medullary cavity), whereas the disseminated form of the disorder may involve skin, lymph nodes, spleen, lung, liver, and bone marrow.

Clinical Syndromes

The nature of involvement and prognosis seem to be related to age, rate of progression, and extent of disease. Several disorders have thus been described that vary significantly in terms of severity and rate of progression. Generally (but not always) younger patients have more aggressive disease. The classical spectrum comprises a fulminant systemic disorder (Letterer-Siwe), multifocal bone disease (Hand-Schuller-Christian), or localized bone involvement (eosinophilic granuloma). Patients develop the character of their involvement at an early stage.

Localized disease usually involves bone (particularly marrow sites) and adjacent tissues, and is rarely seen in soft tissues alone. This presentation is more often encountered in older children (3 to 10 years) and occasionally in young adults. The skull (especially parietal and frontal bones) is preferentially involved and, when affected, the orbit characteristically demonstrates disease in the lateral superior quadrant that has arisen from the sphenoid wing, a feature in four of our five localized cases. (The remaining one arose from the frontal bone [Fig. 10-25].) These lesions typically show focal bony lysis and soft tissue expansion with evidence of central low density necrosis (Fig. 10-26).

Multifocal bone involvement may be relatively limited or quite extensive, with or without associated skin or visceral disease. Bone lesions have either a punched-out lytic or moth-eaten appearance with expansion of adjacent tissues

(Fig. 10-27). Fibrosis may occur accompanied by local arrest of the process with sclerosis of the bone and failure of development (Fig. 10-28). This produces a characteristic shallow orbit and flattened forehead (Fig. 10-29). Radiologically, the sclerotic lesion must be distinguished from fibrous dysplasia, meningioma, dermoid cyst, lacrimal gland tumor, osteoblastic metastatic disease, or Caffey's disease. Skin involvement is characterized by pruritic eczematous yellow-red infiltration of the papillary dermis, especially of the scalp. The involvement of bone and surrounding tissues may lead to the well-described triad of diabetes insipidus, exophthalmos, and bony lesions. The acute spectrum of this disease affects infants and young children almost always under 3 years of age. It is usually associated with onset of fever and localized infections, skin lesions, otitis media, and hepatosplenomegaly. Lymphadenopathy and bony involvement are frequently seen. Bone marrow involvement may lead to anemia, thrombocytopenia, and leukopenia.

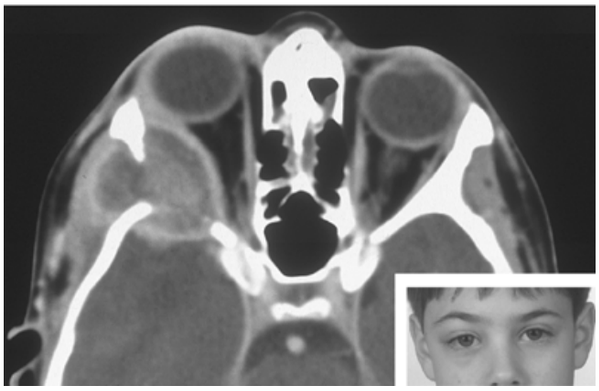

Figure 10-26. This 10-year-old boy presented with a 3-week history of swelling of his right upper lid. He had downward displacement and axial proptosis with an otherwise normal ocular examination. Contrasted CT scan demonstrated a lytic mass with an enhancing rim, suspicious for Langerhans' cell histiocytosis. Fine needle aspiration biopsy confirmed the diagnosis. The lesion was curetted and the patient had postoperative steroids after a negative systemic evaluation. He developed a second lesion of the occipital region 1 year after the primary orbital lesion and this was treated with curettage. He was disease-free 5 years after presentation.

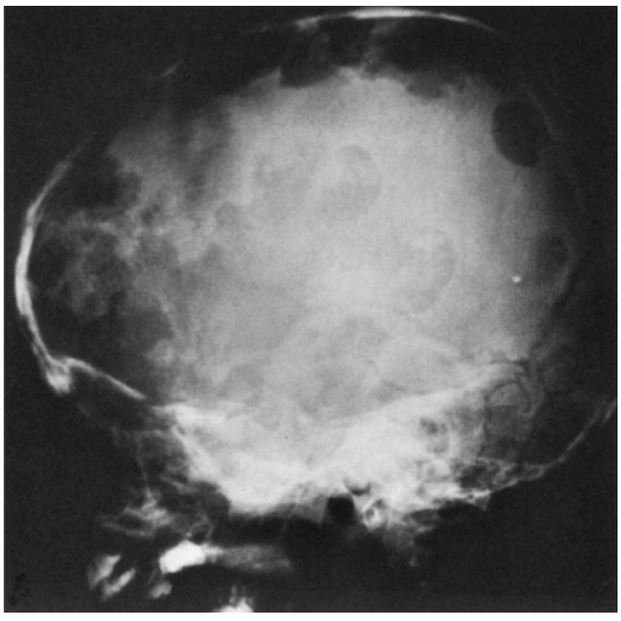

Figure 10-27. Lateral skull radiograph of a 3-year-old boy with Langerhans' cell histiocytosis shows multiple lytic lesions of the cranial vault.

Prognosis is related to the patient's age, disease extent, and progression. Children under 2 years of age have a mortality rate of 55% to 60%, compared with 15% for older children. Disseminated disease correlates with poor survival. Patients with thrombocytopenia, jaundice, hepatosplenomegaly, anemia, and respiratory insufficiency have a high mortality rate. Overall, however, one observes considerable case-to-case variation without any clear correlation between histopathology and prognosis.

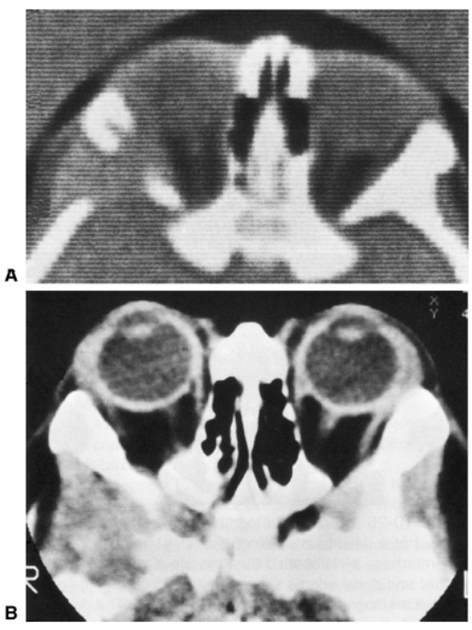

Figure 10-28. (A) Axial CT of a patient with Langerhans' cell histiocytosis demonstrates destruction of the posterior lateral right orbital margin and temporal fossa and a soft tissue mass is visible in the orbit and temporalis fossa. (B) Follow-up CT scan obtained 5 years later demonstrates regrowth and sclerosis of bone after treatment. Residual mass is still present.

The range of treatments for this disorder depends on whether the disease is localized, disseminated, acute, or chronic. Since it may undergo spontaneous regression, some localized lesions can be observed, and may be characterized by evanescent behavior. The other treatment modalities include low-dose local irradiation, cytotoxic agents in disseminated disease, and oral or intralesional steroids. Treatment in children should be supervised by a pediatric oncologist and is usually effective in controlling local disease. The more fulminant and progressive forms fail to show significant response to any form of treatment. Localized periorbital disease will generally respond to low-dose irradiation or local curettage.

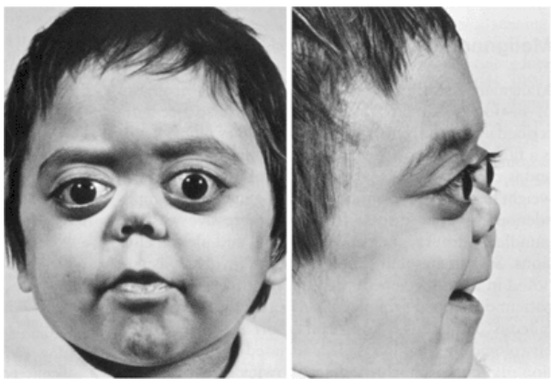

Figure 10-29. This patient has shallow orbits and exophthalmos due to the arrest of bony development following treatment for orbital Langerhans' cell histiocytosis.

Malignant Histiocytosis

Malignant histiocytosis, or true histiocytic lymphoma, represents a systemic neoplasm of histiocytic origin. This disorder has also been described under the term *histiocytic medullary reticulosis*. Many cases classified in the past as true histiocytic lymphomas have been recently reclassified as anaplastic large cell lymphomas. Malignant histiocytosis is a rare, fulminant neoplastic disorder affecting all age groups and is characterized by abrupt onset of fever, weakness, weight loss, hepatosplenomegaly, and generalized lymphadenopathy. The disease leads to progressive wasting, jaundice, purpura, anemia, leukopenia, and pleural effusions. Soft tissues and skin can also be involved, as was seen in one case (Fig. 10-30). The patient developed orbital and periocular disease with cutaneous conjunctival and orbital soft tissue infiltrates. Histologically, the disease is associated with an infiltration of pleomorphic histiocytes showing active erythrophagocytosis. Multinucleated giant cells and bizarre histiocytes are also seen.
Overall, the prognosis is poor and survival, when the disease is untreated, is less than 12 months. In some cases, the use of combination chemotherapy has resulted in remission.

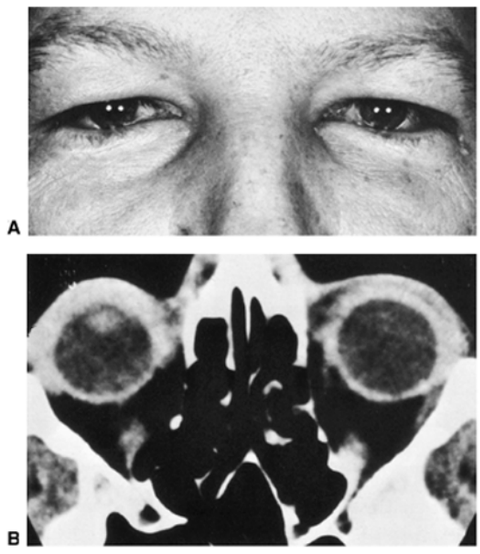

Figure 10-30. (A) Clinical photograph of a 43-year-old man demonstrates periorbital swelling, chemosis, and subconjunctival hemorrhage of 1-months' duration. He also had respiratory difficulty and pedal edema secondary to widespread malignant histiocytosis diagnosed 2 months earlier. He died from the disease 6 months after onset. (B) Axial CT scan demonstrates an irregular bilateral anterior infiltration and thickening of the lids and conjunctiva.

Bibliography

General

Chan JK, Banks PM, Cleary ML, et al. A proposal for classification of lymphoid neoplasms (by the International Lymphoma Study Group). Histopathology 1994;25:517-36.

Duke-Elder S, MacFaul PA. The ocular adnexa. In: Duke-Elder S, ed. System of Ophthalmology. St. Louis: CV Mosby, 1974; v. 13.

Frizzera G. Recent progress in lymphoma classification. Curr Opin Oncol 1997;9:392-402.

Harris NL, Jaffe ES, Diebold J, et al. World Health Organization classification of neoplastic diseases of the hematopoietic and lymphoid tissues: report of the Clinical Advisory Committee Meeting-Airlie House, Virginia, November 1997. J Clin Oncol 1999;17:3835-49.

Harris NL, Jaffe ES, Stein H, et al. A revised European-American classification of lymphoid neoplasms: a proposal from the International Lymphoma Study Group. Blood 1994;84:1361-92.

Henderson JW. Orbital Tumors. 3rd ed. New York: Raven Press, 1994.

Ioachim HL. Lymph Node Biopsy. Philadelphia: JB Lippincott, 1982.

Jones IS, Jakobiec FA. Diseases of the Orbit. New York: Harper & Row, 1979.

Lennert K. Malignant Lymphomas Other Than Hodgkin's Disease: Histology, Cytology, Ultrastructure, Immunology. New York: Springer-Verlag, 1978.

Reese AB. Tumors of the Eye. 3rd ed. New York: Harper & Row, 1976.

Robb-Smith AHT, Taylor CR. Lymph Node Biopsy. New York: Oxford University Press, 1981.

Lymphocytic Tumors

Abo W, Takada K, Kamada M, et al. Evolution of infectious mononucleosis into Epstein-Barr virus carrying monoclonal malignant lymphoma. Lancet 1982;1:1272-6.

Anonymous. National Cancer Institute-sponsored study of classifications of non-Hodgkin's lymphomas: summary and description of a working formulation for clinical usage. Non-Hodgkin's Lymphoma Pathologic Classification Project. Cancer 1982;49:2112-35.

Antle CM, White VA, Horsman DE, Rootman J. Large cell orbital lymphoma in a patient with acquired immune deficiency syndrome. Ophthalmology 1990;97:1494-8.

Argatoff LH, Connors JM, Klasa RJ, Horsman DE, Gascoyne RD. Mantle cell lymphoma: a clinicopathologic study of 80 cases. Blood 1997;89:2067-78.

Astarita RW, Minckler D, Taylor CR, et al. Orbital and adnexal lymphomas: a multiparameter approach. Am J Clin Pathol 1980;73:615-21.

Banerjee D, Ahmad D. Malignant lymphoma complicating lymphocytic interstitial pneumonia: a monoclonal B-cell neoplasm arising in a polyclonal lymphoproliferative disorder. Hum Pathol 1982;13:780-2.

Burke JS, Butler JJ, Fuller LM. Malignant lymphomas of the thyroid: a clinical pathological study of 35 patients including ultrastructural observations. Cancer 1977;39:1587-602.

Cahill M, Barnes C, Moriarty P, et al. Ocular adnexal lymphoma - comparison of MALT lymphoma with other histological types. Br J Ophthalmol 1999;83:742-7.

Chavis RM, Garner A, Wright JE. Inflammatory orbital pseudotumor: a clinicopathologic study. Arch Ophthalmol 1978;96:1817-22.

Cleary ML, Chao J, Warnke R, Sklar J. Immunoglobulin gene rearrangement as a diagnostic criterion of B-cell lymphoma. Proc Natl Acad Sci USA 1984;81:593-7.

Cleary ML, Warnke R, Sklar J. Monoclonality of lymphoproliferative lesions in cardiac-transplant recipients. Clonal analysis based on immunoglobulin-gene rearrangements. N Engl J Med 1984;310:477-82.

Colby TV, Carrington CB. Lymphoreticular tumors and infiltrates of the lung. Pathol Annu 1983;18:27-70.

Colby TV, Carrington CB. Pulmonary lymphomas: current concepts. Hum Pathol 1983;14:884-7.

Compagno J, Oertel JE. Malignant lymphoma and other lymphoproliferative disorders of the thyroid gland. Am J Clin Pathol 1980;74:1-11.

Cossman J, Uppenkamp M, Sundeen J, et al. Molecular genetics and the diagnosis of lymphoma. Arch Pathol Lab Med 1988;112:117-27.

Coupland SE, Krause L, Delecluse H-J, et al. Lymphoproliferative lesions of the ocular adnexa: analysis of 112 cases. Ophthalmology 1998;105:1430-41.

Curtin HD. Pseudotumor. Radiol Clin North Am 1987;25:583-99.

Dolman PJ, Rootman J, Quenville NF. Signet-ring cell lymphoma in the orbit: a case report and review. Can J Ophthalmol 1986;21:242-5.

Dorfman RF, Burke JS, Berard CW. A working formulation of non-Hodgkin's lymphomas: background, recommendations, histological criteria, and relationship to other classifications. In: Rosenberg SA, Kaplan HS, eds. Malignant Lymphomas: Etiology, Immunology, Pathology, Treatment. New York: Academic Press, 1982; 351-68.

Ellis JH, Banks PM, Campbell RJ, Liesegang TJ. Lymphoid tumors of the ocular adnexa. Clinical correlation with the working formulation classification and immunoperoxidase staining of paraffin section. Ophthalmology 1985;92:1311-24.

Evans HL. Extranodal small lymphocytic proliferation: a clinicopathologic and immunocytochemical study. Cancer 1982;49:84-96.

Fisher RI, Dahlberg S, Nathwani BN, et al. A clinical analysis of two indolent lymphoma entities: mantle cell lymphoma and marginal zone lymphoma (including the mucosa-associated lymphoid tissue and monocytoid B-cell subcategories): a Southwest Oncology Group study. Blood 1995;85:1075-82.

Font RL, Shields JA. Large cell lymphoma of the orbit with microvillous projections (“porcupine lymphoma”). Arch Ophthalmol 1985;103:1715-9.

Foran JM, Rohatiner AZS, Cunningham D, et al. European phase II study of Rituximab (chimeric anti-CD-20 monoclonal antibody) for patients with newly diagnosed mantle-cell lymphoma and previously treated mantle-cell lymphoma, immunoctyoma, and small B-cell lymphocytic lymphoma. J Clin Oncol 2000;18:317-24.

Garner A, Rahi AHS, Wright JE. Lymphoproliferative disorders of the orbit: an immunological approach to diagnosis and pathogenesis. Br J Ophthalmol 1983;67:561-9.

Hammer RD, Glick AD, Greer JP, et al. Splenic marginal zone lymphoma. A distinct B-cell neoplasm. Am J Surg Pathol 1996;20:613-26.

Hande KR, Garrow GC. Acute tumor lysis syndrome in patients with high-grade non-Hodgkin's lymphoma. Am J Med 1993;94:133-9.

Harris NL, Pilch BZ, Bhan AK, et al. Immunohistologic diagnosis of orbital lymphoid infiltrates. Am J Surg Pathol 1984;8:83-91.

Harris NL, Jaffe ES, Stein H, et al. A revised European-American classification of lymphoid neoplasms: a proposal from the International Lymphoma Study Group. Blood 1994;84:1361-92.

Hornblass A, Jakobiec FA, Reifler DM, Mines J. Orbital lymphoid tumors located predominantly within extraocular muscles. Ophthalmology 1987;94:688-97.

Isaacson P, Wright DH. Malignant lymphoma of mucosa-associated lymphoid tissue. A distinctive type of B-cell lymphoma. Cancer 1983;52:1410-6.

Isaacson P, Wright DH. Extranodal malignant lymphoma arising from mucosa-associated lymphoid tissue. Cancer 1984;53:2515-24.

Isaacson PG, Spencer J. Malignant lymphoma of mucosa-associated lymphoid tissue. Histopathology 1987;11:445-62.

Jakobiec FA. Ocular inflammatory disease: the lymphocyte redivivus. Am J Ophthalmol 1983;96:384-91.

Jakobiec FA, Iwamoto T, Knowles DM 2nd. Ocular adnexal lymphoid tumors. Correlative ultrastructural and immunologic marker studies. Arch Ophthalmol 1982;100:84-98.

Jakobiec FA, Iwamoto T, Patell M, Knowles DM 2nd. Ocular adnexal monoclonal lymphoid tumors with a favorable prognosis. Ophthalmology 1986;93:1547-57.

Jakobiec FA, Lefkowitch J, Knowles DM 2nd. B- and T-lymphocytes in ocular disease. Ophthalmology 1984;91:635-54.

Jakobiec FA, McLean I, Font RL. Clinicopathologic characteristics of orbital lymphoid hyperplasia. Ophthalmology 1979;86:948-66.

Jakobiec FA, Neri A, Knowles DM 2nd. Genotypic monoclonality in immunophenotypically polyclonal orbital lymphoid tumors. A model of tumor progression in the lymphoid system. The 1986 Wendell Hughes lecture. Ophthalmology 1987;94:980-94.

Jenkins C, Rose GE, Bunce C, et al. Histological features of ocular adnexal lymphoma (REAL classification) and their association with patient morbidity and survival. Br J Ophthalmol 2000;84:907-13.

Johnson TE, Tse DT, Byrne GE Jr, et al. Ocular-adnexal lymphoid tumors: a clincopathologic and molecular genetic study of 77 patients. Ophthal Plast Reconstr Surg 1999;15:171-9.

Knowles DM 2nd, Halper JP, Jakobiec FA. The immunologic characterization of 40 extranodal lymphoid infiltrates: usefulness in distinguishing between benign pseudolymphoma and malignant lymphoma. Cancer 1982;49:2321-35.

Knowles DM 2nd, Jakobiec FA. Cell marker analysis of extranodal lymphoid infiltrates: to what extent does the determination of mono or polyclonality resolve the diagnostic dilemma of malignant lymphoma versus pseudolymphoma in an extranodal site? Semin Diagn Pathol 1985;2:163-8.

Knowles DM 2nd, Jakobiec FA. Ocular adnexal lymphoid neoplasms: clinical, histopathologic, electron microscopic, and immunologic characteristics. Hum Pathol 1982;13:148-62.

Knowles DM 2nd, Jakobiec FA. Orbital lymphoid neoplasms: a clinicopathologic study of 60 patients. Cancer 1980;46:576-89.

Knowles DM 2nd, Jakobiec FA, Halper JP. Immunologic characterization of ocular adnexal lymphoid neoplasms. Am J Ophthalmol 1979;87:603-19.

Knowles DM 2nd, Jakobiec FA, McNally L, Burke JS. Lymphoid hyperplasia and malignant lymphoma occurring in the ocular adnexa (orbit, conjunctiva, and eyelids): a prospective multiparametric analysis of 108 cases during 1977 to 1987. Hum Pathol 1990;21:959-73.

Koss MN, Hockholzer L, Nichols PW, et al. Primary non-Hodgkin's lymphoma and pseudolymphoma of lung: a study of 161 patients. Hum Pathol 1983;14:1024-38.

Lennert K. Malignant Lymphomas Other Than Hodgkin's Disease: Histology, Cytology, Ultrastructure, Immunology. New York: Springer-Verlag, 1978.

Levine RA. Orbital ultrasonography. Radiol Clin North Am 1987;25:447-69.

Lim LC, Koh KP, Tan P. Fatal cytokine release syndrome with chimeric anti-CD20 monoclonal antibody rituximab in a 71-year-old patient with chronic lymphocytic leukemia. J Clin Oncol 1999;17:1962-3.

Lukes RJ, Collins RD. New approaches to the classification of the lymphomata. Br J Cancer 1975;31(Suppl 2):1-28.

Maloney DG, Press OW. Newer treatments for non-Hodgkin's lymphoma: monoclonal antibodies. Oncology 1998;12(Suppl 8):63-76.

McCune SL, Gockerman JP, Rizzieri DA. Monoclonal antibody therapy in the treatment of non-Hodgkin lymphoma. JAMA 2001;286:1149-52.

McNally L, Jakobiec FA, Knowles DM 2nd. Clinical, morphologic, immunophenotypic, and molecular genetic analysis of bilateral ocular adnexal lymphoid neoplasms in 17 patients. Am J Ophthalmol 1987;103:555-68.

Morgan G. Lymphocytic tumors of the orbit. Mod Probl Ophthalmol 1975;14:355-60.

Morgan G, Harry J. Lymphocytic tumors of indeterminate nature: a 5-year follow-up of 98 conjunctival and orbital lesions. Br J Ophthalmol 1978;62:381-3.

Neri A, Jakobiec FA, Pillici P, et al. Immunoglobulin and T cell receptor beta chain gene rearrangement analysis of ocular adnexal lymphoid neoplasms: clinical and biologic implications. Blood 1987;70:1519-29.

O'Connor NTJ, Wainscoat JS, Wetherall DJ, et al. Rearrangement of the T-cell receptor beta-chain gene in the diagnosis of lymphoproliferative disorders. Lancet 1985;1:1295-7.

Onrust SV, Lamb HM, Balfour JAB. Rituximab. Drugs 1999;58:79-90.

Papadimitriou CS, Muller-Hermelink U, Lennert K. Histologic and immunohistochemical findings in the differential diagnosis of chronic lymphocytic leukemia of B-cell type and lymphoplasmacytic/lymphoplasmacytoid lymphoma. Virchows Arch [A] Pathol Anat Hist 1979;384:149-58.

Patel S, Rootman J. Nodular sclerosing Hodgkin's disease of orbit. Ophthalmology 1983;90:1433-6.

Piro LD, White CA, Grillo-Lopez AJ, et al. Extended rituximab (anti-CD20 monoclonal antibody) therapy for relapsed or refractory low-grade or follicular non-Hodgkin's lymphoma. Ann Oncol 1999;10:655-61.

Portlock CS, Rosenberg SA. No initial therapy for stage III and IV non-Hodgkin's lymphomas of favorable histologic types. Ann Intern Med 1979;90:10-3.

Rappaport H. Atlas of Tumor Pathology, Section III, Fascicle 8. Tumors of the Hematopoietic System. Washington, DC: Armed Forces Institute of Pathology, 1966.

Rassiga AL. Advances in adult non-Hodgkin's lymphoma. Current concepts of classification, diagnosis, and management. Arch Intern Med 1980;140:1647-51.

Reifler DM, Warzynski MJ, Blount WR, et al. Orbital lymphoma associated with acquired immune deficiency (AIDS). Surv Ophthalmol 1994;38:371-80.

Risdall R, Hoppe RT, Warnke R. Non-Hodgkin's lymphoma: a study of the evolution of the disease based upon 92 autopsied cases. Cancer 1979;44:529-42.

Rootman J, Patel S, Jewell L. Polyclonal orbital and systemic infiltrates. Ophthalmology 1984;91:1112-7.

Rosenberg SA. Current concepts in cancer: non-Hodgkin's lymphoma - selection of treatment on the basis of histologic type. N Engl J Med 1979;301:924-8.

Sigelman J, Jakobiec FA. Lymphoid lesions of the conjunctiva: relation of histopathology to clinical outcome. Ophthalmology 1978;85:818-43.

Sklar J. What can DNA rearrangements tell us about solid hematolymphoid neoplasms? Am J Surg Pathol 1990;14(Suppl 1):16-25.

Taylor CR. An immunohistological study of follicular lymphoma, reticulum cell sarcoma and Hodgkin's disease. Eur J Cancer 1976;12:61-75.

Turner RR, Colby TV, Doggett RS. Well-differentiated lymphocytic lymphoma. A study of 47 patients with primary manifestation in the lung. Cancer 1984;54:2088-96.

Turner RR, Egbert P, Warnke RA. Lymphocytic infiltrates of the conjunctiva and orbit: immunohistochemical staining of 16 cases. Am J Clin Pathol 1984;81:447-52.

Vogiatzis KV. Lymphoid tumors of the orbit and ocular adnexa: a long-term follow-up. Ann Ophthalmol 1984;16:1046-55.

Warnke R, Pederson M, Williams C, Levy R. A study of lymphoproliferative diseases comparing immunofluorescence with immunohistochemistry. Am J Clin Pathol 1978;70:67-75.

Weisenburger DD, Armitage JO. Mantle cell lymphoma-an entity comes of age. Blood 1996;87:4483-94.

White V, Rootman J, Quenville N, et al. Orbital lymphoproliferative and inflammatory lesions. Can J Ophthalmol 1987;22:362-73.

White VA, Gascoyne RD, McNeil BK, et al. Histopathologic findings and frequency of clonality detected by the polymerase chain reaction in ocular adnexal lymphoproliferative lesions. Mod Pathol 1996;9:1052-61.

White WL, Ferry JA, Harris NL, Grove AS Jr. Ocular adnexal lymphoma: a clinicopathologic study with identification of lymphomas of mucosa-associated lymphoid tissue type. Ophthalmology 1995;102:1994-2006.

Yang H, Rosove MH, Figlin RA. Tumor lysis syndrome occurring after the administration of rituximab in lymphoproliferative disorders: high-grade non-Hodgkin's lymphoma and chronic lymphocytic leukemia. Am J Hematol 1999;62:247-50.

Yeo JH, Jakobiec FA, Abbott GF, Trokel SL. Combined clinical and computed tomographic diagnosis of orbital lymphoid tumors. Am J Ophthalmol 1982;94:235-45.

Zukerberg LR, Medeiros LJ, Ferry JA, Harris NL. Diffuse low-grade B-cell lymphomas. Four clinically distinct subtypes defined by a combination of morphologic and immunophenotypic features. Am J Clin Pathol 1993;100:373-85.

Burkitt's Lymphoma

Banks PM, Arseneau JC, Gralnick HR, et al. American Burkitt's lymphoma: a clinicopathologic study of 30 cases. II. Pathologic correlations. Am J Med 1975;58:322-6.
Burkitt D. A sarcoma involving the jaws in African children. Br J Surg 1958;46:218-23.
Burkitt D, O'Conor GT. Malignant lymphoma in African children. I. A clinical syndrome. Cancer 1961;14:258-69.
de Thé G. Role of Epstein-Barr virus in human diseases: infectious mononucleosis, Burkitt's lymphoma and nasopharyngeal carcinoma. In: Klein G, ed. Viral Oncology. New York: Raven Press, 1980; 769.
Feman SS, Niwayana G, Hepler RS, Foos RY. "Burkitt tumor" with intraocular involvement. Surv Ophthalmol 1969;14:106-11.
Flandrin G, Brouet JC, Daniel MT, Preud'homme JL. Acute leukemia with Burkitt's tumor cells: a study of six cases with special reference to lymphocyte surface markers. Blood 1975;45:183-8.
Henle W, Henle G. Evidence for an oncogenic potential of the Epstein-Barr virus. Cancer Res 1973;33:1419-23.
Histopathological definition of Burkitt's tumor. Bull World Health Organ 1969;40:601-7.
Lukes RJ, Collins RD. New approaches to the classification of the lymphomata. Br J Cancer 1975;31[Suppl 2]:1-28.
Mann RB, Jaffe ES, Berard CW. Malignant lymphomas - a conceptual understanding of morphologic diversity. A review. Am J Pathol 1979;94:105-91.
Mann RB, Jaffe ES, Braylan RC, et al. Non-endemic Burkitt's lymphoma: a B-cell tumor related to germinal centers. N Engl J Med 1976;295:685-91.
Nadal D, Caduff R, Frey E, et al. Non-Hodgkin's lymphoma in four children infected with human immunodeficiency virus. Association with Epstein-Barr virus and treatment. Cancer 1994;73:224-30.
Newkirk MM, Shiroky JB, Johnson N, et al. Rheumatic disease patients, prone to Sjögren's syndrome and/or lymphoma, mount an antibody response to BHRF1, the Epstein-Barr viral homologue of BCL-2. Br J Rheumatol 1996;35:1075-81.
O'Conor GT, Rappaport H, Smith EB. Childhood lymphoma resembling "Burkitt tumor" in the United States. Cancer 1965;18:411-7.
Rooney N, Ramsay AD. Lymphomas of the head and neck. II. The B-cell lymphomas. Eur J Cancer 1994;30B:155-9.
Weisenthal RW, Streeten BW, Dubansky AS, et al. Burkitt lymphoma presenting as a conjunctival mass. Ophthalmology 1995;102:129-34.
Wright DH. Burkitt's lymphoma: a review of the pathology, immunology, and possible etiologic factors. Pathol Annu 1971;6:336-63.
Ziegler JL. Treatment results of 54 American patients with Burkitt's lymphoma are similar to the African experience. New Engl J Med 1977;297:75-80.
Ziegler JL, Magrath IT. Burkitt's lymphoma. Pathobiol Annu 1974;4:129-42.

T-Cell Lymphomas

Bunn PA Jr, Carney DN. Treatment of cutaneous T-cell lymphoma. J Dermatol Surg Oncol 1980;6:383-7.
Chiang AK, Chan AC, Srivastava G, Ho FC. Nasal T/natural killer (NK)-cell lymphomas are derived from Epstein-Barr virus-infected cytotoxic lymphocytes of both NK- and T-cell lineage. Int J Cancer 1997;73:332-8.
Chu AC. The use of monoclonal antibodies in the in situ identification of T-cell subpopulations in cutaneous T-cell lymphoma. J Cutan Pathol 1983;10:479-98.
Coupland SE, Foss H-D, Assaf C, et al. T-cell and T/natural killer-cell lymphomas involving ocular and ocular adnexal tissues. A clinicopathologic, immunohistochemical, and molecular study of seven cases. Ophthalmology 1999;106:2109-20.
Diamandidou E, Cohen PR, Kurzrock R. Mycosis fungoides and Sézary syndrome. Blood 1996;88:2385-409.
Edelson RL. Cutaneous T cell lymphoma: mycosis fungoides, Sézary syndrome, and other variants. J Am Acad Dermatol 1980;2:89-106.
Edelson RL. Cutaneous T-cell lymphoma. J Dermatol Surg Oncol 1980;6:358-68.
Edelson RL, Raafat J, Berger CL, et al. Antithymocyte globulin in the management of cutaneous T cell lymphoma. Cancer Treat Rep 1979;63:675-80.
Epstein EH Jr. Mycosis fungoides: clinical course and cellular abnormalities. J Invest Dermatol 1980;75:103-6.
Epstein EH Jr, Levin DL, Croft JD Jr, Lutzner MA. Mycosis fungoides. Survival, prognostic features, response to therapy, and autopsy findings. Medicine 1972;51:61-72.
Haynes BF, Metzgar RS, Minna JD, Bunn PA. Phenotypic characterization of cutaneous T-cell lymphoma. Use of monoclonal antibodies to compare with other malignant T-cells. N Engl J Med 1981;304:1319-23.
Jaffe ES, Chan JK, Su IJ, et al. Report on the Workshop on Nasal and Related Extranodal Angiocentric T/Natural Killer Cell Lymphomas. Definitions, differential diagnosis, and epidemiology. Am J Surg Pathol 1996;20:103-11.
Kwong YL, Chan AC, Liang R, et al. CD56+ NK lymphomas: clinicopathological features and prognosis. Br J Hematol 1997;97:821-9.
Lauer SA, Fischer J, Jones J, et al. Orbital T-cell lymphoma in human T-cell leukemia virus-I infection. Ophthalmology 1988;95:110-5.
Leidenix MJ, Mamalis N, Olson RJ, et al. Primary T-cell immunoblastic lymphoma of the orbit in a pediatric patient. Ophthalmology 1993;100:998-1002.
Levi JA, Wiernik PH. Management of mycosis fungoides - current status and future prospects. Medicine 1975;54:73-88.
Lutzner M, Edelson R, Schein P, et al. Cutaneous T-cell lymphomas: the Sézary syndrome, mycosis fungoides, and related disorders. Ann Intern Med 1975;83:534-52.
Lipp RW, Sill H, Aigner R, et al. Gallium-67-citrate scintigraphy of high-grade T-cell non-Hodgkin's lymphoma. J Nucl Med 1996;37:1524-5.
Meekins B, Proia AD, Klintworth GK. Cutaneous T cell lymphoma presenting as a rapidly enlarging ocular adnexal tumor. Am Acad Ophthalmol 1985;92:1288-93.
Meyer JH, Scharf B, Gerling J. Midline granuloma presenting as orbital cellulitis. Graefes Arch Clin Exp Ophthalmol 1996;234:137-9.
Rappaport H, Thomas LB. Mycosis fungoides: the pathology of extracutaneous involvement. Cancer 1974;34:1198-229.
Safai B, Good RA. Lymphoproliferative disorders of the T-cell series: a review. Medicine 1980;59:335-51.
Shapiro PE, Pinto FJ. The histologic spectrum of mycosis fungoides/Sezary syndrome (cutaneous T-cell lymphoma). A review of 222 biopsies, including newly described patterns and the earliest pathologic changes. Am J Surg Pathol 1994;18:645-67.
Stenson S, Ramsay DL. Ocular findings in mycosis fungoides. Arch Ophthalmol 1981;99:272-7.
Vonderheid EC. Evaluation and treatment of mycosis fungoides lymphoma. Int J Dermatol 1980;19:182-8.
Zucker JL, Doyle MF. Mycosis fungoides metastatic to the orbit. Arch Ophthalmol 1991;109:688-91.

Leukemia: Granulocytic Sarcoma

Brugo EA, Larkin E, Molina-Escobar J, Contanzi J. Primary granulocytic sarcoma of the small bowel. Cancer 1975;35:1333-40.
Bulas RB, Laine FJ, Das Narla L. Bilateral orbital granulocytic sarcoma (chloroma) preceding the blast phase of acute myelogenous leukemia: CT findings. Ped Radiol 1995;25:488-9.
Cavdar AO, Babacan E, Gozdasoglu S, et al. High risk subgroup of acute myelomonocytic leukemia (AMML) with orbito-ocular granulocytic sarcoma (OOGS) in Turkish children. Retrospective analysis of clinical, hematological, ultrastructural and therapeutical findings of thirty-three OOGS. Acta Haematologica 1989;81:80-5.
Edgerton AE. Chloroma: report of a case and a review of the literature. Trans Am Ophthalmol Soc 1947;45:376-414.

Krause JR. Granulocytic sarcoma preceding acute leukemia. Cancer 1979;44:1017-21.
Leder LD. Ueber die selective Ferment cytochemische Darstellung von neutrophilen myeloischen Zellen und Gewebsmastzellen im Paraffinschnitt. Klin Wschr 1964;42:553
Liu PI, Ishimaru T, McGregor DH, et al. Autopsy study of granulocytic sarcoma (chloroma) in patients with myelogenous leukemia, Hiroshima-Nagasaki 1949-1969. Cancer 1973;31:948-55.
Long JC, Berard CW. Short Course 42: The Pathology of Lymph Nodes. New Orleans: International Academy of Pathology, 1980.
Mason TE, Demaree RS Jr, Margolis CL. Granulocytic sarcoma (chloroma) two years preceding myelogenous leukemia. Cancer 1973;31:423-32.
Specchia G, Palumbo G, Pastore D, et al. Extramedullary blast crisis in chronic myeloid leukemia. Leukemia Res 1996;20:905-8.
Wiernik PH, Serpick AA. Granulocytic sarcoma (chloroma). Blood 1970;35:361-9.
Zimmerman LE, Font RL. Ophthalmologic manifestations of granulocytic sarcoma (myeloid sarcoma or chloroma). The Third Pan American Association of Ophthalmology and American Academy of Ophthalmology lecture. Am J Ophthalmol 1975;80:975-90.

Plasma Cell Tumors

Aboud N, Sullivan T, Whitehead K. Primary extramedullary plasmacytoma of the orbit. Aust N Z J Ophthalmol 1995;23:235-9.
Adkins JW, Shields JA, Shields CL, et al. Plasmacytoma of the eye and orbit. Int Ophthalmol 1996-97;20:339-43.
Azar HA. Pathology of multiple myeloma and related growths. In: Azar H, Potter M, eds. Multiple Myeloma and Related Disorders. New York: Harper & Row, 1973; v. 1; 1-85.
Benjamin I, Taylor H, Spindler J. Orbital and conjunctival involvement in multiple myeloma. Report of a case. Am J Clin Pathol 1975;63:811-7.
Bush SE, Goffinet DR, Bagshaw MA. Extramedullary plasmacytoma of the head and neck. Radiology 1981;140:801-5.
Clarke E. Plasma cell myeloma of the orbit. Br J Ophthalmol 1953;37:543-54.
Dolin S, Dewar JP. Extramedullary plasmacytoma. Am J Pathol 1956;32:83-103.
Fine RS, Amjad H, Schneider JR. Case report. Plasmacytoma presenting as unilateral proptosis. Postgrad Med 1978;64:178-9.
Harwood AR, Knowling MA, Bergsagel DE. Radiotherapy of extramedullary plasmacytoma of the head and neck. Clin Radiol 1981;32:31-6.
Hayes JG, Petersen M, Kakulas BA. Multiple myeloma with bilateral orbital infiltration and polyneuropathy. Med J Aust 1980;2:276-7.
Hellwig CA. Extramedullary plasma cell tumors as observed in various locations. Arch Pathol 1943;36:95-111.
Jonasson F. Orbital plasma cell tumors. Ophthalmologica 1978;177:152-7.
Kennerdell JS, Jannetta PJ, Johnson BL. A steroid-sensitive solitary intracranial plasmacytoma. Arch Ophthalmol 1974;92:393-8.
Kim H, Heller P, Rappaport H. Monoclonal gammopathies associated with lymphoproliferative disorders: a morphologic study. Am J Clin Pathol 1973;59:282-94.
Kincaid MC, Green WR. Diagnostic methods in orbital diseases. Ophthalmology 1984;91:719-25.
Knowles DM 2nd, Halper JA, Trokel S, Jakobiec FA. Immunofluorescent and immunoperoxidase characteristics of IgD lambda myeloma involving the orbit. Am J Ophthalmol 1978;85:485-94.
Knowling MA, Harwood AR, Bergsagel DE. Comparison of extramedullary plasmacytomas with solitary and multiple plasma cell tumor of bone. J Clin Oncol 1983;1:255-62.
Kurzel RB, Mausolf F. Orbital involvement of an extramedullary plasmacytoma. Ophthalmologica 1978;176:241-4.
Kyle RA. Multiple myeloma: review of 869 cases. Mayo Clin Proc 1975;50:29-40.
Levin SR, Spaulding AG, Wirman JA. Multiple myeloma. Orbital involvement in a youth. Arch Ophthalmol 1977;95:642-4.
Lewinski UH, Klein B, Gafter U, Djaldetti M. Acute plasma cell leukemia followed by extramedullary plasmacytoma. Br J Haematol 1980;24:131-6.
Mcfadzean RM. Orbital plasma cell myeloma. Br J Ophthalmol 1975;59:164-5.
Maeda Y, Tani E, Nakano M, Matsumoto T. Plasma cell granuloma of the fourth ventricle. J Neurosurg 1984;60:1291-6.
Mewis-Levin L, Garcia CA, Olson JD. Plasma cell myeloma of the orbit. Ann Ophthalmol 1981;17:477-81.
Mill WB, Griffith R. The role of radiation therapy in the management of plasma cell tumors. Cancer 1980;45:647-52.
Mustoe TA, Fried MP, Goodman ML, et al. Osteosclerotic plasmacytoma of maxillary bone (orbital floor). J Laryngol Otol 1984;98:929-38.
Pasmantier MW, Azar HA. Extraskeletal spread in multiple plasma cell myeloma. Cancer 1969;23:167-74.
Pasternak S, White VA, Gascoyne RD, et al. Monoclonal origin of localised orbital amyloidosis detected by molecular analysis. Br J Ophthalmol 1996;80:1013-7.
Rappaport K, Liesegang TJ, Menke DH, Czervionke LF. Plasmacytoma manifesting as recurrent cellulitis and hematic cyst of the orbit. Am J Ophthalmol 1996;122:595-7.
Rodman HI, Font RL. Orbital involvement in multiple myeloma. Review of the literature and report of three cases. Arch Ophthalmol 1972;87:30-5.
Schreiman JS, McLeod RA, Kyle RA, Beabout JW. Multiple myeloma: evaluation by CT. Radiology 1985;154:483-6.
Sharma MC, Mahapatra AK, Gaikwad S, Biswal A. Primary extramedullary orbital plasmacytoma in a child. Child Nerv Sys 1996;12:470-2.
Tong D, Griffin TW, Laramore GF, et al. Solitary plasmacytoma of bone and soft tissues. Radiology 1980;135:195-8.
Vaquero J, Areitio E, Martinez R. Intracranial parasellar plasmacytoma. Arch Neurol 1982;39:738.
Wiltshaw E. The natural history of extramedullary plasmacytoma and its relation to solitary myeloma of bone and myelomatosis. Medicine 1976;55:217-38.
Woodruff RK, Whittle JM, Malpass JS. Solitary plasmacytoma. I: extramedullary soft tissue plasmacytoma. Cancer 1979;43:2340-3.
Yakulis R, Dawson RR, Wang SE, Kennerdell JS. Fine needle aspiration diagnosis of orbital plasmacytoma with amyloidosis. A case report. Acta Cytologica 1995;39:104-10.

Hodgkin's Lymphoma

Anagnostopoulos I, Hansmann M-L, Franssila K, et al. European Task Force on Lymphoma project on lymphocyte predominance Hodgkin disease: histologic and immunohistologic analysis of submitted cases reveals 2 types of Hodgkin disease with a nodular growth pattern and abundant lymphocytes. Blood 2000;96:1889-99.
Consul BN, Kulshrestha OP. Hodgkin's disease and bilateral exophthalmos. Am J Ophthalmol 1963;56:462.
Fratkin JD, Shammas HF, Miller SD. Disseminated Hodgkin's disease with bilateral orbital involvement. Arch Ophthalmol 1978;96:102-4.
Mason DY, Banks PM, Chan J, et al. Nodular lymphocyte predominance Hodgkin's disease. A distinct clinicopathological entity. Am J Surg Pathol 1994;18:526-30.
Patel S, Rootman J. Nodular sclerosing Hodgkin's disease of the orbit. Ophthalmology 1983;90:1433-6.
Sen DK, Mohan H, Chatterjee PK. Hodgkin's disease of the orbit. Int Surg 1971;55:183-6.

Langerhans' Cell Histiocytosis

Avery ME, McAfee JG, Guild HG. The course and prognosis of reticuloendotheliosis (eosinophilic granuloma, Schüller-Christian disease and Letterer-Siwe disease); a study of forty cases. Am J Med 1957;22:636-52.

Baghdassarian SA, Shammas HF. Eosinophilic granuloma of orbit. Ann Ophthalmol 1977;9:1247-51.

Caputo R. Langerhans cell histiocytosis. In: Freedberg IM, Eisen AZ, Wolff K, et al, eds. Fitzpatrick's Dermatology in General Medicine. 5th ed. New York: McGraw-Hill, 1999; v. 2; 1882-92.

Chawla HB, Cullen JF. Eosinophilic granuloma of the orbit. J Pediatr Ophthalmol 1968;5:93-5.

Enriquez P, Dahlin DC, Hayles AB, Henderson ED. Histiocytosis X: a clinical study. Mayo Clin Proc 1967;42:88-99.

Favara BE, McCarthy RC, Mierau GW. Histiocytosis X. Hum Pathol 1983;14:663-76.

Heuer HE. Eosinophilic granuloma of the orbit. Acta Ophthalmol 1972;50:160-5.

Lichtenstein L. Histiocytosis X. Integration of eosinophilic granuloma of bone, “Letterer-Siwe disease,” and “Schüller-Christian disease” as related manifestations of a single nosologic entity. Arch Pathol 1953;56:84-102.

Lichtenstein L, Jaffe HL. Eosinophilic granuloma of bone, with report of a case. Am J Pathol 1940;16:595-604.

Nesbit ME Jr, Wolfson JJ, Kieffer SA, Peterson HO. Orbital sclerosis in histiocytosis X. Am J Roentgenol Rad Ther Nucl Med 1970;110:123-8.

Oberman HA. Idiopathic histiocytosis: a correlative review of eosinophilic granuloma, Hand-Schüller-Christian disease and Letterer-Siewe disease. J Pediatr Ophthalmol 1968;5:86-92.

Okada K, Minamoto A, Sakata H, Mizote H. Bilateral choroidal osteomas associated with histiocytosis X. Jap J Ophthalmol 1996;40:111-5.

Straatsma BR. Eosinophilic granuloma of bone. Trans Am Acad Ophthalmol Otolaryngol 1958;62:771-6.

Malignant Histiocytosis

Ballard JO, Binder RA, Rath CE, Powell D. Malignant histiocytosis in a patient presenting with leukocytosis, eosinophilia, and lymph node granuloma. Cancer 1975;35:1444-8.

Copie-Bergman C, Wotherspoon AC, Norton AJ, et al. True histiocytic lymphoma: morphologic, immunohistochemical, and molecular genetic study of 13 cases. Am J Surg Pathol 1998;22:1386-92.

Henderson DW, Sage RE. Malignant histiocytosis with eosinophilia. Cancer 1973;32:1421-8.

Ho FCS, Todd D. Malignant histiocytosis: report of 5 Chinese patients. Cancer 1978;42:2450-60.

Lampert IA, Catovsky D, Bergier N. Malignant histiocytosis: a clinico-pathological study of 12 cases. Br J Haematol 1978;40:65-77.

Scott RB, Robb-Smith AHT. Histiocytic medullary reticulosis. Lancet 1939;2:194-8.

Stein H, Mason DY, Gerdes J, et al. The expression of the Hodgkin's disease associated antigen Ki-1 in reactive and neoplastic lymphoid tissue: evidence that Reed-Sternberg cells and histiocytic malignancies are derived from activated lymphoid cells. Blood 1985;66:848-58.

Stein RS, Moran EM, Byrne GE Jr. Malignant histiocytosis: complete remission with combination chemotherapy. Cancer 1976;38:1083-6.

Vilpo JA, Klemi P, Lassila O, et al. Cytological and functional characterization of three cases of malignant histiocytosis. Cancer 1980;46:1795-801.

Warnke RA, Kim H, Dorfman RD. Malignant histiocytosis (histiocytic medullary reticulosis). I. Clinicopathologic study of 29 cases. Cancer 1975;35:215-30.

Zucker JM, Caillaux JM, Vanel D, Gerard-Marchault R. Malignant histiocytosis in childhood. Cancer 1980;45:2821-9.

Chapter 11
Structural Lesions

Structural lesions, which comprise approximately 15% of this series, constitute a variety of disorders of both a congenital and acquired nature. The congenital lesions are hamartomas, choristomas, and teratomas as well as ectopias and bony anomalies, including mesodermal defects. The acquired structural lesions consist of postinflammatory, traumatic, and posttraumatic lesions of the orbit.

Cystic

There are numerous ways to classify cystic lesions of the orbit. They can either be congenital or acquired, with further division based on tissue type, location, and etiology. In terms of the differential diagnosis, there are a wide range of orbital lesions that have cystic elements. Clinically, anterior cysts have a characteristic consistency and contour with smooth edges and in some instances, compressibility. When filled with clear fluid, they may transilluminate. If situated deeper within the orbit, they present as mass lesions and are diagnosed primarily on the basis of imaging characteristics. Cysts share the common feature of a roughly spherical cavity filled with material of a different density than the surrounding tissue. They may be multilocular. Often, there is an abrupt transition from the cyst wall to the cavity, which accounts for features on imaging. When cystic lesions involve bone, the effect may be to excavate and expand locally when they are encapsulated, or cause lysis when they have associated inflammatory responses wherein the margins may be more irregular.

Recognizing cystic from solid lesions is useful in developing a differential diagnosis. For practical purposes, cysts can be divided into those of epithelial and nonepithelial origin (Figs. 11-1 and 11-2). The primary focus in this discussion will be on epithelial cysts of congenital and acquired origin and some of the neurogenic cysts.

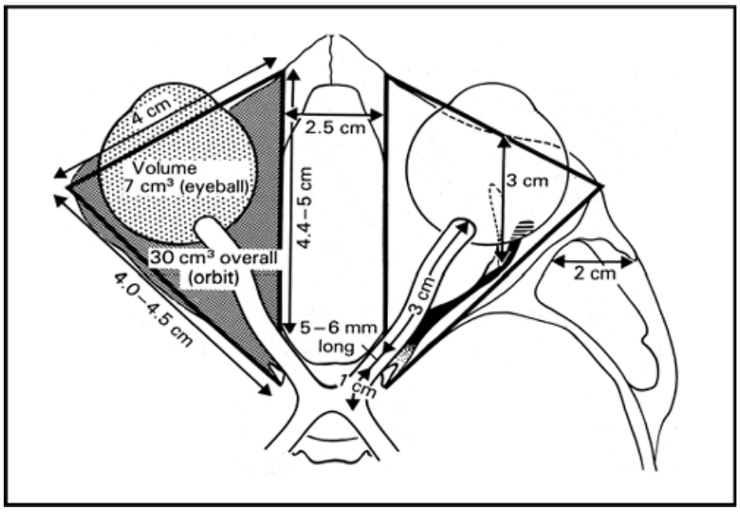

Figure 11-1. Cystic lesions with an epithelial lining are divided into congenital and acquired forms and further defined according to the type of epithelial lining. (Reproduced with permission from Lessner AM, Antle CM, Rootman J, et al. Cystic lesions of the orbit and radiolucent defects of bone. In: Margo CE, Hamed LM, Mames RN, eds. Diagnostic Problems in Clinical Ophthalmology. Philadelphia: WB Saunders, 1994:87-98.)

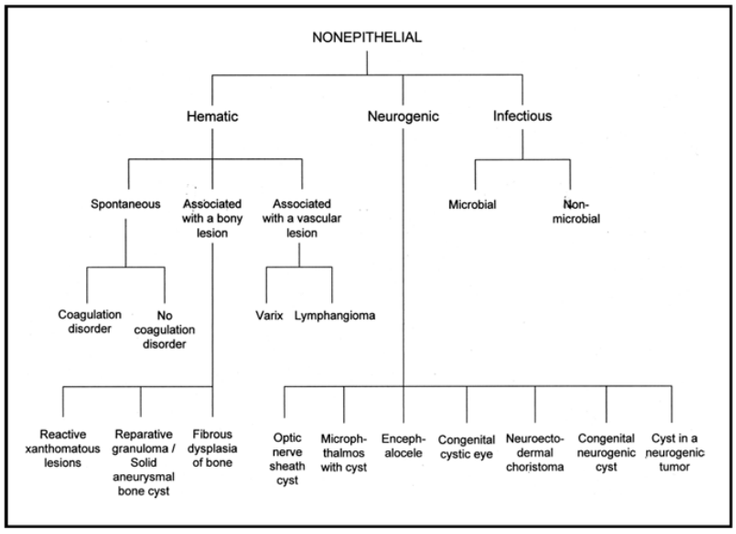

Figure 11-2. Cystic lesions without an epithelial lining fall into three categories: hematic, neurogenic, and infectious. Further subdivisions are based primarily on histopathologic findings or on etiology. (Reproduced with permission from Lessner AM, Antle CM, Rootman J, et al. Cystic lesions of the orbit and radiolucent defects of bone. In: Margo CE, Hamed LM, Mames RN, eds. Diagnostic Problems in Clinical Ophthalmology. Philadelphia: WB Saunders, 1994;87-98.)

Conjunctival Epithelial Cysts

Congenital

Dermoid and Epidermoid Cysts

Orbital and periorbital dermoid cysts present in a variety of ways depending upon the suture of origin, size, rate of growth, and potential for rupture. They are developmental choristomas, representing 2.2% of our overall series and approximately 6.0% of orbital tumors. They are thought to arise from ectodermal rests pinched off at suture lines. They represent 10% of head and neck dermoids, most occurring in the upper outer quadrant, but they may develop virtually anywhere within and adjacent to the orbit. Dermoids typically exert a noninfiltrative mass effect, develop slowly, and displace adjacent structures. Although they often have histologic features of rupture (about 50%), less than 15% in our series were associated clinically with low-grade inflammatory features and they rarely fistulize spontaneously.

Clinically, these cysts can be divided into two groups, superficial (simple, exophytic) and deep (complicated, endophytic). The presentation, progression, complications, and management are related to the type of dermoid.

Dermoids and epidermoids are lined by squamous epithelium. In the case of the dermoid, adnexal structures are also noted in and adjacent to the epithelial lining in contrast to epidermoids that are lined by squamous epithelium alone.

Overall, approximately 70% of dermoids and epidermoids are superotemporal, and 90% are characterized by the presence of a painless subcutaneous mass. Histopathologically, dermoids are lined by keratinized epithelium but rarely can have nonkeratinizing epithelium. Almost all cases have evidence of pilosebaceous structures and hair shafts as well as sebaceous glands. Sweat glands are seen in about 20%.

On imaging, the majority have adjacent bone change and approximately half have differential attenuation that suggests fat. About 15% have calcification and a small percentage have fluid levels. In the majority of cases, there is a well-defined wall; however, significant rupture is associated with irregular walls and spillover into adjacent tissue of multiple fat densities, surrounded by infiltration (see Fig. 11-11). The most common bony change is pressure excavation by the lesion. The presence of a tunnel or channel through the adjacent wall is noted in about one third of cases with fewer having evidence of a blind pit or cleft in the bone. Irregular bony margins suggest rupture with granulomatous destruction of the adjacent bone. A rare clinical feature of a ruptured cyst that we have seen in two of our patients was the presence of subconjunctival fat droplets. Overall, management consists of observation of some of the superficial lesions but the majority require complete extirpation.

Superficial Dermoid Cysts

Superficial dermoids usually present in infancy (up to age three) as localized rounded periorbital masses, often situated temporally (frontozygomatic suture, deep temporalis

fossa) and less frequently medially (Figs. 11-3 and 11-4). In our series, two third had an anterior component and within this group, approximately 60% originated from the frontozygomatic suture, 25% originated medially from the frontolacrimal suture, and 6% in the deep temporalis fossa. They are usually painless, firm, and immobile and cause little ocular or lid displacement. Most are 1 to 2 cm in size, nonfluctuant, and on palpation the posterior edge does not extend around the bony orbital margin.

On imaging, they are rounded and well-defined. About 40% of the time they will have a center of fat density (Fig. 11-4) with little significant bony defect other than indentations or pits with occasional channels producing a dumbbell feature.

They are best managed by direct excision of the entire dermoid including its base, generally between the first and fifth year of life to avoid traumatic rupture. In our experience these have been histologically typical dermoid cysts, usually with intact walls lined by keratinized squamous epithelium. In approximately half, focal areas of granulomatous inflammation line the wall of the cyst replacing the epithelium and spilling over to varying degrees into the adjacent tissues.

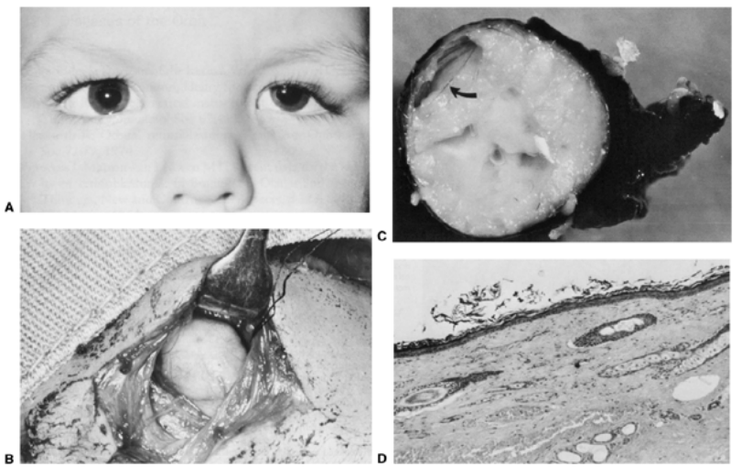

Figure 11-3. (A) A 30-month-old boy with a left superotemporal superficial dermoid arising from the frontozygomatic suture. (B) This was surgically removed and had a smooth contour and pale color. (C) Gross photomicrograph of the dermoid reveals a thin wall, keratin and lipid debris, and hair (arrow). (D) The cyst wall shows keratinized lining, abortive sebaceous structures, and hair (H&E, original magnification × 10). (Reproduced with permission from Sherman RP, Rootman J, Lapointe JS. Orbital dermoids: clinical presentation and management. Br J Ophthalmol 1981;68:642-52.)

Deep Dermoid Cysts

Complicated orbital dermoids (30% of our series) typically arise within the bony orbit and present as insidious masses later in life, which in retrospect are frequently present for many years. They can originate from any of the suture lines (especially frontozygomatic) or even from the diploic sites in the apex. If palpable, they typically have rounded anterior margins with extension of the mass deep into the orbit. Unless they have been previously incised or chronically ruptured, they rarely cause entrapment of adjacent structures and are dominated clinically by mass effect, causing displacement and distortion of the globe. They can rarely present with a fistula that is secondary to partial excision or even spontaneously occurring (Fig. 11-5). In our experience, the extent and complexity of deeper dermoids are frequently underestimated on referral, especially when the anterior margins are palpable superficially (Fig. 11-6).

Careful imaging is important to distinguish the deep lesions, which may have dumbbell components into the temporalis fossa, intracranial cavity, and the sinuses (Figs. 11-7 and 11-8). Rarely temporalis erosion is associated with chewing induced oscillopsia. On imaging, these lesions have a constellation of findings that together may permit specific

diagnosis. Characteristically, the margins are well defined and the central portion may have an intermediate density between fat and muscle. In some instances, the density may be equivalent to fat, but when present is pathognomonic (Fig. 11-9). About 15% have focal, fine areas of calcification in the wall. The bony changes are of particular note and consist of focal or generalized enlargement or excavation of the adjacent bony walls (Fig. 11-10). When the margins are irregular, notched, or associated with thickened walls and adjacent orbital infiltration, rupture and granulomatous inflammation are likely (Fig. 11-11).

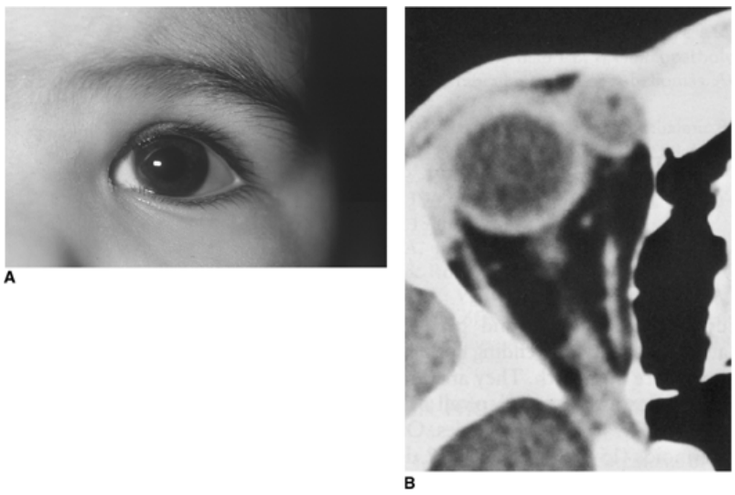

Figure 11-4. (A) A 15-month-old patient presented with a dermoid in the superomedial aspect of the left lid. It had been present since birth but had shown progressive growth over the last 3 months. (B) An axial CT scan shows a well-defined capsule, contents of lower density, and excavation of adjacent bone. Note the small area of fat density in the center of the lesion. (Reproduced with permission from Sherman RP, Rootman J, Lapointe JS. Orbital dermoids: clinical presentation and management. Br J Ophthalmol 1981;68:642-52.)

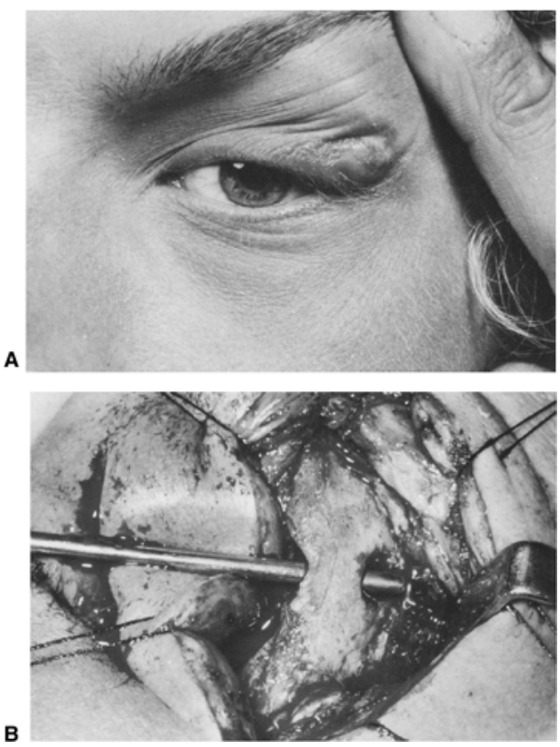

Figure 11-5. (A) A 21-year-old patient presented with a mass and a draining fistula in the superolateral aspect of the left lid after drainage of a so-called chalazion. (B) Photomicrograph taken at surgery shows the suction tip extending through a defect in the frontozygomatic suture into the temporalis fossa, where the outer portion of a dumbbell dermoid lies. (Reproduced with permission from Sherman RP, Rootman J, Lapointe JS. Orbital dermoids: clinical presentation and management. Br J Ophthalmol 1981;68:642-52.)

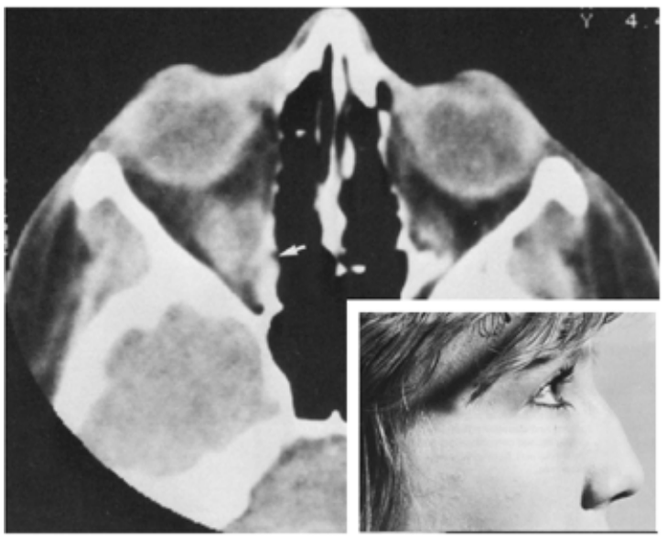

Figure 11-6. This 17-year-old female presented with a thickened right lower lid and elevated globe due to an inferior deep orbital dermoid, which had been excised but recurred repeatedly prior to referral. Her CT scan revealed that the posterior aspect of the orbital mass was immediately inferior to the optic nerve and abutted the medial orbital wall. Note dehiscence in the posterior medial wall (arrow). This was the site of origin noted at the time of excision of the dermoid cyst. (Reproduced with permission from Sherman RP, Rootman J, Lapointe JS. Orbital dermoids: clinical presentation and management. Br J Ophthalmol 1981;68:642-52.)

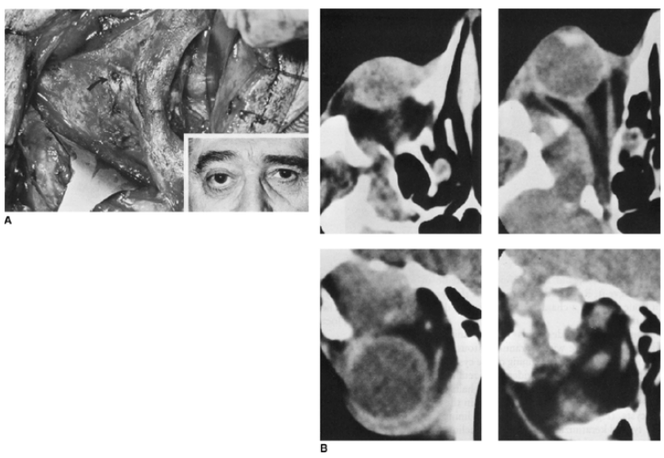

Figure 11-7. (A) This 56-year-old male presented with a long-standing history of progressive proptosis and downward displacement of his right eye due to an extensive deep orbital dermoid. The surgical photograph shows the dermoid in the lateral orbit eroding through the bony wall (arrow). (B) Axial and coronal views of the dermoid show erosion of the superior, lateral, and posterolateral walls of the orbit. Note low-density areas due to the presence of fat as well as irregular calcification and exostosis associated with the dermoid.

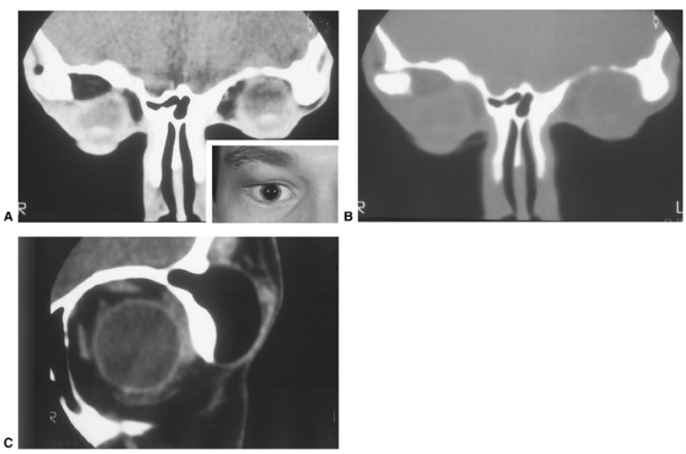

Figure 11-8. This 29-year-old man presented with a 6-week history of a lump in the right upper lid and a long-standing ptosis. (A-inset) He had downward displacement of the globe and an S-shaped deformity of the lid with a palpable mass. (A, B) CT scans demonstrated a low-density dumbbell dermoid in both the orbit and temporalis fossa with a channel through the suture line in the bone. (C) This CT scan demonstrates another dermoid in the temporalis fossa with a deep pit in the bone that did not extend into the orbit or intracranially.

Frontozygomatic dermoids may be difficult to differentiate from solid, malignant, and erosive lacrimal gland lesions. An important distinguishing feature is that the bony change tends to include or extend only to the frontozygomatic suture in dermoids whereas lacrimal tumors extend beyond the sutures. In addition, the well-defined margins on the orbital side associated with relative central lucency are more suggestive of dermoids (Fig. 11-8). Ultrasonography may identify dermoids as cystic but when they contain much debris (including keratin and fat), they may have internal echoes suggestive of a solid tumor, and deeper lesions may be more difficult to characterize.

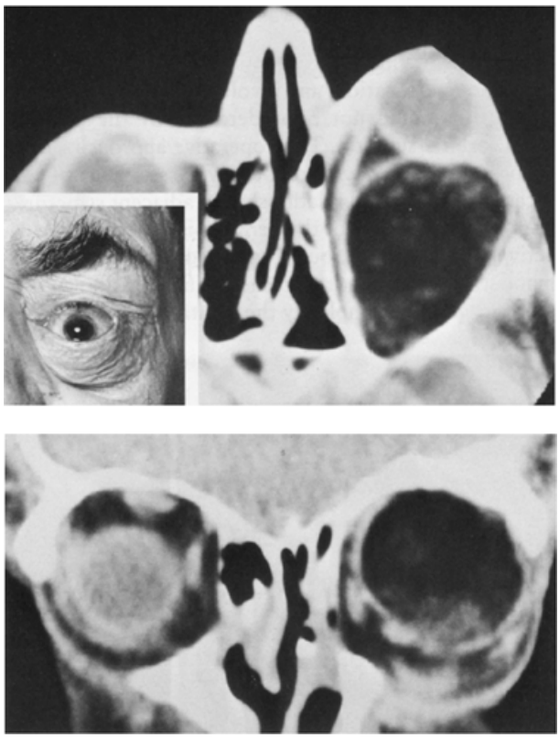

Fig. 11-9. A massive, deep orbital dermoid in a 72-year-old man that had been partially excised 35 years earlier. Note the central lucency due to fat within the lesion. At surgery it was found to be attached to the bone adjacent to the superior orbital fissure.

The differential diagnosis depends in part on the location of the mass. In the lacrimal fossa, primary and secondary lacrimal tumors should be considered; medially, retention cysts or mucoceles can be distinguished by their relationship to the sinuses, evidence of focal destruction of bone, and associated opacification and expansion of the affected sinuses. We have seen several orbitofrontal mucoceles that mimic dermoids in this location, which arose from an old fracture site in the lateral portion of the frontal sinus (which may be noted on scan). Medial encephaloceles can be distinguished by the presence of a focal defect continuous to the cranial cavity; however, this feature is not always present and injection of a contrast medium into the lesion or withdrawal and analysis for evidence of cerebrospinal fluid may help to distinguish cystic lesions involving the orbit, sinuses, and intracranial cavity. Finally, any of the solid orbital tumors and chronic inflammations should be included in the differential diagnosis, especially if there is a focal bony defect.

Management may be complicated and should involve an operative approach based on thorough preoperative assessment of size, location, extent, and relationship to adjacent structures. In principle, the entire dermoid including the active growth center (frequently at the bony interface) needs

to be removed. We first attempt to dissect completely the orbital side of the lesion while it is firm before evacuating it; this allows us to follow the more clearly defined planes when the lesion is intact. Evacuation frequently becomes necessary, which facilitates complete dissection of the lining. Lesions extending intracranially or into adjacent structures require combined orbital approaches. With complete excision of the lining and contents, even with intraoperative rupture, there does not appear to be early or late postoperative morbidity. After excision, the adjacent bone should be smoothed out using a drill to remove any crevices or exostoses. A ruptured dermoid cyst that has eroded adjacent bone produces a characteristic yellowish discoloration of the bone, noted at the time of surgery.

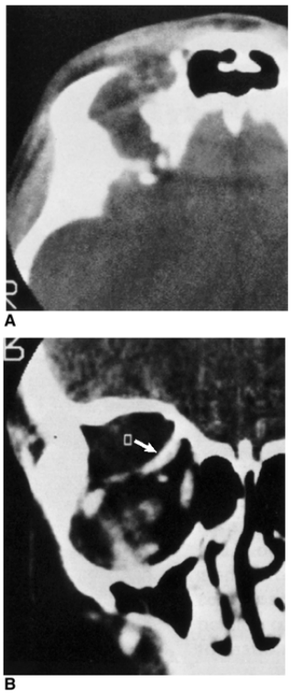

Figure 11-10. Axial (A) and coronal (B) CT scans of a deep dermoid in the orbital roof showing irregular excavation of bone, a lucent center, and rim calcification (arrow).

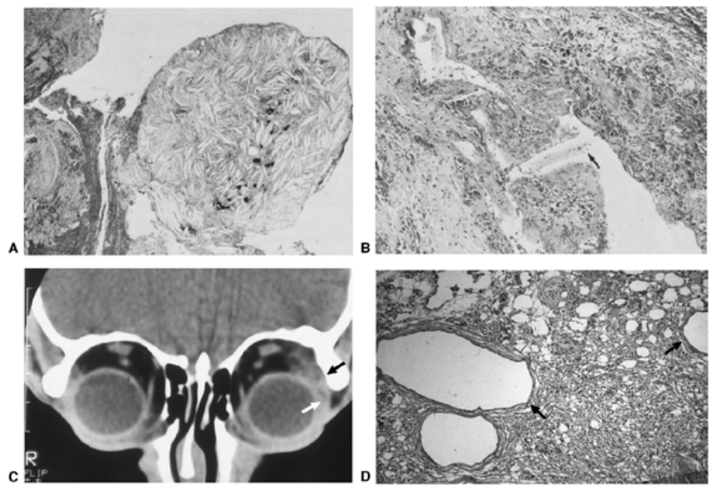

Figure 11-11. (A) A nodule of tissue from the wall of a deep dermoid containing cholesterol clefts surrounded by foreign body reaction (H&E, original magnification × 2.5). (B) Histology of the wall of a deep dermoid showing hair (arrow) surrounded by scar and inflammatory reaction (H&E, original magnification × 10). (C) This CT scan demonstrates a focal excavation of the left lacrimal fossa associated with an adjacent infiltration demonstrating low density areas (arrows). This was seen in a 43-year-old man who presented with a history of two episodes of swelling of his left upper lid. These features suggested a ruptured dermoid, which was excised by lateral orbitotomy along with the adjacent infiltrative area. (D) Histology revealed a granulomatous reaction with multiple fat-containing spaces (arrows) of varying size due to a ruptured dermoid cyst (H&E, original magnification × 10).

Pathologically, deep dermoids almost universally have evidence of rupture with a granulomatous foreign body reaction. In fact, the entire lining of the cyst may be a granulomatous infiltrate with evidence of retained fat, cholesterol clefts, old hemorrhage, and hairs (Fig. 11-11). Calcification may also be noted in the wall of large dermoid cysts. Elsewhere, the lining may consist of typical keratinizing squamous epithelium with adnexal structures, which are sometimes extensive. It is of interest that in spite of histologic evidence of previous rupture, few of our patients (15%) presented with a history of orbital inflammatory signs and symptoms (mostly subacute). The single patient with a fistula had a chronic, low-grade, localized inflammatory reaction.

Rarely, spontaneous squamous cell carcinomas may arise from asymptomatic choristomatous cysts of the orbit.

Conjunctival Dermoid Cysts

Primary conjunctival dermoid cysts often rise medially adjacent to or behind the caruncle (Fig. 11-12). In our series of dermoids, 10% were conjunctival and of these, approximately 42% were medial, 33% lateral, and 9% inferior. They are seen in adolescents or adults and do not have sutural origin or bony abnormalities. They are lined by nonkeratinizing

conjunctival epithelium and contain mucous secreting goblet cells as well as adnexal structures. Management consists of complete extirpation when indicated.

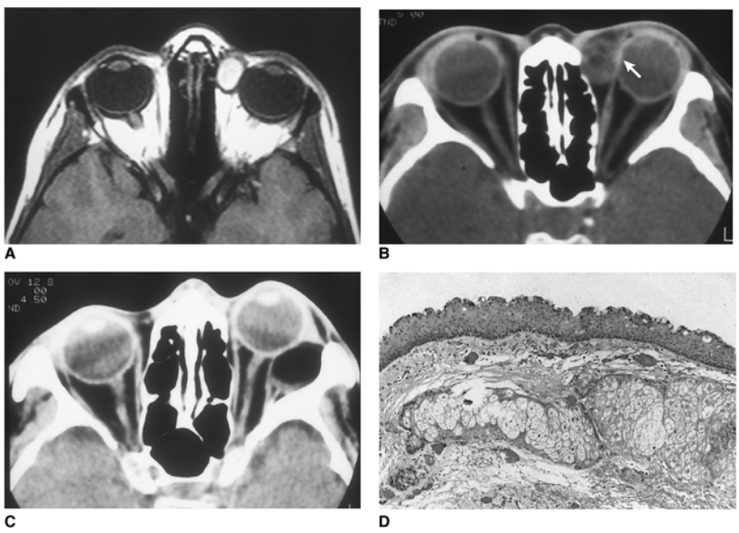

Figure 11-12. Conjunctival dermoids. (A) T1-weighted MR image of a 7-year-old boy demonstrates a medial conjunctival dermoid containing fat. (B) A similar lesion was found in a 50-year-old female. CT scan of the dermoid shows low density changes consistent with fat (arrow). (C) This CT scan of a 43-year-old man demonstrates a deep orbital dermoid in the lacrimal fossa that has excavated the bone and ruptured posteriorly, where the lining was thickened with granulomatous inflammation. (D) Histology of the cyst in (C) demonstrates a nonkeratinizing squamous epithelium with mucin secreting cells and sebaceous glands in the wall of the cyst (H&E, original magnification × 10).

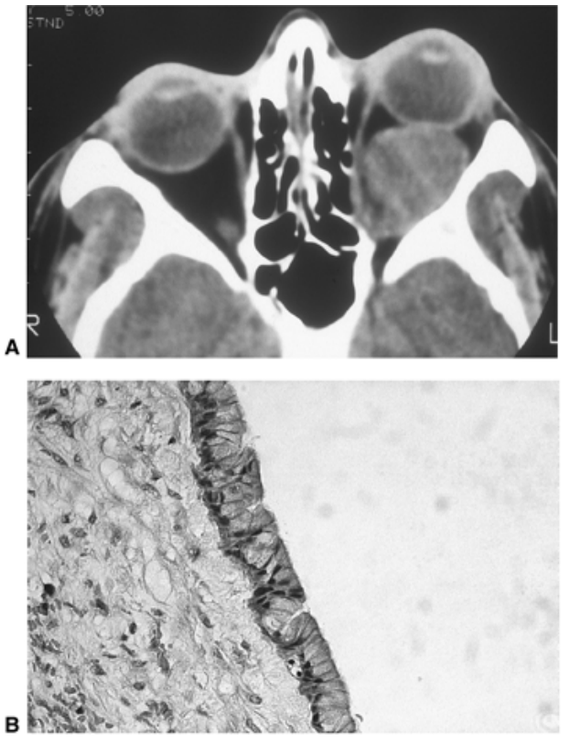

Figure 11-13. (A) The CT scan demonstrates a large intraconal mass with focal excavation of the lateral and medial orbital wall and indentation of the globe, which occurred in a 21-year-old woman who had progressive proptosis and papilledema due to a multilocular respiratory cyst. (B) Histology of the cyst lining is shown. Note the pseudostratified columnar respiratory epithelium (H&E, original magnification × 25).

Epidermoid Cysts

Epidermoid cysts consist of a single layer of epithelium (keratinized or nonkeratinized), without evidence of adnexal structures. These may arise as congenital lesions with clinical features parallel to those described for dermoids, but the majority in a clinical orbital practice are of acquired or traumatic origin.

Miscellaneous Epithelial Cysts

The orbit, eyelid, or ocular adnexa may be affected by a variety of cysts lined by single or multiple types of epithelium. They present with a wide spectrum of clinical features. Respiratory epithelial cysts develop from ectopic rests and in contrast to conjunctival dermoids or epidermoids, they can occur in any part of the orbit. Their lining is made up of pseudostratified columnar epithelium, and they are distinguished from mucoceles by their primary orbital origin and absence of sinus involvement (Fig. 11-13). We have experienced a single case of a Rathke's pouch cyst, which is a rare choristoma derived from a diverticulum of the embryonic buckle cavity (Fig. 11-14). These cysts typically involve the orbit secondarily to other structures such as the skull

base, posterior nasopharynx, and the paranasal sinuses. Pseudoriferous cysts derive from sweat ducts and typically arise from the eyelid but can be encountered in the anterior orbit. Other cysts include those with multiple epithelia, typically nonkeratinizing epithelium with goblet cells and without adnexal structures. We have also seen an apocrine cyst (Fig. 11-15) and have encountered a single case of an epithelial cyst of the lateral rectus muscle (Fig. 11-16). Congenital cysts may also arise from the accessory lacrimal gland but the majority of lacrimal cysts are acquired and arise from the lacrimal ducts.

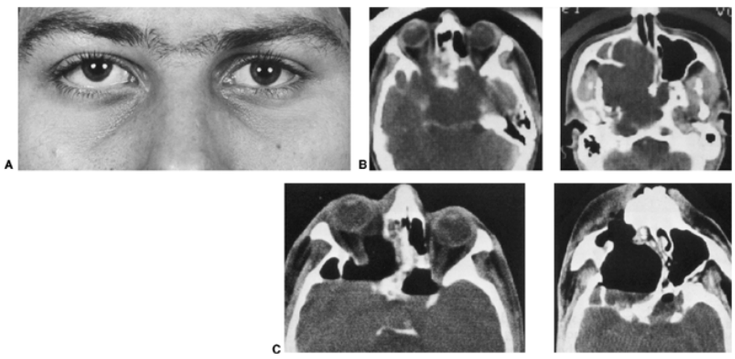

Figure 11-14. (A) A 17-year-old male presented with upward displacement and mild proptosis of the right globe and diplopia in downgaze. (B) Axial CT scans show a large, apparently destructive, lesion of the base of the skull. (C) This axial CT scan was taken after intranasal drainage of the cyst at biopsy. It was diagnosed as a Rathke's pouch cyst. Note air and fluid within the cyst cavity, which extends into the middle cranial fossa.

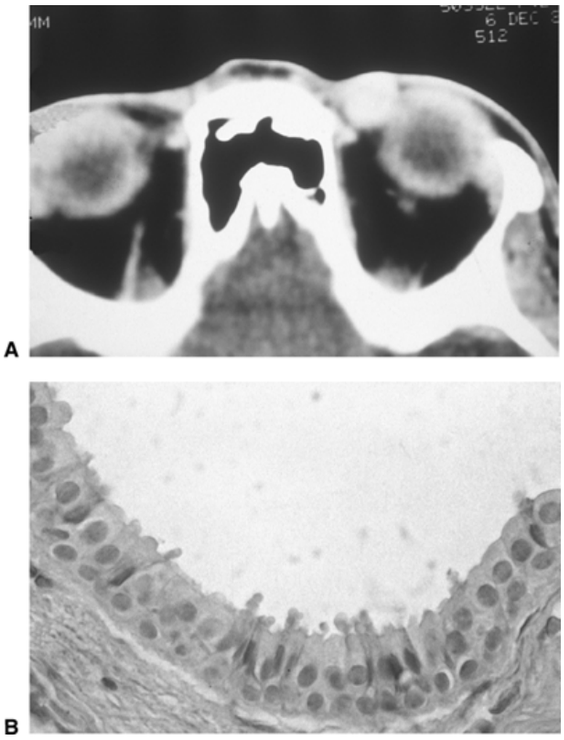

Figure 11-15. (A) This CT scan demonstrates an anterior cystic lesion that occurred in the lid of a 43-year-old woman. Excision revealed an apocrine cyst, the lining of which is shown histologically in (B) (H&E, original magnification × 25).

Acquired Cysts

Mucocele

Pathogenesis and Development

Mucoceles are slowly expanding cystic lesions originating from the sinuses. Their etiology is related to obstruction of the normal sinus ostea and entrapment of the secretory epithelium, which continues to produce mucous, filling the normally aerated space and exerting pressure on the surrounding bony structures. This leads to effacement of the normal septae, expansion of the sinus, thinning of the bony walls, and ultimately extension through the wall into the adjacent orbit, nasopharynx, or cranial cavity. The respiratory epithelium lining the sinus may undergo atrophy with

loss of the normal cilia and goblet cells and replacement by a fibrous capsule (Fig. 11-17). The majority of mucoceles, therefore, contain a clear to slightly yellowish mucoid material. Rarely a pyocele filled with purulent material may be formed when the contents are infected. In the antibiotic era, this is increasingly infrequent. Thus, cyst contents vary from mucoid or viscous to purulent with the majority containing a clear sterile fluid.

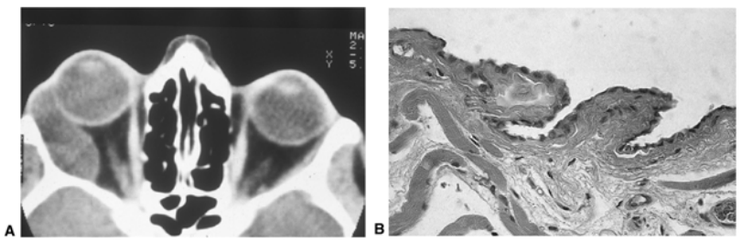

Figure 11-16. (A) This CT scan demonstrates a large lateral orbital cyst within the lateral rectus muscle that presented as a subconjunctival bluish mass in a 48-year-old woman. Excision of the mass revealed a cyst attached within the lateral rectus muscle, which was lined by a single layer of nonkeratinizing squamous epithelium (B) (H&E, original magnification × 25). No adnexal structures were identified and the patient recovered full function after removal of the intramuscular cyst.

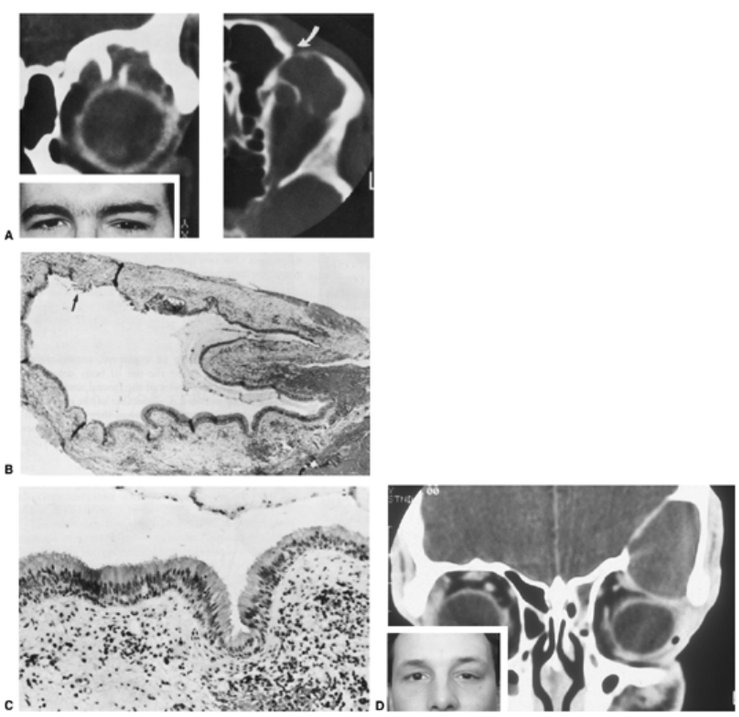

Figure 11-17. (A) This 34-year-old man presented with downward displacement of his left eye. He had also noted diplopia in upgaze. The axial and coronal CT scans show a mucocele arising lateral to a fracture site (arrow) in the frontal sinus and extending inferiorly into the orbit. Note the smooth, scalloped edges and focal calcification. (B, C) Histopathology of the mucocele in (A) shows pseudostratified respiratory epithelium, areas of thinning and loss of epithelium (B, arrow), mucin debris, and surrounding inflammation (H&E, original magnification, B × 2.5, C × 25). (D) This 29-year-old man presented with a history of a relatively acute onset of ptosis and downward displacement of the globe. This had partially resolved and then progressed over approximately a year, leading to severe ptosis and swelling of the upper lid. This was due to a large lateral frontal mucocele that had eroded the roof of the orbit and the adjacent floor of the anterior cranial fossa.

It has been suggested that the usual cause of osteal obstruction is inflammation with secondary scarring, but other contributing factors include fractures (Fig. 11-17), osteomas, polyps, nasal septal deviation, mucous retention cysts, and congenital narrowing of the ostea. Hemorrhage within a mucocele is rare, and associated with brown fluid and cholesterol crystals. A review of the history of patients in our own series suggested that approximately one third had fractures, one third had a history of chronic sinusitis and sinus surgery, and the remaining third had no antecedent history.

Incidence and Distribution

Of the structural lesions in our clinic, mucoceles constituted 10% while overall they represented 1.5% of orbital patients seen. The incidence varies, depending on the series studied, from 2% to 15% but the estimated frequency is 3% or 4% of orbital patients. Most mucoceles involve the frontal or ethmoid sinuses, or both, and occur at any age in both sexes. The majority, however, are seen between the fourth and seventh decades. In this series, the average age was 50.3 years. Rare mucoceles of infancy and childhood may suggest an underlying cystic fibrosis. They develop slowly with an average duration of symptoms of 10 months.

Clinical Features

The clinical features are an expansive, noninfiltrating mass effect dominated by the site of bony erosion or expansion. Thus, mucoceles of the frontal sinus lead to downward and outward displacement of the globe with minimal proptosis, particularly when they occur anteriorly. Posterior extension from the sinus may lead to more downward displacement and proptosis. Psychophysical or oculomotor dysfunction is rare and usually a reflection of an extremely large lesion.

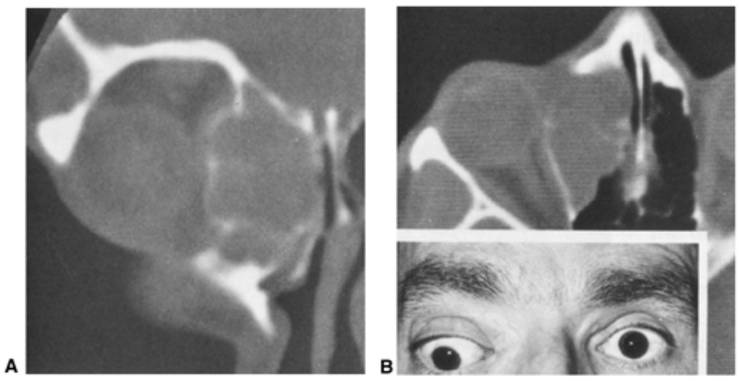

Figure 11-18. This 48-year-old man had down- and outward displacement of his right globe due to a frontoethmoid mucocele, which is shown on coronal (A) and axial (B) CT scans. Note the characteristic expansion of the ethmoid sinus with smooth, scalloped margins and bone formation in the periorbita.

Frontoethmoid mucoceles cause outward and downward displacement, and are often associated with a fullness in the superomedial and medial canthal region with flattening of the nasion and a palpable mass (Fig. 11-18). Rarely, they may be bilateral, leading to a hyperteloric appearance (Fig. 11-19). In our experience ethmoid mucoceles tended to be smaller and characterized by lateral displacement of the globe with minimal exophthalmos. Mucoceles arising from the frontoethmoid complex, when associated with a palpable mass, can be felt above the medial canthal ligament in contrast to lesions of the lacrimal sac, which are generally palpable below the ligament. When they penetrate bone, the periosteal tissues may develop metaplastic bone formation, producing a shell and palpable exostosis at the margin of the lesion (Figs. 11-17A and 11-18). Mucoceles of the frontoethmoid complex, particularly in the young, must be differentiated from cephaloceles. In children, cephaloceles may vary in size with Valsalva maneuver, may be pulsatile, and are usually associated with hypertelorism. On investigation the bony dehiscence from the cranial cavity should be obvious. Nevertheless, the dehiscence may be very tiny, particularly in an adult, and differentiation may be difficult. Fluid aspirate could help to differentiate between cerebrospinal fluid and mucus content.

Mucoceles originating in the sphenoid and posterior ethmoid sinus, because of their intimate relationship to the optic nerve, cavernous sinus, and orbital apex, tend to present with functional abnormalities related to these structures rather than globe displacement and soft tissue changes (Fig. 11-20). Characteristically, the patients have visual symptoms, retrobulbar pain, or nerve palsies, and about half of them have nasal symptoms. Encroachment on the optic canal may cause optic atrophy. Apical orbital and cavernous sinus involvement

lead to extraocular muscle palsies in 50% of the patients (usually third nerve). Sensory nerve compression leads to intermittent apical orbital pain, which may be confused with migraine. The location and ophthalmic manifestations of our series of mucoceles are summarized in Tables 11-1 and 11-2 .

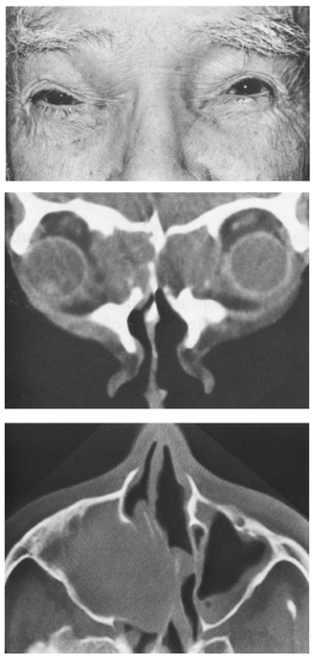

Figure 11-19. This 80-year-old man had progressive hypertelorism due to extensive bilateral mucoceles involving the frontoethmoid and maxillary sinuses.

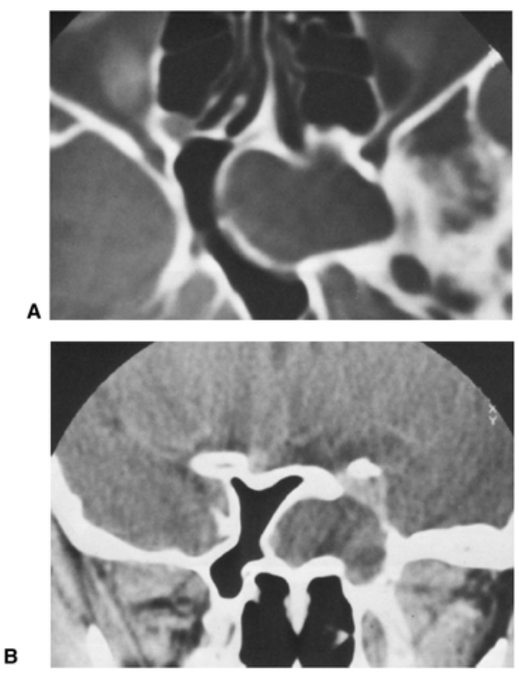

Figure 11-20. Axial (A) and coronal (B) CT scans of a sphenoid sinus mucocele that led to a mild left optic neuropathy, which was due to pressure on the optic nerve.

Table 11-1. Mucoceles classified by sinus involvement, UBC Orbital Clinic, 1976-1999

SINUS	RIGHT	LEFT	BOTH ORBITS	TOTAL
Frontal	6	10	4	20
Fronto-ethmoid	5	4	3	12
Ethmoid	3	5	1	9
Maxillary	2	1		3
Sphenoid	1	1		2
Ethmoid-maxillary		1		1
Fronto-ethmoid-maxillary			1	1
Total				48

An unusual presentation is that of enophthalmos secondary to erosion of the floor of the orbit caused by a maxillary sinus mucocele (silent sinus syndrome) (Fig. 11-21). Maxillary sinus mucoceles are rare and usually lead to upward displacement of the globe; however, erosion of the floor may cause the eye to sink in the expanded orbit. We have seen three such patients. All were characterized by awareness of deepening of the superior sulcus and downward displacement of the globe with enophthalmos, which was usually asymptomatic but intermittent facial pain had been noted in

a few. One patient was aware of a filling of the sulcus on awakening in the morning, brought about by her recumbent position during the night. Imaging demonstrates opacification and implosion of the maxillary sinus, often with erosion of the floor and in some instances, implosion of the lateral wall of the maxillary sinus with an increase in the adjacent cheek fat pad.

Table 11-2. Presenting features of orbital mucoceles, UBC Orbital Clinic, 1976-1999

	SINUS INVOLVED							
CLINCIAL FINDINGS	F	E	M	S	F-E	E-M	F-E-M	TOTAL
Displacement								
Proptosis	6	5	1		5			17
Ptosis	5	2			1			8
Other	3	1	1			1	1	7
Swelling	9	4	1	1	6		1	22
Visual loss or blurring	7	4		2	2			15
Diplopia	7	3	1		2	1		14
Pain	5	3	1		1			10

F = frontal; E = ethmoid; M = maxillary; S = sphenoid

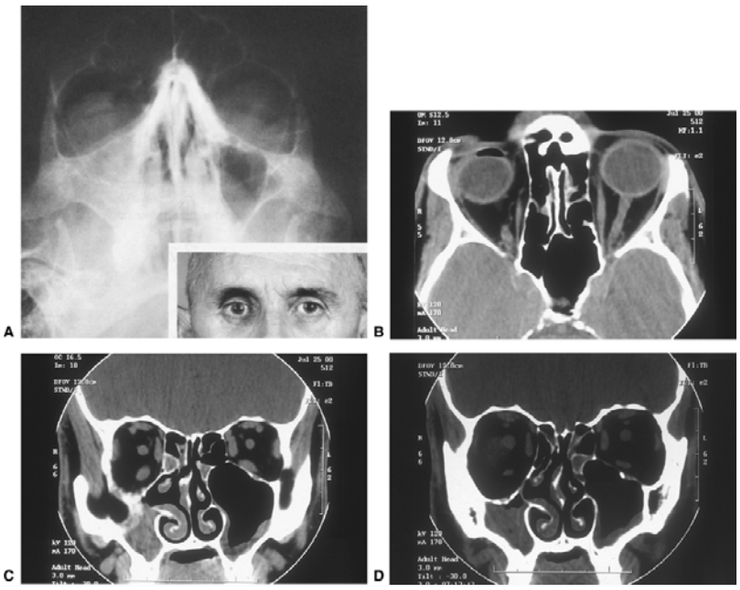

Figure 11-21. Silent sinus syndrome. (A) A 59-year-old man with a right maxillary mucocele that had caused progressive right enophthalmos and globe ptosis. Note the deepened right superior sulcus. These axial (B) and coronal (C, D) scans demonstrate the typical characteristics of the silent sinus syndrome, which is seen in a 35-year-old man who presented with spontaneous enophthalmos. Note the retrusion of the globe (B), enlargement of the orbit due to erosion of the floor (C, D), and implosion of the lateral maxillary wall. (Fig. 11-21A borrowed with permission from Cline RA, Rootman J. Enophthalmos: a clinical review. Ophthalmology 1984;91:22937.)

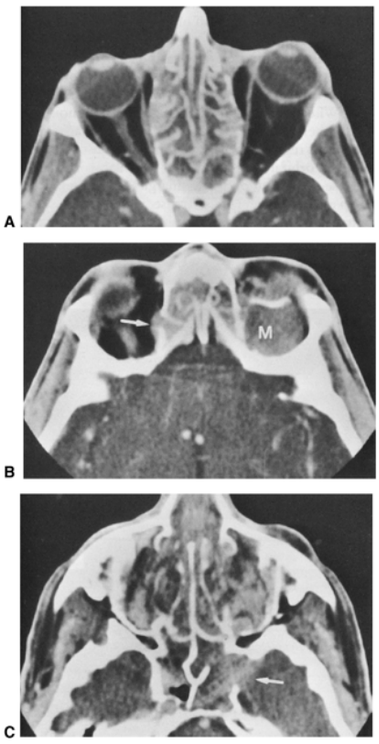

Figure 11-22. Composite CT scan demonstrates widespread sinus polyposis, which involved the frontal, ethmoid, sphenoid, and maxillary sinuses. It was associated with multiple focal areas of erosion (arrows) due to polypoid tissue and the development of a large mucocele (B - “M”) in the roof of the left orbit.

When present for prolonged periods of time, sinus polyposis may cause proptosis by expansion of the sinuses and erosion of the bone. Polyposis usually occurs within the context of very long-standing allergic rhinitis. The polypoid tissue may erode the wall focally, in multiple sites, or may cause diffuse expansion of the sinuses. In addition, polyposis may contribute to the development of mucocele (Fig. 11-22).

Another unusual manifestation of mucocele was exemplified by a patient who developed intermittent exophthalmos and downward displacement of the globe. This was related to a pyocele that had caused a fistula, which extended through the orbit and the upper lid. Intermittent drainage led to resolution of his symptoms. We have seen two patients with chronic sinusitis and pyocele extending into the orbit, causing intermittent and recurrent episodes of orbital cellulitis. Rare cases of sudden hemorrhage and proptosis have also been described.

Very few cases in our series were characterized by acute inflammatory features that were due to active infection within a pyomucocele. In these instances, the patients present with a more dramatic onset associated with inflammatory features and require acute drainage.

Investigations

On imaging, mucoceles expand the sinus cavity while thinning the sinus walls and destroying the normal internal septae (Figs. 11-17 ,11-18 ,11-19). The margin of the mucocele on CT or polytomography may be a thin shell of bone (Figs. 11-17 and 11-18). On CT scan the sinus is homogeneously opacified by material of soft tissue density. The leading margin in the orbit is usually well defined, rarely enhances, and is smooth in contour. An associated old, healed bony fracture may be noted at the margin of the mucocele (Fig. 11-17). MR imaging reveals iso- or high-intensity signals on T1 images and high signals on T2, which help to demonstrate intracranial or intraorbital extension. CT is most effective in defining the bony changes. On ultrasonography, mucoceles are usually smooth in outline, rounded, and clearly defined from surrounding orbital structures. In addition, they have few internal echoes, good sound transmission, and good definition of the deep wall, characteristic of fluid-filled lesions. Those that contain debris may show some internal echoes and be confused with solid lesions.

Management

Management is surgical and directed to complete removal of the cyst lining, reestablishment of normal drainage, or obliteration of the sinus. This is usually the domain of the otorhinolaryngologist, but ophthalmologic expertise may be necessary for management of the orbital portion. Recurrence has been frequently noted in the past and attributed to incomplete excision of the lining or restenosis of the new osteum.

When the mucocele is clearly isolated, we usually completely excise the lining and smooth the bone with a drill to remove any crevices that may be lined by epithelium. When the

mucoceles are large and involve the frontoethmoid complex, either a silastic tube or a nasal flap is placed in the opening to reestablish and maintain it. It is useful to complete the orbital dissection prior to collapse of the cyst because defining the margin of the mucocele is much easier while the mass is tense, facilitating dissection from the periorbita. Usually this margin is dissected free with ease but in instances of recurrent inflammation, careful and meticulous sharp dissection may be necessary because of fibrosis. The development of endonasal fibre optic surgery has led to the use of these techniques in treating mucoceles. It is best restricted to those mucoceles where drainage can be established relatively easily. For patients with the silent sinus syndrome, repair of the orbital floor leads to resolution of the enophthalmos and reconstitution of the superior sulcus. Pyomucoceles require antibiotics in addition to excision and drainage.

Lacrimal Ductal Cysts

Lacrimal ductal cysts are an uncommon consideration in the differential diagnosis of mass lesions of the anterior orbit and lacrimal gland region. Schmidt coined the term dacryops for this condition in 1803. Classically, they are mobile, tense, and fluctuant swellings. Two third of our cases had some degree of irritation or tenderness. In the majority, eversion of the upper lid causes protrusion of the cysts into the conjunctival cul-de-sac where they appear as slightly bluish lesions that transilluminate (Fig. 11-23). They tend to expand slowly and may vary in size due to intermittent discharge. Several of our patients noted swelling of the cyst when crying, and one experienced swelling and pain when deep sea diving. Rarely, they may present with sudden expansion due either to inflammation or hemorrhage within the cyst.

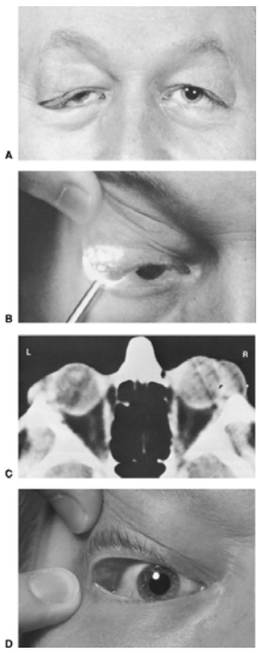

Figure 11-23. (A) Clinical photograph of a 44-year-old man with bilateral lateral lid swelling and marked blepharochalasis. (B) The right upper lid has a large transilluminatable cystic lesion. (C) CT scan demonstrates slight right proptosis and bilateral soft tissue masses adjacent to the globe anteriorly. (D) With the lid distracted superolaterally, the cystic component of this lesion can be viewed in the fornix and characteristically has a bluish coloration. (Figs. 11-23A to C borrowed with permission from Smith S, Rootman J. Lacrimal ductal cysts: presentation and management. Surv Ophthalmol 1986;30:245-50.)

These cysts may be unilateral or bilateral, and single or multiple. Bilateral cysts may be associated with blepharochalasis. Usually the cysts are relatively small and isolated, but they may be sufficiently large to cause globe displacement, and may be multilocular.

Histologically these cysts are lined by a double layer of epithelium; the inner lining is cuboidal and the outer myoepithelial (Fig. 11-24). The intervening stroma is frequently fibrotic with an inflammatory cell infiltrate. Occasionally, intense inflammation and granulation tissue may be seen. The pathogenesis is probably related to trauma or inflammation that weakens the ductal walls, destroying their neuromuscular contractility, and allowing dilatation with blockage even at low secretary pressures. The clinical diagnosis is usually obvious on the basis of the visible cyst. In large lesions, ultrasonography, CT, and MR imaging may

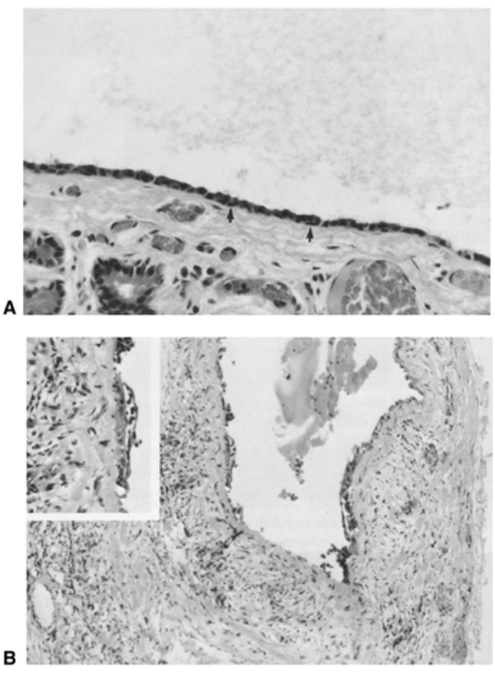

Figure 11-24. (A) Photomicrograph of a portion of the cyst wall obtained from a 44-year-old patient diagnosed with a lacrimal cyst. Note the inner cuboidal layer and outer myoepithelial cells (arrows). The lumen contains inspissated secretions, and the wall of the cyst is somewhat fibrotic. Note also lacrimal structures (H&E, original magnification × 25). (B) Another portion of the cyst wall from the same patient shows degeneration of the epithelial surface associated with more marked inflammation and fibrosis (H&E, original magnification × 25). (B-inset) High power of the same specimen (X 25). (Borrowed with permission from Smith S, Rootman J. Lacrimal ductal cysts: presentation and management. Surv Ophthalmol 1986;30:245-50.)

demonstrate the cystic structure. They must be differentiated from other cystic and noncystic lesions of the lids and lacrimal fossa with which they may be confused. We found the following potentially confusing cystic lesions in this region: dermoid cysts (particularly those that are superficial), laterally located frontal mucoceles, implantation cysts, aneurysmal bone cysts, and a muscle cyst in the lateral rectus. In addition to those seen in our series, the literature cites parasitic cysts and cysts of the lid adnexal structures in the differential diagnosis. The latter are most commonly seen in association with cicatrizing conditions such as pemphigoid and trachoma. Solid tumors of the lacrimal gland may be mistaken for ductal cysts, but are for the most part recognizable with clinical and imaging studies as solid lesions.

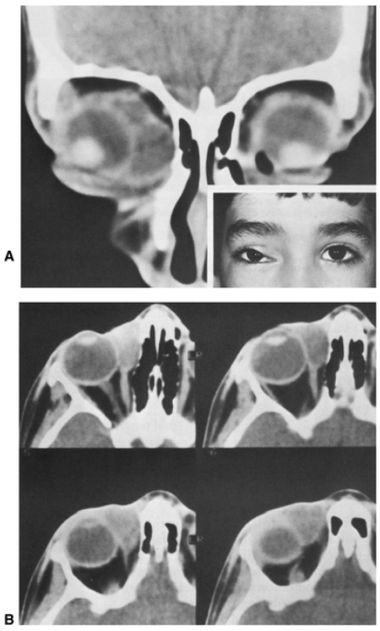

Figure 11-25. A boy presented with a history of progressive swelling of the superior lid and medial canthal region following extraocular muscle surgery, which had been performed 8 months after birth. The coronal (A) and axial (B) CT scans demonstrate a large epithelial cyst, the posterior end of which is attached to the medial rectus muscle.

If symptomatic or cosmetically bothersome, lacrimal ductal cysts may be treated by complete excision or marsupialization; the latter technique is preferred for patients with large cysts or decreased tear production on the affected side as shown on Schirmer's testing, which should be done in all cases. In several instances we have noted that the ductal cysts are multiple at the time of excision. Simple lancing, incomplete excision, or aspiration alone usually results in a recurrence of the cyst.

Implantation Cysts

Orbital implantation cysts are usually the result of previous trauma or surgery. We have encountered a number of cysts that developed following muscle surgery. These can reach significant size and extend deep into the orbit (Fig. 11-25). Management is by excision of the cyst under the microscope, avoiding damage to the usually scarred and partially incorporated muscle. Rarely, implantation cysts may result from penetrating trauma to the orbit.

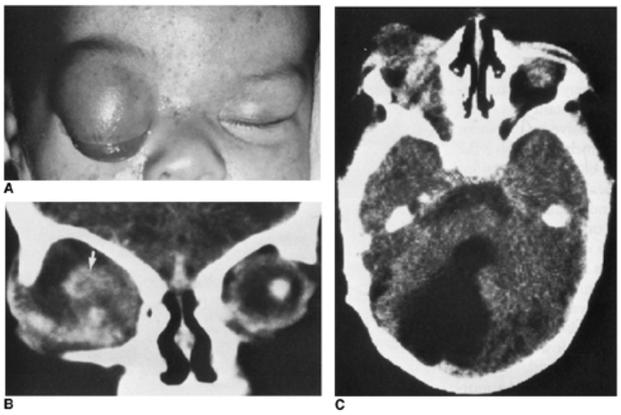

Figure 11-26. An infant born with a large multilocular cystic and solid lesion of the orbit and upper lid. It was associated with a partial absence of the right cerebral hemisphere. (Reproduced with permission from Wilson RD, Traverse L, Hall JG, et al. Oculocerebrocutaneous syndrome. Am J Ophthalmol 1985;99:142-8.)

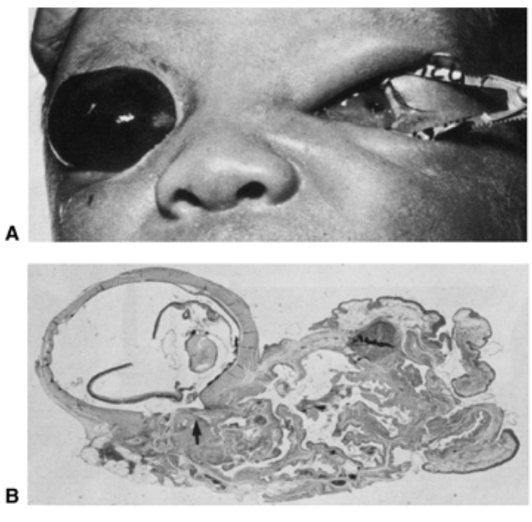

Figure 11-27. (A) An infant born with a massive cyst on the right and a microphthalmic eye on the left. (B) Low-power histologic view of the right microphthalmic eye attached to the extensive neuroepithelial-lined cyst. Note the coloboma in the deformed globe inferiorly (arrow).

Neurogenic Cysts

There are a number of congenital neurogenic cysts that arise as a result of developmental malformations of the globe, optic nerve, or the meninges.

Congenital Cystic Eye & Microphthalmos with Cyst

Congenital cystic eye occurs as a result of arrested development of the optic vesicle. It happens sporadically, can be of variable size, and may be associated with profound malformations of the brain (Fig. 11-26). Microphthalmos with cyst arises as a result of failure of closure of the optic fissure (Fig. 11-27). These patients typically present with a microphthalmic eye and an inferior cyst appearing under the conjunctiva or in the lower lid, as opposed to cystic eye, which appears as lesions in the upper lid. The cyst however may be of variable size with relatively normal looking eyes. They may rarely be associated with massive gliomatosis. The cysts are lined by primitive neuroepithelium continuous with the primary vitreous cavity. Microphthalmos with cyst is usually unilateral. It may be of sporadic occurrence in a healthy infant but can be associated with systemic abnormalities.

These congenital cystic lesions of the orbit should be differentiated from teratomas, which usually develop more rapidly, are associated with a normal appearing but protruding eye, of a denser hue, and although they often have a cystic element on imaging, have a solid component. In addition, they should be distinguished from orbital cephalocele. Management of large lesions is surgical excision of the cyst, globe, and abnormal neuroepithelial structures.

Orbital Cephalocele

Cranial orbital cephaloceles are rare and result from failure of separation of the surface ectoderm and neuroectoderm, which leads to a dehiscence in bone and protrusion of either a dural (meningocele) or an encephalic (encephalocele, meningoencephalocele) cyst. They usually present as congenital lesions but, particularly when in the deep orbit, may appear later in life. They are frequently associated with other congenital facial anomalies that characteristically involve the midline structures. Those that occur anteriorly usually affect the base of the nose, causing hypertelorism and a superomedial mass that either displaces the globe downward and outward or extends anteriorly toward the brow. Deeper orbital cephaloceles may be occult and result in proptosis with or without ocular dysfunction. Those that are visible may fluctuate, transilluminate, pulsate, and change in size with Valsalva maneuver.

The importance of recognizing these cysts is to plan appropriate management rather than have an accidental surgical encounter. On investigation, there may be evidence of a variably sized bony dehiscence suggesting the presence of a cephalocele. If an undiagnosed cyst is encountered at surgery and a cephalocele is suspected, aspiration of the contents will yield cerebrospinal fluid. Management, when the defect is small, consists of excision, closure, and ligation of the base with patching of the bony defect from the orbital side. When large, a transfrontal craniotomy with excision, patching, and closure is necessary.

Other Neurogenic Cysts

Primary orbital arachnoidal cysts have been noted particularly in association with colobomatous defects of the ipsilateral eye. Nerve sheath cysts usually contain cerebrospinal fluid and may be associated with other developmental anomalies of the central nervous system. The diagnosis can be confirmed by analyzing fluid for the isoform of transferrin that is present only in cerebrospinal fluid. We have also encountered a primary choristomatous cyst of the optic nerve in a patient with progressive proptosis and a blind eye from birth (Fig. 11-28).

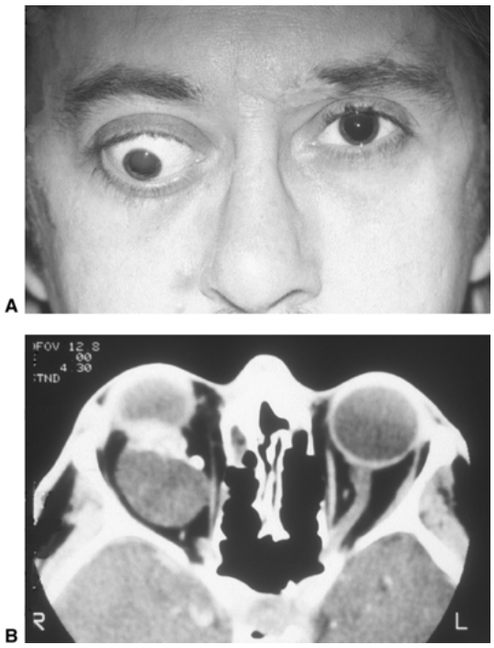

Figure 11-28. (A) This 32-year-old man presented with a long-standing history of progressive proptosis and downward displacement of his right blind eye. (B) On CT scan, we noted a cystic lesion associated with some focal areas of calcification anteriorly that distorted the globe. This lesion was excised for cosmetic reasons and found to be a choristomatous cyst of the optic nerve.

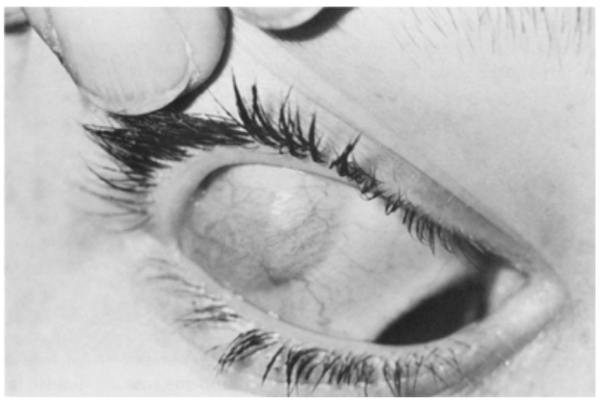

Figure 11-29. A superotemporal conjunctival dermolipoma.

Tumors and Ectopias

Dermolipomas

Dermolipomas are not usually lesions of the deep orbit and are properly described as conjunctival tumors. They are included here because of the frequent clinical confusion with true orbital dermoids. Dermolipomas are an ectopia of skin to the conjunctiva, probably related to sequestration at the time of embryonic development of the lids. They typically occur on the superolateral epibulbar surface and are usually asymptomatic (Fig. 11-29). Clinically, they have a pinkish coloration with focal areas of hair on their surface, and they may demonstrate keratin with a Wood's light. Subconjunctivally, there may be evidence of patches of bright yellow fat lobules. The most commonly confused lesion is fat herniation due to a dehiscence in Tenon's capsule. This typically occurs in elderly patients; have a smooth conjunctival surface; are soft, indentable, freely mobile, and in contrast to dermolipomas, move forward with retropulsion of the globe, and have surface vessels that blanch with epinephrine. The other differentials include subconjunctival lipoma and lacrimal gland prolapse.

Histologically, the surface of a dermolipoma consists of keratinizing squamous epithelium with adnexal structures, including hair, which may be sufficient to cause constant irritation that requires treatment. If asymptomatic, excision is not necessary. Because of their intimate association with the lacrimal duct structures, it is important to avoid damage to the ducts at the time of excision. We usually remove them under the microscope, identify the abnormal epithelium with hairs on it, and excise that portion of the surface as an ellipse, identifying and avoiding the lacrimal ducts. The underlying dermis usually contains fat and connective tissue septae and can be debulked with ease, again avoiding the lacrimal ducts and the underlying lateral rectus muscle. Deep excision is unnecessary because the offending feature consists of the superficial ectopic skin. Aggressive orbital dissection should be avoided.

Lacrimal Ectopia

Although not infrequent in the conjunctiva, caruncle, and epibulbar sites, ectopic lacrimal tissue is rare in the deep orbit. When it occurs here, it is isolated from ductal structures, and accumulated secretions are said to incite a local cicatricial inflammatory response. Depending on the location, there may be evidence of both mass and infiltrative effect with restricted extraocular movements, proptosis, and visual deterioration. Diagnosis requires reliable evidence of lacrimal tissue obtained from a site remote from the lacrimal gland. Some of the cases described have been characterized by progressive chronic inflammatory infiltration of the orbit. Suggested management has been surgical excision. Ectopic lacrimal gland may occur in the orbit and has been described associated with cystic components resulting from the isolated lacrimal ducts.

Other Ectopias

The orbit may be a site for a number of different types of ectopias, particularly heterotopic brain tissue and cartilage.

Orbital Teratoma

A teratoma is a tumor composed of tissues derived from more than one germ layer and usually from all three. They are believed to arise from pluripotential embryonic tissue. Overall, teratomas are said to account for 6.6% of childhood tumors, most commonly occurring in the testes, ovaries, and retroperitoneum. The orbit is a rare site for teratomas, particularly if they are defined as tumors that contain components of elements from all three germ layers.

Characteristically, they present as a rapidly developing unilateral tumor of the infant orbit. In older age groups, they are generally smaller and develop more slowly. The common clinical feature is extreme unilateral proptosis, with marked stretching of the lids by a solid or more frequently cystic mass. The eye is usually of normal size but may be degenerated secondary to protrusion and exposure. The orbit is increased in size. Although massive intracranial teratomas with orbital extension have been described, the vast majority are primary lesions of the orbit.

Histologically, the totipotential cells differentiate along ectodermal, neuroectodermal, mesodermal, and endodermal lines. The presence of gastrointestinal, glandular, and secretary choroid plexus accounts for the frequently cystic and rapidly developing features of these tumors. Although malignant teratomas are not uncommon elsewhere, in the orbit they are extremely rare. They may involve the orbit primarily or secondarily expand into the orbit from adjacent sinus or intracranial sites.

On imaging, teratomas appear heterogenous, due to cystic and solid components, foci of fat, and heterotopic bone or even teeth.

The importance of this tumor lies in the differential diagnosis of a rapidly growing and massive orbital tumor of infancy. This includes benign lesions (orbital hemangioma and lymphangioma) and malignant tumors (rhabdomyosarcoma secondary extension of retinoblastoma and metastatic tumor,

particularly neuroblastoma and leukemia). In addition, congenital anomalies such as microphthalmos with cyst, congenital cystic eyeball, unilateral congenital glaucoma, cephalocele, and plexiform neurofibroma should be ruled out. Inflammatory lesions in this age group rarely mimic tumors.

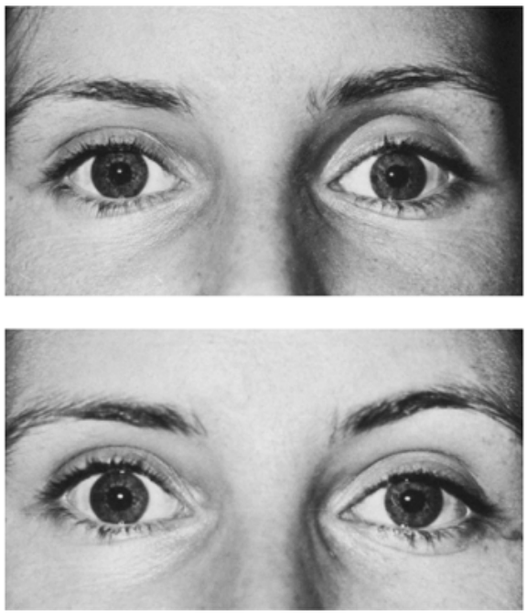

Figure 11-30. (A) A 36-year-old patient with orbital asymmetry and left enophthalmos. Note the deepened superior sulcus. (B) The same patient following augmentation of the orbit with a bone graft in the floor.

In the past, the majority of these have been treated by exenteration. However, with improvements in preoperative diagnostic imaging and surgical technology, excision of the tumor alone is possible. This is particularly true if the tumor is smaller and there is evidence of preservation of ocular function.

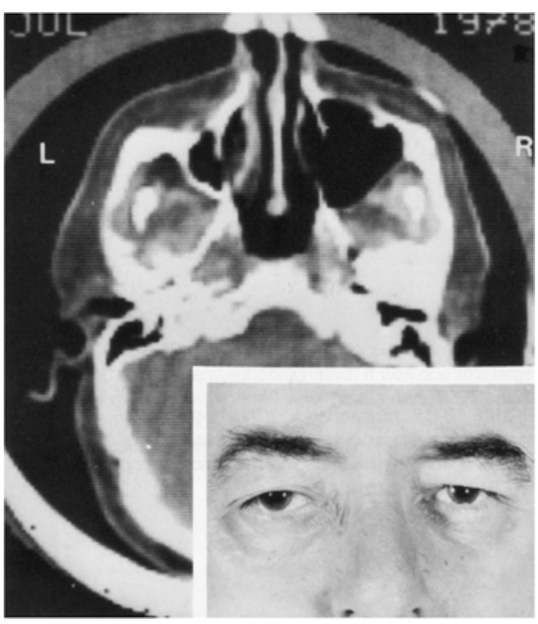

Figure 11-31. This 57-year-old man had a long-standing history of prominence of his right eye. Note, however, left enophthalmos and flattening of the premaxillary area. The CT scan shows left maxillary hypoplasia, which was associated with enophthalmos. (Borrowed with permission from Cline RA, Rootman J. Enophthalmos: a clinical review. Ophthalmology 1984;91:229-37.)

Bony Anomalies & Mesodermal Defects

Orbital Asymmetry

Minor degrees of facial and orbital asymmetry were the most common causes of pseudoproptosis in our series (Fig. 11-30). We have seen a total of 48 patients (1.6% of orbital cases) referred for evaluation of proptosis that were essentially related to varying degrees of structural asymmetry. In almost all instances the asymmetry is identifiable clinically by an associated facial asymmetry. A simple clue to picking this up is to observe the patient from behind while he/she faces a mirror. The reversal of the images makes facial asymmetry particularly noticeable. For the most part, our patients had minor degrees of asymmetry involving all of the hemifacial structures. However, in a few instances the asymmetry was related to maxillary hypoplasia resulting in a relatively retroplaced and small orbit on the affected side (Fig. 11-31). In several instances, familial asymmetry was evident when examining the siblings or parents. Retrospective photographic review is useful to demonstrate how long the patient has had this anomaly.

Craniofacial Dysostosis and Developmental Anomalies of the Skull

Craniofacial dysostosis and developmental anomalies may result in profound orbital abnormalities. The most common orbital abnormality associated with craniofacial dysostosis is extreme shallowing as the result of arrested growth of the affected cranial bones. The flattening of the face and the shallowing of the orbits may produce severe and threatening exophthalmos. In Crouzon's disease there may also be an associated developmental hypoplasia of the superior rectus muscles leading to marked exodeviations,

particularly in upgaze. Narrowing of the optic canal may lead to optic atrophy. The cosmetic and functional disturbances related to the dysostosis, hypertelorism, and exorbitism are in the domain of a multidisciplinary craniofacial team, which should include an ophthalmologist. The craniofacial dysostoses include a multiplicity of craniosynostosis syndromes and the clefting syndromes, many of which have ocular and orbital manifestations. Their definition and management are beyond the scope of this book and constitute a separate medical discipline.

Mesodermal Defects

Part of the abnormality associated with von Recklinghausen's disease (multiple neurofibromatosis) may be a developmental anomaly of the cranial bones, in particular, absence of the sphenoid wing (Fig. 11-32). This may lead to pulsatile exophthalmos or rarely enophthalmos because of the adjacency of the dura and periorbita.

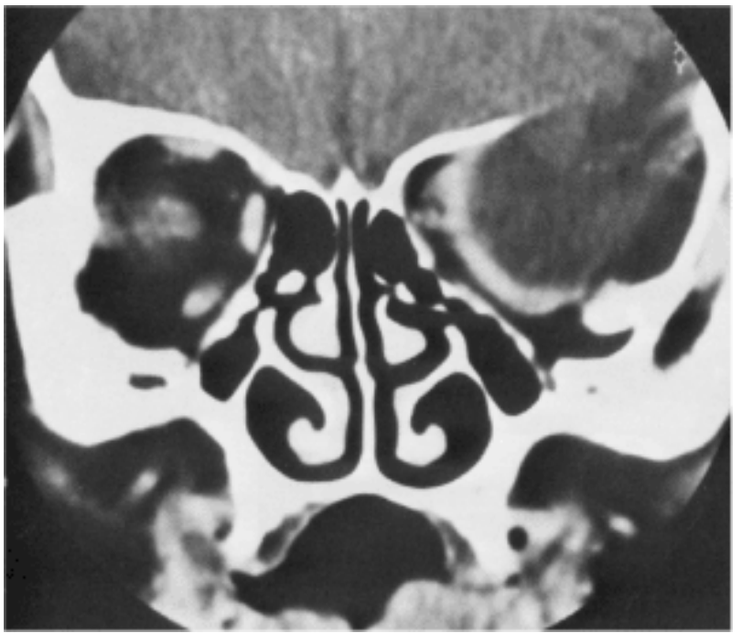

Figure 11-32. Coronal CT scan of a patient with absence of the left sphenoid wing and pulsating exophthalmos due to neurofibromatosis. The temporal lobe has herniated into the orbit through the bony defect.

Trauma

Clinical Presentation and Examination

The algorithm for managing orbital trauma (Fig. 11-33) consists of an evaluation of the general status of the patient before attending to local problems. Key local issues consist of defining those acute injuries that may need immediate care, such as damage to the globe, acute retrobulbar hemorrhage, tense emphysema, and optic nerve damage. After the acute problems are evaluated and managed, attention should then be turned to the assessment of periocular soft tissues and potential fractures, which will require imaging and appropriate mid- and long-term management.

Orbital injury may be isolated, but it often occurs in association with damage to local structures including the globe, paranasal sinuses, nasolacrimal system, nose, and brain. In addition, the injury may be complicated by inebriation, shock, or loss of consciousness. The first priority is establishing an airway, control of bleeding, and restoration of circulation. Once the patient is stabilized, local structures can then be assessed. The globe should be promptly examined before the onset of soft tissue swelling. The minimum requirement is to obtain a visual acuity when possible with the least amount of trauma to the potentially damaged ocular structures. Tightly swollen lids can be gently separated by Desmarres retractors; if they are unavailable, a retractor can be fashioned from paper clips. If there is no significant orbital tension, blepharospasm, or obvious

ocular injury, a speculum may be gently inserted. When necessary, a lid block can be given to reduce blepharospasm in order to perform an adequate ocular examination. In children or restless and pugnacious patients, examination aided either by sedation or anesthesia may be necessary. Major ocular injuries, which are indicated by a soft globe, prolapsing tissue, rupture, hemorrhage, and loss of the red reflex, should be ruled out promptly and dealt with in the operating room.

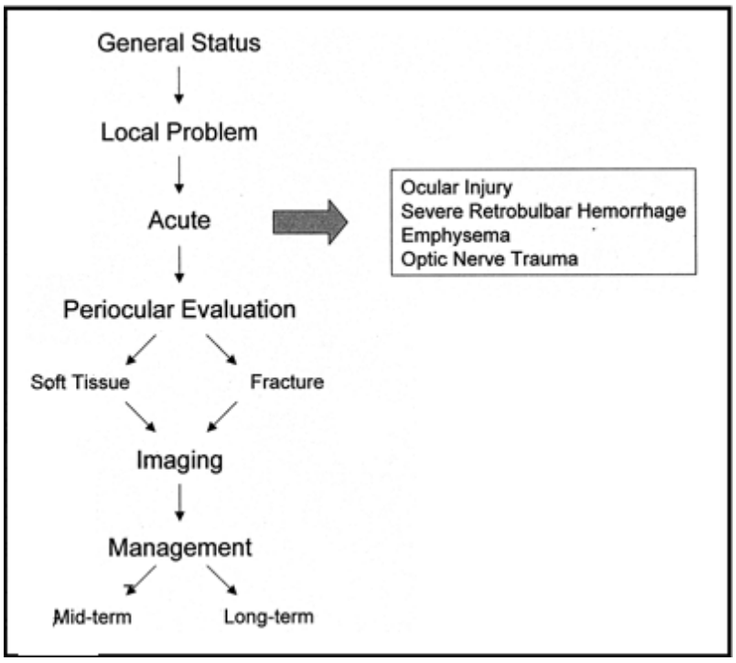

Figure 11-33. Algorithm for the management of trauma to the orbit.

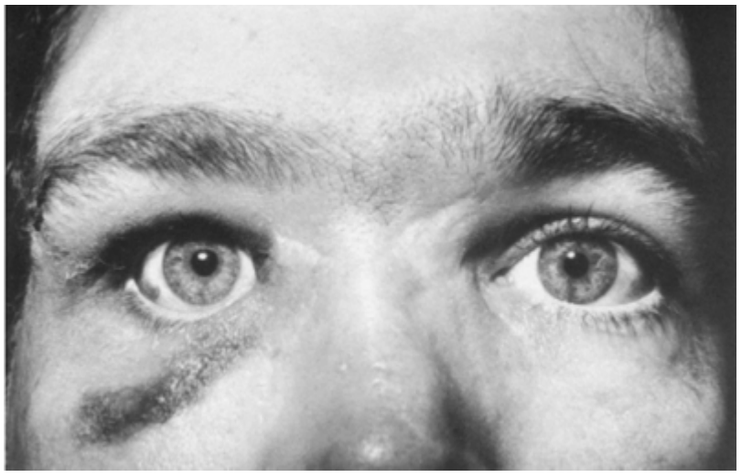

Figure 11-34. Clinical photograph of a patient who had a midfacial fracture, which resulted in flattening of the base of the nose and hypertelorism.

A careful, thorough history is not always possible, but should include circumstances of injury, exact nature of the offending object, distance and direction that it travelled, time of occurrence, any previous ocular disorder, history of surgery, allergies, systemic medical problems, or current medications. Pretrauma photographs may be useful.

Traumatic exophthalmos may result from reduction in orbital volume due to inward displacement of the orbital walls, hemorrhage, and emphysema. Severe orbital tension is characterized by a firm exophthalmos, raised intraocular pressure, and a pulsating retinal artery. Emphysema can be detected by tissue crepitus when present. Pulsating exophthalmos may suggest an orbital roof fracture with secondary herniation of the anterior cranial fossa contents or a high-flow carotid cavernous fistula.

Once the globe has been assessed and severe orbital tension ruled out, a more thorough orbital examination can be done. Gross external inspection of the facial structures is helpful in defining major facial fractures. Horizontal, vertical, and axial displacement of the globe and orbit should be documented. The lids should be checked for abnormality of height, width, inclination, and interpalpebral distance. Lid mobility (levator function), ptosis, and pseudoptosis should be evaluated. The assessment of ptosis may be particularly difficult in the presence of significant lid swelling. The medial and lateral canthal ligaments should be checked for any alteration in level and increase in intercanthal distance (telecanthus). The position of the globe may be altered due to avulsion of the suspensory ligaments or fractures of adjacent sites. Malar flattening with or without globe ptosis, downward displacement of the lateral canthus, and lower lid retraction may be indicative of a displaced trimalar fracture of the zygoma. In contrast, lower lid retraction without flattening may be present with simple orbital rim fractures. Telecanthus, especially when associated with depression of the nasal bridge, can be seen with a midline fracture (Fig. 11-34). Enophthalmos may be due to increased orbital volume secondary to herniation of tissues into adjacent sinuses or disturbances in the periorbital fat, or it may be postraumatically due to an absolute deficiency of fat from liquefaction or subsequent fibrosis (Fig. 11-35). Traumatic exophthalmos can result from reduction in orbital volume due to inward displacement of orbital walls, hemorrhage, tissue swelling, and emphysema. A pseudoproptotic appearance

may occur with a complete third nerve palsy. Another cause of pseudoptosis may be a deepened superior sulcus related to enophthalmos or downward displacement of the globe associated with a blow-out fracture of the floor or medial wall of the orbit. Pulsation and/or a bruit may be present when a traumatic arteriovenous shunt has occurred and the intraocular pressure may be elevated in this circumstance.

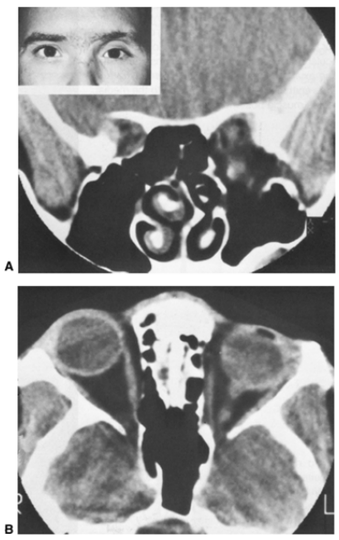

Figure 11-35. Clinical features and coronal (A) and axial (B) CT scans of a blow-out fracture of the orbit, with left enophthalmos and downward displacement of the inferior orbital structures. Note globe ptosis, enophthalmos, and deepened superior sulcus.

Extraocular movements and diplopia should be documented in all fields of gaze, to assess acute motor status and progressive change. If there is any reduction in eye movements, forced duction testing should be performed to distinguish entrapment and muscle contusion from paresis (Fig. 11-36). Topical proparacaine or cocaine is instilled in the eye, and a cotton-tipped applicator or pledget saturated with anesthetic is placed over the insertion of the muscle for 5 minutes. The muscle is then grasped with forceps and the eye is rotated in the affected direction of gaze.

In the trap door syndrome, the patient may have an essentially white eye with marked restriction of up- and downgazes, a positive forced duction, and severe pain, nausea, and vomiting on attempted upgaze due to muscle entrapment in the fracture site. This syndrome is more common in childhood orbital trauma.

Palpation of the orbital rim may reveal local tenderness, displacement, and degree of comminution of the fracture site. Tissue emphysema and crepitus may suggest a paranasal sinus fracture (Figs. 11-37 and 11-38).

Sensation should be tested, particularly in the distribution of the infraorbital, frontal, zygomaticofacial, and zygomaticotemporal nerves. Cerebrospinal fluid rhinorrhea may occur, especially with a significant naso-orbital or roof fracture. Anosmia may be an indication of a dural tear in the roof of the ethmoid sinus or cribriform plate.

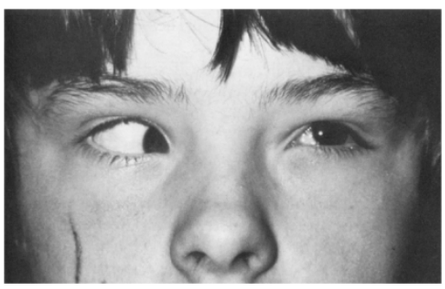

Figure 11-36. Clinical photograph of a patient with a medial wall blow-out fracture, which led to limitation of abduction on the left side.

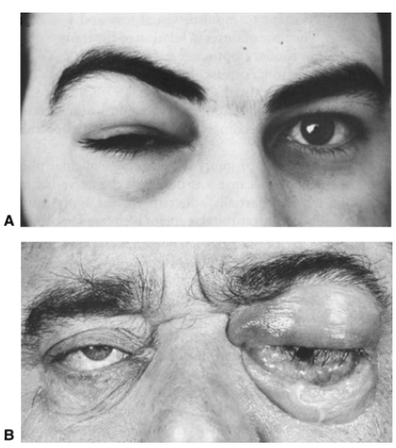

Figure 11-37. Clinical photographs showing orbital emphysema following trauma. (A) The soft tissues of the lid are primarily involved. This occurred 1 day after orbital trauma, when he blew his nose. (B) Massive orbital emphysema following a blow-out fracture of the orbit.

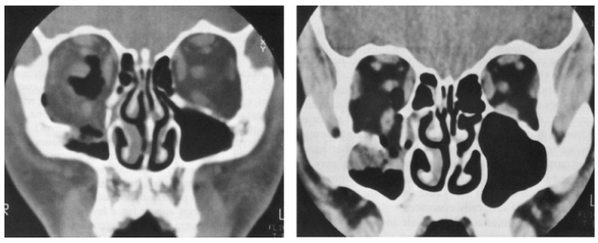

Figure 11-38. Coronal CT scans of a patient with a blow-out fracture of the orbit demonstrate orbital emphysema and downward displacement of the inferior orbital structures, including the inferior rectus muscle. The patient was supine for these direct coronal images, causing fluid in the right maxillary antrum to layer in the superior, dependent portion of the sinus.

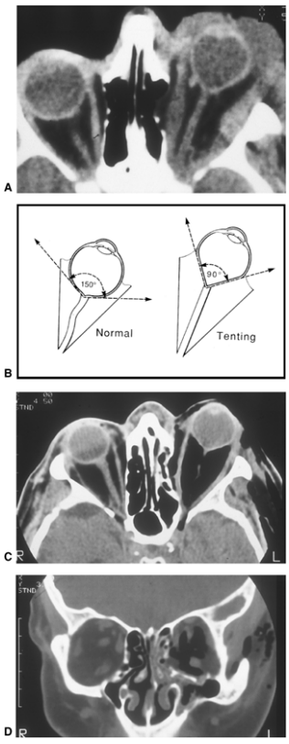

Figure 11-39. Globe tenting. (A) This axial CT scan demonstrates severe globe tenting and stretching of the optic nerve, which occurred in a 42-year-old man who had direct orbital and facial trauma. This resulted in a high-flow carotid cavernous fistula, leading to no light perception and total ophthalmoplegia. (B) This schematic illustrates the optic nerve stretching and tenting of the globe that occurs with severe orbital tension. Globe tenting is defined as a posterior globe angle of less than 130. Progressive reduction of the posterior globe angle correlates with an increase in proptosis and optic nerve stretching, as well as more severe visual impairment. A globe angle of less than 120 with acute proptosis is a surgical emergency. These axial (C) and coronal (D) CT scans of a 57-year-old man demonstrate globe tenting due to emphysema after a blow-out fracture of the medial wall.

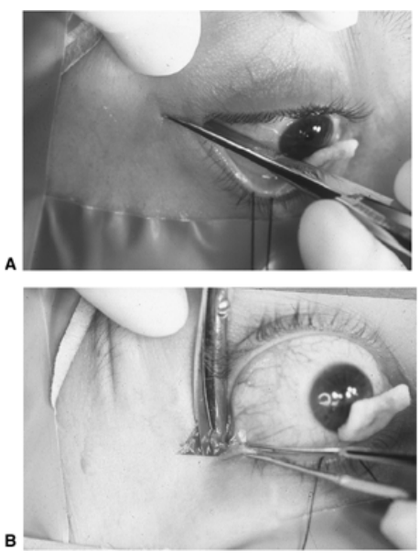

Figure 11-40. (A) A direct lateral canthotomy is demonstrated in this photograph, with an incision of the inferior crus of the lateral canthal ligament and the adjacent septal insertion on the arcus marginalis (B).

Lacerations should be explored to evaluate the integrity of the orbital septum and the major anterior orbital structures, especially the levator muscle and lacrimal structures. In addition, a careful assessment for retained foreign bodies should be made. If possible, photographs or sketches of the injury should be obtained.

Management of Catastrophic Loss of Vision–Acute Rise in Intraorbital Pressure

Soft tissue injury, fracture, avulsion, and contusion may cause an acute rise in intraorbital pressure as blood is trapped in confined spaces. It is a particular risk with extraperiosteal bleeds and those at the orbital apex. The pressure can cause catastrophic ischemia of the optic nerve and retinal hypoperfusion, or direct pressure on the optic nerve. The orbit or extraperiosteal space may act as a closed compartment, leading to an asymptotic rise in pressure when the size limit is reached. Thus small changes in fluid volume can bring about dramatic increases or decreases in pressure.

These patients usually have evidence of severe orbital tension with pain, a firm globe, limitation of ocular movement,

reduced vision, loss of direct pupillary responses, or an afferent defect. Axial displacement may be associated with an intraconal hemorrhage whereas extraperiosteal bleeds lead to out-, down-, or upward displacement depending on which space is involved. The optic nerve head may demonstrate arterial pulsation. Severely raised intraorbital pressure can lead to stretching of the optic nerve and tenting of the globe, the degree of which correlates with visual outcome (Figs. 11-39A and B).

Most orbital hemorrhages are self-limited and can be managed by careful sequential observation. When tense proptosis, raised intraocular pressure, retinal vascular pulsation, reduced motility, and decreased vision occur, management should be urgent. For more moderate degrees of orbital tension, treatment can include acetazolamide, mannitol, and anterior chamber paracentesis. Paracentesis may not be effective if there is a continuing rise in intraorbital pressure. Severe visual threat is a surgical emergency requiring rapid reduction. If there is marked nonaxial displacement of the globe due to an extraperiosteal bleed, this can be reduced by draining or aspirating with an 18- or 20-guage needle with or without orbital ultrasound guidance.

The most straightforward method of relieving orbital pressure is to relax the septal ring with a graded lateral canthotomy. The canthotomy is achieved with lysis of the lateral tendon to the bony rim with sturdy scissors (Fig. 11-40A). If this is effective as reflected in reduction of intraocular pressure, return of vision, or absence of pulsation of the retinal vessels, the patient can be observed. Further relaxation along the arcus marginalis can be obtained by disinserting the inferior, and if necessary, the superior crus of the lateral canthal tendon (Fig. 11-40B). Even further relief can be achieved by continuing to cut the septum at the arcus marginalis on the orbital rim.

If the above measures fail, bony orbital decompression with periorbital fenestration may be necessary. In the emergency situation, it is possible to outfracture the medial wall or floor through a forniceal incision using a sturdy periosteal elevator or a similar instrument. Medial extraperiosteal bleeds may also be decompressed using an endonasal approach.

Another cause of acute orbital tension can be emphysema, which occasionally leads to tenting of the globe (Figs. 11-39C and D). This rarely requires any decompressive measures as air tends to absorb rapidly.

Serious injury is more common with penetration of the medial upper lid than at other sites. Blunt objects need a greater force to penetrate the orbit, creating entry wounds larger than the size of the object. Sharp objects enter with minimal force and often the globe shifts away, preventing direct damage. High-speed missiles frequently perforate the globe before penetrating the orbit. A pointed object may even penetrate the roof of the orbit or pass through the superior orbital fissure and pierce the internal carotid artery within the cavernous sinus, leading to a carotid-cavernous fistula.

Optic Nerve Trauma

Optic nerve injuries can result from contusion, avulsion, fractures of the optic canal, compression secondary to intracanalicular hematoma, intrasheath hemorrhage, and indirect torsional injury within the canal. In addition, the nerve may be damaged intracranially due to sudden deceleration. These types of optic nerve injury result from four different mechanisms: direct orbital trauma, indirect damage to the optic nerve, traumatic chiasmal syndrome, and optic nerve compression due to frontal lobe herniation (gyrus rectus syndrome). Direct optic nerve trauma may be the result of penetrating injuries with small instruments, such as pencils, ice picks, and antennae, which may even have evidence of minimal soft tissue trauma. They carry with them the risk of cranial penetration or carotid injury. High velocity missiles may damage the optic nerve and only require removal if toxic or associated with progressive visual loss. Finally, direct trauma can also cause avulsion of the nerve as well as strangulation. Sometimes, a shearing force will cause an intrasheath hemorrhage, which may be associated with minimal orbital signs and a profound optic neuropathy. With proof on imaging, it is worthwhile to urgently decompress the blood from within the sheath.

Another direct cause of injury to the intracanalicular optic nerve may be fracture in the canal or of the adjacent sinus or orbital walls (Fig. 11-41). Fractures here, especially when displaced, imply profound and permanent visual loss. Apical

hemorrhage may also affect the optic nerve rapidly by occurring within a confined or tight space (Fig. 11-42).

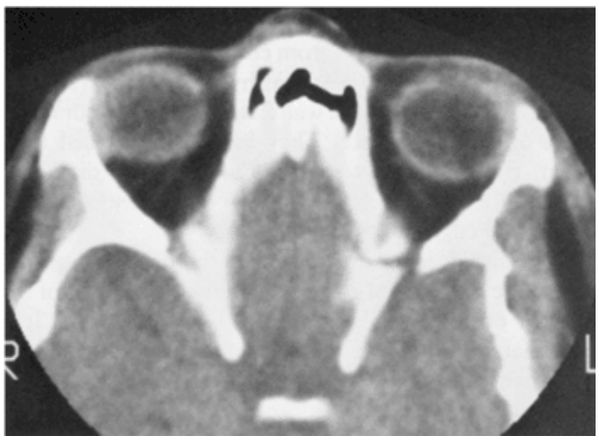

Figure 11-41. Axial CT scan demonstrates a fracture involving the roof of the adjacent optic canal and the tuberculum sellae. This was associated with a left optic neuropathy.

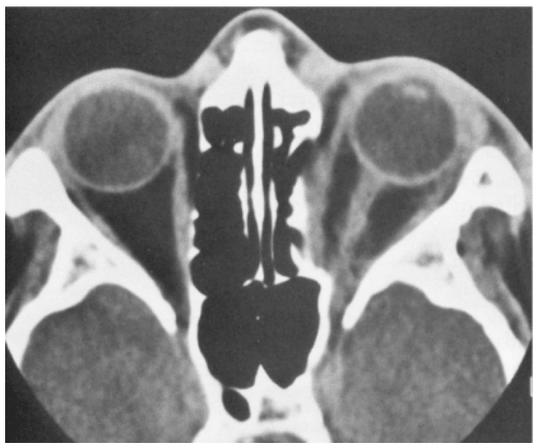

Figure 11-42. CT scan shows a medial blow-out fracture of the orbit and hemorrhage into the orbital apex. The latter accounted for the sudden onset of an optic neuropathy following the trauma.

One of the more difficult and controversial management issues relates to indirect injury to the optic nerve brought about by sudden deceleration of the head, usually with a supraorbital blow but rarely with occipital or parietal injury. There may be an acute, often complete visual loss, or gradual visual deterioration with a sluggish or absent ipsilateral pupillary reflex and normal consensual reaction. The fundus is normal and there may be associated findings of epistaxis and concussion. In our experience, at least 60% to 70% with serious optic nerve injury have other more severe, often life-threatening associated injuries or are unconscious. Thus the opportunity to either assess or intervene for any optic nerve injury is not available. The remaining 30% may have an indirect injury, which presents either with an acute or gradual visual deterioration, sluggish or absent ipsilateral pupillary reflex, and a normal consensual along with an afferent pupillary defect. To date, there are no control data to help in decision making, though anecdotal series suggest possible benefits of high-dose corticosteroids and surgical optic canal decompression. Patients with a delayed loss of vision have a better prognosis and are more likely to respond to therapy. Consensus opinion suggests at this point that the initial treatment with megadose corticosteroids may limit secondary injury and that nonresponders should be followed with consideration for surgical decompression of the bony canal. The recommended megadose of steroids is dexamethasone 0.75 mg/kg initially, then 0.3 mg/kg every 6 hours with treatment up to 5 days. Surgical intervention is recommended when there is demonstrable fracture with impingement or deteriorating visual function following response to megadose steroids. The role of surgery is more controversial with complete visual loss at the time of injury.

The traumatic chiasmal syndrome is associated with severe head trauma, usually to the vertex or upper forehead, which results in an anterior-posterior distortion of the skull and a deceleration injury of the brain and optic nerve. The result is usually one blind eye and a temporal defect in the other field but occasionally, pure bitemporal defects occur. This injury may be associated with cranial nerve palsies, diabetes insipidus, pituitary insufficiency, anosmia, cerebrospinal fluid rhinorrhea, meningitis, and carotid cavernous fistula.

The superior orbital fissure syndrome may occur in isolation without optic nerve injury, secondary to medial displacement of the greater wing of the sphenoid bone. This may require removal of the displaced bone.

Soft Tissue Injury and Orbital Hemorrhage

Blunt or penetrating trauma may result in soft tissue injuries with damage to vital orbital structures. The optic nerve, extraocular muscles, or neurovascular structures may be affected either directly or indirectly by shearing forces. The signs and symptoms of soft tissue injury include ecchymosis, lid swelling, proptosis, and ophthalmoplegia. Orbital hemorrhage can be classified according to the site of accumulated blood.

- Eyelid hemorrhage anterior to the orbital septum
- Hemorrhage posterior to the orbital septum, including subconjunctival hemorrhage
- Hemorrhage within the muscle cone
- Subperiosteal hematoma
- Intracranial hemorrhage that spreads to the orbit through the medial portion of the superior orbital fissure or through the subarachnoid space of the optic nerve.

Abrasions and avulsion of tissue usually produce superficial defects. Simple, anterior closed injuries lead to contusions with tenderness, swelling, and lid ecchymosis, which present as limited or localized bruising, edema, and subconjunctival hemorrhage (the “black eye”). In contrast, subconjunctival hemorrhages secondary to deeper orbital trauma accumulate in the retrobulbar, intraconal, and extraconal spaces and tracks anteriorly or posteriorly. In such situations visible ecchymosis may not appear for a few days, and when present, can be seen in the fornix extending beneath both the bulbar and tarsal conjunctivae in Tenon's capsule. Deeper and cranial hemorrhages may also take a few days to present, either by tracking from the subgaleal space or into the intraconal space through the superior orbital fissure extending extraconally as it tracks forward. The ecchymosis in this instance appears in the palpebral rather than bulbar conjunctiva when intraconal

hemorrhage is not present. Intracranial bleeding may also pass directly into the extraconal space through the medial aspect of the superior orbital fissure.

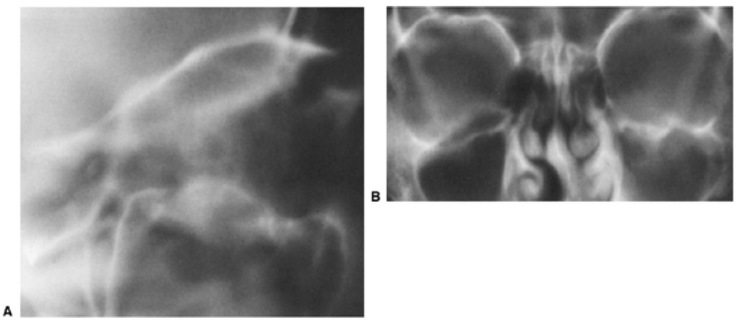

Figure 11-43. Lateral (A) and coronal (B) tomograms of the orbit demonstrate a left orbital blow-out fracture with opacification of the maxillary sinus. The orbital floor is disrupted.

If the periorbita is damaged, the blood may extravasate to appear superficially in the lid or conjunctiva in contrast to subperiosteal or a contained hematoma, which typically present with an abrupt onset of unilateral proptosis and globe displacement or slowly progressive proptosis. Clinically, one may see choroidal striae on fundoscopy and forced ductions may be negative. CT scan may show a mass with a central nonenhancing area of low density surrounded by a thin, isodense soft tissue rim that enhances. Ultrasonography demonstrates an extraconal well-demarcated lesion in the peripheral orbit. Depending on its location, it may affect nerves in the superior orbital fissure or the optic nerve itself. It is usually limited by the firm adherence of the periorbita at bony suture lines.

The management of soft tissue hemorrhage that does not threaten vision is conservative and consists of thorough inspection, cleansing and repair of wounds, and cold compresses in the early phase followed by warm compresses. Hematomas, on the other hand, may appear as swollen fluctuant areas that may occasionally need to be drained or aspirated. In the later stages, hematomas become organized, and if they cause a significant mass effect, they may need to be surgically evacuated.

Penetrating trauma may result in laceration or avulsion of muscles, damage to nerve supply, or both. Avulsion of rectus muscles may lead to anterior ischemic necrosis. An avulsed muscle may be difficult to find when it contracts towards the orbital apex and is best isolated under controlled operating room conditions.

Fractures of the Orbit

Fractures of the orbit may be suggested by a variety of clinical signs and symptoms but usually cannot be clearly defined without accurate imaging. Roof fractures may be associated with hemorrhage into the upper lid and lateral subconjunctiva. Occasionally cerebrospinal fluid rhinorrhea may also be noted when the sinuses are involved. Lateral wall fractures are more likely to be associated with avulsion of the optic nerve. Orbital emphysema may result from medial wall or floor fractures.

The etiology of orbital fractures may be divided into direct (orbital rim) fractures that occur when the force is applied to the bone or group of bones, and indirect (blow-out or blow-in) when the force is transmitted through the orbital soft tissues. Fractures in and around the orbit tend to follow the line of least resistance. Site and extent are dependent on the degree and direction of impact.

Although plain x-rays are rarely used, they can be useful in very rapid assessment. Plain x-rays, including Waters, Caldwell, and lateral views, may demonstrate blow-out and orbital rim fractures as well as those of other facial bones (Fig. 11-43). Opacification of the maxillary antrum is suggestive of floor fracture. Tissue emphysema and opaque foreign bodies may also be noted following sinus fracture.

CT (in the axial and coronal planes) with and without bone settings is the imaging of choice for trauma. This can define the location, extent, and severity of bony and soft tissue injury with and without entrapment of orbital tissues. Imaging findings should be correlated with the clinical features of presentation. When available, MR imaging is useful for noting soft tissue detail and changes in the orbital fat and

extraocular muscles; however, it is less effective in identifying fractures.

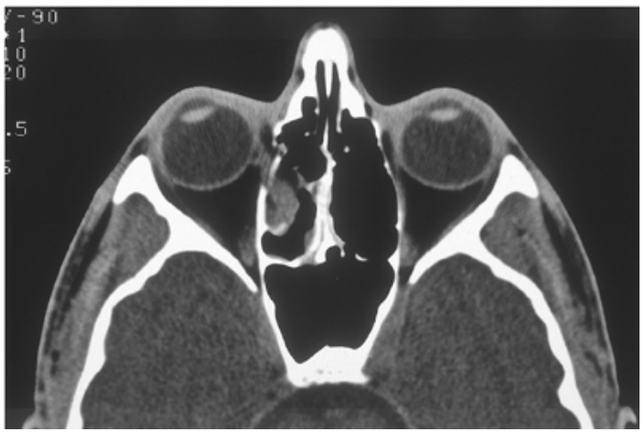

Figure 11-44. This axial CT scan demonstrates displacement of the medial rectus muscle into the ethmoid sinus following a blow to the right eye of a 13-year-old boy. This was associated with an exodeviation due to injury of the motor nerve to the medial rectus.

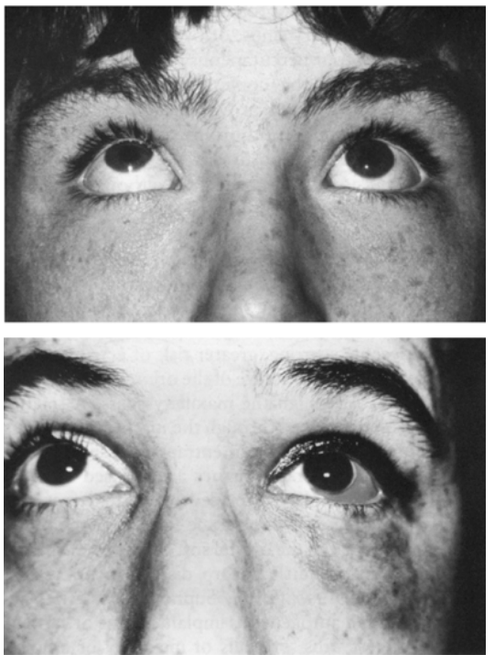

Figure 11-45. These clinical photographs demonstrate features of limitation of supraduction, which was associated with blow-out fractures of the orbit.

Overall, orbital fractures tend to occur more often in males than females and are left sided, reflecting the right-handedness of assailants. The decision to treat acutely is based on the risk of anticipated deformity, evidence of significant displacement of orbital soft tissues, or indeed incarceration of such tissues.

Blow-Out Fractures

Blow-out fractures result from compression of soft tissue due to a sudden increase in orbital hydraulic pressure. The force is transmitted to the walls where fractures occur in the areas of least resistance. They are usually caused by a blunt, rounded object greater than 5 cm in diameter, such as a fist, knee, elbow, hockey puck, tennis ball, or dashboard edge.

The site of least resistance is in the floor medial to the infraorbital groove, immediately in front of the inferior orbital fissure (Figs. 11-35 and 11-38). It is here that the inferior rectus and inferior oblique muscles and their fat and fascial attachments may be displaced or entrapped. The nerve to the inferior oblique, because of its course along the lateral border of the rectus, may be injured without actual muscle entrapment. The medial wall and uncommonly the roof may be involved in a blow-out type fracture (Fig. 11-44).

Physical findings suggestive of a blow-out fracture include orbital rim tenderness, infraorbital hypesthesia, motility disturbances with a positive forced duction, enophthalmos, and pseudoptosis. There is usually extensive edema and ecchymosis and there may be crepitus.

Infraorbital hypesthesia, when present, suggests a fracture of the central portion of the floor of the orbit. A defect medial or lateral to the infraorbital canal may leave sensation intact. Anesthesia in the distribution of the zygomatic nerve may be associated with a lateral fracture.

True muscle incarceration is usually not found at the time of surgery. Most cases of acute movement disturbances are caused by orbital septal disruption or injury to muscles, including laceration, avulsion, hemorrhage, and peripheral nerve injury. The great majority of orbital blow-out fractures lead to impairment of movement in all fields of up and down gaze, reflecting both inferior oblique and inferior rectus involvement (Fig. 11-45). The disruption of the connective tissue septae not only involves the system of the inferior orbit, but can have tractional effects on the medial and lateral rectus muscles, which explains some of the bizarre motility patterns seen following blow-out fractures.

Acute enophthalmos may occur due to prolapse and escape of fat and orbital contents into a sinus or due to increased orbital volume. Initial enophthalmos may be masked by edema or hematoma. Enophthalmos may be associated with a pseudoptosis of the upper eyelid, a deepening of the supratarsal sulcus, and a decrease in the interpalpebral fissure. Late enophthalmos can develop as the result of an enlarged orbit or fat atrophy and necrosis, and the globe may be retracted by short, fibrotic entrapped muscles (see Fig. 11-35).

Facial x-rays may show the teardrop sign due to soft tissue protrusion into the superior portion of the maxillary antrum through the fracture site. A coronal CT scan can help determine soft tissue injuries and recognize entrapped or displaced extraocular muscles and extent of injury (Figs. 11-43 and 11-45). In some cases, tethering of the muscles by connective tissue strands may be seen, along with alterations of the normal rectangular or elliptical contour of the muscle in cross section.

There is a syndrome of orbital floor blow-out with entrapment that tends to occur in children or adolescents. The fracture occurs just medial to the infraorbital nerve allowing the orbital soft tissues to pass through, with the bone acting as an acute trap door and incarcerating the soft tissues. The patient characteristically has minimal evidence of trauma but extreme limitation of ocular movement with a positive forced duction and severe pain, nausea, and vomiting on attempted movement. The CT findings are characteristic (Fig. 11-46). This lesion requires urgent orbital repair.

The management of the remaining orbital blow-out fractures is based on the risk of altered globe position (enophthalmos and hypoglobus), displacement of the muscles, potential restrictive strabismus, and whether there is time for contemplative assessment of the patient. In patients who are initially asymptomatic, the incidence of late complications following untreated blow-out fractures is extremely low. If orbital imaging identifies significant expansion (greater than 2 cm^3), typically large floor fractures or fractures that involve more than one half of the orbital floor, or fractures involving the floor and medial wall), surgery is indicated to restore orbital volume and integrity.

For restrictive strabismus, surgery is indicated when imaging demonstrates significant displacement or entrapment of extraocular muscles. Surgery is directed at reconstituting the orbital shape and volume and freeing the adhesions. Both of the above indications (i.e., risk of enophthalmos and persistent diplopia) do not require acute intervention and are probably best achieved in a few days when some of the soft tissue swelling has decreased.

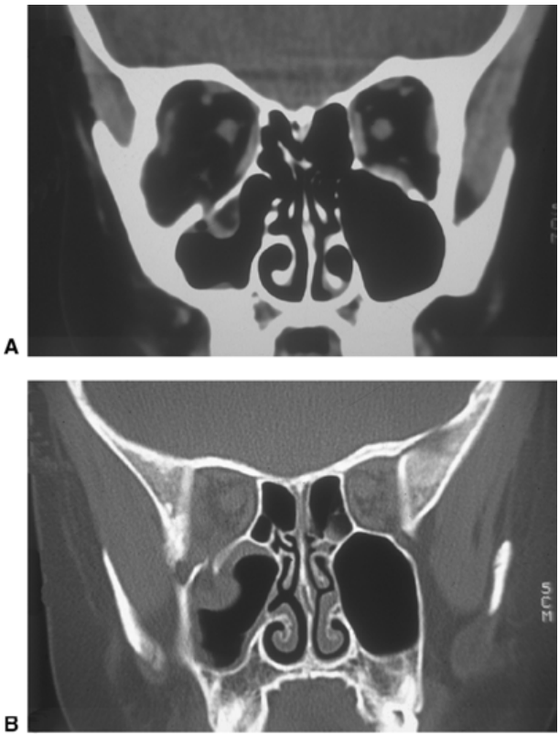

Figure 11-46. These coronal CT scans demonstrate trapdoor entrapment of the right inferior rectus muscle into the right maxillary sinus in a 9-year-old boy, which required immediate surgical repair.

Infraorbital hypesthesia alone is not an indication for acute repair. A number of authors have described long-term hypesthesia relieved by surgically disimpacting the nerve within the infraorbital canal. During the early assessment period, the patient should be warned not to blow his nose or sneeze because of risk of orbital emphysema. There should be careful follow-up for evidence of infection (rare). Early motility exercises may improve ocular excursions and might stimulate the formation of a functional connective tissue system around the muscles.

In summary, the most common presenting symptoms of blow-out fracture are diplopia with restricted extraocular movements and infraorbital hypesthesia. A small percentage of patients demonstrate primary enophthalmos, proptosis, ptosis, or orbital emphysema. Indications for surgery remain entrapment, potential enophthalmos, orbital hemorrhage, and bony spurs.

Treatment of late enophthalmos depends upon the cosmetic results desired and is often difficult. One should wait 4 to 6 months until the enophthalmos stabilizes. To test the likelihood of successful repair, the forward traction test has been advocated. One applies forceps to the medial and lateral

rectus muscle and exerts forward traction. If the globe comes forward, prognosis for repair is better than if the globe cannot be advanced. Globe ptosis and enophthalmos can be repaired by placement of an implant in the floor. This implant should have a greater volume posteriorly in order to increase orbital volume, and advance and elevate the globe. However, if the cosmetic deformity consists of a narrow palpebral fissure or ptosis, one could correct this with appropriate lid surgery. For a deepened superior sulcus one could remove the skin and some orbital fat from the contralateral eye and elevate the crease to provide symmetry.

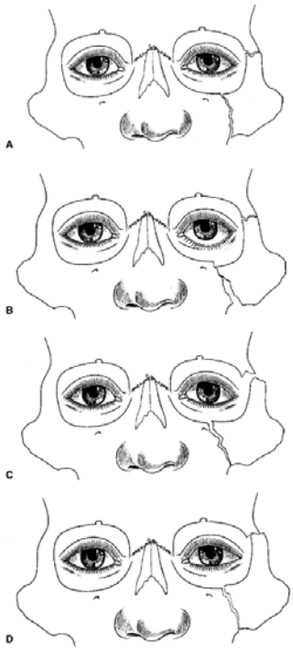

Figure 11-47. Schematic demonstrates the ocular features of trimalar fractures. (A) An undisplaced fracture does not change the lid or eye position. (B) Rotation of the inferolateral orbital margin causes inferior lateral scleral show. (C) A downward displacement of the fracture pulls the lateral canthus down. (D) Upward displacement causes elevation of the canthus and stretching and flattening of the lateral lid.

Complex Fractures

Complex fractures include those that extend beyond the orbit and involve the rim, roof, naso-orbital-ethmoidal region, maxilla, and zygoma. These fractures can result in esthetic and functional disturbances, including diplopia, lid and canthal malposition, lagophthalmos, and disruption of lacrimal out-flow. Zygomatic fractures (Fig. 11-47) commonly occur following a lateral blow to the cheek, which results in dislocation of the zygoma from the frontal bone above, the arch laterally, and the maxilla medially. These fractures usually extend into the floor of the orbit with features of a blow-out fracture (in 33% to 40% of patients). Posterior displacement leads to a step-like deformity and tenderness of the inferior orbital rim. The cheek may be edematous with a depression of the normal convexity, associated with ecchymosis, unilateral epistaxis, and emphysema. When the fracture is rotated, the level of the globe or lateral canthus, or both, will be altered. Surgical repair is almost always necessary. The indications for such are trismus (inability to open the mouth) and unacceptable facial asymmetry with displacement of the canthal ligaments and lower lid. Undisplaced fractures do not require surgical treatment.
Maxillary fractures can be divided into three groups (Fig. 11-48):

- Le Fort I is a low transverse maxillary fracture above the teeth with no orbital involvement.
- Le Fort II has a pyramidal configuration including nasal, lacrimal, and maxillary bones. These involve the medial orbital floor (which also may be blown out).
- Le Fort III involves craniofacial disjunction in which the entire facial skeleton is detached from the base of the skull and suspended only by soft tissues. They involve the medial and lateral orbital walls and orbital floor.

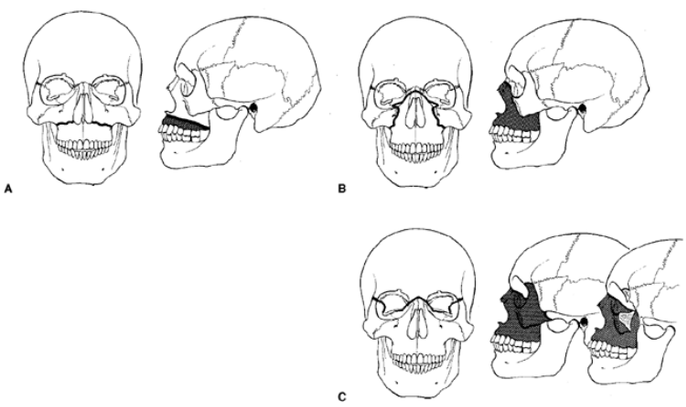

Figure 11-48. Le Fort fractures: (A) Le Fort I; (B) Le Fort II; (C) Le Fort III.

Thus, fractures of the central third of the facial skeleton (Le Fort II and III types) may involve the orbit and are often asymmetric. Comminuted midfacial fractures are one of the most common fractures affecting the facial skeleton. A force that fractures the nasal bones usually fractures the medial orbital walls, ethmoid sinuses, and cribriform plate (which may result in cerebrospinal fluid rhinorrhea) (Fig. 11-49). The most common etiology is a dashboard injury. In minor injuries only the nasal bones and frontal processes of the maxillae are displaced posteriorly and impacted into the interorbital space, collapsing and spreading internally (Fig. 11-50). In more severe trauma the lacrimal and ethmoid bones crumble and telescope, leading to hypertelorism and associated displacement of the medial canthal ligaments with telecanthus (see Fig. 11-34). Severe epistaxis may result from laceration or avulsion of the anterior ethmoid artery. A rare late complication of nasal fracture is incarceration of mucosa with failure of union, which leads to recurrent hemorrhage into the adjacent soft tissues with ecchymosis and hemosiderin deposition.

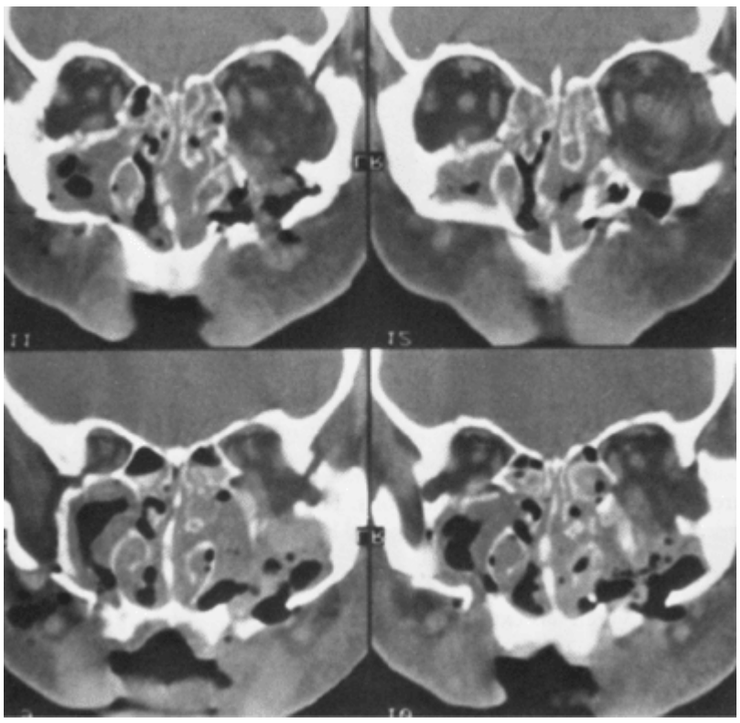

Figure 11-49. Composite of CT scans demonstrates a midfacial fracture with bilateral disruption of the ethmoid and maxillary sinuses, nasal structures, and orbital floor. Note the lateral zygomatic fracture on the left side.

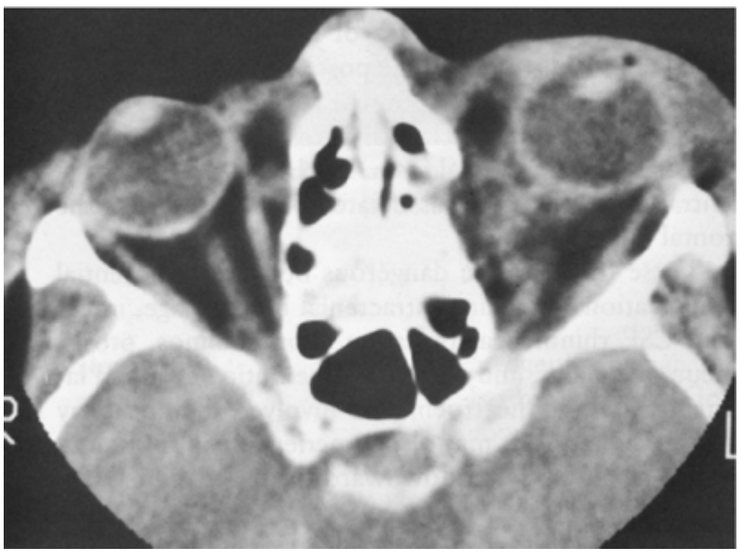

Figure 11-50. Axial CT scan of a midfacial smash, with collapse of the ethmoid sinuses and hemorrhage into the medial half of the left orbit.

Clinically, the patient usually presents with a flattened bridge of the nose and swollen medial canthal areas. Dacryostenosis is a common complication.
Treatment of these injuries should be at one time and consists of correction of the epicanthal folds, restoration of bony contour, repair of the lacrimal system, and medial canthoplasty.

Orbital Apex Fractures

Orbital apex fractures occur alone or in combination with other facial fractures. Injury to the optic nerve with vision loss, cerebrospinal fluid leaks, and carotid cavernous fistulas are possible associated complications. The diagnosis of a fracture of the optic canal is facilitated by using a CT scan with the gantry tilted 10 in order to accurately assess the optic canal. Conventional views will also show a linear fracture of the frontal or temporal bones or of the lesser wing of the sphenoid, which has extended into this region.

Orbital Roof Fractures

Orbital roof fractures may also involve the brain, cribriform plate, and the frontal sinuses. They are usually caused by missiles or blunt trauma. Orbital roof fractures may be divided into three types. The first involves the medial third of the rim, the anterior wall of the frontal sinus, and the subjacent area of the orbital roof (Fig. 11-51). Extension through the posterior wall of the frontal sinus into the anterior cranial fossa may occur. The second type involves the lateral third of the rim, which is weakened by the lacrimal fossa. The last type involves the central third and may be associated with a fracture of the frontal bone.

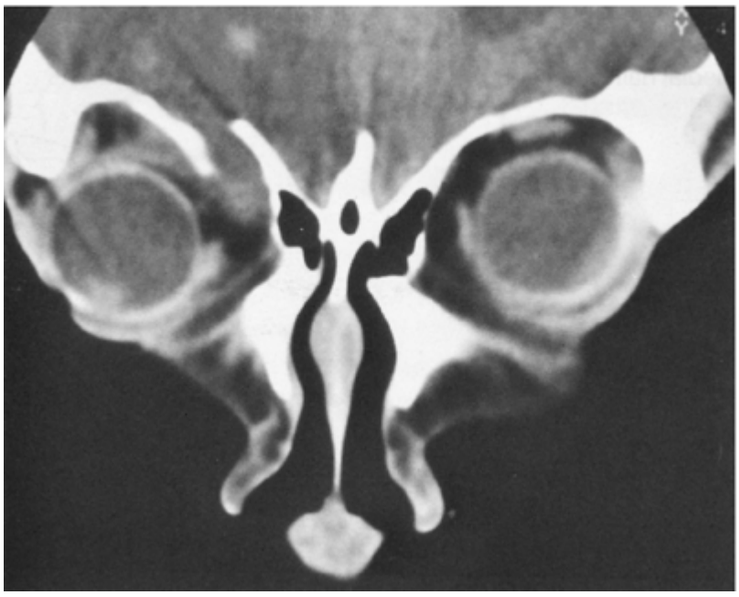

Figure 11-51. Coronal CT scan of an orbital roof fracture with a traumatic encephalocele.

These fractures are serious because of potential complications including intracranial hemorrhage, infection, cerebrospinal fluid rhinorrhea, pulsating exophthalmos, ptosis, pneumocephalus, and injuries to the optic nerve and lacrimal gland. If the trochlea is involved, diplopia may ensue. Patients may also experience painful limitation of upgaze due to downward displaced bone fragments. The brain often sustains a concussion injury and may even be lacerated if there is a comminuted fracture. The supraorbital rim may be depressed with a step-like deformity and may demonstrate point tenderness. Delayed onset of eyelid ecchymosis may follow a roof fracture. Persons with large frontal sinuses are more susceptible. Management of these fractures should use a team approach with a neurosurgeon and ophthalmologist.

Orbital Foreign Bodies

Foreign bodies may enter the orbit either by traversing between the globe and the orbital wall or by double perforation of the globe, as occurs in 7% of intraocular foreign bodies. It should always be kept in mind that there may be more than one foreign body present. Any laceration or puncture site should be explored for a foreign body.
Many orbital foreign bodies are inert and well tolerated. Exceptions to this are copper and organic matter. Copper can incite a purulent inflammatory response even after variable periods of quiescence. Organic foreign bodies such as wood or vegetable matter cannot be seen on conventional x-rays, and CT scan or MRI may be helpful in localizing them. If left in the orbit, they can produce cellulitis, granuloma, fistula to the skin or conjunctiva, abscess, osteomyelitis, or periostitis. Organic foreign bodies may also present with

serious late complications, such as brain abscess (Fig. 11-52).

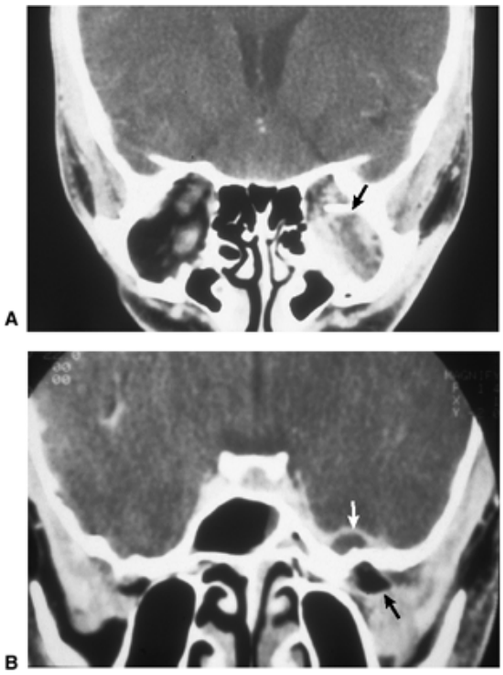

Figure 11-52. Coronal CT scans demonstrate an orbital cellulitis with a bony fracture (A, arrow) in a 30-year-old man due to a penetrating wood foreign body. This had extended into the orbit and pterygopalatine fossa and also caused a subdural abscess (B, white arrow). Because the wood was old and dry, it appeared as an air-filled shadow on CT scan (B, black arrow).

A careful history must be obtained because the initial incident is often forgotten. Management depends on the composition, size, and shape of the foreign body and accurate localization by use of plain orbital x-rays, bone free film, or CT scans, or all three (Figs. 11-53 and 11-54). Ultrasonography is of limited value because it may be difficult to differentiate some foreign bodies from traumatized orbital fat. If there is a chronic fistula, a retained foreign body may sometimes be located surgically by following the fistulous tract posteriorly. It should be noted in passing that magnetic resonance imaging cannot be used in the presence of a suspected magnetic foreign body, because magnetic fragments may move in the magnetic field and damage critical structures.
Once the extent of ocular and orbital damage is assessed, a decision must be made whether or not to remove it. Because there is a good prognosis and removal can be difficult, treatment should be conservative unless there is a significant inflammatory reaction or a compressive effect on a vital orbital structure. Objects located in the orbit posterior to the equator should be left alone to prevent iatrogenic damage. Inert, smooth-edged objects should also be observed. Generally, foreign bodies should be removed if superficial and anterior in location, if they have sharp edges (that threaten adjacent structures), or if they are composed of organic matter or copper. Removal should be as atraumatic as possible to prevent further damage and fragmentation of the object. It is important to explore the complete extent of injury, and cultures should be obtained.

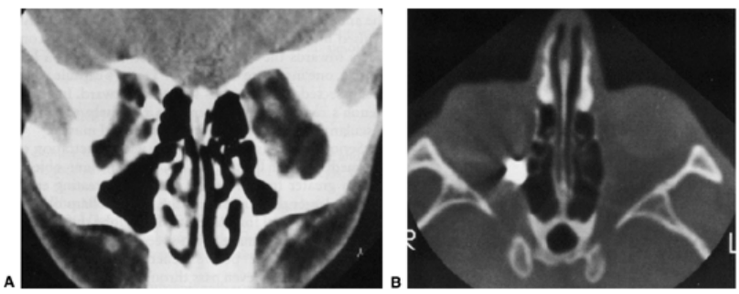

Figure 11-53. Axial (A) and coronal (B) CT scans show a metallic foreign body in the orbit following an air gun injury. It caused pressure on the optic nerve. The foreign body was removed surgically, and visual field returned to normal.

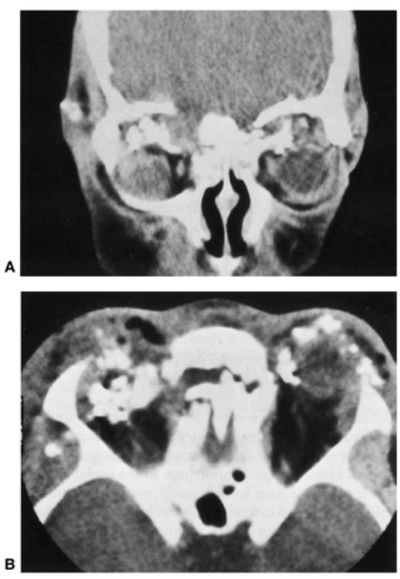

Figure 11-54. Coronal (A) and axial (B) CT scans of multiple foreign bodies in the orbit, which was associated with a gunshot injury.

It must be remembered that a foreign body may enter the orbit and penetrate to the paranasal sinuses, nose, or intracranial cavity (by means of the superior orbital fissure or roof). There is an increased risk of direct penetration of a foreign body into the anterior fossa in children due to the absence of a frontal sinus. There may not be a fracture evident on X-ray. In a series of 42 transorbital cranial penetrations can have about a 10% mortality rate. Immediate and delayed neurological complications should always be anticipated.

Bibliography

Conjunctival Epithelial Cysts

Dermoid and Epidermoid Cysts

Bonavolonta G, Tranfa G, de Conciliis C, Strianese D. Dermoid cysts: 16-year survey. Ophthal Plast Reconstr Surg 1995;11:187-92.

Chawda SJ, Moseley IF. Computed tomography of orbital dermoids: a 20-year review. Clin Radiol 1999;54:821-5.

Cullen JF. Orbital diploic dermoids. Br J Ophthamol 1974;58:105-6.

Eijpe AA, Koornneef L, Verbeeten B Jr, et al. Intradiploic epidermoid cysts of the bony orbit. Ophthalmology 1991;98:1737-43.

Emerick GT, Shields CL, Shields JA, et al. Chewing-induced visual impairment from a dumbbell dermoid cyst. Ophthal Plast Reconstr Surg 1997;13:57-61.

Grove AS Jr. Giant dermoid cysts of the orbit. Ophthalmology 1979;86:1513-20.

Holds JB, Anderson RL, Mamalis N, et al. Invasive squamous cell carcinoma arising from asymptomatic choristomatous cysts of the orbit: two cases and a review of the literature. Ophthalmology 1993;100:1244-52.

Honig JF. A de novo discharging sinus of the fronto-orbital suture: a rare presentation of a dermoid cyst. J Craniofac Surg 1998;9:536-8.

Howard GR, Nerad JA, Bonavolonta G, Tranfa F. Orbital dermoids located within the lateral rectus muscle. Ophthalmology 1994;101:767-71.

Lessner AM, Antle CM, Rootman J, et al. Cystic lesions of the orbit and radiolucent defects of bone. In: Margo CE, Hamed LM, Mames RN, eds. Diagnostic Problems in Clinical Ophthalmology. Philadelphia: WB Saunders, 1994, 87-98.

Meyer DR, Lessner AM, Yeatts RP, Linberg JV. Primary temporal fossa dermoid cysts: characterization and surgical management. Ophthalmology 1999;106:342-9.

Pollard ZF, Calhoun MD. Deep orbital dermoid with draining sinus. Am J Ophthalmol 1975;79:310-3.

Sathananthan N, Moseley IF, Rose GE, Wright JE. The frequency and clinical significance of bone involvement in outer canthus dermoid cysts. Br J Ophthalmol 1993;77:789-94.

Sherman RP, Rootman J, Lapointe JS. Orbital dermoids: clinical presentation and management. Br J Ophthalmol 1984:68:642-52.

Shields JA, Kaden IH, Eagle RC Jr, Shields CL. Orbital dermoid cysts: clinicopathologic correlations, classification, and management. The 1997 Josephine E. Schueler Lecture. Ophthal Plast Reconstr Surg 1997;13:265-76.

Conjunctival Cysts

Goldstein MH, Soparkar CNS, Kersten RC, et al. Conjunctival cysts of the orbit. Ophthalmology 1998;105:2056-60.

Howard GR, Nerad JA, Bonavolonta G, Tranfa F. Orbital dermoid cysts located within the lateral rectus muscle. Ophthalmology 1994;101:767-71.

Shields JA, Augsburger JJ, Donoso LA. Orbital dermoid cyst of conjunctival origin. Am J Ophthalmol 1986;101:726-9.

West JA, Drewe RH, McNab AA. Atypical choristomatous cysts of the orbit. Aust & N Z J Ophthalmol 1997;25:117-23.

Miscellaneous Epithelial Cysts

Ballesteros E, Greenebaum E, Merriam JC. Fine-needle aspiration diagnosis of enterogenous cyst of the orbit: a case report. Diagn Cytopathol 1997;16:450-3.

Eggert JE, Harris GJ, Caya JG. Respiratory epithelial cyst of the orbit. Ophthal Plast Reconstr Surg 1988; 4:101-4.

Leventer DB, Merriam JC, Defendini R, et al. Enterogenous cyst of the orbital apex and superior orbital fissure. Ophthalmology 1994;101:1614-21.

Newton C, Dutton JJ, Klintworth GK. A respiratory epithelial choristomatous cyst of the orbit. Ophthalmol 1985;92:1754-7.

Rose GE, O'Donnell BA. Congenital orbital cysts associated with the common sheath of superior rectus and levator palpebrae superioris muscles. Ophthalmology 1995;102:135-8.

Mucoceles

Aoki H, Tanaka Y, Niki Y, et al. Intraorbital subperiosteal hematoma due to paranasal mucocele-case report. Neurologia Medico-Chirurgica 1997;37:627-9.

Benninger MS, Marks S. The endoscopic management of sphenoid and ethmoid mucoceles with orbital and intranasal extension. Rhinology 1995;33:157-61.

Cline RA, Rootman J. Enophthalmos: a clinical review. Ophthalmology 1984;91:229-37.

Coleman DJ, Jack RL, Franzen LA. B-scan ultrasonography of orbital mucoceles. Eye Ear Nose Throat Mon 1972;51:207-11.

Delfini R, Missori P, Iannetti G, et al. Mucoceles of the paranasal sinuses with intracranial and intraorbital extension: report of 28 cases. Neurosurgery 1993;32:901-6.

Ehrenpreis SJ, Biedlingmaier JF. Isolated third-nerve palsy associated with frontal sinus mucocele. J Neuro Ophthalmol 1995;15:105-8.

Garber PF, Abramsom AL, Stallman PT, Wasserman PG. Globe ptosis secondary to maxillary sinus mucocele. Ophthal Plast Reconstr Surg 1995;11:254-60.

Girard B, Choudat L, Hamelin N, et al. Mucocele fronto-naso-ethmoido-sphenoidl-maxillo-orbitaire a relevation ophtalmologique. J Fr d'Ophtalmol 1999;22:536-40.

Guerry RK, Smith JL. Paranasal sinus carcinoma causing orbital mucocele. Am J Ophthamol 1975;80:943-6.

Iliff CE. Mucoceles in the orbit. Arch Ophthalmol 1973;89:392-5.

Johnson LN, Hepler RS, Yee RD, et al. Sphenoid sinus mucocele (anterior clinoid variant) mimicking diabetic ophthalmoplegia and retrobulbar neuritis. Am J Ophthalmol 1986;102:111-5.

Lund VJ, Rolfe ME. Ophthalmic considerations in fronto-ethmoidal mucoceles. J Laryngol Otol 1989;103:667-9.

Luxenberger W. Anderhuber W. Stammberger H. Mucocele in an orbitoethmoidal (Haller's) cell (accidentally combined with acute contralateral dacryocystitis). Rhinology 1999;37:37-9.

Montgomery WW. Mucocele of the maxillary sinus causing enophthalmos. Eye Ear Nose Throat Mon 1964;43:41-4.

Ormerod LD, Weber AL, Rauch SD, Feldon SE. Ophthalmic manifestations of maxillary sinus mucoceles. Ophthalmology 1987;94:1013-19.

Pia F, Aluffi P, Borello G. Mucocele frontale: open surgery. Acta Otorhinolaryngol Ital 1999;19:155-9.

Pollock JA, Newton TH, Hoyt WF. Transsphenoidal and transethmoidal encephaloceles. A review of clinical and roentgen features in 8 cases. Radiology 1968;90:442-53.

Reese AB. Expanding lesions of the orbit. Trans Ophthalmol Soc U K 1971;91:85-104.

Senior BA, Lanza DC, Kennedy DW, Weinstein GS. Computer-assisted resection of benign sinonasal tumors with skull base and orbital extension. Arch Otoloaryngol Head Neck Surg 1997;123:706-11.

Soparkar CNS, Patrinely JR, Cuaycong MJ, et al. The silent sinus syndrome: a cause of spontaneous enophthalmos. Ophthalmology 1994;101:772-8.

Stewart MG, Patinely JR, Appling WD, Jordan DR. Late proptosis following orbital floor repair. Arch Otolaryngol Head Neck Surg 1995;121:649-52.

Stool S, Kertesz E, Sibinga M, Frayer W. Exophthalmos due to pyocele of the sinus in children with cystic fibrosis. Trans Am Acad Ophthalmol Otolaryngol 1966;70:811-6.

Wilkins RB, Kulwin DR. Spontaneous enophthalmos associated with chronic maxillary sinusitis. Ophthalmology 1981;88:981-5.

Lacrimal Ductal Cysts

Brownstein S, Belin MW, Krohel GB, et al. Orbital dacryops. Ophthalmology 1984;91:1424-8.

Duke-Elder S, MacFaul PA. The ocular adnexa. Part II. Lacrimal, orbital, and para-orbital disease. In: Duke-Elder S, ed. System of Ophthalmology. London: Henry Kimptom, 1974; v. 13:596-1163.

Duran JA, Cuevas J. Cyst of accessory lacrimal gland. Br J Ophthalmol 1983;67:485-6.

Green WR, Zimmerman LE. Ectopic lacrimal gland tissue. Arch Ophthamol 1967;78:318-27.

Harris GJ. Marsupialization of a lacrimal gland cyst. Ophthalmic Surg 1983;14:75-8.

Rush A, Leone CR Jr. Ectopic lacrimal gland cyst of the orbit. Am J Ophthalmol 1981;92:198-201.

Sen DK, Thomas A. Simple dacryops. Am J Ophthalmol 1967;63:161.

Smith S, Rootman J. Lacrimal ductal cysts: presentation and management. Surv Ophthalmol 1986;30:245-50.

Neurogenic Cysts

Microphthalmos with Cyst & Congenital Cystic Eye

Baghdassarian SA, Tabbara KF, Matta CS. Congenital cystic eye. Am J Ophthalmol 1973;76:269-75.

Dollfus MA, Marx P, Langlois J, et al. Congenital cystic eyeball. Am J Ophthalmol 1968;66:504-9.

Ehlers N. Cryptophthalmos with orbito-palpebral cyst and microphthalmos (report of a bilateral case). Acta Ophthalmol 1966;44:84-94.

Fledelius HC, Ultrasonic evaluation of microphthalmos and coloboma. A discussion of 3 cases, with emphasis on microphthalmos with orbital cyst. Acta Ophthalmol Scand Suppl 1996:23-6.

Foxman S, Cameron JD. The clinical implications of bilateral microphthalmos with cyst. Am J Ophthalmol 1984;97:632-8.

Hayashi N, Repka MX, Ueno H, et al. Congenital cystic eye: report of two cases and review of the literature. Surv Ophthalmol 1999;44:173-9.

Helveston EM, Malone E Jr, Lashmet MH. Congenital cystic eye. Arch Ophthalmol 1970;84:622-4.

Jensen OA. Microphthalmia with associated pseudogliomatosis of the retina and pseudogliomatous orbital cyst. Acta Ophthalmol 1965;43:240-4.

Kok-van Alphen CC, Manschot WA, Frederiks E, van Beuseko GT. Microphthalmus with orbital cyst. Ophthalmologica 1973;167:389-92.

Polito E, Leccisotti A, Colobomatous ocular cyst extension with globe preservation. Ophthal Plast Reconstr Surg 1995;11:288-92.

Sherman J, Bass SJ, George A, et al. Optic pit, microphthalmos and orbital cyst. Ophthal Paediatr Genet 1988;9:131-3.

Warburg M. Classification of microphthamos and coloboma. J Med Genet 1993;30:664-9.

Waring GO 3d, Roth AM, Rodrigues MM. Clinicopathologic correlation of microphthalmos with cyst. Am J Ophthalmol 1976;82:714-21.

Wilson RD, Travese L, Hall JG, et al. Oculocerebrocutaneous syndrome. Am J Ophthalmol 1985;99:142-8.

Cephaloceles

Boonvisut S, Ladpli S, Sujatanond M, et al. Morphologic study of 120 skull base defects in frontoethmoidal encephalomeningoceles. Plast Reconstr Surg 1998;101:1784-95.

Clements DB, Kaushal K. A study of the ocular complications of hydrocephalus and meningomyelocele. Trans Ophthalmol Soc U K 1970;90:383-90.

Consul BN, Kulshrestha OP. Orbital meningocele. Br J Ophthalmol 1965;49:374-6.

Dvorak-Theobald G, Middleton WH. Congenital cyst of the optic nerve with encephalocele. Trans Am Acad Ophthalmol Otolaryngol 1951;55:277-9.

Hershewe GL, Corbett JJ, Ossoinig KC, Thompson HS. Optic nerve compression from a basal encephalocele. J Neuro Ophthalmol 1995;15:161-5.

Leone CR Jr, Marlowe JF. Orbital presentation of an ethmoidal encephalocele. Report of a case of a 62-year-old woman. Arch Ophthalmol 1970;83:445-7.

Mortada A. Pulsating frontocele and exophthalmos. Am J Ophthalmol 1968;65:425-7.

Rochels R, Nover A. Papillenanomalien bei (peri)orbitalen Enzephalozelen–Ein Beitrag zur gemeinsamen Pathogenese dieser Fehlbildungen. Klin Monatsbl Augenheilkd 1990;197:311-6.

Songur E, Mutluer S, Gurler T, et al. Management of frontoethmoidal (sincipital) encephalocele. J Craniofac Surg 1999;10:135-9.

Strandberg B. Cephalocele of posterior part of orbit. General survey, with report of case. Arch Ophthalmol 1949;42:254-65.

Sugawara Y, Harii K, Hirabayashi S, et al. A spheno-orbital encephalocele with unilateral exophthalmos. Ann Plast Surg 1996;36:410-2.

Terry A, Patrinely JR, Anderson RL, Smithwick W 4th. Orbital meningoencephalocele manifesting as a conjunctival mass. Am J Ophthalmol 1993;115:46-9.

Other Neurogenic Cysts

Kim KM, Kang SJ, Kim DS, et al. Congenital intraoribtal optic nerve cyst: case report. J Neurosurg 1999;91:325-7.

Tumors and Ectopias

Dermolipomas

Beard C. Dermolipoma surgery, or, “an ounce of prevention is worht a pound of cure.” Ophthal Plast Reconstr Surg 1990;6:153-7.

Eijpe AA, Koornneef L, Bras J, et al. Dermolipoma: characteristic CT appearance. Doc Ophthalmol 1990;74:321-8.

Fry CL, Leone CR Jr. Safe management of dermolipomas. Arch Ophthalmol 1994;112:1114-6.

Hered RW, Hiles DA. Epibulbar osseous choristoma and ectopic lacrimal gland underlying a dermolipoma. J Ped Ophthalmol Strabismus 1987;24:255-8.

Jordan DR, Tse DT. Herniated orbital fat. Can J Ophthalmol 1987;22:173-7.

Kim YD, Goldberg RA. Orbital fat prolapse and dermolipoma: two distinct entities. Korean J Ophthamol 1994;8:42-3.

McNab AA, Wright JE, Caswell AG. Clinical features and surgical management of dermolipomas. Aust N Z J Ophthalmol 1990;18:159-62.

Lacrimal Ectopias

Kao SC, Yeh LK, Tsai CC, Hsu WM. Ectopic lacrimal gland cyst of the orbit. Chung Hua i Hsueh Tsa Chih 2000;63:334-8.

Rao VA, Kwatra V, Puri A. Cyst of ectopic (choristomatous) lacrimal gland. Indian J Ophthalmol 1989;37:189-90.

Other Ectopias

Wilkins RB. Hofmann J, Byrd WA, Font RL. Heterotopic brain tissue in the orbit. Arch Ophthalmol 1987;105:390-2.

Orbital Teratomas

Bilgic S, Dayanir V, Kiratli H, Gungen Y. Congenital orbital teratoma: a clincopathologic case report. Ophthal Plast Reconstr Surg 1997;13:142-6.

Kivela T, Tarkkanen A. Orbital germ cell tumors revisited: a clinicopathological approach to classification. Surv Ophthalmol 1994;38:541-54.

Mamalis N, Garland PE, Argyle JC, Apple DJ. Congenital orbital teratoma: a review and report of two cases. Surv Ophthalmol 1985;30:41-6.

Prause JU, Borgesen SE, Carstensen H, et al. Cranio-orbital teratoma. Acta Ophthalmol Scand Suppl 1996:53-6.

Weiss AH, Greenwald MJ, Margo CE, Myers W. Primary and secondary orbital teratomas. J Pediatr Ophthalmol Strabismus 1989;26:44-9.

Bony Anomalies

Fries PD, Katowitz JA. Congenital craniofacial anomalies of ophthalmic inportance. Surv Ophthalmol 1990;35:87-119.

Trauma

Anderson DP, Ford RM. Visual abnormalities after severe head injuries. Can J Surg 1980;23:163-5.

Anderson RL, Panje WR, Gross CE. Optic nerve blindness following blunt forehead trauma. Ophthalmology 1982;89:445-55.

Bensagi ZC, Meyer DR. Internal orbital fractures in the pediatric age group: characterization and management. Ophthalmology 2000;107:829-36.

Dalley RW, Robertson WD, Rootman J. Globe tenting: a sign of increased orbital tension. A. JNR 1989;10:181-6.

Dutton JJ. Management of blow-out fractures of the orbital floor [editorial]. Surv Ophthalmol 1991;35:279-80.

Egbert JE, May K, Kersten RC, Kulwin DR. Pediatric orbital floor fracture: direct extraocular muscle involvement. Ophthalmology 2000;107:1875-9.

Emery JM, von Noorden GK, Schlernitzauer DA. Orbital floor fractures: long-term follow-up of cases with and without surgical repair. Trans Am Acad Ophthalmol Otolaryngol 1971;75:802-12.

Flanagan JC, McLachlan DL, Shannon GM. Orbital roof fractures: neurologic and neurosurgical considerations. Ophthalmology 1980;87:325-9.

Fleishman JA, Beck RW, Hoffman RO. Orbital emphysema as an ophthalmologic emergency. Ophthalmology 1984;91:1389-91.

Gilbard SM, Mafee MF, Lagouros PA, Langer BG. Orbital blowout fractures. The prognostic significance of computed tomography. Ophthalmology 1985;92:1523-8.

Glatt HJ, Custer PL, Barrett L, Sartor K. Magnetic resonance imaging and computed tomography in a model of wooden foreign bodies in the orbit. Ophthal Plast Reconstr Surg 1990;6:108-14.

Godoy J, Mathog RH. Malar fractures associated with exophthalmos. Arch Otolaryngol 1985;111:174-7.

Green BF, Kraft SP, Carter KD, et al. Intraorbital wood. Detection by magnetic resonance imaging. Ophthalmology 1990;97:608-11.

Harris GJ, Garcia GH, Logani SC, Murphy ML. Correlation of preoperative computed tomography and postoperative ocular motility in orbital blowout fractures. Ophthal Plast Reconstr Surg 2000;16:179-87.

Hawes MJ, Dortzbach RK. Surgery on orbital floor fractures. Influence of time of repair and fracture size. Ophthalmology 1983;90:1066-70.

Hoffman JR, Neuhaus RW, Baylis HI. Penetrating orbital trauma. Am J Emergen Med 1983;1:22-7.

Holt GR, Holt GE. Management of orbital trauma and foreign bodies. Otolaryngol Clin North Am 1988;21:35-52.

Ilankovan V, Hadley D, Moos K, el Attar A. A comparison of imaging techniques with surgical experience in orbital injuries. A prospective study. J Cranio Maxillo Fac Surg 1991;19:348-52.

Jacobs NA, Morgan LH. On the management of retained airgun pellets: a survey of 11 orbital cases. Br J Ophthalmol 1988;72:97-100.

Jordan DR, Allen LH, White J, et al. Intervention within days for some orbital floor fractures: the white-eyed blowout. Ophthal Plast Reconstr Surg 1998;14:379-90.

Joseph MP, Lessell S, Rizzo J, Momose KJ. Extracranial optic nerve decompression for traumatic optic neuropathy. Arch Ophthalmol 1990;108:1091-3.

Klingele TG, Gado MH, Burde RM, Coxe WS. Compression of the anterior visual system by the gyrus rectus. Case report. J Neurosurg 1981;55:272-5.

Koornneef L. Current concepts on the management of orbital blow-out fractures. Ann Plast Surg 1982;9:185-200.

Lahbabi M, Lockhart R, Fleuridas G, et al. Enophtalmies post-traumatriques. Considerations physiopathologiques et therapeutiques actuelles. Rev Stomatol Chir Maxillofac 1999;100:165-74.

Lee AG. Traumatic optic neuropathy. [Letter]. Ophthalmology 2000;107:814.

Lessell S. Indirect optic nerve trauma. Arch Ophthalmol 1989;107:382-6.

Levin LA, Beck RW, Joseph MP, et al. The treatment of traumatic optic neuropathy: the International Optic Nerve Trauma Study. Ophthalmology 1999;106:1268-77.

Liu D. A simplified technique of orbital decompression for severe retrobulbar hemorrhage. Am J Ophthalmol 1993;116:34-7.

Manson PN, Iliff N. Management of blow-out fractures of the orbital floor. II. Early repair for selected injuries. Surv Ophthalmol 1991;35:280-92.

Mauriello JA Jr, Lee HJ, Nguyen L. CT of soft tissue injury and orbital fractures. Radiologic Clin N Am 1999

McLachlan DL, Flanagan JC, Shannon GM. Complications of orbital roof fractures. Ophthalmology 1982;89:1274-8.

Miller GR, Tenzel RR. Ocular complications of midfacial fractures. Plast Reconstr Surg 1967;39:37-42.

Millman AL, Della Rocca RC, Spector S, et al. Steroids and orbital blowout fractures – a new systematic concept in medical management and surgical decision-making. Adv Ophthal Plast Reconstr Surg 1987;6:291-300.

Nasr AM, Haik BG, Fleming JC, et al. Penetrating orbital injury with organic foreign bodies. Ophthalmology 1999;106:523-32.

Paris GL, Spohn WG. Correction of enophthalmos in the anophthalmic orbit. Ophthalmology 1980;87:1301-8.

Pope-Pegram LD, Hamill MB. Post-traumatic subgaleal hematoma with subperiosteal orbital extension. Surv Ophthalmol 1986;30:258-62.

Putterman AM. Management of blow-out fractures of the orbital floor. III. The conservative approach. Surv Ophthalmol 1991;35:292-8.

Putterman AM. Late management of blow-out fractures of the orbital floor. Trans Am Acad Ophthalmol Otolaryngol 1977;83:650-9.

Putterman AM, Stevens T, Urist MJ. Nonsurgical management of blow-out fractures of the orbital floor. Am J Ophthalmol 1974;77:232-9.

Raskin EM, Millman AL, Lubkin V, et al. Prediction of late enophthalmos by volumetric analysis of orbital fractures. Ophthal Plast Reconstr Surg 1998;14:19-26.

Rootman J, Stewart B, Goldberg RA. Orbital Surgery: A Conceptual Approach. Philadelphia: Lippincott-Raven, 1995.

Rosen HM. The response of porous hydroxyapatite to contiguous tissue infection. Plast Reconstr Surg 1991;88:1076-80.

Segrest DR, Dortzbach RK. Medial orbital wall fractures: complications and management. Ophthal Plast Reconstr Surg 1989;5:75-80.

Seiff SR, Berger MS, Guyon J, Pitts LH. Computed tomographic evaluation of the optic canal in sudden traumatic blindness. Am J Ophthalmol 1984;98:751-5.

Seiff SR, Good WV. Hypertropia and the posterior blowout fracture: mechanism and management. Ophthalmology 1996;103:152-6.

Specht CS, Varga JH, Jalali MM, Edelstein JP. Orbitocranial wooden foreign body diagnosed by magnetic resonance imaging. Dry wood can be isodense with air and orbital fat by computed tomography. Surv Ophthalmol 1992;36:341-4.

Stuzin JM, Cutting CB, McCarthy JG, Dufresne CR. Radiographical documentation of direct injury of the intracanalicular segment of the optic nerve in the orbital apex syndrome. Ann Plast Surg 1988;20:368-73.

Tengtrisorn S, McNab AA, Elder JE. Persistent infra-orbital nerve hyperaesthesia after blunt orbital trauma. Aust N Z J Ophthalmol 1998;26:259-60.

Wachler BS, Holds JB. The missing muscle syndrome in blowout fractures: an indication for urgent surgery. Ophthal Plast Reconstr Surg 1998;14:17-8.

Wesley RE, Wahl JW, Loden JP, Henderson RR. Management of wooden foreign bodies in the orbit. South Med J 1982;75:924-32.

Wilson WB, Dreisbach JN, Lattin DE, Stears JC. Magnetic resonance imaging of nonmetallic orbital foreign bodies. Am J Ophthalmol 1988;105:612-7.

Chapter 12

Inflammatory Diseases

Conceptual Model: Definition & Categorization

The clinical presentations of orbital inflammation, based on differing pathologic infiltrates and anatomic locations, were discussed earlier in the context of anatomic and pathophysiologic patterns of disease. Using this model, individual cases can be analyzed by combining features of acute, subacute, and chronic inflammation along with disease location as a framework. This chapter will classify inflammatory disease into the major categories of nonspecific inflammations, infections and infestations, and specific noninfectious inflammations.

The last 20 years of our experience in managing over 3,000 orbital cases has lead to a paradigm shift in terms of nonthyroidal orbital inflammatory disease. This shift reflects the historical trends in medical understanding, which have been characterized by the clinical definition of disease giving way in this century to specific diagnoses based on pathologic, anatomic (imaging), and systemic associations of disease. The final decades of this millennium have seen increasing diagnostic specificity brought about by immunopathologic and molecular genetic techniques, which will link prevention and specific treatment based on the ultimate pathogenesis of disease.

With regard to inflammations of the orbit, our own experience has shifted toward the exclusion of lymphoproliferative processes from the discussion of inflammatory disease, because they are clinically and pathologically distinct from inflammatory disorders. There are, however, some transitional lesions. The orbital inflammatory processes can be viewed as either nonspecific or specific. The frequency of diagnosis of nonspecific orbital inflammatory syndromes is decreasing as we improve our understanding of the pathogenetic and clinical constellations of the specific orbital inflammations. In effect, the nonspecific orbital inflammatory diseases (previously misnamed as “inflammatory orbital pseudotumors”) constitute a shrinking population of our inflammatory cases.

The definition of nonspecific inflammations remains clinical and consists of processes that are acute and subacute, and have specific anatomical localizations within the orbit (Fig. 12-1). In contrast, the specific inflammations represent three possible types of processes:

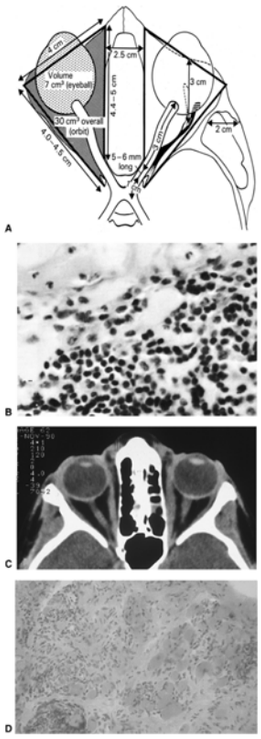

Figure 12-1. Nonspecific inflammations. (A, B) Imaging and histopathologic features of nonspecific anterior orbital inflammation (B, H&E, original magnification × 25). (C, D) CT scan and biopsy of nonspecific myositic inflammation of left medial rectus (D, H&E, original magnification × 10)

- those identified on the basis of a specific pathogen (i.e., infections and infestations) (Fig. 12-2);
- those that have specific local and/or systemic constellations of findings that identify them as distinct entities, including such diseases as vasculitis (Figs. 12-3 and 12-4);
- those disorders that have a specific histopathology that identifies them, such as some of the granulomatous diseases (Fig. 12-4).

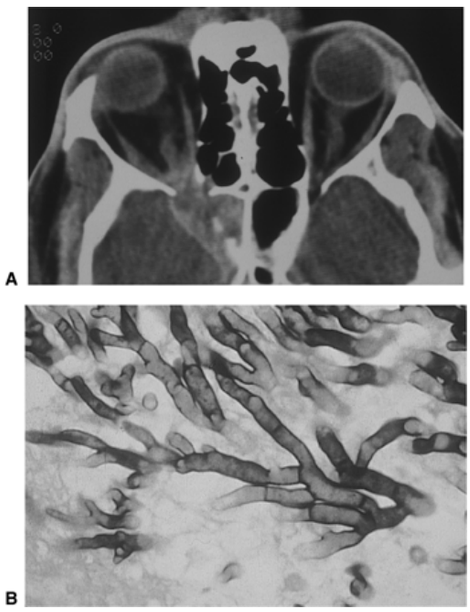

Figure 12-2. Specific inflammation – fungal pathogen. (A) Axial CT scan demonstrates a sphenoid sinus infiltration with erosion of the middle cranial fossa and infiltration of the orbital apex. (B) Biopsy revealed an *Aspergillus* infection. This occurred in a 54-year-old farmer and was characterized by a progressive, downhill course resulting in death (Grocott, original magnification × 25).

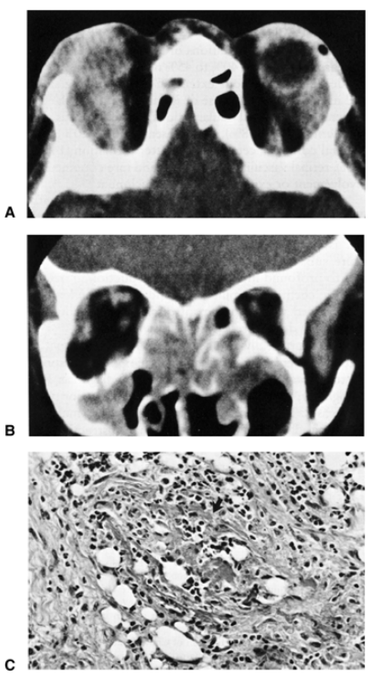

Figure 12-3. Specific inflammation – Wegener's granulomatosis. (A, B) CT scan shows bilateral lateral orbital infiltration with a lacrimal gland epicenter and extensive soft tissue changes with bone destruction of the sinuses and nasal airways. (C) Histopathology of an orbital biopsy showed diffuse infiltration of the tissue by mixed inflammation consisting of lymphocytes, epithelioid cells, occasional giant cells, polymorphic nuclear leukocytes, rare eosinophils, and plasma cells. Also, there were vessels (arrow) that showed necrotizing inflammatory changes with local infiltration by neutrophils. Special stains with PTAH showed numerous areas of fibrinoid necrosis. The overall morphology was in keeping with severe necrotizing angiitis of a granulomatous nature consistent with Wegener's granulomatosis (H&E, original magnification × 25)

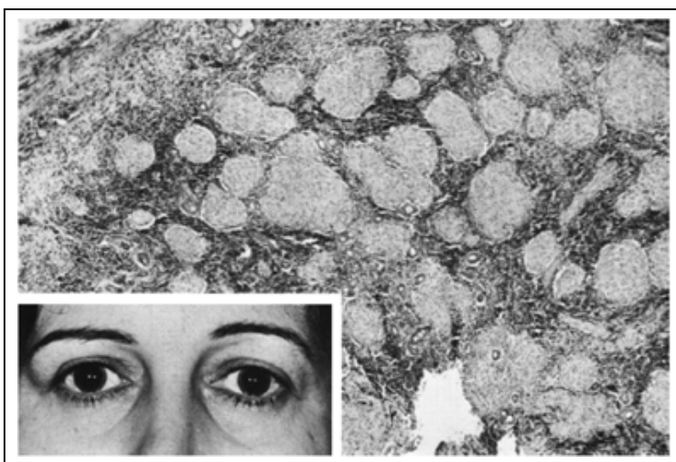

Figure 12-4. Specific inflammation – sarcoid. Histopathology and clinical features of a 50-year-old woman who presented with a progressive right superolateral mass. Histologically, the lacrimal gland was occupied by multiple granulomatous naked tubercles. The patient had bilateral hilar adenopathy (H&E, original magnification × 2.5).

Nonspecific Inflammations of the Orbit

Traditionally, acute and subacute idiopathic inflammatory syndromes have been included with the polyglot of orbital “pseudotumors,” a clinically and histologically confusing category of lesions. The pathologic substrate described for these myriad diseases ranges from nonspecific polymorphous lymphocytic and plasmacytic infiltrates to granulomatous disorders, depending on the source in the literature. The full histologic spectrum, from truly inflammatory to pseudoneoplastic disease, has been described within this rubric. The histologic studies are confusing and may not correlate with the clinical features of the disease. Yet with improved orbital imaging and careful clinical analysis, more specificity is possible in defining the presentation and character of these diseases. The patterns of orbital involvement may not point to pathogenesis, but do provide a clinical framework for diagnosis and management. They are a heterogeneous group etiologically, but in our opinion, their inclusion as inflammatory syndromes is more rational than a broader traditional framework. These entities probably include a number of different organ-specific immunologic disorders of more specific etiologies yet to be defined. Disease defined by the character of presentation and temporal sequence should form the essential diagnostic framework in this situation.

Table 12-1. Comparative features of acute and subacute nonspecific idiopathic inflammations of the orbit

	MYOSITIC	LACRIMAL	ANTERIOR	DIFFUSE	APICAL
CLINICAL					
Number	51	25	23	3	11
Pain	On movement	With tenderness	Moderate	Moderate	Can be severe
Ocular and orbital features	Painful Decreased extra-ocular movement Normal vision Localized injection and chemosis	Lateral swelling S-shaped lid deformity Tenderness Pouting of lacrimal ducts Chemosis and injection localized	Uveitis Retinal detachment Decreased extra-ocular movement Decreased vision Anterior inflammation - Chemosis - Diffuse injection and swelling of lid	Uveitis Retinal detachment Decreased extra-ocular movement Decreased vision Anterior inflammation - Chemosis - Diffuse injection and swelling of lid	Decreased vision Decreased extra-ocular movement Mild proptosis and chemosis
Visual Outcome	Good	Good	Good	Usually positive, rarely negative	Usually positive, rarely negative
IMAGING					
CT & MR	Muscle irregularly enlarged Swelling of tendon Local scleral and Tenon's capsule swelling Fusiform enlargement of whole muscle	Irregular swelling of lacrimal gland and adjacent tissues	Anterior: enhancing with irregular margins intimate to scleral envelope Variable extension along optic nerve Decreased fat density	Diffuse: enhancing with decreased fat density	Apical irregular infiltration Extends along muscle and optic nerve
Ultrasonography	Increased extra-ocular muscle size	Local swelling with increased Tenon's space	Sclerotenonitis with T sign	T sign	Negative

The common feature of these syndromes is that they have the clinical hallmarks of inflammation, are generally acute or subacute in onset, and histologically are composed of polymorphous infiltrations of inflammatory cells. They are associated with an influx of these cells and their chemical by-products that produce pain, vascular dilatation, and edema with or without systemic malaise. They contrast to chronic or progressive infiltrative inflammations and granulomatous disease, which are usually characterized by mass effect associated with insidious destruction and desmoplasia and therefore frequently require biopsy to define them.

The clinical categories of these entities are defined by the location of the inflammation. On imaging, they have a characteristic feature of an irregular margin adjacent to the primary focus. In addition, there is usually evidence of tissue swelling and enhancement with contrast media. The nonspecific acute and subacute inflammatory syndromes can be divided in order of occurrence as myositic, lacrimal, anterior, apical, and diffuse on the basis of difference in presentation and clinical findings. Although this is an arbitrary subdivision, it parallels the clinical situation and allows a framework for diagnosis, categorization, and management. In effect, most patients with nonspecific acute and subacute idiopathic inflammatory syndromes are usually categorized as outlined and managed with nonspecific anti-inflammatory medications (Table 12-1).

Acute & Subacute Nonspecific Myositic Inflammation: Orbital Myositis

Clinical Features

Orbital myositis was the most common nonspecific inflammatory syndrome we encountered. From a purely clinical point of view, it could be divided into three profiles: isolated, recurrent, and atypical. The isolated and recurrent disease typically present with periorbital inflammation and swelling, retrobulbar pain, and pain on movement. Approximately half of patients present with clinical signs and symptoms of diplopia, conjunctival injection (often focal over muscle insertions), and proptosis (Fig. 12-5). In contrast, those patients that are atypical (7%) lack pain, may lack restriction of movement, have unusual or abnormal CT patterns, are progressive, or may be associated with psychophysical changes such as optic neuropathy. The atypical cases may require biopsy and run the gamut, in our experience, from polymorphous infiltrates to sclerosing inflammations, granulomatous disorders, and lymphoproliferative disease.

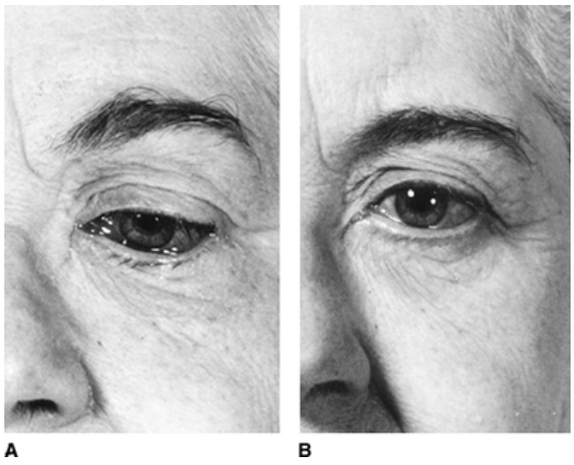

Figure 12-5. (A) Clinical features of a patient with acute medial and inferior idiopathic myositic inflammation. Note downward displacement with inferior and medial chemosis and injection. (B) The same patient after 1 week of steroid therapy. (Reproduced with permission from Rootman J, Nugent R. The classification and management of acute orbital pseudotumors. Ophthalmology 1982;89:1040.)

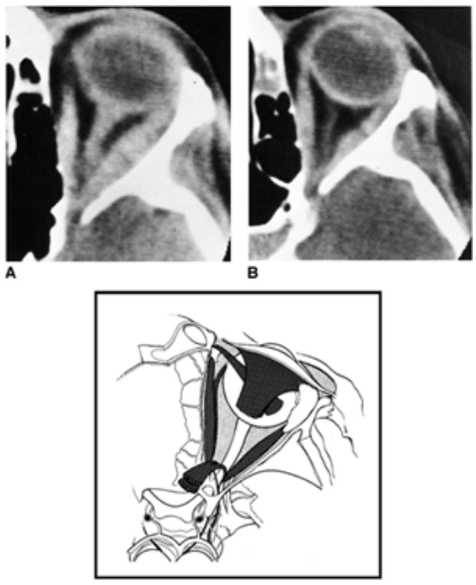

Figure 12-6. (A) Axial CT scan shows orbital myositis. Note thickened lateral rectus muscle and tendon with fuzzy margins and increased orbital fat density. (B) CT scan of the same patient 2 months later following spontaneous clinical resolution. The lateral rectus has decreased in size. Since that time, the patient has had two episodes of orbital myositis. (C) Schematic diagram of myositis.

Most cases of myositis do not typically have direct systemic associations other than with underlying immune disorders in some (allergy, collagen vascular disease, Crohns disease). Rarely, this disorder is associated with giant cell myocarditis or seen as a paraneoplastic syndrome.

The typical profile for myositis consists of sudden presentation of periorbital pain that is exacerbated by movement and associated with clinical inflammation. The major distinguishing features of those cases that are likely to remain isolated versus those that are more likely to be recurrent are that in the majority of instances, isolated cases involve one muscle. Recurrent disease seems to develop multiple muscle involvement and is often bilateral. Review of our experience suggests that virtually all of the vertical and horizontal muscles of the orbit can be involved in almost equal numbers. About one-half of the patients will have some underlying immunologic disorder and may have had an antecedent flu-like illness. Those patients who go on to recurrent episodes usually have involvement of new muscles that differ from the primary presentation and may be either recurrent or progressive in terms of activity. The imaging features of myositis consist of muscle enlargement associated with tendon swelling and a slightly ragged appearance to the borders of the contrast-enhancing affected muscles (Figs. 12-6 ,12-7 ,12-8).

Differential Diagnosis

The major differential diagnosis is Graves' orbitopathy (Table 12-2). However, dysthyroid myopathy is usually painless in onset (unless severe and infiltrative), asymmetric, slowly progressive, and associated with a systemic diathesis. Lid retraction, limitation of gaze in the direction opposite to the muscle involved, and deterioration of visual function (color vision, visual fields, and visual acuity) also may occur in thyroid orbitopathy in contrast to orbital myositis. On CT scan in thyroid orbitopathy, the extraocular muscle enlargement is usually fusiform and tapers toward the muscle insertion on the globe. Ultrasonography will demonstrate enlargement of the extraocular muscle and local infiltration of surrounding structures in myositis. These differences constitute a guideline for the majority of cases since there may be some overlap.

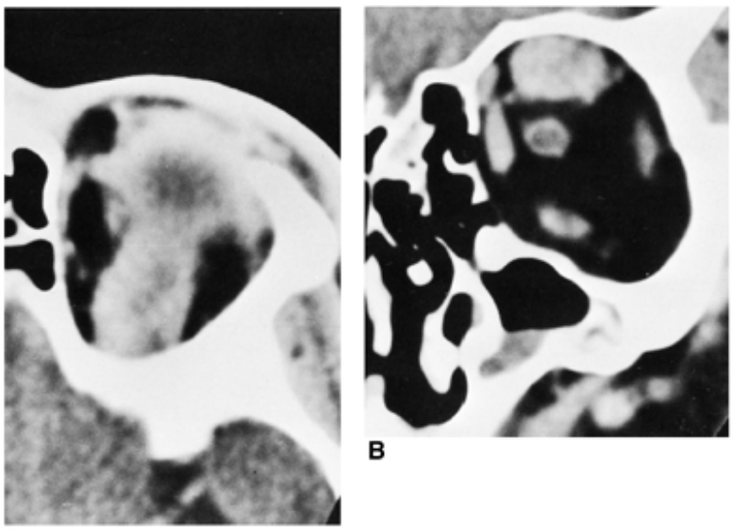

Figure 12-7. Axial (A) and coronal (B) CT scans of a 58-year-old man with a 1-week history of left superotemporal headache, upper lid swelling, tenderness, slight limitation of elevation, abduction, and infraduction. There was injection and chemosis of the superior conjunctiva. Systemic investigation was negative, and the patient responded to low-dose steroids. The scans show enlargement of the superior rectus muscle.

Additional diseases that should be considered in the differential diagnosis include arteriovenous fistulas and malformations, orbital metastases, Tolosa-Hunt syndrome, trichinosis, trochleitis, myasthenia gravis, other nonspecific orbital inflammatory syndromes, sclerosing inflammation (muscle focused), lymphomas, amyloid depositions, and primary tumors of the extraocular muscles. Arteriovenous fistula may be associated with injection of the globe and enlargement of extraocular muscles on CT scan. However, clinical signs differ considerably from acute myositis and are generally unassociated with pain or inflammatory features. Metastatic or locally infiltrative neoplasia to the extraocular muscles may mimic nonspecific inflammation. Sharp pain, however, is a rare clinical feature in metastatic tumors and enophthalmos is frequent. In addition, metastases are rarely characterized by an acute onset, and

imaging tends to define a nodular infiltrative solid mass. Tolosa-Hunt syndrome usually has deeper, more constant orbital pain and multiple neuropathies. Imaging demonstrates either cavernous sinus enlargement or no orbital findings. Trichinosis is usually associated with a dermatopathy. Trochleitis is associated with a very localized tenderness over the trochlea with limitation in elevation and adduction (an acute Brown's syndrome). Myasthenia gravis usually does not have inflammatory signs and has reversible ptosis using edrophonium. However, it should be noted that a small percentage of patients with thyroid orbitopathy have concomitant myasthenia gravis. Anterior and diffuse nonspecific idiopathic orbital inflammations are characteristically associated with ocular findings and have distinctive CT, MR, and ultrasonographic features that allow categorization. Apical nonspecific idiopathic orbital inflammations may mimic myositis and, in fact, commonly involve the muscles at the apex. However, optic neuropathy is characteristic in contrast to the typical features of myositis. Lacrimal nonspecific idiopathic orbital inflammations have a constellation of findings that point to the lacrimal gland. Sclerosing inflammation and lymphomas of the extraocular muscles characteristically have features of spill-over of the process into the adjacent orbit.

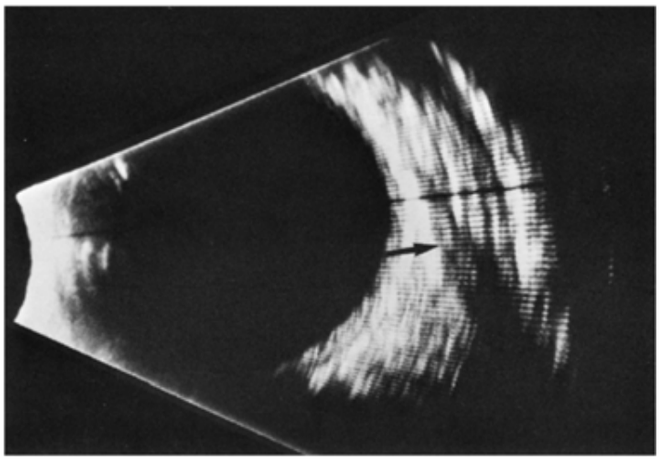

Figure 12-8. B-scan ultra-sonographic findings in orbital myositis demonstrating irregular echoes in the lateral rectus muscle (arrow) with slight infiltration of the adjacent fat. The patient was an 18-year-old boy who had pain on adduction of the right eye, injection, and chemosis over the lateral rectus muscle. He responded to prednisone 40 mg/day tapered over a 1-month period. Systemic investigations were negative.

Table 12-2. Differential diagnosis of Graves' orbitopathy versus orbital myositis

	IDIOPATHIC MYOSITIS	GRAVES' ORBITOPATHY
CLINICAL		
Onset	Rapid-days	Slower-weeks to months
Pain	Frequent especially on extraocular movement	Rare initially; generally gritty irritation
Lid		
Ptosis	Frequent	Rare, except in markedly congested orbits
Retraction		
Stare	Absent	Frequent
Lag	Absent	Frequent
Chemosis	Localized and injected	Generalized, but may be localized
Extraocular movements	Limitation and pain in field of movement of involved muscle or antagonist	Limitation; painless or mildly uncomforTable in field of movement opposite to involved muscle
Visual function	Unimpaired	May be impaired
Response to steroids	Dramatic with complete resolution; may recur	Incomplete and slow
ORBITAL IMAGING		
Bilaterality	Infrequent	Frequent
Number of muscles	More than one in approximately 54%	Typically more than one
Muscle borders	Irregular	Regular
Extension into orbital fat	Frequent	Little or none
Tendon involvement	Frequent	Infrequent
Scleral and Tenon's capsule enhancement	Occasional and localized	None
Site	Any muscle	Inferior, superior, and medial most frequent

Treatment

Patients who present with unilateral single-muscle disease of typical onset can be treated comparatively easily, either with nonsteroidal anti-inflammatory drugs or relatively low-dose corticosteroids. They will improve rapidly and are unlikely to have a recurrence. In contrast, patients who present with bilateral or multiple muscle disease with a typical acute or subacute onset are expected to be prone to recurrences; therefore, they require more follow-up and should be carefully analyzed for potential systemic associations. In addition, this same set of patients should be treated

more aggressively, either with pulsed intravenous corticosteroids or high-dose oral corticosteroids tapered over a 4- to 6-week period. If they fail to respond or persist, the patient should undergo biopsy. Patients who have persistent, recalcitrant, and recurrent disease may require intervention with immunosuppressive drugs. Those cases that have an atypical onset warrant early biopsy and management on the basis of the biopsy results (Fig. 12-9). Radiotherapy is considered to be much less effective in the treatment of myositis.

An algorithm for the management of patients with myositis has three general pathways (Fig. 12-10). In the first instance, the patient presenting with unilateral disease that affects one muscle is likely to have an isolated episode, which if waning may be observed. Alternatively, treatment could be instituted either with nonsteroidal anti-inflammatory drugs or moderate doses of corticosteroids (up to 30-40 mg prednisone tapered rapidly on a symptomatic basis). The expectation would be that in the large majority of these patients, the condition would abate and not recur. On the other hand, if a patient presents either with bilateral or multiple muscle disease or with a significant apical component, more aggressive therapy should be instituted based on the likelihood that there will be recurrent disease. Consideration should be given either to high-dose (80-100 mg prednisone) or pulsed steroids (1 g methylprednisolone IV under supervision) with or without nonsteroidal anti-inflammatories. If the disease continues to lead to recurrent episodes, one should consider the addition of biopsy and immunosuppressives. Other authors have recommended the use of radiotherapy but our single patient's condition recurred after long-term follow-up, and in Mombaerts and Koornneef's series, the condition recurred in all of their patients who had radiotherapy. Perhaps higher doses, as suggested by Kennerdell, should be assessed carefully in a multicentered prospective trial of patients with recurrent or progressive myositis. In addition, patients who have a constellation of findings that suggest a tendency toward recalcitrant or recurrent disease may well be worth studying more carefully from an immunopathologic and biopsy point of view. Finally, patients presenting with features that are atypical for an acute or subacute inflammatory disorder of the muscles should be biopsied and treated according to the results of that biopsy. The foregoing could provide a practical management profile for studying these patients on a prospective basis.

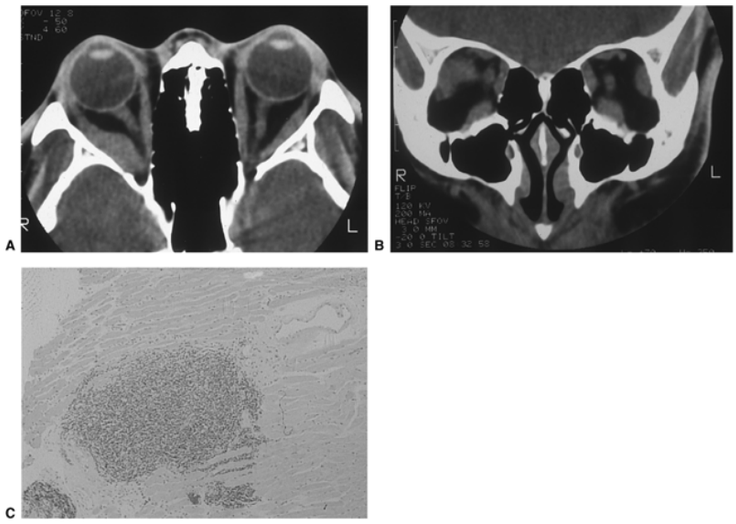

Figure 12-9. (A, B) Axial and coronal scans of a 28-year-old man who presented with a 6-month history of decreased vision, slight discomfort in extremes of horizontal gaze, and no pain or diplopia. Note focal low density areas in the muscles of this atypical myositis. (C) Biopsy demonstrated focal polyclonal lymphorrhages with a diagnosis of reactive lymphoid hyperplasia, which responded to low-dose radiotherapy (H&E, original magnification × 10).

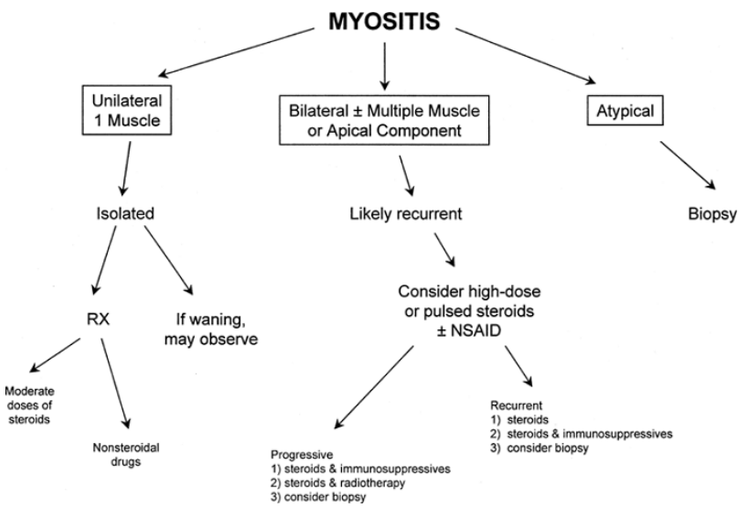

Figure 12-10. Suggested algorithm for the treatment of orbital myositis.

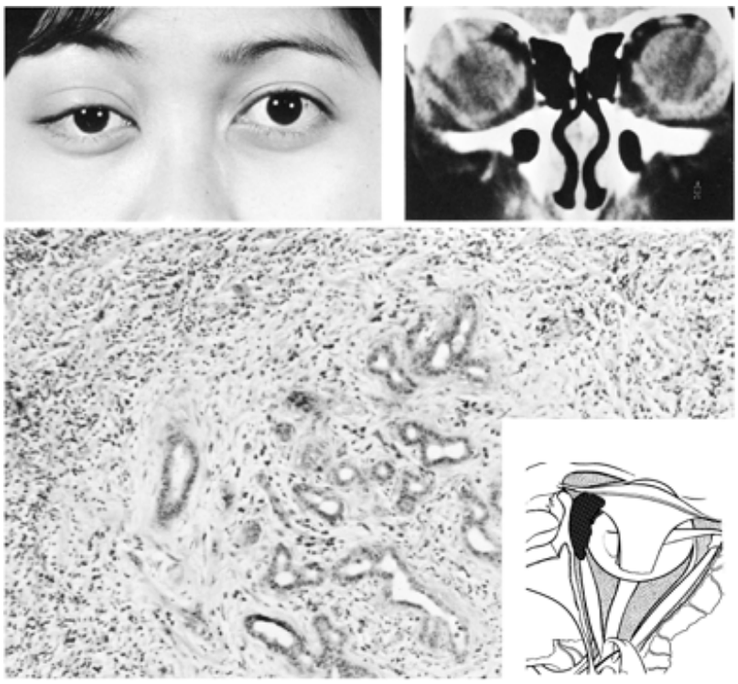

Figure 12-11. A 25-year-old woman had a 1-month history of swelling and slight tenderness of the right upper lid associated with 2 mm downward and 2 mm inward globe displacement. Coronal CT scan shows a mass in the lacrimal fossa. Biopsy shows a chronic polymorphous inflammatory infiltrate associated with sclerosis and destruction of the lacrimal gland and preservation of some ductal structures. She was treated with prednisone 40 mg/day tapered over a 3-month period, and showed rapid improvement. On systemic investigation, she had an elevated ESR (50 mm/hr). She subsequently developed alopecia. The study at that time showed that she had decreased peripheral T-lymphocytes, a high titer of cytomegalovirus antibody, and no other abnormalities (H&E, original magnification × 10).

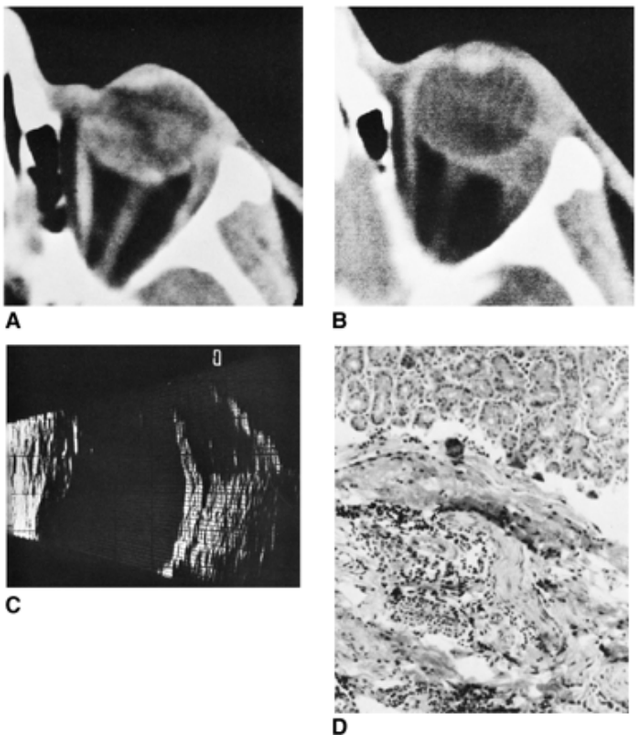

Figure 12-12. (A) Axial CT scan shows an enlarged left lacrimal gland in a 33-year-old man with left mild superotemporal tenderness and swelling, pouting of the lacrimal ducts, diplopia in right gaze only, 3 mm of proptosis, 2 mm of inward and 2 mm of downward displacement, and a narrow interpalpebral fissure. Immunologic study was negative. (B) Repeat CT scan shows the orbit 2 months after initiation of steroid therapy for an acute idiopathic inflammation of the lacrimal gland. Note slight prominence of the lacrimal gland, which has decreased in size. (C) Ultrasonogram shows a superotemporal mass with internal reflectivity and an echolucent area adjacent to the scleral shell. (D) Biopsy reveals perivascular capsular lymphocytic infiltration of the lacrimal gland (H&E, original magnification × 25).

Nonspecific Lacrimal Inflammation

Clinical Features

Dacryoadenitis was our second most common nonspecific inflammatory disease of the orbit. The typical presentation of acute and subacute dacryoadenitis consists of pain, tenderness, and injection of the temporal portion of the upper lid and conjunctival fornix with an associated tender, palpable lacrimal gland, an S-shaped deformity of the lid, and pouting of the lacrimal ducts noted on biomicroscopy of the fornix. There may be some minimal evidence of proptosis with downward, inward displacement of the globe.

Approximately 50% of our patients with so-called nonspecific inflammations of the lacrimal gland have potential for some sort of an associated systemic disorder, a feature that is much more common if the patient has a chronic or tumefactive presentation (Fig. 12-11). Because of this, we tend to recommend more routine biopsy. In our experience, the type of disorders that have been seen with this kind of presentation include lymphoma and hematopoietic malignancy, sarcoid, Sjögren's syndrome, Wegener's granulomatosis, sclerosing inflammation, and a myriad of autoimmune disorders, which prompt us to suggest biopsy because they have significant and serious systemic implications.

On imaging, the lacrimal gland is typically enlarged, enhances with contrast, and has irregular margins (Fig. 12-12). It is confined to the superolateral orbit, obscuring the lateral aspect of the globe and often displacing it inferomedially. On ultrasound, the mass may have internal reflectivity with an echolucent area next to the scleral shell, associated with thickening of the adjacent muscles anteriorly.

Differential Diagnosis

The differential diagnosis of nonspecific lacrimal inflammation includes viral and bacterial dacryoadenitis, rupture of a dermoid cyst (rarely associated with significant acute or subacute inflammation and in our experience is more typically a mass), and the specific lacrimal inflammations already mentioned. On biopsy, the patients with acute inflammatory disorders tend to show polymorphous cellular infiltration with edema and vascular dilatation and do not have a striking degree of destruction of the lacrimal gland (Fig. 12-12). If there is evidence of destruction of the lacrimal gland, consideration should be given to the possibility of organ specific immune disorder (Fig. 12-11).

Treatment

Our overall management suggestion for acute nonspecific dacryoadenitis is to have a high index of suspicion for systemic disease, which may prompt biopsy. We recommend biopsy should be accomplished through a percutaneous route in order avoid the excretory ducts. Treatment of nonspecific

lacrimal inflammation consists of oral corticosteroids, usually moderate tapering doses (40 mg prednisone), with the majority resolving over a 1- to 3-month period.

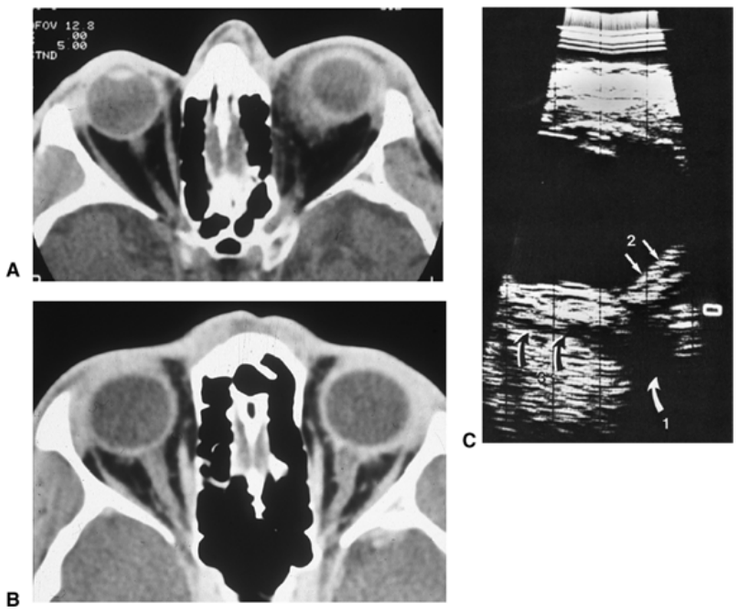

Figure 12-13. (A) Sixty-year-old male with a 1-week history of left lid swelling, ptosis, discomfort, and pain on extraocular movement. CT demonstrates an anterior nonspecific orbital inflammatory syndrome, which responded promptly to a short course of steroids. (B) Twenty-year-old male with a history of right retrobulbar pain and conjunctival and lid injection associated with tenderness. Examination revealed decreased vision, red desaturation, and serous elevation of the retina. His CT demonstrates an anterior orbital infiltrate affecting the distal portion of the optic nerve and the globe. This responded promptly to steroids but the patient suffered 3 additional episodes before the condition resolved. (C) Ultrasonogram shows doubling (squaring off, T sign) of the optic nerve shadow (large white arrows), peripapillary retinal detachment (small white arrow), and accentuation of Tenon's space (black arrows). (Fig. 12-13C reproduced with permission from Rootman J, Nugent R. The classification and management of acute orbital pseudotumors. Ophthalmology 1982;89:1040)

Acute and Subacute Nonspecific Anterior and Diffuse Orbital Inflammation

Clinical Features

In patients with anterior inflammation the main focus involves the globe and the adjacent orbit. Features on presentation consist of pain, proptosis, ptosis, lid swelling, injection, and in some instances decreased vision. The other important findings may be ocular and include uveitis, sclerotenonitis, papillitis, and exudative retinal detachments. This syndrome appears to be more common in children and young adults. The clinical pattern of presentation and severity correlates with the location and degree of involvement noted on CT scan and ultrasonography (Fig. 12-13). Patients with diffuse disease have the same features as those with anterior orbital inflammation, but in addition have involvement of the extraocular muscles and neurosensory structures (Fig. 12-14).

The imaging characteristics consist of an irregular orbital infiltration that is anteriorly located intimate to the eye, and which produces scleral and choroidal thickening with obscuration of the junction of the globe and optic nerve and variable extension along its sheath (Fig. 12-15). When the patient has diffuse involvement, the whole of the orbit is obscured by infiltration. Earlier recognition and referral in the last decade has led to fewer cases of diffuse disease in our clinic. On ultrasonography, there is accentuation of Tenon's space and doubling of the optic nerve shadow (T sign). In the younger group in particular, systemic investigation may show an increased sedimentation rate and cerebrospinal fluid pleocytosis.

Differential Diagnosis

The differential diagnosis of anterior and diffuse nonspecific orbital inflammation includes orbital cellulitis, a sudden event in a preexisting lesion (hemorrhage within a vascular lesion), local ocular inflammation (scleritis, uveitis), and systemic inflammatory syndromes (collagen vascular diseases). In younger patients, leukemic infiltration, metastatic neuroblastoma, and rhabdomyosarcoma can occasionally develop as sudden syndromes and may be confused clinically with idiopathic inflammation.

Treatment

Treatment is with nonspecific anti-inflammatory drugs, generally oral prednisone (usually in doses starting at 60 mg tapered over 2 to 3 months), which usually produces a dramatic reversal of signs and symptoms, in particular pain. The majority of patients improve substantially within weeks. Resolution can be monitored by repeat imaging. Some, particularly younger patients, may have recurrent episodes

requiring adjuvant nonsteroidal anti-inflammatory drugs or more rarely immunosuppressive drugs. Generally, recalcitrant adult cases should be considered for biopsy.

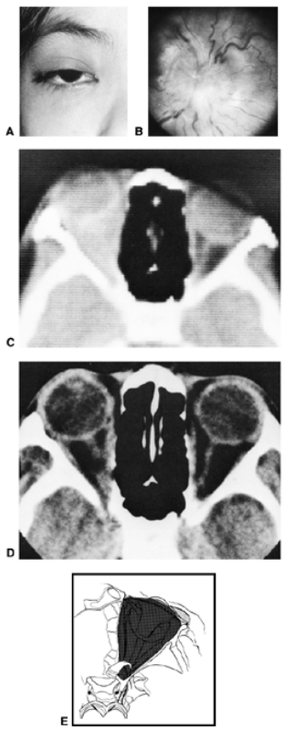

Figure 12-14. (A) Clinical photograph of a 13-year-old patient with an idiopathic diffuse orbital inflammation and a 2-week history of uveitis followed 1 week later by ptosis, diplopia, proptosis, lid injection with edema, signs of optic neuropathy (visual acuity 20/25, afferent pupillary defect, color desaturation), and papilledema. (B) Her optic nerve photograph reveals severe papilledema. (C) Axial CT scan (noncontrast, EMI 1010) shows a soft tissue infiltrate involving the entire right orbit. There is poor visualization of fat, muscles, and the optic nerve. (D) Axial CT scan (noncontrast, GE 8800) performed after intermittent steroid therapy reveals normal fat density, and the extraocular muscles, globe, and optic nerve is now clearly defined. (E) Schematic representation of diffuse involvement of the orbit. (Reproduced with permission from Rootman J, Nugent R. The classification and management of acute orbital pseudotumors. Ophthalmology 1982;89:1040)

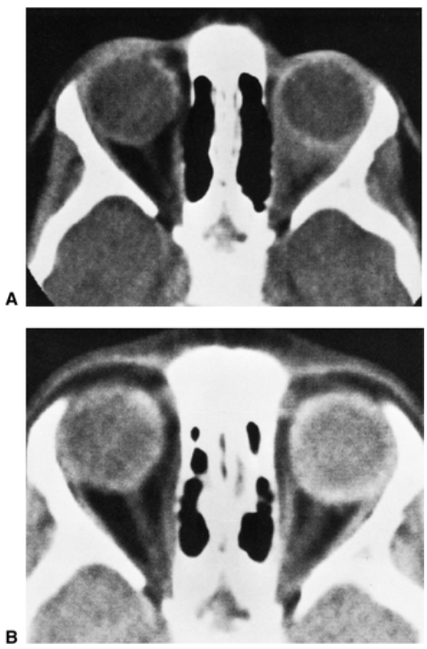

Figure 12-15. (A) Axial CT scan (noncontrast) of left acute idiopathic anterior orbital inflammation. Note soft tissue density involving the posterior globe and anterior orbit with extension along the optic nerve. The soft tissue infiltration obscures the normal definition of the optic nerve and extraocular muscles in the plane just posterior to the globe. (B) Noncontrast CT scan of the same patient 9 months after initiation of therapy. The globe, optic nerve, and anterior orbit are now well-defined.

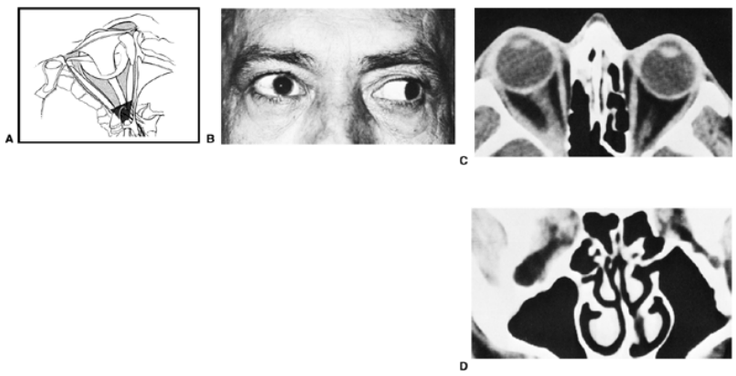

Figure 12-16. (A) Schematic diagram demonstates apical orbital involvement. (B) This 54-year-old man had a 5-week history of right superomedial and periorbital pain with mild injection and swelling of the lid. He had also noted a recent onset of double vision. On physical examination, he had vision of hand movement on the right with a central and inferior visual field loss. In addition, there were decreased extraocular movements in all positions of gaze, 5 mm proptosis, an afferent pupillary defect, and slight injection and chemosis of the conjunctiva. (C, D) CT scan showed apical infiltration with involvement of adjacent muscle, optic nerve, and fat. He was diagnosed as having an idiopathic apical inflammatory process, and was treated with prednisone 80 mg/day. He responded dramatically, and within 1 week had 20/50 vision and increased extraocular movements. Systemic investigations were negative.

Acute and Subacute Nonspecific Apical Orbital Inflammation

Acute and subacute apical inflammation is characterized by an early onset of psychophysical abnormalities associated with more modest signs of inflammation, such as pain on movement or diplopia (Fig. 12-16). Thus, the cardinal features are a disproportionate functional abnormality compared to the degree of inflammatory signs. Imaging demonstrates an apical focus (Fig. 12-17). The differential diagnosis clearly involves the orbital apex syndromes such as Tolosa-Hunt. It is worth noting that apical disease is often a trap for the unwary and should rarely be treated nonspecifically without a very careful follow-up and systemic evaluation, because in our experience a wide variety of disorders can present this way. In our own clinic, the differential diagnoses have included cases of angiosarcoma, Tolosa-Hunt syndrome, lymphoma, secondary tumors from adjacent sinuses, sclerosing inflammation, fungal infections, metastases, Wegener's granulomatosis, angiomeningioma, and mucormycosis. The wide differential diagnosis provides a cautionary note for accepting nonspecific apical inflammation without assiduous follow-up or consideration of biopsy.

Conclusion

The five clinical syndromes of acute and subacute idiopathic orbital inflammation appear to correlate well with location and degree of disease identified on orbital imaging. Nonspecific anti-inflammatory treatment used in these situations effect resolution that appears to be proportional to the length and amount of involvement. The rapid steroid responsiveness (especially as applied to pain) is almost pathognomonic. Imaging is useful, particularly for assessing resolution with therapy. Failure of resolution should suggest alternative diagnoses, and a biopsy may become necessary. Management following biopsy for persistent, recurrent, or inconclusive disease will be governed by the histology of the lesion. In the clinical situation, acute cases often demand rapid action because the patients are frequently extremely uncomfortable, and there may be considerable threat to vision. Many authors have suggested that biopsy in acute anterior and diffuse inflammatory lesions may, in fact, be detrimental to the care of patients. Given the efficacy of current investigative techniques, we can now monitor the course of the diseases accurately. In all patterns, when patients have been

appropriately investigated and treated but show little or poor response, biopsy may then become appropriate. Aside from lacrimal gland lesions, in our experience this is rarely necessary in acute and subacute inflammations, and the patients can be managed by categorization according to clinical presentation and location. Treatment can be monitored by clinical findings and follow-up orbital imaging.

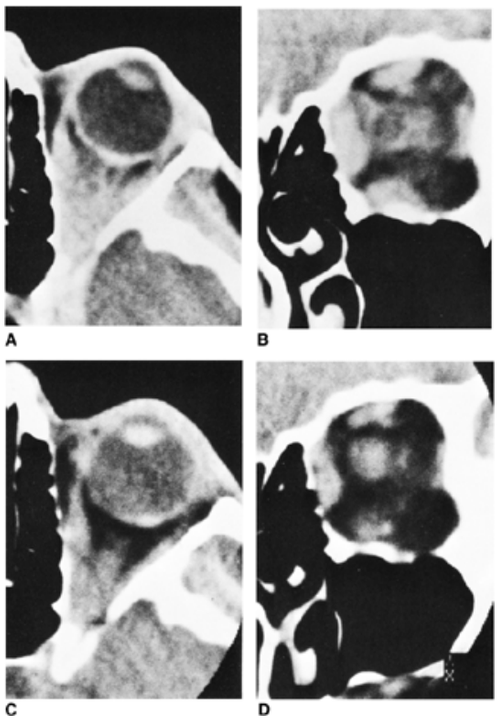

Figure 12-17. CT scans of a 57-year-old woman who presented with a 1-1/2 month history of redness and swelling of the left eye. She had complete ptosis for 3 to 4 days, and was aware of diplopia for 2 days with severe apical pain. On physical examination, her vision was 20/20. She had a 15 D hypertropia, left exotropia of 20 D, 4 mm of proptosis, and tenderness to ballottement. (A, B) CT scans in both axial and coronal planes show soft tissue infiltration of the apex, fat, and adjacent muscles. She responded to 60 mg prednisone daily, tapered slowly over 2 months. (C, D) CT scans were performed 3-1/2 months later when the patient was clinically normal. Systemic investigations were negative.

Specific Inflammations of the Orbit

As noted earlier, the specific inflammations can be divided into three different categories: those with identifiable pathogens (i.e., infections and infestations), specific local and/or systemic constellations of findings, and those with specific histopathology.

Infections and Infestations

Infective cellulitis is an important cause of orbital inflammation and may develop from contiguous inflammatory disease of the sinuses, face, and oropharynx. In addition, it may result from foreign bodies or be secondary to pyemic deposition. Causes include a wide variety of bacterial, viral, fungal, and parasitic pathogens that vary with regional epidemiology. In our experience, the most significant category of orbital cellulitis arise from bacterial infections of the sinuses. It is particularly important to consider the local infectious disease profile (epidemiology) and to be suspicious of unusual pathogens in patients who are immunosuppressed.

Microbial

Orbital Cellulitis and Sinusitis

Clinical Features

Infective orbital cellulitis from sinusitis is extremely important to recognize as the juxtaposition to intracranial structures may lead to rapid and serious consequences. Pathophysiologically, the infection originates from the sinuses and can spread readily to the orbit through the thin bony walls and foramina, or in a retrograde fashion by the interconnecting valveless venous system of the orbit and sinuses. The process frequently develops through a sequence of edema and cellulitis to local and contiguous pyemic destruction of tissue planes with subperiosteal, orbital, and intracranial abscess formation and thrombophlebitis (Table 12-3). From a clinical point of view, cellulitis is generally associated with axial displacement of the globe, whereas

formation of an abscess, particularly in the subperiosteal space, usually causes nonaxial displacement and may ultimately track forward causing subcutaneous induration or fistulization (Figs. 12-18 ,12-19 ,12-20). Posterior subperiosteal tracking may lead to rapid and catastrophic visual loss and neurosensory compromise due to apical compression (Fig. 12-21). Direct contiguity may lead to inflammatory optic nerve damage (Fig. 12-22).

Table 12-3. Cellulitis and sinusitis

	CELLULITIS	ABSCESS	CAVERNOUS SINUS
Clinical Features			
Ocular and orbital	Group 1: Inflammatory edema Lid edema Group 2: Orbital cellulitis Increasing lid swelling Injection Chemosis Axial proptosis Venous congestion (choroid & retina) Increasing pain +/- Increasing intraocular pressure	Group 3: Subperiosteal abscess +/- Induration and fluctuation Increased lid swelling Chemosis +/- Nonaxial displacement Increased intraocular pressure Increased orbital tension Decreased extraocular movement Local tenderness Motor and sensory signs out of proportion to inflammation May be sudden Group 4: Orbital abscess Increased proptosis Increased inflammatory signs Ophthalmoplegia Decreased vision; papilledema Palpable fluctuant mass +/- Perivasculitis	Group 5: Cavernous sinus thrombosis Bilaterality Increased chemosis Increased orbital tension Increased intraocular pressure Cranial nerve palsies (III, IV, V, VI) Decreased sensation Decreased extraocular movement Decreased movements out of proportion to cellulitis Dusky colored lids Increased venous engorgement Papilledema
General	+/- Malaise	Increasing malaise and fever +/- Spiking	Headache Varying consciousness Nausea Vomiting Fever
Imaging			
CT	Groups 1 & 2 Swelling of lid Sinus opacification Mucosal thickening +/- Obscuration and infiltration of orbitat fat	Group 3 Homogeneous subperiosteal accumulation of pus with smooth border on orbital side enhancing capsule +/- Gas Group 4 Homogeneous or heterogenous mass +/- Contrast enhancing capsule +/- Gas in orbit	Group 5 Increased size of superior orbital vein (bilateral) Increased extraocular muscle size Expanded cavernous sinus +/- Cerebral infarct +/- Abscess in central nervous system - subdural/intracerebral
Ultrasonography	Clear spaces Change in fat densities	Irregular, poorly defined lesion of medium or reflectivity	Increased orbital vein size Increased extraocular muscle
Radiography	Sinus opacity +/ Air fluid level	Sinus opacificatio +/- Air fluid level	Sinus opacity +/- Air fluid level

Permanent visual loss can result from profound increased intraorbital tension associated with abscess formation or from direct optic neuritis or vasculitis. The most devastating complication is spread by means of vascular emissaries to the cavernous sinus, leading to cavernous sinus thrombosis (Fig. 12-23). Alternatively, spread through diploic vessels to the intracranial cavity can lead to subdural empyema or intracranial abscesses.

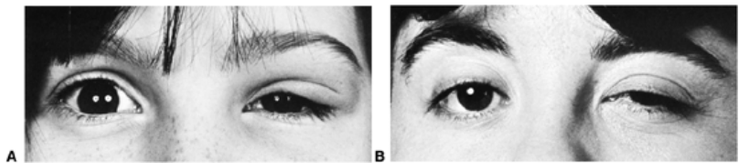

Figure 12-18. (A) This 10-year-old patient has the clinical features of group 1 orbital cellulitis or inflammatory edema (periorbital cellulitis) with mild edema (especially the upper lid) due to ethmoid sinusitis. (B) This 22-year-old woman presented with group 2 orbital cellulitis secondary to ethmoid sinusitis following an upper respiratory illness. She had 4 mm of proptosis, lateral displacement of the globe, pain, and tenderness associated with a slight decrease in vision. Both responded to intravenous antibiotic treatment.

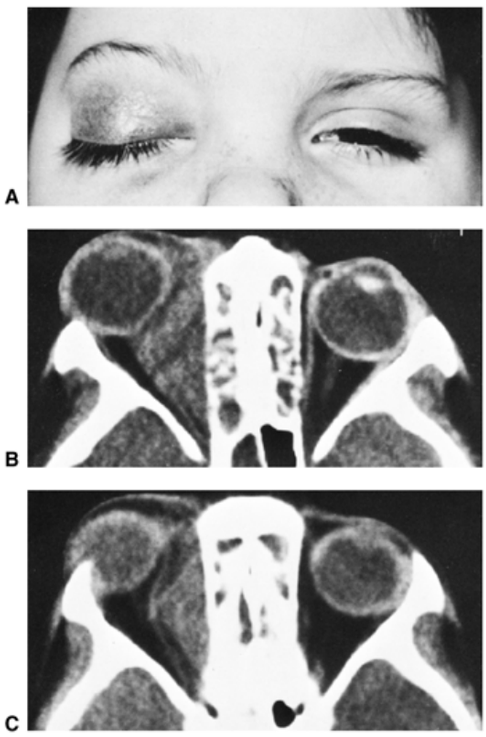

Figure 12-19. Group 3 subperiosteal abscess. (A) This 10-year-old child presented with a 2-day history of sudden onset of right ptosis, lid injection, decreased vision (20/70), marked limitation of ocular movements, malaise, and anorexia following 7 days of lid swelling. He had mild papilledema and a tense orbit due to a medial subperiosteal abscess arising from ethmoid sinusitis, demonstrated on axial CT scans. Note slight tenting of the globe and bowing of the optic nerve (B) and medial rectus (C). He was treated with urgent drainage and systemic antibiotics, and recovered uneventfully.

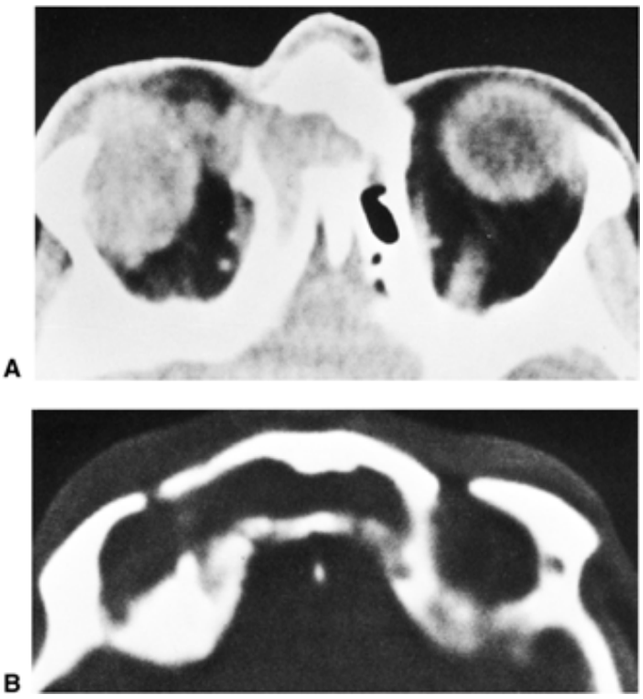

Figure 12-20. Group 4 orbital abscess is seen in axial CT scans (A, B) of an abscess arising from the frontoethmoid complex (different window settings). The patient, a 70-year-old man, had a history of allergic rhinitis and recurrent papillomata removed from the sinus. This episode was preceded by a 3-week history of right supraorbital pain, inflammation, and swelling with intermittent drainage of purulent material “from the corner of the eye.” He had developed a tense orbit with diplopia, ptosis, decreased vision (20/50), reduced extraocular movements, and downward displacement of the globe (5 mm). He was treated by drainage of the orbital abscess and sinuses, and with intravenous antibiotics.

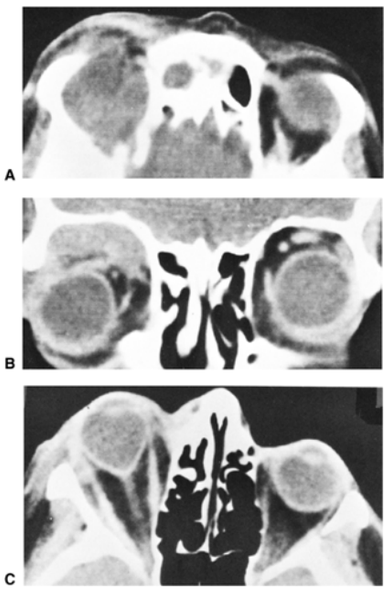

Figure 12-21. Coronal (A) and axial (B, C) CT scans of a 61-year-old woman who presented with an explosive onset of severe proptosis, downward displacement, and vision loss due to a right frontal sinus abscess. There had been an antecedent history of progressive frontal pain for 2 weeks. The abscess penetrated into the right superior subperiosteal space, leading to massive and sudden proptosis. The marked posterior tenting of the globe is a result of severe orbital pressure and forward displacement from the tense abscess. In spite of rapid drainage, visual loss was permanent.

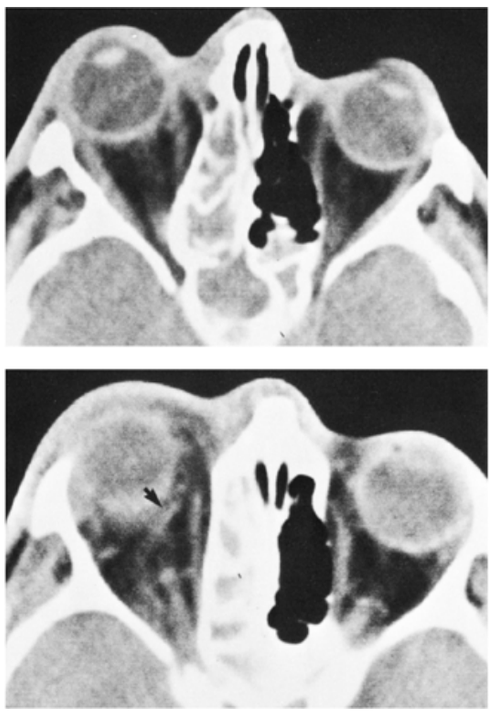

Figure 12-22. Axial CT scans of an 80-year-old patient with right orbital cellulitis secondary to chronic and recurrent ethmoid sinusitis. Note lid edema, apical infiltration of the orbit (B), and dilatation of the right superior ophthalmic vein (arrow). He had suffered profound visual deterioration due to the apical cellulitis.

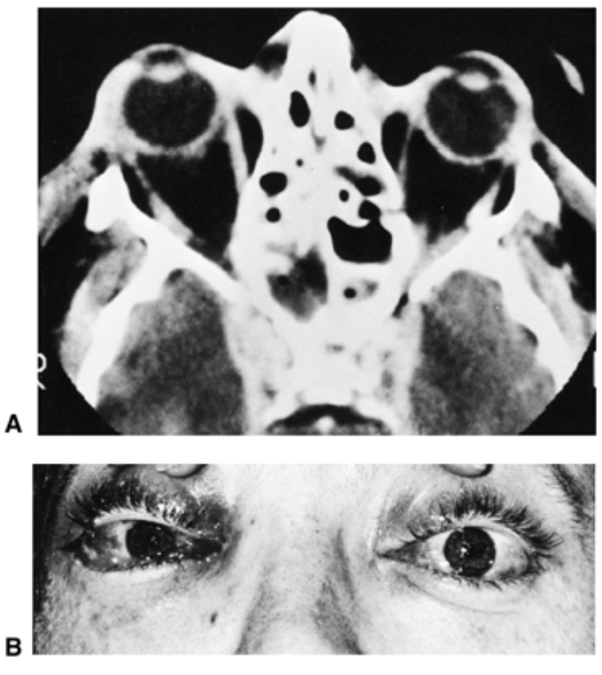

Figure 12-23. Group 5 cavernous sinus thrombosis. (A) Axial CT scan of a patient (B) who presented clinically with catastrophic onset of bilateral proptosis, chemosis, almost total limitation of ocular movement, ptosis, lid edema, profound decrease in vision, and varying levels of consciousness. Note opacification of sphenoid sinus, engorgement of the cavernous sinus, and proptosis. This was preceded by a 2-week history of retrobulbar and frontal pain. The patient responded to systemic antibiotics, sinus drainage, and symptomatic therapy, but he had suffered a right cerebral infarct.

In general, progress is characterized by evidence of increasing malaise, fever, lid injection, proptosis, chemosis, pain, orbital tension, motor dysfunction, raised intraocular pressure, and congestion of the veins of the choroid and retina (with papilloedema and periphlebitis). Cavernous sinus thrombosis is associated with the development of headache, nausea, vomiting, fever, varying levels of consciousness, increased chemosis, bilaterality, nerve palsies, decreased extraocular movements, and development of a blue-purple lid. The ophthalmological danger signals of progression are decreased vision, reduction of extraocular movements (especially if out of proportion to the degree of cellulitis), dilated pupil or afferent pupillary defect, engorged fundus vessels, papilledema, perivasculitis, evidence of spread to the other orbit, a violaceous lid, increasing proptosis, raised intraocular pressure, and decreased sensation (hypesthesia).

The ocular complications of orbital cellulitis are exposure and neurotropic keratitis, conjunctival prolapse, secondary glaucoma, septic uveitis and retinitis, exudative retinal detachment, optic neuropathy, and panophthalmitis.

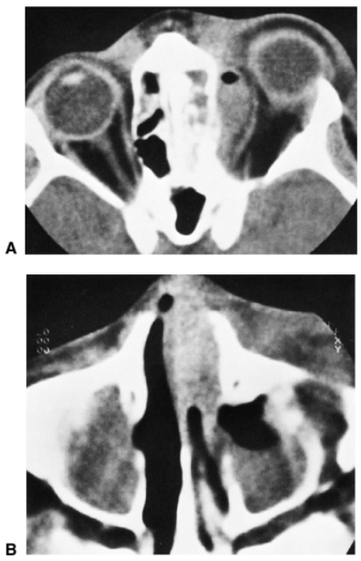

Figure 12-24. This 9-year-old boy presented with progressive left upper lid swelling and injection, decreased vision (20/60), limited upgaze, and chemosis. (A) Axial CT scans show a subperiosteal abscess with bilateral maxillary and left ethmoid sinusitis. Note air in the abscess (should raise suspicion of gas-producing organisms), which is displacing the medial rectus and globe laterally, and the soft tissue swelling over the cheek (B). He was treated successfully with intravenous antibiotics, external ethmoidectomy with drainage, and antral lavage.

Classification

The clinical classification of orbital cellulitis includes five groups originally described by Chandler et al (Table 12-3).

- Group 1: Inflammatory edema (preseptal cellulitis, periorbital cellulitis) is characterized by swelling of the eyelids with mild orbital edema, usually involving the upper eyelid (especially medially) in the initial stages. It reflects slowing and congestion of venous outflow. A slightly more advanced stage includes chemosis (Fig. 12-18A).
- Group 2: Orbital cellulitis. The orbit is infiltrated, leading to variable mass effect and functional defects (edema, congestion, proptosis, motor and visual impairment). This can be a feature of either bacterial or sterile cellulitis (Fig. 12-18B).
- Group 3: Subperiosteal abscess (Figs. 12-19 and 12-24). Purulent foci within the adjacent subperiosteal space may lead to nonaxial displacement, local tenderness, and possible fluctuant masses depending on size and location. The volume of the abscess and speed of development may reflect virulence of the pathogen or the unique pathophysiology of the subperiosteal space. Abscess formation may be rapid, because destruction of soft tissue planes is not a requisite to accumulation of purulent material in this potential space. In fact, a clinical clue to the development of subperiosteal abscess may be profound proptosis with a functional deficit in the absence of striking concomitant inflammatory signs, such as chemosis and lid injection. Displacement of the globe is frequently nonaxial and reflects the site of the abscess.
- Group 4: Orbital abscess (Fig. 12-20). Progression of intraorbital cellulitis or spread from the subperiosteal space leads to intraconal or extraconal loculation. Proptosis, inflammatory signs, ophthalmoplegia, visual deficit, and systemic toxicity are frequently severe at this stage.
- Group 5: Cavernous sinus thrombosis is heralded by profound central nervous system deficits or changes in local inflammatory signs with functional impairment (previously outlined).

Table 12-4. Orbital cellulitis and sinusitis

	CHILD	ADULT
Signs and Symptoms	Lid edema, diplopia, decreased vision, proptosis	Lid edema, diplopia, decreased vision, proptosis, more frequent nonaxial displacement
General	More frequent malaise, fever, anorexia	Less malaise, fever, and anorexia
Location	Ethmoid or pansinusitis	Frontoethmoid
History	Upper respiratory infection	Allergy, sinus problem, dental extraction
Bacteriology	May be no growth, gram-positive, gram-negative, *H. influenzae, S. Aureus*	Frequent growth, gram-positive, gram-negative, *S. aureus*, mixed anaerobes
Management	Systemic antibiotics; drainage rarely necessary	Surgical drainage frequently necessary, plus antibiotics
Outcome	Recovery with few complications	More frequent complications including visual loss, central nervous system abscess, recurrent cellulitis, osteomyelitis

Although this classification suggests an orderly progression, sudden and catastrophic events may occur with virulent pathogens or as a result of acute pressure blowout from a sinus into subperiosteal or orbital spaces (Fig. 12-21). In addition, spread of infection to the cavernous sinus or orbital apex from contiguous disease (especially sphenoid sinusitis) may cause rapid, early, profound deterioration. Another important and frequent cause of variation in this pattern is incomplete or inappropriate treatment. Current imaging technology allows for earlier recognition of orbital and periorbital involvement and is useful for assessing severity and guiding treatment.

Diagnosis

The clinical diagnosis of orbital cellulitis is best substantiated by imaging to identify abscess formation and to get accurate staging and localization of lesions. CT or MR imaging will demonstrate precise location and extent of the inflammatory process, and can be used to follow improvement or worsening of the disease. The sinus pathology is reflected in mucosal wall thickening, opacification, and air fluid levels. Chronic infection of the sinuses may be associated with thickening of the walls, and a persistent inflammatory process (particularly in children) may be due to a foreign body in the nasal passages. Depending upon the major location of the inflammatory process, the disorder can be subclassified into subperiosteal, extraconal, and intraconal abscess formation.

Subperiosteal infection most commonly occurs adjacent to the ethmoid sinuses but may accumulate superiorly along with frontal sinusitis, more readily viewed on coronal scans (Figs. 12-19 , 12-23 , 12-24). The fluid or pus collecting in the subperiosteal space appears as a homogeneous or heterogeneous collection, which may be surrounded by an enhancing border. With progression, it will displace the extraconal fat and extraocular muscles. When the process is immediately retrobulbar or in the intraconal space, the edema leads to an increase in fat density. If the intraconal space is predominantly involved without sinus disease, a foreign body or an immunocompromised state should be suspected. The adjacent soft tissue planes are obscured by the inflammation when diffuse, and an abscess can be identified as a poorly defined mass with contrast enhancement of the rim. Gas producing anaerobes may lead to abscesses with lucent spaces within them. However, in an earlier stage before cavitation, there may be diffuse enhancement. If the globe is involved, the scleral uveal rim may be thickened.

Epidemiology

The most important factors to consider are epidemiologic based on regional pathogens but more particularly on differences between the disease in adults and children (Table 12-4). Because of the delay in development of the sinuses in children, the locus of the disease is ethmoidal and the major predisposing cause of sinusitis in childhood is intercurrent upper respiratory disease. Children under the age of 4 may be prone to infection with *Hemophilus influenzae*, an occurrence that has markedly reduced with the introduction of HI vaccines leading to fewer cases and a wider spectrum of causative bacterial agents. Overall, sinusitis and, for that matter, subperiosteal abscesses in childhood (under age 9) tend to be due to single aerobic organisms such as *Streptococcus pneumoniae*, *moraxella catarrhalis*, and *Hemophilus influenzae*. Subperiosteal abscess formation is less frequent in children and even when the features exist, conservative therapy with antibiotics is suggested as long as there is no threat to vision.

In contrast, adults typically develop frontoethmoid disease with predisposing histories of sinusitis, polyps, allergy, trauma, and recent dental extraction. The infection in adults is typically polymicrobial and frequently contains anaerobic organisms. Nonaxial displacement is more common in adults, reflecting abscess formation. Direct nasopharyngeal, and especially sinus aspiration or abscess cultures, are often positive and relevant. Most patients have significant orbital signs associated with sinusitis and orbital cellulitis, except for those with sphenoid involvement where there may be a disproportionate visual or motor sensory loss because of apical location. Other epidemiologic factors of note are emerging species of resistant bacteria such as methicillin-resistant *Staphyloccus aureus* and penicillin-resistant pneumonococci.

Management

The management and outcome of sinusitis and orbital cellulitis differ in adults and children. The overwhelming majority of children do not need sinus or abscess drainage.

Table 12-5. Initial empiric antimicrobial regimens for orbital cellulitis*

CLINICAL TYPE	PREDOMINANT ORGANISM	RECOMMENDED REGIMENS
Preseptal (periorbital)	Group A streptococci *S. aureus* *H. influenzae***	Child: amoxicillin/clavulanate (po) or ampicillin/sulbactam (IV), or if *H. influenzae* as in adults Adult: cloxacillin (IV, high dose), or cefazolin, or clindamycin
Orbital (sinusitis)	Streptococci *Strep. pneumoniae* *H. influenzae* *M. Catarrhalis* Bacteroides Fusobacterium Anaerobic cocci *S. aureus* (unusual)	Second or third generation cephalosporin (e.g., cefuroxime, cefotaxime, ceftriaxone), or piperacillin/taxobactam, or ticarcillin/clavulanate, or imipenem
Trauma or foreign-body related	*S. aureus* *S. epidermidis* Streptococci Coliforms Anaerobes (if soil contamination)	Vancomycin + gram negative coverage***

* Therapy should be revised according to the results of microbiologic testing, particularly of specimens from surgical drainage of abscesses.
** Much less common since introduction of HI vaccines.
*** Numerous options, for example, ciprofloxacin, ceftazidime, ceftazidime, ceftriaxone, piperacillin or piperacillin/tazobactam, imipenem.

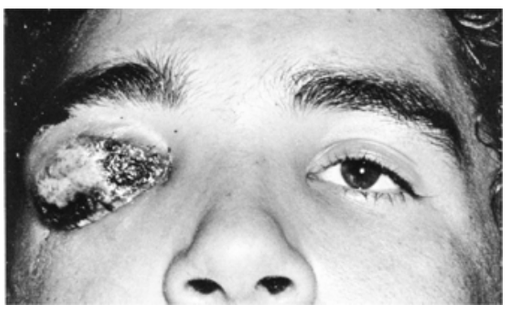

Figure 12-25. A 21-year-old patient with a severe necrotizing preseptal cellulitis 4 days after a minor lid laceration. He responded to systemic and local antibiotics with minimal scarring and no orbital involvement.

In contrast, adults more frequently require such, particularly if there is orbital tension and threat to vision. With adults, it is important to use adequate intravenous antibiotic therapy directed at polymicrobial or cultured-specific infection for a significant period of time in order to be assured of clearance of disease and to avoid complications of recurrence, intracranial extension, and osteomyelitis. The advent of endoscopic sinus surgery allows for minimally invasive drainage of subperiosteal abscesses. Imaging with CT or MR is helpful in predicting the need for, and site of, drainage of abscesses, and can accurately monitor the progress and effect of treatment. Antimicrobial therapy is best directed against a cultured organism and should involve the expertise of an infectious disease consultant. As a guideline, Table 12-5 suggests empiric antimicrobial regimens for orbital cellulitis. It should be noted that in cases without a threat to vision or function, particularly in younger age groups, conservative intravenous antibiotic therapy may be associated with an increase in the size of the subperiosteal abscess in the first few days after the initiation of therapy. Drainage of an abscess should be emergent if there is a threat to the optic nerve, retinal function, or if there is a profoundly tense orbit in patients who have significant pain. In those with intracranial complications of frontal sinusitis, the abscess should be drained.

The role of the ophthalmologist is to establish the diagnosis and monitor ocular function during therapy. It is especially important to recognize increasing orbital tension and threat to ocular function, thus observation and monitoring of visual acuity, degree of proptosis, central nervous system function, horizontal and vertical displacement, extraocular movements, pupillary signs, and fundus examination are extremely important. The main principles of management consist of the prevention of ocular and nonocular complications, the use of appropriate antibiotics, surgical drainage when necessary (i.e., evidence of significant abscess with globe tenting, deterioration of proptosis, vision, or extraocular movements), symptomatic therapy, and careful follow-up.

Other Sources of Microbial Orbital Cellulitis

Contiguous Spread

The majority of infective cellulitides that spread from contiguous structures are preseptal, with involvement of the deeper orbital structures being rare (Fig. 12-25). In some instances, there is antecedent local trauma or infection, such as in dacryocystitis. Usually there is a profound degree of swelling due to the loose subcutaneous tissues. Untreated or severe infections may rarely extend into the deeper orbit (Fig. 12-26) but in most instances, subcutaneous disease can be treated with intravenous antibiotics.

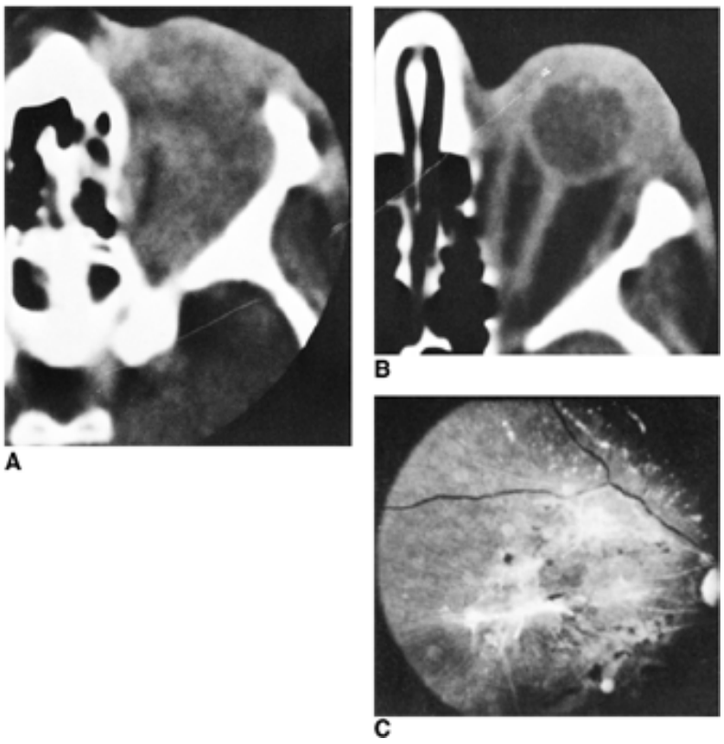

Figure 12-26. (A) CT findings of orbital cellulitis resulting from an infected wound of the lid in a 34-year-old man. (B) Note tenting of the globe due to severe orbital tension. In spite of drainage and systemic antibiotics, he remained blind due to retinitis and infarction. (C) Fundus photograph 3 months after cellulitis.

A large variety of organisms are associated with contiguous spread, including *Staphylococcus aureus* and *Streptococcus pyogenes*. If foul-smelling, anaerobic infections should be considered especially if the wound has been contaminated by soil and bites. *Strep. pyogenes* may be associated with erysipelas, necrotizing fasciitis, or toxic shock, requiring very aggressive treatment.

Management includes careful bacterial isolation, systemic and local antibiotics, and surgical drainage of abscesses. Direct culture and scraping of wounds will usually yield an organism but in the absence of drainage, careful limited aspiration of the subcuticular tissues can aid in isolation of bacteria.

Drug treatment depends on severity of disease, and intravenous treatment is recommended when significant involvement is noted or an aggressive onset has occurred. If the disease is localized and the patient systemically well, oral antibiotics may be sufficient.

Infection of the skin and subcutaneous tissues, especially of the face, are common in children and warrant separate discussion. The immunologic and local predispositions are different in children and produce several special syndromes, including impetigo, *Hemophilus influenzae* cellulitis and conjunctivitis, and maxillary osteomyelitis. Impetigo is a superficial mixed infection with *S. aureus* and group A *Strep. pyogenes*. Characteristically, impetigo involves the head and neck, starting as a reddish macule and progressing to vesicular eruptions that ultimately rupture and drain, producing yellow ocher crusts. When the lids are affected, profound injection and edema may occur. Treatment is with local hygiene, antibiotic ointment, and systemically administered antibiotic appropriate for penicillin-resistant organisms.

Children younger than 3 years of age are prone to a distinctive infection with *H. influenzae*. It is usually associated with an upper respiratory infection, systemic malaise, and fever. Involvement of the conjunctiva produces a mucopurulent discharge, and the lid is characteristically violaceous. The organism may also produce sinusitis and orbital cellulitis, as noted previously. Blood cultures are especially useful in this circumstance because bacteremia is common. Profound and rapid progression may occur, and intravenous systemic antibiotics are mandatory. Because *H. influenzae* organisms are frequently penicillin resistant, the drug of choice is ampicillin, or chloramphenicol if the organisms are ampicillin resistant. Chloramphenicol drops should be applied locally for the conjunctivitis. With the advent of the *H. influenzae* vaccination, this disorder is less frequent in areas of use.

A rare fulminant osteomyelitis of the superior maxilla may occur in children younger than the age of 9 months. The infection is due to *S. aureus* and associated with profound systemic symptoms and rapid progression. Because of rapid spread and potential intracranial, orbital, and systemic involvement, high-dose antimicrobial intravenous therapy is indicated.

Other Contiguous Infections

Conjunctivitis rarely spreads to involve the deeper orbital tissues and has a characteristic history. We have encountered several instances of orbital cellulitis progressing from severe conjunctivitis. A common preseptal cellulitis that may masquerade as bacterial is herpes zoster, particularly noted in an older age group.

Orbital Foreign Bodies

Orbital foreign bodies are another source of infection, the most common in our experience being eroding orbital implants. Foreign bodies tend to induce a rapidly developing cellulitis or produce a localized abscess that may progress to fistulization (Fig. 12-27). Vegetal foreign bodies may also induce a chronic granulomatous response with fistulization

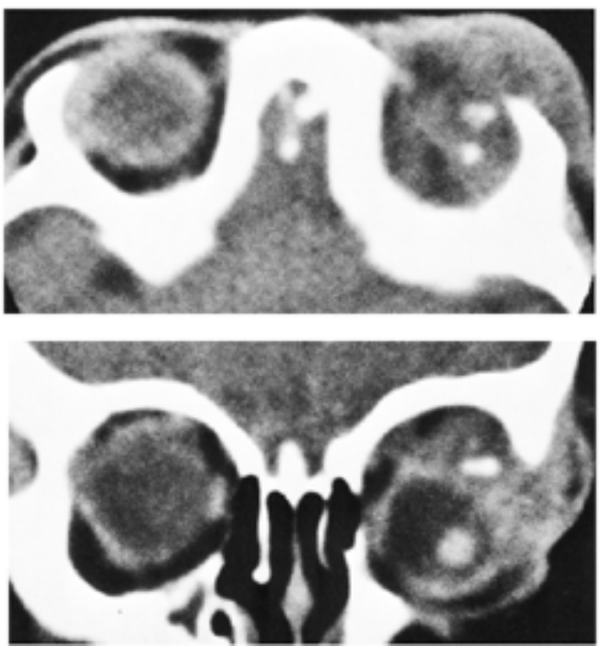

Figure 12-27. Axial and coronal CT scans show an orbital abscess secondary to a foreign body. This was seen in a 1.5-year-old girl who had a small stab wound of the upper lid 10 days earlier after falling on a lead pencil. She presented with a 2-day history of swelling of the lid and purulent drainage. There was no visible lid wound, but a small draining fistula was noted in the superior fornix. The abscess was drained and it cultured mixed organisms (*Streptococcus viridans*, *Hemophilus influenzae*, and anaerobic gram-negative rods).

(Fig. 12-28). Treatment implies mandatory removal of the offending foreign body, local irrigation, and systemic antibiotics.

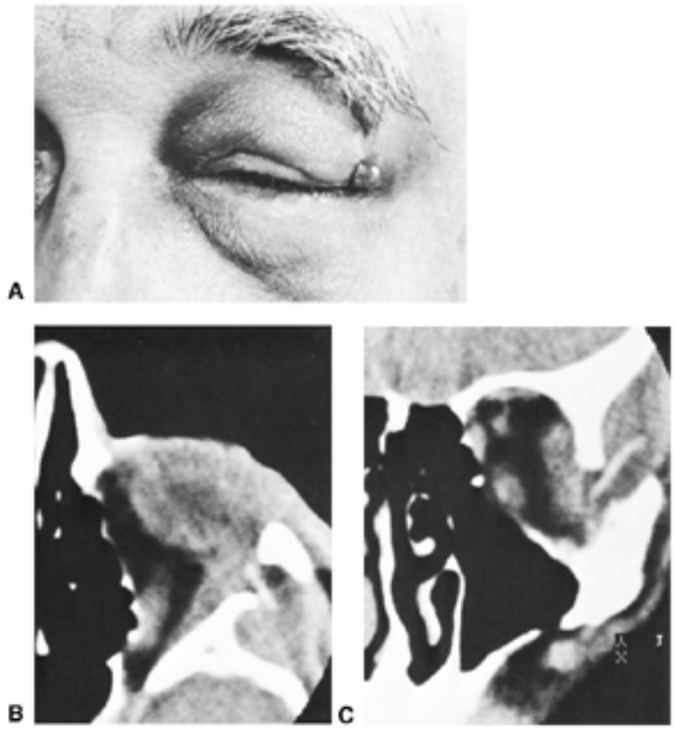

Figure 12-28. (A) This 55-year-old man presented with a chronic draining sinus and low-grade orbital cellulitis associated with trismus. He had fallen 3 months earlier into a thicket of branches. On axial (B) and coronal (C) CT scans, the wooden foreign body that had penetrated the left lateral orbital wall and temporalis fossa is identified as a linear density crossing the wall at right angles. At surgery, the branch that was extracted from the temporalis fossa had extended into the pterygopalatine fossa, accounting for the trismus.

Pyemic Cellulitis

Pyemic orbital cellulitis is rare but may occur especially in compromised hosts. In these instances, local and systemic bacteriologic evaluation is important as unusual organisms may be involved. Predisposition includes immunocompromise, old age, poor nutrition, and chronic alcoholism.

Intraorbital Sources of Cellulitis

Dacryoadenitis, panophthalmitis (Fig. 12-29), and dacryocystitis are additional sources of orbital infection. The microbial infections in these instances may spread beyond the site of origin into the orbit.

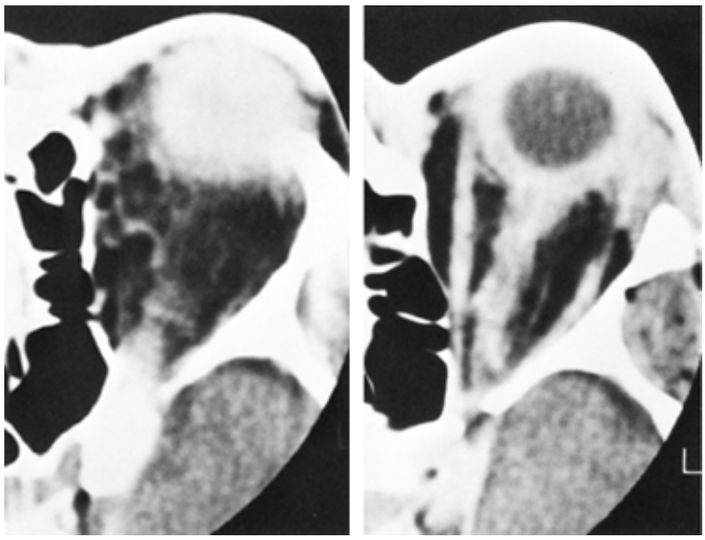

Figure 12-29. Axial CT scans demonstrate the features of severe endophthalmitis and orbital cellulitis following a posterior chamber lens implant. Note marked infiltration of the orbital fat and thickening of the uveoscleral envelope.

Fungus Infections

Rhino-orbital Mucormycosis

Rhino-orbital mucormycosis is an aggressive opportunistic infection that occurs in debilitated patients, particularly individuals with uncontrolled diabetes with ketoacidosis, immunocompromise, and renal disease. Healthy persons are rarely affected (due to normal containment by phagocytes) and if so, usually have localized disease. The orbit is a site in about 10% of patients with hematologic malignancies who have proven mucormycosis, a context in which survival is uncommon.

The sinus and nasopharynx are inoculated by spores (which are ubiquitous in soil, air, skin, body orifices, manure, and food), with growth and spread of the organism into the tissue being associated with invasion by hyphae. This organism has a propensity to invade and occlude vascular lumina leading to infarction, which compounds inflammatory necrosis and forms a characteristic black eschar. Spread to adjacent tissues of the orbit and intracranial cavity may be rapid and devastating, leading to a fatal outcome.

Early diagnosis can allow for containment and successful therapy; thus it is important to recognize the characteristic pattern in a predisposed patient (Fig. 12-30). The earliest orbital sign consists of apical boring pain, and progression is associated with increased cellulitis, proptosis, abrupt visual failure, and apical neuropathies. The presence of a characteristic eschar of skin, palate, or nasal mucosa in the early stages is rare. Imaging will show displacement of orbital structures adjacent to the opacified sinus, with and without bony destruction. There may be increased density of soft tissue and enlargement of the optic nerve.

Treatment requires a well-coordinated and prompt multidisciplinary approach. An early definitive diagnosis is associated with a more favorable outcome. Tissues should be obtained for microscopic examination, fungal culture, and histopathology. Histologically, these large nonseptate branching hyphae can readily be seen with routine staining methods (hematoxylin & eosin) and can be dramatically demonstrated with appropriate special stains. The underlying metabolic disorder should be corrected and a failure to respond metabolically may be a clue to the diagnosis. Wide local excision of the involved tissues with frozen section guidance if possible and adequate postoperative surgical drainage are also required.

If caught sufficiently early in the localized form, treatment need not necessarily imply exenteration. Systemic antifungals along with local irrigation of tissues with such agents is recommended. The extent of surgical excision should be balanced against the threat to life and vision, and the expected deformity. Some have suggested that hyperbaric oxygenation may play a role in treating this disorder.

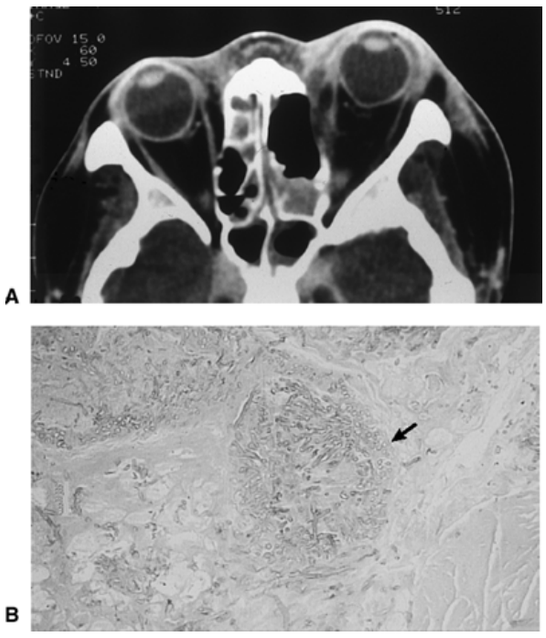

Figure 12-30. Mucormycosis. (A) Axial CT scan and (B) biopsy specimens from 43-year-old patient with a relapsed leukemia post-bone marrow transplant. The orbital tissues demonstrated mucormycosis with intravascular invasion (arrow) (H&E, original magnification × 10). The patient died of intracranial extension of the mucormycosis.

Aspergillosis

Aspergillus is a normally harmless saprophyte that is opportunistic and difficult to culture. This organism is better known to ophthalmologists as a cause of septic endophthalmitis, corneal ulcers, and orbital invasion. There is an increasing frequency related to drug addiction, kidney transplants, and immunosuppression. It is the only fungus aside from *Rhizopus* that stains with hematoxylin-eosin in addition to the specific fungal stains. *Aspergillus*, however, is septate whereas *Rhizopus* is not.

There are two clinical circumstances in which aspergillosis presents. The first is a disseminated form (often occurring in immunocompromised hosts) that causes a widespread necrotizing angiitis due to microscopic foci of fungus in small vessels. Endophthalmitis is a common sequel in this form. The second form of presentation in the orbit is the development of a relatively slow, localized infiltrative mass,

usually originating from an adjacent sinus. When anterior, it primarily leads to proptosis and displacement of the globe, and when apical, causes a painful orbital apex syndrome (Fig. 12-2). This can be an infection in healthy people but is more common in predisposed individuals with recurrent sinusitis and polyps. The usual infiltrate is granulomatous but focal abscess formation and fistulas may occur. It is frequently missed and can lead to devastating local spread and even death.

Disseminated aspergillosis is seldom treatable. Localized disease when recognized early is probably best treated by surgical drainage and debridement along with systemic and local antifungals. Early diagnosis may be aided by the use of aspiration cytology.

We have recently experienced four cases of apical presentation of aspergillosis with minimal sinus involvement. All four cases had a 4- to 6-month history of progressive apical retrobulbar pain associated with deteriorating vision and progressive apical neuropathies. On imaging, they had minimal changes in the sphenoid sinus lining associated with a focal, tiny gap in the sinus wall and infiltration of the apical orbit, which sometimes extended into the cavernous sinus (Fig. 12-31). The apical infiltration was characterized by the presence of fine, focal, low-density areas that turned out to be microabscesses. In spite of extensive debridement, local irrigation with antifungals, and systemic therapy, two of the patients went on to die of intracranial involvement and the remaining two have persistent disease.

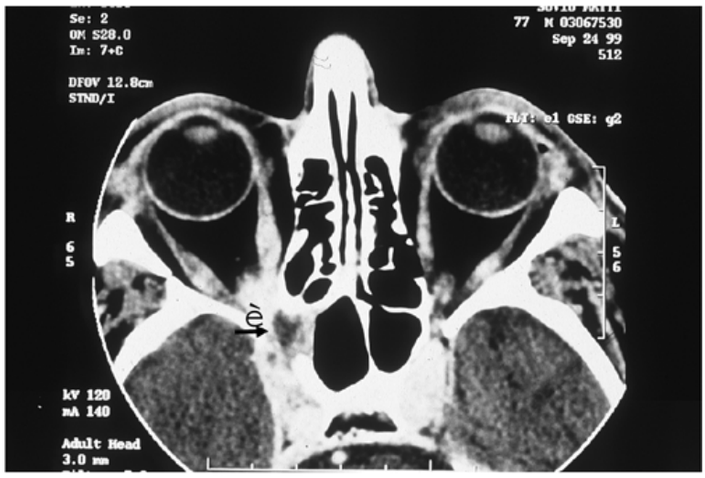

Figure 12-31. This 78-year-old man presented with a 5-month history of right frontal parietal pain and a recent (2 to 3 weeks) decrease in vision that progressed over a 1-week period from 20/25 to 20/40. This was associated with an afferent pupillary defect and color vision defect. Axial CT scan shows erosion of the lateral wall of the sphenoid sinus with a central low density area, which was due to a localized *Aspergillus* abscess arising from the sinus (arrow).

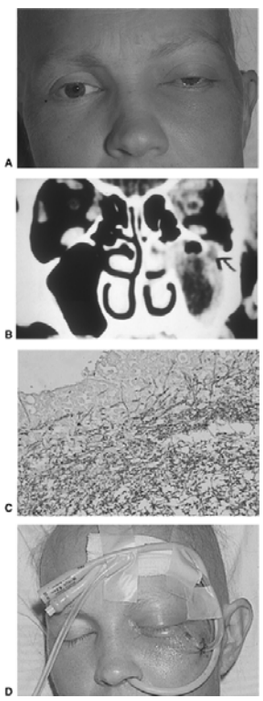

Figure 12-32. Immunocompromised patient. (A) Clinical photo of a 37-year-old woman with cytopenia subsequent to consolidation therapy for acute myelogenous leukemia. She had intermittent fever, left ptosis, and left intraorbital numbness with upward displacement of the globe and premalar injection. (B) CT scan demonstrated maxillary and inferior orbital infiltration. The sinus was explored, its contents removed, and the inferior orbital fat excised. (C) The biopsy and culture demonstrated an infection with *pseudallescheria boydii* (Grocott, original magnification × 10). (D) An irrigating system was left in the sinus and she was treated with antifungals by irrigation and systemically. As her neutropenia recovered, local and systemic symptoms disappeared.

Other Mycotic Infections

There are a number of other fungal organisms that may rarely affect the orbit (Fig. 12-32). Treatment depends on specific identification of the organism and local and systemic fungal therapy. The range of organisms seen include North American blastomycosis, African histoplasmosis (*H. duboisii*), sporotrichosis, rhinosporidiosis, coccidioidomycosis, candidiasis, and bipolaris hawaiiensis. Allergic fungal sinusitis may occur with orbital symptoms but is not invasive and may involve a variety of fungal organisms. It should be recognized so that it may be treated by sinus debridement and steroids (Fig. 12-33).

Tuberculosis and Syphilis

Worldwide, tuberculosis is a persistent and significantly increasing infection. Orbital involvement occurs in two circumstances: either secondary to hematogenous spread or by direct extension from contiguous structures, usually the sinuses. Hematogenous dissemination of the disease can lead to two orbital manifestations. The first, and more common, is periostitis, which characteristically affects the malar bones of people in their first and second decades. Periostitis presents as an insidious, localized inflammatory lesion that leads to cold abscess, sequestration, and fistula formation. The orbital tuberculoma is another manifestation of hematologic spread and is associated with the development of an infiltrative orbital mass, which may cause neurosensory deficit. In both instances, concomitant evidence of active tuberculosis should be sought but may not necessarily be present. Diagnosis may be aided by fine needle aspiration biopsy.

Another source of orbital tuberculosis is from direct spread, either from intraorbital structures or more commonly from adjacent sinuses (Fig. 12-34). The sinus spread causes necrotizing infiltrative lesions that may develop cutaneous fistulas. In all of the above circumstances, growth of acid-fast bacilli from direct biopsy material is rare. Evidence of such a lesion in the presence of a strongly positive tuberculin test may warrant treatment on a presumptive basis while awaiting culture. Recommended therapy is systemic antituberculous drugs.

Orbital involvement with syphilis is rare but the increase in patients with immunosuppressive syndromes has led to more infections. Syphilitic periostitis may cause diffuse or focal involvement of the orbital bones, which appear as either acute or chronic inflammatory disease. Fistulization, bone resorption, and secondary spread into the orbit may occur. When posterior, manifestations of a painful apex syndrome is characteristic. Primary soft tissue gumma may occur within the orbit, extraocular muscles, and lacrimal gland. Appropriate systemic antibiotic therapy should lead to resolution of disease.

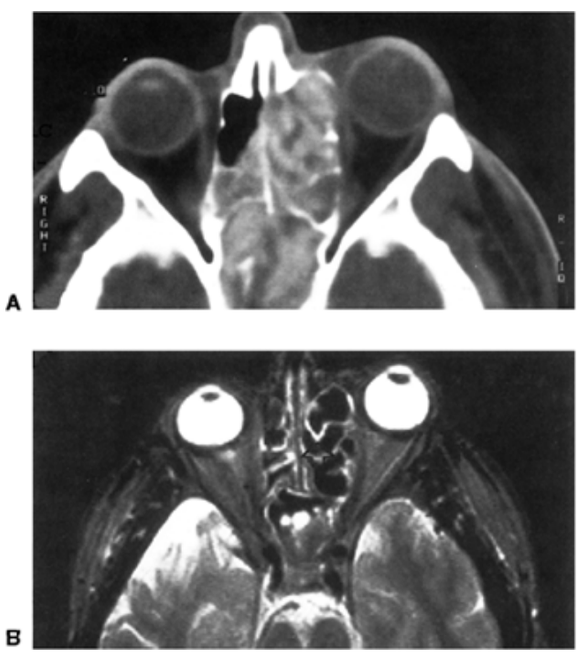

Figure 12-33. Allergic fungal sinusitis. (A) Axial CT scan of the orbits shows a soft tissue mass filling the ethmoid and sphenoid sinuses with extension into the anterior medial left orbit. (B) Axial T2-weighted scan shows increased signal intensity of the ethmoid (arrow) and sphenoid sinus mucosa and a marked decrease in signal intensity within the left ethmoid sinus and anterior sphenoid sinus. The organism was isolated and found to be bipolaris spicifera. (Reproduced with permission from Klapper SR, Lee AG, Patrinely JR, et al. Orbital involvement in allergic fungal sinusitis. Ophthalmology 1997;104:2094-100.)

Parasitic Infestations

Parasitic orbital infections have specific geographic prevalence, with the highest incidence seen in emerging countries or areas of endemic parasitoses. The most common orbital infestation is with echinococcosis but cysticercosis, microfilaria, and trichinosis may also affect the orbit.

Echinococcosis (Hydatid Cyst)

Echinococcus is an infestation of the intestines of dogs, sheep, pigs, cows, and other animals, which may parasitize man during its larval stage and spread to multiple sites of the body forming cystic spaces. The cysts characteristically have a chitinous ectocyst and a cellular endocyst that may contain many scoleces in daughter cysts.

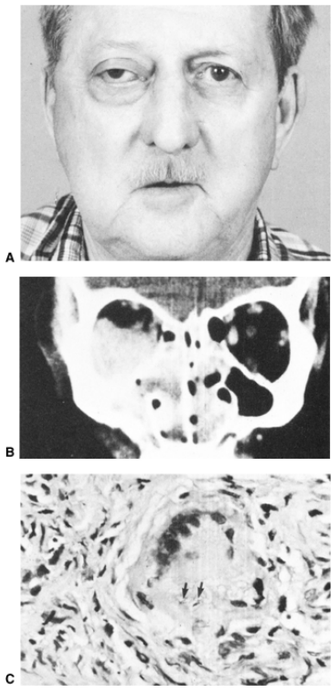

Figure 12-34. (A) October 1983. Right proptosis with swelling of lids, temple and face – chemotic conjunctiva. (B) CT scan taken at that time shows a soft tissue mass involving the inferior rectus, inferior oblique, and lateral rectus muscles as well as the maxillary sinus. Histology of the mass revealed Langerhans giant cell, epithelioid cells, and remnants of bacilli (arrows). (Ziehl-Neelson, original magnification × 400) (Reproduced with permission from Khalil M, Lindley S, Matouk E. Tuberculosis of the orbit. Ophthalmology 1985; 92: 1624-7.)

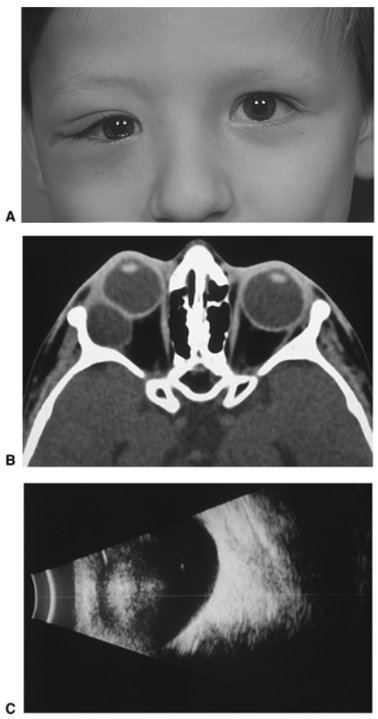

Figure 12-35. This 4-year-old boy from Bosnia presented with a 3-month history of downward, inward displacement of the right globe and a recent onset of periorbital swelling and injection. (B) Axial CT scan shows a cystic mass, also demonstrated on ultrasound (C), which proved on excision to be an echinococcal cyst. Systemic evaluation revealed a single large hepatic cyst, which was treated with albendazole 15 mg/kg/day for 1 month and underwent resolution.

Orbital cysts are seen in 1% of cases of echinococcosis. They tend to occur between the first and fourth decades of life, and are particularly common in the superior and posterior orbit. Onset is usually insidious and dominated by mass effect, but rupture of the cyst can be associated with a more sudden and fulminant inflammatory course and may be a complication of either surgical incision or injury. The cyst rarely may erode intracranially or into the adjacent sinuses.

Diagnosis is made on the basis of imaging a cystic lesion of the orbit, which may have evidence of calcification (Fig. 12-35). This can be substantiated by biological tests including intradermal antigen reaction, complement-fixating, and hemagglutinating antibody tests. Treatment is excision of an intact cyst either by a direct or lateral orbital route. Rupture should be avoided in order to prevent an inflammatory reaction or contamination with daughter cysts. Systemic

antiparasitic therapy is recommended and if a violent local inflammatory response occurs, suppression may be aided by local or systemic corticosteroids. It has been suggested that systemic albendazole is also successful in resolving echinococcal infections. Hydatid cysts have been diagnosed by fine needle aspiration biopsy, aspirated, and injected with a scolicidal in combination with albendazole systematically.

Cysticercosis

Cysticercus cellulosae, the larvae from the tapeworm *Taenia solium*, occur rarely in the orbit in spite of a preference for the eye and brain, the most common sites being the conjunctiva or in the eye itself. Orbital involvement frequently has been noted in the anterior orbit so proptosis is unusual. Presence of eosinophilia, positive complement fixation, and precipitin reactions are often inconclusive. Treatment of anterior subconjunctival parasites consist of excision. Cysticercosis has a propensity to deposit within muscles, and may be encountered as an abscess in extraocular muscle (Fig. 12-36). Diagnosis of cystic muscle involvement may be serological or by fine needle aspiration biopsy. The parasite rarely extrudes from muscle spontaneously. The abscess may be excised but systemic albendazole, with or without corticosteroids if inflamed, is effective in treatment.

Trichinosis

Encystation with trichinosis tends to occur in striated muscles, thus extraocular muscles are a site of preferential occurrence. The patient may present with orbital manifestations of acute inflammation including swelling, chemosis, visual disturbance, and painful myopathy. The ocular muscle involvement is often antecedent to that of the generalized skeletal musculature. On CT imaging, there may be evidence of calcification of the extraocular muscles. Treatment is by thiabendazole and corticosteroids to reduce inflammatory signs and symptoms.

Other Parasitoses

Rare microfilarial infections of the deeper orbit have been described, but the common infestations involves superficial tissues. The other parasites that have been noted include Onchocerca, Ascaris, Schistosoma, and Entamoeba.

Other Infestations

Arthropodal infestation of the orbit is uncommon and usually occurs in conditions of chronic suppuration and debility,

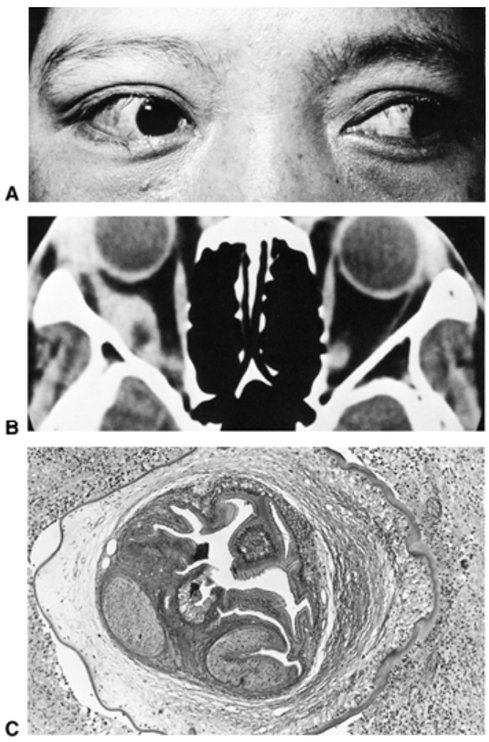

Figure 12-36. (A) This 35-year-old Cambodian woman presented with a 1-week history of right ocular pain and swelling associated with diplopia on right and left gaze. She had pain on eye movement, 7 mm right proptosis with restriction of abduction, and supraduction. In addition, the conjunctiva was injected and chemotic inferolaterally. White blood count was 8.1 with no eosinophils. (B) The axial CT scan shows a mass with central lucency that was contiguous with and obscured the right lateral rectus muscle. Ultrasonographic examination suggested a solid mass in the right lateral rectus muscle. The patient underwent an orbitotomy for biopsy and at surgery, an abscess was found within the right lateral rectus muscle and was excised. (C) Histology reveals cysticercosis with scolex and cyst with zonal inflammation of eosinophils, polymorphonuclear leucocytes, epithelioid cells, and occasional giant cells surrounding the organism.

particularly in the tropics. Orbital myiasis can vary in degree from mild conjunctivitis with a localized larval infestation (*Oestrus ovis*) to full-blown, rapidly destructive lesions of the orbital soft tissues and bones (*Dermatobia noxialis* or *D. hominis*, *Hypoderma bovis*, *Wohlfahrtia magnifica*, and *Calliphora vomitoria*). Infestation with a single larva may produce a fistula and local inflammation that resolves on extrusion of the larva. Treatment consists of removal of the maggots aided by application of topical turpentine. Concomitant bacterial infections are treated with appropriate antibiotics and the tissues allowed to granulate. In severe cases, the dominant systemic debility usually leads to a fatal outcome.

Other (Specific) Orbital Inflammations

The specific inflammatory disorders may also imply a combination of pathologically identifiable infiltrates often with systemic constellations of findings that make them specifically identifiable. They can be broadly divided into vasculitides, granulomatous disorders, and idiopathic sclerosing inflammation.

Vasculitis (Angiitides)

Vasculitis includes a wide range of inflammatory angiodestructive processes, which involve varying calibers of vessels and different types of infiltrates ranging from polymorphonuclear leucocytic with leucocytoclasis (periarteritis nodosa, hypersensitivity angiitis) to necrotizing granulomatous disease (Wegener's granulomatosis). The unifying histopathologic feature is evidence of vessel destruction or significant angiocentric inflammation. Blood vessel damage is characterized by any or all of the following: endothelial damage, vessel wall necrosis, fibrin deposition within and around vessels, or indirect evidence of tissue necrosis. Most are thought to have an immunologic basis varying from immune-complex deposition to delayed hypersensitivity (Table 12-6). The majority are thought to have an immune complex-mediated basis.

Clinically, angiitides express a continuum of inflammatory features from acute and subacute onset to chronic inflammation with vaso-obstructive signs and symptoms. The various entities are classified on the basis of symptoms related to the organs or tissues affected, as well as their principal histopathologic features. It should, however, be noted that some vascular inflammatory syndromes defy classification and may not fit neatly into a specific category. A wide range of disorders are included but the major ophthalmic or orbital diseases include Wegener's granulomatosis, polyarteritis nodosa, and hypersensitivity angiitis. Connective tissue disease may have a significant vasculitic component, including systemic lupus erythematosus, rheumatoid arthritis, scleroderma, and polymyositis.

Table 12-6. Classification of vasculitis based on pathogenesis

- Infectious
  - Bacterial (e.g., Neisseria)
  - Rickettsial (e.g., Rocky Mountain spotted fever)
  - Spirochetal (e.g., syphilis)
  - Fungal (e.g., aspergillosis)
  - Viral (e.g., herpes)
- Immunologic
  - Immune complex-mediated
    - Henoch-Schonlein purpura
    - Essential cryoglobulinemic vasculitis
    - Serum sickness vasculitis
    - Lupus vasculitis
    - Hepatitis B microscopic polyarteritis
  - Direct antibody attack-mediated
    - Goodpasture's syndrome (antibasement membrane antibodies)
    - Kawasaki disease (antiendothelial antibodies)
  - ANCA associated (possibly ANCA-mediated)
    - Wegener's granulomatosis - cANCA
    - Microscopic polyangiitis (microscopic polyarteritis)
    - Churg-Strauss syndrome - pANCA
  - Cell-mediated
    - Allograft organ rejection
  - Unknown
    - Giant cell (temporal) arteritis
    - Takayasu's arteritis
    - Polyarteritis nodosa

ANCA = antineutrophil cytoplasmic antibodies (Reproduced with permission from Schoen FJ. Blood vessels. In Cotran RS, Kumar V, Robbins SL, eds. Robbins Pathologic Basis of Disease, 5th ed. Philadelphia: Saunders, 1994:490)

Vasculitis deserves a special place as a specific orbital inflammation because it reminds us of the protean nature of clinical inflammatory disease and the importance of systemic associations. The necessity for careful initial and prospective systemic analysis and vigilance in orbital inflammation is underlined by this group. Although many of these disorders have relatively distinct systemic symptoms and signs, it may be difficult to diagnose them and to differentiate them from nonspecific inflammatory diseases if restricted to the orbit during the early stages. Because they may have serious or even life-threatening consequences, we must be particularly careful in diagnosing and ruling them out in the face of nonspecific inflammations of the orbit. The major categories of orbital vasculitis include Wegener's granulomatosis, hypersensitivity vasculitis (with the subclasses of orbital vasculitis, vasculitis associated with connective disease, and

Cogan's syndrome), periarteritis nodosa, and other more rare forms of vasculitis (Table 12-7).

Table 12-7. Characteristics of some systemic vasculitis

ANGIITIDES	VESSELS INVOLVED	ORGAN OR TISSUE AFFECTED	PRINCIPLE MORPHOLOGIC FEATURES	OCULAR AND ORBITAL FINDINGS
Polyarteritis nodosa	Medium-sized or small muscular arteries	Gastrointestinal tract, mesentery, liver, gallbladder, kidney, pancreas, lung, muscles, other sites	Lesions of varying ages; all layers of vessels with acute fibrinoid necrosis and extensive periarterial inflammation	Retinal and choroidal infarcts
Allergic granulomatosis (Churg-Strauss syndrome)	Medium and small arteries, adjacent veins, arterioles, capillaries	Widespread, but lungs frequently involved	Necrotizing inflammation with extravascular granulomas, coexistence of acute and healing lesions, giant cells in granulomas, abundant eosinophils	Few with ocular findings including: episcleritis, uveitis, marginal corneal ulcer, lid swelling, and conjunctival granuloma
Hypersensitivity angiitis	Small venules capillaries, arterioles	All organs and tissues (skin, muscles, heart, kidneys, lungs)	Acute necrotizing vasculitis with fibrinoid necrosis of entire wall; often thrombosis of lumen	May rarely have lid and anterior orbital inflammation
Wegener's granulomatosis	Small to medium vessels	Lungs, kidneys, upper respiratory tract; may be “limited”	Acute necrotizing vasculitis with fibrinoid necrosis of vessel wall; often proximate to granulomas in tissues	Ocular manifestations in 40%: 20–38% scleritis 10–20% uveitis 14–28% corneal gutter 7–18% retinal vasculitis 18–22% orbital involvement
Giant cell arteritis (temporal arteritis)	Muscular arteries; large vessels	Usually temporal, ophthalmic, and cranial arteries; may be systemic	Disruption of elastic lamina with most intense reaction in intimal medial layers; giant cells engulf fiber fragments, occasionally thrombosis of lumen	40% with ocular, chiefly visual problems

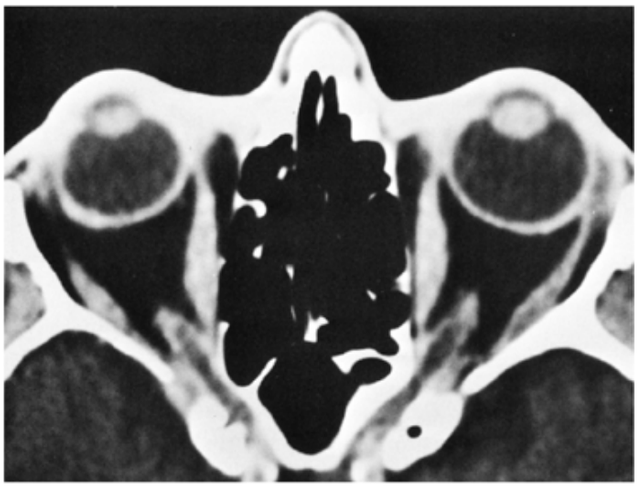

Figure 12-37. Axial CT scan demonstrates bilateral apical optic nerve swelling, mild medial and lateral rectus enlargement, and focal thickening of the scleral envelope. This was seen in a 64-year-old woman who presented with bilateral scleritis and optic neuropathy (vision was hand movement OU). Initial systemic investigations revealed no other abnormalities. A presumptive diagnosis of Wegener's granulomatosis with vasculitis was made, and the patient was treated with high-dose corticosteroids and cyclophosphamide. Vision on the left improved to 20/50, and remained at hand movement on the right. The patient refused to continue therapy, and over the next several months developed multiple renal infarcts, bilateral pulmonary vasculitis, and pleural effusion. The patient died 8 months after the onset of scleritis and optic neuropathy due to Wegener's granulomatosis.

Wegener's Granulomatosis

Wegener's granulomatosis may occur as a systemic or localized (limited) disease. When systemic, it is characterized by widespread inflammatory effects suggestive of connective tissue disease. The dominant features are rapidly progressive multisystem damage with upper and lower respiratory tract involvement followed by renal failure from necrotizing glomerulonephritis. Untreated, the generalized form is fatal, usually within two years.

In cases involving the orbit, patients typically present without systemic evidence since the disease is more commonly part of the limited form of Wegener's that spares the kidneys and may have a chronic remitting course associated with ear, nose, and throat ailments and chest disease, which may be active for many years. Ocular and orbital involvement

is common in both systemic and limited Wegener's granulomatosis and is seen in approximately 50% of cases. The limited form tends to be more indolent, whereas the generalized disorder may follow a course from rapid progression to long-term intermittent activity.

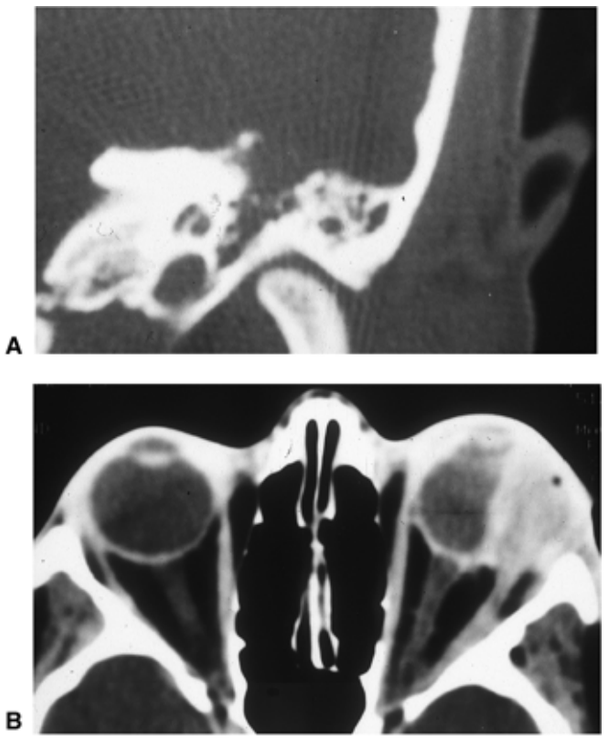

Figure 12-38. (A) CT scan of the inner ear showing bone erosion that was associated with drainage from the ear, hearing loss, and tinnitus. The patient had been referred with a 2-month history of progressive orbital cellulitis and infiltration treated as an infection. (B) Axial scan shows severe necrotizing scleritis and adjacent orbital infiltration on the left, which was associated with clinically minimal scleritis on the right. There was extensive choroidal and retinal detachment. Biopsy results of the orbit showed mixed inflammation with focal microabscesses consistent with features of Wegener's granulomatosis. Systemic results however were negative. The patient was treated with corticosteroids and cyclophosmphmide, and both her ocular and ear, nose, and throat symptoms resolved. The left eye became phthisical. (Reproduced with permission from Perry SR, Rootman J, White VA. The clinical and pathologic constellation of Wegener granulomatosis of the orbit. Ophthalmology 1997;104;683-94.)

The major clinical findings in orbital Wegener's are proptosis associated with a destructive orbital inflammatory mass, ocular inflammation with necrotizing scleritis, and optic neuropathy (Fig. 12-37). These are often bilateral and usually cause an irreversible morbidity if not treated. The disease is best treated with systemic steroids combined with an alkylating agent, preferably cyclophosphamide, which usually halts local and systemic disease. A specific diagnosis is essential before instituting the necessarily aggressive treatment and in the case of the orbit, can be confirmed by biopsy.

The diagnosis of orbital Wegener's should be based on a constellation of clinical, radiologic, and pathologic features. Clinically, the important features that should raise an index of suspicion are bilaterality, involvement of the respiratory

tract or sinuses including the mastoids (which are often missed) (Fig. 12-38), scleritis at the time of onset particularly when associated with the classical features of limbal corneal infiltrates, and systemic associations (Fig. 12-39). Some of the more subtle aspects include hearing loss or draining ears and the characteristic perilimbal clear zone associated with the scleritis and keratitis. In addition, distant episodes of orbital or sinus disease of unknown cause may be recognized historically since the disorder can progress in an episodic and regressing fashion (Fig. 12-40).

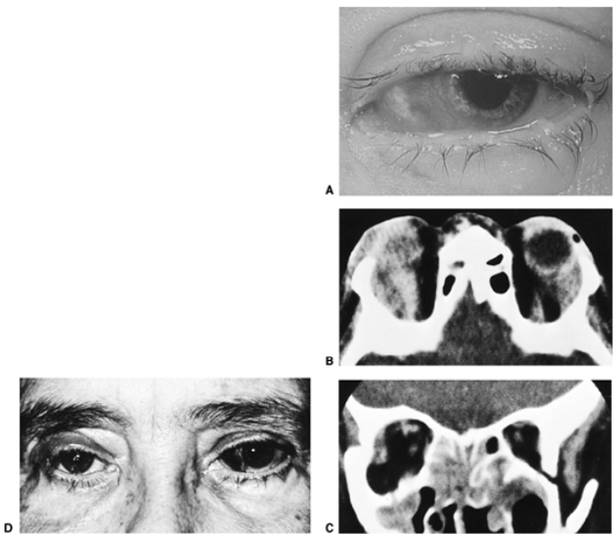

Figure 12-39. (A) A 67-year-old woman presented with a 6-month history of photophobia, tenderness, and inflammation of her eyes, affecting the left more than right. In addition, she had a mild increase in temperature and chronic sinus obstruction that was progressive for 6 months. On physical examination, she had extensive bilateral scleritis with marginal corneal ulcers and limbal corneal infiltrates, reduced vision (20/400 OD, 20/200 OS), scleral ectasia with periocular swelling, proptosis, and edema. (B, C) CT scans shows bilateral lateral orbital infiltration and extensive soft tissue changes with bone destruction of the paranasal sinuses and nasal airways. The overall picture suggested a limited form of Wegener's granulomatosis, which was biopsy proven (see Fig. 12-3). (D) Physical appearance of the same patient 2 months after initiation of therapy, which consisted of cyclophosphamide and prednisone. At this time, her vision was 20/40 OD, and counting fingers at 6 feet OS. Systemic investigation was negative. (Fig. 14-39A reproduced with permission from Perry SR, Rootman J, White VA. The clinical and pathologic constellation of Wegener granulomatosis of the orbit. Ophthalmology 1997;104;683-94.)

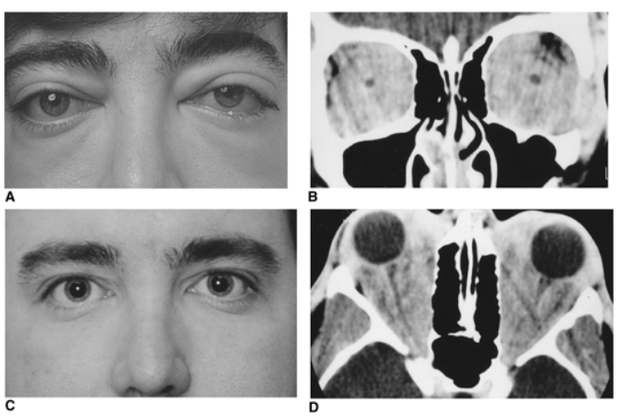

Figure 12-40. (A) A 21-year-old male presented in January 1987 with a 1-year history of recurrent, progressive, bilateral lid swelling associated with injection and proptosis. He also had noted some persistent nasal obstruction. Visual acuity was 20/20 in each eye with normal pupils, and he had markedly injected conjunctiva with chemosis and brawny lid edema. His proptosis measured 29 mm in the right eye and 30 mm in the left. He had symmetrical but moderate reduction of ocular movements. His general health was otherwise good. (B, D) Axial and coronal CT scans showed diffuse bilateral infiltration replacing orbital fat, obliterating other structures, and causing proptosis, with swelling in his inferior and middle turbinates. Although suspicious for Wegener's granulomatosis, biopsy evidence was not definitive. Nevertheless, he was treated with steroids and cyclophosphamide with improvement as shown, 8 months post-treatment (C). His ocular situation remained stable until 1991, when a nasal obstruction developed. Repeat CT scans showed reduced proptosis but persistent obliteration of all fat planes. He remained clinically stable until November 1992, when he was seen for nasal obstruction, shortness of breath, and sore throat. Systemic investigation at that point showed bilateral, ill-defined densities in the chest, and he had a subglottic inflammatory mass, of which a biopsy was done. Results showed only chronic inflammation. At this point, his c-ANCA test result was positive and a definitive diagnosis of Wegener's granulomatosis was made. He began receiving trimethoprim-sulfamethoxazole (Septra) and corticosteroids. Within 6 weeks, he stopped taking steroids; his breathing had improved because of decreased obstruction of his airway and nasal passages and reduction of the pulmonary infiltrates. In 1996, he developed left exophoria for which he underwent lateral rectus recession. He was later diagnosed with advanced keratoconus OU and early cataracts OU in 1997. At the time of his last follow-up, he was completely stable while taking trimethoprim-sulfamethoxazole (Septra) with no respiratory or orbital symptoms. (Reproduced with permission from Perry SR, Rootman J, White VA. The clinical and pathologic constellation of Wegener granulomatosis of the orbit. Ophthalmology 1997;104;683-94.)

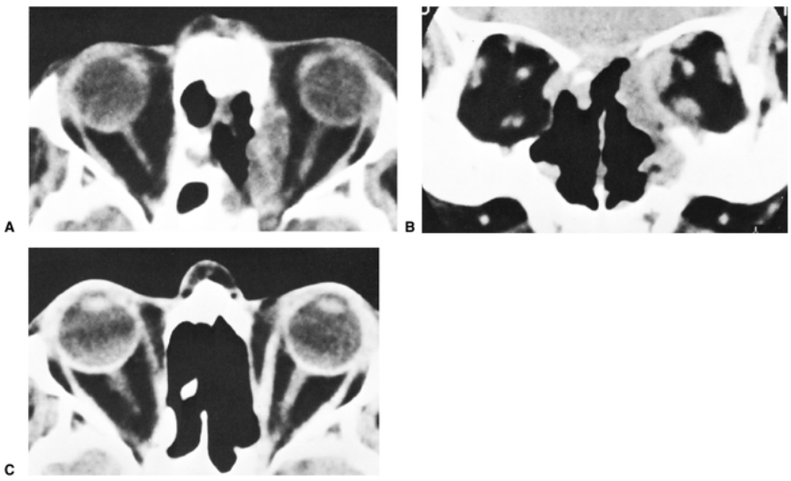

Figure 12-41. This 48-year-old man had a 15-year history of progressive destructive granulomatous inflammatory lesions involving his nasopharyngeal and sinus structures. He had multiple sinus procedures, and had developed a saddle-nose. (A, B) The overall clinical picture is a midline granulomatous process without systemic association, and a presumptive diagnosis of Wegener's granulomatosis was made. The patient was treated with cyclophosphamide and prednisone. (C) This axial CT scan demonstrates resolution of the orbital lesion after 6 months of therapy.

A wide age range from childhood to old age is associated with Wegener's. It is particularly important to recognize that it can occur in young people.

Major clinical and CT findings tend to form three relatively distinct patterns: diffuse orbital involvement (which may be bilateral) (Fig. 12-40), lacrimal involvement, or midline involvement associated with visual deterioration (Fig. 12-41). Lid swelling with brawny discoloration is particularly notable in those with lacrimal gland involvement (Fig. 12-42). Lacrimal involvement may not have contiguous orbital or midline disease. Extensive orbital infiltration may be associated with yellowing of the lids.

The CT features that are suggestive include involvement of the sinus (including mastoids) (Fig. 12-38) and a tendency for the orbital masses to be associated with infiltration and obliteration of the adjacent fat planes. Midline orbital involvement is associated with bone erosion. Optic neuropathy is the result of intraorbital involvement and is not infrequent.

Another important finding is the potential for acute progression of the chronic disease. We noted this in our patients, in which the majority had a relatively mild prodromal disease followed by episodes of dramatic deterioration. Orbital biopsy may be difficult to interpret and should be studied in light of the constellation of clinical features, which include careful clinical systemic study, c-ANCA testing (not often positive initially in the “limited” form), and imaging of the orbit, paranasal, and mastoid sinuses. The suggestive histopathologic features include mixed inflammation with lymphocytes, eosinophils, and polymorphonuclear leukocytes; mixed granulomatous inflammation or stellate microabscesses; areas of fat necrosis and lipid-laden macrophages; acute inflammation affecting vessel walls (vasculitis), and fibroplasia. These histopathologic features are characteristic of Wegener's in other extravascular soft tissue sites.

It is important to recognize this disorder within this constellation of clinical and biopsy findings because treatment can be dramatically effective using the combination of cyclophosphamide and corticosteroids. The use of

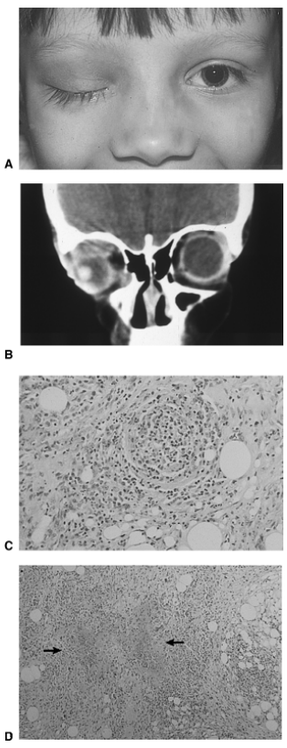

Figure 12-42. (A) A 5-year-old female was seen on referral of pathology evidence of a lacrimal inflammatory mass and brawny induration of the lid. (B) CT scan demonstrates a superolateral orbital mass. Her biopsy specimen showed necrotizing vasculitis (C, H&E, original magnification, × 25) associated with areas of microabscess formation that were either stellate (arrows) (D, H&E, original magnification, × 10) or focal with fibrosis and mixed inflammation. Upon presentation in November 1990, no other systemic findings were noted and a diagnosis of Wegener's granulomatosis was made. The patient was treated with reducing doses of prednisolone and cyclophosphamide. Over the next year, she improved substantially; the prednisolone was discontinued in August 1991 and the cyclophosphamide discontinued in February 1992 without any evidence of recurrence. (Reproduced with permission from Perry SR, Rootman J, White VA. The clinical and pathologic constellation of Wegener granulomatosis of the orbit. Ophthalmology 1997;104;683-94.)

trimethoprim-sulfamethoxazole (Septra) has been advocated in some cases, and anti-TNFs (tumor necrosis factors), such as Etanercept and Inflixamab, may also play a role. A nonrestrictive clinical and pathologic definition can lead to earlier diagnosis, rapid treatment, and prevention of sometimes catastrophic local or systemic outcome.

Other Respiratory Vasculitides

Two other respiratory vasculitides are Churg-Strauss syndrome and lymphomatoid granulomatosis. Churg-Strauss syndrome (allergic granulomatosis and angiitis) more closely resembles polyarteritis nodosa histologically, but clinically is associated with lower respiratory disease and eosinophilia. Histologically, there may be a polymorphonuclear leucocytic vasculitis with or without granulomas. The systemic manifestations of Churg-Strauss syndrome are varied and involve many organ systems. Peripheral eosinophilia is seen in up to 85% of cases.

The differentiation of Churg-Strauss syndrome from Wegener's granulomatosis is based on frequent association of allergy and asthma, eosinophilia, and responsiveness to corticosteroids alone in contrast to Wegener's.

The few cases of ocular involvement with Churg-Strauss syndrome consist chiefly of episcleritis, panuveitis, marginal corneal ulceration, lid swelling, and conjunctival granuloma. In addition, ischemic optic neuropathy has been described.

Management is usually with corticosteroids, and the large majority of patients respond. Azathioprine or cyclophosphamide should be added for resistant cases.

Lymphomatoid granulomatosis is now considered an evolving, diffuse large B-cell lymphoma rich in reactive T-cells. It is commonly associated with Epstein-Barr virus. These lymphomas typically involve the lung, skin, and central nervous system, but may secondarily involve the orbit. Lesions previously referred to as lethal midline granuloma or polymorphic reticulosis are now considered neoplastic lesions from inception. Typically they involve the nasal region, but more importantly have a propensity to involve the midline of the face. Most demonstrate an angiocentric histology and are either of T-cell or natural killer cell lineage.

Polyarteritis Nodosa (Periarteritis Nodosa)

Polyarteritis nodosa is a vasculitis of the medium and small arteries, adjacent veins, and occasionally arterioles and venules. It is segmental and has a predilection for bifurcations leading to nodular aneurysms. Lesions in a single patient may vary from acute inflammation with fibrinoid necrosis to stages of both healing and healed vasculitis. Sites of predilection are kidney, heart, liver, and gastrointestinal tract. It may also occur in the skin, peripheral nerves, pancreas, testes, and skeletal muscle.

The systemic disorder has a predilection for males in the second to fourth decades. The clinical manifestations are nonspecific and protean with fever, malaise, leucocytosis, and multisystem involvement. Up to two thirds of untreated patients will die within 1 year as a result of renal, cerebral, myocardial, and gastrointestinal involvement.

Ophthalmologically, the major findings are retinal and choroidal infarcts with exudative detachment due to tissue necrosis. Orbital involvement is unusual and associated with nonspecific orbital inflammatory features, which may be anteceded by systemic disease. Corneal and scleral necrosis as well as scleritis may occur.

Definitive diagnosis requires biopsy of involved tissues but aneurysms may be noted on angiography. Treatment is with systemic steroids and cyclophosphamide, and a survival rate of 80% at 5 years is obtainable.

Hypersensitivity (Leucocytoclastic) Angiitis

Hypersensitivity angiitis resembles periarteritis nodosa microscopically but affects smaller vessels and is more widely uniform in involvement. Pathologically the arterioles, venules, and capillaries are usually, but not necessarily, necrotic or may simply have perivascular infiltration with neutrophils undergoing karyolysis (leucocytoclasis). This is a frequent form of vasculitis and typically involves the skin, lungs, mucous membranes, heart, gastrointestinal tract, kidney, and muscle. In most instances, drugs, microorganisms, or tumor antigens have been identified as precipitating the vasculitis. The angiitides associated with the collagen diseases and essential cryoglobulinemia are examples that also fit into this category. Because smaller vessels are involved, the signs and symptoms relate to hemorrhagic and microinfarctive lesions. The spectrum of clinical disease varies from widespread multisystem involvement to primary dermatologic lesions. Many patients may have a history of recent respiratory infection or drug ingestion. Patients may have arthralgia, arthritis, myalgia, pulmonary lesions with effusion, pericarditis, myocarditis, peripheral neuropathy, and encephalopathy. Gastrointestinal and renal involvement may also be noted.

Specific diagnosis is established by biopsy. The prognosis is difficult to predict for the group overall because of heterogeneity. Removal of the inciting cause, if related to drugs

or toxins, will lead to reversal of the process. The signs and symptoms of the disease can be abated with corticosteroid therapy. It is important to rule out the possibility of underlying collagen diseases. We have divided our personal experience with leucocytoclastic vasculitis into three different groups: orbital vasculitis, vasculitis associated with connective tissue disorders, and Cogan's syndrome. All of these have similar histologic features consistent with a hypersensitivity angiitis, but have different associations.

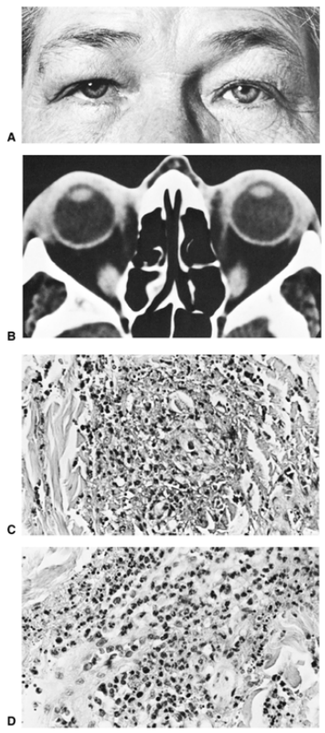

Figure 12-43. (A) This 39-year-old woman noted swelling of the upper eyelids for a 2-month period, affecting the right more than the left. (B) On axial CT scan, there was increased soft tissue of the lids and apparent enlargement of the lacrimal glands. (C, D) On biopsy, the muscle and soft tissue were pale and thickened and the lacrimal structures appeared normal (C and D, H&E, original magnifications × 10). Histologically, there was evidence of leukocytoclastic vasculitis. The vasculitis involved small vessels within skeletal muscle and adjacent connective tissue including capillaries, precapillary arterioles, and postcapillary venules. The inflammatory infiltrate in and surrounding the blood vessel wall consisted of a mixture of neutrophils associated with nuclear dusting, consistent with leucocytoclastic vasculitis. Systemic investigation was negative, and the patient was treated with 25 mg/day of prednisone tapered over a 3-week period with marked and complete improvement. There was no recurrence at 1-year follow-up.

Orbital Vasculitis

The histology of orbital vasculitis, described by Henderson and Garrity and colleagues, parallels that of hypersensitivity angiitis with fibrinoid change, vascular disruption, hemorrhage, necrosis, and fatty destruction.

Clinically, patients present with a nonspecific acute and subacute inflammation of the orbit of varying severity. At diagnosis, few have systemic associations and rarely develop it. In our experience, this disorder tends to involve the anterior orbit and lids, and it responds rapidly to systemic steroid treatment. It is the anterior acute cases that seem to be more easily treated (Fig. 12-43). Henderson and more recently, Garrity et al. have suggested that there are some lesions that may be recalcitrant, requiring immunosuppressive therapy.

Vasculitis Associated with Connective Tissue Disorders

Any of the connective tissue disorders may be associated with systemic vasculitis, including systemic lupus erythematosus, rheumatoid arthritis, and dermatomyositis. The vasculitis resembles hypersensitivity angiitis. Twenty percent of patients with lupus have ocular involvement, primarily retinal vasculitis. Involvement of the orbit is infrequent and usually secondary to conjunctival or ocular vasculitis. A few cases of orbital vasculitis and orbital myositis have been described. We have seen several, including a case of acute anterior orbital congestion secondary to vasculitis involving the sclera and intraocular structures (Fig. 12-44). This responded to aggressive systemic treatment. We have also seen patients with known diagnosis of systemic lupus present with acute, self-limited, anterior orbital inflammation or orbital myositis.

Cogan's Syndrome

Cogan's syndrome is divided into typical and atypical forms. Typical Cogan's syndrome was originally defined as interstitial keratitis associated with auditory symptoms and

vertigo. The atypical form consists of ocular and orbital disease without corneal involvement. However, it has been suggested with careful study that many patients have a transient steroid-sensitive superficial (nummular) keratitis, which is typically in the peripheral cornea. The atypical syndrome may involve the sclera and periocular tissues leading to lid swelling, chemosis, injection, and anterior orbital inflammatory disease. Identifying this entity is important, because the systemic necrotizing vasculitis occasionally associated with it may be very severe and involve multiple sites, endangering life. Early treatment with immunotherapy may be helpful in preventing deafness. We have seen one patient with this syndrome who presented with severe anterior orbital infiltration and inflammation as a primary symptom (Fig. 12-45). Within 1 week she developed the subepithelial nummular infiltrations and hearing problems. Biopsy of the conjunctiva revealed a perivascular infiltrate. This disorder will respond to systemic corticosteroids; however, in some instances, it can be fulminant and unresponsive.

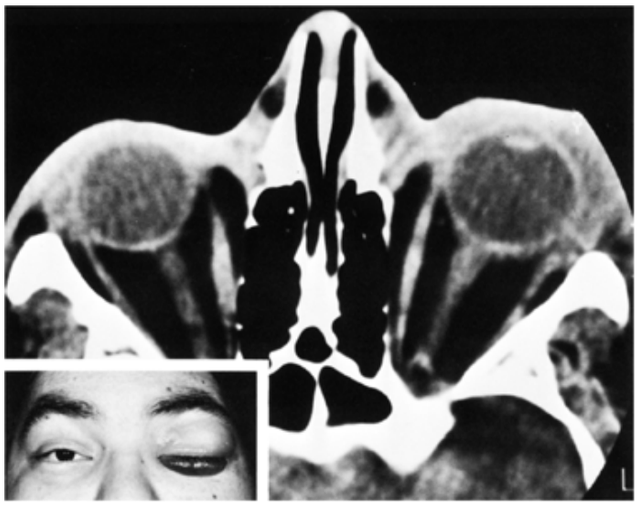

Figure 12-44. This 22-year-old man with systemic lupus erythematosus and nephrotic syndrome presented with sudden onset of left central visual loss, profound lid edema, and chemosis. His vision was counting fingers at 6 feet OS, and he had marked reduction in extraocular movements. His exophthalmometry measurements were 20 mm OD and 22 mm OS, and he had marginal corneal infiltrates as well as multiple choroidal infarcts with a shallow exudative detachment. Axial CT scan shows marked left anterior orbital soft tissue swelling with a lateral component contiguous with the left lacrimal gland and insertions of the superior and lateral rectus muscles. In addition, there was evidence of thickening of the scleral envelope. The patient had a small choroidal infarct on the right side; within 2 to 3 days he developed similar soft tissue findings. His local findings responded to intensive immunosuppressive therapy and plasmapheresis.

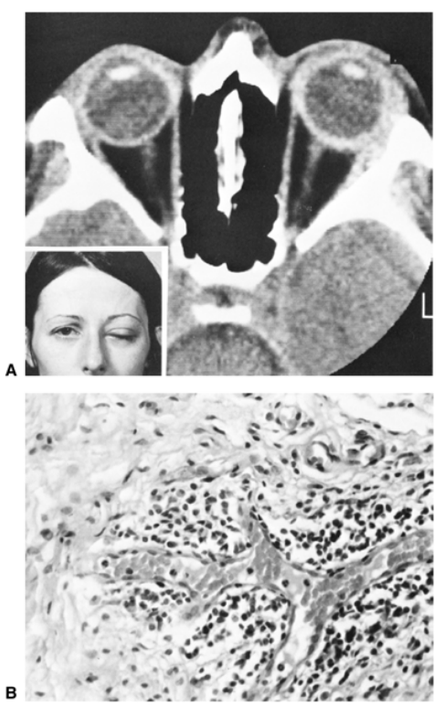

Figure 12-45. (A) This patient presented with severe left anterior orbital inflammation with lid edema, chemosis, ptosis, and superficial ocular inflammation associated with mild proptosis. Within 1 week, she developed subepithelial nummular infiltrations of the cornea and hearing problems. The axial CT scan shows thickening and enhancement of scleral coats on the left globe with increased anterior soft tissues. The patient was diagnosed as having Cogan's syndrome (atypical) and responded to high-dose corticosteroid therapy. (B) Biopsy of the conjunctiva showed an intense nonspecific perivascular lymphocytic and plasmacytic infiltrate (H&E, original magnification × 10).

Temporal Arteritis

Temporal arteritis is most frequently associated with the complication of ischemic optic neuropathy and rarely is associated with orbital soft tissue features.

Idiopathic Sclerosing Inflammations of the Orbit

Idiopathic sclerosing inflammation is a unique clinicopathologic entity that shares histopathologic similarities to retroperitoneal fibrosis (*c.f.* Pathology chapter). It is characterized by primary, chronic, immunologically mediated fibrosis and a poor response to corticosteroid treatment and radiotherapy, leading to frequent visual disability. This entity accounted for about 5% of nonthyroid inflammatory lesions seen in our institution.

The clinical features are dominated by a cicatricial infiltration associated with mass effect and mild inflammation. Patients present with pain, proptosis, mild lid swelling, injection, restriction of ocular movements, and ptosis, and a significant number have visual deterioration. The disease may be bilateral, in which case it is usually asymmetrical. Three anatomical subgroups have been noted: diffuse, lacrimal, and apical. Most commonly, the process develops in the anterior superolateral orbit involving the lacrimal gland. Twenty percent, however, begin as an apical lesion. We have also experienced several cases beginning as a myositic disorder (Fig. 12-46). With progression, diffuse orbital involvement is common and may go on to intracranial and bone involvement, affecting the cavernous sinus region and even the pterygopalatine fossa (Fig. 12-47). This disorder may be associated with similar fibrosclerosis in the retroperitoneum and elsewhere as part of multifocal mediastinal or retroperitoneal fibrosclerosis, a feature noted in 3 of our patients.

The characteristic imaging findings are a homogeneously enhancing mass with irregular margins, which obliterate the adjacent extraocular muscles, lacrimal gland, or orbital structures (Fig. 12-48).

The differential diagnosis includes conditions that may be characterized by orbital desmoplasia and pain with mild inflammation. These include thyroid orbitopathy, sarcoid, Wegener's granulomatosis, sinus disease, tuberculosis, Erdheim-Chester disease, primary and secondary neoplasms (especially breast, bowel, or prostate carcinoma), meningioma, and more rarely lymphoma.

The characteristic histopathologic feature is fibrosis with a paucicellular inflammatory infiltrate that has the immunopathologic profile of retroperitoneal fibrosis.

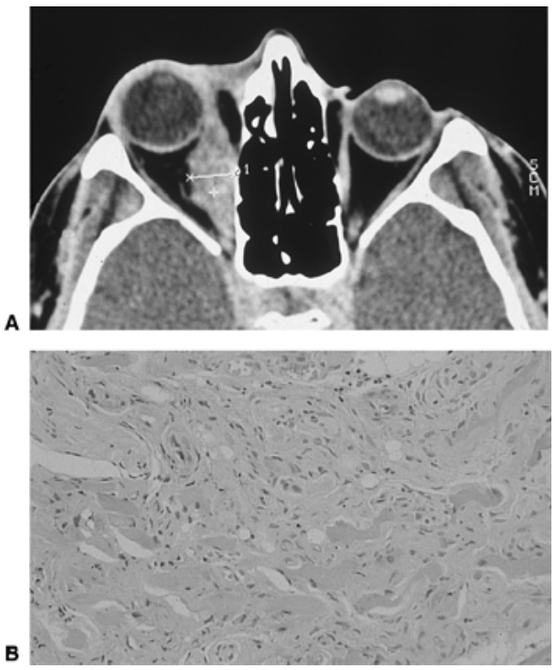

Figure 12-46. This 30-year-old woman with a long-standing history of right amblyopia presented with a sudden onset of swelling, pain, and redness surrounding the right eye. On examination, she had 4 mm proptosis on the right with moderate restriction of right adduction. There was mild scleral injection and conjunctival chemosis. (A) CT scan demonstrated a progressive fibrosing lesion involving the right medial rectus muscle, its tendon, and the adjacent fat. (B) Histology of the muscle revealed a sclerosing inflammation incoporating the muscle (H&E, original magnification × 10). She was treated with high-dose steroids and radiotherapy with no effect on the inflammatory disease. Her condition continued to worsen and she eventually developed marked optic nerve compromise with disc swelling and visual deterioration to 20/200. A right decompression was performed, and the patient started on azathioprine and a nonsteroidal antiinflammatory drug, which led to settling of her inflammatory process. Significant volume deficit of her right orbit resulted with the resolution of her proptosis, requiring orbital augmentation. She also developed a severe retinal neovascularization and rubeosis iridis, which were treated with panretinal photocoagulation.

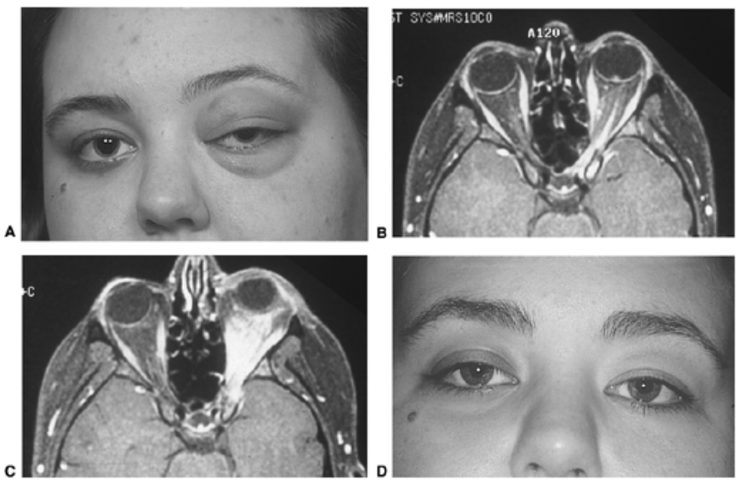

Figure 12-47. This 23-year-old woman presented in April 1995 with a sudden onset of painless central visual loss, which was diagnosed as a nonspecific orbital inflammatory syndrome involving the superior orbital fissure and the anterior cavernous sinus as demonstrated on MRI. She was treated with steroids and had a prompt response but by August, she had a recurrence that led to the introduction of naproxyn (Naprosyn) and methotrexate as well as radiotherapy. She developed marked steroid side effects and progressive proptosis with ptosis. (A) On referral in January 1997 her vision was 20/20 OD and 20/40 OS with a paracentral scotoma, relative afferent pupillary defect, and evidence of brawny induration of the left upper lid. Her exophthalmometry measurements were 19 mm OD and 26 mm OS with decreased movements, mild temporal pallor, and macular folds. (B) MRI (post-gadolinium with fat subtraction) demonstrates an apical, ill-defined optic nerve sheath infiltration associated with medial rectus enlargement and extension into the cavernous sinus, which had progressed (C) by December 1996 to demonstrate extensive involvement of the orbit (post-gadolinium). She underwent a biopsy which demonstrated sclerosing inflammation. She was treated by a rheumatologist with an aggressive regimen of pulsed steroids, cyclosporine, and cyclophosphamide, which led to a rapid response with resolution of the proptosis, increased extraocular movements, and a vision of 20/25 over the next 6 months (D). The medications were reduced and withdrawn over a 1-year period. This disorder has recurred as a more focal involvement of the medial rectus, requiring reinduction.

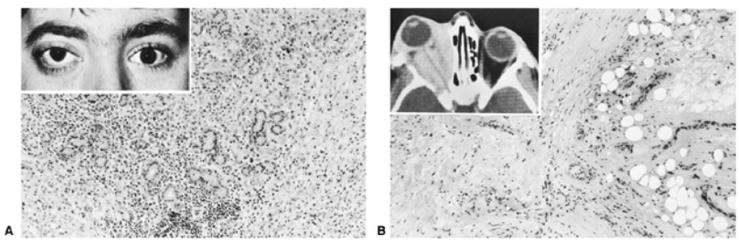

Figure 12-48. (A, inset) This 18-year-old boy had progressive right proptosis over a 2-year period due to sclerosing inflammation, which started superolaterally in the right orbit. In addition, on presentation he had papilledema, reduced extraocular movements, reduced vision, a right afferent pupillary defect, and choroidal striae. (B, inset) His CT scan shows extensive orbital involvement with encasement of the optic nerve and extraocular muscles. Histologically, it was a sclerosing inflammation that incorporated lacrimal structures (A) and invaded the orbit (B) (A and B, H&E, original magnification × 2.5). Systemically, he had increased circulating immune complexes, increased IgM levels, and a history of three bouts of aseptic arthritis. He responded clinically with arrest and improvement of his proptosis and extraocular movements following orbital radiotherapy (3000 rad over 10 days). His vision did not recover.

Historically, the treatment of this disorder has been associated with poor outcome in up to 30% of cases. Since our description of the immunopathologic profile of this disorder, we have developed a more aggressive approach to sclerosing inflammation that consists of biopsy for prompt, early diagnosis, and early intervention. Such intervention involves a combination of corticosteroids with other drugs directed against T-cells (cyclosporine) and B-cells (methotrexate, cyclophosphamide, azothioprine depending on age). Since instituting this regimen, we have had 6 cases which have been abruptly arrested without progression. This management profile requires the multidisciplinary involvement of a rheumatologist and chemotherapist.

Granulomatous Inflammations

Nonvasculitic granulomatous disorders have been grouped together on the basis of their fundamental underlying histopathologic infiltration by histiocytes. As the clinical picture often involves a low grade infiltrative process with mild inflammatory features and varying clinical constellations, they almost universally come to biopsy. Thus from a practical point of view, they can be grouped together histologically and clinically. The granulomatous inflammations of note in the orbit include foreign body granulomas, ruptured dermoid cysts, sarcoid and sarcoidal reactions, xanthogranulomatous disorders, and fibro-osseous processes.

Foreign Body Granulomas

The most common intrinsic origin for a foreign body granuloma is rupture of a dermoid cyst (Fig. 12-49). In our experience, although histologic evidence of rupture of a dermoid cyst is present in more than 50% of the cases examined, clinical inflammation only occurs in about 15% of cases. The inflammatory subgroup are typically associated on imaging with an irregular infiltrative margin often containing lucent areas on CT scans, suggesting dispersion of fat within the inflammatory response. Treatment is by excision. The margins of such lesions are often irregular and fibrotic, and care should be taken to avoid destroying adjacent structures. A small residuum of the fibrotic portion but not the cyst may be left behind and treated with corticosteroids.

Vegetal foreign bodies may also be a source of orbital granulomatous inflammation and are typically associated with an antecedent history of trauma and a persistent low-grade inflammatory response that may lead to fistulization (Fig. 12-28).

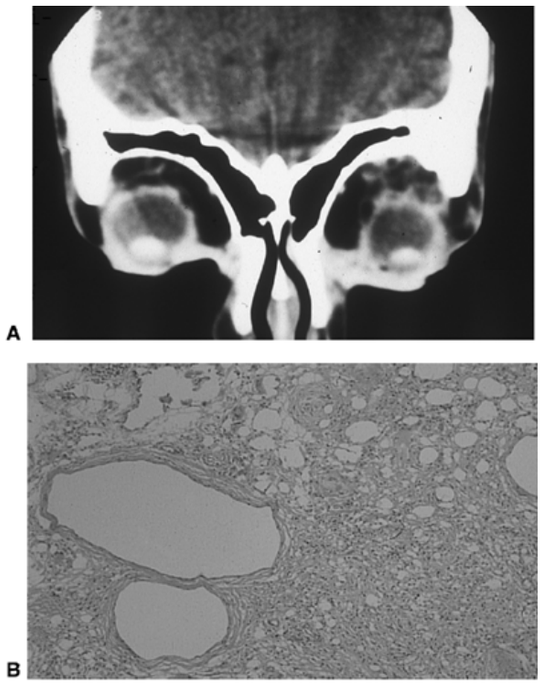

Figure 12-49. Ruptured dermoid cyst causing foreign body granuloma. A 43-year-old man had 2 episodes of swelling, irritation, and injection of the left upper lid with some tenderness and slight limitation of elevation. (A) CT scan demonstrated a superior and superolateral infiltrate with characteristic low density material and focal bony erosion. Excision revealed a fibrous mass attached to a cyst adjacent to the bone erosion. (B) Histology of the orbital infiltration demonstrates lipid-filled spaces surrounded by a granulomatous reaction, consistent with a ruptured dermoid cyst (H&E, original magnification × 2.5).

Another foreign body granuloma of note is the paraffinoma, a lesion that results from injection of a petrolatum-based material into the soft tissues of the orbit (Fig. 12-50). The most common instances that we have noted have been secondary to sinus surgery and firm packing with excessive amounts of petrolatum-soaked gauze. Treatment implies excising as much as possible of the foreign body material along with anti-inflammatories. This disorder can be prevented by not using petrolatum-soaked gauze. We have also experienced several cases of bone wax granulomas following its use in orbital surgery, and others have reported similar experiences with avitene.

Sarcoid and Sarcoidal Reactions

When the orbit is involved with a sarcoid granuloma, in our experience there is almost an even split between an isolated sarcoidal reaction and a reaction associated with sarcoidosis.

Overall the clinical presentation consists of a mass effect, rarely associated with evidence of inflammation, with more than half of the patients presenting with lacrimal involvement (Fig. 12-51). When the lacrimal gland is involved, half are bilateral, which is dominantly an isolated reaction, but at least one third have been associated with sarcoidosis. Generally, 7% of patients with known sarcoidosis have lacrimal involvement but only 0.6% present primarily with lacrimal involvement (Table 12-8). On imaging, the lesions typically are circumscribed but occasionally have infiltrative margins.

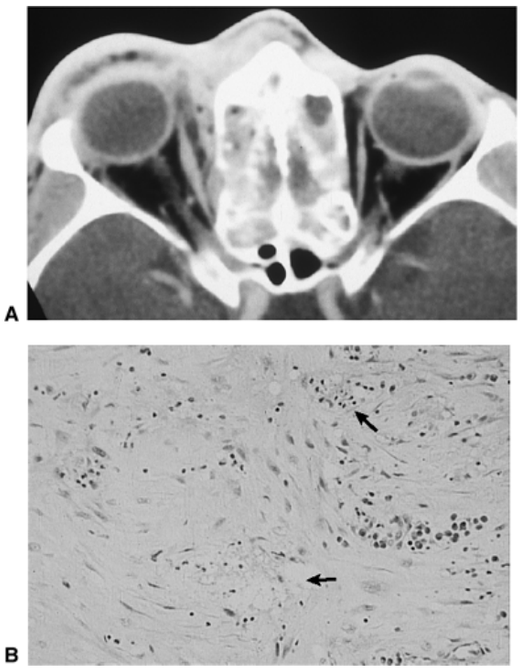

Figure 12-50. This 45-year-old man presented with orbital cellulitis after having an ethmoidectomy and polypectomy that was associated with postoperative subcutaneous emphysema on the right side. He had been treated with corticosteroids for a nonspecific orbital inflammatory syndrome and presented to us with recurrence of disease after discontinuing steroids. (A) The orbital inflammation was associated with an anterior subperiosteal and extraperiosteal infiltration, which demonstrated focal areas of radiolucence both within the orbit and adjacent sinuses. (B) A diagnosis of paraffinoma was confirmed by biopsy (arrows – lipid spaces) (H&E, original magnification × 10). The patient underwent partial resection of the involved tissues with a total period of 12 weeks of steroids to control inflammation. He subsequently had persistent lid scarring and nodularity with a slight ptosis and restriction of ocular movements. Systemically, he developed a painful bilateral post-steroidal hip syndrome, which resolved over a 12-month period.

Table 12-8. Presentation and clinical features of sarcoidosis

NATURE OF PRESENTATION	FEATURES IN KNOWN SARCOIDOSIS	OPHTHALMIC SERIES
40% on routine chest X-ray	90% radiographic bilateral hilar adenopathy	50% ocular involvement
15% acute polyarthritis (frequently associated with erythema nodosum and iridocyclitis)	40% extrapulmonary manifestations	15% present with ocular
11% erythema nodosum	33%–50% skin lesions	30% with posterior uveitis have CNS disease
6% skin sarcoid	20% hepatosplenomegaly	
7% ocular sarcoid	20% ocular	
0.6% lacrimal	20% bone change on X-ray 8% salivary 7% lacrimal mass 13% reduced lacrimal secretions 17%-33% positive conjunctival (on biopsy) 4% CNS 0.2% orbital Lung involvement: Stage 1, 50% Stage 2, 25% Stage, 3, 15%	

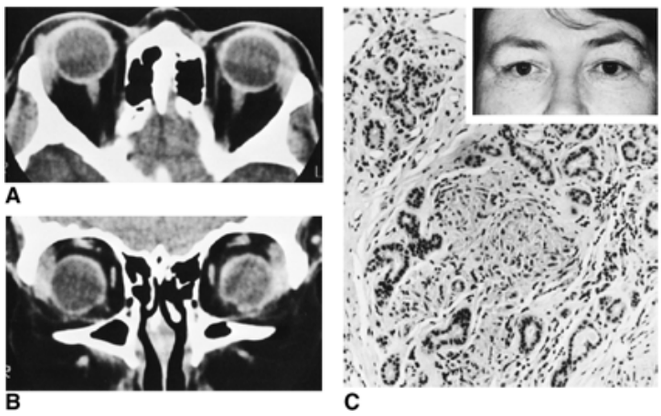

Figure 12-51. (A, B) Axial and coronal CT scans demonstrate bilateral enlargement and protrusion of the lacrimal glands, which had been slowly progressive over a 2- to 3-month period. (C) Histology demonstrates a naked tubercle within the lacrimal acini. The patient had bilateral hilar adenopathy, and the final diagnosis was sarcoidosis (H&E, original magnification × 25)

Patients with sarcoidosis may also have other ocular findings including uveitis, chorioretinitis, conjunctival inflammatory nodules, or optic nerve sheath sarcoid (Fig. 12-52). Treatment is usually with oral corticosteroids and/or immunosuppressives when clinically indicated.

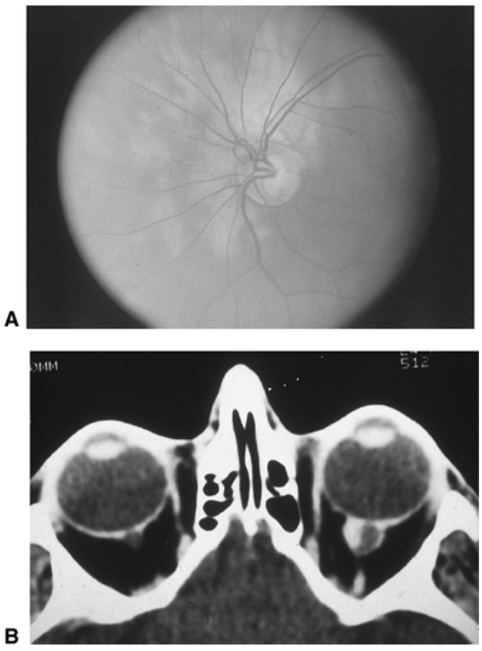

Figure 12-52. This fundus photograph (A) and CT scan (B) were obtained from a 65-year-old woman who presented with a history of intermittent and progressive visual loss, assumed to be due to optic nerve meningioma because of the dural thickening noted on CT scan. The patient initially refused biopsy, and was treated with steroids with dramatic improvement of vision. She was maintained on a very low dose of steroids but then began to develop a peripapillary choroidal infiltrate (shown), which was suspicious for a differential diagnosis of sarcoid, lymphoma, or meningioma. She underwent a medial conjunctival approach to biopsy of the anterior optic nerve dura, which revealed a sarcoidal reaction. Treatment with steroids has led to resolution with a 5-year follow-up. (Reproduced with permission from Kao SCS, Rootman J. Unusual ophthalmic presentations of dural sheath sarcoid: report of two cases. Can J Ophthalmol 1996;31:195-200.)

There is one other type of sarcoidal reaction that is worthy of note and that is involvement of the dura with sarcoid. We have seen three cases of optic nerve dural involvement with sarcoidal granuloma that were characterized by a relatively sudden onset of visual disability associated with imaging findings of multifocal dural-enhancing lesions and, in one instance, choroidal infiltration. In addition, we have also had a case of dural sarcoid that involved the skull base, periorbita, and the extraocular muscles. All of the dural cases required aggressive intervention with anti-inflammatories and/or immunosuppressives. The optic neuropathy is reversible in dural sarcoid if recognized and treated early.

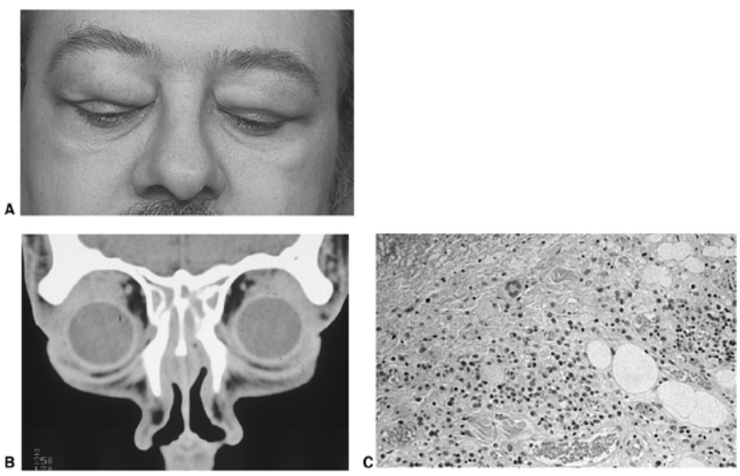

Figure 12-53. Xanthogranulomatous lesion associated with adult-onset asthma. (A) A 45-year-old man with a 5-year history of progressive infiltration of the upper lids and orbit by a nontender, noninflamed xanthomatous mass with mild proptosis and diplopia on upgaze. He had also developed adult-onset asthma. (B) His CT demonstrates anterior and superior dense, irregular infiltration, which on biopsy (C) was a xanthogranuloma with Touton giant cells (H&E, original magnification × 25).

Xanthogranulomatous Disorders of the Orbit

Orbital xanthogranulomas consist of a chronic inflammatory infiltrate with lipid-laden histiocytes that have small, round nuclei and abundant clear or vacuolated cytoplasm. A characteristic finding is the presence of scattered, multinucleated giant cells of the Touton type. These histiocytes give rise to the typical yellow-orange coloration of the lids in the xanthomatous lesions, which may occur both in childhood and adult life.

Juvenile xanthogranuloma more commonly affects the eyelid, anterior uveal tract, and nonocular skin sites with few cases involving the anterior orbit.

The adult-onset orbital xanthogranulomas are rare, frequently bilateral, and may be associated with hematologic abnormalities. Periocular xanthogranulomas in adults have been reported in the context of Erdheim-Chester disease, necrobiotic xanthogranuloma, or juvenile xanthogranuloma. In addition, there are several recent cases of bilateral periocular xanthogranulomatosis in adults without systemic disease or an association with asthma. We have also seen 3 cases of xanthogranulomas associated with adult-onset asthma and benign reactive hyperplasia of the lymph nodes (Fig. 12-53). Recently, we have noted responses to combined treatment with steroid induction and cyclosporine with or without an immunosuppressive (Fig. 12-54).

Necrobiotic xanthogranuloma is characterized by the presence of multiple, rather indurated xanthomatous subcutaneous nodules in patients who have paraproteinemia (Fig. 12-55). Ophthalmic involvement is common and usually involves the eyelid, orbit, and in some instances conjunctiva. A few cases with episcleritis, scleritis, uveitis, and keratitis have been described. They have a tendency to ulcerate and progress in size. Approximately 47% have a risk of later malignancy, including multiple myeloma, plasma-proliferative disorders, lymphoproliferative disorders, and lymphocytic leukemia. Histopathologically, there are poorly formed granulomas with sheets of histiocytes, many of which are lipidized, and evidence of Touton and foreign body type giant cells. These usually are associated with areas of necrobiotic collagen. Cholesterol clefts and lymphoid nodules may be noted. The majority of patients demonstrate monoclonal gammopathies, although few of them have overt multiple myeloma. The clinical picture is associated with waxy, firm infiltrates occurring in the sixth decade. Systemic treatment of an associated lymphoma when present may lead to response of the local lesions.

The importance of recognizing the xanthogranulomatous lesions relates to their frequent association with systemic disorder, which in some cases may be life threatening.

Erdheim-Chester disease rarely involves the orbit with a lipogranulomatous process. Systemic involvement of bones, heart, lungs, or retroperitoneum has been reported with these

cases. The orbital cases have shown diffuse involvement leading to infiltration, scarring, compressive, and restrictive effects associated with subcuticular xanthelasma-like lesions. These may respond in part to systemic steroids.

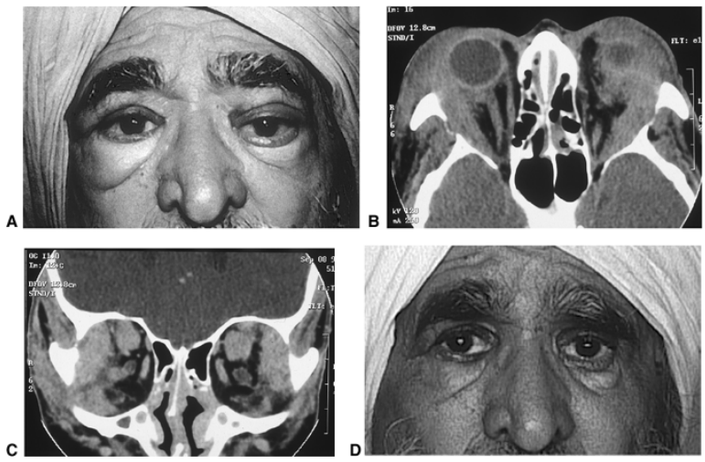

Figure 12-54. (A) This 72-year-old man had a 5-year history of progressive infiltration of the orbit. On examination, he had reduced vision to 20/30 OD and 20/60 OS with firm xanthochromic subcutaneous masses, proptosis, and reduced ocular movements as well as an enlarged, firm parotid gland. (B, C) His CT scans showed extensive irregular infiltration of the orbit. Our review of previous biopsies diagnosed as Erdheim-Chester disease suggested an alternative diagnosis of xanthogranulomatous disorder with lymphadenopathy and adult-onset asthma. (D) He has responded dramatically to a regimen of corticosteroids and cyclosporine with recovery of vision and reduction of proptosis from 18 mm OD and 23 mm OS to 11 mm OU. In addition, he has recovered his ocular movements and his asthma has significantly improved over a 6-month period.

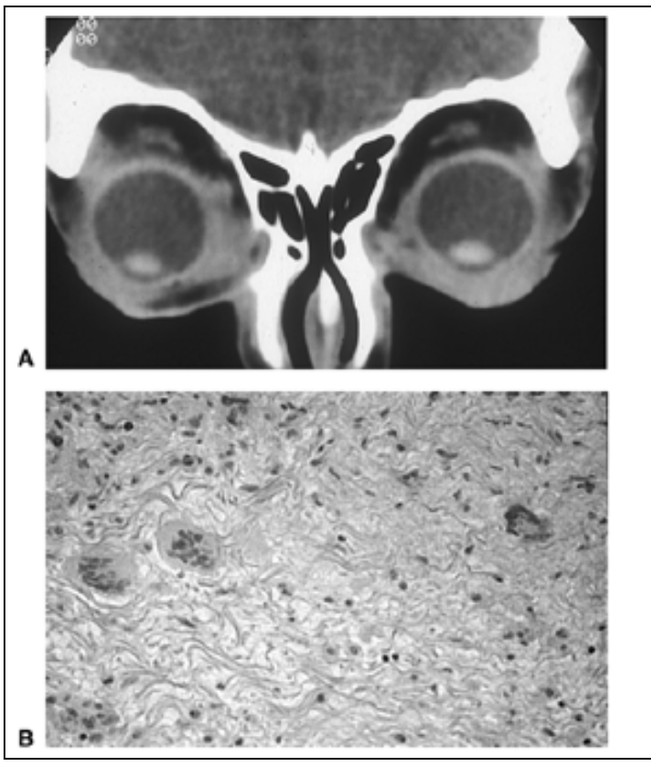

Figure 12-55. CT scan (A) and biopsy (B) from a 69-year-old woman with a 1-year history of progressive injection of the globes, which was associated with xanthomatous lid lesions. She has a firm, rubbery infiltrate of the lids and Tenon's capsule with mild restriction of movement. Biopsy demonstrated a lipogranuloma in Tenon's capsule with Touton giant cells, consistent with necrobiotic xanthogranuloma (H&E, original magnification × 25). She also had a paraproteinemia and was treated with diminishing doses of steroids with some improvement.

Pseudorheumatoid nodules occasionally can appear as focal, yellowish subcutaneous masses in the dermis of children. They may occur in the periorbital region but not in the deep orbit and thus occasionally affect the anterior orbit. They consist of zonular granulomas surrounding necrobiotic collagen and are managed by simple excision.

Fibro-osseous Processes

There are a number of fibro-osseous processes, including aneurysmal bone cyst, giant cell reparative granuloma, and cholesterol granulomas, that may occur in the periorbital region and secondarily involve the soft tissues of the orbit. They however belong more in a discussion of bone tumors than with inflammatory conditions of the orbit.

Idiopathic Lipogranuloma

Although described in the older literature, this is in my experience an increasingly rare entity and may represent an incomplete diagnosis related to any lipidizing process that has led to granuloma formation, many of which have already been discussed.

Melkersson-Rosenthal Syndrome

Melkersson-Rosenthal syndrome has been described in the literature since 1929 as a syndrome characterized by relapsing orofacial edema (75% of patients) and recurrent facial nerve or other paralyses (33%), which may or may not be associated with a fissured tongue (lingua plicata). The triad occurs in about 8% of patients only. The clinical picture is characterized by a nonpitting, relatively firm swelling of the orofacial tissues with focal brawny induration (Fig. 12-56). Numerous patients have been described with preseptal eyelid findings with an indurated peau d'orange appearance. The histopathologic characteristics consist of epithelioid cell granulomas or lymphonodular plasmacytic-type granulomas, with a characteristic perilymphatic subendothelial component associated with lymphangiectasia and dermal edema. Treatment is not curative and focuses on the use of nonsteroidal anti-inflammatories, systemic corticosteroids, and excision and reconstruction if there is persistent functional or aesthetic problems with the lids.

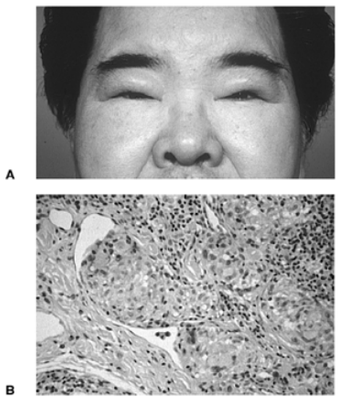

Figure 12-56. (A) This 63-year-old man presented with a long-standing history of progressive thickening and induration of his lids. On examination, he had firm, nonpuffy, brawny lids and similar thickening of his premalar skin. His remaining ocular exam was unremarkable. (B) Histology demonstrated multiple nonnecrotizing granulomas, including many in the subendothelial space of lymphatic vessels, which is characteristic of Melkersson-Rosenthal syndrome (H&E, original magnification × 25).

Transitional Lesions

There are a number of lesions that may occur in the orbit, which are characterized clinically primarily by mass effect and infiltration of orbital structures, sometimes with low-grade features of inflammation. These may be identified as part of the differential diagnosis on biopsy of orbital inflammatory conditions or lymphoproliferative disorders. This includes Kimura's disease, Sjögren's syndrome, and sinus histiocytosis with massive lymphadenopathy. In my view, they belong more to the lymphoproliferative spectrum and could also be discussed under these categories of disease. Their inclusion here is a matter of completing the differential diagnosis for inflammatory disorders that are characterized by low-grade mass and infiltrative effects.

Kimura's Disease

Kimura's disease, sometimes called angiolymphoid hyperplasia with eosinophilia, is a benign disorder of young adults characterized by the development of inflammatory angiomas of the skin, chiefly of the head and neck and often with regional lymphadenopathy. It is believed to be a reactive inflammatory disorder that may be associated with systemic eosinophilia and may occasionally undergo spontaneous resolution. These features support the concept of an inflammatory pathogenesis. It is frequently seen in Asia where it is often associated with peripheral eosinophilia and elevated serum IgE levels. Numerous orbital cases have been described.

Histologically, the striking feature is a well-circumscribed lesion consisting of a mixture of vascular channels with plump vacuolated endothelial cells and zonal polymorphic inflammatory infiltrate with many eosinophils. Lymphoid follicles and disrupted inflamed larger vessels may be noted.

A number of studies support the easy distinction between Kimura's disease and angiolymphoid hyperplasia with eosinophilia but the larger reviews of ocular cases suggest that this distinction cannot always be made.

Orbital involvement consists primarily of well-defined soft tissue masses of the anterior orbit, canthus, or lids (Fig. 12-57). This lesion, which is essentially a benign disorder, is included because of the inflammatory, lymphoproliferative, and vascular component, necessitating a differentiation of this from a number of important orbital lesions. The differential diagnosis includes angiosarcomas, epithelioid hemangioendotheliomas, nonspecific orbital inflammations, insect bite, pyogenic granuloma, eosinophilic granuloma, angiomatous lymphoid hamartoma, and granuloma faciale.

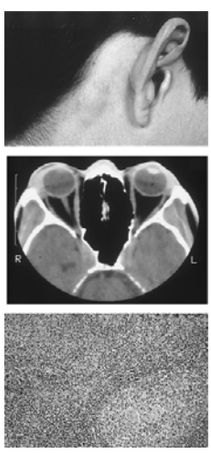

Figure 12-57. Kimura's disease. This 31-year-old Vietnamese man had bilateral episodic lacrimal enlargement associated with retro-auricular and cervical adenopathy. The lymph node and lacrimal biopsy demonstrated follicles with giant cells surrounded by lymphocytes, histiocytes, numerous eosinophils, and plasma cells, which was consistent with Kimura's disease (H&E, original magnification × 10).

If the lesion is well-defined and focal, it may be treated by local excision alone. For lesions that are incompletely excised of significant size, recurrent, or persistent, radiotherapy has been advocated.

Sjögren's Syndrome

Sjögren's syndrome is defined by the presence of any two of the triad of keratoconjunctivitis sicca, xerostomia, and autoimmune disease. The primary or isolated form consists of the ocular and oral changes alone and is called the *sicca syndrome.* More commonly, however, patients have an associated autoimmune disease including rheumatoid arthritis (most common), systemic lupus erythematosus, polymyositis, vasculitis, scleroderma, mixed connective tissue disease, autoimmune liver disease, and hemolytic anemia.

Pathogenesis

Lymphocytic infiltration and sclerosis of the lacrimal and salivary glands account for the decrease in tears and saliva. The organ-specific damage may be due to factors both of cytotoxic T-cell infiltration and the presence of autoantibodies. Three quarters of patients have detectable rheumatoid factor even in the absence of clinical arthritis (50% of patients with sicca syndrome and almost all patients when they have the associated rheumatoid arthritis). In addition, about 70% have antinuclear antibody (ANA) and 25% a positive LE test. A multiplicity of organ-specific autoantibodies have been identified, including those to salivary duct cells, gastric parietal cells, and thyroid. There are two antinuclear antibodies associated with the syndrome, anti-SS-A and anti-SS-B. The SS-B antibodies are felt to be highly specific for Sjögren's syndrom, and are found in 60% to 70% of patients with the primary disorder. Anti-SS-A antibodies are seen in only 14% of patients and are not considered specific. The patients with associated autoimmune disorders appear to make up a distinctive subset with some difference in serologic and immunologic studies. Patients with Sjögren's syndrome may be at a higher risk of autoimmune thyroid disorders.

Pathologically, the glands (major and minor lacrimal and salivary, as well as other exocrine glands) are characterized by early periductal lymphocytic infiltration (with and without lymphoid follicles) followed by atrophy of the acini, hyalinization, and fibrosis. The ductal elements may undergo proliferation, forming epimyoepithelial islands. The early disappearance of lysozyme from the tears (versus an increase in sarcoidosis) may help in a diagnosis of Sjögren's syndrome.

Clinical Features

The keratoconjunctivitis sicca is characterized by an insidious onset of burning, dryness, photophobia, and mucus secretion. This may lead to fluctuations in vision and blepharospasm. Clinically, it is associated with a filamentary keratopathy with multiple filaments and gray punctate lesions of the cornea. A thick mucus discharge may be noted in the fornix, and the keratitis is demonstrable with rose Bengal (1%) stain. Associated follicular or Meibomian gland infection is frequent. There is a rapid breakup of the tear film and a reduced Schirmer test. Palpable enlargement of the lacrimal gland may be evident and may fluctuate when present (Fig. 12-58). Clinically, lacrimal gland involvement may appear as a mild dacryoadenitis with variable enlargement of the lacrimal gland and in some instances spill-over

into orbital soft tissues, decreased tear secretion, and features of a sicca syndrome (Fig. 12-59).

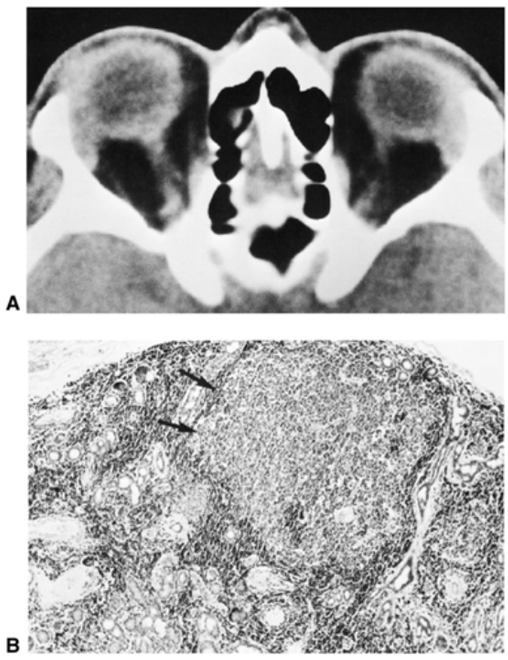

Figure 12-58. (A) Axial CT scan demonstrates bilateral enlargement of the lacrimal glands in a 50-year-old woman with a 3-month history of nontender upper lid swelling associated with ocular grittiness. There was reduced tear secretion on Schirmer's test. (B) Histopathology shows dense lymphocytic infiltration with partial destruction of the gland. Note large follicular centers (arrows) (H&E, original magnification × 10). Systemically, the patient had bilateral modest effusions of her knees and a right submandibular salivary gland enlargement. The diagnosis was consistent with Sjögren's syndrome. The patient responded to systemic prednisone 30 mg/day with improvement in tear secretion and reduction in lacrimal swelling. Her prednisone was tapered over a 3-month period and replaced by chloroquine 200 mg/day for 6 months. There has been no recurrence during a 2-year follow-up.

Salivary involvement leads to difficulty swallowing, reduction in taste, and thinning of the buccal mucosa. It may be associated with parotid gland enlargement (50%), which may fluctuate. Involvement of the nasopharynx and respiratory passages leads to epistaxis, reduced sense of smell, hoarseness, and recurrent bronchitis. In addition to the autoimmune disorders associated with sicca syndrome, patients may develop a lymphoproliferative disorder. It is usually a pseudolymphoma and may be difficult to differentiate from a malignant lymphoma. In fact, some patients go on to develop both salivary and extrasalivary malignant lymphomas (40-fold higher risk). In addition to the wide variety of autoimmune disorders, patients may suffer from Raynaud's phenomena, hypergammaglobulinemic purpura, hyperviscosity syndrome, and peripheral neuropathies. The neuropathies frequently affect the cranial nerves, in particular, the trigeminal.

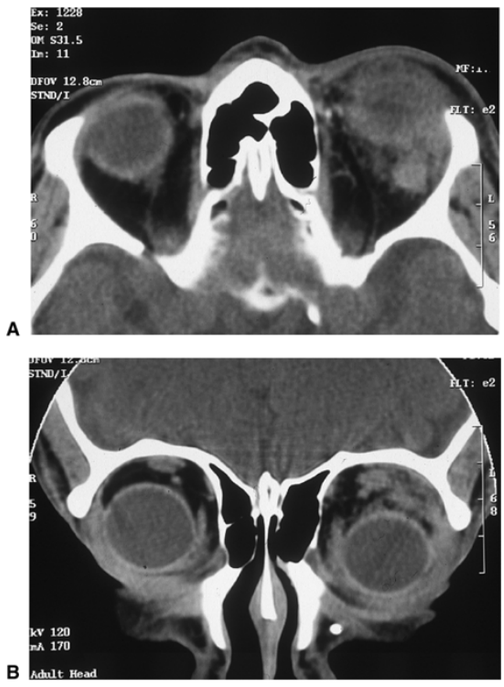

Figure 12-59. This 61-year-old man developed left conjunctival and lid swelling, which had been persistent for 3 months on presentation in our clinic. He had 3 mm downward and 1 mm inward displacement with 4 mm axial proptosis. There was a good range of ocular movements and no palpable mass in the superior or superolateral fornix. He had reduced tear secretion to 2 mm on the right and 4 mm on the left at 5 minutes. (A) Axial and (B) coronal CT scans demonstrated enlargement of the lacrimal gland with irregular infiltration of the adjacent orbit. Biopsy revealed histologic features typical of Sjögren's disease.

Imaging

Imaging in the lacrimal gland in patients with Sjögren's disease may show either normal, enlarged, or atrophic lacrimal glands. On MRI, the hypertrophic glands may be relatively homogeneous whereas normal sized glands may be more heterogenous with high signal intensity spots (T1-weighted, which were suppressed after fat saturation) throughout the parenchyma. In contrast, the atrophic glands are heterogeneous due to accelerated fat deposition. The normal sized glands have a wide range of reduced lacrimal flow as do the hypertrophic glands. Atrophic glands, on the other hand, have significantly lower lacrimal flow rates.

Differential Diagnosis

Inflammatory involvement of the lacrimal and salivary gland was once called Mikulicz's disease. The term now has been broadened to include all causes of lacrimal and salivary gland enlargement including sarcoidosis, Sjögren's syndrome, lymphoma, leukemia, tuberculosis, syphilis, and other specific and nonspecific inflammations. Therefore, Mikulicz's syndrome is a broad, nonspecific term incorporating a wide variety of diseases.

Management

The glandular disease appears to be resistant to treatment and is progressive. Systemic steroids and immunosuppressive agents are used in the presence of significant systemic disease. The mainstay of local management consists in the treatment of the keratoconjunctivitis sicca and xerostomia. We had a patient who responded to steroids followed by chloroquine therapy. Low-dose (2500 rad) radiotherapy may be used to control recalcitrant local disease. Recent studies suggest that the new monoclonal antibodies against lymphocytes may be of use in treating this syndrome.

Sinus Histiocytosis with Massive Lymphadenopathy (Rosai-Dorfman's Disease)

This disease seen in young adults is usually associated with cervical adenopathy and involves the orbit in approximately 10% cases. The serum gammaglobulin levels and erythrocytes sedimentation rates are often elevated. Histopathologically, there are masses of large histiocytes surrounded by lymphocytes and plasma cells. They are frequently divided into lobules by fibrous tissue. Extranodal orbital involvement with Rosai-Dorfman's disease can occur in the orbit and can even progress to blindness. This disorder may be recalcitrant to treatment, requiring steroids and immunosuppressives. The use of radiotherapy for treatment is controversial.

Castleman's Disease

Castleman's disease is another rare atypical and perhaps transitional lymphoproliferative disorder. Morphologically, it has been subdivided into hyalin vascular and plasma cell types on the basis of histology, with some intermediate histologic types. The hyalin vascular type tends more frequently to be localized to the mediastinum. The plasma cell type often involves lymph nodes, may be multicentric, and is often associated with systemic symptoms, autoimmune disease, and a more aggressive course, leading to infections and malignancies such as Kaposi's sarcoma, malignant lymphoma, or epithelial neoplasia. The localized type is treatable by surgical excision, whereas multicentric disease requires combined chemotherapy.

In the orbit this is an extremely rare disorder with a case of localized involvement of the lacrimal gland having been described. A second patient has been reported who presented with left perioptic nerve and bilateral lacrimal involvement as part of a multicentric disorder associated with abnormal serum immunoglobulins. This is another lymphoproliferative disorder, similar to those described that are part of the differential diagnosis of orbital lymphoma but appear to be transitional in character.

Guide to Analysis of Noninfectious Inflammation

Persistent or low-grade orbital inflammatory conditions often proceed to biopsy. It is this group of lesions that constitute many of the diseases included in the differential diagnosis of specific noninfectious orbital inflammatory conditions. The differential diagnosis is aided by imaging that allows for definition of location and associated orbital and periorbital findings. Once a biopsy is obtained, the type and focus of infiltration gives some guidance with regard to categorization of the lesions (Fig. 12-60).

The different types of infiltrate for these inflammatory conditions include lymphocytic, granulomatous, leucocytic, mixed, and xanthogranulomatous as demonstrated by many of the lesions discussed. As to focus, the presence of angiocentric change, desmoplasia, and necrotizing features may point to more specific inflammations that have characteristic pathologic patterns. In addition, the types and focus of reactions may lead to definition of the disorder based on associated systemic or local features of the disease. This paradigm will help in the diagnosis and differential diagnosis of many of the perplexing inflammatory conditions of the orbit.

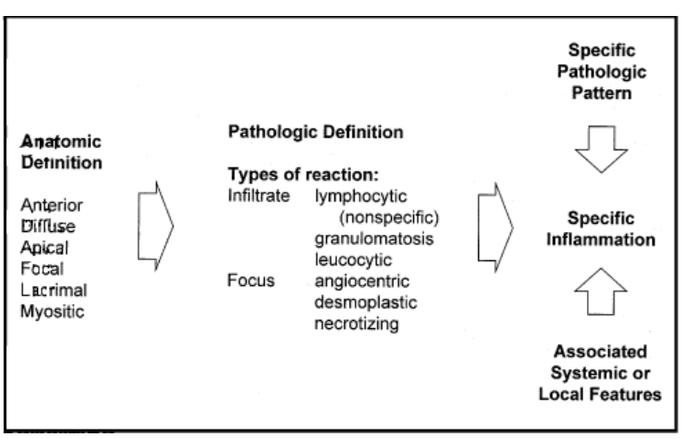

Figure 12-60. Algorithm for analysis of inflammation.

Bibliography

General

Henderson JW. Orbital Tumors. 3rd ed. Philadelphia: Lippincott-Raven, 1994.

White VA, Rootman J. Orbital pathology. In: Albert DM, Jakobiec FA, eds. Principles and Practice of Ophthalmology, vol 4. Philadelphia: WB Saunders, 1994: 2303-59.

Nonspecific Inflammation of the Orbit

General

Chavis RM, Garner A, Wright JE. Inflammatory orbital pseudotumor. A clinicopathologic study. Br J Ophthalmol 1978; 96: 1817-22.

Garner A. Pathology of “pseudotumours” of the orbit: a review. J Clin Pathol 1973; 26: 639-48.

Jakobiec FA, McLean I, Font RL. Clinicopathologic characteristics of orbital lymphoid hyperplasia. Ophthalmology 1979; 86: 948-66.

Kennerdell JS, Dresner SC. The nonspecific orbital inflammatory syndromes. Surv Ophthalmol 1984; 29: 93-103.

Knowles DM 2nd, Jakobiec FA, Halper JP. Immunologic characterization of ocular adnexal lymphoid neoplasms. Am J Ophthalmol 1979; 87: 603-19.

Knowles DM 2nd, Jakobiec FA. Ocular adnexal lymphoid neoplasms: clinical, histopathologic, electron microscopic, and immunologic characteristics. Hum Pathol 1982; 13: 148-62.

Mottow LS, Jakobiec FA. Idiopathic inflammatory orbital pseudotumor in childhood. I. Clinical characteristics. Arch Ophthalmol 1978; 96: 1410-7.

Mottow-Lippa L, Jakobiec FA, Smith M. Idiopathic inflammatory orbital pseudotumor in childhood. II. Results of diagnostic tests and biopsies. Ophthalmology 1981; 88: 565-74.

Nugent RA, Rootman J, Robertson WD, et al. Acute orbital pseudotumors: classification and CT features. AJNR 1981; 2: 431-6.

Myositis

Brenner EH, Shock JP. Proptosis secondary to systemic lupus erythematosus. Arch Ophthalmol 1978; 91: 81-2.

Bullen CL, Younge BR. Chronic orbital myositis. Arch Ophthalmol 1982; 100: 1749-51.

Dunnington JH, Berke RN. Exophthalmos due to chronic orbital myositis. Arch Ophthalmol 1943; 30: 446-66.

Durno CA, Ehrlich R, Taylor R, et al. Keeping an eye on Crohn's disease: orbital myositis as the presenting symptom. Can J Gastroenterol 1997; 11: 497-500.

Grimson BS, Simons KB. Orbital inflammation, myositis, and systemic lupus erythematosus. Arch Ophthalmol 1983; 101: 736-8.

Harris GJ, Murphy ML, Schmidt EW, et al. Orbital myositis as a paraneoplastic syndrome. Arch Ophthalmol 1994; 112: 380-6.

Hemady R, Tauber J, Foster CST. Immunosuppressive drugs in immune and inflammatory ocular disease. Surv Ophthalmol 1991; 35: 369-85.

Jellinek EH. The orbital pseudotumor syndrome and its differentiation from endocrine exophthalmos. Brain 1977; 92: 35-58.

Kennerdell JS. Discussion. Outcome of orbital myositis: clinical features associated with recurrence. Ophthalmology 1997; 104: 414.

Lanciano R, Fowble B, Sergott RC, et al. The results of radiotherapy for orbital pseudotumor. Int J Radiat Oncol Biol Phys 1990; 18: 407-11.

Leib ML, Odel JG, Cooney MJ. Orbital polymyositis and giant cell myocarditis. Ophthalmology 1994; 101: 950-4.

Mannor GE, Rose GE, Moseley IF, Wright JF. Outcome of orbital myositis. Clinical features associated with recurrence. Ophthalmology 1997; 104: 409-13.

Mombaerts I, Koornneef L. Current status in the treatment of orbital myositis. Ophthalmology 1997; 104: 402-8.

Orcutt JC, Garner A, Henk JM, Wright JE. Treatment of idiopathic inflammatory orbital pseudotumors by radiotherapy. Br J Ophthalmol 1983; 67: 570-4.

Purcell JJ Jr, Taulhee WA. Orbital myositis after upper respiratory tract infection. Arch Ophthalmol 1981; 99: 437-8.

Sanchez-Roman J, Varela-Aguilar JM, Bravo-Ferrer J, et al. Idiopathic orbital myositis: treatment with cyclosporin. Ann Rheum Dis 1993; 52: 84-5.

Scott IU, Siatkowski RM. Idiopathic orbital myositis. Curr Opin Rheumatol 1997; 9: 504-12.

Sergott RC, Glaser JS, Charyulu K. Radiotherapy of idiopathic inflammatory orbital pseudotumor. Indications and results. Arch Ophthalmol 1981; 99: 853-6.

Shah SS, Lowder CY, Schmitt MA, et al. Low-dose methotrexate therapy for ocular inflammatory disease. Ophthalmology 1992; 99: 1419-23.

Siatkowski RM, Capo H, Byrne SF, et al. Clinical and echographic findings in idiopathic orbital myositis. Am J Ophthalmol 1994; 118: 343-50.

Slavin ML, Glaser JS. Idiopathic orbital myositis: report of six cases. Arch Ophthalmol 1982; 100: 1261-5.

Stevens AW, Grossman ME, Barr ML. Orbital myositis, vitiligo, and giant cell myocarditis. J Am Acad Dermatol 1996; 35: 310-2.

Trokel SL, Hilal SK. Recognition and differential diagnosis of enlarged extraocular muscles in computed tomography. Am J Ophthalmol 1979; 87: 503-12.

Weinstein GS, Dresner SC, Slamovits TL, Kennerdell JS. Acute and subacute orbital myositis. Am J Ophthalmol 1983; 96: 209-17.

Wolter JR, Hoy JE, Schmidt DM. Chronic orbital myositis. Its diagnostic difficulties and pathology. Am J Ophthalmol 1966; 62: 292-8.

Lacrimal NSOIS

Blodi FC, Gass JDM. Inflammatory pseudotumor of the orbit. Br J Ophthalmol 1968; 52: 79-93.

Blodi FC. Orbital inflammations. Orbit 1982; 1: 1-19.

Coop ME. Pseudotumor of the orbit. A clinical and pathological study of 47 cases. Br J Ophthalmol 1961; 45: 513-42.

Harr DL, Quencer RM, Abrams GW. Computed tomography and ultrasound in the evaluation of orbital infection and pseudotumor. Radiology 1982; 142: 395-401.

Kennerdell JS, Dresner SC. The nonspecific orbital inflammatory syndromes. Surv Ophthalmol 1984; 29: 93-103.

Nugent RA, Rootman J, Robertson WD, et al. Acute orbital pseudotumors: classification and CT features. AJNR 1981; 2: 431-6.

Anterior and Diffise NSOIS

Gunalp I, Gunduz K, Yazar Z. Idiopathic orbital inflammatory disease. Acta Ophthalmol Scand 1996; 74: 191-3.

Kenney AH, Hafner JN. Ultrasonic evidence of inflammatory thickening and fluid collection with the retrobulbar fascia: the T sign. Ann Ophthalmol 1977; 9: 1557-63.

Mombaerts I, Schlingemann RO, Goldschmeding R, Koornneef L. Are systemic corticosteroids useful in the management of orbital pseudotumors? Ophthalmology 1996; 103: 521-8.

Mombaerts I, Goldschmeding R, Schlingemann RO, Koornneef L. What is orbital pseudotumor? Surv Ophthalmol 1996; 41: 66-78.

Mottow LS, Jakobiec FA. Idiopathic inflammatory orbital pseudotumor in childhood. I. Clinical characteristics. Arch Ophthalmol 1978; 96: 1410-7.

Mottow-Lippa L, Jakobiec FA, Smith M. Idiopathic inflammatory orbital pseudotumor in childhood. II. Results of diagnostic tests and biopsies. Ophthalmology 1981; 88: 565-74.

Nugent R, Belkin R, Neigel J, et al. Graves' orbitopathy: correlation of CT and clinical findings. Radiology 1990; 177: 675-82.

Rootman J, Nugent RA. The classification and management of acute orbital pseudotumours. Ophthalmology 1982; 89: 1040-8.

Specific Inflammations of the Orbit

Cellulitis

Ambati BK, Ambati J, Azar N, et al. Periorbital and orbital cellulitis before and after the advent of haemophilus influenzae type B vaccination. Ophthalmology 2000;107:1450-3

Arjmand EM, Lusk RP, Muntz HR. Pediatric sinusitis and subperiosteal orbital abscess formation: diagnosis and treatment. Otolaryngol Head Neck Surg 1993; 109: 886-94.

Bilaniuk LT, Zimmerman RA. Computer-assisted tomography: sinus lesions with orbital involvement. Head Neck Surg 1980; 2: 293.

Brook I. Bacteriologic features of chronic sinusitis in children. JAMA 1981; 246: 967-9.

Brook I, Friedman EM, Rodriguez WJ, Controni G. Complications of sinusitis in children. Pediatrics 1980; 66: 568-72.

Brook I, Frazier EH. Microbiology of subperiosteal orbital abscess and associated maxillary sinusitis. Laryngoscope 1996; 106: 1010-3.

Canadian Medical Association. A practical guide for the diagnosis and treatment of acute sinusitis. CMAJ 1997; 156(6; Suppl): S1-S14.

Catalano RA, Smoot CN. Subperiosteal orbital masses in children with orbital cellulitis: time for a reevaluation? J Pediatr Ophthalmol Strabismus 1990; 27: 141-2.

Chandler JR, Langenbrunner DJ, Stevens ER. The pathogenesis of orbital complications in acute sinusitis. Laryngoscope 1970; 80: 1414-28.

Clairmont AA, Per-Lee JH. Complications of acute frontal sinusitis. Am Fam Physcian 1975; 11: 80-4.

Clary RA, Cunningham MJ, Eavey RD. Orbital complications of acute sinusitis: comparison of computed tomography scan and surgical findings. Ann Otol Rhinol Laryngol 1992; 101: 598-600.

Clunc JP. Septic thrombosis within the cavernous chamber. Am J Ophthalmol 1963; 56: 33-9.

Donahue SP, Schwartz G. Preseptal and orbital cellulitis in childhood: a changing microbiologic spectrum. Ophthalmology 1998; 105:1902-6.

El Shewy TM. Acute infarction of the choroid and retina. A complication of orbital cellulitis. Br J Ophthalmol 1973; 57: 204-5.

el-Toukhy E, Szal M, Levine MR, Levine HL. Osteomyelitis of the orbit. Ophthalmic Plastic and Reconstructive Surgery 1997; 13: 68-71.

Fleisher G, Ludwig S, Campos J. Cellulitis: bacterial etiology, clinical features, and laboratory findings. J Pediatr 1980; 97.

Garcia GH, Harris GJ. Criteria for nonsurgical management of subperiosteal abscess of the orbit: analysis of outcomes 1988-1998. Ophthalmology 2000;107:1454-8

Gellady AM, Shulman ST, Ayoub EM. Periorbital and orbital cellulitis in children. Pediatrics 1978; 61: 272-7.

Goodwin WJ Jr, Weinshall M, Chandler JR. The role of high resolution computerized tomography and standardized ultrasound in the evaluation of orbital cellulitis. Laryngoscope 1982; 92: 729-31.

Hamory BH, Sande MA, Sydnor A, Jr, et al. Etiology and antimicrobial therapy of acute maxillary sinusitis. J Infect Dis 1979; 139: 197-202.

Handler LC, Davey IC, Hill JC, Lauryssen C. The acute orbit: differentiation of orbital cellulitis from subperiosteal abscess by computerized tomography. Neuroradiology 1991; 33: 15-8.

Harris GJ. Subperiosteal abscess of the orbit. Arch Ophthalmol 1983; 101: 751-7.

Harris GJ. Age as a factor in the bacteriology and response to treatment of subperiosteal abscess of the orbit. Trans Am Ophth Soc 1993; 91: 441-516.

Harris GJ. Subperiosteal abscess of the orbit. Age as a factor in the bacteriology and response to treatment. Ophthalmology 1994; 101: 585-95.

Harris GJ. Subperiosteal abscess of the orbit: computed tomography and the clinical course. Ophthalmic Plastic and Reconstructive Surgery 1996; 12: 1-8.

Lerman SJ, Brunken JM, Bollinger M. Prevalence of ampicillin resistant strains of Haemophilus influenzae causing systemic infection. Antimicrob Agents Chemother 1980; 18: 474-5.

Leo JS, Halpern J, Sachler JRL. Computed tomography in the evaluation of orbital infections. Comput Tomogr 1980; 4: 133-8.

Lew D, Southwick FS, Montgomery WW, et al. Sphenoid sinusitis. A review of 30 cases. N Engl J Med 1983; 309: 1149-54.

Mann W, Amedee RG, Maurer J. Orbital complications of pediatric sinusitis: treatment of periorbital abscess. Am J Rhinol 1997; 11: 149-53.

Morgan PR, Morrison WV. Complications of frontal and ethmoid sinusitis. Laryngoscope 1980; 90: 661-6.

Mortimore S, Wormald PJ. The Groote Schuur hospital classification of the orbital complications of sinusitis. J Laryngol Otol 1997; 111: 719-23.

Noel LP, Clarke WN, Peacocke TA. Periorbital and orbital cellulitis in childhood. Can J Ophthalmol 1981; 16: 178-80.

Noel LP, Clarke WN, MacDonald N. Clinical management of orbital cellulitis in children. Can J Ophthalmol 1990; 25: 11-6.

Page EL, Wiatrak BJ. Endoscopic vs external drainage of orbital subperiosteal abscess. Arch Otolaryngol Head Neck Surg 1996; 122: 737-40.

Patt BS, Manning SC. Blindness resulting from orbital complications of sinusitis. Otolaryngol Head Neck Surg 1991; 104: 789-95.

Pereira KD, Mitchell RB, Younis RT, Lazar RH. Management of medial subperiosteal abscess of the orbit in children–a 5 year experience. Int J Pediatr Ophthalmol 1997; 38: 247-54.

Schramm VL, Jr, Curtin HD, Kennerdell JS. Evaluation of orbital cellulitis and results of treatment. Laryngoscope 1982; 92: 732-8.

Schwartz GR, Wright SW. Changing bacteriology of periorbital cellulitis. Ann Emerg Med 1996; 28: 617-20.

Shapiro ED, Wald ER, Brozanski BA. Periorbital cellulitis and paranasal sinusitis: a reappraisal. Pediatr Infect Dis 1982; 1: 91-4.

Singh B. The management of sinogenic orbital complications. J Laryngol Otol 1995; 109: 300-3.

Tarazi AE, Shikani AH. Irreversible unilateral visual loss due to acute sinusitis. Arch Otolaryngol Head Neck Surg 1991; 117: 1400-1.

Wald ER, Milmoe GJ, Bowen A, et al. Acute maxillary sinusitis in children. N Engl J Med 1981; 304: 749-54.

Weiss A, Friendly D, Eglin K, et al. Bacterial periorbital and orbital cellulitis in childhood. Ophthalmology 1983; 90: 195-203.

Williams SR, Carruth JA. Orbital infection secondary to sinusitis in children: diagnosis and management. Clin Otolaryngol 1992; 17: 550-7.

Yarington CT, Jr. Cavernous sinus thrombosis revisited. Proc R Soc Med 1977; 70: 456-9.

Zalzal GH. Periorbital hematoma secondary to sinusitis in a child. Arch Otolaryngol Head Neck Surg 1991; 117: 557-9.

Zimmerman RA, Bilaniuk LT. CT of orbital infection and its cerebral complications. Am J Roentgenol 1980; 134: 45-50.

Other Sources of Cellulitis

Campolattaro BN, Lueder GT, Tychsen L. Spectrum of pediatric dacryocystitis: medical and surgical management of 54 cases. J Pediatr Ophthalmol Strabismus 1997; 34: 143-53.

Frederick J, Braude AI. Anaerobic infections of the paranasal sinuses. N Engl J Med 1974; 290: 135-7.

Ingraham HJ, Ryan ME, Burns JT, et al. Streptococcal preseptal cellulitis complicated by the toxic Streptococcus syndrome. Ophthalmology 1995; 102: 1223-6.

Meyer MA. Streptococcal toxic shock syndrome complicating preseptal cellulitis. Am J Ophthalmol 1997; 123: 841-3.

Shayegani A, MacFarlane D, Kazim M, Grossman ME. Streptococcal gangrene of the eyelids and orbit. Am J Ophthalmol 1995; 120: 784-92.

Mucormycosis

Bodenstein NP, McIntosh WA, Vlantis AC, Urquhart AC. Clinical signs of orbital ischemia in rhino-orbitocerebral mucormycosis. Laryngoscope 1993; 103: 1357-61.

Ferry AP. Cerebral mucormycosis (phycomycosis). Ocular findings and review of the literature. Surv Ophthalmol 1961; 6: 1-24.

Ferry AP, Abedi S. Diagnosis and management of rhino-orbitocerebral mucormycosis (phycomycosis). A report of 16 personally observed cases. Ophthalmology 1983; 90: 1096-104.

Gass JDM. Ocular manifestations of acute mucormycosis. Arch Ophthalmol 1961; 65: 226-37.

Kohn R, Hepler R. Management of limited rhino-orbital mucormycosis without exenteration. Ophthalmology 1985; 92: 1440-4.

Langford JD, McCartney DL, Wang RC. Frozen section-guided surgical debridement for management of rhino-orbital mucormycosis. Am J Ophthalmol 1997; 124: 265-7.

Nussbaum ES, Hall WA. Rhinocerebral mucormycosis: changing patterns of disease. Surg Neurol 1994; 41: 152-6.

O'Brien TJ, McKelvie P. Rhinocerebral mucormycosis presenting as periorbital cellulitis with blindness: report of 2 cases. Clin Experiment Neurol 1994; 31: 68-78.

Pagano L, Ricci P, Tonso A, et al. Mucormycosis in patients with haematological malignancies: a retrospective clinical study of 37 cases. GIMEMA Infection Program (Gruppo Italiano Malattie Ematologiche Maligne dell'Adulto). Br J Haematol 1997; 99: 331-6.

Press GA, Weindling SM, Hesselink JR, et al. Rhinocerebral mucormycosis: MR manifestations. J Comp Assist Tomogr 1988; 12: 744-9.

Straatsma BR, Zimmerman LE, Gass JDM. Phycomycosis. A clinicopathologic study of fifty-one cases. Lab Invest 1962; 11: 963-85.

Yohai RA, Bullock JD, Aziz AA, Markert RJ. Survival factors in rhino-orbital-cerebral mucormycosis. Surv Ophthalmol 1994; 39: 3-22.

Aspergillosis

Cahill KV, Hogan CD, Koletar SL, Gersman M. Intraorbital injection of amphotericin B for palliative treatment of Aspergillus orbital abscess. Ophthal Plast Reconstr Surg 1994; 10: 276-7.

Chandra P, Ahluwalia BK, Chugh TD. Primary orbital aspergilloma. Br J Ophthalmol 1970; 54: 693-6.

Crivelli G, Riviera L. Unilateral blindness from aspergilloma at the right optic foramen. J Neurosurg 1970; 33: 207-11.

Fisher EW, Toma A, Fisher PH, Cheesman AD. Rhinocerebral mucormycosis: use of liposomal amphotericin B. J Laryngol Otol 1991; 105: 575-7.

Fraser DW, Ward JI, Ajello L, Plikaytis BD. Aspergillosis and other systemic mycoses. The growing problem. JAMA 1979; 242: 1631-5.

Green WR, Font RL, Zimmerman LE. Aspergillosis of the orbit. Report of ten cases and review of the literature. Arch Ophthalmol 1969; 82: 302-13.

Harris GJ, Will BR. Orbital aspergillosis. Conservative debridement and local amphotericin irrigation. Ophthal Plast Reconstr Surg 1989; 5: 207-11.

Johnson R, Rootman J. Bilateral retinal infarction in disseminated aspergillosis. Can J Ophthalmol 1982; 17: 233-6.

Levin LA, Avery R, Shore JW, et al. The spectrum of orbital aspergillosis: a clinicopathological review. Surv Ophthalmol 1996; 41: 142-54.

Oneson RH, Feldman PS, Newman SA. Aspiration cytology and immunohistochemistry of an orbital aspergilloma. Diagn Cytopathol 1988; 4: 59-61.

Wolter JR. Diagnosis and management of orbital aspergillosis. Ann Ophthalmol 1976; 8: 17-20.

Young RC, Bennett JE, Vogel CL, et al. Aspergillosis. The spectrum of the disease in 98 patients. Medicine 1970; 49: 147-73.

Other Mycotic Infections

Ajayi BG, Osuntokun B, Olurin O, et al. Orbital histoplasmosis due to Histoplasma capsulatum var. duboisii: successful treatment with Septrin. J Trop Med Hyg 1986; 89: 179-87.

Klapper SR, Lee AG, Patrinely JR, et al. Orbital involvement in allergic fungal sinusitis. Ophthalmology 1997; 104: 2094-100.

Maskin SL, Fetchick RJ, Leone CR, Jr, et al. Bipolaris hawaiiensis-caused phaeohyphomycotic orbitopathy. A devastating fungal sinusitis in an apparently immunocompetent host. Ophthalmology 1989; 96: 175-9.

Streeten BW, Rabuzzi DD, Jones D. Sporotrichosis of the orbital margin. Am J Ophthalmol 1974; 77: 750-5.

Vida L, Moel SA. Systemic North American blastomycosis with orbital involvement. Am J Ophthalmol 1974; 77: 240-2.

Tuberculosis of the Orbit

Baghdassarian SA, Zakharia H, Asdourian KK. Report of a case of bilateral caseous tuberculous dacryoadenitis. Am J Ophthalmol 1972; 74: 744-6.

D'Souza P, Garg R, Dhaliwal RS, et al. Orbital-tuberculosis. Int Ophthalmol 1994; 18: 149-52.

Jain MR, Chundawat HS, Batra V. Tuberculosis of the maxillary antrum and of the orbit. Indian J Ophthalmol 1979; 27: 18-20.

Khalil M, Lindley S, Matouk E. Tubercolosis of the orbit. Ophthalmology 1985; 92: 1624-7.

Oakhill A, Shah KJ, Thompson AG, et al. Orbital tuberculosis in childhood. Br J Ophthalmol 1982; 66: 396-7.

Pillai S, Malone TJ, Abad JC. Orbital tuberculosis. Ophthal Plast Reconstr Surg 1995; 11: 27-31.

Sheridan PH, Edman JB, Starr SE. Tuberculosis presenting as an orbital mass. Pediatrics 1981; 67: 874-5.

Spoor TC, Harding SA. Orbital tuberculosis. Am J Ophthalmol 1981; 91: 644-7.

Echinococcosis (Hydatid Cyst)

Ergun R, Okten AI, Yuksel M, et al. Orbital hydatid cysts: report of four cases. Neurosurg Rev 1997; 20: 33-7.

Gelisken F, Erda S, Kreissig I. Exsudative netshautablosung bei intraorbitaler Echinokokkuszyste. Klin Monatsbl Augenheilkunde 1994; 205: 109-11.

Gil-Grande LA, Rodriguez-Caabeiro F, Prieto JG, et al. Ramdomised controlled trial of efficacy of albendazole in intra-abdominal hydatid disease. Lancet 1993; 342: 1269-72.

Gomez Morales A, Croxatto JO, Crovetto L, Ebner R. Hydatid cysts of the orbit. A review of 35 cases. Ophthalmology 1988; 95: 1027-32.

Ozek MM, Pamir MN, Sav A. Spontaneous rupture of an intraorbital hydatid cyst. A rare cause of acute visual loss. J Clin Neuro Ophthalmol 1993; 13: 135-7.

Richards KS, Morris DL. Effect of albendazole on human hydatid cysts: an ultrastructural study. HPB Surg 1990; 2: 105-13.

Saenz-Santamaria J, Moreno-Casado J, Nunez C. Role of fine-needle biopsy in the diagnosis of hydatid cyst. Diagn Cytopathol 1995; 13: 229-32.

Sami A, Achouri M, Harouch M, et al. Kystes hydatiques intra-orbitaires. 10 cas. Neuro-Chirurgie 1995; 41: 398-402.

Schipper HG, Kager PA. Diagnostiek en behandeling van cysteuze echinokokkose (infectie met Echinococcus granulosus). Nederlands Tijdschrift voor Geneeskunde 1997; 141: 984-9.

Sperryn CW, Corr PD. CT evaluation of orbital hydatid disease: a review of 10 cases. Clin Radiol 1994; 49: 703-4.

Cysticercosis

Arora VK, Gupta K, Singh N, Bhatia A. Cytomorphologic panorama of cysticercosis on fine needle aspiration. A review of 298 cases. Acta Cytol 1994; 38: 377-80.

Atul K, Kumar TH, Mallika G, Sandip M. Socio-demographic trends in ocular cysticercosis. Acta Ophthalmol Scand 1995; 73: 438-41.

Bansal RK, Gupta A, Grewal SP, Mohan K. Spontaneous extrusion of cysticercosis: report of three cases. Indian J Ophthalmol 1992; 40:59-60.

DiLoreto DA, Kennedy RA, Neigel JM, Rootman J. Infestation of extraocular muscles by Cysticercus cellulosae. Br J Ophthalmol 1990; 74: 751-2.

Kapila K, Verma K. Diagnosis of parasites in fine needle breast aspirates. Acta Cytol 1996; 40: 653-5.

Sekhar GC, Lemke BN. Orbital cysticercosis. Ophthalmology 1997; 104: 1599-604.

Srivastava VK, Srivastava A, Singhal KC. Albendazole therapy in orbital cysticercosis. Ind J Physiol Pharmacol 1996; 40: 265-6.

Trichinosis

Behrens-Baumann W, Freissler G. Retinochorioidiopathie bei einem Patienten mit seropositiver Trichinose. Klin Monatsbl Augenheilkunde 1991; 199: 114-7.

Other Infestations

Agarwal DC, Singh B. Orbital myiasis - a case report. Indian J Ophthalmol 1990; 38: 187-8.

Grammer J, Erb C, Kamin G, et al. Ophthalmomyiasis externa due to the sheep botfly Oestrus ovis (Diptera: Oestridae) in southwest Germany. Ger J Ophthalmol 1995; 4: 188-95.

Mariotti JM, Vacheret G. Les myiases conjonctivales, une pathologie frequente en Corse. J Fr Ophthalmol 1992; 15: 679-82.

Wolfelschneider P, Wiedemann P. Ophthalmomyiasis externa durch Oestrus ovis (Schafs- und Ziegenbremse). Klin Monatsbl Augenheilkunde 1996; 209: 256-8.

Other Specific Inflammations of the Orbit

Wegener's Granulomatosis

Austin P, Green WR, Sallyer DC, et al. Peripheral comeal degeneration and occlusive vasculitis in Wegener's granulomatosis. Am J Ophthalmol 1978; 85: 311-7.

Belden CJ, Hamed LM, Mancuso AA. Bilateral isolated retrobulbar optic neuropathy in limited Wegener's granulomatosis. J Clin Neuro Ophthalmol 1993; 13: 119-23.

Bullen CL, Liesegang TJ, McDonald TJ, DeRemee RA. Ocular complications of Wegener's granulomatosis. Ophthalmology 1983; 90: 279-90.

Carrington CB, Liebow A. Limited forms of angiitis and granulomatosis of Wegener's type. Am J Med 1966; 41: 497-527.

Cassan SM, Divertie MB, Hollenhorst RW, Harrison EG Jr. Pseudotumor of the orbit and limited Wegener's granulomatosis. Ann Intern Med 1970; 72: 687-93.

Cassan SM, Coles DT, Harrison EG, Jr. The concept of limited forms of Wegener's granulomatosis. Am J Med 1970; 49: 366-79.

Courcoutsakis NA, Langford CA, Sneller MC, et al. Orbital involvement in Wegener granulomatosis: MR findings in 12 patients. J Comp Assist Tomogr 1997; 21: 452-8.

Coutu RE, Klein M, Lessell S, et al. Limited form of Wegener's granulomatosis. Eye involvement as a major sign. JAMA 1975; 233: 868-71.

Fahey JL, Leonard E, Churg J, Godman GC. Wegener's granulomatosis. Am J Med 1954; 17: 168-79.

Fauci AS, Haynes B, Katz P. The spectrum of vasculitis: clinical, pathologic, immunologic, and therapeutic considerations. Ann Intern Med 1978; 89: 660-76.

Fauci AS, Haynes BF, Katz P, Wolff SM. Wegener's granulomatosis: prospective and therapeutic experience with 85 patients for 21 years. Ann Intern Med 1983; 98: 76-85.

Faulds JS, Wear AR. Pseudotumor of the orbit and Wegener's granuloma. Lancet 1960; 2: 955-7.

Harcourt RB. Orbital granulomata associated with widespread angiitis. Br J Ophthalmol 1964; 48: 673-7.

Haynes BF, Fishman MI, Fauci AS, Wolff SM. The ocular manifestations of Wegener's granulomatosis. Fifteen years experience and review of the literature. Am J Med 1977; 63: 131-41.

Hoekstra JA, Fauci AS. The granulomatous vasculitides. Clin Rheum Dis 1980; 6: 373.

Kalina PH, Lie JT, Campbell RJ, Garrity JA. Diagnostic value and limitations of orbital biopsy in Wegener's granulomatosis. Ophthalmology 1992; 99: 120-4.

Muhle C, Reinhold-Keller E, Richter C, et al. MRI of the nasal cavity, the paranasal sinuses and orbits in Wegener's granulomatosis. Eur Radiol 1997; 7: 566-70.

Nolle B, Coners H, Duncker G. ANCA in ocular inflammatory disorders. Adv Exp Med Biol 1993; 336: 305-7.

Novack SN, Pearson CM. Cyclophosphamide therapy in Wegener's granulomatosis. N Engl J Med 1971; 284: 938-42.

Perry SR, Rootman J, White VA. The clinical and pathologic constellation of Wegener's granulomatosis of the orbit. Ophthalmology 1997; 104: 683-94.

Piercey S, Montanaro A. Recurrent Wegener's granulomatosis: a case report and review. Ann Allergy Asthma Immunol 1996; 76: 317-20.

Provenzale JM, Mukherji S, Allen NB, et al. Orbital involvement by Wegener's granulomatosis: imaging findings. Am J Roentgenol 1996; 166: 929-34.

Provenzale JM, Allen NB. Wegener granulomatosis: CT and MR findings. AJNR 1996; 17: 785-92.

Robin JB, Schanzlin DJ, Meisler DM, et al. Ocular involvement in the respiratory vasculitides. Surv Ophthalmol 1985; 30: 127-40.

Spalton DJ, Graham EM, Page NGR, Sanders MD. Ocular changes in limited forms of Wegener's granulomatosis. Br J Ophthalmol 1981; 65: 553-63.

Tullo AB, Durrington P, Graham E, et al. Florid xanthelasmata (yellow lids) in orbital Wegener's granulomatosis. Br J Ophthalmol 1995; 79: 453-6.

Weiter J, Farkas TG. Pseudotumor of the orbit as a presenting sign in Wegener's granulomatosis. Surv Ophthalmol 1972; 17: 106-19.

Wolff SM, Fauci AS, Horn RG, Dale PC. Wegener's granulomatosis. Ann Intern Med 1974; 81: 513-25.

Other Respiratory Syndromes

Chumbley LC, Harrison EG, Jr, DeRemee RA. Allergic granulomatosis and angiitis (Churg-Strauss syndrome). Report and analysis of 30 cases. Mayo Clin Proc 1977; 52: 477-84.

Churg J, Strauss L. Allergic granulomatosis, allergic angiitis, and periarteritis nodosa. Am J Pathol 1951; 27: 277-301.

Churg J. Allergic granulomatous and granulomatous-vascular syndromes. Ann Allergy 1963; 21: 619.

Cury D, Breakey AS, Payne BF. Allergic granulomatous angiitis associated with uveoscleritis and papilledema. Arch Ophthalmol 1956; 55: 261-6.

Hardy WR, Anderson RE. The hypereosinophilic syndromes. Ann Intern Med 1968; 68: 1220-9.

Heine A, Beck R, Stropahl G, et al. Entzundlicher pseudotumor der anterioren orbita. Ein symptom bei einer allergisch-granulomatosen angiits Churg-Strauss-Syndrome). Ophthalmologe 1995; 92: 870-3.

Khan NA, Shenoy PK, McClymont L, Palmer TJ. Exophthalmos and facial swelling: a case of limited Churg-Strauss syndrome. J Laryngol Otol 1996; 110: 578-82.

Lanham JG, Elkon KB, Pusey CD, Hughes GR. Systemic vasculitis with asthma and eosinophilia: a clinical approach to the Churg-Strauss syndrome. Medicine 1984; 63: 65-81.

Meisler DM, Stock EL, Wertz RD, et al. Conjunctival inflammation and amyloidosis in allergic granulomatosis and angiitis (Churg-Strauss syndrome). Am J Ophthalmol 1981; 91: 216-9.

Nissim F, Von der Valde J, Czernobilsky B. A limited form of Churg-Strauss syndrome: ocular and cutaneous manifestations. Arch Path Lab Med 1982; 106: 305-7.

Polyarteritis Nodosa

Astrom K, Lidholm S. Extensive intracranial lesions in a case of orbital nonspecific granuloma combined with polyarteritis nodosa. J Clin Pathol 1963; 16: 137.

Boeck J. Ocular changes in periarteritis nodosa. Am J Ophthalmol 1956; 42: 567-77.

Calabrese LH, Hoffman GS, Clough JD. Systemic vasculitis. In: Young JR, Olin JW, Bartholemew JR, eds. Peripheral Vascular Diseases. St. Louis: Mosby, 1996; 382-5.

Cogan DG. Corneoscleral lesions in periarteritis nodosa and Wegener's granulomatosis. Trans Am Ophth Soc 1955; 53: 321-44.

Goar EL, Smith LS. Polyarteritis nodosa of the eye. Am J Ophthalmol 1952; 35: 1619-25.

Ingalls RG. Bilateral uveitis and keratitis accompanying periarteritis nodosa. Trans Am Acad Ophthalmol Otolaryngol 1951; 55: 630-1.

Kielar RA. Exudative retinal detachment and scieritis in polyarteritis. Am J Ophthalmol 1976; 82: 694-8.

Koike R, Yamada M, Matsunaga T, et al. Polyarteritis nodosa (PN) complicated with unilateral exophthalmos. Intern Med 1993; 32: 232-6.

Robinowitz M. Histopathologic features of nonarteriosclerotic diseases of the aorta and arteries. In: Sidaway AN, Sumpio BE, DePalma RG, eds. The Basic Science of Vascular Disease. Armonk, NY: Futura Publishing, 1997: 357-60.

van Wien S, Merz EH. Exophthalmos secondary to polyarteritis nodosa. Am J Ophthalmol 1963; 56: 204-7.

Walton EW. Pseudotumor of the orbit and polyarteritis nodosa. J Clin Pathol 1959; 12: 410-26.

Zeek PM. Medical progress: periarteritis nodosa and other forms of necrotizing angiitis. N Engl J Med 1953; 248: 764-72.

Zeek PM. Periarteritis nodosa: a critical review. Am J Clin Pathol 1952; 22: 777-90.

Hypersensitivity (Leucocytoclastic) Angiitis

Bohndorf M, Baykal HE, Plinkert PK, et al. Audiovestibulare, ophthalmologische Befunde und Therapie bei 6 Patientinnen. HNO 1996; 44: 302-6.

Brenner EH, Shock JP. Proptosis secondary to systemic lupus erythematosus. Arch Ophthalmol 1978; 91: 81-2.

Cogan DG. Syndrome of nonsyphilitic interstitial keratitis and vestibuloauditory symptoms. Arch Ophthalmol 1945; 33: 144-9.

Cogan DG. Nonsymphilitic interstitial keratitis with vestibuloauditory symptoms. Report of four additional cases. Arch Ophthalmol 1949; 42: 42-9.

Cogan DG, Dickersin GR. Nonsymphilitic interstitial keratitis with vestibulo-auditory symptoms. A case with fatal aortitis. Arch Ophthalmol 1964; 71: 172-5.

Dicken CH. Periorbital edema: an important physical finding in dermatomyositis. Cutis 1991; 48: 116-7.

Fisher ER, Hellstrom HR. Cogan's syndrome and systemic vascular disease. Analysis of pathologic features with reference to its relationship to thromboangiitis obliterans (Buerger). Arch Ophthalmol 1961; 72: 572-92.

Garrity JA, Kennerdell JS, Johnson BL, Ellis LD. Cyclophosphamide in the treatment of orbital vasculitis. Am J Ophthalmol 1986; 102: 97-103.

Ghanchi FD, Williamson TH, Lim CS, et al. Colour Doppler imaging in giant cell (temporal) arteritis: serial examination and comparison with non-arteritic anterior ischaemic optic neuropathy. Eye 1996; 10: 459-64.

Gold DH, Morris DA. Ocular findings in systemic lupus erythematosus. Br J Ophthalmol 1972; 56: 800-4.

Haynes BF, Kaiser-Kupfer MI, Mason P, Fauci AS. Cogan's syndrome: studies in thirteen patients, long-term follow-up, and a review of the literature. Medicine 1980; 59: 426-41.

Haynes BF, Pikus A, Kaiser-Kupfer M, Fauci AS. Successful treatment of sudden hearing loss in Cogan's syndrome with corticosteroids. Arthritis Rheum 1981; 24: 501-3.

Henderson JW. Orbital Tumors. 3rd ed. Philadelphia: Lippincott-Raven, 1994.

Jordan DR, McDonald H, Olberg B, et al. Orbital panniculitis as the initial manifestation of systemic lupus erythematosus. Ophthal Plast Reconstr Surg 1993; 9: 71-5.

McNeil NF, Berke M, Reingold IM. Polyarteritis nodosa causing deafness in an adult. Report of a case with special reference to concepts about the disease. Ann Intern Med 1952; 37: 1253.

Nassani S, Cocito L, Arcuri T, Favale E. Orbital pseudotumor as a presenting sign of temporal arteritis. Clin Exp Rheum 1995; 13: 367-9.

Norton EWD, Cogan DG. Syndrome of nonsyphilitic interstitial keratitis and vestibuloauditory symptoms. A long-term follow-up. Arch Ophthalmol 1959; 61: 695-7.

Oliner L, Taubenhaus M, Shapira TM, Leshin N. Nonsymphilitic interstitial keratitis and bilateral deafness (Cogan's syndrome) associated with essential polyangitis (periarteritis nodosa). A review of the syndrome with consideration of a possible pathogenic mechanism. N Engl J Med 1953; 248: 1001-8.

Peitersen E, Carlsen BH. Hearing impairment as the initial sign of polyarteritis nodosa. Acta Otolaryngol 1966; 61: 189-95.

Serop S, Vianna RN, Claeys M, De Laey JJ. Orbital myositis secondary to systemic lupus erythematosus. Acta Ophthalmol 1994; 72: 520-3.

Wilkinson LS, Panush RS. Exophthalmos associated with systemic lupus erythematosus. Arthritis Rheum 1975; 18: 188-9.

Sclerosing Inflammation of the Orbit

Aylward GW, Sullivan TJ, Garner A, et al. Orbital involvement in multifocal fibrosclerosis. Br J Ophthalmol 1995; 79: 246-9.

Cervellini P, Volpin L, Curri D, et al. Sclerosing orbital pseudotumor. Ophthalmologica 1986; 193: 39-44.

Kennerdell JS. The management of sclerosing nonspecific orbital inflammation. Ophthalmic Surg 1991; 22: 512-8.

Levey JM, Mathai J. Diffuse pancreatic fibrosis: an uncommon feature of multifocal idiopathic fibrosclerosis. Am J Gastroenterol 1998; 93: 640-2.

Levine MR, Kaye L, Mair S, Bates J. Multifocal fibrosclerosis. Report of a case of bilateral idiopathic sclerosing pseudotumor and retroperitoneal fibrosis. Arch Ophthalmol 1993; 111: 841-3.

Manassero A, Cracco C, Terrone C, Rossetti SR. Coexistence of orbital and retroperitoneal involvement in multifocal fobrosclerosis: case report. Archivo Italiano di Urologia, Andrologia 1998; 70: 11-4.

McCarthy JM, White VA, Harris G, et al. Idiopathic sclerosing inflammation of the orbit: immunohistologic analysis and comparison with retroperitoneal fibrosis. Mod Pathol 1993; 6: 581-7.

Richards AB, Shalka HW, Roberts FJ, Flint A. Pseudotumor of the orbit and retroperitoneal fibrosis. A form of multifocal fibrosclerosis. Arch Ophthalmol 1980; 98: 1617-20.

Rootman J, McCarthy J, White V, et al. Idiopathic sclerosing inflammation of the orbit: a distinct clinicopathologic entitity. Ophthalmology 1994; 101: 570-84.

Schonder AA, Clift RC, Brophy JW, Dane LW. Bilateral recurrent orbital inflammation associated with retroperitoneal fibrosclerosis. Br J Ophthalmol 1985; 69: 783-7.

Van Hoe L, Oyen R, Gryspeerdt S, et al. Case report: pseudotumoral pelvic retroperitoneal fibrosis associated with orbital fibrosis. Br J Radiol 1995; 68: 421-3.

Granulomatous Inflammation of the Orbit

Mombaerts I, Schlingemann RO, Goldschmeding R, Koornneef L. Idiopathic granulomatous orbital inflammation. Ophthalmology 1996; 103: 2135-41.

Satorre J, Antle CM, O'Sullivan R, et al. Orbital lesions with granulomatous inflammation. Can J Ophthalmol 1991; 26: 174-95.

Foreign Body Granuloma

Abramson DH, Andracchi S. Orbital avitene granuloma formation after enucleation for intraocular retinoblastoma. Am J Ophthalmol 1997; 123: 567-9.

Feldmann R, Harms M, Chavaz P, et al. Orbital and palpebral paraffinoma. J Am Acad Dermatol 1992; 26: 833-5.

Hintschich CR, Beyer-Machule CK, Stefani FH. Paraffinoma of the periorbit - a challenge for the oculoplastic surgeon. Ophthal Plast Reconstr Surg 1995; 11: 39-43.

Katz SE, Rootman J. Adverse effects of bone wax in surgery of the orbit. Ophthal Plast Reconstr Surg 1996; 12: 121-6.

Witschel H, Geiger K. Paraffin induced sclerosing lipogranuloma of eyelids and anterior orbit following endonasal sinus surgery. Br J Ophthalmol 1994; 78: 61-5.

Sarcoid and Sarcoidosis

Bronson LJ, Fisher YL. Sarcoidosis of the paranasal sinuses with orbital extension. Arch Ophthalmol 1976; 94: 243-4.

Cook JR, Brubaker RF, Savell J, Sheagren J. Lacrimal sarcoidosis treated with corticosteroids. Arch Ophthalmol 1972; 88: 513-7.

Crick RP, Hoyle C, Smellie H. The eyes in sarcoidosis. Br J Ophthalmol 1961; 45: 461-81.

Crystal GG, Roberts RC, Hunninghake GW, et al. Pulmonary sarcoidosis: a disease characterized and perpetuated by activated lung T lymphocytes. Ann Intern Med 1981; 94: 73-94.

Daniele RP. Sarcoidosis: diagnosis and management. Hosp Pract 1983; 18: 113-5.

Fanburg BL. Sarcoidosis and Other Granulomatous Diseases of the Lung. New York: Marcel Dekker, 1983.

Fisher OE, Burton GG, Bryan WE. Sarcoidosis involving the lacrimal sac. Am Rev Respir Dis 1971; 103: 708-10.

James DG. The diagnosis and treatment of ocular sarcoidosis. Acta Med Scand Suppl 1964; 425: 203-8.

James DG, Neville E, Langley DA. Ocular sarcoidosis. Trans Ophthalmol Soc UK 1976; 96: 133-9.

Jensen VJ. Sarcoidosis of the orbit. Acta Ophthalmol [Kbh] 1957; 35: 416-9.

Kao SCS, Rootman J. Unusual ophthalmic presentations of dural sheath sarcoid: report of two cases. Can J Ophthalmol 1996; 31: 195-200.

Karma A. Diagnosing sarcoidosis by transconjunctival biopsy of the lacrimal gland. Am J Ophthalmol 1984; 98: 640-2.

Karma A, Poukkula A, Ruokonen A. Gallium^{67} citrate scanning in patients with lacrimal gland and conjunctival sarcoidosis. A report on three cases. Acta Ophthalmol 1984; 62: 549-55.

Katz P, Fauci AS, Yeager H Jr, Reen BM. Serum angiotensin-converting enzyme and lysozyme in granulomatous diseases of unknown cause. Ann Intern Med 1981; 94: 359-60.

Khan F, Wessely Z, Chazin SR, Seriff NS. Conjunctival biopsy in sarcoidosis: a simple, safe, and specific diagnostic procedure. Ann Ophthalmol 1977; 9: 671-6.

Lauver JW, Gooneratne NS. Lacrimal, parotid and mediastinal uptake of gallium 67 in sarcoidosis. Br J Radiol 1976; 52: 582-4.

Mayock RL, Bertrand P, Morrison CE. Manifestations of sarcoidosis. Analysis of 145 patients, with a review of nine series selected from the literature. Am J Med 1963; 35: 67-89.

Melmon KL, Goldberg JS. Sarcoidosis with bilateral exophthalmos as the initial symptom. Am J Med 1962; 33: 158-60.

Moller DR. Systemic sarcoidosis. In: Fishman AP, ed. Pulmonary Diseases and Disorders, vol 1. New York: McGraw-Hill, 1998: 1055-68.

Nessan VJ, Jacoway JR. Biopsy of minor salivary glands in the diagnosis of sarcoidosis. N Engl J Med 1979; 301: 922-4.

Nichols CW, Mishkin M, Yanoff M. Presumed orbital sarcoidosis: report of a case followed by computerized axial tomography and conjunctival biopsy. Trans Am Ophth Soc 1978; 76: 67-75.

Nowinski T, Flanagan J, Ruchman M. Lacrimal gland enlargement in familial sarcoidosis. Ophthalmology 1983; 90: 909-13.

Obenauf CD, Shaw HE, Sydnor CF, Klintworth GK. Sarcoidosis and its ophthalmic manifestations. Am J Ophthalmol 1978; 86: 648-55.

Papo I, Beltrami CA, Salvolini U, Caruselli G. Sarcoidosis simulating a glioma of the optic nerve. Surg Neurol 1977; 8: 353-5.

Satorre J, Antle M, White V, Rootman J. Inflamaciones sarcoideas de la orbita. Archivos de la Sociedad Espanol de Oftalmologia 1991; 60: 609-16.

Sharma OP, Vita JB. Determination of angiotensin-converting enzyme activity in tears. A noninvasive test for evaluation of ocular sarcoidosis. Arch Ophthalmol 1983; 101: 559-61.

Silverstein A, Feuer MM, Siltzbach LE. Neurologic sarcoidosis. Study of 18 cases. Arch Neurol 1965; 12: 1-11.

Thrasher DR, Briggs DD, Jr. Pulmonary sarcoidosis. Clin Chest Med 1982; 3: 537-63.

Weinreb RN, Yavitz EQ, O'Connor GR, Barth RA. Lacrimal gland uptake of gallium citrate Ga 67. Am J Ophthalmol 1981; 92: 216-20.

Wolk RB. Sarcoidosis of the orbit with bone destruction. AJNR 1984; 5: 204-5.

Xanthogranulomatous Disorders of the Orbit

Alper MG, Zimmerman LE, LaPiana FG. Orbital manifestations of Erdheim-Chester disease. Trans Am Ophth Soc 1983; 81: 64-85.

Bullock JD, Bartley GB, Campbell RJ, et al. Necrobiotic xanthogranuloma with paraproteinemia: case report and a pathogenetic theory. Ophthalmology 1986; 93: 1233-6.

Codere F, Lee RD, Anderson RL. Necrobiotic xanthogranuloma of the eyelid. Arch Ophthalmol 1983; 101: 60-3.

Cornblath WT, Dotan SA, Trobe JD, Headington JT. Varied clinical spectrum of necrobiotic xanthogranuloma. Ophthalmology 1992; 99: 103-7.

Floyd BB, Brown B, Isaacs H, Minckler DS. Pseudorheumatoid nodule involving the orbit. Arch Ophthalmol 1982; 100: 1478-80.

Jakobiec FA, Mills MD, Hidayat AA, et al. Periocular xanthogranulomas associated with severe adult-onset asthma. Trans Am Ophth Soc 1993; 91: 99-129.

Kossard S, Winkelmann RK. Necrobiotic xanthogranuloma with paraproteinemia. J Am Acad Dermatol 1980; 3: 257-70.

Macfarlane AW, Verbov JL. Necrobiotic xanthogranuloma with paraproteinaemia. Br J Dermatol 1985; 113: 339-43.

Nasr AM, Johnson T, Hidayat A. Adult onset primary bilateral orbital xanthogranuloma. Orbit 1991; 10: 13-22.

Robertson DM, Winkelmann RK. Ophthalmic features of necrobiotic xanthogranulorna with paraproteinemia. Am J Ophthalmol 1984; 97: 173-83.

Rose GE, Patel BC, Garner A, Wright JE. Orbital xanthogranuloma in adults. Br J Ophthalmol 1991; 75: 680-4.

Ross MJ, Cohen KL, Peiffer RL Jr, Grimson BS. Episcleral and orbital pseudorheumatoid nodules. Arch Ophthalmol 1983; 101: 418-21.

Shields JA, Karcioglu ZA, Shields CL, et al. Orbital and eyelid involvement with Erdheim Chester disease. Arch Ophthalmol 1991; 109: 850-4.

Zimmerman LE. Ocular lesions of juvenile xanthogranuloma: nevoxanthoendothelioma. Trans Am Acad Ophthalmol Otolaryngol 1965; 69: 412-39.

Fibro-osseous Lesions

O'Sullivan RM, Nugent RA, Satorre J, Rootman J. Granulomatous orbital lesions: computed tomographic features. Can Assoc Radiol J 1992; 43: 349-58.

Satorre J, Antle CM, O'Sullivan R, et al. Orbital lesions with granulomatous inflammation. Can J Ophthalmol 1991; 26: 174-95.

Melkersson-Rosenthal Syndrome

Cockerham KP, Hidayat AA, Cockerham GC, et al. Melkersson-Rosenthal syndrome: new clinicopathologic findings in 4 cases. Arch Ophthalmol 2000;118:227-32.

Yeatts RP, White WL. Granulomatous blepharitis as a sign of Melkersson-Rosenthal syndrome. Ophthalmology 1997;104:1185-90.

Kimura's Disease

Archer KF, Hurwitz JJ, Heathcote G. Orbital angiolymphoid hyperplasia with eosinophilia. Presentation as chalazion. Ophthalmic Plastic & Reconstructive Surgery 1991; 7: 208-21.

Buggage RR, Spraul CW, Wojno TH, Grossniklaus HE. Kimura disease of the orbit and ocular adnexa. Surv Ophthalmol 1999;44:79-91.

Cook HY, Stafford ND. Angiolymphoid hyperplasia with eosinophilia involving the lacrimal gland: case report. Br J Ophthalmol 1988; 72: 710-2.

Francis IC, Kappagoda MB, Smith J, Kneale K. Kimura's disease of the orbit. Ophthalmic Plastic & Reconstructive Surgery 1988; 4: 235-9.

Fu KK. Orbital Kimura's disease. J Roy Soc Med 1993; 86: 234-5.

Hareyama M, Oouchi A, Nagakura H, et al. Radiotherapy for Kimura's disease: the optimum dosage. Int J Rad Oncol Biol Phys 1998; 40: 647-51.

Hidayat AA, Cameron JD, Font RL, Zimmerman LE. Angiolymphoid hyperplasia with eosinophilia (Kimura's disease) of the orbit and ocular adnexa. Am J Ophthalmol 1983; 96: 176-89.

Hui PK, Chang JK, Ng CS, et al. Lymphadenopathy of Kimura's disease. Am J Surg Pathol 1989; 13(3): 177-86.

Jayamanne DGR, Webber SK, Ridley REW, et al. Angiolymphoid hyperplasia with eosinophilia (Kimura's disease) of the conjunctiva. Br J Ophthalmol 1995; 79: 1053-4.

Kennedy SM, Pitts JF, Lee WR, Gibbons DC. Bilateral Kimura's disease of the eyelids. Br J Ophthalmol 1992; 76: 755-7.

Kim GE, Kim WC, Yang WI, et al. Radiation treatment in patients with recurrent Kimura's disease. Int J Rad Oncol Biol Phys 1997; 38: 607-12.

Kuo T, Shih L, Chan H. Kimura's disease. Am J Surg Pathol 1988; 12(11): 843.

Moroz I, Rosen N, Rosner M. Bilateral Kimura's disease with devastating visual outcome. Eye 1998; 12: 102-3.

Nomura K, Sasaki C, Murai T, et al. Angiolymphoid hyperplasia with eosinophilia: successful treatment with indomethacin farnesil. Br J Dermatol 1996; 134: 189-90.

Senel MF, Van Buren CT, Etheridge WB, et al. Effects of cyclosporine, azathioprine and prednisone on Kimura's disease and focal segmental glomerulosclerosis in renal transplant patients. Clinical Nephrology 1996; 45: 18-21.

Sheren SB, Custer PH, Smith ME. Angiolymphoid hyperplasia with eosinophilia of the orbit associated with obstructive airway disease. Am J Ophthalmol 1989; 108: 167-9.

Smith DL, Kincaid MC, Nicolitz E. Angiolymphoid hyperplasia with eosinophilia (Kimura's disease) of the orbit. Arch Ophthalmol 1988; 106: 793-5.

Sjogren's Syndrome

Adamson TC 3rd, Fox RI, Frisman, DN, Howell FV. Immunohistologic analysis of lymphoid infiltrates in primary Sjogren's syndrome using monoclonal antibodies. J Immunol 1983; 130: 203-8.

Bloch KJ, Buchanan WW, Wohl MJ, Bunim JJ. Sjogren's syndrome: a clinical, pathological and serological study of 62 cases. Medicine 1965; 44: 187.

Chisholm DM, Mason DK. Labial salivary gland biopsy in Sjogren's disease. J Clin Pathol 1968; 21: 656-60.

Fauci AS, Moutsopoulos HM. Polyclonally triggered B cells in the peripheral blood and bone marrow of normal individuals and in patients with systemic lupus erythematosus and primary Sjogren's syndrome. Arthritis Rheum 1981; 24: 577-83.

Heaton JM. Sjogren's syndrome and systemic lupus erythematosus. Br Med J 1959; 1: 466.

Izumi M, Eguchi K, Uetani M, et al. MR features of the lacrimal gland in Sjogren's syndrome. AJR 1998;170:1661-6.

Kolsi R, Abid M, Rebai T, et al. Syndrome de Gougerot-Sjogren associe aux dysthyroidies. Revue du Rhumatisme et des Maladies Osteo-Articulaires 1990; 57: 805-8.

Moutsopoulos HM (moderator). NIH Conference. Sjogren's syndrome (sicca syndrome): current issues. Ann Intern Med 1980; 92(Part 1): 212-26.

Scofield RH. Autoimmune thyroid disease in systemic lupus erythematosus and Sjogren's syndrome. Clinical & Experimental Rheumatology 1996; 14: 321-30.

Shearn MA. Sjogren's Syndrome. Philadelphia: WB Saunders, 1971.

Shearn MA. Sjogren's syndrome. Med Clin N Am 1977; 61: 271-82.

Talal N, Bunim JJ. The development of malignant lymphoma in the course of Sjogren's syndrome. Am J Med 1964; 36: 529.

Talal N, Sokoloff L, Barth WF. Extrasalivary lymphoid abnormalities in Sjogren's syndrome (reticulum cell sarcoma, pseudolymphoma, macroglobulinemia). Am J Med 1967; 43: 50-65.

Sinus Histiocytosis

Foucar E, Rosai J, Dorfman R. Sinus histiocytosis with massive lymphadenopathy (Rosai-Dorfman disease): review of the tentity. Sem Diagn Pathol 1990; 7: 19-73.

Remadi S, Anagnostopoulou ID, Jlidi R, et al. Extranodal Rosai-Dorman disease in childhood. Pathology, Research & Practice 1996; 192:

1007-15.

Resnick DK, Johnson BL, Lovely TJ. Rosai-Dorfman disease presenting with multiple orbital and intracranial masses. Acta Neuropathologica 1996; 91: 554-7.

Castleman's Disease

Herrada J, Cabanillas F, Rice L, et al. The clinical behavior of localized and multicentric Castleman disease. Ann Intern Med 1998;128:657-62.

Kurokawa T, Suzuki S, Kawaguchi K, et al. Castleman diseaes presenting with ophthalmic signs and symptoms. Am J Ophthalmol 1999;128:114-6.

Palestro G, Turrini F, Pagano M, Chiusa L. Castleman's disease. Adv Clin Path 1999;3:11-22.

Snead MP, James JN, Snead DRJ, et al. Orbital lymphomas and Castleman's disease. Eye 1993;7:84-8.

Chapter 13
Vascular Lesions

Jack Rootman

Tom R. Marotta

Douglas A. Graeb

Conceptual Model

Understanding vascular lesions of the orbit requires familiarity with a number of embryologic, pathophysiologic, and hemodynamic concepts that influence their biologic behavior, clinical features, and treatment strategies. Historically, vascular lesions in the orbit or elsewhere have been defined based on strictly descriptive nosology and models. As knowledge increased, their anatomic and pathologic basis has become clearer. Broadly speaking, they can be divided into malformations, shunts, and new growths. In terms of pathogenesis, the normal embryology and anatomy of the vascular system strongly influences their type and development. Finally, the overriding factor for understanding and managing vascular lesions is the nature of the hemodynamics of individual cases.

In order to comprehend these lesions, it is important to understand the difference between a new growth and a malformation (Table 13-1). New growths are usually not present at birth and develop as a result of a proliferation with or without a superimposed involutional process. In contrast, malformations are present at birth even though they may be occult, and tend to grow commensurate with the growth of the overall organism. New growths are characterized at a cellular level by proliferating, often plump cells, which are frequently endothelial in this instance. Further, neoplasia may be transferred to the in vitro environment and continue to grow. In terms of their hemodynamics, they connect to in-flow and out-flow vessels of the normal vascular system. Malformations, on the other hand, tend to have flat endothelial cells, do not grow in vitro, and have a substratum of dysplastic vessels. Radiologically, new growths are usually well circumscribed, may or may not be lobular, and are characterized by parenchymal staining. Malformations, on the other hand, tend to be diffuse, usually do not stain parenchymally or do so in a patchy fashion, and may be associated with ectatic, irregular, often enlarged vessels and focal calcification. There is also a difference in terms of effect on the adjacent skeletal structures. New growths tend to either have a mass effect (expanding the adjacent skeletal structures and displacing soft tissue) or infiltrate the skeleton and soft tissue. Malformations, on the other hand, may be associated with distortion, hypertrophy, or destruction brought about primarily by incorporation into, and alteration of the hemodynamics of the adjacent skeletal system, and soft tissue.

Table 13-1. Comparison of vascular neoplasia and malformations

NEOPLASIA	MALFORMATION
Clinical	
Usually not present at birth	All present at birth (may be occult)
Proliferation ± involute	Commensurate growth
Cellular	
Growing cells (especially plump endothelial)	Flat endothelium
May grow in vitro	Does not grow in vitro
Normal in-flow and out-flow vessels	Dysplastic vessels
Radiologic (Angio)	
Well circumscribed ± lobular shape	Diffuse
Parenchymal staining	No staining Low-flow - phleboliths and ectatic channels High-flow - enlarged vessels No flow
Skeletal	
Mass effect	May be distortion, hypertrophy, or destruction

During embryogenesis, the regional circulation develops in three stages. An undifferentiated capillary network is formed from chords of mesenchymal cells. Later, interconnecting channels develop the retiform plexus through which blood begins to flow from the arterial to the venous side. Remodeling occurs with the onset of blood flow, leading to closure of some vessels and persistence or expansion of others, resulting in the establishment of the mature circulatory complex. Because embryonic vascular development is integrated, anomalies of one part may be associated with similar lesions elsewhere, since malformations occur as a result of an event in time. It is therefore not surprising that vascular malformations may include abnormalities that are purely venous, arterial, lymphatic, or capillary in nature, or consist of any combination of these elements, and that they may occur in multiple sites.

The clinical properties of orbital vascular malformations are determined by their relationship with a major vessel type (arterial, venous, or lymphatic). The same is true of shunts and new growths. Shunts can be either of a congenital, malformative, or acquired nature. By definition, new growths are proliferative lesions derived from the vascular system, either as a dysgenesis or a dedifferentiation.

The final and **clinically most important** conceptual issue is the nature of the hemodynamics of the various lesions, which can significantly affect presentation and treatment strategies. One can view hemodynamics in terms of the relationship between, and the effect of, in-flow (arterial or venous) and out-flow (arterial or venous) of blood or serum from any lesion, whether a malformation, shunt, or new growth. This is perhaps best understood when considering specific lesions. For instance, the arteriovenous malformation has in-flow from dedicated vessels of the normal arterial system and out-flow through a normal vein downstream. In the case of a orbital arteriovenous malformation, this would be arterial flow into the malformation and principally out through the superior ophthalmic vein or inferior ophthalmic vein to the cavernous sinus. Because of the lack of intervening capillaries, this lesion acts to shunt blood in an antigrade fashion into the normal venous system; when it is high-flow, it is characterized by pulsation, turbulence, progressive arterialization, and potential thrombosis. In contrast, an acquired shunt between the arterial and venous system may occur either spontaneously or secondary to trauma. Those that occur secondary to trauma usually are high-flow resulting from a blowout of an artery into the venous system. In the case of the orbit, a post-traumatic carotid cavernous fistula is an excellent example of such a shunt. Because the flow is from the arterial to venous channels, all of the out-flow feeds in a retrograde fashion via the venous network to normal structures, leading to swelling, leakage, increased pressure, pulsation, and bruit. In contrast, the acquired low-flow dural fistula is a result of thrombosis within smaller venous channels, leading to shunting through fewer and fewer veins. The increased venous pressure in this circumstance is much less than in high-flow shunts and results in turbulence, thrombosis, and leakage (edema).

The specific symptoms in acquired shunts tend to reflect the underlying hemodynamics. Lesions associated with large (rapid) shunts from the normal arterial to the normal venous system are characterized by pulsatile bruit, visible and palpable orbital pulsations, and the effects of increased venous pressure (dilatation of episcleral veins, elevation of intraocular pressure, chemosis, orbital tissue swelling, and engorgement of the retinal circulation). Lesions in which the arteriovenous shunt is less vigorous present with milder symptoms and signs. Exophthalmos may be present but is generally nonpulsatile; bruit is frequently absent, and elevation of intraocular pressure is less. However, these low-flow shunts are prone to the development of episodes of venous thrombosis, which may either alleviate or aggravate the symptoms depending upon the alteration in hemodynamics produced by such an event.

On the venous side of the circulation, the most obvious abnormality hemodynamically is the distensible venous malformation. This lesion is characterized by the presence of a rich network of anomalous veins directly connected to the venous system. Increasing the pressure within the system (with a Valsalva maneuver or increased thoracic pressure) leads to distention of the malformation. Alternatively, compressing out-flow also leads to distention.

From a practical clinical point of view, the remaining vascular malformations of the orbit that derive from the venous anlage behave in a fashion that is dominated by nonvisible or indiscernible distensibility and episodes of recurrent hemorrhage, expansion, and swelling. This reflects a lack of, or minimal hemodynamic relationship to, the venous and arterial sides of the system, and includes the category of nondistensible varices and so-called lymphangiomas, which probably represent a combined venous-lymphatic lesion. Pure lymphatic malformations are rare in the orbit, are anteriorly located, and demonstrate no direct hemodynamic connection clinically or on imaging.

New growths also have a hemodynamic component affecting the proliferative element. For example, the capillary hemangioma at its peak acts as a sump from the arterial side thus increasing flow to the lesion, manifest as pulsation and injection. Reducing out-flow of a capillary hemangioma (with increased jugular venous pressure, i.e., crying) leads to expansion and perhaps increased pulsation and bluish discoloration brought about by reduced oxygenation of blood.

Most lesions present with mass effect, which may be positive (proptosis or displacement of the globe), negative (enophthalmos – frequent in distensible varices), or intermittent (the pulsatile exophthalmos of post-traumatic carotid-cavernous fistulas and congenital high-flow arteriovenous malformations, or the proptosis seen with the Valsalva maneuver in distensible venous malformations).

In summary, the clinical pictures that lead one to suspect vascular lesions are individual features or combinations of tumefaction, vascular engorgement (due either to arteriovenous shunting, dilatation, or venous thrombosis), spontaneous hemorrhage (with or without history of an antecedent anomaly), orbital pulsation, intermittent exophthalmos, or spontaneous hemorrhage.

This chapter will discuss the major orbital vascular lesions. In the category of **malformations**, these can be divided into arterial, venous, combined, lymphatic, and miscellaneous congenital vascular lesions. We have also included cavernous hemangioma as a malformation because of its fundamental biologic characteristics. The next major orbital vascular lesions are acquired **shunts**, which may be post-traumatic or spontaneous. The remaining sections will deal with **new growths** , **aneurysms** , **obstructive lesions**, and a number of **unclassified vascular events** in the orbit.

Malformations

Vascular malformations need to be understood differently from the acquired arteriovenous shunts or fistulae in terms of pathogenesis and hemodynamics. They derive either from the arterial system, venous system, or both. Arterially-derived malformations may develop as arteriovenous shunts that bypass the capillary bed and flow directly (antigrade) from the arterial side through the malformation into the venous out-flow channels. On the other hand, venous-side malformations may consist of simple ectasias of the veins or complex venous anomalies with abnormal out-flow channels. Finally, lymphatic lesions derive from the venous anlage and may consist of isolated, purely lymphatic channels or more commonly, a combination of venous and lymphatic components. As stated earlier, any combination of venous, arterial, lymphatic, or capillary lesions may occur.

The Orbital Society has adopted a classification of orbital vascular malformations based on their hemodynamic relationships. This classification promotes clinical differentiations based on blood flow that would help to determine their signs and symptoms and would dictate appropriate management. Before assigning a given case to any of these categories, numerous clinical and imaging features should be considered including postural expansion, clinical evidence of pulsation or bruit, expansion with Valsalva maneuver, directional echography or Doppler flow imaging (which can demonstrate no-flow, venous flow, or arterial flow), intrinsic opacification with contrast-enhanced CT or CT angiography, changes in the size of the malformation between axial and coronal CT scans, flow characteristic using MRI or MR angiography, and intrinsic flow characteristics using invasive venography (direct or indirect) or arteriography. On the basis of these features, one should be able to categorize orbital vascular malformations into the following (Table 13-2):

- Type 1 – **No-flow** (hemodynamically isolated). An example of this would be the true lymphatic vascular malformations and some venous lymphatic lesions.
- Type 2 – **Venous flow**. This category includes distensible venous vascular malformations characterized by clinical and imaging features of enlargement with increased venous pressure. Combined distensible venous-lymphatic vascular malformations may have characteristics of Type 1 and Type 2 features. The categories of nondistensible venous and combined nondistensible venous-lymphatic lesions are identified more often by recurrent bouts of bleeding, expansion, and inflammation, and blend indistinguishably from a clinical point of view. Distensible venous lesions tend to behave in a more innocuous fashion.
- Type 3 – **Arterial flow**. Lesions in this category are distinguished by evidence of arterial flow. The primary examples are arteriovenous malformations that have a direct flow from the arterial side, through a malformation, and then to the venous-side of the circulation.

Finally, vascular malformations tend to distribute themselves anatomically into four different groups: superficial lesions that typically consist of visible vascular malformations of the conjunctiva or lid alone; deep lesions that usually have no surface manifestations and are entirely retrobulbar; combined lesions that have both superficial and deep components, and complex lesions that involve the orbit, periorbital and intracranial tissues, and may involve multifocal sites (Fig. 13-1).

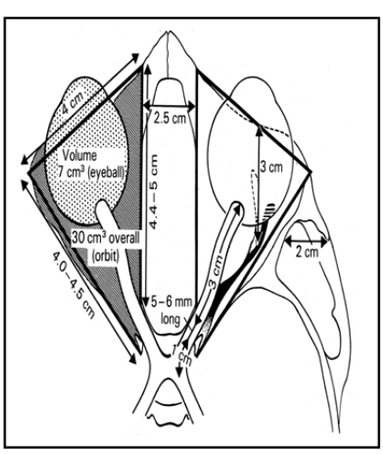

Figure 13-1. Schematic of orbit demonstrates major local anatomic subtypes of vascular tumors, including superficial (cutaneous, preseptal, and conjunctival), deep (behind the septum or intraconal), and combined with superficial and deep components.

Table 13-2. Hemodynamic classification of vascular lesions

TYPE	HEMODYNAMICS	CLINICAL FEATURES	IMAGING	HISTOLOGY
Type 1 - NO FLOW Lymphangioma (or combined venous-lymphatic malformations)		Recurrent bouts of hemorrhage Frequently ill-defined margins	Irregular, patchy uptake on contrast CT MRI may evidence blood-filled cysts both recent and old Direct injection stays within lesion	Ectatic, thin-walled, dysplastic, serous-containing vessels with lymphorrhages
Type 2 - VENOUS FLOW Distensible	Direct and rich communication with venous system	Enlarged with Valsalva maneuver or bending May be painful on expansion May be multiple	Expand on coronal CT Demonstrate flow (Doppler) Uniform contrast enhancement Direct injection can demonstrate connection to the venous system Retrograde injection fills the lesion Type 1: ectasias with normal out-flow Type 2: malformations with tangled normal out-flow Type 3: single or multiple vessels	Dysmorphic venous channels containing blood without evidence of thrombosis or interstitial hemorrhage
Nondistensible	Direct but minimal communication with the venous system	Do not enlarge on Valsalva maneuver Subject to recurrent hemorrhage Similar to Type 1	Direct injection leads to out-flow Retrograde injection partially fills lesion With CT or MRI tend to enhance uniformly May have focal areas of recent and old hemorrhage	Irregular, dysmorphic veins with varying amounts of new and old blood
Combined lymphatic venous-distensible	Features of distensible and nondistensible lesions (Types 1 and 2)	Features of Type 1 and Type 2-distensible	Features of Type 1 and Type 2-distensible	Dysmorphic lymphatic and venous channels New and old blood Smooth muscle bundles
Type 3 ARTERIAL FLOW Arteriovenous malformation	Direct antigrade flow through malformation to venous side Intraorbital Extraorbital - collateral flow to extraorbital shunt	Clinical pulsation Pain on Valsalva Rarely hemorrhage Gradual expansion with time	CT & CT angiography show uniform enhancement MRI demonstrates flow voids Occasional old and new hemorrhage Doppler echography shows pulsation and flow May increase in size with increased venous pressure Direct injection leads to a rapid flow through normal or arterialized veins Intra-arterial injection (selective) demonstrates tangled vascular mass with high-flow into distinctive out-flow channels	Thick-walled, irregular arterial channels with and without stromal bleeding
Cavernous hemangioma	Direct low-flow through the malformation	Painless expansion	Patchy to uniform enhancement of a well-defined regular lesion Arteriography shows late pooling Direct injection fills the lesion	Thin-walled, blood-filled vessels Smooth muscle and fibrous stroma
Acquired arteriovenous shunts **High-flow**	Retrograde flow arterial to orbital veins	Pulsation Swelling Bruit Raised intraocular pressure Dilated episcleral veins Occasional ischemic retinopathy	CT and MRI demonstrate enlarged superior ophthalmic vein and extraocular muscles, and dural and cavernous vascular lesions Doppler ultrasonography shows pulsation Ultrasound demonstrates dilated superior ophthalmic vein and expanded extraocular muscles Selective angiography shows shunt	Arterialized veins
Low-flow	Retrograde flow arterial to venous side	Same as high-flow but to a lesser degree	Same as high-flow but to a lesser degree	Thinner arterialized veins

Arteriovenous Malformations

High-flow Lesions

Clinical

Arteriovenous malformations in the orbit are characterized by high arterial flow directly into the anomaly that exits through the normal venous channels, which may arterialize (Fig. 13-2). Thus, they bypass the orbital system and more commonly act to shunt blood away from the system rather than into the normal vascular channels because they flow into preexisting channels. Clinically, they are associated with pulsating exophthalmos, occasional episodes of hemorrhage or thrombosis, or a caput medusae effect as they flow out through arterialized venous channels. Elsewhere in the body, they may shunt so much blood away from the down-flow system that they lead to tissue ischemia as a result of a steal syndrome. They may also lead to cardiac failure, particularly if large or multiple, as a result of shunting. The high-flow orbital arteriovenous malformations are often associated with evidence of a bruit and may cause pain when engorged with straining or Valsalva maneuver.

Imaging

Orbital arteriovenous malformations are characterized by irregular, rapidly enhancing masses that may have high-flow characteristics on Doppler studies and flow voids on MR scanning. Direct selective angiography will demonstrate

the engorged, rapidly filling proximal arterial system, the malformation, and the distal venous out-flow (Fig. 13-3).

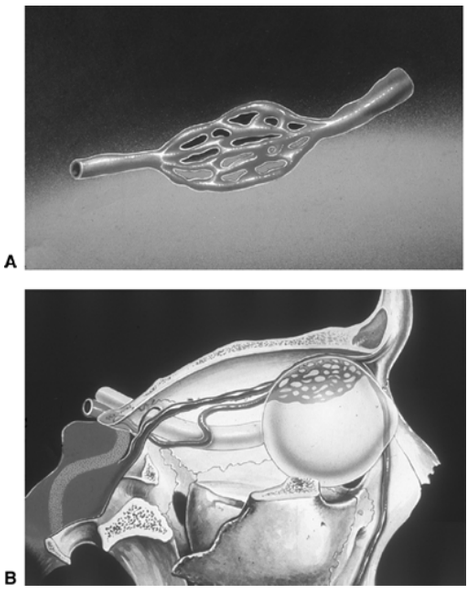

Figure 13-2. Demonstration of the direct in- and out-flow systems of an arteriovenous malformation originating from a branch of the ophthalmic artery and flowing back through the superior ophthalmic venous system into the cavernous sinus (see Fig. 13-3).

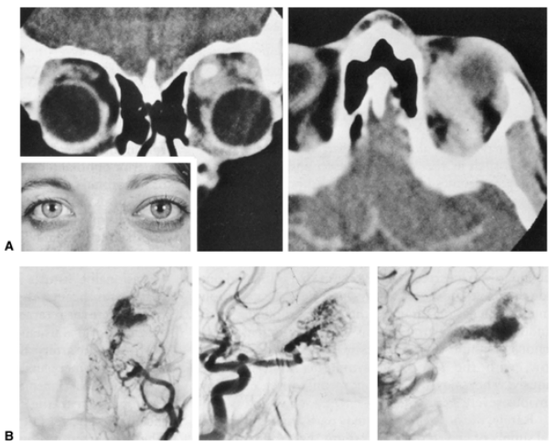

Figure 13-3. (A) A primary orbital arteriovenous malformation in a 17-year-old girl with a 3-year history of proptosis. Close clinical observation demonstrated orbital pulsation synchronous with the pulse. CT scan shows calcification within a poorly-defined, enhancing mass and marked enlargement of the superior ophthalmic vein. (B) Arteriography of this patient demonstrates enlarged ophthalmic artery (center) and external carotid branches (left supplying a tangle of anomalous vessels, with early drainage to the markedly enlarged superior ophthalmic vein (right).

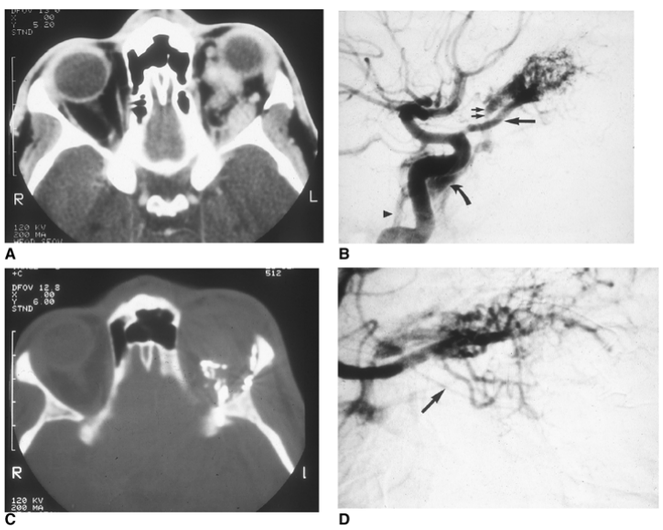

Figure 13-4. This composite demonstrates the CT and angiographic features of an arteriovenous malformation of the orbit that was selectively embolized with glue prior to resection. (A) CT scan demonstrates the superior and lateral location of the anomaly. (B) This is also shown in a lateral subtracted view of the left internal carotid injection, which shows a fairly diffuse arteriovenous malformation nidus of small vessels fed by an enlarged ophthalmic artery (straight arrow). Venous drainage is posteriorly via the superior ophthalmic vein (double arrow) to the cavernous sinus (curved arrow) and inferior petrosal sinus (arrowhead). (C) CT scan demonstrates glue in the feeding vessels postembolization. (D) Angiography immediately after embolization of three branches with bucrylate shows marked reduction of the arteriovenous malformation nidus and reduced opacification of the superior ophthalmic vein. The posterior ciliary artery is patent (arrow). (Figs. 13-4B and D reproduced with permission from Rootman J, Kao SCS, Graeb DA. Multidisciplinary approaches to complicated vascular lesions of the orbit. Ophthalmology 1992;99:1440-6.)

Management

Management of some high-flow arteriovenous malformations can take advantage of newer radiologic interventional vascular techniques. Selective catheter positioning distal to the posterior ciliary and central retinal vessels, along with provocative lidocaine testing are mandatory when the lesions occur within the orbit. Selective gluing can then be carried out followed by excision (Fig. 13-4). For those lesions with feeding vessels that are outside the orbit, a direct cut-down followed by embolization and surgery is also a safe and very direct approach. The more complex arteriovenous malformations may be part of multisystem congenital vascular malformations, which will be discussed later.

Low-flow Malformations

Cavernous Hemangiomas

Hemodynamics

Cavernous hemangiomas are usually considered vascular hamartomas but in some respects behave more like low-flow arteriovenous vascular malformations; that is, they usually have a direct, relatively small arterial in-flow and similar out-flow mechanisms. Direct post-excision injection into these lesions demonstrate that they are made up of interconnected vascular channels, usually containing blood that perfuses very slowly, and are not associated with focal areas of thrombosis as a rule (Fig. 13-5D).

Histopathology reveals a fine capsule that surrounds a tumor consisting of large endothelially lined channels with abundant, loosely distributed smooth muscle in the vascular walls and stroma. The cavernous hemangioma is histologically and hemodynamically a low-flow, arterial-side, hamartomatous malformation. Evidence for this is multifold and relates to several clinical and imaging features. Clinically, these tumors are soft and on ultrasound can be compressed, demonstrating slow refilling. On examination, they have a typical scintigraphic pattern similar to hepatic hemangiomas and on MRI with gadolinium, the lesions initially show central patchy enhancement with later total and homogeneous fill-up (20 to 60 minutes). The fact that they are more frequently located laterally is also consistent with arterial origin. Direct arteriography typically reveals a few small intratumoral collections or puddles of contrast, which appear late in the arterial phase and persist well into the venous phase (Fig. 13-5C). The main tumor mass does not opacify, and the ophthalmic artery and its branches may be displaced or stretched but not enlarged. Direct injection demonstrates that the channels are interconnected and rarely do we see focal areas of thrombosis. Conceptually, therefore, these lesions can be thought of as having very small arterial input and very slow flow through them into minimal venous out-flow channels.

Clinical Features

Cavernous hemangiomas are benign noninfiltrative lesions that exert a slowly progressive, noninfiltrative mass effect. Although they may undergo evolution with time, only a few in our series were noted to have evidence of scarring, hemosiderin deposition, thrombosis, or significant inflammatory infiltrates. Thus, sudden change reflecting either clinical evidence of inflammation or hemorrhage is the exception and not the rule; rather, the history is one of progressive slow mass effect.

We have seen 44 cavernous hemangiomas, all occurring in adults between the third and seventh decades. These tumors are typically intraconal and lateral, causing little motor dysfunction and producing a mass effect (i.e., proptosis, posterior pole indentation, choroidal striae, and optic nerve elevation) (Fig. 13-5). Twenty-five of our 44 (57%) patients complained of some form of visual symptoms (often progressive hyperopia). Because the tumors grow slowly, the patient is frequently unaware of the duration of the disease but examination of old photographs often reveals proptosis of many years' duration. Very large cavernous hemangiomas or those located within the orbital apex may, however, produce optic nerve compression, diplopia, or orbital pain (Fig. 13-6). Two of our patients had the unusual feature of transient amauroses in extremes of gaze due to gaze-evoked optic nerve compression induced in this position.

Imaging

CT scan typically shows a very well-defined oval or rounded intraconal mass with smooth margins, which enhances with intravenous contrast. Occasionally, a small portion of the lesion extends to the extraconal compartment but the greatest bulk of the tumor is almost always intraconal. The majority arise laterally causing medial displacement of the optic nerve; proptosis is generally present and the globe is frequently indented by the rounded anterior margin of the tumor. About one half will show subtle outward bowing of the lateral orbital wall, consistent with a longstanding, slowly growing mass. The enhancement pattern may be homogeneous or somewhat inhomogeneous with approximately equal frequency. The position of the nonenhancing optic nerve can be seen on good quality scans in the majority of cases; the nerve is typically displaced rather than surrounded by the tumor. Small areas of calcification are occasionally seen.

B-scan ultrasonography shows rounded, intraconal, well-circumscribed masses with well-delineated posterior

surfaces (Fig. 13-5C). The acoustic texture is echogenic and the adjacent extraocular muscles may be accentuated. A-scan ultrasonography shows medium reflectivity between regular highly reflective spikes and medium sound attenuation. The borders are usually well defined with a posterior high reflective spike marking the capsule.

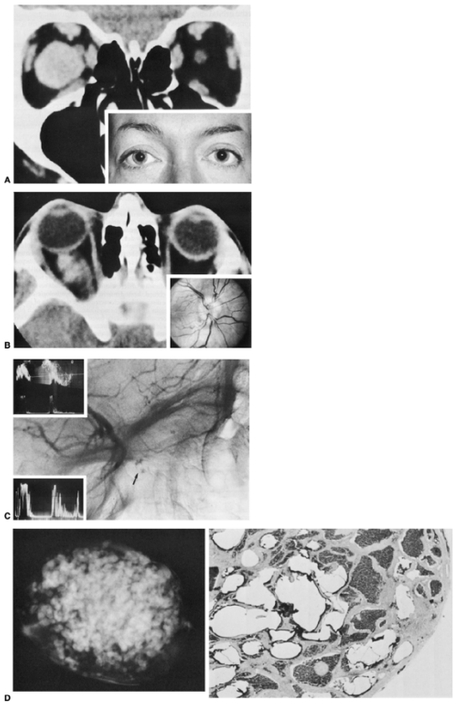

Figure 13-5. (A) Right orbital mass noted for 6 months proved on CT scan to consist of a well-defined intraconal enhancing lesion immediately behind the globe. (A, B) Note displacement of the optic nerve leading to disc swelling (B, inset) and obscured vision on right lateral gaze. (C) Venous phase of angiogram demonstrates the characteristic small “puddles” of contrast (arrow). Ultrasonograms (C, insets) demonstrate a well-circumscribed echogenic mass on B-scan (top) with high and medium internal reflectivity and well-defined highly reflective borders on A-scan. (D) Specimen from the same patient injected with radio-opaque contrast after excision. Note the well-defined capsule and interconnected vascular endothelially-lined network, not all of which have filled as shown on the right. This suggests multiple sources of blood supply (H&E, original magnification × 2.5).

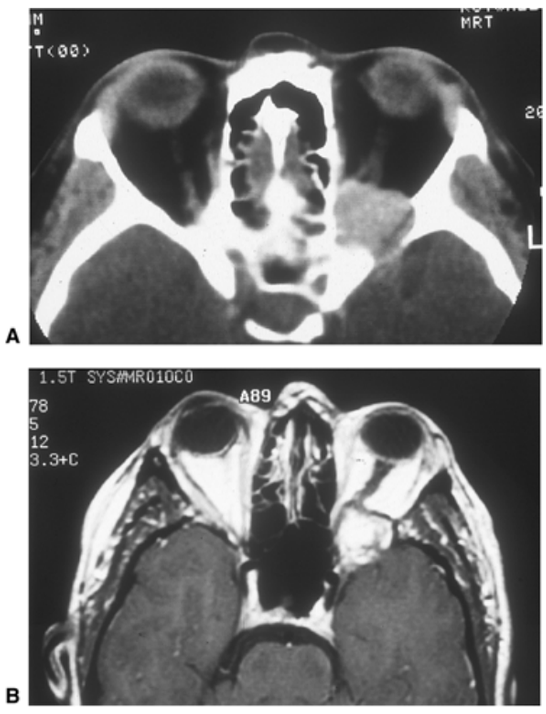

Figure 13-6. (A) This CT scan demonstrates an apical hemangioma in a 36-year-old woman who presented with a 9-month history of decreased vision and an afferent pupillary defect with mild optic atrophy. (B) T1-weighted MR scan with gadolinium injection demonstrates the smooth contours of the lesion associated with patchy central early uptake of dye. This tumor was removed via a combined cranio-orbitotomy approach.

Internal carotid angiography typically reveals a few small intratumoral collections or puddles of contrast, which appear late in the arterial phase and persist well into the venous phase (Fig. 13-5C). The main tumor mass does not opacify. The ophthalmic artery and its branches may be displaced or stretched but they are not enlarged and supply from external carotid branches is infrequent. Although the angiographic appearance of cavernous hemangiomas is characteristic, angiography is rarely necessary. In occasional instances, however, contrast puddling is not seen and the angiogram may be entirely normal or show only vascular displacement.

On MRI, cavernous hemangiomas are isointense to muscle on T1-weighted sequences and hyperintense to muscle on T2-weighted sequences. With gadolinium, the lesions show initial central patchy enhancement and between 20 to 60 minutes, they fill up homogeneously (Fig. 13-6). On MR scan, they enhance with contrast (Fig. 13-7).

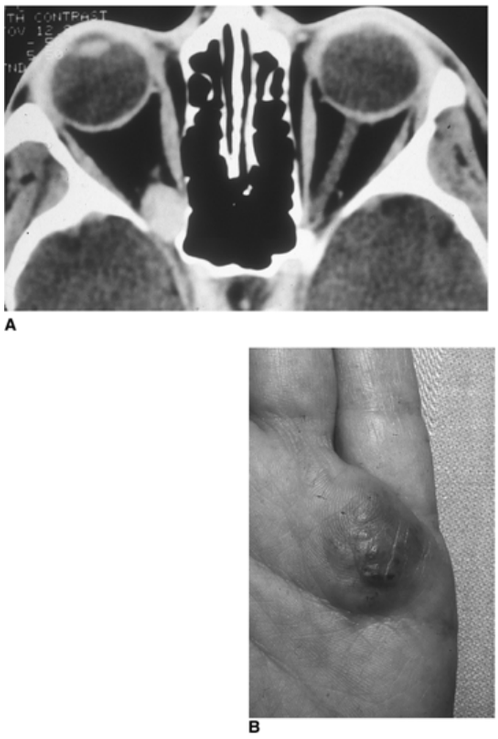

Figure 13-7. (A) Axial CT scan demonstrates an apical hemangioma with uniform contrast enhancement. This appeared in a 30-year-old woman with Usher's syndrome, which had led to a significant reduction of her already decreased vision. The lesion was inferior to the optic nerve. (B) She was also noted to have a hemangioma in the palm of her left hand.

Management

The biologic behavior of these lesions is that they probably expand slowly with time; they are now frequently being discovered on CT or MR scan done for other reasons, suggesting that they exist much more commonly than is clinically apparent. Generally speaking, intervention is unnecessary unless there is some functional or cosmetic concern. From a clinical point of view, the effects of cavernous hemangiomas are dominated by location. When directly behind the globe, they may cause elevation of the disk, stria in the posterior pole, and progressive hyperopia. On the other hand

when located apically, they can cause optic neuropathy; indeed, some of these may extend through the superior orbital fissure with excavation of the adjacent bone. The treatment strategy for cavernous hemangioma may be observation, particularly if it is not interfering with function and is not unsightly.

The cavernous hemangioma is a classic surgical lesion, and few orbital tumors are removed with greater ease and satisfaction. When surgical indications exist, the strategy at the time of surgery can be based on the low-flow nature of the lesion, which allows for dissection, puncture to exsanguinate, and reduction of the lesion size permitting excision from tighter spaces without interfering with adjacent tissues. When exposed, the tumor is a plump, nodular, plum-colored mass with vascular channels on its well-defined surface. It can be removed by blunt dissection of the surface to free it of adjacent orbital structures. Any connecting vascular strands can then be easily identified and cauterized. There is frequently an apical vascular tag, which is best left to the final stage of the procedure because rupture earlier may cause more bleeding and obscure the field. When these vessels are transected, preferably at the end of removal, there may be a slow gush of blood, which can be controlled with simple gentle tamponade or can be avoided by identifying the vessels and using bipolar cautery. A transconjunctival or modified swinging eyelid approach can be utilized in excising these lesions, particularly if anterior, combined with exsanguination of the tumor.

Cavernous Hemangioma of Bone

Another so-called cavernous hemangioma can occur in the bones adjacent to the orbit. Histologically, they resemble involuted capillary hemangiomas, consisting of large diaphanous thin-walled vessels without the stromal components of cavernous hemangioma. Because of their rigid encasement, resection can lead to significant bleeding. They cause slow expansion of the bone adjacent to the orbit and may ultimately require excision (Fig. 13-8). The CT findings are characteristic with a star burst appearance, and preoperative angiography allows for recognition of the in- and out-flow characteristics of the lesion. Selected embolization can then be used to obstruct the lesion, which allows for bloodless excision.

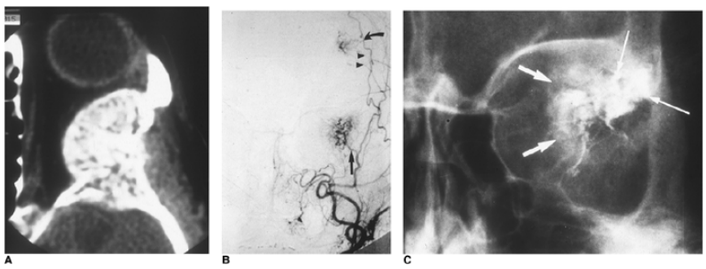

Figure 13-8. This 66-year-old woman presented with a history of slowly progressive left proptosis. She had exophthalmometry of 17.5 mm on the left, 2 mm downward and 3 mm inward displacement, and slight limitation of elevation. (A) Axial CT shows a bony mass arising from the greater wing of sphenoid extending into the orbit. A coarsened trabecular pattern with parallel striations (star burst) and areas of fat density can be seen, features characteristic of cavernous hemangioma of bone. The lesion was embolized and (B) angiography shows supply arising from a sphenoidal branch of the middle meningeal artery (vertical arrow). The tortuous dilated tumor vessels with slow flow are characteristic of hemangioma of bone. A second lesion is seen in the left frontal bone supplied by branches of the superficial temporal (curved arrow) and middle meningeal (arrowhead) arteries. (C) Plain film after embolization shows diffuse hazy opacification resulting from stasis of contrast in the tumor (large arrows) as well as the more dense bucrylate occluding the larger vessels (small arrows), reproducing the vascular pattern seen at angiography. (Reproduced with permission from Rootman J, Kao SCS, Graeb DA. Multidisciplinary approaches to complicated vascular lesions of the orbit. Ophthalmology 1992;99:1440-6.)

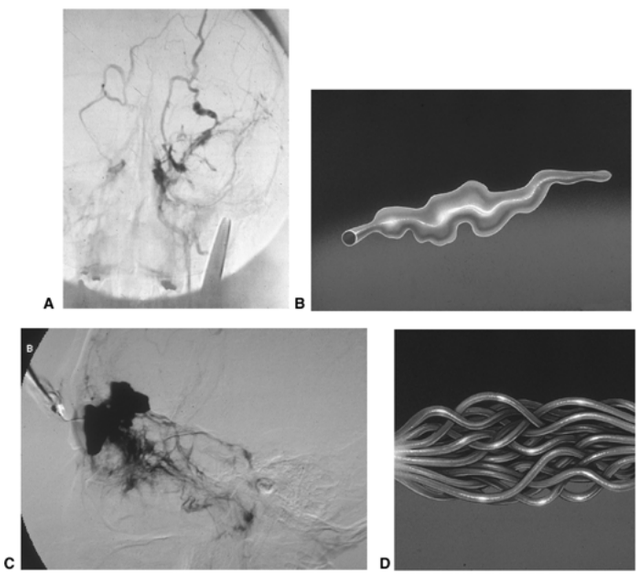

Figure 13-9. (A) Direct venogram demonstrates a venous orbital malformation. This is characterized by an ectatic venous out-flow channel that is part of the superior ophthalmic vein, schematically shown in (B). (C) A direct injection to a multichannel, sacular, distensible venous anomaly flows out through a complex dysplastic venous network to the pterygopalatine fossa and superior and inferior ophthalmic venous system, which is represented schematically in (D).

Venous Vascular Malformations

Venous Anomalies

Hemodynamics

The venous anomalies consist of either segmental irregular dilatations of the venous out-flow system or a tangled mass of abnormal venous channels with or without dysmorphic out-flow channels (Fig. 13-9). They appear to be associated with two different clinical syndromes, which can be explained on the basis of the size of functioning connections to the venous system. Lesions with large connections respond to changes in venous pressure and are readily distensible. In our experience, these constitute the majority of so-called purely venous vascular malformations. Patients may describe proptosis and pain that increases with activities such as straining, bending forward, or Valsalva maneuver. In contrast, lesions with little or small functioning systemic venous connections are clinically and radiographically nondistensible, do not respond in an obvious way to changes in systemic venous pressure, and are characterized more by stagnant blood flow, which leads to thrombosis or hemorrhage, or both. These nondistensible lesions may blend imperceptibly from a clinical and management point of view into the so-called “lymphangiomas” as part of the spectrum of venous-lymphatic lesions dominated by a lack of, or minimal communication with, the venous out-flow system. Spontaneous hemorrhage may occur in all types of vascular malformations; however, the hemodynamic properties of distensible venous lesions are such that thrombosis or hemorrhage is uncommon, compared with the nondistensible malformations which have relatively stagnant blood flow.

Distensible Venous Vascular Malformations

Clinical Features

In a review of our distensible vascular malformations, the overwhelming majority were pure venous anomalies as demonstrated by clinical, imaging, and either indirect or direct venography. Four of 30 of these malformations were combined venous-lymphatic in character and behaved more like nondistensible venous malformations with recurrent hemorrhages. However, they demonstrated either clinical or imaging evidence of distensibility.

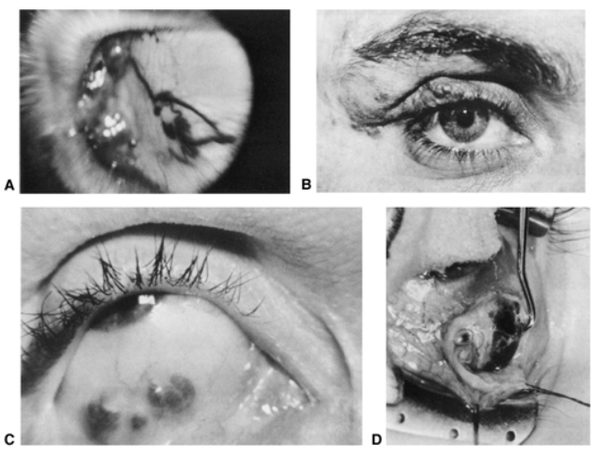

Figure 13-10. Clinical photograph of conjunctival (A) and lid (B) varix. Note tortuous blood-filled aneurysmal venous network. (C) Epibulbar component of a deep orbital varix. (D) Surgical photograph of a superficial varix demonstrates involvement of the inferior anterior orbit.

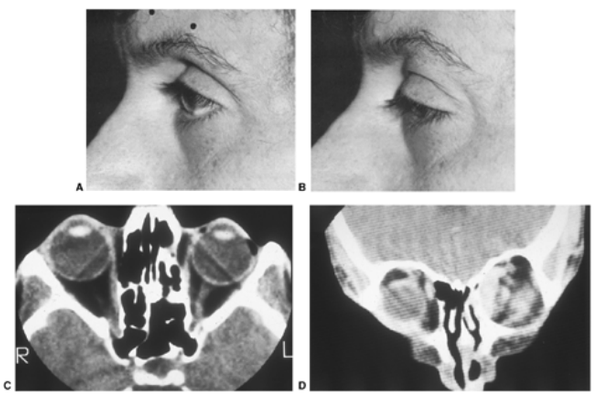

Figure 13-11. Clinical photographs of a normally enophthalmic patient with a distensible orbital varix before (A) and after (B) Valsalva maneuver, leading to proptosis and fullness of the lid. The 33-year-old patient had noted the intermittent proptosis since childhood. In addition, she had similar distensible venous lesions on her neck and back. Note on the axial scan (C) that only the enophthalmos (due to fat atrophy) not the lesion is demonstrated but on coronal view (D) with the associated increased venous pressure, the medial distensible varix appears. (Figs. 13-11A and B reproduced with permission from Cline RA, Rootman J. Enophthalmos: a clinical review. Ophthalmology 1984; 91:229-37.)

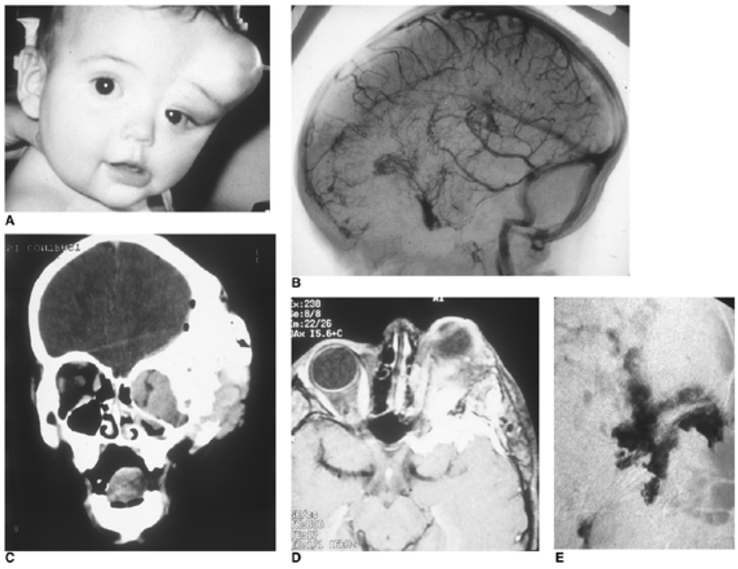

Figure 13-12. (A) This infant presented with a complex, easily collapsible malformation of her left orbit, forehead, and scalp. It distended markedly on crying. (B) The venous phase of her cerebral angiogram showed multiple areas of venous puddling in the brain adjacent to the orbital venous malformation. (C) On coronal CT, the extensive lesion was seen to involve the face, orbit, and dural lining. (D) Axial T1-weighted MRI with gadolinium enhancement revealed the extent of the orbital and cranial involvement. (E) A late phase direct venogram (lateral image) demonstrates the malformation extending from the orbit intracranially over the base of the frontal and parietal lobes. In addition, there is flow into the pterygopalatine fossa. (Figs. 13-12A and C reproduced with permission from Rootman J, Kao SCS, Graeb DA. Multidisciplinary approaches to complicated vascular lesions of the orbit. Ophthalmology 1992;99:1440-6.)

Distensible varices can appear as superficial, deep, combined, or complex lesions. The superficial lesions are easily visible as dark, tortuous epibulbar or lid lesions (Fig. 13-10). In contrast (Fig. 13-11), the deeper distensible varices are characterized by intermittent, sometimes uncomfortable proptosis, frequent evidence of enophthalmos (due to fat atrophy), occasional bruising, and pain on expansion brought about by either physical effort or bending. The combined lesions have features of direct surface visibility and significant proptosis on Valsalva maneuver with or without enophthalmos. The complex lesions are characterized by frequently extensive involvement of the periorbital tissues and scalp, and may show evidence of intracranial vascular anomalies as a result of a complex venous malformation of the brain (Fig. 13-12). In addition complex lesions may demonstrate venous malformations elsewhere.

Imaging

The major imaging features of distensible venous vascular malformations consist of enlargement on coronal CT scan, expansion with Valsalva maneuver during dynamic CT or MR scanning, increased size demonstrated on A- and B-scan ultrasonography, or flow on Doppler echography. Direct injection, either through proximal veins or intralesionally, demonstrate either ectatic dysmorphic vessels flowing out through normal venous channels or more commonly saccular tangles of malformed vessels extending out through multiple venous out-flow channels, including those of the pterygopalatine fossa, face, and cavernous sinus (Figs. 13-9C and 13-12).

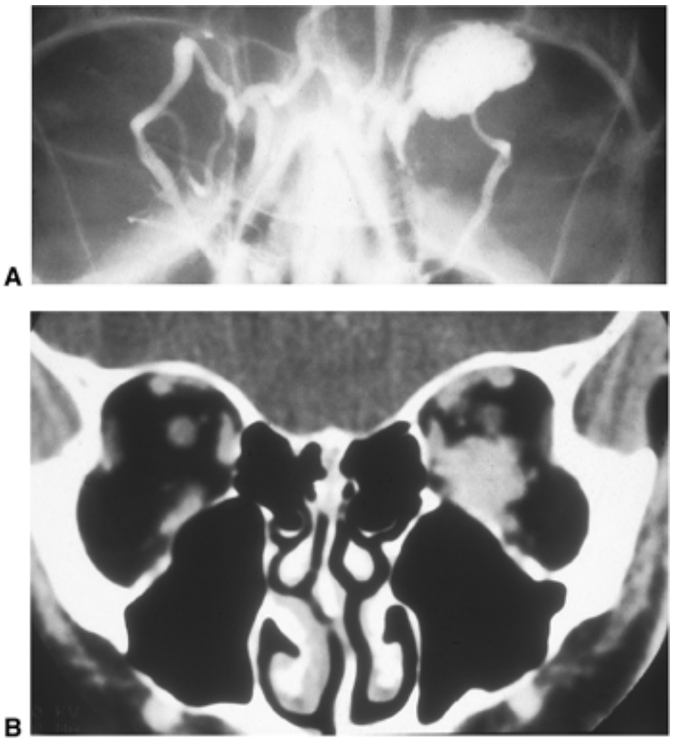

Figure 13-13. (A) Standard venography reveals a complex multichannel venous malformation in the left superomedial orbit. No other lesions were identified on this venogram. (B) Coronal CT scan of the left orbit reveals a separate, slightly irregular, enhancing intraconal mass just inferior to the optic nerve. (NB: standard venography failed to reveal the intraconal venous lesion inferior to the optic nerve because it was not connected to the superior ophthalmic venous system. (Reproduced with permission from Lacey B, Rootman J, Marotta TR. Distensible venous malformations of the orbit. Clinical and hemodynamic features and a new technique of management. Ophthalmology 1999;106:1197-209.)

Management

For the most part, distensible venous lesions are not of serious consequence and do not require any intervention. The indications for surgical treatment are usually related to pain, cosmesis, or progressive expansion. We have only had one patient with optic nerve compromise as an indication for excision.

The direct surgical treatment of distensible venous malformations of the orbit is difficult due to the tortuous tangles of fragile, thin-walled, malformed vessels and their tendency to rupture and bleed excessively (Fig. 13-13). Excision has traditionally required hypotensive anesthesia and skill in all methods of hemostasis, including isolation and ligation or clipping of abnormal vessels. Direct surgical excision can be fraught with hemorrhage due to multiple and complex relationships with anomalous vessels that may pass into the orbit and adjacent tissues, including the pterygopalatine fossa, face, bones, and intracranial space. Direct excision is best reserved for superficial lesions.

Attempts to reduce the vascularity of these lesions prior to surgical excision include intralesional thrombosis using thermoelectric desiccation and retrograde venous catheterization and embolization with platinum microcoils. Our approach has been to perform intraoperative venography and controlled glue embolization combined with intraoperative obstruction of out-flow followed by excision of the glued mass. The embolization with a mixture of n-butyl-2-cyanoacrylate,

lipoidal, and tantalum powder produces a radio-opaque cast of the malformation, which can then be excised in a relatively blood-free manner (Fig. 13-14). It is extremely important that the hemodynamics of a distensible venous malformation are understood prior to embolization by a multidisciplinary team. Occlusion of the drainage pathways of a lesion or lesions will lead to expansion or stasis within any remaining portion if not completely excised. Such altered hemodynamics may favor postoperative thrombosis or hemorrhage.

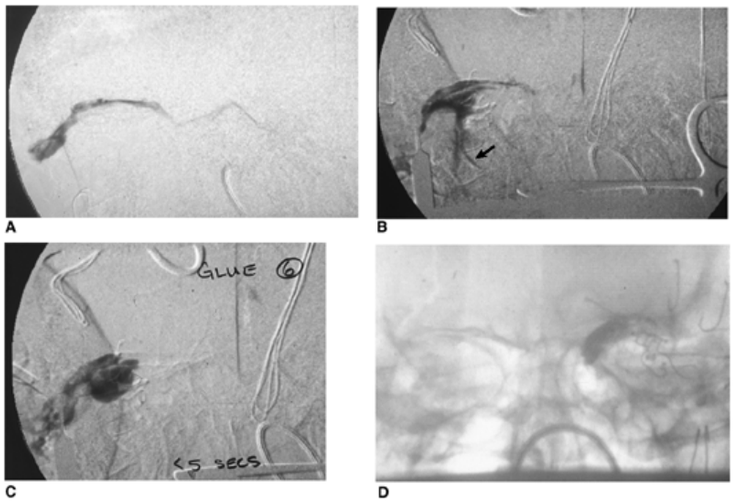

Figure 13-14. (A) Intraoperative direct intralesional lateral venogram demonstrates filling of a lesion and its out-flow through a single venous channel at the superior orbital fissure to the cavernous sinus. (B) With pressure applied at the superior orbital fissure, control of out-flow is confirmed venographically prior to injection of the glue mixture. An apparent opacified component inferiorly (arrow) represents artifact. (C) The glue cast is seen in situ following embolization and (D) intraoperative fluoroscopic anterior-posterior view confirmed the presence of the glue cast within the superior orbital venous malformation, which was then excised. (Figs. 13-17A and B reproduced with permission from Lacey B, Rootman J, Marotta TR. Distensible venous malformations of the orbit. Clinical and hemodynamic features and a new technique of management. Ophthalmology 1999;106:1197-209.)

Nondistensible Venous Vascular Malformations

Nondistensible venous malformations may appear as superficial, deep, or combined lesions. Clinically, they are characterized by syndromes consisting of episodes of acute exacerbation and remission, which are related to hemorrhage or thrombosis within the lesion (Fig. 13-15). Hemorrhage or thrombosis within deeper lesions leads to sudden proptosis, pain, and increased pressure in the orbital tissues. In addition, there may be a mechanical restriction of ocular movements or visual deficit. There may be subconjunctival extension of the ecchymosis following these deep orbital hemorrhages. The superficial components may be associated with swelling and disfigurement of the lid and conjunctiva, which may or may not extend into the deep orbit.

In some respects, the distinction between nondistensible varices and lymphangiomas is difficult on clinical grounds, but in our opinion, there may be a number of differing features. The superficial component of lymphangiomas is generally more striking with evidence of varying types of tortuous vascular channels, some of which contain blood, menisci, or clear fluid, compared with the larger, blood-filled channels of a varix. In addition, lymphangiomas may be associated with expansion during intercurrent illness, and similar lesions may be seen elsewhere in the skin and mucous membranes of the head and neck. The histopathological distinction between these two lesions may also be difficult; however, the varix is clearly a venous lesion in character with well-defined venous channels, whereas the lymphangioma is composed of thin-walled endothelially lined vessels, stromal lymphorrhages, and both serous or blood-filled channels (some occasionally dysplastic) with the less uniform presence of smooth muscle in the walls and stroma. It is not surprising that the clinical syndromes are similar when the varix is nondistensible, because both lesions have either very slow or no flow and are probably of similar embryologic origin. However, the varix can be demonstrated to have venous connections on direct injection or injection of tributary veins (periorbital or internal jugular venography). In contrast, we have shown that direct injection of lymphangiomas

fails to reveal any connection to either the arterial or the venous system. B-scan ultrasonography and CT scan may show abnormally dilated irregular veins or when there has been hemorrhage and multilobular lesions. A-scan ultrasonography shows well-delineated regular structures with low internal reflectivity and minimal attenuation due to the congested pools of blood in the dilated veins. In our experience, the described appearance on CT scan and ultrasonography is not pathognomonic. As noted, many of these lesions may be combined venous-lymphatic in character.

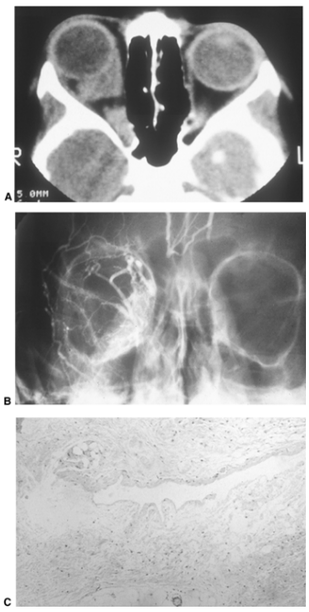

Figure 13-15. (A) This 10-year-old child presented with a history of recurrent, sudden onset of painful proptosis followed by the appearance within days of subconjunctival blood. (B) On venography, she demonstrates a complex venous vascular malformation, which was excised following a visually threatening episode. (C) Histology shows a complex dysmorphic venous channel (H&E, original magnification × 10). She subsequently developed macroaneurysms in the peripheral retina of her right eye.

Management

The two indications for intervention in nondistensible orbital venous vascular malformations are the same as those for the so-called lymphangiomas. One is extreme orbital pressure with functional deficit and the other is cosmetic disfigurement. Profound orbital hemorrhage leading to visual deterioration and severe pain may necessitate surgical intervention but in many cases, these can be managed conservatively either by observation or aspiration of intracyst contents. Surgical management consists of deep orbital exposure with evacuation of clotted blood and excision of the associated lesion. This can be aided by the use of CO_2 laser. These lesions may not be well defined and may contain clotted blood and a mixture of spaces filled with fresh unclotted old blood at the time of surgery. The originating varix and out-flow channels may be impossible to find, in which case only evacuation and decompression can be performed. Preoperative recognition of a significant venous component aids in preventing unexpected hemorrhage. The more superficial components can be handled by subcutaneous or anterior orbital dissection with either frequent use of bipolar cauterization or CO_2 laser.

Lymphatic and Combined Venous-Lymphatic Vascular Malformations

Combined venous-lymphatic malformations are for the most part hemodynamically isolated vascular hamartomas, aside from the previously noted instances of combined distensible venous-lymphatic lesions. The concept of this lesion in the orbit seems incongruous since evidence suggests that postseptal or deeper portions of the orbit do not normally have lymphatic channels. In spite of this, lymphangiomas consistently described in the orbit have been the center of considerable controversy; in particular, separation of lymphangiomas from orbital varices have been a source of confusion with a failure to emphasize the importance of hemodynamic considerations. However, we believe the fundamental differentiation (particularly from distensible lesions) should be based on clinical, hemodynamic, and histopathologic criteria. The distinguishing characteristic of this group of lesions consists of relative hemodynamic isolation with clinical features based on extent and location. These combined venous-lymphatic lesions are congenital vascular malformations arising from the venous anlage and have a unique combination of clinical, radiologic, and histologic characteristics. They are combined vascular malformations within the spectrum of arterial, venous, and lymphatic lesions that have characteristics of lymphatic and venous components.

The four patterns of occurrence are based on location: superficial, deep, and combined, and there may be complex lesions that involve combined orbital components along with facial, intracranial, and systemic features. The location of these lesions governs differences in clinical presentation, noncontiguous associations, complications, and management.

Histopathologically, lymphangiomas are better understood as a spectrum of vascular hamartomas with similar fundamental components and relative hemodynamic isolation. Features include diaphanous, serous-filled vascular channels, collagenous stromal network, evidence of recurrent and old hemorrhage, lymphorrhages (accumulations of lymphocytes), dysplastic vessels, and randomly occurring bundles of smooth muscle (Fig. 13-16). For the most part, the endothelially-lined channels contain serous fluid but may also contain blood or an admixture of blood and blood products, especially in the deeper combined components. Ultrastructurally, a mixture of abnormal vessels is found with characteristics of both blood and lymph vessels (Fig. 13-17).

Superficial Lesions

Superficial lymphangiomas typically are visible lesions of the conjunctiva or lid alone. They consist of multiple clear cystic structures or may contain an admixture of xanthochromic or partially blood-filled cysts (Fig. 13-18A). On the other hand, they may simply consist of a transilluminatable bluish cyst just beneath the skin. The isolated superficial lesions are probably the only category that can be purely lymphatic in character. If cosmetically unacceptable they can be removed with relative ease because of their limited location and small size.

Deep Lesions

Deep lymphangiomas may present with sudden proptosis due to spontaneous hemorrhage into what was a previously unrecognized lesion (Figs. 13-19 and 13-20). In our experience, the majority of them occurred in childhood, and in all

cases the clinical picture was similar. Only four demonstrated significant features of venous connection, either by expansion on Valsalva maneuver or change in size on coronal CT scan. The remainder (34) did not demonstrate features of deep vascular connection. The majority of patients in this category presented with a spontaneous hemorrhage associated with exophthalmos, which may be sudden or develop over several weeks. Occasionally, they develop as gradually increasing proptosis. A significant number of these patients (over half) have compressive symptoms with decreased visual acuity, papilledema, and optic nerve conduction defects.

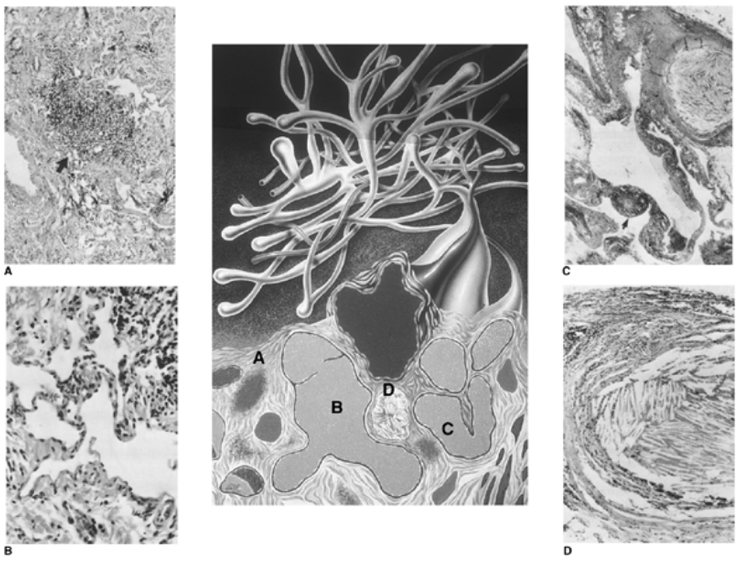

Figure 13-16. Histopathologic and schematic spectrum of components of lymphangiomas, showing large, diaphanous, endothelially-lined vascular channels (B, C) with stromal connective tissue and lymphorrhages (A, C: arrows). Note evidence of old bleeding with formation of cholesterol clefts (C, D) (H&E, original magnifications: A, × 10; B, × 25; C, × 2.5; D, × 10). (Reproduced with permission from Rootman J, Hay E, Graeb D, Miller R. Orbital-adnexal lymphangiomas: a spectrum of hemodynamically isolated vascular hamartomas. Ophthalmology 1986;93:1558-70.)

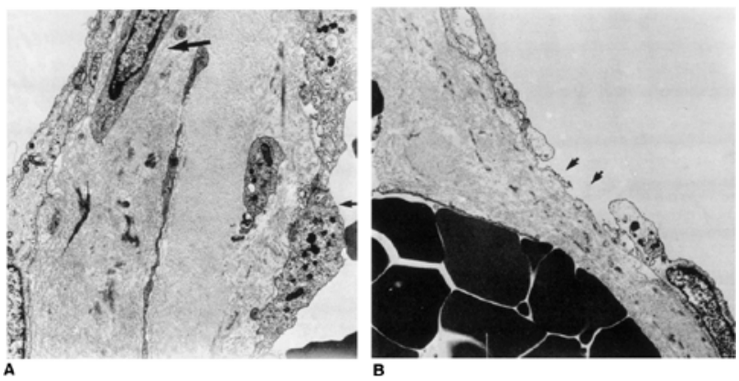

Figure 13-17. Electron micrographs of tissue obtained from a combined venous-lymphatic malformation (lymphangioma). (A) Stroma between two ectatic lumina of a blood vessel-like capillary. Note tight endothelial apposition (short arrows) and pericytes (long arrows). (B) Lymphatic-like space next to a red cell-containing vascular channel. Note absence of pericytes, and endothelial gap typical of a lymphatic vessel (short arrows) adjacent to fluid-containing lumen (original magnifications: A, × 7280; B, × 5600). (Reproduced with permission from Rootman J, Hay E, Graeb D, Miller R. Orbital-adnexal lymphangiomas: a spectrum of hemodynamically isolated vascular hamartomas. Ophthalmology 1986;93:1558-70.)

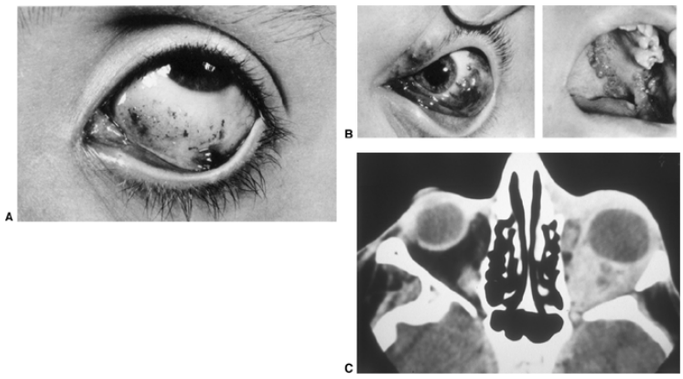

Figure 13-18. Combined lymphangioma. (A) Clinical photograph shows multiple characteristic conjunctival cysts present since birth, some of which contain clear or xanthochromic fluid while others contain blood. A deep component was noted behind the globe on CT scan. Biopsy showed a series of fine, endothelially lined vascular channels with only connective tissue stroma. (B, left) Epibulbar surface and (B, right) mouth of a patient who had a histologically confirmed complex venous-lymphatic malformation. Note typical multicystic oral lesions, some with blood and others with clear or xanthochromic fluid. (C) CT scan demonstrates intra- and extraconal components as well as orbital expansion associated with this massive malformation.

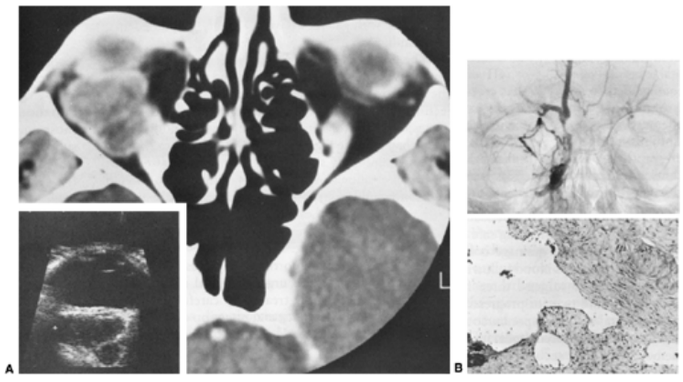

Figure 13-19. (A) CT scan after contrast injection shows a right-sided deep lymphangioma presenting as a low-density cystlike mass with rim enhancement. (A, inset) Ultrasonogram demonstrates a lobular mass with few internal echoes, causing flattening of the globe. The patient presented with a 6-week history of rapid onset of orbital mass effect, which was exacerbated by a needle aspiration several days before referral. (B) Orbital venogram of this patient demonstrates only slight stretching and displacement of the superior ophthalmic vein with no connection to the lesion. Histology of the margin shows large, thin-walled, endothelially lined vascular channels without a smooth muscle layer surrounded by a loose collagenous stroma with little intraluminal blood. The central cavity contained decomposed blood products. (Reproduced with permission from Rootman J, Hay E, Graeb D, Miller R. Orbital-adnexal lymphangiomas: a spectrum of hemodynamically isolated vascular hamartomas. Ophthalmology 1986;93:1558-70.)

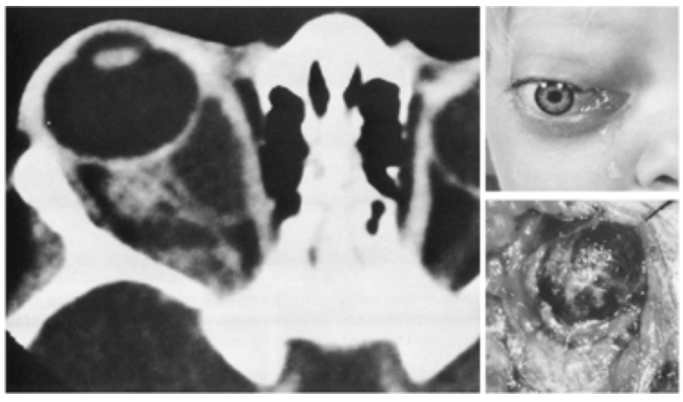

Figure 13-20. Deep combined venous-lymphatic malformation (lymphangioma). Clinical photograph shows massive proptosis progressing over a 2-week period and leading to papilledema with choroidal folds. CT scan after injection of contrast demonstrates a large, medial cystlike area with posterior rim enhancement and a mottled, lateral, irregularly enhancing component. Bottom inset demonstrates the hemorrhagic cystic component at surgery. (Reproduced with permission from Rootman J, Hay E, Graeb D, Miller R. Orbital-adnexal lymphangiomas: a spectrum of hemodynamically isolated vascular hamartomas. Ophthalmology 1986;93:1558-70.)

We have recently noted a subgroup of orbital venous lymphatic malformations (lymphangiomas) that can mimic cavernous hemangiomas (Fig. 13-21). Patients in this group presented with very slowly evolving proptosis. On CT, there was a relatively homogeneous intraconal mass that was well defined anteriorly. On contrast enhancement using MR imaging, there was heterogeneous enhancement. The clinical picture and CT findings suggested cavernous hemangioma and intraoperatively the lesion resembled cavernous hemangioma. However, posterior dissection was difficult in all patients due to dense adhesions and irregular extension of the lesion. Histologically, they were all characteristic of orbital venous lymphatic malformations.

Imaging

The CT scans of patients in the deep category show low-density cystlike masses behind the orbital septum in the intraconal and extraconal spaces. With contrast injection, a thin rim of enhancement may be noted, which corresponds histologically to abnormal endothelially lined channels (Fig. 13-20). In addition, some of the patients may show focal enhancing areas outside the cystlike region and enlargement of the bony orbit. On ultrasonography, retrobulbar cystic masses are noted. Both angiography and orbital venography fail to demonstrate a vascular component, showing only displacement of normal vessels. Direct injection leads to persistent pooling of contrast medium. MRI delineates the structure of the lesion with evidence of subacute and chronic hemorrhagic cysts by differing paramagnetic qualities (Fig. 13-21B). As well, it identifies the solid component of the lesion and is the imaging modality of choice.

Management

Acute orbital hemorrhage may cause optic nerve compression and require urgent surgical management. They can be successfully treated by careful dissection, evacuation of hematic cysts, and resection of the offending vascular anomaly (Fig. 13-20). Contrast CT scan can give some guidance to the area of a vascular anomaly, because it appears as either rim or irregular focal enhancement. Nevertheless, the surrounding orbital tissues are not infrequently densely scarred and interdigitated with the malformation; differentiation of normal and abnormal tissues at the time of surgery may thus be very difficult, making safe total excision complicated. Postoperative drainage is recommended to avert any sequestration of blood following surgery. Twelve of our patients underwent surgery, six for progressive proptosis and six for compressive optic neuropathy. One had slow (several months) spontaneous resorption. Five of our patients have required repeat intervention for recurrent hemorrhage on a second occasion, a reflection of the indistinct margins and

difficulty of complete excision. Some authors suggest repeat drainiage of cysts as a conservative measure to reduce intraorbital pressure and volume.

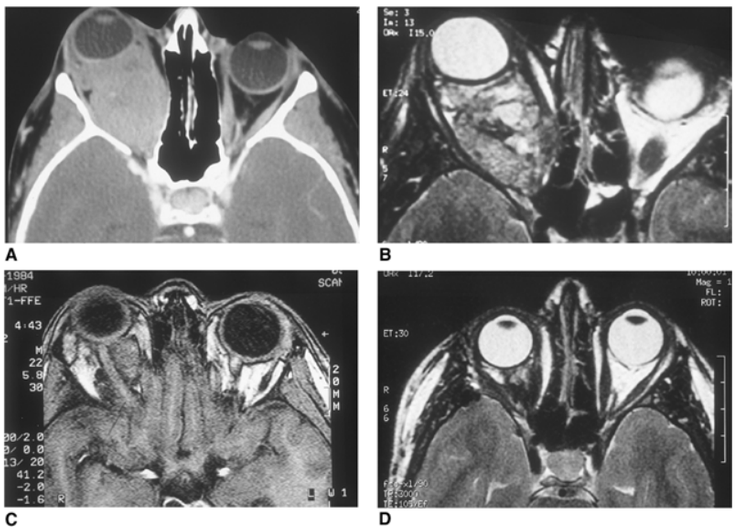

Figure 13-21. (A) CT scan demonstrates a massive venous-lymphatic malformation of the orbit in a 15-year-old with a 3-year history of progressive right proptosis and decreasing vision. On examination, the vision was 20/60 with an afferent pupillary defect, widened interpalpebral fissure, 3 mm of downward displacement, and 10 mm of exophthalmos, which was the same on Valsalva maneuver. She had a 30 diopter esotropia with an 8 diopter hypotropia, and there was evidence of papilledema. There is a large, multilobular lesion with expansion of the orbit, which on MRI (B) shows focal, hyperintense areas on T2-weighted scans. It displaces the optic nerve superiorly (C). She underwent an extended circumferential panorbitotomy in July 1999 with excision of the mass. (D) This T2-weighted MRI demonstrates the orbit 3 months postoperatively. Her vision at that time was 20/40 without an afferent pupillary defect; exophthalmometry was 11 mm on the right and 15 mm on the left with a 25 diopter right hypotropia and 14 diopter esotropia. At 14 months postoperatively, her vision was 20/25-2 with an exophthalmometry measurement of 14 mm on the right and 16 on the left. She had a 20 diopter right hypotropia and a 14 diopter esotropia and will undergo strabismus surgery.

Combined and Complex Lesions

Because of their extent, combined lymphangiomas are usually recognized within the first year of life and enlarge over many years. They may have intermittent spontaneous bleeds. Hemorrhages into the deep portion can cause optic nerve dysfunction; those into the superficial component cause recurrent subconjunctival hemorrhages, periorbital ecchymosis, and swelling. However, unlike the deep type, the diagnosis of lymphangioma is made obvious by the visible component. The superficial portion consists of multiple conjunctival and lid cysts, some of which are filled with clear or xanthochromic fluid and others with blood or menisci. In addition, in a third of these cases (two of six in our series) similar cystic lesions of the mucous membranes of the mouth may be noted (Fig. 13-18B). The combined lesions are frequently massive in size, involving the intraconal, extraconal, preseptal, and postseptal spaces. The very large lesions produce significant cosmetic disfigurement and frequently decreased vision from either optic atrophy (as a result of spontaneous hemorrhages in the orbit) or amblyopia. Two of our patients have had cerebral hemorrhages due to an isolated intracranial vascular anomaly (Figs. 13-22 and 13-23). These two patients led us to explore the intracranial contents of these lesions and we noted that 27% (7/26) had radiologic evidence of noncontiguous intracranial vascular anomalies, a feature not previously noted and worthy of recognition. The intracranial lesions had the radiologic characteristics of developmental venous anomalies. It should be noted that the overwhelming majority of these cases were associated with diffuse orbital lesions with superficial and deep components that demonstrated orbital bony expansion, intraconal and extraconal components, as well as evidence of extension through the superior fissure or into the pterygopalatine fossa.

Imaging

Imaging demonstrates large soft tissue masses that cross boundaries of both pre- and postseptal spaces as well as intra- and extraconal compartments. The diffuse lesions are frequently poorly defined at their margins and on contrast injection show inhomogeneous enhancement and some rounded cystlike nonenhancing areas within the tumor mass with different paramagnetic qualities. Enlargement of the orbit is frequent. No connection to the arterial or venous system can be demonstrated clinically or by contrast studies (Fig. 13-24).

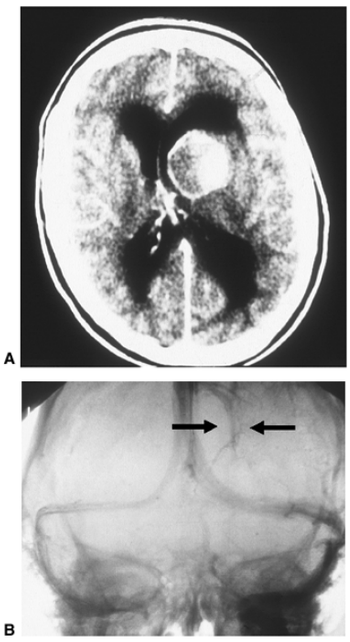

Figure 13-22. This 22-year-old female had bare light perception on presentation with a diffuse left orbital lymphangioma (demonstrated in Figs. 15-18B and C). At age 27, obstructive hydrocephalus developed due to a left basal ganglia hemorrhage (A), which required bilateral intraventricular shunts. (B) Angiography showed a developmental venous anomaly in the left hemisphere (arrows). A retrospective review of prior enhanced CT scans showed a developmental venous anomaly in the left basal ganglia. (Reproduced with permission from Katz SE, Rootman J, Vangveeravong S, Graeb D. Combined venous lymphatic malformations of the orbit (so-called lymphangiomas): association with noncontiguous intracranial vascular anomalies. Ophthalmology 1998;105:176-84.)

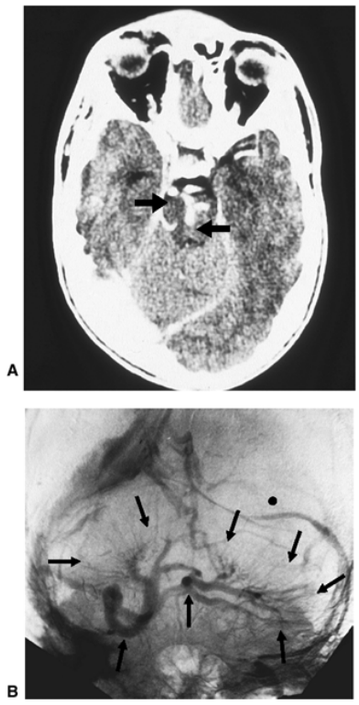

Figure 13-23. (A) Noncontiguous anomalous right perimesencephalic and transmesencephalic vessels (arrows) are noted in this 14-year-old male with a right orbital lymphangioma. (B) Angiogram demonstrates an extensive posterior fossa developmental venous anomaly with absence of the left transverse sinus (dot). (Reproduced with permission from Katz SE, Rootman J, Vangveeravong S, Graeb D. Combined venous lymphatic malformations of the orbit (so-called lymphangiomas): association with noncontiguous intracranial vascular anomalies. Ophthalmology 1998;105:176-84.)

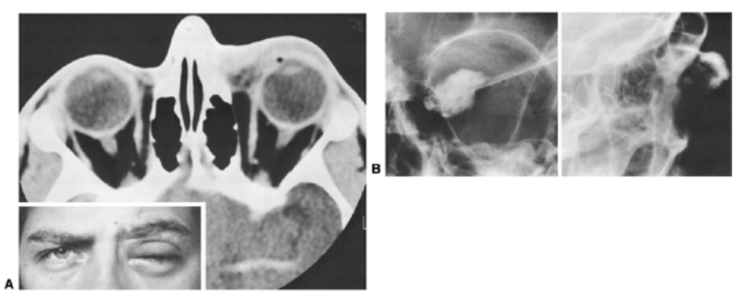

Figure 13-24. Combined lymphangioma. (A, inset) This 19-year-old man had a history of a mass lesion of the lid, conjunctiva, and anterior orbit that had been present since infancy, leading to amblyopia and esotropia. The conjunctival portion had typical cystic elements. He had multiple lid procedures. (A) CT scan with contrast demonstrates a variably enhancing mass in the anterior orbit, lid, and conjunctiva. (B) Preoperative intralesional injection of contrast demonstrated multiple fine vascular channels with no dispersion or connection to the venous system, demonstrated on both early and late films (done at 30 minutes). (Reproduced with permission from Rootman J, Hay E, Graeb D, Miller R. Orbital-adnexal lymphangiomas: a spectrum of hemodynamically isolated vascular hamartomas. Ophthalmology 1986;93:1558-70.)

Management

Combined lesions require orbital surgery either on an urgent basis, when there is an acute retrobulbar hemorrhage with optic nerve compression, or on an elective basis to deal with cosmetic disfigurement or chronic compression. Because of the large size and widespread orbital involvement, the prognosis for successful management is more guarded than for superficial lesions. Carbon dioxide laser surgery may aid in the management of these lesions. We have in a number of cases done a circumferential panorbitotomy in an attempt to excise as much of the offending lesion as possible.

In summary, combined venous-lymphatic vascular malformations (lymphangiomas) present a spectrum of vascular hamartomas with histopathologic features that identify them as a group paralleling the histology of similar lesions elsewhere in the head and neck. This includes the presence of diaphanous, serous-filled vascular channels, a loose connective tissue stroma, lymphorrhages, features of old hemorrhage, randomly distributed smooth muscle bundles, and dysplastic vessels. There is usually no clinical evidence of active hemodynamic connection (i.e., no bruit or change on Valsalva maneuver), and there is minimal or no direct arterial or venous connection on radiographic studies or direct or indirect contrast injection studies. The relative hemodynamic isolation of these thin-walled vascular channels explains the pathophysiology of this lesion. Bleeding may result from sludging, minimal trauma with rupture of a component vessel, or possibly spontaneous hemorrhage from fragile neovascular tufts. In addition, the intermittent and slow expansion of the mass may be related to an osmotic process with imbibed tissue fluids. It should be emphasized that the differentiation of these lesions from nondistensible venous varices on clinical and imaging grounds may be impossible and that they really represent part of the lymphatic venous spectrum of the vascular malformations. Overall, the constellation of clinical and investigative features may be sufficiently distinctive to warrant an attempt to separate these lesions into a category of their own that can be divided into superficial, deep, combined, and complex types. A minority (only four in our series) had both lymphatic and distensible venous components. The clinical manifestations, prognosis, and management directly correlate with the pathophysiology and location of the lesions.

Other Congenital Vascular Malformations

Of the four congenital vascular anomalies discussed in this section, one (Sturge-Weber syndrome) is a phakomatosis as originally described. (The other conditions are tuberous sclerosis, neurofibromatosis, and von Hippel-Lindau disease.) The phakomatoses are characterized by the presence of cutaneous

or mucosal nevi, hamartomas, or neoplastic growths. The central nervous system and eyes are most prominently involved, but abnormalities are frequently seen in other organ systems as well.

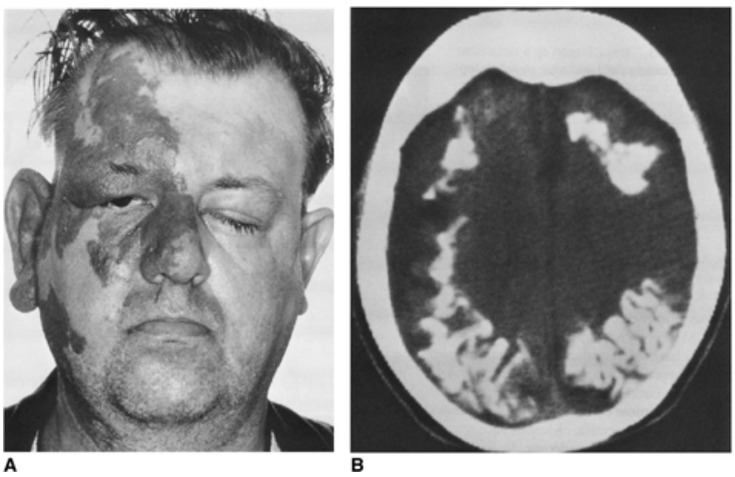

Figure 13-25. (A) Clinical photograph of a patient with Sturge-Weber syndrome (meningofacial angiomatosis). Note that the facial nevus flammeus does not conform to the midline. The patient had ipsilateral glaucoma. The left eye is closed secondary to recent radioactive plaque surgery for an unrelated uveal melanoma. (B) CT scan demonstrates characteristic serpiginous calcifications conforming to the sulcal convolutions.

The term *phakomatosis* is purely morphologic and descriptive and does not imply any pathogenetic link among these disorders. More recently, many new syndromes, including the three other conditions discussed in this section (hereditary hemorrhagic telangiectasia, Wyburn-Mason syndrome, and Klippel-Trenaunay syndrome) have been added to the phakomatoses, and the term *neurocutaneous syndromes* applied to all of them.

These conditions are all rare. Sturge-Weber syndrome is the most common, followed by hereditary hemorrhagic telangiectasia, Klippel-Trenaunay syndrome, and Wyburn-Mason syndrome. In all of them, ophthalmologic involvement is more frequent and integral to the diagnosis than is orbital involvement. Aditionally, these complex vascular malformations may occur in combinations.

Sturge-Weber Syndrome

A multitude of descriptive terms exist for Sturge-Weber syndrome, the most widely accepted being *encephalofacial angiomatosis.* However, it is the mesodermal coverings of the brain, meninges, and cranial bone that are involved by the angiomatous malformation, rather than the brain itself. The term *meningofacial angiomatosis* would more accurately describe this syndrome.

The minimum criteria for the diagnosis consist of a port wine nevus (nevus flammeus) of the face with ipsilateral leptomeningeal angiomatosis. The angiomatosis is responsible for the highly characteristic intracranial calcification and also very frequently results in focal seizures and contralateral hemiparesis. Ipsilateral glaucoma and buphthalmos are very common. Although incomplete forms have been reported in families, the heredity of this syndrome is uncertain.

The facial nevus is present at birth. It is usually flat, reddish-violet, and blanches on pressure. There are no case reports of the Sturge-Weber syndrome in which the nevus did not involve at least the upper eyelid or the supraorbital face and scalp. This anomaly is usually unilateral but frequently the medial boundary does not conform strictly to the midline. Occasionally, it may cross the midline or be present to a more or less equal extent bilaterally (Fig. 13-25). Similar dermal lesions are frequently found in the oropharynx, trunk, and limbs. Pathologically, they consist of dilated endothelially lined vessels situated in the mid- and deep dermis.

The leptomeningeal angiomatosis is almost always unilateral and most commonly in the occipital or parieto-occipital region, although infrequently the entire hemisphere may be involved. The thickened meninges contain a dense tangle of malformed vessels several layers thick. Frequent areas of hyalinized connective tissue are seen in their walls. Hypervascularity of the underlying cerebral cortex and subcortical white matter is frequently found without frank vascular malformations.

The cortex underlying the malformation is generally atrophic with microscopic evidence of nerve cell loss, degeneration, and gliosis. Associated cerebral malformations are invariable, including microgyria, agyria, polygyria, heterotopias, and ectopias. Capsular hypertrophy and ectopia of the ipsilateral gasserian ganglion have also been described, implying a topographic coordination between the meningofacial malformation and the trigeminal sensory root ganglion. Meningeal hypervascularity has also been described in the spinal cord along with ectopic dorsal root ganglion cells and glial proliferation. Capillary angiomas may also be found in the kidneys, spleen, ovaries, intestine, adrenals, thyroid, pancreas, and lung.

Microscopically, two kinds of calcification are noted, consisting of fine granular deposition in the walls of small vessels and large coarse calcifications that are free within the cortex, predominantly in layers two and three (the molecular and pyramidal layers). These calcifications are seldom radiologically apparent before the age of 2 years, but become almost universal by adolescence. The finding of paired parallel serpiginous calcifications conforming to the sulcal convolutions on either plain films or CT is diagnostic (Fig. 13-25). The calcifications are believed to be secondary to vascular stasis and tissue hypoxia.

Nevi confined to the forehead tend to be associated with angiomatosis overlying the occipital lobe, whereas nevi involving the maxillary area are associated with parietal angiomatosis. This is explained by the anatomic relationship of these areas during early fetal life when the primitive circulation to the brain and its coverings is being differentiated. A congenital lack of vasomotor innervation has been thought to be a contributing factor in the secondary vascular abnormalities, leading to hyperplasia and dilatation of the abnormal vessels. It has been postulated that the deficiency is in the parasympathetic supply, which is distributed by means of sensory branches of the trigeminal nerve.

At angiography, the leptomeningeal angiomatosis does not opacify or is opacified only faintly, presumably due to very slow flow. A decreased number of superficial cortical veins has been described in the region of the angiomatosis with a corresponding increase in the deep venous system, which serves as a collateral route of drainage.

Homonymous hemianopia can be seen because of involvement of the visual cortex by leptomeningeal angiomatosis, although this sign may be difficult to elicit in many of these patients owing to intellectual abnormalities.

Seizures, both focal and generalized, usually begin in infancy and ultimately affect 90% of patients. Subnormal mentality is also present in about 50%. Hemiparesis and intellectual impairment may progress with uncontrolled seizures, and early lobectomy has been recommended by some for controlling seizures and preventing progressive neurologic and intellectual deficit.

From the ophthalmologic point of view, lid involvement, buphthalmos, and/or glaucoma are the most common abnormalities, found in about 30% of patients. Although not entirely agreed upon, the cause is thought to be related to both elevated episcleral venous pressure secondary to episcleral hemangiomas and angle cleavage anomalies. If the patient develops retinal detachment for a long period of time, neovascular glaucoma may ensue.

Diffuse choroidal angiomas, or hypertrophy, are also frequently found and recognized as a dark posterior pole or “tomato catsup” fundus. There may be secondary retinal detachment and/or some additional focal areas of angiomatous thickening with a background of diffuse angioma. Occasional instances of focal angiomas have been noted. Microscopically, these are cavernous hemangiomas consisting of large, dilated, endothelially lined channels separated by scanty connective tissue. When extensive, treatment with external beam radiotherapy may control progression. If localized, plaque radiotherapy may be useful. Atrophy and cystic degeneration of the overlying retina are frequently present. The angiomas may calcify, occasionally sufficiently to be seen radiographically. Angiomas may also be seen in the conjunctiva or episclera. Glial proliferation of the optic nerve and generalized hypervascularity of the globe and nerve may also be found.

Hereditary Hemorrhagic Telangiectasia (Osler-Weber-Rendu Syndrome)

Hereditary hemorrhagic telangiectasia is a rare autosomal dominant disorder that is characterized by the presence of numerous telangiectasias of skin and mucous membranes and associated with progression and repeated episodes of hemorrhage. The telangiectasias range in size from pinpoint lesions to spider nevi several millimeters in diameter; they are usually flat but may occasionally be nodular. Varying in color from bright red to purple or violet, they are seldom seen before the second or third decade, and increase in size and number thereafter. In addition to the skin, frequent sites of involvement include the nasal, oral, and gastrointestinal mucosa. Repeated episodes of epistaxis and gastrointestinal hemorrhage are common.

Widespread visceral involvement is also frequent, with pulmonary arteriovenous fistulas and malformations being the most important clinically. These are often multiple, predominate in the lower lobes, and are responsible for polycythemia, paradoxic embolism, and brain abscess. Hemoptysis

is also seen and may rarely be associated with air embolism. About 15% of patients with hereditary hemorrhagic telangiectasia have demonstrable pulmonary arteriovenous fistulas; 40% to 60% of patients with pulmonary arteriovenous fistulas or malformations have hereditary hemorrhagic telangiectasia.

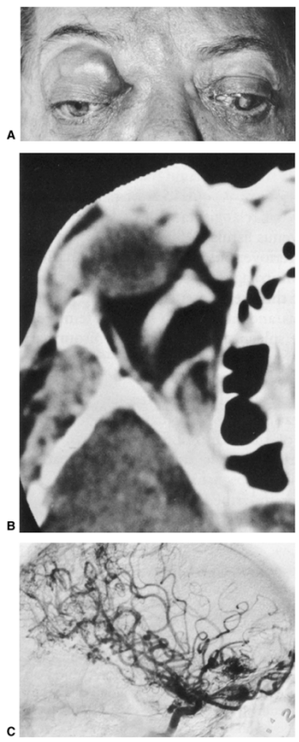

Figure 13-26. Clinical, CT, and angiographic features of a case of Rendu-Osler-Weber syndrome. (A) Clinical photograph shows a massively enlarged pulsatile vein in the right upper lid. (B) CT scan shows enlarged superior ophthalmic and lid veins. (C) Arteriogram demonstrates multiple arteriovenous malformations, aneurysms, and fistulas including an arteriovenous malformation in the orbit.

Involvement of the liver is associated with a process resembling cirrhosis and rarely with portosystemic encephalopathy. The spleen, pancreas, and genitourinary tract may also be involved.

In the central nervous system, a wide range of vascular abnormalities may be seen, the most frequent being small punctate telangiectatic lesions. They may be single or multiple, in any part of the brain, and are almost always asymptomatic. Arteriovenous malformations, aneurysms, dural arteriovenous fistulas, and cavernous angiomas have all been described.

Orbital involvement is uncommon. Scattered case reports describe conjunctival telangiectasia, varix-like ectatic formations of the retinal veins, telangiectasia of the optic nerve, and orbital arteriovenous malformations (Fig. 13-26). A proliferative vascular retinopathy has also been described.

The telangiectatic lesion has a similar pathology in all organs studied and consists of proliferation and dilatation of small venules. Electron microscopic studies have shown defective overlapping of terminal villi of the endothelial cells, with many endothelial gaps plugged with thrombi. These small venules lack perivascular support due to an absence of pericytes, smooth muscles, and elastic fibers thus increasing their tendency to hemorrhage. Local hyperfibrinolysis has also been described in these lesions.

Wyburn-Mason Syndrome

The rare Wyburn-Mason syndrome consists of the association of retinal arteriovenous communications with deep-seated ipsilateral cerebral arteriovenous malformations involving the visual pathway. Arteriovenous malformations may also be found in the facial soft tissues, mandible, or maxilla. Facial nevi are the least constant element in this syndrome and are usually ipsilateral within the trigeminal nerve distribution. They most commonly consist of a faint reddish blush with scattered punctate red spots but typical portwine pigmented nevi may also be found.

The retinal lesion consists of a direct communication between a retinal artery and vein, usually without any intervening vascular network. Retinal arteriovenous communications may also occur rarely as an isolated abnormality.

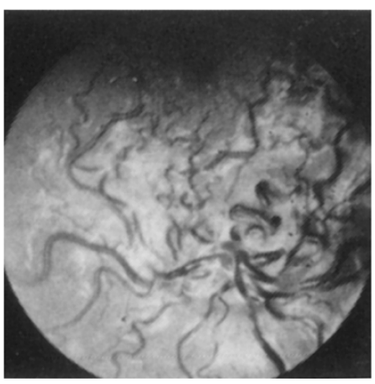

Figure 13-27. Fluorescein angiogram of a patient with Wyburn-Mason syndrome demonstrates the complicated arteriovenous communication of the retinal vessels in this disorder.

There is a broad spectrum of abnormality, ranging from barely visible single communications to multiple complex communications with strikingly prominent findings. The more complex lesions tend to be associated with the Wyburn-Mason syndrome (Fig. 13-27).

The involved arteries and draining veins are enlarged and tortuous, sometimes reaching 500 to 600 meters in diameter, and it may be difficult to distinguish arteries from veins on fundoscopy. Fluorescein angiography demonstrates rapid flow through the feeding artery. The site of arteriovenous communication is usually evident as an abrupt increase in vessel caliber when the dye reaches the venous side. Laminar flow is usually seen in the draining vein, with rapidly flowing shunted blood occupying the central portion of the blood vessel column.

The larger, complex communications are associated with visual impairment or total visual loss, retinal edema and exudates, and cystic retinal degeneration. Retinal hemorrhages also occur and may be related to thrombosis of a draining vein.

Cerebral arteriovenous malformations may occupy part or all of the ipsilateral visual pathway from the optic nerve to the visual cortex. There is frequent extension into the dorsal midbrain, pons, cerebellum, and thalamus. These lesions may in fact be bilateral.

Clinical findings are related to the amount and site of involvement. There is usually some impairment of visual acuity with the large malformations seen in the Wyburn-Mason syndrome, although the smaller isolated arteriovenous communications are frequently incidental. The patient frequently presents in childhood with unilateral amblyopia, esotropia, or both. Later in life visual failure may develop, either suddenly or gradually. Involvement of the optic nerve and orbital soft tissues may be associated with pulsatile proptosis. Hemianopia is frequent owing to involvement of the optic chiasm or post-chiasmatic visual pathway. The cerebral AVM may lead to hemiparesis, hemiplegia, seizures, or subarachnoid hemorrhage.

Plain orbital radiographs and CT scans will show enlargement of the optic canal and occasionally of the bony orbit, which is due to involvement of the optic nerve and orbital structures with arteriovenous malformation. The arteriovenous malformation itself will be seen on CT scan as a poorly defined enhancing mass. Contrast-enhanced CT or CT angiography of the head and orbits followed by confirmatory angiography should be performed in all patients with retinal arteriovenous communications to diagnose the full extent of the abnormality, particularly the intracranial component.

Klippel-Trenaunay Syndrome

Klippel-Trenaunay syndrome consists of the association of cutaneous hemangiomas and venous varicosities, usually confined to a single limb, with bony and soft tissue hypertrophy of that limb. There are rare reports of associated orbital vascular anomalies, which include varices, conjunctival telangiectasia, retinal varicosities, and angiomas of the conjunctiva, sclera, and choroid. A single case of enlarged optic nerve and medial rectus muscle has been reported in association with this syndrome.

Acquired Arteriovenous Shunts (Dural Carotid Cavernous Fistulas)

The orbital vessels may be involved in acquired arteriovenous shunts to varying degrees and by different mechanisms. The arteriovenous fistulas or shunts can be classified pathogenetically into spontaneous or traumatic fistulas, hemodynamically into high- or low-flow, and angiographically into direct or dural fistulas.

Anatomy and Classification

A dural carotid cavernous fistula is an abnormal communication between meningeal branches of the internal and/or external carotid arteries and cavernous sinus. They may arise from the intracavernous branches of the internal carotid

artery (typically the meningeal hypophyseal trunk or artery of the inferior cavernous sinus) or from the external carotid system via the internal maxillary, ascending pharyngeal, and occipital arteries, which provides meningeal supply in the region of the cavernous sinus.

Table 13-3. Table of Barrow's types of carotid cavernous fistula.

BARROW TYPE	ORIGIN	VESSELS INVOLVED	OUR EXPERIENCE	MANAGEMENT
Type A	Trauma, rarely ruptured aneurysm	Internal carotid	13/26	Balloon or surgical occlusion
Type B	Spontaneous	Meningeal branches of the internal carotid	0/26	Selective or retrograde embolization; 20% to 50% close spontaneously
Type C	Spontaneous	Meningeal branches of the external carotid to cavernous sinus	3/26	Selective embolization or retrograde venous occlusion; 20-50% close spontaneously
Type D	Spontaneous	Meningeal branches of the internal and external carotid	10/26	Selective embolization or retrograde venous occlusion; 20-50% close spontaneously

The cavernous sinus is normally purely venous and drains in an anterior-posterior direction. Blood from the orbit and periorbital regions drain via the superior and inferior ophthalmic veins and the sphenoparietal sinus to collect in the cavernous sinus. Drainage from the cavernous sinus travels via the superior or inferior petrosal sinus into the lateral and sigmoid sinus or internal jugular vein, or via the basilar sinus into the pterygoid plexus.

Barrow has classified carotid cavernous fistula into four types (Table 13-3). Type A are direct, high-flow, internal carotid to cavernous sinus fistulas, which are usually post-traumatic but may be spontaneous from rupture of an aneurysm. The remaining dural fistulas are largely of spontaneous origin. Type B fistulas are shunts between meningeal branches of the internal carotid artery and the cavernous sinus. Type C fistulas are between meningeal branches of the external carotid artery and the cavernous sinus. Type D fistulas are shunts between the meningeal branches of both the internal and external carotid arteries and the cavernous sinus. Generally, type B fistulas are extremely rare while type C is slightly more common. Type D fistulas are by far the most common of the spontaneous dural fistulas (Table 13-3).

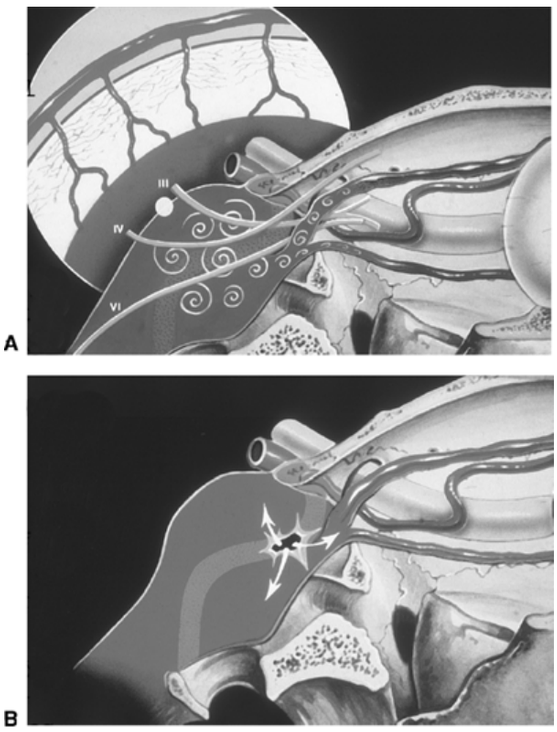

Figure 13-28. These schematic diagrams demonstrate the essential hemodynamics of dural (A) and carotid cavernous fistulas (B). The dural fistulas are characterized by in-flow from multiple dural arteries, which characteristically creates turbulence in these low-flow entities and accounts for their frequency of spontaneous thrombosis. The carotid cavernous fistula usually results from trauma but may be due to a ruptured aneurysm leading to a high-flow lesion in the cavernous sinus and retrograde flow through the orbital venous system.

Pathogenesis and Hemodynamics

Although there is some controversy concerning the pathogenesis of dural fistulas, venous thrombosis in the cavernous sinus is probably the initiating factor in the arteriovenous shunts of spontaneous onset (usually low-flow), and may also play an important role in the subsequent clinical course. It is postulated that as the thrombosed sinus (in this case, the cavernous sinus) becomes recanalized, pre-existing microscopic arteries in the wall of the dural sinus become enlarged sufficiently to constitute a significant hemodynamic shunt (Fig. 13-28A). Thrombosis of the superior ophthalmic vein will lead to eventual resolution of the orbital symptoms. On the other hand, thrombosis of the other venous exit routes of the cavernous sinus may increase the flow of blood to the superior ophthalmic vein and aggravate the symptoms. The remaining theories of origin of spontaneous arteriovenous fistulas propose that shunts occur secondary to rupture of intracavernous arterial vessels, or are congenital and remain asymptomatic while flow is in a posterior direction. Post-traumatic carotid cavernous fistulas (usually high-flow) result from a tear within the cavernous portion of the internal carotid artery itself or more rarely, from spontaneous rupture of an aneurysm (Fig. 13-28B).

The effect that acquired arteriovenous shunts have on orbital structures is directly related to the site and degree of shunting and is proportional to the volume of flow. Increased arteriovenous flow and pressure leads to venous dilatation, fluid transudation, and vascular turbulence, which may result in sludging and thrombosis. Higher-flow shunts have a greater effect, resulting in orbital swelling, chemosis, increased episcleral venous pressure (therefore, increased intraocular pressure), retinal vascular dilatation, pulsatile exophthalmos, and bruit. In contrast, low-flow shunts tend to manifest lesser signs and symptoms, consisting of edema and vascular dilatation with or without increased intraocular pressure (Fig. 13-29). Primary orbital shunts, defined as those where the arterial venous shunt is situated within the orbit, have already been described under congenital arteriovenous malformation, which may occur alone or as part of congenital syndromes. These flow in an antegrade fashion in contrast to the acquired shunts, which flow in an retrograde fashion.

Rarely, the orbital arteries may participate in the arterial supply of an arteriovenous shunt that occurs outside the orbit. In these cases, the main feature is arterial engorgement and there may in fact be a steal or ischemic syndrome.

Post-traumatic carotid cavernous fistulas (Barrow type A) result from a tear within the cavernous portion of the internal carotid artery itself (Figs. 13-28B and 13-30). The tear is the result of major head trauma, often associated with basal skull fracture. Occasionally, fistulas may follow a penetrating injury that passes through the orbit and superior orbital fissure to perforate the internal carotid artery. In either instance, a sizable hole is usually produced in the intracavernous portion of the artery. Because this portion of the artery is encased within a plexus of veins, an arteriovenous fistula results, which transmits increased blood flow and elevated pressure to the cavernous sinus and its tributaries, including retrograde drainage to the ophthalmic veins. The large arteriovenous shunt that ensues produces the signs and symptoms of a high-flow vascular lesion. The patient is usually aware of a pulsatile bruit from the time of the injury. Pulsatile exophthalmos is frequent and is associated with chemosis, orbital swelling, episcleral venous congestion, and elevated intraocular pressure. Cranial nerve palsies (usually third, sixth, or both) may result from pressure on the distended cavernous sinus but may also occur as the direct effect of trauma. Symptoms are frequently bilateral but are milder in the contralateral eye. Occasionally, if the hole in the internal carotid artery is quite small, post-traumatic carotid cavernous fistulas may present as a low-flow shunt.

The Barrow types B and D shunts (Figs. 13-31 and 13-32) are probably of spontaneous thrombotic origin. In contrast, the type C fistula between the meningeal branches of the external carotid artery and the cavernous sinus may result directly from minor trauma (Fig. 13-33). In these lesions, rather than the network of arteries, one sees only a single meningeal-feeding artery with a small shunt into the cavernous sinus. It has been postulated that minor trauma, hypertension, or straining may result in rupture of normal meningeal arteries to cause this variety of spontaneous arteriovenous shunt.

Shunts in other portions of the intracranial dural sinus network may occasionally cause orbital symptoms if the elevated pressure is transferred to the superior ophthalmic vein. Very rarely, the rapid venous drainage from an intracerebral arteriovenous malformation may cause similar symptoms.

In summary, the acquired arteriovenous shunts are either high-flow or low-flow. The high-flow lesions are usually post-traumatic carotid cavernous fistulas or more rarely, of spontaneous origin. The low-flow shunts are dural arteriovenous fistulas of the cavernous sinus region and are usually spontaneous or less often post-traumatic.

Clinical Features

The major manifestations of dural shunts consist of red eye, pain, diplopia, and bruit, and the mean duration of symptoms prior to diagnosis is about 3 to 4 months. Clinical signs consist of injection, proptosis, elevated intraocular pressure, sometimes retinal venous dilatation, and bruit (Fig. 13-29).

Episcleral injection is due to dilated episcleral vessels and if chronic, is associated with dilated iris vessels. Less frequently, we have noted flame hemorrhages, choroidal detachment, and cystoid macular edema, which may lead to visual loss (Fig. 13-34). Only about one third of the patients demonstrate bruit. Diplopia may result from orbital congestion or cranial nerve palsy related to increased pressure or thrombosis in the cavernous sinus. Major coexisting diseases are systemic hypertension and diabetes. Type C fistulas tend to occur in a younger age group.

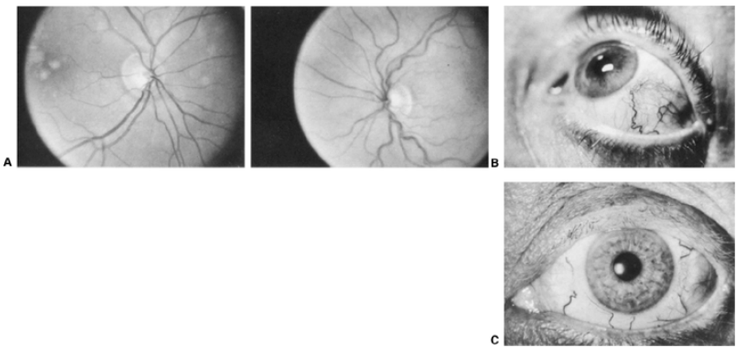

Figure 13-29. Clinical manifestations of low-flow arteriovenous shunts. (A) Vascular dilatation and tortuousity in the left posterior pole (versus normal right posterior pole). (B) This was associated clinically with epibulbar vascular dilatation and 3 mm of proptosis, which occurred spontaneously in a 72-year-old woman. (C) Epibulbar vascular dilatation and tortuousness in a 74-year-old woman who presented with a mild sixth nerve palsy, raised intraocular pressure (34 mmHg), and 2 mm of proptosis due to a low-flow shunt.

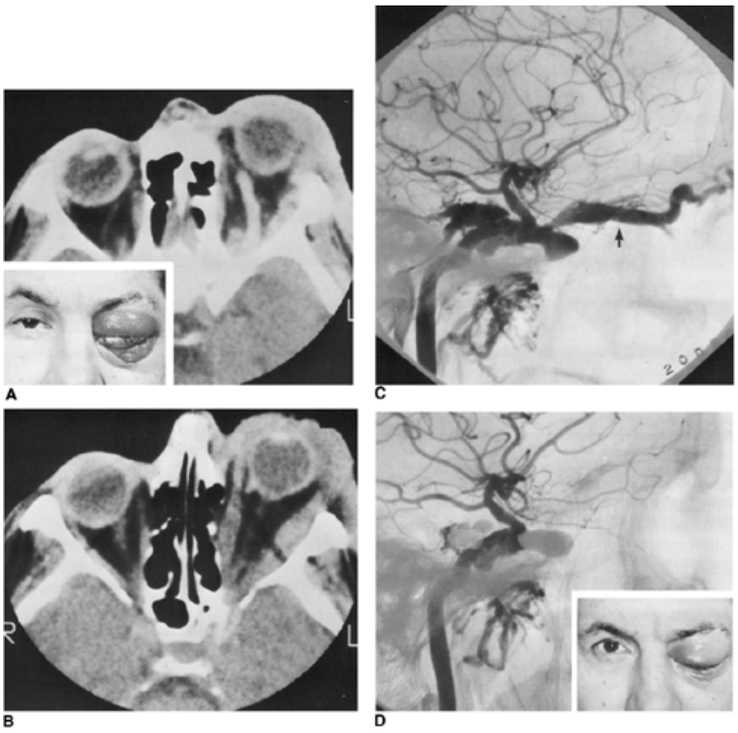

Figure 13-30. (A, B) CT and clinical features of a high-flow shunt (Barrow type A) following head trauma with marked orbital engorgement both clinically and on CT scan. Note enlarged superior ophthalmic vein, marked proptosis with tethering of the globe, and markedly enlarged extraocular muscles. (C) Arteriogram of the same patient shows a post-traumatic carotid cavernous fistula, with high-flow shunt into the cavernous sinus and retrograde drainage into the superior ophthalmic vein (arrow). (D) Angiogram following detachable balloon embolization of two separate fistulas with occlusion of the shunt to the superior ophthalmic vein. (D, inset) Early resolution 1 week after embolization.

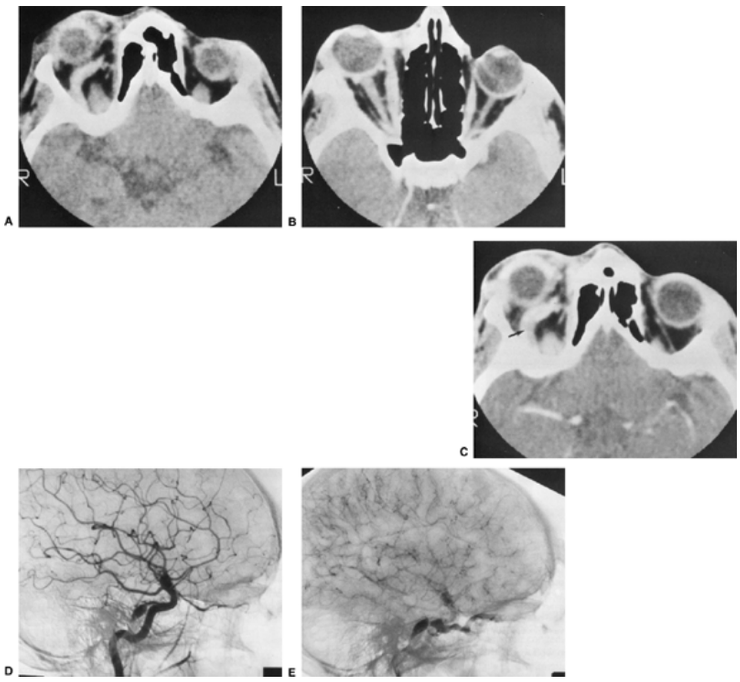

Figure 13-31. Contrast CT scan and angiographic features of a low-flow spontaneous arteriovenous shunt that demonstrates dilated superior ophthalmic (A) and vortex veins (B). (B) Note moderate enlargement of extraocular muscles and proptosis. (C) Contrast-enhanced CT scan taken 1 month later demonstrates partial resolution of symptoms, 2 days after angiography. Note intraluminal nonenhancing area consistent with a spontaneous thrombus (arrow). (D, E) Angiographic features of the carotid cavernous shunt of the same patient (Barrow type D). Note initial filling of the posterior cavernous sinus (D) with delayed retrograde opacification of the anterior cavernous sinus and the enlarged superior ophthalmic vein (E).

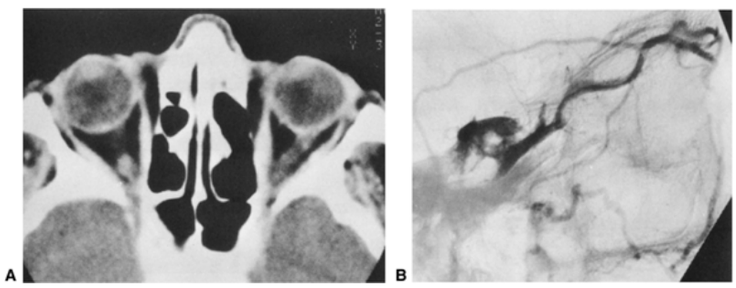

Figure 13-32. CT and angiographic features of a spontaneously occurring low-flow arteriovenous shunt (Barrow type D) in a 59-year-old woman. Note mild extraocular muscle enlargement on CT scan (A), and a shunt from the external carotid branches to the cavernous sinus with retrograde drainage into a relatively normal-size superior ophthalmic vein on angiography (B). This was associated with 3 mm of proptosis, normal intraocular pressure, slightly dilated retinal veins, and episcleral venous dilatation.

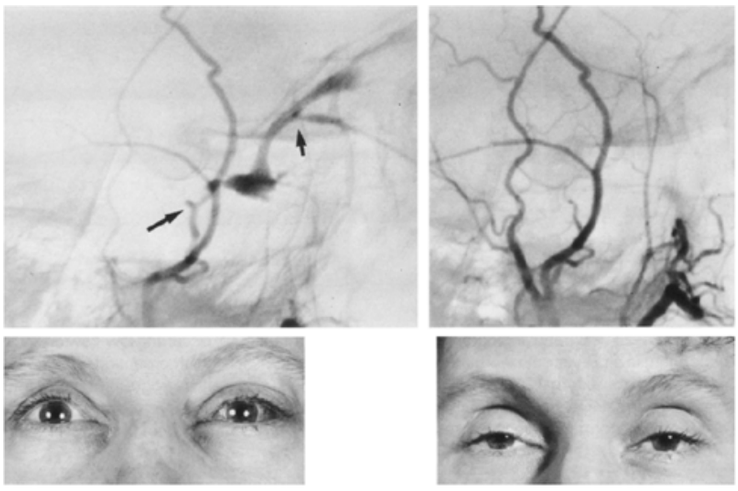

Figure 13-33. (Left) Angiography of a low-flow arteriovenous shunt (Barrow type C). The 54-year-old patient had a history of left lid swelling, mild proptosis, chemosis, decreased abduction, slightly raised intraocular pressure (22 mmHg), and epibulbar injection. Note slow filling of cavernous sinus from the accessory meningeal artery (long arrow) and retrograde drainage to a mildly dilated superior ophthalmic vein (short arrow). (Right) The same patient is shown 6 months later following embolization of the shunt, with absence of flow in the superior ophthalmic vein. Note resolution of ocular signs.

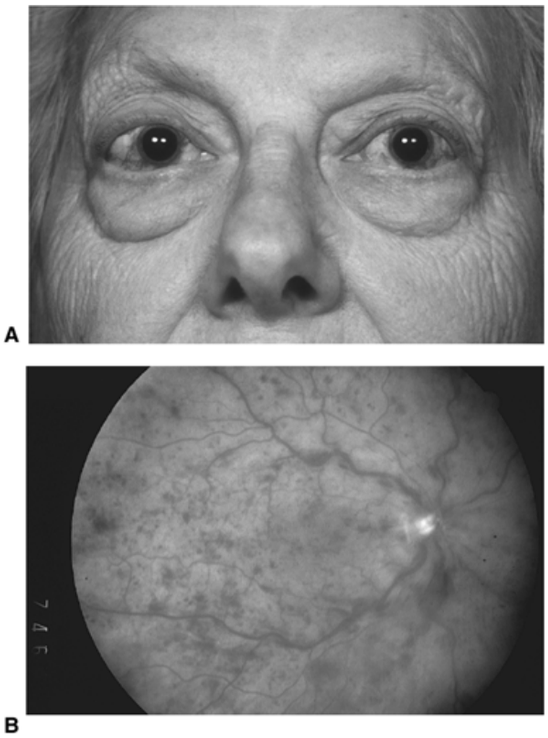

Figure 13-34. This 69-year-old woman had undergone embolization by an external carotid approach for a spontaneous dural fistula, which had caused raised intraocular pressure. She presented 1 year later with persistent epibulbar venous dilatation and reduced vision (20/300 right eye, 20/70 left eye) due to a venous ischemic-hypoxic retinopathy. This resolved spontaneously over the next 9 months with a final vision of 20/200 on the right and 20/50 on the left.

Imaging

CT and MR imaging are useful screening tools, which may show dilatation of the superior ophthalmic vein (80%), increased extraocular muscle size (65%), or enlargement of the cavernous sinus (35%). In our series, only 1 patient of 20 showed none of these signs. Orbital ultrasound may also demonstrate engorgement of the superior ophthalmic vein, pulsation, enlargement of the extraocular muscles, or choroidal detachment.

The definitive test is bilateral selective internal and external carotid artery angiography. Bilateral angiography is necessary because the clinical appearance is not predictive of the side on which the afferent flow is present or whether the flow is unilateral or bilateral. Selective angiography determines whether the in-flow is from internal, external, or both carotid systems. In our series of angiographically studied cases of spontaneous dural fistulas, 23% were Barrow type C and 77% were Barrow type D.

Management

Type A patients with high-flow fistula are best treated with a detachable balloon since the overwhelming majority will not close spontaneously (Fig. 13-30). Failure may require direct surgical exposure with obliteration of the cavernous sinus or trapping of the arteries.

The majority of spontaneous carotid cavernous fistulas are dural arteriovenous malformations, and between 20% to 50% will close spontaneously. In these circumstances, we follow the patients conservatively unless they experience debilitating pain, medically untreatable ocular hypertension, severe retinal venous stasis, or visual loss. It is important to note that within this group, demonstration of out-flow via the middle cerebral venous system on angiography has been associated with a significant number developing cerebral hemorrhage, and these patients should be treated to prevent this. Fistulizing surgery for glaucoma in patients with dural fistulas has an elevated risk of choroidal and expulsive hemorrhage. Type B fistulas are rare while type C are supplied by single feeders and can be nicely obliterated by selective embolization. Type D fistulas with feeders from both the internal and external carotid arteries are more challenging and require embolization of all feeding branches, which will eradicate fistulas in about 50% of cases. Alternatively, failure in this circumstance can prompt retrograde obliteration of the cavernous sinus (Fig. 13-35). The most convenient transvenous approach is usually via the superior ophthalmic vein but can be achieved through the internal jugular vein where coils are deposited to generate thrombosis. In our own series, 5 of 10 type D fistulas closed on initial attempt of external carotid artery embolization. Of the remaining five, one closed with repeat external carotid artery embolization, and two closed with superior ophthalmic vein cannulation and cavernous sinus trapping. The final two improved with initial treatment but did not completely resolve. They are being followed conservatively. It should be noted that thrombosis of the superior ophthalmic vein precedes clinical resolution of a fistula and may be heralded by acute worsening of the ophthalmic manifestations. These signs improve spontaneously over weeks.

Complications following endovascular embolization or transvenous cavernous sinus trapping are rare but include vascular perforation and hemorrhage, local or systemic infection, and transient or permanent neurologic deficit ranging from isolated cranial nerve deficits to hemispheric dysfunction. In our series, of 13 patients who underwent external carotid embolization, two experienced transient V_2 palsy and one had a frontal infarct with full clinical recovery. Of three patients who underwent superior ophthalmic vein cannulation and cavernous sinus trapping with platinum coils, one developed a middle cerebral artery infarct with long-term sequelae. Overall, 40% of our patients with

fistulas had spontaneous closure, 50% had successful closure with treatment, two are being managed conservatively following treatment, and one refused recommended treatment and has not had spontaneous improvement.

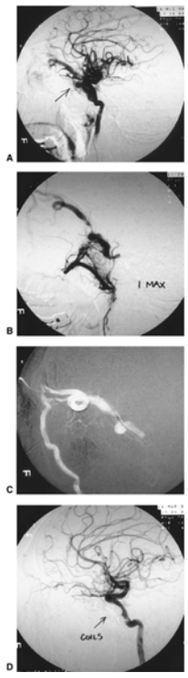

Figure 13-35. This 67-year-old man developed a spontaneous high-flow fistula and had undergone embolization on two previous occasions by traditional route. (A) Left carotid angiogram demonstrates the high-flow fistula draining through the superior ophthalmic vein. (B) The superior ophthalmic vein was directly cannulated and (C, D) the clinically detachable coils placed in the cavernous sinus. He recovered uneventfully.

New Growths

We have divided the vascular tumors into hamartomas and neoplasms. All are characterized by development of mass effect modified by their hemodynamics. Tumors may be high-flow (infantile hemangiomas), low-flow, or reflect little or no-flow (some solid neoplasms). Malignant lesions may be complicated by local infiltrative features in addition to the mass and hemodynamic effect.

Hamartomas

Although nosologic argument exists, we have classified capillary hemangiomas as hamartomas rather than neoplasms. We have also classified cavernous hemangiomas and so-called lymphangiomas as malformations. Infantile hemangiomas have a history of rapid onset and a rich blood supply with or without dermal and/or systemic features.

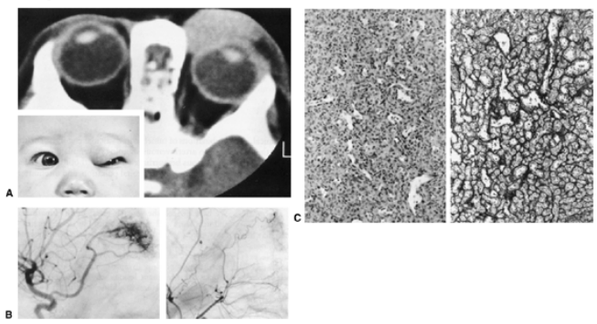

Figure 13-36. (A, inset) This 11-month-old infant had a history of a left upper lid mass, noted at 10 weeks of age. The size of the mass increased rapidly over 6 weeks. It was a rubbery, slightly violaceous tumor of the upper lid and anterior orbit behind the septum. It was associated with 4 diopters of astigmatism, and the child acted amblyopic. Contrast-enhanced CT scan (A) reveals a uniformly enhancing, smooth, contoured mass displacing the globe posteriorly. Failure to respond to corticosteroids and the child's significant astigmatism led to excision of the mass under hypotensive anesthesia. (B) Preoperative angiography of the mass demonstrates rapid filling of a fine vascular network primarily supplied by the internal carotid system (left) with minor external carotid supply (right). (C, left) Photomicrographs of the excised lesion shown in (A) and (B) demonstrates a dense hypercellular net of fine endothelially-lined vascular channels (H&E, original magnification × 10). (C, right) Reticulin stain shows organization of the capillary channels characteristic of infantile hemangiomas (reticulin, original magnification × 10).

Capillary Hemangioma

Infantile capillary hemangiomas represent an abnormal growth of blood vessels with varying degrees of endothelial proliferation. The more densely endotheliomatous lesions generally demonstrate more rapid growth and regression. These endothelial cells are organized into a network of basement membrane-lined vascular channels of varying density and size (Fig. 13-36).

Capillary hemangiomas have a female predominance and usually present within the first months of life, starting as small flat foci that undergo rapid expansion over weeks to months and then typically involute. The regression may take months to years depending upon the size and histopathology. (On average, in three quarters of patients, the hemangioma involutes by the time the patient is 7 years.). Lesions undergoing involution are characterized histologically by fewer endothelial cells, larger and less numerous vascular channels, increasing collagen deposition, intralesional fat, and in some instances, inflammatory cell infiltrates (Fig. 13-37). Many are associated with dermal hemangiomas in the head and neck and throughout the body, or with deep visceral capillary tumors. When visceral lesions are of great size, they may lead to sequestration of thrombocytes and red blood cells with at

tendant thrombocytopenia and bleeding diathesis (the Kasabach-Merritt syndrome).

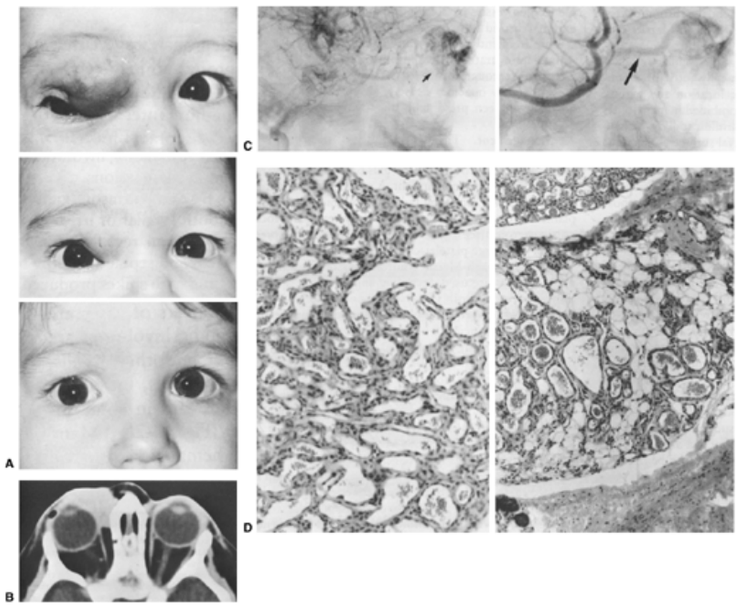

Figure 13-37. (A, top) Clinical photograph of an 11-month-old child demonstrates an anterior postseptal hemangioma. It responded to corticosteroids (A, center), but rebounded and was associated with 5 diopters of astigmatism. Postoperative results of anterior resection (A, bottom) had a return to emmetropia. (B) CT scan shows a mass with distinct margins causing lateral and posterior displacement of the globe. (C) Angiography of the lesion demonstrates hyperdynamic blood flow through an enlarged ophthalmic artery with rapid shunting into the superior ophthalmic vein (right, large arrow). Note patchy (inhomogeneous) filling of the posterior portion reflecting regressive features (left, small arrow). (D) Photomicrographs of the lesion show evidence of maturation of larger channels, increased collagen, and intralesional fat deposition (H&E, original magnification × 10).

Our series consisted of 31 infantile capillary hemangiomas, which were divided clinically into four subgroups on the basis of anatomic location and extent including superficial, deep, combined, and complex or systemic capillary hemangiomas. The superficial infantile capillary hemangioma affects the lid or conjunctival surface alone, deep lesions affect the orbit behind the septum, combined lesions involve both superficial and deep components, and complex hemangiomas are multicentric.

Deep Infantile Hemangioma

Clinical Features

These hemangiomas are posterior to the orbital septum and may therefore lie in the deep tissues of the lid and anterior orbit or may occur solely within the retrobulbar orbit (Figs. 13-36 ,13-37 ,13-38). The main clinical features of proptosis or displacement of the globe are caused by their mass effect. Because of their rich blood supply, some will exhibit subtle pulsation if examined carefully. They may also enlarge with crying or the Valsalva maneuver. Obvious dilatation of the overlying lid or facial vessels and a blue-violet discoloration of the lids or conjunctiva may be noted. When palpable, they have a rubbery to soft consistency and a smooth contour, and may be collapsed to a degree with modest pressure. The size and location of these lesions often cause distortion or obstruction of the visual axis with subsequent amblyopia and strabismus. The associated refractive abnormalities are astigmatism and myopia and may be of sufficient degree to risk amblyopia if not recognized and treated.

Imaging

On CT and MR scans (Fig. 13-39), the margins of these lesions vary from moderately well defined to infiltrating. They may occur in any compartment and frequently cross boundaries, being both intraconal and extraconal, postseptal and preseptal. Those with a significant retrobulbar component cause displacement and occasionally globe indentation. The enhancement seen with intravenous contrast varies from moderate to intense and may be homogeneous or inhomogeneous (Figs. 13-36 and 13-38). This variable pattern presumably reflects the histology of these lesions as they involute, with the less intense, more inhomogeneous pattern seen in lesions undergoing involution. We have not noted calcification.

On MRI, capillary hemangiomas are usually well defined but may have some irregular margins with both homogeneous and heterogeneous low signal intensity on T1-weighted images compared to fat. The signal intensity

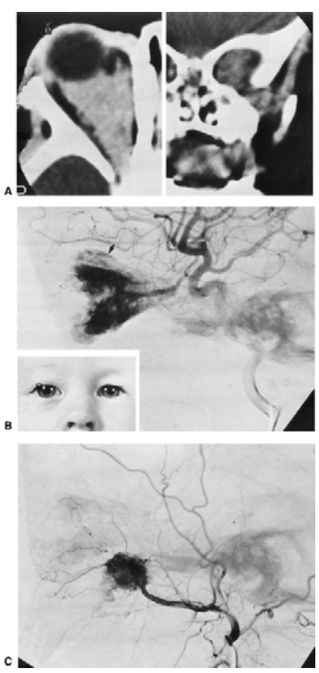

Figure 13-38. (A, left) Contrast-enhanced axial CT scan of a 5-month-old infant demonstrates right pulsatile proptosis due to a diffuse, enhancing, deep, intraconal infantile hemangioma. Coronal scan (A, right) demonstrates mass in the pterygopalatine fossa. (B) Internal carotid angiogram of the same patient demonstrates early dense opacification of a diffuse retrobulbar mass via an enlarged ophthalmic artery. The negative shadow is created by the superior muscle mass (arrow). (C) The mass in the pterygopalatine fossa has a supply separate from the internal maxillary artery.

with respect to extraocular muscles is high. On T2-weighted images they show high signal intensity with respect to fat and extraocular muscles, and there may be multiple areas of flow voids. With gadolinium-enhanced T1-weighted images, capillary hemangiomas may demonstrate diffuse, either heterogeneous or homogeneous, enhancement that is best demonstrated with fat suppression.

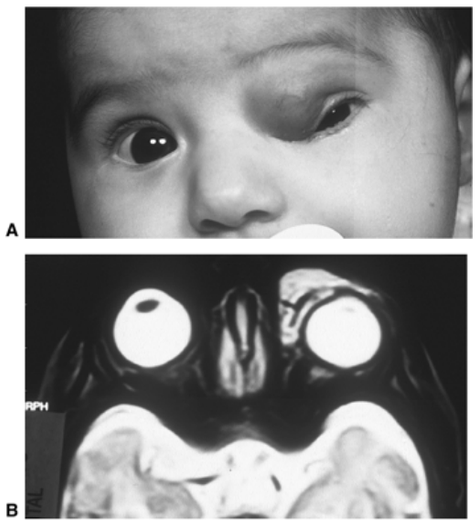

Figure 13-39. (A) This 7-month-old infant developed a progressive, enlarging capillary hemangioma, which partially occluded her visual access and led to significant astigmatism. (B) The T2-weighted MRI demonstrates a central flow void. The lesion was surgically resected, which cleared the visual axis and reduced the astigmatism.

B-scan ultrasonography demonstrates either a smooth lobular or irregular contour and high echogenicity. A-scan ultrasonography reveals some irregularity due to vascular spaces and septae with low to medium internal reflectivity and high spikes produced by the septae. Blood flow is frequently fast and may be demonstrated on Doppler echography.

At angiography, they frequently have multiple feeding vessels from both the ophthalmic artery and external carotid branches (see Fig. 13-36). The feeding vessels are frequently enlarged and early draining veins are often demonstrated, reflecting a hemodynamically rapid shunt through the tumor (see Fig. 13-37). The tumor mass generally opacifies densely, although less vascular areas may be seen, presumably due to involution (see Fig. 13-37).

Management

The vast majority of deep infantile hemangiomas regress; therefore, this outcome can usually be obtained without surgical intervention. However, larger lesions with considerable proptosis or with associated astigmatism or visual axis obstruction may require more aggressive treatment. A number of modalities have been tried, including radiotherapy (radon seed implantation or external beam therapy), systemic and local corticosteroids (see Fig. 13-37), and surgery. In the presence of very large platelet-consuming lesions associated with the Kasabach-Merrit syndrome, systemic antifibrinolytic agents are used, including aminocaproic acid or tranexamic acid. Both the systemic corticosteroids and antifibrinolytic agents should be monitored by a pediatrician familiar with their use. We use systemic and locally injected corticosteroids to treat large nonresectable lesions or to shrink resectable lesions. The systemic dosage used is 1.5 mg/kg to 2.5 mg/kg prednisone daily over a few weeks with titration downward depending on response. Local injection is also used in doses of 40 mg to 80 mg triamcinolone with 25 mg methylprednisolone (Solu-Medrol) directly into the lesion. This produces local tension in the lesion, which rapidly dissipates, and is usually followed by reduction in the size of the mass. In our experience, corticosteroids are effective in a high percentage of cases, but recurrence and regrowth with diminution of the steroid dose is not infrequent (a rebound phenomenon). More recently, some cases have been treated with recombinant interferon alpha-2a and 2b with variable results.

We have performed surgical resection in selected circumstances such as significant threat to vision with failure to respond to corticosteroids, rebound on steroid withdrawal, severe steroidal side effects, and severe proptosis, or if the lesion is clearly isolated and well defined with functional deficits. Operative removal requires detailed preoperative investigation (including systemic survey, CT, and sometimes angiography), hypotensive anesthesia (when necessary), and meticulous surgical technique. In these circumstances, a controlled resection can be performed with constant hemostasis. At surgery, these tumors may have fine pseudopodal extensions, which can be cauterized or followed depending upon the surrounding structures. These extensions frequently insinuate themselves between structures and required microdissection. Surgery has produced rapid resolution and gratifying results in these selected cases (see Fig. 13-37).

We have not used radiation because of the risk of many long-term side effects; however, several other institutions favor judicious use of either radon seed implantation or external beam therapy and report clinical resolution.

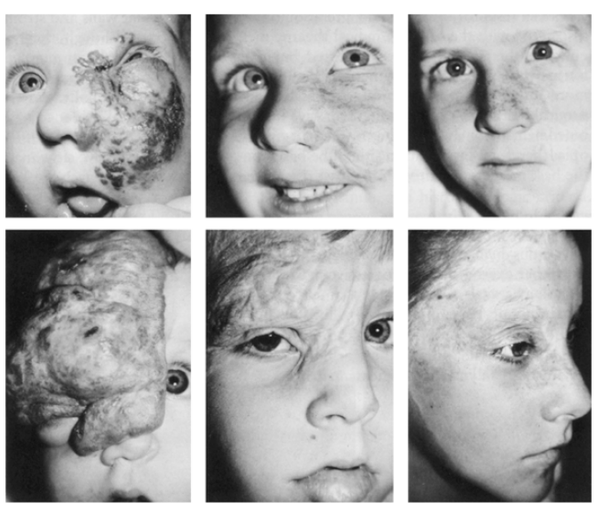

Figure 13-40. (Top, left) Massive facial and orbital hemangioma in a 5-month-old child. (Top, center) Three years later, the hemangioma has regressed following observation only. (Top, right) The patient at age 12 years after cosmetic facial surgery and strabismus repair. (Bottom, left) Massive infantile hemangioma of a second patient at 10 months. (Bottom, center) Following spontaneous regression 53 months later. (Bottom, right) The patient at age 11 years following surgical repair. (Photos courtesy of Drs. A.J. Stewart and R.J. Cowan.)

Superficial Infantile Hemangioma

Superficial capillary hemangiomas are the so-called strawberry nevi and are confined to the dermis. They may be single or multiple, can occur anywhere on the body, and undergo the same pattern of growth and resolution described earlier. An important clinical feature that indicates resolution is the appearance in a previously vascular strawberry-like lesion of fine stellate areas of pale scarring (herald spot). It is very reassuring to point out this feature to the parents of affected children. These lesions are best treated with benign neglect when no functional abnormalities are associated. Larger hemangiomas may need therapy if they bleed frequently or lead to visual obstruction. Therapy includes steroids, dermal laser, cryotherapy, and surgery.

Combined Infantile Hemangioma

Combined hemangiomas have both dermal and deep components. Clinically, the dermal component is associated with a palpable deeper mass or displacement of the globe. When massive, these lesions are the most startling and tragic of the infantile hemangiomas. The widespread involvement produces marked deformity of both the skin and the orbit, and they are frequently associated with amblyopia. Management is again governed by the potential visual function risks, and involves corticosteroids, perhaps interferon, systemic antifibrinolytic agents, selective angiographic embolization, or perhaps radiotherapy with adjunctive local measures. Cosmetic surgery for skin redundancy and persistent deformities should await resolution of the primary lesion. We have seen seven cases of this type with long-term follow up, all of which were treated with cosmetic surgery following spontaneous resolution with reasonable cosmetic results (Fig. 13-40). Functional amblyopia was unfortunately present in all cases as a result of the profound alteration of visual axis associated with them. More radical therapy early in the course of this tumor has been advocated, but in our opinion may not produce better functional results and may be more disfiguring. No uniformly successful medical or surgical treatment exists for these massive lesions. However, early aggressive systemic intervention with steroids appears to be effective in treating extensive lesions. Combined hemangiomas have a high attendant risk of amblyopia; therefore, intervention should be based on getting the best cosmetic result with the least risk to the child.

Neoplasia

Hemangiopericytoma

Hemangiopericytomas are uncommon tumors which infrequently occur in the head and neck in adults. It is difficult to predict biologic behavior on the basis of histopathology. Because the pericyte is a spindle-shaped cell with a moderate amount of cytoplasm and an indistinct border, routine histopathologic differentiation from endothelial cells, histiocytes, and fibroblasts may be difficult. Distinction on a cellular basis may be best achieved by electron microscopy and immunohistochemistry. Since the identification of this entity by Stout, the tumor has been well delineated throughout the body, where it tends to occur in the retroperitoneum and lower limbs. Orbital occurrences have been repeatedly described in multiple case reports where the behavior and morphology is similar to those noted at other sites.

The fundamental histopathology consists of a uniformly cellular tumor with a sinusoidal vascular component often forming branching (stag horn) channels. The reticulin and Factor VIII-related pattern forms a dense network or mesh around individual cells, in contrast to that of capillary hemangiomas. Pericytes stain for vimentin only. Additional features noted in hemangiopericytomas include myxoid, cellular, storiform, and cystic components. In addition, giant cells may be noted as well as areas of necrosis, hemorrhage, and hyalinization. Three patterns have been described, sinusoidal, solid, and mixed types. Hemangiopericytomas can be divided into benign, intermediate (borderline), and malignant tumors on the basis of histopathologic criteria. The benign pattern demonstrates minimal atypia with few mitotic figures whereas borderline and malignant patterns demonstrate increasing mitosis, compression of vascular spaces, pleomorphism, necrosis, hemorrhage, and infiltrative margins. In spite of these distinctions, it remains difficult to reliably predict the biology on the basis of histopathologic criteria although rates of spread are higher in borderline and malignant varieties. A recently described variant that can be confused with well-defined liposarcomas is the histologically benign lipomatous hemangiopericytoma.

Clinical Features

The median age of occurrence is in the fourth decade, but hemangiopericytomas have been noted from 20 months of age to 87 years. The major clinical features are proptosis and mass effect, predominantly in the superior part of the orbit, unassociated with pain, features of infiltration, or entrapment (Fig. 13-41A). Hemodynamically, they have been shown to have a rapid circulation with a significant amount of shunting of blood. Angiography shows dilated feeding arteries, an early tumor blush, and a rapid venous out-flow (Fig. 13-41B). In spite of this, clinical evidence of active hemodynamics is rare and can be demonstrated on all three phases of angiography. Patients will usually have symptoms for less than 1 year on presentation; however, there is wide variation from 1 month to 26 years. On CT and MR imaging, these tumors tend to present as well-defined masses with homogeneous enhancement and show a blush on angiography (Fig. 13-42).

The major differential diagnosis in the orbit, besides infantile capillary hemangiomas, includes fibrous histiocytoma, solitary fibrous tumor, and mesenchymal chondrosarcomas. When they have arisen from the dural sheath, the differential diagnosis includes optic nerve meningioma and dural sarcoid. Fibrous histiocytomas are dominated by a storiform, highly cellular pattern without a significant vascular component, and mesenchymal chondrosarcomas contain areas of chondroid or cartilaginous tissue. Ultrastructurally, the pericyte has a number of distinct characteristics including frequent pinocytotic vesicles, poorly developed and rare desmosomes, and a striking, frequently multilayered basal lamina.

Management

About one third of hemangiopericytomas of the orbit will recur, and 10% to 15% may develop metastases. It is worth noting that hemangiopericytomas may occur as a lesion of the optic nerve. Local recurrence correlates most closely with incomplete or piecemeal excision. In addition, there is an increased incidence of recurrence in the malignant and borderline groups. Nevertheless, histologically benign tumors may also recur or metastasize. Because local recurrence and metastatic disease are a significant risk in these tumors and may occur after many years, long-term follow-up (at least 10 years) is necessary to ensure complete cure. Since these tumors usually have a pseudocapsule, careful and complete local excision is the recommended form of therapy but is often difficult because of friability. Elsewhere in the body, high-dose radiotherapy has been used in treatment of these tumors when recurrent or aggressive in behavior, but carries attendant morbidity in the orbit. Aggressive local behavior may require exenteration. Systemic chemotherapy has been used in too small a number of cases to comment on its efficacy.

At the time of surgery, most of these tumors appear to be reasonably well-circumscribed pinkish or violaceous masses, and they may have large draining telangiectatic vessels. We have seen seven such tumors. Two have recurred following excision, one arising from the optic nerve (Fig. 13-41B) and the other arising from the orbital apex (Fig. 13-42). At surgery, the mass itself appears to be quite friable; however, the majority have been described as having circumscribed borders with rare grossly infiltrative lesions noted. In the

literature, the majority have been about 3 cm in size but range all the way from 1.7 cm to 5.5 cm. Some patients have had large intracranial components.

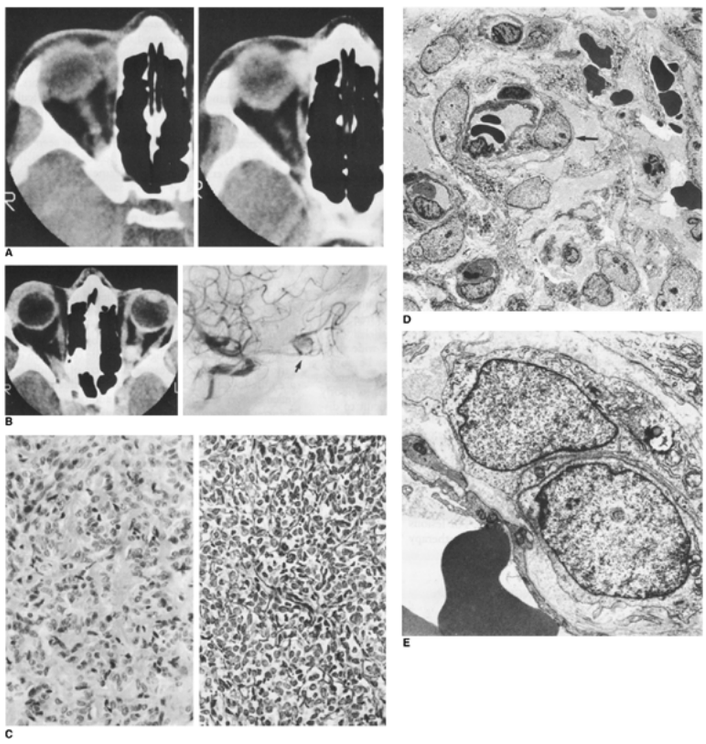

Figure 13-41. Hemangiopericytoma. (A) Axial CT scan without (left) and with (right) contrast injection. Note well-defined homogeneously enhancing anterior orbital mass. (B) The contrast-enhancing apical orbital mass displaced the optic nerve and led to optic neuropathy. Angiogram (B, right) demonstrates an early uniform fine mesh of enhancing vessels (arrow). (C) Histopathology of a solid hemangiopericytoma (shown in B). This demonstrates a spindle cell population (C, left) and dense reticulin pattern surrounding individual cells (C, right) (left: H&E, original magnification × 25; right: reticulin, original magnification × 25). (D, E) Ultrastructural features of hemangiopericytoma (from patient shown in A). Note characteristic wrapping of pericytes around a vascular channel (D, arrow). Additional features consistent with pericytes include the presence of basement membrane, few intracytoplasmic filaments, and pinocytotic vesicles (original magnifications: D, × 2000; E, × 9400).

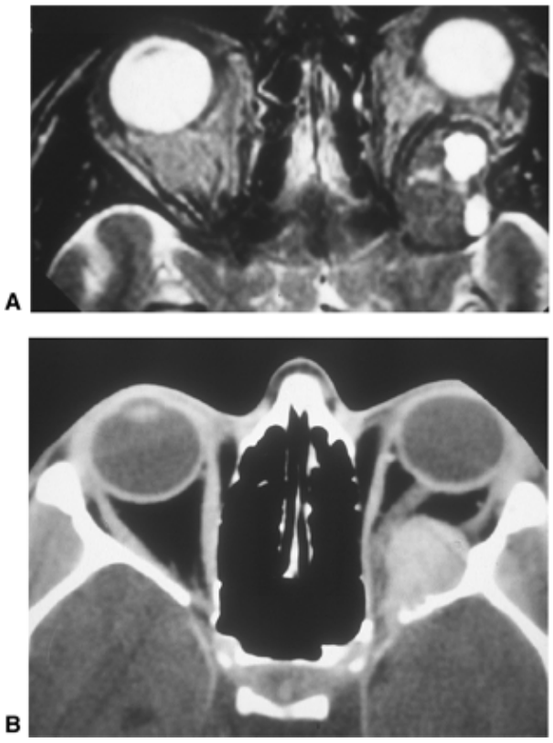

Figure 13-42. These MR (A) and CT (B) scans demonstrate an apical orbital mass excavating the adjacent posterolateral wall of the orbit and causing an optic neuropathy. (A) The T1-weighted image (with fat suppression and Gadolinium injection) demonstrates some large fluid-containing areas in an essentially solid tumor. This was removed by a combined craniotomy-orbitotomy and was histologically confirmed to be a hemangiopericytoma. The patient has had a focal dural recurrence after 5 years of follow-up.

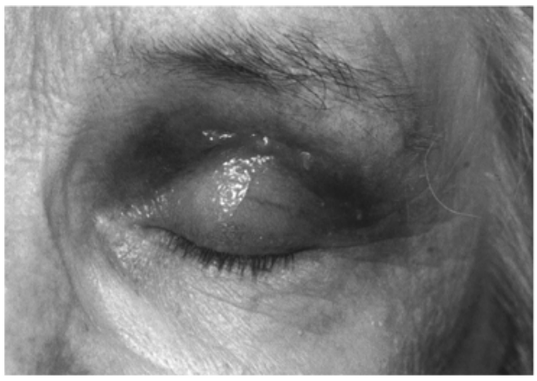

A

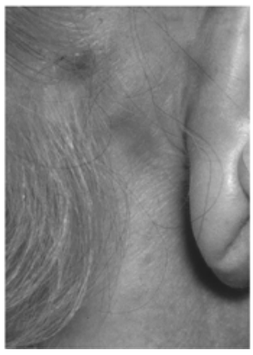

B

Figure 13-43. (A) This 79-year-old woman presented with spontaneous hemorrhaging of her left upper lid, which on biopsy proved to be an angiosarcoma. This was noted to be present in multiple sites on her scalp and behind her ear (B).

In summary, orbital hemangiopericytomas are unusual vascular tumors that tend to present as well-circumscribed noninfiltrative superior masses. They have an unpredictable pattern of behavior and are best handled by careful local excision, unless they demonstrate biologically aggressive behavior. In this instance, a more radical approach is required, which may include preoperative embolization, wider excision, and radiotherapy.

Malignant Hemangioendothelioma: Angiosarcoma

Malignant, endothelially-derived vascular tumors are extremely rare, representing 1% of all sarcomas. Typically, they occur in the skin with a predilection for the head and neck of males in later life. Often, they are ill-defined and multifocal, involving the skin and subcutaneous tissues of the scalp and lids (Fig. 13-43). They may be multiple and aggressive both locally and systemically. The structural spectrum is diverse, partly accounting for a lack of standardized nomenclature. The fundamental histologic features are the presence of irregular lumina (frequently containing blood) lined by atypical endothelial cells, which may be papillary in configuration. A wide spectrum of differentiation of these tumors may be noted, from well-defined vascular groupings of atypical endothelial cells with a vascular reticulin pattern to poorly differentiated (epithelioid) cells that are difficult to distinguish from carcinomas. Ultrastructurally, the morphologic spectrum reflects this diversity but fundamental endothelial features (basal lamina, luminal pinocytotic vesicles, tight junctions, cytofilaments, and Weibel-Palade bodies) may be noted. Factor VIII-related antigen and *Ulex europaeus-1* may be noted.

About a dozen cases have been reported as primary in the orbit as opposed to the more common multifocal origin in the head and neck region. We have seen two that were multifocal and progressive. The dominant presentation has been the development of sometimes hemorrhagic mass effect over

a relatively short period (2 to 3 months). No sex predilection has been noted and the median age was 24 years. One quarter of the reported patients had local sensory or motor neurologic signs and symptoms, including a Tolosa-Hunt syndrome. Overall, these tumors have been typically locally aggressive, and wide surgical excision is recommended (but not always achievable) to prevent recurrence or metastases.

Kaposi's Sarcoma

Multifocal hemorrhagic sarcoma was first described in 1872 by Kaposi. Three related clinical syndromes appear to exist, varying with demography, genetic factors, and immune status. The classic syndrome is development of discrete violaceous lesions on the extremities (especially the lower) of elderly males (seventh decade) and immune-compromised patients. It typically occurs in patients of eastern European or Mediterranean origin. Progression is characterized by increasing numbers of lesions, nodularity, hemorrhage, and gastrointestinal, genitourinary, lymph node, and visceral involvement. Mortality in this form is between 10% and 20%, typically with a long clinical course over 8 to 10 years. Second malignancies, especially those of reticuloendothelial origin, are frequent with 25% of patients succumbing.

A second more aggressive syndrome is seen in Central Africa, typically in the fourth decade. Visceral, lymph node, and internal mucosal involvement is more frequent early in the course of the disease, and progression is therefore more rapid. Finally, a particularly aggressive form develops in persons afflicted by the acquired immune deficiency syndrome (AIDS).

Clinically, the disease can be staged into nodular, locally aggressive, and generalized, correlating with the prognosis. Ocular involvement is usually of the skin, lids, or conjunctiva. The African form has been noted in the lacrimal gland.

Histologically, this tumor is believed to arise from a primitive perithelial cell giving rise to a spectrum of findings. Earlier, less aggressive lesions may be dominated by inflammatory cells and resemble pyogenic granuloma with a background of malignant spindle cells. With evolution of the lesion, increasing numbers of spindle cells are noted with increasing atypia and a reduction in the inflammatory cell background. Features of recurrent hemorrhage and slit-like vascular channels can also be noted.

Treatment depends on staging. Local lesions may be resected or treated with injectable chemotherapeutic agents. Multifocal disease or visceral involvement is treated by systemic chemotherapy and extended field radiation.

Vascular Leiomyoma (Angiomyoma)

Vascular leiomyoma is a rare, usually subcuticular tumor that arises from the smooth muscle of blood vessels. The few cases described in the orbit have been slow growing, encapsulated masses occurring chiefly in the fourth and fifth decades of life. The differential diagnoses for these well-encapsulated orbital masses include cavernous hemangioma, schwannoma, and neurofibroma. Although the dominant clinical feature is mass effect, pain and change on Valsalva maneuver may be noted. Histologically, they consist of fascicular interwoven bundles of spindle cells with a significant vascular pattern. Myxoid areas may be noted. Densely vascular lesions may be confused with hemangiopericytoma. The diagnosis is substantiated by identification of smooth muscle origin by means of histochemistry or electron microscopy. Because they are well encapsulated and benign, the treatment of choice is complete excision. Incomplete removal may lead to recurrence locally.

Epithelioid Hemangioendothelioma

Epithelioid hemangioendothelioma is a less malignant variant of angiosarcoma and has been described in less than 10 cases in the orbit, one of which occurred in the adjacent orbital bone.

Aneurysms

Arterial aneurysms within the vascular network of the orbit may be noted as incidental findings on angiography done for other reasons. Rarely do aneurysms in the orbit cause functional deficits. However, we have encountered one orbital aneurysm (Fig. 13-44) that occurred as a complication of an arteriovenous shunt and led to a tumefaction in the apex of the orbit. This mass effect caused some associated pressure on the apical structures and ultimately led to the development of an optic neuropathy. We have also encountered a dramatic cranio-orbital aneurysm (Fig. 13-45).

Thrombotic Lesions

Many of the foregoing lesions, including arteriovenous fistulas, orbital varices, and some of the tumors, have thrombotic (obstructive) elements either on the arterial or venous side. On the other hand, arterial and venous obstructive processes can be complications of other systemic and local diseases, such as orbital vein thrombosis secondary

to sphenoid sinusitis. Rarely, orbital vein thrombosis has been described as a spontaneous phenomenon presenting as a sudden hemorrhage, chemosis, edema, and retinal venous dilatation due to a superior orbital vein obstruction. With recanalization, the signs and symptoms abate spontaneously. We have encountered four cases of women who developed spontaneous venous thrombosis of the anterior superior orbital vein. They presented with a sudden onset of painless upper lid swelling and an anterior, superior orbital mass was palpable through the medial third of the upper lid. In addition, hypoglobus, variable proptosis, and mild limitation of upgaze was also noted (Fig. 13-46). Two of these patients underwent partial or total surgical removal of the venous thrombosis. Once the syndrome was identified, we were able to manage the two most recent cases by observation alone and they resolved spontaneously. In addition, we have seen a case of superior ophthalmic vein thrombosis following marked orbital inflammation subsequent to repeated ocular surgery.

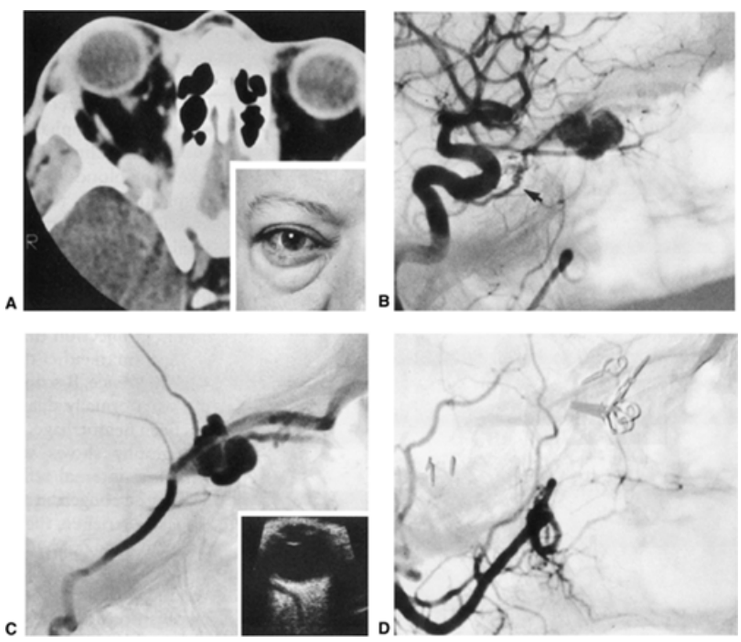

Figure 13-44. (A, inset) This 53-year-old woman presented with an apical orbital venous aneurysm due to an arteriovenous shunt causing edema, chemosis, raised intraocular pressure (24 mmHg versus 10 mmHg), 7 mm of proptosis, and reduced vision. An audible temporal bruit was present. (A) CT scan shows venous aneurysm associated with a bony defect due to enlargement of the canal of Hyrtl. (B) Angiogram shows internal carotid supply to the shunt (arrow) and straightening of the ophthalmic artery due to proptosis. (C) Right-selective middle meningeal angiogram also demonstrates supply to the venous aneurysm. (C, inset) Ultrasonogram shows dilated superior ophthalmic vein. (D) Angiogram after surgical closure of the middle meningeal supply and clipping of the orbital aneurysm, which led to resolution of symptoms.

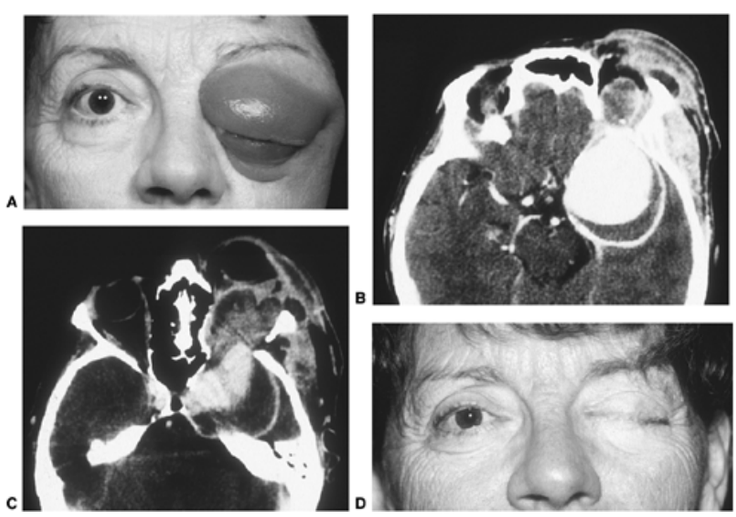

Figure 13-45. (A) This 41-year-old female had a history of left progressive visual loss over a 2-year period. She had developed II, III, IV, and V cranial nerve palsies with progressive proptosis, periorbital edema, and chemosis due to a massive internal carotid aneurysm that extended into the orbit (B, C). The aneurysm was partially thrombosed. She underwent a permanent balloon occlusion of the internal carotid artery after a balloon trial occlusion, which led to resolution of her signs and symptoms (D). (Figs. 13-45B to D reproduced with permission from Marotta TR, Lingawi SS, Katz SE, et al. Intraorbital rupture of a cavernous internal carotid artery aneurysm: therapeutic options. Ophthal Plast Reconstr Surg 2001;17:67-72.)

Unclassified Spontaneous and Post-Traumatic Orbital Hemorrhages

Orbital hemorrhage may be a feature of trauma and may be of sufficient degree to lead to functional visual, sensory, or motor threat. Management in the acute situation may require emergency canthotomy, CT- or ultrasound-guided aspiration, or even decompression. We have encountered several cases of spontaneous orbital hemorrhage of an idiopathic variety, an occurrence which has also been described in the literature. However, the majority of cases of spontaneous hemorrhage that we have encountered have been related to underlying vascular, hemodynamic, and hematologic abnormalities.

An important but rare cause of spontaneous orbital hemorrhage is a postoperative hemorrhage that occurs approximately 3 to 4 days following orbital surgery. (We have seen none.) The hemorrhage may be due to dissolution of intravascular clots. In part it could be related to postoperative inflammation or the release of proteolytic enzymes that result from damage to the orbital fat.

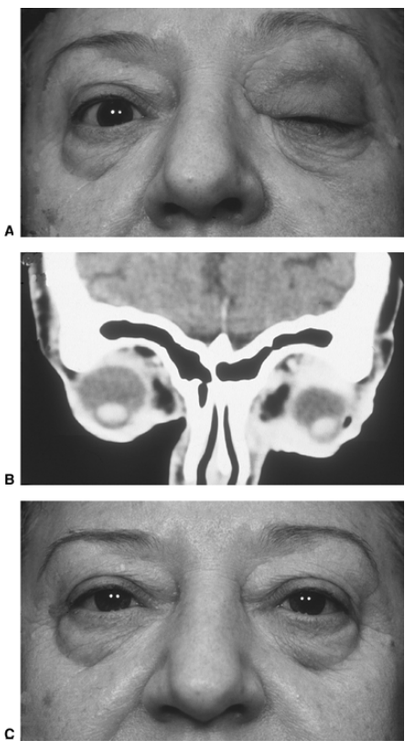

Figure 13-46. (A) This 61-year-old woman presented with a sudden onset 1 week earlier of left upper lid swelling unassociated with pain or other visual findings. She had an edematous left upper lid with a palpable nodule recognized as arising from a thrombosed superior ophthalmic vein (B). She underwent simple observation and the lesion spontaneously resolved over several weeks (C).

Bibliography

General

Duke-Elder S, MacFaul PA. The ocular adnexa. Part II. Lacrimal, orbital and para-orbital diseases. In: Duke-Elder S, ed. System of Ophthalmology, Vol 13. St. Louis: CV Mosby, 1974.

Enzinger FM, Weiss SW. Soft Tissue Tumors, 3rd ed. St. Louis: CV Mosby, 1995.

Henderson JW. Orbital Tumors, 3rd ed. New York: Raven Press, 1994:89-133.

Jakobiec FA, Jones IS. Vascular tumors, malformations, and degenerations. In: Jones IS, Jakobiec FA, eds. Diseases of the Orbit. Philadelphia: Harper & Row, 1979:269-308.

Mulliken J, Young AE. Vascular Birthmarks: Hemangiomas and Malformations. Philadelphia: WB Saunders, 1988.

Reese AB. Tumors of the Eye, 3rd ed. Philadelphia: Harper & Row, 1976.

Malformations

Cavernous Hemangioma

Coleman DJ, Jack RL, Franzen LA. High resolution B-scan ultrasonography of the orbit. 2. Hemangiomas of the orbit. Arch Ophthalmol 1972;88:368-74.

Deol AK, Terry JE, Seibert DA, et al. Hemangioma of the apical orbit diagnosed by radionuclide imaging. Optom Vis Sci 1994;71:57-9.

Dilenge D. Arteriography in angiomas of the orbit. Radiology 1974;113:355-61.

Forbes GS, Sheedy PF, Waller RR. Orbital tumors evaluated by computed tomography. Radiology 1980;136:101-11.

Fries PD, Char DH. Bilateral orbital cavernous hemangiomas. Br J Ophthalmol 1988;72:871-3.

Fries PD, Char DH, Norman D. MR imaging of orbital cavernous hemangioma. J Comput Assist Tomogr 1987;11:418-51.

Harris GJ, Jakobiec FA. Cavernous hemangioma of the orbit: a clinicopathologic analysis of sixty-six cases. In: Jakobiec FA, ed. Ocular and Adnexal Tumors. Birmingham, AL: Aesculapius, 1978:741-81.

Hassler W, Schaller C, Farghaly F, Rohde V. Transconjunctival approach to a large cavernoma of the orbit. Neurosurgery 1994;34:859-61.

Henderson JW, Farrow GM, Garrity JA. Clinical course of an incompletely removed cavernous hemangioma of the orbit. Ophthalmology 1990;97:625-8.

Johnson TE, Nasr AM, Nalbandian RM, Cappelen-Smith J. Enchondromatosis and hemangioma (Maffucci's syndrome) with orbital involvement. Am J Ophthalmol 1990;110:153-9.

Ki WW, Shin JW, Won KS, et al. Diagnosis of orbital cavernous hemangioma with Tc-99m RBC SPECT. Clin Nucl Med 1997;22:546-9.

Kopelow SM, Foos RY, Straatsma BR, et al. Cavernous hemangioma of the orbit. Int Ophthalmol Clin 1971;11:113-24.

McNab AA, Wright JE. Cavernous hemangioma of the orbit. Aust N Z J Ophthalmol 1989;17:337-45.

Ohbayashi M, Tomita K, Agawa S, et al. Multiple cavernous hemangiomas of the orbits. Surg Neurol 1988;29:32-4.

Ohtsuka K, Hashimoto M, Akiba H. Serial dynamic magnetic resonance imaging of orbital cavernous hemangioma. Am J Ophthalmol 1997;123:396-8.

Orcutt JC, Wulc AE, Mills RP, Smith CH. Asymptomatic orbital cavernous hemangiomas. Ophthalmology 1991;98:1257-60.

Reese AB. Expanding lesions of the orbit. Trans Ophthalmol Soc UK 1971;91:85-104.

Sood S, Vashisht S, Betharia SM, Berry M. CT evaluation of orbital osseous hemangioma. Australas Radiol 1992;36:124-6.

Sullivan TJ, Aylward GW, Wright JE, et al. Bilateral multiple cavernous hemangiomas of the orbit. Br J Ophthalmol 1992;76:627-9.

Wende S, Kazner E, Grumme T. The diagnostic value of computed tomography in orbital disease: a cooperative study of 520 cases. Neurosurg Rev 1980;3:43-9.

Wilms G, Raat H, Dom R, et al. Orbital cavernous hemangioma: findings on sequential Gd-enhanced MRI. J Comput Assist Tomogr 1995;19:548-51.

Wolin MJ, Holds JB, Anderson RL, Mamalis N. Multiple orbital tumors were cavernous hemangiomas. Ann Ophthalmol 1990;22:426-8.

Wright JE. Orbital vascular anomalies. Trans Am Acad Ophthalmol Otolaryngol 1980;78:OP606-16.

Venous Vascular Malformations

Lacey B, Rootman J, Marotta TR. Distensible venous malformations of the orbit. Clinical and hemodynamic features and a new technique of management. Ophthalmology 1999;106:1197-1209.

Wright JE, Sullivan TJ, Garner A, et al. Orbital venous anomalies. Ophthalmology 1997;104;905-13.

Wright JE. Orbital vascular anomalies. Trans Am Acad Ophthalmol Otolaryngol 1974;78:606-16.

Lymphatic and Combined Venous-Lymphatic Vascular Malformations

Batsakis JG. Tumors of the Head and Neck - Clinical and Pathological Considerations, 2nd ed. Baltimore: Williams & Wilkins, 1979:301.

Brent Bond J, Haik BG, Taveras JL, et al. Magnetic resonance imaging of orbital lymphangioma with and without gadolinium contrast enhancement. Ophthalmology 1992;99:1318-24.

Cline RA, Rootman J. Enophthalmos: a clinical review. Ophthalmology 1984;91:229-37.

Harris GJ, Sakol PJ, Bonavolonta G, DeConciliis C. An analysis of thirty caes of orbital lymphangioma: pathophysiologic considerations and management recommendations. Ophthalmology 1990;97:1583-92.

Iliff WJ, Green WR. Orbital lymphangiomas. Ophthalmology 1979;86:914-29.

Jakobiec FA, Jones IS. Vascular tumors, malformations, and degenerations. In: Jones IS, Jakobiec FA, eds. Diseasesof the Orbit. Philadelphia: Harper & Row, 1979:269-308.

Jones IS. Lymphangiomas of the ocular adnexa: analysis of 62 cases. Am J Ophthalmol 1961;51:481-509.

Katz SE, Rootman J, Vangveeravong S, Graeb D. Combined venous-lymphatic malformations of the orbit (so-called lymphangiomas). Ophthalmology 1998;105:176-84.

Kazim M, Kennerdell JS, Rothfus W, Marquardt M. Orbital lymphangioma: correlation of magnetic resonance images and intraoperative findings. Ophthalmology 1992;99:1588-94.

Pang P, Jakobiec FA, Iwamoto T, Hornblass A. Small lymphangiomas of the eyelids. Ophthalmology 1984;91:1278-84.

Rootman J, Stewart B, Goldberg RA. Orbital Surgery: A Conceptual Approach. Philadelphia: Lippincott-Raven, 1995.

Rootman J, Hay E, Graeb D, Miller R. Orbital-adnexal lymphangiomas: a spectrum of hemodynamically isolated vascular hamartomas. Ophthalmology 1986;93:1558-70.

Selva D, Strianese D, Bonavolonta G, Rootman J. Orbital venous-lymphatic malformations (lymphangiomas) mimicking cavernous hemangiomas. Am J Ophthalmol 2001;131:364-70.

Waldo ED, Vuletin JC, Kaye GI. The ultrastructure of vascular tumors: additional observations and a review of the literature (part 2). Pathol Annu 1977;12:279-308.

Williams HB. Hemangiomas and lymphangiomas. Adv Surg 1981;15:317-49.

Other Congenital Vascular Malformations

Sturge-Weber Syndrome

Gass JDM. Stereoscopic Atlas of Macular Disease: Diagnosis and Treatment, 4th ed. St. Louis: Mosby, 1997:213.

Jorgensen JS, Guthoff R. Die Rolle des episkleralen Venendrucks bei der Entstehung von Sekundarglaukomen. Klin Monatsbl Augenheilkd 1988;193:471-5.

Nellhaus G, Haberland C, Hill BJ. Sturge-Weber disease with bilateral intracranial calcifications at birth and unusual pathologic findings. Acta Neurol Scand 1967;43:314-47.

Phelps CD. The pathogenesis of glaucoma in Sturge-Weber syndrome. Ophthalmology 1978;85:276-86.

Susac JO, Smith JL, Scelfo RJ. The "tomato catsup" fundus in Sturge-Weber syndrome. J Pediatr Ophthalmol Strabismus 1974;92:69-70.

Victor M, Ropper AH. Adams and Victor's Principles of Neurology, 7th ed. New York: McGraw Hill, 2001:1069-80.

Wohlwill FJ, Yakovlev PI. Histopathology of meningo-facial angiomatosis (Sturge-Weber's disease). J Neuropathol Exp Neurol 1957;16:341.

Hereditary Hemorrhagic Telangiectasia

Davis DG, Smith JL. Retinal involvement in hereditary hemorrhagic telangiectasia. Arch Ophthalmol 1971;85:618-21.

Hashimoto K, Pritzker MS. Hereditary hemorrhagic telangiectasia. Oral Surg Oral Med Oral Pathol 1972;34:751-68.

Hieshima GB, Cahan LD, Berlin MS, Pribram HW. Calvarial, orbital and dural vascular anomalies in hereditary hemorrhagic telangiectasia. Surg Neurol 1977;8:263-7.

Hodgson CH, Burchell HB, Allen GC, Clagett OT. Hereditary hemorrhagic telangiectasia and pulmonary arteriovenous fistula: a survey of a large family. N Engl J Med 1959;261:625-36.

Roman G, Fisher M, Perl DP, Poser CM. Neurological manifestations of hereditary hemorrhagic telangiectasia (Rendu-Osler-Weber disease): report of 2 cases and review of the literature. Ann Neurol 1978;4:130-44.

Swensson B, Swensson O, Haring G. Progressive disseminierte essentielle Teleangiektasien mit konjunktivaler Beteiligung. Klin Monatsbl Augenheilkd 1998;212:116-9.

Wyburn-Mason Syndrome

Archer DB, Deutman A, Ernest JT, Krill AE. Arteriovenous communications of the retina. Ophthalmology 1973;75:224-41.

Danis R, Appen RE. Optic atrophy and the Wyburn-Mason syndrome. J Clin Neuroohthalmol 1984;4:91-5.

Fujita H, Nakano K, Kumon Y, et al. [A case of Wyburn-Mason syndrome]. Rinsho Shinkeigaku 1989;29:1039-44.

Kim J, Kim OH, Suh JH, Lew HM. Wyburn-Mason syndrome: an unusual presentation of bilateral orbital and unilateral brain arteriovenous malformations. Pediatr Radiol 1998;28:161.

Maeda H, Fujieda M, Morita H, Kurashige T. [Wyburn-Mason syndrome: a case report]. No To Hattatsu 1992;24:65-9.

Theron J, Newton TH, Hoyt WF. Unilateral retinocephalic vascular malformations. Neuroradiology 1974;7:185-96.

Wyburn-Mason R. Arteriovenous aneurysm of mid-brain and retina, facial naevi and mental changes. Brain 1943;66:163-203.

Klippel-Trenaunay Syndrome

Good WV, Hoyt CS. Optic nerve shadow enlargement in the Klippel-Trenaunay-Weber syndrome. J Pediatr Ophthalmol Strabismus 1989;26:288-9.

Limaye SR, Doyle HA, Tang RA. Retinal varicosity in Klippel-Trenaunay syndrome. J Pediatr Ophthalmol Strabismus 1979;16:371-3.

Rathbun JE, Hoyt WF, Beard C. Surgical management of orbitofrontal varix in Klippel-Trenaunay-Weber syndrome. Am J Ophthalmol 1970;70:109-12.

Arteriovenous Shunts (Dural Carotid Cavernous Fistulas)

Barrow DL, Spector RH, Braun IF, et al. Classification and treatment of spontaneous carotid-cavernous sinus fistulas. J Neurosurg 1985;62:248-56.

Brismar G, Brismar J. Spontaneous carotid-cavernous fistulas: phlebographic appearance and relation to thrombosis. Acta Radiol [Diagn] (Stockh) 1976;17:180-92.

Chaudhary MY, Sachdev VP, Cho SH, et al. Dural arteriovenous malformation of the major venous sinuses: an acquired lesion. AJNR 1982;3:13-9.

Davies MA, TerBrugge K, Willinsky R, et al. The validity of classification for the clinical presentation of intracranial dural arteriovenous fistulas. J Neurosurg 1996;85:830-7.

Debrun GM, Vinuela F, Fox AJ, et al. Indications for treatment and classification of 132 carotid-cavernous fistulas. Neurosurgery 1988;22:285-9.

Grove AS Jr. The dural shunt syndrome: pathophysiology and clinical course. Ophthalmology 1984;91:31-44.

Houser OW, Campbell JK, Campbell RJ, Sundt TM Jr. Arteriovenous malformation affecting the transverse dural venous sinus: an acquired lesion. Mayo Clin Proc 1979;54:651-61.

Lasjaunias P, Chiu M, Ter Brugge K, et al. Neurological manifestations of intracranial dural arteriovenous malformations. J Neurosurg 1986;64:724-30.

Newton TH, Hoyt WF. Spontaneous arteriovenous fistula between dural branches of the internal maxillary artery and the posterior cavernous sinus. Radiology 1968;91:1147-50.

Seeger JF, Gabrielsen TO, Giannotta SL, Lotz PR. Carotid-cavernous sinus fistulas and venous thrombosis. AJNR 1980;1:141-8.

Siu K, Henderson K. Dural arteriovenous shunts in the region of the cavernous sinus. Aust N Z J Surg 1974;44:264-9.

Taki W, Nakahara I, Nishi SH, et al. Pathogenetic and therapeutic considerations of carotid-cavernous sinus fistulas. Acta Neurochir (Wien) 1994;127:6-14.

Talusan ED, Fishbein SL, Schwartz B. Increased pressure of dilated episceral veins with open-angle glaucoma without exophthalmos. Ophthalmology 1983;90:257-65.

Vinuela F, Fox AJ, Debrun GM, et al. Spontaneous carotid-cavernous fistulas: clinical, radiological, and therapeutic considerations. J Neurosug 1984; 60:976-84.

Wright JE. Orbital vascular anomalies. Trans Am Acad Ophthalmol Otolaryngol 1974;78:606-16.

New Growths

Hamartomas

Capillary Hemangioma

Haik BG, Jakobiec FA, Ellsworth RM, Jones IS. Capillary hemangioma of the lids and orbit: an analysis of the clinical features and therapeutic results in 101 cases. Ophthalmology 1979;86:760-92.

Henriksson P, Nilsson IM, Bergentz SE, et al. Giant hemangioma with a disorder of coagulation. Acta Paediatr Scand 1971;60:227-34.

Kasabach HH, Merritt KK. Capillary hemangioma with extensive purpura: report of a case. Am J Dis Child 1940;59:1063-70.

Kennedy RE. Arterial embolization of orbital hemangiomas. Trans Am Ophthalmol Soc 1978;76:266-77.

Kushner BJ. Intralesional corticosteroid injection for infantile adnexal hemangioma. Am J Ophthalmol 1982;93:496-506.

Lang PG, Dubin HV. Hemangioma-thrombocytopenia syndrome: a disseminated intravascular coagulopathy. Arch Dermatol 1975;111:105-7.

Neidhart JA, Roach RW. Successful treatment of skeletal hemangioma and Kasabach-Merritt syndrome with aminocaproic acid. Am J Med 1982;73:434-8.

Pasyk KA, Dingman RO, Argenta LC, Sandall GS. The management of hemangiomas of the eyelid and orbit. Head Neck 1984;6:851-7.

Pearce RL, Summers L, Herrmann RP. The management of patients with the Kasabach-Merritt syndrome. Br J Oral Surg 1975;13:188-95.

Plesner-Rasmussen HJ, Marushak D, Goldschmidt E. Capillary hemangiomas of the eyelids and orbit. Acta Ophthalmol 1983;61:645-54.

Steahly LP, Almquist HT. Steroid treatment of an orbital or periocular hemangioma. J Pediatr Ophthalmol 1977;14:35-7.

Stigmar G, Crawford JS, Ward CM, Thomson HG. Ophthalmic sequelae of infantile hemangiomas of the eyelids and orbit. Am J Ophthalmol 1978;85:806-13.

Teske S, Ohlrich SJ, Gole G, et al. Treatment of orbital capillary hemangioma with interferon. Aust N Z J Ophthalmol 1994;22:13-7.

Walker RS, Custer PL, Nerad JA. Surgical excision of periorbital capillary hemangiomas. Ophthalmology 1994;101:1333-40.

Wisnicki JL. Hemangiomas and vascular malformations. Ann Plast Surg 1984;12:41-59.

Neoplasia

Hemangiopericytoma

Angervall L, Kindblom LG, Nielsen JM, et al. Hemangiopericytoma: a clinicopathologic, angiographic and microangiographic study. Cancer 1978;42:2412-27.

Brown DN, MacCarty CS, Soule EH. Orbital hemangiopericytoma: review of the literature and report of four cases. J Neurosurg 1965;22:354-61.

Croxatto JO, Font RL. Hemangiopericytoma of the orbit: a clinicopathologic study of 30 cases. Hum Pathol 1982;13:210-8.

Enzinger FM, Smith BH. Hemangiopericytoma: an analysis of 106 cases. Hum Pathol 1976;7:61-82.

Folpe AL, Devaney K, Weiss SW. Lipomatous hemangiopericytoma: a rare variant of hemangiopericytoma that may be confused with liposarcoma. Am J Surg Pathol 1999;23:1201-7.

Fox SA. Hemangiopericytoma of the orbit. Am J Ophthalmol 1955;40:786-9.

Francois J, Hassens M. Hemangiopericytome de l'orbite. Ann Oculist 1963;196:873-911.

Geisinger KR, Silverman JF, Cappellari JO, Dabbs DJ. Fine-needle aspiration cytology of malignant hemangiopericytomas with ultrastructural and flow cytometric analyses. Arch Pathol Lab Med 1990;114:705-10.

Gensler S, Caplan LH, Laufman H. Giant benign hemangiopericytoma functioning as an arteriovenous shunt. JAMA 1966;198:203-6.

Goodman SA. Hemangiopericytoma of the orbit. Am J Ophthalmol 1955;40:237-43.

Henderson JW, Farrow GM. Primary orbital hemangiopericytoma: an aggressive and potentially malignant neoplasm. Arch Ophthalmol 1978;96:666-73.

Jakobiec FA, Howard GM, Jones IS, Wolff M. Hemangiopericytoma of the orbit. Am J Ophthalmol 1974;78:816-34.

Kikuchi K, Kowada M, Sageshima M. Orbital hemangiopericytoma: CT, MR, and angiographic findings. Comput Med Imaging Graph 1994;18:217-22.

Macoul KL. Hemangiopericytoma of the lid and orbit. Am J Ophthalmol 1968;86:731-3.

McMaster MJ, Soule EH, Ivins JC. Hemangiopericytoma: a clinicopathologic study and long-term follow-up of 60 patients. Cancer 1975;36:2232-44.

Rice CD, Kersten RC, Mrak RE. An orbital hemangioperictyoma recurrent after 33 years. Arch Ophthalmol 1989;107:552-6.

Shields JA, Shields CA, Rashid RC. Clincopathologic correlation of choroidal folds: secondary to massive cranioorbital hemangiopericytoma. Ophthal Plast Reconstr Surg 1992;8:62-8.

Sugar HS, Fishman GR, Kobernick S, Goodman P. Orbital hemangiopericytoma or vascular meningioma? Am J Ophthalmol 1970;70:103-9.

Sullivan TJ, Wright JE, Wulc AE, et al. Haemangiopericytoma of the orbit. Aust N Z J Ophthlamol 1992;20:325-32.

Malignant Hemangioendothelioma: Angiosarcoma

Carelli PV, Cangelosi JP. Angiosarcoma of the orbit. Am J Ophthalmol 1948;31:453-6.

Hufnagel T, Ma L, Kuo TT. Orbital angiosarcoma with subconjunctival presentation. Report of a case and literature review. Ophthalmology 1987;94:72-7.

Maddox JC, Evans HL. Angiosarcoma of skin and soft tissue: a study of forty-four cases. Cancer 1981;48:1907-21.

Messmer EP, Font RL, McCrary JA 3rd, Murphy D. Epithelioid angiosarcoma of the orbit presenting as Tolosa-Hunt syndrome. A clinicopathologic case report with review of the literature. Ophthalmology 1983;90:1414-21.

Sekimoto T, Nakaseko H, Kondo K, et al. A case of malignant hemangioendothelioma in the orbit. Nippon Ganka Kiyo 1971;22:535-8.

Stout AP. Hemangio-endothelioma: a tumor of blood vessels featuring vascular endothelial cells. Ann Surg 1943;118:445-64.

Treheux A, Reny A, Picard JL, et al. Tumeur rare de l'orbite chez l'enfant. J Radiol Electrol Med Nucl 1975;56:279-80.

Tsuda N, Takaku I. A case report of malignant vascular tumor of the orbit in a newborn. Folio Ophthalmol Japonica 1970;21:728.

Kaposi's Sarcoma

Dayan AD, Lewis PD. Origin of Kaposi's sarcoma from the reticuloendothelial system. Nature 1967;213:889-90.

Giraldo G, Beth E, Cocur P, et al. Kaposi's sarcoma: a new model in the search for viruses associated with human malignancies. J Natl Cancer Inst 1972;49:1495-507.

Giraldo G, Beth E, Huang ES. Kaposi's sarcoma and its relationship to cytomegalovirus (CMNV). III. CMV, DNA and CMV early antigens in Kaposi's sarcoma. Int J Cancer 1980;26:23-9.

Holland GN, Gottlieb MS, Yee RD, et al. Ocular disorders associated with a new severe acquired cellular immunodeficiency syndrome. Am J Ophthalmol 1982;93:393-402.

Holecek MJ, Harwood AR. Radiotherapy of Kaposi's sarcoma. Cancer 1978;41:1733-8.

Howard GM, Jakobiec FA, DeVoe AG. Kaposi's sarcoma: the subconjunctival hemorrhage that never clears. Am J Ophthalmol 1975;79:420-3.

Kalinske M, Leone CR Jr. Kaposi's sarcoma involving eyelid and conjunctiva. Ann Ophthalmol 1982;14:497-9.

Lanzotti VJ, Campos LT, Sinkovrics JG, Samuels ML. Chemotherapy for advanced Kaposi's sarcoma. Arch Dermatol 1975;111:1331-3.

Macher AM, Palestine A, Masur H, et al. Multicentric Kaposi's sarcoma of the conjunctiva in a male homosexual with the acquired immunodeficiency syndrome. Ophthalmology 1983;90:879-84.

O'Brien PH, Brasfield RD. Kaposi's sarcoma. Cancer 1966;19:1497-502.

Odom RB, Goette DK. Treatment of cutaneous Kaposi's sarcoma with intralesional vincristine. Arch Dermatol 1978;114:1693-4.

Sezer N, Ercikan C. Kaposi's sarcoma with ocular manifestations. Br J Ophthalmol 1964;48:223-6.

Templeton AC, Bhana D. Prognosis in Kaposi's sarcoma. J Natl Cancer Inst 1975;55:1301-4.

Vascular Leiomyoma

Carrier DA, Mawad ME, Kirkpatrick JB. MR appearance of an orbital leiomyoma. AJNR 1993;14:473-4.

Duhig JT, Ayer JP. Vascular leiomyoma. A study of 61 cases. Arch Pathol 1959;68:424-30.

Henderson JW, Harrison EG Jr. Vascular leiomyoma of the orbit: report of a case. Trans Am Acad Ophthalmol Otolaryngol 1970;74:970-4.

Jakobiec FA, Howard GM, Rosen M, Wolff M. Leiomyomas and leiomyosarcoma of the orbit. Am J Ophthalmol 1975;80:1028-42.

Jakobiec FA, Jones IS, Tannenbaum M. Leiomyoma: an unusual tumor of the orbit. Br J Ophthalmol 1973;57:825-31.

Nath K, Shukla BR. Orbital leiomyoma and its origin. Br J Ophthalmol 1963;47:369.

Sanborn GE, Valenzuela RE, Green WR. Leiomyoma of the orbit. Am J Ophthalmol 1979;87:371-5.

Wolter JR. Hemangio-leiomyoma of the orbit. Eye Ear Nose Throat Mon 1965;44:42-6.

Epithelioid Hemangioendothelioma

Lyon DB, Tang TT, Kidder TM. Epithelioid hemangioendothelioma of the orbital bones. Ophthalmology 1992;99:1773-8.

Messmer EP, Font RL, McCrary JA IIIrd, Murphy D. Epithelioid angiosarcoma of the orbit presenting as Tolosa-Hunt syndrome. Ophthalmology 1983;90:1414-21.

Aneurysms

Kikuchi K, Kowada M. Case report: saccular aneurysm of the intraorbital ophthalmic artery. Br J Radiol 1994;67:1134-5.

Marotta TR, Lingawa SS, Katz SE, Woodhurst WB, Rootman J. Intraorbital rupture of a cavernous internal carotid artery aneurysm: therapeutic options. Ophthal Plast Reconstr Surg 2001;17:67-72.

Ogawa A, Tominaga T, Yoshimoto T, Kiyosawa M. Intraorbital ophthalmic artery aneurysm: case report. Neurosurgery 1992;31:1102-4.

Chapter 14

Degenerations and Depositions

Patients with degenerations and depositions were the smallest group (1.6%) encountered in the UBC orbital practice. Patients in this category have a range of atrophies and abiotrophies that lead to changes of the orbit or its contents. They may present clinically with pseudoproptosis (myopia, buphthalmos; Fig. 14-1), enophthalmos (fat atrophies), ocular motor abnormalities (progressive external ophthalmoplegia, mitochondrial dystrophies, amyloid deposition), or mass effect (amyloid deposition, orbital fat prolapse).

Degenerations

Myopia was a frequent cause of pseudoproptosis in patients seen in our orbital practice. In such patients, pseudoproptosis may occur spontaneously, either bilaterally or unilaterally, or secondary to atrophy following injury or childhood inflammation of the contralateral orbit. Other degenerative causes of pseudoproptosis include failure of recognition of facial asymmetry, unilateral bony hypoplasia, ptosis, buphthalmos (Fig. 14-1), spontaneous lid retraction, and staphyloma.

Orbital Atrophy

Orbital atrophy can be secondary to fatty degeneration following severe orbital trauma, hemorrhage, inflammation, or radiotherapy. Orbital radiotherapy (particularly when delivered in childhood) causes fat atrophy and enophthalmos; unfortunately, this is a common consequence of retinoblastoma and rhabdomyosarcoma treatment with external beam radiotherapy (Fig. 14-2).

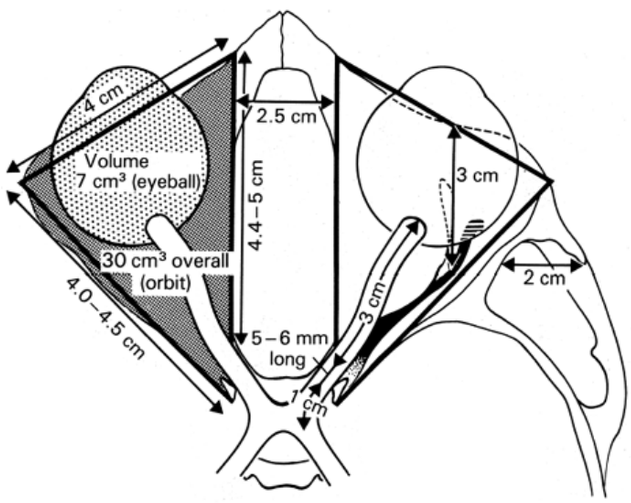

Figure 14-1. Axial CT scan demonstrates a buphthalmic left eye in a 67-year-old man who presented with a history of childhood amblyopia and strabismus, and a recent awareness of increasing prominence of the left eye. On physical examination, the left globe was 2 mm more prominent than the right, and displaced downward 3 mm with an 18 diopter right hypertropia. On fundus examination, there was left peripapillary atrophy and old chorioretinal scars. The CT scan supports a diagnosis of a large globe causing the appearance of proptosis.

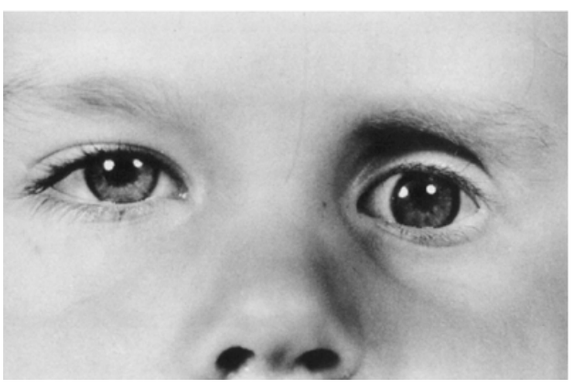

Figure 14-2. This child with bilateral retinoblastoma had been treated several years earlier with left orbital radiotherapy and local therapy on the right side. The radiotherapy led to obvious orbital shrinkage. (Reproduced with permission from Cline RA, Rootman J. Enophthalmos: a clinical review. Ophthalmology 1984;91:229-37.)

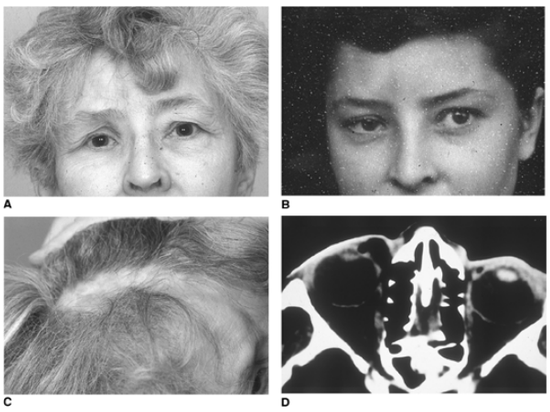

Figure 14-3. (A) This 57-year-old woman was referred for examination because of right enophthalmos. She had noted that the right eye was always smaller but it had become more obvious in the last 12 years. (B) A photograph of the patient at age 14 years demonstrates the deepened right superior sulcus. Note that in both A and B, there is evidence of an atrophic linear scar of the forehead and scalp (en coup de sabre) with loss of hair in the same dermatome (C). On physical examination, the interpalpebral fissure was 8 mm on the right and 9 mm on the left with a reduction of right maximum levator function by 3 mm compared with the left. There was evidence of slight lagophthalmos, and exophthalmometry was 6 mm on the right and 14 mm on the left with a deepened superior sulcus and reduced elevation, infraduction, and abduction. (D) Her CT scan demonstrated enophthalmos with fat atrophy. The final diagnosis was linear scleroderma. (Fig. 14-3D reproduce with permission from Lacey B, Chang W, Rootman J. Nonthyroid causes of extraocular muscle disease. Surv Ophthalmol 1999;44: 187-213.)

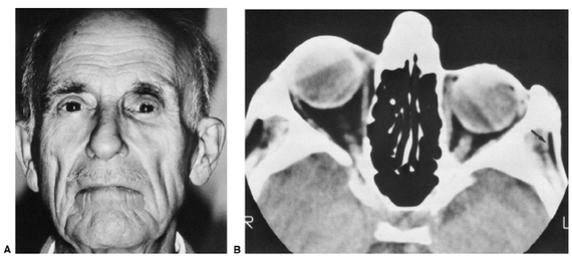

Figure 14-4. (A) This 78-year-old man had noted “sinking” of his left eye for 1 to 2 years. He was otherwise healthy with no known sinus problems or other ocular symptoms. His vision was normal, as were extraocular movements. There was a markedly deepened left superior sulcus and temporalis fossa. From a clinical viewpoint, he appeared to have some orbital fat atrophy and similar atrophy in the temporalis fossa. Old photographs revealed that this atrophy had been progressive for the past 3 years. (B) Axial CT scan shows left enophthalmos with reduced orbital fat and a diminution of fat in the temporalis fossa (arrow) when compared with the right side.

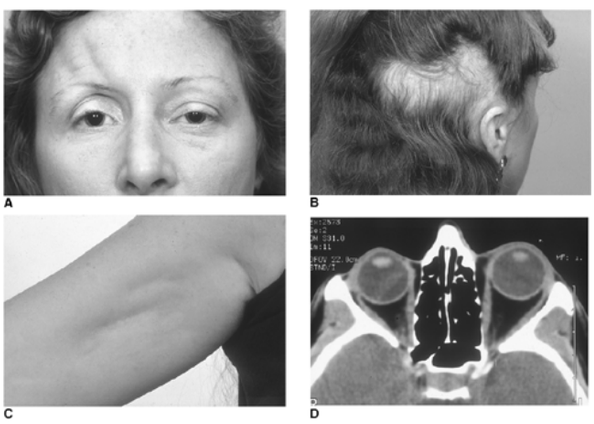

Figure 14-5. (A, B) This 33-year-old woman presented with a 15-year history of right enophthalmos, a deepened superior sulcus, and atrophy of the bony forehead and scalp with loss of hair. She also had a history of granulomatous uveitis and iritis. Other findings included a smaller right hand and focal areas of skin and muscle atrophy (C). The interpalpebral fissure was 10 mm on the right and 7 mm on the left, and there was a deep superior sulcus with linear thinning of the scalp and forehead with absence of brow and scalp hair. Exophthalmometry was 10 mm on the right and 14 mm on the left. There was also palpable underlying bony change and no evidence of cicatricial involvement of the orbit with a full range of ocular movements. She was neurologically normal on primary assessment, and CT scan (D) demonstrated orbital fat atrophy. She was diagnosed with Parry-Romberg syndrome. Five years later, she developed some balance problems with increasing shrinkage of the muscles in the right arm and scapula, a weak shoulder girdle, and depressed reflexes with numbness of the dorsum of her foot. An MRI was performed and showed a parietal lesion.

Abiotrophies

Orbital volume loss may be a part of a regional disorder, such as linear scleroderma (Fig. 14-3), an idiopathic syndrome in the elderly (Fig. 14-4), or related to Parry-Romberg syndrome (Fig. 14-5). Linear scleroderma is characterized by a progressive (Figs. 14-3A and B) atrophy of the subcutaneous tissues, usually in the V_1 dermatome (Fig. 14-3C). It is often associated with hair loss from the head or brow, producing the classic “en coup de sabre” picture. It is unassociated with changes in the underlying bone, neurologic problems, or lateralization elsewhere in the body. We have seen several patients with these classical features who also demonstrated cicatricial atrophy of the lid and extraocular muscles on the affected side along with fat atrophy, resulting in enophthalmos (Fig. 14-3).

In contrast to linear scleroderma, Parry-Romberg syndrome (or progressive facial hemiatrophy - PFK) consists of a hemifacial progressive atrophy of the subcutaneous fat that starts early in life and is associated with atrophy of the dermal, muscular, and skeletal tissues on the affected side of the face. In addition, it has been described with involvement of the ipsilateral upper extremities and half of the body, with rare contralateral involvement. Bone atrophy tends to be associated with an earlier onset of this syndrome. The disorder may be associated with generalized epilepsy and neurological features. Besides enophthalmos, Horner's syndrome, heterochromic iritis, retinitis, and uveitis have been described. There is evidence of cicatricial atrophy of the dermis and subdermal fat with some inflammatory features

histologically. Imaging of the central nervous system has suggested in some instances that vascular abnormalities, malformations, and dysplasias may be associated with this neurocutaneous syndrome. The inflammatory features may suggest a immunogenic neurovascular disorder. Some of the features bear resemblance to linear scleroderma but clinical ocular inflammation and neurocutaneous changes, as well as bony anomalies, are not seen in linear scleroderma.

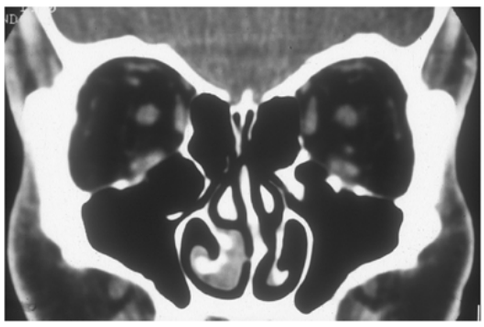

Figure 14-6. This CT scan demonstrates extraocular atrophy in a 24-year-old male. The patient manifested marked restriction of ocular movements, particularly in elevation and adduction, with positive forced ductions of his inferior recti. He was aware of some weakness affecting the muscles of the upper part of his body. Additionally, he suffered from weakness of his shoulders and thighs. Careful evaluation including biopsy was not diagnostic for mitochondrial myopathy but suggested a generalized myopathy. (Reproduced with permission from Lacey B, Chang W, Rootman J. Nonthyroid causes of extraocular muscle disease. Surv Ophthalmol 1999;44:187-213.)

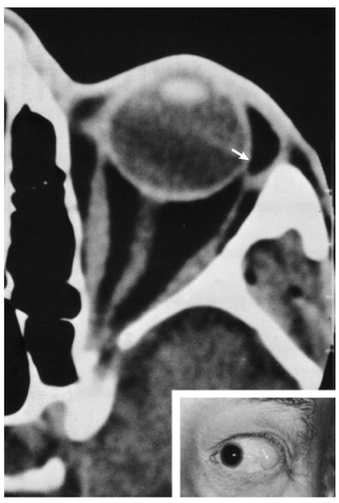

Figure 14-7. Clinical photograph and axial CT scan demonstrate lateral prolapse of orbital fat through Tenon's capsule (arrow), a clinical syndrome that often presents as an apparent anterior orbital mass.

The primary orbital fat atrophies, particularly those associated with the aging process, do not affect muscle balance. We have also encountered several cases of muscle atrophy associated with restriction of extraocular movement (Fig. 14-6), two of which were due to mitochondrial dystrophy.

Another commonly seen degenerative condition is in the patient who presents with a mass, usually in the region of the lacrimal gland, due to a prolapse of fat through the weakened Tenon's capsule. This, of course, is a disorder of the elderly. It may be diagnosed on the basis of ease of retropulsion of the orbital fat prolapse, evidence of fat seen through Tenon's capsule on slit-lamp examination, normal conjunctiva, and normal ocular motor and orbital findings. It is frequently associated with other features of periorbital fat prolapse. On CT scan, this has a dramatic appearance of a focal area of radiolucency adjacent to the sclera anteriorly (Fig. 14-7).

Depositions

Orbital Amyloid Deposition

Given what is known about pathogenesis, it could be argued that amyloid belongs in the category of inflammatory or lymphoproliferative disease processes. However, we have included it here as a deposition because of its varied and overlapping distribution and its distinctive nature. Amyloid diseases have in common the deposition of several types of abnormal fibrillar proteins with similar physical chemical properties. The characterization of the different types of proteins in amyloid deposits has led to a classification based on not only clinicopathologic features but the nature of the amyloid protein (Table 14-1). The symptoms associated with deposition depend on the site, distribution, and magnitude of amyloid, with renal involvement being the most serious. The diagnosis is by biopsy evidence of amyloid in the involved tissues.

These proteins appear as an amorphous, eosinophilic, hyaline material on routine light microscopy. A pathognomonic feature is positive congophilia (Congo red stain) with blue-green birefringence (dichroism) on polarizing microscopy. In addition, these deposits may be defined histochemically

by metachromasia with crystal or methyl violet and fluorescence in ultraviolet light following thioflavin T or thioflavin S staining. Ultrastructurally, amyloid consists of parallel rows of fibers 75 nm to 100 nm in diameter (Fig. 14-8D) that show a cross beta-pleated sheet structure on X-ray diffraction.

Table 14-1. Clinical amyloidosis syndromes and corresponding amyloid fibril

CLINICAL SYNDROME	FIBRIL PROTEIN	ORIGIN
Primary amyloidosis	AL	Monoclonal immunoglobulin light chains
Amyloidosis associated with multiple myeloma	AL	Monoclonal immunoglobulin light chains
Reactive amyloidosis (secondary amyloidosis)	AA	Serum amyloid A (SAA) = acute phase reactant
Familial Mediterranean fever	AA	Serum amyloid A (SAA) = acute phase reactant
Familial amyloid polyneuropathy (type I, II)	ATTR	Transthyretin
Familial amyloidotic cardiomyopathy	ATTR	Transthyretin
Senile systemic amyloidosis	ATTR	Transthyretin
Familial amyloid polyneuropathy (type III) (Iowa)	AApoAI	Apolipoprotein AI
Familial amyloid polyneuropathy (type IV) (Finnish)	AGel	Gelsolin
Hereditary cerebral hemorrhage with amyloidosis (Icelandic)	ACys	Cystatin C
Alzheimer's disease	A	Protein
Down's syndrome	A	Protein
Hereditary cerebral hemorrhage with amyloidosis (Dutch)	A	Protein
Dialysis-related amyloidosis	2-microglobulin	2-microglobulin
Amyloidosis associated with medullary carcinoma of the thyroid	Precalcitonin	Precalcitonin

From Table 1 of Pasternak S, White VA, Gascoyne RD, Perry SR, Johnson RLC, Rootman J. Monoclonal origin of localised orbital amyloidosis detected by molecular analysis. Br J Ophthalmol 1996;80:1013-7.

Amyloid deposition can be categorized on the basis of distribution into systemic and localized disease. The systemic type can be divided into immunocyte-related (primary), secondary (related to inflammatory disease), and familial. In the immunocyte-related (i.e., primary systemic amyloidosis without underlying disease) and lymphoma-related amyloidosis, the fibrils are composed of fragments from a variable region of proteins derived from monoclonal immunoglobulin light chains and are termed *AL amyloid*. They are typically deposited around blood vessels, in skin, nerve, and muscle of the tongue, heart, and gastrointestinal tract. Skin is a characteristic site in so-called primary amyloidosis, where amyloid deposits as yellow plaques.

Secondary amyloidosis occurs in conjunction with a variety of inflammatory conditions including rheumatoid arthritis (14% to 26% of patients with arthritis), dermatomyositis, scleroderma, inflammatory bowel disease, osteomyelitis, lung abscess, and leprosy. The protein fibrils in secondary amyloidosis (*AA amyloid*) are derived from an acute-phase reactant, serum amyloid A protein. Both overproduction and defective degradation of precursor proteins are involved in the pathogenesis of fibril deposition in both types of systemic amyloidosis. The organs commonly affected in secondary amyloidosis are liver, spleen, kidneys, and adrenals. The heredofamilial systemic amyloidosis syndromes are rare. They are usually described on the basis of geographic origin of the cases and can be divided into neuropathies (Portuguese), nephropathies (familial Mediterranean fever), cardiopathies, and miscellaneous (including lattice corneal dystrophy, medullary tumor of the thyroid, and cerebral amyloidosis). The neuropathies have *AF amyloid* derived from pre-albumin.

In the orbit, amyloidosis may be localized or part of a systemic disorder. The systemic form, when it involves the orbit, may be primary or associated with multiple myeloma. It is usually associated with deposition of *AL amyloid*. From a clinical point of view, the orbital appearance in systemic disorder is characterized by involvement of the skin of the eyelids with a waxy yellow subcutaneous deposit, frequently associated with spontaneous hemorrhage and ecchymosis. This contrasts with localized, diffuse, or nodular amyloidosis,

which do not have cutaneous involvement. Immunocyte-related systemic amyloidosis (primary and lymphoma-related) may also infiltrate cranial nerves or extraocular muscles and will rarely involve the vitreous, retina, choroid, and sclera.

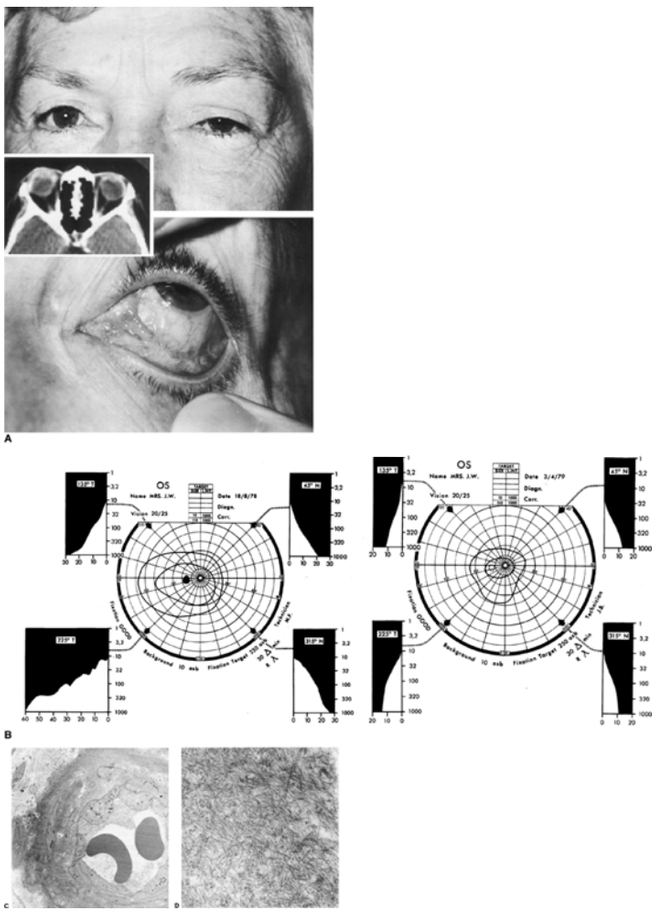

Figure 14-8. (A, top) This 62-year-old woman had left orbital aching and drooping of the lid, which had been present for 18 months. In addition, she was aware of inferior conjunctival thickening and injection. On physical examination, the lower lid and orbit had a doughy consistency. The tissues of the semilunar fold and both inferior and superior conjunctival fornices were thickened by a firm, yellowish, subconjunctival infiltrate (A, bottom). There was reduced corneal sensation, full extraocular movement, normal exophthalmometry, and normal fundus examination. The CT scan (A, inset) shows an increased density of the left upper lid and thickening of the anterior portion of the sclera and orbit. (B) Visual fields demonstrate a general constriction on the left side, which progressed over the next year. The anterior orbital and subconjunctival amyloid mass was debulked. (C) Electron microscopy of the orbital specimen demonstrates extracellular amyloid filaments in close relation to endothelial and smooth muscle cells. The amyloid encases perivascular cells (original magnification × 5600). (D) High power electron micrograph demonstrates extracellular amyloid filaments forming a dense meshwork (original magnification × 94000). We postulated that peripheral amyloid deposition had affected the pial vessels, leading to the extremely steep profile of the constricted isopters demonstrated on static perimetry in (B).

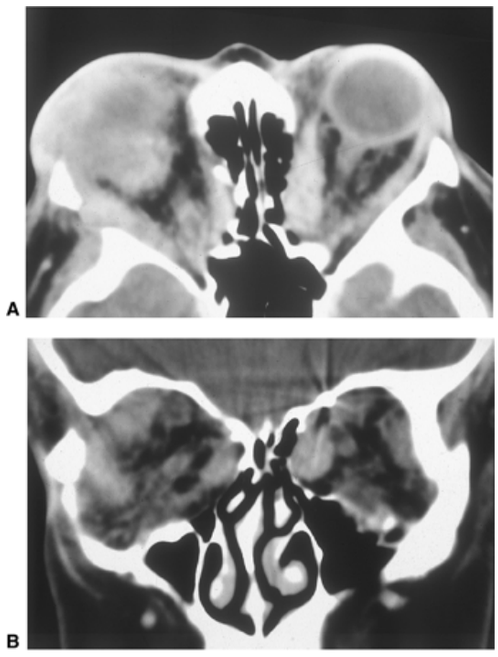

Figure 14-9. The axial (A) and coronal (B) CT scans demonstrate nodular enlargement of the extraocular muscles and infiltration of the adjacent tissues in a 44-year-old woman who had undergone decompression for progressive exophthalmos thought to be associated with thyroid orbitopathy. Biopsy showed localized amyloid that proved on PCR analysis to be a monoclonal immunoglobulin. The patient was treated with 3000 cGy to the orbits, leading to disease regression. (Fig. 14-9B reproduced with permission from Lacey B, Chang W, Rootman J. Nonthyroid causes of extraocular muscle disease. Surv Ophthalmol 1999;44:187-213.)

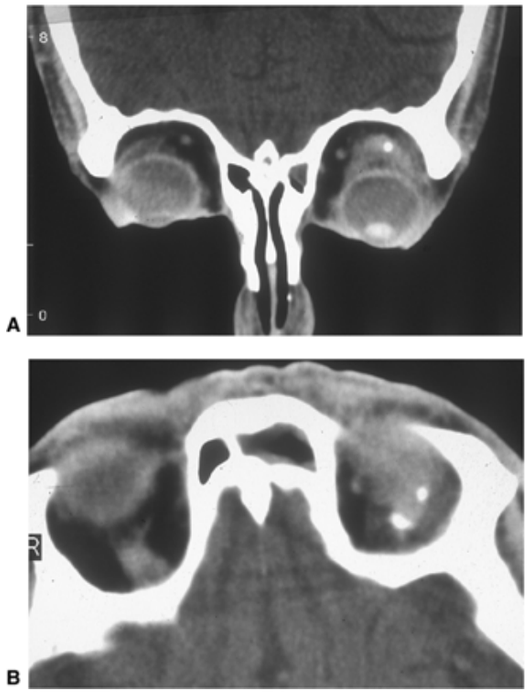

Figure 14-10. This focally calcified, irregular anterior orbital lesion occurred in an 85-year-old man who presented with ptosis, downward displacement of the globe, and mild proptosis. The granular lesion was removed piecemeal via an orbitotomy and proved to be an amyloidoma with a sparse cellular component. One year later, he is free of recurrent disease.

We have seen two types of localized orbital amyloidosis that parallels those described in the literature. One was a case of bilateral nodular infiltration of the extraocular muscles and adjacent orbital tissues, associated with progressive proptosis and restriction of extraocular movements (Fig. 14-9). The second type was two cases of amyloidoma. Both occurred in the anterior orbit adjacent to the lacrimal gland, which is the usual location described in the literature. Focal calcification may be noted in amyloidomas and provides a differential feature. At the time of surgery, these lesions are characteristically waxy yellow in appearance and extremely friable (almost curettable) (Fig. 14-10).

On pathologic investigation using polymerase chain reaction (PCR) analysis, we were able to establish a monoclonal origin of the plasma cells in two cases (Fig. 14-9). Both of the patients were treated with radiotherapy successfully after the diagnosis was established. A final case that we have encountered involved the forniceal conjunctiva and extended into the deep orbit, leading to visual field contraction (Fig. 14-8).

A primary localized amyloid has been frequently reported in the cornea and conjunctiva and does not usually involve the orbit. Localized amyloid secondary to chronic inflammation or infections of the conjunctiva or cornea usually is subclinical and identified only at the time of microscopy; it also does not involve the orbit. Amyloid is less common in the orbit and when present, may appear as a slowly expanding mass anywhere within the soft tissues. When it affects the extraocular muscles, it characteristically causes a nodular enlargement (Fig. 14-9). Immunoamyloidosis may be due to a production of amyloidogenic light-chain immunoglobulin protein by a proliferating clone of plasma cells, which may be localized or disseminated in distribution. The benign localized form of this disease has been found in various organs, particularly the bronchopulmonary tree and ocular sites such as the orbit, eyelid, and conjunctiva. We have also reported an example of localized ocular immunoamyloidosis involving the caruncle due to a single clone of plasma cells.

In summary, orbital infiltration by amyloid is most often primary and localized, although it may be part of a systemic syndrome where the lid is usually involved as well. Deposits of primary amyloid may initially occur in the conjunctiva and rarely will subsequently extend to involve more posterior tissues. This may cause proptosis or infiltrate the extraocular muscles to produce motility disturbances or ptosis. In the late stages, complete fixation of the globe occasionally occurs. Lacrimal gland involvement can lead to expansion of the lacrimal fossa and tumefaction with associated keratoconjunctivitis indistinguishable from a slow-growing tumor of the lacrimal gland. Orbital pain secondary to nerve infiltration has been described. In addition, recurrent orbital hemorrhages and eyelid purpura from perivascular deposits have been noted.

Infiltrates usually develop so insidiously that the diagnosis is often late. Biopsy and histopathologic examination with special stains (including immunohistochemistry) are mandatory. Evaluation for systemic involvement includes a thorough physical examination, blood and urine protein immunoelectrophoresis, 24-hour urine assessment for Bence Jones proteins (immunoglobulin light chain fragments), and bone marrow aspirate in cases of suspected multiple myeloma. Rectal and abdominal fat biopsies may help rule out the presence of systemic disease.

Definitive treatment for localized amyloidosis is surgical excision and reconstruction where possible but as noted, radiotherapy may play a role in treatment. Damage is restricted to the involved tissue, because localized amyloidosis apparently never systematizes. Therefore, the prognosis is favorable for most orbital cases. However, the systemic variety has a more serious course. In some cases of secondary amyloidosis, elimination of chronic infection or removal of the inciting neoplasm may result in resorption of the deposits. However, most primary and secondary systemic cases progress inexorably to cause major organ failure with a mean survival following diagnosis of between 1 and 4 years. Death is on average within 14 months, but may occur any time between that period and 10 years. Patients with myeloma and amyloidosis usually die within 6 months. There have been attempts to treat familial Mediterranean fever and primary systemic amyloidosis with colchicine and dimethylsulfoxide (DMSO).

Bibliography

Parry-Romberg Syndrome

Bilen N, Efendi H, Apaydin R, et al. Progressive facial hemiatrophy (Parry-Romberg syndrome). Aust J Dermatol 1999;40:223-5.

Chapman MS, Peraza JE, Spencer SK. Parry-Romberg syndrome with contralateral and ipsilateral extremity involvement. J Cutan Med Surg 1999;3:260-2.

Cory RC, Clayman DA, Faillace WJ, et al. Clinical and radiologic findings in progressive facial hemiatrophy (Parry-Romberg syndrome). AJNR 1997;18:751-7.

Dupont S, Catala M, Hasboun D, et al. Progressive facial hemiatrophy and epilepsy: a common underlying dysgenetic mechanism. Neurology 1997;48:1013-8.

Fernandez O, Romero F, Salazar JA, Rodriguez-Barrionuevo C. El sindrome de Parry-Romberg: una forma de vasculitis focal. Neurologia 1998;13:54-7.

Goldberg-Stern H, deGrauw T, Passo M, Ball WS Jr. Parry-Romberg syndrome: follow-up imaging during suppressive therapy. Neuroradiology 1997;39:873-6.

Matthias C, Terstegge K, Siemes H. Otorhinolaryngological complications of progressive facial hemiatrophy (Romberg's disease). Ann Otol Rhinol Laryngol 1995;104:853-7.

Miedziak AI, Stefanyszyn M, Flanagan J, Eagle RC Jr. Parry-Romberg syndrome associated with intracranial vascular malformations. Arch Ophthalmol 1998;116:1235-7.

Miller MT, Spencer MA. Progressive hemifacial atrophy. A natural history study. Trans Am Ophthalmol Soc 1995;93:203-17.

Ong K, Billson FA, Pathirana DS, Clifton-Bligh P. A case of progressive hemifacial atrophy with uveitis and retinal vasculitis. Aust N Z J Ophthalmol 1991;19:295-8.

Pensler JM, Murphy GF, Mulliken JB. Clinical and ultrastructural studies of Romberg's hemifacial atrophy. Plast Reconstr Surg 1990;85:669-74.

Taylor HM, Robinson R, Cox T. Progressive facial hemiatrophy: MRI appearance. Dev Med Child Neurol 1997;39:484-6.

Terstegge K, Kunath B, Felber S, et al. MR of brain involvement in progressive facial hemiatrophy (Romberg disease): reconsideration of a syndrome. AJNR 1994;15:145-50.

Woolfenden AR, Tong DC, Norbash AM, Albers GW. Progressive facial hemiatrophy: abnormality of intracranial vasculature. Neurology 1998;50:1915-7.

Amyloidosis

Borodic GE, Beyer-Machule CK, Millin J, et al. Immunoglobulin deposition in localized conjunctival amyloidosis. Am J Ophthalmol 1984;98:617-22.

Campos EC, Melato M, Manconi R, Antonutto G. Pathology of ocular tissues in amyloidosis. Ophthalmologica 1980;181:31-40.

Cline RA, Rootman J. Enophthalmos: a clinical review. Ophthalmology 1984;91:229-37.

Cohen AS, Connors LH. The pathogenesis and biochemistry of amyloidosis. J Pathol 1987;151:1-10.

Cohen AS, Shirahama T, Sipe JD, Skinner M. Editorial. Amyloid proteins, precursors, mediator, and enhancer. Lab Invest 1983;48:1-4.

Cooper JH, Ramsey M, Rootman J. Extramedullary plasmacytoma (amyloid tumor) of the caruncle. Can J Ophthalmol 1989;24:166-8.

Cotran RS, Kumar V, Collins T. Diseases of immunity. In: Cotran RS, Kumar V, Collins T, eds. Robbins Pathologic Basis of Disease. 6th ed. Philadelphia: WB Saunders, 1999:188-259.

Erie JC, Garrity JA, Norman ME. Orbital amyloidosis involving the extraocular muscles. Arch Ophthalmol 1989;107:1428-9.

Finlay KR, Rootman J, Dimmick J. Optic neuropathy in primary orbital amyloidosis. Can J Ophthalmol 1980;15:189-92.

Gean-Marton AD, Kirsch CF, Vezina LG, Weber AL. Focal amyloidosis of the head and neck: evaluation with CT and MR imaging. Radiology 1991;181:521-5.

Glenner GG. Amyloid deposits and amyloidosis: the beta-fibrilloses I. N Engl J Med 1980;302:1283-92.

Glenner GG. Amyloid deposits and amyloidosis: the beta-fibrilloses II. N Engl J Med 1980;302:1333-43.

Husby G, Sletten K. Chemical and clinical classification of amyloidosis. Scand J Immunol 1986;23:253-65.

Kaiser-Kupfer MI, McAdam KPWJ, Kuwabara T. Localized amyloidosis of the orbit and upper respiratory tract. Am J Ophthalmol 1977;84:721-8.

Kisilevsky R. Amyloidosis: a familiar problem in the light of current pathogenetic developments. Lab Invest 1983;49:381-90.

Klintworth GK. Proteins in ocular disease. In: Garner A, Klintworth DG, eds. Pathobiology of Ocular Disease. New York: Marcel Dekker, 1994:993-1007.

Knowles D, Jakobiec F, Rosen M, Howard G. Amyloidosis of the orbit and adnexae. Surv Ophthalmol 1975;19:367-84.

Kyle RA, Greipp PR. Amyloidosis (AL). Clinical and laboratory features in 229 cases. Mayo Clin Proc 1983;58:665-83.

Levine MR, Buckman G. Primary localized orbital amyloidosis. Ann Ophthalmol 1986;18:165-7.

Lucas DR, Knox F, Davies S. Apparent monoclonal origin of lymphocytes and plasma cells infiltrating ocular adnexal amyloid deposits: report of 2 cases. Br J Ophthalmol 1982;66:600-6.

Marsh WM, Streeten BW, Hoepner JA, et al. Localized conjunctival amyloidosis associated with extranodal lymphoma. Ophthalmology 1987;94:61-4.

Murdoch IE, Sullivan TJ, Moseley I, et al. Primary localised amyloidosis of the orbit. Br J Ophthalmol 1996;80:1083-6.

Okamoto K, Ito J, Emura I, et al. Focal orbital amyloidosis presenting as rectus muscle enlargement: CT and MR findings. AJNR 1998;19:1799-801.

Pasternak S, White VA, Gascoyne RD, Perry SR, Johnson RLC, Rootman J. Monoclonal origin of localised orbital amyloidosis detected by molecular analysis. Br J Ophthalmol 1996;80:1013-7.

Raflo GT, Farrell TA, Sioussat RS. Complete ophthalmoplegia secondary to amyloidosis associated with multiple myeloma. Am J Ophthalmol 1981;92:221-4.

Schaldenbrand JD, Keren DF. IgD amyloid in IgD-lambda monoclonal conjunctival amyloidosis. A case report. Arch Pathol Lab Med 1983;107:626-8.

Simpson GT 2nd, Skinner MS, Strong M, Cohen AS. Localized amyloidosis of the head and neck and upper aerodigestive and lower respiratory tracts. Ann Otol Rhinol Laryngol 1984;93:374-9.

Tan SY, Pepys MB. Amyloidosis. Histopathology 1994;25:403-14.

Tan SY, Murdoch IE, Sullivan TJ, et al. Primary localized orbital amyloidosis composed of immunoglobulin gamma heavy chain CH3 domain. Clin Sci 1994;87:487-91.

Subject Index

A

B

C

D

E

I

K

L

M

N

O

P

R

S

T

U

V

W

X

Z